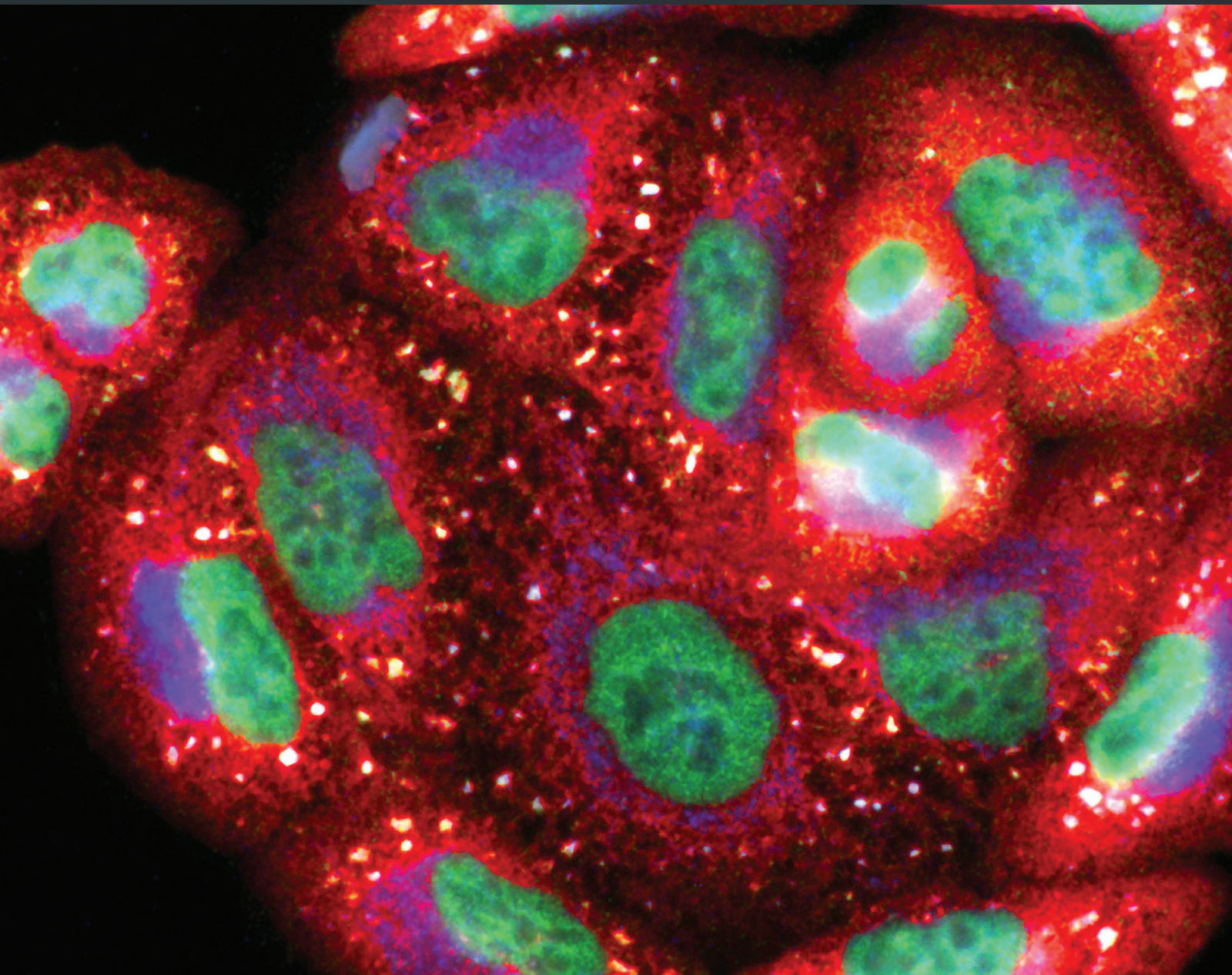


Oxidative Medicine and Cellular Longevity

Bioactive Compounds of Food: Their Role in the Prevention and Treatment of Diseases

Lead Guest Editor: Anderson J. Teodoro

Guest Editors: Germán Gil and Felipe L. de Oliveira





Bioactive Compounds of Food: Their Role in the Prevention and Treatment of Diseases

Oxidative Medicine and Cellular Longevity

Bioactive Compounds of Food: Their Role in the Prevention and Treatment of Diseases

Lead Guest Editor: Anderson J. Teodoro

Guest Editors: Germán Gil and Felipe L. de Oliveira



Copyright © 2019 Hindawi. All rights reserved.

This is a special issue published in "Oxidative Medicine and Cellular Longevity." All articles are open access articles distributed under the Creative Commons Attribution License, which permits unrestricted use, distribution, and reproduction in any medium, provided the original work is properly cited.

Editorial Board

- Fabio Altieri, Italy
Fernanda Amicarelli, Italy
José P. Andrade, Portugal
Cristina Angeloni, Italy
Antonio Ayala, Spain
Elena Azzini, Italy
Peter Backx, Canada
Damian Bailey, UK
Sander Bekeschus, Germany
Ji C. Bihl, USA
Consuelo Borrás, Spain
Nady Braidy, Australia
Darrell W. Brann, USA
Ralf Braun, Germany
Laura Bravo, Spain
Amadou Camara, USA
Gianluca Carnevale, Italy
Roberto Carnevale, Italy
Angel Catalá, Argentina
Giulio Ceolotto, Italy
Shao-Yu Chen, USA
Ferdinando Chiaradonna, Italy
Zhao Zhong Chong, USA
Alin Ciobica, Romania
Ana Cipak Gasparovic, Croatia
Giuseppe Cirillo, Italy
Maria R. Ciriolo, Italy
Massimo Collino, Italy
Graziamaria Corbi, Italy
Manuela Corte-Real, Portugal
Mark Crabtree, UK
Manuela Curcio, Italy
Andreas Daiber, Germany
Felipe Dal Pizzol, Brazil
Francesca Danesi, Italy
Domenico D'Arca, Italy
Sergio Davinelli, USA
Claudio De Lucia, Italy
Yolanda de Pablo, Sweden
Sonia de Pascual-Teresa, Spain
Cinzia Domenicotti, Italy
Joël R. Drevet, France
Grégory Durand, France
Javier Egea, Spain
- Ersin Fadillioglu, Turkey
Ioannis G. Fatouros, Greece
Qingping Feng, Canada
Gianna Ferretti, Italy
Giuseppe Filomeni, Italy
Swaran J. S. Flora, India
Teresa I. Fortoul, Mexico
Jeferson L. Franco, Brazil
Rodrigo Franco, USA
Joaquin Gadea, Spain
Juan Gambini, Spain
José Luís García-Giménez, Spain
Gerardo García-Rivas, Mexico
Janusz Gebicki, Australia
Alexandros Georgakilas, Greece
Husam Ghanim, USA
Rajeshwary Ghosh, USA
Eloisa Gitto, Italy
Daniela Giustarini, Italy
Saeid Golbidi, Canada
Aldrin V. Gomes, USA
Tilman Grune, Germany
Nicoletta Guaragnella, Italy
Solomon Habtemariam, UK
Eva-Maria Hanschmann, Germany
Tim Hofer, Norway
John D. Horowitz, Australia
Silvana Hrelia, Italy
Stephan Immenschuh, Germany
Maria Isagulians, Latvia
Luigi Iuliano, Italy
Vladimir Jakovljevic, Serbia
Marianna Jung, USA
Peeter Karihtala, Finland
Eric E. Kelley, USA
Kum Kum Khanna, Australia
Neelam Khaper, Canada
Thomas Kietzmann, Finland
Demetrios Kouretas, Greece
Andrey V. Kozlov, Austria
Jean-Claude Lavoie, Canada
Simon Lees, Canada
Ch. Horst Lillig, Germany
Paloma B. Liton, USA
- Ana Lloret, Spain
Lorenzo Loffredo, Italy
Daniel Lopez-Malo, Spain
Antonello Lorenzini, Italy
Nageswara Madamanchi, USA
Kenneth Maiese, USA
Marco Malaguti, Italy
Tullia Maraldi, Italy
Reiko Matsui, USA
Juan C. Mayo, Spain
Steven McAnulty, USA
Antonio Desmond McCarthy, Argentina
Bruno Meloni, Australia
Pedro Mena, Italy
Víctor M. Mendoza-Núñez, Mexico
Maria U Moreno, Spain
Trevor A. Mori, Australia
Ryuichi Morishita, Japan
Fabiana Morroni, Italy
Luciana Mosca, Italy
Ange Mouithys-Mickalad, Belgium
Iordanis Mourouzis, Greece
Danina Muntean, Romania
Colin Murdoch, UK
Pablo Muriel, Mexico
Ryoji Nagai, Japan
David Nieman, USA
Hassan Obied, Australia
Julio J. Ochoa, Spain
Pál Pacher, USA
Pasquale Pagliaro, Italy
Valentina Pallottini, Italy
Rosalba Parenti, Italy
Vassilis Paschalis, Greece
Visweswara Rao Pasupuleti, Malaysia
Daniela Pellegrino, Italy
Ilaria Peluso, Italy
Claudia Penna, Italy
Serafina Perrone, Italy
Tiziana Persichini, Italy
Shazib Pervaiz, Singapore
Vincent PIALoux, France
Ada Popolo, Italy
José L. Quiles, Spain



Walid Rachidi, France
Zsolt Radak, Hungary
Namakkal S. Rajasekaran, USA
Kota V. Ramana, USA
Sid D. Ray, USA
Hamid Reza Rezvani, France
Alessandra Ricelli, Italy
Paola Rizzo, Italy
Francisco J. Romero, Spain
Joan Roselló-Catafau, Spain
Gabriele Saretzki, UK
Nadja Schroder, Brazil
Sebastiano Sciarretta, Italy
Ratanesh K. Seth, USA

Honglian Shi, USA
Cinzia Signorini, Italy
Mithun Sinha, USA
Carla Tatone, Italy
Frank Thévenod, Germany
Shane Thomas, Australia
Carlo Tocchetti, Italy
Angela Trovato Salinaro, Jamaica
Paolo Tucci, Italy
Rosa Tundis, Italy
Giuseppe Valacchi, Italy
Jeannette Vasquez-Vivar, USA
Daniele Vergara, Italy
Victor M. Victor, Spain

László Virág, Hungary
Natalie Ward, Australia
Philip Wenzel, Germany
Anthony R. White, Australia
Georg T. Wondrak, USA
Michal Wozniak, Poland
Sho-ichi Yamagishi, Japan
Liang-Jun Yan, USA
Guillermo Zalba, Spain
Jacek Zielonka, USA
Mario Zoratti, Italy
H. P. Vasantha Rupasinghe, Canada

Contents

Bioactive Compounds of Food: Their Role in the Prevention and Treatment of Diseases

Anderson Junger Teodoro 

Editorial (4 pages), Article ID 3765986, Volume 2019 (2019)

Effects and Underlying Mechanisms of Bioactive Compounds on Type 2 Diabetes Mellitus and Alzheimer's Disease

Rongzi Li, Yuxian Zhang, Suhail Rasool, Thangiah Geetha, and Jeganathan Ramesh Babu 

Review Article (25 pages), Article ID 8165707, Volume 2019 (2019)

Curcumin Suppresses Hepatic Stellate Cell-Induced Hepatocarcinoma Angiogenesis and Invasion through Downregulating CTGF

Shan Shao, Wanxing Duan, Qinhong Xu , Xuqi Li , Liang Han, Wei Li, Dong Zhang, Zheng Wang , and Jianjun Lei 

Research Article (12 pages), Article ID 8148510, Volume 2019 (2019)

Shepherd's Purse Polyphenols Exert Its Anti-Inflammatory and Antioxidative Effects Associated with Suppressing MAPK and NF- κ B Pathways and Heme Oxygenase-1 Activation

Jinming Peng, Tianyong Hu , Jin Li, Jing Du, Kerui Zhu, Baohui Cheng, and Kaikai Li 

Research Article (14 pages), Article ID 7202695, Volume 2019 (2019)

Goji Berries as a Potential Natural Antioxidant Medicine: An Insight into Their Molecular Mechanisms of Action

Zheng Fei Ma , Hongxia Zhang, Sue Siang Teh, Chee Woon Wang, Yutong Zhang , Frank Hayford, Liuyi Wang, Tong Ma, Zihan Dong, Yan Zhang, and Yifan Zhu

Review Article (9 pages), Article ID 2437397, Volume 2019 (2019)

Structural Characterization and Antitumor Activity of Polysaccharides from *Kaempferia galanga* L.

Xu Yang, Haiyu Ji, Yingying Feng, Juan Yu, and Anjun Liu 

Research Article (10 pages), Article ID 9579262, Volume 2018 (2019)

Genetically Engineered Resveratrol-Enriched Rice Inhibits Neuroinflammation in Lipopolysaccharide-Activated BV2 Microglia Via Downregulating Mitogen-Activated Protein Kinase-Nuclear Factor Kappa B Signaling Pathway

Lalita Subedi , So-Hyeon Baek , and Sun Yeou Kim 

Research Article (14 pages), Article ID 8092713, Volume 2018 (2019)

A Double-Blind Placebo-Controlled Randomized Trial Evaluating the Effect of Polyphenol-Rich Herbal Congee on Bone Turnover Markers of the Perimenopausal and Menopausal Women

Jintanaporn Wattanathorn , Woralak Somboonporn, Sudarat Sungkamanee, Wipawee Thukummee, and Supaporn Muchimapura 

Clinical Study (11 pages), Article ID 2091872, Volume 2018 (2019)

Antioxidant Activities and Repair Effects on Oxidatively Damaged HK-2 Cells of Tea Polysaccharides with Different Molecular Weights

Xin-Yuan Sun , Jian-Min Wang, Jian-Ming Ouyang , and Li Kuang

Research Article (17 pages), Article ID 5297539, Volume 2018 (2019)

Sulforaphane Modulates AQP8-Linked Redox Signalling in Leukemia Cells

Cecilia Prata , Carlotta Facchini, Emanuela Leoncini, Monia Lenzi , Tullia Maraldi ,
Cristina Angeloni , Laura Zambonin, Silvana Hrelia , and Diana Fiorentini 
Research Article (10 pages), Article ID 4125297, Volume 2018 (2019)

Identification of Hypotensive Biofunctional Compounds of *Coriandrum sativum* and Evaluation of Their Angiotensin-Converting Enzyme (ACE) Inhibition Potential

Farieha Hussain, Nazish Jahan , Khalil-ur- Rahman , Bushra Sultana, and Saba Jamil
Research Article (11 pages), Article ID 4643736, Volume 2018 (2019)

Omega-9 Oleic Acid, the Main Compound of Olive Oil, Mitigates Inflammation during Experimental Sepsis

Isabel Matos Medeiros-de-Moraes, Cassiano Felipe Gonçalves-de-Albuquerque, Angela R. M. Kurz, Flora Magno de Jesus Oliveira, Victor Hugo Pereira de Abreu , Rafael Carvalho Torres ,
Vinícius Frias Carvalho, Vanessa Estado, Patrícia Torres Bozza, Markus Sperandio,
Hugo Caire de Castro-Faria-Neto , and Adriana Ribeiro Silva 
Research Article (13 pages), Article ID 6053492, Volume 2018 (2019)

Anti-Inflammatory and Antioxidant Properties of Black Mulberry (*Morus nigra* L.) in a Model of LPS-Induced Sepsis

Karine de Pádua Lúcio, Ana Carolina Silveira Rabelo , Carolina Morais Araújo, Geraldo Célio Brandão, Gustavo Henrique Bianco de Souza, Regislainy Gomes da Silva, Débora Maria Soares de Souza, André Talvani , Frank Silva Bezerra , Allan Jefferson Cruz Calsavara, and Daniela Caldeira Costa 
Research Article (13 pages), Article ID 5048031, Volume 2018 (2019)

***Polysiphonia japonica* Extract Attenuates Palmitate-Induced Toxicity and Enhances Insulin Secretion in Pancreatic Beta-Cells**

Seon-Heui Cha , Hyun-Soo Kim, Yongha Hwang, You-Jin Jeon, and Hee-Sook Jun 
Research Article (8 pages), Article ID 4973851, Volume 2018 (2019)

Procyanidins Extracted from Lotus Seedpod Ameliorate Amyloid- β -Induced Toxicity in Rat Pheochromocytoma Cells

Hao Huang, Peipei Yan, Taoping Sun, Xiaoxing Mo, Jiawei Yin, Peiyun Li, Yalun Zhu, Shuang Rong, Wei Yang, Xiaoyi Chen , and Liegang Liu 
Research Article (14 pages), Article ID 4572893, Volume 2018 (2019)

Multifunctional Phytochemicals in *Cotoneaster* Fruits: Phytochemical Profiling, Cellular Safety, Anti-Inflammatory and Antioxidant Effects in Chemical and Human Plasma Models *In Vitro*

Agnieszka Kicel , Joanna Kolodziejczyk-Czepas, Aleksandra Owczarek, Magdalena Rutkowska, Anna Wajs-Bonikowska, Sebastian Granica, Pawel Nowak, and Monika A. Olszewska 
Research Article (16 pages), Article ID 3482521, Volume 2018 (2019)

An Overview on the Anti-inflammatory Potential and Antioxidant Profile of Eugenol

Joice Nascimento Barboza, Carlos da Silva Maia Bezerra Filho, Renan Oliveira Silva, Jand Venes R. Medeiros , and Damião Pergentino de Sousa 
Review Article (9 pages), Article ID 3957262, Volume 2018 (2019)

Falcarinol Is a Potent Inducer of Heme Oxygenase-1 and Was More Effective than Sulforaphane in Attenuating Intestinal Inflammation at Diet-Achievable Doses

Amanda L. Stefanson  and Marica Bakovic 

Research Article (14 pages), Article ID 3153527, Volume 2018 (2019)

Neuroprotective Effect of *Caryocar brasiliense* Camb. Leaves Is Associated with Anticholinesterase and Antioxidant Properties

Thiago Sardinha de Oliveira, Douglas Vieira Thomaz, Hiasmin Franciely da Silva Neri, Letícia Bonancio Cerqueira, Luane Ferreira Garcia, Henric Pietro Vicente Gil, Roberto Pontarolo , Francinete Ramos Campos, Elson Alves Costa, Fernanda Cristina Alcantara dos Santos, Eric de Souza Gil , and Paulo César Ghedini 

Research Article (12 pages), Article ID 9842908, Volume 2018 (2019)

Inhibitory Effects of Momordicine I on High-Glucose-Induced Cell Proliferation and Collagen Synthesis in Rat Cardiac Fibroblasts

Po-Yuan Chen , Neng-Lang Shih, Wen-Rui Hao, Chun-Chao Chen , Ju-Chi Liu , and Li-Chin Sung 

Research Article (11 pages), Article ID 3939714, Volume 2018 (2019)

Gamma Oryzanol Treats Obesity-Induced Kidney Injuries by Modulating the Adiponectin Receptor 2/PPAR- α Axis

Fabiane Valentini Francisqueti , Artur Junio Togneri Ferron, Fabiana Kurokawa Hasimoto, Pedro Henrique Rizzi Alves, Jéssica Leite Garcia, Klinsmann Carolo dos Santos , Fernando Moreto, Vanessa dos Santos Silva , Ana Lúcia A. Ferreira, Igor Otávio Minatel, and Camila Renata Corrêa 

Research Article (9 pages), Article ID 1278392, Volume 2018 (2019)

The Protective Effect of the Total Flavonoids of *Abelmoschus esculentus* L. Flowers on Transient Cerebral Ischemia-Reperfusion Injury Is due to Activation of the Nrf2-ARE Pathway

Yang Luo, Hong-Xin Cui , An Jia, Shan-Shan Jia, and Ke Yuan 

Research Article (11 pages), Article ID 8987173, Volume 2018 (2019)

Protocatechuic Acid Attenuates Trabecular Bone Loss in Ovariectomized Mice

Seon-A Jang, Hae Seong Song, Jeong Eun Kwon, Hyun Jin Baek, Hyun Jung Koo, Eun-Hwa Sohn, Sung Ryul Lee , and Se Chan Kang 

Research Article (11 pages), Article ID 7280342, Volume 2018 (2019)

The Antidiabetic and Antinephritic Activities of *Tuber melanosporum* via Modulation of Nrf2-Mediated Oxidative Stress in the db/db Mouse

Xue Jiang, Shanshan Teng, Xue Wang, Shan Li, Yaqin Zhang, and Di Wang 

Research Article (14 pages), Article ID 7453865, Volume 2018 (2019)

Editorial

Bioactive Compounds of Food: Their Role in the Prevention and Treatment of Diseases

Anderson Junger Teodoro 

Universidade Federal do Estado do Rio de Janeiro (UNIRIO), Laboratory of Functional Foods, Rio de Janeiro, Brazil

Correspondence should be addressed to Anderson Junger Teodoro; atteodoro@gmail.com

Received 3 February 2019; Accepted 3 February 2019; Published 11 March 2019

Copyright © 2019 Anderson Junger Teodoro. This is an open access article distributed under the Creative Commons Attribution License, which permits unrestricted use, distribution, and reproduction in any medium, provided the original work is properly cited.

The aim of this special issue on “Bioactive Compounds of Food: Their Role in the Prevention and Treatment of Diseases” is to provide a representation of the new trends of bioactive compounds of food involved in different pathologies. Food bioactive compounds are extranutritional constituents that typically occur in small quantities in foods. In summary, numerous bioactive compounds appear to have beneficial health effects. Much scientific research needs to be conducted before we can begin to make science-based dietary recommendations. Despite this, there is sufficient evidence to recommend consuming food sources rich in bioactive compounds. From a practical perspective, this translates to recommending a diet rich in a variety of fruits, vegetables, whole grains, legumes, oils, and nuts. Therefore, the current issue will be focused on identifying as well as understanding the mechanistic role of food bioactive compounds in a range of human pathologies. This issue is logically divided into four main areas: (a) bioactive compounds and inflammation, (b) functional food in chronic diseases, (c) bone health and polyphenols, and (d) neuroprotective effects of bioactive compounds. Forty-four papers were selected through our routine rigorous double-blind external peer review by qualified experts. Due to the capacity limitation, some papers have already appeared earlier in the last issue (volume 2019, No. 2019). Some papers are briefly introduced below.

1. Bioactive Compounds and Inflammation

Inflammation is the major cause and aggravating factor of various acute or chronic pathological conditions, including

photoaging, diabetes, and cancer. The inflammatory response promotes the activation of transcriptional factors and proinflammatory cytokines, which can lead to an unresolved inflammatory response associated with an inhibition of insulin signaling and high risk for cardiovascular events. Epidemiological and intervention studies have been carried out to find out dietary patterns, foods, and bioactive compounds with protective anti-inflammatory actions. Thus, a way to prevent inflammation which can lead to carcinogenesis or cardiovascular diseases is through the use of bioactive food compounds of spices and herbs which show both antioxidant and anti-inflammatory properties. For this reason, anti-inflammatory phytochemicals could represent an exogenous aid crucial for the prevention of chronic diseases mediated by inflammatory processes.

An important paper by A. Kicel et al. (published in Vol. 2018) entitled “Multifunctional Phytocompounds in *Cotoneaster* Fruits: Phytochemical Profiling, Cellular Safety, Anti-Inflammatory and Antioxidant Effects in Chemical and Human Plasma Models *In Vitro*” provide a more detailed insight into the chemical composition and activity of *Cotoneaster* fruits. To this end, the fruits from nine species of *Cotoneaster* cultivated in Poland were analyzed for a range of lipophilic and hydrophilic (polyphenolic) constituents with acknowledged health-promoting properties using a combination of chromatographic and spectroscopic methods (GC-FID-MS, UHPLC-PDA-ESI-MS3, and UV-Vis spectrophotometry). The most promising polyphenolic fractions were then subjected to an analysis of antioxidant activity comprising eight complementary *in vitro* tests (both chemical and biological plasma models) covering some of the

mechanisms crucial for reducing the level of oxidative damage in the human organism, that is, scavenging of free radicals, enhancement of the nonenzymatic antioxidant capacity of blood plasma, and protection of its lipid and protein components against oxidative/nitrative changes. Additionally, the inhibitory effects of the fruit extract on the proinflammatory enzymes, that is, lipoxygenase and hyaluronidase, were also measured. Hence, *Cotoneaster* fruits appear to be promising candidates for the production of pharma- and nutraceuticals associated with preventing and treating oxidative stress and inflammatory-related chronic diseases; they may also contribute to a balanced and varied diet comprising food rich in bioactive compounds.

Falcarinol (FA) and falcarindiol (FD) are the most abundant carrot-derived polyacetylenes and have a demonstrated anti-inflammatory effect, in part by the suppression of NF κ B. FD has been shown to activate Nrf2 by S-alkylation of its inhibitor protein Keap1. A. Stefanson and M. Bakovic (published in Vol. 2018) evaluate for the first time the protective effect of diet-achievable levels of FA against intestinal inflammation in comparison to sulforaphane (SF)—widely recognized as the most potent natural compound activator of the Nrf2/ARE pathway. The results are described in the paper “Falcarinol Is a Potent Inducer of Heme Oxygenase-1 and Was More Effective than Sulforaphane in Attenuating Intestinal Inflammation at Diet-Achievable Doses.”

Sepsis is an organ dysfunction that results from a dysregulated host response to infection. It is known that there is an interrelation between redox processes and inflammation and that reactive species can activate inflammatory signaling pathways and that inflammatory cells can produce more reactive species, resulting in a vicious cycle leading to a redox and inflammatory disequilibrium, and thus may be a determining factor in the sepsis outcome. Thus, the interaction between redox processes and inflammation would be a determining factor for the antioxidant selection with therapeutic potential to minimize systemic damage and improve the septic animal's survival. K. P. Lúcio et al. (published in Vol. 2018) evaluate the anti-inflammatory and antioxidant properties of *Morus nigra* L. in a sepsis model induced by LPS. Male C57BL/6 mice were distributed into four groups: ?control, sepsis, sepsis treated with leaf extract of mulberry, and sepsis treated with mulberry pulp. The animals were treated with 100 μ L of their respective treatments for twenty-one days. Sepsis was induced at the 21st day with lipopolysaccharide (LPS) by intraperitoneal injection. The results of the paper “Anti-Inflammatory and Antioxidant Properties of Black Mulberry (*Morus nigra* L.) in a Model of LPS-Induced Sepsis” showed that the treatment with the extracts of leaves and the pulp of *Morus nigra* produced beneficial effects on the modulation of important parameters that are normally altered in sepsis.

Different strategies for the treatment of sepsis have emerged in the last few years, but none of them has proven to be beneficial in clinical trials. Lipids can modulate leukocyte function and therefore the immune response. Omega-9 is a natural agonist of peroxisome proliferator-activated receptor (PPAR). PPAR gamma ligands had been demonstrated to protect septic animals against microvascular

dysfunction and enhance bacterial elimination through neutrophil extracellular trap formation. The paper entitled “Omega-9 Oleic Acid, the Main Compound of Olive Oil, Mitigates Inflammation during Experimental Sepsis” by I. M. Medeiros-de-Moraes et al. (published in Vol. 2018) investigated the effect of Omega-9 on systemic corticosterone levels, inflammatory markers, cell migration, bacterial clearance, and nuclear receptor PPAR gamma expression in both liver and adipose tissues during experimental sepsis. The authors also studied Omega-9 effects on leukocyte rolling in vivo. It has been demonstrated that Omega-9 modulated the immune response in septic mice. Omega-9 decreased the production of proinflammatory cytokines, increased IL-10 production, reduced neutrophil migration and accumulation in the site of infection, and also improved bacterial clearance. Omega-9 treatment affected leukocyte trafficking in septic animals and inflamed cremaster muscle postcapillary venules by decreasing selectin-dependent leukocyte rolling in vivo.

2. Functional Food in Chronic Diseases

Obesity, insulin resistance, hypertension, chronic inflammation, dyslipidemia, and oxidative stress are considered the major risk factors for different pathologies. The paper entitled “Gamma Oryzanol Treats Obesity-Induced Kidney Injuries by Modulating the Adiponectin Receptor 2/PPAR- α Axis” evaluated the effect of γ Oz to recover renal function in obese animals by high sugar-fat diet by the modulation of the adiponectin receptor 2/PPAR- α axis. F. V. Francisqueti et al. (published in Vol. 2018) concluded that Oz is able to modulate PPAR- α expression, inflammation, and oxidative stress pathways improving obesity-induced renal disease.

Hypertension is a dominant risk factor for chronic diseases, including cardiovascular disorders, stroke, renal diseases, and diabetes. Hypertension is the second leading cause of disability around the world. Bioactive phytoconstituents, available as natural components in foods and medicinal plants, provide preventive and curative health benefits to improve cardiovascular health. The functionalities of bioactives from green resources, including the inhibition of the activity of enzymes or the formation of complexes with metals, which catalyze the oxidation reaction and the capacity to modulate metabolic processes, may result in the eradication and management of cardiovascular diseases. F. Hussain et al. (published in Vol. 2018) investigated these themes by identifying and characterizing the bioactive compounds of *Coriandrum sativum* responsible for the treatment of hypertension through LC-ESI-MS/MS and by exploring their mechanism of action as angiotensin-converting enzyme (ACE) inhibitors in the work “Identification of Hypotensive Biofunctional Compounds of *Coriandrum sativum* and Evaluation of Their Angiotensin-Converting Enzyme (ACE) Inhibition Potential.”

The incidence of diabetes mellitus (DM), a metabolic ?disturbance disease characterized by chronic hyperglycemia, has increased rapidly worldwide. Currently, a global population of 382 million people is diagnosed with DM and this number is predicted to rise to 592 million by 2035. Current antidiabetic therapies have some limitations. Moreover, DM

is a chronic disease with miscellaneous complications that require long-term treatment. Some effective Western medicines for diabetes are associated with high cost and adverse effects. Therefore, it is necessary to find alternative agents for the treatment of diabetes and its complications that have lower costs and fewer side effects. Phytochemicals are regarded as an important source for treating human health problems, including DM. Foods are composed of a variety of bioactive substances such as polysaccharides, pigments, minerals, peptides, and polyphenols, which have valuable pharmaceutical and biomedical potential. In these context, the papers “*Polysiphonia japonica* Extract Attenuates Palmitate-Induced Toxicity and Enhances Insulin Secretion in Pancreatic Beta-Cells” (S.-H. Cha et al., published in Vol. 2018), “The Antidiabetic and Antinephritic Activities of *Tuber melanosporum* via Modulation of Nrf2-Mediated Oxidative Stress in the db/db Mouse” (X. Jiang et al., published in Vol. 2018), and “Inhibitory Effects of Momordicine I on High-Glucose-Induced Cell Proliferation and Collagen Synthesis in Rat Cardiac Fibroblasts” (P.-Y. Chen et al., published in Vol. 2018) explored the antidiabetic properties of bioactive compounds with different matrices and found that the effects may be related to the modulation of oxidative stress and inflammation-related cytokines via Nrf2 signaling and may improve insulin secretion. The effects may provide these compounds with a candidacy for a natural nutritional product for adjunct DM therapy.

Cancer is a major global disease where abnormal cells rapidly proliferate, having the ability to migrate to different parts of the human body via a process called metastasis. Cancer is also one of the leading causes of death worldwide and is a burden financially and on the quality of human lives in both well-developed and less-developed countries, especially as the population is increasing. Until now, cancer research has focused on the search for curative treatments, and few studies have aimed at developing preventive strategies. Chemoprevention is an old concept that consists in the use of drugs, vitamins, or nutritional supplements to reduce the risk of developing or having a recurrence of cancer. The consumption of whole plant foods as chemopreventive agents is highly recommended in the dietary guidelines on the basis of health benefits from dietary phytochemicals observed in epidemiological studies. The paper entitled “Sulforaphane Modulates AQP8-Linked Redox Signaling in Leukemia Cells” of the authors C. Prata et al. (published in Vol. 2018) evaluate the potential anticancer activity of sulforaphane (SFN) in the B1647 leukemia cell line, focusing on AQP8 function and expression. The authors also investigated the effect of SFN on Nox2, Nox4, and peroxiredoxin expression and on the phosphorylation state of VEGFR-2 and Akt. X. Yang et al. (published in Vol. 2018), through another approach, investigated the antitumor activity and structural characteristics of water-soluble polysaccharides from *Kaempferia galanga* L. (KGPs) in the paper “Structural Characterization and Antitumor Activity of Polysaccharides from *Kaempferia galanga* L.”. The results showed that KGPs were acidic polysaccharides (total sugar of 85.23%, uronic acid of 24.17%) with skeletal modes of pyranose rings and mainly composed of arabinose and galactose with the average molecular weight

of 8.5×10^5 Da. The in vivo antitumor test showed that KGPs could effectively protect the thymus and spleen of tumor-bearing mice from solid tumors and enhance the immunoregulatory capability of CD4+ T cells and the cytotoxic effects of CD8+ T cells and NK cells, finally leading to the inhibitory effects on H22 solid tumors.

3. Bone Health and Polyphenols

Bone is a dynamic organ that undergoes continuous remodeling by the coordination and balance between resorption and the formation activities of osteoclast and osteoblast cells. It is well established that women are vulnerable to bone loss especially during and after menopause. The paper entitled “A Double-Blind, Placebo-Controlled Randomized Trial Evaluating the Effect of Polyphenol-Rich Herbal Congee on Bone Turnover Markers of the Perimenopausal and Menopausal Women”, by J. Wattanathorn et al. (published in Vol. 2018), tested the hypothesis that the polyphenol-rich herbal congee containing the combined extract of *Morus alba* and *Polygonum odoratum* leaves should improve bone turnover markers in menopausal women. The authors performed a randomized, double-blind, placebo-controlled study. The study demonstrates the antiosteoporotic effect of the polyphenol-rich herbal congee by a possible mechanism via the improved bone turnover via increased bone formation and decreased bone resorption.

Osteoporosis is a disease related to excessive bone resorption due to estrogen insufficiency that occurs post menopause. Primary osteoporosis, which is classified as type I (postmenopausal osteoporosis) and is frequently associated with fenestrated trabecular bone resorption, occurs between the ages of 50 and 65 years in postmenopausal women. Estrogen deficiency induces receptor activator of nuclear factor κ B ligand (RANKL), the key molecule required for osteoclast differentiation, leading to enhanced osteoclast activation and reduced osteoclast apoptosis. Several studies have shown that protocatechuic acid (PCA) has beneficial effects on osteoblast and osteoclast cells in vitro. S.-A. Jang et al. investigated the antiosteoporotic activity of PCA supplementation, which was determined in ovariectomized (OVX) female ICR mice at 12 weeks after OVX. In the paper “Protocatechuic Acid Attenuates Trabecular Bone Loss in Ovariectomized Mice” (published in Vol. 2018), the authors demonstrated an inhibitory potential of PCA against osteoclastogenesis, which augments bone resorption in OVX or postmenopausal conditions. This was demonstrated in the OVX mouse model. The underlying mechanism of PCA in the suppression of bone loss in OVX mice may be associated with the following effects: (1) reduction of the serum level of RANKL and increase in OPG; (2) blocking the RANK signaling pathway via downregulation of TRAF6 and NFATc1 expression; and (3) attenuation of cathepsin K and calcitonin receptor expression.

4. Neuroprotective Effects of Bioactive Compounds

Neuroinflammation is the key mediator of secondary brain damage in most of the neurological disorders, such as

Alzheimer's disease (AD), Prion disease, Parkinson's disease (PD), multiple sclerosis (MS), ischemic stroke, experimental autoimmune encephalomyelitis (EAE), and neuropathic pain. Neuroinflammation is induced by aging-dependent conditions and aging-independent pathological events, which share similar inflammatory cascades. Ischemic cardiovascular disease (also known as "ischemic stroke") is the third leading cause of death and disability worldwide. The number of patients suffering from cerebral ischemic disease worldwide has increased by 2 million per year, and the morbidity associated with this disease can affect young people. Therefore, searching for natural products for the protection and treatment of transient cerebral ischemia-reperfusion injury (TCI-RI) and exploring their mechanism of action are a rational approach. The paper entitled "The Protective Effect of the Total Flavonoids of *Abelmoschus esculentus* L. Flowers on Transient Cerebral Ischemia-Reperfusion Injury is Due to Activation of the Nrf2-ARE Pathway". Therefore, Y. Luo et al. (published in Vol. 2018) examined the protective effect of an extract of the total flavonoids of *A. esculentus* flowers (AFF) on TCI-RI and its potential mechanism. The authors demonstrated that AFF had protective effects against TCI-RI possibly by direct (scavenging free radicals) and indirect (activating the neuronal Nrf2-ARE pathway to modulate damage by oxidative stress) actions.

Alzheimer's disease (AD), a progressive neurodegenerative disease, is characterized by extracellular senile plaque deposits, intracellular neurofibrillary tangles, and neuronal apoptosis. Oxidative damage is known to play an important role in neuronal damage, due to the neurodegeneration promoted by highly reactive compounds. Amongst the potential neuroprotective phytomedicines is *Caryocar brasiliense* (Camb), a Caryocaraceae family member popularly known as "pequi." T. S. de Oliveira et al. (published in Vol. 2018) investigated the antioxidant and anticholinesterase activities as well as the neuroprotective effects of *C. brasiliense* leaf extracts, in order to provide new information on the potential use of this plant against neurodegenerative disorders in the work "Neuroprotective Effect of *Caryocar brasiliense* Camb. Leaves Is Associated with Anticholinesterase and Antioxidant Properties". Progressive loss of memory and other cognitive functions are typical symptoms in AD. According to the amyloid hypothesis, amyloid- β - ($A\beta$ -) related toxicity and imbalance are cardinal reasons that contribute to synaptic dysfunction and subsequent neurodegeneration in AD. Therefore, $A\beta$ has been suggested as a potential therapeutic target for AD treatment. Thus, within this context the paper of the authors H. Huang et al. entitled "Procyanidins Extracted from Lotus Seedpod Ameliorate Amyloid- β -Induced Toxicity in Rat Pheochromocytoma Cells" (published in Vol. 2018) verify the anti- $A\beta$ effects and protective mechanisms as a promising natural product for AD treatment. The authors evaluated the amelioration of LSPC in $A\beta$ 25-35-induced damage on rat pheochromocytoma (PC12) cells. CREB/BDNF signaling and antioxidant activity were studied as possible pathways. We used LC-MS/MS to analyze its distribution in vivo.

Microglia, neurons, astrocytes, and oligodendrocytes are the basic cells of the brain. Microglia and astrocytes, as glial

cells, have a role to defend against brain injury, to maintain homeostasis, and to repair brain injury. In aging-dependent conditions and aging-independent disorders such as AD and stroke, neuroinflammation can be initiated by chronic microglial activation. Activated microglia are required for basic immune defense in the brain; however, chronic microglial activation is toxic to the central nervous system (CNS). Hence, natural compounds or nutraceuticals with the potential to regulate these steps to control microglial activation will be promising candidates for inhibiting neuroinflammation and neurodegenerative conditions. L. Subedi et al. (published in Vol. 2018) compared the efficacy of normal Dongjin rice (NR), modified resveratrol-enriched rice (RR), and resveratrol in terms of cytotoxicity and anti-inflammatory potential in activated microglia and elucidated the possible mechanisms underlying the antineuroinflammatory potential of RR in lipopolysaccharide- (LPS-) stimulated BV2 murine microglial cells. The paper "Genetically Engineered Resveratrol-Enriched Rice Inhibits Neuroinflammation in Lipopolysaccharide-Activated BV2 Microglia via Downregulating Mitogen-Activated Protein Kinase-Nuclear Factor Kappa B Signaling Pathway" not only discovered the safe and effective role of RR against aging and neuroinflammation, but also identified the anti-neuroinflammatory potential of NR itself because of the presence of active phytochemicals such as α -tocopherol and γ -tocopherol in rice. The anti-inflammatory effect of RR treatment seems to be mediated through the inhibition of nitrite production, MAPK phosphorylation, NF κ B-mediated production of proinflammatory cytokines, and expression of inflammatory proteins.

Conflicts of Interest

The Lead Guest Editor and Guest Editors declare no conflict of interest in the issue.

Acknowledgments

We would like to thank all the authors for their fine contributions to this special issue, the guest editors Prof. Dr. Germán Gil and Prof. Dr. Felipe L. de Oliveira, and all the external specialist reviewers who upheld the quality of this special issue by critically evaluating the papers and reviewing several revisions. Advices from the participating editorial team members are greatly appreciated.

Anderson Junger Teodoro

Review Article

Effects and Underlying Mechanisms of Bioactive Compounds on Type 2 Diabetes Mellitus and Alzheimer's Disease

Rongzi Li, Yuxian Zhang, Suhail Rasool, Thangiah Geetha, and Jeganathan Ramesh Babu 

Department of Nutrition, Dietetics, and Hospitality Management, Auburn University, Auburn, Alabama 36849, USA

Correspondence should be addressed to Jeganathan Ramesh Babu; jeganrb@auburn.edu

Received 6 July 2018; Revised 15 October 2018; Accepted 24 October 2018; Published 17 January 2019

Guest Editor: Germán Gil

Copyright © 2019 Rongzi Li et al. This is an open access article distributed under the Creative Commons Attribution License, which permits unrestricted use, distribution, and reproduction in any medium, provided the original work is properly cited.

Type 2 diabetes mellitus is a complicated metabolic disorder characterized by hyperglycemia and glucose intolerance. Alzheimer's disease is a progressive brain disorder characterized by a chronic loss of cognitive and behavioral function. Considering the shared characteristics of both diseases, common therapeutic and preventive agents may be effective. Bioactive compounds such as polyphenols, vitamins, and carotenoids found in vegetables and fruits can have antioxidant and anti-inflammatory effects. These effects make them suitable candidates for the prevention or treatment of diabetes and Alzheimer's disease. Increasing evidence from cell or animal models suggest that bioactive compounds may have direct effects on decreasing hyperglycemia, enhancing insulin secretion, and preventing formation of amyloid plaques. The possible underlying molecular mechanisms are described in this review. More studies are needed to establish the clinical effects of bioactive compounds.

1. Introduction

Diabetes is a complex metabolic disorder that is characterized by hyperglycemia due to insulin insufficiency and/or insulin dysfunction. Globally, an estimated 425 million adults were living with diabetes mellitus in 2017. By 2045, projections show this number rising to 629 million diabetics globally [1]. In type 1 diabetes, hyperglycemia is caused by autoimmune destruction of the pancreas beta cells [2]. Type 2 diabetes mellitus (T2DM) is the more common type of diabetes where peripheral insulin resistance and compensatory increased insulin secretion may accelerate the decrease in pancreatic islet secretory function, eventually leading to insulin deficiency [2]. Diabetes is associated with several complications, including nephropathy, retinopathy, neuropathy, and atherosclerosis [2]. About 60% to 70% of all people with diabetes will eventually develop peripheral neuropathy [3]. Increasing epidemiological evidence suggests that diabetes neuropathy and T2DM may be related to increased risk of Alzheimer's disease (AD) [4]. AD is a progressive brain disorder that gradually impairs a person's memory and ability to learn, communicate, and perform daily activities [5]. An estimated 5.7 million Americans are living with AD in 2018 [6]. Considering the high prevalence and tremendous social

and economic burden, it is imperative to identify an effective, safe, and inexpensive approach to delay the progression or prevent the symptoms of these diseases. However, existing antidiabetic drugs have various adverse effects, and currently, no treatment has been identified to prevent or reverse AD progression [7, 8]. Considering the biochemical association between AD and T2DM [9, 10], it is possible that there may be a common therapeutic target for AD and T2DM. Natural bioactive compounds may be alternative treatment for diabetes and a novel promising therapy for AD due to their efficacy, fewer side effects, and easy availability [11]. Researches have shown that the beneficial effects of bioactive compounds may be due to various properties such as antioxidant, anti-inflammatory, and antiapoptotic effects [11, 12]. Herein, we review the multiple beneficial effects of bioactive compounds and their underlying mechanism of actions in cell culture and animal models of AD and T2DM.

2. Pathophysiology of T2DM and AD

The pathophysiology of T2DM is characterized by peripheral insulin resistance, increased hepatic glucose production, and impaired β -cell function, eventually resulting in β -cell failure [13]. Insulin resistance is a condition in which cells fail to

respond to normal levels of insulin that occurs mainly within the liver, muscle, and fat tissues [14]. Normally, insulin can inhibit hepatic glucose production in both postprandial and fasting states, whereas postprandial glucose production is increased in the situation of hepatic insulin resistance [15]. Elevated lipid breakdown within fat may also contribute to increased hepatic glucose production [16]. Insulin resistance initially stimulates compensatory β -cell proliferation and improved insulin secretion; however, long-term exposure to hyperglycemia-induced oxidative stress, endoplasmic reticulum (ER) stress, and various cytokines may contribute to β -cell failure due to apoptosis, autophagy, and impaired proliferation [17, 18]. The progressive degeneration of β -cell function leads to reduced insulin secretion and disruption of glucose homeostasis [18].

The pathological features of AD include extracellular deposition of misfolded amyloid plaques ($A\beta$ peptide) in senile plaques, intracellular neurofibrillary tangles (NFTs), inflammation, and brain atrophy [19]. $A\beta$, a 38-43 amino acid residue peptide, originates from proteolysis of the amyloid precursor protein (APP) [20]. In the nondisease state, APP produces nonamyloidogenic $A\beta$ products by α -secretase, but in the AD brain, $A\beta$ is produced from APP by the sequential enzymatic actions of β -site APP cleaving enzymes 1 (BACE-1, a β -secretase) and γ -secretase [20, 21]. The imbalance between the production and clearance of $A\beta$ leads to $A\beta$ accumulation and its subsequent aggregation and neurotoxicity [22]. $A\beta$ spontaneously aggregates into different forms, including 3-50 $A\beta$ monomers, oligomers, fibrils, and plaques [22]. Soluble oligomers appear to be the most toxic form [23]. NFT primarily consists of hyperphosphorylated tau, which is insoluble and loses the ability to bind to microtubules, and hyperphosphorylated tau self-aggregates into toxic, helical filament structures [21].

3. Possible Links between T2DM and AD

T2DM and AD share many characteristics, including chronic inflammation, oxidative stress, impaired insulin signaling, insulin resistance, glucose intolerance, and cognitive impairment [9].

3.1. Insulin Resistance. Increasing evidence has shown that insulin deficiency and resistance, the markers of T2DM, are also important in AD pathology [24]. Moreover, it was proposed that AD may be a brain-specific form of diabetes mellitus, a “type 3 diabetes” [10]. Insulin receptors (IR) are expressed in the peripheral systems as well as central nervous system, especially in the hippocampus, which is the earliest affected structure in AD [25, 26]. The binding of insulin to IR leads to tyrosine phosphorylation and activation of insulin receptor substrate (IRS), which then activates phosphatidylinositol-3 kinase (PI3 kinase) and Akt, and Akt then mediates phosphorylation or inactivation of glycogen synthase kinase 3 β (GSK3 β) [20]. Impaired insulin signaling results in increased GSK3 β activity, which causes hyperphosphorylation of tau, formation of NFTs, and increased production of $A\beta$ [20, 27]. In the AD brain, $A\beta$ oligomers lead to abnormal activation of tumor necrosis factor- α

(TNF- α)/c-Jun N-terminal kinase pathway (JNK) and cause the inhibition of IRS1 and the disruption of insulin signaling [9, 28]. Moreover, the insulin-degrading enzyme (IDE) is responsible for the degradation of APP and $A\beta$ [29]. Under conditions of insulin resistance, there is competition between insulin and $A\beta$ for IDE that eventually reduces $A\beta$ degradation [12].

3.2. Chronic Inflammation. Chronic inflammation may also contribute to the association between T2DM and AD. Increased levels of various proinflammatory cytokines such as TNF- α , interleukin-6 (IL-6), and interleukin-1 β (IL-1 β) have been observed in T2DM [30]. These cytokines are associated with β -cell damage, apoptosis, and impaired insulin secretion [31, 32]. Certain proinflammatory cytokines could also cross the blood brain barrier (BBB) and act on the central nervous system; these effects have been hypothesized to contribute to the initiation and progression of AD [33]. For example, studies have shown that increased levels of IL-1 in the brain reduced hippocampal acetylcholine (ACh) release, reduced mRNA expression of hippocampal nerve growth factor (NGF), and caused memory deficits [34]. Advanced glycation end products (AGEs) are produced via nonenzymatic glycation of amine residues on proteins, lipids, or nucleic acids by reducing sugars [35]. In diabetes, chronic hyperglycemia may promote the generation of AGEs [35], which interact with RAGE receptors, inducing the activation of different intracellular inflammatory pathways, including the nuclear factor-kappa B (NF- κ B) signaling cascade and inflammatory mediators such as TNF- α , IL-6, and C-reactive protein (CRP) [36]. AGEs may be implicated in AD pathology. In particular, $A\beta$ has been reported to be a RAGE ligand where the binding of $A\beta$ to RAGE promotes $A\beta$ influx across BBB leading to the accumulation of $A\beta$ in the brain [37, 38]. In addition, the interaction of RAGE with $A\beta$ is associated with the activation of microglia and increased levels of oxidative stress, an augmented proinflammatory response, and neuronal injury and cell death [39].

3.3. Oxidative Stress. Oxidative stress, the result of the imbalance between the production of reactive nitrogen species (RNS) and reactive oxygen species (ROS), and intracellular antioxidant defense [40], is involved in the onset or progression of T2DM and AD. ROS, such as nitric oxide synthase (iNOS), cyclooxygenase-2 (COX-2), and hydroxyl radicals, are involved in causing damage to membrane polyunsaturated fatty acids, proteins, and DNA [41]. This ROS-mediated lipid peroxidation leads to loss of plasma membrane integrity and increases its permeability to Ca^{2+} [2]. Excessive ROS/RNS production plays an important role in the onset of T2DM and its complications [42]. In T2DM, increased glucose concentrations may induce glucose autooxidation, mitochondria dysfunction, and increased production of ROS [42]. The overproduction of ROS further mediates lipid peroxidation, leading to β -cell dysfunction, and impairs several biochemical pathways, including NF- κ B, JNK/stress-activated protein kinase (SARK), and p38-mitogen-activated protein kinase (p38-MAPK), which may in turn contribute to insulin resistance and late complications of T2DM [42, 43]. Oxidative

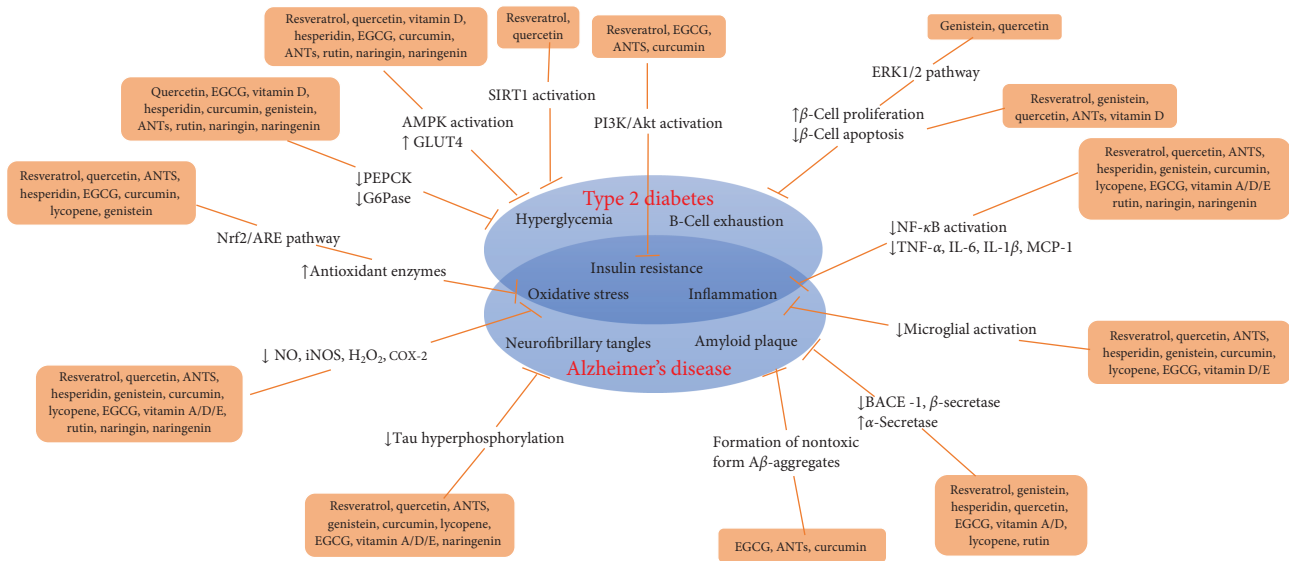


FIGURE 1: Functions of bioactive compounds in T2DM and AD pathogenesis. (1) Shared characteristics of T2DM and AD including insulin resistance, inflammation, and oxidative stress. (2) Some bioactive compounds can ameliorate hyperglycemia by activating AMPK, increasing GLUT4 translocation, inhibiting PEPCK and G6Pase activities, or activating SIRT1. (3) Some bioactive compounds can preserve functional β -cell mass by increasing β -cell proliferation or decreasing apoptosis. (4) Through activation of the PI3K/Akt pathway, some bioactive compounds improved insulin resistance. (5) Bioactive compounds attenuate oxidative stress via reducing NO, iNOS, and COX-2 levels or/and increasing the expression of antioxidant enzymes. (6) Most bioactive compounds could ameliorate inflammation which in turn improves T2DM and AD pathology. (7) Bioactive compounds can decrease $A\beta$ production or assemble them into nontoxic aggregates, thereby decreasing formation of amyloid plaques. (8) Some bioactive compounds reduce NFT levels by inhibiting tau hyperphosphorylation. References: [46, 47, 50, 54, 55, 59, 61, 62, 64, 72, 75, 77, 81, 89, 93, 98, 101, 103, 108, 110, 116, 117, 121, 123, 126, 132, 133, 139, 140, 147, 149, 151, 152, 159, 162, 169, 175, 180, 183, 186, 189, 194–196, 200, 204, 215, 217, 227, 231, 234].

stress and mitochondria dysfunction also play a critical role in AD pathogenesis [42, 44]. Neurons depend on mitochondria for ATP utilization and maintenance of calcium homeostasis; oxidative stress-induced mitochondria bioenergetic depletion can cause neuronal injury and death [44]. Moreover, mitochondria dysfunction amplifies the production of ROS, which then enhances tau hyperphosphorylation, NFT formation, and $A\beta$ aggregation [42]. $A\beta$ and NFT are also involved in the generation and promotion of oxidative stress [42]. All these together accelerate the progression of AD. Considering the biochemical link between T2DM and AD, it is possible that common therapeutic and preventive agents may be effective treatments for both diseases.

4. Effects of Bioactive Compounds on T2DM and AD and Their Mechanisms of Action

Bioactive compounds are defined as components of foods that can regulate metabolic processes in humans or animals and improve health [45]. They are found largely in vegetables, fruits, and whole grains and can be consumed daily [45]. Beneficial effects of bioactive compounds have been identified in both cell and animal studies, including decreasing inflammation, scavenging free radicals, and regulating cell signaling pathways [46, 47] (Figure 1). Because of their rich availability, safety, and few side effects, use of bioactive compounds has been proposed to reduce the incidence or delay the progression of several diseases, including T2DM and AD

[11, 12]. Examples of bioactive compounds include polyphenols, carotenoids, phytosterols, prebiotics, and vitamins.

4.1. Polyphenols

4.1.1. Resveratrol. Resveratrol is a polyphenolic compound found in grape skins, seeds, and red wines that exhibits antioxidant and anti-inflammatory properties; it also increases mitochondrial function and maintains metal homeostasis [19]. Both cell and animal studies suggested that resveratrol may have therapeutic potential in the treatment of T2DM [49]. SIRT1, an NAD^+ -dependent deacetylase, has been shown to regulate many factors that influence T2DM, and resveratrol was reported to be an activator of SIRT1 [50]. In insulin-secreting cells, resveratrol treatment potentiated glucose-stimulated insulin secretion and glucose metabolism as well as mitochondrial activity [51]. These effects were dependent on active SIRT1, which induced upregulation of key genes for β -cell function [51]. Moreover, resveratrol has been shown to normalize hyperglycemia, improve insulin sensitivity, and lower hepatic glucose production through the activation of SIRT1 [50]. A recent study suggested that resveratrol improved T2DM by regulating mitochondrial biogenesis, lipid metabolism, and β cells through activation of SIRT1 [52]. Manganese superoxide dismutase (Mn-SOD) is an important antioxidant enzyme in mitochondria, and Mn-SOD dysfunction could increase ROS production and induce tissue damage [53]. A recent study showed that resveratrol treatment ameliorated the functional and histological

abnormalities and mitochondria biogenesis in the kidney of obese leptin receptor-deficient mice (db/db) mice, which is a well-accepted mouse model of type 2 diabetes, and these effects should primarily contribute to the improvement of oxidative stress via normalization of Mn-SOD function and glucose-lipid metabolism by resveratrol [53]. In addition, Lee et al. [54] reported that resveratrol treatment improved glucose tolerance, reduced high glucose-induced oxidative stress, and also attenuated β -cell loss in db/db mice. Further, resveratrol has been shown to reduce hyperglycemia and ameliorate dysregulated insulin signaling. Specifically, treatment of streptozotocin- (STZ-) induced diabetic rats with resveratrol increased glucose uptake through enhanced GLUT4 translocation by regulating the AMP-activated protein kinase (AMPK)/Akt/iNOS signaling pathway [55].

The beneficial effect of resveratrol in AD were also reported in both cell and animal studies. Feng et al. [56] reported that resveratrol protected P12 cells against A β -induced cell apoptosis through the upregulation of SIRT1 and the downregulation of rho-associated kinase 1 (ROCK1) by SIRT1 (Table 1). In addition, treatment with resveratrol in Tg2576 neuron cultures reduced the accumulation of A β peptides and promoted α -secretase activity, thereby inducing nonamyloidogenic APP processing, and these effects were partly dependent upon the activation of SIRT1 by resveratrol [57]. Activation of microglia in the brain triggers neuronal inflammation and cell death, and A β could trigger microglial activation by interacting with toll-like receptors (TLR) such as TLR4. It was reported that resveratrol prevented lipopolysaccharide- (LPS-, a TLR4 ligand) induced activation of murine RAW 264.7 macrophages and microglial BV-2 cells by inhibiting the TLR4/NF- κ B/STAT (signal transducer and activation of transcription) signaling cascade [58]; therefore, the anti-inflammatory effects of resveratrol protect microglia against A β -induced inflammation. Moreover, the antioxidant effects of resveratrol protected rats against A β -induced neurotoxicity by attenuating iNOS and lipid peroxidation and increasing the production of heme oxygenase-1 (HO-1) [46]. In addition, a recent study [59] suggested that resveratrol treatment reduced microtubule-associated ubiquitin ligase (MID1) protein expression *in vitro* and *in vivo*, which in turn resulted in increased activity of microtubule-associated protein phosphatase 2A (PP2A) and further improved dephosphorylation of tau.

4.1.2. Quercetin. Quercetin is a flavonoid that is naturally found in a variety of foods, including red onions, broccoli, tea, and apples [60]. Exhibiting antioxidant, anti-inflammatory, and antiapoptotic effects, quercetin has been reported to have the potential for treatment of diabetes and its complications [61–63]. Quercetin could influence glucose homeostasis in both the liver and skeletal muscle; specifically, in cultured skeletal muscle cells, quercetin increased glucose uptake through stimulation of GLUT4 translocation by activating AMPK [61]. Similarly, in hepatocytes, quercetin also activated AMPK, and this was related to the suppression of glucose-6-phosphatase (G6Pase), eventually reducing hepatic glucose production (Table 2) [61]. Youl et al. [62] reported

that quercetin potentiated glucose-induced insulin secretion and protected β -cell function and viability from H₂O₂-induced oxidative damage in INS-1 cells. These effects were mediated by phosphorylation of extracellular signal-regulated kinase (ERK1/2), suggesting that ERK1/2 activation was involved in the action of quercetin [62]. Moreover, a recent study showed that quercetin treatment improved glucose and lipid metabolism and also alleviated hepatic histomorphological injury in STZ-induced diabetic rats, which probably associated with the upregulation of SIRT1 activity by quercetin and its influence on the Akt signaling pathway [63]. The vascular complications are responsible for most of the morbidity and mortality in patients with diabetes [64]. In STZ-induced diabetic rats, quercetin administration ameliorated the progression of diabetes-induced hypertension and abrogated diabetes-induced vasoconstriction [47]. These effects may be due to the inhibitory effects of quercetin on inflammatory pathways, via inhibition of NF- κ B and amelioration of the serum TNF- α and C-reactive protein (CRP) levels in the aorta of diabetic rats (Table 3) [47].

Several *in vivo* and *in vitro* studies have shown that quercetin exerts neuroprotective effects in diabetic neuropathy [65–67]. Qu et al. [65] reported that high concentrations of glucose impaired the proliferation of rat RSC96 cells and primary rat Schwann cells; inhibited the expression of beclin-1 and light chain (LC3), which are the biomarkers for autophagy; and decreased the numbers of autophagosomes in both cell types. All these effects were rescued after treatment with quercetin. Schwann cells are important for neuronal function and structure [65]; therefore, quercetin may have neuroprotective effects in diabetic peripheral neuropathy. Xia et al. [66] reported that quercetin supplement could reverse cognitive decline in mice fed a high-fat diet, possibly by altering Nrf2 signaling and eventually improving cognitive function. Additionally, a recent study indicated that quercetin reduced oxidative stress and alleviated inflammation and protein glycation in the brain of diabetic rats [67]. These effects may be related to the upregulation of glyoxalase, which is a ubiquitous cellular enzyme that participates in the detoxification of the cytotoxic byproduct of glycolysis and has been implicated in the pathogenesis of diabetic encephalopathy [67].

The beneficial effects of quercetin in AD were also confirmed in both cell and animal studies [68–70]. In cultured neurons, pretreatment with quercetin ameliorated A β 1-42-induced protein oxidation, lipid peroxidation, cytotoxicity, and apoptosis; however, high doses were nonneuroprotective and toxic (Table 1) [68]. In *Drosophila* models, Kong et al. [69] found that quercetin could extend lifespan and rescue the climbing ability of AD flies, and mechanistic studies showed that cell cycle-related proteins were interrupted by A β accumulation and that quercetin could rescue these cell cycle-related signaling pathways. In a triple transgenic AD (3xTg-AD) mouse model, 3-month treatment with quercetin decreased extracellular β -amyloidosis and ameliorated microglial and astroglial activation in the brain, as evidenced by decreased levels of A β 1-40, A β 1-42, and BACE1-mediated cleavage of APP. Additionally, performance on learning and memory tasks was also improved (Table 4) [70]. Moreover, administration of quercetin to APPsw/

TABLE 1: Effects of bioactive compounds on Alzheimer's disease (*in vitro* studies).

Bioactive compounds	Models	Treatment	Effects	Specific mechanism of action	Reference
<i>Polyphenols</i>					
Resveratrol	PC12 cells	12.5, 25, 50, and 100 μM , 2 h prior to the A β 25–35, 24 or 48 h	<p>↓Cell viability</p> <p>↓Aβ25–35-induced intracellular Ca$^{2+}$ level</p> <p>↓Cell apoptosis</p>	<p>↑SIRT1</p> <p>↓ROCK1</p>	[56]
Quercetin	Primary rat neuronal cells	Low dose: 5 and 10 μM , High dose: 20 and 40 μM , 24 h	<p>↓Aβ1–42-induced apoptotic cell death and cell toxicity at low dose</p> <p>↑Toxic at high dose</p>	<p>↓Lipid peroxidation</p> <p>↓Oxidative stress</p>	[68]
Genistein	BV-2 microglia cells	50 μM , 2 h before incubation with A β 25–35, 24 h	<p>↓Cell viability</p> <p>↓Aβ25–35-induced inflammatory damage</p>	<p>↓The expression of TLR4, NF-κB,</p> <p>↓The activity of NF-κB</p>	[80]
EGCG	HEK-293 cells	15 and 20 μM , 1–3 days	Convert large, mature amyloid- β fibrils into smaller, amorphous, and nontoxic aggregates	Directly binds to β -sheet-rich aggregates and mediates the conformational change	[103]
Hesperidin	Neuro-2A cells	20 μM , 6 h pretreatment before exposure to A β 1–42	↓A β -induced impairment of insulin signaling and glucose uptake	↓A β -induced autophagy	[115]
Anthocyanins	Neuro-2A cells	50 μM malvidin or ononin with A β , 48 h	↓A β -induced neurotoxicity, cell cycle arrest	<p>↑Ca$^{2+}$ homeostasis</p> <p>↓Aβ-induced ROS</p>	[125]
Curcumin	Macrophages from AD patients	0.1 μM	↓A β aggregates	↑A β uptake by macrophages	[238]
Rutin	APPswe cells	1, 5, and 10 μM	<p>↓The formation of Aβ fibrils and disaggregated Aβ fibrils</p> <p>↓Neurotoxicity</p>	Free-radical scavenger activity	[152]
Carotenoid					
Lycopene	Rat cortical neurons	0.1, 1, 2, and 5 μM , 4 h pretreatment before exposure to A β	<p>↓Cell viability</p> <p>↓Apoptotic rate</p>	<p>↓Aβ-induced ROS</p> <p>↓Mitochondrial membrane potential depolarization</p>	[192]
<i>Vitamins</i>					
Vitamin A	—	100, 150, and 250 μM retinoid acid	<p>↓Aβ42 and Aβ40 oligomerization</p> <p>↓Cell toxicity</p>	Specific binding of retinoic acid to the C-terminal portion of A β	[204]
Vitamin D	ROS 17/2.8 cell	10 $^{-6}$, 10 $^{-8}$, 10 $^{-10}$, and 10 $^{-12}$ M, 6 h	↑NGF expression	↑AP-1 binding activity in the NGF promoter	[222]
Vitamin E	Rat cortical neurons	1 mM of Trolox (vitamin E derivative) with A β	↓A β -induced tau phosphorylation	↓P38 MAPK	[231]

TABLE 2: Effects of bioactive compounds on type 2 diabetes mellitus (*in vitro* studies).

Bioactive compounds	Models	Treatment	Effects	Specific mechanism of action	Reference
<i>Polyphenols</i>					
Resveratrol	INS-1E, β cells, and human islets	25 μ M, 24 h	<ul style="list-style-type: none"> ↑Glucose-stimulated insulin secretion ↑Glucose metabolism ↑Mitochondrial activation 	↑The activation of SIRT1	[51]
Quercetin	L6 skeletal muscle cells, murine H4IIE cells, human HepG2 hepatocytes	50 μ M, 18 h	<ul style="list-style-type: none"> ↑Glucose uptake ↑GLUT4 translocation ↓Hepatic glucose production 	<ul style="list-style-type: none"> ↑The activation of AMPK ↓The activity of G6Pase 	[61]
Genistein	INS-1 cells, human islets	0.1, 1, and 5 μ M 24 h	↑ β -cell proliferation	↑cAMP/PKA-dependent ERK1/2 signaling pathway	[75]
EGCG	RIN5mF cells	20, 50, 100, and 200 μ g/ml, 24 h	↓Cytokine-induced β -cell destruction	↓NO ↓iNOS expression through the inhibition of NF- κ B activation	[90]
Hesperidin	Pancreatic islets cells	0.2 and 1 mg/ml, 24 h	<ul style="list-style-type: none"> ↑Insulin synthesis and secretion ↑Cell function 	↓Oxidative stress induced by IL-1 β	[109]
Anthocyanins	HepG2 cells	50, 100, and 250 μ g/ml, 24 h	<ul style="list-style-type: none"> ↓Insulin resistance ↑Glucose uptake ↑Glycogen content 	<ul style="list-style-type: none"> ↑PI3K/Akt pathways ↓G6Pase, PEPCK activity 	[121]
Curcumin	STZ-induced islets	10 μ M, 24 h	<ul style="list-style-type: none"> ↑Islet viability ↑Insulin secretion 	<ul style="list-style-type: none"> ↓ROS, NO ↓Poly ADP-ribose polymerase-1 	[131]
Rutin	Rat soleus muscle	10 and 500 μ M	↑Glucose uptake	Via the PI3K, atypical protein kinase C and MAPK pathways ↑GLUT4 synthesis	[237]
Naringin	Human umbilical vein endothelial cells	12.5, 25, 50, 100, and 200 μ M, 5 days	↓High-glucose-induced damage	<ul style="list-style-type: none"> ↑Mitochondrial function ↓Expression of CX3CL1 	[161]
<i>Vitamins</i>					
Vitamin A	Fetal and adult rats' pancreatic islets	10 ⁻⁶ M retinoic acid, 24 h	<ul style="list-style-type: none"> ↑Insulin mRNA level ↑Insulin secretion 	↑Glucokinase through activation of glucokinase promoter	[198]
Vitamin D	Rat RINm5F, human islets	10 ⁻⁶ or 10 ⁻⁸ M 1,25(OH) ₂ D ₃ , 48 h	↓Cytokine-induced apoptosis	<ul style="list-style-type: none"> ↑Antiapoptotic A20 gene ↓NF-κB 	[215]
Vitamin E	Alloxan-treated mice pancreatic islets	0.01 and 0.1 mM α -tocopherol with glucose	↑Insulin secretion	<ul style="list-style-type: none"> ↓Oxidative stress ↓Apoptosis 	[54]

TABLE 3: Effects of bioactive compounds on type 2 diabetes mellitus (*in vivo* studies).

Bioactive compounds	Models	Treatment	Effects	Specific mechanism of action	Reference
<i>Polyphenols</i>					
Resveratrol	db/db mice	20 mg/kg/day, 12 weeks	↓Glucose tolerance ↓Pancreatic islet fibrosis ↑Islet mass	↓Oxidative stress	[228]
Quercetin	STZ-induced diabetic rats	50 mg/kg/day, orally for 6 weeks	↓Diabetes-induced hypertension and vasoconstriction	↓TNF- α , CRP, NF- κ B	[47]
Genistein	STZ-induced diabetic rats	250 mg/kg of diet, 6 weeks	↓STZ-induced hyperglycemia ↑Blood insulin level ↑Glucose tolerance	↑ β -cell proliferation ↓ β -cell apoptosis	[75]
EGCG	Male db/db mice	250, 500, or 1000 mg/kg of diet, 5 weeks or orally by gavage 30 or 100 mg/kg/d	↑Blood insulin level ↑Glucose tolerance ↓Blood glucose	↑mRNA expression of glucokinase ↓mRNA expression of PEPCK, G6Pase, and fatty acid synthase ↑Pancreatic function	[93]
Hesperidin	HFD/STZ-induced diabetic rats	50 mg/kg/day, orally for 4 weeks	↓HbA1c, glucose level ↑Serum insulin level	↑Antioxidants (vitamin C and vitamin E) and GSH ↓NO, TNF- α , and IL-6	[109]
Anthocyanins	STZ-induced diabetic rats	One-time i.p. injection 3 mg/kg bodyweight	↑Blood insulin level ↑Glucose tolerance ↓Blood glucose ↓Oxidative stress	↓Hemoglobin glycation, iron-mediated free radical reactions ↑Hemoglobin-mediated iron release	[122]
Curcumin	STZ-induced diabetic rats	100 mg/kg body weight for 8 weeks	↓Body weight, glucose ↑Blood insulin level ↓Pancreatic β -cell damage	↓TNF- α , IL1- β , and IFN- γ ↑Nrf-2, HO-1, and GLUT2 ↓ER/mitochondrial-related apoptosis	[133]
Rutin	S961-treated C57BL/6 mice	Oral gavaged (25 mg/kg body weight) and metformin (100 mg/kg body weight)	↓Blood glucose	↑IRK activity ↑GLUT4 translocation	[147]
Naringin	STZ-induced type 2 diabetic rats	100 mg/kg body weight for 4 weeks	↓Blood glucose ↓Total lipid, triglycerides, and total cholesterol	↑G6Pase activity ↑Insulin receptor, GLUT4, and adiponectin ↓Oxidative stress	[159]
Naringenin	STZ-induced diabetic rats	100 mg/kg body weight for 15 days	↓Blood glucose ↓Total lipid, triglycerides, and LDL and VLDL ↓Oxidative stress	↑Expression of GLUT4 and PPAR γ	[172]

TABLE 3: Continued.

Bioactive compounds	Models	Treatment	Effects	Specific mechanism of action	Reference
<i>Carotenoid</i>					
Lycopene	STZ-induced diabetic rats	10, 30, 60, or 90 mg/kg body weight for 30 days	<ul style="list-style-type: none"> ↑Blood insulin level ↓Blood glucose ↓Total lipid, triglycerides, and total cholesterol 	<ul style="list-style-type: none"> ↑Activities of antioxidant enzymes ↓NO, H₂O₂ 	[185]
<i>Vitamins</i>					
Vitamin A	High-fat/high-sucrose diet-induced obese mouse	Direct pipetting (0.16 mg RA/50 μ l in oil) into the mouths	<ul style="list-style-type: none"> ↓Adipose lipid stores ↑Muscle mitochondrial content ↑Glucose tolerance ↓Insulin resistance 	<ul style="list-style-type: none"> ↑PPARβ/δ expression ↑RAR expression 	[200]
Vitamin D	Alloxan-induced diabetic rats	1,25(OH) ₂ D ₃ intraperitoneal (7 ng/gm/day) for 15 days	<ul style="list-style-type: none"> ↓Pancreatic and liver damage ↓Hyperglycemia 	<ul style="list-style-type: none"> ↑DNA tail length of liver and pancreas ↓Serum calcium levels ↓G6Pase, FBPase 	[219]
Vitamin E	Alloxan-induced mouse	50 mg α -tocopherol, per 100 g diet, 14 weeks	<ul style="list-style-type: none"> ↓Alloxan-induced hyperglycemia ↑Insulin secretion 	<ul style="list-style-type: none"> ↓Oxidative stress ↓Pancreas apoptosis 	[228]

TABLE 4: Effects of bioactive compounds on Alzheimer's disease (*in vivo* studies).

Bioactive compound	Models	Treatment	Effects	Specific mechanism of action	Reference
<i>Polyphenols</i>					
Resveratrol	SAMP8 and SAMR1 mice	Transresveratrol 1 g/kg in diet, 7 months	↑Life expectancy ↓Cognitive impairment in SAMP8 ↓Amyloid deposition	↑AMPK pathways ↑SIRT1 ↑Nonamyloidogenic ADAM-10 enzyme	[239]
Quercetin	3xTg-AD mice	i.p. injection 25 mg/kg every 48 hours for 3 months	↑Learning and memory function	↓Aβ1-40, Aβ1-42, and BACE1 ↓Microglial activation	[70]
Genistein	Intrahippocampal Aβ1-40-injected rats	10 mg/kg, one hour before surgery	↑Short-term spatial recognition memory in a Y-maze test ↑Learning and memory	↓Oxidative stress	[86]
EGCG	APPsw mice	i.p. 20 mg/kg, 60 days, or orally 50 mg/kg, 6 months	↑Memory performance ↓Aβ levels ↓Tau hyperphosphorylation	↓α-secretase	[104]
Hesperidin	APP/PS1 mice	Intragastric administration 40 mg/kg for 90 days	↑Learning and memory function	↓Oxidative stress via activation of Akt/Nrf2 ↓Inflammation via inhibition of RAGE/NF-κB	[116]
Anthocyanins	APPsw mice	ANT-rich blackcurrant extracts 5.6 mg/day, 6 weeks	↑Spatial working memory	↓Oxidative stress	[127]
Curcumin	Alzheimer transgenic APPsw mouse model	Low dose: 160 ppm or high dose: 5000 ppm, 6 months	↓Overall insoluble and soluble amyloid, and plaque burden (low dose) ↓Oxidative stress and inflammation	↓IL1-β, IL-6, and ApoE ↓NF-κB, iNOS, and COX-2 ↓Plasma and tissue cholesterol	[139]
Rutin	Aβ1-42-injected rats	100 mg/kg body weight/day, 3 weeks	↓Aβ-induced learning and memory deficits ↓Aβ-induced neurotoxicity	↑Activation of MAPK pathway ↑BDNF gene expression	[156]
Naringin	APPswe/PS1dE9 transgenic mouse	50 or 100 mg/kg body weight/day, 16 weeks	↑Learning and memory ability	↑CaMKII activity	[167]
Naringenin	Aβ1-40-injected Wistar rats	Orally by gavage at a dose of 100 mg/kg one hour before surgery	↓Aβ-induced learning and memory deficits	↓Lipid peroxidation ↓Apoptosis estrogenic pathway	[179]
<i>Carotenoid</i>					
Lycopene	Aβ1-42-injected Wistar rats	1, 2, and 4 mg/kg, orally 14 days	↓Aβ-induced learning and memory deficits	↓NF-κB, TNF-α, and IL-1β	[193]
<i>Vitamins</i>					
Vitamin A	APP/PS1 mice	i.p. 20 mg/kg all-trans-retinoic acid, 3 times/week, 8 weeks	↓Spatial learning and memory ↓Aβ accumulation ↓Tau hyperphosphorylation	↓APP processing ↓CDK5 activity ↓Activated microglia and astrocytes	[207]
Vitamin D	APP/PS1 mice	0 (deficiency diet), 2.4 (control diet), and 12 IU/g (surplus diet), 5 months	↓Amyloid plaques ↓Aβ peptides	↓Neuroinflammation ↑NGF	[240]
Vitamin E	Tg2576 mice	8 IU/g/day, 6 months	↓Aβ peptide formation in young but not in old Tg2576 mice	↓Oxidative stress	[241]

PS1dE9 mice alleviated learning and memory deficits as well as decreased plaque burden compared to control mice; the protective effects of quercetin might function by reducing mitochondrial dysfunction through the activation of AMPK [71]. A recent work also suggested an anti-inflammatory role of quercetin in AD mice [72]. Specifically, quercetin treatment reduced β-amyloid plaque aggregation as well as

decreased IL-1β/COX-2/iNOS proinflammatory signaling in the hippocampal CA1 region of 3xTg-AD mice [72].

4.1.3. Genistein. Genistein is an isoflavone found in a variety of plants, including chickpeas, fava beans, and soybeans [73]. Several health benefits are attributed to isoflavones, and recent evidence suggests that genistein may be a potential

preventative and therapeutic treatment for diabetes and AD [74–76].

Loss of functional β -cell mass, which decreases insulin secretion, is crucial for the development of T2DM. The mass of β cells is controlled by the balance between neogenesis, transdifferentiation, proliferation, and apoptosis [74]. Fu et al. [75] reported that genistein incubation induced increase of both INS-1 and human islet β -cell proliferation via the activation of the cAMP/PKA-dependent ERK1/2 signaling pathway (Table 2). Animal studies also showed an antidiabetic effect of genistein. Specifically, Fu et al. [75] found that induction of diabetes by STZ decreased β -cell mass and disrupted the cell architecture (Table 3). However, dietary supplementation of genistein improved β -cell mass by increasing β -cell proliferation and reducing apoptosis; accordingly, supplementation with genistein alleviated STZ-induced hyperglycemia and improved glucose tolerance and insulin levels [75]. Ae Park et al. [76] evaluated the antidiabetic effects of genistein on C57BL/Ks)-db/db mice, which share metabolic features that are like human T2DM. Blood glucose and HbA1c were significantly lower in the genistein groups, while glucose tolerance and the insulin/glucagon ratio were also improved in the genistein group compared to the control group [76]. In addition, the genistein supplements improved the plasma triglyceride, HDL-cholesterol, free fatty acid, and total cholesterol levels in these mice. These effects might be associated with increased hepatic glucokinase activity as well as decreased hepatic fatty acid synthase, β -oxidation, and G6Pase activities [76]. Therefore, genistein may exert an antidiabetic role in T2DM by improving the lipid and glucose metabolism. Furthermore, Dkhar et al. [77] reported that genistein reduced fasting glucose, inhibited cytosolic phosphoenolpyruvate carboxykinase (PEPCK), and activated AMPK and ERK1/2 pathway in alloxan-induced diabetic mice, which may in turn improve dysfunction in hepatic gluconeogenesis in T2DM. Furthermore, recent studies have shown that genistein might also be a prospective therapeutic approach for the management of T2DM complications [78, 79]. For example, Rajput et al. [78] reported that genistein treatment recovered cognitive decline in diabetic mice by modulating acetylcholinesterase, antioxidant levels, and neuroinflammation. Another interesting study indicated that genistein pretreatment improved obsessive-compulsive disorder in STZ-induced diabetic mice by increasing serotonergic neurotransmission [79].

The antioxidant, anti-inflammatory, and antiapoptosis qualities of genistein might also apply to AD. Zhou et al. [80] reported that A β 25-35 induced inflammatory damage in BV-2 microglia, possibly through the TLR4- and NF- κ B-mediated signal pathway, which could be attenuated by genistein injection (Table 1). Another study indicated that pretreatment with genistein prevented the increase of inflammatory and oxidant mediators such as COX-2, iNOS, IL-1 β , and TNF- α stimulated by A β in cultured astrocytes and that these effects may be mediated by increasing expression of peroxisome proliferator-activated receptors (PPARs) [81]. The activation of PPARs has been shown to suppress inflammation in AD [82]. Furthermore, genistein protected PC12 cells from A β 25-35-induced neurotoxicity and neuron death

by interfering with the activation of JNK, which could stimulate the transcription of the death inducer Fas ligand [83]. Moreover, recent studies indicated that genistein protected P12 cells against A β 25-35-induced injury as well as protected AD rats against hippocampal neuron injury by regulating calcium/calmodulin-dependent protein kinase IV (CaM-CaMKIV) and tau protein expression [84, 85]. In addition, genistein as a phytoestrogen can bind estrogen receptors and impact estrogen-mediated processes [86]. In A β 1-40-injected rats, pretreatment of genistein improved learning and memory function of rats via an estrogenic pathway and by reducing oxidative stress (Table 4) [86]. However, some studies indicated that genistein exerted toxic effects in AD pathology. For instance, in SHSY5Y cells, genistein enhanced A β 42 accumulation by increasing mRNA expression and activities of both APP and β -secretase and by decreasing levels of the A β 42-degrading enzyme IDE [87]. Considering the mixed results of the effects of genistein from *in vitro* studies, it is imperative to verify these toxic effects in experimental models.

4.1.4. Epigallocatechin-3-Gallate. Epigallocatechin-3-gallate (EGCG) is a polyphenolic compound derived from a variety of plants, particularly green tea. In recent years, the beneficial effects of green tea have been studied and the health benefits are attributed to its most abundant component, EGCG [88]. EGCG exhibits strong antioxidant activity. Cytokines produced by immune cells may induce β -cell damage in insulin-dependent diabetes mellitus, and it is associated with the generation of iNOS and NO within the cell [89]. Han [90] reported that EGCG protected RINn5F cells against cytokine-induced β -cell destruction and that the molecular mechanism may involve the suppression of iNOS expression through the inhibition of NF- κ B activation (Table 2). Thus, EGCG may lead to enhanced pancreatic function. However, the supposed antioxidant effects of EGCG are controversial, and there is evidence suggesting that EGCG has prooxidant effects [91, 92]. For instance, Suh et al. [92] reported that EGCG mediated the production of H₂O₂ and triggered Fe²⁺-dependent formation of toxic radicals, which further decreased cell viability and induced apoptotic cell death in HIT-T15 pancreatic β cells.

Animal studies also suggest that EGCG may play a role in preventing the development of diabetes and its complications, although the evidence is not consistent [93–95]. In a db/db mouse model, EGCG consumption improved glucose-stimulated insulin secretion, oral glucose tolerance, and blood glucose in a dose-dependent manner. The increase in insulin secretion could be caused by a protective effect of EGCG on the pancreas [93]. Furthermore, the study implied that EGCG supplementation influenced the expression of genes that are involved in glucose and lipid metabolism in the liver, for example, by increasing mRNA expression of glucose kinase and decreasing mRNA expression of PEPCK, G6Pase, and fatty acid synthase (Table 3) [93]. Oršolić et al. [94] reported that administration of EGCG resulted in increased survival, decreased lipid peroxidation, and reduced DNA damage in diabetic mice and that the beneficial effects of EGCG might be associated with its

antioxidant and anti-inflammatory potential. By contrast, Yun et al. [95] reported that EGCG acted as a prooxidant in β cells, which impaired β -cell function and insulin secretion by increasing oxidative stress. In biological systems, the anti- or prooxidant activity of EGCG may be different depending upon its concentration, the cellular environment, the presence of red blood cells or metal ions, and the characteristics of the cell line under investigation [92, 96, 97]; thus, additional studies are needed to determine the adverse effects of EGCG in different cell lines and pathophysiological conditions. In addition to its antioxidant property, new studies have investigated the other possible mechanism of EGCG in the treatment of T2DM [98, 99]. For instance, Zhang et al. [98] reported that EGCG improved insulin resistance in HepG2 cells through ameliorating glucose-induced inflammation and lipotoxicity via the GLUT2/peroxisome proliferator-activated receptor γ coactivator (PGC-1 β)/sterol regulatory element-binding-1c (SREBP-1c)/FAS pathway.

EGCG may have the potential to improve cognitive function and attenuate the hallmarks of AD. For instance, in an *in vitro* study where cultured hippocampal neuronal cells were treated with EGCG, a protective effect against A β -induced neuron injury and death through scavenging ROS was found, as evidenced by decreased levels of malonyldialdehyde (MDA) and caspase, which were likely a result of decreased ROS [100]. EGCG could also prevent the development of AD by inhibiting the formation of the biomarkers of AD pathology [101]. The assembly of amyloid fibrils is involved in converting native, unfolded polypeptides A β into a β -sheet formation [102]. The presence of EGCG could directly bind the unfolded polypeptides A β and then assemble them into unstructured, nontoxic A β -oligomers instead of β -sheet-rich aggregates, inhibiting the fibrillogenesis of A β [101]. Moreover, Bieschke et al. [103] reported that EGCG could remodel the large, mature β fibrils into smaller, nontoxic amorphous protein aggregates, further reducing cellular toxicity (Table 1). In AD transgenic mice, chronic EGCG injections decreased A β levels and plaques and promoted nonamyloidogenic APP processing by increasing α -secretase activity (Table 4) [104]. Moreover, EGCG administered orally in drinking water (50 mg/kg, 6 months) reduced A β deposition, regulated the tau profile, and suppressed the phosphorylated tau isoforms in AD transgenic mice [105]. Radial-arm water-maze tests also indicated EGCG provided cognitive benefits [105]. A recent study suggested that EGCG facilitated the degradation of extracellular A β in astrocytes, by increasing neprilysin secretion via ERK and the phosphoinositide 3-kinase (PI3K) pathway [106]. Furthermore, Du et al. [107] indicated that EGCG attenuated the neurotoxicity in both SH-SY5Y cells and the APP/PS1 transgenic mice model, via a novel mechanism that involves suppression of ER-stress-mediated neuronal apoptosis.

4.1.5. Hesperidin. Hesperidin is a flavonoid glycoside abundant in citrus fruits such as lemons and oranges. Recently, evidence from *in vitro* and *in vivo* studies has shown that hesperidin possesses beneficial effects for the prevention and treatment of T2DM and its complications, through its

antioxidant, anti-inflammatory, and antidepressant properties [108–111]. In rat pancreatic islet cells, hesperidin was protective against oxidative stress induced by IL-1 β , thereby improving the function of islet cells and restoring biosynthesis and secretion of insulin [108]. Treatment of high fat diet (HFD)/STZ-induced diabetic rats with hesperidin reduced hyperglycemia by increasing peripheral glucose uptake, which might be associated with the upregulation of GLUT4 mRNA expression (Table 2) [108]. Oral administration of hesperidin significantly decreased glucose and HbA1c levels and increased serum insulin, vitamin C, and vitamin E levels in HFD/STZ-induced diabetic rats [109]. These effects were possibly due to a decline in production of oxidants and proinflammatory cytokines such as TNF- α and IL-6 (Table 3) [109]. Moreover, in STZ-induced diabetic rats, hesperidin treatment attenuated retina and plasma abnormalities, including reduced retina thickness and increased blood-retina breakdown, via its antioxidant and anti-inflammatory properties, and the inhibition of the production of AGEs and elevated aldose reductase [110]. Hesperidin could attenuate experimental diabetic neuropathy. Treatment of STZ-induced diabetic rats with hesperidin significantly attenuated neuropathic pain and improved nerve conduction velocity by downregulating the production of free radical generation and proinflammatory cytokine [111]. The antidepressant effect of hesperidin was demonstrated in STZ-induced diabetic rats, which also was mediated by its antioxidant and anti-inflammatory activities as well as increased neurogenesis [112]. Furthermore, a recent study implied the protective effects of hesperidin in diabetic nephropathy, possibly through the inhibition of transforming growth factor- β 1- (TGF- β 1-) integrin-linked kinase (ILK-) Akt signaling [113].

Additionally, several studies provided evidence that hesperidin may be a novel therapeutic agent for the treatment of AD [114–116]. In PC12 cells, hesperidin protected cells against A β 25-35-induced cytotoxicity and apoptosis by attenuating mitochondria dysfunction [114]. Further study indicated that hesperidin mediated the voltage-dependent anion channel 1- (VDACV-1-) regulated mitochondria apoptotic pathway [114]. Huang et al. [115] reported that hesperidin administration ameliorated A β 1-42-impaired glucose utilization, partly by decreasing A β -induced cellular autophagy in neuro-2A cells (Table 1). In APP/PS1 mice, intragastric administration of hesperidin improved learning and memory deficits by attenuating inflammation and oxidative stress through inhibition of RAGE/NF- κ B signaling and activation of Akt/Nrf2 signaling (Table 4) [116]. Moreover, in the transgenic APP/PS1-21 mice, hesperidin treatment significantly restored deficits in nesting and social interactions and attenuated A β deposition, microglial activation, and TNF- α , iNOS, and IL-1 β levels in the brains of mice [117]. These results suggested that reduced A β deposition and alleviation of neuroinflammatory reactions by hesperidin might contribute to the improvement of behavior [117]. Taken together, studies suggest that hesperidin might be a potential candidate for the treatment and prevention of T2DM and AD; however, more studies on the clinical effects of hesperidin should be performed.

4.1.6. Anthocyanins. Anthocyanins (ANTs) are flavonoids responsible for the blue, red, and purple colors of vegetables, fruits, and flowers [118]. Most ANTs act as strong antioxidants, which may contribute to their antidiabetic properties. Zhang et al. [119] reported that ANTs from Chinese bayberry extract upregulated HO-1 expression via activation of PI3K/Akt and ERK1/2 signaling in INS-1 cells. As a result, ANTs protect cells against H₂O₂-induced β -cell injury. Furthermore, Zhang et al. [120] found that pretreatment with ANTs attenuated H₂O₂-mediated β -cell autophagy by activating the antioxidant transcription factor Nrf2. Additionally, in HepG2 cells, mulberry ANT extract was reported to mitigate insulin resistance via activation of PI3K/Akt pathways (Table 2) [121]. In STZ-induced diabetic rats, injection of the ANT pelargonidin improved serum insulin levels, normalized elevated blood glucose levels, and glucose tolerance. It also relieved oxidative stress, including the hemoglobin-(Hb-) induced iron-mediated oxidative reaction, by releasing iron from the Hb and decreasing Hb glycation (Table 3) [122]. ANTs from black soybean seed coats also yield antidiabetic effects such as decreasing blood glucose levels and improving hemodynamic parameters and insulin levels in STZ-induced diabetic mice [123]. These effects were partly due to the regulation of GLUT4 transporter, the activation of the phosphorylation of insulin receptor, and the prevention of pancreatic apoptosis [123]. Recently, Luna-Vital et al. [124] demonstrated that ANT from purple corn improved insulin secretion and hepatic glucose uptake *in vitro*, by enhancing the activity of the free fatty acid receptor-1 (FFAR1) and glucokinase.

Growing evidence suggests that ANTs may have beneficial effects on AD. Shih et al. [125] reported that exposure of A β ₁₋₄₀ and A β ₂₅₋₃₅ to neuro-2A cells resulted in ROS formation, the perturbation of calcium balance, and influenced the expression of genes involved in apolipoprotein E (ApoE) metabolism. All these effects could be blocked by ANT treatment, eventually leading to reduction of A β -induced neurotoxicity (Table 1). In addition, treatment of neuro-2A cells with *Vaccinium myrtillus* anthocyanoside, a heterogeneous mixture of ANTs, promoted the formation of nontoxic forms of A β aggregates instead of the toxic amyloid fibrils [126]. The molecular mechanism may involve the direct binding between ANT and A β molecules to suppress amyloid fibril formation, a function similar to that of EGCG [101]. Moreover, APdE9 mouse fed a diet rich in ANT from bilberry or blackcurrant supplementation showed altered APP processing and A β levels. Specifically, both bilberry and blackcurrant extracts decreased APP-C-terminal fragment levels in the cerebral cortex compared to animals fed the control diet [127]. Soluble A β ₄₀ and A β ₄₂ levels were decreased in bilberry-fed mice but not blackcurrant-fed mice, and by contrast, the ratio of insoluble A β _{42/40} was significantly decreased in blackcurrant-fed mice but not in bilberry-fed mice. Both berry diets attenuated behavioral abnormalities of aged mice as compared to control diet-fed mice (Table 4) [127].

Although several studies have demonstrated the beneficial effects of ANTs on T2DM and AD, further studies are needed to clarify what type of ANT is most appropriate for

a given purpose, because different sources of ANTs were used in studies.

4.1.7. Curcumin. Curcumin is a polyphenolic compound extracted from the dried roots of turmeric plants [128]. More than 500 published articles were retrieved when searching the PubMed database using the terms “curcumin and diabetes.” In these articles, various pharmacological properties of curcumin were noted. Its antioxidant and anti-inflammatory properties are the most well known [129]. Hepatic stellate cells (HSCs) are the major effectors during T2D-associated hepatic fibrogenesis [130], and AGEs have been shown to induce gene expression of RAGE in HSCs, which could stimulate the activation of HSCs [130]. Lin et al. [129] reported that curcumin eliminated the stimulation of AGE probably by increasing gene expression of PPAR γ , which attenuated the gene expression of RAGE, and alleviated the oxidative stress. Furthermore, curcumin protected pancreatic islets against STZ-induced oxidative stress by scavenging free radicals [131]. Curcumin increased islet viability and insulin secretion and decreased ROS concentration and the generation of NO as well as prevented the overactivation of poly ADP-ribose polymerase-1 (Table 2) [131]. In db/db mice, oral curcumin mitigated hyperglycemia-induced liver and kidney damage through normalization of mitochondrial function, by suppressing NO synthesis and lipid peroxidation [132]. Another study indicated that oral treatment with curcumin decreased body weight and blood glucose levels and increased plasma insulin levels [133]. In addition, curcumin attenuated hyperglycemia-induced oxidative stress, ER stress and its related inflammation, and protected β cells from apoptotic damage. These effects might be associated with the activation of HO-1 and the inhibition of NF- κ B signaling through a PI3K/Akt-mediated pathway, as well as the suppression of multiple apoptotic signaling (ER-mediated and mitochondrial-dependent or mitochondrial-independent apoptotic pathways) (Table 3) [133]. Curcumin has been shown to exhibit antihyperlipidemic activity. Pari and Murugan [134] reported that treatment of STZ-induced diabetic rats with intragastric tetrahydrocurcumin, one of the active metabolites of curcumin, resulted in a significant reduction of serum-free fatty acids, triglycerides, VLDL, LDL, and cholesterol and an increase of HDL cholesterol. Furthermore, curcumin inhibited hepatic gluconeogenesis by inhibiting hepatic G6Pase and PEPCK activities and activating AMP kinase [135]. Moreover, a recent study showed that curcumin improved insulin resistance and also ameliorated the metabolic disorder of glucose and lipid in T2DM rats; these effects might be associated with the reduction of the free fatty acid and TNF- α in serum [136].

Curcumin also emerged as a promising therapeutic option for AD. Huang et al. [137] reported that curcumin inhibited A β -induced tau hyperphosphorylation in human neuroblastoma SH-SY5Y cells, which is involved in the phosphatase and tension homolog (PTEN)/Akt/GSK3 β pathway. Qian et al. [138] showed that curcumin treatment protected P12 cells from A β -induced reduction in MDA production, cell viability, and apoptosis, by increasing the expression of the N-methyl-D-aspartate receptor (NMDAR) subunit

NR2A. In an Alzheimer transgenic APPsw mouse model, curcumin decreased overall insoluble and soluble amyloid and plaque burden, and it reduced oxidative stress and suppressed the inflammatory cytokine IL-1 β and astrocytic inflammatory marker glial fibrillary acidic protein (GFAP) (Table 4) [139]. Moreover, increasing evidence suggests that curcumin could bind A β and shift its aggregation pathway. For instance, Rao et al. [140] found that curcumin binding to A β promoted the formation of nontoxic forms of A β aggregates. Similarly, another study indicated that curcumin could bind to highly aggregated A β as well as to abnormal tau protein in the brain of aged AD animals; therefore, curcumin might be used as a specific marker for A β detection [141]. Overall, these findings highlight the potential utility of curcumin in T2DM and AD protection fields. However, there are some limitations to its therapeutic use, including poor bioavailability, rapid metabolism, and rapid systemic elimination [142]. Additional approaches are needed to enhance its bioavailability, and more clinical trials are needed to confirm its potential in prevention of AD and T2DM.

4.1.8. Rutin. Rutin is a flavonoid in many vegetables and fruits, such as apples, figs, buckwheat, and asparagus [143]. It has a wide range of biological effects including antioxidant, anti-inflammatory, antihyperglycemic, and neuroprotective [144, 145]. All these properties support the potential of rutin to prevent or treat diabetes and its complications. For example, in nicotinamide- (NA-) STZ-induced diabetic rats, administration of rutin significantly ameliorated glucose tolerance; decreased serum glucose levels; produced improvement of the increased serum lipid variables, such as LDL-cholesterol, VLDL-cholesterol, triglycerides, and serum total lipids; and also improved the oxidative stress [146]. The possible mechanisms for the antihyperglycemic and antihyperlipidemia effect of rutin were investigated in further studies. It has been shown that rutin decreased the activity of G6Pase and glycogen phosphorylase, as well as increased the activity of hepatic hexokinase activity; therefore, rutin may reduce hepatic glucose output [146]. Furthermore, the decrease in glucose level can be achieved by improving glucose uptake by tissues [145]. Hsu et al. [147] reported that rutin reduced blood glucose level in insulin-resistant mice through enhancement of insulin-dependent receptor kinase (IRK) activity and GLUT4 translocation (Table 3). In adipose tissue and skeletal muscle, rutin has been shown to increase expression of PPAR γ , which further improve insulin resistance, affect insulin sensitivity, and improve glucose uptake [146, 148]. Moreover, rutin treatment increased β -cell viability and reduced the glucotoxicity through activating AMPK and IRS2 signaling [149]. Furthermore, it has been shown that rutin improved insulin secretion in isolated rat pancreatic islets [146]. Taken together, the antihyperglycemic effect of rutin may be achieved by increasing glucose uptake by peripheral tissue, improving insulin resistance, suppressing gluconeogenesis in the liver, and stimulating insulin secretion.

In addition to antihyperglycemia and antihyperlipidemia, rutin also exhibits antidiabetic effects by decreasing

oxidative stress and suppressing the inflammatory cytokine in STZ-induced diabetic rats [150]. Moreover, a very recent study showed that rutin exhibited protective effect on the liver of db/db mice by activating the IRS2/PI3K/Akt/GSK3 β signal pathway, improving hepatocyte proliferation, and decreasing generation of AGEs [151]. Overall, several cell and animal studies support the beneficial effects of rutin on T2DM. Further clinical studies are suggested to evaluate the efficiency and safety of rutin.

The therapeutic potential of rutin for AD has also been shown in both cell and animal studies [152, 153]. The possible mechanisms involved are eliminating the inflammatory component of neurodegeneration, decreasing oxidative stress which relates to neuronal cell loss, and preventing A β aggregation [154]. For example, in APPsw (APP Swedish mutation) cells, rutin treatment prevented A β 25-35 fibril formation and inhibited BACE activity [152] (Table 1). Furthermore, rutin ameliorated the neurotoxic effect, including declined cell viability and reduced GSH levels induced by overexpression of APP in APPsw cells [152]. Similarly, Wang et al. [153] indicated that rutin inhibited A β 42 fibrillization and improved A β 42-induced cytotoxicity in SH-SY5Y cells. Additionally, rutin attenuated mitochondrial damage and decreased the generation of ROS, GSSG, NO, iNOS, and proinflammatory cytokines, as well as enhanced the activities of SOD and catalase [153]. Moreover, a recent study showed that *Nelumbo nucifera* extracts exhibited protective effect on A β -induced apoptosis in PC12 cells; further purification of these extracts identified them to be flavonoids, such as rutin [155]. In A β -injected rats, administration of rutin significantly enhanced memory retrieval compared to the control group, possibly through activation of the MAPK pathway and brain derived neurotrophic factor (BDNF) gene expression and reduction of oxidative stress and neurotoxicity induced by A β (Table 4) [156]. Furthermore, Choi et al. [157] found that the impaired cognition and memory of A β -induced AD mouse was alleviated by oral administration of rutin.

4.1.9. Naringin. Naringin, a flavonoid mostly found in grape fruit and related citrus species, has been reported for its antioxidant, anti-inflammatory, and antihyperglycemic properties [158, 159]. Recently, several new investigations indicated that naringin could improve T2DM and mitigate the severity of T2DM complications [159–161], and the underlying mechanism has been elucidated. In NA/STZ-induced type 2 diabetic rats, naringin produced a significant amelioration of the serum glucose level and lipid profile, such as LDL-cholesterol, LDL, and free fatty acids (Table 3) [159]. These effects may be mediated by elevating liver G6Pase and glycogen phosphorylase activities, improving the insulin secretory response, and enhancing the expression of GLUT4, insulin receptor, and adiponectin as well as decreasing oxidative stress [159]. In *in vitro* studies, it has also been shown that naringin protected the cell against high glucose-induced damage. For instance, Chen et al. [160] reported that naringin inhibited the high glucose-induced inflammatory reaction by mediating the nucleotide-binding and oligomerization domain-like receptor family pyrin domain-

containing 3 (NLRP3) inflammasome in the rat mesangial cell. Furthermore, Li et al. [161] indicated that naringin protected the human endothelial cell against high glucose-induced damage through inhibition of oxidation, downregulation of the chemokine (C-X3-C motif) ligand 1 (CX3CL1), and improvement of mitochondrial function (Table 2).

Furthermore, several studies have demonstrated the beneficial effect of naringin on diabetic complications including diabetes-associated anemia, kidney damage, cognitive decline, and atherosclerosis [162–164]. For instance, Mahmoud [162] reported that naringin protected HFD/STZ diabetic rats from diabetes-associated anemia by decreasing proinflammatory cytokine production and stimulating adiponectin expression. Sharma et al. [163] demonstrated that naringin attenuated hepatic steatosis and kidney damage, and also ameliorated insulin resistance and β -cell dysfunction by decreasing oxidative stress and inflammation through upregulation of PPAR γ , heat shock protein-27, and heat shock protein-72. In addition, the effects of naringin on oxidative stress, proinflammatory factors, and the PPAR γ signaling pathway may be involved in ameliorating cognitive deficits in the type 2 diabetic rat model [164]. Recently, an interesting study showed that naringin exhibited antiatherogenic effect in a T2DM rat model; the underlying mechanism may be involved in the enhancement of HDL-mediated reverse cholesterol transport and the improvement of paraoxonase activity [165].

The potent neuroprotective effects of naringin have been well characterized, and increasing attention has been focused on its protective effects on AD. In an APP/PS transgenic mouse model, naringin consumption enhanced learning and memory ability of mice, ameliorated cognitive deficits, and also reduced senile plaque formation and reversed glucose uptake defect in the brain. The inhibition of GSK3 β activity may be the possible mechanism [166]. Another study suggested that the enhancement of CaMKII activity may be one of the mechanisms by which naringin improved cognitive function in the AD mouse model (Table 4) [167]. Moreover, naringin treatment restored intracerebroventricular STZ-induced cognitive deficits in rats, the mitigation of mitochondrial dysfunction mediated oxidative stress, and the suppression of acetylcholinesterase activity and the TNF- α level by naringin may contribute to its function on cognitive impairment [168]. A recent study has investigated the effects of naringin dihydrochalcone (NDC) on neuropathology in APP/PS1 transgenic mice [169]. NDC is a naringin derivative and acts as an artificial sweetener with antioxidant activity in food and medicine [170]. The results suggested that NDC attenuated A β deposition and neuroinflammation and enhanced neurogenesis as well as ameliorated cognitive deficits in AD mice [169].

4.1.10. Naringenin. Naringenin is a flavonoid abundantly found in citrus fruits such as oranges, lemons, grapefruits, and tomatoes [171]. In recent years, there has been increased attention on the benefits of naringenin on T2DM and its complications. In STZ-induced diabetic rats, oral administration of naringenin decreased the blood glucose level, normalized LDL, and VLDL concentrations and also normalized

oxidative stress parameters in both the liver and pancreas; these effects may be attributed to the increased expression of mRNA and protein levels of GLUT4 and PPAR γ by naringenin [172] (Table 3). Many studies have been designed to evaluate the role of naringenin in diabetes-associated complications, such as nephropathy, cardiac hypertrophy, vascular disease, hepatotoxicity, and neuropathy [173–175]. For instance, Kapoor et al. [173] demonstrated that the altered activity of liver and kidney enzymes, altered antioxidant status, increased generation of ROS, mitochondria dysfunction, and increased expression of apoptotic proteins could induce liver damage and diabetic hepatopathy in diabetic rats; all these effects were rescued after naringenin treatment; therefore, naringenin has potential for the management of diabetic hepatopathy. Roy et al. [174] showed that naringenin alleviated renal impairment and structural changes such as glomerulosclerosis in STZ-induced diabetic rats, possibly through downregulation of TGF- β 1 and IL-1 by reducing oxidative stress, modulating proinflammatory cytokine production and apoptotic events. Moreover, researchers found that naringenin ameliorated high glucose-induced endothelial dysfunction by decreasing oxidative stress and apoptosis via the ROS/caspase-3 and NO pathway in endothelial cells [175]. Furthermore, naringenin acted as an antioxidant and cholinesterase inhibitor and ameliorated diabetes-induced memory dysfunction in rats [176]. Moreover, in a recent study, naringenin has been shown to improve cardiac hypertrophy in diabetic mice; these effects may be related to the upregulation of cytochrome P450 2J3 and the activation of PPARs [177]. Overall, the beneficial effects of naringenin on diabetes and its complications have been investigated, partly through its antioxidant, anti-inflammatory, and antiapoptotic properties.

In recent years, a few studies have explored the possible role of naringenin in prevention and treatment of AD. For instance, in an AD rat model, the expression of A β 40 and A β 42 were downregulated, and the learning and memory ability were improved after naringenin administration [178]. Another study has investigated the underlying mechanisms in A β -injected rats; the results suggested that naringenin pretreatment alleviated A β -induced impairment of memory and learning through downregulation of lipid peroxidation and apoptosis and also through mediation of the estrogenic pathway (Table 4) [179]. In PC12 cells, naringenin suppressed A β 25-35-induced nerve damage by improving cell viability, stimulating Akt and GSK3 β activation, inhibiting cell apoptosis, and regulating the estrogen receptor [180]. The collapsin response mediator protein-2 (CRMP-2) has been implicated in the pathogenesis of AD; phosphorylation leads to its inactivity, which in turn inhibits axonal outgrowth and results in neuronal loss and memory deficits [181, 182]. A recent study reported that naringenin could bind to CRMP-2 then decrease its phosphorylation, which in turn alleviates AD-like pathology [181]. Even though naringenin has a wide range of activities, due to its low water solubility and poor bioavailability, the clinical development of naringenin has been hampered [182]. A recent study has developed naringenin-loaded nanoemulsions, which protected SH-SY5Y cells against A β -induced neurotoxicity,

possibly by reducing amyloidogenesis and tau hyperphosphorylation; also, it showed a better neuroprotective effect than free naringenin [183]. Overall, naringenin might be a potential agent for treatment of AD; further studies are needed to identify more underlying mechanisms and develop an optimal form of naringenin.

4.2. Carotenoid

4.2.1. Lycopene. Lycopene is a carotenoid occurring naturally in tomatoes and pink grapefruits that is responsible for the red color [184]. Although there is little evidence regarding the possible antidiabetic effects of lycopene from *in vitro* studies, many *in vivo* studies have shown the beneficial effects of lycopene on diabetes and its associated complications [185–187]. Ali and Agha [185] conducted a study with STZ-induced diabetic rats where supplementation with lycopene (Table 3) caused a dose-dependent decrease in H_2O_2 , NO, and lipid peroxidation, as well as increased activity of antioxidant enzymes, which further contributed to the decreased glucose levels, increased insulin levels, and improved serum lipid profiles (Table 3). The antioxidant properties of lycopene also have been shown to rescue diabetic endothelial dysfunction in STZ-induced diabetic rats [186]. To study the specific therapeutic effect of lycopene on diabetic nephropathy, Li et al. [187] conducted a study with STZ-induced diabetic rats. The results indicated that lycopene protected kidneys against diabetes mellitus-induced morphological destruction and function impairments by improving oxidative status, increasing Akt phosphorylation, and regulating connective tissue growth factor. Another study indicated that lycopene ameliorated renal function by interrupting the AGE-RAGE axis [188]. In addition, lycopene has been tested for its ability to attenuate diabetes-associated cognitive decline. Kuhad et al. [189] reported a dose-dependent response to chronic treatment with lycopene that alleviated cognitive impairment and cholinergic dysfunction, decreased NO and TNF- α , and increased acetylcholinesterase activity in STZ-induced diabetic rats. The dysfunction of endothelial progenitor cells (EPCs) has been implicated in diabetes-associated vascular complications [190]; Zeng et al. [191] showed that lycopene ameliorated AGE-induced EPC apoptosis and oxidative autophagy, further impairing the number and function of EPCs. Therefore, lycopene may have potential to improve T2DM vascular complications. Taken together, the antidiabetic function of lycopene might be associated with its antioxidant and anti-inflammatory properties.

Recent interest has focused on lycopene as a potential useful agent in the management of AD. The antioxidant, anti-inflammatory, and antiapoptotic effects of lycopene may directly link to its neuroprotective function. In primary cultured rat cortical neurons, pretreatment with lycopene attenuated A β ₂₅₋₃₅-induced neurotoxicity, as evidenced by improved cell viability and decreased rate of apoptosis in a dose-dependent manner; these effects were attributed to the inhibition of the A β ₂₅₋₃₅-induced generation of ROS and mitochondrial membrane potential collapse (Table 1) [192]. Furthermore, Qu et al. [193] reported that lycopene protected mitochondria against A β -induced damage in cultured

rat cortical neurons, and its effects in part resulted by decreasing mitochondrial oxidative stress and improving mitochondrial function. Chen et al. [194] found that lycopene could reduce A β ₁₋₄₂ secretion by inhibiting APP expression in APPsw cells. Moreover, administration of oral lycopene improved A β -induced learning and memory in an AD mouse model. Mitigation of NF- κ B activity and the downregulation of TNF- α and IL-1 β by lycopene might be the underlying mechanism (Table 4) [195]. In tau transgenic mice expressing P301L mutation, lycopene supplementation ameliorated the memory impairment by inhibiting oxidative stress as well as attenuating tau hyperphosphorylation [196]. Although several studies have assessed the antidiabetic and neuroprotective function of lycopene in cell and animal models, few clinical studies have been performed. To establish proper dietary recommendations, large-scale human studies are necessary.

4.3. Vitamins

4.3.1. Vitamin A. Vitamin A or retinol is an essential dietary nutrient that is necessary for vision, reproduction, and normal growth. Intracellularly, retinol can be converted to retinal all-trans-retinoic acid (RA) or 9-cis-retinoic acid [197]. The potential mechanisms through which vitamin A can impact T2DM include chelation of oxide radicals, increasing insulin sensitivity, regeneration of β cells, and regulation of obese and adipose biology [197]. For instance, it was suggested that all-trans-RA could improve insulin signaling by inhibiting protein kinase C (PKC) activity through binding to PKC isozymes. PKC was found to be elevated in diabetes and abrogated insulin signaling [197]. RA also increased insulin secretion and insulin mRNA levels in cultured islets, by increasing pancreatic glucokinase through activation of the glucokinase promoter (Table 2) [198]. Moreover, retinol and RA are positive regulators of uncoupling protein 1 (UCP-1), and the overexpression of UCP-1 could improve skeletal muscle glucose transport and insulin resistance [199]. Additionally, Berry and Noy [200] reported that all-trans-RA suppressed obesity and insulin resistance by inducing expression of PPAR β/δ and retinoid acid receptor (RAR) genes (Table 3). A recent study [201] suggested that vitamin A-deficient diet-fed rats displayed reduced stearoyl-CoA desaturase 1 (SCD1) and monounsaturated fatty acid levels, which in turn increase ER stress-mediated apoptosis and alter the structure and function of the pancreas. However, there is controversy about the effects of vitamin A on the treatment of T2DM. It was reported that the metabolic availability of retinoid could be reversed by insulin treatment [202]; therefore, vitamin A may not be an effective intervention for diabetic individuals with altered retinoid biology. Additionally, large-dose intakes of vitamin A interfere with bone metabolism and are associated with osteoporosis [197].

Vitamin A could also play an important role in nerve regeneration, neural development, neural plasticity, and neurodegenerative diseases, including AD [203]. Several studies have been shown the potential effects of vitamin A on amyloid pathology, neurotransmission, oxidative stress, and inflammation. *In vitro*, in a dose-dependent manner, vitamin

A inhibited oligomerization and fibrillation of A β 40 and A β 42 (Table 1) [204]. Vitamin A was also reported to regulate the expression of genes involved in the production of A β , including BACE1 and presenilin 1/2 [205, 206]. Treatment of APP/PS1 transgenic mice with all-trans-RA attenuated A β deposit accumulation and tau hyperphosphorylation and improved spatial learning and memory when compared with the control mice (Table 4) [207]. Deficiency in cholinergic transmission is the major underlying feature of AD, which may be attributed to the decreased expression of choline acetyltransferase (ChAT). It was reported that all-trans-RA administration upregulated the expression and activity of ChAT in a neuronal cell line [208]. Zeng et al. [209] established a marginal vitamin A deficiency (MVAD) rat model from maternal MVAD rats, then injected rats with A β 1-42; the results showed that MVAD feeding exacerbated A β 1-42-induced learning and memory deficits; therefore, long-term MVAD may result in an increased risk of AD. In contrast, a recent study [210] showed that increased availability of retinol at levels above the cellular physiological concentrations increased oxidative stress; the levels of α -synuclein, A β , and tau phosphorylation in human SH-SY5Y neuronal cell term MVAD may result in an increased risk of AD.

4.3.2. Vitamin D. Vitamin D exists in two forms, cholecalciferol (VD₃) and ergocalciferol (VD₂). VD₃ can be obtained from diet or synthesized in the skin from 7-dehydrocholesterol during exposure to solar UVB radiation. In the kidney, it is converted to 1,25-(OH)₂ VD₃, the active form of vitamin D [211]. Vitamin D is mediated by its nuclear receptor, vitamin D receptor (VDR). Vitamin D plays a crucial role in modulating the risk of T2DM by influencing insulin sensitivity, β -cell function, and inflammation [146, 149]. In peripheral insulin-target cells, vitamin D may affect insulin sensitivity by stimulating the expression of insulin receptor through interaction with VDR or by activating PPAR κ [212, 213]. Calcium is important for insulin-mediated intracellular processes [214], and vitamin D could regulate intracellular and extracellular calcium concentrations to affect insulin sensitivity. Moreover, vitamin D may promote β -cell survival by modulating the generation and activity of cytokines through the downregulation of NF- κ B (Table 2) [215] or the Fas-related pathway [216]. A recent study suggested that vitamin D increased glucose-stimulated insulin secretion by enhancing calcium influx through upregulation of expression of R-type voltage-gated calcium channel (VGCC) gene in mouse and human islets [217]. Treatment of STZ-induced diabetic mice with a vitamin D-supplemented diet decreased the fasting blood glucose levels, increased insulin levels, and restored pancreatic islets damaged by STZ [218]. Meerza et al. [219] (Table 3) also demonstrated that the treatment of 1,25-(OH)₂ VD₃ significantly changed blood calcium and glucose concentrations, as well as the activities of glucose metabolic enzymes, including G6Pase, hexokinase, and fructose 1,6-bisphosphatase (FBPase) in type 2 diabetic mice.

Recent studies showed that VDR is widely expressed in the brain [220]. Prospective studies have reported that vitamin D deficiency was associated with increased risk of AD

[221]. Therefore, vitamin D may exhibit neuroprotective functions such as regulation of neurotransmitters, NGF synthesis, calcium homeostasis, A β metabolism, oxidative stress, and inflammation [222, 223]. For instance, NGF signaling interruption has been shown to upregulate APP and β -secretase leading to an increased level of A β [224]. In mouse fibroblasts, 1,25-(OH)₂ VD₃ was reported to induce NGF expression by increasing AP-1 binding activity in the NGF promoter (Table 1) [222]. Furthermore, vitamin D could stimulate A β clearance by macrophages of AD patients [223]. In the TgCRND8 mouse model of AD, treatment of vitamin D resulted in reduced soluble and insoluble plaque-related A β , primarily in the hippocampus in which the VDR is abundant, and improved memory function [225]. In addition, a recent study reported that vitamin D supplementation was efficient in improving endogenous neurogenesis and working memory in transgenic AD-like male mice when administered before the onset of the symptoms, while in female mice, vitamin D was efficient when delivered during the symptomatic phase of the disease [226]. Overall, further studies are needed to test the safety and efficacy of long-term use of vitamin D and to identify what type of vitamin D supplement is more beneficial for T2DM and AD patients, according to their age, gender, and disease stage.

4.3.3. Vitamin E. Vitamin E is an important component of the antioxidant system in all body tissues, and α -tocopherol is the most active form. Due to its antioxidant activity, vitamin E has been considered to be a promising therapeutic option for AD and T2DM. *In vivo*, STZ-induced diabetic rats were reported to have significantly decreased glucose levels and improved activities of antioxidant enzymes such as catalase, glutathione peroxidase, and glutathione reductase after supplementation with vitamin E [227]. In addition, vitamin E supplementation ameliorated alloxan-induced mouse hyperglycemia by enhancing insulin secretion from the alloxan-treated islets (Table 3) [228]. However, the results from human studies are inconsistent, and a systematic review concluded that there were no beneficial effects of vitamin E supplementation in improving glycemic control in the full set of T2D patients. It was effective only in patients with low-serum vitamin E concentrations or inadequate glycemic control at baseline [229].

Previous studies have reported that the antioxidant and anti-inflammatory properties of vitamin E contribute to its neuroprotective effects. An animal study showed that depletion of α -tocopherol resulted in increased lipid peroxidation, which in turn impaired A β clearance from the brain and blood of AD transgenic model mice, eventually causing A β accumulation in the brain and plasma of mice [230]. Moreover, both *in vivo* and *in vitro* studies showed that vitamin E protects against the formation of A β -induced tau phosphorylation through the inhibition of the activation of p38-MAPK by reducing oxidative stress (Table 1) [231]. Beyond antioxidant activity, recent studies have identified the role of vitamin E in gene regulation, signaling, and membrane fluidity [232]. Rats fed a vitamin E-deficient diet showed changes in hippocampus gene expression. These genes were associated with apoptosis, NGF, A β clearance,

and the onset or progression of AD [233]. For example, the expression of APP binding protein 1, which binds and stabilizes APP, was decreased after treatment with a vitamin E-deficient diet [233]. In addition, α -tocopherol was shown to inhibit the activation of PKC and improve the activity of PP2A, an enzyme that is implicated in AD pathology [234, 235]. A recent study [236] investigated that vitamin E had positive characteristics with respect to AD in neuronal cell lines, including reduction of ROS, cholesterol, and cholesterol ester levels; however, it also had negative effects such as enhancement of A β production and inhibition of A β degradation. Overall, *in vivo* and *in vitro* studies have established plausible effects of vitamin E on AD pathology, but more clinical research are needed for conclusive results.

5. Conclusion

T2DM and AD are complex disorders with high prevalence and heavy social and economic burdens. The ineffectiveness of the current therapeutic agents in management of AD and long-term diabetes complications require the development of safe and effective complementary approaches. The therapeutic potential of various bioactive compounds such as resveratrol, curcumin, and lycopene has attracted the interest of researchers. It is important to identify the molecular mechanisms underlying the antidiabetic and neuroprotective effects of bioactive compounds in cell cultures and animal models of T2DM and AD. Published data indicate that there might be beneficial effects of bioactive compounds on decreasing hyperglycemia, enhancing insulin secretion, improving β -cell function, decreasing A β accumulation, and improving cognitive function in those afflicted. The mechanisms of action may involve their antioxidant, anti-inflammatory, and antiapoptotic properties. Moreover, some studies of these bioactive compounds have yielded controversial results, which may be attributed to different experimental designs, dosages, and types of bioactive compounds examined. Additional carefully designed clinical trials are needed to provide better evidence for the potential therapeutic application of bioactive compounds in the treatment of T2DM and AD.

Conflicts of Interest

The authors confirm that this article content has no conflict of interest.

Acknowledgments

This work was supported by the Alabama Agricultural Experiment Station (AAES) Hatch/Multistate Funding Program and AAES Award for Interdisciplinary Research (AAES-AIR) to JRB.

References

- [1] *Percentage of Diabetics in the Global Adult Population in 2017 and 2045*, Statista, 2018, <https://www.statista.com/statistics/271464/percentage-of-diabetics-worldwide/>.
- [2] J. M. Forbes and M. E. Cooper, "Mechanisms of diabetic complications," *Physiological Reviews*, vol. 93, no. 1, pp. 137–188, 2013.
- [3] *Peripheral Neuropathy and Diabetes*, WebMD, 2017, <https://www.webmd.com/diabetes/peripheral-neuropathy-risk-factors-symptoms#1>.
- [4] K. Akter, E. A. Lanza, S. A. Martin, N. Myronyuk, M. Rua, and R. B. Raffa, "Diabetes mellitus and Alzheimer's disease: shared pathology and treatment?," *British Journal of Clinical Pharmacology*, vol. 71, no. 3, pp. 365–376, 2011.
- [5] *Alzheimer's Disease Fact Sheet*, National Institute of Health, U.S. Department of Health & Human Services, 2016, <https://www.nia.nih.gov/health/alzheimers-disease-fact-sheet>.
- [6] *Alzheimer's Disease Facts and Figures*, Alzheimer's Association, 2018, <https://www.alz.org/alzheimers-dementia/facts-figures>.
- [7] S. A. Mohammed, A. G. Yaqub, K. A. Sanda et al., "Review on diabetes, synthetic drugs and glycemic effects of medicinal plants," *Journal of Medicinal Plants Research*, vol. 7, no. 36, pp. 2628–2637, 2013.
- [8] T. Ma, M.-S. Tan, J.-T. Yu, and L. Tan, "Resveratrol as a therapeutic agent for Alzheimer's disease," *BioMed Research International*, vol. 2014, Article ID 350516, 13 pages, 2014.
- [9] J. M. Walker and F. E. Harrison, "Shared neuropathological characteristics of obesity, type 2 diabetes and Alzheimer's disease: impacts on cognitive decline," *Nutrients*, vol. 7, no. 9, pp. 7332–7357, 2015.
- [10] S. M. De la Monte and J. R. Wands, "Alzheimer's disease is type 3 diabetes—evidence reviewed," *Journal of Diabetes Science and Technology*, vol. 2, no. 6, pp. 1101–1113, 2008.
- [11] S. Gothai, P. Ganesan, S. Y. Park, S. Fakurazi, D. K. Choi, and P. Arulselvan, "Natural phyto-bioactive compounds for the treatment of type 2 diabetes: inflammation as a target," *Nutrients*, vol. 8, no. 8, 2016.
- [12] B. McAnany and D. Martirosyan, "The effects of bioactive compounds on Alzheimer's disease and mild cognitive impairment," *Functional Foods in Health and Disease*, vol. 6, no. 6, pp. 329–343, 2016.
- [13] R. J. Mahler and M. L. Adler, "Type 2 diabetes mellitus: update on diagnosis, pathophysiology, and treatment," *The Journal of Clinical Endocrinology & Metabolism*, vol. 84, no. 4, pp. 1165–1171, 1999.
- [14] U. Masharani and M. S. German, "Pancreatic hormones & diabetes mellitus," *Greenspan's Basic & Clinical Endocrinology*, vol. 8, 2011.
- [15] S. V. Gelding, N. Coldham, R. Niththyananthan, V. Anyaoku, and D. G. Johnston, "Insulin resistance with respect to lipolysis in non-diabetic relatives of European patients with type 2 diabetes," *Diabetic Medicine*, vol. 12, no. 1, pp. 66–73, 1995.
- [16] M. A. Charles, E. Eschwege, N. Thibault et al., "The role of non-esterified fatty acids in the deterioration of glucose tolerance in Caucasian subjects: results of the Paris Prospective Study," *Diabetologia*, vol. 40, no. 9, pp. 1101–1106, 1997.
- [17] T. Kitamura, "The role of FOXO1 in β -cell failure and type 2 diabetes mellitus," *Nature Reviews Endocrinology*, vol. 9, no. 10, pp. 615–623, 2013.
- [18] S. Fischbach and G. K. Gittes, "The role of TGF- β signaling in β -cell dysfunction and type 2 diabetes: a review," *Journal of Cytology & Histology*, vol. 5, no. 6, 2014.

- [19] A. Granzotto and P. Zatta, "Resveratrol and Alzheimer's disease: message in a bottle on red wine and cognition," *Frontiers in Aging Neuroscience*, vol. 6, p. 95, 2014.
- [20] G. S. Desai, C. Zheng, T. Geetha et al., "The pancreas-brain axis: insight into disrupted mechanisms associating type 2 diabetes and Alzheimer's disease," *Journal of Alzheimer's disease*, vol. 42, no. 2, pp. 347–356, 2014.
- [21] H. W. Querfurth and F. M. LaFerla, "Alzheimer's disease," *The New England Journal of Medicine*, vol. 362, no. 4, pp. 329–344, 2010.
- [22] P. R. Bharadwaj, A. K. Dubey, C. L. Masters, R. N. Martins, and I. G. Macreadie, "A β aggregation and possible implications in Alzheimer's disease pathogenesis," *Journal of Cellular and Molecular Medicine*, vol. 13, no. 3, pp. 412–421, 2009.
- [23] V. H. Finder and R. Glockshuber, "Amyloid- β aggregation," *Neurodegenerative Diseases*, vol. 4, no. 1, pp. 13–27, 2007.
- [24] X. Li, D. Song, and S. X. Leng, "Link between type 2 diabetes and Alzheimer's disease: from epidemiology to mechanism and treatment," *Clinical Interventions in Aging*, vol. 10, pp. 549–560, 2015.
- [25] L. Li and C. Hölscher, "Common pathological processes in Alzheimer disease and type 2 diabetes: a review," *Brain Research Reviews*, vol. 56, no. 2, pp. 384–402, 2007.
- [26] H. Braak, E. Braak, and J. Bohl, "Staging of Alzheimer-related cortical destruction," *European Neurology*, vol. 33, no. 6, pp. 403–408, 1993.
- [27] C. J. Phiel, C. A. Wilson, V. M.-Y. Lee, and P. S. Klein, "GSK-3 α regulates production of Alzheimer's disease amyloid- β peptides," *Nature*, vol. 423, no. 6938, pp. 435–439, 2003.
- [28] T. R. Bomfim, L. Forný-Germano, L. B. Sathler et al., "An anti-diabetes agent protects the mouse brain from defective insulin signaling caused by Alzheimer's disease-associated A β oligomers," *The Journal of Clinical Investigation*, vol. 122, no. 4, pp. 1339–1353, 2012.
- [29] I. V. Kurochkin and S. Goto, "Alzheimer's β -amyloid peptide specifically interacts with and is degraded by insulin degrading enzyme," *FEBS Letters*, vol. 345, no. 1, pp. 33–37, 1994.
- [30] S. Mirza, M. Hossain, C. Mathews et al., "Type 2-diabetes is associated with elevated levels of TNF-alpha, IL-6 and adiponectin and low levels of leptin in a population of Mexican Americans: a cross-sectional study," *Cytokine*, vol. 57, no. 1, pp. 136–142, 2012.
- [31] J. Spranger, A. Kroke, M. Mohlig et al., "Inflammatory cytokines and the risk to develop type 2 diabetes: results of the prospective population-based European Prospective Investigation into Cancer and Nutrition (EPIC)-Potsdam study," *Diabetes*, vol. 52, no. 3, pp. 812–817, 2003.
- [32] J. P. Palmer, S. Helqvist, G. A. Spinass et al., "Interaction of β -cell activity and IL-1 concentration and exposure time in isolated rat islets of Langerhans," *Diabetes*, vol. 38, no. 10, pp. 1211–1216, 1989.
- [33] W. A. Banks, "Blood-brain barrier transport of cytokines: a mechanism for neuropathology," *Current Pharmaceutical Design*, vol. 11, no. 8, pp. 973–984, 2005.
- [34] P. Taepavaraprak and C. Song, "Reductions of acetylcholine release and nerve growth factor expression are correlated with memory impairment induced by interleukin-1 β administrations: effects of omega-3 fatty acid EPA treatment," *Journal of Neurochemistry*, vol. 112, no. 4, pp. 1054–1064, 2010.
- [35] S. Y. Goh and M. E. Cooper, "The role of advanced glycation end products in progression and complications of diabetes," *The Journal of Clinical Endocrinology & Metabolism*, vol. 93, no. 4, pp. 1143–1152, 2008.
- [36] G. Abate, M. Marziano, W. Rungratanawanich, M. Memo, and D. Uberti, "Nutrition and AGE-ing: focusing on Alzheimer's disease," *Oxidative Medicine and Cellular Longevity*, vol. 2017, Article ID 7039816, 10 pages, 2017.
- [37] M. O. Chaney, W. B. Stine, T. A. Kokjohn et al., "RAGE and amyloid beta interactions: atomic force microscopy and molecular modeling," *Biochimica et Biophysica Acta (BBA) - Molecular Basis of Disease*, vol. 1741, no. 1–2, pp. 199–205, 2005.
- [38] R. Deane and B. V. Zlokovic, "Role of the blood-brain barrier in the pathogenesis of Alzheimer's disease," *Current Alzheimer Research*, vol. 4, no. 2, pp. 191–197, 2007.
- [39] C. Matrone, M. Djelloul, G. Tagliatela, and L. Perrone, "Inflammatory risk factors and pathologies promoting Alzheimer's disease progression: is RAGE the key?," *Histology and Histopathology*, vol. 30, no. 2, pp. 125–139, 2015.
- [40] V. P. Reddy, X. Zhu, G. Perry, and M. A. Smith, "Oxidative stress in diabetes and Alzheimer's disease," *Journal of Alzheimer's Disease*, vol. 16, no. 4, pp. 763–774, 2009.
- [41] M. Nita and A. Grzybowski, "The role of the reactive oxygen species and oxidative stress in the pathomechanism of the age-related ocular diseases and other pathologies of the anterior and posterior eye segments in adults," *Oxidative Medicine and Cellular Longevity*, vol. 2016, Article ID 3164734, 23 pages, 2016.
- [42] W. Ahmad, B. Ijaz, K. Shabbiri, F. Ahmed, and S. Rehman, "Oxidative toxicity in diabetes and Alzheimer's disease: mechanisms behind ROS/ RNS generation," *Journal of Biomedical Science*, vol. 24, no. 1, p. 76, 2017.
- [43] J. L. Evans, I. D. Goldfine, B. A. Maddux, and G. M. Grodsky, "Are oxidative stress-activated signaling pathways mediators of insulin resistance and β -cell dysfunction?," *Diabetes*, vol. 52, no. 1, pp. 1–8, 2003.
- [44] X. Zhu, G. Perry, M. A. Smith, and X. Wang, "Abnormal mitochondrial dynamics in the pathogenesis of Alzheimer's disease," *Journal of Alzheimer's Disease*, vol. 33, no. s1, pp. S253–S262, 2013.
- [45] C. M. Galanakis, *Nutraceutical and Functional Food Components*, Academic Press, 2017.
- [46] T.-C. Huang, K.-T. Lu, Y.-Y. P. Wo, Y.-J. Wu, and Y.-L. Yang, "Resveratrol protects rats from A β -induced neurotoxicity by the reduction of iNOS expression and lipid peroxidation," *PLoS One*, vol. 6, no. 12, article e29102, 2011.
- [47] M. F. Mahmoud, N. A. Hassan, H. M. El Bassossy, and A. Fahmy, "Quercetin protects against diabetes-induced exaggerated vasoconstriction in rats: effect on low grade inflammation," *PLoS One*, vol. 8, no. 5, article e63784, 2013.
- [48] S. Gothai, P. Ganesan, S. Y. Park, S. Fakurazi, D. K. Choi, and P. Arulselvan, "Natural phyto-bioactive compounds for the treatment of type 2 diabetes: inflammation as a target," *Nutrients*, vol. 8, no. 8, p. 461, 2016.
- [49] T. Szkudelski and K. Szkudelska, "Resveratrol and diabetes: from animal to human studies," *Biochimica et Biophysica Acta (BBA) - Molecular Basis of Disease*, vol. 1852, no. 6, pp. 1145–1154, 2015.

- [50] M. Kitada and D. Koya, "SIRT1 in type 2 diabetes: mechanisms and therapeutic potential," *Diabetes & Metabolism Journal*, vol. 37, no. 5, pp. 315–325, 2013.
- [51] L. Vetterli, T. Brun, L. Giovannoni, D. Bosco, and P. Maechler, "Resveratrol potentiates glucose-stimulated insulin secretion in INS-1E β -cells and human islets through a SIRT1-dependent mechanism," *Journal of Biological Chemistry*, vol. 286, no. 8, pp. 6049–6060, 2011.
- [52] M.-M. Cao, X. Lu, G. D. Liu, Y. Su, Y. B. Li, and J. Zhou, "Resveratrol attenuates type 2 diabetes mellitus by mediating mitochondrial biogenesis and lipid metabolism via sirtuin type 1," *Experimental and Therapeutic Medicine*, vol. 15, no. 1, pp. 576–584, 2018.
- [53] M. Kitada, S. Kume, N. Imaizumi, and D. Koya, "Resveratrol improves oxidative stress and protects against diabetic nephropathy through normalization of Mn-SOD dysfunction in AMPK/SIRT1-independent pathway," *Diabetes*, vol. 60, no. 2, pp. 634–643, 2011.
- [54] Y.-E. Lee, J.-W. Kim, E.-M. Lee et al., "Chronic resveratrol treatment protects pancreatic islets against oxidative stress in db/db mice," *PLoS One*, vol. 7, no. 11, article e50412, 2012.
- [55] S. V. Penumathsa, M. Thirunavukkarasu, L. Zhan et al., "Resveratrol enhances GLUT-4 translocation to the caveolar lipid raft fractions through AMPK/Akt/eNOS signalling pathway in diabetic myocardium," *Journal of Cellular and Molecular Medicine*, vol. 12, no. 6a, pp. 2350–2361, 2008.
- [56] X. Feng, N. Liang, D. Zhu et al., "Resveratrol inhibits β -amyloid-induced neuronal apoptosis through regulation of SIRT1-ROCK1 signaling pathway," *PLoS One*, vol. 8, no. 3, article e59888, 2013.
- [57] V. Vingtdeux, U. Dreses-Werringloer, H. Zhao, P. Davies, and P. Marambaud, "Therapeutic potential of resveratrol in Alzheimer's disease," *BMC Neuroscience*, vol. 9, article s6, Supplement 2, 2008.
- [58] H. Capiralla, V. Vingtdeux, H. Zhao et al., "Resveratrol mitigates lipopolysaccharide- and $A\beta$ -mediated microglial inflammation by inhibiting the TLR4/NF- κ B/STAT signaling cascade," *Journal of Neurochemistry*, vol. 120, no. 3, pp. 461–472, 2012.
- [59] S. Schweiger, F. Matthes, K. Posey et al., "Resveratrol induces dephosphorylation of tau by interfering with the MID1-PP2A complex," *Scientific Reports*, vol. 7, no. 1, article 13753, 2017.
- [60] R. J. Nijveldt, E. van Nood, D. E. C. van Hoorn, P. G. Boelens, K. van Norren, and P. A. M. van Leeuwen, "Flavonoids: a review of probable mechanisms of action and potential applications," *The American Journal of Clinical Nutrition*, vol. 74, no. 4, pp. 418–425, 2001.
- [61] H. M. Eid, A. Nachar, F. Thong, G. Sweeney, and P. S. Haddad, "The molecular basis of the antidiabetic action of quercetin in cultured skeletal muscle cells and hepatocytes," *Pharmacognosy Magazine*, vol. 11, no. 41, pp. 74–81, 2015.
- [62] E. Youl, G. Bardy, R. Magous et al., "Quercetin potentiates insulin secretion and protects INS-1 pancreatic β -cells against oxidative damage via the ERK1/2 pathway," *British Journal of Pharmacology*, vol. 161, no. 4, pp. 799–814, 2010.
- [63] J. Peng, Q. Li, K. Li et al., "Quercetin improves glucose and lipid metabolism of diabetic rats: involvement of Akt signaling and SIRT1," *Journal of Diabetes Research*, vol. 2017, Article ID 3417306, 10 pages, 2017.
- [64] A. Ergul, "Endothelin-1 and diabetic complications: focus on the vasculature," *Pharmacological Research*, vol. 63, no. 6, pp. 477–482, 2011.
- [65] L. Qu, X. Liang, B. Gu, and W. Liu, "Quercetin alleviates high glucose-induced Schwann cell damage by autophagy," *Neural Regeneration Research*, vol. 9, no. 12, pp. 1195–1203, 2014.
- [66] S. F. Xia, Z. X. Xie, Y. Qiao et al., "Differential effects of quercetin on hippocampus-dependent learning and memory in mice fed with different diets related with oxidative stress," *Physiology & Behavior*, vol. 138, pp. 325–331, 2015.
- [67] X. Zhu, Y. Q. Cheng, Q. Lu, L. du, X. X. Yin, and Y. W. Liu, "Enhancement of glyoxalase 1, a polyfunctional defense enzyme, by quercetin in the brain in streptozotocin-induced diabetic rats," *Naunyn-Schmiedeberg's Archives of Pharmacology*, vol. 391, no. 11, pp. 1237–1245, 2018.
- [68] M. A. Ansari, H. M. Abdul, G. Joshi, W. O. Opii, and D. A. Butterfield, "Protective effect of quercetin in primary neurons against $A\beta$ (1–42): relevance to Alzheimer's disease," *The Journal of Nutritional Biochemistry*, vol. 20, no. 4, pp. 269–275, 2009.
- [69] Y. Kong, K. Li, T. Fu et al., "Quercetin ameliorates $A\beta$ toxicity in *Drosophila* AD model by modulating cell cycle-related protein expression," *Oncotarget*, vol. 7, no. 42, pp. 67716–67731, 2016.
- [70] A. M. Sabogal-Guáqueta, J. I. Muñoz-Manco, J. R. Ramírez-Pineda, M. Lamprea-Rodríguez, E. Osorio, and G. P. Cardona-Gómez, "The flavonoid quercetin ameliorates Alzheimer's disease pathology and protects cognitive and emotional function in aged triple transgenic Alzheimer's disease model mice," *Neuropharmacology*, vol. 93, pp. 134–145, 2015.
- [71] D. M. Wang, S. Q. Li, W. L. Wu, X. Y. Zhu, Y. Wang, and H. Y. Yuan, "Effects of long-term treatment with quercetin on cognition and mitochondrial function in a mouse model of Alzheimer's disease," *Neurochemical Research*, vol. 39, no. 8, pp. 1533–1543, 2014.
- [72] F. Vargas-Restrepo, A. M. Sabogal-Guáqueta, and G. P. Cardona-Gómez, "Quercetin ameliorates inflammation in CA1 hippocampal region in aged triple transgenic Alzheimer's disease mice model," *Biomédica*, vol. 38, pp. 69–76, 2018.
- [73] Y. S. Oh and H. S. Jun, "Role of bioactive food components in diabetes prevention: effects on beta-cell function and preservation," *Nutrition and Metabolic Insights*, vol. 7, pp. 51–59, 2014.
- [74] E. Tarabra, S. Pelengaris, and M. Khan, "A simple matter of life and death—the trials of postnatal beta-cell mass regulation," *International Journal of Endocrinology*, vol. 2012, Article ID 516718, 20 pages, 2012.
- [75] Z. Fu, W. Zhang, W. Zhen et al., "Genistein induces pancreatic β -cell proliferation through activation of multiple signaling pathways and prevents insulin-deficient diabetes in mice," *Endocrinology*, vol. 151, no. 7, pp. 3026–3037, 2010.
- [76] S. Ae Park, M. S. Choi, S. Y. Cho et al., "Genistein and daidzein modulate hepatic glucose and lipid regulating enzyme activities in C57BL/KsJ-db/db mice," *Life Sciences*, vol. 79, no. 12, pp. 1207–1213, 2006.
- [77] B. Dkhar, K. Khongsti, D. Thabab, D. Syiem, K. Satyamoorthy, and B. Das, "Genistein represses PEPCK-C expression in an insulin-independent manner in HepG2 cells and in alloxan-induced diabetic mice," *Journal of*

- Cellular Biochemistry*, vol. 119, no. 2, pp. 1953–1970, 2018.
- [78] M. S. Rajput and P. D. Sarkar, “Modulation of neuro-inflammatory condition, acetylcholinesterase and antioxidant levels by genistein attenuates diabetes associated cognitive decline in mice,” *Chemico-Biological Interactions*, vol. 268, pp. 93–102, 2017.
- [79] P. Phadnis, P. Dey Sarkar, and M. S. Rajput, “Improved serotonergic neurotransmission by genistein pretreatment regulates symptoms of obsessive-compulsive disorder in streptozotocin-induced diabetic mice,” *Journal of Basic and Clinical Physiology and Pharmacology*, vol. 29, no. 4, pp. 421–425, 2018.
- [80] X. Zhou, L. Yuan, X. Zhao et al., “Genistein antagonizes inflammatory damage induced by β -amyloid peptide in microglia through TLR4 and NF- κ B,” *Nutrition*, vol. 30, no. 1, pp. 90–95, 2014.
- [81] S. L. Valles, P. Dolz-Gaiton, J. Gambini et al., “Estradiol or genistein prevent Alzheimer’s disease-associated inflammation correlating with an increase PPAR γ expression in cultured astrocytes,” *Brain Research*, vol. 1312, pp. 138–144, 2010.
- [82] M. Heneka and G. Landreth, “PPARs in the brain,” *Biochimica et Biophysica Acta (BBA) - Molecular and Cell Biology of Lipids*, vol. 1771, no. 8, pp. 1031–1045, 2007.
- [83] Y. Morishima, Y. Gotoh, J. Zieg et al., “ β -Amyloid induces neuronal apoptosis via a mechanism that involves the c-Jun N-terminal kinase pathway and the induction of Fas ligand,” *The Journal of Neuroscience*, vol. 21, no. 19, pp. 7551–7560, 2001.
- [84] S. Ye, T. T. Wang, B. Cai et al., “Genistein protects hippocampal neurons against injury by regulating calcium/calmodulin dependent protein kinase IV protein levels in Alzheimer’s disease model rats,” *Neural Regeneration Research*, vol. 12, no. 9, pp. 1479–1484, 2017.
- [85] B. Cai, S. Ye, Y. Wang et al., “Protective effects of genistein on $A\beta_{25-35}$ -induced PC12 cell injury via regulating CaM-CaMKIV signaling pathway,” *Zhongguo Zhong Yao Za Zhi*, vol. 43, no. 3, pp. 571–576, 2018.
- [86] M. Bagheri, M. T. Joghataei, S. Mohseni, and M. Roghani, “Genistein ameliorates learning and memory deficits in amyloid $\beta_{(1-40)}$ rat model of Alzheimer’s disease,” *Neurobiology of Learning and Memory*, vol. 95, no. 3, pp. 270–276, 2011.
- [87] G. Chatterjee, D. Roy, V. Kumar Khemka, M. Chattopadhyay, and S. Chakrabarti, “Genistein, the isoflavone in soybean, causes amyloid beta peptide accumulation in human neuroblastoma cell line: implications in Alzheimer’s disease,” *Aging and Disease*, vol. 6, no. 6, pp. 456–465, 2015.
- [88] J. V. Higdon and B. Frei, “Tea catechins and polyphenols: health effects, metabolism, and antioxidant functions,” *Critical Reviews in Food Science and Nutrition*, vol. 43, no. 1, pp. 89–143, 2003.
- [89] M. Tannous, R. Amin, M. R. Popoff, C. Fiorentini, and A. Kowluru, “Positive modulation by Ras of interleukin-1 β -mediated nitric oxide generation in insulin-secreting clonal β (HIT-T15) cells,” *Biochemical Pharmacology*, vol. 62, no. 11, pp. 1459–1468, 2001.
- [90] M. K. Han, “Epigallocatechin gallate, a constituent of green tea, suppresses cytokine-induced pancreatic β -cell damage,” *Experimental & Molecular Medicine*, vol. 35, no. 2, pp. 136–139, 2003.
- [91] L. Elbling, R.-M. Weiss, O. Teufelhofer et al., “Green tea extract and (–)-epigallocatechin-3-gallate, the major tea catechin, exert oxidant but lack antioxidant activities,” *The FASEB Journal*, vol. 19, no. 7, pp. 807–809, 2005.
- [92] K. S. Suh, S. Chon, S. Oh et al., “Prooxidative effects of green tea polyphenol (–)-epigallocatechin-3-gallate on the HIT-T15 pancreatic beta cell line,” *Cell Biology and Toxicology*, vol. 26, no. 3, pp. 189–199, 2010.
- [93] S. Wolfram, D. Raederstorff, M. Preller et al., “Epigallocatechin gallate supplementation alleviates diabetes in rodents,” *The Journal of Nutrition*, vol. 136, no. 10, pp. 2512–2518, 2006.
- [94] N. Oršolić, D. Sirovina, G. Gajski, V. Garaj-Vrhovac, M. Jazvinšćak Jembrek, and I. Kosalec, “Assessment of DNA damage and lipid peroxidation in diabetic mice: effects of propolis and epigallocatechin gallate (EGCG),” *Mutation Research/Genetic Toxicology and Environmental Mutagenesis*, vol. 757, no. 1, pp. 36–44, 2013.
- [95] S. Y. Yun, S. P. Kim, and D. K. Song, “Effects of (–)-epigallocatechin-3-gallate on pancreatic beta-cell damage in streptozotocin-induced diabetic rats,” *European Journal of Pharmacology*, vol. 541, no. 1-2, pp. 115–121, 2006.
- [96] N. Salah, N. J. Miller, G. Paganga, L. Tijburg, G. P. Bolwell, and C. Riceevans, “Polyphenolic flavanols as scavengers of aqueous phase radicals and as chain-breaking antioxidants,” *Archives of Biochemistry and Biophysics*, vol. 322, no. 2, pp. 339–346, 1995.
- [97] S. Oikawa, A. Furukawa, H. Asada, K. Hirakawa, and S. Kawanishi, “Catechins induce oxidative damage to cellular and isolated DNA through the generation of reactive oxygen species,” *Free Radical Research*, vol. 37, no. 8, pp. 881–890, 2003.
- [98] Q. Zhang, H. Yuan, C. Zhang et al., “Epigallocatechin gallate improves insulin resistance in HepG2 cells through alleviating inflammation and lipotoxicity,” *Diabetes Research and Clinical Practice*, vol. 142, pp. 363–373, 2018.
- [99] X. Li, S. Li, M. Chen, J. Wang, B. Xie, and Z. Sun, “(–)-Epigallocatechin-3-gallate (EGCG) inhibits starch digestion and improves glucose homeostasis through direct or indirect activation of PXR/CAR-mediated phase II metabolism in diabetic mice,” *Food & Function*, vol. 9, no. 9, pp. 4651–4663, 2018.
- [100] Y. T. Choi, C. H. Jung, S. R. Lee et al., “The green tea polyphenol (–)-epigallocatechin gallate attenuates β -amyloid-induced neurotoxicity in cultured hippocampal neurons,” *Life Sciences*, vol. 70, no. 5, pp. 603–614, 2001.
- [101] D. E. Ehrnhoefer, J. Bieschke, A. Boeddrich et al., “EGCG redirects amyloidogenic polypeptides into unstructured, off-pathway oligomers,” *Nature Structural & Molecular Biology*, vol. 15, no. 6, pp. 558–566, 2008.
- [102] D.-S. Yang, C. M. Yip, T. H. J. Huang, A. Chakrabartty, and P. E. Fraser, “Manipulating the amyloid- β aggregation pathway with chemical chaperones,” *Journal of Biological Chemistry*, vol. 274, no. 46, pp. 32970–32974, 1999.
- [103] J. Bieschke, J. Russ, R. P. Friedrich et al., “EGCG remodels mature α -synuclein and amyloid- β fibrils and reduces cellular toxicity,” *Proceedings of the National Academy of Sciences of the United States of America*, vol. 107, no. 17, pp. 7710–7715, 2010.
- [104] K. Rezai-Zadeh, D. Shytle, N. Sun et al., “Green tea epigallocatechin-3-gallate (EGCG) modulates amyloid precursor protein cleavage and reduces cerebral amyloidosis in

- Alzheimer transgenic mice," *The Journal of Neuroscience*, vol. 25, no. 38, pp. 8807–8814, 2005.
- [105] K. Rezaei-Zadeh, G. W. Arendash, H. Hou et al., "Green tea epigallocatechin-3-gallate (EGCG) reduces β -amyloid mediated cognitive impairment and modulates tau pathology in Alzheimer transgenic mice," *Brain Research*, vol. 1214, no. 12, pp. 177–187, 2008.
- [106] N. Yamamoto, M. Shibata, R. Ishikuro et al., "Epigallocatechin gallate induces extracellular degradation of amyloid β -protein by increasing neprilysin secretion from astrocytes through activation of ERK and PI3K pathways," *Neuroscience*, vol. 362, pp. 70–78, 2017.
- [107] K. Du, M. Liu, X. Zhong et al., "Epigallocatechin gallate reduces amyloid β -induced neurotoxicity via inhibiting endoplasmic reticulum stress-mediated apoptosis," *Molecular Nutrition & Food Research*, vol. 62, no. 8, 2018.
- [108] A. M. Mahmoud, O. M. Ahmed, M. B. Ashour, and A. Abdel-Moneim, "In vivo and in vitro antidiabetic effects of citrus flavonoids; a study on the mechanism of action," *International Journal of Diabetes in Developing Countries*, vol. 35, no. 3, pp. 250–263, 2015.
- [109] A. M. Mahmoud, M. B. Ashour, A. Abdel-Moneim, and O. M. Ahmed, "Hesperidin and naringin attenuate hyperglycemia-mediated oxidative stress and proinflammatory cytokine production in high fat fed/streptozotocin-induced type 2 diabetic rats," *Journal of Diabetes and its Complications*, vol. 26, no. 6, pp. 483–490, 2012.
- [110] X. Shi, S. Liao, H. Mi et al., "Hesperidin prevents retinal and plasma abnormalities in streptozotocin-induced diabetic rats," *Molecules*, vol. 17, no. 11, pp. 12868–12881, 2012.
- [111] A. Visnagri, A. D. Kandhare, S. Chakravarty, P. Ghosh, and S. L. Bodhankar, "Hesperidin, a flavanoglycone attenuates experimental diabetic neuropathy via modulation of cellular and biochemical marker to improve nerve functions," *Pharmaceutical Biology*, vol. 52, no. 7, pp. 814–828, 2014.
- [112] S. A. El-Marasy, H. M. I. Abdallah, S. M. el-Shenawy, A. S. el-Khatib, O. A. el-Shabrawy, and S. A. Kenawy, "Anti-depressant effect of hesperidin in diabetic rats," *Canadian Journal of Physiology and Pharmacology*, vol. 92, no. 11, pp. 945–952, 2014.
- [113] Y. Zhang, B. Wang, F. Guo, Z. Li, and G. Qin, "Involvement of the TGF β 1- ILK-Akt signaling pathway in the effects of hesperidin in type 2 diabetic nephropathy," *Biomedicine & Pharmacotherapy*, vol. 105, pp. 766–772, 2018.
- [114] D. M. Wang, S. Q. Li, X. Y. Zhu, Y. Wang, W. L. Wu, and X. J. Zhang, "Protective effects of hesperidin against amyloid- β (A β) induced neurotoxicity through the voltage dependent anion channel 1 (VDAC1)-mediated mitochondrial apoptotic pathway in PC12 cells," *Neurochemical Research*, vol. 38, no. 5, pp. 1034–1044, 2013.
- [115] S. M. Huang, S. Y. Tsai, J. A. Lin, C. H. Wu, and G. C. Yen, "Cytoprotective effects of hesperetin and hesperidin against amyloid β -induced impairment of glucose transport through downregulation of neuronal autophagy," *Molecular Nutrition & Food Research*, vol. 56, no. 4, pp. 601–609, 2012.
- [116] Y. Hong and Z. An, "Hesperidin attenuates learning and memory deficits in APP/PS1 mice through activation of Akt/Nrf2 signaling and inhibition of RAGE/NF- κ B signaling," *Archives of Pharmacal Research*, vol. 41, no. 6, pp. 655–663, 2018.
- [117] C. Li, C. Zug, H. Qu, H. Schluesener, and Z. Zhang, "Hesperidin ameliorates behavioral impairments and neuropathology of transgenic APP/PS1 mice," *Behavioural Brain Research*, vol. 281, no. 15, pp. 32–42, 2015.
- [118] R. A. S. Sancho and G. M. Pastore, "Evaluation of the effects of anthocyanins in type 2 diabetes," *Food Research International*, vol. 46, no. 1, pp. 378–386, 2012.
- [119] B. Zhang, M. Kang, Q. Xie et al., "Anthocyanins from Chinese bayberry extract protect β cells from oxidative stress-mediated injury via HO-1 upregulation," *Journal of Agricultural and Food Chemistry*, vol. 59, no. 2, pp. 537–545, 2011.
- [120] B. Zhang, M. Buya, W. Qin et al., "Anthocyanins from Chinese bayberry extract activate transcription factor Nrf2 in β cells and negatively regulate oxidative stress-induced autophagy," *Journal of Agricultural and Food Chemistry*, vol. 61, no. 37, pp. 8765–8772, 2013.
- [121] F. Yan, G. Dai, and X. Zheng, "Mulberry anthocyanin extract ameliorates insulin resistance by regulating PI3K/AKT pathway in HepG2 cells and db/db mice," *The Journal of Nutritional Biochemistry*, vol. 36, pp. 68–80, 2016.
- [122] M. Roy, S. Sen, and A. S. Chakraborti, "Action of pelargonidin on hyperglycemia and oxidative damage in diabetic rats: implication for glycation-induced hemoglobin modification," *Life Sciences*, vol. 82, no. 21–22, pp. 1102–1110, 2008.
- [123] I. T. Nizamutdinova, Y. C. Jin, J. I. Chung et al., "The anti-diabetic effect of anthocyanins in streptozotocin-induced diabetic rats through glucose transporter 4 regulation and prevention of insulin resistance and pancreatic apoptosis," *Molecular Nutrition & Food Research*, vol. 53, no. 11, pp. 1419–1429, 2009.
- [124] D. A. Luna-Vital and E. Gonzalez de Mejia, "Anthocyanins from purple corn activate free fatty acid-receptor 1 and glucokinase enhancing in vitro insulin secretion and hepatic glucose uptake," *PLoS One*, vol. 13, no. 7, article e0200449, 2018.
- [125] P. H. Shih, C. H. Wu, C. T. Yeh, and G. C. Yen, "Protective effects of anthocyanins against amyloid β -peptide-induced damage in neuro-2A cells," *Journal of Agricultural and Food Chemistry*, vol. 59, no. 5, pp. 1683–1689, 2011.
- [126] M. Y. Yamakawa, K. Uchino, Y. Watanabe et al., "Anthocyanin suppresses the toxicity of A β deposits through diversion of molecular forms in in vitro and in vivo models of Alzheimer's disease," *Nutritional Neuroscience*, vol. 19, no. 1, pp. 32–42, 2016.
- [127] S. Vepsäläinen, H. Koivisto, E. Pekkarinen et al., "Anthocyanin-enriched bilberry and blackcurrant extracts modulate amyloid precursor protein processing and alleviate behavioral abnormalities in the APP/PS1 mouse model of Alzheimer's disease," *The Journal of Nutritional Biochemistry*, vol. 24, no. 1, pp. 360–370, 2013.
- [128] J. Thomas, "Extraction of curcumin," <https://www.livestrong.com/article/289939-extraction-of-curcumin/>.
- [129] J. Lin, Y. Tang, Q. Kang, and A. Chen, "Curcumin eliminates the inhibitory effect of advanced glycation end-products (AGEs) on gene expression of AGE receptor-1 in hepatic stellate cells in vitro," *Laboratory Investigation*, vol. 92, no. 6, pp. 827–841, 2012.
- [130] J. Lin, Y. Tang, Q. Kang, Y. Feng, and A. Chen, "Curcumin inhibits gene expression of receptor for advanced glycation end-products (RAGE) in hepatic stellate cells in vitro by elevating PPAR γ activity and attenuating oxidative stress," *British Journal of Pharmacology*, vol. 166, no. 8, pp. 2212–2227, 2012.

- [131] K. Meghana, G. Sanjeev, and B. Ramesh, "Curcumin prevents streptozotocin-induced islet damage by scavenging free radicals: a prophylactic and protective role," *European Journal of Pharmacology*, vol. 577, no. 1–3, pp. 183–191, 2007.
- [132] M. G. Soto-Urquieta, S. López-Briones, V. Pérez-Vázquez, A. Saavedra-Molina, G. A. González-Hernández, and J. Ramírez-Emiliano, "Curcumin restores mitochondrial functions and decreases lipid peroxidation in liver and kidneys of diabetic *db/db* mice," *Biological Research*, vol. 47, no. 1, p. 74, 2014.
- [133] K. Rashid and P. C. Sil, "Curcumin enhances recovery of pancreatic islets from cellular stress induced inflammation and apoptosis in diabetic rats," *Toxicology and Applied Pharmacology*, vol. 282, no. 3, pp. 297–310, 2015.
- [134] L. Pari and P. Murugan, "Antihyperlipidemic effect of curcumin and tetrahydrocurcumin in experimental type 2 diabetic rats," *Renal Failure*, vol. 29, no. 7, pp. 881–889, 2007.
- [135] H. Fujiwara, M. Hosokawa, X. Zhou et al., "Curcumin inhibits glucose production in isolated mice hepatocytes," *Diabetes Research and Clinical Practice*, vol. 80, no. 2, pp. 185–191, 2008.
- [136] L.-q. Su, Y.-d. Wang, and H.-y. Chi, "Effect of curcumin on glucose and lipid metabolism, FFAs and TNF- α in serum of type 2 diabetes mellitus rat models," *Saudi Journal of Biological Sciences*, vol. 24, no. 8, pp. 1776–1780, 2017.
- [137] H. C. Huang, D. Tang, K. Xu, and Z. F. Jiang, "Curcumin attenuates amyloid- β -induced tau hyperphosphorylation in human neuroblastoma SH-SY5Y cells involving PTEN/Akt/GSK-3 β signaling pathway," *Journal of Receptors and Signal Transduction*, vol. 34, no. 1, pp. 26–37, 2014.
- [138] W. Qian, H. Li, N. Pan, and C. Zhang, "Curcumin treatment is associated with increased expression of the N-methyl-D-aspartate receptor (NMDAR) subunit, NR2A, in a rat PC12 cell line model of Alzheimer's disease treated with the acetyl amyloid- β peptide, A β (25–35)," *Medical Science Monitor*, vol. 24, pp. 2693–2699, 2018.
- [139] G. P. Lim, T. Chu, F. Yang, W. Beech, S. A. Frautschy, and G. M. Cole, "The curry spice curcumin reduces oxidative damage and amyloid pathology in an Alzheimer transgenic mouse," *The Journal of Neuroscience*, vol. 21, no. 21, pp. 8370–8377, 2001.
- [140] P. P. N. Rao, T. Mohamed, K. Teckwani, and G. Tin, "Curcumin binding to beta amyloid: a computational study," *Chemical Biology & Drug Design*, vol. 86, no. 4, pp. 813–820, 2015.
- [141] M. Mutsuga, J. K. Chambers, K. Uchida et al., "Binding of curcumin to senile plaques and cerebral amyloid angiopathy in the aged brain of various animals and to neurofibrillary tangles in Alzheimer's brain," *Journal of Veterinary Medical Science*, vol. 74, no. 1, pp. 51–57, 2012.
- [142] P. Anand, A. B. Kunnumakkara, R. A. Newman, and B. B. Aggarwal, "Bioavailability of curcumin: problems and promises," *Molecular Pharmacology*, vol. 4, no. 6, pp. 807–818, 2007.
- [143] *The Potential Health Benefits of Rutin*, Health line, 2017, <https://www.healthline.com/health/potential-benefits-of-rutin#diet>.
- [144] J. Yang, J. Guo, and J. Yuan, "In vitro antioxidant properties of rutin," *LWT - Food Science and Technology*, vol. 41, no. 6, pp. 1060–1066, 2008.
- [145] A. Ghorbani, "Mechanisms of antidiabetic effects of flavonoid rutin," *Biomedicine & Pharmacotherapy*, vol. 96, pp. 305–312, 2017.
- [146] O. M. Ahmed, A. A. Moneim, I. A. Yazid, and A. M. Mahmoud, "Antihyperglycemic, antihyperlipidemic and antioxidant effects and the probable mechanisms of action of *Ruta graveolens* infusion and rutin in nicotinamide-streptozotocin-induced diabetic rats," *Diabetologia Croatica*, vol. 39, no. 1, pp. 15–35, 2010.
- [147] C. Y. Hsu, H. Y. Shih, Y. C. Chia et al., "Rutin potentiates insulin receptor kinase to enhance insulin-dependent glucose transporter 4 translocation," *Molecular Nutrition & Food Research*, vol. 58, no. 6, pp. 1168–1176, 2014.
- [148] A. L. Hevener, W. He, Y. Barak et al., "Muscle-specific Pparg deletion causes insulin resistance," *Nature Medicine*, vol. 9, no. 12, pp. 1491–1497, 2003.
- [149] E. P. Cai and J. K. Lin, "Epigallocatechin gallate (EGCG) and rutin suppress the glucotoxicity through activating IRS2 and AMPK signaling in rat pancreatic β cells," *Journal of Agricultural and Food Chemistry*, vol. 57, no. 20, pp. 9817–9827, 2009.
- [150] N. T. Niture, A. A. Ansari, and S. R. Naik, "Anti-hyperglycemic activity of rutin in streptozotocin-induced diabetic rats: an effect mediated through cytokines, antioxidants and lipid biomarkers," *Indian Journal of Experimental Biology*, vol. 52, no. 7, pp. 720–7, 2014.
- [151] W. Liang, D. Zhang, J. Kang et al., "Protective effects of rutin on liver injury in type 2 diabetic db/db mice," *Biomedicine & Pharmacotherapy*, vol. 107, pp. 721–728, 2018.
- [152] K. Jiménez-Aliaga, P. Bermejo-Bescós, J. Benedí, and S. Martín-Aragón, "Quercetin and rutin exhibit antiamyloidogenic and fibril-disaggregating effects in vitro and potent antioxidant activity in APP^{swe} cells," *Life Sciences*, vol. 89, no. 25–26, pp. 939–945, 2011.
- [153] S. W. Wang, Y. J. Wang, Y. J. Su et al., "Rutin inhibits β -amyloid aggregation and cytotoxicity, attenuates oxidative stress, and decreases the production of nitric oxide and pro-inflammatory cytokines," *NeuroToxicology*, vol. 33, no. 3, pp. 482–490, 2012.
- [154] S. Habtemariam, "Rutin as a natural therapy for Alzheimer's disease: insights into its mechanisms of action," *Current Medicinal Chemistry*, vol. 23, no. 9, pp. 860–873, 2016.
- [155] A. Kumaran, C. C. Ho, and L. S. Hwang, "Protective effect of *Nelumbo nucifera* extracts on beta amyloid protein induced apoptosis in PC12 cells, in vitro model of Alzheimer's disease," *Journal of Food and Drug Analysis*, vol. 26, no. 1, pp. 172–181, 2018.
- [156] S. Moghbelinejad, M. Nassiri-Asl, T. Naserpour Farivar et al., "Rutin activates the MAPK pathway and BDNF gene expression on beta-amyloid induced neurotoxicity in rats," *Toxicology Letters*, vol. 224, no. 1, pp. 108–113, 2014.
- [157] J. Y. Choi, J. M. Lee, D. G. Lee et al., "The *n*-butanol fraction and rutin from Tartary buckwheat improve cognition and memory in an in vivo model of amyloid- β -induced Alzheimer's disease," *Journal of Medicinal Food*, vol. 18, no. 6, pp. 631–641, 2015.
- [158] M. A. Mamdouh and A. A. E. K. Monira, "The influence of naringin on the oxidative state of rats with streptozotocin-induced acute hyperglycaemia," *Zeitschrift für Naturforschung C*, vol. 59, no. 9–10, pp. 726–733, 2004.
- [159] O. M. Ahmed, M. A. Hassan, S. M. Abdel-Twab, and M. N. Abdel Azeem, "Navel orange peel hydroethanolic extract, naringin and naringenin have anti-diabetic potentials in type 2 diabetic rats," *Biomedicine & Pharmacotherapy*, vol. 94, pp. 197–205, 2017.

- [160] F. Chen, G. Wei, J. Xu, X. Ma, and Q. Wang, "Naringin ameliorates the high glucose-induced rat mesangial cell inflammatory reaction by modulating the NLRP3 inflammasome," *BMC Complementary and Alternative Medicine*, vol. 18, no. 1, p. 192, 2018.
- [161] G. Li, Y. Xu, X. Sheng et al., "Naringin protects against high glucose-induced human endothelial cell injury via antioxidant and CX3CL1 downregulation," *Cellular Physiology and Biochemistry*, vol. 42, no. 6, pp. 2540–2551, 2017.
- [162] A. M. Mahmoud, "Hematological alterations in diabetic rats - role of adipocytokines and effect of citrus flavonoids," *EXCLI Journal*, vol. 12, p. 647, 2013.
- [163] A. K. Sharma, S. Bharti, S. Ojha et al., "Up-regulation of PPAR γ , heat shock protein-27 and -72 by naringin attenuates insulin resistance, β -cell dysfunction, hepatic steatosis and kidney damage in a rat model of type 2 diabetes," *The British Journal of Nutrition*, vol. 106, no. 11, pp. 1713–1723, 2011.
- [164] Z. Qi, Y. Xu, Z. Liang et al., "Naringin ameliorates cognitive deficits via oxidative stress, proinflammatory factors and the PPAR γ signaling pathway in a type 2 diabetic rat model," *Molecular Medicine Reports*, vol. 12, no. 5, pp. 7093–7101, 2015.
- [165] S. O. Rotimi, I. B. Adelani, G. E. Bankole, and O. A. Rotimi, "Naringin enhances reverse cholesterol transport in high fat/low streptozocin induced diabetic rats," *Biomedicine & Pharmacotherapy*, vol. 101, pp. 430–437, 2018.
- [166] D. Wang, K. Gao, X. Li et al., "Long-term naringin consumption reverses a glucose uptake defect and improves cognitive deficits in a mouse model of Alzheimer's disease," *Pharmacology Biochemistry and Behavior*, vol. 102, no. 1, pp. 13–20, 2012.
- [167] D.-M. Wang, Y.-J. Yang, L. Zhang, X. Zhang, F.-F. Guan, and L.-F. Zhang, "Naringin enhances CaMKII activity and Improves long-term memory in a mouse model of Alzheimer's disease," *International Journal of Molecular Sciences*, vol. 14, no. 3, pp. 5576–5586, 2013.
- [168] A. K. Sachdeva, A. Kuhad, and K. Chopra, "Naringin ameliorates memory deficits in experimental paradigm of Alzheimer's disease by attenuating mitochondrial dysfunction," *Pharmacology Biochemistry and Behavior*, vol. 127, pp. 101–110, 2014.
- [169] W. Yang, K. Zhou, Y. Zhou et al., "Naringin dihydrochalcone ameliorates cognitive deficits and neuropathology in APP/PS1 transgenic mice," *Frontiers in Aging Neuroscience*, vol. 10, p. 169, 2018.
- [170] Y. Nakamura, S. Watanabe, N. Miyake, H. Kohno, and T. Osawa, "Dihydrochalcones: evaluation as novel radical scavenging antioxidants," *Journal of Agricultural and Food Chemistry*, vol. 51, no. 11, pp. 3309–3312, 2003.
- [171] V. Rao, S. Venkateswara, and S. Vinu Kiran, "Flavonoid: a review on naringenin," *Journal of Pharmacognosy and Phytochemistry*, vol. 6, no. 5, pp. 2778–2783, 2017.
- [172] A. K. Singh, V. Raj, A. K. Keshari et al., "Isolated mangiferin and naringenin exert antidiabetic effect via PPAR γ /GLUT4 dual agonistic action with strong metabolic regulation," *Chemico-Biological Interactions*, vol. 280, pp. 33–44, 2018.
- [173] R. Kapoor and P. Kakkar, "Naringenin accords hepatoprotection from streptozotocin induced diabetes in vivo by modulating mitochondrial dysfunction and apoptotic signaling cascade," *Toxicology Reports*, vol. 1, pp. 569–581, 2014.
- [174] S. Roy, F. Ahmed, S. Banerjee, and U. Saha, "Naringenin ameliorates streptozotocin-induced diabetic rat renal impairment by downregulation of TGF- β 1 and IL-1 via modulation of oxidative stress correlates with decreased apoptotic events," *Pharmaceutical Biology*, vol. 54, no. 9, pp. 1616–1627, 2016.
- [175] W. Qin, B. Ren, S. Wang et al., "Apigenin and naringenin ameliorate PKC β II-associated endothelial dysfunction via regulating ROS/caspase-3 and NO pathway in endothelial cells exposed to high glucose," *Vascular Pharmacology*, vol. 85, pp. 39–49, 2016.
- [176] A. Rahigude, P. Bhutada, S. Kaulaskar, M. Aswar, and K. Otari, "Participation of antioxidant and cholinergic system in protective effect of naringenin against type-2 diabetes-induced memory dysfunction in rats," *Neuroscience*, vol. 226, pp. 62–72, 2012.
- [177] J. Zhang, H. Qiu, J. Huang et al., "Naringenin exhibits the protective effect on cardiac hypertrophy via EETs-PPARs activation in streptozocin-induced diabetic mice," *Biochemical and Biophysical Research Communications*, vol. 502, no. 1, pp. 55–61, 2018.
- [178] J. Ma, W. Q. Yang, H. Zha, and H. R. Yu, "Effect of naringenin on learning and memory ability on model rats with Alzheimer disease," *Zhong Yao Cai*, vol. 36, no. 2, pp. 271–276, 2013.
- [179] S. Ghofrani, M. T. Joghataei, S. Mohseni et al., "Naringenin improves learning and memory in an Alzheimer's disease rat model: insights into the underlying mechanisms," *European Journal of Pharmacology*, vol. 764, pp. 195–201, 2015.
- [180] N. Zhang, Z. Hu, Z. Zhang et al., "Protective role of naringenin against A β ₂₅₋₃₅-caused damage via ER and PI3K/Akt-mediated pathways," *Cellular and Molecular Neurobiology*, vol. 38, no. 2, pp. 549–557, 2018.
- [181] M. Lawal, F. A. Olotu, and M. E. S. Soliman, "Across the blood-brain barrier: neurotherapeutic screening and characterization of naringenin as a novel CRMP-2 inhibitor in the treatment of Alzheimer's disease using bioinformatics and computational tools," *Computers in Biology and Medicine*, vol. 98, pp. 168–177, 2018.
- [182] J.-N. Zhang and J. C. Koch, "Collapsin response mediator protein-2 plays a major protective role in acute axonal degeneration," *Neural Regeneration Research*, vol. 12, no. 5, pp. 692–695, 2017.
- [183] A. W. Khan, S. Kotta, S. H. Ansari, R. K. Sharma, and J. Ali, "Self-nanoemulsifying drug delivery system (SNEDDS) of the poorly water-soluble grapefruit flavonoid naringenin: design, characterization, in vitro and in vivo evaluation," *Drug Delivery*, vol. 22, no. 4, pp. 552–561, 2015.
- [184] T. Rissanen, S. Voutilainen, K. Nyssönen, and J. T. Salonen, "Lycopene, atherosclerosis, and coronary heart disease," *Experimental Biology and Medicine*, vol. 227, no. 10, pp. 900–907, 2002.
- [185] M. M. Ali and F. G. Agha, "Amelioration of streptozotocin-induced diabetes mellitus, oxidative stress and dyslipidemia in rats by tomato extract lycopene," *Scandinavian Journal of Clinical and Laboratory Investigation*, vol. 69, no. 3, pp. 371–379, 2009.
- [186] J. Zhu, C. G. Wang, and Y. G. Xu, "Lycopene attenuates endothelial dysfunction in streptozotocin-induced diabetic rats by reducing oxidative stress," *Pharmaceutical Biology*, vol. 49, no. 11, pp. 1144–1149, 2011.

- [187] W. Li, G. Wang, X. Lu, Y. Jiang, L. Xu, and X. Zhao, "Lycopene ameliorates renal function in rats with streptozotocin-induced diabetes," *International Journal of Clinical and Experimental Pathology*, vol. 7, no. 8, pp. 5008–5015, 2014.
- [188] S. Tabrez, K. Z. Al-Shali, and S. Ahmad, "Lycopene powers the inhibition of glycation-induced diabetic nephropathy: a novel approach to halt the AGE-RAGE axis menace," *BioFactors*, vol. 41, no. 5, pp. 372–381, 2015.
- [189] A. Kuhad, R. Sethi, and K. Chopra, "Lycopene attenuates diabetes-associated cognitive decline in rats," *Life Sciences*, vol. 83, no. 3-4, pp. 128–134, 2008.
- [190] M. F. Lombardo, P. Iacopino, M. Cuzzola et al., "Type 2 diabetes mellitus impairs the maturation of endothelial progenitor cells and increases the number of circulating endothelial cells in peripheral blood," *Cytometry Part A*, vol. 81A, no. 10, pp. 856–864, 2012.
- [191] Y.-C. Zeng, L.-S. Peng, L. Zou et al., "Protective effect and mechanism of lycopene on endothelial progenitor cells (EPCs) from type 2 diabetes mellitus rats," *Biomedicine & Pharmacotherapy*, vol. 92, pp. 86–94, 2017.
- [192] M. Qu, L. Li, C. Chen et al., "Protective effects of lycopene against amyloid β -induced neurotoxicity in cultured rat cortical neurons," *Neuroscience Letters*, vol. 505, no. 3, pp. 286–290, 2011.
- [193] M. Qu, Z. Jiang, Y. Liao, Z. Song, and X. Nan, "Lycopene prevents amyloid [beta]-induced mitochondrial oxidative stress and dysfunctions in cultured rat cortical neurons," *Neurochemical Research*, vol. 41, no. 6, pp. 1354–1364, 2016.
- [194] W. Chen, L. Mao, H. Xing et al., "Lycopene attenuates $A\beta_{1-42}$ secretion and its toxicity in human cell and *Caenorhabditis elegans* models of Alzheimer disease," *Neuroscience Letters*, vol. 608, pp. 28–33, 2015.
- [195] A. K. Sachdeva and K. Chopra, "Lycopene abrogates $A\beta(1-42)$ -mediated neuroinflammatory cascade in an experimental model of Alzheimer's disease," *The Journal of Nutritional Biochemistry*, vol. 26, no. 7, pp. 736–744, 2015.
- [196] L. Yu, W. Wang, W. Pang, Z. Xiao, Y. Jiang, and Y. Hong, "Dietary lycopene supplementation improves cognitive performances in tau transgenic mice expressing P301L mutation via inhibiting oxidative stress and tau hyperphosphorylation," *Journal of Alzheimer's Disease*, vol. 57, no. 2, pp. 475–482, 2017.
- [197] S. Iqbal and I. Naseem, "Role of vitamin A in type 2 diabetes mellitus biology: effects of intervention therapy in a deficient state," *Nutrition*, vol. 31, no. 7-8, pp. 901–907, 2015.
- [198] G. Cabrera-Valladares, M. S. German, F. M. Matschinsky, J. Wang, and C. Fernandez-Mejia, "Effect of retinoic acid on glucokinase activity and gene expression and on insulin secretion in primary cultures of pancreatic islets," *Endocrinology*, vol. 140, no. 7, pp. 3091–3096, 1999.
- [199] A.-L. Poher, C. Veyrat-Durebex, J. Altirriba et al., "Ectopic UCP1 overexpression in white adipose tissue improves insulin sensitivity in Lou/C rats, a model of obesity resistance," *Diabetes*, vol. 64, no. 11, pp. 3700–3712, 2015.
- [200] D. C. Berry and N. Noy, "All-trans-retinoic acid represses obesity and insulin resistance by activating both peroxisome proliferation-activated receptor β/δ and retinoic acid receptor," *Molecular and Cellular Biology*, vol. 29, no. 12, pp. 3286–3296, 2009.
- [201] M. Raja Gopal Reddy, S. Mullapudi Venkata, U. K. Putcha, and S. M. Jeyakumar, "Vitamin A deficiency induces endoplasmic reticulum stress and apoptosis in pancreatic islet cells: implications of stearoyl-CoA desaturase 1-mediated oleic acid synthesis," *Experimental Cell Research*, vol. 364, no. 1, pp. 104–112, 2018.
- [202] T. K. Basu and C. Basualdo, "Vitamin A homeostasis and diabetes mellitus," *Nutrition*, vol. 13, no. 9, pp. 804–806, 1997.
- [203] M. Chakrabarti, A. J. McDonald, J. Will Reed, M. A. Moss, B. C. Das, and S. K. Ray, "Molecular signaling mechanisms of natural and synthetic retinoids for inhibition of pathogenesis in Alzheimer's disease," *Journal of Alzheimer's Disease*, vol. 50, no. 2, pp. 335–352, 2015.
- [204] J. Takasaki, K. Ono, Y. Yoshiike et al., "Vitamin A has anti-oligomerization effects on amyloid- β in vitro," *Journal of Alzheimer's Disease*, vol. 27, no. 2, pp. 271–280, 2011.
- [205] H.-P. Lee, G. Casadesus, X. Zhu et al., "All-trans retinoic acid as a novel therapeutic strategy for Alzheimer's disease," *Expert Review of Neurotherapeutics*, vol. 9, no. 11, pp. 1615–1621, 2009.
- [206] M. Obulesu, M. R. Dowlathabad, and P. V. Bramhachari, "Carotenoids and Alzheimer's disease: an insight into therapeutic role of retinoids in animal models," *Neurochemistry International*, vol. 59, no. 5, pp. 535–541, 2011.
- [207] Y. Ding, A. Qiao, Z. Wang et al., "Retinoic acid attenuates β -amyloid deposition and rescues memory deficits in an Alzheimer's disease transgenic mouse model," *The Journal of Neuroscience*, vol. 28, no. 45, pp. 11622–11634, 2008.
- [208] J. P. T. Corcoran, P. L. So, and M. Maden, "Disruption of the retinoid signalling pathway causes a deposition of amyloid beta in the adult rat brain," *European Journal of Neuroscience*, vol. 20, no. 4, pp. 896–902, 2004.
- [209] J. Zeng, T. Li, M. Gong et al., "Marginal vitamin A deficiency exacerbates memory deficits following $A\beta_{1-42}$ injection in rats," *Current Alzheimer Research*, vol. 14, no. 5, pp. 562–570, 2017.
- [210] A. Kunzler, E. A. Kolling, J. D. da Silva-Jr et al., "Retinol (vitamin a) increases α -synuclein, β -amyloid peptide, tau phosphorylation and RAGE content in human SH-SY5Y neuronal cell line," *Neurochemical Research*, vol. 42, no. 10, pp. 2788–2797, 2017.
- [211] S. D. Rege, T. Geetha, T. L. Broderick, and J. R. Babu, "Can diet and physical activity limit Alzheimer's disease risk?," *Current Alzheimer Research*, vol. 14, no. 1, pp. 76–93, 2017.
- [212] J. Mitri and A. G. Pittas, "Vitamin D and diabetes," *Endocrinology and Metabolism Clinics of North America*, vol. 43, no. 1, pp. 205–232, 2014.
- [213] T. W. Dunlop, S. Väisänen, C. Frank, F. Molnár, L. Sinkkonen, and C. Carlberg, "The human peroxisome proliferator-activated receptor δ gene is a primary target of $1\alpha,25$ -dihydroxyvitamin D_3 and its nuclear receptor," *Journal of Molecular Biology*, vol. 349, no. 2, pp. 248–260, 2005.
- [214] E. O. Ojuka, "Role of calcium and AMP kinase in the regulation of mitochondrial biogenesis and GLUT4 levels in muscle," *Proceedings of the Nutrition Society*, vol. 63, no. 02, pp. 275–278, 2004.
- [215] R. Riachy, B. Vandewalle, J. Kerr Conte et al., "1,25-Dihydroxyvitamin D_3 protects RINm5F and human islet cells against cytokine-induced apoptosis: implication of the antiapoptotic protein A20," *Endocrinology*, vol. 143, no. 12, pp. 4809–4819, 2002.
- [216] R. Riachy, B. Vandewalle, E. Moerman et al., "1,25-Dihydroxyvitamin D_3 protects human pancreatic islets against

- cytokine-induced apoptosis via down-regulation of the Fas receptor," *Apoptosis*, vol. 11, no. 2, pp. 151–159, 2006.
- [217] L. Kjalarsdottir, S. A. Tersey, M. Vishwanath et al., "1,25-Dihydroxyvitamin D₃ enhances glucose-stimulated insulin secretion in mouse and human islets: a role for transcriptional regulation of voltage-gated calcium channels by the vitamin D receptor," *The Journal of Steroid Biochemistry and Molecular Biology*, 2018.
- [218] G. Wang, C. Hu, C. Hu, L. Ruan, Q. Bo, and L. Li, "Impact of oral vitamin D supplementation in early life on diabetic mice induced by streptozotocin," *Life, Earth & Health Science*, vol. 42, no. 3, pp. 455–459, 2014.
- [219] D. Meerza, I. Naseem, and J. Ahmed, "Effect of 1, 25(OH)₂ vitamin D₃ on glucose homeostasis and DNA damage in type 2 diabetic mice," *Journal of Diabetic Complications*, vol. 26, no. 5, pp. 363–368, 2012.
- [220] D. W. Eyles, S. Smith, R. Kinobe, M. Hewison, and J. J. McGrath, "Distribution of the vitamin D receptor and 1 α -hydroxylase in human brain," *Journal of Chemical Neuroanatomy*, vol. 29, no. 1, pp. 21–30, 2005.
- [221] C. Annweiler, Y. Rolland, A. M. Schott et al., "Higher vitamin D dietary intake is associated with lower risk of Alzheimer's disease: a 7-year follow-up," *The Journals of Gerontology Series A: Biological Sciences and Medical Sciences*, vol. 67, no. 11, pp. 1205–1211, 2012.
- [222] T. D. Veenstra, M. Fahnestock, and R. Kumar, "An AP-1 site in the nerve growth factor promoter is essential for 1,25-dihydroxyvitamin D₃-mediated nerve growth factor expression in osteoblasts," *Biochemistry*, vol. 37, no. 17, pp. 5988–5994, 1998.
- [223] A. Masoumi, B. Goldenson, S. Ghirmai et al., "1 α ,25-Dihydroxyvitamin D₃ interacts with curcuminoids to stimulate amyloid- β clearance by macrophages of Alzheimer's disease patients," *Journal of Alzheimer's Disease*, vol. 17, no. 3, pp. 703–717, 2009.
- [224] P. Calissano, C. Matrone, and G. Amadoro, "Nerve growth factor as a paradigm of neurotrophins related to Alzheimer's disease," *Developmental Neurobiology*, vol. 70, no. 5, pp. 372–383, 2010.
- [225] M. R. Durk, K. Han, E. C. Y. Chow et al., "1 α ,25-Dihydroxyvitamin D₃ reduces cerebral amyloid- β accumulation and improves cognition in mouse models of Alzheimer's disease," *The Journal of Neuroscience*, vol. 34, no. 21, pp. 7091–7101, 2014.
- [226] M. Morello, V. Landel, E. Lacassagne et al., "Vitamin D improves neurogenesis and cognition in a mouse model of Alzheimer's disease," *Molecular Neurobiology*, vol. 55, no. 8, pp. 6463–6479, 2018.
- [227] M. C. Garg, D. P. Chaudhary, and D. D. Bansal, "Effect of vitamin E supplementation on diabetes induced oxidative stress in experimental diabetes in rats," *Indian Journal of Experimental Biology*, vol. 43, no. 2, pp. 177–180, 2005.
- [228] K. Takemoto, W. Doi, and N. Masuoka, "Protective effect of vitamin E against alloxan-induced mouse hyperglycemia," *Biochimica et Biophysica Acta (BBA) - Molecular Basis of Disease*, vol. 1862, no. 4, pp. 647–650, 2016.
- [229] N. Suksomboon, N. Poolsup, and S. Sinprasert, "Effects of vitamin E supplementation on glycaemic control in type 2 diabetes: systematic review of randomized controlled trials," *Journal of Clinical Pharmacy and Therapeutics*, vol. 36, no. 1, pp. 53–63, 2011.
- [230] Y. Nishida, S. Ito, S. Ohtsuki et al., "Depletion of vitamin E increases amyloid β accumulation by decreasing its clearances from brain and blood in a mouse model of Alzheimer disease," *Journal of Biological Chemistry*, vol. 284, no. 48, pp. 33400–33408, 2009.
- [231] E. Giraldo, A. Lloret, T. Fuchsberger, and J. Viña, "A β and tau toxicities in Alzheimer's are linked via oxidative stress-induced p38 activation: protective role of vitamin E," *Redox Biology*, vol. 2, pp. 873–877, 2014.
- [232] G. Fata, P. Weber, and M. Mohajeri, "Effects of vitamin E on cognitive performance during ageing and in Alzheimer's disease," *Nutrients*, vol. 6, no. 12, pp. 5453–5472, 2014.
- [233] C. Rota, G. Rimbach, A. M. Miniñane, E. Stoecklin, and L. Barella, "Dietary vitamin E modulates differential gene expression in the rat hippocampus: potential implications for its neuroprotective properties," *Nutritional Neuroscience*, vol. 8, no. 1, pp. 21–29, 2005.
- [234] R. Ricciarelli, A. Tasinato, S. Clément, N. K. Ozer, D. Boscoboinik, and A. Azzi, " α -Tocopherol specifically inactivates cellular protein kinase C α by changing its phosphorylation state," *Biochemical Journal*, vol. 334, no. 1, pp. 243–249, 1998.
- [235] L. Martin, X. Latypova, C. M. Wilson, A. Magnaudeix, M. L. Perrin, and F. Terro, "Tau protein phosphatases in Alzheimer's disease: the leading role of PP2A," *Ageing Research Reviews*, vol. 12, no. 1, pp. 39–49, 2013.
- [236] M. O. W. Grimm, L. Regner, J. Mett et al., "Tocotrienol affects oxidative stress, cholesterol homeostasis and the amyloidogenic pathway in neuroblastoma cells: consequences for Alzheimer's disease," *International Journal of Molecular Sciences*, vol. 17, no. 11, p. 1809, 2016.
- [237] V. D. Kappel, L. H. Cazarolli, D. F. Pereira et al., "Involvement of GLUT-4 in the stimulatory effect of rutin on glucose uptake in rat soleus muscle," *Journal of Pharmacy and Pharmacology*, vol. 65, no. 8, pp. 1179–1186, 2013.
- [238] L. Zhang, M. Fiala, J. Cashman et al., "Curcuminoids enhance amyloid- β uptake by macrophages of Alzheimer's disease patients," *Journal of Alzheimer's Disease*, vol. 10, no. 1, pp. 1–7, 2006.
- [239] D. Porquet, G. Casadesús, S. Bayod et al., "Dietary resveratrol prevents Alzheimer's markers and increases life span in SAMP8," *Age*, vol. 35, no. 5, pp. 1851–1865, 2013.
- [240] J. Yu, M. Gattioni-Celli, H. Zhu et al., "Vitamin D₃-enriched diet correlates with a decrease of amyloid plaques in the brain of A β PP transgenic mice," *Journal of Alzheimer's Disease*, vol. 25, no. 2, pp. 295–307, 2011.
- [241] S. Sung, Y. Yao, K. Uryu et al., "Early vitamin E supplementation in young but not aged mice reduces A β levels and amyloid deposition in a transgenic model of Alzheimer's disease," *The FASEB Journal*, vol. 18, no. 2, pp. 323–325, 2004.

Research Article

Curcumin Suppresses Hepatic Stellate Cell-Induced Hepatocarcinoma Angiogenesis and Invasion through Downregulating CTGF

Shan Shao,¹ Wanxing Duan,² Qinhong Xu ,² Xuqi Li ,³ Liang Han,² Wei Li,² Dong Zhang,¹ Zheng Wang ,² and Jianjun Lei ²

¹From the Department of Oncology, First Affiliated Hospital of Xi'an Jiaotong University, 277 West Yanta Road, Xi'an, 710061 Shaanxi Province, China

²From the Department of Hepatobiliary Surgery, First Affiliated Hospital of Xi'an Jiaotong University, 277 West Yanta Road, Xi'an, 710061 Shaanxi Province, China

³From the Department of General Surgery, First Affiliated Hospital of Xi'an Jiaotong University, 277 West Yanta Road, Xi'an, 710061 Shaanxi Province, China

Correspondence should be addressed to Zheng Wang; zheng.wang11@mail.xjtu.edu.cn and Jianjun Lei; james.lee1987@stu.xjtu.edu.cn

Received 28 March 2018; Revised 16 September 2018; Accepted 8 October 2018; Published 16 January 2019

Guest Editor: Anderson J. Teodoro

Copyright © 2019 Shan Shao et al. This is an open access article distributed under the Creative Commons Attribution License, which permits unrestricted use, distribution, and reproduction in any medium, provided the original work is properly cited.

Microenvironment plays a vital role in tumor progression; we focused on elucidating the role of hepatic stellate cells (HSCs) in hepatocarcinoma (HCC) aggressiveness and investigated the potential protective effect of curcumin on HSC-driven hepatocarcinoma angiogenesis and invasion. Our data suggest that HSCs increase HCC reactive oxygen species (ROS) production to upregulate hypoxia-inducible factor-1 α (HIF-1 α) expression to promote angiogenesis, epithelial to mesenchymal transition (EMT) process and invasion. And HSCs could secrete soluble factors, such as interleukin-6 (IL-6), vascular endothelial cell growth factor (VEGF), and stromal-derived factor-1 (SDF-1) to facilitate HCC progression. Curcumin could significantly suppress the above HSC-induced effects in HCC and could abrogate ROS and HIF-1 α expression in HCC. HIF-1 α or connective tissue growth factor (CTGF) knockdown could abolish the aforementioned curcumin affection. Moreover, CTGF is a downstream gene of HIF-1 α . In addition, nuclear factor E2-related factor 2 (Nrf2) and glutathione (GSH) are involved in curcumin protection of HCC. These data indicate that curcumin may induce ROS scavenging by upregulating Nrf2 and GSH, thus inhibiting HIF-1 α stabilization to suppress CTGF expression to exhibit its protection on HCC. Curcumin has a promising therapeutic effect on HCC. CTGF is responsible for curcumin-induced protection in HCC.

1. Introduction

Hepatocellular carcinoma (HCC) represents the fifth most common cancer worldwide and is the third most common cause of cancer-related deaths [1]. Its high tendency to metastasize is considered to partially account for the extremely poor clinical prognosis of HCC. HCCs are typically highly vascularized [2, 3]. Transarterial chemoembolization (TACE) using the anthracycline antibiotic doxorubicin is the standard treatment for unresectable intermediate HCC and has survival benefit in asymptomatic patients with multifocal disease

without vascular invasion or extrahepatic spread. Sorafenib, lenvatinib, which is noninferior to sorafenib, and regorafenib increase survival and are the standard treatments in advanced hepatocellular carcinoma. However, several clinical trials have revealed that sorafenib has limited anticancer effects to improving patient survival [4, 5]. Thus, it is an urgent need for a greater understanding of the molecular mechanism of HCC progression and seeking for new therapeutic targets for the treatment.

The stroma is closely involved in both hepatic fibrosis and carcinogenesis and is a vital player in the cellular and

molecular mechanisms associated with these processes [6, 7]. Hepatic stellate cells (HSCs) are an important component in the liver, and its activation with subsequent phenotypic alterations is a critical event for fibrosis. Besides, HSCs can affect the initiation and progression of HCC. Previous studies have revealed that HSCs facilitate cancer cell invasion and proliferation through secreting growth factors and cytokines [8]. In addition, HSCs exhibit biological effect on regulating immune evasion and angiogenesis.

Curcumin, commonly known as turmeric, is a polyphenol derived from the *Curcuma longa* plant. It has been broadly used for centuries [9, 10], on account of its nontoxic and various therapeutic properties including antiseptic activity, antioxidant, and anti-inflammatory [9]. Recent studies have shown that curcumin exhibits anticancer activities through its effect on some biological pathways associated with cell cycle regulation, tumorigenesis, and metastasis [11, 12]. Curcumin has an inhibition effect on the transcription factor nuclear factor- κ B (NF- κ B) [13] and its downstream gene products (including cyclooxygenase-2, matrix metalloproteinase (MMP-9), interleukins, and Cyclin D1) [14, 15]. Moreover, curcumin regulates the expression of many growth cell adhesion molecules and factor receptors linking tumor angiogenesis and metastasis [9, 16].

Here, we investigated whether oxidative stress plays a vital role in HCC progression and evaluated the potential beneficial effects of curcumin on HSC-induced HCC invasiveness and angiogenesis. We revealed that curcumin has a promising therapeutic effect on HSC-induced HCC invasion and angiogenesis. CTGF is responsible for curcumin induce protection in HCC. Curcumin may induce ROS scavenging by upregulating Nrf2 and GSH, thus inhibiting HIF-1 α stabilization to suppress CTGF expression to exhibit its protection on HCC.

2. Materials and Methods

2.1. Cell Lines and Cell Culture. The HCC cell line (HepG2) and human umbilical vein endothelial cells (HUVECs) were obtained from the Shanghai Institution for Biological Science (Shanghai, China). Human hepatic stellate cell lines (HSCs) were purchased from ScienCell Research Laboratory (Carlsbad, CA, USA). All cell lines were cultured at 37°C, 5% CO₂, and 95% air in Dulbecco's modified Eagle's medium (DMEM) (high glucose) (HyClone, Logan, USA) containing 10% heat-inactivated fetal bovine serum (FBS) plus 100 μ g/ml ampicillin and 100 μ g/ml streptomycin.

2.2. Reagents. Anti-HIF-1 α was obtained from Bioworld (St. Louis, MO, USA). The other antibodies, namely, anti-E-cadherin, anti-MMP-9, anti-vimentin, anti-CTGF, anti-Nrf2, and anti- β -actin, were purchased from Cell Signaling Technology Biotechnology (Danvers, MA, USA). Curcumin was purchased from Sigma-Aldrich (St. Louis, MO, USA) and DCF-DA was purchased from Molecular Probes (Eugene, OR, USA).

2.3. Real-Time Quantitative PCR (RT-qPCR). TRIzol reagent was used to isolate total RNA, and the reverse transcription was developed using a PrimeScript RT reagent Kit

(TaKaRa, Dalian, China). The iQ5 Multicolor Real-Time PCR Detection System (Bio-Rad, Hercules, CA, USA) was carried out to perform real-time PCR. The $\Delta\Delta$ CT method was applied to determine fold changes in gene expression as normalized to those of GAPDH. The following PCR primers were as follows: MMP-9, forward: 5'-GAACCAATCTCACC GACAGG-3' and reverse: 5'-GCCACCCGAGTGTAACC ATA-3'; E-cadherin, forward: 5'-ATTCTGATTCTGCTGC TCTTG-3' and reverse: 5'-AGTCCTG GTCCTCTTCTCC-3'; vimentin, forward: 5'-AATGACCGCTTCGCCAAC-3' and reverse: 5'-CCGCATCTCCTCCTCGTAG-3'; VEGF, forward: 5'-TGCAGATTATGCGGATCAAACC-3' and reverse: 5'-TGCATTACATTT GTTGTGCTGTAG-3'; HIF-1 α , forward: 5'-AAGTCTAGGGATGCAGCA-3' and reverse: 5'-CAAGATCACC AGCATCATG-3'; IL-6, forward: 5'-A GTTCCTGCAGTCCAGCCTGAG-3' and reverse: 5'-TC AAAGTGCATAGCCACTTTC C-3'; CTGF, forward: 5'-A CCTGTGGGATGGGCATCT-3' and reverse 5'-CAGGCG GCTCTGCTTCTCTA-3'; and GAPDH, forward: 5'-ACCA CAGTCCATGCCATCAC-3' and reverse: 5'-TCCACCAC CCTGTTGCTGAT-3'.

2.4. Western Blot Analysis. Total cellular protein of indicated cells was extracted and heated for 15 min at 75°C. 100 μ g of cellular proteins was separated on a 10% SDS-PAGE gel and then transferred to the PVDF membranes. The membranes were incubated with the following primary antibodies: anti-HIF-1 α , anti-E-cadherin, anti-MMP-9, and anti-vimentin. The membrane was subsequently incubated with HRP-conjugated secondary antibodies, and an enhanced chemiluminescence detection system was used to perform the peroxidase reaction to visualize the immunoreactive bands.

2.5. HUVEC Tubule Formation Assay. 200 μ l of Matrigel was used to coat each well of a 24-well plate. HUVECs (2×10^4) from each group were resuspended into 200 μ l of conditioned media (CM) in each well and incubated at 37°C under 5% CO₂ for 24 h. A light microscope were used to capture the image under at 100x magnification, and the number of capillary tubes were measured by calculating the total tube length of each image. We randomly chose three different fields per well and photographed the image using a light microscope. The total length of all tubing with each field was measured after calibration with a stage micrometer, and Prism 5 software (GraphPad Software, San Diego, CA, USA) was used to analyze the data.

2.6. Cell Invasion Assay. A chamber-based invasion assay (Millipore Co., Billerica, MA, USA) was used to determine HCC cell invasion. The upper surface of the membrane was coated with 25 ml of Matrigel (BD Biosciences, Franklin Lakes, NJ, USA). HepG2 cells (1×10^5) from the indicated groups were resuspended in the upper chamber in serum-free media to allow migration towards a serum gradient (10%) in the lower chamber for 20 h. The noninvading cells were scraped from the top of the Matrigel, and the invading cells on the bottom surface were fixed with 4%

paraformaldehyde and stained with crystal violet. The numbers of migrated cells were calculated in ten randomly selected fields under a light microscope at $\times 100$ magnification.

2.7. Assay of Intracellular ROS. Intracellular H_2O_2 production assay is described in previous publications [17, 18]. Briefly, $5 \mu\text{g/ml}$ DCF-DA was used to incubate the cells from the indicated groups for 5 minutes and then 1 ml of RIPA buffer was used to lyse the cells after washing with PBS. Fluorimetric analysis at 510 nm was applied to detect H_2O_2 concentrations. The data were normalized to total protein content.

2.8. RNA Interference. A negative control shRNA (sc-108060) (Santa Cruz, Dallas, Texas, USA) and shRNA against HIF-1 α (sc-400036) (Santa Cruz) were obtained from Santa Cruz Biotechnology and were applied to transfect the HCC cells. RNA interference was performed using Lipofectamine (Invitrogen, Carlsbad, CA, USA), according to the manufacturer's instructions. After interference, puromycin was used to select the silenced cells. Then, the stably transfected cells were selected for further use.

2.9. Enzyme-Linked Immunosorbent Assay (ELISA). HCC cells from the indicated groups were incubated with serum-free medium for 72 h. The concentrations of IL-6, VEGF, and SDF-1 in the CM were detected using an enzyme-linked immunosorbent assay (ELISA) kit (R&D, Minneapolis, MN, USA), according to the manufacturer's instructions.

2.10. Measurement of Glutathione Content. GSH and GSSG levels were measured in CGN extracts using the GSH reductase enzyme method. This assay is based on the reaction of GSH and thiol-mediated which produces the 5,5'-dithio-bis (2 nitrobenzoic acid) (DTNB) to 5-thio-2-nitrobenzoic acid (TNB), detectable at $\lambda = 412 \text{ nm}$. The test is specific to GSH due to the specificity of the GSH reductase enzyme to GSH: the rate of accumulation of TNB is proportional to the concentration of GSH in the sample. Briefly, cell extract was diluted 1:2 with KPE buffer (0.1 M potassium phosphate, 5 mM disodium EDTA, pH 7.5) prior to the addition of freshly prepared DTNB (2.5 mM) and GSH reductase solutions (250 U/ml). Following the addition of β -NADPH, the absorbance ($\lambda = 412 \text{ nm}$) was measured immediately at 30 s intervals for 2 min. The rate of change in absorbance was compared to that for GSH standards. The measurement of GSSG in each sample was identical to that used for the measurement of GSH, but with a previous treatment of the sample with 2-VP, which reacts out with GSH.

2.11. Statistical Analysis. The data were presented as the mean \pm SD from at least three independent experiments. Statistical comparisons of more than 2 groups were performed using one-way analysis of variance with Bonferroni's post hoc test. Statistical comparisons between 2 samples were performed using the Student's *t*-test. Significance was defined as $p < 0.05$.

3. Results

3.1. Curcumin Suppresses HCC Angiogenesis Induced by HSCs through HIF-1 α . To investigate the effect of curcumin on HCC-induced angiogenesis, HUVECs were applied to conduct a tube formation assay. As shown in Figures 1(a) and 1(b), conditioned medium from HepG2 + HSCs (CM group) significantly increased tube formation, as compared with conditioned medium from HepG2 cells (St Med group). However, curcumin obviously abolished HSC-enhanced angiogenesis. Intriguingly, NAC, an oxidant scavenger, also abrogated HSC-mediated enhancements of angiogenesis, which indicate that oxidative stress is involved in HSC-enhanced HCC angiogenesis. Moreover, curcumin has a similar oxidant scavenger ability, as it could abrogate ROS production in HepG2 cells induced by HSCs (Figure 1(e)). These data indicate that HSC-induced oxidative stress plays a key role in HCC angiogenesis. And curcumin may inhibit HSC-induced HCC angiogenesis by eliminating ROS production.

Previous study shows that oxidative stress has been largely associated with molecular stabilization of HIF-1 α . Here, we want to examine whether HIF-1 α is involved in HCC angiogenesis; we knockdown HIF-1 α in HepG2 cells using sh-RNA (Figures 1(c) and 1(d)). We found that HSC conditioned medium (CM) could not increase HUVEC tube formation when HIF-1 α was knockdown in HepG2 cells (Figures 1(a) and 1(b)). Moreover, curcumin or NAC could not influence HUVEC tube formation after HIF-1 α knockdown in HepG2 cells. In addition, HIF-1 α knockdown significantly inhibited ROS production in HepG2 cells induced by HSCs. HSC conditioned medium (CM) could not increase ROS production in HepG2 cells when HIF-1 α was knockdown in HepG2 cells (Figures 1(a) and 1(b)). And curcumin or NAC could not influence ROS production after HIF-1 α knockdown in HepG2 cells. These data indicate that HSCs induce the proangiogenesis activity of HCC cells. Oxidative stress exhibits a pivotal role in this process. This HSC-induced proangiogenesis in HepG2 cells can be suppressed by curcumin and NAC, and the suppression appears to be dependent on the expression of HIF-1 α .

3.2. Curcumin Abrogates VEGF, IL-6, and SDF-1 Expression in HCC through HIF-1 α . Previous studies suggested that the activated stroma secretes large amounts of IL-6, VEGF, and SDF-1, resulting in a significant enhancement in invasion of the surrounding cancer cells [17–20]. Here, we showed that VEGF, IL-6, and SDF-1 expression levels in HSCs obviously increased after the cells had been cultured in HepG2-derived CM (CM group) (Figure 2). However, curcumin or NAC could abolish the upregulation in VEGF, IL-6, and SDF-1 expression induced by HepG2-derived CM (CM group) (Figure 2), suggesting that curcumin has a similar effect as NAC scavenging oxidative stress to suppress the inflammatory and angiogenic responses in HSCs exposed to HepG2-derived CM.

However, curcumin could not inhibit VEGF, IL-6, and SDF-1 production when HIF-1 α was knocked down by

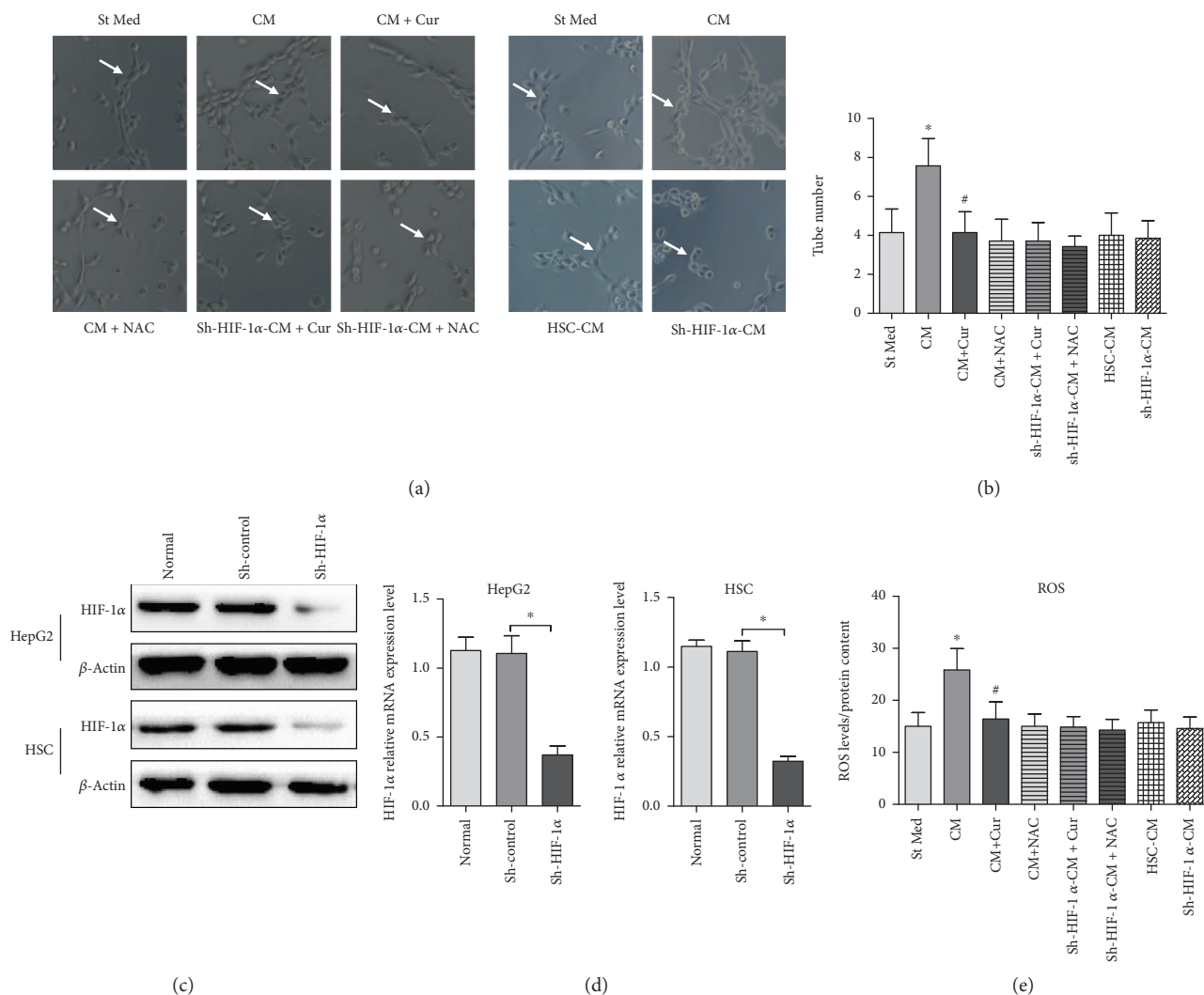


FIGURE 1: Curcumin inhibits HSC-induced HCC angiogenesis by suppressing HIF-1 α . HUVECs were incubated with conditioned medium from the HepG2 (St Med), HepG2 + HSC (CM), HepG2 + HSC + curcumin (CM + Cur), HepG2 + HSC + NAC (CM + NAC), sh-HIF-1 α -HepG2 + HSC + curcumin (sh-HIF-1 α -CM + Cur), sh-HIF-1 α -HepG2 + HSC + NAC (sh-HIF-1 α -CM + NAC) groups, HSC only (HSC-CM), and sh-HIF-1 α -HepG2 only (sh-HIF-1 α -CM). Cur stands for Curcumin. 50 μ M Curcumin was added into the medium for 24 h in CM + Cur group or sh-HIF-1 α -CM + Cur group. 20 mM NAC was added into the medium for 24 h in CM + NAC group or sh-HIF-1 α -CM + NAC group. (a) Angiogenesis was evaluated based on tube formation (indicated by arrows). (b) Tube numbers were counted. * $p < 0.05$ versus St Med group ($n = 6$), # $p < 0.05$ versus CM group ($n = 6$). (c) HIF-1 α in HepG2 cells or HSCs was silenced by sh-RNA. HIF-1 α and β -actin expression levels were determined by immunoblotting. * $p < 0.05$, sh-control versus sh-HIF-1 α , $n = 3$. (d) HepG2 or HSCs were treated as in (c), and HIF-1 α and β -actin expression levels were determined by qRT-PCR. * $p < 0.05$, sh-control versus sh-HIF-1 α , $n = 3$. All data are representative of at least three independent experiments. (e) Hydrogen peroxide production in HepG2 cells was determined using DCF-DA, and total protein content was used to normalize the data. * $p < 0.05$ versus St Med group ($n = 6$), # $p < 0.05$ versus CM ($n = 6$).

shRNA in HSCs (Figure 2), suggesting that the inhibition effects of curcumin on VEGF, IL-6, and SDF-1 expression are dependent on HIF-1 α downregulation (Figure 2).

3.3. Curcumin Abolishes HCC EMT and Invasion Induced by HSCs through HIF-1 α . Tumor microenvironment exhibits great promotion effects in liver carcinogenesis [11]. Here, we examined whether curcumin could inhibit HSC-induced HCC EMT process and invasion. HepG2 cells were treated with CM from HSCs with or without curcumin or NAC

and the expression of associated EMT proteins (e.g., E-cadherin and vimentin) in HepG2 cells were evaluated. Furthermore, a chamber invasion assay was applied to evaluate the invasive ability of the HCC cells. We showed that curcumin or NAC could abrogate the E-cadherin decrease and vimentin increase induced by HSC-derived CM in HepG2 cells (Figure 3). However, we noticed that curcumin or NAC could not influence E-cadherin and vimentin expression when HIF-1 α was knocked down by shRNA (Figure 3). Similar results were observed in the invasive

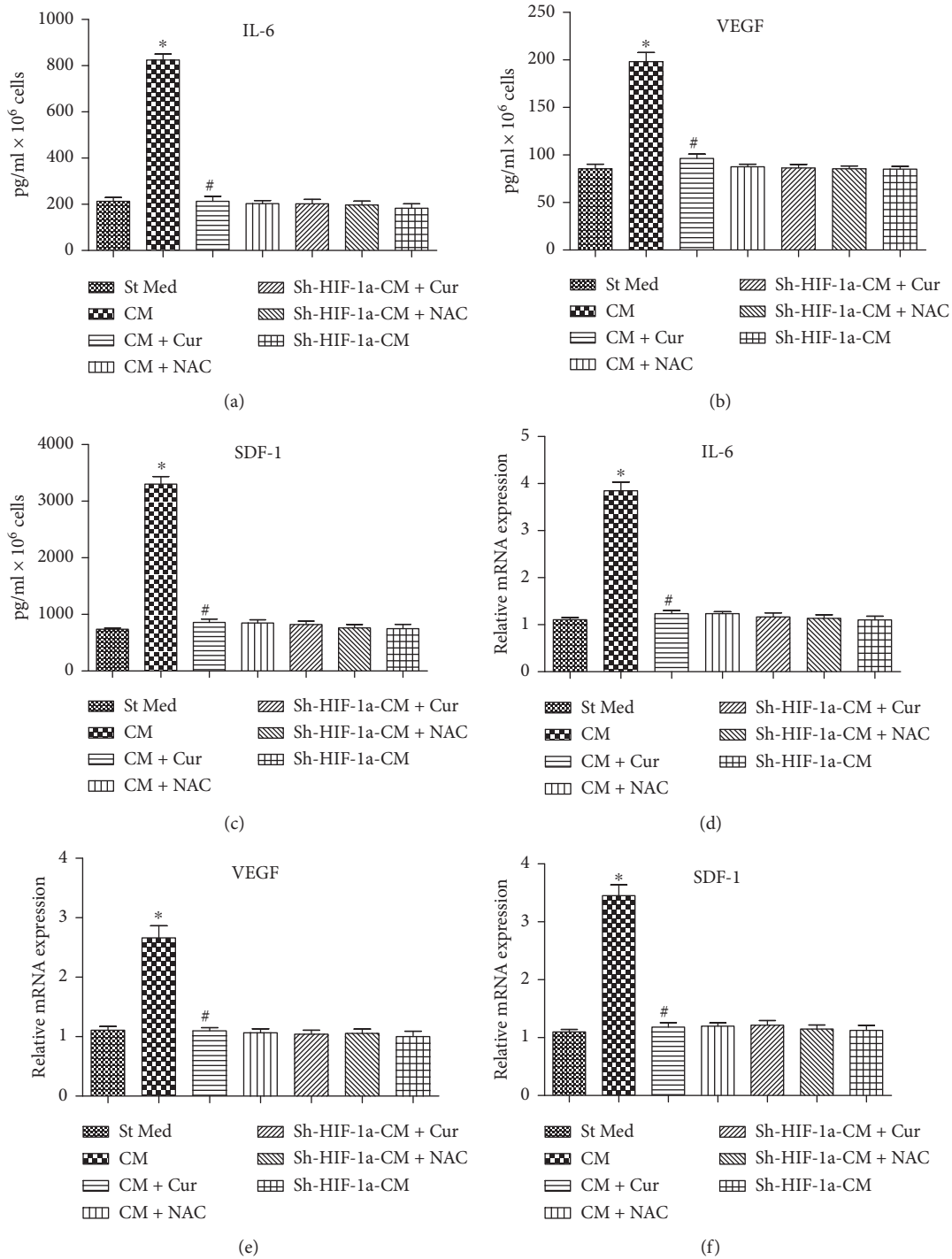


FIGURE 2: Curcumin decreased VEGF, IL-6, and SDF-1 expression in HCC via inhibiting HIF-1 α . St Med stands for standard media of PSC cells, CM stands for conditioned media from HepG2 cells, CM+Cur stands for conditioned media from HepG2 cells pretreated with curcumin, CM+NAC stands for conditioned media from HepG2 cells pretreated with NAC, sh-HIF-1 α -CM+Cur stands for HSC cell knockdown with sh-HIF-1 α and cultured with conditioned media from HepG2 cells pretreated with curcumin, sh-HIF-1 α -CM+NAC stands for HSC knockdown with sh-HIF-1 α and cultured with conditioned media from HepG2 cells pretreated with NAC, and sh-HIF-1 α -CM stands for HSC cell knockdown with sh-HIF-1 α and cultured with conditioned media from HepG2 cells. ELISA was assayed to assess IL-6 (a), VEGF (b), and SDF-1 (c) expression in the conditioned medium of the indicated groups. IL-6 (d), VEGF (e), and SDF-1 (f) mRNA expression in HSCs was detected by qRT-PCR, as described in the Materials and Methods. * $p < 0.05$ versus St Med group ($n = 6$), # $p < 0.05$ versus CM ($n = 6$). All data are representative of at least three independent experiments.

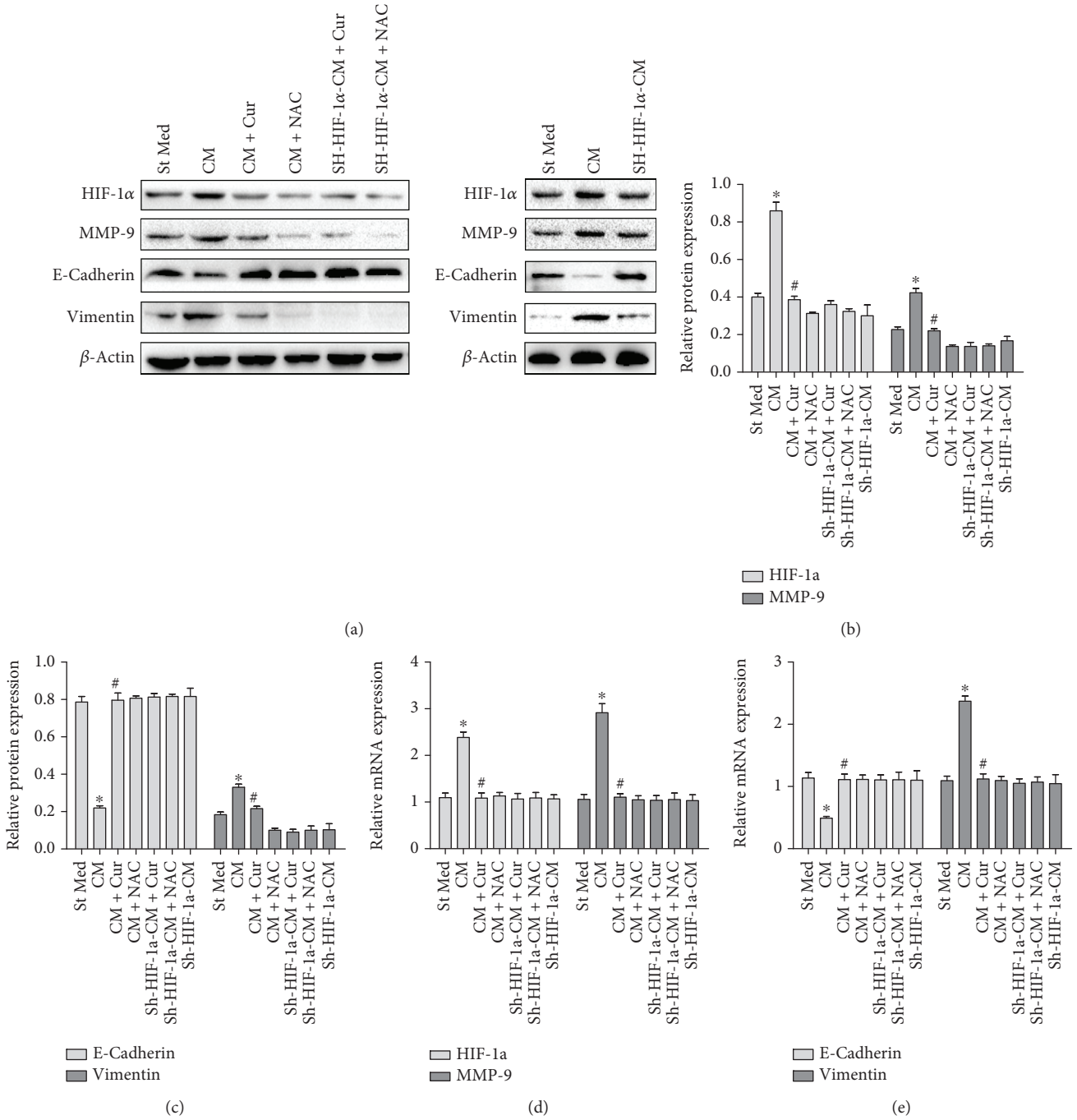


FIGURE 3: Curcumin abrogated HSC-induced increases in HIF-1α, MMP-9 expression and EMT process in HepG2 cells through down-regulating HIF-1α. St Med stands for standard media of HepG2 cells, CM stands for conditioned media from HSCs, CM + Cur stands for conditioned media from HSCs with curcumin exposure, CM + NAC stands for conditioned media from HSCs pretreated with NAC exposure, sh-HIF-1α-CM + Cur stands for sh-HIF-1α knockdown HepG2 cells treated with conditioned media from HSCs pretreated with curcumin, sh-HIF-1α-CM + NAC stands for sh-HIF-1α knockdown HepG2 cells treated with conditioned media from HSCs pretreated with NAC, and sh-HIF-1α-CM stands for sh-HIF-1α knockdown HepG2 cells treated with conditioned media from HSCs. (A&B&C) HIF-1α, MMP-9, E-cadherin, vimentin, and β-actin protein expression levels were evaluated by immunoblotting. **p* < 0.05 versus St Med group (*n* = 3), #*p* < 0.05 versus CM group (*n* = 3). (d, e) HIF-1α, MMP-9, E-cadherin, vimentin, and β-actin mRNA expression levels were determined by qRT-PCR. **p* < 0.05 versus St Med group (*n* = 3); #*p* < 0.05 versus CM (*n* = 3). All data are representative of at least three independent experiments.

capacity of HepG2 cells. Curcumin or NAC abolished HSC-derived CM enhanced invasion of HepG2 cell (Figure 4). However, when HIF-1α was knocked down in HepG2 cells,

curcumin or NAC could not affect HepG2 cell invasiveness (Figure 4). Similar results were found in the expression of MMP-9, an invasion-associated enzyme (Figure 3). These

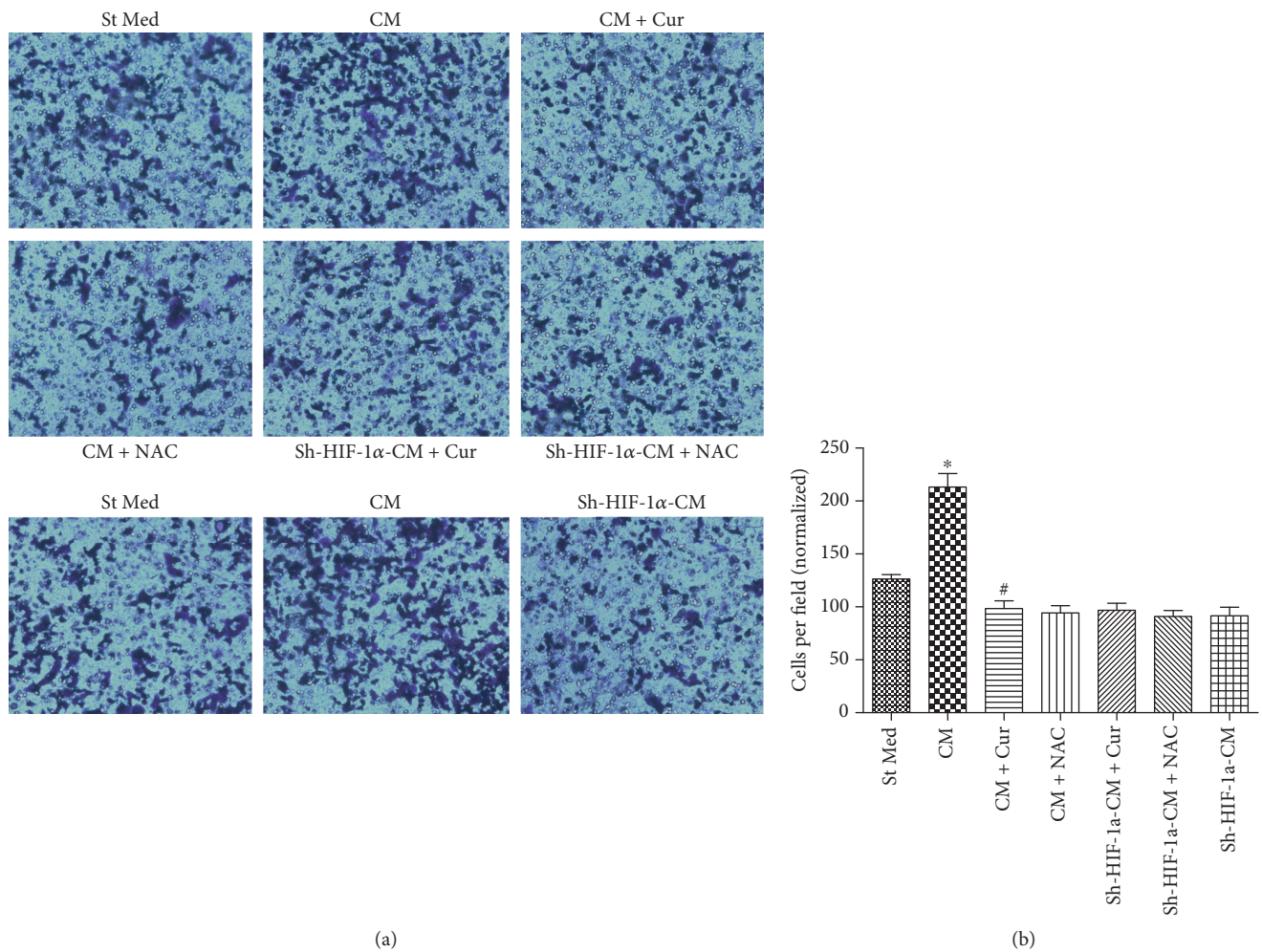


FIGURE 4: Curcumin suppressed HSC-induced invasion in HepG2 cells through decreasing HIF-1 α . St Med stands for standard media of HepG2 cells, CM stands for conditioned media from HSCs, CM + Cur stands for conditioned media from HSCs with curcumin exposure, CM + NAC stands for conditioned media from HSCs with NAC exposure, sh-HIF-1 α -CM + Cur stands for sh-HIF-1 α knockdown HepG2 cells treated with conditioned media from HSCs pretreated with curcumin, sh-HIF-1 α -CM + NAC stands for sh-HIF-1 α knockdown HepG2 cells treated with conditioned media from HSCs pretreated with NAC, and sh-HIF-1 α -CM stands for sh-HIF-1 α knockdown HepG2 cells treated with conditioned media from HSCs. The cells were placed in a Matrigel-coated invasion chamber for 20 h. (a, b) We evaluated invasion ability by counting the numbers of migrated cells in ten randomly selected fields under a light microscope at $\times 100$ magnification. * $p < 0.05$ versus St Med group ($n = 6$), # $p < 0.05$ versus CM ($n = 6$). All data are representative of at least three independent experiments.

findings indicate that curcumin inhibits HSC-induced HCC invasion, and this inhibition seems to be dependent on oxidative stress and HIF-1 α expression.

Intriguingly, CM from HSCs could induce HIF-1 α expression in HepG2 cells, and NAC, a ROS scavenger, significantly reduced HIF-1 α expression. As CM from HSCs could obviously upregulate ROS production in HepG2 cells, we speculate that ROS may stabilize HIF-1 α expression to promote HSC-induced HCC invasion.

3.4. CTGF Is Responsible for the Observed Effects of HIF-1 α on HSC Activation and HCC Invasion. As shown in Figure 5(a), CM derived from HSCs could increase CTGF expression in HepG2 cells, which could be inhibited by curcumin. When HIF-1 α was knocked down in HepG2 cells, CTGF expression decreased significantly. And CM derived from HSCs could not affect CTGF expression after HIF-1 α interference. In

tumor cells, CTGF has been reported to regulate growth, migration, invasion, and angiogenesis [21]. We investigated whether CTGF is responsible for the observed effects of curcumin and HIF-1 α on HSC activation and HCC invasion. CTGF shRNA was used to target CTGF expression in both HSCs and HepG2 cells (Figures 5(b) and 5(c)). And then the HIF-1 α and VEGF expression in HSCs and the E-cadherin and vimentin expression in HepG2 cells were tested. CTGF shRNA significantly suppressed VEGF expression in HSCs (Figure 5(d)). However, HIF-1 α expression was not affected by CTGF shRNA (Figures 5(d) and 5(e)). Moreover, CTGF knockdown in HepG2 cells increased E-cadherin expression and decreased vimentin expression in HepG2 cells cultured with CM from HSCs (Figures 5(f) and 5(g)). Furthermore, when CTGF was knocked down in HepG2 cells, curcumin could not affect HSC activation or HepG2 cell invasiveness (Figure 5). Since CTGF shRNA could not

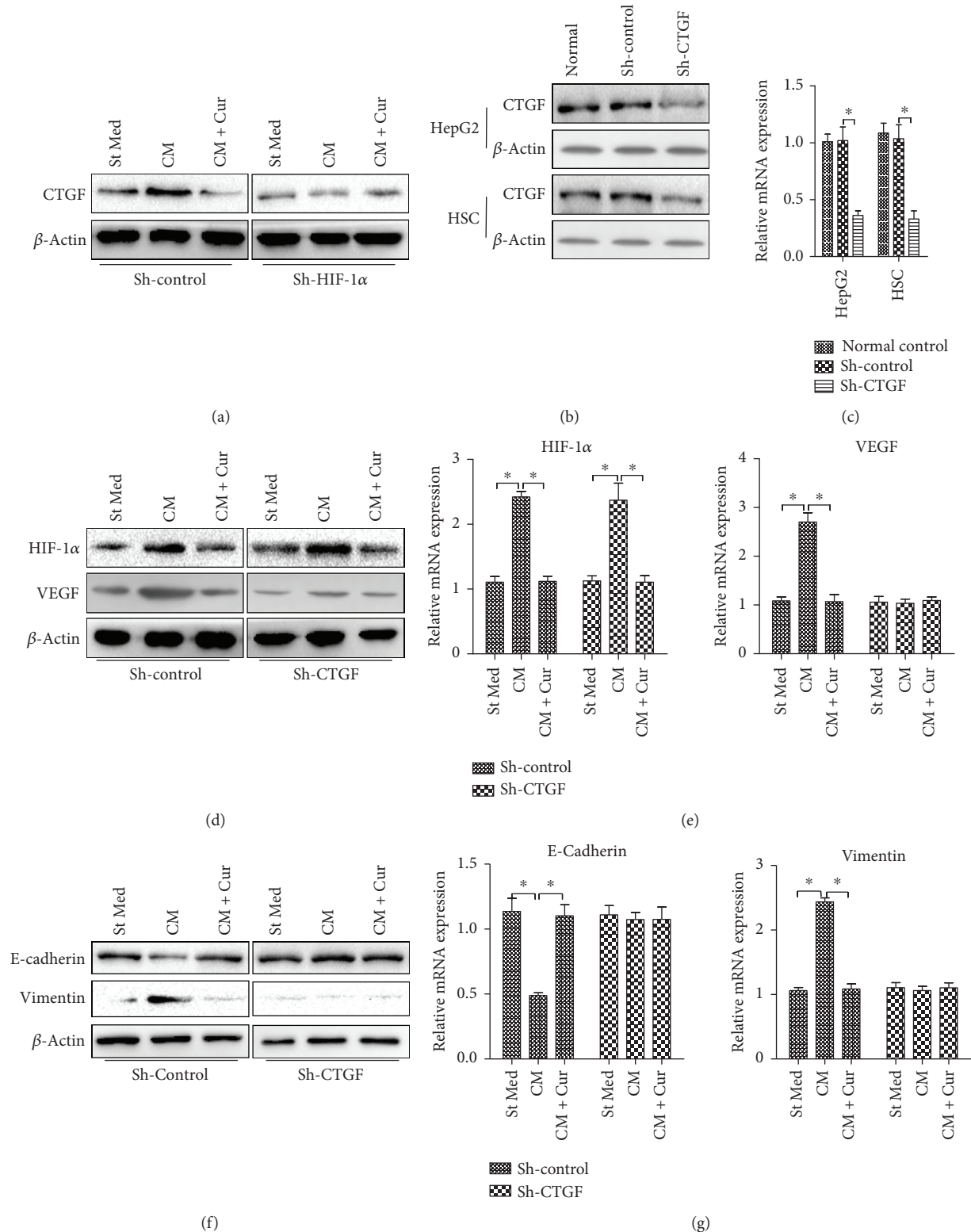


FIGURE 5: CTGF interference abrogates the observed effects of HIF-1 α silencing and curcumin on HSC activation and HCC invasion. (a) HepG2 cells were silenced by control shRNA (sh-control) or shRNA targeting HIF-1 α (sh-HIF-1 α); CTGF protein levels of HepG2 cells were analyzed by western blot. CTGF interference efficiency in HSCs and HepG2 cells were analyzed by western blot (b) and qRT-PCR (c). (d, e) HSCs transfected with shRNA were cultured with or without curcumin for 12 h and serum starved for an additional 24 h. (d) HIF-1 α and VEGF protein level of HSCs were analyzed by western blot. (e) HIF-1 α and VEGF mRNA level of HSCs were analyzed by qRT-PCR. HepG2 cells transfected with CTGF shRNA were incubated with the conditioned media (CM) from HSCs with or without curcumin for 24 h. The cells were lysed, and E-cadherin and vimentin expression levels were analyzed by western blot (f) and qRT-PCR (g). * $p < 0.05$. All data are representative of at least three independent experiments.

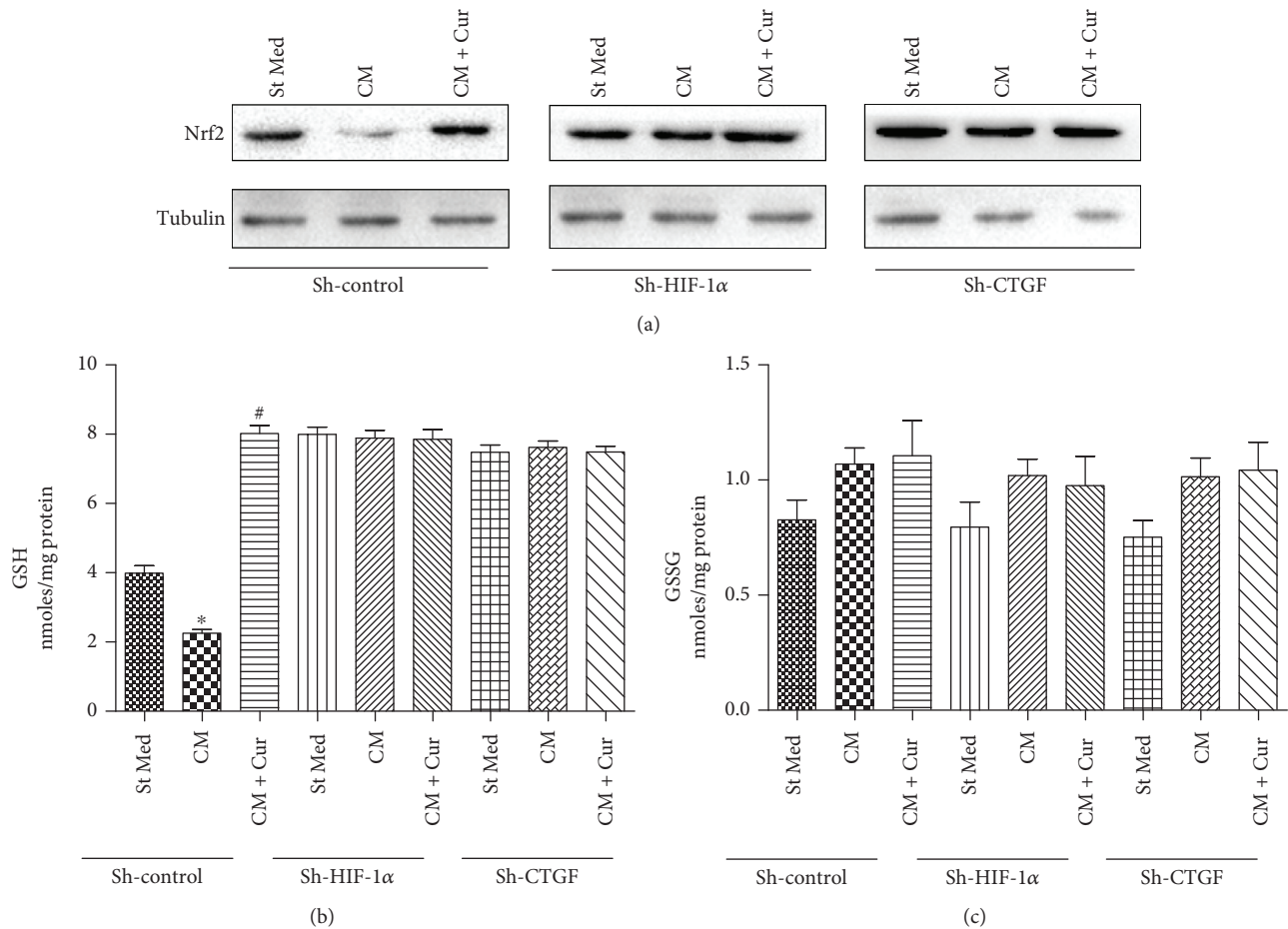


FIGURE 6: Nrf2 and GSH participate in curcumin-induced HCC protection. (a) HepG2 cells were silenced by control shRNA (sh-control), shRNA targeting HIF-1 α (sh-HIF-1 α), or shRNA targeting CTGF (sh-CTGF); nuclear Nrf2 protein levels of HepG2 cells were analyzed by western blot. (b) Glutathione (GSH) and glutathione disulfide (GSSG) levels were evaluated in HepG2 cells. * $p < 0.05$ versus St Med group ($n = 3$), # $p < 0.05$ versus CM ($n = 3$). All data are representative of at least three independent experiments.

influence HIF-1 α expression in HSCs and HIF-1 α knock-down could downregulate CTGF expression, these data indicate that CTGF is a downstream gene of HIF-1 α and is responsible for the observed effects of curcumin and HIF-1 α on HSC activation and HCC invasion.

3.5. Curcumin Induces Nrf2 and GSH Expression in HCC Protection. To elucidate possible mechanisms of HCC protection by curcumin, we tested nuclear Nrf2 and total GSH and GSSG expression in HepG2 cells. As shown in Figure 6, curcumin induced significant Nrf2 and GSH expression in HepG2 cells without affect GSSG expression. However, when HIF-1 α or CTGF was knocked down in HepG2 cells, curcumin could not influence Nrf2 or GSH expression. These data indicate that curcumin may induce ARE by upregulating Nrf2 and GSH expression in HCC protection. This effect is dependent on HIF-1 α and CTGF expression.

4. Discussion

As is well known, HCC stroma and peritumoural tissue were infiltrated with activated HSCs, and HSCs are located at tumor sinusoids, tumor capsule, and fibrous

septae [7, 22, 23]. Moreover, activated HSCs have also been found in the periphery of dysplastic nodules within the liver [24]. In response to liver injury, quiescent HSCs activated into matrix-secreting myofibroblasts and are the major producer of ECM proteins in the process of liver fibrogenesis [25–27]. As master regulators of fibrosis, HSC may hence directly affect HCC formation through effects on the tumor stroma. In addition, the interaction between tumors and cancer-associated fibroblasts is well established in other systems that complex intercellular signaling networks is involved in this process, contributing to cancer initiation, growth, and progression [26, 28–31]. In our study, we added evidence that HSCs promoted HCC oxidative stress, angiogenesis, invasion, and EMT process. ROS and HIF-1 α exhibit very important function in mediating the HSC and HCC cell interplay. CTGF is responsible for HIF-1 α effects on HSC activation and HCC invasion.

VEGF, SDF-1, and CTGF, which are associated with angiogenesis and chemoattraction of cancer and endothelial cells, and IL-6, which is associated with the proinflammatory response, have already been proven to be a downstream gene of HIF-1 [32, 33]. Our recent studies have shown that exogenous SDF-1 could increase CXCR4-positive pancreatic

cancer invasion and EMT [34], and activated pancreatic cancer stellate cells could secrete SDF-1 and IL-6 to induce EMT in pancreatic cancer [18]. This study revealed that coculture of HepG2 and HSCs elicited much more VEGF, SDF-1, and IL-6 secretion in HSCs, suggesting that HCC cells surrounded by HSCs may more likely metastasize to other sites than other cells. Therefore, activated HSCs are active players in attracting hepatocarcinoma cells to different locations. Active factors in this chemoattraction include CTGF, SDF-1, VEGF, and IL-6, confirming their pleiotropic role in hepatocarcinoma progression. Hence, the surrounding stroma might play a role in attracting metastatic hepatocarcinoma cells from the primary lesions, thereby facilitating satellite metastases.

Angiogenesis is closely related to HCC initiation, progression, and metastasis [35], as sorafenib could efficiently target these processes [36, 37]. Multiple proangiogenic factors stimulate new vessel formation to sustain the rapid growth pattern of malignant hepatocytes which in turn facilitates tumor progression and metastasis [38]. However, the molecular mechanisms underlying angiogenesis remain poorly understood [39]. In our study, we revealed that HSCs promoted tube formation and VEGF expression via upregulating HIF-1 α expression, suggesting that HIF-1 α is a potential target for HCC therapy. Furthermore, curcumin inhibited tube formation and VEGF expression, and knockdown of HIF-1 α abrogated these effects, suggesting that curcumin has prominent therapeutic effects on HCC through targeting HIF-1 α . In addition, CTGF is a downstream gene of HIF-1 α and is responsible for the observed effects of curcumin and HIF-1 α on HSC activation and HCC invasion.

Curcumin and NAC eliminated ROS production in HCC cocultured with HSCs, and also suppressed HCC progression, suggesting that ROS plays a key role in curcumin inhibitory effect on HCC. ROS is significantly associated with tumor aggression via several pathways. They can regulate the activity of transcription factors through inducing DNA damage and genome instability and can also affect gene expression. Also, ROS production is associated with EMT process in several tumors [18, 40, 41]. Here, we showed that curcumin induced Nrf2 and GSH expression without affecting GSSG expression. Nrf2 and GSH are well known to have ability to induce antioxidant response element (ARE). Thus, curcumin may induce ARE by upregulating Nrf2 and GSH expression. However, curcumin could not influence Nrf2 and GSH expression when HIF-1 α or CTGF was knocked down, as curcumin could inhibit HIF-1 α expression and CTGF is a downstream gene of HIF-1 α . These data indicate that curcumin may induce ROS scavenging by upregulating Nrf2 and GSH, thus inhibiting HIF-1 α stabilization to suppress CTGF expression to exhibit its protection on HCC.

It has been shown that curcumin has protective potential in multiple human carcinomas including prostate, head and neck, melanoma, breast, colon, and pancreatic cancers [6], such as inhibiting cancer growth, metastasis, and increasing chemopreventive effect of other anticancer medicines [16, 42, 43]. Epidemiological studies revealed that the low incidence of colon cancer in India is due to the chemopreventive

and antioxidant properties of curcumin [44]. The underlying mechanisms of its anticancer effects are comprehensive and diverse. Our data revealed that curcumin suppressed IL-6 and SDF-1 expression and ROS production and inhibited HCC invasion. Moreover, our results suggest that curcumin inhibits VEGF expression to reduce HCC angiogenesis. However, VEGF, IL-6 expression or ROS production could not be inhibited by curcumin when HIF-1 α was knocked down in HSCs, which suggest that HIF-1 α is a vital factor in curcumin-mediated inhibition of HCC progression. Furthermore, CTGF is a downstream gene of HIF-1 α and is responsible for the observed effects of curcumin and HIF-1 α on HSC activation and HCC invasion.

Data Availability

The data used to support the findings of this study are included within the article.

Conflicts of Interest

The authors declare that they have no competing interests.

Acknowledgments

This study was funded by the National Natural Science Foundation of China (No. 81502066, No. 81472248, and No. 81672434).

References

- [1] A. Forner, "Hepatocellular carcinoma surveillance with miRNAs," *The Lancet Oncology*, vol. 16, no. 7, pp. 743–745, 2015.
- [2] G. K. Abou-Alfa and A. P. Venook, "The antiangiogenic ceiling in hepatocellular carcinoma: does it exist and has it been reached?," *The Lancet Oncology*, vol. 14, no. 7, pp. e283–e288, 2013.
- [3] C. Bowyer, A. L. Lewis, A. W. Lloyd, G. J. Phillips, and W. M. Macfarlane, "Hypoxia as a target for drug combination therapy of liver cancer," *Anti-Cancer Drugs*, vol. 28, no. 7, pp. 771–780, 2017.
- [4] A. Forner, J. M. Llovet, and J. Bruix, "Hepatocellular carcinoma," *Lancet*, vol. 379, no. 9822, pp. 1245–1255, 2012.
- [5] A. Forner, M. Reig, and J. Bruix, "Hepatocellular carcinoma," *Lancet*, vol. 391, no. 10127, pp. 1301–1314, 2018.
- [6] K. Q. Han, X. Q. He, M. Y. Ma et al., "Inflammatory microenvironment and expression of chemokines in hepatocellular carcinoma," *World Journal of Gastroenterology*, vol. 21, no. 16, pp. 4864–4874, 2015.
- [7] A. I. Thompson, K. P. Conroy, and N. C. Henderson, "Hepatic stellate cells: central modulators of hepatic carcinogenesis," *BMC Gastroenterology*, vol. 15, no. 1, p. 63, 2015.
- [8] W. Li, S. Miao, M. Miao et al., "Hedgehog signaling activation in hepatic stellate cells promotes angiogenesis and vascular mimicry in hepatocellular carcinoma," *Cancer Investigation*, vol. 34, no. 9, pp. 424–430, 2016.
- [9] R. Wilken, M. S. Veena, M. B. Wang, and E. S. Srivatsan, "Curcumin: a review of anti-cancer properties and therapeutic activity in head and neck squamous cell carcinoma," *Molecular Cancer*, vol. 10, no. 1, p. 12, 2011.

- [10] B. B. Aggarwal, C. Sundaram, N. Malani, and H. Ichikawa, "Curcumin: the Indian solid gold," *Advances in Experimental Medicine and Biology*, vol. 595, pp. 1–75, 2007.
- [11] S. Chikara, L. D. Nagaprashantha, J. Singhal, D. Horne, S. Awasthi, and S. S. Singhal, "Oxidative stress and dietary phytochemicals: role in cancer chemoprevention and treatment," *Cancer Letters*, vol. 413, pp. 122–134, 2018.
- [12] W. Li, Y. Guo, C. Zhang et al., "Dietary phytochemicals and cancer chemoprevention: a perspective on oxidative stress, inflammation, and epigenetics," *Chemical Research in Toxicology*, vol. 29, no. 12, pp. 2071–2095, 2016.
- [13] D. Wang, M. S. Veena, K. Stevenson et al., "Liposome-encapsulated curcumin suppresses growth of head and neck squamous cell carcinoma *in vitro* and in xenografts through the inhibition of nuclear factor κ B by an AKT-independent pathway," *Clinical Cancer Research*, vol. 14, no. 19, pp. 6228–6236, 2008.
- [14] S. M. Plummer, K. A. Holloway, M. M. Manson et al., "Inhibition of cyclo-oxygenase 2 expression in colon cells by the chemopreventive agent curcumin involves inhibition of NF- κ B activation via the NIK/IKK signalling complex," *Oncogene*, vol. 18, no. 44, pp. 6013–6020, 1999.
- [15] C. Jobin, C. A. Bradham, M. P. Russo et al., "Curcumin blocks cytokine-mediated NF- κ B activation and proinflammatory gene expression by inhibiting inhibitory factor I- κ B kinase activity," *Journal of Immunology*, vol. 163, no. 6, pp. 3474–3483, 1999.
- [16] Y. U. E. F. E. N. G. du, Q. Long, L. Zhang et al., "Curcumin inhibits cancer-associated fibroblast-driven prostate cancer invasion through MAOA/mTOR/HIF-1 α signaling," *International Journal of Oncology*, vol. 47, no. 6, pp. 2064–2072, 2015.
- [17] G. Comito, E. Giannoni, P. D. Gennaro, C. P. Segura, G. Gerlini, and P. Chiarugi, "Stromal fibroblasts synergize with hypoxic oxidative stress to enhance melanoma aggressiveness," *Cancer Letters*, vol. 324, no. 1, pp. 31–41, 2012.
- [18] J. Lei, X. Huo, W. Duan et al., " α -Mangostin inhibits hypoxia-driven ROS-induced PSC activation and pancreatic cancer cell invasion," *Cancer Letters*, vol. 347, no. 1, pp. 129–138, 2014.
- [19] P. A. Cronin, J. H. Wang, and H. P. Redmond, "Hypoxia increases the metastatic ability of breast cancer cells via upregulation of CXCR4," *BMC Cancer*, vol. 10, no. 1, p. 225, 2010.
- [20] A. Toullec, D. Gerald, G. Despouy et al., "Oxidative stress promotes myofibroblast differentiation and tumour spreading," *EMBO Molecular Medicine*, vol. 2, no. 6, pp. 211–230, 2010.
- [21] F. Hall-Glenn, R. A. de Young, B. L. Huang et al., "CCN2/connective tissue growth factor is essential for pericyte adhesion and endothelial basement membrane formation during angiogenesis," *PLoS One*, vol. 7, no. 2, article e30562, 2012.
- [22] S. Faouzi, B. L. Bail, V. Neaud et al., "Myofibroblasts are responsible for collagen synthesis in the stroma of human hepatocellular carcinoma: an *in vivo* and *in vitro* study," *Journal of Hepatology*, vol. 30, no. 2, pp. 275–284, 1999.
- [23] L. Dubuisson, S. Lepreux, P. Bioulac-Sage et al., "Expression and cellular localization of fibrillin-1 in normal and pathological human liver," *Journal of Hepatology*, vol. 34, no. 4, pp. 514–522, 2001.
- [24] Y. N. Park, C. P. Yang, O. Cubukcu, S. N. Thung, and N. D. Theise, "Hepatic stellate cell activation in dysplastic nodules: evidence for an alternate hypothesis concerning human hepatocarcinogenesis," *Liver*, vol. 17, no. 6, pp. 271–274, 1997.
- [25] N. C. Henderson and J. P. Iredale, "Liver fibrosis: cellular mechanisms of progression and resolution," *Clinical Science*, vol. 112, no. 5, pp. 265–280, 2007.
- [26] S. L. Friedman, "Hepatic stellate cells: protean, multifunctional, and enigmatic cells of the liver," *Physiological Reviews*, vol. 88, no. 1, pp. 125–172, 2008.
- [27] C. J. Weston, E. L. Shepherd, L. C. Claridge et al., "Vascular adhesion protein-1 promotes liver inflammation and drives hepatic fibrosis," *The Journal of Clinical Investigation*, vol. 125, no. 2, pp. 501–520, 2015.
- [28] C. Eberlein, C. Rooney, S. J. Ross, M. Farren, H. M. Weir, and S. T. Barry, "E-cadherin and EpCAM expression by NSCLC tumour cells associate with normal fibroblast activation through a pathway initiated by integrin α v β 6 and maintained through TGF β signalling," *Oncogene*, vol. 34, no. 6, pp. 704–716, 2015.
- [29] N. A. Bhowmick, E. G. Neilson, and H. L. Moses, "Stromal fibroblasts in cancer initiation and progression," *Nature*, vol. 432, no. 7015, pp. 332–337, 2004.
- [30] S. Busch, A. Acar, Y. Magnusson, P. Gregersson, L. Rydén, and G. Landberg, "TGF-beta receptor type-2 expression in cancer-associated fibroblasts regulates breast cancer cell growth and survival and is a prognostic marker in pre-menopausal breast cancer," *Oncogene*, vol. 34, no. 1, pp. 27–38, 2015.
- [31] C. Jedszko, B. C. Victor, I. Podgorski, and B. F. Sloane, "Fibroblast hepatocyte growth factor promotes invasion of human mammary ductal carcinoma *in situ*," *Cancer Research*, vol. 69, no. 23, pp. 9148–9155, 2009.
- [32] G. L. Semenza, "Oxygen homeostasis," *Wiley Interdisciplinary Reviews. Systems Biology and Medicine*, vol. 2, no. 3, pp. 336–361, 2010.
- [33] S. W. Youn, S. W. Lee, J. Lee et al., "COMP-Ang1 stimulates HIF-1 α -mediated SDF-1 overexpression and recovers ischemic injury through BM-derived progenitor cell recruitment," *Blood*, vol. 117, no. 16, pp. 4376–4386, 2011.
- [34] X. Li, Q. Ma, Q. Xu et al., "SDF-1/CXCR4 signaling induces pancreatic cancer cell invasion and epithelial-mesenchymal transition *in vitro* through non-canonical activation of Hedgehog pathway," *Cancer Letters*, vol. 322, no. 2, pp. 169–176, 2012.
- [35] P. Magistri, S. Y. Leonard, C. M. Tang, J. C. Chan, T. E. Lee, and J. K. Sicklick, "The glypican 3 hepatocellular carcinoma marker regulates human hepatic stellate cells via Hedgehog signaling," *The Journal of Surgical Research*, vol. 187, no. 2, pp. 377–385, 2014.
- [36] J. M. Llovet, S. Ricci, V. Mazzaferro et al., "Sorafenib in advanced hepatocellular carcinoma," *The New England Journal of Medicine*, vol. 359, no. 4, pp. 378–390, 2008.
- [37] A. L. Cheng, Y. K. Kang, Z. Chen et al., "Efficacy and safety of sorafenib in patients in the Asia-Pacific region with advanced hepatocellular carcinoma: a phase III randomised, double-blind, placebo-controlled trial," *The Lancet Oncology*, vol. 10, no. 1, pp. 25–34, 2009.
- [38] A. X. Zhu, O. Rosmorduc, T. R. J. Evans et al., "SEARCH: a phase III, randomized, double-blind, placebo-controlled trial of sorafenib plus erlotinib in patients with advanced hepatocellular carcinoma," *Journal of Clinical Oncology*, vol. 33, no. 6, pp. 559–566, 2015.
- [39] D. Hanahan and J. Folkman, "Patterns and emerging mechanisms of the angiogenic switch during tumorigenesis," *Cell*, vol. 86, no. 3, pp. 353–364, 1996.

- [40] J. B. Wu, C. Shao, X. Li et al., "Monoamine oxidase A mediates prostate tumorigenesis and cancer metastasis," *The Journal of Clinical Investigation*, vol. 124, no. 7, pp. 2891–2908, 2014.
- [41] C. Jue, C. Lin, Z. Zhisheng et al., "Notch1 promotes vasculogenic mimicry in hepatocellular carcinoma by inducing EMT signaling," *Oncotarget*, vol. 8, no. 2, pp. 2501–2513, 2017.
- [42] P. Wang, B. Wang, S. Chung, Y. Wu, S. M. Henning, and J. V. Vadgama, "Increased chemopreventive effect by combining arctigenin, green tea polyphenol and curcumin in prostate and breast cancer cells," *RSC Advances*, vol. 4, no. 66, pp. 35242–35250, 2014.
- [43] L. Cao, J. Liu, L. Zhang, X. Xiao, and W. Li, "Curcumin inhibits H₂O₂-induced invasion and migration of human pancreatic cancer via suppression of the ERK/NF- κ B pathway," *Oncology Reports*, vol. 36, no. 4, pp. 2245–2251, 2016.
- [44] K. M. Mohandas and D. C. Desai, "Epidemiology of digestive tract cancers in India. V. Large and small bowel," *Indian Journal of Gastroenterology*, vol. 18, no. 3, pp. 118–121, 1999.

Research Article

Shepherd's Purse Polyphenols Exert Its Anti-Inflammatory and Antioxidative Effects Associated with Suppressing MAPK and NF- κ B Pathways and Heme Oxygenase-1 Activation

Jinming Peng,¹ Tianyong Hu ,² Jin Li,¹ Jing Du,¹ Kerui Zhu,¹ Baohui Cheng,² and Kaikai Li ^{1,3}

¹College of Food Science and Technology, Huazhong Agricultural University, Wuhan 430070, China

²Shenzhen Key Laboratory of ENT, Longgang ENT Hospital & Institute of ENT, Shenzhen 518172, China

³Key Laboratory of Environment Correlative Food Science (Huazhong Agricultural University), Ministry of Education, Wuhan 430070, China

Correspondence should be addressed to Kaikai Li; kaikailii@163.com

Received 29 June 2018; Revised 15 October 2018; Accepted 22 November 2018; Published 13 January 2019

Guest Editor: Germán Gil

Copyright © 2019 Jinming Peng et al. This is an open access article distributed under the Creative Commons Attribution License, which permits unrestricted use, distribution, and reproduction in any medium, provided the original work is properly cited.

Shepherd's purse (*Capsella bursa-pastoris* (L.) Medik.), a wild herb as a traditional herbal medicine, has been proved with multiple healthy benefits. In this study, the chemical constituents of shepherd's purse were identified by UPLC-QTOF-MS/MS. The antioxidative and anti-inflammatory potential of shepherd's purse extract (SPE) were also investigated applying lipopolysaccharide- (LPS-) induced inflammation in RAW 264.7 macrophages and a carrageenan-induced mice paw edema model. Twenty-four chemical compounds were identified mainly including phenolic acids and flavonoids. The data also indicated SPE inhibited the productions of NO, PGE₂, TNF- α , and IL-6 stimulated with LPS. In addition, SPE inhibited the increase of reactive oxygen species (ROS) and upregulated the expression of heme oxygenase-1 (HO-1). We further found that SPE inhibited the phosphorylation of P38 MAPK and activation of NF- κ B. *In vivo* mice model also indicated that SPE showed strong antioxidative and anti-inflammatory activity.

1. Introduction

Inflammation which existed in obesity, elder bodies, is accompany with many diverse chronic diseases, such as insulin resistance, type 2 diabetes, vascular disease, chronic renal failure, several cancers, endocrine [1–3]. To counteract this chronic inflammatory status, nonsteroidal anti-inflammatory drugs (NSAIDs) were usually proposed as a treatment strategy [4]. However, the side effects associated with long-term use of NSAIDs and steroids stimulate the development of novel anti-inflammatory therapies [5, 6]. Thus, the functional foods, for instance, some edible wild herbs, which with special health benefits, unique flavor, and also with high nutritional values, may be a good choice for improvement of the chronic low-grade inflammation and its related diseases. More importantly, these functional

foods also showed higher biosafety and also can be easily and well accepted.

Shepherd's purse (*Capsella bursa-pastoris* (L.) Medik.), a wild herb (Figure 1) with high nutritional value and has been eaten raw or cooked as a vegetable for thousands of years in many countries, is getting more and more attention. Shepherd's purse has been used as traditional herbal medicine for a long history which has been recorded in TCM ancient books "Ben Cao Gang Mu," "Ming Yi Bie Lu," and so on. Previous studies found that shepherd's purse contained a wide range of chemicals including flavonoids, alkaloids, polypeptides, choline, acetylcholine, histamine, tyramine, fatty acids, sterols, organic acids, amino acids, sulforaphane, many trace elements, vitamins, and many other compounds [7–11]. Furthermore, pharmacological studies also proved that shepherd's purse with various bioactivities, including

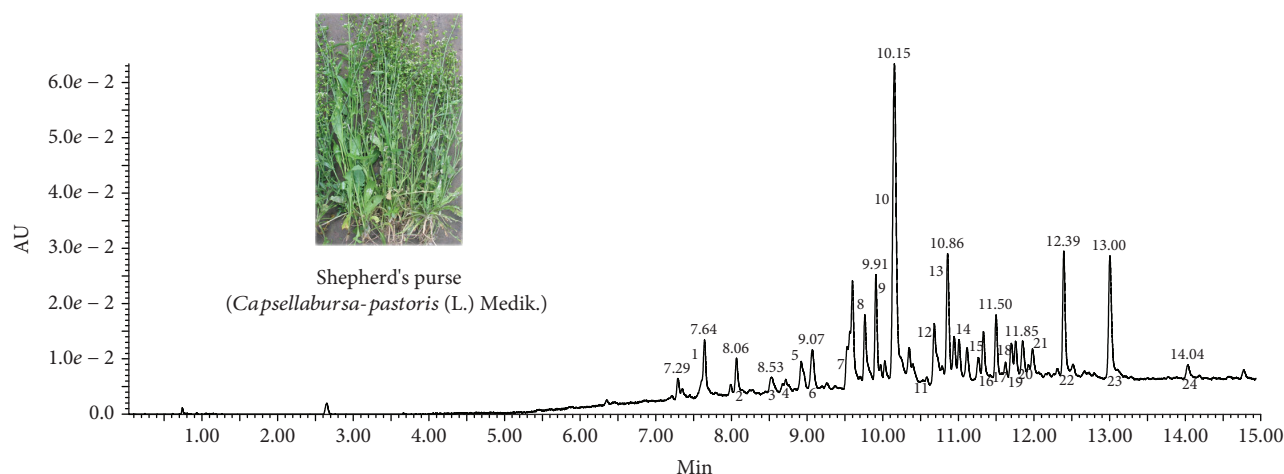


FIGURE 1: The picture of shepherd's purse and DAD chromatogram at 320 nm of shepherd's purse extracts.

anti-inflammatory, antioxidative, antiallergic, AChE inhibitory activity, and anticancer effects in previous studies [12–16]. Choi et al. prepared a sulforaphane-containing solution component from shepherd's purse and found it had significant anti-inflammatory activity [13]. Lan et al. found that the EtOAc extract of *Capsella bursa-pastoris* which with apigenin-7-O- β -D-glucopyranoside, luteolin-7-O- β -D-glucopyranoside, α -adenosine, and uridine showed stronger anti-inflammatory activities in carrageenan-induced paw edema experiment and egg-albumin-induced inflammation experiment [17]. Even though little studies found shepherd's purse with anti-inflammatory activity, the chemical composition, antioxidative and anti-inflammatory activities of the extract of shepherd's purse, and its underlying mechanisms have not been systematically studied. Therefore, the aim of the present study was to systematically investigate the chemical composition, anti-oxidative and anti-inflammatory activities of shepherd's purse extract, and their underlying mechanisms using LPS-induced RAW 264.7 cells and an *in vivo* carrageenan-induced mouse paw edema model.

2. Material and Methods

2.1. Plant Materials and Preparation of Shepherd's Purse Extracts (SPE). Fresh shepherd's purse was collected from Xiaogan, Hubei province of China, in March 2017. The specimen of the whole plant was deposited in College of Food Science and Technology in Huazhong Agricultural University (the voucher specimen number: 2016-02). The raw materials were dry in the shade and then were pulverized with a grinder. For extraction, 100 g raw materials were soaked with 2000 mL 95% ethanol at 100°C for 1 h for twice. The extract solution was combined and concentrated under reduced pressure and then freeze-dried using a vacuum freeze drying. The yield of extract was about 12.8% (*w/w*). The extracts were stored at -20°C for further use.

2.2. UPLC-QTOF-MS/MS System and Conditions. Chemical analysis of the SPE was performed by UPLC-QTOF-MS/MS analysis that was equipped with Waters Acquity UPLC

system and MS system (Waters Corp., MA, USA). The UPLC analysis was performed with an Acquity UPLC BEH C18 column (2.1 \times 100 mm, 1.7 μ m). The mobile phases composed of water with 0.01% formic acid (A) and methanol (B); the elution was performed with a gradient procedure according to the following conditions: 0-0.5 min, 1% B; 0.5-30 min, 1% B -99% B, with a flow rate of 0.4 mL/min. 1 mg/mL of SPE in ethanol was prepared and filtered through 0.22 μ m nylon micropore membranes prior to use. The injection volume was 1 μ L. Parameters for ESI MS are as follows: negative mode; source temperature 120°C; desolvation gas flow 800 L/h; desolvation temperature 450°C; cone gas flow 50 L/h; sampling cone and capillary voltages were 30 and 2500 V, respectively. A scan ranges from *m/z* 100 to 1500 were applied.

2.3. Antioxidant Activity of SPE. The radical scavenging ability of SPE was evaluated using ABTS assay. The stock solution of ABTS⁺ was prepared by admixing ABTS (7 mM) with K₂S₂O₈ solution. To obtain the ABTS⁺ working solution, the above stock solution was further diluted with water until the acceptable absorbance (0.7 \pm 0.02) achieved at 734 nm. Ascorbic acid (Vc) was selected as a positive control and Vc equivalent antioxidant capacity was calculated. 10 μ L sample with different concentration and 200 μ L of the working solution were mixed thoroughly, incubated for about 10 min, and the absorbances were determined at 734 nm using a microplate reader.

2.4. Cell Culture. The mouse macrophage cell line RAW 264.7 (ATCC, USA) was grown in DMEM culture medium (ATCC, USA) supplemented with 10% fetal bovine serum (FBS) (Gibco, USA) in a 5% CO₂ humidified incubator at 37°C.

2.5. Cell Viability Assay. RAW 264.7 macrophages were seeded with a density of 4 \times 10³ cells/well into a 96-well plate. After incubation overnight, the cells were treated with SPE (0-320 μ g/mL) and LPS for 20 h. Then, 20 μ L of 5 mg/mL of methylthiazole tetrazolium (MTT) was added into each well and then incubated for another 4 h. After that, the supernatant

TABLE 1: Identification of compounds in shepherd's purse extract by UPLC-QTOF-MS/MS.

No.	t_R (min)	$[M-H]^-$ (m/z)	Major fragment ions (m/z)	Tentative identification	References
1	7.64	353.0882	191.0553 160.8414 135.0285	5- <i>O</i> -Caffeoylquinic acid	[21]
2	8.06	367.1030	193.0493 134.0362	1- <i>O</i> -Feruloylquinic acid	[22]
3	8.51	337.0929	191.0554 173.0448	4- <i>p</i> -Coumaroylquinic acid	[23]
4	8.77	337.0924	191.0552	5- <i>p</i> -Coumaroylquinic acid	[24]
5	8.91	337.0924	173.0450	3- <i>p</i> -Coumaroylquinic acid	[23]
6	9.07	163.0392	163.0386 119.0492	<i>p</i> -Coumaric acid	[25]
7	9.56	367.1028	298.0486 191.0551 173.0448	5- <i>O</i> -Feruloylquinic acid	[24]
8	9.60	579.1343	459.0821 429.0771 357.0613 327.0504 309.0403 285.0396	Luteolin-6- <i>C</i> -pentoside-8- <i>C</i> -hexoside	[22]
9	9.91	447.0930	357.0610 327.0508 298.0470 285.0399 269.0452	Luteolin-6- <i>O</i> -glucoside	[26]
10	10.15	563.1392	473.0954 443.1048 383.0755 353.0662	Apigenin-6- <i>C</i> -hexoside-8- <i>C</i> -pentoside	[27]
11	10.57	431.1925	293.0453 284.0307 255.0252	Kaempferol- <i>O</i> -rhamnoside	[28]
12	10.68	609.1446	463.0859 301.0340 300.0273 271.0247 255.0301	Quercetin-3- <i>O</i> -rutinoside	[29]
13	10.85	463.0882	300.0269 301.0331 271.0244	Quercetin-3- <i>O</i> -glucoside	[28]
14	11.01	593.1501	443.0973 323.0554 285.0405	Kaempferol-3- <i>O</i> -rutinoside	[30]
15	11.33	505.0986	300.0272 271.0244 255.0292	Quercetin-3-(6- <i>O</i> -acetyl- β -glucoside)	[28]

TABLE 1: Continued.

No.	t _R (min)	[M-H] ⁻ (m/z)	Major fragment ions (m/z)	Tentative identification	References
16	11.499	593.1499	285.0396	Kaempferol-3- <i>O</i> -beta-D-rutinoside	[28]
			284.0320		
			255.0298		
17	11.62	725.1710	725.1678	Kaempferol triglycoside	[26]
			605.1277		
			429.0818		
			327.0488		
			309.0392		
18	11.68	447.0938	285.0387	Kaempferol- <i>O</i> -glucoside	[28]
			447.0905		
			429.0782		
			284.0313		
19	11.75	623.1604	255.0290	Isorhamnetin-3-rutinoside	[24]
			227.0341		
			531.0240		
			427.9770		
			315.0495		
			314.0418		
20	11.85	755.1802	271.0243	Diosmetin-7- <i>O</i> -triglycoside	[31]
			255.0283		
			635.1353		
			579.1293		
21	11.93	623.1611	429.0812	Quercetin rhamnoside glucuronate	[32]
			357.0258		
			309.0400		
			501.1388		
			447.1135		
22	12.39	607.1674	429.1028	Chryseoriol- -rutinoside	[21]
			337.0923		
			269.0453		
			551.1418		
23	13.00	461.1088	515.0217	Chryseoriol-7- <i>O</i> -glucoside	[23]
			429.1035		
			299.0561		
			284.0328		
24	14.04	299.1850	299.0558	Chrysoeriol	[29]
			284.0325		
			256.0376		
			116.9280		
			299.1852		
			284.0325		
			255.0302		

was discarded and 100 μ L DMSO was added. Plates were shaken for 1 min and the absorbance was measured at 570 nm using a microplate reader (Thermo Fisher, USA).

2.6. Determination of NO and Proinflammatory Cytokines. RAW 264.7 macrophages were treated as previously described

[18]. Briefly, the cells were stimulated with 1 μ g/mL of LPS with or without SPE for 16 h. The cell-free supernatant was collected with different treatment times (1, 2, 4, 8, and 16 h). NO concentration was measured using Griess reagent (Sigma, USA) and NaNO₂ were applied as standard. The contents of PGE₂, TNF- α , and IL-6 were measured

using specific ELISA kit (Cayman Chemical, Ann Arbor, Michigan, USA; R&D, Minneapolis, MN, USA) according to the manufacturer's guidelines.

2.7. Measurements of ROS Production. The intracellular generation of ROS was determined using a 2', 7'-dichlorofluorescein diacetate (DCFH-DA) as previously described [18]. RAW 264.7 macrophage cells were first incubated with LPS and SPE for 16 h; after that, cells were treated with 20 μ M DCFH-DA at 37°C for 30 min in the dark. After that, DCF fluorescence intensity was measured by microplate fluorometer at wavelengths of 488 nm (excitation) and 535 nm (emission).

2.8. Western Blot Analysis. The treatment method was the same as described above. For iNOS, COX 2, and HO-1 determination, macrophages were stimulated with 1 μ g/mL LPS and SPE for 16 h. For signaling molecule analysis (NF- κ B and MAP kinase signaling), cells were treated with 1 μ g/mL LPS and SPE for just one hour. Protein samples with or without MG132, a proteasome inhibitor, were also collected for 0.25, 0.5, and 1 h. After that, the cells were harvested and protein was collected. The detailed information of the western blot method was the same as previous reports [19]. The blots were detected using enhanced chemiluminescence assay kit (GE Healthcare, UK) and visualized by the chemiluminescent method (BioRad Laboratories, Hercules, CA, USA). β -Actin was used as a control.

2.9. Carrageenan-Induced Mouse Hind Paw Edema. C57BL/6 mice (20–22 g) were obtained from Laboratory Animal Center of Huazhong Agricultural University (Wuhan, China). All the procedures were approved by the Experimental Animal Review Committee of Huazhong Agricultural University of China. First, 100–400 mg/kg of SPE were administered orally; after 1 h, 30 μ L of 1% carrageenan was injected into their right hind paw to induce edema. The thickness of the paw was evaluated at 1, 2, and 4 h. At last, mice were euthanized and the paw tissues were collected and kept at -80°C for the next study. The inflammatory cytokines including IL 6 and TNF- α were measured using specific ELISA kits (R&D, Minneapolis, MN, USA). SOD activity and MDA content were investigated using special test kits (Nanjing Jiancheng Bioengineering Institute, China).

2.10. Statistical Analysis. All data were presented as means \pm S.D. Statistical significance was analyzed using one-way ANOVA with Tukey multiple comparison test applied GraphPad Prism 5 Software (GraphPad Software, San Diego, CA). $p < 0.05$ was recognized as statistically significant.

3. Results

3.1. UPLC-QTOF-MS/MS Analysis of SPE. In the present study, a qualitative analysis of the composition of SPE was performed using UPLC-DAD-ESI-QTOF-MS. The DAD chromatogram at 320 nm of SPE was shown in Figure 1. As listed in Table 1, twenty-four chemical compounds were identified in the SPE. The compounds of SPE were tentatively

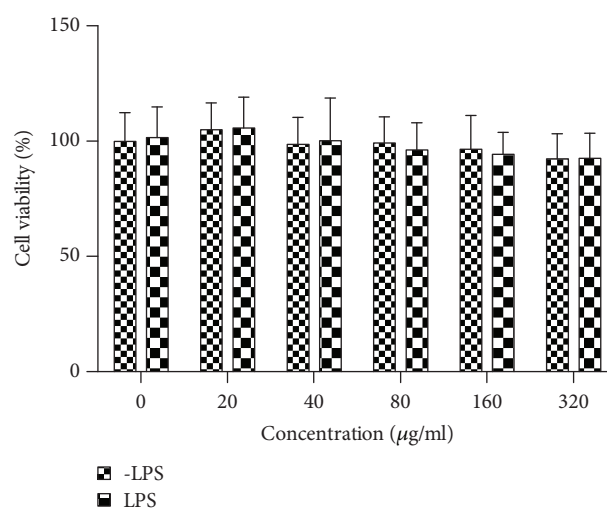


FIGURE 2: Effect of SPE on RAW 264.7 macrophage cell viability. Macrophages were cultured with SPE with or without LPS for 24 h, and cell viability was analyzed using the MTT assay.

identified with the MS data and by comparing with published literatures [20–31]. In brief, these compounds including 7 phenolic acids and their derivatives, 17 flavonoids belonged to the groups of flavones, flavonols, and flavanones.

3.2. Effect of SPE on Viability of RAW 264.7 Macrophages. MTT assay was performed to calculate the cellular cytotoxicity of SPE with or without LPS. The results indicated SPE with no cytotoxicity even at a high concentration (160 $\mu\text{g/ml}$) on RAW 264.7 no matter the existence of LPS (Figure 2). Therefore, in this study 10, 20, 40, and 80 $\mu\text{g/ml}$ of SPE were selected for next study.

3.3. Effect of SPE on the Inflammatory Cytokine Production and Their Related Gene Expression. We first investigated whether SPE could inhibit the production of NO, which is the main proinflammatory mediator in LPS-induced inflammation in macrophages. As the results illustrated in Figure 3(a), LPS could induce large amount of NO; 40 $\mu\text{g/ml}$ of SPE could significantly reduce the NO production ($p < 0.05$) with an IC_{50} of 91.09 $\mu\text{g/ml}$. For PGE_2 , similar to the NO production, with the increased concentration of SPE, the level of PGE_2 was significantly decreased with an IC_{50} of 150.37 $\mu\text{g/ml}$ (Figure 3(b)). Similarly, treatment with SPE resulted in a concentration-dependent reduction of IL 6 and TNF- α with IC_{50} of 129.4 and 136.2 $\mu\text{g/ml}$ (Figures 3(c) and 3(d)). Further western blot assay (Figures 3(e) and 3(f)) also indicated that SPE showed significantly inhibitory effects on the expression of iNOS and COX-2.

3.4. Effects of SPE on Proinflammatory Cytokine Secretion. To further investigate the influences of SPE on the secretion of specific cytokines stimulated by LPS in different treatment times, the contents of NO, IL-6, PGE_2 , and TNF- α were measured at 1, 2, 4, 8, and 16 h. As the results illustrated in Figure 4, with the induction of LPS, the productions of all

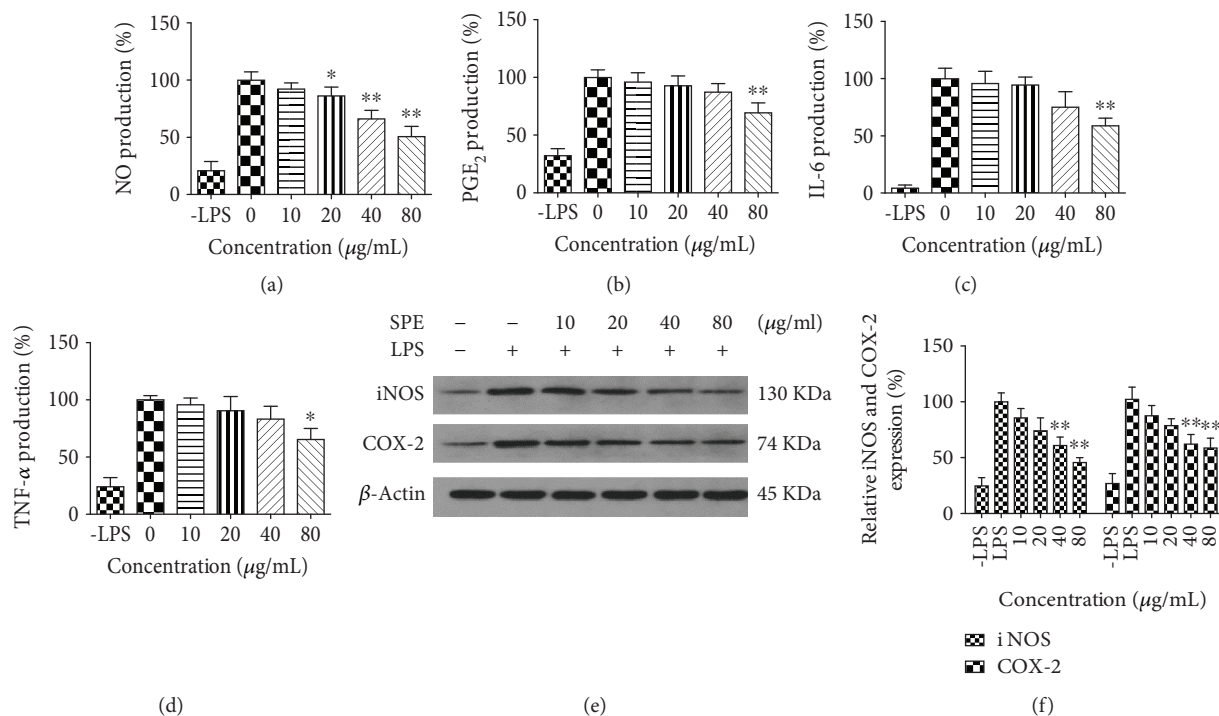


FIGURE 3: Influences of SPE on the production of proinflammatory cytokines and related protein expression. Mouse macrophages were induced with LPS in the presence of SPE for 16 h. Culture supernatant was removed and centrifuged to remove particulates and analyzed for production of these cytokines: (a) NO; (b) PGE₂; (c) IL-6; and (d) TNF- α . (e) The expression levels of iNOS and COX2 were analyzed by western blot. (f) The band intensity of iNOS or COX2 was normalized with β -actin. * $p < 0.05$ and ** $p < 0.01$ versus LPS alone group.

of these four main proinflammatory cytokines were increasing with the time increased of LPS stimulation. 80 μ g/mL SPE could significantly inhibit the generation of these specific proinflammatory cytokines ($p < 0.01$) at 8 h and 16 h.

3.5. Effect of SPE on MAPK Phosphorylation and Activation of NF- κ B. The NF- κ B and MAP kinase signaling (p38, JNK, and ERK) pathways regulate the LPS-induced inflammatory response and also played key roles in the occurrence and development of inflammation [32]. To further clarify the underlying mechanism of the anti-inflammatory ability, influences of SPE on activation of NF- κ B and phosphorylation of MAPKs were evaluated using western blot assays. As the data presented in Figures 5(a) and 5(b), SPE showed a significant reduction on the phosphorylation of p38. In this study, SB 203580, a p-38 MAPK inhibitor, also showed a significantly inhibitory activity on the NO production in LPS-induced RAW264.7 cells (32.06 ± 3.14 vs $18.51 \pm 2.37 \mu$ M). Furthermore, the phosphorylation of I κ B α and p65 appeared after LPS stimulation for 60 min (Figures 5(c) and 5(d)). The phosphorylation of p65 was significantly decreased with the treatment of SPE; the phosphorylation of I κ B- α also decreased with the treatment of 80 μ g/mL SPE even though there was no significant difference. These data indicated that the inhibitory effect of SPE on LPS-induced phosphorylation of p 38 MAPKs and activation of NF- κ B was partly associated with its anti-inflammatory potential. In this study, we also used

MG132, a proteasome inhibitor, to clarify the effect of SPE. As the results illustrated in Figure 6, MG132 showed significantly inhibitory effect on the LPS-induced inflammatory (Figure 6(a)). And as the results showed in Figure 6(b), LPS could significantly induce the phosphorylation of IKK and I κ B and induce the degradation of I κ B α . However, SPE could reverse this to reduce the development of inflammatory process.

3.6. Antioxidative Activities of SPE. Previous studies have indicated that *in vitro* ABTS radical scavenging activity can potentially be used as marker for evaluating the anti-inflammatory activity of flavonoids [33]. Therefore, the antioxidant activity of SPE was firstly investigated using the ABTS assay. As the data presented in Figure 7(a), the ABTS radical scavenging activity of SPE increased with the increasing of SPE concentration with an EC₅₀ value of 61.6 μ g/mL. At the concentration of 160 μ g/ml, about 80% of the ABTS free radical was scavenged. The Vc equivalent antioxidant capacity of SPE was calculated as 0.18 g per gram SPE. Figure 7(b) showed that with the stimulation of LPS, the intracellular ROS were accumulated in RAW 264.7 cells, whereas SPE showed a strong inhibitory effect on the ROS production.

HO-1 has been reported as a stress-inducible protein induced by many stimuli such as oxidative stress and UV light [34, 35], and upregulation of the expression of HO-1 has been proved as a useful approach to improve oxidative

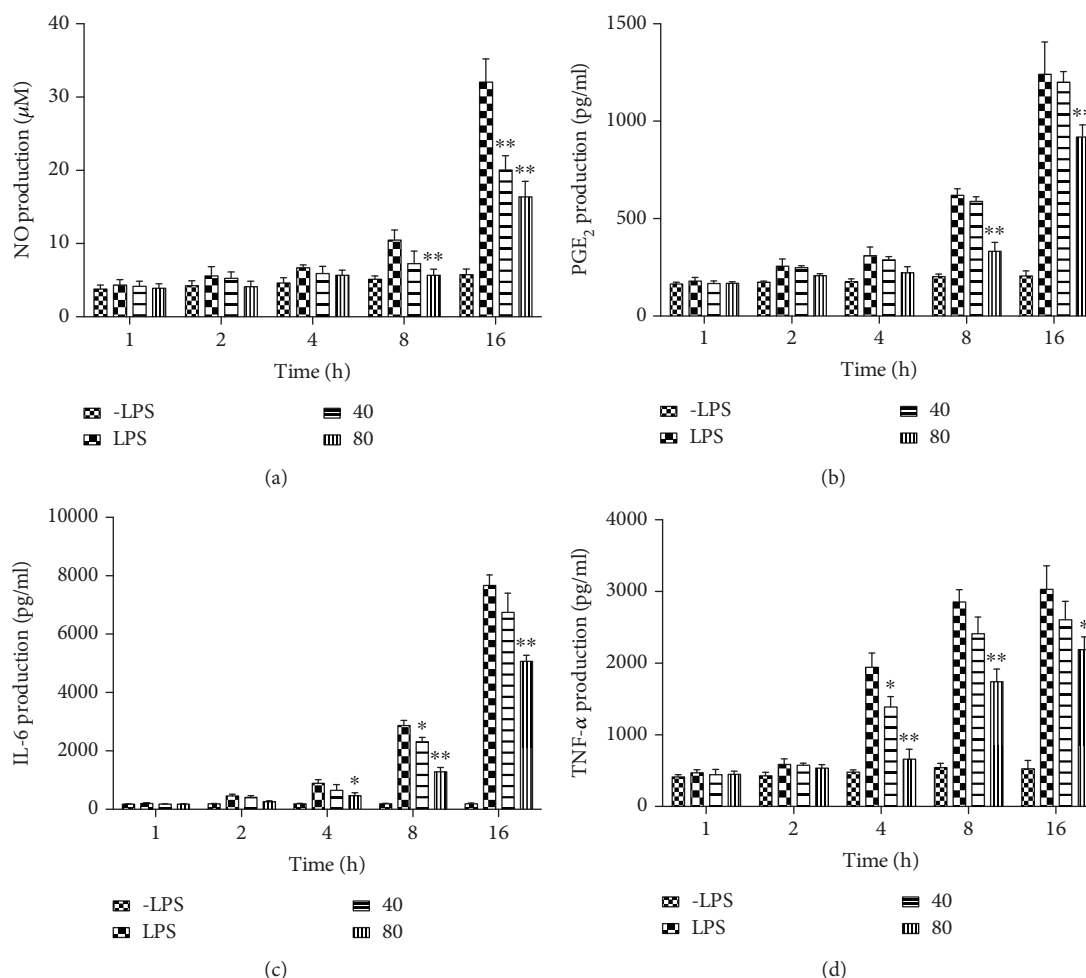


FIGURE 4: Influences of SPE on the secretion of proinflammatory cytokines with different LPS stimulation time. (a) NO; (b) PGE₂; (c) IL-6; and (d) TNF-α. Cells were incubated with 1 μg/ml LPS with the addition of 40 and 80 μg/ml of SPE at 1, 2, 4, 8, and 16 h timepoints; culture supernatant was removed and centrifuged to remove particulates and analyzed for production of these cytokines. **p* < 0.05 and ***p* < 0.01 versus LPS alone group.

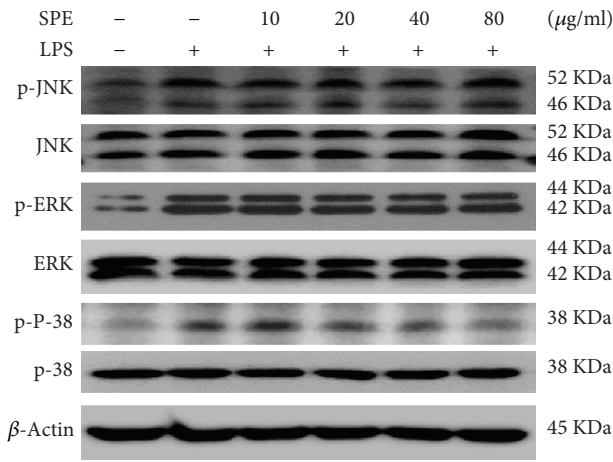
injury and macrophage activation [35–38]. Therefore, the expression of HO-1 with SPE treatment was also evaluated in this study (Figures 7(c) and 7(d)). These results indicated that the expression of HO-1 was increased with the treatment of SPE.

3.7. In Vivo Anti-Inflammatory Activity of SPE. The anti-inflammation potential of SPE was further investigated using an *in vivo* mouse paw edema model. As the data illustrated in Figure 8, the paw thickness significantly increased after the carrageenan injection, and 400 mg/kg of SPE showed a significantly inhibitory activity of paw edema (Figure 8). With the oral administration of 400 mg/kg of SPE, the paw thickness significantly decreased, which was 0.30 ± 0.02 and 0.32 ± 0.02 cm compared with 0.37 ± 0.01 and 0.39 ± 0.03 cm at 2 h and 4 h, respectively. For TNF-α and IL-6, a large amount of TNF-α and IL-6 were induced with the injection of carrageenan (Figures 9(a) and 9(b)); 400 mg/kg of SPE could significantly decrease the generation of TNF-α and IL-6, which was 170.23 ± 19.58 and

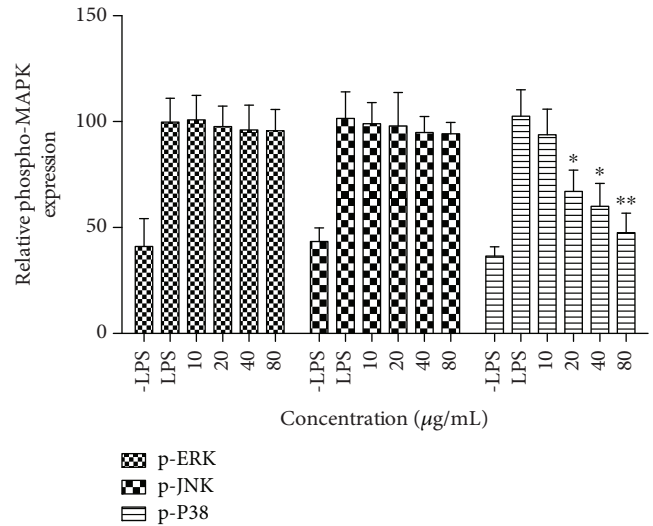
1728.21 ± 237.69 pg/mg protein compared with 226.01 ± 38.70 and 2314.41 ± 409.04 pg/mg protein (*p* < 0.05), respectively. In addition, 400 mg/kg of SPE also could significantly decrease the MDA content (19.82 ± 4.36 vs 39.71 ± 5.30 nmol/mg protein, *p* < 0.01) (Figure 9(c)). These *in vivo* results were also in accordance with the result from cell culture model. Meanwhile, SOD activity assay also indicated that the decrease of SOD activity by the carrageenan injection was reversed with the treatment of SPE (50.53 ± 6.59 vs 32.19 ± 4.28 U/mg protein) (Figure 9(d)).

4. Discussion

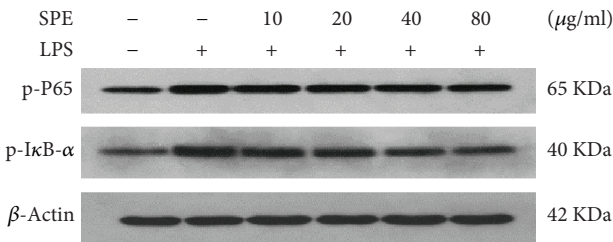
In recent years, the functional foods have received increasing attention worldwide. It can not only supply the nutrients but also provide many phytochemicals which play as a functional factor for human health, especially for these people with chronic disease or in the state of subhealth, such as chronic low-grade inflammation; these functional foods may be the best choice to improve their healthy rather than treatment



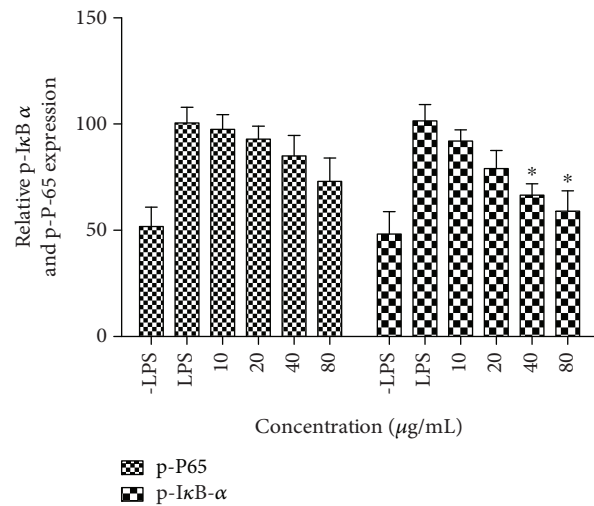
(a)



(b)



(c)



(d)

FIGURE 5: SPE inhibited the activation of LPS-induced MAPK (JNK, ERK, and p38) and NF- κ B ($I\kappa$ B α and p65). Cells were incubated with 1 $\mu\text{g/ml}$ LPS with the addition of different concentration of SPE for 1 h; the protein were extracted and the phosphorylation of JNK, ERK, p 38, p 65, and $I\kappa$ B α were analyzed with western blot assay. (a, c) Western blot assay of activation of MAPKs and NF- κ B were analyzed by and (b, d) The band intensity of phosphorylation MAPKs and NF- κ B were normalized with nonphosphorylation of MAPKs and β -actin. * $p < 0.05$ and ** $p < 0.01$ versus LPS alone group.

with drugs [39, 40]. Previous studies have proved that shepherd's purse (*Capsella bursa-pastoris*) exerts multihealthy benefits, such as antimicrobial [41], anti-inflammatory [13], cardiovascular, reproductive, anticancer [16, 42], hepatoprotective, sedative, and other pharmacological effects [43]. Therefore, the chemical components of shepherd's purse ethanol extract were first characterized by UPLC-QTOF-MS/MS, and then the anti-inflammatory effects and its underlying mechanisms of SPE in LPS-induced RAW 264.7 inflammation model and *in vivo* mouse model were also systemically investigated in this study.

Macrophages play key roles in the immune system; the activation of macrophages induced the secretion of many inflammatory mediators, and also coupled with a high degree of oxidative stress [44]. SPE showed significantly inhibitory on the production of NO and PGE₂. The overexpression of circulating inflammatory factors, including IL-6, IL-1 β , TNF- α , and MCP-1, transforming growth factor (TGF)-a, TGF-b, and IFN-c also have been proved associated with low-grade, chronic inflammation [45, 46]. In this study, the results indicated that the production of TNF- α and IL-6 were significantly inhibited with the treatment of SPE from 4 h.

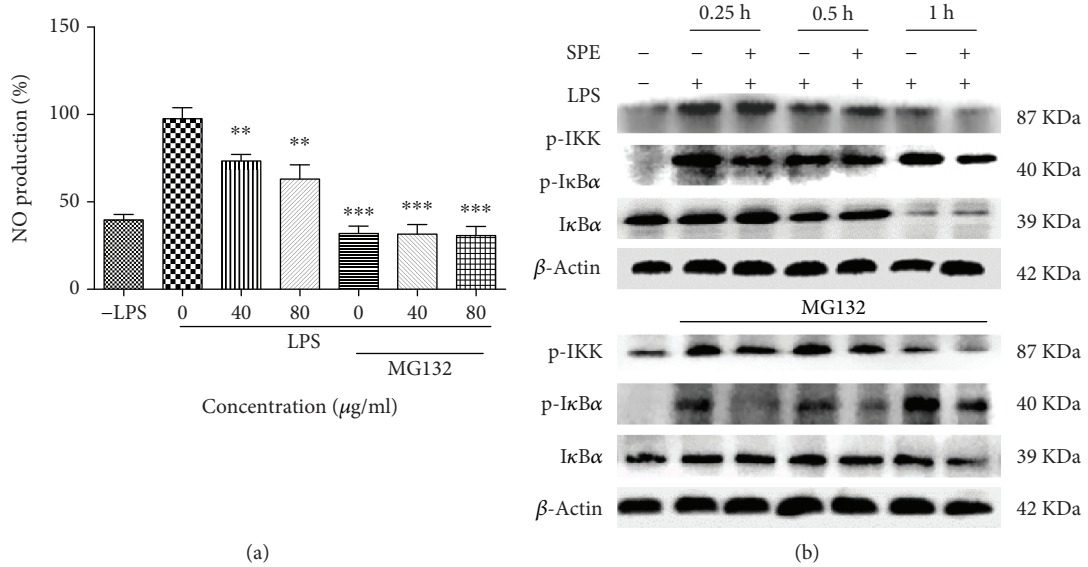


FIGURE 6: SPE reduced the activation of IKK and IκB α and reversed the degradation of IκB α during its inhibition of LPS-induced inflammation. (a) The NO production in the LPS induced RAW 264.7 cells with or without the treatment of SPE and MG 132. RAW 264.7 cells were first incubated with or without MG132 for 1 h and then treatment with LPS or LPS+SPE for 16 h. Culture supernatant was collected and NO production was measured using Griess reagent. (b) The phosphorylation of IKK and IκB α in macrophages. Apart treatment with LPS and SPE, Raw 264.7 cell were also incubated with or without MG132, at 0.25 h, 0.5 h, and 1 h; the proteins were extracted and were analyzed using western blot assay. ** $p < 0.01$ and *** $p < 0.001$ versus LPS alone.

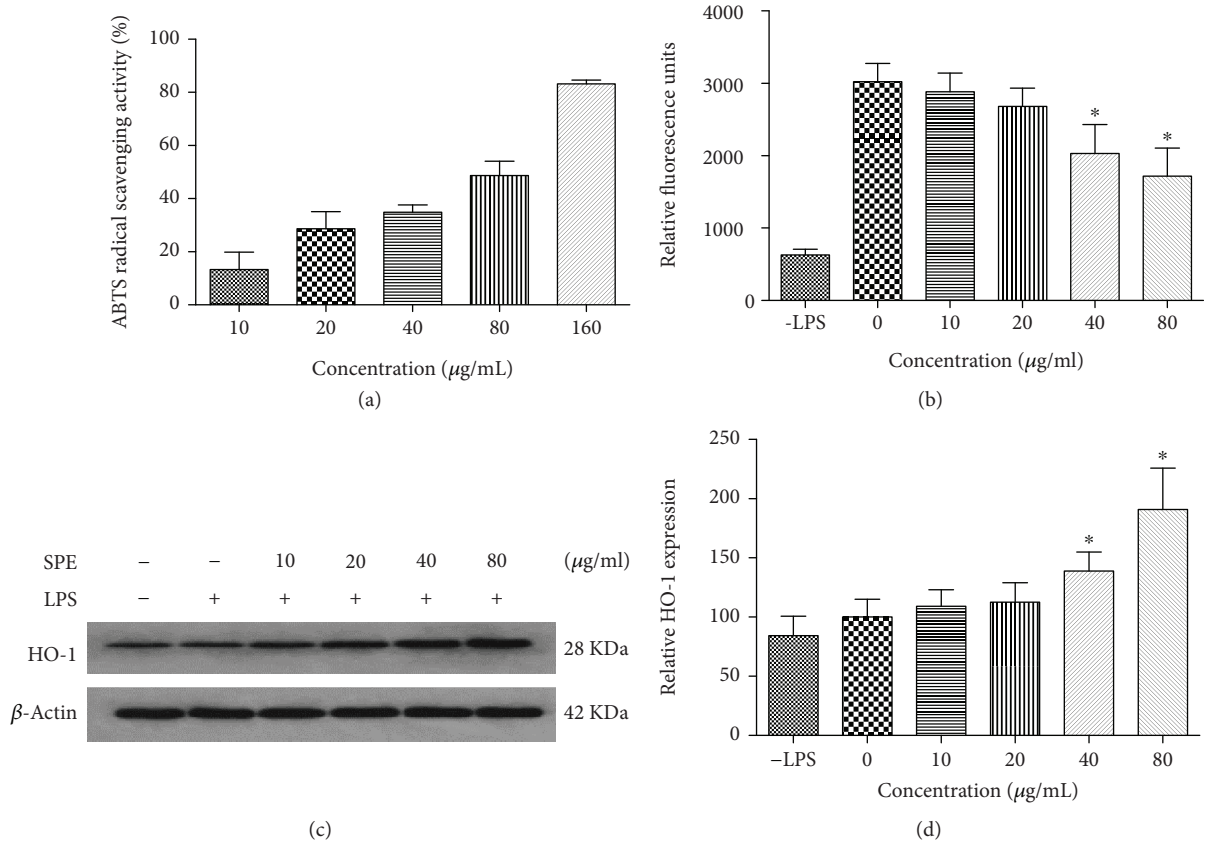


FIGURE 7: SPE showed strong antioxidative potential *in vitro* chemical and cell models. (a) The ABTS⁺ scavenging activity of SPE. (b) SPE inhibited ROS production in LPS-stimulated macrophages. (c, d) SPE enhanced the HO-1 expression. * $p < 0.05$ versus LPS alone group.

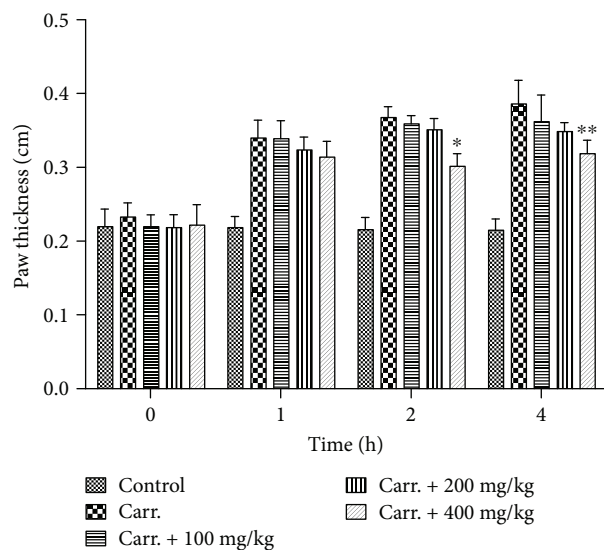


FIGURE 8: SPE inhibited the development of the paw edema induced by carrageenan injection. The edema model was induced with 30 μ L of 1% carrageenan. Different doses of SPE were administered orally 1 h prior to carrageenan injection. * $p < 0.05$ and ** $p < 0.01$ versus carrageenan group.

These findings demonstrated that SPE could attenuate LPS-induced macrophage activation, which indicated that SPE possesses potential anti-inflammatory activity.

Inflammation is regulated by many proinflammatory mediators and cell signal pathways [47]. In this process, NF- κ B, MAPKs, and Nrf 2/HO-1 pathway have been proved that played key roles in mediating the inflammatory responses [19, 48–52]. Therefore, these pathways are potential targets for pharmacological intervention in the treatment of inflammation [49, 50]. This study found that SPE could inhibit the phosphorylation of p38 MAPK and reduce the subsequent inflammatory response. Similarly, NF- κ B is also an important signal pathway involved in immune and inflammatory responses [53, 54]. In addition, following treatment with SPE, LPS induced the phosphorylation of I κ B and P-65 was also inhibited in RAW 264.7 macrophages with the treatment of SPE, which indicated that SPE could prevent the activation of NF- κ B to exert its anti-inflammatory potential. Furthermore, there were very close connections between these two signal pathways. From the above results, we could find that both of the activation of p 38 MAPKs and NF- κ B signal pathways were blocked by the treatment of SPE. Therefore, these data suggested SPE exerts its anti-inflammatory potential at least partly associated with its regulation on the activation of MAPKs and NF- κ B pathways.

It has been proved that there was a connection between chronic inflammation and oxidative stress, and free radical-induced damage also could induce many chronic health problems [55–57]. In the inflammatory process, ROS have been proved to participate in the LPS-stimulated inflammation process by activating specific signaling pathways, resulting in the production of many specific cytokines

[35, 57–60]. In addition, the upregulation of HO-1 was recognized as a pivotal response to different kinds of stress, it could exert its anti-inflammatory potential through inhibiting the excessive production of specific cytokines, and also through its regulation on macrophage switching to an M2-phenotype [61]. In this study, the data indicated SPE with strong antioxidative activity; meanwhile SPE could inhibit ROS production in macrophage cells whereas enhanced the expression of HO-1. These data proved the strong antioxidant activity also played an important role in the anti-inflammatory effect of SPE.

Carrageenan-induced paw edema animal model is usually applied to assess the different phases of inflammation reaction and evaluate the anti-inflammatory agents; it can induce acute inflammation, release of inflammatory mediators, and production of free radicals [62–64]. Therefore, this animal model was also used in this study. The results proved that SPE could inhibit the development of the carrageenan-induced edema, which was consisted with the *in vitro* findings. Meanwhile, the induction of inflammation by carrageenan was compared by generation of ROS and increased oxidative stress [64]. The animal study indicated that there was a significant increase of MDA content along with a distinct decrease of SOD activity with the injection of carrageenan in the model group. However, with the treatment of 400 mg/kg SPE, increase of SOD activity and the decrease of MDA in paw edema tissue were observed. These results indicated that SPE also showed strong anti-inflammatory and antioxidative potential *in vivo*.

In this study, about 24 chemical compounds were identified from the extracts of *Capsella bursa-pastoris*. As the HPLC-MS results, SPE contain a high amount of flavonoids, such as quercetin, kaempferol-7-O-rhamnopyranoside, quercetin-3-O-glucopyranoside, quercetin-6-C-glucopyranoside, and kaempferol-3-O-rutinoside; these results were also consistent with some previous findings [43, 65, 66]. Many studies had investigated the health benefits of these components, for example, antioxidative, ant-obesity, and anticancer activities [64, 67, 68]. Therefore, the flavonoid constituents presented in SPE could play key roles for its antioxidative and anti-inflammatory activity. However, since the extract contained many compounds, further works are still needed to be undertaken to investigate the anti-inflammatory properties of single compounds to further clear the anti-inflammatory potential of SPE.

5. Conclusion

In conclusion, in this study, the chemical composition, anti-inflammatory potential of shepherd's purse, and its underlying mechanisms were first systematically evaluated. Our findings indicated that *Capsella bursa-pastoris* (L.) Medik might reduce NO and PGE₂ production and also inhibited the production of TNF- α and IL-6 in inflammatory development process. The underlying mechanism study proved that the anti-inflammatory potential of *Capsella bursa-pastoris* (L.) Medik was through the inhibition of the activation of p-38 MAPKs and NF- κ B pathways. Taken together, besides the good nutritional value and delicious

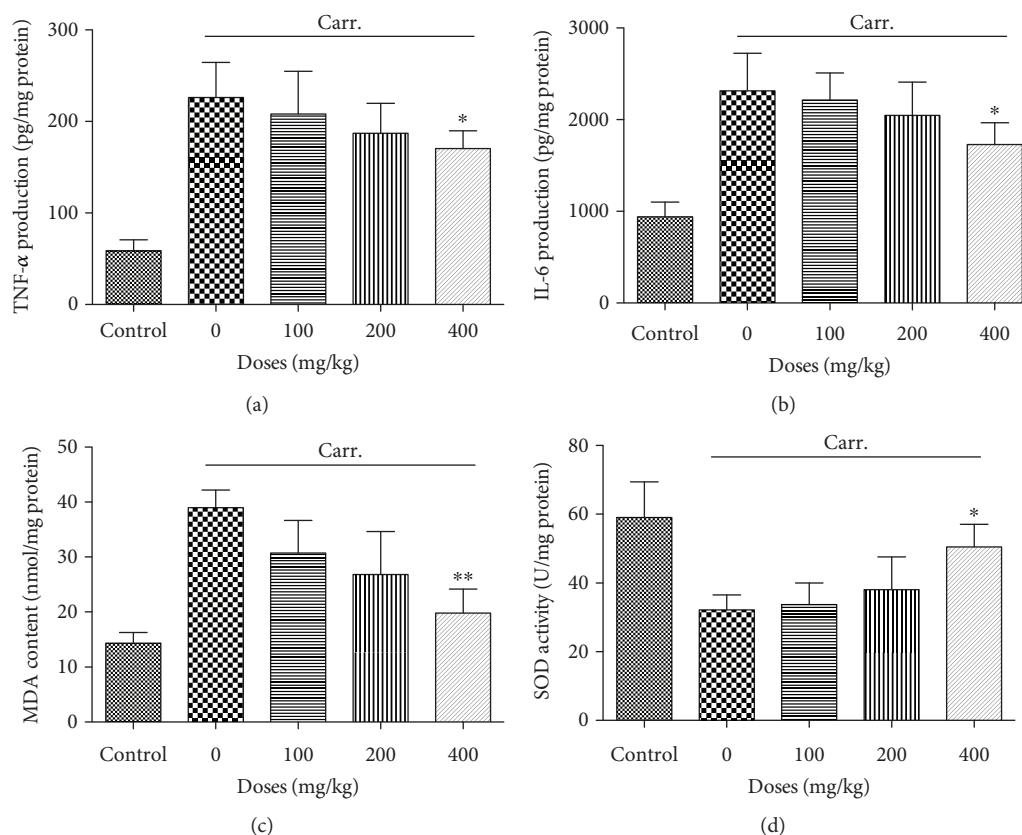


FIGURE 9: Influence of SPE on the production of inflammatory biomarkers and oxidative stress parameters in paw tissue. The edema was induced with $30 \mu\text{L}$ of 1% carrageenan. Different doses of SPE were administered orally 1 h prior to carrageenan injection. (a) TNF- α expression levels. (b): IL-6 expression levels. (c) MDA level. (d) SOD activity in edema tissue. * $p < 0.05$ and ** $p < 0.01$ versus model group.

taste already described in the previous studies, *Capsella bursa-pastoris* (L.) Medik also showed special health benefits, suggesting that it may be interesting not only for human health but also as food additive.

Data Availability

The data used to support the findings of this study are available from the corresponding author upon request.

Conflicts of Interest

The authors have declared no conflict of interest.

Authors' Contributions

Jinming Peng and Tianyong Hu are co-first authors who contributed equally to this work.

Acknowledgments

This work was supported by the Natural Science Foundation of China (31701712), Hubei Provincial Natural Science Foundation of China (2017CFB197), Fundamental Research Funds for the Central Universities (2662016QD035), Longgang Science and Technology programs (no. 20160607142024828),

and Shenzhen Innovation of Science and Technology Commission programs (nos. ZDSYS201506050935272).

References

- [1] U. C. Adler, "Low-grade inflammation in chronic diseases: an integrative pathophysiology anticipated by homeopathy?," *Medical Hypotheses*, vol. 76, no. 5, pp. 622–626, 2011.
- [2] J. Lee, S. J. Ha, H. J. Lee et al., "Protective effect of Tremella fuciformis Berk extract on LPS-induced acute inflammation via inhibition of the NF- κ B and MAPK pathways," *Food & Function*, vol. 7, no. 7, pp. 3263–3272, 2016.
- [3] A. M. Castro, L. E. Macedo-de la Concha, and C. A. Pantoja-Meléndez, "Low-grade inflammation and its relation to obesity and chronic degenerative diseases," *Revista Médica del Hospital General de México*, vol. 80, no. 2, pp. 101–105, 2017.
- [4] E. Cevenini, C. Caruso, G. Candore et al., "Age-related inflammation: the contribution of different organs, tissues and systems. How to face it for therapeutic approaches," *Current Pharmaceutical Design*, vol. 16, no. 6, pp. 609–618, 2010.
- [5] H. Süleyman, B. Demircan, and Y. Karagöz, "Anti-inflammatory and side effects of cyclooxygenase inhibitors," *Pharmacological Reports*, vol. 59, no. 3, pp. 247–258, 2007.
- [6] S. C. Manson, R. E. Brown, A. Cerulli, and C. F. Vidaurre, "The cumulative burden of oral corticosteroid side effects and the

- economic implications of steroid use," *Respiratory Medicine*, vol. 103, no. 7, pp. 975–994, 2009.
- [7] J. L. Guil-Guerrero, J. J. Gimenez-Martinez, and M. E. Torija-Isasa, "Nutritional composition of wild edible crucifer species," *Journal of Food Biochemistry*, vol. 23, no. 3, pp. 283–294, 1999.
- [8] J. M. Cha, W. S. Suh, T. H. Lee, L. Subedi, S. Y. Kim, and K. R. Lee, "Phenolic glycosides from *Capsella bursa-pastoris* (L.) Medik and their anti-inflammatory activity," *Molecules*, vol. 22, no. 6, article 1023, 2017.
- [9] M. Pehlivan, H. Akgulo, and F. yayla, "The some nutrient and trace elements content of wild plants using as ethno botanical and grown in the Gaziantep region," *Journal of Applied Pharmaceutical Science*, vol. 3, no. 4, pp. 143–145, 2013.
- [10] Q. H. Wang, E. Q. Wu, and N. Y. T. Dai, "Study on chemical constituents of *Capsella bursa-pastoris*. Chemical composition and anti-inflammatory effects of the EtOAc extract from *Capsella bursa-pastoris* (L.) Medic," *Natural Product Research and Development*, vol. 26, pp. 50–52, 2014.
- [11] A. E. Al-Snafi, "The chemical constituents and pharmacological effects of *Capsella bursa-pastoris* - a review," *International Journal of Pharmacology & Toxicology*, vol. 5, no. 2, pp. 76–81, 2015.
- [12] E. A. Goun, V. M. Petrichenko, S. U. Solodnikov et al., "Anti-cancer and antithrombin activity of Russian plants," *Journal of Ethnopharmacology*, vol. 81, no. 3, pp. 337–342, 2002.
- [13] W. J. Choi, S. K. Kim, H. K. Park, U. D. Sohn, and W. Kim, "Anti-inflammatory and anti-superbacterial properties of sulfuraphane from shepherd's purse," *Korean J Physiol Pharmacol.*, vol. 18, no. 1, pp. 33–39, 2014.
- [14] H. K. Choi, E. J. Shin, S. J. Park et al., "Ethanol extract of *Capsella bursa-pastoris* improves hepatic steatosis through inhibition of histone acetyltransferase activity," *Journal of Medicinal Food*, vol. 20, no. 3, pp. 251–257, 2017.
- [15] K. Kuroda, M. Akao, M. Kanisawa, and K. Miyaki, "Inhibitory effect of *Capsella bursa-pastoris* extract on growth of Ehrlich solid tumor in mice," *Cancer Research*, vol. 36, no. 6, pp. 1900–1903, 1976.
- [16] K. E. Lee, J. A. Shin, I. S. Hong, N. P. Cho, and S. D. Cho, "Effect of methanol extracts of *Cnidium officinale* Makino and *Capsella bursa-pastoris* on the apoptosis of HSC-2 human oral cancer cells," *Experimental and Therapeutic Medicine*, vol. 5, no. 3, pp. 789–792, 2013.
- [17] X. Lan, W. Qing-Hu, B. Baiyinmuqier, and B. Agula, "Chemical composition and anti-inflammatory effects of the EtOAc extract from *Capsella bursa-pastoris* (L.) Medic," *African Journal of Pharmacy and Pharmacology*, vol. 11, no. 15, pp. 186–190, 2017.
- [18] K. K. Li, S. S. Shen, X. Deng et al., "Dihydrofisetin exerts its anti-inflammatory effects associated with suppressing ERK/p 38 MAPK and heme oxygenase-1 activation in lipopolysaccharide-stimulated RAW 264.7 macrophages and carrageenan-induced mice paw edema," *International Immunopharmacology*, vol. 54, pp. 366–374, 2018.
- [19] K. K. Li, J. M. Peng, W. Zhu, B. H. Cheng, and C. M. Li, "Gallic acid inhibits 3T3-L1 differentiation and lipopolysaccharide induced inflammation through MAPK and NF- κ B signaling," *Journal of Functional Foods*, vol. 30, pp. 159–167, 2017.
- [20] N. Martins, L. Barros, C. Santos-Buelga, S. Silva, M. Henriques, and I. C. Ferreira, "Decoction, infusion and hydroalcoholic extract of cultivated thyme: antioxidant and antibacterial activities, and phenolic characterisation," *Food Chemistry*, vol. 167, pp. 131–137, 2015.
- [21] Z. L. Lv, J. Dong, and B. L. Zhang, "Rapid identification and detection of flavonoids compounds from bamboo leaves by LC-(ESI)-IT-TOF/MS," *BioResources*, vol. 7, no. 2, pp. 1405–1418, 2012.
- [22] L. Z. Lin, S. Lu, and J. M. Harnly, "Detection and quantification of glycosylated flavonoid malonates in celery, Chinese celery, and celery seed by LC-DAD-ESI/MS," *Journal of Agricultural and Food Chemistry*, vol. 55, no. 4, pp. 1321–1326, 2007.
- [23] C. Bergantin, A. Maietti, A. Cavazzini et al., "Bioaccessibility and HPLC-MS/MS chemical characterization of phenolic antioxidants in red chicory (*Cichorium intybus*)," *Journal of Functional Foods*, vol. 33, pp. 94–102, 2017.
- [24] Y. Zhao, X. Li, X. Zeng, S. Huang, S. Hou, and X. Lai, "Characterization of phenolic constituents in *Lithocarpus polystachyus*," *Analytical Methods*, vol. 6, no. 5, pp. 1359–1363, 2014.
- [25] E. J. Llorent-Martínez, P. Ortega-Barrales, G. Zengin et al., "Evaluation of antioxidant potential, enzyme inhibition activity and phenolic profile of *Lathyrus cicera* and *Lathyrus digitatus*: potential sources of bioactive compounds for the food industry," *Food and Chemical Toxicology*, vol. 107, Part B, pp. 609–619, 2017.
- [26] M. Zhu, X. Dong, and M. Guo, "Phenolic profiling of *Duchesnea indica* combining macroporous resin chromatography (MRC) with HPLC-ESI-MS/MS and ESI-IT-MS," *Molecules*, vol. 20, no. 12, pp. 22463–22475, 2015.
- [27] Q. Sun, J. Zhu, F. Cao, and F. Chen, "Anti-inflammatory properties of extracts from *Chimonanthus nitens* Oliv. leaf," *PLoS One*, vol. 12, no. 7, article e0181094, 2017.
- [28] F. Sánchez-Rabeneda, O. Jáuregui, R. M. Lamuela-Raventós, J. Bastida, F. Viladomat, and C. Codina, "Identification of phenolic compounds in artichoke waste by high-performance liquid chromatography-tandem mass spectrometry," *Journal of Chromatography A*, vol. 1008, no. 1, pp. 57–72, 2003.
- [29] F. Ferreres, A. Gil-Izquierdo, P. B. Andrade, P. Valentão, and F. A. Tomás-Barberán, "Characterization of C-glycosyl flavones O-glycosylated by liquid chromatography-tandem mass spectrometry," *Journal of Chromatography A*, vol. 1161, no. 1-2, pp. 214–223, 2007.
- [30] A. Karioti, E. Giocaliere, C. Guccione et al., "Combined HPLC-DAD-MS, HPLC-MS (n) and NMR spectroscopy for quality control of plant extracts: the case of a commercial blend sold as dietary supplement," *Journal of Pharmaceutical and Biomedical Analysis*, vol. 88, pp. 7–15, 2014.
- [31] R. Torres-Carro, M. I. Isla, S. Thomas-Valdes, F. Jiménez-Aspee, G. Schmeda-Hirschmann, and M. R. Alberto, "Inhibition of pro-inflammatory enzymes by medicinal plants from the Argentinean highlands (Puna)," *Journal of Ethnopharmacology*, vol. 205, pp. 57–68, 2017.
- [32] M. Gaestel, A. Kotlyarov, and M. Kracht, "Targeting innate immunity protein kinase signalling in inflammation," *Nature Reviews Drug Discovery*, vol. 8, no. 6, pp. 480–499, 2009.
- [33] W. Chanput, N. Krueyos, and P. Ritthiruangdej, "Antioxidative assays as markers for anti-inflammatory activity of flavonoids," *International Immunopharmacology*, vol. 40, pp. 170–175, 2016.
- [34] C. J. Lee, S. S. Lee, S. C. Chen, F. M. Ho, and W. W. Lin, "Oregonin inhibits lipopolysaccharide-induced iNOS gene

- transcription and upregulates HO-1 expression in macrophages and microglia," *British Journal of Pharmacology*, vol. 146, no. 3, pp. 378–388, 2005.
- [35] K. Asehnoune, D. Strassheim, S. Mitra, J. Y. Kim, and E. B. Abraham, "Involvement of reactive oxygen species in Toll-like receptor 4-dependent activation of NF- κ B," *The Journal of Immunology*, vol. 172, no. 4, pp. 2522–2529, 2004.
- [36] N. G. Abraham and A. Kappas, "Pharmacological and clinical aspects of heme oxygenase," *Pharmacological Reviews*, vol. 60, no. 1, pp. 79–127, 2008.
- [37] J. W. Lee, C. J. Bae, Y. J. Choi et al., "3, 4, 5-trihydroxycinnamic acid inhibits lipopolysaccharide (LPS) - induced inflammation by Nrf 2 activation in vitro and improves survival of mice in LPS-induced endotoxemia model in vivo," *Molecular and Cellular Biochemistry*, vol. 390, no. 1-2, pp. 143–153, 2014.
- [38] H. L. Yang, S. W. Lin, C. C. Lee et al., "Induction of Nrf2-mediated genes by *Antrodia salmonea* inhibits ROS generation and inflammatory effects in lipopolysaccharide-stimulated RAW264.7 macrophages," *Food & Function*, vol. 6, no. 1, pp. 229–240, 2015.
- [39] M. Y. Lee, J. A. Lee, C. S. Seo et al., "Anti-inflammatory activity of Angelica dahurica ethanolic extract on RAW264.7 cells via upregulation of heme oxygenase-1," *Food and Chemical Toxicology*, vol. 49, no. 5, pp. 1047–1055, 2011.
- [40] X. Wang, C. Zhang, Y. Peng et al., "Chemical constituents, antioxidant and gastrointestinal transit accelerating activities of dried fruit of *Crataegus dahurica*," *Food Chemistry*, vol. 246, pp. 41–47, 2018.
- [41] S. Soleimanpour, F. S. Sedighinia, A. S. Afshar, R. Zarif, J. Asili, and K. Ghazvini, "Synergistic antibacterial activity of *Capsella bursa-pastoris* and *Glycyrrhiza glabra* against oral pathogens," *Jundishapur Journal of Microbiology*, vol. 6, no. 8, p. 7262, 2013.
- [42] A. B. Yildirim, F. B. Karakas, and A. U. Turker, "In vitro antibacterial and antitumor activities of some medicinal plant extracts, growing in Turkey," *Asian Pacific Journal of Tropical Medicine*, vol. 6, no. 8, pp. 616–624, 2012.
- [43] C. Grosso, J. Vinholes, L. R. Silva et al., "Chemical composition and biological screening of *Capsella bursa-pastoris*," *Revista Brasileira de Farmacognosia*, vol. 21, no. 4, pp. 635–643, 2011.
- [44] V. Khajuria, S. Gupta, N. Sharma et al., "Anti-inflammatory potential of hentriacontane in LPS stimulated RAW 264.7 cells and mice model," *Biomedicine & Pharmacotherapy*, vol. 92, pp. 175–186, 2017.
- [45] G. S. Youn, K. W. Lee, S. Y. Choi, and J. Park, "Overexpression of HDAC6 induces pro-inflammatory responses by regulating ROS-MAPK-NF- κ B/AP-1 signaling pathways in macrophages," *Free Radical Biology & Medicine*, vol. 97, pp. 14–23, 2016.
- [46] D. R. Germolec, R. P. Frawley, and E. Evans, "Markers of inflammation," *Methods in Molecular Biology*, vol. 598, pp. 53–73, 2010.
- [47] R. Medzhitov, "Origin and physiological roles of inflammation," *Nature*, vol. 454, no. 7203, pp. 428–435, 2008.
- [48] Y. Y. Choo, S. Lee, P. H. Nguyen et al., "Caffeoylglycolic acid methyl ester, a major constituent of sorghum, exhibits anti-inflammatory activity via the Nrf 2/heme oxygenase-1 pathway," *RSC Advances*, vol. 5, no. 23, pp. 17786–17796, 2015.
- [49] S. C. Gupta, C. Sundaram, S. Reuter, and B. B. Aggarwal, "Inhibiting NF- κ B activation by small molecules as a therapeutic strategy," *Biochimica et Biophysica Acta*, vol. 1799, no. 10–12, pp. 775–787, 2010.
- [50] F. Jiang, H. Guan, D. Liu, X. Wu, M. Fan, and J. Han, "Flavonoids from sea buckthorn inhibit the lipopolysaccharide-induced inflammatory response in RAW 264.7 macrophages through the MAPK and NF- κ B pathways," *Food & Function*, vol. 8, no. 3, pp. 1313–1322, 2017.
- [51] N. R. Bhat, P. Zhang, J. C. Lee, and E. L. Hogan, "Extracellular signal-regulated kinase and p 38 subgroups of mitogen-activated protein kinases regulate inducible nitric oxide synthase and tumor necrosis factor-alpha gene expression in endotoxin-stimulated primary glial cultures," *The Journal of Neuroscience*, vol. 18, no. 5, pp. 1633–1641, 1998.
- [52] V. Waetzig, K. Czeloth, U. Hidding et al., "c-Jun N-terminal kinases (JNKs) mediate pro-inflammatory actions of microglia," *Glia*, vol. 50, no. 3, pp. 235–246, 2005.
- [53] Q. Li and I. M. Verma, "NF- κ B regulation in the immune system," *Nature Reviews Immunology*, vol. 2, no. 10, pp. 725–734, 2002.
- [54] A. Salminen, A. Kauppinen, and K. Kaarniranta, "Phytochemicals suppress nuclear factor- κ B signaling: impact on health span and the aging process," *Current Opinion in Clinical Nutrition and Metabolic Care*, vol. 15, no. 1, pp. 23–28, 2012.
- [55] T. Persson, B. O. Popescu, and A. Cedazo-Minguez, "Oxidative stress in Alzheimer's disease: why did antioxidant therapy fail?," *Oxidative Medicine and Cellular Longevity*, vol. 2014, Article ID 427318, 11 pages, 2014.
- [56] H. Li, Y. Ge, Z. Luo et al., "Evaluation of the chemical composition, antioxidant and anti-inflammatory activities of distillate and residue fractions of sweet basil essential oil," *Journal of Food Science and Technology*, vol. 54, no. 7, pp. 1882–1890, 2017.
- [57] S. Qi, Z. Feng, Q. Li, Z. Qi, and Y. Zhang, "Myricitrin modulates NADPH oxidase-dependent ROS production to inhibit endotoxin-mediated inflammation by blocking the JAK/STAT1 and NOX2/p47phox pathways," *Oxidative Medicine and Cellular Longevity*, vol. 2017, Article ID 9738745, 20 pages, 2017.
- [58] R. Kacimi, R. G. Giffard, and M. A. Yenari, "Endotoxin-activated microglia injure brain derived endothelial cells via NF- κ B, JAK-STAT and JNK stress kinase pathways," *Journal of Inflammation*, vol. 8, no. 1, p. 7, 2011.
- [59] H. Y. Zhou, E. M. Shin, L. Y. Guo et al., "Anti-inflammatory activity of 4-methoxyhonokiol is a function of the inhibition of iNOS and COX-2 expression in RAW 264.7 macrophages via NF- κ B, JNK and p38 MAPK inactivation," *European Journal of Pharmacology*, vol. 586, no. 1–3, pp. 340–349, 2008.
- [60] G. Y. Sun, Z. Chen, K. J. Jasmer et al., "Quercetin attenuates inflammatory responses in BV-2 microglial cells: role of MAPKs on the Nrf 2 pathway and induction of heme oxygenase-1," *PLoS One*, vol. 10, no. 10, article e0141509, 2015.
- [61] Y. Naito and T. Takagi, "Heme oxygenase-1 and anti-inflammatory M2 macrophages," *Archives of Biochemistry and Biophysics*, vol. 564, pp. 83–88, 2014.
- [62] M. H. Huang, B. S. Wang, C. S. Chiu et al., "Antioxidant, antinociceptive, and anti-inflammatory activities of *Xanthii Fructus* extract," *Journal of Ethnopharmacology*, vol. 135, no. 2, pp. 545–552, 2011.
- [63] M. Ben Salem, H. Affes, K. Athmouni et al., "Chemical compositions, antioxidant and anti-inflammatory activity of *Cynara scolymus* leaves extracts, and analysis of major

- bioactive polyphenols by HPLC,” *Evidence-based Complementary and Alternative Medicine*, vol. 2017, Article ID 4951937, 14 pages, 2017.
- [64] T. N. Chang, S. S. Huang, Y. S. Chang et al., “Analgesic effects and mechanisms of anti-inflammation of taraxeren-3-one from *Diospyros maritima* in mice,” *Journal of Agricultural and Food Chemistry*, vol. 59, no. 17, pp. 9112–9119, 2011.
- [65] N. Song, W. Xu, H. Guan, X. Liu, Y. Wang, and X. Nie, “Several flavonoids from *Capsella bursa-pastoris* (L.) Medic,” *Asina Journal Of Traditional Medicines*, vol. 2, no. 5, pp. 218–222, 2007.
- [66] R. Kubínová, V. Spačková, E. Svajdlenka, and K. Lučivjanská, “Antioxidant activity of extracts and HPLC analysis of flavonoids from *Capsella bursa-pastoris* (L.) Medik,” *Ceska a Slovenska Farmacie*, vol. 62, no. 4, pp. 174–176, 2013.
- [67] L. Zhao, Q. Zhang, W. Ma, F. Tian, H. Shen, and M. Zhou, “A combination of quercetin and resveratrol reduces obesity in high-fat diet-fed rats by modulation of gut microbiota,” *Food & Function*, vol. 8, no. 12, pp. 4644–4656, 2017.
- [68] Y. H. Cho, N. H. Kim, I. Khan et al., “Anti-inflammatory potential of quercetin-3-O- β -D-(“2”-galloyl)-glucopyranoside and quercetin isolated from *Diospyros kaki* calyx via suppression of MAP signaling molecules in LPS-induced RAW 264.7 macrophages,” *Journal of Food Science*, vol. 81, no. 10, pp. C2447–C2456, 2016.

Review Article

Goji Berries as a Potential Natural Antioxidant Medicine: An Insight into Their Molecular Mechanisms of Action

Zheng Fei Ma ^{1,2} Hongxia Zhang,³ Sue Siang Teh,^{3,4} Chee Woon Wang,⁵ Yutong Zhang ⁶ Frank Hayford,⁷ Liuyi Wang,¹ Tong Ma,⁸ Zihan Dong,¹ Yan Zhang,¹ and Yifan Zhu¹

¹Department of Health and Environmental Sciences, Xi'an Jiaotong-Liverpool University, Suzhou 215123, China

²School of Medical Sciences, Universiti Sains Malaysia, Kota Bharu, 15200 Kelantan, Malaysia

³Department of Food Science, University of Otago, Dunedin 9054, New Zealand

⁴Department of Food Science, Faculty of Applied Sciences, Tunku Abdul Rahman University College, Kuala Lumpur 53300, Malaysia

⁵Department of Biochemistry, Faculty of Medicine, MAHSA University, Bandar Saujana Putra, Jenjarom, 42610 Selangor, Malaysia

⁶Jinzhou Medical University, Jinzhou 121000, China

⁷Department of Nutrition and Dietetics, School of Biomedical and Allied Health Sciences, College of Health Sciences, University of Ghana, P. O. Box KB143, Korle-Bu, Accra, Ghana

⁸Department of Integrative Medicine and Neurobiology, School of Basic Medical Sciences, Shanghai Medical College, Institutes of Integrative Medicine of Fudan University, Shanghai 200032, China

Correspondence should be addressed to Zheng Fei Ma; zhengfeima@gmail.com and Yutong Zhang; zhangyutong730@hotmail.com

Received 30 June 2018; Revised 1 October 2018; Accepted 17 December 2018; Published 9 January 2019

Guest Editor: Germán Gil

Copyright © 2019 Zheng Fei Ma et al. This is an open access article distributed under the Creative Commons Attribution License, which permits unrestricted use, distribution, and reproduction in any medium, provided the original work is properly cited.

Goji berries (*Lycium* fruits) are usually found in Asia, particularly in northwest regions of China. Traditionally, dried goji berries are cooked before they are consumed. They are commonly used in Chinese soups and as herbal tea. Moreover, goji berries are used for the production of tincture, wine, and juice. Goji berries are high antioxidant potential fruits which alleviate oxidative stress to confer many health protective benefits such as preventing free radicals from damaging DNA, lipids, and proteins. Therefore, the aim of the review was to focus on the bioactive compounds and pharmacological properties of goji berries including their molecular mechanisms of action. The health benefits of goji berries include enhancing hemopoiesis, antiradiation, antiaging, anticancer, improvement of immunity, and antioxidation. There is a better protection through synergistic and additive effects in fruits and herbal products from a complex mixture of phytochemicals when compared to one single phytochemical.

1. Introduction

Goji berries (*Lycium* fruits) are obtained from two closely related plants, *Lycium chinense* and *Lycium barbarum*. They are usually found in Asia, particularly in northwest regions of China. *Lycium* belongs to the Solanaceae family that yields numerous foods, including some fruits that are yellow to red, ranging from potatoes and tomatoes to eggplants. Both of these *Lycium* species are generally marketed as goji berry as well as wolfberry. It is a 1-2 cm long berry, bright

orange-red ellipsoid colour with a sweet and tangy flavor [1]. After harvesting in late summer-early autumn, it is sun-dried as a dried fruit.

Traditionally, dried goji berries are cooked before they are consumed. They are commonly used in Chinese soups and as herbal tea. Moreover, goji berries are used for the production of tincture, wine, and juice [2]. Many pharmacological functions related to the eyes, kidney, and liver particularly have been promoted by the consumption of goji berry in populations [3]. Goji berries are often incorporated into

herb formulas. The dose of goji berries is in the range of 6-18 g. However, if goji berries are used as a single herb remedy, this dose may be insufficient. This is because the other herbs in the specific formulation may contain same components as goji berries such as polysaccharides and carotenoids. Goji berries could be used as a major component in a formulation or as a single herb. One of the recommended therapies in the treatment of atrophic gastritis is to consume twice daily with 10 g *Lycium* fruits each time. Besides that, 15 g of goji berries per day is considered beneficial to supply adequate zeaxanthin which is estimated at 3 mg/day as a dietary supplement for eye health [4]. A 20 g *Lycium* fruit in a simple tea is able to improve decreased visual perception [5]. Hence, the dosage range of goji berry alters to 15-30 grams (2- to 5-fold increases) when it is the main herb apart from that in the complex formula where the dosage range is around 6-18 g [4].

Goji berries are gradually being regarded as a functional food in many Asian countries as well as throughout Europe [3]. They also have been marketed as a health food in the western countries [6]. Goji berries recently gained a growing popularity as a “superfruit” in North America and European countries because of their potential health-promoting properties. For example, goji berries have been used to increase longevity and for the benefits to liver, kidney, and vision since ancient times [2]. Due to the rich medical properties and chemical composition, goji berry has been consumed as an important food of a health-promoting diet for hundreds of years.

2. Bioactive Compounds of Goji Berries

There are many bioactive compounds distinguished by high antioxidant potential in goji berries. The nutrients in goji berries are included 46% of carbohydrate, 16% of dietary fiber, 13% of protein, and 1.5% of fat. Thus, goji berries can be an excellent source of macronutrients. Micronutrients which included minerals and vitamins can be found in goji berries as well. There are studies that reported the presence of riboflavin, thiamine, nicotinic acid, and minerals such as copper, manganese, magnesium, and selenium in goji berries [7]. The bioactive compounds responsible for health benefits have been evaluated based on the macronutrients and micronutrients of goji berries. The high biological activity components in goji berries are polysaccharides, carotenoids, and phenolics [8]. These functional components are related with the health-promoting properties of goji berries.

The most important group of compounds present in goji berries is polysaccharides. Polysaccharides comprise 5–8% of dried fruits, and they are found in the water-soluble form of highly branched *L. barbarum* polysaccharides [1]. These six kinds of monosaccharides (i.e., arabinose, galactose, glucose, rhamnose, mannose, xylose, and galacturonic acid) are found in goji berries [5].

A group of carotenoids are the colour components of *Lycium* fruit. Carotenoids are the second highly significant group of biologically active compounds with health benefit properties present in goji berry. The total carotenoid content of different goji berries ranged from 0.03 to 0.5% of dried fruits. Being responsible for the characteristic bright and

TABLE 1: Some chemical compounds of goji berries.

Composition	
Moisture (%)	10.3
Crude protein (%)	8.9
Crude oil (%)	4.1
Fiber (%)	7.3
Total phenol (mg GAE/100 mL)	3.4
Antioxidant activity (%)	20.8
Myristic acid (%)	0.1
Stearic acid (%)	2.9
Palmitic acid (%)	8.2
Arachidic acid (%)	1.8
Oleic acid (%)	21.7

vivid orange to red colouration, the lipid soluble carotenoids occur at extremely high levels in goji berries [2]. One of the most common carotenoids found in goji berries is zeaxanthin in the form of dipalmitin zeaxanthin. In ripening goji berries, the content of zeaxanthin can reach around 77.5% of total carotenoids. Zeaxanthin palmitate (phasalien) contains 31–56% of the total carotenoids. As for now, the best natural source of dipalmitin zeaxanthin is goji berries. The fractions of beta-carotene (35.9 $\mu\text{g/g}$), cryptoxanthin, and neoxanthin (72.1 $\mu\text{g/g}$) are also detected in goji berry extracts [8].

Phenolic acids and flavonoids are examples of the phenolic compounds found in goji berries. Some phenolic compounds in goji berries are caffeic acid (3.73 $\mu\text{g/g}$), caffeoylquinic acid (0.34 $\mu\text{g/g}$), chlorogenic acid (12.4 $\mu\text{g/g}$), p-coumaric acid (6.06 $\mu\text{g/g}$), quercetin-diglucoside (66.0 $\mu\text{g/g}$), kaempferol-3-*O*-rutinoside (11.3 $\mu\text{g/g}$), and rutin (42.0 $\mu\text{g/g}$) [8]. These phenolic compounds have a very high antioxidant capacity [8]. Table 1 summarises some chemical compounds found in goji berries [9].

3. Pharmacological Properties of Goji Berries

Goji berries have become popular over the years due to its public acceptance as a “superfood” with highly advantageous antioxidant and nutritive properties. A superfood is a “nutrient-rich” food considered to be especially beneficial for health or well-being. The carotenoid content of goji berries had been drawn a lot of attention due to its beneficial effects including antioxidant property on vision, retinopathy, and macular degeneration.

In very recent years, interest of consumers about the health benefits of different berry-type fruits, their resultant juices, and their capsules has quickly increased [10]. Berry fruits are rich in antioxidant phytochemicals [11, 12], and these antioxidants are capable of performing a number of functions. The present interest about the properties of several kinds of berries is also shown by the numerous scientific articles published in journals in the last few years. The biennial International Berry Health Benefits Symposium started in 2005 and in their latest research also focused on berry consumption in relation to human health as a key component of their symposium [13, 14]. The most extensively consumed

berry-type products are derived from goji (*Lycium barbarum*), chia (*Salvia hispanica*), açai (*Euterpe oleracea* Martius), jujuba (*Ziziphus jujuba*), pomegranate (*Punica granatum*), and mangosteen (*Garcinia mangostana*) [10]. The dietary intake of berry fruits has been shown to have a positive impact on human health, performance, and disease [15–24]. All these fruits support the immune system and are rich in nutrients. Overall, they have a significant concentration of phytoosterols, monounsaturated fats, antioxidants, essential amino acids, trace minerals, dietary fiber, and fat- and water-soluble vitamins [25].

Goji berry polysaccharides, for instance, are a well-known traditional Chinese medicine and tonic food for many years. In connection with its health benefits, *Lycium barbarum* polysaccharides (LBPs) are one of the most valuable functional components [5, 26]. In recent years, *L. barbarum* is being used not only in China but also worldwide as a health dietary supplement in several forms including juice and tea [27]. Consuming products made from *L. barbarum* might help to decrease blood lipid concentration, promote fertility, and improve immunity [17, 19, 27–29].

3.1. Vision-Protective Effect. The mixture of highly branched polysaccharides and proteoglycans in LBPs has been reported to exert ocular neuroprotective effects [30, 31]. Goji berries, which contain a specific profile of carotenoid species [2, 32], have high carotenoid metabolites, with zeaxanthin making up almost 60% of the total carotenoids in the fruit [33]. Carotenoids are main natural pigments accountable for the yellow, red, and orange colours of many types of fruits and vegetables [34]. They also have many biological actions including the pro-vitamin A's antioxidant activity.

LBPs are the active components which may improve visual function. Chu et al. [28] reported an animal study investigating the effects of LBPs (1 mg/kg) on localised changes of rats' retinal function in a partial optic nerve transection (PONT) model. The multifocal electroretinograms (mfERG) were obtained from Sprague-Dawley rats. One week later, a substantial decrease of major positive component (P1) and photopic negative response (PhNR) amplitudes of mfERG were detected in all retinal regions. Feeding with LBPs prior to PONT preserved the functions of retina. All mfERG responses were reported to be within the normal range in the superior retina, and most of the inferior retinal responses were considerably increased at week 4. The retina ventral part had secondary degeneration which affected the ganglion cell layer and outer retina. LBPs caused alterations to the functional reduction caused by PONT by regulating the signal from the outer retina. Zhu et al. reported that LBPs inhibited the N-methyl-N-nitrosourea-induced rat photoreceptor cell apoptosis [35]. In addition, LBPs also protected the retinal structure by regulating the expressions of caspase and PARP [35].

The protective characteristics of goji berry extracts on retina cells have been shown in the early stage of the retina degeneration in both human and animal studies [1]. Consumption of dietary *L. barbarum* has been shown to be retinoprotective. A study by Yu et al. in 2013 showed that 1% (kcal) wolfberry upregulated carotenoid metabolic genes

of zeaxanthin and luteolin and also improved the biogenesis of mitochondria in the retina of db/db diabetic mice [36]. It has been suggested that inhibited expression of these zeaxanthin and luteolin-metabolizing genes can cause hyperglycaemia, which increases the risk of retinopathy [1].

Using Royal College of Surgeons (RCS) rats as a hereditary retinal dystrophy model, Ni et al. examined the potential neuroprotective effects of aqueous extract of dried *L. barbarum* [37]. The results indicated that the aqueous extract of dried *L. barbarum* might possess a neuroprotective activity on the retinal tissue of RCS rats at the initial stage by hindering apoptosis involving caspase-2 protein and protecting photoreceptors [37]. Prior studies had established that apoptosis is the dominant mechanism of photoreceptor degeneration in RCS rats [38, 39]. The contribution of polysaccharide fractions of *L. barbarum* to the prevention of glaucoma was further demonstrated on the retinal ganglion cells (RGC) in rats with high intraocular pressure (IOP), indicating the neuroprotective effect of *L. barbarum* [40]. Further research work by Tang et al. [41] and Hu et al. [42] also established the protective effect of *L. barbarum* on diabetic retinal injury.

Goji berries have also been shown to exhibit macular benefits in a randomized controlled study of healthy elderly participants [43]. It was observed that after 90 days of daily dietary supplementation with 13.7 g lacto-wolfberry (LWB) (a proprietary milk-based formulation of goji berry) elevated plasma antioxidant and zeaxanthin levels goji, by 26% and 57%, respectively, in supplemented subjects [43]. It is also suggested that taurine, a nonessential free amino acid in goji extracts, may hinder the diabetic retinopathy progress through elevated cAMP levels and enhanced PPAR- γ activity in retinal cells [44]. Taurine is found abundantly in goji. Goji powder extracted with methanol contains $10.7 \pm 0.1\%$ taurine (*w/w*). Elevated cAMP levels have been known as protective against the dysfunction of the endothelial barrier [45, 46]. Results from Pavan et al. [47] strongly suggested that in high glucose-treated cells, elevated cAMP concentrations mediate the impairment of the epithelial barrier and goji berries could be used to achieve their reversal. The protective property of *L. barbarum* extract was also confirmed by Shen et al. using human retina neuron cells [48].

3.2. Lipid-Lowering Effect. The lipid-lowering health benefit of LBP and its purified constituents have been demonstrated in animals with limited clinical studies in humans. Besides having antioxidant activity in vitro [8, 49, 50] and in vivo [49, 51], they have also shown to have the ability to lower the blood lipid concentrations of alloxan-induced diabetic rabbits [7] and mice fed by high-fat diet (HFD) [52]. Ming et al.'s research showed that abnormal lipid peroxidation parameters were returned to near normal level and lipid peroxidation accumulation was inhibited after administering LPS to mice fed on HFD. This suggests that LBP seems to play an imperative role in lipid metabolism [52]. The results were consistent with previous findings, where mice and rats fed with polysaccharide fractions supplemented with HFD were characterized by lowered concentration of total cholesterol, LDL-cholesterol, and triglycerides and increased

concentration of HDL-cholesterol compared to mice and rats on high-fat diets without polysaccharide fractions [53–55]. The evaluation of the lipid profile of diabetic mice and rats fed on goji extract also showed the same results compared with the diabetic controls [1, 7]. However, clinical studies on the lipid-lowering properties of goji berries were limited and almost exclusively performed in China. More so, original data are hardly accessible, and studies were mostly small-sized and may not have been adequately controlled. A study of 25 Chinese subjects aged 64–80 years had their blood lipid peroxides significantly decreased by 65% after 10 days of ingestion of 50 g/d dry goji berries [56, 57]. However, the small size of the study ($N = 25$) and the subjectivity of most parameters must be critically pointed out. An *in vivo* investigation of the effects of serum LBP-standardized *L. barbarum* preparation (GoChi) in a randomized, double-blind, placebo-controlled clinical study involving 50 Chinese healthy adults aged 55–72 years showed a significant decrease in lipid peroxidation (shown by lower concentrations of malondialdehyde (MDA)) by 8.7% and 6.0% pre-intervention and post-intervention in the GoChi group compared with the placebo group, respectively. This was after they were given GoChi or placebo (120 mL/d) for 30 days [26].

3.3. Hypoglycaemic Effect. Diabetes mellitus is characterized by abnormally high levels of blood glucose, and it is also known as hyperglycaemia [58]. Due to the high cost and adverse side effects of many oral hypoglycaemic agents, the exploration and discovery of safer and more effective substitutes have become very important and significant. This has led to the investigation for hypoglycaemic activity in other more traditionally edible food sources such as goji berries which have been shown to have a hypoglycaemic effect in cell and animal studies [1]. A cell experiment on hypoglycaemic effects for instance proved that LBP3b (an extraction from *L. barbarum* fruit) showed a concentration-dependent effect on glucose uptake [59]. Male Wistar HFD-STZ-induced diabetic rats administered with immunoglobulin (Ig) LBP and LBP-IV once daily for 4 continuous weeks and treated with LBP (100 mg/kg) and LBP-IV (200, 100, and 50 mg/kg) after showed significantly decreased concentrations of HbA1 and blood glucose of diabetic rats compared to the diabetic control group [60]. Alloxan-induced diabetic rabbits fed with crude LBP and purified polysaccharide fraction (LBP-X) from *L. barbarum* for 10 days also showed a significant reduction in blood glucose level [7, 61]. Similar results were observed after a 28-day treatment in alloxan-induced diabetic mice with LBP [62–64]. This was consistent with Zou et al.'s [65] findings where the rat insulinoma cell line was used. Very limited or no clinical human studies exist, however.

3.4. Allergic and Anaphylactic Reactions. Monzon-Ballarín et al. [66] described two clinical cases who reported allergic symptoms after goji berry ingestion. The patients had a positive skin prick test and a detection of specific immunoglobulin (Ig) E to goji berry. An analysis of the allergenic profile of the two patients showed a 9 kDa band, suggesting that

the corresponding protein might be related to lipid transfer proteins (LTPs). Larramendi et al. [67] further reported a study involving 31 subjects in Spain. The subjects included five patients reporting allergic symptoms on intake of goji berries, six tolerating the berries, and 20 never having eaten goji berries. All subjects underwent skin prick tests with goji berries, as well as with peach peel and plant food panallergens as biomarkers of cross-reactivity between unrelated foods. They reported that the skin tests to goji berries were positive in 24 subjects (77%). Positivity to goji berries was related with positivity to peach peel and to the panallergen-nonspecific LTPs.

3.5. Anticancer, Antitumour, Immunostimulatory, and Modulatory Effects. Goji berries have been utilised in traditional Chinese medicine to prevent the onset and progression of cancer for so many years, due to its rich phytochemical and antioxidant composition [1]. Some of its ingredients might have a better therapeutic effect on cancer than other foods. Hsu et al. [68] have reported that the *L. barbarum* carotenoid nanoemulsion was more effective in inhibiting HT-29 cancer cells as compared to that of the carotenoid extract. Furthermore, both nanoemulsion and extract could upregulate p53 and p21 expression and downregulate CDK1, CDK2, cyclin A, and cyclin B expression and arrest the cell cycle at G2/M. Moreover, attributing to most of the biological effects of the fruits including anticancer, antitumour, and immunomodulatory and properties, goji berries are unusually rich in water-soluble peptide-conjugated polysaccharides (i.e., LBPs) [69–71]. They have the ability to enhance or potentiate the host defence mechanisms in a way to inhibit tumour growth without harming the host. Research work conducted by Tang et al. [41] and Gan et al. [69] established that compounds in goji berries have proapoptotic and antiproliferative activity against cancer cells.

3.6. Neurological Protective Effect. The neurological protective effect of goji berries has been demonstrated in an experimental study including human clinical trial. Glutamate has been shown to be excitotoxic and is being implicated in many neurodegenerative diseases including Parkinson's disease and Alzheimer's disease [61, 72]. Thus, reduction of glutamate toxicity is considered a therapeutic strategy for those neurodegenerative diseases.

A study by Yang et al. [73] showed that LBP pretreatment significantly improved neurological deficits by decreasing the infarct size, hemispheric swelling, and water content in an experimental stroke model C57BL/6N male mice fed with either vehicle (PBS) or LBP (1 or 10 mg/kg) daily for 7 days, indicating the neuroprotective effect of LBP. LBP again improved the survival rate and promoted the growth of mixed cultured retinal ganglion cells, from neonatal Sprague-Dawley rats [74]. The first double-blind randomized control study performed outside China to assess the general effects of goji juice (GoChi™) in young healthy adults concluded that consumption of GoChi™ for 14 days improved neurological performance generally [75]. It should be noted

however that assessment of most parameters was subjective and the sample size was small in this study ($N = 34$).

3.7. Cardiovascular Protective Effect. In an experiment to investigate the role of LBP in the reduction of myocardial injury in ischemia/reperfusion among rats, the rat heart LBP significantly reduced the myocardium Bax-positive rate; also, through dose-dependent methods, the apoptosis of myocardial cell and increase in Bcl-2 positive rate suggest that LBP can prevent further development and deterioration of CVD [76]. Regarding the effects on renal vascular tension of LBP, Jia et al. [77] tested the one-clip hypertension model among rats with hypertension. It was observed that compared to rats not treated for hypertension, in isolated aortic rings of LBP-treated rats, the reduced phenylephrine contraction was observed, causing that LBP-treated rats were significantly prevented from elevated blood pressure. Another experiment was that rats with hyperlipidemia were administered to take different concentrations (1 g/kg to 4 g/kg) of *L. barbarum* decoction for 10 consecutive days by gastric perfusion. The authors reported that in the serum and liver of rats, total cholesterol and triglyceride levels were reduced; also, the level of serum low-density lipoprotein-(LDL-) C was decreased [5, 78]. A similar result was observed in a study by Luo et al. [7]. LBPs lowered serum total cholesterol and triglyceride levels; meanwhile, the high-density lipoprotein (HDL) cholesterol level was increased after a 10-day treatment among rabbits.

3.8. Antiaging Effects. In a recent review, Gao et al. [79] have discussed the various components contributing to the antiaging properties of *L. barbarum*. These notable components are LBPs, betaine, β -carotene, zeaxanthin, 2-O- β -D-glucopyranosyl-L-ascorbic acid (AA- 2β G), and flavanoids [79]. *L. barbarum* contains betaine (a natural amino-acid). The Lycium Chinese Miller fruit extract containing betaine has been shown to mitigate carbon tetrachloride- (CCl₄-) induced hepatic injury by increasing antioxidative activity and lowering inflammatory mediators such as COX-1/COX-2 and iNOS. Histopathological examination was employed to confirm the ameliorative effects of the extract and betaine [80].

Betaine has been shown to be an anti-inflammation agent associated with colon carcinogenesis. It also has been shown to possess a tumour-preventing effect on colitis-associated cancer in mice induced by azoxymethane. Administration with betaine significantly lowered the incidence of tumour formation with downregulation of inflammation. Treatment with betaine also inhibited the production of the ROS and GSSG level in colonic mucosa and inhibited inflammatory cytokines including IL-6, iNOS, TNF- α , and COX-2 [81]. Betaine has been shown to have preventive effects on ultraviolet B (UVB) irradiation-induced skin damage in mice. UVB is a common kind of free radical that can cause extrinsic aging, such as skin aging. Betaine has been proved to reduce photodamage caused by UVB irradiation. Betaine can be used to suppress the formation of UVB-induced wrinkle and collagen damage by inhibiting the extracellular signal-regulated kinase (ERK), protein kinase (MEK), and matrix metalloproteinase 9 (MMP-9) [82].

3.9. Adverse Effects of Goji Berries. Apart from the allergic and anaphylactic reactions, other side effects that consumers should be aware of are to be mentioned. These include the presence of organic toxic substances and risk of interactions with other prescriptions besides allergy. Atropine, a toxic alkaloid, is naturally present in goji berry. The content was reported to be at toxic level. In a further work by Adam and co-workers, the atropine concentration in eight samples of goji berries using HPLC-MS was found to be maximally 19 ppb (*w/w*). Therefore, its content is far below toxic levels (Adam et al., 2006).

Patients who experienced interactions between goji berries and warfarin have been described in three published case reports. Warfarin is prescribed as a common anticoagulation therapy. The international normalized ratio (INR) was observed to elevate in patients after drinking goji tea [83]. Increased bleeding from the rectum and nose was observed in another patient who drank goji berry juice [84]. Most recently, a study by Zhang et al. reported that an elderly man taking a prolonged maintenance dose of warfarin after drinking goji berry wine experienced an increased international normalized ratio (INR) with associated bleeding [85]. Other possible interactions between goji berries and prescription medications are still unknown. It is important to take into consideration the possible risks of taking goji berries in individuals taking medications with a narrow therapeutic index.

Arroyo-Martinez et al. described a case report of toxic hepatitis related to the use of goji. The symptoms reported included nonbloody diarrhea, asthenia, and colic abdominal pain. The patient had a mild mucocutaneous jaundice and a generalized erythematous and pruriginous maculopapular rash. The patient consumed goji berry tea 3 times a day [86]. The liver function tests were elevated. Goji berries have been shown to modulate the expression of CYP2C9 and CYP2E1 and have an immunomodulatory property [2]. However, another possible change in goji composition is contamination, during its production and post-marketing. Thus, the toxic side effects of post-marketing surveillance are another area of concern.

4. Conclusion

Similar to other plants [87–91], goji berries are a high antioxidant potential fruits which alleviate oxidative stress to confer many health protective benefits such as preventing free radicals from damaging DNA, lipids, and proteins. There is a better protection through synergistic and additive effects in fruits and herbal products from a complex mixture of phytochemicals than from a single phytochemical. The health benefits of goji berries include enhancing hemopoiesis, anti-radiation, antiaging, anticancer, improvement of immunity, and antioxidation.

Conflicts of Interest

The authors declare that they have no conflicts of interest.

Acknowledgments

Zheng Feei Ma would like to thank Siew Poh Tan, Peng Keong Ma, Zheng Xiong Ma, Siew Huah Tan, and Feng Yuan Lau for their active encouragement and support of this work.

References

- [1] B. Kulczyński and A. Gramza-Michałowska, "Goji berry (*Lycium barbarum*): composition and health effects—a review," *Polish Journal of Food and Nutrition Sciences*, vol. 66, no. 2, pp. 67–76, 2016.
- [2] O. Potterat, "Goji (*Lycium barbarum* and *L. chinense*): phytochemistry, pharmacology and safety in the perspective of traditional uses and recent popularity," *Planta Medica*, vol. 76, no. 1, pp. 7–19, 2010.
- [3] J. Cheng, Z.-W. Zhou, H.-P. Sheng et al., "An evidence-based update on the pharmacological activities and possible molecular targets of *Lycium barbarum* polysaccharides," *Drug Design, Development and Therapy*, vol. 9, pp. 33–78, 2015.
- [4] C. Y. Cheng, W. Y. Chung, Y. T. Szeto, and I. F. F. Benzie, "Fasting plasma zeaxanthin response to *Fructus barbarum* L. (wolfberry; Kei Tze) in a food-based human supplementation trial," *British Journal of Nutrition*, vol. 93, no. 1, pp. 123–130, 2007.
- [5] H. Amagase and N. R. Farnsworth, "A review of botanical characteristics, phytochemistry, clinical relevance in efficacy and safety of *Lycium barbarum* fruit (goji)," *Food Research International*, vol. 44, no. 7, pp. 1702–1717, 2011.
- [6] T. Xin, H. Yao, H. Gao et al., "Super food *Lycium barbarum* (Solanaceae) traceability via an internal transcribed spacer 2 barcode," *Food Research International*, vol. 54, no. 2, pp. 1699–1704, 2013.
- [7] Q. Luo, Y. Cai, J. Yan, M. Sun, and H. Corke, "Hypoglycemic and hypolipidemic effects and antioxidant activity of fruit extracts from *Lycium barbarum*," *Life Sciences*, vol. 76, no. 2, pp. 137–149, 2004.
- [8] C. Wang, S. Chang, B. S. Inbaraj, and B. Chen, "Isolation of carotenoids, flavonoids and polysaccharides from *Lycium barbarum* L. and evaluation of antioxidant activity," *Food Chemistry*, vol. 120, no. 1, pp. 184–192, 2010.
- [9] Z. Endes, N. Uslu, M. M. Özcan, and F. Er, "Physico-chemical properties, fatty acid composition and mineral contents of goji berry (*Lycium barbarum* L.) fruit," *Journal of Agroalimentary Processes and Technologies*, vol. 21, no. 1, pp. 36–40, 2015.
- [10] E. Llorent-Martínez, M. Fernández-de Córdova, P. Ortega-Barrales, and A. Ruiz-Medina, "Characterization and comparison of the chemical composition of exotic superfoods," *Microchemical Journal*, vol. 110, pp. 444–451, 2013.
- [11] J. Lachman, M. Orsák, and V. Pivec, "Antioxidant contents and composition in some vegetables and their role in human nutrition," *Zahradnictví (Horticultural Science)*, vol. 27, no. 2, pp. 65–78, 2000.
- [12] J. Lachman, M. Orsák, and V. Pivec, "Antioxidant contents and composition in some fruits and their role in human nutrition," *Zahradnictví (Horticultural Science)*, vol. 27, no. 3, pp. 103–117, 2000.
- [13] N. P. Seeram, "Berry fruits: compositional elements, biochemical activities, and the impact of their intake on human health, performance, and disease," *Journal of Agricultural and Food Chemistry*, vol. 56, no. 3, pp. 627–629, 2008.
- [14] N. P. Seeram, "Recent trends and advances in berry health benefits research," *Journal of Agricultural and Food Chemistry*, vol. 58, no. 7, pp. 3869–3870, 2010.
- [15] J. H. Xie, X. Liu, M. Y. Shen et al., "Purification, physicochemical characterisation and anticancer activity of a polysaccharide from *Cyclocarya paliurus* leaves," *Food Chemistry*, vol. 136, no. 3–4, pp. 1453–1460, 2013.
- [16] J. H. Xie, F. Zhang, Z. J. Wang, M. Y. Shen, S. P. Nie, and M. Y. Xie, "Preparation, characterization and antioxidant activities of acetylated polysaccharides from *Cyclocarya paliurus* leaves," *Carbohydrate Polymers*, vol. 133, pp. 596–604, 2015.
- [17] D.-F. Huang, Y.-F. Tang, S.-P. Nie, Y. Wan, M.-Y. Xie, and X.-M. Xie, "Effect of phenylethanoid glycosides and polysaccharides from the seed of *Plantago asiatica* L. on the maturation of murine bone marrow-derived dendritic cells," *European Journal of Pharmacology*, vol. 620, no. 1–3, pp. 105–111, 2009.
- [18] D. Changbo and S. Zhaojun, "Supplementation of *Lycium barbarum* polysaccharides protection of skeletal muscle from exercise-induced oxidant stress in mice," *African Journal of Pharmacy and Pharmacology*, vol. 6, no. 9, pp. 643–647, 2012.
- [19] X. Xu, B. Shan, C. H. Liao, J. H. Xie, P. W. Wen, and J. Y. Shi, "Anti-diabetic properties of *Momordica charantia* L. polysaccharide in alloxan-induced diabetic mice," *International Journal of Biological Macromolecules*, vol. 81, pp. 538–543, 2015.
- [20] Y.-P. Chin, S.-F. Chang, C.-C. Tseng, and M.-C. Chen, "Escherichia coli capsular polysaccharide synthesis, antibiotic susceptibility, and red blood cell agglutination," *Journal of Experimental & Clinical Medicine*, vol. 6, no. 1, pp. 16–20, 2014.
- [21] J.-H. Xie, M.-Y. Shen, M.-Y. Xie et al., "Ultrasonic-assisted extraction, antimicrobial and antioxidant activities of *Cyclocarya paliurus* (Batal.) Iljinskaja polysaccharides," *Carbohydrate Polymers*, vol. 89, no. 1, pp. 177–184, 2012.
- [22] S. M. Al-Reza, J. I. Yoon, H. J. Kim, J. S. Kim, and S. C. Kang, "Anti-inflammatory activity of seed essential oil from *Zizyphus jujuba*," *Food and Chemical Toxicology*, vol. 48, no. 2, pp. 639–643, 2010.
- [23] C. J. Liu and J. Y. Lin, "Anti-inflammatory and anti-apoptotic effects of strawberry and mulberry fruit polysaccharides on lipopolysaccharide-stimulated macrophages through modulating pro-/anti-inflammatory cytokines secretion and Bcl-2/Bax protein ratio," *Food and Chemical Toxicology*, vol. 50, no. 9, pp. 3032–3039, 2012.
- [24] H. Zhang, Z. F. Ma, X. Luo, and X. Li, "Effects of mulberry fruit (*Morus alba* L.) consumption on health outcomes: a mini-review," *Antioxidants*, vol. 7, no. 5, p. 69, 2018.
- [25] M. Jeszka-Skowron, A. Zgola-Grzeskowiak, E. Stanisz, and A. Waskiewicz, "Potential health benefits and quality of dried fruits: goji fruits, cranberries and raisins," *Food Chemistry*, vol. 221, pp. 228–236, 2017.
- [26] H. Amagase, B. Sun, and C. Borek, "*Lycium barbarum* (goji) juice improves in vivo antioxidant biomarkers in serum of healthy adults," *Nutrition Research*, vol. 29, no. 1, pp. 19–25, 2009.
- [27] J.-H. Xie, W. Tang, M.-L. Jin, J.-E. Li, and M.-Y. Xie, "Recent advances in bioactive polysaccharides from *Lycium barbarum*

- L., *Zizyphus jujuba* Mill, *Plantago* spp., and *Morus* spp.: structures and functionalities,” *Food Hydrocolloids*, vol. 60, pp. 148–160, 2016.
- [28] P. H. Chu, H. Y. Li, M. P. Chin, K. F. So, and H. H. Chan, “Effect of lycium barbarum (wolfberry) polysaccharides on preserving retinal function after partial optic nerve transection,” *PLoS One*, vol. 8, no. 12, article e81339, 2013.
- [29] W. Liu, Y. Liu, R. Zhu et al., “Structure characterization, chemical and enzymatic degradation, and chain conformation of an acidic polysaccharide from *Lycium barbarum* L,” *Carbohydrate Polymers*, vol. 147, pp. 114–124, 2016.
- [30] S. Y. Li, D. Yang, C. M. Yeung et al., “Lycium barbarum polysaccharides reduce neuronal damage, blood-retinal barrier disruption and oxidative stress in retinal ischemia/reperfusion injury,” *PLoS One*, vol. 6, no. 1, article e16380, 2011.
- [31] X. S. Mi, Q. Feng, A. C. Lo et al., “Protection of retinal ganglion cells and retinal vasculature by *Lycium barbarum* polysaccharides in a mouse model of acute ocular hypertension,” *PLoS One*, vol. 7, no. 10, article e45469, 2012.
- [32] I. Bondia-Pons, O. Savolainen, R. Törrönen, J. A. Martinez, K. Poutanen, and K. Hanhineva, “Metabolic profiling of goji berry extracts for discrimination of geographical origin by non-targeted liquid chromatography coupled to quadrupole time-of-flight mass spectrometry,” *Food Research International*, vol. 63, pp. 132–138, 2014.
- [33] B. S. Inbaraj, H. Lu, C. F. Hung, W. B. Wu, C. L. Lin, and B. H. Chen, “Determination of carotenoids and their esters in fruits of *Lycium barbarum* Linnaeus by HPLC-DAD-APCI-MS,” *Journal of Pharmaceutical and Biomedical Analysis*, vol. 47, no. 4–5, pp. 812–818, 2008.
- [34] Q. Zhang, W. Chen, J. Zhao, and W. Xi, “Functional constituents and antioxidant activities of eight Chinese native goji genotypes,” *Food Chemistry*, vol. 200, pp. 230–236, 2016.
- [35] Y. Zhu, Q. Zhao, H. Gao, X. Peng, Y. Wen, and G. Dai, “Lycium barbarum polysaccharides attenuates N-methyl-N-nitrosourea-induced photoreceptor cell apoptosis in rats through regulation of poly (ADP-ribose) polymerase and caspase expression,” *Journal of Ethnopharmacology*, vol. 191, pp. 125–134, 2016.
- [36] H. Yu, L. Wark, H. Ji et al., “Dietary wolfberry upregulates carotenoid metabolic genes and enhances mitochondrial biogenesis in the retina of db/db diabetic mice,” *Molecular Nutrition & Food Research*, vol. 57, no. 7, pp. 1158–1169, 2013.
- [37] T. Ni, G. Wei, X. Yin, X. Liu, and D. Liu, “Neuroprotective effect of *Lycium barbarum* on retina of Royal College of Surgeons (RCS) rats: a preliminary study,” *Folia Neuropathologica*, vol. 51, no. 2, pp. 158–163, 2013.
- [38] G. H. Travis, “Mechanisms of cell death in the inherited retinal degenerations,” *American Journal of Human Genetics*, vol. 62, no. 3, pp. 503–508, 1998.
- [39] M. O. Tso, C. Zhang, A. S. Abler et al., “Apoptosis leads to photoreceptor degeneration in inherited retinal dystrophy of RCS rats,” *Investigative Ophthalmology & Visual Science*, vol. 35, no. 6, pp. 2693–2699, 1994.
- [40] K. Chiu, Y. Zhou, S. C. Yeung et al., “Up-regulation of crystallins is involved in the neuroprotective effect of wolfberry on survival of retinal ganglion cells in rat ocular hypertension model,” *Journal of Cellular Biochemistry*, vol. 110, no. 2, pp. 311–320, 2010.
- [41] L. Tang, Y. Zhang, Y. Jiang et al., “Dietary wolfberry ameliorates retinal structure abnormalities in db/db mice at the early stage of diabetes,” *Experimental Biology and Medicine*, vol. 236, no. 9, pp. 1051–1063, 2011.
- [42] C. K. Hu, Y. J. Lee, C. M. Colitz, C. J. Chang, and C. T. Lin, “The protective effects of *Lycium barbarum* and *Chrysanthemum morifolium* on diabetic retinopathies in rats,” *Veterinary Ophthalmology*, vol. 15, pp. 65–71, 2012.
- [43] P. Bucheli, K. Vidal, L. Shen et al., “Goji berry effects on macular characteristics and plasma antioxidant levels,” *Optometry and Vision Science*, vol. 88, no. 2, pp. 257–262, 2011.
- [44] M. K. Song, N. K. Salam, B. D. Roufogalis, and T. H. W. Huang, “Lycium barbarum (goji berry) extracts and its taurine component inhibit PPAR- γ -dependent gene transcription in human retinal pigment epithelial cells: possible implications for diabetic retinopathy treatment,” *Biochemical Pharmacology*, vol. 82, no. 9, pp. 1209–1218, 2011.
- [45] S. L. Sayner, M. Alexeyev, C. W. Dessauer, and T. Stevens, “Soluble adenylyl cyclase reveals the significance of cAMP compartmentation on pulmonary microvascular endothelial cell barrier,” *Circulation Research*, vol. 98, no. 5, pp. 675–681, 2006.
- [46] R. Fischmeister, “Is cAMP good or bad?: depends on where it’s made,” *Circulation Research*, vol. 98, no. 5, pp. 582–584, 2006.
- [47] B. Pavan, A. Capuzzo, and G. Forlani, “High glucose-induced barrier impairment of human retinal pigment epithelium is ameliorated by treatment with goji berry extracts through modulation of cAMP levels,” *Experimental Eye Research*, vol. 120, pp. 50–54, 2014.
- [48] Z. J. Shen, J. J. Wang, and G. L. Li, “Effect of extract of *Lycium barbarum* L. on adult human retinal nerve cells,” *Zhonghua Yan Ke Za Zhi*, vol. 48, no. 9, pp. 824–828, 2012.
- [49] B. Liang, M. Jin, and H. Liu, “Water-soluble polysaccharide from dried *Lycium barbarum* fruits: isolation, structural features and antioxidant activity,” *Carbohydrate Polymers*, vol. 83, no. 4, pp. 1947–1951, 2011.
- [50] M. Ke, X.-J. Zhang, Z.-H. Han et al., “Extraction, purification of *Lycium barbarum* polysaccharides and bioactivity of purified fraction,” *Carbohydrate Polymers*, vol. 86, no. 1, pp. 136–141, 2011.
- [51] J. Xiao, E. C. Liang, Y. P. Ching et al., “Lycium barbarum polysaccharides protect mice liver from carbon tetrachloride-induced oxidative stress and necroinflammation,” *Journal of Ethnopharmacology*, vol. 139, no. 2, pp. 462–470, 2012.
- [52] M. Ming, L. Guanhua, Y. Zhanhai, C. Guang, and Z. Xuan, “Effect of the *Lycium barbarum* polysaccharides administration on blood lipid metabolism and oxidative stress of mice fed high-fat diet in vivo,” *Food Chemistry*, vol. 113, no. 4, pp. 872–877, 2009.
- [53] X. M. Li, Y. L. Ma, and X. J. Liu, “Effect of the *Lycium barbarum* polysaccharides on age-related oxidative stress in aged mice,” *Journal of Ethnopharmacology*, vol. 111, no. 3, pp. 504–511, 2007.
- [54] B. Cui, S. Liu, X. Lin et al., “Effects of *Lycium barbarum* aqueous and ethanol extracts on high-fat-diet induced oxidative stress in rat liver tissue,” *Molecules*, vol. 16, no. 11, pp. 9116–9128, 2011.
- [55] P. G. Pai, P. U. Habeeba, S. Ullal, P. A. Shoeb, M. Pradeepti, and K. Ramya, “Evaluation of hypolipidemic effects of *Lycium barbarum* (goji berry) in a murine model,” *Journal of natural remedies*, vol. 13, no. 1, pp. 4–8, 2013.

- [56] W. Li, S. Z. Dai, W. Ma, and L. Gao, "Effects of oral administration of wolfberry on blood superoxide dismutase (SOD), hemoglobin (Hb) and lipid peroxide (LPO) levels in old people," *Chinese Traditional and Herbal Drugs*, vol. 22, pp. 96–99, 1991.
- [57] D. Burke, C. Smidt, and L. Vuong, "Momordica cochinchinensis, Rosa roxburghii, wolfberry, and sea buckthorn-highly nutritional fruits supported by tradition and science," *Current Topics in Nutraceutical Research*, vol. 3, no. 4, p. 259, 2005.
- [58] A. F. Amos, D. J. McCarty, and P. Zimmet, "The rising global burden of diabetes and its complications: estimates and projections to the year 2010," *Diabetic Medicine*, vol. 14, no. S5, pp. S1–85, 1997.
- [59] H.-L. Tang, C. Chen, S.-K. Wang, and G.-J. Sun, "Biochemical analysis and hypoglycemic activity of a polysaccharide isolated from the fruit of *Lycium barbarum* L.," *International Journal of Biological Macromolecules*, vol. 77, pp. 235–242, 2015.
- [60] R. Zhao, R. Jin, Y. Chen, and F.-M. Han, "Hypoglycemic and hypolipidemic effects of *Lycium barbarum* polysaccharide in diabetic rats," *Chinese herbal medicines*, vol. 7, no. 4, pp. 310–315, 2015.
- [61] M. Jin, Q. Huang, K. Zhao, and P. Shang, "Biological activities and potential health benefit effects of polysaccharides isolated from *Lycium barbarum* L.," *International Journal of Biological Macromolecules*, vol. 54, pp. 16–23, 2013.
- [62] L. Jing, G. Cui, Q. Feng, and Y. Xiao, "Evaluation of hypoglycemic activity of the polysaccharides extracted from *Lycium Barbarum*," *African Journal of Traditional, Complementary, and Alternative Medicines*, vol. 6, no. 4, pp. 579–584, 2009.
- [63] L. Jing and L. Yin, "Antihyperglycemic activity of polysaccharide from *Lycium barbarum*," *Journal of Medicinal Plants Research*, vol. 4, no. 1, pp. 23–26, 2010.
- [64] Z. Zhou, L. Jing, G. Cui, Q. Feng, and Y. Xiao, "Effects of polysaccharide from *Lycium barbarum* in alloxan-induced diabetic mice," *African Journal of Biotechnology*, vol. 8, no. 23, 2009.
- [65] S. Zou, X. Zhang, W. Yao, Y. Niu, and X. Gao, "Structure characterization and hypoglycemic activity of a polysaccharide isolated from the fruit of *Lycium barbarum* L.," *Carbohydrate Polymers*, vol. 80, no. 4, pp. 1161–1167, 2010.
- [66] S. Monzon Ballarin, M. A. Lopez-Matas, D. Saenz Abad, N. Perez-Cinto, and J. Carnes, "Anaphylaxis associated with the ingestion of goji berries (*Lycium barbarum*)," *Journal of Investigational Allergology & Clinical Immunology*, vol. 21, no. 7, pp. 567–570, 2011.
- [67] C. H. Larramendi, J. L. Garcia-Abujeta, S. Vicario et al., "Goji berries (*Lycium barbarum*): risk of allergic reactions in individuals with food allergy," *Journal of Investigational Allergology & Clinical Immunology*, vol. 22, no. 5, pp. 345–350, 2012.
- [68] H. J. Hsu, R. F. Huang, T. H. Kao, B. S. Inbaraj, and B. H. Chen, "Preparation of carotenoid extracts and nanoemulsions from *Lycium barbarum* L. and their effects on growth of HT-29 colon cancer cells," *Nanotechnology*, vol. 28, no. 13, article 135103, 2017.
- [69] L. Gan, S. Hua Zhang, X. Liang Yang, and H. Bi Xu, "Immunomodulation and antitumor activity by a polysaccharide-protein complex from *Lycium barbarum*," *International Immunopharmacology*, vol. 4, no. 4, pp. 563–569, 2004.
- [70] L. Gan, S. H. Zhang, Q. Liu, and H. B. Xu, "A polysaccharide-protein complex from *Lycium barbarum* upregulates cytokine expression in human peripheral blood mononuclear cells," *European Journal of Pharmacology*, vol. 471, no. 3, pp. 217–222, 2003.
- [71] V. E. Ooi and F. Liu, "Immunomodulation and anti-cancer activity of polysaccharide-protein complexes," *Current Medicinal Chemistry*, vol. 7, no. 7, pp. 715–729, 2000.
- [72] Y.-S. Ho, M.-S. Yu, S.-Y. Yik, K.-F. So, W.-H. Yuen, and R. C.-C. Chang, "Polysaccharides from wolfberry antagonizes glutamate excitotoxicity in rat cortical neurons," *Cellular and Molecular Neurobiology*, vol. 29, no. 8, pp. 1233–1244, 2009.
- [73] D. Yang, S.-Y. Li, C.-M. Yeung et al., "Lycium barbarum extracts protect the brain from blood-brain barrier disruption and cerebral edema in experimental stroke," *PLoS One*, vol. 7, no. 3, article e33596, 2012.
- [74] M. Yang, N. Gao, Y. Zhao, L.-X. Liu, and X.-J. Lu, "Protective effect of *Lycium barbarum* polysaccharide on retinal ganglion cells *in vitro*," *International Journal of Ophthalmology*, vol. 4, no. 4, pp. 377–379, 2011.
- [75] H. Amagase and D. M. Nance, "A randomized, double-blind, placebo-controlled, clinical study of the general effects of a standardized *Lycium barbarum* (goji) juice, GoChi," *Journal of Alternative and Complementary Medicine*, vol. 14, no. 4, pp. 403–412, 2008.
- [76] S. P. Lu and P. T. Zhao, "Chemical characterization of *Lycium barbarum* polysaccharides and their reducing myocardial injury in ischemia/reperfusion of rat heart," *International Journal of Biological Macromolecules*, vol. 47, no. 5, pp. 681–684, 2010.
- [77] Y. X. Jia, J. W. Dong, X. X. Wu, T. M. Ma, and A. Y. Shi, "The effect of lycium barbarum polysaccharide on vascular tension in two-kidney, one clip model of hypertension," *Sheng Li Xue Bao*, vol. 50, no. 3, pp. 309–314, 1998.
- [78] D. Wang, Y. Xiao, and Z. Xu, "The dose-effect relation in Gou Qi Zi's effect of counteracting experimental hyperlipidemia and liver lipid peroxidation," *Journal of Applied Integrated Medicine*, vol. 11, no. 3, pp. 199–200, 1998.
- [79] Y. Gao, W. Yifo, W. Yuqing, G. Fang, and C. Zhigang, "Lycium barbarum: a traditional Chinese herb and a promising anti-aging agent," *Aging and Disease*, vol. 8, no. 6, pp. 778–791, 2017.
- [80] M. Ahn, J. S. Park, S. Chae et al., "Hepatoprotective effects of *Lycium chinense* Miller fruit and its constituent betaine in CCl₄-induced hepatic damage in rats," *Acta Histochemica*, vol. 116, no. 6, pp. 1104–1112, 2014.
- [81] D. H. Kim, B. Sung, Y. J. Kang et al., "Anti-inflammatory effects of betaine on AOM/DSS-induced colon tumorigenesis in ICR male mice," *International Journal of Oncology*, vol. 45, no. 3, pp. 1250–1256, 2014.
- [82] A. R. Im, H. J. Lee, U. J. Youn, J. W. Hyun, and S. Chae, "Orally administered betaine reduces photodamage caused by UVB irradiation through the regulation of matrix metalloproteinase-9 activity in hairless mice," *Molecular Medicine Reports*, vol. 13, no. 1, pp. 823–828, 2016.
- [83] H. Leung, A. Hung, A. C. Hui, and T. Y. Chan, "Warfarin overdose due to the possible effects of *Lycium barbarum* L.," *Food and Chemical Toxicology*, vol. 46, no. 5, pp. 1860–1862, 2008.
- [84] C. A. Rivera, C. L. Ferro, A. J. Bursua, and B. S. Gerber, "Probable interaction between *Lycium barbarum* (goji) and warfarin," *Pharmacotherapy*, vol. 32, no. 3, pp. e50–e53, 2012.
- [85] J. Zhang, L. Tian, and B. Xie, "Bleeding due to a probable interaction between warfarin and Gouqizi (*Lycium Barbarum* L.)," *Toxicology Reports*, vol. 2, pp. 1209–1212, 2015.

- [86] Q. Arroyo-Martinez, M. J. Sáenz, F. A. Arias, and M. S. J. Acosta, "Lycium barbarum: a new hepatotoxic "natural" agent?," *Digestive and Liver Disease*, vol. 43, no. 9, p. 749, 2011.
- [87] Y. Cao, Z. F. Ma, H. Zhang, Y. Jin, Y. Zhang, and F. Hayford, "Phytochemical properties and nutrigenomic implications of Yacon as a potential source of prebiotic: current evidence and future directions," *Food*, vol. 7, no. 4, p. 59, 2018.
- [88] Z. F. Ma and H. Zhang, "Phytochemical constituents, health benefits, and industrial applications of grape seeds: a mini-review," *Antioxidants*, vol. 6, no. 3, p. 71, 2017.
- [89] K. Ravichanthiran, Z. F. Ma, H. Zhang et al., "Phytochemical profile of brown rice and its nutrigenomic implications," *Antioxidants*, vol. 7, no. 6, p. 71, 2018.
- [90] Z. F. Ma and Y. Y. Lee, "Virgin coconut oil and Its cardiovascular health benefits," *Natural Product Communications*, vol. 11, no. 8, pp. 1151-1152, 2016.
- [91] H. Zhang and Z. F. Ma, "Phytochemical and pharmacological properties of *Capparis spinosa* as a medicinal plant," *Nutrients*, vol. 10, no. 2, p. 116, 2018.

Research Article

Structural Characterization and Antitumor Activity of Polysaccharides from *Kaempferia galanga* L.

Xu Yang,¹ Haiyu Ji,^{1,2} Yingying Feng,^{1,2} Juan Yu,^{1,2} and Anjun Liu¹ 

¹Key Laboratory of Food Nutrition and Safety, Ministry of Education, School of Food Engineering and Biotechnology, Tianjin University of Science and Technology, Tianjin 300457, China

²QingYunTang Biotech (Beijing) Co. Ltd., Beijing 100176, China

Correspondence should be addressed to Anjun Liu; laj1456@163.com

Received 11 May 2018; Revised 13 November 2018; Accepted 22 November 2018; Published 30 December 2018

Guest Editor: Germán Gil

Copyright © 2018 Xu Yang et al. This is an open access article distributed under the Creative Commons Attribution License, which permits unrestricted use, distribution, and reproduction in any medium, provided the original work is properly cited.

The water-soluble polysaccharides from *Kaempferia galanga* L. (KGPs) were extracted and purified, and their structural characteristics and antitumor activity were further investigated. The UV spectrum, high-performance gel permeation chromatography (HPGPC), Fourier-transform infrared spectroscopy (FTIR), and ion chromatography (IC) were employed to evaluate the structural characteristics, and H22 tumor-bearing mice model was established to demonstrate the antitumor activity. Physicochemical analysis and UV spectrum results showed that the proportions of total sugar, protein, and uronic acid in KGPs were 85.23%, 0.54%, and 24.17%, respectively. HPGPC, FTIR, and IC indicated that KGPs were acidic polysaccharides with skeletal modes of pyranose rings and mainly composed of arabinose and galactose with the average molecular weight of 8.5×10^5 Da. The *in vivo* antitumor experiments showed that KGPs could effectively protect the thymus and spleen of tumor-bearing mice from solid tumors and enhance the immunoregulatory ability of CD4⁺ T cells, the cytotoxic effects of CD8⁺ T cells and NK cells, and finally resulting in the inhibitory effects on H22 solid tumors. This study provided a theoretical foundation for the practical application of KGPs in food and medical industries.

1. Introduction

Kaempferia galanga L. is an acaulescent perennial plant growing in China [1], and the rhizome has been widely used as indigenous medicine due to the various bioactive compounds, including essential oils [2] and other extracts by methanol [3], hexane [4], and ethanol [5, 6]. As reported, these bioactive substances have exhibited antioxidant, sedative, antitumor, anti-inflammatory, and antimicrobial activities [7], which would contribute to the application on curing many diseases. The methanol extract of *Kaempferia galanga* L. rhizome significantly reduced viable Ehrlich ascites carcinoma (EAC) cells and weight gain, increased life span, and restored all hematological parameters, such as RBC, WBC, and hemoglobin of EAC-bearing mice towards normal level [8]. In addition, the ethanolic extract of *Kaempferia galanga* L. rhizome, ethyl-p-methoxycinnamate, exhibited promising anticholangiocarcinoma activity in CL6-xenografted nude mice as determined by significant inhibitory activity

on tumor growth and lung metastasis, as well as prolongation of survival time [5], which could inhibit the proliferation of human hepatocellular liver carcinoma cells in a dose-dependent manner by inducing cells to enter into apoptosis [6]. However, there are few researches concerning the polysaccharides from the rhizome of *Kaempferia galanga* L. and their *in vivo* antitumor activities.

Polysaccharides commonly exist in various animals, plants, fungus, and algae as polymeric carbohydrate molecule and have exhibited anticoagulant, antioxidant, antitumor, and immunoregulatory activities [9–11] with relatively low toxicity [12]. As is known to us, the properties and bioactivities of polysaccharides were directly associated with their chemical characteristics [13], which could be influenced by extraction techniques [14, 15]. Hot water extraction has been commonly employed to extract crude polysaccharides due to the simple process and low cost [16, 17].

Hepatocellular carcinoma (HCC) is the third leading cause of cancer-related mortality worldwide as one of the

most common malignant tumors, which has been a major public health problem [18, 19]. Modern therapeutic methods of treating HCC patients are chemotherapy [20], but the curative effects are poor due to the relapse of disease and resistance to chemotherapeutics [21]. Therefore, many natural products with stronger antitumor activity and lower toxicity were studied in recent years.

Previous studies mainly focused on the extracts from *Kaempferia galanga* L. by organic reagents and their bioactivities, while the relevant researches about the polysaccharides have not been reported yet. In the present study, the water-soluble polysaccharides from *Kaempferia galanga* L. (KGPs) were extracted with hot water, and their structural characteristics and antitumor effects were further evaluated.

2. Materials and Methods

2.1. Materials and Reagents. The rhizomes (*Kaempferia galanga* L.) were collected from Zhanjiang city (Guangdong, China) and shattered after dried to constant weight. H22 hepatoma cells were obtained from the Shanghai Institute of Biological Sciences at the Chinese Academy of Sciences (Shanghai, China). Bovine serum albumin (BSA), glucuronic acid, trifluoroacetic acid (TFA), standard monosaccharides, dimethyl sulfoxide (DMSO), 3-(4,5-dimethylthiazol-2-yl)-2,5-diphenyltetrazolium bromide (MTT), and 5-fluorouracil (5-FU) were purchased from Solarbio (Beijing, China). Fetal bovine serum (FBS) was obtained from Hangzhou Sijiqing Co. (Hangzhou, China). All other chemicals and agents were of analytical grade.

2.2. Preparation of Polysaccharides. The powder of rhizomes (100 g) was soaked in distilled water (3 L) for 4 h at 80°C two times. Then, the insoluble components were removed by centrifugation, supernatant was collected, and 4 volumes of ethanol were added for precipitating. The precipitations were kept and redissolved in deionized water; Sevag method (1-butanol and chloroform (1:4, v/v) for 5 times) was used to remove proteins [22]. Finally, the mixture was purified by a Sephadex G-200 column (1.6 cm × 35 cm) eluted with distilled water at 1 mL/min and lyophilized to obtain the *Kaempferia galanga* L. polysaccharides (KGPs, ~2.56 ± 0.12 g per 100 g dry weight of rhizomes) for further research.

2.3. Chemical Composition and Structural Analysis. Total sugar content was determined by phenol/H₂SO₄ assay and glucose was used as standard [23]. The content of uronic acid was detected according to the carbazole-sulfuric method using glucuronic acid as the standard [24]. The protein content was evaluated by the Coomassie brilliant blue method with bovine serum albumin as the standard [25]. The samples (5 mg) were dissolved in deionized water (1 mg/mL) and scanned from 200 to 800 nm with a spectrum-2102 UV spectrophotometer.

HPGPC (Agilent-1200) and FTIR (Bruker VECTOR-22, Karlsruhe, Germany) were employed to determine the average molecular weight and bonded states of the polysaccharides following the previous methods [26]. The standard

curve of average molecular weight was established using the T-series dextrans (T-10, T-40, T-70, T-500, and T-2000).

The monosaccharide constituents and proportions were determined by IC, a Dionex ICS2500 chromatographic system (CA, USA) with a Dionex pulsed amperometric detector with an Au electrode and an efficient anion exchange column of Dionex Carbopac PA20 column (150 mm × 3 mm) [27]. The polysaccharide sample (5 mg) was added into 1 mL of 2 M trifluoroacetic acid (TFA) and hydrolyzed at 110°C for 4 h in a sealed tube. Then TFA was absolutely removed by adding methanol and N₂ was used as the carrier gas. The dried hydrolysate was dissolved in 1 mL of distilled water, diluted 10 times with distilled water. The solution was eluted with NaOH (6 mM) and NaAC (100 mM) solutions at a flow rate of 0.45 mL/min. D-fucose, D-rhamnose, L-arabinose, D-galactose, D-glucose, L-xylose, D-mannose, D-glucuronic acid, and D-galacturonic acid were used as the standards for calibration and quantification.

2.4. Antitumor Animal Experiment

2.4.1. Design of Animal Model. Female KM mice of SPF-level (6–8 weeks old, 18–22 g) were purchased from the Center of Experimental Animals of Academy of Military Science (Beijing, China). They were raised under pathogen-free conditions with the 22 ± 2°C temperature, 50 ± 10% humidity, and 12 h light/12 h dark cycle. All mice were permitted free access to tap water and fed with standard pellet diet and to acclimate to new environments for 1 week before the experiment. All animal experimental procedures were conducted in accordance with the principles of Laboratory Animal Care and approved by the Local Ethics Committee for Animal Care and Use at Tianjin University of Science and Technology.

60 healthy female mice were randomly separated into six groups with 10 mice each group: blank group, model group, KGPs groups (100, 200, and 300 mg/kg KGPs) and positive group (5-Fu, 30 mg/kg, which has been in use against cancer for about 40 years [28]). The blank and model group mice were orally administrated with saline, while KGP groups were gavaged with different concentrations of KGPs, the positive group was intraperitoneally infused with 5-Fu. On day 15, 0.2 mL murine H22 hepatoma cells (1 × 10⁷ cells/mL) were inoculated in the subcutaneous right forelimb armpit of mice except the blank group. Then all mice were sequentially treated for another 15 days. Finally, they were all sacrificed by cervical dislocation and the tumors, spleens, and thymuses were weighed immediately. Meanwhile, the blood, spleen, and thymus samples were prepared and analyzed.

The immune organ indexes were expressed as the organ weight relative to body weight, and tumor inhibitory ratio was calculated by the following formula: Inhibitory rate (%) = [(W₁ - W₂)/W₁] × 100 [29], W₁ represents the average tumor weight of the model group and W₂ represents the average tumor weight of the treated group.

2.4.2. Blood Routine Parameter Examination. Anticoagulant (EDTA-K₂) was added into the blood sample to prevent clot

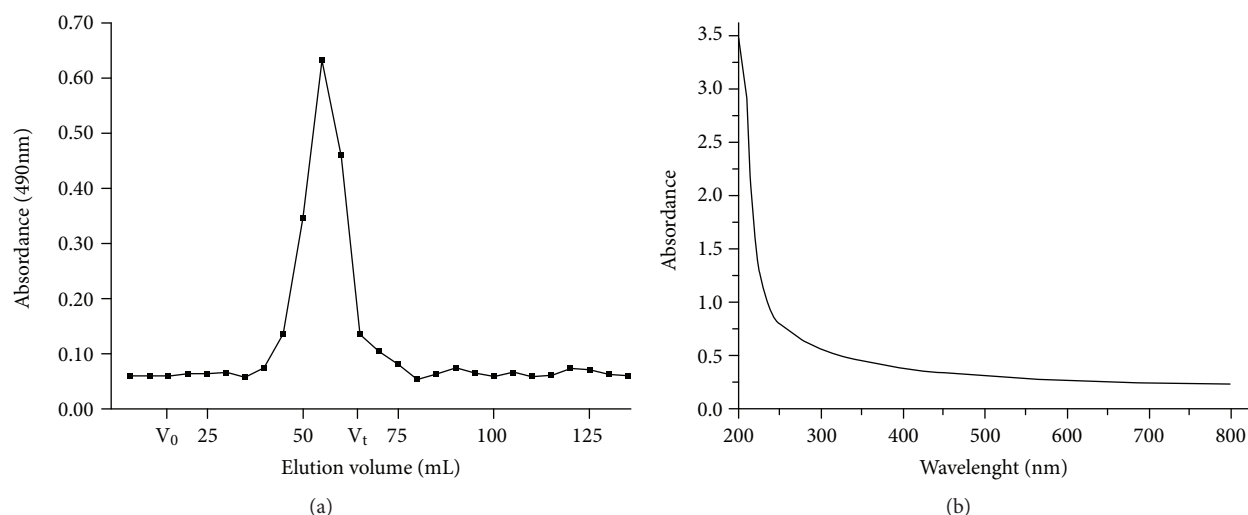


FIGURE 1: The elution curve via Sephadex G-200 column (a) and UV spectrum in the range of 200-800 nm of KGPs (b). V_0 and V_t are the void volume 15.1 mL and total column volume 62.2 mL, respectively.

forming, and all samples were analyzed on the XFA-6130 automatic blood analyzer.

2.4.3. Splenic Lymphocyte Proliferation and NK Cell Activity. Splenic lymphocyte proliferative activity (T cells and B cells stimulated with ConA and LPS, respectively) and NK cell activity (killing activity on H22 hepatoma cells) were performed as described previously [30].

2.4.4. Assessment of Lymphocyte Subsets in Peripheral Blood. The proportions of lymphocyte subsets in the peripheral blood were detected using FCM assay. The bloods were obtained and stained with monoclonal antibodies (mAb) against CD3-FITC, CD19-PE, CD4-PE, and CD8-FITC for 30 min on ice in the dark. Then the erythrocytes and uncombined antibodies were removed by red blood cell lysis buffer and phosphate buffer washing, and finally, a flow cytometry (BD FACSCalibur, Becton Dickinson, Franklin Lakes, NJ, USA) performed with CellQuest Pro software (version 5.1, Becton Dickinson, Franklin Lakes, NJ, USA) was employed to measure the fluorescently labeled lymphocyte subsets (counting 10,000 events).

2.4.5. Histological Observations of the Thymus and Spleen Organ. The thymus and spleen organs of the mice were fixed in 10% neutral formaldehyde solution and dehydrated in gradient ethanol solution. After embedding in paraffin, 4 μ m sections were obtained and stained with hematoxylin and eosin (H&E) for microscopic examination.

2.5. Statistical Analysis. All values were presented as the mean \pm standard deviation (S.D.) of three independent experiments performed in triplicate and statistically analyzed using SPSS for windows, version 19.0 (SPSS Inc., Chicago, IL, USA). The significance of difference was analyzed by one-way analysis of variance (ANOVA) followed by Duncan's test and $p < 0.05$ of the data was considered to be significant.

3. Results

3.1. Chemical Composition of KGPs. The proportions of total sugar, protein, and uronic acid in KGPs were 85.23%, 0.54%, and 24.17%, respectively, which indicated that KGPs were acidic polysaccharides with little amount of protein. Figure 1(a) shows the elution curve via Sephadex G-200 column and UV spectrum in the range of 200-800 nm of KGPs; the results indicated that KGPs were purified well with little proteins due to no absorptions at 260 nm and 280 nm [31].

3.2. Molecular Weight Distribution and FTIR Spectra Analysis. The average molecular weight of KGPs was determined by HPGPC method, and the result is shown in Figure 2(a). The HPGPC profiles of KGPs presented one main peak at 8.029 min, which occupied 93.15% of the total area. The molecular weight of KGPs was 8.5×10^5 Da according to the standard curve performed by glucans. Figure 2(b) exhibited the major functional groups and the chemical bounds of the polysaccharides. As shown, the broad absorption at 3405.03 cm^{-1} corresponded to the O-H stretching vibration [32], and the strong band at 2929.76 cm^{-1} was ascribed to stretching vibrations of C-H [33]. Two strong bands at 1639.87 and 1420.26 cm^{-1} were assigned to the absorbance of the deprotonated carboxylic group (COO-) [34]. These characteristics indicated that KGPs were typical acidic polysaccharides, which agreed with the content of uronic acid (24.17%). The absorptions at $500\text{-}900 \text{ cm}^{-1}$ and 1077.07 cm^{-1} were assigned to the skeletal modes of pyranose rings [35, 36].

3.3. Monosaccharide Analysis of KGPs. IC was used to evaluate the monosaccharide composition of KGPs, and the results are shown in Figure 3. As shown, KGPs were composed of fucose, arabinose, xylose, galactose, glucose, rhamnose, mannose, glucuronic acid, and galacturonic acid in a molar ratio of 0.37 : 3.12 : 1.23 : 6.39 : 1.36 : 3.09 : 1.00 : 0.91 : 1.27, strongly

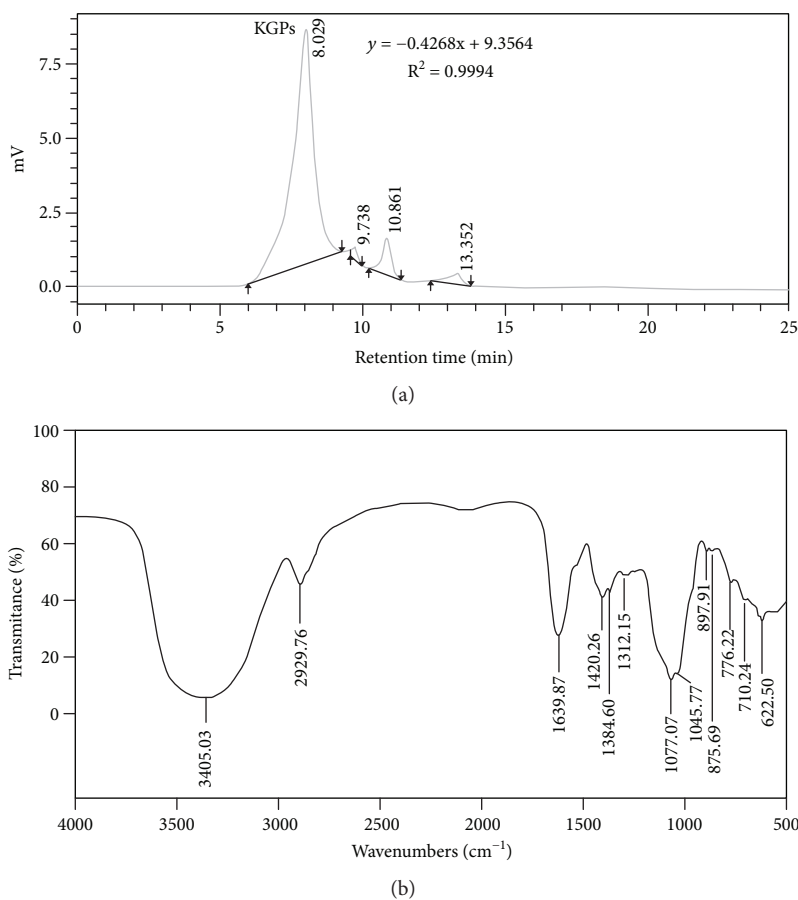


FIGURE 2: The results of HPGPC (a) and FTIR spectra (b) in the range of 500-4000 cm^{-1} of KGPs.

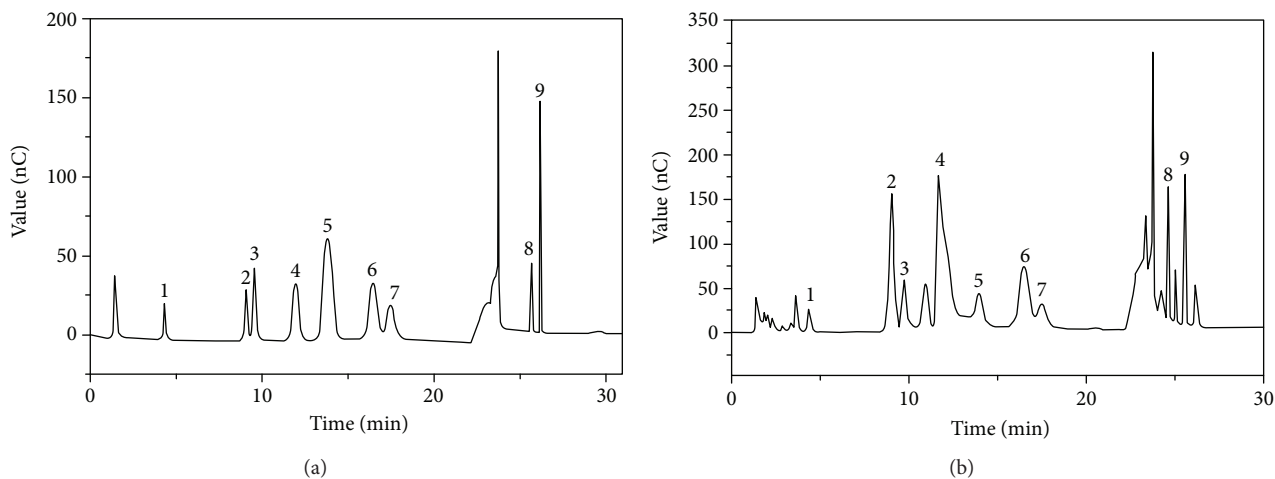


FIGURE 3: The IC results of standard monosaccharides (a) and KGPs (b). 1: fucose; 2: arabinose; 3: xylose; 4: galactose; 5: glucose; 6: rhamnose; 7: mannose; 8: glucuronic acid; 9: galacturonic acid.

suggesting that KGPs were heterogeneous acidic polysaccharides and mainly composed of arabinose and galactose.

3.4. Antitumor Animal Experiment

3.4.1. Organ Indexes and Inhibitory Rate. The antitumor activity of KGPs *in vivo* was further investigated on H22

tumor-bearing mice. The antitumor activities of 5-Fu and different dosages of KGPs are summarized in Figure 4. The thymus indexes of the model group were significantly reduced compared to those of the blank group ($p < 0.05$), while their spleen indexes were remarkably increased ($p < 0.05$), indicating that the proliferation of H22 cells *in vivo* could destroy immune organs. KGPs could effectively

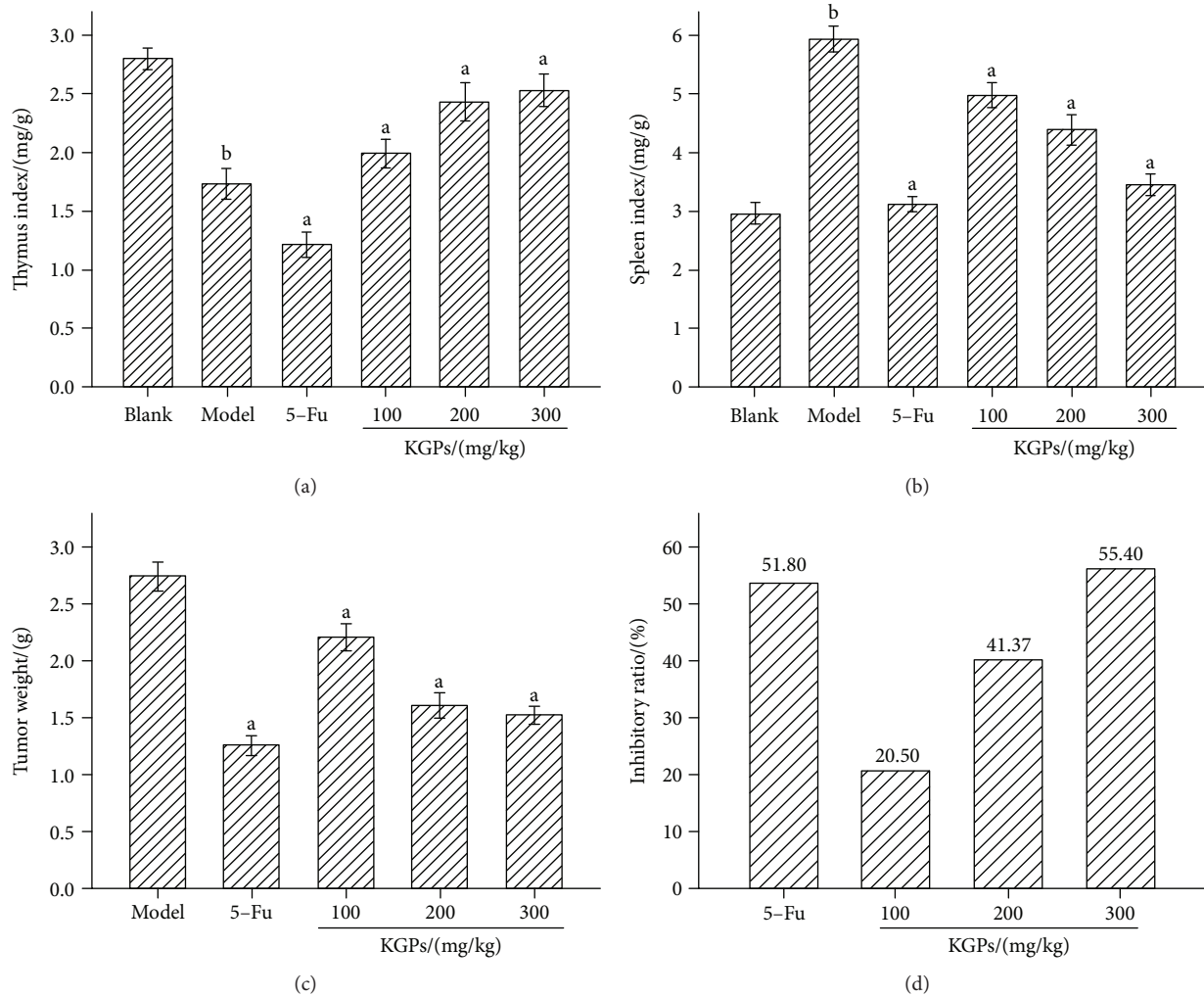


FIGURE 4: The organ indexes and inhibitory rate of H22 tumor-bearing mice. (a) Thymus index. (b) Spleen index. (c) Tumor weight. (d) Inhibitory rate. ^a $p < 0.05$ compared to the model group; ^b $p < 0.05$ compared to the blank group.

protect the thymus and spleen from solid tumors in the host, while 5-Fu exhibited strong inhibitory effects on both tumors and immune organs. The inhibition rates of tumor growth of 5-Fu and KGP treatments (100, 200, and 300 mg/kg) were 51.80%, 20.50%, 41.37%, and 55.40%, respectively. As shown in Figure 5, the H22 solid tumor volume of the model group trended to increase continually with the time varied from 7 d to 19 d, while that of the KGP group raised slowly as the time changed from 7 d to 13 d and reached to the maximum at 13 d, then decrease gradually. The H22 solid tumor volume became significant differences ($p < 0.05$) between the model group and the KGP group at 15 d. The results showed that KGPs could significantly inhibit the proliferation of tumors and protect the immune system of tumor-bearing mice, dose-dependently.

3.4.2. Results of Blood Routine Examination. The blood routine examination of tumor-bearing mice was detected in the present study, and the results are shown in Figure 6. As shown, the percentage of lymphocytes, erythrocyte counts, and content of hemoglobin in the peripheral blood of the

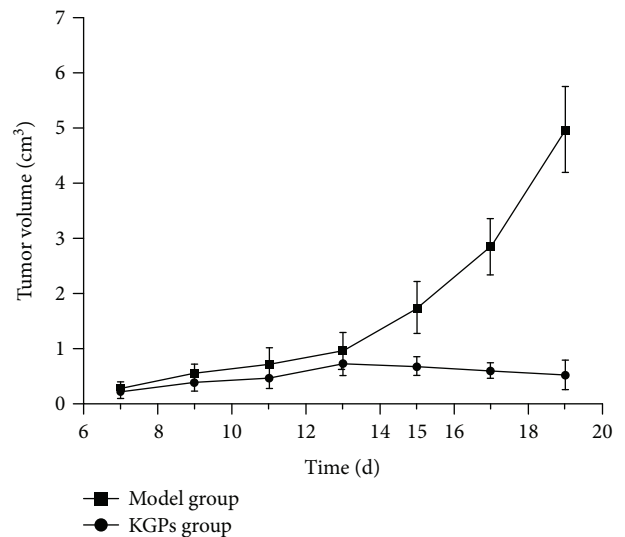


FIGURE 5: The changes of tumor volume of H22 tumor-bearing mice.

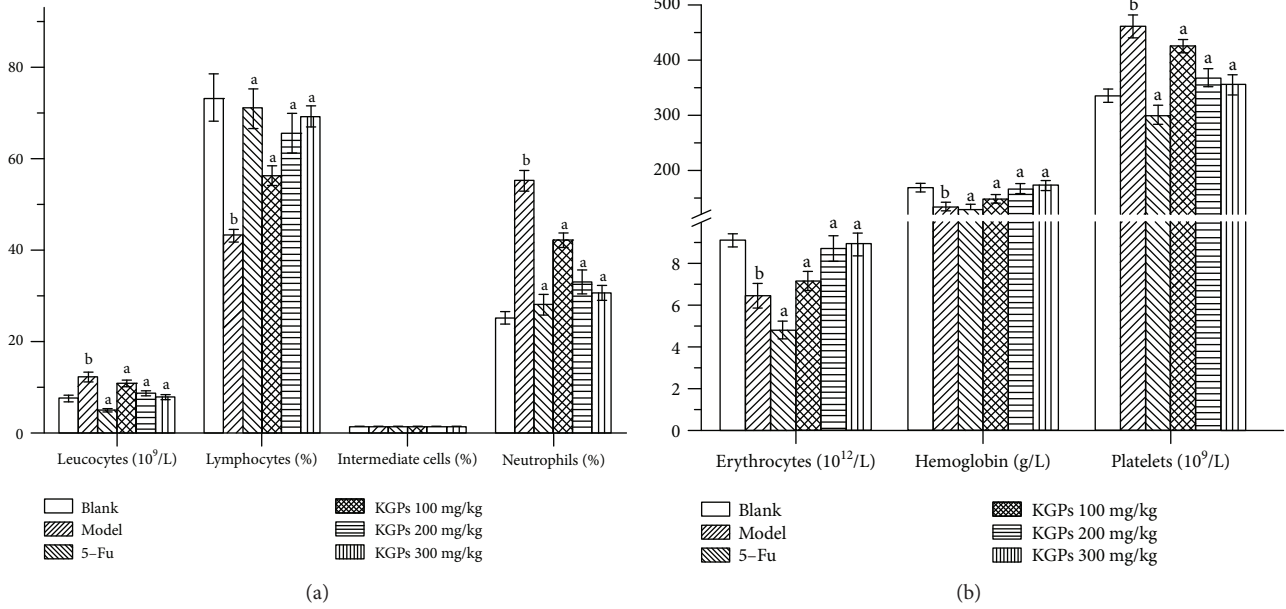


FIGURE 6: The blood routine examination of H22 tumor bearing-mice. ^a $p < 0.05$ compared to the model group; ^b $p < 0.05$ compared to the blank group.

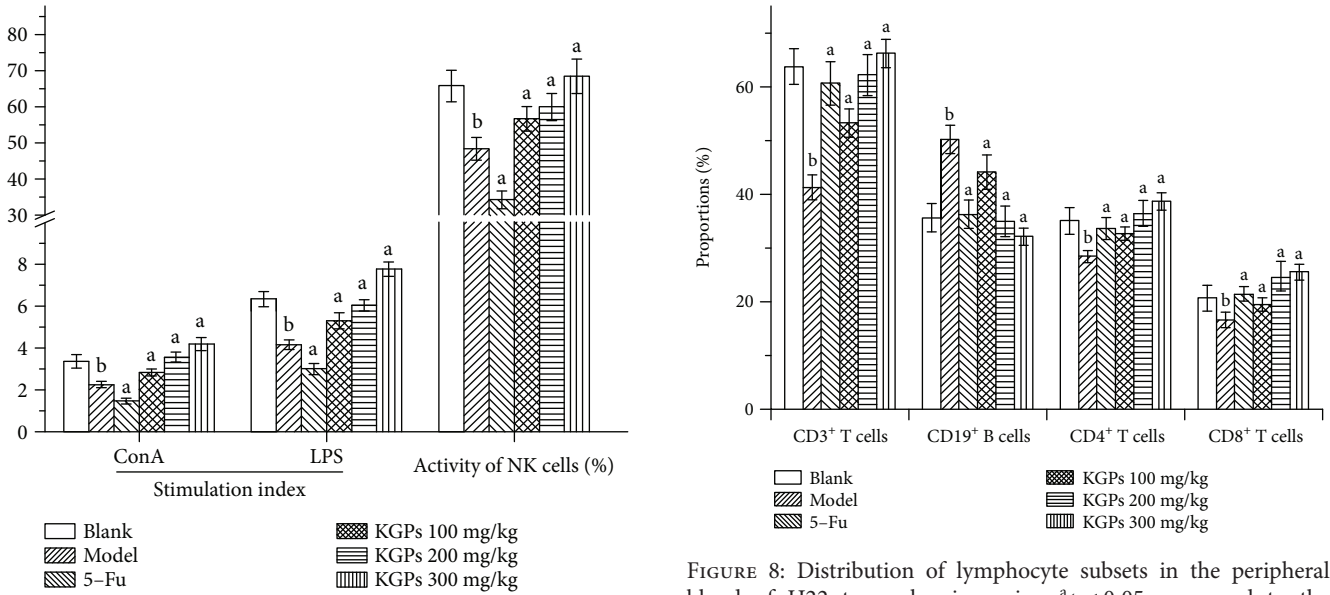


FIGURE 7: Effects of KGPs on the spleen lymphocyte proliferation and NK cell activity. ^a $p < 0.05$ compared to the model group; ^b $p < 0.05$ compared to the blank group.

model group were significantly decreased compared to those of the blank group ($p < 0.05$), whereas the leucocyte counts, neutrophil percentage, and platelet counts remarkably ascended ($p < 0.05$), indicating that the tumor-bearing mice in the model group had signs of inflammation and anemia. These indicators in the 5-Fu group were all lower than those in the model group, suggesting its severely toxic side effects. However, KGPs could remarkably alleviate the symptoms and improve the percentage of lymphocytes in H22 tumor-bearing mice with a dose-dependent manner.

FIGURE 8: Distribution of lymphocyte subsets in the peripheral blood of H22 tumor-bearing mice. ^a $p < 0.05$ compared to the model group; ^b $p < 0.05$ compared to the blank group.

3.4.3. Spleen Lymphocyte Proliferation and NK Cell Killing Activity. The proliferation ability of splenic lymphocytes induced by ConA and LPS and the NK cell killing activity in H22 tumor-bearing mice were determined by MTT assay. Figure 7 shows that the stimulation indexes (ConA and LPS) and NK cell activity of the model group were significantly reduced compared with those of the blank group ($p < 0.05$); these indicators in the 5-Fu group were even lower than those in the model group. In contrast, KGPs could dramatically improve the proliferation ability of T cells and B cells and the killing activity of NK cells compared with the model group ($p < 0.05$) in a dose-dependent manner,

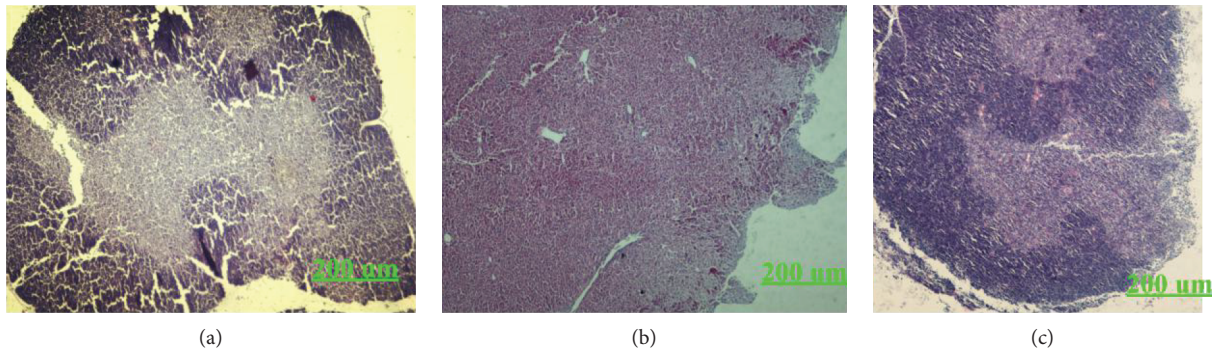


FIGURE 9: H&E staining of the thymus of H22 tumor-bearing mice. (a) Blank group. (b) Model group. (c) KGP group.

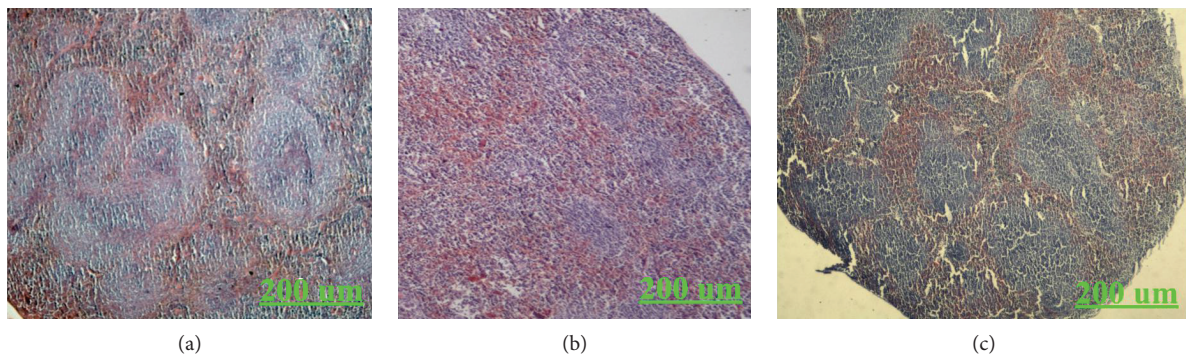


FIGURE 10: H&E staining of the spleen of H22 tumor-bearing mice. (a) Blank group. (b) Model group. (c) KGP group.

suggesting that KGPs could enhance the antitumor immunity of tumor-bearing host.

3.4.4. Distribution of Lymphocyte Subsets. The proportions of lymphocyte subsets in the peripheral bloods of H22 tumor-bearing mice were researched and the results are shown in Figure 8. The percentages of T cells ($CD3^+$, $CD4^+$, and $CD8^+$) in the model group were markedly decreased ($p < 0.05$) in relation to the blank group, which would contribute to the higher level of B cells ($CD19^+$). Mice in 5-Fu showed a relatively balanced distribution of lymphocyte subsets, suggesting that 5-Fu had similar toxicity on both T cells and B cells considering the decrease in lymphocyte counts (Figure 6). The proportions of T cells in the KGP group were significantly increased ($p < 0.05$) compared to those in the model group, dose-dependently, especially the proportion of $CD8^+$ T cells.

3.4.5. H&E Staining of the Thymus and Spleen. The histological observations of the thymus of H22 tumor-bearing mice are shown in Figure 9. Compared to the blank group, the thymus lobules of the model group were differentiated indistinctly. There was no clear boundary between the medullae. While the thymus lobules of KGP group were split obviously, the cortical area was increased conspicuously and the structure of the thymus was recovered gradually. As shown in Figure 10, the boundary between the red and white medullae of the KGP group was evident, and there was no significant difference with that of the blank group. It was indicated that KGPs could protect the thymus and spleen organs of H22 tumor-bearing mice.

4. Discussion

Radical surgery including chemotherapy has traditionally been the medical treatments for liver cancer. However, it would make the patients suffer high costs and recurrence [37]. Therefore, more effective drugs need to be investigated. Multiple polysaccharides have exhibited strong antitumor activity *in vivo* with relatively low toxicity [38, 39]. As reported, the antitumor activity of polysaccharides was closely related to their molecular weight, functional groups, monosaccharide composition, and so on [40]. Previous studies have proved that polysaccharides with the pyranose form and uronic acid would exhibit strong antitumor and immunomodulatory activities on tumor-bearing mice [26, 41, 42]. In the present study, KGPs were acidic polysaccharides (uronic acid of 24.17%) with skeletal modes of pyranose rings and mainly composed of arabinose and galactose with the average molecular weight of 8.5×10^5 Da, which were consistent with characteristics of bioactive polysaccharides reported.

The thymus is a primary lymphoid organ that takes charge of differentiation and maturation of immunocompetent T lymphocytes [43], and T lymphocytes are the main protagonists in orchestrating the antitumor response including $CD8^+$ T cells and $CD4^+$ T cells [44]. The spleen, as a peripheral lymphoid organ, plays a central role in host defense. The damage of the spleen is related to immunodeficiency, resulting in overwhelming infections and insufficient hematopoiesis [45]. In this study, the growth of solid tumor cells *in vivo* would destroy the structure and function of the thymus and spleen, leading to the immunosuppression, inflammation, and hypohemia of the host. KGP treatment

could protect these immune organs from solid tumors and balance the proportions and quantities of leukocytes, thus enhance the antitumor immunity of tumor-bearing mice.

CD4⁺ T cells can modulate antitumor immune response in antitumor immunity via activating CD8⁺ T cells and NK cells; CD8⁺ T cells impart cytolytic activity on tumor cells [46]. NK cells belong to the innate lymphoid cell family and participate in damaging infected and cancerous cells [47]. Inflammation would increase the degree of CD19⁺ B cells as reported [48]. Our results showed that mice of the model group were infected due to the malignant proliferation of H22 hepatoma cells, which was consistent with the higher proportion of CD19⁺ B cells. KGPs could notably enhance the immunoregulation capability of CD4⁺ T cells and the cytotoxic effects of CD8⁺ T cells and NK cells, finally leading to the inhibitory effects on the growth of H22 solid tumors.

5. Conclusions

In conclusion, we extracted and purified the polysaccharides from *Kaempferia galanga* L. (KGPs) and researched the structural characteristics and antitumor activity on H22 tumor-bearing mice. Our results showed that KGPs were acidic polysaccharides (total sugar of 85.23%, uronic acid of 24.17%) with skeletal modes of pyranose rings and mainly composed of arabinose and galactose with the average molecular weight of 8.5×10^5 Da. The *in vivo* antitumor test showed that KGPs could effectively protect the thymus and spleen of tumor-bearing mice from solid tumors and enhance the immunoregulatory capability of CD4⁺ T cells and the cytotoxic effects of CD8⁺ T cells and NK cells, finally leading to the inhibitory effects on H22 solid tumors. This study provided a theoretical basis for the practical application of the novel acidic polysaccharides in food and medical industries.

Data Availability

Data of the compounds are not available from the authors.

Conflicts of Interest

The authors declare that there is no conflict of interest regarding the publication of this paper.

Authors' Contributions

Xu Yang, Haiyu Ji, and Yingying Feng contributed equally to this work.

References

- [1] P. C. Jagadish, K. P. Latha, J. Mudgal, and G. K. Nampurath, "Extraction, characterization and evaluation of *Kaempferia galanga* L. (Zingiberaceae) rhizome extracts against acute and chronic inflammation in rats," *Journal of Ethnopharmacology*, vol. 194, pp. 434–439, 2016.
- [2] A. P. Raina, Z. Abraham, and N. Sivaraj, "Diversity analysis of *Kaempferia galanga* L. germplasm from South India using DIVA-GIS approach," *Industrial Crops and Products*, vol. 69, pp. 433–439, 2015.
- [3] W. Ridditid, C. Sae-wong, W. Reanmongkol, and M. Wongnawa, "Antinociceptive activity of the methanolic extract of *Kaempferia galanga* Linn. in experimental animals," *Journal of Ethnopharmacology*, vol. 118, no. 2, pp. 225–230, 2008.
- [4] L. Huang, T. Yagura, and S. Chen, "Sedative activity of hexane extract of *Kaempferia galanga* L. and its active compounds," *Journal of Ethnopharmacology*, vol. 120, no. 1, pp. 123–125, 2008.
- [5] A. Amuamuta, T. Plengsuriyakarn, and K. Na-Bangchang, "Anticholangiocarcinoma activity and toxicity of the *Kaempferia galanga* Linn. rhizome ethanolic extract," *BMC Complementary and Alternative Medicine*, vol. 17, no. 1, pp. 213–223, 2017.
- [6] B. Liu, F. Liu, C. Chen, and H. Gao, "Supercritical carbon dioxide extraction of ethyl p-methoxycinnamate from *Kaempferia galanga* L. rhizome and its apoptotic induction in human HepG2 cells," *Natural Product Research*, vol. 24, no. 20, pp. 1927–1932, 2010.
- [7] Q. Ma, X. D. Fan, X. C. Liu, T. Q. Qiu, and J. G. Jiang, "Ultrasound-enhanced subcritical water extraction of essential oils from *Kaempferia galanga* L. and their comparative antioxidant activities," *Separation and Purification Technology*, vol. 150, pp. 73–79, 2015.
- [8] H. Ali, R. Yesmin, M. A. Satter, R. Habib, and T. Yeasmin, "Antioxidant and antineoplastic activities of methanolic extract of *Kaempferia galanga* Linn. rhizome against Ehrlich ascites carcinoma cells," *Journal of King Saud University-Science*, vol. 30, no. 3, pp. 386–392, 2018.
- [9] D. L. Diehl, S. R. S. Mok, H. S. Khara, A. S. Johal, H. L. Kirchner, and F. Lin, "Heparin priming of EUS-FNA needles does not adversely affect tissue cytology or immunohistochemical staining," *Endoscopy International Open*, vol. 6, no. 3, pp. E356–E362, 2018.
- [10] K. Nagai, Y. Ueno, S. Tanaka, R. Hayashi, K. Shinagawa, and K. Chayama, "Polysaccharides derived from *Ganoderma lucidum* fungus mycelia ameliorate indomethacin-induced small intestinal injury via induction of GM-CSF from macrophages," *Cellular Immunology*, vol. 320, pp. 20–28, 2017.
- [11] P. Shao, X. Chen, and P. Sun, "In vitro antioxidant and antitumor activities of different sulfated polysaccharides isolated from three algae," *International Journal of Biological Macromolecules*, vol. 62, pp. 155–161, 2013.
- [12] Y. Liu, J. Zhang, and Z. Meng, "Purification, characterization and anti-tumor activities of polysaccharides extracted from wild *Russula griseocarnosa*," *International Journal of Biological Macromolecules*, vol. 109, pp. 1054–1060, 2018.
- [13] J. H. Lee, Y. K. Lee, Y. R. Choi, J. Park, S. K. Jung, and Y. H. Chang, "The characterization, selenylation and anti-inflammatory activity of pectic polysaccharides extracted from *Ulmus pumila* L.," *International Journal of Biological Macromolecules*, vol. 111, pp. 311–318, 2018.
- [14] Y. Chi, Y. Li, G. Zhang et al., "Effect of extraction techniques on properties of polysaccharides from *Enteromorpha prolifera* and their applicability in iron chelation," *Carbohydrate Polymers*, vol. 181, pp. 616–623, 2018.
- [15] X.-m. Wang, R.-g. Sun, J. Zhang, Y.-y. Chen, and N.-n. Liu, "Structure and antioxidant activity of polysaccharide POJ-U1a extracted by ultrasound from *Ophiopogon japonicus*," *Fitoterapia*, vol. 83, no. 8, pp. 1576–1584, 2012.
- [16] Y. G. Cao, Y. Hao, Z. H. Li, S. T. Liu, and L. X. Wang, "Antiviral activity of polysaccharide extract from *Laminaria japonica*

- against respiratory syncytial virus,” *Biomedicine & Pharmacotherapy*, vol. 84, pp. 1705–1710, 2016.
- [17] G. Pan, Z. Xie, S. Huang et al., “Immune-enhancing effects of polysaccharides extracted from *Lilium lancifolium* Thunb,” *International Immunopharmacology*, vol. 52, pp. 119–126, 2017.
- [18] N. Ling, X. Zhou, Y. Ji, W. Li, C. Ji, and Z. Qi, “Immuno-modulatory and cellular antioxidant activities of κ -selenocarrageenan in combination with Epirubicin in H22 hepatoma-bearing mice,” *Biomedicine & Pharmacotherapy*, vol. 91, pp. 132–137, 2017.
- [19] F. Chen, Y. Sun, S. L. Zheng et al., “Antitumor and immunomodulatory effects of ginsenoside Rh2 and its octyl ester derivative in H22 tumor-bearing mice,” *Journal of Functional Foods*, vol. 32, pp. 382–390, 2017.
- [20] F. H. Sarkar and Y. Li, “Using chemopreventive agents to enhance the efficacy of cancer therapy,” *Cancer Research*, vol. 66, no. 7, pp. 3347–3350, 2006.
- [21] J. Wang, W. Liu, Z. Chen, and H. Chen, “Physicochemical characterization of the oolong tea polysaccharides with high molecular weight and their synergistic effects in combination with polyphenols on hepatocellular carcinoma,” *Biomedicine & Pharmacotherapy*, vol. 90, pp. 160–170, 2017.
- [22] J.-H. Xie, M. Y. Shen, S. P. Nie et al., “Simultaneous analysis of 18 mineral elements in *Cyclocarya paliurus* polysaccharide by ICP-AES,” *Carbohydrate Polymers*, vol. 94, no. 1, pp. 216–220, 2013.
- [23] M. DuBois, K. A. Gilles, J. K. Hamilton, P. A. Rebers, and F. Smith, “Colorimetric method for determination of sugars and related substances,” *Analytical Chemistry*, vol. 28, no. 3, pp. 350–356, 1956.
- [24] T. Bitter and H. M. Muir, “A modified uronic acid carbazole reaction,” *Analytical Biochemistry*, vol. 4, no. 4, pp. 330–334, 1962.
- [25] H. Barbosa, N. K. H. Slater, and J. C. Marcos, “Protein quantification in the presence of poly(ethylene glycol) and dextran using the Bradford method,” *Analytical Biochemistry*, vol. 395, no. 1, pp. 108–110, 2009.
- [26] A. J. Liu, J. Yu, H. Y. Ji, H. C. Zhang, Y. Zhang, and H.-P. Liu, “Extraction of a novel cold-water-soluble polysaccharide from *Astragalus membranaceus* and its antitumor and immunological activities,” *Molecules*, vol. 23, no. 1, 2018.
- [27] Y. Wang, Y. Li, Y. Liu, X. Chen, and X. Wei, “Extraction, characterization and antioxidant activities of Se-enriched tea polysaccharides,” *International Journal of Biological Macromolecules*, vol. 77, pp. 76–84, 2015.
- [28] X. Wang and Z. Zhang, “The antitumor activity of a red alga polysaccharide complexes carrying 5-fluorouracil,” *International Journal of Biological Macromolecules*, vol. 69, pp. 542–545, 2014.
- [29] B. Yang, B. Xiao, and T. Sun, “Antitumor and immunomodulatory activity of *Astragalus membranaceus* polysaccharides in H22 tumor-bearing mice,” *International Journal of Biological Macromolecules*, vol. 62, pp. 287–290, 2013.
- [30] J. Yu, H. Ji, and A. Liu, “Preliminary structural characteristics of polysaccharides from pomelo peels and their antitumor mechanism on S180 tumor-bearing mice,” *Polymers*, vol. 10, no. 4, 2018.
- [31] J. Yu, M. Hu, Y. Wang, Q. Zhang, W. Xu, and W. Su, “Extraction, partial characterization and bioactivity of polysaccharides from *Senecio scandens* Buch.-Ham,” *International Journal of Biological Macromolecules*, vol. 109, pp. 535–543, 2018.
- [32] F. Liu, Y. Wang, K. Zhang et al., “A novel polysaccharide with antioxidant, HIV protease inhibiting and HIV integrase inhibiting activities from *Fomitiporia punctata* (P. karst.) murrill (Basidiomycota, hymenochaetales),” *International Journal of Biological Macromolecules*, vol. 97, pp. 339–347, 2017.
- [33] S. Zou, X. Zhang, W. Yao, Y. Niu, and X. Gao, “Structure characterization and hypoglycemic activity of a polysaccharide isolated from the fruit of *Lycium barbarum* L,” *Carbohydrate Polymers*, vol. 80, no. 4, pp. 1161–1167, 2010.
- [34] G. D. Manrique and F. M. Lajolo, “FT-IR spectroscopy as a tool for measuring degree of methyl esterification in pectins isolated from ripening papaya fruit,” *Postharvest Biology and Technology*, vol. 25, no. 1, pp. 99–107, 2002.
- [35] X. Yang, M. Huang, C. Qin, B. Lv, Q. Mao, and Z. Liu, “Structural characterization and evaluation of the antioxidant activities of polysaccharides extracted from Qingzhuan brick tea,” *International Journal of Biological Macromolecules*, vol. 101, pp. 768–775, 2017.
- [36] J. Gao, T. Zhang, Z. Y. Jin et al., “Structural characterisation, physicochemical properties and antioxidant activity of polysaccharide from *Lilium lancifolium* Thunb,” *Food Chemistry*, vol. 169, pp. 430–438, 2015.
- [37] X. Yang, X. Li, Z. Guo, T. Si, H. Yu, and W. Xing, “Immunological response induced by cryoablation against murine H22 hepatoma cell line *in vivo*,” *Cryobiology*, vol. 80, pp. 114–118, 2018.
- [38] J. M. Leiro, R. Castro, J. A. Arranz, and J. Lamas, “Immunomodulating activities of acidic sulphated polysaccharides obtained from the seaweed *Ulva rigida* C. Agardh,” *International Immunopharmacology*, vol. 7, no. 7, pp. 879–888, 2007.
- [39] Y. Fan, W. Wang, W. Song, H. Chen, A. Teng, and A. Liu, “Partial characterization and anti-tumor activity of an acidic polysaccharide from *Gracilaria lemaneiformis*,” *Carbohydrate Polymers*, vol. 88, no. 4, pp. 1313–1318, 2012.
- [40] G. Zhao, J. Kan, Z. Li, and Z. Chen, “Structural features and immunological activity of a polysaccharide from *Dioscorea opposita* Thunb roots,” *Carbohydrate Polymers*, vol. 61, no. 2, pp. 125–131, 2005.
- [41] X. Sun, R. L. Gao, Y. K. Xiong, Q. C. Huang, and M. Xu, “Antitumor and immunomodulatory effects of a water-soluble polysaccharide from *Lilii Bulbus* in mice,” *Carbohydrate Polymers*, vol. 102, pp. 543–549, 2014.
- [42] L. Sun, J. Chu, Z. Sun, and L. Chen, “Physicochemical properties, immunomodulation and antitumor activities of polysaccharide from *Pavlova viridis*,” *Life Sciences*, vol. 144, pp. 156–161, 2016.
- [43] Q. Ge and Y. Zhao, “Evolution of thymus organogenesis,” *Developmental and Comparative Immunology*, vol. 39, no. 1–2, pp. 85–90, 2013.
- [44] E. Nakayama, Y. Shiratsuchi, Y. Kobayashi, and K. Nagata, “The importance of infiltrating neutrophils in SDF-1 production leading to regeneration of the thymus after whole-body X-irradiation,” *Cellular Immunology*, vol. 268, no. 1, pp. 24–28, 2011.
- [45] R. Golub, J. Tan, T. Watanabe, and A. Brendolan, “Origin and immunological functions of spleen stromal cells,” *Trends in Immunology*, vol. 39, no. 6, pp. 503–514, 2018.
- [46] S. Sun, H. Ji, Y. Feng, Y. Kang, J. Yu, and A. Liu, “A novel mechanism of tumor-induced thymic atrophy in mice bearing H22 hepatocellular carcinoma,” *Cancer Management and Research*, vol. 10, pp. 417–424, 2018.

- [47] A. Poli, T. Michel, N. Patil, and J. Zimmer, "Revisiting the functional impact of NK cells," *Trends in Immunology*, vol. 39, no. 6, pp. 460–472, 2018.
- [48] J. Dai, L. Bi, J. Lin, and F. Qi, "Evaluation of interleukin-10 producing CD19⁺ B cells in human gingival tissue," *Archives of Oral Biology*, vol. 84, pp. 112–117, 2017.

Research Article

Genetically Engineered Resveratrol-Enriched Rice Inhibits Neuroinflammation in Lipopolysaccharide-Activated BV2 Microglia Via Downregulating Mitogen-Activated Protein Kinase-Nuclear Factor Kappa B Signaling Pathway

Lalita Subedi ¹, So-Hyeon Baek ², and Sun Yeou Kim ¹

¹College of Pharmacy, Gachon University, #191 Hambakmoero, Yeonsu-gu, Incheon 21936, Republic of Korea

²Department of Well-being Resources, Sunchon National University, Sunchon, Jeonnam 57922, Republic of Korea

Correspondence should be addressed to So-Hyeon Baek; baeksh@scnu.ac.kr and Sun Yeou Kim; sunnykim@gachon.ac.kr

Received 15 June 2018; Revised 30 August 2018; Accepted 10 September 2018; Published 3 December 2018

Guest Editor: Anderson J. Teodoro

Copyright © 2018 Lalita Subedi et al. This is an open access article distributed under the Creative Commons Attribution License, which permits unrestricted use, distribution, and reproduction in any medium, provided the original work is properly cited.

Resveratrol, a natural stilbenoid, is produced by several plants, especially grape vines. Its strong potency against obesity, metabolic disorders, vascular disease, inflammation, and various cancers has already been reported. Large amounts of wine or grapes need to be consumed to obtain the amount of resveratrol required for biological activity. Pure resveratrol at concentrations as low as 10 μ M induces cytotoxicity to normal cells. To overcome these limitations, we prepared genetically modified resveratrol-enriched rice (RR). We previously reported the strong antiaging potential of RR against ultraviolet B/reactive oxygen species-induced toxicity in normal human dermal fibroblasts (NHDF). As aging is characterized by neuroinflammation and neurodegeneration, we further evaluated the role of RR against LPS-induced neuroinflammation. RR inhibited nitric oxide production and the expression of inflammatory proteins such as iNOS and COX-2. RR significantly modulated mitogen-activated protein kinase signaling, activator protein AP-1 signaling, and nuclear factor kappa B (NF- κ B) mediated transcription of inflammatory proteins via inhibition of NF- κ B translocation, I κ B phosphorylation, and proinflammatory cytokine productions such as interleukin IL-6, IL-1 β , tumor necrosis factor alpha (TNF- α), and prostaglandin E2 (PGE2). These findings show that the strong antineuroinflammatory effects of RR can be beneficial for aging-mediated neurodegenerative conditions as well as disorders of the central nervous system caused by neuroinflammation.

1. Introduction

Inflammation is the major cause and aggravating factor of various acute or chronic pathological conditions, including photoaging, diabetes, and cancer [1, 2]. Similarly, neuroinflammation is the key mediator of secondary brain damage in most of the neurological disorders, such as Alzheimer's disease (AD), Prion disease, Parkinson's disease (PD), multiple sclerosis (MS), ischemic stroke, experimental autoimmune encephalomyelitis (EAE), and neuropathic pain [3–5]. Neuroinflammation is induced by aging-dependent conditions and aging-independent pathological events, which share similar inflammatory cascades [6–8]. Microglia, neurons, astrocytes, and oligodendrocytes are the

basic cells of the brain. Microglia and astrocytes, as glial cells, have a role to defend against brain injury to maintain homeostasis and repair brain injury. In aging-dependent conditions and aging-independent disorders such as AD, PD, and stroke, neuroinflammation can be initiated by chronic microglial activation. Activated microglia are required for basic immune defense in the brain; however, chronic microglial activation is toxic to the central nervous system (CNS) [9]. Conversion of normal microglia to toxic microglial M1 phenotype is responsible for the initiation of inflammation in the CNS through the production of reactive oxygen species (ROS), nitric oxide (NO), proteases, arachidonic acids, excitatory amino acids, and cytokines [10]. These neurotoxic substances are responsible for the disruption of architecture

and function of neurons, synaptic degeneration, neuronal loss, and ultimately neurodegeneration [11]. The production of ROS and other inflammatory mediators and oxidative stress are closely related to mitogen-activated protein kinase (MAPK) signaling, as well as nuclear factor kappa B (NF- κ B) and activator protein-1 (AP-1)-mediated transcription [12–16]. Hence, natural compounds or nutraceuticals with the potential to regulate these steps to control microglial activation will be promising candidates for inhibiting neuroinflammation and neurodegenerative conditions. Although advances have been made to treat such neuroinflammatory conditions, there is a lack of effective therapeutic strategy to cure these disease conditions. In the past few decades, there has been a growing interest toward alternative medicines, especially phytochemicals, as therapeutic agents for neurological disorders involving activated microglia-mediated neuroinflammation [17–20].

Resveratrol has been studied for decades for its multifunctional potency against many human ailments [21], including neuroinflammatory conditions [22, 23]. Resveratrol is widely present in a number of grape species, berries, peanuts, soy, and red wine [24]; however, we have to consume a large amount of these foods to get the sufficient amount of resveratrol required for its biological activity [25]. Additionally, the cytotoxic nature of resveratrol on normal cells overshadows its extensive potential against human ailments [26]. To overcome this limitation and achieve therapeutic potential, resveratrol-enriched rice (RR) was developed by taking advantage of genetic engineering [27].

In this study, we developed RR through genetic engineering techniques, as described previously [27]. Rice is a main food component among Asian population, and therefore, rice consumption is higher than other food components. Resveratrol biosynthesis gene was transcribed into normal dongjin rice (NR) to produce RR. We previously reported that RR has a better potency to inhibit ultraviolet B (UVB)/ROS-induced aging by maintaining matrix metalloproteinase (MMP1)/procollagen I (PIP) balance an inhibiting inflammation and apoptosis, without any cellular toxicity [28].

RR can be used safely and more effectively in cases where resveratrol shows efficacy to treat or control neuroinflammatory conditions. Therefore, in this study, we compared the efficacy of NR, RR, and resveratrol in terms of cytotoxicity and anti-inflammatory potential in activated microglia and elucidated the possible mechanisms underlying the antineuroinflammatory potential of RR in lipopolysaccharide- (LPS-) stimulated BV2 murine microglial cells. We hope our research clearly revealed the additive role of RR from NR and resveratrol which could be the best alternative treatment for the neuronal disorders induced by neuroinflammation like AD, PD, and MS lesions.

2. Materials and Methods

2.1. Materials. Dulbecco's modified Eagle medium (DMEM), fetal bovine serum (FBS), and penicillin-streptomycin were purchased from Invitrogen (Carlsbad, CA, USA). LPS, NG-mono-methyl-L-arginine (L-NMMA), and trans-resveratrol were purchased from Sigma-Aldrich (St. Louis, MO, USA).

A normal rice (NR) (*Oryza sativa* var. japonica) and resveratrol-enriched rice (RR) were supplied by the Rural Development Administration (RDA) of South Korea as mentioned in our previous paper [28]. Enzyme-linked immunosorbent assay (ELISA) development kits for tumor necrosis factor alpha (TNF- α), interleukin-6 (IL-6), prostaglandin E2 (PGE2), and IL-1 β were purchased from R&D Systems (Minneapolis, MN, USA). Primary and secondary antibodies against inducible nitric oxide synthase (iNOS), cyclooxygenase (COX-2), extracellular signal-regulated kinases (ERK), C-Jun N-terminal kinase (JNK), p38, NF- κ B, Histone-3, β -Actin, I κ B, pI κ B, C-Fos, p-C-Fos, C-Jun, p-C-Jun, and tubulin were purchased from Cell Signaling (Beverly, MA, USA). All other chemicals and reagents were purchased from Sigma Chemical (St. Louis, MO).

2.2. NR and RR Extraction. NR and RR received from RDA were extracted in methanol (MeOH). The rice grains (10 g) were incubated with 100 mL of MeOH for 60 min. During this period, the extraction mixture was placed in an ultrasonic water bath with sonication. After 60 min incubation of the extraction mixture with sonication, the mixture was filtered (HYUNAI Micro N0.20 filter paper, Korea) and then evaporated using a rotary evaporator at 40°C for the removal of methanol. The evaporated extract yield was further freeze-dried for complete lyophilization of the extract. The final yield of the extract powder was stored and used for experiment. A stock solution (100 mg/mL) was prepared in dimethyl sulfoxide (DMSO). This stock solution was diluted in DMEM and used for cell treatment during experiments.

2.3. Cell Culture. BV-2 murine microglia were used to study the anti-inflammatory effects of NR, RR, and resveratrol. The BV-2 microglial cell lines were obtained as gift samples from Dr. E. Choi, Korea University (Seoul, Korea). BV2 cells were maintained in DMEM supplemented with 10% heat-inactivated FBS, penicillin (1×10^5 U/L), and streptomycin (100 mg/L) in a humidified incubator with 5% CO₂ at 37°C.

2.4. Cell Treatment and Cell Viability Assay. The effect of NR, RR, and resveratrol on the cytotoxicity of BV2 cells was measured using 3-(4,5-dimethylthiazol-2-yl)-2,5-diphenyl-tetrazolium bromide (MTT) assay. The cells cultured in 96-well plates were treated with different concentrations of samples (NR, RR, and resveratrol) with or without LPS. In the pretreatment condition, the samples were pretreated in the seeded plates, and LPS (100 ng/mL) was added 30 min after sample treatment. The cells were incubated for 24 h after LPS activation for nitrite assay and cell viability assay. After incubation for 24 h, the media were removed and MTT solution was added to the cells at a final concentration of 0.5 mg/mL. After an additional 1 h incubation, the media were carefully removed and 200 μ L of DMSO was added to each well. The optical density (OD) was measured on a plate reader at 570 nm. Cell viability was evaluated by observing the ability of viable cells to reduce yellow-colored MTT to purple-colored formazan. The results were expressed as the percentage of LPS-treated group (LPS-treated cells).

2.5. Nitric Oxide Assay. The inhibitory effect of NR, RR, and resveratrol on NO synthesis was determined using BV-2 microglial cells activated with 100 ng/mL LPS. BV2 cells were seeded at a density of 4×10^4 cells/well in a 96-well plate 24 h before treatment. The seeded cells were treated with NR, RR, and resveratrol the next day. The cells were activated with LPS after 30 min [9] and further incubated for 24 h. After 24 h incubation, the nitrite level was measured in the culture media using Griess reagent (1% sulfanilamide and 0.1% N-1-naphthylethylenediamine dihydrochloride in 5% phosphoric acid). The conditioned medium (50 μ L) was transferred to a new 96-well plate and mixed with an equal volume of Griess reagent. This mixture gives a pink color because of the presence of NO. The colorimetric change was quantified by measuring the OD of the solution in 96-well plates using a microplate reader at 540 nm. NG-mono-methyl-L-arginine (L-NMMA), a well-known NOS inhibitor [10], was used as a positive control. NaNO₂ was used as the standard to compare the amount of nitrite in the conditioned medium. Acute microglial activation was performed by LPS treatment for 6 h, and chronic microglial activation was performed by LPS treatment for 24 h.

2.6. Measurement of PGE₂, TNF- α , IL-1 β , and IL-6 Production. BV2 microglial cells were treated with the samples (NR, RR, and R) and activated with LPS to measure TNF- α , IL-1 β , PGE₂, and IL-6 levels under neuroinflammatory conditions. BV2 cells were seeded at a density of 1.5×10^6 cells/well in DMEM and incubated for 24 h. The seeded cells were treated with the samples, followed by LPS treatment for microglial activation, and incubated for 24 h. After 24 h of incubation, conditioned medium from the treated plate was collected and used for measuring the levels of PGE₂, TNF- α , IL-1 β , and IL-6. The collected conditioned medium can be stored at -20°C until later use. PGE₂ was measured using a competitive enzyme immunoassay kit (Cayman Chemical, Ann Arbor, MI, USA). TNF- α , IL-1 β , and IL-6 levels were measured using ELISA development kits (R&D Systems, Minneapolis, MN, USA).

2.7. NF- κ B Assay. BV2 cells were seeded at a density of 1.5×10^6 cells/well in a 6-well plate and treated with NR, RR, and resveratrol, followed by LPS treatment for microglial activation and NF- κ B translocation and transcription. The cells treated with the samples and LPS were incubated for 1 h and then harvested. Nuclear and cytosolic extracts from the harvested microglial cells were prepared using a Nuclear/Cytosolic Extraction Kit (Active Motif, Carlsbad, CA) according to the manufacturer's protocol. The protein levels of NF- κ B, histone-3, I κ B, and p-I κ B were evaluated by Western blot analysis. The expression of nucleolar and cytosolic NF- κ B was measured using histone-3 and β -actin as loading controls, respectively. The expression of I κ B and p-I κ B was observed in the cytosolic fraction. The absence of β -actin expression in the nuclear fraction suggests the clear separation of nuclear and cytosolic fractions during fractionation without any contamination. Densitometry analysis of the bands was performed using ImageMaster™ 2D Elite

software (version 3.1, Amersham Pharmacia Biotech, Buckinghamshire, UK).

2.8. Western Blot Analysis. BV-2 cells were seeded at a density of 6×10^5 cells/well in a 6-well plate and treated with the samples. LPS was incubated for the desired period based on the protein activation pattern according to target protein location in the cells. The cells were harvested with ice-cold phosphate-buffered saline (PBS) and centrifuged at 7500 rpm for 5 min. PBS was removed, and the cell pellets were lysed with lysis buffer [50 mM Tris-HCl (pH 8.0), 0.1% sodium dodecyl sulfate (SDS), 150 mM NaCl, 1% NP-40, 0.02% sodium azide, 0.5% sodium deoxycholate, 100 μ g/mL phenylmethylsulfonyl fluoride (PMSF), and 1 g/mL aprotinin] [29]. This mixture was incubated in ice for 2 h. The cell lysate/protein extract was obtained after ultracentrifugation of the cell and lysis buffer mixture at 12,000 rpm for 30 min at 4°C . Total proteins (30 μ g) from each group were separated by 10% SDS-polyacrylamide gel electrophoresis (PAGE), transferred to nitrocellulose membranes, and incubated with primary antibodies against tubulin, iNOS, COX-2, ERK, pERK, JNK, pJNK, p38, pP38, NF- κ B, histone-3, β -actin, I κ B, pI κ B, C-Fos, p-C-Fos, C-Jun, p-C-Jun, and α -tubulin. The membranes were incubated with horseradish peroxidase-conjugated secondary antibodies, and the protein bands were visualized using ECL Western blotting detection reagents (Amersham Pharmacia Biotech). Densitometry analysis of the bands was performed using ImageMaster™ 2D Elite software (version 3.1, Amersham Pharmacia Biotech).

2.9. Statistical Analysis. The results were evaluated using the Statistical Analysis System (GraphPad Prism 5, La Jolla, CA, USA). The results are presented as mean \pm standard error of the mean (SEM), and all results are the mean of at least three independent experiments. A statistical comparison of different treatment groups was performed by one-way analysis of variance (ANOVA), followed by Newman-Keuls multiple comparison test. A value of $p < 0.05$ was considered statistically significant.

3. Results

3.1. NR, RR, and Resveratrol Significantly Inhibit Nitrite Production in LPS-Activated Microglia. NO production is an important biomarker for almost all types of inflammation, especially LPS-induced neuroinflammation. We evaluated the nitrite oxide level of NR, RR, and resveratrol with L-NMMA as the positive control against LPS-activated BV2 microglial NO production. NR and RR showed the highest potency to inhibit nitrite production. Also, a resveratrol showed excellent potency at a high concentration (100 μ g/mL). However, NR and RR showed better potency than resveratrol at concentrations of 1 and 10 μ g/mL. Although RR extract has lesser amount of pure resveratrol than resveratrol, it has higher potency with lower IC₅₀ value, suggesting that RR does not cause cellular toxicity. The effect of RR (100 μ g/mL) on nitrite production is statistically significant to that of NR alone suggesting that RR has better potency

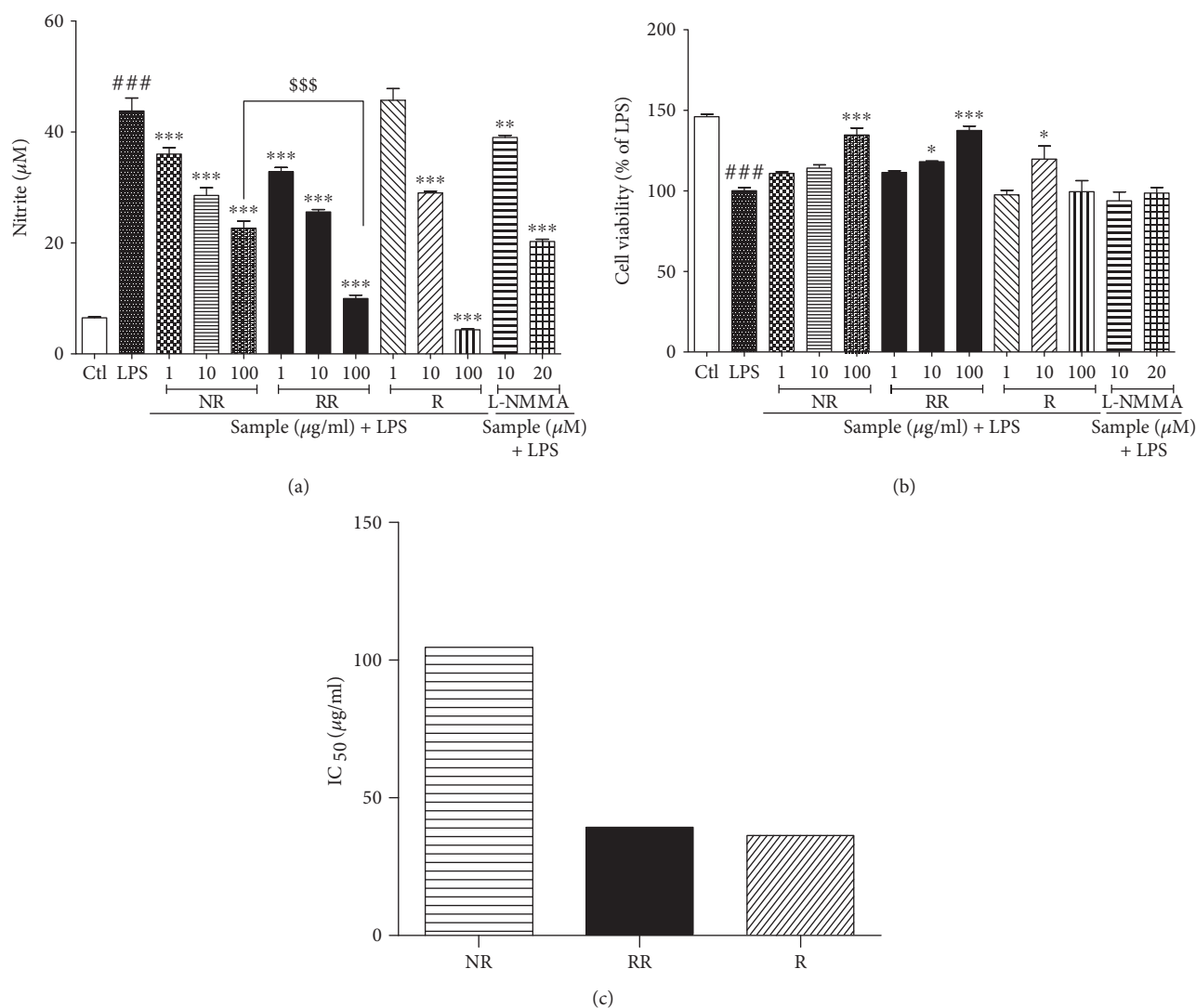


FIGURE 1: Treatment with resveratrol-enriched rice inhibits nitrite production in lipopolysaccharide-activated BV2 microglial cells without cellular toxicity. BV2 microglial cells were pretreated with normal rice (NR), resveratrol-enriched rice (RR), and resveratrol after 30 min of LPS (100 ng/mL) stimulation. (a, b) Nitrite production and cell viability after NR, RR, and resveratrol treatment. (c) IC_{50} value of NR, RR, and resveratrol samples. The concentration of samples was given in μM . All data are presented as the mean \pm standard error of the mean of three independent experiments. * $P < 0.05$, ** $P < 0.01$, and *** $P < 0.001$ indicate significant differences compared with LPS treatment alone. # $P < 0.05$, ## $P < 0.01$, and ### $P < 0.001$ indicate significant differences compared with untreated control group. \$\$\$ $P < 0.001$ indicate significant differences to RR compared to NR. Ctl, untreated control and LPS, lipopolysaccharide.

than that of the NR. NR and RR treatment protected against LPS-induced toxicity, especially up to a concentration 100 $\mu\text{g/ml}$, by increasing the number of viable cells. In case of resveratrol treatment, only 10 $\mu\text{g/ml}$ protected against LPS toxicity by increasing the viable cells, but not 100 $\mu\text{g/ml}$. NR and RR treatment at concentrations of 1 $\mu\text{g/ml}$ and 10 $\mu\text{g/ml}$ demonstrated higher potency in inhibiting nitrite production than L-NMMA, suggesting that NR and RR are better alternatives than L-NMMA for nitrite production inhibition as shown in (Figure 1).

3.2. RR Treatment Inhibits the Expression of iNOS and COX-2 in Acute and Chronic LPS Activation.

As iNOS and COX-2

proteins are precursors of NO production and inflammatory cascades, we further evaluated the role of NR and RR in regulating the expression of iNOS and COX-2 in LPS-activated BV2 microglial cells for acute as well as chronic activation conditions. LPS treatment in BV2 cells significantly increased the expression of iNOS and COX-2. We performed acute microglial activation, which is the incubation of cells with a compound and LPS for 6 h, to determine the altered expression of iNOS and COX-2 in LPS-activated BV2 microglial cells. We also performed incubation for 24 h, which is defined as chronic microglial activation, and evaluated the expression of iNOS and COX-2. We found that NR and resveratrol showed a high potency to inhibit COX-2 expression in acute

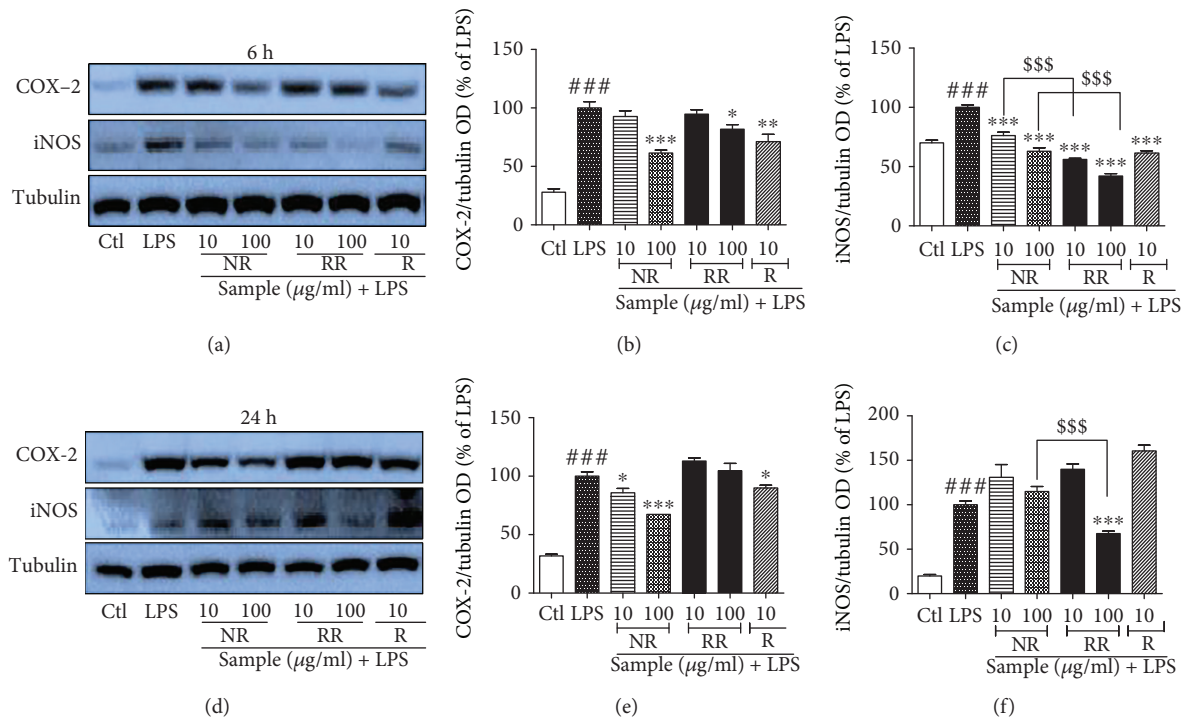


FIGURE 2: Treatment with resveratrol-enriched rice inhibits the expression of iNOS and COX-2 in lipopolysaccharide-activated (acute and chronic) BV2 microglial cells. BV2 microglial cells were pretreated with normal rice (NR), resveratrol-enriched rice (RR), and resveratrol after 30 min of LPS (100 ng/mL) stimulation. (a–c) iNOS and COX-2 expression and their band intensity in LPS-activated BV2 microglial cells after 6 h of sample treatment and LPS activation. (d–f) iNOS and COX-2 expression and their band intensity in LPS-activated BV2 microglial cells after 24 h of sample treatment and LPS activation. Tubulin was used as loading control. All data are presented as the mean \pm standard error of the mean of three independent experiments. * $P < 0.05$, ** $P < 0.01$, and *** $P < 0.001$ indicate significant differences compared with LPS treatment alone. ### $P < 0.001$ indicates significant differences compared with untreated control group. \$\$\$ $P < 0.001$ indicates significant differences to RR compared to NR. Ctl, untreated control and LPS, lipopolysaccharide.

and chronic activation conditions. When compared with NR and R, RR demonstrated poor but significant efficacy in acute activation, but no significant activity in chronic activation. In contrast, RR exhibited the highest potency to inhibit iNOS expression in both acute and chronic activation conditions. NR and resveratrol did not demonstrate significant inhibition of iNOS in chronic activation condition, while a significant potency was observed in acute activation condition as shown in (Figure 2). The effect of RR on inhibition of iNOS expression is statistically significant in comparison to the NR. This result suggests that additive effect of NR and R on RR is more significant than that on NR and R alone for the inhibition of iNOS expression. We hypothesized that the potent iNOS/NO inhibiting ability of RR might be responsible for its anti-inflammatory effects.

3.3. Bioactive-Phytochemicals from NR, Namely, α -Tocopherol and γ -Tocopherol, Inhibit the Nitrite Production and Expression of iNOS and COX-2 against LPS-Activated Microglia. We expected that the safety and compatibility of normal rice and the resveratrol together can show the similar potency of RR against neuroinflammation. However, interestingly, normal rice alone also showed the antineuroinflammatory effect against LPS-treated BV2 cells. To further confirm this effect and to find the responsible bioactive phytochemical in NR, we selected α -tocopherol and γ -

tocopherol to evaluate its role against neuroinflammation in LPS-treated BV2 cells. We observed that treatment of the α -tocopherol and γ -tocopherol significantly inhibited the production of nitrite in LPS-activated microglia. As we treated the sample of 1, 10, 100, and 1000 $\mu\text{g/mL}$ concentration, potency of sample shows concentration-dependent manner and did not show any cellular toxicity as evidenced by cell viability assay. Although γ -tocopherol has been reported to inhibit LPS-induced macrophage cell toxicity previously [30], here, we found the similar potency of α -tocopherol and γ -tocopherol to inhibit the inflammatory mediators against LPS-activated microglia as shown in Figure 3.

3.4. NR, RR, and R Can Modulate MAPK Signaling in Acute LPS-Activated BV2 Microglial Cells. MAPKs are activated by phosphorylation of tyrosine and threonine residues, which in turn leads to a signaling cascade that upregulates the production of inflammatory mediators as well as proinflammatory cytokines in activated microglia or under other inflammatory conditions. Therefore, we evaluated the role of NR and RR in altering the activation/phosphorylation of MAPK proteins (p38, JNK, and ERK). LPS-activated microglia showed significantly increased phosphorylation of JNK, ERK, and P38, which might be responsible for the induction of transcription of inflammatory mediators. Treatment of LPS-activated BV2 cells with NR and RR significantly

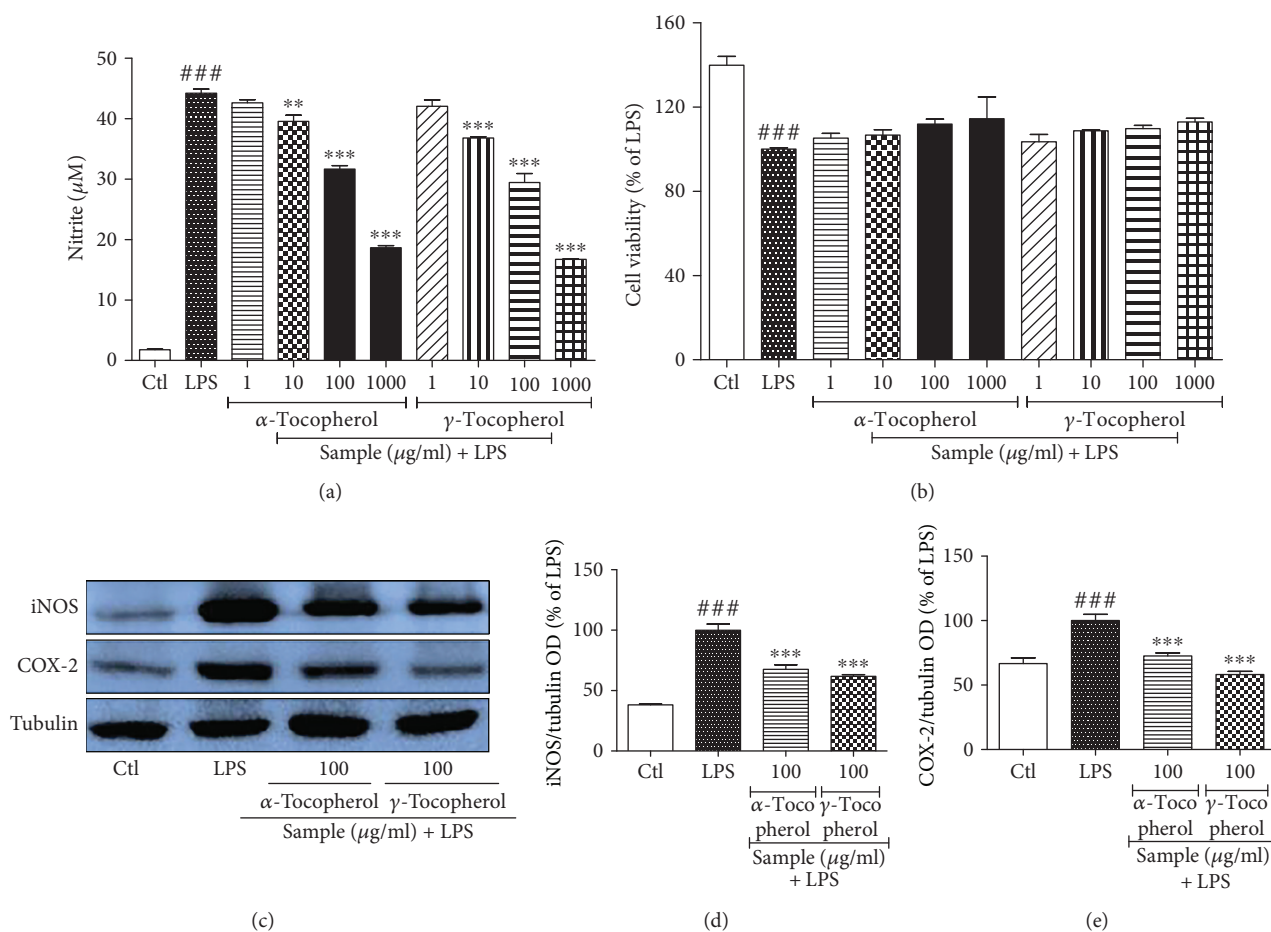


FIGURE 3: Treatment α -tocopherol and γ -tocopherol inhibits the nitrite production and expression of iNOS and COX-2 against LPS-activated microglia cells. BV2 microglial cells were activated with LPS (100 ng/mL) 30 min before sample treatment, and samples of different concentrations were added under the same condition. Incubation of LPS and sample was performed for 6 h for iNOS and COX-2 expression and 24 h for nitrite production assay. (a, b) Nitrite production and cell viability of LPS-activated BV2 microglial cells after treatment of α -tocopherol and γ -tocopherol (c–e) iNOS and COX-2 expression and their respective band intensity. Tubulin was used as loading control. All data are presented as the mean \pm standard error of the mean of three independent experiments. ** $P < 0.01$ and *** $P < 0.001$ indicate significant differences compared with LPS treatment alone. ### $P < 0.001$ indicates significant differences compared with untreated control group. Ctl, untreated control and LPS, lipopolysaccharide.

reduced expression of phosphorylated JNK and P38. In case of ERK phosphorylation, only RR showed high efficacy, while NR did not demonstrate significant inhibition. The effect of RR is statistically significant in both the treated concentration to inhibit the ERK phosphorylation in comparison to the NR alone. This data suggested that additive effect of NR and resveratrol in RR is more significant than in NR and R alone. Resveratrol showed slightly different pattern in the MAPK modulation where it showed increase of JNK phosphorylation although it is not significant. Also, it did not show any changes in ERK phosphorylation whereas it significantly inhibited the p38 phosphorylation. NR and RR exhibited high potency to inhibit P38 phosphorylation than that of the ERK and JNK as shown in (Figure 4). Among all, RR showed the highest potency to inhibit the phosphorylation of all the MAPK's specially at 100 μ g/mL. These findings suggest that RR treatment inhibits pJNK, pERK, and pP38 nonspecifically and its potency is higher than NR and resveratrol itself.

3.5. NR, RR, and R Modulate AP-1 Signaling in LPS-Activated BV2 Microglial Cells. Next, we assessed the expression of AP-1 proteins. Toxicant-induced activation of MAPK is responsible for the activation of AP-1 (C-Fos and C-Jun) in inflammatory response and other conditions [31]. In this study, we observed that the significant inhibition of pERK, pJNK, and pP38 by RR treatment was further confirmed by the downregulated expression of p-C-Fos and p-C-Jun under the similar treatment conditions as that for NF- κ B. NR and RR treatment at a concentration of 100 μ g/mL inhibited the expression of p-C-Fos where NR and RR significantly inhibited the expression of p-C-Jun at both the treated concentrations (10 and 100 μ g/mL). The effect of RR is statistically significant on both the treated concentration in comparison to the NR alone suggesting that additive effect of NR and resveratrol in RR is more significant than the NR and R alone. P38, JNK, and ERK activation is required for C-Jun activation. RR treatment downregulated p-C-Jun expression, indicating its strong

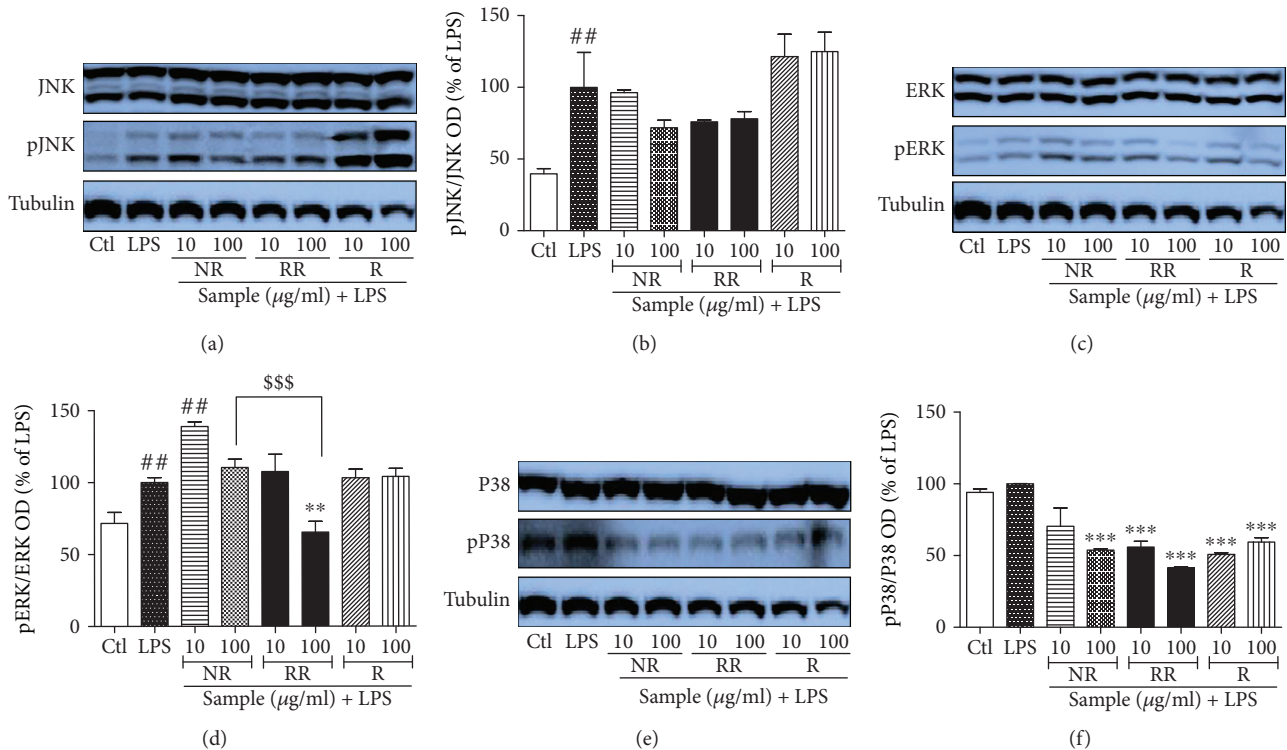


FIGURE 4: Treatment with resveratrol-enriched rice modulates MAPK signaling in lipopolysaccharide-activated (acute) BV2 microglial cells. BV2 microglial cells were activated with LPS (100 ng/mL) 30 min before sample treatment, and samples of different concentrations were added under the same condition. Incubation of LPS and sample was performed for 30 min. MAPK expression was measured in pretreatment in LPS-activated BV2 cells. (a, b) JNK/pJNK expression and band intensity. (c, d) ERK/pERK expression and band intensity. (e, f) p38/pP38 expression and band intensity in LPS-activated BV2 microglia. All data are presented as the mean \pm standard error of the mean of three independent experiments. * $P < 0.05$, ** $P < 0.01$, and *** $P < 0.001$ indicate significant differences compared with LPS treatment alone. ## $P < 0.01$ indicates significant differences compared with untreated control group. \$\$\$ $P < 0.001$ indicates significant differences to RR compared to NR. Ctl, untreated control and LPS, lipopolysaccharide.

anti-inflammatory effects against activated microglia as shown in Figure 5. As resveratrol did not significantly change the JNK and ERK phosphorylation, that result was further supported by the unchanged phosphorylation of C-Fos and C-Jun after resveratrol treatment. This data supported the fact that C-Jun and C-Fos phosphorylation were correlated with JNK and ERK phosphorylation.

3.6. NR, RR, and Resveratrol Modulate NF- κ B Translocation in LPS-Activated BV2 Microglial Cells. Transcription factors play an important role in the increased production of inflammatory proteins and proinflammatory cytokines. NF- κ B and AP-1 play the key roles as transcription factors under inflammatory conditions. In this study, we evaluated the role of NR, RR, and resveratrol against activated microglia-induced NF- κ B translocation and I- κ B phosphorylation. LPS treatment to BV2 cells significantly increased the translocation of NF- κ B from the cytosol to the nucleus, as well as the phosphorylation of I- κ B. These events together can increase transcription. However, NR, RR, and resveratrol treatment reversed these events. LPS-activated BV2 cells treated with RR showed the highest expression of cytosolic NF- κ B and the lowest expression of nucleolar NF- κ B. RR treatment significantly increased the cytosolic NF- κ B and decreased the nuclear one which is

statistically significant to that of NR-treated group as shown in Figure 6, suggesting the better potency of RR to that of NR alone. The inhibition of translocation was further supported by the significant inhibition of phosphorylated I- κ B as shown in (Figure 6). In all these cases, RR demonstrated the highest potency at both the treated concentrations, suggesting its anti-inflammatory effect via inhibition of NF- κ B translocation and NF- κ B/I- κ B-mediated transcription of inflammatory proteins.

3.7. NR and RR Can Modulate MAPK Signaling in Chronic LPS-Activated BV2 Microglial Cells. We evaluated the role of NR, RR, and resveratrol in altering the activation/phosphorylation of MAPK proteins (p38, JNK, and ERK) under chronic (24 h) LPS activation condition in BV2 cells. Inhibition of pJNK by NR and RR was more significant in chronic activation than in acute activation. None of the samples inhibited ERK phosphorylation in chronic activation condition, rather NR treatment significantly increased pERK expression that might suggest for its cell survival capacity against chronic activation of microglia. RR treatment also showed a slight increase in pERK expression, but it was not significant when compared with LPS-only-treated group. In case of P38 phosphorylation, although all the treated samples

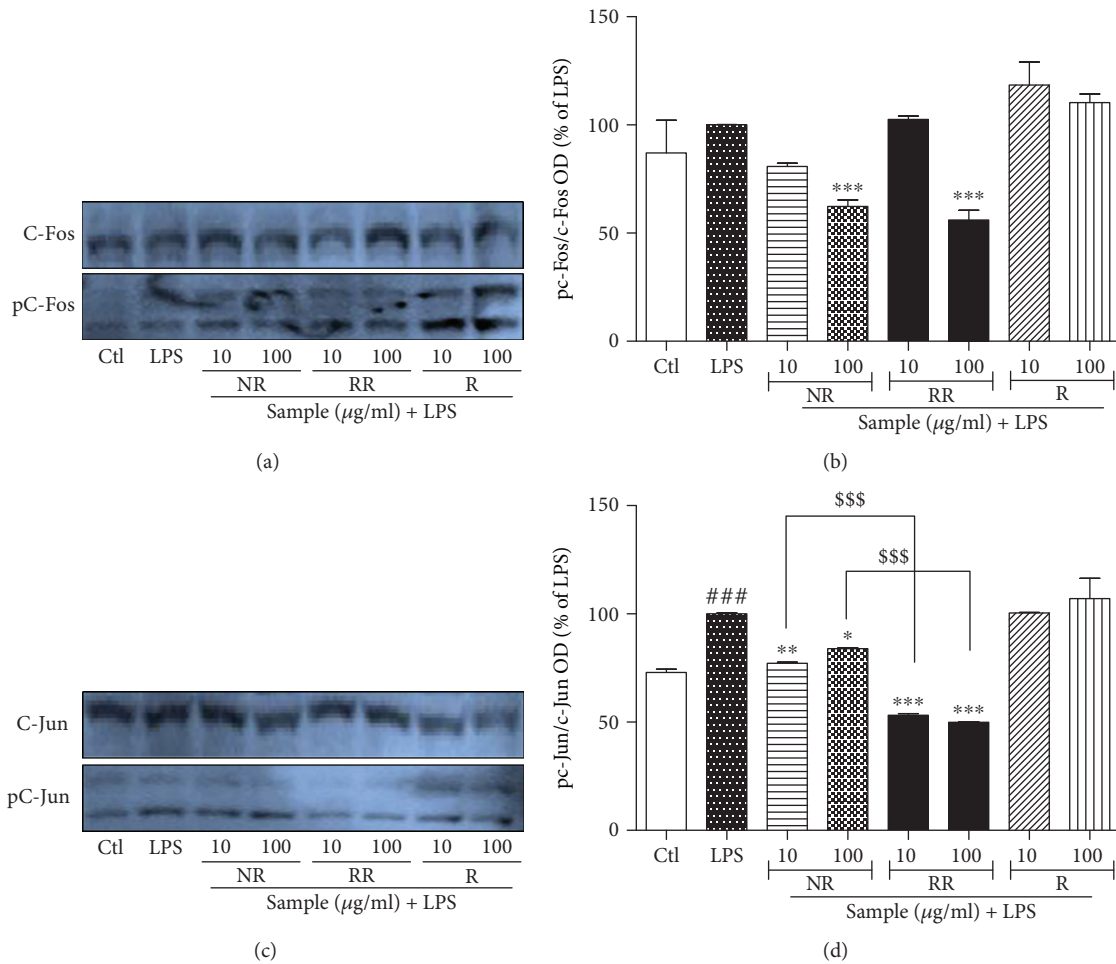


FIGURE 5: Resveratrol-enriched rice modulates AP-1 effector signaling in lipopolysaccharide-activated BV2 microglial cells. BV2 microglial cells were treated with samples, followed by LPS (100 ng/mL) activation. AP-1 signaling was evaluated after incubation of cells for 1 h. AP-1 expression was measured pretreatment in LPS-activated BV2 cells. (a, b) p-C-Fos/C-Fos protein expression and band intensity, and (c, d) p-C-Jun/c-Jun expression and band intensity after incubation with LPS and samples for 1 h in BV2 cells. All data are presented as the mean \pm standard error of the mean of three independent experiments. * $P < 0.05$, ** $P < 0.01$, and *** $P < 0.001$ indicate significant differences compared with LPS treatment alone. ## $P < 0.01$ and ### $P < 0.001$ indicate significant differences compared with untreated control group. \$\$\$ $P < 0.001$ indicates significant differences to RR compared to NR. Ctl, untreated control and LPS, lipopolysaccharide.

inhibited pP38 expression, only RR treatment showed significant inhibition when compared with LPS-only-treated group as shown in (Figure 7).

3.8. NR, RR, and Resveratrol Treatment Inhibits Production of Proinflammatory Cytokines. RR-mediated inhibition of NF- κ B translocation and NF- κ B/I- κ B transcription revealed the reason for the marked inhibition of nitrite levels and iNOS/COX-2 expression. This was further confirmed through the measurement of proinflammatory cytokine levels in LPS-activated BV2 microglial cells. NR, RR, and resveratrol demonstrated almost similar potency to inhibit PGE2 secretion, while resveratrol showed the highest potency for inhibition of TNF- α and IL-6 production as shown in (Figure 8). The effect of RR for the inhibition of the inflammatory cytokines is significantly higher in comparison to the NR alone as shown in Figure 8, suggesting the better potency of RR to that of NR alone. As resveratrol,

the pure compound, and extracts of NR and RR demonstrated almost equipotent ability to inhibit proinflammatory cytokine production, it can be suggested that RR is sufficiently capable to inhibit the production of not only inflammatory mediators but also proinflammatory cytokines.

4. Discussion

In this study, we reported the antineuroinflammatory properties of RR for the first time. We compared the cytotoxicity of RR with NR and resveratrol in LPS-stimulated BV2 microglia. In addition, we determined the effects of RR, NR, and resveratrol on the various parameters of neuroinflammation, including COX2, iNOS, nitric oxide, MAPK signaling in both acute and chronic conditions of activated microglia, AP-1 and NF- κ B signaling, and inflammatory mediator production in activated microglia. Our findings revealed that

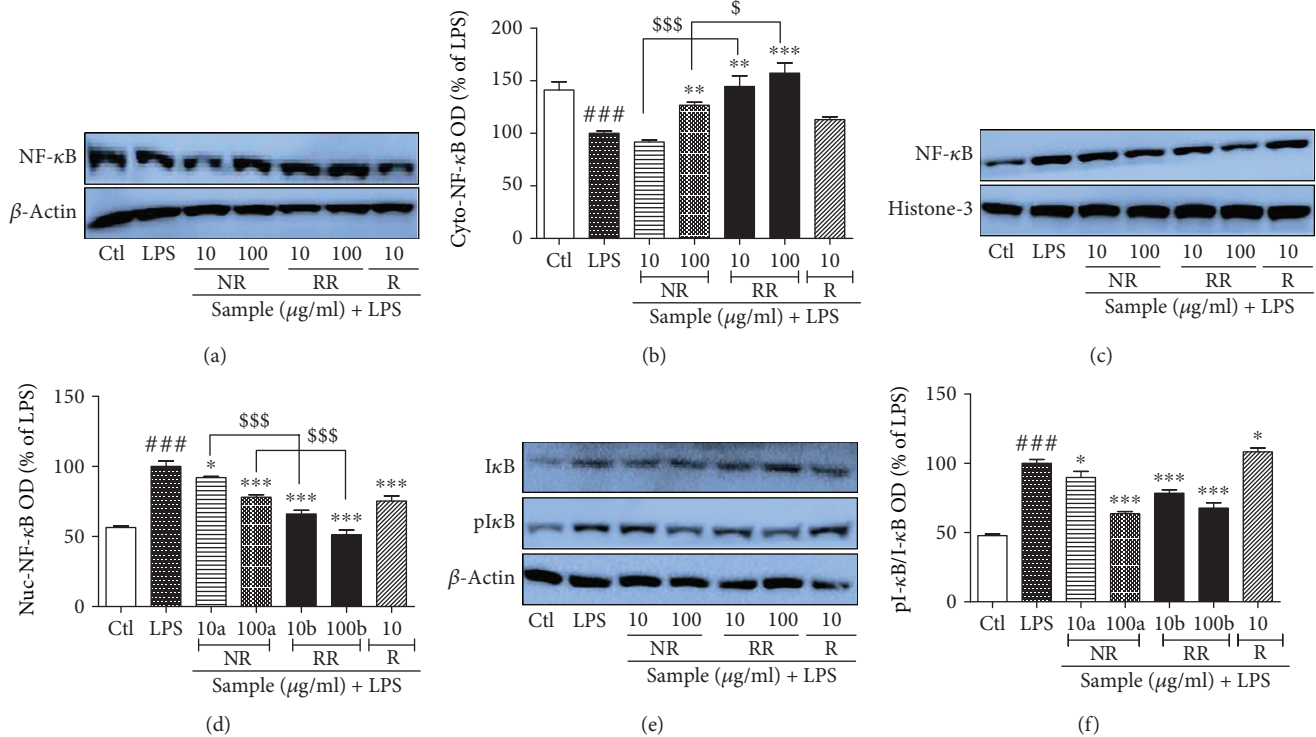


FIGURE 6: Treatment with resveratrol-enriched rice inhibits NF- κ B translocation and I- κ B phosphorylation in lipopolysaccharide-activated BV2 cells. BV2 microglial cells were pretreated with normal rice (NR), resveratrol-enriched rice (RR), and resveratrol after 30 min of LPS (100 ng/mL) stimulation. NF- κ B and I- κ B/pI- κ B expression was determined after 1 h of LPS activation. (a, b) Cytosolic NF- κ B expression and band intensity. β -Actin was used as loading control. (c, d) Nucleolar NF- κ B expression and band intensity. Histone-3 was used as loading control. (e, f) Cytosolic I- κ B and pI- κ B expression and band intensity. β -Actin was used as loading control. All data are presented as the mean \pm standard error of the mean of three independent experiments. * P < 0.05, ** P < 0.01, and *** P < 0.001 indicate significant differences compared with LPS treatment alone. # P < 0.05 and ### P < 0.001 indicate significant differences compared with untreated control group. \$ P < 0.05 and \$\$\$ P < 0.001 indicate significant differences to RR compared to NR. Ctl, untreated control and LPS, lipopolysaccharide.

RR showed equal or higher anti-inflammatory efficacy than resveratrol alone, without any cytotoxicity.

Neuroinflammation and brain aging leads to continuous degeneration of brain function [32]. Aging process specifically targets the brain, cardiovascular system, and metabolic system, either in intrinsic or extrinsic aging [33]. Aging as well as neuroinflammation is the key mediator of neurodegenerative conditions such as AD and PD [34]. As RR treatment significantly attenuated UVB-induced skin aging, metabolic disorders, and hyperpigmentation both *in vitro* and *in vivo* in our previous study, we further designed an experiment to determine their effect against neuroinflammation, which is a major cause of almost all neurological disorders [28]. Potent inhibition of inflammation by RR treatment in UVB/ROS-induced dermal fibroblasts in our previous report serves as a cue for this experiment [28]. As neuroinflammation caused by overactivated microglia can aggravate neurodegeneration in AD, PD, MS, and ischemic stroke, [35], controlling microglial activation could be a potential strategy for the management of these disorders. Acute but strong activation of microglia is observed in ischemic stroke, while chronic microglial activation and neuroinflammation are observed in AD, PD, and MS [36], indicating that inhibition of microglial activation and its

inflammatory cascades is the key therapy against such CNS disorders. Resveratrol, a multifunctional phytochemical, has a proven efficacy against diabetes, cardiovascular disease, obesity, and asthma via alterations in the gut microbiome [37]. Human gut microbiota play an important role in the treatment of various CNS disorders, including neuroinflammation regulation in dementia [38]. It is also possible that the RR-mediated antineuroinflammatory effect might be exerted through the alteration of gut microbiome. Resveratrol at high concentrations might be toxic to the gut microbiome, but RR is completely safe to normal cells as shown in our previous study.

NO production by overactivated microglia is a key biomarker for neuroinflammation in CNS disorders. In a preliminary study, the treatment of NR, RR, and resveratrol showed significant inhibition of nitrite production in LPS-activated BV2 microglial cells, without cellular toxicity. Therefore, we decided to perform a mechanistic study. The inhibition of nitrite production and the IC_{50} value for nitrite release was lower in the RR-treated group than in NR-, resveratrol-, and L-NMMA-treated groups. Increased expression of iNOS is necessary for the increased production and release of NO by activated microglia, whereas COX2 expression is required for its induction of arachidonic acid

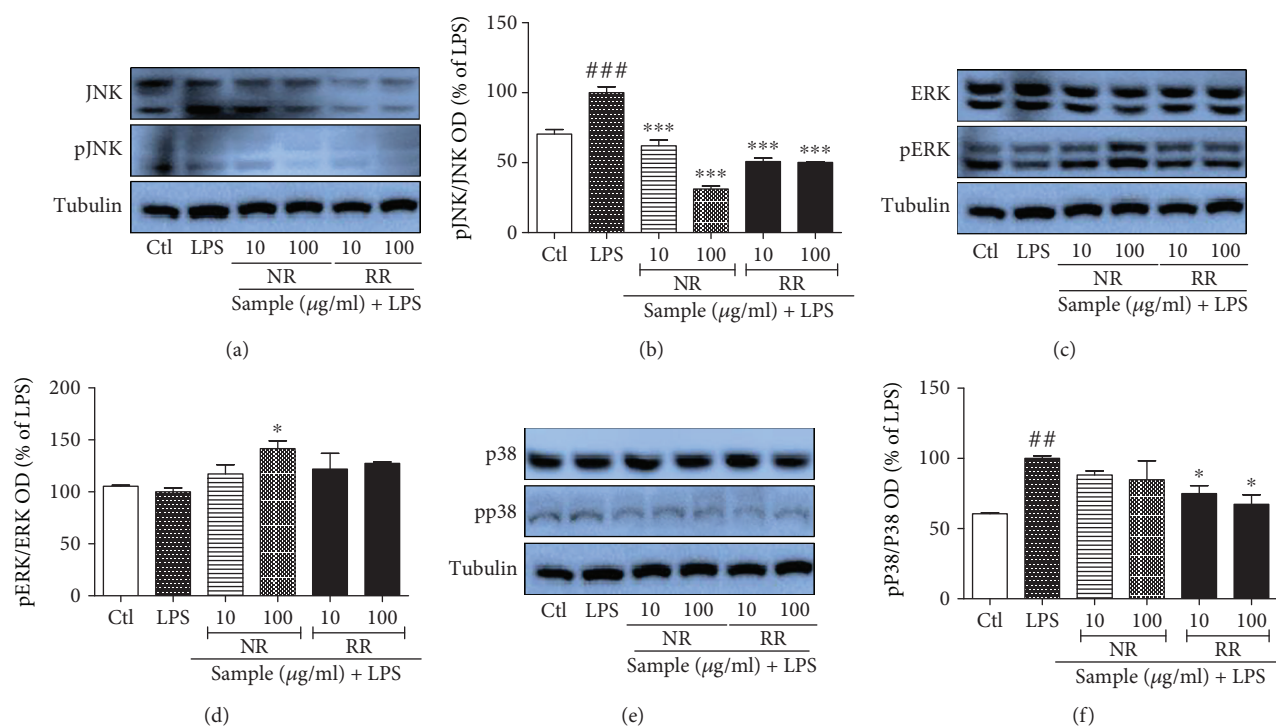


FIGURE 7: Treatment with resveratrol-enriched rice modulates MAPK signaling lipopolysaccharide-activated BV2 cells. BV2 microglial cells were pretreated with normal rice (NR), resveratrol-enriched rice (RR), and resveratrol 30 min prior to LPS (100 ng/mL) treatment. MAPK modulation was observed after 24 h of sample treatment and LPS activation. (a, b) JNK/pJNK expression and band intensity, (c, d) ERK/pERK expression and band intensity, (e, f) p38/pp38 expression and band intensity in LPS-activated BV2 microglia. All data are presented as the mean \pm standard error of the mean of three independent experiments. * $P < 0.05$, and *** $P < 0.001$ indicate significant differences compared with LPS treatment alone. ## $P < 0.01$, and ### $P < 0.001$ indicate significant differences compared with the untreated control group. Ctl, untreated control and LPS, lipopolysaccharide.

pathway via increased PGE2 production. In different edible plants, phytochemicals such as sulforaphane, resveratrol, and curcumin have antineuroinflammatory role either through the Sirt1 and NRF2 activation or inhibition of the NF- κ B translocation and transcription of the inflammatory proteins [17, 39]. Similarly, NR also possesses the antioxidative, anti-inflammatory phytochemicals such as phenolic acids, flavonoids, anthocyanins, proanthocyanidins, tocopherols, γ -oryzanol, and phytic acid [40]. NR contains the α -tocopherol, γ -tocopherol, and tocotrienol as active ingredients [40, 41] which have the potential to inhibit the cytotoxicity against LPS [42]. In specific, γ -tocopherol and its metabolites inhibited the cyclooxygenase activity followed by the inhibition of PGE2 in macrophages and epithelial cells [30]. This finding is also supported by our data that treatment of NR containing α -tocopherol and γ -tocopherol significantly inhibited the COX-2 expression as well as PGE2 production in acute and chronic microglial activation. In addition, we evaluated the effect of α -tocopherol and γ -tocopherol and found that treatment of α -tocopherol and γ -tocopherol not only inhibited the nitrite production but also attenuated the expression of iNOS and COX-2 without cellular toxicity up to the concentration of 1 mg/mL. This data revealed that phytochemicals such as α -tocopherol and γ -tocopherol in NR were responsible for the anti-inflammatory potential. In addition to this, their presence and their effectiveness/safety profile over

resveratrol toxicity make RR a better candidate against neuroinflammation. As inhibition of COX-2 by NR and its phytochemicals is more prominent and COX-2 is involved in the induction of pain [43, 44], the applicability of NR might be highly promising in neuropathic pain model. RR exhibited a minor role in inhibiting COX-2 expression; however, its potency to inhibit iNOS under acute and chronic neuroinflammatory conditions was higher than that of resveratrol and NR. These results collectively support the fact that the higher potency of RR in inhibiting iNOS expression was responsible for its higher potency in inhibiting nitrite production. For a compound or sample to inhibit inflammatory cascades, they must control the inflammatory signaling pathways such as MAPK signaling. This in turn helps in regulating NF- κ B translocation, followed by I- κ B degradation and AP-1 signaling, and these events facilitate the transcription of inflammatory proteins and proinflammatory cytokines [9, 15]. Treatment of activated microglia with RR significantly inhibited the expression of MAPK proteins as evidenced by attenuated phosphorylation of JNK, ERK, and P38 under acute activation condition. Resveratrol treatment significantly increased the expression of JNK, probably because of its cytotoxic nature to normal cells, while RR downregulated the expression of JNK. These results collectively symbolize the superiority of RR over resveratrol in modulating MAPK signaling. This effect was further confirmed in chronic activation condition. LPS exposure to

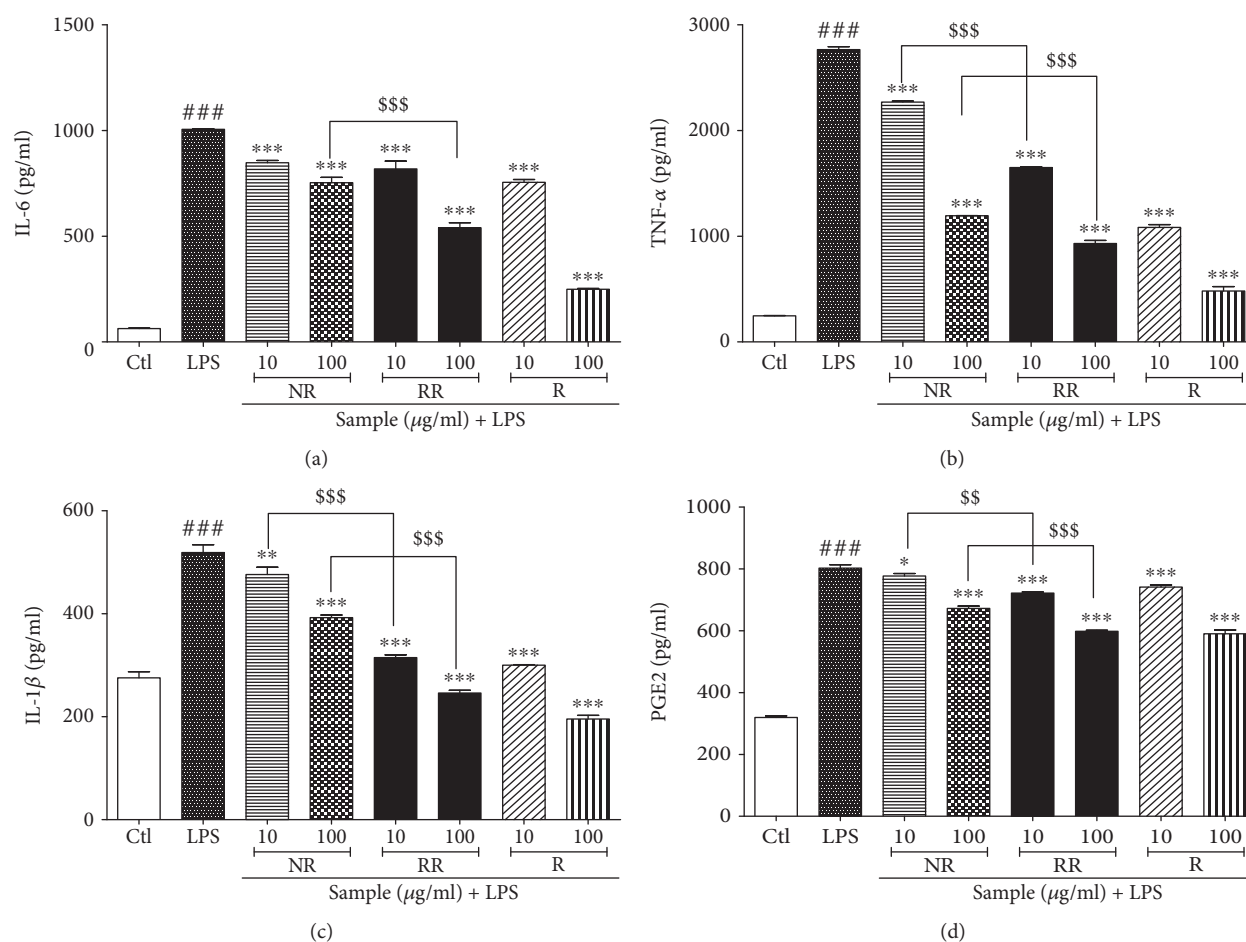


FIGURE 8: Treatment with resveratrol-enriched rice inhibits proinflammatory cytokine production in lipopolysaccharide-activated BV2 cells. BV2 microglial cells were pretreated with normal rice (NR), resveratrol-enriched rice (RR), and resveratrol 30 min prior to lipopolysaccharide (LPS; 100 ng/mL) stimulation. Proinflammatory cytokine levels were measured in the conditioned medium of treated cells using ELISA assay after 24 h of LPS activation. The proinflammatory cytokine levels in NR-, RR-, and resveratrol-treated BV2 cells were evaluated. (a) IL-6 production, (b) TNF- α secretion, (c) IL-1 β secretion, and (d) PGE2 secretion. All data are presented as the mean \pm standard error of the mean of three independent experiments. * P < 0.05, ** P < 0.01, and *** P < 0.001 indicate significant differences compared with LPS treatment alone. ### P < 0.001 indicates significant differences compared with untreated control group. \$\$ P < 0.01 and \$\$\$ P < 0.001 indicate significant differences in RR compared with NR group. Ctl, untreated control.

microglia up to 24 h results in chronic activation and induces continuous cascades of neuroinflammation via inflammatory signaling and inflammatory protein production [45, 46]. RR treatment significantly inhibited the activation of JNK and p38, but it did not show any significant effect on ERK phosphorylation. MAPK signaling takes place within a very short time of toll-like receptor 4 (TLR4) activation; however, in chronic microglial activation, JNK and p38 phosphorylation play imperative roles in inflammatory cascade maintenance and induction [19, 47, 48]. In our study, RR treatment inhibited JNK and p38 phosphorylation with a higher potency than resveratrol treatment. Notably, the potency of NR to inhibit pJNK expression in acute and chronic activation conditions was higher than that of RR and resveratrol alone, which could explain the increase in pJNK expression by resveratrol and significant inhibition of pJNK expression by RR. ERK activation has a dual role: short-term activation occurs during inflammation and long-term activation occurs during cell survival [49]. The increase/insignificant inhibition of

pERK expression by NR suggests its role against LPS-induced toxicity by increasing the survival of microglia. Interventions that can control JNK and ERK activation will alter the expression of AP-1 signaling [50, 51]. Resveratrol increased the expression of pJNK and p-C-Jun expression, while RR treatment inhibited the phosphorylation of pJNK and p-C-Jun. Both NR and RR inhibited p-C-Jun and p-C-Fos expression, but resveratrol did not show a similar effect. Furthermore, we assessed the role of RR against NF- κ B translocation and I- κ B degradation. We observed significantly higher amounts of NF- κ B in the cytosol and lower amounts in the nucleus in the RR-treated group, indicating that RR inhibited the translocation of NF- κ B from the cytosol to the nucleus. Additionally, significantly low levels of phosphorylated I- κ B in the cytosol confirmed that RR inhibited the degradation of I- κ B in activated microglia, suggesting the strong antineuroinflammatory effects of RR against activated microglia. Although the resveratrol is a pure compound, we used here to compare the effectiveness of RR (extract of

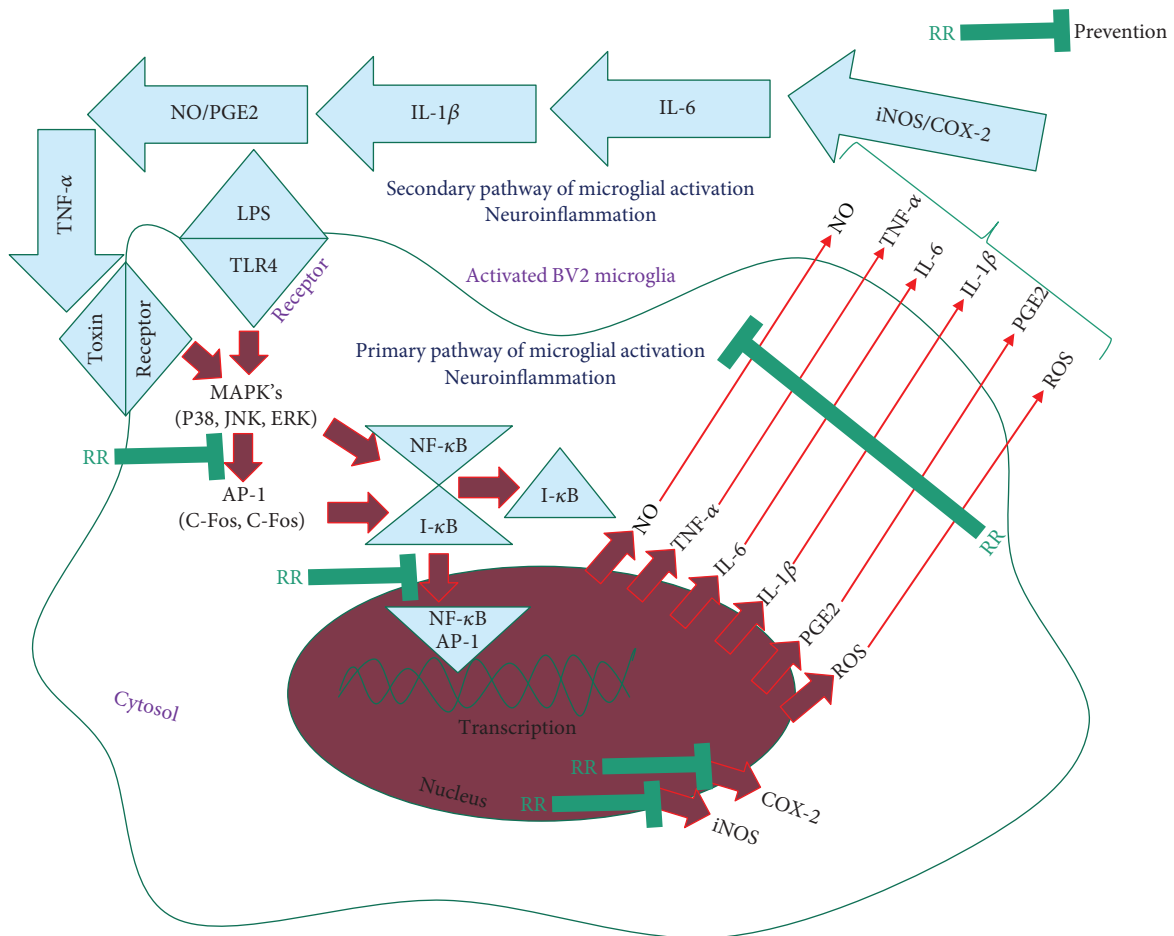


FIGURE 9: Schematic diagram for the antineuroinflammatory effect of resveratrol-enriched rice (RR) against LPS-induced microglia activation.

resveratrol-enriched rice) in comparison to NR (extract of normal rice) and resveratrol alone. NR, RR, and R treatment showed the different potencies in different concentrations for inhibition of inflammatory parameters. The highest concentration of resveratrol, i.e., 100 μ g/mL, showed the highest potency but it also possessed the cellular toxicity. We found the potential effect of RR that seems to act in synergistic effect of NR and resveratrol. NR also showed good potency to inhibit the inflammatory cascades. Therefore, we hypothesized that the presence of phytochemicals α -tocopherol and γ -tocopherol in NR can boost the activity of RR either they can help for the protection of cells against resveratrol-mediated cell death or morphological changes. We evaluated the potential antineuroinflammatory effect of α -tocopherol and γ -tocopherol in rice and found that treatment of α -tocopherol and γ -tocopherol inhibited not only the nitrite production but also the expression of iNOS and COX-2 without cellular toxicity up to the concentration of 1 mg/mL. This data supports that active phytochemicals including α -tocopherol and γ -tocopherol in NR are responsible for the anti-inflammatory potential in LPS-treated BV2 cells. Also, we found that the RR-treated group significantly showed the higher potency of RR than resveratrol-treated group alone in experimental group. Hence, the most notable

achievement of this study was the improved efficacy of resveratrol following preparation of pharmaceutical crops (rice) containing resveratrol, which showed negligible toxicity on microglial cells.

In this study, we not only discovered the safe and effective role of RR against aging and neuroinflammation but also identified the antineuroinflammatory potential of NR itself is because of the presence of active phytochemicals such as α -tocopherol and γ -tocopherol in rice. The anti-inflammatory effect by RR treatment seems to be mediated through inhibition of nitrite production, MAPK phosphorylation, NF- κ B mediated production of proinflammatory cytokines, and expressions of inflammatory proteins which are shown in Figure 9 as a summarized figure. Thus, consumption of RR as a functional food will not only act as a nutritional food component but also as a medicinal ambrosia for the prevention and treatment of various human disorders. Further research should be performed to evaluate the antineuroinflammatory potential of RR in various neuroinflammatory disorders through both *in vitro* and *in vivo* studies.

Data Availability

All the data are included within the manuscript.

Conflicts of Interest

The authors declare that there is no conflict of interests regarding the publication of this paper.

Acknowledgments

This work was supported by a grant from the National Research Foundation of Korea (NRF) funded by the Korean government (MSIP) (no. NRF-2017R1A4A 1015594), the Cooperative Research Program for Agriculture Science & Technology Development (project no. 01118803) of the Rural Development Administration, and the Next-Generation BioGreen 21 Program (project no. PJ01369101), RDA, Republic of Korea.

References

- [1] P. Hunter, "The inflammation theory of disease. The growing realization that chronic inflammation is crucial in many diseases opens new avenues for treatment," *EMBO Reports*, vol. 13, no. 11, pp. 968–970, 2012.
- [2] N. Khansari, Y. Shakiba, and M. Mahmoudi, "Chronic inflammation and oxidative stress as a major cause of age-related diseases and cancer," *Recent Patents on Inflammation & Allergy Drug Discovery*, vol. 3, no. 1, pp. 73–80, 2009.
- [3] S. Amor, F. Puentes, D. Baker, and P. van der Valk, "Inflammation in neurodegenerative diseases," *Immunology*, vol. 129, no. 2, pp. 154–169, 2010.
- [4] P. Eikelenboom, C. Bate, W. A. Van Gool et al., "Neuroinflammation in Alzheimer's disease and prion disease," *Glia*, vol. 40, no. 2, pp. 232–239, 2002.
- [5] R. Fu, Q. Shen, P. Xu, J. J. Luo, and Y. Tang, "Phagocytosis of microglia in the central nervous system diseases," *Molecular Neurobiology*, vol. 49, no. 3, pp. 1422–1434, 2014.
- [6] I. Bardou, H. M. Brothers, R. M. Kaercher, S. C. Hopp, and G. L. Wenk, "Differential effects of duration and age on the consequences of neuroinflammation in the hippocampus," *Neurobiology of Aging*, vol. 34, no. 10, pp. 2293–2301, 2013.
- [7] C. Franceschi and J. Campisi, "Chronic inflammation (inflammaging) and its potential contribution to age-associated diseases," *The Journals of Gerontology Series A: Biological Sciences and Medical Sciences*, vol. 69, Supplement 1, pp. S4–S9, 2014.
- [8] D. Raj, Z. Yin, M. Breur et al., "Increased white matter inflammation in aging- and Alzheimer's disease brain," *Frontiers in Molecular Neuroscience*, vol. 10, p. 206, 2017.
- [9] S. K. Ha, E. Moon, M. S. Ju et al., "6-Shogaol, a ginger product, modulates neuroinflammation: a new approach to neuroprotection," *Neuropharmacology*, vol. 63, no. 2, pp. 211–223, 2012.
- [10] D. W. Reif and S. A. McCreedy, "N-nitro-L-arginine and N-monomethyl-L-arginine exhibit a different pattern of inactivation toward the three nitric oxide synthases," *Archives of Biochemistry and Biophysics*, vol. 320, no. 1, pp. 170–176, 1995.
- [11] M. E. Lull and M. L. Block, "Microglial activation and chronic neurodegeneration," *Neurotherapeutics*, vol. 7, no. 4, pp. 354–365, 2010.
- [12] S. Reuter, S. C. Gupta, M. M. Chaturvedi, and B. B. Aggarwal, "Oxidative stress, inflammation, and cancer: how are they linked?," *Free Radical Biology & Medicine*, vol. 49, no. 11, pp. 1603–1616, 2010.
- [13] S. Ramachandiran, Q. Huang, J. Dong, S. S. Lau, and T. J. Monks, "Mitogen-activated protein kinases contribute to reactive oxygen species-induced cell death in renal proximal tubule epithelial cells," *Chemical Research in Toxicology*, vol. 15, no. 12, pp. 1635–1642, 2002.
- [14] H. Khalaf, J. Jass, and P. E. Olsson, "Differential cytokine regulation by NF- κ B and AP-1 in Jurkat T-cells," *BMC Immunology*, vol. 11, no. 1, p. 26, 2010.
- [15] S. Fujioka, J. Niu, C. Schmidt et al., "NF- κ B and AP-1 connection: mechanism of NF- κ B-dependent regulation of AP-1 activity," *Molecular and Cellular Biology*, vol. 24, no. 17, pp. 7806–7819, 2004.
- [16] R. H. Shih, C. Y. Wang, and C. M. Yang, "NF-kappaB signaling pathways in neurological inflammation: a mini review," *Frontiers in Molecular Neuroscience*, vol. 8, p. 77, 2015.
- [17] G. Corbi, V. Conti, S. Davinelli, G. Scapagnini, A. Filippelli, and N. Ferrara, "Dietary phytochemicals in neuroimmunology: a new therapeutic possibility for humans?," *Frontiers in Pharmacology*, vol. 7, p. 364, 2016.
- [18] R. Venkatesan, E. Ji, and S. Y. Kim, "Phytochemicals that regulate neurodegenerative disease by targeting neurotrophins: a comprehensive review," *BioMed Research International*, vol. 2015, Article ID 814068, 22 pages, 2015.
- [19] L. Subedi, R. Venkatesan, and S. Kim, "Neuroprotective and anti-inflammatory activities of allyl isothiocyanate through attenuation of JNK/NF- κ B/TNF- α signaling," *International Journal of Molecular Sciences*, vol. 18, no. 7, 2017.
- [20] L. Subedi, B. P. Gaire, M. H. Do, T. H. Lee, and S. Y. Kim, "Anti-neuroinflammatory and neuroprotective effects of the *Lindera neesiana* fruit in vitro," *Phytomedicine*, vol. 23, no. 8, pp. 872–881, 2016.
- [21] K. P. L. Bhat, J. W. Kosmeder II, and J. M. Pezzuto, "Biological effects of resveratrol," *Antioxidants & Redox Signaling*, vol. 3, no. 6, pp. 1041–1064, 2001.
- [22] C. Moussa, M. Hebron, X. Huang et al., "Resveratrol regulates neuro-inflammation and induces adaptive immunity in Alzheimer's disease," *Journal of Neuroinflammation*, vol. 14, no. 1, p. 1, 2017.
- [23] R. Y. Tsai, J. C. Wang, K. Y. Chou, C. S. Wong, and C. H. Cherng, "Resveratrol reverses morphine-induced neuroinflammation in morphine-tolerant rats by reversal HDAC1 expression," *Journal of the Formosan Medical Association*, vol. 115, no. 6, pp. 445–454, 2016.
- [24] J. Burns, T. Yokota, H. Ashihara, M. E. J. Lean, and A. Crozier, "Plant foods and herbal sources of resveratrol," *Journal of Agricultural and Food Chemistry*, vol. 50, no. 11, pp. 3337–3340, 2002.
- [25] S. Weiskirchen and R. Weiskirchen, "Resveratrol: how much wine do you have to drink to stay healthy?," *Advances in Nutrition*, vol. 7, no. 4, pp. 706–718, 2016.
- [26] A. Fujimoto, Y. Sakanashi, H. Matsui et al., "Cytometric analysis of cytotoxicity of polyphenols and related phenolics to rat thymocytes: potent cytotoxicity of resveratrol to normal cells," *Basic & Clinical Pharmacology & Toxicology*, vol. 104, no. 6, pp. 455–462, 2009.
- [27] S. H. Baek, W. C. Shin, H. S. Ryu et al., "Creation of resveratrol-enriched rice for the treatment of metabolic syndrome and related diseases," *PLoS One*, vol. 8, no. 3, article e57930, 2013.
- [28] L. Subedi, T. H. Lee, H. M. Wahedi, S. H. Baek, and S. Y. Kim, "Resveratrol-enriched Rice attenuates UVB-ROS-induced skin

- aging via downregulation of inflammatory cascades,” *Oxidative Medicine and Cellular Longevity*, vol. 2017, Article ID 8379539, 15 pages, 2017.
- [29] J. Chae, L. Subedi, M. Jeong et al., “Gomisin N inhibits melanogenesis through regulating the PI3K/Akt and MAPK/ERK signaling pathways in melanocytes,” *International Journal of Molecular Sciences*, vol. 18, no. 2, 2017.
- [30] Q. Jiang, I. Elson-Schwab, C. Courtemanche, and B. N. Ames, “ γ -Tocopherol and its major metabolite, in contrast to α -tocopherol, inhibit cyclooxygenase activity in macrophages and epithelial cells,” *Proceedings of the National Academy of Sciences of the United States of America*, vol. 97, no. 21, pp. 11494–11499, 2000.
- [31] S. P. M. Reddy and B. T. Mossman, “Role and regulation of activator protein-1 in toxicant-induced responses of the lung,” *American Journal of Physiology-Lung Cellular and Molecular Physiology*, vol. 283, no. 6, pp. L1161–L1178, 2002.
- [32] I. Stambler, “Recognizing degenerative aging as a treatable medical condition: methodology and policy,” *Aging and Disease*, vol. 8, no. 5, pp. 583–589, 2017.
- [33] G. R. Boss and J. E. Seegmiller, “Age-related physiological changes and their clinical significance,” *The Western Journal of Medicine*, vol. 135, no. 6, pp. 434–440, 1981.
- [34] E. T. Ang, Y. K. Tai, S. Q. Lo, R. Seet, and T. W. Soong, “Neurodegenerative diseases: exercising toward neurogenesis and neuroregeneration,” *Frontiers in Aging Neuroscience*, vol. 2, 2010.
- [35] C. K. Glass, K. Saijo, B. Winner, M. C. Marchetto, and F. H. Gage, “Mechanisms underlying inflammation in neurodegeneration,” *Cell*, vol. 140, no. 6, pp. 918–934, 2010.
- [36] A. R. Patel, R. Ritzel, L. D. McCullough, and F. Liu, “Microglia and ischemic stroke: a double-edged sword,” *International Journal of Physiology, Pathophysiology and Pharmacology*, vol. 5, no. 2, pp. 73–90, 2013.
- [37] J. K. Bird, D. Raederstorff, P. Weber, and R. E. Steinert, “Cardiovascular and antiobesity effects of resveratrol mediated through the gut microbiota,” *Advances in Nutrition*, vol. 8, no. 6, pp. 839–849, 2017.
- [38] R. Alkadir, J. Li, X. Li, M. Jin, and B. Zhu, “Human gut microbiota: the links with dementia development,” *Protein & Cell*, vol. 8, no. 2, pp. 90–102, 2017.
- [39] S. Davinelli, M. Maes, G. Corbi, A. Zarrelli, D. C. Willcox, and G. Scapagnini, “Dietary phytochemicals and neuro-inflammation: from mechanistic insights to translational challenges,” *Immunity & Ageing*, vol. 13, no. 1, p. 16, 2016.
- [40] P. Goufo and H. Trindade, “Rice antioxidants: phenolic acids, flavonoids, anthocyanins, proanthocyanidins, tocopherols, tocotrienols, γ -oryzanol, and phytic acid,” *Food Science & Nutrition*, vol. 2, no. 2, pp. 75–104, 2014.
- [41] B. Shammugasamy, Y. Ramakrishnan, H. M. Ghazali, and K. Muhammad, “Tocopherol and tocotrienol contents of different varieties of rice in Malaysia,” *Journal of the Science of Food and Agriculture*, vol. 95, no. 4, pp. 672–678, 2015.
- [42] K. Nishio, M. Horie, Y. Akazawa et al., “Attenuation of lipopolysaccharide (LPS)-induced cytotoxicity by tocopherols and tocotrienols,” *Redox Biology*, vol. 1, no. 1, pp. 97–103, 2013.
- [43] E. Ricciotti and G. A. FitzGerald, “Prostaglandins and inflammation,” *Arteriosclerosis, Thrombosis, and Vascular Biology*, vol. 31, no. 5, pp. 986–1000, 2011.
- [44] Y. Lee, C. Rodriguez, and R. Dionne, “The role of COX-2 in acute pain and the use of selective COX-2 inhibitors for acute pain relief,” *Current Pharmaceutical Design*, vol. 11, no. 14, pp. 1737–1755, 2005.
- [45] X. J. Dai, N. Li, L. Yu et al., “Activation of BV2 microglia by lipopolysaccharide triggers an inflammatory reaction in PC12 cell apoptosis through a toll-like receptor 4-dependent pathway,” *Cell Stress and Chaperones*, vol. 20, no. 2, pp. 321–331, 2015.
- [46] L. Subedi, O. W. Kwon, C. Pak et al., “N,N-disubstituted azines attenuate LPS-mediated neuroinflammation in microglia and neuronal apoptosis via inhibiting MAPK signaling pathways,” *BMC Neuroscience*, vol. 18, no. 1, p. 82, 2017.
- [47] U. Namgung and Z. Xia, “Arsenite-induced apoptosis in cortical neurons is mediated by c-Jun N-terminal protein kinase 3 and p38 mitogen-activated protein kinase,” *The Journal of Neuroscience*, vol. 20, no. 17, pp. 6442–6451, 2000.
- [48] W. He, M. F. Zhang, J. Ye, T. T. Jiang, X. Fang, and Y. Song, “Cordycepin induces apoptosis by enhancing JNK and p38 kinase activity and increasing the protein expression of Bcl-2 pro-apoptotic molecules,” *Journal of Zhejiang University SCIENCE B*, vol. 11, no. 9, pp. 654–660, 2010.
- [49] C. Cruz and F. Cruz, “The ERK 1 and 2 pathway in the nervous system: from basic aspects to possible clinical applications in pain and visceral dysfunction,” *Current Neuropharmacology*, vol. 5, no. 4, pp. 244–252, 2007.
- [50] M. Karin and C. J. Marshall, “The regulation of AP-1 activity by mitogen-activated protein kinases,” *Philosophical Transactions of the Royal Society of London. Series B, Biological Sciences*, vol. 351, no. 1336, pp. 127–134, 1996.
- [51] A. J. Whitmarsh and R. J. Davis, “Transcription factor AP-1 regulation by mitogen-activated protein kinase signal transduction pathways,” *Journal of Molecular Medicine*, vol. 74, no. 10, pp. 589–607, 1996.

Clinical Study

A Double-Blind Placebo-Controlled Randomized Trial Evaluating the Effect of Polyphenol-Rich Herbal Congee on Bone Turnover Markers of the Perimenopausal and Menopausal Women

Jintanaporn Wattanathorn ^{1,2}, Woraluk Somboonporn,³ Sudarat Sungkamane,^{2,4} Wipawee Thukumtee,^{1,2} and Supaporn Muchimapura ^{1,2}

¹Department of Physiology, Faculty of Medicine, Khon Kaen University, Khon Kaen 40002, Thailand

²Integrative Complementary Alternative Medicine Research and Development Center, Khon Kaen University, Khon Kaen 40002, Thailand

³Department of Obstetrics and Gynaecology, Faculty of Medicine, Khon Kaen University, Khon Kaen 40002, Thailand

⁴Department of Physiology (Neuroscience Program), Faculty of Medicine, Khon Kaen University, Khon Kaen 40002, Thailand

Correspondence should be addressed to Jintanaporn Wattanathorn; jinwat05@gmail.com

Received 13 March 2018; Revised 24 September 2018; Accepted 16 October 2018; Published 21 November 2018

Guest Editor: Anderson J. Teodoro

Copyright © 2018 Jintanaporn Wattanathorn et al. This is an open access article distributed under the Creative Commons Attribution License, which permits unrestricted use, distribution, and reproduction in any medium, provided the original work is properly cited.

Based on the benefit of polyphenolic compounds on osteoporosis, we hypothesized that the polyphenol-rich herbal congee containing the combined extract of *Morus alba* and *Polygonum odoratum* leaves should improve bone turnover markers in menopausal women. To test this hypothesis, a randomized double-blind placebo-controlled study was performed. A total of 45 menopausal participants were recruited in this study. They were randomly divided into placebo, D1, and D2 groups, respectively. The subjects in D1 and D2 groups must consume the congee containing the combined extract of *M. alba* and *P. odoratum* leaves at doses of 50 and 1500 mg/day, respectively. At the end of an 8-week consumption period, all subjects were determined serum bone markers including calcium, alkaline phosphatase, osteocalcin, and beta CTX. In addition, the hematological and blood clinical chemistry changes, and total phenolic content in the serum were also determined. The results showed that the menopausal women in D2 group increased serum alkaline phosphatase, osteocalcin, and total phenolic compounds content but decreased CTX level. Clinical safety assessment failed to show toxicity and adverse effects. Therefore, herbal congee containing the combined extract of *M. alba* and *P. odoratum* leaves is the potential functional food that can decrease the risk of osteoporosis.

1. Introduction

Bone is a dynamic organ that undergoes continuous remodeling by the coordination and balance between resorption and the formation activities of osteoclast and osteoblast cells [1]. It is well established that women are vulnerable to bone loss especially during and after menopause. Postmenopausal women lose trabecular bone mineral density (BMD) rapidly in their vertebrae, pelvis, and ultradistal wrist. After menopause, the cortical bone loss in the long bones and vertebrae

also occurs, but the rate of bone loss is slower than that in trabecular bone [2]. It has been reported that bone resorption assessed by using the bone resorption markers as indicator increases around 90% during this period [3]. Therefore, this situation increases bone fracture risk.

Currently, a noninvasive instrument such as dual energy X-ray absorptiometry (DXA) can be used as a tool to measure the body composition including bone density. However, it still has a limitation, and bone markers are more sensitive for detecting the change of bone dynamic [4]. Therefore,

the application of bone turnover markers (BTM) as the indices indicating bone dynamic has gained much attention. BTM are classified as the formation or resorption markers depending on their origins. It has been demonstrated that BTM changes occur in parallel with bone turnover process, so their alterations can reflect bone turnover state. Among various BTM, osteocalcin and alkaline phosphatase are regarded as bone formation markers, whereas C-telopeptide of type I collagen (CTX) and N-telopeptide of type I collagen (NTX) and tartrate-resistant acid phosphatase (TR-ACP) are regarded as bone resorption markers [5–8]. Recent studies have clearly demonstrated that polyphenolic compounds provide beneficial effect to bone health by decreasing oxidative stress and inflammation. In addition, they can also modulate osteoblastogenesis and osteoclastogenesis [9]. Based on the previous finding in experimental menopause that the combined extract of *Morus alba* and *Polygonum odoratum* showed the antiosteoporotic effect [10], the positive modulation effect of the congee containing the combined extract of *P. odoratum* and *M. alba* on bone turnover has been raised.

However, recent study has demonstrated that polyphenol substance can exert prooxidant activity [11] and interactions with other agents which in turn produces numerous detrimental effects [12]. Therefore, the adverse effects and toxicities can possibly occur especially in the repetitive administration of the polyphenol-rich product. To assure that the repetitive administration of the congee containing the combined extract of *P. odoratum* and *M. alba* exert the positive modulation effect on the bone turnover and safe for repetitive consumption, the effect of the congee mentioned earlier on bone formation and bone resorption markers together with the hematological and clinical chemistry values in the perimenopausal and menopausal women were determined.

2. Materials and Methods

This study was designed as the randomized controlled trial. All experiments were conducted at the Integrative Complementary Alternative Medicine Research and Development Center, Faculty of Medicine, Khon Kaen University. The study (code number UAPSBS201401) was conducted in accordance with the International Conference of Harmonization (ICH) for Good Clinical Practice (GCP) and in compliance with the Declaration of Helsinki and its further amendments. All protocols were approved by the Khon Kaen University Ethical Committee on Human Research (HE571373); ClinicalTrials.gov was approved ID NCT02562274.

2.1. Participants. Forty-five healthy Thai perimenopausal and postmenopausal women at the age between 45–60 years old (<5 years menstruation cessation) who lived in northeastern of Thailand were recruited to participate this study via advertisements at menopause clinic at Srinagarind Hospital, Faculty of Medicine, Khon Kaen University, Thailand. All subjects in this study were subjected to a physical examination and interviewed using a structured questionnaire to obtain information concerning demographic data, smoking, alcohol intake, physical activity, and dietary status. Subjects were excluded from this study if they were diagnosed with

hypertension, cancer, autoimmune diseases, gout or high uric acid, and disorders as described as follows: heart, liver, kidney, lung, mental, and endocrinological disorders such as thyroid, parathyroid, and diabetes. In addition, they should not have a history of drug use that could affect bone turnover and bone mineral density, pesticide exposure during one week before the test, hysterectomy and/or oophorectomy, alcohol or cigarettes addiction (cigarettes smoking >10 pieces/day), regular exercise (more than 3 time/weeks), unable to follow the study instructions during the trial and the participation in other projects.

2.2. A Polyphenol-Rich Congee Preparation. The aerial parts of *Polygonum odoratum* and *M. alba* leaves were collected from Amphoe Mueang Khon Kaen, Thailand, during April 2013 and prepared as water extract by decoction method. Then, they were filtered and lyophilized as powder. The combination extract of *P. odoratum* and *M. alba* was prepared according to petty patent number 9314, Department of Intellectual Property, Thailand, and used as the functional ingredient in herbal porridge. Each package (25 g/package) contained rice (dried mashed) 90.71%, chicken (dried mashed) 7.26%, and green shallot and coriander (dried mashed) 0.73%. Both placebo and herbal congee were prepared with the same procedure and contained the same ingredients except that the herbal congee contained the combined extract of *P. odoratum* and *M. alba* at doses of 50 and 1500 mg/pack, respectively (the selected doses were obtained from our preclinical data [10] by calculating the human equivalent doses). The placebo, D1, and D2 had the same appearance and smell. The congee containing high and low doses of the combined extract of *P. odoratum* and *M. alba* failed to show the significant calorie from placebo (placebo provided 94.24 whereas the herbal congee containing low and high doses of the combined extract of *P. odoratum* and *M. alba* provided 95.50 and 97.25 Kcal, respectively). Each package contained carbohydrate 20 grams, protein 2 grams, total fat 0 gram, cholesterol 0 mg, and fiber less than 1 gram. In addition, the fingerprint chromatogram of the herbal congee was determined via high performance liquid chromatography which consisted of 515 HPLC pump and 2998 photodiode array detector (Water Company, USA). Chromatographic separation was performed using C-18 end-capped Purospher® STAR column (250 × 4 mm; particle size; 5 μm) and guard column HPLC-Cartridge, Sorbet Lot No. HX255346 (Merck, Germany). Two mobile phases consisting of 2.5% acetic acid in deionized (DI) water (B) and methanol (A) were used to induce gradient elution. The gradient elution was carried out at a flow rate of 1.0 mL/min with the following gradient: 0 min, 10% A; 17 min, 70% A; 18–22 min, 100% A; 25, 50% A; 26–30 min, 10% A. The sample was filtered (0.2 μm, Whatman), and a direct injection of tested sample at the volume of 20 μL on the column was performed. The chromatograms were recorded at 280 nm using UV detector, data analysis was performed using EmpowerTM3, and the results were shown in Figure 1.

2.3. Experimental Design. Eligibility was evaluated by using the semistructure questionnaire, physical examination, and

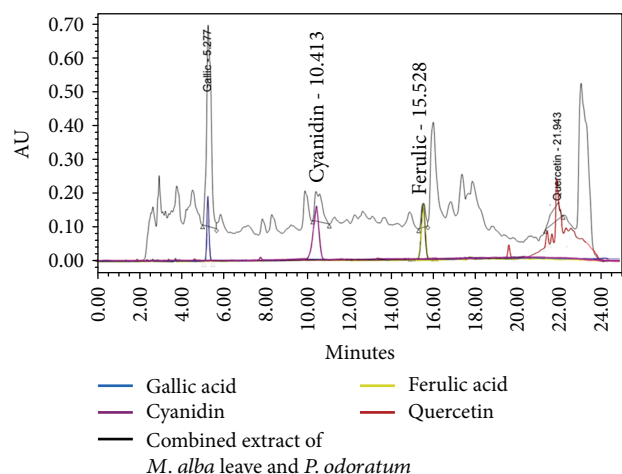


FIGURE 1: Fingerprint chromatogram of herbal congee containing the combined extract of *M. alba* and *P. odoratum*.

the results of the prestudy laboratory tests. Then, they were randomly allocated into placebo group and D1- and D2-treated groups. Subjects in D1- and D2-treated groups must consume the herbal congee containing the combined extract of *P. odoratum* and *M. alba* at doses of 50 and 1500 mg/day, respectively. Prior to the study participation, the participants must fill the informed consent form.

On the experimental day, all participants should not drink tea or coffee or alcohol beverages at least 12 hours before their appointments. In addition, the participants must consume the assigned substance once daily in the morning before breakfast for 8 weeks in a double-blind fashion. All subjects collected blood for the determination of bone markers consisting of serum levels of calcium, osteocalcin, alkaline phosphatase, and beta CTX together with the safety parameters including hematological and clinical chemistry changes prior to the study and at the end of an 8-week study period.

All volunteers were kept blind about treatments. The data interpretation and analysis were performed by blinded investigators, and the code numbers and the group allocation were revealed after the assessment of the last subject. All volunteers were instructed to call the study center in case of any adverse effect occurred during the study. Volunteers had the opportunity to withdraw from the study at any time. All the volunteers were contacted at definite intervals to ensure that they consumed the assigned substance regularly.

2.4. Blood Collection. Blood samples were collected from the participants after an overnight fast by venipuncture and allowed to clot and spun at 3000 rpm for 10 minutes in order to separate cells from serum. Then, the serum was transferred into dry well-labeled specimen plastic tubes and analyzed.

2.5. Determination of Bone Markers. The assessment of serum osteocalcin concentration was carried out by using human Gla-OC High sensitive EIA Kit with the intra- and interassay coefficient of variations (CVs) <5%. In brief, an aliquot of 100 μ L standard or sample was added to an appropriate well and incubated at room temperature for 2 hours.

Then, the sample solution was removed, and the well was washed 3 times with 400 μ L of PBS. 100 μ L total of antibody-POD conjugate solution was added into the wells and incubated for 1 hour. At the end of the incubation period, the solution was aspirated from the wells, and the wells were washed again for 4 times with washing buffer (100 μ L/well). After this step, the substrate solution at the volume of 100 μ L was added to each well and incubated at room temperature for 15 minutes. At the end of incubation period, 100 μ L of the stop solution was added into all wells and mixed gently. Then, an absorbance at 450 nm was recorded via microplate reader. All assays were performed in triplicate.

In this study, the concentration of beta-carboxy-terminal cross-linking telopeptide of type I collagen (CTX) levels was measured by using commercial human Micro ELISA Kit with intra- and interassay coefficients of variations 8 and 10%, respectively. In brief, all reagents and samples were left at room temperature before used. After thawing, samples were centrifuged again before the assay. All the reagents were mixed thoroughly by gently swirling before pipetting. An aliquot of 50 μ L of biotinylated detection Ab working solution was added to each well, covered with plate sealer, gently tapped to mix a solution, and incubated at 37°C for 45 minutes. Each well was aspirated and washed with wash buffer for three times. After washing, the remaining wash buffer was removed by aspirating, and the plate was inverted and patted against thick clean absorbent paper. Then, 100 μ L of HRP conjugate working solution was added to each well, covered with a new plate sealer, and incubated at 37°C for 30 minutes. After the incubation, washing was performed for five times. Then, 90 μ L of substrate solution was added to each well, covered with a new plate sealer, and incubated at 37°C for 15 minutes with light protection. The reaction time can be shortened or extended according to the actual color change, but not more than 30 minutes. Then, add 50 μ L of stop solution to each well and the optical density at 450 nm was monitored via microplate reader.

2.6. Determination of Total Phenolic Compounds. The total phenolics compounds of vegetables were measured by using Folin-Ciocalteu colorimetric method (Quettier-Deleu et al., 2000). Briefly, 20 μ L of each plant extracts was mixed with 0.2 mL of Folin-Ciocalteu reagent and 2 mL of distilled water and incubated at room temperature for 5 minutes. Then, 1 mL of 20% sodium carbonate was added and incubated at room temperature for 2 hours. The total polyphenolic compounds were determined by measuring the absorbance at 765 nm with spectrophotometer. Gallic acid was used as a standard, and the total phenolics were expressed as gallic acid equivalents (mg/L GAE/mg extract). All determinations were performed in triplicate.

2.7. Determination of Calcium and Alkaline Phosphatase in Serum. Blood was collected, and the determinations of calcium and alkaline phosphatase changes were performed at Srinagarind Hospital, Faculty of Medicine, Khon Kaen University, Khon Kaen, Thailand. The coefficient of variation

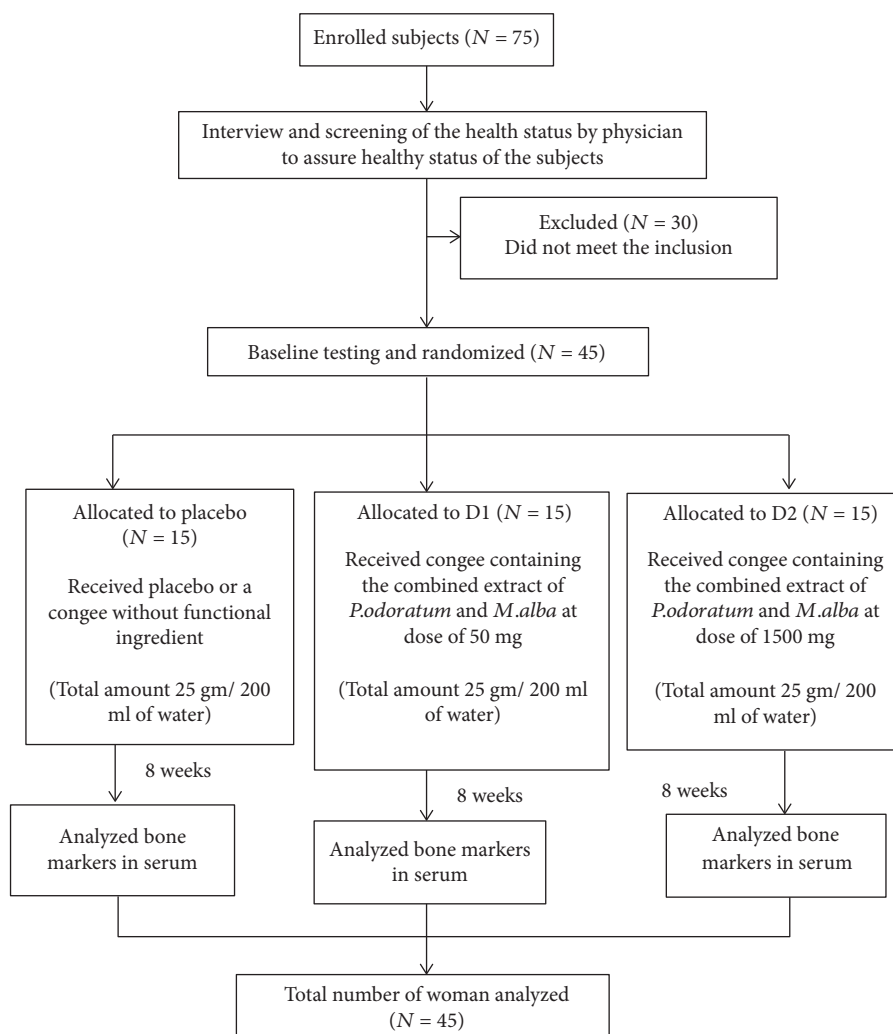


FIGURE 2: Flow diagram of subjects.

TABLE 1: The demographic data of subjects. Data were presented as mean \pm SD ($n = 15$ /group).

Parameters	Placebo	MP 50 mg/day	MP1500 mg/day	<i>P</i> value
Age (years)	51.41 \pm 4.21	50.47 \pm 3.20	50.47 \pm 3.64	0.697
Education (years)	7.73 \pm 4.89	7.73 \pm 4.13	7.47 \pm 4.50	0.983
Body mass index (kg/m ²)	24.27 \pm 2.91	25.23 \pm 3.52	24.91 \pm 3.81	0.742
Blood sugar (mg/dL)	87.33 \pm 13.50	84.67 \pm 6.89	88.93 \pm 15.04	0.635
Uric acid (mg/dL)	5.34 \pm 0.77	5.05 \pm 0.76	5.43 \pm 0.92	0.422
Heart rate (beats/min)	77.00 \pm 12.86	73.20 \pm 9.20	74.27 \pm 8.66	0.455
Respiratory rate (times/min)	19.80 \pm 2.40	18.00 \pm 1.98	18.80 \pm 1.82	0.070
Systolic blood pressure (mmHg)	115.80 \pm 11.48	118.67 \pm 13.84	119.13 \pm 13.06	0.745
Diastolic blood pressure (mmHg)	75.87 \pm 8.93	78.00 \pm 9.38	76.33 \pm 8.47	0.791

(% CV) of calcium (Ca²⁺) and alkaline phosphatase (ALP) was 1.7% and 0.6%, respectively.

2.8. Blood Collection and Toxicity Assessment. Blood was taken from each volunteer and prepared as plasma in order to assess

the changes of hematological and clinical chemistry parameters. All parameters were assessed at Srinagarind Hospital.

2.9. Statistical Analysis. All data were expressed as mean \pm SD. Comparisons between groups were performed using

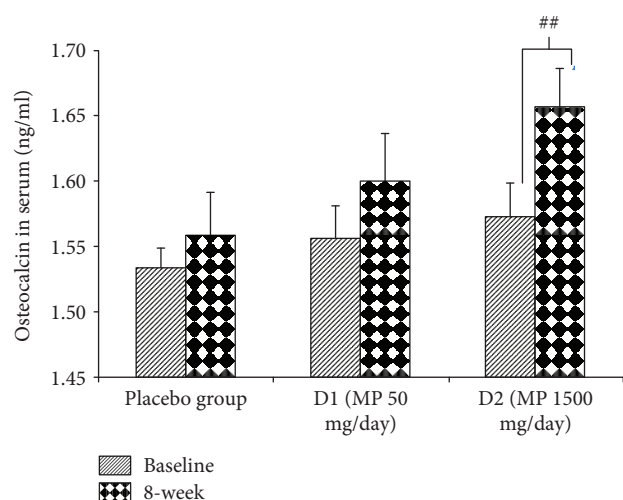


FIGURE 3: The effect of various doses of the herbal congee containing the combined extract of *M. alba* leaves and *P. odoratum* on the serum osteocalcin level ($n = 15/\text{group}$) $^{##}P$ value < 0.01 ; compared to baseline. D1 = MP 50 mg/day; D2 = MP 1500 mg/day.

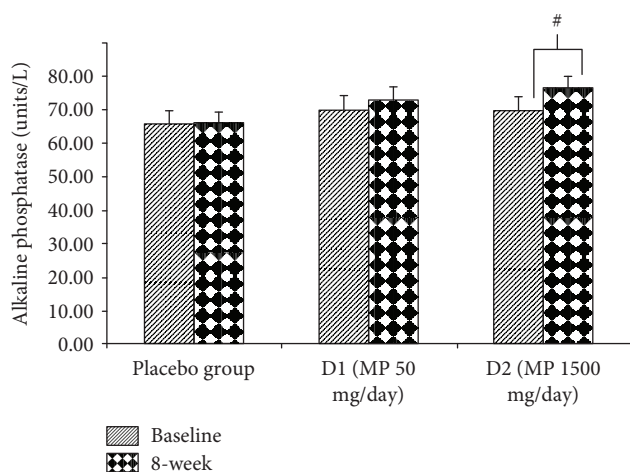


FIGURE 4: The effect of various doses of the herbal congee containing the combined extract of *M. alba* leaves and *P. odoratum* on the level of alkaline phosphatase in serum ($n = 15/\text{group}$) $^{\#}P$ value < 0.05 ; compared to baseline. D1 = MP 50 mg/day; D2 = MP 1500 mg/day.

one-way analysis of variance (ANOVA) followed by post hoc (LSD) multiple comparison tests and Kruskal-Wallis one-way analysis of variance test by using SPSS statistical software. P value < 0.05 was considered significant.

3. Results

3.1. Demographic Data of Subjects. Seventy-five menopause women were enrolled to participate in this study via the advertisements at menopause clinic, Srinagarind Hospital, Faculty of Medicine, Khon Kaen University, Khon Kaen, Thailand. After the interview and the screening of health status by the physician, it was found that only 45 subjects met the inclusion criteria and were allocated to placebo, D1, and D2 groups as shown in Figure 2. The baseline demographic

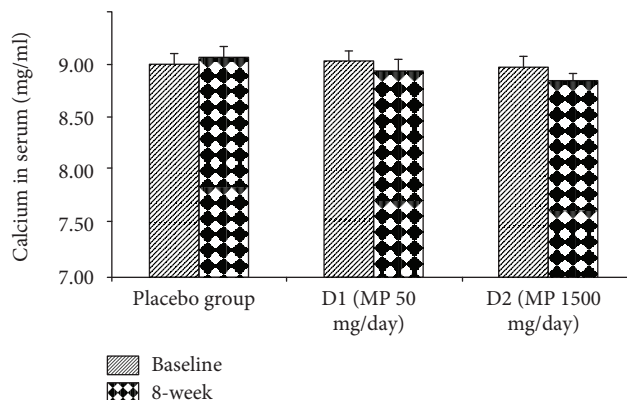


FIGURE 5: The effect of various doses of the herbal congee containing the combined extract of *M. alba* leaves and *P. odoratum* on the level of calcium in serum ($n = 15/\text{group}$). D1 = MP 50 mg/day; D2 = MP 1500 mg/day.

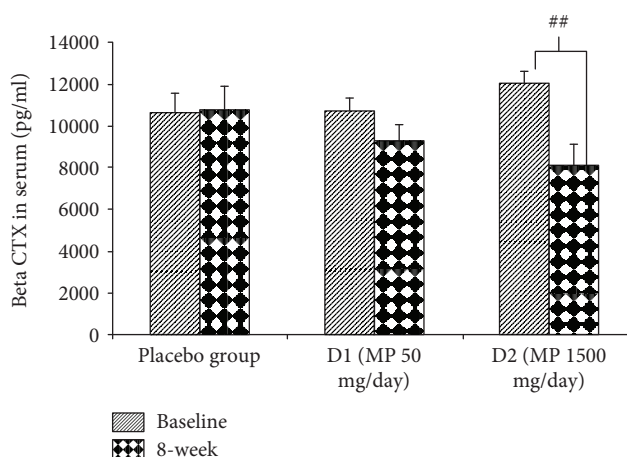


FIGURE 6: The effect of various doses of the herbal congee containing the combined extract of *M. alba* leaves and *P. odoratum* on the level of serum beta CTX ($n = 15/\text{group}$). $^{##}P$ value < 0.01 ; compared to baseline. D1 = MP 50 mg/day; D2 = MP 1500 mg/day.

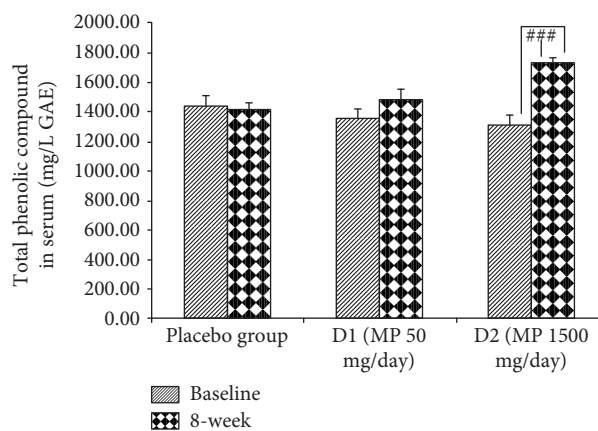


FIGURE 7: The effect of various doses of the herbal congee containing the combined extract of *M. alba* leaves and *P. odoratum* on the level of phenolic compounds in serum of all subjects ($n = 15/\text{group}$) $^{###}P$ value < 0.001 ; compared to baseline. D1 = MP 50 mg/day; D2 = MP 1500 mg/day.

TABLE 2: Effect of various doses of herbal congee containing the combined extract of *M. alba* leaves and *P. odoratum* or MP on blood clinical chemistry values ($N = 45$). Values are expressed as mean \pm SD; * P value < 0.05 , ** P value < 0.01 ; compared to placebo group.

Blood chemistry	Normal value	Group	Baseline Mean \pm SD	8 weeks Mean \pm SD
Glucose (mg/dL)	70–100 mg/dL	Placebo	87.33 \pm 13.50	88.27 \pm 12.19
		MP 50 mg/day	84.67 \pm 6.89 F (1,28) = 0.00, $P = 0.983$	81.47 \pm 7.79 F (1,28) = 2.777, $P = 0.096$
		MP 1500 mg/day	88.93 \pm 15.04 F (1,28) = 0.23, $P = 0.989$	88.60 \pm 15.80 F (1,28) = 2.814, $P = 0.245$
Uric acid (mg/dL)	2.7–7.0 mg/dL	Placebo	5.34 \pm 0.77	4.96 \pm 0.81
		MP 50 mg/day	5.05 \pm 0.76 F (1,28) = 1.097, $P = 0.304$	4.53 \pm 1.08 F (1,28) = 0.656, $P = 0.418$
		MP 1500 mg/day	5.43 \pm 0.92 F (1,28) = 0.078, $P = 0.782$	4.74 \pm 1.17 F (1,28) = 0.622, $P = 0.733$
Bicarbonate (mEq/L)	20.6–28.2 mEq/L	Placebo	26.41 \pm 1.78	25.07 \pm 1.34
		MP 50 mg/day	27.68 \pm 2.56 F (1,28) = 0.520, $P = 0.477$	24.79 \pm 1.99 F (1,28) = 0.124, $P = 0.724$
		MP 1500 mg/day	27.07 \pm 2.42 F (1,28) = 0.741, $P = 0.37$	24.11 \pm 3.24 F (1,28) = 0.149, $P = 0.928$
Blood urea nitrogen (mg/dL)	20.6–28.2 mEq/L	Placebo	11.40 \pm 2.73	11.53 \pm 2.57
		MP 50 mg/day	11.61 \pm 3.18 F (1,28) = 0.039, $P = 0.085$	12.19 \pm 2.57 F (1,28) = 0.496, $P = 0.487$
		MP 1500 mg/day	10.89 \pm 2.39 F (1,28) = 0.292, $P = 0.593$	11.41 \pm 2.87 F (1,28) = 0.013, $P = 0.910$
Creatinine (mg/dL)	0.5–1.5 mg/dL	Placebo	0.66 \pm 0.09	0.69 \pm 0.10
		MP 50 mg/day	0.68 \pm 0.11 F (1,28) = 0.538, $P = 0.463$	0.68 \pm 0.08 F (1,28) = 0.072, $P = 0.788$
		MP 1500 mg/day	0.65 \pm 0.09 F (1,28) = 0.905, $P = 0.608$	0.66 \pm 0.12 F (1,28) = 0.195, $P = 0.550$
Sodium (mEq/L)	130–147 mEq/L	Placebo	140.47 \pm 2.00	138.20 \pm 2.60
		MP 50 mg/day	140.80 \pm 1.66 F (1,28) = 0.400, $P = 0.527$	133.40 \pm 18.73 F (1,28) = 0.256, $P = 0.613$
		MP 1500 mg/day	139.67 \pm 2.13 F (1,28) = 0.303, $P = 0.992$	138.27 \pm 2.46 F (1,28) = 0.319, $P = 0.852$
Potassium (mEq/L)	3.4–4.7 mEq/L	Placebo	4.67 \pm 0.24	4.78 \pm 0.57
		MP 50 mg/day	4.69 \pm 0.38 F (1,28) = 0.421, $P = 0.517$	5.03 \pm 0.68 F (1,28) = 1.216, $P = 0.270$
		MP 1500 mg/day	4.71 \pm 0.62 F (1,28) = 0.822, $P = 0.663$	4.97 \pm 0.55 F (1,28) = 1.444, $P = 0.468$
Chloride (mEq/L)	96–107 mEq/L	Placebo	94.70 \pm 23.34	94.32 \pm 23.24
		MP 50 mg/day	100.73 \pm 1.22 F (1,28) = 0.550, $P = 0.815$	100.47 \pm 1.51 F (1,28) = 0.542, $P = 0.461$
		MP 1500 mg/day	100.27 \pm 2.79 F (1,28) = 0.514, $P = 0.773$	101.33 \pm 2.38 F (1,28) = 1.872, $P = 0.392$
Cholesterol (mg/dL)	127–262 mg/dL	Placebo	214.00 \pm 50.96	195.53 \pm 48.86
		MP 50 mg/day	217.27 \pm 48.77 F (1,28) = 0.032, $P = 0.859$	208.07 \pm 42.55 F (1,28) = 0.362, $P = 0.547$
		MP 1500 mg/day	266.80 \pm 32.03 F (1,28) = 0.215, $P = 0.647$	203.44 \pm 24.42 F (1,28) = 0.650, $P = 0.723$

TABLE 2: Continued.

Blood chemistry	Normal value	Group	Baseline Mean \pm SD	8 weeks Mean \pm SD
Albumin (g/dL)	3.8–5.4 g/dL	Placebo	3.90 \pm 1.41	4.46 \pm 0.40
		MP 50 mg/day	3.52 \pm 1.59 F (1,28) = 0.789, P = 0.382	4.19 \pm 0.02* F (1,28) = 6.404, P = 0.010
		MP 1500 mg/day	3.13 \pm 1.63 F (1,28) = 0.050, P = 0.824	4.41 \pm 26* F (1,28) = 8.348, P = 0.015
Globulin (g/dL)	2.6–3.4 g/dL	Placebo	2.69 \pm 0.90	2.83 \pm 0.35
		MP 50 mg/day	2.42 \pm 1.05 F (1,28) = 0.520, P = 0.477	3.01 \pm 0.44 F (1,28) = 2.718, P = 0.099
		MP 1500 mg/day	2.14 \pm 1.08 F (1,28) = 0.058, P = 0.811	2.95 \pm 0.28 F (1,28) = 3.079, P = 0.215
Bilirubin total (mg/dL)	0.3–1.5 mg/dL	Placebo	0.61 \pm 0.39	0.51 \pm 0.12
		MP 50 mg/day	0.67 \pm 0.35 F (1,28) = 0.000, P = 0.983	0.49 \pm 0.16 F (1,28) = 0.776, P = 0.387
		MP 1500 mg/day	0.66 \pm 0.36 F (1,28) = 0.246, P = 0.881	0.51 \pm 0.24 F (1,28) = 0.566, P = 0.754
Bilirubin direct (mg/dL)	0–0.5 mg/dL	Placebo	0.21 \pm 0.09	0.19 \pm 0.09
		MP 50 mg/day	0.21 \pm 0.09 F (1,28) = 0.178, P = 0.673	0.16 \pm 0.07 F (1,28) = 0.741, P = 0.387
		MP 1500 mg/day	0.20 \pm 0.10 F (1,28) = 0.276, P = 0.871	0.15 \pm 0.09 F (1,28) = 1.233, P = 0.540
Alanine aminotransferase or ALT (U/L)	4–36 U/L	Placebo	21.93 \pm 10.85	26.33 \pm 13.71
		MP 50 mg/day	16.67 \pm 7.21 F (1,28) = 2.005, P = 0.157	18.53 \pm 9.04 F (1,28) = 3.492, P = 0.062
		MP 1500 mg/day	17.00 \pm 5.54 F (1,28) = 2.129, P = 0.345	18.87 \pm 5.60 F (1,28) = 4.192, P = 0.123
Aspartate aminotransferase or AST (U/L)	12–32 U/L	Placebo	22.00 \pm 5.01	24.93 \pm 7.27
		MP 50 mg/day	19.93 \pm 3.79 F (1,28) = 0.919, P = 0.338	22.20 \pm 7.31 F (1,28) = 1.716, P = 0.190
		MP 1500 mg/day	24.40 \pm 6.45 F (1,28) = 0.934, P = 0.623	23.93 \pm 7.45 F (1,28) = 2.329, P = 0.312
Lactic acid dehydrogenase or LDH (U/L)	89–221 U/L	Placebo	214.07 \pm 42.39	218.50 \pm 49.20
		MP 50 mg/day	202.40 \pm 37.44 F (1,28) = 0.990, P = 0.340	219.54 \pm 36.49 F (1,28) = 0.097, P = 0.756
		MP 1500 mg/day	197.38 \pm 24.93 F (1,28) = 0.879, P = 0.391	219.67 \pm 47.83 F (1,28) = 0.586, P = 0.743
Creatine kinase–MB or CK-MB (U/L)	0–25 U/L	Placebo	19.30 \pm 5.12	18.53 \pm 5.05
		MP 50 mg/day	18.91 \pm 6.34 F (1,28) = 1.781, P = 0.182	21.53 \pm 5.90 F (1,28) = 1.883, P = 0.170
		MP 1500 mg/day	17.71 \pm 7.51 F (1,28) = 1.879, P = 0.396	20.53 \pm 9.20 F (1,28) = 1.657, P = 0.437
Triglyceride (mg/dL)	10–200 mg/dL	Placebo	141.53 \pm 57.48	148.60 \pm 54.76
		MP 50 mg/day	137.53 \pm 62.04 F (1,28) = 2.755, P = 0.097	97.20 \pm 45.88** F (1,28) = 8.434, P = 0.004
		MP 1500 mg/day	117.93 \pm 48 F (1,28) = 3.092, P = 0.213	119.07 \pm 50.23* F (1,28) = 8.792, P = 0.011

TABLE 2: Continued.

Blood chemistry	Normal value	Group	Baseline Mean \pm SD	8 weeks Mean \pm SD
High density lipoprotein-cholesterol or HDL-C (mg/dL)	>35 mg/dL	Placebo	48.79 \pm 17.40	52.07 \pm 9.18
		MP 50 mg/day	41.95 \pm 16.44 F (1,28) = 2.90, <i>P</i> = 0.089	60.27 \pm 12.06 F (1,28) = 0.491, <i>P</i> = 0.045
		MP 1500 mg/day	36.93 \pm 16.46 F (1,28) = 2.571, <i>P</i> = 0.276	64.47 \pm 18.80* F (1,28) = 5.267, <i>P</i> = 0.029
Low density lipoprotein-cholesterol or LDL-cholesterol (mg/dL)	0–150 mg/dL	Placebo	121.49 \pm 40.8	141.80 \pm 24.29
		MP 50 mg/day	109.19 \pm 47.47 F (1,28) = 0.007, <i>P</i> = 0.934	156.20 \pm 47.27 F (1,28) = 0.001, <i>P</i> = 0.980
		MP 1500 mg/day	100.82 \pm 51.02 F (1,28) = 0.107, <i>P</i> = 0.948	141.47 \pm 24.23 F (1,28) = 0.001, <i>P</i> = 1.000

data of all participants were presented in Table 1. No significant differences in all parameters were observed.

3.2. Effect of Herbal Congee on Bone Makers. The effect of various doses of the herbal congee containing the combined extract of *M. alba* leaves and *P. odoratum* on the level of osteocalcin, alkaline phosphatase, calcium, and beta CTX in serum was shown in Figures 3–6. Subjects who consumed the herbal congee containing the combined extract of *M. alba* leaves and *P. odoratum* showed the elevations of serum osteocalcin and alkaline phosphatase levels (*P* value < 0.01 and 0.05; compared to placebo group) as shown in Figures 3 and 4. However, the serum calcium level failed to show the significant change, while the serum beta CTX showed the significant reduction (*P* value < 0.01; compared to placebo group) as shown in Figures 5 and 6, respectively.

3.3. Effect of Herbal Congee on the Total Phenolic Compounds. The effect of various doses of the herbal congee containing the combined extract of *M. alba* leaves and *P. odoratum* on the level of total phenolic compounds was shown in Figure 7. It was found that after 2 months of administration, subjects who consumed the herbal congee containing the combined extract of *M. alba* leaves and *P. odoratum* at dose of 1500 mg per day showed the significant elevation of total phenolic compound (*P* value < 0.001; compared to placebo, *P* value < 0.001; compared to baseline level).

3.4. Effect of Herbal Congee on the Blood Chemistry Parameters. Table 2 showed the effect of various doses of herbal congee containing the combined extract of *M. alba* leaves and *P. odoratum* on blood chemistry values. It was found that no significant differences of the parameters were observed at baseline level. At the end of an 8-week consumption period, subjects who consumed herbal congee containing the combined extract of *M. alba* leaves and *P. odoratum* at doses of 50 and 1500 mg per day showed the significant reduction of triglyceride (*P* value < 0.01 and 0.05, respectively; compared to placebo group) together with the elevations of albumin (*P* value < 0.05; compared to placebo-treated group). In addition, the elevation of high-density lipoprotein cholesterol (HDL-C) was also observed in

subjects who consumed the high dose of the herbal congee at the end of experimental period (*P* value < 0.05; compared to placebo-treated group).

3.5. Effect of Herbal Congee on the Hematological Changes. Table 3 showed the effect of various doses of herbal congee containing the combined extract of *M. alba* leaves and *P. odoratum* on the hematological values. It was found that at baseline consumption period, no significant changes of all parameters were observed. At the end of an 8-week consumption period, subjects who consumed herbal congee containing the combined extract of *M. alba* leaves and *P. odoratum* at dose of 1500 mg per day showed the significant reduction of platelets (*P* value < 0.05; compared to placebo group). However, the changes of all parameters were also in the normal range. No changes of other parameters were observed.

4. Discussion

This study clearly revealed that no major side effects or clinically significant symptoms were reported from any of the volunteers. No data of clinical chemistry and hematological values showed the significant toxicity. Therefore, these data support the consumption safety for healthy menopausal women. In addition, this study clearly revealed that subjects who consumed the herbal congee containing the combined extract of *M. alba* leaves and *P. odoratum* at dose of 1500 mg per day increased the total phenolic compounds in serum and improved bone formation markers including osteocalcin and alkaline phosphatase (ALP) but decreased bone resorption marker including serum collagen type 1 cross-linked C-telopeptide (beta CTx).

Osteoblasts which are responsible for bone formation are located on the bone surface. Bone formation is enhanced by the osteoproduction action of osteoblasts. During bone formation process, alkaline phosphatase is produced by osteoblasts during the synthesis of the collagen matrix [13]. In addition to alkaline phosphatase, osteocalcin, a 5.8 kDa hydroxyapatite-binding bone-specific protein, is also produced by osteoblasts [14]. In contrast to both parameters mentioned earlier, beta CTx is released into the bloodstream

TABLE 3: Effect of various doses of the herbal congee containing the combined extract of *M. alba* leaves and *P. odoratum* (MP) on the hematological parameters ($N = 45$). Values are expressed as mean \pm SD.

CBC	Normal value	Group	Baseline Mean \pm SD	8 weeks Mean \pm SD
Red blood cell or RBC ($\times 10^6/\mu\text{L}$)	4.0–5.20 ($\times 10^6/\mu\text{L}$)	Placebo	3.92 \pm 1.71	4.13 \pm 1.33
		MP 50 mg/day	3.15 \pm 1.97 F (1,28) = 1.284, $P = 0.267$	3.65 \pm 1.62 F (1,28) = 2.048, $P = 0.163$
		MP 1500 mg/day	2.69 \pm 1.03 F (1,28) = 2.138, $P = 0.155$	3.19 \pm 1.77 F (1,28) = 1.845, $P = 0.185$
Hemoglobin or HGB (g/dL)	12.0–14.3 g/dL	Placebo	10.87 \pm 4.91	10.99 \pm 3.69
		MP 50 mg/day	8.41 \pm 5.19 F (1,28) = 0.208, $P = 0.648$	10.12 \pm 4.49 F (1,28) = 0.761, $P = 0.383$
		MP 1500 mg/day	7.35 \pm 2.84 F (1,28) = 1.215, $P = 0.545$	8.34 \pm 4.49 F (1,28) = 0.947, $P = 0.623$
Hematocrit or HCT (%)	36.0–47.7%	Placebo	32.34 \pm 14.70	36.58 \pm 12.48
		MP 50 mg/day	25.10 \pm 15.77 F (1,28) = 1.399, $P = 0.237$	33.95 \pm 15.42 F (1,28) = 0.291, $P = 0.590$
		MP 1500 mg/day	21.98 \pm 8.34 F (1,28) = 0.862, $P = 0.239$	29.48 \pm 16.79 F (1,28) = 0.323, $P = 0.851$
White blood cells or WBC ($\times 10^3/\mu\text{L}$)	4.60–10.60 $\times 10^3/\mu\text{L}$	Placebo	6.19 \pm 3.25	5.41 \pm 1.91
		MP 50 mg/day	4.65 \pm 1.99 F (1,28) = 0.950, $P = 0.330$	5.66 \pm 1.15 F (1,28) = 0.692, $P = 0.329$
		MP 1500 mg/day	4.02 \pm 1.87	5.94 \pm 1.13
Platelet or PLT ($\times 10^3/\mu\text{L}$)	173–383 $\times 10^3/\mu\text{L}$	Placebo	248.01 \pm 105.23 F (1,28) = 1.049, $P = 0.592$	274.20 \pm 85.65 F (1,28) = 4.229, $P = 0.409$
		MP 50 mg/day	183.86 \pm 95.34 F (1,28) = 1.304, $P = 0.263$	245.65 \pm 104.49 F (1,28) = 0.071, $P = 0.792$
		MP 1500 mg/day	158.11 \pm 71.84 F (1,28) = 0.134, $P = 0.717$	206.37 \pm 108.42* F (1,28) = 6.935, $P = 0.031$
Mean platelet volume or MPV (fl)	8.5–12.8 fl	Placebo	7.28 \pm 3.07	8.10 \pm 2.55
		MP 50 mg/day	5.65 \pm 3.39 F (1,28) = 0.000, $P = 0.983$	7.07 \pm 3.02 F (1,28) = 0.070, $P = 0.935$
		MP 1500 mg/day	4.85 \pm 1.99 F (1,28) = 0.218, $P = 0.897$	5.96 \pm 3.20 F (1,28) = 0.008, $P = 0.927$
Neutrophil or NE (%)	43.7–70.9%	Placebo	48.36 \pm 21.50	42.54 \pm 14.71
		MP 50 mg/day	37.54 \pm 20.67 F F (1,28) = 0.001, $P = 0.971$	37.56 \pm 16.97 F (1,28) = 0.292, $P = 0.593$
		MP 1500 mg/day	32.02 \pm 13.38 F (1,28) = 0.002, $P = 0.966$	33.72 \pm 17.88 F (1,28) = 0.155, $P = 0.337$
Lymphocyte or LY (%)	20.1–44.5%	Placebo	29.21 \pm 13.61	37.29 \pm 12.32
		MP 50 mg/day	23.96 \pm 12.03 F (1,28) = 0.035, $P = 0.852$	33.91 \pm 15.01 F (1,28) = 0.108, $P = 0.744$
		MP 1500 mg/day	19.70 \pm 8.25 F (1,28) = 0.032, $P = 0.859$	27.70 \pm 14.12 F (1,28) = 0.267, $P = 0.609$
Monocyte or MO (%)	3.4–9.8%	Placebo	5.78 \pm 1.95	6.10 \pm 1.92
		MP 50 mg/day	4.88 \pm 2.71 F (1,28) = 1.00, $P = 0.326$	5.26 \pm 2.06 F (1,28) = 0.466, $P = 0.500$
		MP 1500 mg/day	3.83 \pm 1.80 F (1,28) = 0.037, $P = 0.848$	4.44 \pm 2.12 F (1,28) = 0.005, $P = 0.942$

TABLE 3: Continued.

CBC	Normal value	Group	Baseline Mean \pm SD	8 weeks Mean \pm SD
Eosinophil or EO (%)	0.7–9.2%	Placebo	3.49 \pm 1.97	5.16 \pm 3.23
		MP 50 mg/day	3.24 \pm 0.89 F (1,28) = 1.765 <i>P</i> = 0.184	4.72 \pm 3.02 F (1,28) = 1.255, <i>P</i> = 0.263
		MP 1500 mg/day	3.40 \pm 1.21 F (1,28) = 2.131, <i>P</i> = 0.344	3.82 \pm 8.09 F (1,28) = 1.788, <i>P</i> = 0.409
Basophil or BA (%)	0.0–2.6%	Placebo	0.44 \pm 0.21 F (1,28) = 0.757, <i>P</i> = 0.384	0.78 \pm 0.47 F (1,28) = 0.373, <i>P</i> = 0.545
		MP 50 mg/day	0.38 \pm 0.17 F (1,28) = 0.519, <i>P</i> = 0.477	0.68 \pm 0.42 F (1,28) = 373, <i>P</i> = 0.541
		MP 1500 mg/day	0.29 \pm 0.12 F (1,28) = 0.911, <i>P</i> = 0.348	0.62 \pm 0.29 F (1,28) = 0.794, <i>P</i> = 0.672
Mean corpuscular volume or MCV (fl)	80.0–97.8 fl	Placebo	71.33 \pm 31.11	78.58 \pm 25.49
		MP 50 mg/day	54.06 \pm 31.73 F (1,28) = 0.363, <i>P</i> = 0.548	70.17 \pm 31.05 F (1,28) = 0.450, <i>P</i> = 0.529
		MP 1500 mg/day	47.06 \pm 19.38 F (1,28) = 0.517, <i>P</i> = 0.772	56.01 \pm 28.70 F (1,28) = 0.553, <i>P</i> = 0.463
Mean corpuscular hemoglobin MCH (pg)	25.2–32.0 pg	Placebo	23.98 \pm 10.43	25.39 \pm 8.20
		MP 50 mg/day	18.10 \pm 10.34 F (1,28) = 2.559, <i>P</i> = 0.110	22.81 \pm 10.10 F (1,28) = 0.100, <i>P</i> = 0.922
		MP 1500 mg/day	15.71 \pm 6.60 F (1,28) = 0.273, <i>P</i> = 0.873	18.25 \pm 9.39 F (1,28) = 0.219, <i>P</i> = 0.644
Mean corpuscular hemoglobin concentration or MCHC (g/dL)	31.3–33.4 g/dL	Placebo	29.97 \pm 13.75	29.30 \pm 10.07
		MP 50 mg/day	22.75 \pm 13.62 F (1,28) = 3.604, <i>P</i> = 0.068	26.18 \pm 12.08 F (1,28) = 1.533, <i>P</i> = 0.226
		MP 1500 mg/day	20.02 \pm 7.89 F (1,28) = 0.992, <i>P</i> = 0.328	22.02 \pm 12.56 F (1,28) = 0.003, <i>P</i> = 0.959
Red blood cells distribution width or RDW (%)	11.9–14.8%	Placebo	12.57 \pm 3.49	12.51 \pm 3.96
		MP 50 mg/day	10.16 \pm 5.27 F (1,28) = 0.011, <i>P</i> = 0.917	10.98 \pm 4.60 F (1,28) = 3.822, <i>P</i> = 0.051
		MP 1500 mg/day	7.87 \pm 4.22 F (1,28) = 2.650, <i>P</i> = 0.266	9.25 \pm 4.89 F (1,28) = 0.170, <i>P</i> = 0.075

during bone resorption and serves as a specific marker for the degradation of mature type I collagen. Therefore, an elevated serum concentration of beta-CTX is reported to reflect bone resorption [15]. It has been reported that the rapid increase in serum beta CTX concentration is related to the secretion activity of osteoclasts [16]. The current data showed the elevation of alkaline phosphatase and osteocalcin but decreased beta-CTX level in serum of subjects who consumed MP at dose of 1500 mg/day. These results indicated the positive modulation effect of the herbal congee on the bone turn over which enhanced the bone formation but decreased bone resorption. Our data were in agreement with the previous study which showed the positive modulation effect of the combined extract of *M. alba* and *P. odoratum* (MP) on bone turnover in animal model of menopause [10].

Recent finding has demonstrated that polyphenolic compounds inhibit receptor activator of nuclear factor- κ B ligand- (RANKL-) induced osteoclast formation [17]. Since the herbal congee containing the combination extract of *P.*

odoratum and *M. alba* contained high concentration of polyphenol, this substance may possibly be active constituent which contributes a role on an antiosteoclastogenic effect of the herbal congee containing the combination extract of *P. odoratum* and *M. alba*. However, further researches concerning depth analysis for active ingredient and the detail mechanism of action are still essential.

Although the current results clearly showed that the congee containing *P. odoratum* and *M. alba* is safe for consumption, the cholesterol showed the increasing trends. Therefore, the long-term application of the product should be a caution about hypercholesterolemia. However, studies which focused on the effect of long-term treatment should also be performed in order to assure that no side effect on hypercholesterolemia occurs. In addition, drug interaction is also possible during long-term application especially the interaction with the drugs commonly used in daily life such as paracetamol. Thus, the information concerning this aspect still requires further researches. The limitation of this study is that no data

concerning the bone density can be demonstrated because the treatment duration is not long enough to produce the changes of bone density.

5. Conclusion

The present study demonstrates the antiosteoporotic effect of the polyphenol-rich herbal congee which contained the combined extract of *P. odoratum* and *M. alba*. The possible underlying mechanism may occur via the improved bone turnover via the increased bone formation and the decreased bone resorption. Therefore, the herbal congee containing the combined extract of *P. odoratum* and *M. alba* may be useful for the prevention and treatment of osteoporosis in menopause. However, long-term treatment study is still required to assure that no side effect on hypercholesterolemia.

Data Availability

The data used to support the findings of this study are available from the corresponding author upon request.

Conflicts of Interest

No competing financial interests exist.

Acknowledgments

This study was supported by the National Research Council of Thailand, Research Division of Faculty of Medicine and the Integrative Complementary Alternative Medicine Research and Development Center, Khon Kaen University, Thailand (Research Fund Year 2014).

References

- [1] C. Cervellati, G. Bonaccorsi, E. Cremonini et al., "Oxidative stress and bone resorption interplay as a possible trigger for postmenopausal osteoporosis," *BioMed Research International*, vol. 2014, Article ID 569563, 8 pages, 2014.
- [2] B. L. Clarke and S. Khosla, "Physiology of bone loss," *Radiologic Clinics of North America*, vol. 48, no. 3, pp. 483–495, 2010.
- [3] P. Garnero, E. Sornay-Rendu, M. C. Chapuy, and P. D. Delmas, "Increased bone turnover in late postmenopausal women is a major determinant of osteoporosis," *Journal of Bone and Mineral Research*, vol. 11, no. 3, pp. 337–349, 1996.
- [4] D. C. Bauer, P. Garnero, J. P. Bilezikian et al., "Short-term changes in bone turnover markers and bone mineral density response to parathyroid hormone in postmenopausal women with osteoporosis," *The Journal of Clinical Endocrinology & Metabolism*, vol. 91, no. 4, pp. 1370–1375, 2006.
- [5] I. Cepelak and D. Cvorisec, "Biochemical markers of bone remodeling – review," *Biochemia Medica*, vol. 19, no. 1, pp. 17–35, 2009.
- [6] H. Rosenbrock, V. Seifert-Klauss, S. Kaspar, R. Busch, and P. B. Lippa, "Changes of biochemical bone markers during the menopausal transition," *Clinical Chemistry and Laboratory Medicine*, vol. 40, no. 2, pp. 143–151, 2002.
- [7] C. Kleinhans, F. F. Schmid, F. V. Schmid, and P. J. Kluger, "Comparison of osteoclastogenesis and resorption activity of human osteoclasts on tissue culture polystyrene and on natural extracellular bone matrix in 2D and 3D," *Journal of Biotechnology*, vol. 205, pp. 101–110, 2015.
- [8] P. Dreyer and J. G. H. Vieira, "Bone turnover assessment: a good surrogate marker?," *Arquivos Brasileiros de Endocrinologia & Metabologia*, vol. 54, no. 2, pp. 99–105, 2010.
- [9] L. Đudarić, A. Fužinac-Smojver, D. Muhvić, and J. Giacometti, "The role of polyphenols on bone metabolism in osteoporosis," *Food Research International*, vol. 77, Part 2, pp. 290–298, 2015.
- [10] S. Sungkamane, J. Wattanathorn, S. Muchimapura, and W. Thukham-mee, "Antiosteoporotic effect of combined extract of *Morus alba* and *Polygonum odoratum*," *Oxidative Medicine and Cellular Longevity*, vol. 2014, Article ID 579305, 9 pages, 2014.
- [11] S. Eghbaliferiz and M. Iranshahi, "Prooxidant activity of polyphenols, flavonoids, anthocyanins and carotenoids: updated review of mechanisms and catalyzing metals," *Phytotherapy Research*, vol. 30, no. 9, pp. 1379–1391, 2016.
- [12] L. I. Mennen, R. Walker, C. Bennetau-Pelissero, and A. Scalbert, "Risks and safety of polyphenol consumption," *The American Journal of Clinical Nutrition*, vol. 81, no. 1, pp. 326S–329S, 2005.
- [13] E. J. Mackie, "Osteoblasts: novel roles in orchestration of skeletal architecture," *The International Journal of Biochemistry & Cell Biology*, vol. 35, no. 9, pp. 1301–1305, 2003.
- [14] C. M. Gundberg, J. B. Lian, and S. L. Booth, "Vitamin K-dependent carboxylation of osteocalcin: friend or foe?," *Advances in Nutrition*, vol. 3, no. 2, pp. 149–157, 2012.
- [15] C. de la Piedra, M. L. Traba, C. D. Cabrera, and M. S. Henríquez, "New biochemical markers of bone resorption in the study of postmenopausal osteoporosis," *Clinica Chimica Acta*, vol. 265, no. 2, pp. 225–234, 1997.
- [16] S. A. Nesbitt and M. A. Horton, "Trafficking of matrix collagens through bone-resorbing osteoclasts," *Science*, vol. 276, no. 5310, pp. 266–269, 1997.
- [17] K. S. Shim, T. Kim, H. Ha et al., "Water extract of *Magnolia officinalis* cortex inhibits osteoclastogenesis and bone resorption by downregulation of nuclear factor of activated T cells cytoplasmic 1," *Integrative Medicine Research*, vol. 4, no. 2, pp. 102–111, 2015.

Research Article

Antioxidant Activities and Repair Effects on Oxidatively Damaged HK-2 Cells of Tea Polysaccharides with Different Molecular Weights

Xin-Yuan Sun , Jian-Min Wang, Jian-Ming Ouyang , and Li Kuang

Institute of Biomineralization and Lithiasis Research, Jinan University, Guangzhou 510632, China

Correspondence should be addressed to Jian-Ming Ouyang; toyjm@jnu.edu.cn

Received 4 April 2018; Revised 7 August 2018; Accepted 10 September 2018; Published 21 November 2018

Guest Editor: Anderson J. Teodoro

Copyright © 2018 Xin-Yuan Sun et al. This is an open access article distributed under the Creative Commons Attribution License, which permits unrestricted use, distribution, and reproduction in any medium, provided the original work is properly cited.

This study aims at investigating the antioxidant activity and repair effect of green tea polysaccharide (TPS) with different molecular weights (Mw) on damaged human kidney proximal tubular epithelial cells (HK-2). Scavenging activities on hydroxyl radical ($\cdot\text{OH}$) and ABTS radical and reducing power of four kinds of TPS with Mw of 10.88 (TPS0), 8.16 (TPS1), 4.82 (TPS2), and 2.31 kDa (TPS3) were detected. A damaged cell model was established using 2.6 mmol/L oxalate to injure HK-2 cells. Then, different concentrations of TPSs were used to repair the damaged cells. Index changes of subcellular organelles of HK-2 cells were detected before and after repair. The four kinds of TPSs possessed radical scavenging activity and reducing power, wherein TPS2 with moderate Mw presented the strongest antioxidant activity. After repair by TPSs, cell morphology of damaged HK-2 cells was gradually restored to normal conditions. Reactive oxygen species production decreased, and mitochondrial membrane potential ($\Delta\psi\text{m}$) of repaired cells increased. Cells of G1 phase arrest were inhibited, and cell proportion in the S phase increased. Lysosome integrity improved, and cell apoptotic rates significantly reduced in the repaired group. The four kinds of TPSs with varying Mw displayed antioxidant activity and repair effect on the mitochondria, lysosomes, and intracellular DNA. TPS2, with moderate Mw, showed the strongest antioxidant activity and repair effect; it may become a potential drug for prevention and treatment of kidney stones.

1. Introduction

Tea originated from China features a long history of over 4000 years; it is also the most popular nonalcoholic beverage and common food ingredient in Asia [1]. Tea polysaccharide (TPS) is an acid polysaccharide extracted from tea leaves [2]. TPS displays antioxidant, hypoglycemic, hypolipidemic, antihypertensive, immunological, antitumor, anticoagulant, and protective effects [3]. Chen et al. [4] have confirmed that TPS isolated from green tea manifests the scavenging activity of superoxide radicals, hydroxyl radicals ($\cdot\text{OH}$), and lipid radicals in vitro. TPS exerts protective effects against cellular damage induced by oxidative stress.

Many studies have shown that tea polyphenol has inhibitory effects on calcium oxalate urolithiasis due to its antioxidative effects [5, 6]. Tea polyphenol decreases osteopontin

expression and cell apoptosis and increases superoxide dismutase activity in rat kidney tissues, thus inhibits the formation of calcium oxalate stones [5]. Polyphenols mainly act as antioxidants through phenolic hydroxyl groups. By contrast, TPSs contain not only hydroxyl groups but also more carboxyl groups. The binding ability of carboxyl groups to calcium ions is obviously higher than that of hydroxyl groups [7], so it has a better potential to inhibit the formation of stones. At the same time, the structure of plant polysaccharides is similar to glycosaminoglycans (GAG), which are potent inhibitors of growth and aggregation of calcium oxalate crystals in vitro [8]. Research has shown that semisynthetic polysaccharides are more effective in preventing crystal-cell interactions than are GAGs [9].

The molecular weight (Mw) and structure of TPS are related to tea species and purification [10, 11]. Chen et al.

[12] revealed that the TPS extracted from green tea, with Mw of 120 kDa, comprises arabinose, ribose, xylose, glucose, galactose, and uronic acid at a molar ratio of 1.00:0.77:2.65:0.88:0.42:2.13. Wang et al. [13] extracted from green tea a water-soluble polysaccharide (7WA), with an average Mw of 7.1×10^4 Da. 7WA mainly contains arabinose and galactose at a molar ratio of 1.0:0.96 and possesses a backbone consisting of 1,3- and 1,6-linked galactopyranosyl residues, with branches attached to O-3 of 1,6-linked galactose residues and O-4 and O-6 of 1,3-linked galactose residues. Wang et al. [14] achieved a polysaccharide component (ZTPs) from green tea with a Mw of 8000 Da by hot-water extraction and ethanol precipitation. ZTPs consist of mannose, ribose, rhamnose, glucuronic acid, galacturonic acid, glucose, xylose, galactose, arabinose, and fucose, with molar percentages of 4.3%, 1.4%, 4.1%, 2.6%, 3.0%, 31.4%, 4.6%, 21.8%, 23.5%, and 3.3%, respectively.

Polysaccharide bioactivity is closely related with molecular structure, including Mw, active group content, structure of the main chain and branched chain, monosaccharide composition and sequence, glycosidic bond type and position, conformation, and solubility [15–17]. For the same kind of polysaccharides, Mw is the most important indicator of biological activity [18–21]. Lei et al. [19] showed that three sulfated glucans from *Saccharomyces cerevisiae*, with Mw of 12.9 (sGSC1), 16.5 (sGSC2), and 19.2 kDa (sGSC3), displayed antioxidant and immunological activities in vitro. Results showed that sGSC1, sGSC2, and sGSC3 can scavenge 1,1-diphenyl-2-picryl-hydrazyl (DPPH), superoxides, and hydroxyl radicals, and strength of radical scavenging effects of sGSCs followed the order sGSC1 > sGSC2 > sGSC3. Sun et al. [20] performed degradation of *Porphyridium cruentum* (EPS-0) with Mw of 2918.7 kDa to obtain three polysaccharide fractions with low Mw of 256.2 (EPS-1), 60.66 (EPS-2), and 6.55 kDa (EPS-3). EPS-0 showed no remarkable antioxidant activity, but polysaccharide fractions after degradation exerted inhibitory effects on hemolysis injury induced by Fe^{2+}/Vc in mouse liver hemocytes; half maximal inhibitory concentration (IC_{50}) value of EPS-1, EPS-2, and EPS-3 measured 1.09, 0.91, and 0.81 mg/mL, respectively. Results suggested that EPS-3, with the lowest Mw, showed the strongest protective effect on oxidative damage of liver hemocytes in mice. Ying et al. [21] extracted and obtained three Liubao TPS sections with Mw of 7.1 kDa (LTPS-30), 6.9 kDa (LTPS-50), and 6.6 kDa (LTPS-70). LTPS-70, with the smallest Mw, exhibited the strongest antioxidant activity and repair effect on damaged human umbilical vascular endothelial cells in the concentration range of 12.5–400 $\mu\text{g}/\text{mL}$.

Oxidative injury is one of the main factors that cause various diseases. Formation of kidney stones is related to oxidative damage of kidney epithelial cells [22–24]. TPS presents good antioxidant activity, which can reduce oxidative damage and can repair cells [25]. Therefore, TPS may be used to reduce incidences and prevent formation of kidney stones. We extracted four kinds of green TPSs with Mw of 10.88, 8.16, 4.82, and 2.31 kDa and comparatively investigated their antioxidant activity and repair effect on damaged kidney epithelial cells to provide basis for prevention and treatment of kidney stones.

2. Materials and Methods

2.1. Reagents and Apparatus. Green tea polysaccharide (TPS) was purchased from Shaanxi Ciyuan Biological Co., Ltd.; D_2O (99.9%, Sigma), other conventional reagents were purchased from Guangzhou Chemical Reagent Company (Guangzhou, China).

Human kidney proximal tubular epithelial (HK-2) cells were purchased from Shanghai Cell Bank, Chinese Academy of Sciences (Shanghai, China). Fetal bovine serum and cell culture medium (DMEM) were purchased from HyClone Biochemical Products Co. Ltd. (Beijing, China). Cell culture plates of 6-, 12-, and 96-well (NEST, China). Cell proliferation assay kit (Cell Counting Kit-8, CCK-8) was purchased from Dojindo Laboratory (Kumamoto, Japan). Acridine orange (AO) was purchased from Siam (USA). Hematoxylin and eosin (HE) staining kit, reactive oxygen species assay kit (DCFH-DA), and mitochondrial membrane potential assay kit (JC-1) were purchased from Shanghai Beyotime Bio-Tech Co., Ltd. (Shanghai, China). Carbonyl cyanide 3-chlorophenylhydrazone (CCCP) and cell apoptosis and necrosis assay kit were purchased from 4A Biotech Co., Ltd. (Beijing, China).

The apparatus included ultraviolet-visible spectrophotometer (Cary 500, Varian company, USA), inverted fluorescence microscope (Olympus company, Japan), flow cytometry (Beckman, Gallios, USA), enzyme mark instrument (safireZ, Tecan, Switzerland), nuclear magnetic resonance spectrometer (Varian Bruker-300 MHz, Germany), and Fourier-transform IR spectra (FT-IR) (EQUINOX55, Bruker, Germany).

2.2. Degradation of Tea Polysaccharide. About 1.2 g of crude tea polysaccharide (TPS0) was weighted accurately and dissolved in 20 mL distilled water. The reaction system was quickly added with hydrogen peroxide (H_2O_2) and allowed to proceed for 2 h at 90°C ; at which point, the solution PH was adjusted to 7.0 by adding 2 mol/L NaOH solution. The degraded solution was concentrated to one-third of its original volume at 60°C . The product was precipitated by adding anhydrous ethanol three times. The solution was stored overnight and filtered. The filtrate was dried in vacuum to obtain the degraded polysaccharide. Degraded tea polysaccharides with different molecular weight can be gained by changing the concentration of H_2O_2 at 4%, 8%, and 14%, respectively.

2.3. Molecular Weight Determination of Tea Polysaccharide. According to reference [26], the Ubbelohde viscosity was used to measure the molecular weight of tea polysaccharide. The intrinsic viscosity $[\eta]$ and molecular weight M could be described by the Mark-Houwink empirical equation $[\eta] = \kappa M^\alpha$. For tea polysaccharide, the κ and α are 0.0416 and 0.49, respectively.

2.4. Analysis of Carboxylic Group Content of Tea Polysaccharide. The carboxylic group ($-\text{COOH}$) content of TPS was measured by conductometric titration [27]. The final value was the average of three parallel experiments.

2.5. Fourier-Transform Infrared Spectroscopy (FT-IR) Analysis of Tea Polysaccharide. The dried polysaccharide sample (2.0 mg each) was mixed with 200 mg of potassium bromide (KBr) and compressed for scanning the spectrum in the region of 4000 cm^{-1} to 400 cm^{-1} with a resolution of 4 cm^{-1} .

2.6. ^1H NMR and ^{13}C NMR Spectrum of Tea Polysaccharide. According to reference [28], approximately 40 mg of tea polysaccharide was dissolved in 0.5 mL deuterium oxide (D_2O , 99.9%) in NMR tube. After the polysaccharide was dissolved completely, the ^1H and ^{13}C NMR spectrum was performed using the Varian Bruker-600 MHz spectrophotometer.

2.7. Hydroxyl Radical ($\cdot\text{OH}$) Scavenging Activity of TPS with Different Molecular Weight. The $\cdot\text{OH}$ scavenging ability of polysaccharide in vitro was detected by $\text{H}_2\text{O}_2/\text{Fe}$ system method [19, 29]. 38 EP tubes (10 mL) were prepared, and the reaction mixture in the EP tube that contained different concentrations of polysaccharides (0.15, 0.5, 0.8, 1.0, 2.0, and 3.0 g/L) was incubated with FeSO_4 (2.5 mmol/L, 1 mL) and phenanthroline (2.5 mmol/L, 1 mL) in a phosphate buffer (20 mmol/L, 1 mL, pH 6.6) for 90 min at 37°C . The absorbance measured at 580 nm repeatedly took average value. The ascorbic acid (Vc) was used as a positive control group. The ability to scavenge hydroxyl radicals was calculated using the following equation:

$$\text{Scavenging effect (\%)} = \frac{(A_3 - A_1)}{(A_2 - A_1)} \times 100, \quad (1)$$

where A_1 is the blank group; A_2 is the control group with H_2O_2 ; and A_3 is the experiment group with polysaccharide.

2.8. ABTS Radical Scavenging Activity of TPS with Different Molecular Weight. The ABTS radical scavenging activity of polysaccharides was performed according to [30] with slight modification. 7 mmol/L ABTS solution was mixed with 2.45 mmol/L potassium persulfate aqueous solution, and then, the mixture was incubated in the dark at room temperature for 14 h. Then, 3.0 mL mixture solution was added to 1 mL of various polysaccharide solutions in a test tube. After reacting for 6 min at room temperature, the absorbance was measured at 734 nm.

$$\text{Scavenging effect (\%)} = \left[1 - \frac{(A_1 - A_2)}{A_0} \right] \times 100, \quad (2)$$

where A_0 is the control group without polysaccharide; A_1 is the experiment group; and A_2 is the blank group without reagents.

2.9. Reducing Power of TPS with Different Molecular Weight. The reducing power of polysaccharides was determined referring to reference [31] with some modifications. 2 mL of four polysaccharide samples with different molecular weights in different concentrations (0.15, 0.5, 0.8, 1.0, 2.0, and 3.0 g/L) was mixed with 2 mL phosphate buffer (PBS, pH = 6.6) and

2 mL potassium ferricyanide (1.0%, w/v). The mixture was incubated at 50°C for 20 min and cooled to room temperature. 2 mL trichloroacetic acid (10%, w/v) was added to the mixture which was then centrifuged for 10 min at 3000 r/min. The supernatant (2 mL) was mixed with 0.5 mL FeCl_3 (0.1%, w/v) solution and 2 mL distilled water. The mixture was fully mixed and stood for 10 min. The absorbance was measured at 700 nm. The phosphate buffer was used as a negative control group. The ascorbic acid (Vc) was used as a positive control group and for comparison.

2.10. Cytotoxicity Measurement of TPS on HK-2 Cells. HK-2 cells were cultured in DMEM-F12 medium containing 10% fetal bovine serum, 100 $\mu\text{g}/\text{mL}$ streptomycin antibiotic-100 U/mL penicillin with pH 7.4 in a 5% CO_2 humidified environment at 37°C . Upon reaching a monolayer of 80%–90% confluence, cells were gently blown after trypsinization to form a cell suspension for subsequent cell experiments.

Cell suspension with a cell concentration of 1×10^5 cells/mL was inoculated per well in 96-well plates and incubated for 24 h. Afterward, the culture medium was removed, and 100 μL of 0, 20, 60, and 100 $\mu\text{g}/\text{mL}$ TPSs with various molecular weights was added and each concentration was repeated in three parallel wells. After incubation for 24 h, 10 μL CCK-8 was added to each well and incubated for 1.5 h. Absorbance (A) was measured by using the enzyme mark instrument at 450 nm according to the CCK-8 kit instruction. Cell viability was determined using the following equation:

$$\text{Cell viability (\%)} = \frac{A(\text{treatment group})}{A(\text{control group})} \times 100. \quad (3)$$

2.11. Repair Effect of TPS on Damaged HK-2 Cells by CCK-8. 100 μL of cells suspension with a concentration of 1×10^5 cells/mL was inoculated per well in 96-well plates. The cells were divided into four groups: (1) control group of background: cell-free culture medium group, (2) normal control group: in which only serum-free culture medium was added, (3) damaged group: in which serum-free culture medium with 2.6 mmol/L oxalate was added and incubated for 3.5 h, and (4) repair groups, including TPS0, TPS2, and TPS3 repair groups, in which different concentrations of TPS0 (10.88 kDa), TPS2 (4.82 kDa), and TPS3 (2.31 kDa), respectively, were added into the cells of damaged groups and repaired for 10 h. After the repair was completed, 10 μL CCK-8 was added to each well and incubated for 1.5 h. The absorbance values were measured using the enzyme mark instrument at 450 nm to detect the repair capacity of polysaccharide.

2.12. Cell Morphology Observation by Hematoxylin-Eosin (HE) Staining. According to our previous study [32], changes of cell morphology were observed under an optical microscope after HE staining. 1 mL of cell suspension with a cell concentration of 1×10^5 cells/mL was inoculated per well in 12-well plates and incubated for 24 h. The cells were divided into three groups: (1) normal control group: in which only serum-free culture medium was added, (2) damaged group:

in which serum-free culture medium with 2.6 mmol/L oxalate was added and incubated for 3.5 h, and (3) repair groups, including TPS0, TPS2, and TPS3 repair groups, in which 80 $\mu\text{g}/\text{mL}$ of TPS0, TPS2, and TPS3, respectively, was added into the cells of damaged groups and repaired for 10 h. The supernatant was then removed by aspiration and the cells were washed twice with PBS. Cells were fixed with 4% paraformaldehyde for 15 min and stained with hematoxylin and eosin according to the manufacturer's instructions. Morphological changes of the cells were observed under a microscope, and the nuclei were stained in violet and cytoplasm in pink or red.

2.13. Changes in Reactive Oxygen Species (ROS). The density of seeded cells and experimental grouping was the same as those in Section 2.12. The positive reagent (Rosup, 100 $\mu\text{mol}/\text{L}$) of reagent kit was used as a positive control. After repair for 10 h, the cells were washed with PBS; 500 μL DCFH-DA diluted with serum-free culture medium at 1 : 1000 was added and incubated for 30 min at 37°C. Then, the cells were washed 3 times with PBS to remove excess DCFH-DA. ROS distribution was observed under fluorescent microscope; the fluorescence intensity of intracellular ROS was quantitatively detected by a microplate reader.

For fluorescence quantitative detection by a microplate reader, 100 μL of cells suspension with a concentration of 1×10^5 cells/mL was inoculated per well in 96-well plates. After repair for 10 h, the cells were washed with PBS; then, 100 μL DCFH-DA was added and incubated for 30 min at 37°C. The fluorescence intensity of intracellular ROS was quantitatively detected at 502 nm.

2.14. Measurement of Mitochondria Membrane Potential ($\Delta\psi_m$). The density of seeded cells and experimental grouping were the same as those in Section 2.12. As a known mitochondrial membrane potential disrupter, 50 $\mu\text{mol}/\text{L}$ CCCP was used as a positive control. After the repair was completed, the cells were collected and centrifuged at 1000 rpm/min for 5 min. After that, the supernatant was removed by suction, and cells were rinsed twice with PBS. The $\Delta\psi_m$ was detected according to JC-1 kit. Then the cells were stained with 200 μL JC-1 dye, thoroughly mixed, and incubated in darkness at 37°C for 15 min. After treatment, the cells were detected by flow cytometer.

2.15. Changes in Lysosomal Integrity before and after Repair. Cell suspension with a cell concentration of 1×10^5 cells/mL was inoculated per well in 12-well plates with coverslips and incubated for 24 h. The experimental grouping was the same as those in Section 2.12. The cells were washed twice with PBS and then loaded with 5 $\mu\text{g}/\text{mL}$ AO in DMEM for 15 min. After being repaired for 10 h, the cells were rinsed three times with PBS, and the distribution of AO in the cells was observed under fluorescence microscope.

For fluorescence quantitative detection by a microplate reader, cells (1×10^5 cells/mL) were cultured in a 96-well plate (100 $\mu\text{L}/\text{well}$) and were stained with AO. The red and green fluorescence were detected under enzyme mark instrument with excitation at 485 nm and emission at

530 nm (green cytoplasmic AO) and 620 nm (red lysosomal AO). Normal lysosomal integrity = (total red fluorescence intensity of normal lysosome)/(total green fluorescence intensity of normal lysosome). Lysosomal integrity = (total red fluorescence intensity)/[(total green fluorescence intensity) \times (normal lysosomal integrity)].

2.16. Cell Cycle Assay. According to our previous study [32], changes of cell cycle progression were analyzed by flow cytometry. 2 mL of cell suspension with a cell concentration of 1×10^5 cells/mL was inoculated per well in 6-well plates and incubated for 24 h. After the cells were confluent, the medium was changed to serum-free culture media and then incubated for another 12 h to achieve synchronization. The experimental grouping was the same as those in Section 2.12. After being repaired for 10 h, the cells were collected with trypsin digestion. The collected cells were washed twice with PBS and centrifuged (1000 rpm) for 5 minutes and then fixed with 70% ethanol at 4°C for 12 hours. The ethanol was removed by centrifugation (2000 rpm, 5 minutes), and the cells were washed twice with PBS. The cells were then resuspended in 200 μL of propidium iodide and kept at 37°C for 15 minutes. The cell cycle was analyzed by flow cytometry to measure the amount of PI-labeled DNA in the fixed cells.

2.17. Changes in Apoptosis Rate before and after Repair. According to our previous study [33], apoptosis and necrosis in HK-2 cells before and after repair were measured by flow cytometer with Annexin V-FITC/PI double staining assay. The density of seeded cells and experimental grouping were the same as those in Section 2.12. The apoptosis inducer (CCCP, 50 $\mu\text{mol}/\text{L}$) was used as a positive control. After the repair was completed, the cells were harvested and then stained using Annexin V-FITC/PI cell death assay kit according to the manufacturer's instructions. The cells were resuspended in 200 μL of binding buffer. Then, 5 μL of Annexin V-FITC was added, followed by incubation in the dark for 10 min at room temperature. The cells were resuspended in 200 μL of binding buffer and stained with 5 μL of PI. The prepared cells were then analyzed using a flow cytometer.

2.18. Statistical Analysis. The experimental data were expressed by mean \pm standard deviation ($\bar{x} \pm \text{SD}$). The experimental results were analyzed statistically using SPSS 13.0 software. Multiple group comparisons were performed using one-way ANOVA, followed by the Tukey post hoc test. If $p < 0.05$, there was a significant difference; if $p < 0.01$, the difference was extremely significant; if $p > 0.05$, there was no significant difference.

3. Results

3.1. Degradation of TPS. Three degraded TPS fractions, namely, TPS1, TPS2, and TPS3, were obtained from crude TPS (TPS0) at 4%, 8%, and 14% concentrations, respectively, of H_2O_2 . Mean Mw of TPS0, TPS1, TPS2, and TPS3 reached 10.88, 8.16, 4.82, and 2.31 kDa, respectively (Table 1). TPSs are enriched with polysaccharides.

Degradation reaction of H_2O_2 is moderate, and the extent of degradation can be controlled without changing the

TABLE 1: Degradation conditions and physicochemical properties of TPSs with different Mw.

Polysaccharide abbreviation	H ₂ O ₂ concentration C _{(H₂O₂)/%}	Intrinsic viscosity [η]/mL/g	Mean molecular weights Mr/kDa	-COOH content/%	Solubility (25°C) g/100 g
TPS0	0	3.952 ± 0.130	10.88 ± 0.73	11.2	10.0
TPS1	4	3.434 ± 0.086	8.16 ± 0.42	12.3	12.5
TPS2	8	2.653 ± 0.072	4.82 ± 0.27	12.7	25.0
TPS3	14	1.842 ± 0.188	2.31 ± 0.48	11.0	33.3

structure of the main chain of polysaccharides [34–37]. For instance, Xizhen et al. [36] performed degradation of natural soybean polysaccharide by controlling the concentration of H₂O₂ to obtain four polysaccharide fractions with Mw of 550, 347, 285, and 21 kDa. All degraded polysaccharide fractions had basically similar structure of the functional group. Hou et al. [37] performed degradation of *Laminaria japonica* fucoidan by changing H₂O₂ concentration, reaction temperature, and pH and obtained seven degraded fractions with Mw of 1.0, 3.8, 8.3, 13.2, 35.5, 64.3, and 144.5 kDa. No significant changes were observed in the major backbone structure and sulfate group content of all polysaccharide fractions.

No significant change was observed in carboxyl content of TPS before and after degradation. When concentrations of H₂O₂ totaled 4% and 8%, carboxyl contents of degraded TPS1 and TPS2 products reached 12.3% and 12.7%, which were slightly higher than that of TPS0 (11.2%) before degradation. The above results were attributed to the increased solubility of degraded polysaccharides (Table 1); the increase in solubility exposed numerous -COOH groups [38]. When H₂O₂ concentration was increased to 14%, carboxyl content of TPS3 measured 11.0% and was slightly lower than that of TPS0. This result can be explained by oxidative decarboxylation of polysaccharides induced by free oxygen atoms originating from high concentrations of H₂O₂ at high temperature [39].

3.2. Fourier-Transform Infrared (FT-IR) Spectrum of TPS.

Figure 1 shows the FT-IR spectra of the four TPS fractions. The polysaccharide fractions presented similar spectra before and after degradation. No new peaks appeared, indicating the similar structure of the four polysaccharide fractions. The polysaccharide samples displayed strong absorption peak at 3401–3423 cm⁻¹, corresponding to the stretching vibration of the hydroxyl group. Intermolecular and/or intramolecular hydrogen bonding was also observed. The absorption peak at 3000–2800 cm⁻¹ was related to C–H stretching vibration. The signal at about 1608 cm⁻¹ was related to C=O stretching vibration of the carboxyl group, and the signal at 1105 cm⁻¹ suggested α-glucose pyranose ring [40].

Each polysaccharide sample manifested the same amount (2.0 mg). Thus, absorption peak intensity can reflect the content of characteristic functional groups [41]. Compared with the undegraded TPS0 fraction, absorption peaks for -OH (3412 and 3417 cm⁻¹) and -COOH (1602.1 and 1610.5 cm⁻¹) in degraded TPS1 and TPS2 fractions were notably stronger, respectively, indicating that TPS1 and TPS2 exposed numerous -OH and -COOH groups [38]. The absorption peak for -COOH in TPS3 weakened and

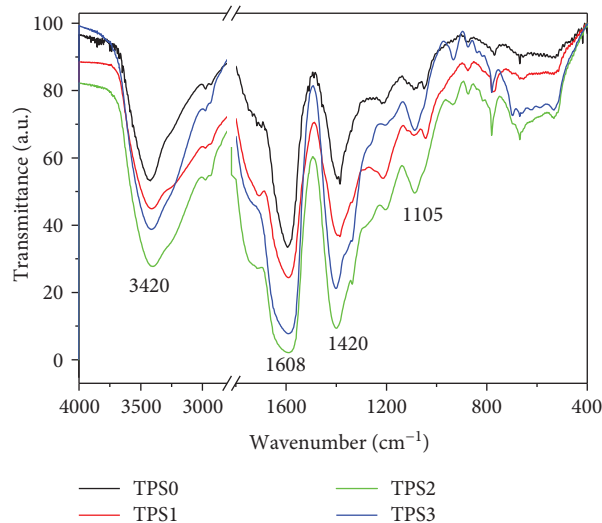


FIGURE 1: FT-IR spectra of TPSs with different molecular weights.

showed consistency with the slightly reduced carboxylic group content (Table 2).

3.3. ¹H Nuclear Magnetic Resonance (NMR) and ¹³C NMR Spectrum Analysis of TPS. As shown in FT-IR spectra, the basic structure of TPS remained undamaged during H₂O₂ degradation. Therefore, as representative for TPS0, ¹H and ¹³C NMR spectra of polysaccharide were characterized, and the spectra are shown in Figure S1. The ¹³C NMR and ¹H NMR signal assignment of TPS0 is shown in Table S1.

In ¹H NMR spectrum, signals in the range of δ 4.5–5.5 ppm were assigned to the sugar ring of polysaccharides. H⁻¹ proton signals derived from α-configuration sugar ring are detected at more than 4.95 ppm, whereas most of β-configuration protons will appear at less than 4.95 ppm. Thus, β- and α-configuration existed in TPS simultaneously [42]. The signals at δ 5.0, 3.74, 3.95, 4.25, 4.37, and 4.37 ppm corresponded to H-1 to H-6, respectively, of (1→4)-α-GalpA in TPS [43]. The signals at δ 4.63, 3.75, 3.56, 3.77, 3.60, and 3.91 ppm were attributed to H-1 to H-6 of (1→6)-β-Galp, whereas the signals at δ 5.24, 4.17, 4.09, 4.11, and 3.85 ppm were assigned to H-1 to H-5 of (1→2, 3, 5)-Araf, respectively [43]. The signals at δ 3.08, 3.10, 3.17, and 3.45 ppm were assigned to H-2, H-4, H-5, and H-6 of (1→)-β-D-Glcp, respectively [43]. The signals at δ 4.89 and 3.64 ppm were assigned to H-1 and H-6 of (1→4)-α-D-Glcp, respectively [44].

In the ¹³C NMR spectrum, the signals in the region of δ 100–104 ppm indicated that monosaccharides existed in the

TABLE 2: FT-IR characteristic absorption peak of original and degraded TPS.

Polysaccharide abbreviation	Mean molecular weights M_r /kDa	-COOH content/%	Relative intensity of -COOH absorption peak	Functional groups characteristic absorption peak		
				-OH	-COOH	Sugar ring
TPS0	10.88	11.2	1.3	3423	1609.9	1391.1, 1142.3, 1093.9, 765.9
TPS1	8.12	12.3	2.0	3417	1602.1	1385.4, 1213.4, 778.6
TPS2	4.82	12.7	2.7	3412	1610.5	1399.2, 1087.5, 780.6
TPS3	2.31	11.0	1	3401	1608.1	1401.4, 1087.3, 780.4

[\ast] $(100 - T_{TPS0}) : (100 - T_{TPS1}) : (100 - T_{TPS2}) : (100 - T_{TPS3})$, where T represents the light transmittance.

form of pyranose ring. The signals at δ 170–180 ppm were attributed to the uronic acid of polysaccharides [45]. The signals at δ 98.9, 68.2, 68.9, 77.8, 72.7, and 173.4 ppm were assigned to C-2 to C-6 of (1 \rightarrow 4)- α -GalpA, respectively. The signals at δ 107.1, 73.1, 74.7, 71.5, 75.4, and 70.5 ppm corresponded to C-1 to C-6 of (1 \rightarrow 6)- β -Galp, respectively [43]. The signals at δ 109.5, 81.3, 77.8, 85.3, and 70.1 ppm were assigned to C-1 to C-5 of (1 \rightarrow 2,3,5)-Araf, whereas δ 74.3, 76.6, 70.3, 76.7, and 60.8 ppm were assigned to C-2 to C-6 of (1 \rightarrow)- β -D-Glcp, respectively [13]. The signals at δ 99.5 and 61.2 ppm were attributed to C-1 and C-6 of (1 \rightarrow 4)- α -D-Glcp, respectively [44].

3.4. Comparison of Antioxidant Activity of TPS with Different Mw

3.4.1. Hydroxyl Radical (OH) Scavenging Capacity. Fenton reactions were used to investigate the OH radical scavenging ability of TPS. As shown in Figure 2(a), radical scavenging activity improved with increasing polysaccharide concentration. At the same concentration, TPS2 with mid-level Mw featured the strongest scavenging activity. For example, at the concentration of 3.0 mg/mL of TPS, OH scavenging rates of TPS0, TPS1, TPS2, and TPS3 reached 51%, 62%, 79.4%, and 37%, respectively. These values were all lower than 95.3% of Vc.

3.4.2. ABTS Radical Scavenging Capacity. As shown in Figure 2(b), four TPSs showed scavenging capacity for ABTS radical in a concentration-dependent manner. At the same concentration, TPS2 exhibited the strongest scavenging ability. At 3.0 mg/mL concentration of TPS, ABTS radical scavenging rates of TPS0, TPS1, TPS2, and TPS3 totaled 88.1%, 90.0%, 93.3%, and 82.2%, respectively.

3.4.3. Reducing Power. The reducing power of four TPSs followed the order TPS2 > TPS1 > TPS0 > TPS3 (Figure 2(c)). TPS2 still featured the strongest reducing power, whereas the weakest was observed for TPS3, which possessed the smallest Mw. However, reducing powers of both TPS2 and TPS3 were lower than Vc. Reducing power of the four TPSs changed concentration-dependent manner. For different polysaccharides, reducing power strengthened with increasing TPS concentration.

3.5. Toxicity Assessment of TPSs on Human Kidney Proximal Tubular Epithelial Cells (HK-2) Cells.

Antioxidant activities

of TPS1 (8.16 kDa) and TPS0 (10.8 kDa) showed minimal difference due to their similar Mw (Figure 2(a)–2(c)). Therefore, we only selected TPS0, TPS2, and TPS3 for the following cytotoxicity and repair experiments. As shown in Figure 3, these TPSs can promote cell proliferation within the range of 20–100 μ g/mL, and TPS2 exhibited the strongest promotion effect. The above results showed that these TPSs caused no cytotoxicity on HK-2 cells and promoted cell growth.

3.6. Repair Effect of TPS on Damaged HK-2 Cells

3.6.1. Improvement of Cell Viability. The effects of oxalate concentration and injury time on the viability of HK-2 cells were shown in Figure S2. The toxicity was gradually increased with increasing oxalate concentration and exposure time. We selected the oxalate concentration of 2.6 mmol/L and the treatment time of 3.5 h for the subsequent damage experiments.

Repair effects of TPS0, TPS2, and TPS3 on damaged HK-2 cells were compared at concentrations of 20, 40, 60, 80, and 100 μ g/mL (Figure 4). The best repair effect in all polysaccharides was observed at 80 μ g/mL concentration and decreased at concentrations higher or lower than 80 μ g/mL.

At the same concentration, TPS2 showed the best repair effect. For instance, cell viability of damaged HK-2 cells increased from 59.4% before repair to 89.4%, 92.8%, and 84.8% after being repaired by 80 μ g/mL TPS0, TPS2, and TPS3, respectively. The above results suggested that repair ability of TPSs was correlated with their Mw and is consistent with antioxidant activity.

3.6.2. Repair Effect on Cell Morphology. Morphological changes in damaged HK-2 cells before and after repair were observed by hematoxylin and eosin staining. As shown in Figure 5, the junctions between normal HK-2 cells were tight, and the cells were plump. When HK-2 cells were exposed to 2.6 mmol/L oxalate for 3.5 h, the cells lost their natural shape, their volume reduced, eosinophilic staining enhanced, and a large number of apoptotic cells with dense staining were formed. After repair by TPS with different Mw, cell number increased, and cell morphology was gradually restored to normal conditions. After the damaged cells were repaired by TPS2, their morphology resembled closely that of normal cells. By comparison, repair effect of TPS3 with lower Mw and TPS0 with higher Mw were weaker than that of TPS2.

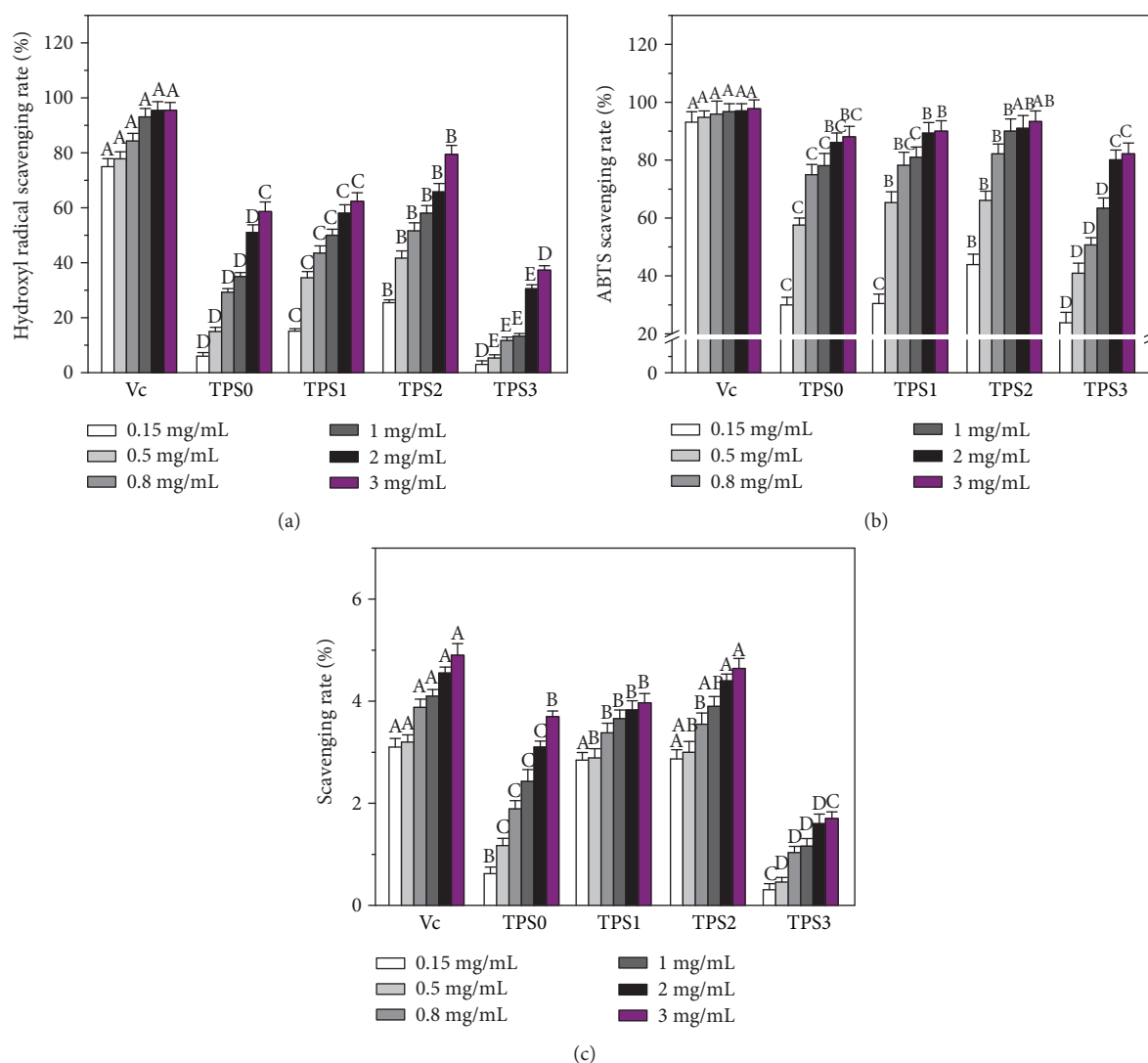


FIGURE 2: The comparison of antioxidant capacity of TPS0, TPS1, TPS2, and TPS3 at different concentrations. (a) Hydroxyl radical scavenging ability; (b) ABTS radical scavenging ability; (c) reducing power. Data were expressed as mean \pm SD of five independent experiments. Different letters (A, B, C, D, E) indicate a significant difference ($p < 0.05$) between different TPSs of the same concentration.

3.6.3. Changes in Intracellular Reactive Oxygen Species (ROS) after Repair by Different TPSs. A large amount of ROS in the body can cause oxidative damage to biological molecules (including DNA, lipids, and proteins), therefore mediating the occurrence of a series of inflammatory responses and causing cell dysfunction or death [46, 47]. The antioxidant capacity of TPS can reduce oxidative damage of cells in different degrees.

Figure 6 illustrates the intracellular ROS changes in all cell groups as detected by DCFH-DA. Following treatment of HK-2 cells with Rosup (positive control) and 2.6 mmol/L oxalate (damage control) for 3.5 h, the bright green fluorescence images were observed, indicating the high levels of intracellular ROS. After the damaged cells were repaired by TPS, fluorescent intensity displayed attenuation at different degrees, and this effect was most notable in the TPS2 treatment group (Figure 6(b)). The above results indicated that TPSs can reduce the production of intracellular ROS and alleviate oxidative damage in cells.

3.6.4. Repair Effect on Mitochondrial Membrane Potential ($\Delta\psi_m$). Figure 7 shows changes in $\Delta\psi_m$ of the damaged HK-2 cells before and after repair. The red/green fluorescence intensity ratio in the mitochondria of the normal control group reached 67.5. When cells were damaged by 2.6 mmol/L oxalate, the red/green fluorescence ratio reduced to 3.8, indicating that $\Delta\psi_m$ was reduced evidently. However, after the damaged cells were repaired by TPS0, TPS2, and TPS3, $\Delta\psi_m$ increased at different degrees. After the damaged cells were repaired by TPS2, the red/green fluorescence ratio in the mitochondria reached 22.9, which was higher than that of the TPS0 treatment group (19.8) and TPS3 treatment group (9.3). Thus, TPS2 showed the strongest repair effect on damaged mitochondria.

3.6.5. Changes in Lysosomal Integrity before and after Repair. Acridine orange (AO), a metachromatic fluoroprobe, is a lysosomotropic component that accumulates in lysosomes by proton trapping. AO accumulation changes fluorescence

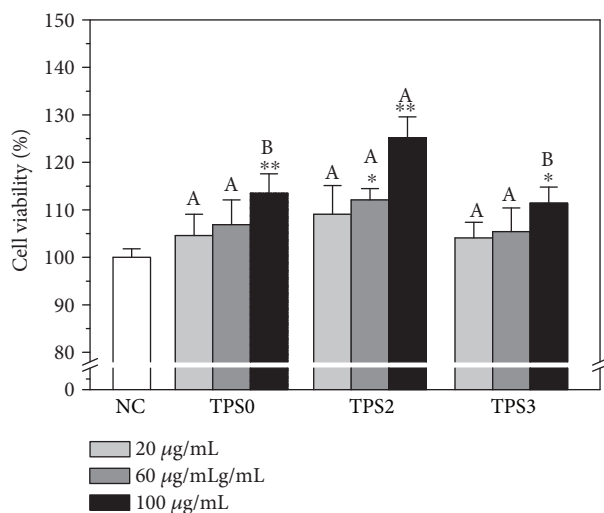


FIGURE 3: Cytotoxicity detection of TPSs with different Mw on HK-2 cells. NC: normal control. Treatment time: 24 h. Data were expressed as mean \pm SD of five independent experiments. Compared with NC group, * $p < 0.05$; ** $p < 0.01$. Different letters (A, B) indicate a significant difference ($p < 0.05$) between different TPSs of the same concentration.

emission from green in the cytoplasm to red in lysosomes [48]. Therefore, AO can be used to determine lysosomal integrity by measuring the ratio of red and green fluorescence. A low intensity of red fluorescence implies serious damage in lysosomes.

As shown in Figure 8, lysosome structure was complete (100%), and superposition of red and green fluorescence showed a strong orange-red color in normal control cells. Integrity of lysosome in damaged cells was significantly reduced (51.80%) (Figure 8(b)). However, after the damaged cells were repaired by TPS0, TPS2, and TPS3, lysosome integrity increased to 81.91%, 88.90%, and 75.03%, respectively. Therefore, TPS2 exhibited the strongest repair effect on lysosomes of cells.

3.6.6. Changes in Cell Cycle before and after Repair. Cell cycle mainly includes early DNA synthetic phase (G1 phase), DNA synthetic phase (S phase), and late DNA synthetic phase (G2 phase). Arrest of the cell cycle reflects the degree of DNA damage [49].

As shown in Figure 9, when normal HK-2 cells were damaged by oxalate, the percentage of cells in the S phase evidently decreased from 59.4% to 31.1% (Figure 9(b)), whereas that of cells in the G1 phase increased from 26.3% to 52.5% (Figure 9(c)). Results indicated that oxalate led to the arrest of HK-2 cells in the G1 phase. After the damaged cells were repaired by TPS0, TPS2, and TPS3, the percentage of cells arrested in the S phase increased to 40.6%–54.3%, which was higher than 31.1% observed for the damage control group. The increasing degree was related to the Mw of TPS. After the repair by TPS2, the percentage of cells in the S phase increased the most. Thus, TPS2 exhibited the strongest repair effect on DNA in damaged cells.

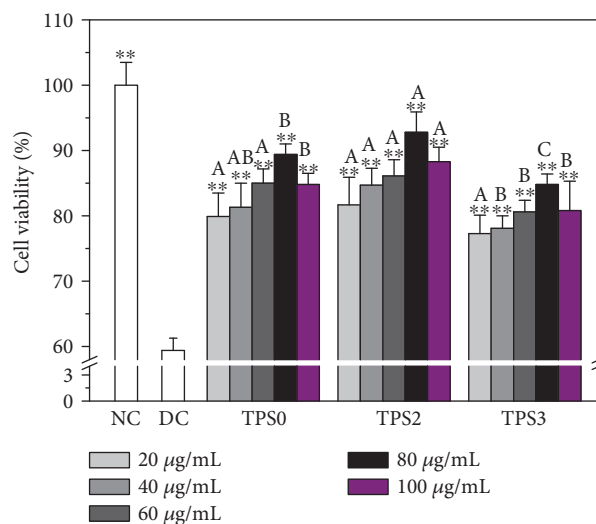


FIGURE 4: Cell viability of the damaged HK-2 cells after exposing to four TPSs with Mw. NC: normal control; DC: oxalate damaged control. Oxalate concentration: 2.6 mmol/L. Injury time: 3.5 h; repaired time: 10 h. Data were expressed as mean \pm SD of five independent experiments. Compared with DC group, * $p < 0.05$; ** $p < 0.01$. Different letters (A, B, C) indicate a significant difference ($p < 0.05$) between different TPSs of the same concentration.

3.6.7. Changes in Cell Apoptosis before and after Repair. We performed flow cytometric analysis to quantify apoptotic and necrotic cells using Annexin V/propidium iodide (PI) double staining. Annexin V staining was applied to reveal surface exposure of phosphatidylserine (apoptosis) and PI to reveal the loss of plasma membrane integrity (necrosis) [50, 51].

Figure 10(a) displays the dot plot of cellular apoptosis of the observed cells. Quadrants Q1, Q2, Q3, and Q4 denote the ratio of necrotic cells, late-stage apoptotic cells, normal cells, and early stage apoptotic cells, respectively, whereas Q2+Q4 denotes the total cell apoptotic rate. When normal HK-2 cells were damaged by oxalate, total cell apoptotic rate (Q2+Q4) increased from 2.5% to 16.7% (Figure 10(b)). After the damaged HK-2 cells were repaired by TPS0, TPS2, and TPS3, cell apoptotic rates reached 8.2%, 6.5%, and 11.7%, respectively. These rates were all lower than the 16.0% noted in the damage group. The above results indicate that TPS can reduce cell apoptosis, and TPS2 with moderate Mw exhibited the strongest repair effect.

4. Discussion

4.1. Chemical Structure Analysis of TPS. From the results of ^1H NMR and ^{13}C NMR spectrum (Figure S1), TPS comprises glucose, galactose, glucuronic acid, and arabinose. The main sugar residues included (1 \rightarrow 4)- α -GalpA, (1 \rightarrow 4)- α -D-Glcp, (1 \rightarrow)- β -D-Glcp, (1 \rightarrow 6)- β -Galp, and (1 \rightarrow 2,3,5)-Araf, which were consistent with the results clarified by Wang et al. [52] and Scoparo et al. [53].

FT-IR results revealed that the four polysaccharide fractions featured a similar backbone structure, but characteristic

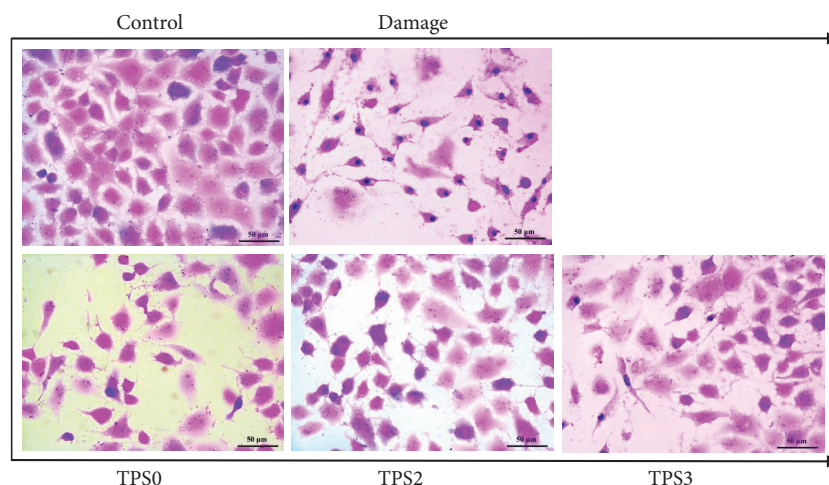


FIGURE 5: Cell morphological changes of damaged HK-2 cells after repair by TPS fractions with different Mw. Oxalate damage concentration: 2.6 mmol/L. Damaged time: 3.5 h; TPS concentration: 80 $\mu\text{g}/\text{mL}$; repaired time: 10 h.

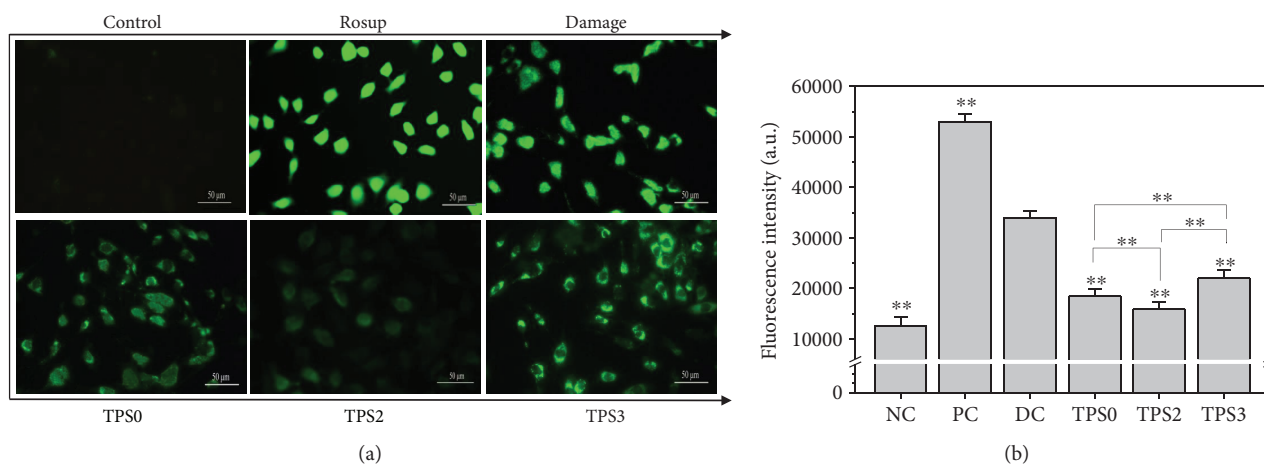


FIGURE 6: Changes in intracellular ROS of damaged HK-2 cells after being repaired by TPSs with different Mw. (a) The image of ROS distribution observed under fluorescence microscope. (b) Quantitative analysis of ROS fluorescence intensity. The green fluorescence intensity represents ROS production. NC: normal control; PC: positive control (Rosup); DC: damaged control (oxalate). TPS concentration: 80 $\mu\text{g}/\text{mL}$; oxalate damage concentration: 2.6 mmol/L. Damaged time: 3.5 h; repaired time: 10 h. Data were expressed as mean \pm SD of three independent experiments. Compared with DC group, * $p < 0.05$; ** $p < 0.01$.

absorption peak intensities of $-\text{COOH}$ and $-\text{OH}$ of polysaccharide differed. This result may explain why the hydroxyl radicals produced by H_2O_2 degradation can attack glucosidic linkages. Oxidative scission produced diverse termini, which can be further oxidized to produce carboxyl acid. Splitting of C-C bonds within sugar residues also occurred, leading to ring-opening oxidation and formation of carboxyl groups [54]. For instance, Tian et al. [55] prepared water-soluble chitosan with low Mw (LWCS) with H_2O_2 . FT-IR and NMR suggested no distinct change in the structures of 1,4- β -D-glucose main chain, whereas changes only occurred in the side chain of LWCS.

4.2. Effects of Mw of TPS on Antioxidant Activity In Vitro. For different types of plant polysaccharides, the best bioactivity is attributed to different ranges of Mw. For example, Xing et al.

[56] reported that $\text{O}_2^{\cdot-}$ -scavenging effect of LWCS (9 kDa) was more effective than that of high-molecular-weight chitosan (760 kDa). However, Ma et al. [57] observed that antitumor activity of high-Mw *Pleurotus eryngii* polysaccharide (413 kDa) against HepG-2 cells was better than that of low-Mw fraction (12 kDa).

4.2.1. Causes of Low Antioxidant Activity and Cell Repair Ability of Low-Mw TPS. The antioxidant activity of polysaccharides is closely correlated with Mw. As shown in Figure 2, $\cdot\text{OH}$, ABTS scavenging rates, and reducing power of low-Mw TPS3 (2.31 kDa) were weaker than those of moderate Mw TPS2 (4.82 kDa). This phenomenon possibly caused the significant destruction in the chain structure of TPS3 (with the lowest Mw); TPS3 featured the most loose molecular structure. The number of

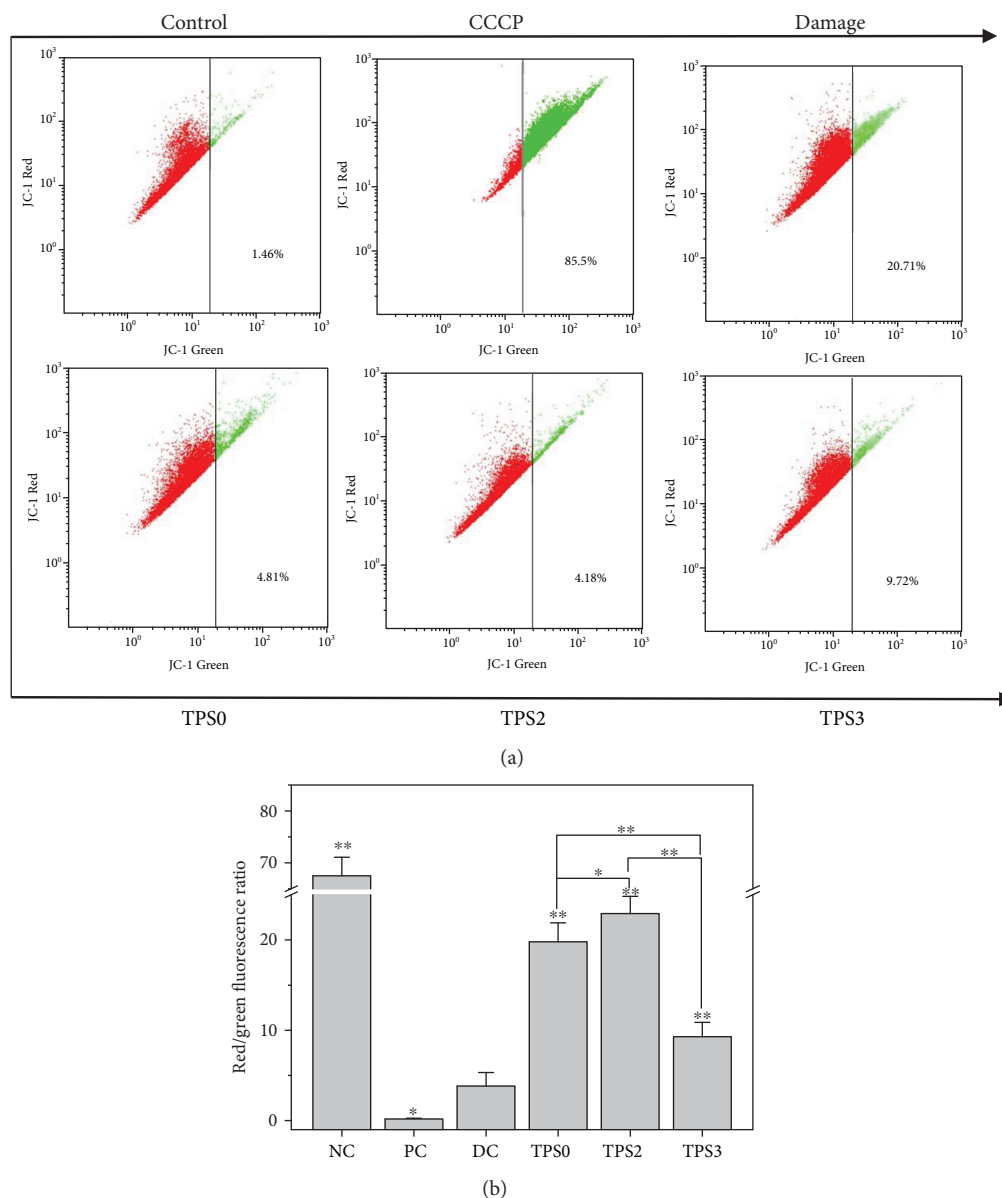


FIGURE 7: Changes in mitochondrial membrane potential of damaged HK-2 cells after being repaired by TPSs with different Mw. (a) Dot plot of $\Delta\psi_m$ detected by flow cytometry. (b) The quantitative results of the red/green fluorescence intensity ratio. NC: normal control; PC: positive control (CCCP); DC: damaged control (oxalate). TPS concentration: 80 $\mu\text{g}/\text{mL}$; oxalate damage concentration: 2.6 mmol/L . Damaged time: 3.5 h; repaired time: 10 h. Data were expressed as mean \pm SD of three independent experiments. Compared with DC group, * $p < 0.05$; ** $p < 0.01$.

effective hydroxyl groups capable of chelating metal ions reduced [58, 59]. Therefore, TPS3 featured the weakest free radical scavenging ability.

Many studies have also reported similar results. Sheng and Sun [58] performed degradation of *Athyrium multidentatum* (Doll.) Ching polysaccharide and obtained four polysaccharide fractions with Mw of 14,528 (CPA-1), 12,370 (CPA-2), 11,548 (CPA-3), and 6403 Da (CPA-4). At a concentration of 0.2 mg/mL , DPPH-free radical scavenging rate of CPA-1, CPA-2, CPA-3, and CPA-4 totaled 0.687, 0.605, 0.429, and 0.420, respectively. In other words, polysaccharides with low Mw show weak antioxidant activity. Lai et al. [60] extracted two Mw of mung bean polysaccharides

by ethanol precipitation. At a concentration of 0.8 mg/mL , DPPH-free radical scavenging rate (70.2%) of mung bean polysaccharide with low Mw (45 kDa) was weaker than that of mung bean polysaccharide (91.6%) with high Mw (83 kDa).

4.2.2. Causes of Low-Antioxidant Activity and Cell Repair Ability in High-Mw TPS. Polysaccharides can supply single electrons or hydrogen atoms to terminate free radical chain reaction and achieve radical scavenging activity [61, 62]. In comparison with low-Mw polysaccharides, high-Mw polysaccharides feature stronger winding function, a more compact structure, stronger hydrogen bond, and less exposed

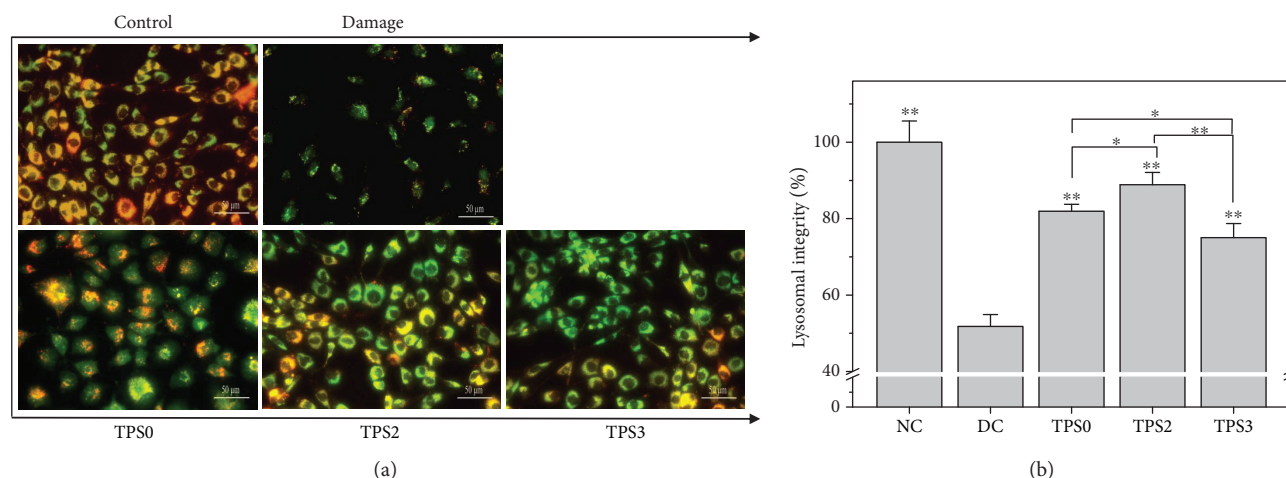


FIGURE 8: Changes in integrity of lysosomes of damaged HK-2 cells after being repaired by TPSs with different Mw. (a) The image of the integrity of lysosome observed under fluorescence microscope; (b) quantitative analysis of intracellular lysosome integrity. The cells were stained by acridine orange. TPS concentration: 80 $\mu\text{g}/\text{mL}$; oxalate damage concentration: 2.6 mmol/L. Damaged time: 3.5 h; repaired time: 10 h. Data were expressed as mean \pm SD of three independent experiments. Compared with DC group, * $p < 0.05$; ** $p < 0.01$.

external active group and thus possess weaker ability to terminate free radical chain reaction.

Polysaccharide bioactivity depends on helical structure of the main chain and the presence of hydrophilic groups (hydroxyl group) located on the outside surface of the polysaccharide helix [63]. High-Mw polysaccharides possess several branched chains, large molecular volume, and steric hindrance, resulting in the easily disintegrated bioactive triple-helical polymerization structure [58, 59, 64, 65]. High-Mw of polysaccharides also exhibit limited physical properties, such as low water solubility and high viscosity, affecting their bioactivities. The repair effect in cell also reduces due to the significant increase in resistance of large volume of polysaccharide molecules into cells [66].

Many studies have reported the weak antioxidant activity of polysaccharides with high Mw [67, 68]. For example, Zha et al. [67] extracted and obtained three polysaccharide fractions from rice bran with hot-water method; the Mw ranged from 1.2×10^5 Da to 6.3×10^5 Da (PW1), 3.5×10^4 Da to 7.4×10^4 Da (PW2), and 5.3×10^3 Da to 2.3×10^4 Da (PW3). IC_{50} values of scavenging ABTS radical of PW1, PW2, and PW3 measured 0.35, 0.2, and 0.04 mg/mL, respectively. The above results indicate the weak antioxidant activity of high-Mw polysaccharides. Sun et al. [68] performed H_2O_2 degradation of k-carrageenan polysaccharide with Mw of 350,000 Da and obtained four fractions with Mw of 3.25, 5.82, 15.08, and 20.9 kDa. IC_{50} values of scavenging superoxide anion free radicals of the four degraded fractions totaled 2.65, 3.22, 6.66, and 8.13 mg/mL. As for hydroxyl radical scavenging, IC_{50} values reached 0.014, 0.049, 0.062, and 0.110 mg/mL.

4.2.3. Causes of the Highest Antioxidant Activity and Cell Repair Ability in Moderate-Mw TPS. When high-Mw polysaccharides are degraded into a certain range of Mw, they can achieve optimal bioactivity. Polysaccharides with

moderate Mw can not only possess sufficient spatial scale to form three-helical polymerization structure [58, 59, 64] and maintain bioactivity but also destruct highly compact molecular conformation to expose several active groups to increase hydrophilicity and stability of the structure. Steric hindrance of polysaccharides is suitable when reacting with biological receptors. Therefore, polysaccharides can exhibit strong antioxidant activity and desirable cell repair ability. TPS2 with moderate Mw can chelate with metal ions (such as Fe^{2+} and Cu^{2+}) that are necessary in producing $\cdot\text{OH}$ radicals to form complexes. Therefore, generation of radicals and initiation or progress of lipid chain reaction is inhibited [69].

Xu et al. [70] degraded crude polysaccharides from *Camellia* seed cake (COP-C) using ultrasonic wave and obtained four polysaccharide fractions, namely, COP-1, COP-2, COP-3, and COP-4, with molecular weights of 7.9, 36, 83, and 225 kDa, respectively. At the concentration of 2 mg/mL, radical scavenging capacity and reducing power order followed the order of COP-2 > COP-3 > COP-4 > COP-1. Only the polysaccharide with moderate Mw of 36–83 kDa exhibited the strongest antioxidant activity. Trombetta et al. [71] have shown that moderate Mw of polysaccharide from *Opuntia ficus-indica* (L.) cladodes also benefits enhancement of ability to repair damaged cells. The polysaccharide fraction with Mw higher than 10^4 Da showed a wound-healing effect on damaged skin epithelium cells in mice. Wound-healing effect is more remarkable for polysaccharides with Mw ranging 10^4 – 10^6 Da than those with Mw > 10^6 Da.

4.3. Polysaccharides with Strong Antioxidant Activity Feature Strong Cell Repair Ability. The four studied TPSs exhibited repair effect on damaged HK-2 cells induced by oxalate, and repair ability was positively related with antioxidant activity. TPS2, which presented the strongest antioxidant activity, also showed the strongest cell repair ability.

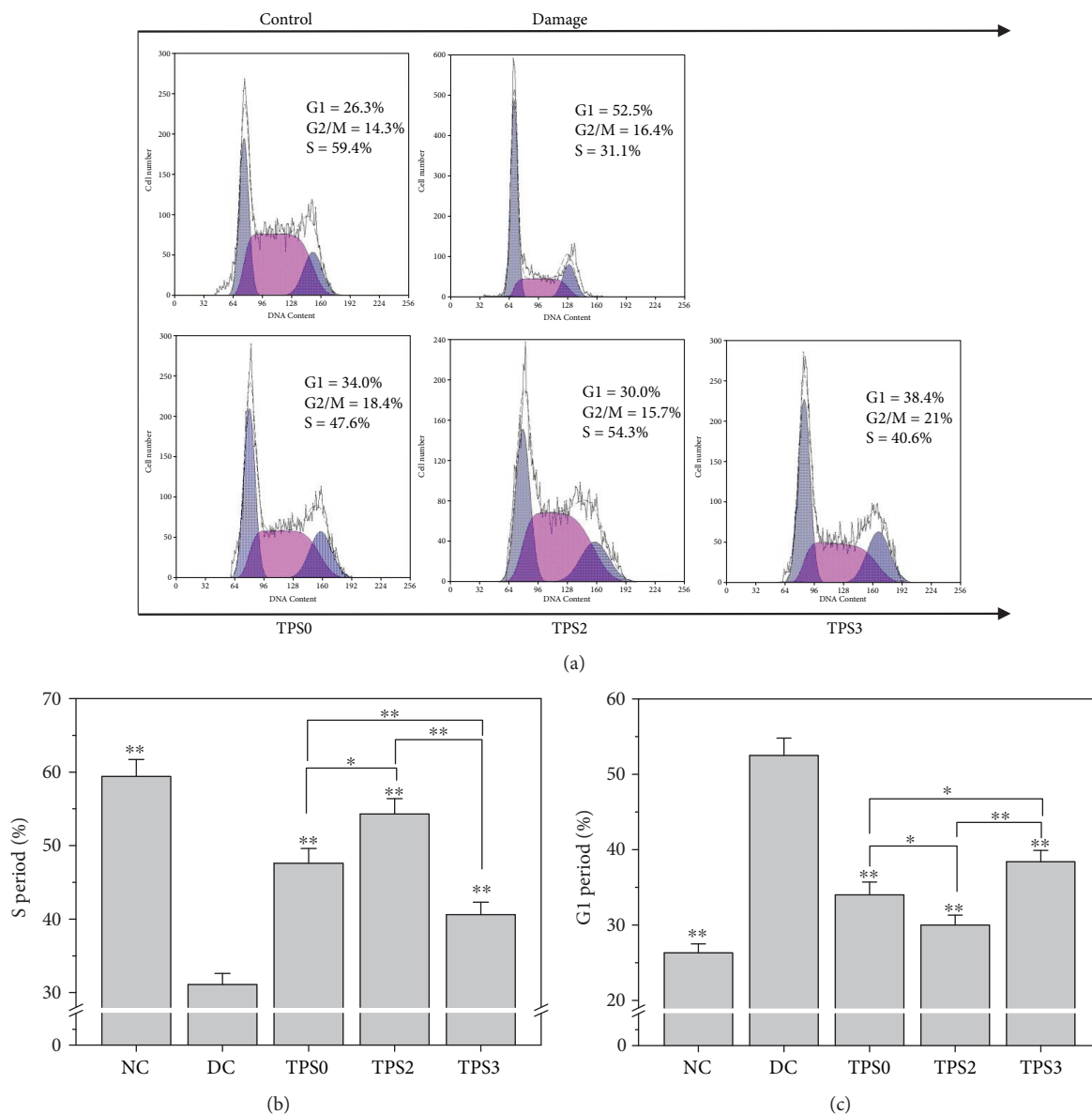


FIGURE 9: Changes in cell cycle of damaged HK-2 cells after being repaired by TPS fractions with different Mw. (a) Representative images of cell cycle; (b) the percentage of cells in the S phase; (c) the percentage of cells in the G1 phase. Oxalate damage concentration: 2.6 mmol/L. TPS concentration: 80 μ g/mL; Damaged time: 3.5 h; repaired time: 10 h. Data were expressed as mean \pm SD of three independent experiments. Compared with DC group, * $p < 0.05$; ** $p < 0.01$.

In living organisms, small molecules can pass through the plasma membrane directly or through the help of carrier proteins or ion channels [72], while some macromolecules, such as proteins, polynucleotides, and lipoprotein particles, are difficult to directly cross the cell membrane and needs to be transported on both sides of the cell membrane by endocytosis and efflux [73]. Sun et al. [74] confirmed that masson pine pollen polysaccharide, which has a molecular weight of 316 kDa, mainly entered RAW264.7 macrophages through receptor-regulated endocytosis rather than phagocytosis. Cobb et al. [75] indicated that polysaccharide A (PS-A) from *Bacteroides fragilis* with the molecular weight of larger than 100 kDa is endocytosed by antigen-presenting cells (APCs) and localizes to the conventional MHCII compartment (MIIC). This observation was also confirmed in

primary mouse splenocytes, human THP-1 monocytes, and mouse B1 B cells. Time course studies indicated that entry and surface localization of PS-A was visible in 30 min and peaked at 6 h. Therefore, the TPS polysaccharide (2.31 ~ 10.88 kDa) used in this study can access to the HK-2 cells.

Numerous studies have shown that accumulation of ROS in vivo can attack cells and cause protein oxidation, lipid peroxidation, and nucleic acid fracture, which can affect normal cell functions and result in the occurrence of chronic diseases [46, 47, 76]. As antioxidants, polysaccharides can scavenge radicals, reduce oxidative damage of cells, and exhibit protective effects on cells [77]. For instance, *Lycium barbarum* polysaccharides can protect tissue cells from DNA damage induced by oxidative stress [78]. *Hericium erinaceus*

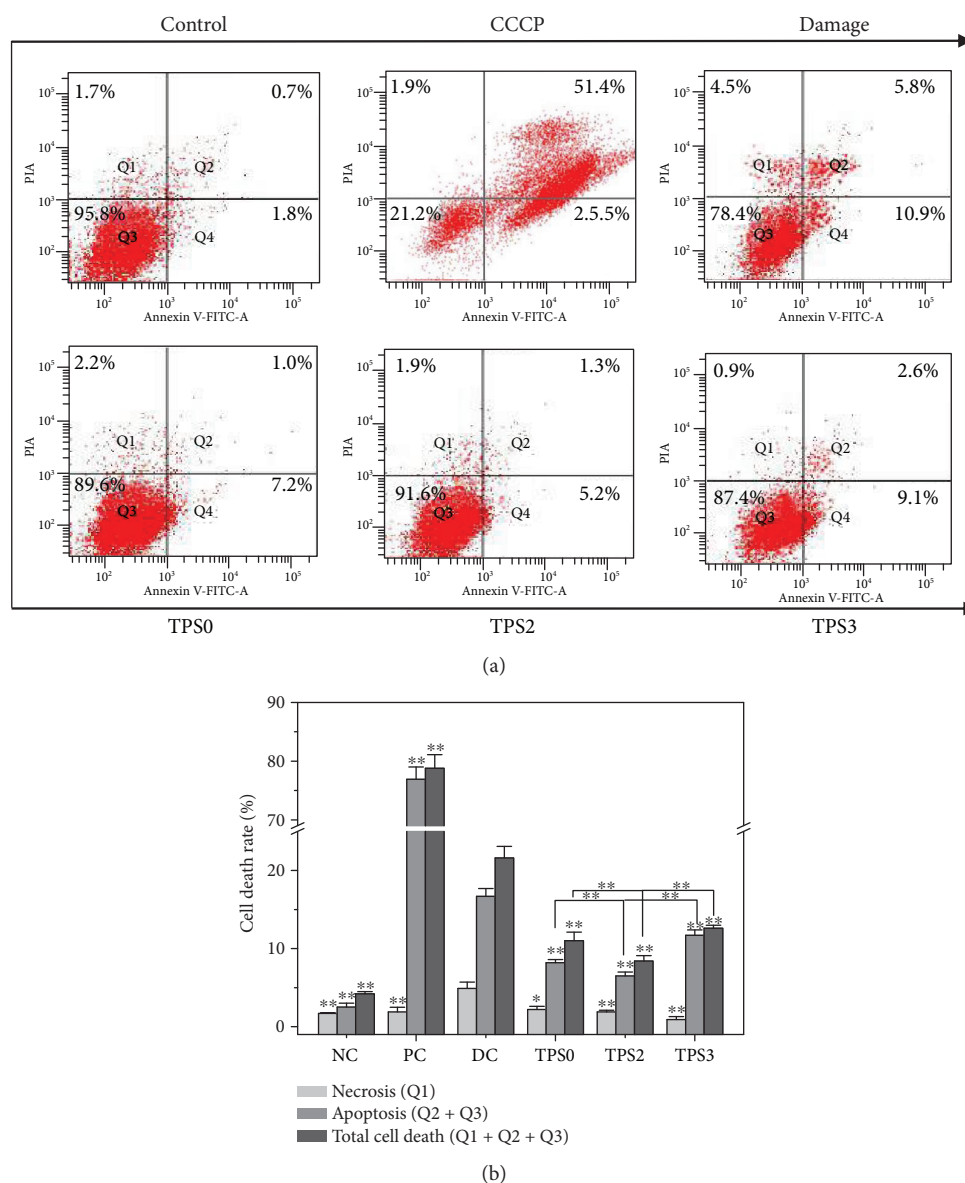


FIGURE 10: Changes in cell apoptosis and necrosis rate of damaged HK-2 cells after being repaired by TPSs with different Mw. (a) Dot plots of cell apoptosis and necrosis detected by flow cytometry. (b) Quantitative analysis of cell apoptosis and necrosis. NC: normal control; PC: positive control (CCCP); DC: damaged control (oxalate). TPS concentration: 80 μ g/mL; oxalate damage concentration: 2.6 mmol/L. Damaged time: 3.5 h; repaired time: 10 h. Data were expressed as mean \pm SD of three independent experiments. Compared with DC group, * p < 0.05; ** p < 0.01.

polysaccharides can scavenge DPPH free radical, reduce ROS production, improve cell viability, inhibit reduction of mitochondrial membrane potential, and exhibit protective effects on amyloid beta-induced neurotoxicity in PC12 cells [79]. *Salvia brachyantha* extract reduces H9C2 cell apoptosis induced by xanthine oxidase/xanthine by preventing generation of toxic-free radicals and by enhancing the intracellular antioxidant defense system [80]. Kim et al. [81] revealed that *Psidium guajava* leaf polysaccharides can scavenge radicals to relieve H₂O₂-induced oxidative stress and DNA injury in Vero cells and inhibit lipid peroxidation. After cell repair by 12.5, 25, and 50 μ g/mL of *Psidium guajava* leaf polysaccharides,

intracellular ROS production decreased from 129.5% in the damage group to 118.9%, 109.7%, and 99.7%, respectively. A polysaccharide from *Lonicera japonica* flowers remarkably reduced malondialdehyde levels, elevated superoxide dismutase and glutathione peroxidase activities, and protected the rat brain against ischemia/reperfusion injury [82].

On the basis of our research results, a proposed repair mechanism of damaged HK-2 cells by TPS is illustrated in Figure 11. High concentration of oxalate in urine will cause lipid peroxidation; this phenomenon leads to excessive production of ROS and damage to renal epithelial cells. TPS polysaccharides exhibit a strong ability to scavenge ROS;

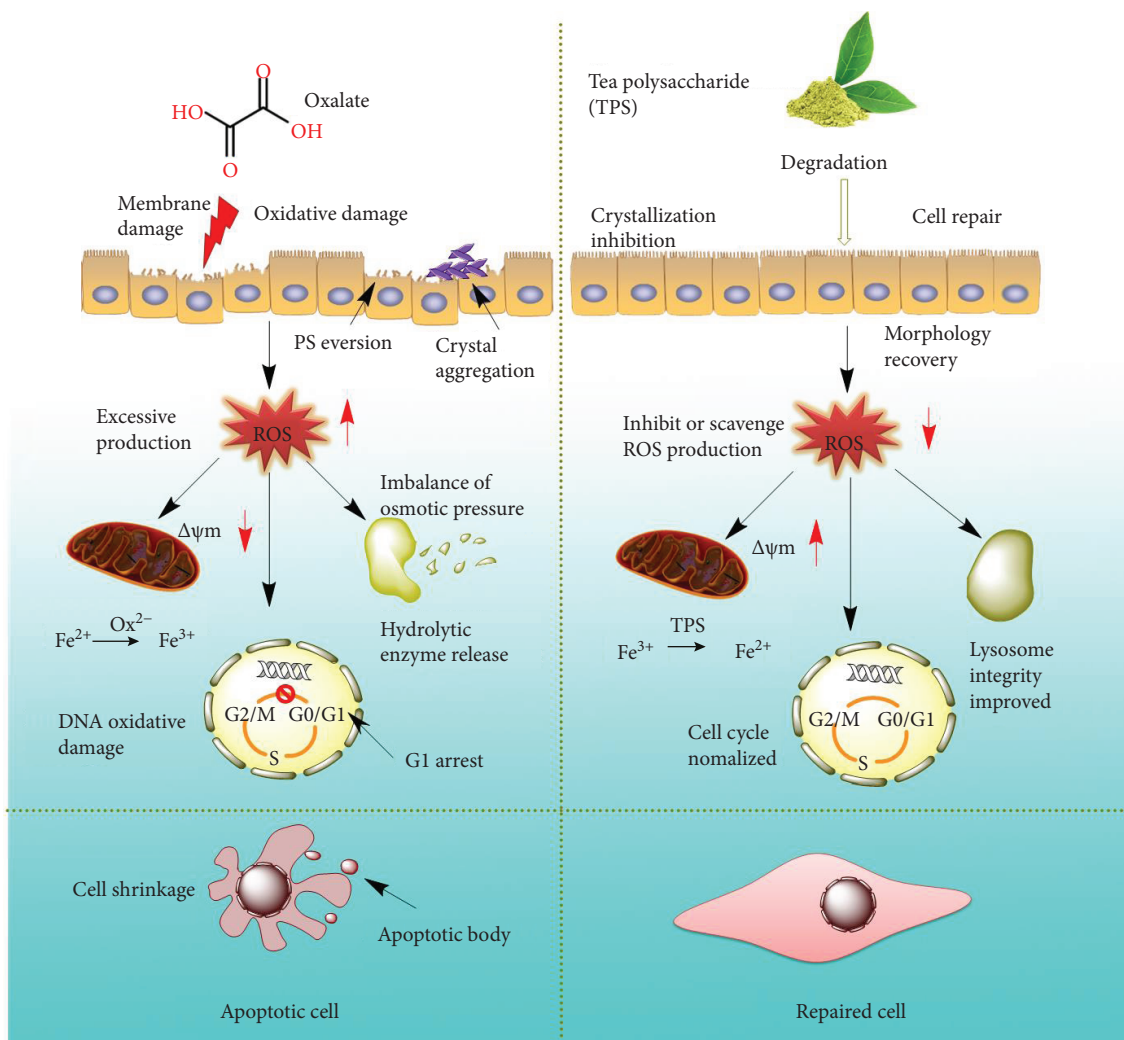


FIGURE 11: A proposed schematic illustration of the repair mechanism of damaged HK-2 cells after the treatment of TPS with different molecular weights.

therefore, TPS elicited repair effect on damaged HK-2 cells. After the damaged HK-2 cells were repaired through treatment with TPS with different molecular weights, the cell viability increased, the amount of LDH released decreased, and the cell morphology was improved. When the cells were oxidatively damaged by oxalate, the permeability of the mitochondrial membrane increased, resulting in decreased $\Delta\psi_m$. TPS can repair the membrane potential of cells and increase $\Delta\psi_m$. In damaged cells, the percentage of cells in the S phase decreased but that in the G1 phase increased. After treatment with TPS, TPS promoted cell cycle progression from the G1 phase to the S phase and repaired DNA replication. Finally, TPS alleviated cell apoptosis induced by oxidative stress and decreased the underlying risk of stone formation.

5. Conclusions

Four TPS fractions (TPS0, TPS1, TPS2, and TPS3) with Mw of 10.88, 8.16, 4.82, and 2.31 kDa, respectively, were

obtained. All TPS fractions exhibited antioxidant activity. The order of hydroxyl radical scavenging, ABTS radical scavenging activity, and reducing power was as follows: TPS2 > TPS1 > TPS0 > TPS3. The four TPSs also showed repair effects on HK-2 cells with damage induced by 2.6 mmol/L oxalate. Repair effect of TPSs was positively related with antioxidant activity. TPS2, featuring a moderate Mw, displayed the strongest antioxidant activity and cell repair ability. Compared with the damage group, cell morphology in the repaired group was closer to that of normal cells. The treated groups also yielded the following results: cell viability strengthened, mitochondrial membrane potential and integrity of lysosome improved, ROS production decreased, cells were arrested in the G1 phase, and cell apoptosis rate was reduced. All these findings indicate that these TPSs show repair effect on cell morphology, mitochondria, DNA, and other subcellular organelles in damaged HK-2 cells. Our results suggest that these TPS fractions, especially TPS2, may become potential drugs for prevention and cure of kidney stones.

Data Availability

All the data supporting the results were shown in the paper and can be applicable from the corresponding author.

Conflicts of Interest

The authors declare no competing financial interest.

Acknowledgments

This research work was granted by the Natural Science Foundation of China (Nos. 81670644 and 21701050).

Supplementary Materials

The ^{13}C NMR and ^1H NMR attribution and spectra of TPS0 used for structural elucidation are presented in Table S1 and Figure S1. The effects of oxalate concentration and injury time on the viability of HK-2 cells are presented in Figure S2. (*Supplementary Materials*)

References

- [1] G. Chen, Q. Yuan, M. Saeeduddin, S. Ou, X. Zeng, and H. Ye, "Recent advances in tea polysaccharides: extraction, purification, physicochemical characterization and bioactivities," *Carbohydrate Polymers*, vol. 153, pp. 663–678, 2016.
- [2] M. Nakamura, S. Miura, A. Takagaki, and F. Nanjo, "Hypolipidemic effects of crude green tea polysaccharide on rats, and structural features of tea polysaccharides isolated from the crude polysaccharide," *International Journal of Food Sciences and Nutrition*, vol. 68, no. 3, pp. 321–330, 2017.
- [3] L. L. Du, Q. Y. Fu, L. P. Xiang et al., "Tea polysaccharides and their bioactivities," *Molecules*, vol. 21, no. 11, p. 1449, 2016.
- [4] H. Chen, M. Zhang, Z. Qu, and B. Xie, "Antioxidant activities of different fractions of polysaccharide conjugates from green tea (*Camellia sinensis*)," *Food Chemistry*, vol. 106, no. 2, pp. 559–563, 2008.
- [5] Y. Itoh, T. Yasui, A. Okada, K. Tozawa, Y. Hayashi, and K. Kohri, "Examination of the anti-oxidative effect in renal tubular cells and apoptosis by oxidative stress," *Urological Research*, vol. 33, no. 4, pp. 261–266, 2005.
- [6] B. C. Jeong, B. S. Kim, J. I. Kim, and H. H. Kim, "Effects of green tea on urinary stone formation: an in vivo and in vitro study," *Journal of Endourology*, vol. 20, no. 5, pp. 356–361, 2006.
- [7] W. Fang, H. Zhang, J. Yin et al., "Hydroxyapatite crystal formation in the presence of polysaccharide," *Crystal Growth & Design*, vol. 16, no. 3, pp. 1247–1255, 2016.
- [8] Y. M. Michelacci, R. Q. Glashan, and N. Schor, "Urinary excretion of glycosaminoglycans in normal and stone forming subjects," *Kidney International*, vol. 36, no. 6, pp. 1022–1028, 1989.
- [9] E. R. Boeve, L. C. Cao, C. F. Verkoelen, J. C. Romijn, W. C. De Bruijn, and F. H. Schroder, "Glycosaminoglycans and other sulphated polysaccharides in calculogenesis of urinary stones," *World Journal of Urology*, vol. 12, no. 1, pp. 43–48, 1994.
- [10] Z. Y. Zhao, L. T. Huangfu, L. L. Dong, and S. L. Liu, "Functional groups and antioxidant activities of polysaccharides from five categories of tea," *Industrial Crops and Products*, vol. 58, pp. 31–35, 2014.
- [11] X. Zhang, H. Chen, N. Zhang et al., "Extrusion treatment for improved physicochemical and antioxidant properties of high-molecular weight polysaccharides isolated from coarse tea," *Food Research International*, vol. 53, no. 2, pp. 726–731, 2013.
- [12] H. Chen, M. Zhang, and B. Xie, "Components and antioxidant activity of polysaccharide conjugate from green tea," *Food Chemistry*, vol. 90, no. 1-2, pp. 17–21, 2005.
- [13] H. Wang, S. Shi, B. Bao, X. Li, and S. Wang, "Structure characterization of an arabinogalactan from green tea and its anti-diabetic effect," *Carbohydrate Polymers*, vol. 124, pp. 98–108, 2015.
- [14] D. Wang, Y. Zhao, Y. Sun, and X. Yang, "Protective effects of Ziyang tea polysaccharides on CCl_4 -induced oxidative liver damage in mice," *Food Chemistry*, vol. 143, pp. 371–378, 2014.
- [15] P. Zhou, M. Xie, S. Nie, and X. Wang, "Primary structure and configuration of tea polysaccharide," *Science in China Series C: Life Sciences*, vol. 47, no. 5, pp. 416–424, 2004.
- [16] C. Li, Q. Huang, X. Fu, X. J. Yue, R. H. Liu, and L. J. You, "Characterization, antioxidant and immunomodulatory activities of polysaccharides from *Prunella vulgaris* Linn," *International Journal of Biological Macromolecules*, vol. 75, pp. 298–305, 2015.
- [17] F. Yu, X. Cao, Y. Li et al., "Diels–Alder crosslinked HA/PEG hydrogels with high elasticity and fatigue resistance for cell encapsulation and articular cartilage tissue repair," *Polymer Chemistry*, vol. 5, no. 17, pp. 5116–5123, 2014.
- [18] R. You, K. Wang, J. Liu, M. Liu, L. Luo, and Y. Zhang, "A comparison study between different molecular weight polysaccharides derived from *Lentinus edodes* and their antioxidant activities in vivo," *Pharmaceutical Biology*, vol. 49, no. 12, pp. 1298–1305, 2011.
- [19] N. Lei, M. Wang, L. Zhang et al., "Effects of low molecular weight yeast β -glucan on antioxidant and immunological activities in mice," *International Journal of Molecular Sciences*, vol. 16, no. 9, pp. 21575–21590, 2015.
- [20] L. Sun, C. Wang, Q. Shi, and C. Ma, "Preparation of different molecular weight polysaccharides from *Porphyridium cruentum* and their antioxidant activities," *International Journal of Biological Macromolecules*, vol. 45, no. 1, pp. 42–47, 2009.
- [21] L. Ying, Y. Pan, Y. Wang, and P. Xu, "Physicochemical properties, in vitro antioxidant activities and protective effects of Liubao tea polysaccharides on HUVEC," *Journal of Tea Science*, vol. 37, no. 1, pp. 25–37, 2017.
- [22] X.-Y. Sun, J.-M. Ouyang, and K. Yu, "Shape-dependent cellular toxicity on renal epithelial cells and stone risk of calcium oxalate dihydrate crystals," *Scientific Reports*, vol. 7, no. 1, p. 7250, 2017.
- [23] Q.-Z. Gan, X.-Y. Sun, and J.-M. Ouyang, "Adhesion and internalization differences of COM nanocrystals on Vero cells before and after cell damage," *Materials Science and Engineering: C*, vol. 59, pp. 286–295, 2016.
- [24] H. Tsuji, W. Wang, J. Sunil et al., "Involvement of renin–angiotensin–aldosterone system in calcium oxalate crystal induced activation of NADPH oxidase and renal cell injury," *World Journal of Urology*, vol. 34, no. 1, pp. 89–95, 2016.
- [25] Y. Sun, X. Yang, X. Lu, D. Wang, and Y. Zhao, "Protective effects of Keemun black tea polysaccharides on acute carbon tetrachloride-caused oxidative hepatotoxicity in mice," *Food and Chemical Toxicology*, vol. 58, pp. 184–192, 2013.

- [26] J.-Y. Yin, S.-P. Nie, Q.-B. Guo, Q. Wang, S.-W. Cui, and M.-Y. Xie, "Effect of calcium on solution and conformational characteristics of polysaccharide from seeds of *Plantago asiatica* L.," *Carbohydrate Polymers*, vol. 124, pp. 331–336, 2015.
- [27] P. Bhadja, C. Y. Tan, J. M. Ouyang, and K. Yu, "Repair effect of seaweed polysaccharides with different contents of sulfate group and molecular weights on damaged HK-2 cells," *Polymers*, vol. 8, no. 5, p. 188, 2016.
- [28] R. Li, W. Chen, W. Wang, W. Tian, and X. Zhang, "Antioxidant activity of *Astragalus* polysaccharides and antitumour activity of the polysaccharides and siRNA," *Carbohydrate Polymers*, vol. 82, no. 2, pp. 240–244, 2010.
- [29] J. Jiang, F. Kong, N. Li, D. Zhang, C. Yan, and H. Lv, "Purification, structural characterization and in vitro antioxidant activity of a novel polysaccharide from *Boshuzhi*," *Carbohydrate Polymers*, vol. 147, pp. 365–371, 2016.
- [30] L. Yang, T. Zhao, H. Wei et al., "Carboxymethylation of polysaccharides from *Auricularia auricula* and their antioxidant activities in vitro," *International Journal of Biological Macromolecules*, vol. 49, no. 5, pp. 1124–1130, 2011.
- [31] K. I. Berker, B. Demirata, and R. Apak, "Determination of total antioxidant capacity of lipophilic and hydrophilic antioxidants in the same solution by using ferric–ferricyanide assay," *Food Analytical Methods*, vol. 5, no. 5, pp. 1150–1158, 2012.
- [32] X. Y. Sun, K. Yu, and J. M. Ouyang, "Time-dependent subcellular structure injuries induced by nano-/micron-sized calcium oxalate monohydrate and dihydrate crystals," *Materials Science and Engineering: C*, vol. 79, pp. 445–456, 2017.
- [33] X. Y. Sun, M. Xu, and J. M. Ouyang, "Effect of crystal shape and aggregation of calcium oxalate monohydrate on cellular toxicity in renal epithelial cells," *ACS Omega*, vol. 2, no. 9, pp. 6039–6052, 2017.
- [34] B. W. Jo and S.-K. Choi, "Degradation of fucoidans from *Sargassum fulvellum* and their biological activities," *Carbohydrate Polymers*, vol. 111, no. 13, pp. 822–829, 2014.
- [35] B. C. Pierce, J. Wichmann, T. H. Tran, R. Cheetamun, A. Bacic, and A. S. Meyer, "Formation of water-soluble soybean polysaccharides from spent flakes by hydrogen peroxide treatment," *Carbohydrate Polymers*, vol. 144, pp. 504–513, 2016.
- [36] H. Xizhen, N. Yanning, J. Mingfei et al., "Characterization and antioxidant study of different molecular weight of soluble soybean polysaccharides," *Soybean Science*, vol. 35, no. 5, pp. 805–809, 2016.
- [37] Y. Hou, J. Wang, W. Jin, H. Zhang, and Q. Zhang, "Degradation of *Laminaria japonica* fucoidan by hydrogen peroxide and antioxidant activities of the degradation products of different molecular weights," *Carbohydrate Polymers*, vol. 87, no. 1, pp. 153–159, 2012.
- [38] M. A. Chaouch, J. Hafsa, C. Rihouey, D. Le Cerf, and H. Majdoub, "Depolymerization of polysaccharides from *Opuntia ficus indica*: antioxidant and antiglycated activities," *International Journal of Biological Macromolecules*, vol. 79, pp. 779–786, 2015.
- [39] L. Winer, R. Goren, and J. Rivov, "Stimulation of the oxidative decarboxylation of indole-3-acetic acid in citrus tissues by ethylene," *Plant Growth Regulation*, vol. 32, no. 2/3, pp. 231–237, 2000.
- [40] R. Xu, H. Ye, Y. Sun, Y. Tu, and X. Zeng, "Preparation, preliminary characterization, antioxidant, hepatoprotective and anti-tumor activities of polysaccharides from the flower of tea plant (*Camellia sinensis*)," *Food and Chemical Toxicology*, vol. 50, no. 7, pp. 2473–2480, 2012.
- [41] L. Sun, L. Wang, J. Li, and H. Liu, "Characterization and antioxidant activities of degraded polysaccharides from two marine Chrysophyta," *Food Chemistry*, vol. 160, no. 1–7, pp. 1–7, 2014.
- [42] Y. G. Xia, J. Liang, B. Y. Yang, Q. H. Wang, and H. X. Kuang, "Structural studies of an arabinan from the stems of *Ephedra sinica* by methylation analysis and 1D and 2D NMR spectroscopy," *Carbohydrate Polymers*, vol. 121, pp. 449–456, 2015.
- [43] L. Yang, S. Fu, X. Zhu et al., "Hyperbranched acidic polysaccharide from green tea," *Biomacromolecules*, vol. 11, no. 12, pp. 3395–3405, 2010.
- [44] J. Fu, L. Huang, H. Zhang, S. Yang, and S. Chen, "Structural features of a polysaccharide from *Astragalus membranaceus* (Fisch.) Bge. var. *mongholicus* (Bge.) Hsiao," *Journal of Asian Natural Products Research*, vol. 15, no. 6, pp. 687–692, 2013.
- [45] H. Chen, Z. Wang, X. Lu, and B. Xie, "Isolation and chemical characterisation of a polysaccharide from green tea (*Camellia sinensis* L.)," *Journal of the Science of Food and Agriculture*, vol. 88, no. 14, pp. 2523–2528, 2008.
- [46] J. P. E. Spencer, A. Jenner, O. I. Aruoma et al., "Intense oxidative DNA damage promoted by l-DOPA and its metabolites implications for neurodegenerative disease," *FEBS Letters*, vol. 353, no. 3, pp. 246–250, 1994.
- [47] S. Thamilselvan and M. Menon, "Vitamin E therapy prevents hyperoxaluria-induced calcium oxalate crystal deposition in the kidney by improving renal tissue antioxidant status," *BJU International*, vol. 96, no. 1, pp. 117–126, 2005.
- [48] F. Yu, Z. Chen, B. Wang et al., "The role of lysosome in cell death regulation," *Tumor Biology*, vol. 37, no. 2, pp. 1427–1436, 2016.
- [49] J. A. Seiler, C. Conti, A. Syed, M. I. Aladjem, and Y. Pommier, "The intra-S-phase checkpoint affects both DNA replication initiation and elongation: single-cell and -DNA fiber analyses," *Molecular and Cellular Biology*, vol. 27, no. 16, pp. 5806–5818, 2007.
- [50] S. Arur, U. E. Uche, K. Rezaul et al., "Annexin I is an endogenous ligand that mediates apoptotic cell engulfment," *Developmental Cell*, vol. 4, no. 4, pp. 587–598, 2003.
- [51] A. Ishaque and M. Al-Rubeai, "Use of intracellular pH and annexin-V flow cytometric assays to monitor apoptosis and its suppression by *bcl-2* over-expression in hybridoma cell culture," *Journal of Immunological Methods*, vol. 221, no. 1–2, pp. 43–57, 1998.
- [52] Y. Wang, X. Wei, and Z. Jin, "Structure analysis of an acidic polysaccharide isolated from green tea," *Natural Product Research*, vol. 23, no. 7, pp. 678–687, 2009.
- [53] C. T. Scoparo, L. M. Souza, N. Dartora et al., "Chemical characterization of heteropolysaccharides from green and black teas (*Camellia sinensis*) and their anti-ulcer effect," *International Journal of Biological Macromolecules*, vol. 86, pp. 772–781, 2016.
- [54] S. Trombotto, A. Bouchu, G. Descotes, and Y. Queneau, "Hydrogen peroxide oxidation of palatinose and trehalulose: direct preparation of carboxymethyl α -D-glucopyranoside," *Tetrahedron Letters*, vol. 41, no. 43, pp. 8273–8277, 2000.
- [55] F. Tian, Y. Liu, K. Hu, and B. Zhao, "The depolymerization mechanism of chitosan by hydrogen peroxide," *Journal of Materials Science*, vol. 38, no. 23, pp. 4709–4712, 2003.

- [56] R. Xing, S. Liu, Z. Guo et al., "Relevance of molecular weight of chitosan and its derivatives and their antioxidant activities in vitro," *Bioorganic & Medicinal Chemistry*, vol. 13, no. 5, pp. 1573–1577, 2005.
- [57] G. Ma, W. Yang, A. M. Mariga et al., "Purification, characterization and antitumor activity of polysaccharides from *Pleurotus eryngii* residue," *Carbohydrate Polymers*, vol. 114, pp. 297–305, 2014.
- [58] J. Sheng and Y. Sun, "Antioxidant properties of different molecular weight polysaccharides from *Athyrium multidentatum* (Doll.) Ching," *Carbohydrate Polymers*, vol. 108, pp. 41–45, 2014.
- [59] H. Saitō, Y. Yoshioka, N. Uehara, J. Aketagawa, S. Tanaka, and Y. Shibata, "Relationship between conformation and biological response for (1→3)- β -D-glucans in the activation of coagulation Factor G from limulus amebocyte lysate and host-mediated antitumor activity. Demonstration of single-helix conformation as a stimulant," *Carbohydrate Research*, vol. 217, no. 1, pp. 181–190, 1991.
- [60] F. Lai, Q. Wen, L. Li, H. Wu, and X. Li, "Antioxidant activities of water-soluble polysaccharide extracted from mung bean (*Vigna radiata* L.) hull with ultrasonic assisted treatment," *Carbohydrate Polymers*, vol. 81, no. 2, pp. 323–329, 2010.
- [61] H. Qi, T. Zhao, Q. Zhang, Z. Li, Z. Zhao, and R. Xing, "Antioxidant activity of different molecular weight sulfated polysaccharides from *Ulva pertusa* Kjellm (Chlorophyta)," *Journal of Applied Phycology*, vol. 17, no. 6, pp. 527–534, 2005.
- [62] M. Jiangwei, Q. Zengyong, and X. Xia, "Optimisation of extraction procedure for black fungus polysaccharides and effect of the polysaccharides on blood lipid and myocardium antioxidant enzymes activities," *Carbohydrate Polymers*, vol. 84, no. 3, pp. 1061–1068, 2011.
- [63] J. A. Bohn and J. N. BeMiller, "(1→3)- β -D-Glucans as biological response modifiers: a review of structure-functional activity relationships," *Carbohydrate Polymers*, vol. 28, no. 1, pp. 3–14, 1995.
- [64] S.-Q. Huang, S. Ding, and L. Fan, "Antioxidant activities of five polysaccharides from *Inonotus obliquus*," *International Journal of Biological Macromolecules*, vol. 50, no. 5, pp. 1183–1187, 2012.
- [65] X. Li and L. Wang, "Effect of extraction method on structure and antioxidant activity of *Hohenbuehelia serotina* polysaccharides," *International Journal of Biological Macromolecules*, vol. 83, pp. 270–276, 2016.
- [66] S. Chen, R. Ding, Y. Zhou, X. Zhang, R. Zhu, and X. D. Gao, "Immunomodulatory effects of polysaccharide from marine fungus *Phoma herbarum* YS4108 on T cells and dendritic cells," *Mediators of Inflammation*, vol. 2014, Article ID 738631, 13 pages, 2014.
- [67] X.-Q. Zha, J. H. Wang, X. F. Yang et al., "Antioxidant properties of polysaccharide fractions with different molecular mass extracted with hot-water from rice bran," *Carbohydrate Polymers*, vol. 78, no. 3, pp. 570–575, 2009.
- [68] T. Sun, H. Tao, J. Xie, S. Zhang, and X. Xu, "Degradation and antioxidant activity of κ -carrageenans," *Journal of Applied Polymer Science*, vol. 117, no. 1, pp. 194–199, 2010.
- [69] Y. Zhang, S. Li, X. Wang, L. Zhang, and P. C. K. Cheung, "Advances in lentinan: isolation, structure, chain conformation and bioactivities," *Food Hydrocolloids*, vol. 25, no. 2, pp. 196–206, 2011.
- [70] Z. Xu, X. Li, S. Feng et al., "Characteristics and bioactivities of different molecular weight polysaccharides from camellia seed cake," *International Journal of Biological Macromolecules*, vol. 91, pp. 1025–1032, 2016.
- [71] D. Trombetta, C. Puglia, D. Perri et al., "Effect of polysaccharides from *Opuntia ficus-indica* (L.) cladodes on the healing of dermal wounds in the rat," *Phytomedicine*, vol. 13, no. 5, pp. 352–358, 2006.
- [72] J. C. Skou, "Enzymatic basis for active transport of Na^+ and K^+ across cell membrane," *Physiological Reviews*, vol. 45, no. 3, pp. 596–618, 1965.
- [73] L. Bareford and P. Swaan, "Endocytic mechanisms for targeted drug delivery," *Advanced Drug Delivery Reviews*, vol. 59, no. 8, pp. 748–758, 2007.
- [74] M. Sun, F. Su, J. Yang, Z. Gao, and Y. Geng, "Fluorescent labeling of polysaccharides from masson pine pollen and its effect on RAW264.7 macrophages," *Polymers*, vol. 10, no. 4, p. 372, 2018.
- [75] B. A. Cobb, Q. Wang, A. O. Tzianabos, and D. L. Kasper, "Polysaccharide processing and presentation by the MHCII pathway," *Cell*, vol. 117, no. 5, pp. 677–687, 2004.
- [76] A. A. Alfadda and R. M. Sallam, "Reactive oxygen species in health and disease," *BioMed Research International*, vol. 2012, Article ID 936486, 14 pages, 2012.
- [77] C. Y. Zhang, T. Kong, W. H. Wu, and M. B. Lan, "The protection of polysaccharide from the brown seaweed *Sargassum graminifolium* against ethylene glycol-induced mitochondrial damage," *Marine Drugs*, vol. 11, no. 12, pp. 870–880, 2013.
- [78] Q. Luo, Z. Li, X. Huang, J. Yan, S. Zhang, and Y. Z. Cai, "*Lycium barbarum* polysaccharides: protective effects against heat-induced damage of rat testes and H_2O_2 -induced DNA damage in mouse testicular cells and beneficial effect on sexual behavior and reproductive function of hemicastrated rats," *Life Sciences*, vol. 79, no. 7, pp. 613–621, 2006.
- [79] J.-H. Cheng, C.-L. Tsai, Y.-Y. Lien, M.-S. Lee, and S.-C. Sheu, "High molecular weight of polysaccharides from *Hericium erinaceus* against amyloid beta-induced neurotoxicity," *BMC Complementary and Alternative Medicine*, vol. 16, no. 1, 2016.
- [80] M. A. Esmaili and A. Sonboli, "Antioxidant, free radical scavenging activities of *Salvia brachyantha* and its protective effect against oxidative cardiac cell injury," *Food and Chemical Toxicology*, vol. 48, no. 3, pp. 846–853, 2010.
- [81] S. Y. Kim, E. A. Kim, Y. S. Kim et al., "Protective effects of polysaccharides from *Psidium guajava* leaves against oxidative stresses," *International Journal of Biological Macromolecules*, vol. 91, pp. 804–811, 2016.
- [82] D. Su, S. Li, W. Zhang, J. Wang, J. Wang, and M. Lv, "Structural elucidation of a polysaccharide from *Lonicera japonica* flowers, and its neuroprotective effect on cerebral ischemia-reperfusion injury in rat," *International Journal of Biological Macromolecules*, vol. 99, pp. 350–357, 2017.

Research Article

Sulforaphane Modulates AQP8-Linked Redox Signalling in Leukemia Cells

Cecilia Prata ¹, Carlotta Facchini,¹ Emanuela Leoncini,² Monia Lenzi ¹, Tullia Maraldi ³,
Cristina Angeloni ⁴, Laura Zambonin,¹ Silvana Hrelia ² and Diana Fiorentini ¹

¹Department of Pharmacy and Biotechnology, Alma Mater Studiorum, University of Bologna, Via Irnerio, 48-40126 Bologna, Italy

²Department for Life Quality Studies, Alma Mater Studiorum, University of Bologna, Corso d'Augusto, 237-47921 Rimini, Italy

³Department of Surgery, Medicine, Dentistry and Morphological Sciences, University of Modena and Reggio Emilia, Policlinico, Via del Pozzo, 71-41124 Modena, Italy

⁴School of Pharmacy, University of Camerino, Via Gentile III da Varano, 62032 Camerino, Macerata, Italy

Correspondence should be addressed to Diana Fiorentini; diana.fiorentini@unibo.it

Received 5 July 2018; Revised 21 September 2018; Accepted 2 October 2018; Published 18 November 2018

Guest Editor: Germán Gil

Copyright © 2018 Cecilia Prata et al. This is an open access article distributed under the Creative Commons Attribution License, which permits unrestricted use, distribution, and reproduction in any medium, provided the original work is properly cited.

Sulforaphane, a biologically active isothiocyanate compound extracted from cruciferous vegetables, has been shown to exert cytotoxic effects on many human cancer cells, including leukemia. However, the exact molecular mechanisms behind the action of sulforaphane in hematological malignancies are still unclear. Like other cancer cells, leukemia cells produce high level of reactive oxygen species; in particular, hydrogen peroxide derived from Nox family is involved in various redox signal transduction pathways, promoting cell proliferation and survival. Recent evidence show that many tumour cell types express elevated level of aquaporin isoforms, and we previously demonstrated that aquaporin-8 acts as H₂O₂ transport facilitator across the plasma membrane of B1647 cells, a model of acute myeloid human leukemia. Thus, the control of AQP8-mediated H₂O₂ transport could be a novel strategy to regulate cell signalling and survival. To this purpose, we evaluated whether sulforaphane could somehow affect aquaporin-8-mediated H₂O₂ transport and/or Nox-mediated H₂O₂ production in B1647 cell line. Results indicated that sulforaphane inhibited both aquaporin-8 and Nox2 expression, thus decreasing B1647 cells viability. Moreover, the data obtained by coimmunoprecipitation technique demonstrated that these two proteins are linked to each other; thus, sulforaphane has an important role in modulating the downstream events triggered by the axis Nox2-aquaporin-8. Cell treatment with sulforaphane also reduced the expression of peroxiredoxin-1, which is increased in almost all acute myeloid leukemia subtypes. Interestingly, sulforaphane concentrations able to trigger these effects are achievable by dietary intake of cruciferous vegetables, confirming the importance of the beneficial effect of a diet rich in bioactive compounds.

1. Introduction

The consumption of whole plant foods as chemopreventive agents is highly recommended in the dietary guidelines on the basis of health benefits from dietary phytochemicals observed in epidemiological studies [1]. Among edible plants, cruciferous vegetables have been proved to exert potent anticarcinogenic effects owing to the presence of isothiocyanates, which are the hydrolytic products of glucosinolates. Among cruciferous vegetables, broccoli contains the highest concentration of the glucosinolate glucoraphanin, which is hydrolysed by myrosinase and gut microbiota,

releasing sulforaphane, SFN (4-methylsulfinylbutyl isothiocyanate). In addition to its well-known anticancer activity [2], SFN has been demonstrated to possess cardioprotective [3], neuroprotective [4], and anti-inflammatory activities [5], suggesting a pleiotropic protective role for this nutraceutical compound.

The potent chemopreventive effect of SFN is based on its ability to target multiple mechanisms within the cell to control carcinogenesis. Many reports have shown that SFN prevents tumour initiation by both inhibiting phase I enzymes [6] and activating phase II detoxifying enzymes [7]. Moreover, SFN prevents uncontrolled cancer cell

proliferation through the modulation of genes involved in apoptosis and cell cycle arrest [5, 8], angiogenesis [9, 10], and metastasis [11, 12].

SFN cytotoxic effects have also been demonstrated on hematological malignancies [13], and it has been reported that SFN treatment of HL-60 and acute lymphoblastic leukemia cells triggered apoptosis or cell cycle arrest [14–17]. Leukemia is one of the main cause of cancer-associated death, and the high susceptibility to treatment-related toxicity is still the major limit to the therapeutic success. Therefore, the identification and development of novel agents from natural products to counteract this disease are needed in order to maximize the therapeutic benefit and minimize antineoplastic drug resistance and treatment-related toxicity in patients treated with intensified doses of multiple drugs.

In the human erythromegakaryocytic cell line B1647, a model of acute myeloid leukemia, constitutively producing VEGF and expressing its tyrosine kinase receptor, VEGFR-2 [18], we demonstrated that VEGF signalling is coupled to NAD(P)H oxidase (Nox) activity [19]. In particular, H₂O₂ generated via Nox2- and Nox4-dependent pathways is involved in early signalling events, such as the maintenance of the VEGFR-2 phosphorylation state, and also in the modulation of downstream events leading to cell proliferation and survival [20, 21]. It has to be pointed out that H₂O₂-derived Nox is formed outside the cell and have to cross the membrane to reach its cytosolic targets. To this regard, it has been reported that specific aquaporin isoforms are capable of funneling H₂O₂ across the plasma membrane in many cell types [22, 23]. In particular, AQP8 isoform has demonstrated the ability to channel H₂O₂ through the plasma membrane in B1647 cell line [24, 25], HeLa [26], and B [27] cells.

Furthermore, tumour cells overexpress AQPs, and a positive correlation exists between histological tumour grade and the AQP expression as compared to normal tissues [28–30].

The inhibition of AQP8-mediated H₂O₂ entry into the cell, or the decreased AQP8 expression, entails that Nox-derived H₂O₂ cannot exert its growth-promoting effects. Therefore, the control of AQP8-mediated H₂O₂ transport provides a novel mechanism to regulate cell signalling and survival.

This study aimed at evaluating the potential anticancer activity of SFN in B1647 leukemia cell line, focusing on AQP8 function and expression. We also investigated the effect of SFN on Nox2, Nox4, and peroxiredoxin expression and on the phosphorylation state of VEGFR-2 and Akt.

2. Materials and Methods

2.1. Chemicals and Reagents. Dulbecco's modified Eagle's medium (DMEM), Roswell Park Memorial Institute (RPMI) 1640 medium, penicillin, streptomycin, L-glutamine, phytohaemagglutinin (PHA), 3-(4,5-dimethylthiazol-2-yl)-2,5-diphenyltetrazolium bromide (MTT), DAPI, RIPA lysis buffer, 10% SDS solution, mammalian protease inhibitor mixture, phosphatase inhibitor cocktail PhosSTOP (Roche), Laemmli sample buffer containing 2-mercaptoethanol, Tris-HCl, bovine serum albumin (BSA), Hank's Balanced Salt

Solution (HBSS), 2,7-dichlorodihydrofluorescein diacetate (DCFH-DA), plumbagin from *Plumbago indica* (5-hydroxy-2-methyl-1,4-naphthoquinone), and all other chemicals were purchased from Sigma-Aldrich. Iscove's Modified Dulbecco's medium (IMDM) with L-glutamine, foetal bovine serum (FBS), and human serum AB male (HS) were purchased from Biowest. DL-Sulforaphane (SFN) (LKT Laboratories) was dissolved in DMSO and stored at -20°C at a stock concentration of 10 mM. Absolute RNA Miniprep Kit was from Agilent Technologies; RNA-to-cDNA conversion kit was from Applied Biosystems; SsoAdvanced™ Universal SYBR Green Supermix was from Bio-Rad Laboratories; and RT-PCR primers for AQP8, β -2-microglobulin, and actin were manufactured from Sigma-Aldrich. SiRNA against Nox4 and scrambled were obtained from Ambion by Life Technologies (USA). Mini-PROTEAN® TGX™ precast gels 4–20%, Precision Plus Protein™ Unstained Standards, Clarity™ Western ECL Substrate, and DC™ protein assay were from Bio-Rad Laboratories. Nitrocellulose membranes were from GE Healthcare. Primary antibodies against: AQP8 (#WH0000343) and β -actin (#A5441) were from Sigma-Aldrich, phospho-Akt (Ser473) (#4058) and Prx-1 (#8499) from Cell Signalling Technologies, phospho-VEGFR-2 from Thermo Scientific, gp91-phox (Nox2) from Millipore, and Nox4 from Santa-Cruz. Secondary antibodies: horseradish peroxidase-conjugated secondary antibodies anti-rabbit (#7074) and anti-mouse (#7076) were purchased from Cell Signalling Technologies; goat anti-Mouse IgG (H+L) Highly Cross-Adsorbed Secondary Antibody, Alexa Fluor® Plus 488 (#A32723) was from Thermo Scientific.

2.2. Cell Culture. B1647 erythromegakaryocytic cell line, established from the bone marrow of a patient with acute myelogenous leukaemia (AML), is cultured in IMDM supplemented with 5% (v/v) heat inactivated HS, L-glutamine, 100 U/mL penicillin, and 100 μ g/mL streptomycin in a humidified incubator maintained at 37°C and 5% CO₂.

Human fibroblasts were grown and kindly provided by Professor A. Lorenzini, University of Bologna.

Peripheral blood lymphocytes (PBL) were isolated by density gradient centrifugation with Histopaque-1077 from whole peripheral blood of healthy donors. PBL were cultured at 37°C and 5% CO₂ in RPMI-1640 supplemented with 1% penicillin/streptomycin, 15% heat inactivated FBS, 1% L-glutamine, and 0.5% PHA.

2.3. Cell Viability. Cell viability was evaluated by the MTT assay. Cells were treated with increasing concentrations of SFN (5, 10, or 30 μ M) for 24 h in 96-well plates, then incubated with 0.5 mg/mL MTT for 4 h at 37°C. The blue-violet formazan salt crystals formed were dissolved with a solubilisation solution (10% SDS, 0.01 M HCl) keeping the plates overnight at 37°C and 5% CO₂ in a humidified atmosphere. The absorbance at 570 nm was measured using a multiwell plate reader (Wallac Victor², PerkinElmer).

2.4. Analysis of mRNA Expression by RT-PCR. After 24 h treatment with SFN (1, 5, or 10 μ M), total RNA was extracted

from B1647 cells using Absolutely RNA Miniprep Kit according to the manufacturer's recommendations. RNA quantification was performed using a NanoVue spectrophotometer (GE Healthcare). mRNA was reverse-transcribed into cDNA starting from 1 μ g of total RNA using a high capacity RNA-to-cDNA Conversion Kit. PCR was carried out in a total volume of 20 μ L containing 2 μ L of cDNA, 10 μ L SsoAdvanced™ Universal SYBR Green Supermix, and 1 μ L (500 nM) of each primer. The specific primers used were produced by Sigma-Aldrich: AQP8 (forward sequence: TTCTCCATCGGCTT TGCCGTC A; reverse sequence: CAGCCAGTAGATCCAG TGGAAG; amplicon of 135 pb), β -actin (forward sequence: 5'-AAGACCTCTATGCCAACAC-3'; reverse sequence: 5'-TGATCTTCATGGTGCTAGG-3'), and β 2-microglobulin (forward sequence: 5'-ACTGGTCTTTCTACATCCTG-3'; reverse sequence: 5'-AGATGATTCAGAGCTCCATAG-3'). β -Actin and β 2-microglobulin were used as reference genes. The reaction mixtures were kept for 45 min at 45°C, 2 min at 94°C, then cycled 35 times through a program of 30 s at 94°C, 1 min at 56°C, and 1 min at 72°C; finally, the reaction was incubated for an extra 7 min at 68°C. Normalized expression levels were calculated relative to control cells according to the $2^{-\Delta\Delta CT}$ method.

2.5. Cell Transfection. B1647 cells were nucleofected with Cell Line Nucleofector™ Kit V (Amaxa Biosystems, Cologne, Germany) with Program T-019 following the manufacturer's instructions. siRNA against Nox4 (sequence 5'-3': CAACUC AUAUGGGACAAGAtt; antisense UCUUGUCCCAUAUG AGUUGtt) and scrambled were obtained from Ambion by Life Technologies (USA). RNA silencing was obtained with 300 nM siRNA. Subsequently, cells were immediately suspended in a complete medium and incubated in a humidified 37°C/5% CO₂ incubator. After 24 h, cells were used for the experiments: evaluation of Nox4 expression by Western blot analysis and intracellular ROS level measurement.

2.6. Electrophoresis and Western Blot Analysis. After 24 h treatment with SFN (1, 5, or 10 μ M), B1647 cells (1×10^6 /mL) were washed with ice-cold PBS and lysed with RIPA buffer containing mammalian protease and phosphatase inhibitor mixtures. Protein concentration of the cleared lysates was determined by Bio-Rad DC™ protein assay. Proteins (10 μ g per lane) were electrophoretically separated on 4–20% SDS-PAGE Mini-Protean® TGX™ precast gels using a Mini-Protean II apparatus (Bio-Rad Laboratories) and transferred to Hybond-C nitrocellulose membrane. Nonspecific binding was avoided by incubating membranes in blocking buffer containing 5% (w/v) albumin in Tris-buffered saline (TBS)/Tween, then the nitrocellulose membranes were probed overnight at 4°C with primary antibodies (anti-AQP8, anti-Nox2, anti-phospho-VEGFR-2, anti-phospho-Akt, anti-Nox4, or anti- β -actin as internal normalizer). Nitrocellulose membranes were washed with TBS/Tween and incubated at room temperature for 1 h with horseradish peroxidase-conjugated secondary antibodies in TBS/Tween containing 5% nonfat dried milk or 5% albumin and successively washed with TBS/Tween. Chemiluminescence detection was performed using Clarity™ Western ECL Substrate.

Bands were acquired with a CCD imager (ChemiDoc™ MP System, Bio-Rad Laboratories), and relative densitometric analysis were performed by using Image Lab analysis software (Bio-Rad Laboratories).

2.7. Immunofluorescence Confocal Microscopy. B1647 cells were treated with 10 μ M SFN for 24 h, loaded into cytospin chambers, and centrifuged at 450 rpm for 10 min. Cells were then fixed in formaldehyde 3.7% for 15 min, washed twice with PBS, blocked with PBS/BSA 1% (w/v) for 1 h, and incubated with mouse anti-AQP8 antibody for 1 h. Consecutively, cells were treated with fluorescent goat anti-Mouse Secondary Antibody, Alexa Fluor® Plus 488 conjugated for 1 h in the dark, nuclei were stained with DAPI, and coverslips were mounted on slides. Confocal imaging was acquired by a Nikon A1 confocal laser scanning microscope (Nikon Instruments, Japan).

2.8. Measurement of Intracellular ROS Level. B1647 cells were treated with 5 or 10 μ M SFN for 24 h and, when specified, with 1 μ M plumbagin for 30 min. To evaluate intracellular ROS level, 1×10^6 cells/mL were washed twice in HBSS and incubated for 20 min with 5 μ M DCFH-DA at 37°C. DCFH-DA is a small, nonpolar, and nonfluorescent molecule that passes through the cell membrane into the cells by diffusion; in the cytosol, it is enzymatically deacetylated by intracellular esterases to a polar nonfluorescent compound, which is oxidised by intracellular ROS to the highly green fluorescent 2,7-dichlorofluorescein (DCF). DCF fluorescence was measured using a multiwell plate reader (Wallac Victor2, PerkinElmer). Excitation wavelength was 485 nm, and emission wavelength was 535 nm. Fluorescence values were reported as the percentage of intracellular ROS in respect to controls.

2.9. Immunoprecipitation. Control or SFN-treated B1647 cells (1×10^6 cells/mL) were lysed as described above. Lysates containing equal protein amounts were incubated overnight with anti-AQP8 antibody. Then, samples were incubated with protein G-agarose for 1.5 h at 4°C and pelleted at 12,000 \times g for 30 min. Pellets were washed 5 times with buffer (pH=8) and centrifuged at 12,000 \times g for 5 min. Samples were subjected to SDS-PAGE and Western blotting analysis with anti-Nox2 as described above. Bands were acquired with a CCD imager (ChemiDoc™ MP System, Bio-Rad Laboratories), and relative densitometric analysis were performed by using Image Lab analysis software (Bio-Rad Laboratories).

2.10. Statistical Analysis. Each experiment was performed at least three times, and all values are represented as means \pm SD. One-way ANOVA was used to compare differences among groups followed by Bonferroni's test (Prism 5; Graph-Pad Software). Values of $p < 0.05$ were considered as statistically significant.

3. Results

It has been reported that SFN is able to selectively exert cytotoxic effects in many human cancer cells without affecting

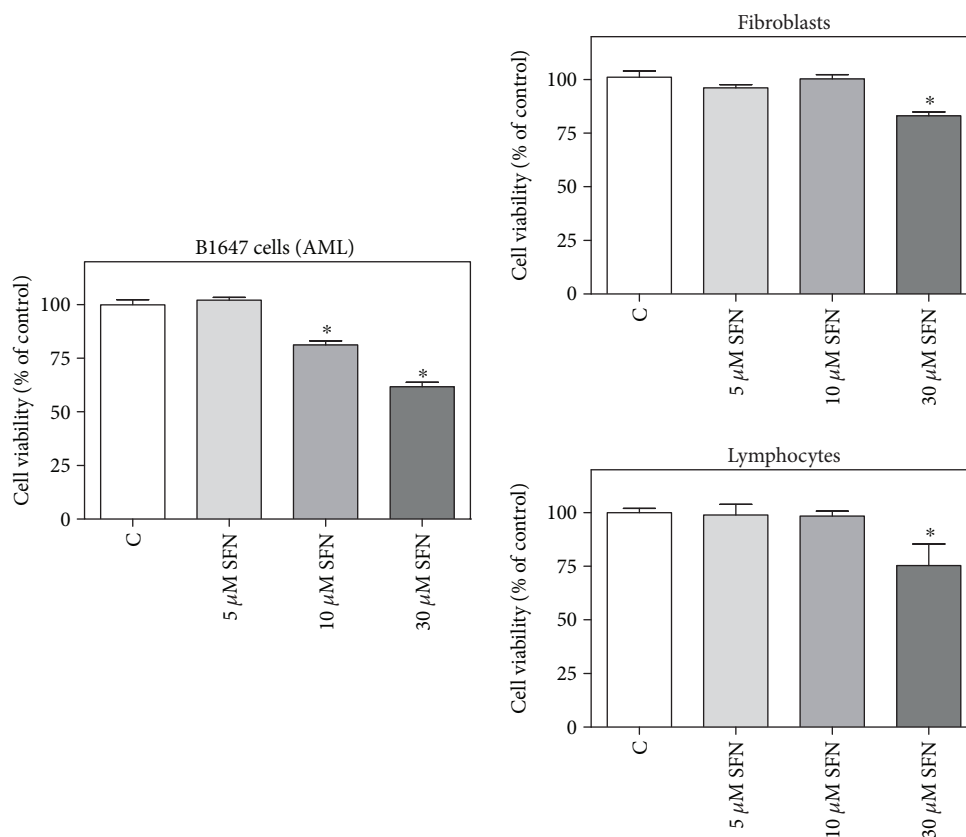


FIGURE 1: Effect of SFN on the viability of transformed and nontransformed human cells. B1647 cells, human lymphocytes or fibroblasts were incubated for 24 h with increasing SFN concentrations. Viability was evaluated by MTT test, as reported in Materials and Methods section. Results are expressed as means \pm SD of three independent experiments. Statistical analysis was performed by Bonferroni multiple comparison test following one-way ANOVA. * $p < 0.05$, significantly different from control cells.

normal cells [8]. On these bases, leukemia B1647 cells and human lymphocytes or fibroblasts, chosen as model of non-transformed cells, were incubated with increasing SFN concentrations, and cell viability was evaluated by MTT assay (Figure 1). Both 10 and 30 μ M SFN showed cytotoxic effects in B1647, as cell viability was significantly lower compared to control cells. In human lymphocytes and fibroblasts, 30 μ M SFN significantly reduced cell viability; meanwhile, 10 μ M SFN did not show any cytotoxic effect. Therefore, SFN concentrations below or at least the same as 10 μ M were used in the subsequent experiments.

To investigate the mechanism underpinning the observed cytotoxic effect of SFN in B1647 cells, we evaluated AQP8 expression after SFN treatment, as we hypothesized that SFN could impair the cellular redox status affecting H_2O_2 transport through AQP8 channel. In order to verify this hypothesis, B1647 cells were treated with different SFN concentrations for 24 h, and the expression of AQP8 was evaluated by RT-PCR (Figure 2(a)) and Western blot (Figure 2(b)) analyses.

Results show that AQP8 was significantly decreased both at transcriptional and protein level upon cell treatment with 10 μ M SFN, whereas 1 or 5 μ M SFN did not cause any significant change.

To corroborate these findings, B1647 cells were treated with 10 μ M SFN, then AQP8 content in plasma membrane

was evaluated using an immune-fluorescence technique and visualized through confocal microscopy (Figure 3).

As expected, SFN treatment strongly reduced green fluorescence in B1647 plasma membrane, confirming the ability of SFN to reduce AQP8 level, in agreement with RT-PCR and Western blot data.

Since SFN decreases AQP8 level, it is reasonable that a smaller amount of H_2O_2 is transported into the cell. To investigate this aspect, B1647 cells were incubated for 24 h with increasing SFN concentrations and then assayed for ROS level by using the fluorescent DCF probe. Results in Figure 4 show that only 10 μ M SFN treatment causes a significant decrease of ROS intracellular levels in respect to control cells, according to previous observations.

To better elucidate the mechanisms behind SFN ability to reduce ROS intracellular level, we investigated SFN influence on the sources of H_2O_2 present in B1647 cells. To this regard, we have previously demonstrated that the main sources of H_2O_2 in B1647 cell line are Nox2 and Nox4 isoforms [19]. Nox-derived ROS are involved in early signalling events, such as the auto-phosphorylation of VEGFR-2 leading to downstream events, including the maintenance of the active phosphorylated form of Akt [20]. Therefore, the possible effect of SFN on Nox isoforms expression and the phosphorylation level of VEGFR-2 and Akt were investigated in B1647 cell line (Figure 5).

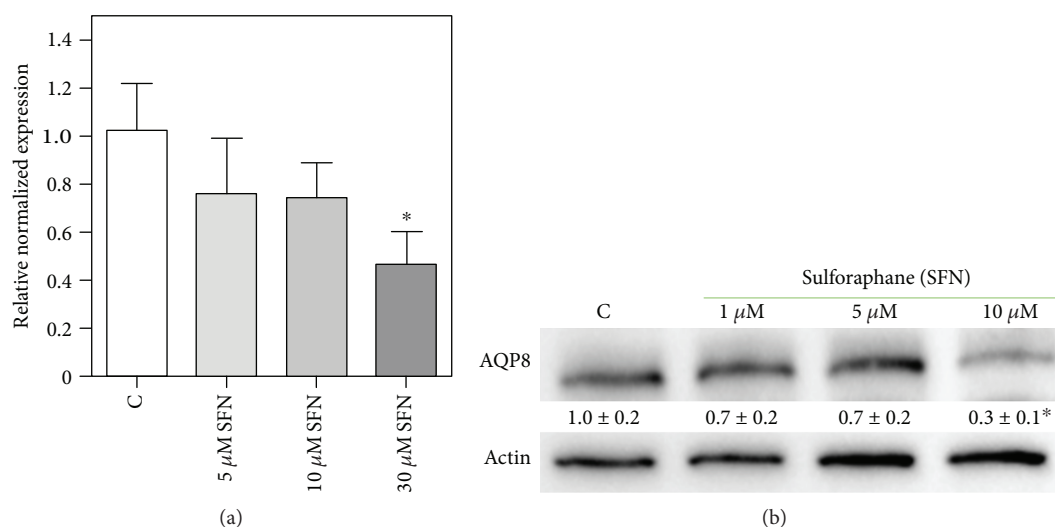


FIGURE 2: Effect of SFN on AQP8 expression in B1647 cell line. B1647 cells were incubated for 24 h with different SFN concentrations and (a) RNA was extracted from the cells and samples subjected to RT-PCR analysis using specific primers as described in Materials and Methods section. Normalized expression levels were calculated relative to control cells according to the $2^{-\Delta\Delta C_q}$ method; (b) proteins were extracted, separated by SDS-PAGE, transferred to nitrocellulose membrane, and immunoassayed using anti-AQP8 and anti- β -actin antibodies as reported in Materials and Methods section. Immunoblot is the representative of three independent experiments, and densitometric analysis, normalized to β -actin, is expressed as fold decrease with respect to control. * $p < 0.05$, significantly different from control cells.

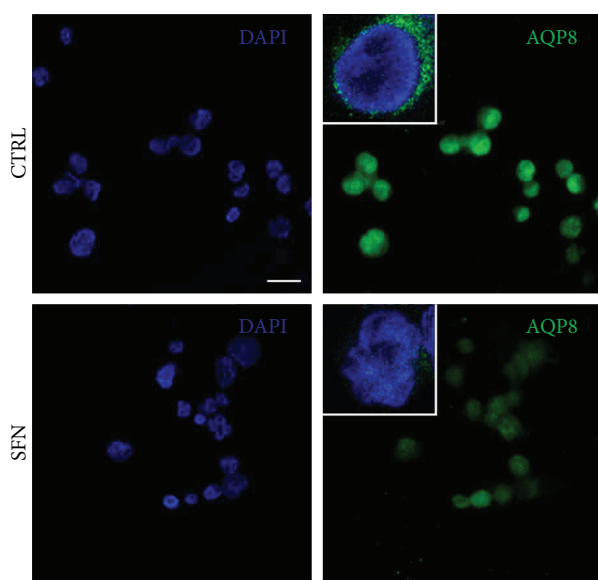


FIGURE 3: Effect of SFN on AQP8 content in plasma membrane of B1647 cell line. Representative confocal images of B1647 cells treated (SFN) or not (CTRL) with 10 μM sulforaphane for 24 h and labelled with DAPI (blue) and anti-aquaporin 8, AQP8, (green). Cells were not permeabilized in order to exclude intracellular signals. Scale bar = 10 μm. Triple magnification of representative superimposed 3 central slices is shown in white squares. Images were acquired by Nikon A1 confocal laser scanning microscope (Nikon Instruments, Japan). The results are the representative of two independent experiments.

Western blot analysis reveals that, when treated with 10 μM SFN, B1647 cells express Nox2 to a lesser extent than controls and exhibit a diminished phosphorylation level of both VEGFR-2 and Akt. On the other hand, the amount of

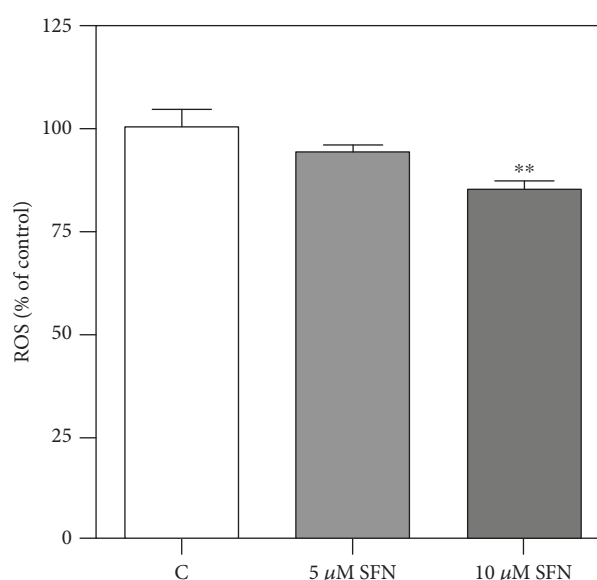


FIGURE 4: Effect of SFN on intracellular ROS level in B1647 cell line. B1647 cells were incubated for 24 h with different SFN concentrations. Intracellular ROS level was evaluated as DCF fluorescence as reported in Materials and Methods section. Data are expressed as % of control and represent means \pm SD of at least three independent experiments. Data were analysed by one-way ANOVA followed by Bonferroni's test. ** $p < 0.01$, significantly different from control cells.

Nox4 was significantly increased. This result could explain the slight decrease in the level of intracellular ROS observed upon SFN treatment. To better appreciate SFN effect on Nox2, Nox4 isoform was inhibited by plumbagin, a Nox4 inhibitor [31], or by silencing with siRNA against Nox4.

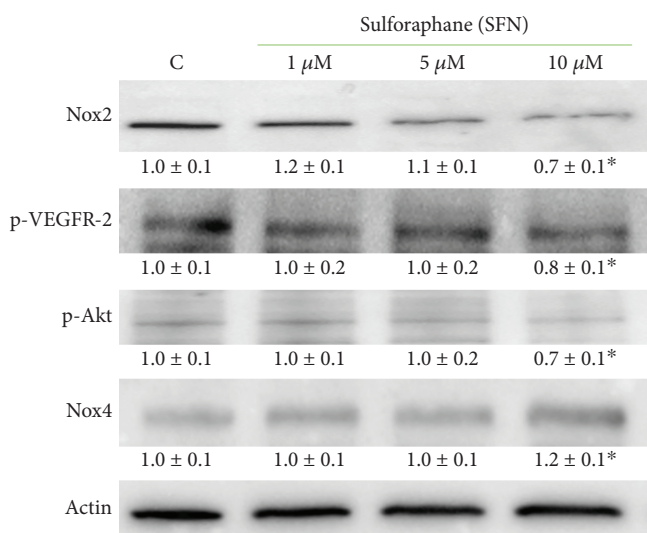


FIGURE 5: Effect of SFN on Nox2 and Nox4 expression and phosphorylation level of VEGFR-2 and Akt in B1647 cell line. B1647 cells were incubated for 24h with different SFN concentrations. At the end of incubation, cells were lysed, and proteins were separated by SDS-PAGE, transferred to nitrocellulose membrane, and immunoassayed using specific antibodies as reported in Materials and Methods section. Immunoblots are the representative of three independent experiments, and densitometric analysis, normalized to β -actin, is expressed as fold decrease with respect to control. * $p < 0.05$, significantly different from control cells.

Figure 6 shows the evaluation of intracellular ROS level in the presence of plumbagin (Figure 6(a)) or after specific Nox4 silencing (Figure 6(b)). Interestingly, SFN treatment led to a more pronounced reduction of intracellular ROS content when Nox4 was inhibited or silenced.

It has been recently reported that aquaporins can have protein interaction partners [31]; therefore, the possible interaction between AQP8 and Nox2, the main ROS source in B1647 cells, was investigated by immunoprecipitation technique. Results in Figure 7 show that Nox2 coprecipitates with AQP8, indicating a strong link between these two proteins. As expected, upon the 10 μ M SFN treatment, the band corresponding to Nox2 significantly lost intensity, according to the decreasing SFN effect on AQP8 and Nox2 expression. To corroborate this result, the “*vice-versa*” immunoprecipitation was performed, i.e., IP for Nox2 and WB for AQP8, and also, in this case, the coprecipitation of the two proteins was observed (not shown).

Peroxiredoxins (Prxs) have catalytic cysteines exhibiting great susceptibility to oxidation by hydrogen peroxide [32]; therefore, they are important regulators of peroxide-dependent signalling pathways. Furthermore, Prxs have been found to be elevated in many human cancer cells and tissues, where they enhance the aggressive survival phenotype and confer increased resistance to chemo- and radio-therapy [33]. In order to ascertain whether SFN could affect Prx-1 expression, B1647 cells were incubated with SFN for 24h, then subjected to Western blot analysis, as reported in Figure 8.

The results show that the cell treatment with 10 μ M SFN for 24 h significantly decreased Prx-1 expression.

4. Discussion

In a previous study carried out in B1647 cell line, we have demonstrated that AQP8 expression modulates the amplitude of the downstream VEGF signalling, which proceeds through the involvement of Nox-produced H_2O_2 as a second messenger [25]. Thus, this AQP isoform has gained an important role as a fine level regulator in the transduction of the redox signal. It has been reported that living cells can regulate the permeability of AQP8 to H_2O_2 and water through a temporary modification of functional cysteines, particularly during cell stress conditions [34, 35]. It seems of great interest the identification of molecules able to modulate the activity and/or expression of AQP8 isoform in order to influence the cellular response. In particular, the attention points toward the identification of natural products or food-derived molecules to be used as chemopreventive agents. On these premises, we investigated the potential effect of the isothiocyanate SFN on the modulation of AQP8 and Nox expression in the leukemic B1647 cell line. As a result of many *in vivo* and *in vitro* studies, it was stated that SFN is able to selectively exert cytotoxic effects in various human cancer cells, while having no cytotoxic effects, or being even cytoprotective in normal cells [5, 8]. The treatment of HL-60 cells with increasing concentrations of SFN (0–100 μ M) was reported to induce a dose-dependent decrease in cell viability, with a IC_{50} value determined as 49.5 μ M [36]; in pre-B ALL (acute lymphoblastic leukemia) and T-ALL cell lines, it was observed that SFN induce cytotoxicity at concentration ranging from 4 to 10 μ M in contrast to 90 μ M for nonleukemic controls [37]. These data evidence that high SFN concentrations are needed to exert cytotoxic effects on normal cells, whereas low concentrations provoke a selective effect on transformed cells. Our data show that 30 μ M SFN significantly reduced the viability of both leukemic and normal cells, while 10 μ M exerted a cytotoxic effect only in cancer cells. Therefore, SFN concentrations below or equal to 10 μ M were used in all the experiments. Interestingly, concentrations of similar order of magnitude can be really achieved in human plasma through dietary intake of cruciferous vegetables. Since it has been estimated that 40 g of fresh broccoli sprouts yield a transient serum level of SFN of about 2 μ mol/L [38], a serving of 200 g of broccoli can provide the desired SFN plasma level of about 10 μ mol/L.

As our results show that SFN is able to downregulate AQP8 expression, we can speculate that the lower level of intracellular ROS we measured by DCFH-DA is due to a smaller amount of H_2O_2 transported into the cell. DCFH-DA is not specific for H_2O_2 but reacts with all oxidants present in biological systems [39, 40]. However, in a previous paper of us, reporting data performed in the same leukemic cell line, i.e., B1647, we measured the intracellular ROS level with both DCFH-DA and PF1, a boronate dye more selective for H_2O_2 than DCFH-DA, obtaining similar results [24]. Furthermore, in the subsequent paper, we detected the intracellular thiol redox state of B1647 cells with a dimedone

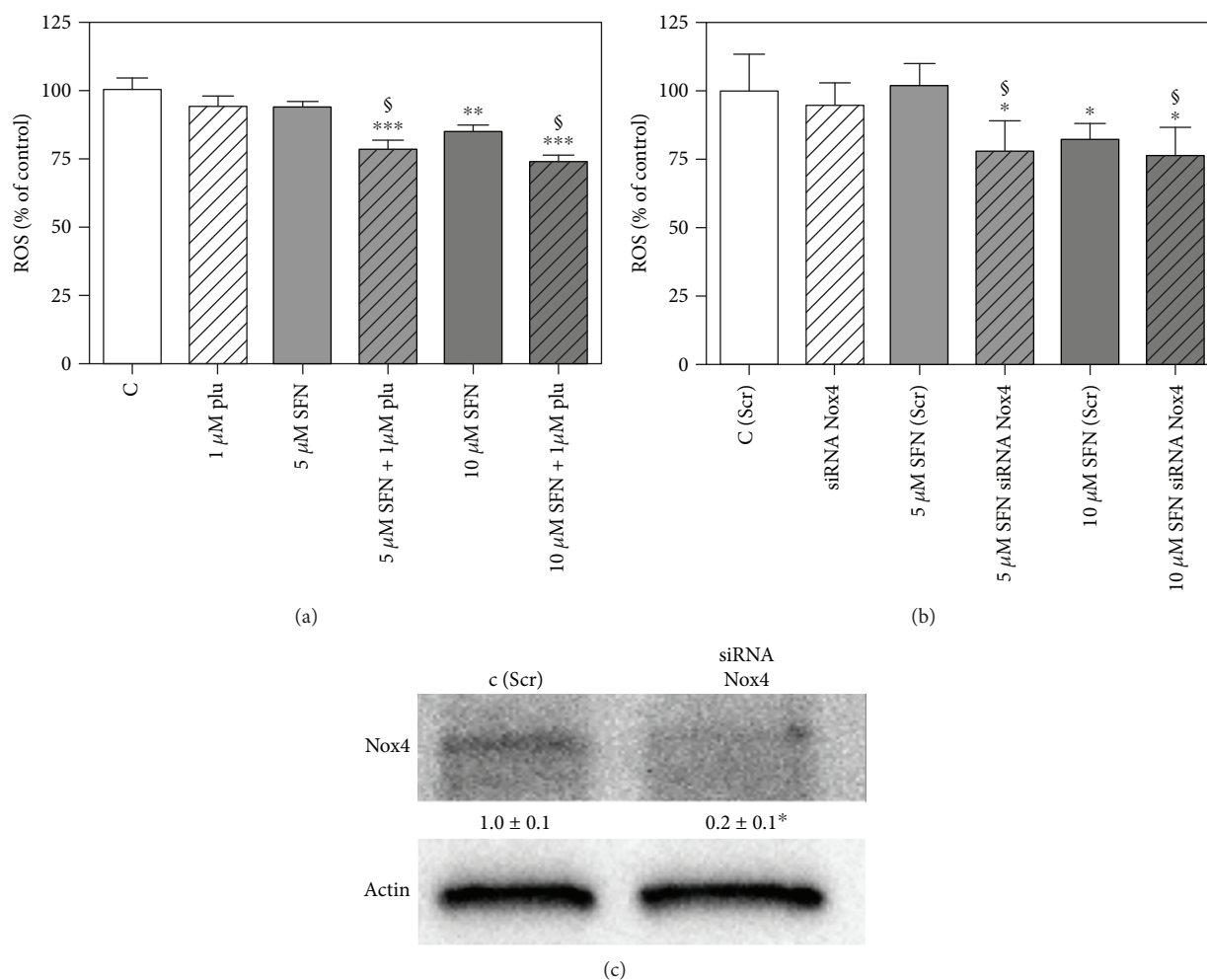


FIGURE 6: Effect of SFN on intracellular ROS level in B1647 cell line after Nox4 inhibition or silencing. (a) B1647 cells were incubated for 24 h with different SFN concentrations, then treated or not with 1 μ M plumbagin for 30 min. (b) B1647 cells were transfected with specific siRNA against Nox4 or a random RNA sequence (scrambled) as negative control, C (Scr). 24 h after transfection with siRNA, B1647 cells were incubated for 24 h with different SFN concentrations. Intracellular ROS level was then evaluated as DCF fluorescence as reported in Materials and Methods section. Data are expressed as % of control and represent means \pm SD of three independent experiments. Data were analysed by one-way ANOVA followed by Bonferroni's test. *** p < 0.001; ** p < 0.01; * p < 0.05, significantly different from relative control cells. § p < 0.05, significantly different from the corresponding bars in the absence of plumbagin (a) or in Nox4-silenced cells (b). (c) B1647 cells were transfected by electroporation with siRNA against Nox4 or a random RNA sequence (scrambled) as negative control. Effect of RNA interference of Nox4 was confirmed by Western blot analysis with specific antibodies against Nox4.

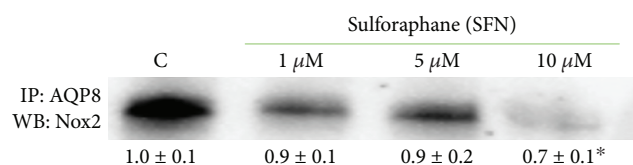


FIGURE 7: Effect of SFN on the interaction between AQP8 and Nox2 in B1647 cell line. B1647 cells were incubated for 24 h with different SFN concentrations. At the end of incubation, cells were subjected to immunoprecipitation with anti-AQP8. Proteins were then extracted, separated by SDS-PAGE, immunoblotted, and revealed for anti-Nox2 as described in Materials and Methods section. Immunoblot is the representative of three independent experiments, and densitometric analysis is expressed as fold decrease with respect to control. * p < 0.05, significantly different from control cells.

method, which is able to react with cysteine sulfenic acid, which is formed upon H_2O_2 action as a signalling molecule. We observed a linear correlation between the protein thiol redox state and the applied stimulus, i.e., H_2O_2 10–100 μ M. This technique allowed us to demonstrate that the amplitude of intracellular cysteine oxidation is dependent on AQP8 expression level, which modulates the amount of H_2O_2 that is able to reach its intracellular targets [25].

The decrease of Nox2 expression observed in this study is, in part, counterbalanced by a significant increase in Nox4 expression. Indeed, we have previously demonstrated that B1647 cell line expresses Nox2 and the constitutively active Nox4, but not other isoforms [19]. It could be argued that cell undergoing SFN treatment might deploy mechanisms to counteract the limited H_2O_2 production (by Nox2) and transport (by AQP8) through the strengthening

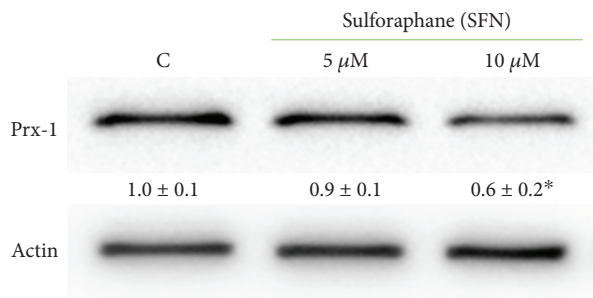


FIGURE 8: Effect of SFN on peroxiredoxin-1 (Prx-1) in B1647 cell line. B1647 cells were incubated with 5 or 10 μ M SFN for 24 h. At the end of incubation, cells were lysed, and proteins were separated by SDS-PAGE, immunoblotted, and revealed for anti-Prx-1 as reported in Materials and Methods section. Immunoblot is the representative of three independent experiments, and densitometric analysis, normalized to β -actin, is expressed as fold decrease with respect to control. * $p < 0.05$, significantly different from control cells.

of Nox4 expression. Blocking Nox4 activity by the inhibitor plumbagin or knocking down this isoform by specific Nox4 silencing led to a more pronounced SFN effect on intracellular ROS content (Figure 6). In this condition, Nox2 remains the main ROS source in B1647 cells, and SFN effect can be better appreciated. Although it was reported that 10 μ M plumbagin greatly inhibited Nox4 activity in HEK293 and LN229 cells [41], in our conditions, this plumbagin concentration markedly decreased B1647 cell viability (data not shown), and therefore, we used 1 μ M plumbagin, according to Guida and coworkers [42].

By using a coimmunoprecipitation technique, we also demonstrated that Nox2 and AQP8 are linked to each other, confirming the existence of a Nox2-AQP8 axis in B1647 cell line. The evidence of the interaction between AQP8 and Nox2 supports the importance of these two partners in the redox signalling cascade. The activity of Nox2-AQP8 axis is also a determinant in B cell activation and differentiation [27]. Many isoforms of aquaporins have protein-protein interactions, specifically found for AQP0, AQP2, AQP4, and AQP5 [31]. The characteristics of these interaction partners are strikingly different, but they generally influence the translocation, trafficking, internalization, or phosphorylation of AQP isoforms. B1647 is a self-producing VEGF cell line, which is subjected to continuous VEGF signalling; therefore, the axis Nox2-AQP8 has a central role in modulating the downstream events supporting their viability and proliferation. This distinctive feature of these cells could explain the observed SFN-induced intracellular ROS decrease. Although other reports, obtained in different cell types, demonstrate a SFN-induced ROS increase [43–45], it has been shown that SFN inhibits VEGF expression [8, 9], which is strictly linked to Nox activation. Therefore, VEGF inhibition coupled with SFN-induced decrease of both Nox2 and AQP8 expression may contribute to the observed decrease in intracellular ROS level in B1647 cell line. Moreover, SFN is known to induce changes in the intracellular redox state, and, depending on its concentration, exposure

time, or cell type, it may promote antioxidant or prooxidant response. From the data of the literature, it can be summarized that a predominantly antioxidant response has been reported at low SFN concentration, i.e., up to 5 μ M SFN for up to 24 h, which is close to our conditions, whereas higher SFN concentrations and long-lasting exposure periods produce a prooxidant effect [45, 46].

The ability of SFN to interfere with the redox signalling is confirmed also by its effect on VEGFR-2 and Akt phosphorylation status, which is significantly reduced in SFN-treated cells. The decreased amount of p-VEGFR-2 was an expected result, since ROS source involved in VEGFR-2 activation has been identified in Nox activity [20]. The smaller amount of p-Akt observed in SFN-treated cells indicates that this isothiocyanate exerts its action also on the downstream H_2O_2 targets, among which Akt represents a key enzyme controlling many hallmarks of cancer. Indeed, the active phosphorylated form of this enzyme plays a pivotal role in tumour cell survival, proliferation, and invasiveness [47].

Prxs are abundant thiol-dependent peroxidases highly efficient at reducing hydrogen peroxide, peroxynitrite, and other hydroperoxides [48]. Due to their high reactivity and abundance, Prxs will be the major targets of intracellular hydrogen peroxide [49] and, therefore, important regulators of peroxide-dependent signalling pathways [50]. Besides their antioxidant activity, recently, evidence indicates that Prxs have a significant influence on the development and progression of cancer. Prx-knock-out mice often exhibit increased carcinogenesis, whereas elevated Prx expression is commonly observed in human tumours [49]. In leukemia cells, Prxs display variable expression, suggesting difference in functional significance depending on the cellular context [51]. In particular, a proteomic analysis has demonstrated that Prxs are significantly increased in almost all acute myeloid leukemia (AML) subtypes; thus, they were proposed as potential targets for AML patients [52]. Our results show that B1647 cell line expresses Prx-1, which is significantly reduced upon SFN treatment, indicating an additional protective role of this isothiocyanate against malignancy. However, further studies are needed to elucidate a definitive role for Prx family in leukemia.

5. Conclusions

The data reported here show that SFN downregulates AQP8 and Nox2 expression in B1647 cell line, limiting both H_2O_2 production and entry into the cells. Consequently, the amount of hydrogen peroxide able to reach its intracellular targets is decreased, and leukemia cell viability significantly reduced. Indeed, by decreasing the effect of Nox2-AQP8 axis, SFN causes profound effects on the transduction of the redox signalling and, consequently, on cell survival and proliferation, opening the way to unforeseen opportunities in the fighting of acute myeloid leukemia. Of note, SFN concentrations able to trigger these effects are comparable to plasma concentrations measured after cruciferous vegetables dietary intake.

Abbreviations

SFN:	Sulforaphane
AQP8:	Aquaporin-8
VEGF:	Vascular endothelial growth factor
VEGFR-2:	Vascular endothelial growth factor receptor-2
Nox:	NAD(P)H oxidase
Prx:	Peroxiredoxin.

Data Availability

The data used to support the findings of this study are available from the corresponding author upon request.

Disclosure

The funders had no role in study design, data collection and analysis, decision to publish, or paper preparation.

Conflicts of Interest

The authors declare that no conflict of interest and no competing financial interest exist.

Acknowledgments

The authors would like to thank Professor Laura Bonsi who kindly provided B1647 cell line used in this study. This work was supported by grants from Italian Ministry of Education, University and Research (MIUR) and from Fondazione del Monte di Bologna e Ravenna, Italy.

References

- [1] A. K. Singh, N. Sharma, M. Ghosh, Y. H. Park, and D. K. Jeong, "Emerging importance of dietary phytochemicals in fight against cancer: role in targeting cancer stem cells," *Critical Reviews in Food Science and Nutrition*, vol. 57, no. 16, pp. 3449–3463, 2016.
- [2] M. Lenzi, C. Fimognari, and P. Hrelia, "Sulforaphane as a promising molecule for fighting cancer," *Cancer Treatment and Research*, vol. 159, pp. 207–223, 2014.
- [3] C. Angeloni, E. Leoncini, M. Malaguti, S. Angelini, P. Hrelia, and S. Hrelia, "Modulation of phase II enzymes by sulforaphane: implications for its cardioprotective potential," *Journal of Agricultural and Food Chemistry*, vol. 57, no. 12, pp. 5615–5622, 2009.
- [4] A. Tarozzi, C. Angeloni, M. Malaguti, F. Morroni, S. Hrelia, and P. Hrelia, "Sulforaphane as a potential protective phytochemical against neurodegenerative diseases," *Oxidative Medicine and Cellular Longevity*, vol. 2013, Article ID 415078, 10 pages, 2013.
- [5] A. Briones-Herrera, D. Eugenio-Pérez, J. G. Reyes-Ocampo, S. Rivera-Mancía, and J. Pedraza-Chaverri, "New highlights on the health-improving effects of sulforaphane," *Food & Function*, vol. 9, no. 5, pp. 2589–2606, 2018.
- [6] S. Langouët, L. L. Furge, N. Kerriguy, K. Nakamura, A. Guillouzo, and F. P. Guengerich, "Inhibition of human cytochrome P 450 enzymes by 1, 2-dithiole-3-thione, oltipraz and its derivatives, and sulforaphane," *Chemical Research in Toxicology*, vol. 13, no. 4, pp. 245–252, 2000.
- [7] M.-K. Kwak, N. Wakabayashi, and T. W. Kensler, "Chemoprevention through the Keap1–Nrf 2 signaling pathway by phase 2 enzyme inducers," *Mutation Research/Fundamental and Molecular Mechanisms of Mutagenesis*, vol. 555, no. 1–2, pp. 133–148, 2004.
- [8] R. Bayat Mokhtari, N. Baluch, T. S. Homayouni et al., "The role of Sulforaphane in cancer chemoprevention and health benefits: a mini-review," *Journal of Cell Communication and Signaling*, vol. 12, no. 1, pp. 91–101, 2018.
- [9] E. Bertl, H. Bartsch, and C. Gerhauser, "Inhibition of angiogenesis and endothelial cell functions are novel sulforaphane-mediated mechanisms in chemoprevention," *Molecular Cancer Therapeutics*, vol. 5, no. 3, pp. 575–585, 2006.
- [10] D. H. Kim, B. Sung, Y. Kang et al., "Sulforaphane inhibits hypoxia-induced HIF-1 α and VEGF expression and migration of human colon cancer cells," *International Journal of Oncology*, vol. 47, no. 6, pp. 2226–2232, 2015.
- [11] H. G. Jee, K. E. Lee, J. B. Kim, H. K. Shin, and Y. K. Youn, "Sulforaphane inhibits oral carcinoma cell migration and invasion in vitro," *Phytotherapy Research*, vol. 25, no. 11, pp. 1623–1628, 2011.
- [12] C.-S. Lee, H. Cho, Y. Jeong et al., "Isothiocyanates inhibit the invasion and migration of C6 glioma cells by blocking FAK/JNK-mediated MMP-9 expression," *Oncology Reports*, vol. 34, no. 6, pp. 2901–2908, 2015.
- [13] C. Fimognari, E. Turrini, P. Sestili et al., "Antileukemic activity of sulforaphane in primary blasts from patients affected by myelo- and lympho-proliferative disorders and in hypoxic conditions," *PLoS One*, vol. 9, no. 7, article e101991, 2014.
- [14] D. O. Moon, M. O. Kim, S. H. Kang, Y. H. Choi, and G. Y. Kim, "Sulforaphane suppresses TNF- α -mediated activation of NF- κ B and induces apoptosis through activation of reactive oxygen species-dependent caspase-3," *Cancer Letters*, vol. 274, no. 1, pp. 132–142, 2009.
- [15] H. S. Shang, Y. L. Shih, C. H. Lee et al., "Sulforaphane-induced apoptosis in human leukemia HL-60 cells through extrinsic and intrinsic signal pathways and altering associated genes expression assayed by cDNA microarray," *Environmental Toxicology*, vol. 32, no. 1, pp. 311–328, 2017.
- [16] K. Suppipat, C. S. Park, Y. Shen, X. Zhu, and H. D. Lacorazza, "Sulforaphane induces cell cycle arrest and apoptosis in acute lymphoblastic leukemia cells," *PLoS One*, vol. 7, no. 12, article e51251, 2012.
- [17] J. Jakubikova, Y. Bao, and J. Sedlak, "Isothiocyanates induce cell cycle arrest, apoptosis and mitochondrial potential depolarization in HL-60 and multidrug-resistant cell lines," *Anti-cancer Research*, vol. 25, no. 5, pp. 3375–3386, 2005.
- [18] L. Bonsi, L. Pierdomenico, M. Biscardi et al., "Constitutive and stimulated production of VEGF by human megakaryoblastic cell lines: effect on proliferation and signaling pathway," *International Journal of Immunopathology and Pharmacology*, vol. 18, no. 3, pp. 445–455, 2005.
- [19] C. Prata, T. Maraldi, D. Fiorentini, L. Zambonin, G. Hakim, and L. Landi, "Nox-generated ROS modulate glucose uptake in a leukaemic cell line," *Free Radical Research*, vol. 42, no. 5, pp. 405–414, 2009.
- [20] T. Maraldi, C. Prata, C. Caliceti et al., "VEGF-induced ROS generation from NAD(P)H oxidases protects human leukemic cells from apoptosis," *International Journal of Oncology*, vol. 36, no. 6, pp. 1581–1589, 2010.

- [21] C. Caliceti, L. Zamboni, B. Rizzo et al., "Role of plasma membrane caveolae/lipid rafts in VEGF-induced redox signaling in human leukemia cells," *BioMed Research International*, vol. 2014, Article ID 857504, 13 pages, 2014.
- [22] G. P. Bienert, J. K. Schjoerring, and T. P. Jahn, "Membrane transport of hydrogen peroxide," *Biochimica et Biophysica Acta (BBA) - Biomembranes*, vol. 1758, no. 8, pp. 994–1003, 2006.
- [23] G. P. Bienert, A. L. B. Møller, K. A. Kristiansen et al., "Specific aquaporins facilitate the diffusion of hydrogen peroxide across membranes," *The Journal of Biological Chemistry*, vol. 282, no. 2, pp. 1183–1192, 2007.
- [24] F. Vieceli Dalla Sega, L. Zamboni, D. Fiorentini et al., "Specific aquaporins facilitate Nox-produced hydrogen peroxide transport through plasma membrane in leukaemia cells," *Biochimica et Biophysica Acta (BBA) - Molecular Cell Research*, vol. 1843, no. 4, pp. 806–814, 2014.
- [25] F. Vieceli Dalla Sega, C. Prata, L. Zamboni et al., "Intracellular cysteine oxidation is modulated by aquaporin-8-mediated hydrogen peroxide channeling in leukaemia cells," *BioFactors*, vol. 43, no. 2, pp. 232–242, 2016.
- [26] M. Bertolotti, S. Bestetti, J. M. García-Manteiga et al., "Tyrosine kinase signal modulation: a matter of H₂O₂ membrane permeability?," *Antioxidants & Redox Signaling*, vol. 19, no. 13, pp. 1447–1451, 2013.
- [27] M. Bertolotti, G. Farinelli, M. Galli, A. Aiuti, and R. Sitia, "AQP8 transports NOX2-generated H₂O₂ across the plasma membrane to promote signaling in B cells," *Journal of Leukocyte Biology*, vol. 100, no. 5, pp. 1071–1079, 2016.
- [28] D. Ribatti, G. Ranieri, T. Annese, and B. Nico, "Aquaporins in cancer," *Biochimica et Biophysica Acta (BBA) - General Subjects*, vol. 1840, no. 5, pp. 1550–1553, 2014.
- [29] A. S. Verkman, M. Hara-Chikuma, and M. C. Papadopoulos, "Aquaporins—new players in cancer biology," *Journal of Molecular Medicine*, vol. 86, no. 5, pp. 523–529, 2008.
- [30] M. C. Papadopoulos and S. Saadoun, "Key roles of aquaporins in tumor biology," *Biochimica et Biophysica Acta (BBA) - Biomembranes*, vol. 1848, no. 10, pp. 2576–2583, 2015.
- [31] J. Sjöhamn and K. Hedfalk, "Unraveling aquaporin interaction partners," *Biochimica et Biophysica Acta (BBA) - General Subjects*, vol. 1840, no. 5, pp. 1614–1623, 2014.
- [32] S. G. Rhee, H. A. Woo, and D. Kang, "The role of peroxiredoxins in the transduction of H₂O₂ signals," *Antioxidants & Redox Signaling*, vol. 28, no. 7, pp. 537–557, 2018.
- [33] Y. Zhang, "Cancer-preventive isothiocyanates: measurement of human exposure and mechanism of action," *Mutation Research*, vol. 555, no. 1-2, pp. 173–190, 2004.
- [34] I. Medraño-Fernandez, S. Bestetti, M. Bertolotti et al., "Stress regulates aquaporin-8 permeability to impact cell growth and survival," *Antioxidants & Redox Signaling*, vol. 24, no. 18, pp. 1031–1044, 2016.
- [35] S. Bestetti, I. Medraño-Fernandez, M. Galli et al., "A persulfidation-based mechanism controls aquaporin-8 conductance," *Science Advances*, vol. 4, no. 5, article eaar5770, 2018.
- [36] C. Fimognari, M. Lenzi, G. Cantelli-Forti, and P. Hrelia, "Induction of differentiation in human promyelocytic cells by the isothiocyanate sulforaphane," *In Vivo*, vol. 22, no. 3, pp. 317–320, 2008.
- [37] K. Suppipat and H. Lacorazza, "From the table to the bedside: can food-derived sulforaphane be used as a novel agent to treat leukemia?," *Current Cancer Drug Targets*, vol. 14, no. 5, pp. 434–445, 2014.
- [38] J. D. Clarke, A. Hsu, K. Riedl et al., "Bioavailability and inter-conversion of sulforaphane and erucin in human subjects consuming broccoli sprouts or broccoli supplement in a cross-over study design," *Pharmacological Research*, vol. 64, no. 5, pp. 456–463, 2011.
- [39] H. Maeda, Y. Fukuyasu, S. Yoshida et al., "Fluorescent probes for hydrogen peroxide based on a non-oxidative mechanism," *Angewandte Chemie International Edition*, vol. 43, no. 18, pp. 2389–2391, 2004.
- [40] B. Kalyanaraman, V. Darley-Usmar, K. J. A. Davies et al., "Measuring reactive oxygen and nitrogen species with fluorescent probes: challenges and limitations," *Free Radical Biology & Medicine*, vol. 52, no. 1, pp. 1–6, 2012.
- [41] Y. Ding, Z. J. Chen, S. Liu, D. Che, M. Vetter, and C. H. Chang, "Inhibition of Nox-4 activity by plumbagin, a plant-derived bioactive naphthoquinone," *The Journal of Pharmacy and Pharmacology*, vol. 57, no. 1, pp. 111–116, 2005.
- [42] M. Guida, T. Maraldi, E. Resca et al., "Inhibition of nuclear Nox4 activity by plumbagin: effect on proliferative capacity in human amniotic stem cells," *Oxidative Medicine and Cellular Longevity*, vol. 2013, Article ID 680816, 12 pages, 2013.
- [43] Z. Miao, F. Yu, Y. Ren, and J. Yang, "d,l-Sulforaphane induces ROS-dependent apoptosis in human glioblastoma cells by inactivating STAT3 signaling pathway," *International Journal of Molecular Sciences*, vol. 18, no. 1, 2017.
- [44] P. J. Amin and B. S. Shankar, "Sulforaphane induces ROS mediated induction of NKG2D ligands in human cancer cell lines and enhances susceptibility to NK cell mediated lysis," *Life Sciences*, vol. 126, pp. 19–27, 2015.
- [45] J. M. P. Ferreira de Oliveira, M. Costa, T. Pedrosa et al., "Sulforaphane induces oxidative stress and death by p53-independent mechanism: implication of impaired glutathione recycling," *PLoS One*, vol. 9, no. 3, article e92980, 2014.
- [46] I. Misiewicz, K. Skupinska, and T. Kasprzycka-Guttman, "Differential response of human healthy lymphoblastoid and CCRF-SB leukemia cells to sulforaphane and its two analogues: 2-oxohexyl isothiocyanate and allysin," *Pharmacological Reports*, vol. 59, no. 1, pp. 80–87, 2007.
- [47] N. Koundouros and G. Poulogiannis, "Phosphoinositide 3-kinase/Akt signaling and redox metabolism in cancer," *Frontiers in Oncology*, vol. 8, 2018.
- [48] Z. A. Wood, E. Schröder, J. Robin Harris, and L. B. Poole, "Structure, mechanism and regulation of peroxiredoxins," *Trends in Biochemical Sciences*, vol. 28, no. 1, pp. 32–40, 2003.
- [49] M. B. Hampton, K. A. Vick, J. J. Skoko, and C. A. Neumann, "Peroxiredoxin involvement in the initiation and progression of human cancer," *Antioxidants & Redox Signaling*, vol. 28, no. 7, pp. 591–608, 2018.
- [50] C. C. Winterbourn and M. B. Hampton, "Thiol chemistry and specificity in redox signaling," *Free Radical Biology & Medicine*, vol. 45, no. 5, pp. 549–561, 2008.
- [51] M. E. Irwin, N. Rivera-del Valle, and J. Chandra, "Redox control of leukemia: from molecular mechanisms to therapeutic opportunities," *Antioxidants & Redox Signaling*, vol. 18, no. 11, pp. 1349–1383, 2013.
- [52] C. López-Pedrerá, J. M. Villalba, E. Siendones et al., "Proteomic analysis of acute myeloid leukemia: identification of potential early biomarkers and therapeutic targets," *Proteomics*, vol. 6, Supplement 1, pp. S293–S299, 2006.

Research Article

Identification of Hypotensive Biofunctional Compounds of *Coriandrum sativum* and Evaluation of Their Angiotensin-Converting Enzyme (ACE) Inhibition Potential

Farieha Hussain,¹ Nazish Jahan ¹, Khalil-ur- Rahman ², Bushra Sultana,¹ and Saba Jamil¹

¹Department of Chemistry, University of Agriculture, Faisalabad 38000, Pakistan

²Department of Biochemistry, University of Agriculture, Faisalabad 38000, Pakistan

Correspondence should be addressed to Nazish Jahan; nazishjahanuaf@yahoo.com

Received 6 July 2018; Revised 2 October 2018; Accepted 9 October 2018; Published 15 November 2018

Guest Editor: Felipe L. de Oliveira

Copyright © 2018 Farieha Hussain et al. This is an open access article distributed under the Creative Commons Attribution License, which permits unrestricted use, distribution, and reproduction in any medium, provided the original work is properly cited.

The aim of this study was to identify and characterize the bioactive compounds of *Coriandrum sativum* responsible for the treatment of hypertension and to explore their mechanism of action as angiotensin-converting enzyme (ACE) inhibitors. Bioactive fractions like alkaloids, flavonoids, steroids, and tannins were extracted and evaluated for their ACE inhibition potential. Among them, only flavonoid-rich fraction showed high ACE inhibition potential with IC_{50} value of $28.91 \pm 13.42 \mu\text{g}/\text{mL}$. The flavonoids were characterized through LC-ESI-MS/MS. Seventeen flavonoids were identified in this fraction of *Coriandrum sativum* in negative ionization mode which includes pinocembrin, apigenin, pseudobaptigenin, galangin-5-methyl ether, quercetin, baicalein trimethyl ether, kaempferol dimethyl ether, pinobanksin-5-methylether-3-O-acetate, pinobanksin-3-O-pentanoate, pinobanksin-3-O-phenylpropionate, pinobanksin-3-O-pentanoate, apigenin-7-O-glucuronide, quercetin-3-O-glucoside, apigenin-3-O-rutinoside, rutin, isorhamnetin-3-O-rutinoside, and quercetin dimethyl ether-3-O-rutinoside, while six flavonoids including daidzein, luteolin, pectolarigenin, apigenin-C-glucoside, kaempferol-3-7-dimethyl ether-3-O-glucoside, and apigenin-7-O-(6-methyl-beta-D-glucoside) were identified in positive ionization mode. The results of this study revealed that *Coriandrum sativum* is a valuable functional food that possesses a number of therapeutic flavonoids with ACE inhibition potential that can manage blood pressure very efficiently.

1. Introduction

Hypertension is a dominant risk factor for chronic diseases, including cardiovascular disorders, stroke, renal diseases, and diabetes. Hypertension is the second leading cause of disability around the world, and its prevalence has doubled in the last 5 years in all social strata of Pakistan. Globally, the overall prevalence of hypertension is approximately 40% in adults. Among them, almost 57% of human population is well aware about their blood pressure, from which about 40.6% have access to antihypertensive medicines. Still, there is a huge gap between the number of hypertensive patients and the availability of treatment facilities. The health facilities for the management of hypertension is more alarming in the middle and low income countries as more than 80% of deaths due to cardiovascular diseases occur in

these countries [1]. The prevalence of hypertension in Pakistan is very high and is considered as a top alarming physiological disorder in the community [2]. Not to speak of Pakistan, hypertension has become a health menace all over the world. Owing to the high prevalence and increased mortality and morbidity due to hypertension and associated complications, there is a dire need to explore the alternatives including food components for the management of this health menace.

Bioactive phytoconstituents, available as natural components in foods and medicinal plants, provide preventive and curative health benefits to improve cardiovascular health. Functionalities of bioactives from green resources including inhibition of activity of enzymes or form complexes with metals, which catalyse the oxidation reaction and the capacity to modulate metabolic processes, may result in the

eradication and management of cardiovascular diseases [3]. Angiotensin I-converting enzyme (ACE) plays a fundamental role in the management of hypertension as it converts angiotensin I to the potent angiotensin II which is vasoconstrictor. Moreover, it inactivates the vasodilator bradykinin. By inhibiting these processes, synthetic ACE inhibitors have long been used as antihypertensive agents. However, the unwanted side effects of these drugs are taking their toll in the form of side effects with high rate. Bioactive food components like alkaloids, peptides flavonoids, flavanols, anthocyanins, phenolic acids, polyphenols, tannins, resveratrol, polysaccharides, and sterol have been identified as green ACE inhibitors [4]. These nutritional components have received considerable attention for their effectiveness in both the prevention and the treatment of hypertension. The recent research emphasis is on the characterization of the bioactive constituent of foods and identification of their molecular mechanism of action for the development of drugs from green natural resources. Flavonoids are reported to exhibit the capacity to inhibit different zinc metalloproteinases, including ACE. Indeed, the micromolar concentrations of various flavonoids, such as anthocyanins, flavones, flavonols, and flavanols, have been reported to exhibit more than 50% of ACE inhibition potential. Therefore, different bioactive flavonoids, including catechin, epicatechin, rutin, myricetin, luteolin, apigenin, and naringenin, were identified from the leaves of *Mentha spicata* [5]. 2-(3,4-dihydroxy-5-methoxy-phenyl) and 3,5-dihydroxy-6,7-dimethoxychromen-4-one were extracted from the leaves of *Euphorbia nerifolia*. Epicatechin, (-)-(2S)-6-Methoxy-[2'',3'': 7,8]-furanoflavanone, kaempferol-3-O-sulphate-7-O-c-arabinopyranoside, vidalenolone, (2S)-7, 8, bi's-3', 4'-(2,2-dimethyl-chromano)-5-hydroxy flavanone, 3,7-dihydroxy-4',8-dimethoxy flavone, 14-Hydroxy artonin E, and kaempferol were extracted from the leaves and flowers of *Cassia angustifolia* [6]. Rutin and kaempferol were also extracted from *Ficus carica* and evaluated for their therapeutic potential [4, 7, 8]. Many flavonoids of *Coriander sativum* with known ACE inhibition mode of action were explored for the first time in this study.

Coriandrum sativum L. belonged to the family Apiaceae (Umbelliferae) and mainly cultivated throughout the year. It is an important functional food that is traditionally used as nutrition and taste enhancer with additional medicinal benefits including antioxidant, antihypertensive, lipid lowering, and analgesic [9]. *Coriandrum sativum*, being a treasure of bioactive compounds, may contribute its exceptional pharmaceutical potential to combat cardiovascular diseases [10]. Therefore, *Coriandrum sativum* was explored for the identification and characterization of more bioactive compounds with known ACE inhibition mechanism of action against hypertension.

2. Materials and Method

All analytical grade chemicals and reagents were purchased from Sigma-Aldrich, USA, and Merck, Germany.

Coriandrum sativum (fresh leaves) was purchased from the local market and identified from a taxonomist of Department of Botany, University of Agriculture Faisalabad (voucher no. 227-4-2016).

2.1. Extraction of Bioactive Fractions of Phytochemicals. Four bioactive fractions of phytoconstituents were extracted from *Coriandrum sativum*.

2.1.1. Extraction of Flavonoids. The extraction of partially purified flavonoid fraction was made through Soxhlet apparatus by using multiple solvents from least to most polar with the order of n-hexane, chloroform, ethyl acetate, and methanol (500 mL of each). Each fraction was examined for the presence of flavonoid with the appearance of orange-pink color through Shibata reaction [11, 12]. Flavonoid positive ethyl acetate fraction was dried by evaporating solvent through rotary evaporator (BUCHI Rotavapor II) at 50°C to obtain brownish mass. About 1 mg of brownish mass was dissolved in 10 mL of distilled water and used for the evaluation of ACE inhibition potential of flavonoids.

2.1.2. Extraction of Tannins. Defatted plant material was shaken for four days at ambient temperature with mixture of acetone and water (70:30 V/V) in a capped flask. Acetone was evaporated by using rotary evaporator, and remaining aqueous extract was further partitioned with dichloromethane (2 × 50 mL) and diethyl acetate (4 × 50 mL) separately. The organic layers were dried by evaporating the solvent under reduced pressure at 50°C, and the presence of tannins were confirmed with the formation of greenish-black precipitate by adding 5% ferric chloride [11].

2.1.3. Extraction of Alkaloids. Dried powder of *Coriandrum sativum* (20 g) was extracted with benzene for 6 hours. This benzene extract was shaken with three successive portions of 5% sulphuric acid (25 cm³) and decolorized with activated charcoal. The hot solution was filtered. The pH of the filtrate was maintained at 8.5 with ammonia solution. Filtrate was transferred into a separatory funnel and extracted with three successive portions of chloroform (20 cm³). All three portions were combined, and chloroform layer was distilled off to get alkaloids. The presence of alkaloids was confirmed by the appearance of reddish precipitate with Dragendorff's reagent [11].

2.1.4. Extraction of Steroids. The grinded plant material (40 g) was soaked in 200 mL of ethanol for 7 days, and the gummy material was obtained after ethanol evaporation under reduced pressure at 40°C by using rotary evaporator. This gummy material was redissolved in 90% ethanol and partitioned successively with n-hexane, chloroform, and ethyl acetate through Soxhlet apparatus. All three fractions were tested for presence of steroids by adding acetic anhydride and H₂SO₄ [13]. The ethyl acetate fraction showed positive results for presence of steroid.

2.2. Evaluation of ACE Inhibition Potential

2.2.1. Preparation of Lung Acetone Powder. The lungs, separated from freshly slaughtered rabbits, were washed with

0.8% saline solution and centrifuged at 4000 rpm for 10 minutes with phosphate saline buffer. The supernatant was removed, and the residue was washed with acetone with continuous stirring on a magnetic stirrer. After overnight drying, this material was grinded to fine powder and stored at 4°C as lung acetone powder [14].

2.2.2. Extraction of ACE from Lung Acetone Powder. The extraction of enzyme was carried out by mixing lung acetone powder (0.5 g) and 10 mL of borate buffer (100 mM, pH 8.3) with continuous overnight stirring. Then this mixture was centrifuged at 4000 rpm for 45 minutes. Supernatant was dialyzed with borate buffer by using dialyzing membrane (pore size 20 Å). The ACE enzyme, collected after lyophilization, was stored at -20°C [15].

2.2.3. ACE Activity Assay. ACE activity was determined by the following method of Belovic et al. [16] with some modifications. The solution of angiotensin-converting enzyme (50 µL of 100 mU/mL) was incubated with 50 µL borate buffer at 37°C for 10 minutes and was reincubated for 80 minutes at 37°C after adding substrate, Hip-His-Leu (150 µL, 8.3 mM in borate buffer). The reaction was stopped with 250 µL of 1 M HCl. The resulting hippuric acid was extracted with 1500 µL of ethyl acetate after centrifugation at 3000 rpm for 15 minutes. Supernatant (750 µL) was dried under air flow at 7°C. In this dried powder, 1 mL of distilled water was mixed, and the absorption of hippuric acid released after action of ACE was measured at 228 nm by using UV/Visible double beam spectrophotometer. The reaction blank was prepared with the same procedure except the addition of HCl before adding substrate.

2.2.4. ACE Inhibition Potential of Partially Purified Bioactive Fractions. The inhibition percentages were determined by the same modified enzyme assays only by replacing 50 µL of buffer with the same volume and concentration of partially purified bioactive fractions (100 µg/mL) and standard captopril (100 µg/mL). The decrease in concentration of hippuric acid in test sample as compared to control was expressed in terms of percentage ACE inhibition.

ACE inhibition was calculated according to the following equation: %ACE = 100[(A - B) - (C - D)]/(A - B), where A represents absorbance in the presence of ACE, B absorbance of reaction blank, C absorbance in the presence of ACE and inhibitors, and D absorbance of sample blank.

2.3. LC-ESI-MS/MS Analysis of Secondary Metabolites. Secondary metabolites of *Coriandrum sativum* with the highest ACE inhibition activity were subjected to chemical characterization by LC-ESI-MS/MS analysis to find out the bioactive compounds actually involved in ACE inhibition potential. This analysis was carried out on liquid chromatography coupled with electrospray ionization (Linear Ion Trap, LTQ XL) mass spectrometer (ESI-LC/MS) (Thermo Fisher Scientific, San Jose, CA, USA).

In order to get chromatographic separations, 5 µL of each sample was injected via auto sampler (Surveyor Auto-sampler Plus) into the HPLC system (Surveyor) equipped with Luna reverse phase C-18 column (250 × 4.6 mm, 5 µm

particle size) (Phenomenex, USA). The elution of sample from column was carried out at a flow rate of 0.5 mL/min using gradient elution.

Solvent A and B were prepared by mixing water, acetonitrile, and trifluoroacetic acid (TFA) with a ratio of 90:10:0.1% (v/v) and 10:90:0.06% (v/v), respectively, for positive ionization mode. Solvent A and B were prepared by mixing water, acetonitrile, and formic acid with a ratio of 90:10:0.1% (v/v) and 10:90:0.06% (v/v), respectively, for negative ionization mode. Gradient elution was programmed as follows: from 10% to 25% A and 90 to 75% B from 0 to 05 min followed by 25 to 50% A and 75 to 50% B in the next 10 min. This flow was maintained till the end of analysis. A photodiode array was used as the detector, and prominent peaks were further analyzed by mass spectrometer. The compounds corresponding to these peaks were ionized using atmospheric pressure electrospray ionization (ESI) probe at negative and positive ionization mode. ESI MS/MS conditions were selected as sheath gas flow rate 45 (arb) or 9 liter/min, auxiliary gas flow rate 10 (arb) or 2 liter/min. APCI vaporization temperature was maintained at 300°C, corona source voltage 4.5 KV, source current 4.10 µA, ion transfer capillary temperature 275°C, capillary voltage 45 V, and tube lens voltage 110 V.

The identification of flavonoids was performed under full scan mode at different ranges of *m/z*. MS² analysis for each parent ion peak at different collision-induced dissociation (CID) powers. Xcalibur 1.4 software was applied for calibration of MS data [17–21].

Qualitative analysis was performed by comparing the retention time of identical peaks in LC-ESI-MS/MS chromatogram of present analysis with those of reference standards, literature reports, and library. The chemical nature of the compounds was proposed on the basis of MS and MS² analysis fragmentation data. The fragmentation pattern gave tentative confirmation about the presence of a compound.

2.4. Statistical Analysis. The results were presented as mean ± SE of three concordant readings. The means were analyzed by one-way ANOVA followed by Tukey's test. IC₅₀ values for % ACE inhibition of different extracts were calculated using linear regression analysis.

3. Results

3.1. Extraction of Bioactive Fractions and Evaluation of Their ACE Inhibition Potential. Four bioactive fractions including flavonoids, tannins, alkaloids, and steroids were extracted from *Coriandrum sativum* and evaluated for ACE inhibition potential, and the results have been presented in Table 1. Flavonoid fraction of *Coriandrum sativum* showed 81.4 ± 0.48% inhibition of ACE, while the potential of tannin fraction (2.3 ± 0.64%) to inhibit the ACE was very small. Alkaloid and steroid fractions of *Coriandrum sativum* have not revealed any ACE inhibitory activity. This high ACE inhibition potential of flavonoid fraction of *Coriandrum sativum* certifies that no other phytoconstituents including tannins, alkaloids, and steroids but only the flavonoids of this plant may manage hypertension

TABLE 1: ACE inhibition potential of bioactive compounds extracted from *Coriandrum sativum*.

Treatments (100 $\mu\text{g}/\text{mL}$)	ACE inhibition (%)
Steroids fraction	$-0.9 \pm 1.47\text{C}$
Alkaloids fraction	$-32.79 \pm 1.97\text{D}$
Flavonoids fraction	$81.4 \pm 0.48\text{A}$
Tannins fraction	$2.3 \pm 0.64\text{B}$

Means sharing different letter are statistically significant ($P > 0.05$).

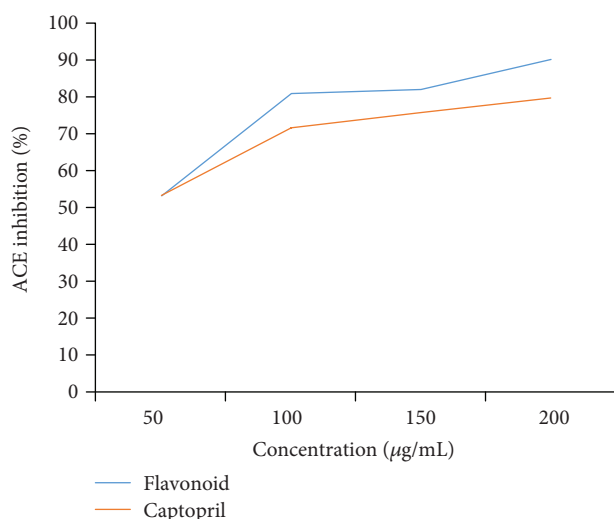


FIGURE 1: ACE inhibition (%) of flavonoids fraction of *Coriandrum sativum* and captopril at different concentrations.

TABLE 2: IC_{50} values of flavonoid fraction of *Coriandrum sativum* and captopril.

Sr. no.	Extracts	IC_{50} ($\mu\text{g}/\text{mL}$)
1	Flavonoid fraction	28.91 ± 13.42
2	Captopril	4.68 ± 15.42

through ACE inhibition mode of action. The studies reported the antihypertensive potential of tannins and alkaloids of some other plants may be due to the mode of action other than ACE inhibition, like calcium channel blocker or beta blockers [22].

Therefore, only the flavonoid fraction was further evaluated at its various concentrations to find its dose-dependent response and IC_{50} of ACE inhibition. Standard synthetic drug captopril was also evaluated for ACE inhibition at different concentrations (Figure 1). The results revealed that the ACE inhibition potential of flavonoid fractions was increased with the increase of its concentration. The partially purified fraction of flavonoid and captopril exhibited almost equal ACE inhibition potential at 50 $\mu\text{g}/\text{mL}$, but flavonoids depicted higher ACE inhibition potential at all other studied concentrations than the standard synthetic drug.

As for as IC_{50} values are concerned, the studied flavonoid-rich fraction of *Coriandrum sativum* showed higher IC_{50} value as compared to the captopril (Table 2).

3.2. LC-ESI-MS/MS Analysis of Flavonoid Fraction of *Coriandrum sativum*. In order to identify the specific compounds, the flavonoid fraction of *Coriandrum sativum* was further characterized through LC-ESI-MS/MS in both negative and positive ionization mode. Identification of the flavonoids was confirmed by comparing retention times and mass spectra with authentic standards available in the literature. In case of unavailability of any standards, the compounds were identified on the basis of accurate mass data of $[\text{M}-\text{H}]^-$ and $[\text{M}+\text{H}]^+$ ions.

Seventeen flavonoid compounds were identified in negative ionization mode of LC-ESI-MS/MS (Figures 2 and 3). MS spectrum showed peak at 255.33 $[\text{M}-\text{H}]^-$. This peak was identified as pinocembrin ($\text{C}_{15}\text{H}_{12}\text{O}_4$) (Figure 2), which showed MS/MS fragment ion peaks at m/z 237.17 with the elimination of $[\text{M}-\text{H}-\text{OH}]^-$, at m/z 213.17 after elimination of $[\text{M}-\text{H}-\text{C}_2\text{H}_2\text{O}]^-$, and at m/z 211.17 with the removal of $[\text{M}-\text{H}-\text{CO}_2]^-$ from the molecular ion (Table 3). Similar fragment ion peaks for pinocembrin have also been reported by Falcão et al. [23] and Falcão et al. [24] in the earlier literature.

A molecular ion peak at m/z 269.25 was identified as apigenin ($\text{C}_{15}\text{H}_{10}\text{O}_5$) in mass spectrum (Figure 2). Apigenin produced fragment ion peaks in the MS^2 spectrum at m/z 153.08 correspond to the removal of $[\text{M}-\text{H}-116\text{amu}]^-$ and at m/z 119.17 attributed to the loss of $[\text{M}-\text{H}-150\text{amu}]^-$ (Table 3). The fragment ions identified for apigenin in this study are in good harmony with fragment ions observed by Aldini et al. [25] in another study.

Peak at m/z 281.25 $[\text{M}-\text{H}]^-$ ($\text{C}_{16}\text{H}_{10}\text{O}_5$) in mass spectrum was proposed as pseudobaptigenin. MS/MS spectrum showed a fragment ion peak at m/z 263.25 that corresponds to the loss of a water molecule and at m/z 237.17 produced by the loss of CO_2 .

The precursor ion showed peak at m/z 283.33 $[\text{M}-\text{H}]^-$ ($\text{C}_{16}\text{H}_{12}\text{O}_5$) identified as galangin-5-methylether $[\text{M}-\text{H}]^-$ ($\text{C}_{16}\text{H}_{12}\text{O}_5$) in mass spectrum (Figure 2). MS/MS spectrum showed fragment ion peaks at m/z 268.08 by the loss of methyl radical $[\text{M}-\text{H}-\text{CH}_3]^-$, at m/z 239.25 that corresponds to the loss of $[\text{M}-\text{H}-\text{CO}_2]^-$, and at m/z 211.17 by the elimination of $[\text{M}-\text{H}-72]^-$ (Table 3). These fragment ion peaks are in good agreement with previously identified peaks by Pellati et al. [26].

Peak at m/z 301.33 in mass spectrum (Figure 2) was identified as quercetin $[\text{M}-\text{H}]^-$ ($\text{C}_{15}\text{H}_{10}\text{O}_7$). Quercetin was further confirmed through its specific fragmentation pattern in the MS/MS spectrum. The MS/MS spectrum of quercetin showed fragment ion peaks at m/z 273 by the loss of $[\text{M}-\text{H}-\text{CO}]^-$, at m/z 257.25 with the elimination of $[\text{M}-\text{H}-\text{CO}_2]^-$, and at m/z 151.17 found after the elimination of $[\text{M}-\text{H}-150\text{amu}]^-$ (Table 3).

Peak at m/z 311.25 $[\text{M}-\text{H}]^-$ ($\text{C}_{18}\text{H}_{16}\text{O}_5$) in mass spectrum (Figure 2) was identified as baicalein trimethyl ether, which showed fragment ion peaks in the MS/MS spectrum at m/z 257.17 that corresponds to the loss of $[\text{M}-\text{H}-\text{CO}_2]^-$, at m/z 249.25 due to the loss of $[\text{M}-\text{H}-\text{CH}_3\text{OH}]^-$, and at m/z 153.00 by the loss of $[\text{M}-\text{H}-\text{B}\&\text{C ring}]^-$ (Table 3).

Peak at m/z 313.75 in mass spectrum (Figure 2) was identified as kaempferol dimethyl ether $[\text{M}-\text{H}]^-$ ($\text{C}_{17}\text{H}_{14}\text{O}_6$),

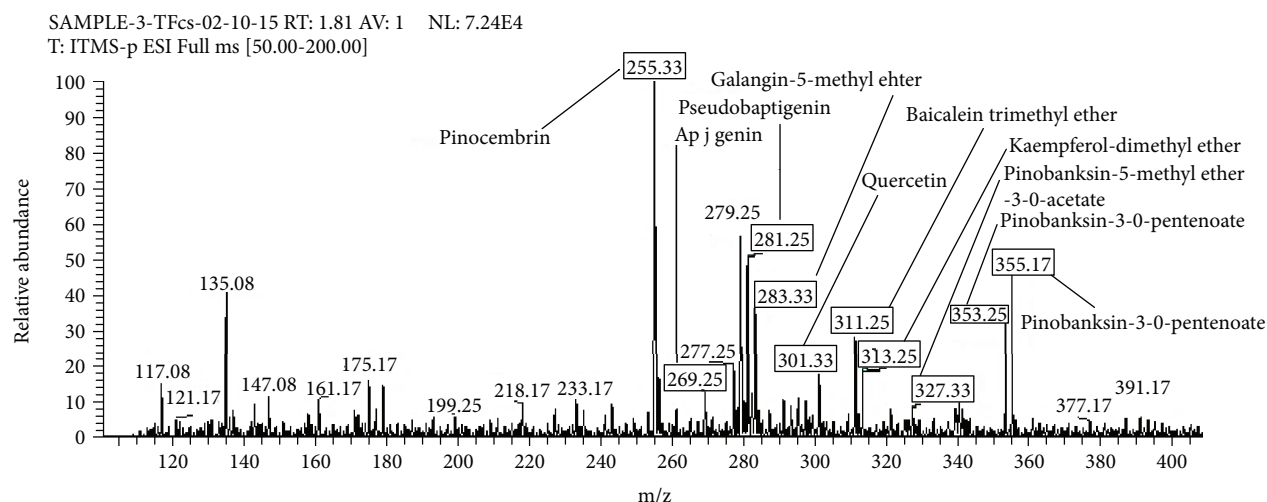


FIGURE 2: LC-MS/MS spectrum (m/z 120–400) of flavonoid fraction of *Coriandrum sativum* generated through negative ionization mode.

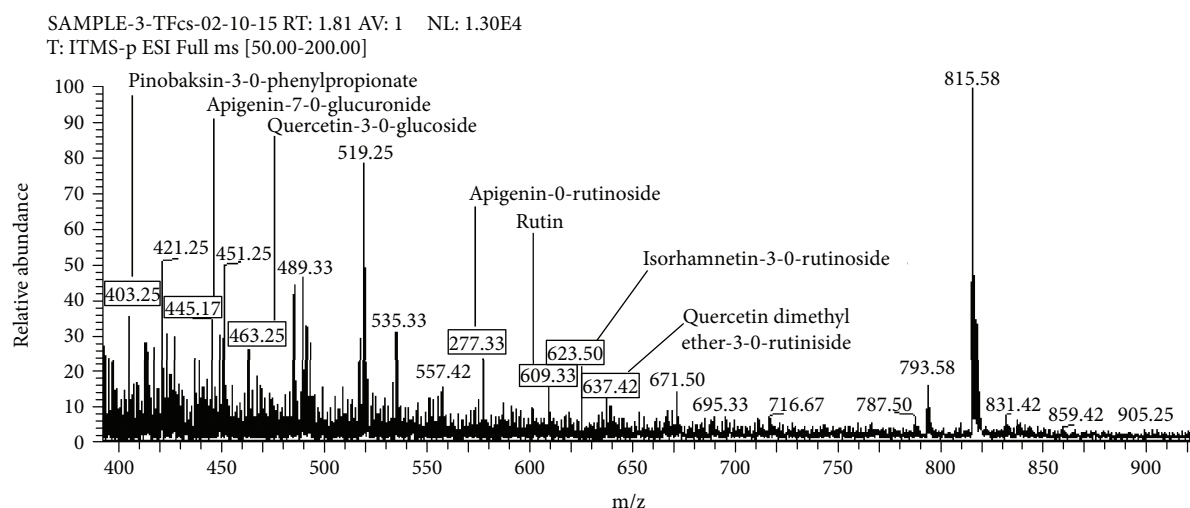


FIGURE 3: LC-MS/MS spectrum (m/z 400–900) of flavonoid fraction of *Coriandrum sativum* generated through negative ionization mode.

which showed MS² fragment ion peaks at m/z 298.08 with the elimination of $[M-H-CH_3]^-$ (Table 3). Similar fragment ion peaks for kaempferol dimethyl ether were also previously reported by Falcão et al. [23] and Falcão et al. [24].

Peak related to m/z 327.33 $[M-H]^-$ ($C_{18}H_{16}O_6$) in mass spectrum (Figure 2) was identified as pinobanksin-5-methyl ether-3-O-acetate, which was further confirmed by MS² fragment ion peaks at m/z 285.33 $[M-H-CH_3CHO]^-$, at m/z 267.08 that corresponds to the loss of $[M-H-CH_3COOH]^-$, and at m/z 239.25 that corresponds to the loss of $[M-H-CH_3COOH-CO]^-$ (Table 3), as peaks identified for pinobanksin-5-methyl ether-3-O-acetate is in good agreement with the peaks described by Gardana et al. [27] and Falcão et al. [24] in previous data.

In the mass spectrum, peak that corresponds to m/z 353.25 $[M-H]^-$ ($C_{20}H_{18}O_6$) was identified as pinobanksin-3-O-pentanoate. The molecular ion peak of pinobanksin-3-O-pentanoate was confirmed through MS/MS fragment ion peaks at m/z 271.33 by the loss of $[M-H-pentanal]^-$ and at m/z 253.08 by the loss of $[M-H-pentanoic acid]^-$ (Table 3).

These peaks are in harmony with peaks previously mentioned by Falcão et al. [28] and Falcão et al. [29].

Peak at m/z 355.17 $[M-H]^-$ ($C_{20}H_{20}O_6$) in the same mass spectrum was identified as pinobanksin-3-O-pentanoate, which was further confirmed by MS/MS fragment ion peak at m/z 271.33 by the loss of $[M-H-pentanal]^-$ and at m/z 253.08 by the loss of $[M-H-pentanoic acid]^-$ (Table 3). This fragmentation pattern showed harmony with earlier reported data by Falcão et al. [23] and Falcão et al. [24].

Peak at m/z 403.25 $[M-H]^-$ ($C_{24}H_{20}O_6$) in mass spectrum (Figure 3) was identified as pinobanksin-3-O-phenyl propionate. The molecular ion peak exhibited MS/MS fragment ion peaks at m/z 271.25 by the loss of $[M-H-phenyl propanol]^-$ and at m/z 253.17 by the loss of $[M-H-phenyl propanoic acid]^-$ (Table 3). The similar pattern of fragments ions also described in some other studies reported by Gardana et al. [27] and Falcão et al. [23].

A precursor ion at m/z 445.17 $[M-H]^-$ ($C_{21}H_{18}O_{11}$) in mass spectrum (Figure 3) was identified as apigenin-7-O-glucuronide. The MS/MS spectrum of this ion showed a

TABLE 3: Name and structure of flavonoids identified from the flavonoid fraction of *Coriandrum sativum* through LC-MS in negative ionization mode.

Sr. no.	Name of compounds	MW	R _t (Min)	λ _{max} (nm)	HPLC/ESI-MS <i>m/z</i> [M-H] ⁻	HPLC/ESI-MS/MS <i>m/z</i> [M-H] ⁻
1	Pinocembrin	256.25	6.20	288	255.25	237.17, 213.17, 211.17
2	Apigenin	270.24	7.39	325	269.33	153.08
3	Pseudobaptigenin	282.24	7.56	—	281.25	263.25, 237.17
4	Glangin-5-methyl ether	284.27	7.60	259,350	283.33	268.08, 239.25, 211.17
5	Quercetin	302.24	7.69	256	301.33	273.25, 257.25, 151.17
6	Baicalein trimethyl ether	312.32	7.75	—	311.17	257.17, 249.25, 153
7	Kaempferol dimethyl ether	314.29	7.79	339	313.75	298.08
8	Pinobanksin-5-methyl ether-3-O-acetate	328	7.84	292	327.33	285.33, 267.08, 239.05
9	Pinobanksin-3-O-pentenoate	354.11	7.98	291	353.25	271.33, 253.08
10	Pinobanksin-3-O-pentanoate	356.11	8.02	292	355.42	271.33, 253.08
11	Pinobanksin-3-O-phenyl propionate	404.25	8.36	292	403.25	325.17, 253.17
12	Apigenin-7-O-glucuronide	446	8.42	325	445.17	269.08, 175.17
13	Quercetin-3-O-glucoside	464	8.49	256,354	463.17	301.17, 300.17
14	Apigenin-3-O-rutinoside	578	8.96	325	577.33	559.33, 269.33
15	Rutin	612	9.29	256,353	611.40	609.25, 301.17
16	Isorhamnetin-3-O-rutinoside	624	9.46	253,346	623.50	315.00, 300.33
17	Quercetin dimethyl ether-3-O-rutinoside	638	9.60	253,349	637.25	301.17

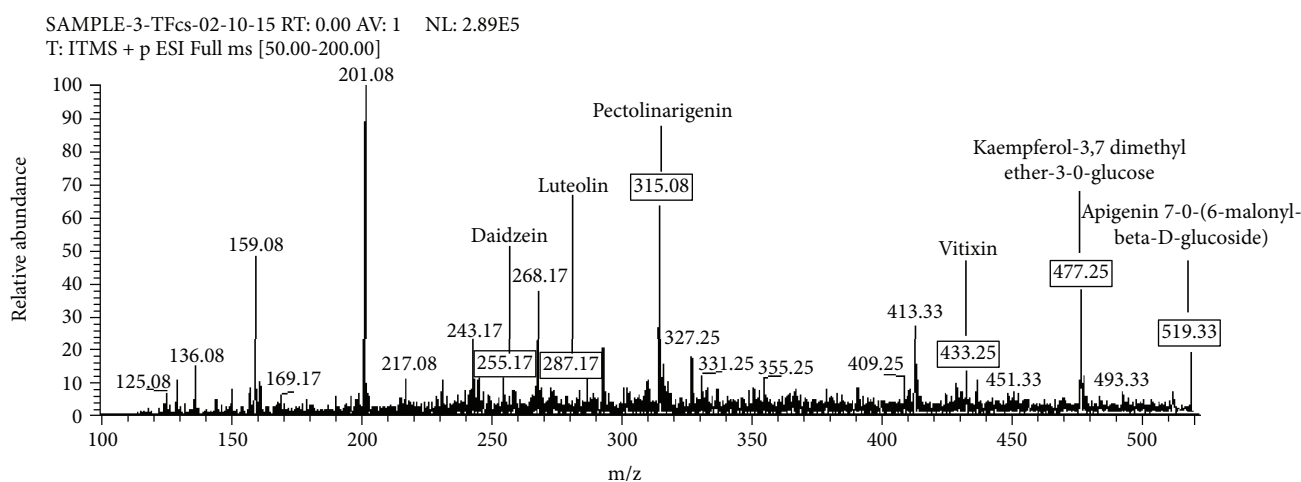


FIGURE 4: LC-MS/MS spectrum (*m/z* 100–500) of flavonoid fraction of *Coriandrum sativum* generated through positive ionization mode.

product ion peak at *m/z* 269.08 that was corresponding to the loss of [M-H-glucuronide]⁻ and product ion at *m/z* 175.17 that corresponds to the loss of [M-H-glucuronide-C ring]⁻ (Table 3). Jeyadevi et al. [30] was also reported the fragment ion peaks at *m/z* 269 and *m/z* 175 for apigenin-7-O-glucuronide.

The same mass spectrum (Figure 3) showed that a precursor ion peak at *m/z* 463.25 [M-H]⁻ (C₂₁H₂₀O₁₂) was led to the identification of quercetin-3-O-glucoside which was further collaborated by comparison of MS/MS fragmentation of the precursor ion at *m/z* 301.17 resulted due to the loss of [M-H-glucoside]⁻ and at *m/z* 300.17 produced by the elimination of [M-H-glucoside radical]⁻ (Table 3). The fragmentation pattern for quercetin-3-O-

glucoside identified in this study is in good agreement with some other studies presented by Falcão et al. [23] and Falcão et al. [24].

Peak at *m/z* 577.33 [M-H]⁻ (C₂₇H₃₀O₁₄) in mass spectrum (Figure 3) was identified as apigenin-O-rutinoside, which was further confirmed by MS/MS fragment ion peaks at *m/z* 559.33 that corresponds to the elimination of [M-H-H₂O]⁻ and at *m/z* 269.33 due to the elimination of [M-H-rutinoside]⁻ (Table 3).

A precursor ion at *m/z* 609.33 [M-H]⁻ (C₂₇H₃₀O₁₅) in the negative ionization mode of mass spectrum (Figure 3) and its MS/MS spectrum showed fragment ion peak at *m/z* 301.17, characteristic peak of rutin, formed after the loss of hexose residue (162 amu) or the direct loss of rutinoside

TABLE 4: Name and structure of flavonoids identified from the flavonoid fraction of *Coriandrum sativum* through LC-MS in positive ionization mode.

Sr. no.	Name of compounds	MW	R _t (Min)	λ _{max} (nm)	HPLC/ESI-MS m/z [M-H] ⁻	HPLC/ESI-MS/MS m/z [M-H] ⁻
1	Daidzein	254	0.75	—	255.17	237.17, 227.17
2	Luteolin	286	0.91	253,350	287.17	153.08
3	Pectolinarigenin	314	1.23	—	315.08	297.17, 243.08
4	Apigenin-C-glucoside	432	1.72	268, 325	433.25	415.25, 271.08
5	Kaempferol-3,7-dimethyl ether-3-O-glucoside	476	1.98	265,346	477.17	315.17
6	Apigenin 7-O-(6-malonyl-beta-d-glucoside)	518	2.39	325	519.33	271.08

residue [M-H-rutinoside]⁻. Therefore, these data and comparison with the literature produced by Cuyckens and Claeys, [31] led to the identification of peak as quercetin-3-O-rutinoside (rutin). The peak at *m/z* 301 for rutin was also reported by Ibrahim et al. [32].

A peak at *m/z* 623.50 [M-H]⁻ (C₂₈H₃₂O₁₆) in mass spectrum (Figure 3) was identified as isorhamnetin-3-O-rutinoside, which showed MS/MS fragmentation ion peaks at *m/z* 315 by the elimination of [M-H-rutinoside]⁻ and at *m/z* 300.33 by the loss of [M-H-rutinoside-CH₃]⁻ (Table 3). The fragment ion peaks identified in this study resembled the previous data reported by Falcão et al. [23] and Falcão et al. [24].

A peak at *m/z* 637.42 in mass spectrum (Figure 3) was identified as quercetin dimethyl ether-3-O-rutinoside, which showed MS/MS fragment ion peak at *m/z* 301.17 [M-H-2CH₃-rutinoside]⁻ (Table 3). The present finding is in good agreement with the previously described fragment ions of quercetin dimethyl ether-3-O-rutinoside by Falcão et al. [23] and Falcão et al. [24].

Six flavonoids including daidzein, luteolin, pectolinarigenin, apigenin-C-glucoside, kaempferol-3-7-dimethyl ether-3-O-glucoside, and apigenin-7-O-(6-methyl-beta-D-glucoside) were identified in the bioactive fraction of *Coriander sativum* when analyzed through positive ionization mode of LC-ESI-MS/MS. The fragmentation pattern of these flavonoids presented with their MS² spectra was comparable with previously reported literature [33, 34]. Precursor ion peak at *m/z* 255.17 [M+H]⁺ (C₁₅H₁₀O₄) in the mass spectrum (Figure 4) was identified as daidzein which produced fragment ion peaks at *m/z* 237.17 that corresponds to the loss of [M+H-OH]⁺ and at *m/z* 227.17 by the loss of [M+H-CO]⁺ in MS/MS spectrum specific for daidzein molecule (Table 4).

Luteolin (C₁₅H₁₀O₆) produced precursor ion peak at *m/z* 287.17 [M+H]⁺ in mass spectrum (Figure 4) and further confirmed from MS/MS fragment ion peaks at *m/z* 269.08 after the elimination of [M+H-H₂O]⁺ and at *m/z* 259.17 after the removal of [M+H-CO]⁺ (Table 4). The fragment ion peaks were in agreement with the fragment ion peaks of luteolin described by Santos et al. [34] and Ibrahim et al. [32].

The precursor ion peak at *m/z* 315.08 [M+H]⁺ (C₁₇H₁₄O₆) in mass spectrum (Figure 4) was detected as pectolinarigenin. This peak was further confirmed through MS/MS fragment ion peaks produced at *m/z* 297.17 by the loss of [M+H-H₂O]⁺ and at *m/z* 243.08 by the elimination of [M+H-C₃H₄O₂]⁺ (Table 4).

A precursor ion at *m/z* 433.25 [M+H]⁺ (C₂₁H₂₀O₁₀) was identified as apigenin-8-C-glycoside (apigenin-C-glucoside) in mass spectrum (Figure 4). The main product ion peaks in the MS/MS spectrum during positive ionization mode produced at *m/z* 415.25 due to dehydrations [M+H-H₂O]⁺ and at *m/z* 271.08 due to the cleavage of the sugar ring [M+H-glucoside]. These product ion peaks were also resembled to the peaks of apigenin-C-glucoside described in another study by Abad-Garcia et al. [33] (Table 4). The peak at *m/z* 477.25 [M+H]⁺ (C₂₃H₂₄O₁₁) corresponds to kaempferol 3,7-dimethyl ether-3-O-glucoside in mass spectrum (Figure 4), which was further confirmed through the fragment ion peaks produced at *m/z* 315.17 by the loss of glucoside unit [M+H-glucoside]⁺ in the MS/MS spectrum (Table 4). A molecular ion peak at *m/z* 519.33 [M+H]⁺ (C₂₄H₂₂O₁₃) was identified as apigenin-7-O-(6-malonyl-beta-d-glucoside) in mass spectrum (Figure 4), which produced fragment ion peaks at *m/z* 271.08 after the removal of [M+H-malonyl-glucoside]⁺ in the MS/MS spectrum (Table 4).

4. Discussion

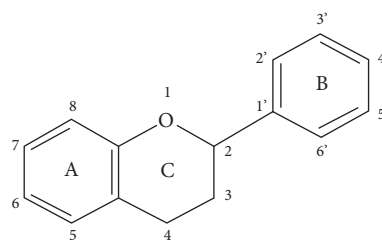
In the present study, four secondary metabolites including flavonoids, tannins, alkaloids, and steroids were fractionated from *Coriandrum sativum* and evaluated for ACE inhibition potential to find out the actual bioactive compounds responsible for ACE inhibition. Extraction and isolation of desired components from the plants is not only necessary for purification and characterization purpose but also important for the identification of particular bioactive compounds used as ACE inhibitors. The ACE inhibition potential of the flavonoid-rich fraction of *Coriandrum sativum* was higher than all other studied fractions. Higher ACE inhibition potential of only flavonoid might be due to the presence of ACE inhibitor bioactive compounds in this fraction. The leaves of *Coriandrum sativum* possess a significant ACE inhibition potential, while the seeds of this plant did not show any ACE inhibition potential [8]. The high ACE inhibition potential of fresh leaves than the seeds of *Coriandrum sativum* is because of variation in nature and concentration of bioactive compounds in different parts of the same plant. Moreover, the frequency distribution of variety of phytoconstituents in various parts of the plants may be different due to species and geonetical variations [35–37].

Peptides and flavonoids are the most investigated classes of phytochemicals for their ACE inhibition potential. Plant peptides commonly have IC_{50} values in the range of 16–310 $\mu\text{g}/\text{mL}$ [28, 38, 39]. The flavonoid fraction extracted from *Coriandrum sativum* showed IC_{50} value 28.91 $\mu\text{g}/\text{mL}$ which confirmed that ACE inhibition potential of flavonoid fraction of *Coriandrum sativum* is comparable to ACE inhibition potential of peptides of other plants.

Flavonoids are considered as chief antioxidants in the medicinal plants and can play a pivotal role in the prevention of cardiovascular and other oxidative stress-related disorders. Other than combating free radicals, flavonoids are also having antihypertensive, antihistamine, antimicrobial, memory enhancing, and even mood-boosting properties. A large number of experimental studies have been available to prove the use of flavonoid-rich food, supplements, or herbal preparation for the protection and treatment of atherosclerosis and cardiovascular diseases [29, 40–44]. Natural flavonoids, including hesperidin, rutin, and diosmetin, are utilized as basic ingredient in more than hundred herbal medicines that are being sold throughout the world [45]. Remedial properties of flavonoids have been attributed to their ability to act as antioxidants, free radical scavengers, and chelators of divalent cations. The biological mechanisms of flavonoids to control vascular function and hypertension seem to be concomitant with the accomplishment of nitric oxide (NO). Although the mechanism involved in increased production of NO is not fully understood, but it is expected that NO production might be controlled by the regulation of the renin angiotensin aldosterone system in endothelial cells. ACE, being a key regulator of the renin-angiotensin-aldosterone system (RAAS), is if inhibited with flavonoids, can easily manage the blood pressure and related cardiovascular disorders. ACE has been reported for exhibiting three active sites: a zinc ion, carboxylate-binding functionality, and a pocket that chelates a hydrophobic side chain of C-terminal amino acid residues. ACE binds to the substrate through coordination with zinc ion present in the structure of the substrate; as a result of this binding, the carbonyl group becomes polarized and facilitate the nucleophilic attack. Therefore, some flavonoids were reported to show *in vitro* ACE inhibition activity through chelation with zinc ion present on the active site of ACE. Free hydroxyl groups of flavonoids have also been reported for the formation of chelate with zinc ions present on ACE [46]. Possibly, flavonoids have functional groups which are able to form hydrogen bridges with the amino acids near at the active site [47–49].

Quercetin, rutin, apigenin, and luteolin have already been identified in *Coriandrum sativum* [50–52], and many others have been identified through this study. Furthermore, the leaves of *Coriandrum sativum* as a source of important therapeutic flavonoids particularly with ACE inhibition mechanism to combat with various cardiovascular diseases were explored for the first time in this study.

The ACE inhibition potential of different flavonoids is based on three principle structural features which include the presence of the double bond between C2 and C3 at C-



SCHEME 1

ring, the presence of OH group at position 3', 4' of B ring [53, 54], and the carbonyl (CO) group on the C4 carbon in the C-ring [55] (Scheme 1).

The presence of a double bond between C2 and C3 is essential to maintain the planar structure of flavonoids responsible for inhibition of ACE. The presence of the different hydroxyl groups also has prominent importance for the establishment of ACE inhibition potential of flavonoids [53]. The exact position and number of the hydroxyl and carbonyl functional groups are key factors for ACE inhibition potential [56, 57]. All the identified flavonoids of *Coriandrum sativum* possess the essential structural features required for the activity to regulate the ACE to ultimate control and manage blood pressure and other related cardiovascular diseases.

Some of the flavonoid including pinocembrin, apigenin, quercetin, and rutin have already been reported as ACE inhibitors [5, 58], while many other important flavonoids were explored in this study including pseudobaptigenin, galangin-5-methyl ether, baicalein trimethyl ether, kaempferol dimethyl ether, pinobanksin-5-methylether-3-O-acetate, pinobanksin-3-O-pentenoate, pinobanksin-3-O-phenylpropionate, pinobanksin-3-O-pentanoate, apigenin-7-O-glucuronide, quercetin-3-O-glucoside, apigenin-3-O-rutinoside, isorhamnetin-3-O-rutinoside, quercetin dimethyl ether-3-O-rutinoside, daidzein, luteolin, pectolinarigenin, apigenin-C-glucoside, kaempferol-3-7-dimethyl ether-3-O-glucoside, and apigenin-7-O-(6-methyl-beta-D-glucoside) that have never been evidenced earlier as ACE inhibitors. All the flavonoids identified in *Coriandrum sativum* except pinocembrin, pinobanksin-5-methylether-3-O-acetate, pinobanksin-3-O-pentenoate, pinobanksin-3-O-phenylpropionate, and pinobanksin-3-O-pentanoate exhibited key structural features required for structural activity relationship to act as ACE inhibitors [58].

5. Conclusion

In addition to some already reporting flavonoids, many other new flavonoids like pseudobaptigenin, galangin-5-methyl ether, baicalein trimethyl ether, kaempferol dimethyl ether, apigenin-7-O-glucuronide, quercetin-3-O-glucoside, apigenin-3-O-rutinoside, isorhamnetin-3-O-rutinoside, quercetin dimethyl ether-3-O-rutinoside, daidzein, luteolin, pectolinarigenin, apigenin-C-glucoside, kaempferol-3-7-dimethyl ether-3-O-glucoside, and apigenin-7-O-(6-methyl-beta-D-glucoside) identified in the leaves of *Coriandrum sativum* exhibited such structural features which are essential

to inhibit the activity of angiotensin-converting enzyme. Therefore, the leaves of *Coriandrum sativum*, as a source of therapeutic flavonoids, can manage blood pressure very efficiently. *Coriandrum sativum*, a common functional food, if used in an appropriate way, can prevent and even combat a variety of cardiovascular disorders.

Data Availability

The data in the form of figures/tables and MS spectrum used to support the findings of this study are included within the article.

Conflicts of Interest

The authors do not have any conflict of interests with other people or organizations.

Acknowledgments

We are grateful to the Pakistan Academy of Sciences (No. 5-9/PAS/724) and Higher Education Commission of Pakistan for the financial support of this study.

References

- [1] F. P. Cappuccio and M. A. Miller, "Cardiovascular disease and hypertension in sub-Saharan Africa: burden, risk and interventions," *Internal and Emergency Medicine*, vol. 11, no. 3, pp. 299–305, 2016.
- [2] S. T. Shafi and T. Shafi, "A survey of hypertension prevalence, awareness, treatment, and control in health screening camps of rural Central Punjab, Pakistan," *Journal of Epidemiology and Global Health*, vol. 7, no. 2, pp. 135–140, 2017.
- [3] W.-Y. Huang, S. T. Davidge, and J. Wu, "Bioactive natural constituents from food sources—potential use in hypertension prevention and treatment," *Critical Reviews in Food Science and Nutrition*, vol. 53, no. 6, pp. 615–630, 2013.
- [4] R. H. Liu, "Health benefits of fruit and vegetables are from additive and synergistic combinations of phytochemicals," *The American Journal of Clinical Nutrition*, vol. 78, no. 3, pp. 517S–520S, 2003.
- [5] D. Ojeda, E. Jiménez-Ferrer, A. Zamilpa, A. Herrera-Arellano, J. Tortoriello, and L. Alvarez, "Inhibition of angiotensin converting enzyme (ACE) activity by the anthocyanins delphinidin- and cyanidin-3-O-sambubiosides from *Hibiscus sabdariffa*," *Journal of Ethnopharmacology*, vol. 127, no. 1, pp. 7–10, 2010.
- [6] W. Cai, X. Gu, and J. Tang, "Extraction, purification, and characterization of the flavonoids from *Opuntia milpa alta* skin," *Czech Journal of Food Science*, vol. 28, no. 2, pp. 108–116, 2010.
- [7] K. Hieda, Y. Sunagawa, Y. Katanasaka, K. Hasegawa, and T. Morimoto, "Antihypertensive effects of foods," *World Journal of Hypertension*, vol. 5, no. 2, pp. 53–62, 2015.
- [8] A. Kouchmeshky, S. B. Jameie, G. Amin, and S. A. Ziai, "Investigation of angiotensin-converting enzyme inhibitory effects of medicinal plants used in traditional Persian medicine for treatment of hypertension: screening study," *Thrita*, vol. 1, no. 1, pp. 13–23, 2012.
- [9] F. Darughe, M. Barzegar, and M. A. Sahari, "Antioxidant and antifungal activity of coriander (*Coriandrum sativum* L.) essential oil in cake," *International Food Research Journal*, vol. 19, no. 3, pp. 1253–1260, 2012.
- [10] C. U. Rajeshwari, R. I. Shobha, and B. Andallu, "Antihemolytic activity of various fractions of methanolic extract of coriander (*Coriandrum sativum* L.) leaves and seeds: a comparative study," *Pakistan Journal of Food Sciences*, vol. 22, no. 1, pp. 1–6, 2012.
- [11] O. M. Kolawole, S. O. Oguntoye, O. Agbede, and A. B. Olayemi, "Studies on the efficacy of *Bridelia ferruginea* Benth. Bark extract in reducing the coliform load and BOD of domestic waste water," *Ethnobotanical Leaflets*, vol. 10, pp. 228–238, 2006.
- [12] I. Javed and M. Aslam, "Isolation of a flavonoid from the roots of *Citrus sinensis*," *Malaysian Journal of Pharmaceutical Sciences*, vol. 7, no. 1, pp. 1–8, 2009.
- [13] Y. Ahmed, S. Rahman, P. Akthar, F. Islam, M. Rahman, and Z. Yaqoob, "Isolation of steroids from n-hexane extract of the leave of *Saurauia roxburghi*," *International Food Research Journal*, vol. 20, no. 5, pp. 2939–2943, 2013.
- [14] H. Luna, A. Pacheco, A. Solis, I. H. Perez, N. Manjarrez, and J. Cassani, "Study towards the improvement of the enantioselective hydrolysis of naproxen esters by sheep liver acetone powder," *Journal of Biotech Research*, vol. 1, pp. 21–27, 2009.
- [15] J.-H. Kim, D.-H. Lee, S.-C. Jeong, K.-S. Chung, and J.-S. Lee, "Characterization of antihypertensive angiotensin I-converting enzyme inhibitor from *Saccharomyces cerevisiae*," *Journal of Microbiology and Biotechnology*, vol. 14, no. 6, pp. 1318–1323, 2004.
- [16] M. B. Belovic, I. M. Nebojša, T. N. Taleksandra, and S. M. Zdravko, "Selection conditions for angiotensin-converting enzyme inhibition assay: influence of sample preparation and buffer," *Food and Feed Research*, vol. 40, no. 1, pp. 11–15, 2013.
- [17] J. Sun, F. Liang, Y. Bin, P. Li, and C. Duan, "Screening non-colored phenolics in red wines using liquid chromatography/ultraviolet and mass spectrometry/mass spectrometry libraries," *Molecules*, vol. 12, no. 3, pp. 679–693, 2007.
- [18] M. Kajdžanoska, V. Gjamovski, and M. Stefova, "HPLC-DAD-ESI-MSn identification of phenolic compounds in cultivated strawberries from Macedonia," *Macedonia Journal of Chemistry and Chemical Engineering*, vol. 29, no. 2, pp. 181–194, 2010.
- [19] M. R. Maqsood, M. Hanif, M. Rafiq et al., "Some pyridyl- and thiophenyl-substituted 1,2,4-triazolo[3,4-b]1,3,4-thiadiazole derivatives as potent antibacterial," *Bulletin of the Korean Chemical Society*, vol. 33, no. 12, pp. 4180–4184, 2012.
- [20] M. Imran, A. M. Revol-Junelles, M. de Bruin, C. Paris, E. Breukink, and S. Desobry, "Fluorescent labeling of Nisin Z and assessment of anti-listerial action," *Journal of Microbiological Methods*, vol. 95, no. 2, pp. 107–113, 2013.
- [21] S. Sadiq, M. Imran, M. N. Hassan, M. Iqbal, Y. Zafar, and F. Y. Hafeez, "Potential of bacteriocinogenic *Lactococcus lactis* subsp. *lactis* inhabiting low pH vegetables to produce nisin variants," *LWT - Food Science and Technology*, vol. 59, no. 1, pp. 204–210, 2014.
- [22] A. M. Abdulazeez, O. S. Ajiboye, A. M. Wudil, and H. Abubakar, "Partial purification and characterization of angiotensin converting enzyme inhibitory alkaloids and flavonoids from the leaves and seeds of *Moringa oleifera*," *Journal of Advances in Biology & Biotechnology*, vol. 5, no. 2, pp. 1–11, 2016.
- [23] S. I. Falcão, M. Vilas-Boas, L. M. Estevinho, C. Barros, M. R. M. Domingues, and S. M. Cardoso, "Phenolic characterization of

- northeast Portuguese propolis: usual and unusual compounds," *Analytical and Bioanalytical Chemistry*, vol. 396, no. 2, pp. 887–897, 2010.
- [24] S. I. Falcão, N. Vale, P. Gomes et al., "Phenolic profiling of Portuguese propolis by LC–MS spectrometry: uncommon propolis rich in flavonoid glycosides," *Phytochemical Analysis*, vol. 24, no. 4, pp. 309–318, 2013.
- [25] G. Aldini, L. Regazzoni, A. Pedretti et al., "An integrated high resolution mass spectrometric and informatics approach for the rapid identification of phenolics in plant extract," *Journal of Chromatography A*, vol. 1218, no. 20, pp. 2856–2864, 2011.
- [26] F. Pellati, G. Orlandini, D. Pinetti, and S. Benvenuti, "HPLC-DAD and HPLC-ESI-MS/MS methods for metabolite profiling of propolis extracts," *Journal of Pharmaceutical and Biomedical Analysis*, vol. 55, no. 5, pp. 934–948, 2011.
- [27] C. Gardana, M. Scaglianti, P. Pietta, and P. Simonetti, "Analysis of the polyphenolic fraction of propolis from different sources by liquid chromatography tandem mass spectrometry," *Journal of Pharmaceutical and Biomedical Analysis*, vol. 45, no. 3, pp. 390–399, 2007.
- [28] A. Pihlanto, S. Akkanen, and H. J. Korhonen, "ACE-inhibitory and antioxidant properties of potato (*Solanum tuberosum*)," *Food Chemistry*, vol. 109, no. 1, pp. 104–112, 2008.
- [29] J. Rojas, S. Ronceros, R. Palomino et al., "Efecto coadyuvante del extracto liofilizado de *Passiflora edulis* (maracuyá) en la reducción de la presión arterial en pacientes tratados con Enalapril," *Anales de la Facultad de Medicina*, vol. 70, no. 2, pp. 103–108, 2009.
- [30] R. Jeyadevi, T. Sivasudha, A. Rameshkumar, and L. Dinesh Kumar, "Anti-arthritis activity of the Indian leafy vegetable *Cardiospermum halicacabum* in Wistar rats and UPLC–QTOF–MS/MS identification of the putative active phenolic components," *Inflammation Research*, vol. 62, no. 1, pp. 115–126, 2013.
- [31] F. Cuyckens and M. Claeys, "Mass spectrometry in the structural analysis of flavonoids," *Journal of Mass Spectrometry*, vol. 39, no. 1, pp. 1–15, 2004.
- [32] R. M. Ibrahim, A. M. el-Halawany, D. O. Saleh, E. M. B. E. Naggari, A. E. R. O. el-Shabrawy, and S. S. el-Hawary, "HPLC-DAD-MS/MS profiling of phenolics from *Securigera securidaca* flowers and Its anti-hyperglycemic and anti-hyperlipidemic activities," *Revista Brasileira de Farmacognosia*, vol. 25, no. 2, pp. 134–141, 2015.
- [33] B. Abad-Garcia, S. Garmon-Lobato, L. A. Berrueta, B. Gallo, and F. Vicente, "New features on the fragmentation and differentiation of C-glycosidic flavone isomers by positive electrospray ionization and triple quadrupole mass spectrometry," *Rapid Communications in Mass Spectrometry*, vol. 22, no. 12, pp. 1834–1842, 2008.
- [34] L. Santos-Zea, J. A. Gutiérrez-Urbe, and S. O. Serna-Saldivar, "Comparative analyses of total phenols, antioxidant activity, and flavonol glycoside profile of cladode flours from different varieties of *Opuntia* spp.," *Journal of Agricultural and Food Chemistry*, vol. 59, no. 13, pp. 7054–7061, 2011.
- [35] A. Adsersen and H. Adsersen, "Plants from Réunion Island with alleged antihypertensive and diuretic effects—an experimental and ethnobotanical evaluation," *Journal of Ethnopharmacology*, vol. 58, no. 3, pp. 189–206, 1997.
- [36] R. A. Restrepo, N. Loango, M. V. Moncada, and P. Landazuri, "Angiotensin-converting enzyme inhibitory activity of *Passiflora edulis* f. *flavicarpa* and *Petroselinum crispum* (mill) fuss," *British Journal of Pharmaceutical Research*, vol. 3, no. 4, pp. 776–785, 2013.
- [37] H. Li, P. Zhou, Q. Yang et al., "Comparative studies on anxiolytic activities and flavonoid compositions of *Passiflora edulis* 'edulis' and *Passiflora edulis* 'flavicarpa'," *Journal of Ethnopharmacology*, vol. 133, no. 3, pp. 1085–1090, 2011.
- [38] C. Daskaya-Dikmen, A. Yucetepe, F. Karbancioglu-Guler, H. Daskaya, and B. Ozelik, "Angiotensin-I-converting enzyme (ACE)-inhibitory peptides from plants," *Nutrients*, vol. 9, no. 4, p. 316, 2017.
- [39] M. Liu, M. Du, Y. Zhang et al., "Purification and identification of an ACE inhibitory peptide from walnut protein," *Journal of Agricultural and Food Chemistry*, vol. 61, no. 17, pp. 4097–4100, 2013.
- [40] G. Schmeda-Hirschmann and A. R. de Arias, "A screening method for natural products on triatomine bugs," *Phytotherapy Research*, vol. 6, no. 2, pp. 68–73, 1992.
- [41] K. Hansen, A. Adsersen, S. B. Christensen, S. R. Jensen, U. Nyman, and U. W. Smitt, "Isolation of an angiotensin converting enzyme (ACE) inhibitor from *Olea europaea* and *Olea lancea*," *Phytomedicine*, vol. 2, no. 4, pp. 319–325, 1996.
- [42] M. da Silva Pinto, Y. I. Kwon, E. Apostolidis, F. M. Lajolo, M. I. Genovese, and K. Shetty, "Potential of *Ginkgo biloba* L. leaves in the management of hyperglycemia and hypertension using *in vitro* models," *Bioresource Technology*, vol. 100, no. 24, pp. 6599–6609, 2009.
- [43] G. Oboh and A. O. Ademosun, "Shaddock peels (*Citrus maxima*) phenolic extracts inhibit α -amylase, α -glucosidase and angiotensin-I converting enzyme activities: a nutraceutical approach to diabetes management," *Diabetes & Metabolic Syndrome: Clinical Research & Reviews*, vol. 5, no. 3, pp. 148–152, 2011.
- [44] A. O. Ademiluyi and G. Oboh, "In vitro anti-diabetes and antihypertension potential of phenolic extracts of selected underutilized tropical legumes," *Journal of Basic and Clinical Physiology and Pharmacology*, vol. 23, no. 1, pp. 17–25, 2012.
- [45] G. Oboh, A. O. Ademiluyi, A. J. Akinyemi, T. Henle, J. A. Saliu, and U. Schwarzenbolz, "Inhibitory effect of polyphenol-rich extracts of jute leaf (*Corchorus olitorius*) on key enzyme linked to type-2 diabetes (α -amylase and α -glucosidase) and hypertension (angiotensin I converting) *in vitro*," *Journal of Functional Foods*, vol. 4, no. 2, pp. 450–458, 2012.
- [46] M. R. Loizzo, A. Said, R. Tundis et al., "Inhibition of angiotensin converting enzyme (ACE) by flavonoids isolated from *Ailanthus excelsa* (Roxb) (Simaroubaceae)," *Phytotherapy Research*, vol. 21, no. 1, pp. 32–36, 2007.
- [47] C.-H. Chen, J. Y. Lin, C. N. Lin, and S. Y. Hsu, "Inhibition of angiotensin-I-converting enzyme by tetrahydroxyxanthones isolated from *Tripterospermum lanceolatum*," *Journal of Natural Products*, vol. 55, no. 5, pp. 691–695, 1992.
- [48] H. Bormann and M. F. Melzig, "Inhibition of metalloproteinases by flavonoids and related compounds," *Pharmazie*, vol. 55, no. 2, pp. 129–132, 2000.
- [49] M. A. Lacaille-Dubois, U. Franck, and H. Wagner, "Search for potential angiotensin converting enzyme (ACE)-inhibitors from plants," *Phytomedicine*, vol. 8, no. 1, pp. 47–52, 2001.
- [50] C. U. Rajeshwari and B. Andallu, "Isolation and simultaneous detection of flavonoids in the methanolic and ethanolic extracts of *Coriandrum sativum* L. seeds by RP-HPLC," *Pakistan Journal of Food Sciences*, vol. 21, no. 1–4, pp. 13–21, 2011.

- [51] K. Msaada, M. B. Jemia, N. Salem et al., "Antioxidant activity of methanolic extracts from three coriander (*Coriandrum sativum* L.) fruit varieties," *Arabian Journal of Chemistry*, vol. 10, pp. S3176–S3183, 2017.
- [52] P. Nazni and R. Dharmaligam, "Original article isolation and separation of phenolic compound from coriander flowers," *International Journal of Agricultural and Food Science*, vol. 4, no. 1, pp. 13–21, 2014.
- [53] Y. C. Xu, S. W. S. Leung, D. K. Y. Yeung et al., "Structure–activity relationships of flavonoids for vascular relaxation in porcine coronary artery," *Phytochemistry*, vol. 68, no. 8, pp. 1179–1188, 2007.
- [54] A. C. Saragusti, M. G. Ortega, J. L. Cabrera, D. A. Estrin, M. A. Marti, and G. A. Chiabrande, "Inhibitory effect of quercetin on matrix metalloproteinase 9 activity molecular mechanism and structure–activity relationship of the flavonoid–enzyme interaction," *European Journal of Pharmacology*, vol. 644, no. 1–3, pp. 138–145, 2010.
- [55] L. Sartor, E. Pezzato, I. Dell'Aica, R. Caniato, S. Biggin, and S. Garbisa, "Inhibition of matrix-proteases by polyphenols: chemical insights for anti-inflammatory and anti-invasion drug design," *Biochemical Pharmacology*, vol. 64, no. 2, pp. 229–237, 2002.
- [56] L. Navarro-Núñez, J. Castillo, M. L. Lozano et al., "Tromboxane A_2 receptor antagonist by flavonoids: structure–activity relationships," *Journal of Agricultural and Food Chemistry*, vol. 57, no. 4, pp. 1589–1594, 2009.
- [57] L. Guerrero, J. Castillo, M. Quiñones et al., "Inhibition of angiotensin-converting enzyme activity by flavonoids: structure–activity relationship studies," *PLoS One*, vol. 7, no. 11, article e49493, 2012.
- [58] F. C. Braga, C. P. Serra, N. S. Viana Júnior, A. B. Oliveira, S. F. Côrtes, and J. A. Lombardi, "Angiotensin-converting enzyme inhibition by Brazilian plants," *Fitoterapia*, vol. 78, no. 5, pp. 353–358, 2007.

Research Article

Omega-9 Oleic Acid, the Main Compound of Olive Oil, Mitigates Inflammation during Experimental Sepsis

Isabel Matos Medeiros-de-Moraes,¹ Cassiano Felipe Gonçalves-de-Albuquerque,^{1,2} Angela R. M. Kurz,^{1,3,4} Flora Magno de Jesus Oliveira,¹ Victor Hugo Pereira de Abreu ², Rafael Carvalho Torres ⁵, Vinícius Frias Carvalho,⁵ Vanessa Estado,¹ Patrícia Torres Bozza,¹ Markus Sperandio,^{3,6} Hugo Caire de Castro-Faria-Neto ^{1,7} and Adriana Ribeiro Silva ¹

¹Laboratório de Imunofarmacologia, Instituto Oswaldo Cruz, FIOCRUZ, Rio de Janeiro, RJ, Brazil

²Laboratório de Imunofarmacologia, Instituto Biomédico, Universidade Federal do Estado do Rio de Janeiro, Rio de Janeiro, RJ, Brazil

³Walter Brendel Centre, Ludwig Maximilians University München, Klinikum der Universität, Germany

⁴The Centenary Institute, Camperdown, New South Wales, Australia

⁵Laboratório de Inflamação, Instituto Oswaldo Cruz, FIOCRUZ, Rio de Janeiro, RJ, Brazil

⁶German Center for Cardiovascular Research (DZHK) Partner Site, Munich Heart Alliance, Munich, Germany

⁷Universidade Estácio de Sá, Programa de Produtividade Científica, Rio de Janeiro, RJ, Brazil

Correspondence should be addressed to Adriana Ribeiro Silva; arsilva71@gmail.com

Received 6 July 2018; Revised 26 September 2018; Accepted 10 October 2018; Published 13 November 2018

Guest Editor: Germán Gil

Copyright © 2018 Isabel Matos Medeiros-de-Moraes et al. This is an open access article distributed under the Creative Commons Attribution License, which permits unrestricted use, distribution, and reproduction in any medium, provided the original work is properly cited.

The Mediterranean diet, rich in olive oil, is beneficial, reducing the risk of cardiovascular diseases and cancer. Olive oil is mostly composed of the monounsaturated fatty acid omega-9. We showed omega-9 protects septic mice modulating lipid metabolism. Sepsis is initiated by the host response to infection with organ damage, increased plasma free fatty acids, high levels of cortisol, massive cytokine production, leukocyte activation, and endothelial dysfunction. We aimed to analyze the effect of omega-9 supplementation on corticosteroid unbalance, inflammation, bacterial elimination, and peroxisome proliferator-activated receptor (PPAR) gamma expression, an omega-9 receptor and inflammatory modulator. We treated mice for 14 days with omega-9 and induced sepsis by cecal ligation and puncture (CLP). We measured systemic corticosterone levels, cytokine production, leukocyte and bacterial counts in the peritoneum, and the expression of PPAR gamma in both liver and adipose tissues during experimental sepsis. We further studied omega-9 effects on leukocyte rolling in mouse cremaster muscle-inflamed postcapillary venules and in the cerebral microcirculation of septic mice. Here, we demonstrate that omega-9 treatment is associated with increased levels of the anti-inflammatory cytokine IL-10 and decreased levels of the proinflammatory cytokines TNF- α and IL-1 β in peritoneal lavage fluid of mice with sepsis. Omega-9 treatment also decreased systemic corticosterone levels. Neutrophil migration from circulation to the peritoneal cavity and leukocyte rolling on the endothelium were decreased by omega-9 treatment. Omega-9 also decreased bacterial load in the peritoneal lavage and restored liver and adipose tissue PPAR gamma expression in septic animals. Our data suggest a beneficial anti-inflammatory role of omega-9 in sepsis, mitigating leukocyte rolling and leukocyte influx, balancing cytokine production, and controlling bacterial growth possibly through a PPAR gamma expression-dependent mechanism. The significant reduction of inflammation detected after omega-9 enteral injection can further contribute to the already known beneficial properties facilitated by unsaturated fatty acid-enriched diets.

1. Introduction

Sepsis is a cause of morbidity and mortality in intensive care units and associated with increased hospital-related costs [1, 2]. According to the Third International Consensus definitions, sepsis is a life-threatening organ dysfunction caused by unbalanced host response to infection [3].

Different strategies for the treatment of sepsis have emerged in the last few years, but none of them has proven to be beneficial in clinical trials [4]. Lipids can modulate leukocyte function and therefore the immune response [5]. The Mediterranean diet, characterized by high ingestion of olive oil, is associated to a reduction in the mortality of vascular diseases and cancer [6–8]. Oleic acid, a ω -9 monounsaturated fatty acid, is the main constituent of olive oil [9, 10]. We have previously shown that mice fed with chow rich in olive oil had increased survival rates, decreased neutrophil accumulation, lowered plasma TNF- α , prostaglandin E₂, and leukotriene B₄ levels in the peritoneal cavity after LPS-induced endotoxemic shock [11].

Omega-9 is a natural agonist of peroxisome proliferator-activated receptor (PPAR) [12]. Three PPAR isotypes were described so far: PPAR alpha, PPAR gamma, and PPAR delta/beta. PPARs modulate metabolism, inflammation, and infection [13–15]. PPAR gamma ligands had been demonstrated to protect septic animals against microvascular dysfunction [16] and enhance bacterial elimination through neutrophil extracellular trap formation [17]. Furthermore, we showed that omega-9 decreased nonesterified fatty acids in mice after enteric injection [18] and pretreatment with omega-9 improved lipid metabolism acting on PPAR target genes with increasing survival of septic mice [19].

Here, we investigated the effect of omega-9 on systemic corticosterone levels, inflammatory markers, cell migration, bacterial clearance, and nuclear receptor PPAR gamma expression in both liver and adipose tissues during experimental sepsis. We also studied omega-9 effects on leukocyte rolling *in vivo*.

2. Materials and Methods

2.1. Animals. Male Swiss mice weighing between 18 and 20 g were obtained from FIOCRUZ (Rio de Janeiro, Brazil) and were purchased from Janvier Lab (Saint Berthevin, France). The animals were accommodated in a room at 22°C, with free access to water and food and alternating light/dark cycle of 12 h. All experiments were approved by the Oswaldo Cruz Foundation Animal Welfare Committee under license number LW-36/10 and L-015/2015 and by the Regierung von Oberbayern, 002-08. The weight of the animals was measured on days 1, 7, and 14, and the food intake was quantified for each cage. We divided the amount of chow that was consumed by the number of animals in each cage, and then, we estimate the food intake per animal.

2.2. Omega-9 or Palmitic Acid Treatment. Mice were given a daily dose of omega-9 (oleic acid, 18:1 (n-9), Sigma) or palmitic acid (16:0, Sigma) for 14 days before CLP. For the intravital microscopy experiments, the animals received omega-9 for 8 days. We prepared oleate solution by water

addition according to previous works [20–22]. Briefly, we added NaOH to reach pH 12.0 and sonicated; after oleate solubilization, we adjusted the pH to 7.6 with HCl. We gave by gavage 0.28 mg of omega-9 (100 μ L) or 0.26 mg of palmitic acid (100 μ L) per day. Control mice received 100 μ L of saline.

2.3. Cecal Ligation and Puncture (CLP). Mice received omega-9 or saline for 14 days orally. On the 15th day, we induced polymicrobial sepsis by CLP, as we previously described [19]. Briefly, we anesthetized mice through intraperitoneal injection of ketamine (100 mg/kg) (Cristália) and xylazine (10 mg/kg) (Syntec). We made an incision through the linea alba; the cecum was exposed, ligated with sterile 3-0 silk, and perforated through and through twice with an 18 gauge needle. We extruded a small amount of fecal material through the hole, and the cecum was softly pushed into the abdomen. We sutured the area with nylon 3-0 (Shalon) in two layers. All mice received 1 mL of sterile 0.9% saline subcutaneously. For 24 h experiments, six hours after CLP, we treated mice with antibiotic imipenem (10 mg/kg) intraperitoneally. We submitted sham mice to the same procedures described above, but the cecum was not ligated nor punctured.

2.4. Peritoneal Lavage. Mice were submitted to euthanasia with isoflurane (Cristália) 6 h or 24 h after surgery. The peritoneal cavity was washed with saline (3 mL) under sterile conditions. Aliquots from the peritoneal washes were plated in tryptic soy for count of colony forming units (CFU) and used for total cell count in Turk solution (2% acetic acid), in Neubauer chambers. Differential leukocyte count was done in cytocentrifuged smears stained with panoptic (Laborclin). The remaining peritoneal wash was centrifuged, and the supernatant was collected and stored at –20°C for further cytokine quantification. We also counted total leukocytes in blood samples taken from a tail vein and analyzed differential leukocyte counts in blood smears.

2.5. Cytokine Analysis. TNF- α , IL-10, and IL-1 β were detected by enzyme-linked immunosorbent assay (ELISA, DuoSet kit, R&D systems, Minneapolis, MN, USA) according to the instructions of the manufacturer.

2.6. Western Blot Analysis. Detection of PPAR gamma was performed as previously described [22] with minor modifications. Briefly, we perfused organs with 20 mM ethylenediaminetetraacetic acid (EDTA) pH 7.4. We cut liver tissues into small pieces and mixed with lysis buffer (with a cocktail of protease inhibitors) at 4°C in (Complete, Roche AG, Basel, Switzerland). We lysed periepididymal adipose tissues at 4°C in RIPA buffer with protease inhibitors (Roche AG, Basel, Switzerland) and phosphatase inhibitor cocktail (Roche). We stored tissues at –20°C for further protein quantification by BCA. Western blot analysis was done with whole liver and adipose tissue lysates (40 μ g of proteins) using anti-PPAR gamma (1:1000, Santa Cruz) and anti- β -actin (1:15000 dilution, Sigma), and detection was performed with the “SuperSignal Chemiluminescence” kit (Pierce), after exposing the membrane to an autoradiograph film

(GE Healthcare). Bands were digitalized and quantified by the ImageMaster 2D Elite program.

2.7. Corticosterone Levels. Animals were euthanized using an overdose of isoflurane (Cristália), during the nadir (08:00 h) of the circadian rhythm [23, 24], and blood was straightway collected through cardiac puncture with saline with heparin (400 U/mL). Plasma was obtained after sample centrifugation for 10 min at 1000×g and stored at -20°C until use. Corticosterone plasma levels were evaluated using radioimmunoassay (MP Biomedicals, Solon, OH, USA) following the guidelines of the manufacturer.

2.8. Intravital Microscopy of the Cremaster Muscle. Intravital microscopy of the mouse cremaster muscle postcapillary venules was used to study leukocyte rolling under different inflammatory conditions as previously described [25]. Briefly, we anesthetized the animals with intraperitoneal injection of ketamine (125 mg/kg, Ketanest®, Pfizer GmbH, Karlsruhe, Germany) and xylazine (12.5 mg/kg; Rompun®, Bayer, Leverkusen, Germany). Afterward, they were transferred the animals to a heating pad to keep temperature at 37°C . After surgical insertion of a tracheal tube, the carotid artery was cannulated to take the blood sample and for systemic application of antibodies. We used the P-selectin-blocking mAb RB40.34 and the E-selectin-blocking mAb 9A9 which were generous gifts from Dietmar Vestweber (MPI Münster) and Barry Wolitzky (MitoKor, San Diego), respectively. The scrotum was surgically opened, to exteriorize the cremaster muscle. After longitudinal incision and distribution of the muscle over a cover glass, the cremaster muscle was superfused with 35°C bicarbonate-buffered saline. We observed cremaster muscle postcapillary venules via an upright microscope (Olympus BX51) with an objective ($\times 40/0.8$ NA). We measured venular centerline red blood cell velocity during the experiment via an online cross-correlation program (CircuSoft Instrumentation, Hockessin, Delaware, USA). We recorded the experiments via a CCD camera system (model CF8/1; Kappa, Gleichen, Germany) on a Panasonic S-VHS recorder and performed offline the analysis of experiments using the used videotapes. We measured diameter and segment length of postcapillary venules using a digital image processing system [26]. Postcapillary venules were recorded to calculate rolling flux fraction (percentage of rolling leukocytes relative to the number of leukocytes passing the vessel). Leukocytes with a displacement of $>15\ \mu\text{m}$ were tracked by using ImageJ (National Institutes of Health, Bethesda, MD). In some experiments, TNF- α (500 ng) was injected intrascrotally 2.5 h before intravital imaging.

2.9. Intravital Microscopy of Brain Microcirculation. The cerebral microcirculation in mice was assessed as previously described [16]. Briefly, we anesthetized the animals with ketamine (75 mg/kg, i.p.) and xylazine (10 mg/kg, i.p.) and fixed in a stereotaxic frame. Then, the left parietal bone was exposed by a midline skin incision; a cranial window overlying the right parietal bone (1–5 mm lateral, between the coronal suture and the lambdoid suture) was created with a

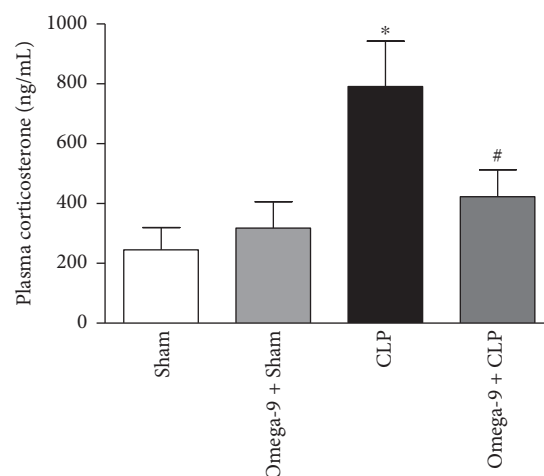


FIGURE 1: Omega-9 decreased cortisol levels in septic mouse plasma. Animals were treated with omega-9 for 14 days. On the 15th day, CLP was performed, and 24 h after, the plasma was collected for the quantification corticosterone. Each bar represents the mean \pm SEM of at least 7 animals. * and + $p < 0.05$ compared to sham and sham + omega-9, respectively, and # compared to CLP.

high-speed drill, and the dura mater and the arachnoid membranes were excised and withdrawn to expose the cerebral microcirculation. The cranial window was suffused with artificial cerebrospinal fluid (in mmol: KCl, 2.95; NaCl, 132, CaCl_2 , 1.71; MgCl_2 , 0.64; NaHCO_3 , 24.6; dextrose, 3.71; and urea, 6.7; at 37°C , pH 7.4). Animals were then placed under an upright fixed-stage intravital microscope equipped with a LED lamp (Zeiss, model Axio Scope) coupled to a Zeiss Axiocam and processed using ZEN software (Zeiss). Water immersion objective 20x were used in the experiments and produced total magnifications of 200x.

The visualization of brain microvascular surface was facilitated by intravenous administration of 0.1 mL 2% fluorescein isothiocyanate- (FITC-) labeled dextran (molecular weight 150,000) and by epi-illumination at 460–490 nm using a 520 nm emission filter. Leukocytes were labeled using the fluorescent dye rhodamine 6G (0.3 mg/kg) and visualized by epi-illumination at 536–556 nm excitation using a 615 nm emission wavelength. Analysis of leukocyte-endothelium interactions was carried out by analyzing four randomly selected venular segments (30 to 100 μm in diameter) in each preparation. Rolling leukocytes were counted as the number of cells crossing the venular segment at speed less than the red blood cells for 1 minute. Adherent leukocytes were defined as the total number of leukocytes that were firmly attached to the endothelium and did not change position during 1 minute of observation and expressed as a number of cells/ $\text{mm}^2/100\ \mu\text{m}$.

2.10. Statistical Analysis. Results were analyzed by “one-way” ANOVA followed by Newman-Keuls using GraphPad Prism 5.0. Values of $p < 0.05$ were considered significant. Data are presented as mean \pm SEM or individual values with a median.

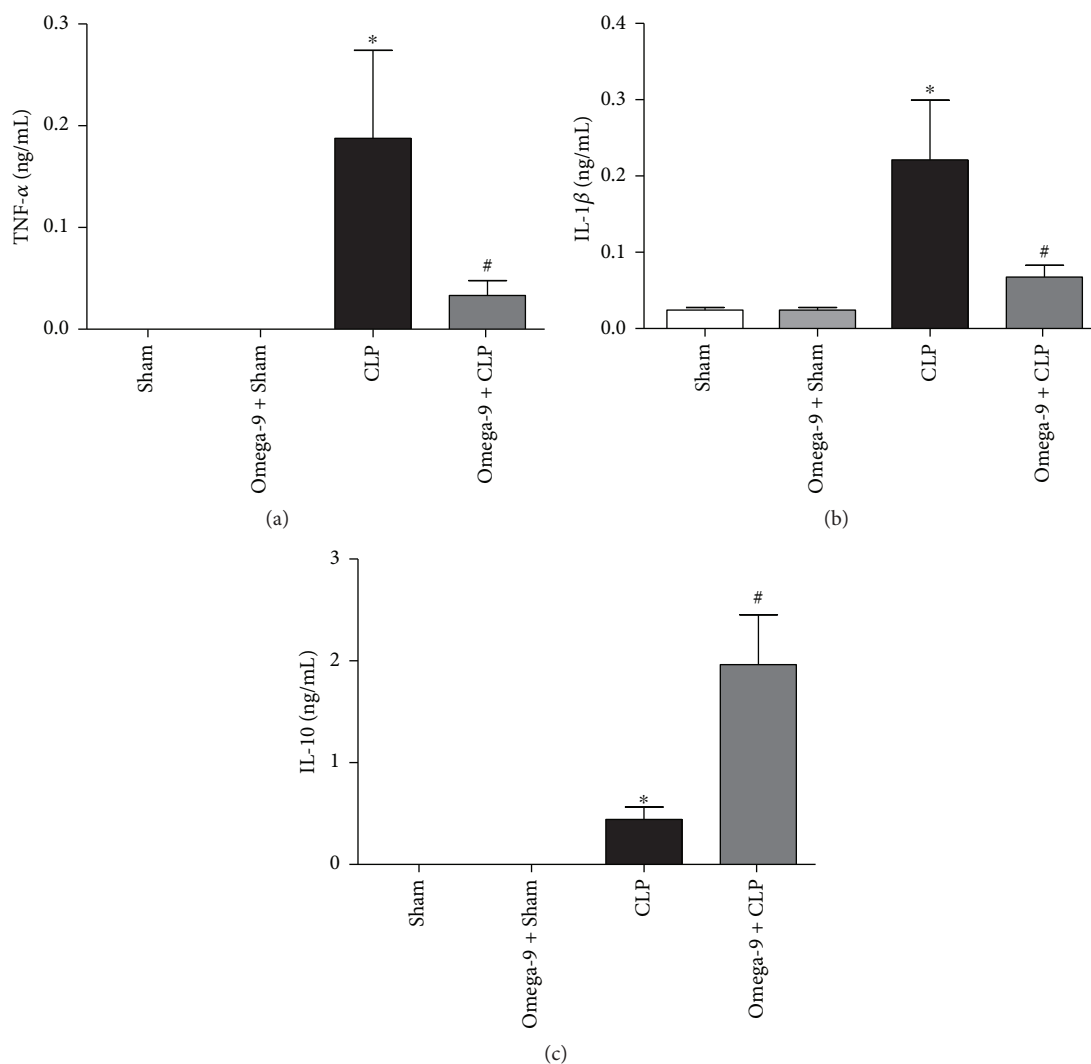


FIGURE 2: Omega-9 reduced proinflammatory cytokines but increases the level of the anti-inflammatory cytokine IL-10 in the peritoneal lavage of mice submitted to CLP. Animals were treated with omega-9 for 14 days. On the 15th day, CLP was performed, and 24 h after, the peritoneal lavage was collected for the quantification of TNF- α (a), IL-1 β (b), and IL-10 (c). Each bar represents the mean \pm SEM of at least 7 animals. * and # $p < 0.05$ compared to sham and sham + omega-9, respectively, and # compared to CLP.

3. Results

3.1. Omega-9 Treatment Decreased Corticosterone Serum Levels in Septic Mice. We previously demonstrated that omega-9 treatment increased survival and ameliorated clinical scores after CLP-induced sepsis [19]. In the present work, we continue to investigate the mechanisms behind the protective effects of omega-9.

High cortisol levels (a 10-fold increase compared to health volunteers) [27] are linked to disease severity and hyperinflammation during sepsis. Here, we observed high levels of corticosterone in septic mice. Omega-9 treatment prevented the increase in plasma corticosterone levels (Figure 1), reinforcing our previous data where omega-9 pretreatment decreased biochemical markers of organ dysfunction [19].

3.2. Omega-9 Reduced IL-1 β and TNF- α and Increased IL-10 Production in Septic Mice. Monocytes and neutrophils

produce IL-1 β , tumor necrosis factor- α (TNF- α), and IL-10, cytokines constituting the storm during sepsis [27–29]. Septic mice had higher levels of TNF- α , IL- β , and IL-10 in the peritoneal lavage compared to the control (Figures 2(a)–2(c)) while omega-9 pretreatment strongly decreased the levels of TNF- α (Figure 2(a)) and IL-1 β (Figure 2(b)) in septic mice. Interestingly, IL-10 increased in the peritoneal lavage of septic mice receiving omega-9 (Figure 2(c)).

3.3. Omega-9 Decreased Neutrophil Migration in the Peritoneum of Septic Mice. One of the main steps of the immune response during inflammation is the recruitment of myeloid cells into inflamed tissue. We evaluated the effect of omega-9 pretreatment on cell migration and accumulation into the peritoneal cavity of septic mice. Septic mice presented higher leukocyte numbers in the peritoneal cavity, characterized by an increase in neutrophil numbers when compared to sham animals in both time points analyzed, 6 h

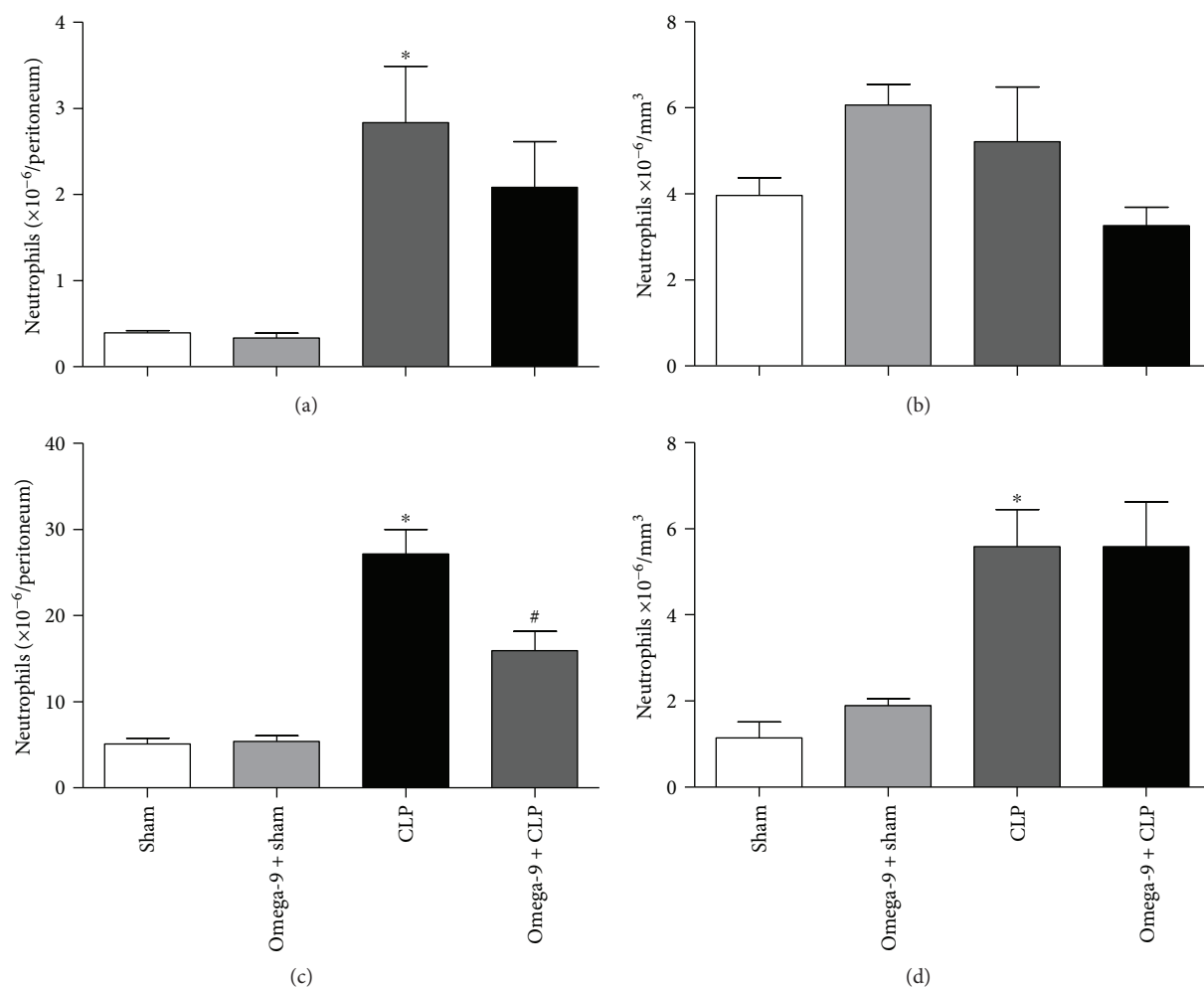


FIGURE 3: Omega-9 reduced leukocyte migration to the peritoneal cavity in septic mice. Animals were treated with omega-9 for 14 days. On the 15th day, CLP was performed; 6 h and 24 h after, the peritoneal lavage was collected for the leukocyte counts. Counts of peritoneal neutrophils (a) and systemic neutrophils (b) 6 h after CLP and counts of peritoneal neutrophils (c) and systemic neutrophils (d). Control groups received the same volume of saline. Results are mean \pm SEM from at least 7 animals. * and # $p < 0.05$ compared to sham and sham + omega-9, respectively, and # compared to CLP.

and 24 h after CLP (Figures 3(a) and 3(c)). Neutrophil accumulation in the peritoneal cavity was reduced in septic mice treated with omega-9 only 24 h after CLP (Figure 3(c)), showing no significant effect at an earlier time point (Figure 3(a)).

3.4. Omega-9 Impaired Leukocyte Rolling in Inflamed Microvessels In Vivo. To analyze the role of omega-9 in leukocyte rolling *in vivo*, we used intravital microscopy in surgically prepared mouse cremaster muscle postcapillary venules [30, 31]. Leukocyte rolling is induced by the surgery of the cremaster and is exclusively dependent on P-selectin (<45 min after surgery) [32–35]. We showed a decrease in rolling in omega-9-treated mice compared to the control (Figure 4(a) and Supplemental Movies 2 and 1, respectively). Systemic injection of P-selectin-blocking antibody RB40.34 abolished leukocyte rolling (Figure 4(a)) endorsing the dependence of P-selectin on rolling in the trauma model. Next, we used TNF- α stimulation of the mouse cremaster muscle in Swiss mice pretreated with omega-9 to study leukocyte rolling. In TNF- α -stimulated mice, leukocyte rolling

is P- and E-selectin dependent [35]. We found that rolling flux fraction was significantly diminished in omega-9-treated animals compared to that in controls (Figure 4(b)). There was no alteration in neutrophil blood counts comparing omega-9-treated and untreated animals (data not shown). Microvascular injection of anti-P-selectin and anti-E-selectin-blocking antibodies Rb40.34 and 9A9, respectively, abolished rolling completely demonstrating that rolling in this model is indeed dependent on P- and E-selectins, as shown previously [35]. Hemodynamic conditions were alike between the different treatment groups (Supplemental Table 1).

3.5. Omega-9 Impaired Leukocyte Rolling in Septic Mice. Figure 5 illustrates the leukocyte-endothelium interaction in cerebral venules of mice subjected to sham or CLP with (omega-9 + CLP) or without (CLP) omega-9 treatment. Rolling leukocytes in the CLP group were significantly increased when compared to the sham group. Pretreatment with omega-9 significantly attenuated the CLP-induced leukocyte rolling in the cerebral microcirculation compared with the

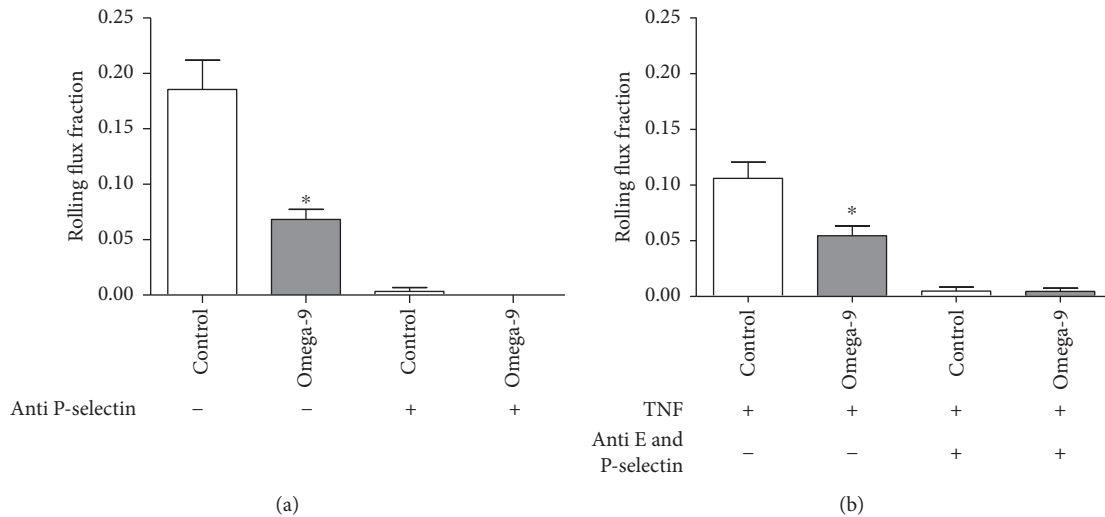


FIGURE 4: Omega-9 reduced rolling flux fraction in cremaster in trauma and TNF models. We treated the animals with omega-9 for 8 days prior to the experiments. On the day 9, we analyzed rolling in postcapillary venules of mouse cremaster muscle in two models: trauma (a) and TNF (b) models. We also treated animals of the trauma model with anti-P-selectin and of the TNF model with anti-P- and E-selectins. Rolling flux fraction was analyzed. Each bar is mean from at least 5 animals. * and # $p < 0.05$ compared to sham and sham + omega-9, respectively, and # compared to CLP.

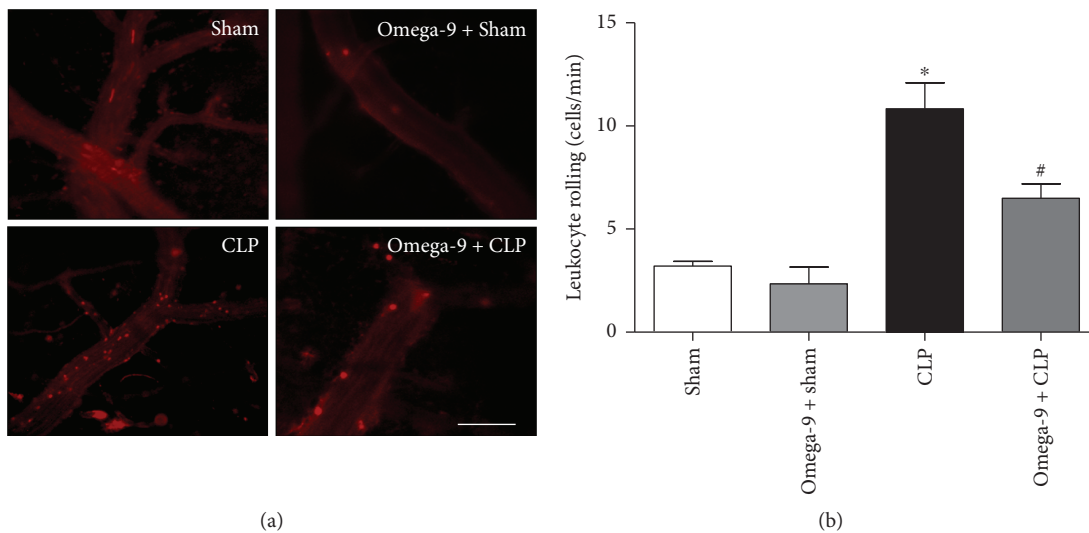


FIGURE 5: Omega-9 reduced leukocyte rolling in mice submitted to CLP. Fluorescent intravital microscopy images showing leukocyte-endothelium interaction in the cerebral postcapillary venules after 24 h of sepsis in mice (a). Animals were treated with vehicle (CLP) or omega-9 (omega-9 + CLP) compared to sham operated pretreated with vehicle (sham) or omega-9 (omega-9 + sham) mice. Rolling of leukocytes in the microvasculature was expressed as number of cells per minute (b). Data indicate mean \pm SEM, 5 mice per group. * $p < 0.001$ versus the sham group; # $p < 0.05$ versus the CLP group.

CLP-untreated group. Omega-9 pretreatment did not induce any effect in cerebral venules of sham mice.

3.6. Omega-9 Increased Bacterial Killing in the Mouse Peritoneal Cavity after CLP. Because omega-9 treatment modulated cytokine response and neutrophil accumulation in the peritoneal cavity, we decided to evaluate the impact of omega-9 treatment on the bacterial load after CLP. We observed that despite decreasing neutrophil accumulation in the peritoneal cavity, omega-9 pretreatment did not

impair the bacterial elimination by the innate immune response. To our surprise, omega-9 pretreatment increased bacterial clearance in the peritoneum (Figure 6).

3.7. Omega-9 Restored PPAR Gamma Expression in the Liver and Adipose Tissue in Septic Mice. Omega-9 is a PPAR ligand and the treatment displayed an anti-inflammatory profile, so we investigate the levels of PPAR gamma in the liver and adipose tissues. We confirmed the reduction of PPAR gamma expression in both liver and adipose tissues from septic mice.

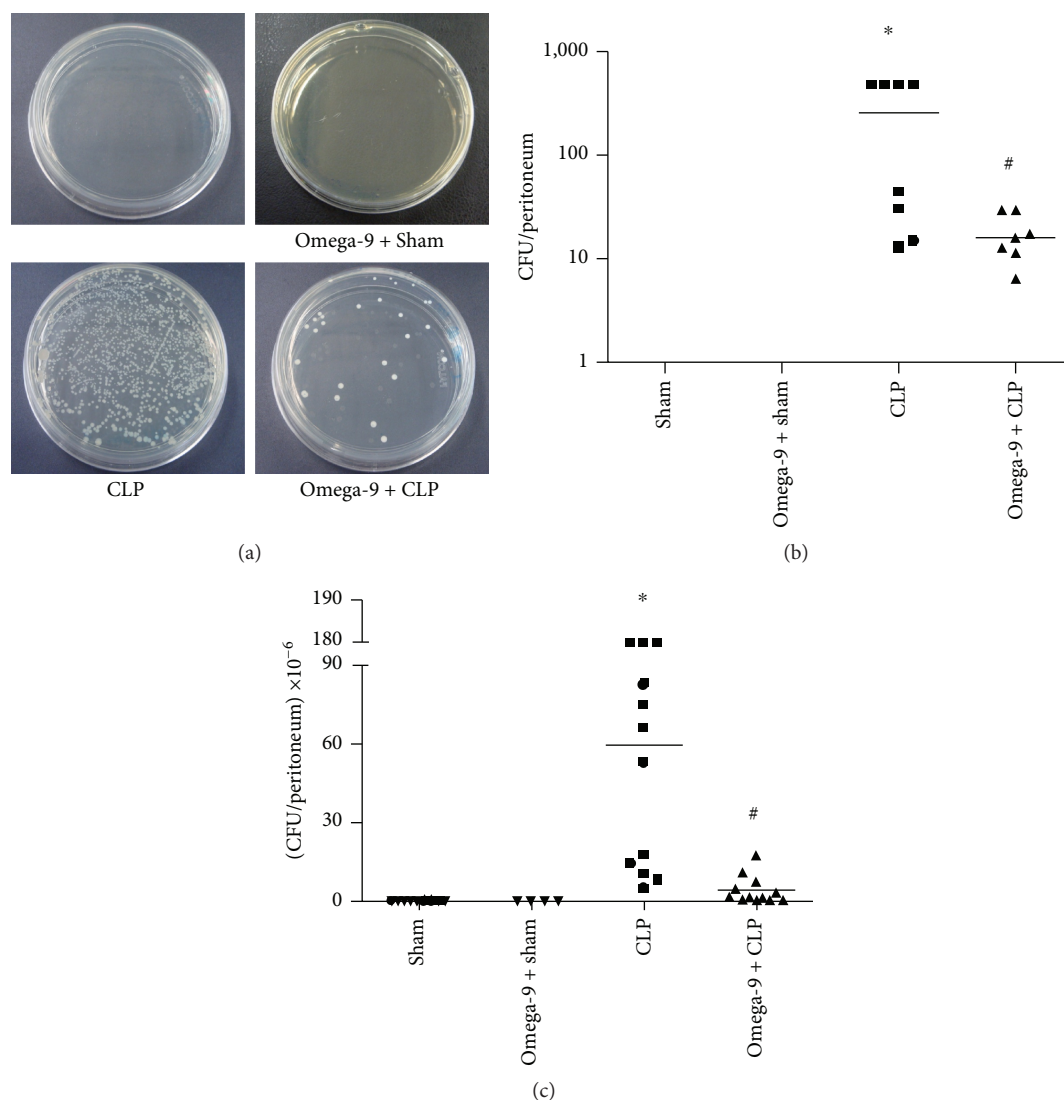


FIGURE 6: Omega-9 improved bacterial clearance in Swiss mice submitted to CLP. Animals were treated with omega-9 for 14 days. On the 15th day, CLP was performed, and 6 h (b) and 24 h (c) after, the peritoneal lavage was collected and plated on TSA-coated plates for CFU counts. Results are represented as individual values and median from at least 7 animals. In (a), there are representative photos of the exposed graph (c). * and + compared to sham and sham + omega-9, respectively, and # compared to CLP.

In contrast, omega-9-pretreated animals maintained PPAR gamma expression levels similar to sham mice in the liver (Figure 7), and it was even higher in adipose tissue (Figure 8).

4. Discussion

Mortality from sepsis varies from 30 to 50%, and incidences are rising due to a rising elderly population and an increased number of patients with immunosuppression [36–39]. The number of patients with sepsis rose from 387,330 to 1.1 million from 1996 to 2011 and probably will reach 2 million by 2020 in the US [40]. Sepsis mortality is similar to heart attacks and exceeds stroke deaths. Therapeutic procedures are urgently needed [41]. Hence, infections leading to damage in the microcirculation can compromise the multiple organ function, including the lungs, heart, liver, gut, kidneys, and brain, causing hypotension and myocardial dysfunction,

microvascular leak, thrombocytopenia, disseminated intravascular coagulation (DIC), acute respiratory distress syndrome (ARDS), acute kidney injury (AKI), and acute brain injury [42–45].

Therapies with anti-Toll-like receptor 4, anti-TNF- α , and activated protein C failed in clinical trials, requiring a rethinking of sepsis pathophysiology [29, 46–51]. Food intake can influence the immune response [52–57]. The Mediterranean diet, composed of olive oil as the main source of fat, is an example of how lipids can influence the inflammatory response [7, 58]. This diet has been linked with a reduced risk of cancer and vascular illnesses and also with a decreased chronic disease incidence, such as Parkinson [6, 8, 59]. Omega-9 is a monounsaturated fatty acid, the main olive oil component [9, 10]. Omega-9 protects from insulin resistance and prevents endothelial dysfunction in response to proinflammatory signals. Omega-9 also

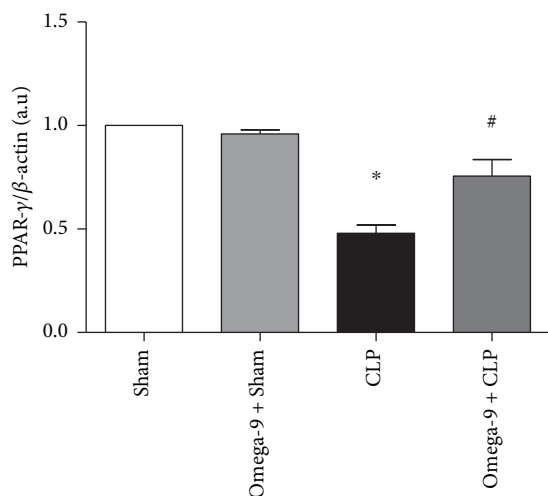


FIGURE 7: Omega-9 treatment restored the expression of PPAR gamma in the liver of CLP mice. Animals were treated with omega-9 for 14 days. On the 15th day, CLP was performed, and liver was removed from animals 24 h after CLP. Graphics in this figure represent the rate between densitometric analyses of PPAR gamma and β -actin bands. * and + $p < 0.05$ compared to sham and sham + omega-9, respectively, and # compared to CLP.

reduces vascular smooth muscle cell proliferation and apoptosis, suggesting a beneficial role in atherosclerosis [60]. Furthermore, omega-9 decreases the release of cytokines, increases the killing ability of neutrophils, and improves bacterial elimination [61].

We previously have shown that omega-9 prevents organ dysfunction and increases survival during sepsis [19]. Some reports associated kidney and liver dysfunction during sepsis with an increase in plasma cortisol levels and decreased ability to metabolize cortisol. Both the adrenal gland activation to produce glucocorticoid and catecholamine and the diminished ability to break down cortisol by suppressed expression and impaired cortisol-metabolizing enzyme activity are characteristic of host innate reaction to aggression [62, 63]. Here, we showed that septic animals had increased corticosterone plasma levels which could be decreased by omega-9 treatment. We suggest that omega-9 protective effect on organ dysfunction may be at least partially related to its effect on normalizing corticosterone levels in our animal model.

Neutrophils are the highest leukocyte population in the blood of humans (50–70% of leukocytes). They can be quickly mobilized from bone marrow into the circulation after immune activation and physical exercise or caused by the release of corticoids and adrenaline [64]. Reservoir organs may contribute to fast mobilization during inflammatory processes. Recruitment of neutrophil to the inflammatory site is a process that comprehends tethering, rolling, adhesion, crawling, and extravasation. A spatial and temporal expression and adhesion molecule interaction on neutrophils (i.e., L-selectin, PSGL-1, LFA-1, and Mac-1) and their ligands on endothelial cells (i.e., E- and P-selectin, and ICAM-I) are crucial for effective extravasation of neutrophils into the tissues [65]. Negatively modulating the expression of

these adhesion molecules, in turn, will influence leukocyte migration into the inflamed tissue.

Ingestion of the monounsaturated fatty acid-rich diet decreased the expression of ICAM-I [66]. Human embryonic endothelial cells (HUVECs) treated with omega-9 had diminished expression of LPS-stimulated VCAM-I, E-selectin, and ICAM-I [67]. Mice fed with chow rich in olive oil decreased neutrophil accumulation in the peritoneal cavity 24 h after LPS injection [11]. Our data add to this as they showed a decrease of neutrophil influx into the peritoneum in omega-9-treated animals, preventing exacerbated inflammation. Interestingly, just the treatment with unsaturated fatty acid was effective in controlling neutrophil influx, because supplementation with a saturated fatty acid palmitic acid did not affect neutrophil accumulation in septic mice (Supplemental Figure 1). Using the trauma model, where rolling depends on P-selectin, omega-9-treated animals showed a decrease in rolling that could be confirmed in the TNF model suggesting that omega-9 regulates selectin-dependent rolling *in vivo*. Omega-9 effect reducing leukocyte rolling extended to septic animals. In the sepsis model, omega-9 was also very effective in inhibiting rolling of leukocytes on endothelial cells of septic mice.

Neutrophils fight and destroy invading microorganisms by diverse mechanisms such as phagocytosis, production of ROS, and formation of neutrophil extracellular trap (NET) [68]. Neutrophils produce proinflammatory cytokines and release nitric oxide and ROS [69], and the excess of these mediators can increase vascular permeability leading to organ damage [70, 71]. By attenuating the accumulation of neutrophils in the peritoneum, there is a decrease in organ damage caused by the excessive overactivated neutrophil numbers. Interestingly, we also detected increased bacterial clearance in the peritoneal lavage in omega-9-treated septic animals. Similar results have been obtained recently by our group using low dose dasatinib treatment in septic mice [72]. Neutrophils increase their ability to produce ROS after treatment with omega-9 [73]. Supplementation for only 5 days is enough for omega-9 to incorporate into neutrophil membranes [74]. Also, omega-9 enhanced phagocytosis by neutrophils 30 min after incubation and improved the microorganism elimination *in vitro* [75]. These effects are not achieved using omega 3 or 6 [65]. Our results showed that omega-9 was effective in increasing the bacterial elimination by the host during sepsis. Intake of omega-3 daily for 14 days alters gut flora decreasing species diversity, but several butyrate-producing bacteria increased [76]. Similarly, a decrease in Faecalibacterium, often linked to an increase in the Bacteroidetes and butyrate-producing bacteria belonging to the Lachnospiraceae, has been observed following omega-3 supplementation [77]. Accordingly, a study suggests that PUFA supplementation improves gut function and microbiome composition [78]. Concerning infection models, neutrophils treated with omega-3 showed enhanced antiparasitic activity against *Plasmodium falciparum* [79] and dietary omega-3 decreased bacterial load and increased the survival rate in septic mice [80]. In our sepsis model, it is possible that although there were fewer neutrophils in the peritoneum, they are still able to fight the infection efficiently, actively

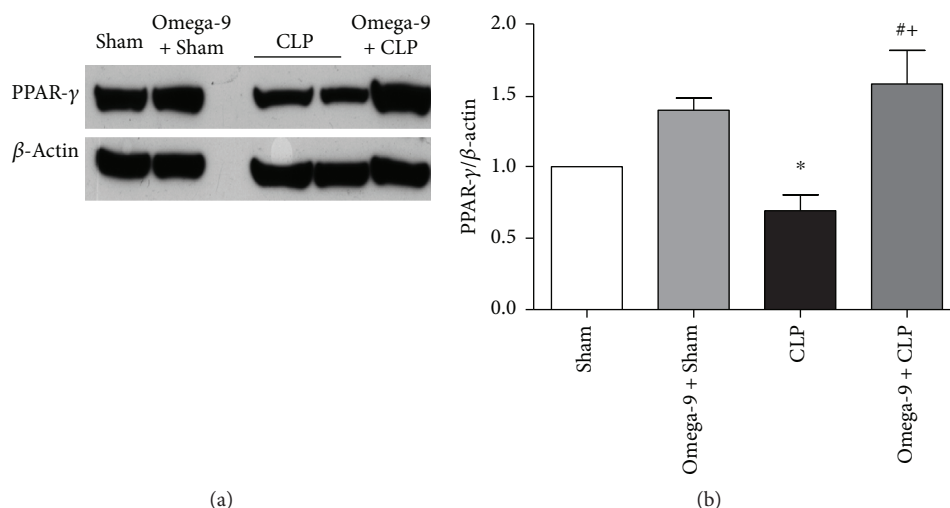


FIGURE 8: Omega-9 treatment restored PPAR gamma expression in the adipose tissue of CLP mice. Animals were treated with omega-9 for 14 days. On the 15th day, CLP was performed, and adipose tissue was removed from animals 24 h after CLP. Graphics in this figure represent the rate between densitometric analyses of PPAR gamma and β -actin bands. * and + $p < 0.05$ compared to sham and sham + omega-9, respectively, and # compared to CLP.

killing bacteria without causing excessive tissue damage. Omega-9 just prevented excessive neutrophil influx, because it did not affect early neutrophil migration to the peritoneal cavity but inhibited exacerbated neutrophil influx 24 h after CLP. CFU counts corroborate because bacterial elimination was effective even in earlier time point in omega-9-treated septic animals. We do not exclude the macrophage role on bacterial killing. So far, our data only allow us to conclude that omega-9 has not altered mononuclear cell counts (data not shown).

Omega-9 can bind to PPAR, known as lipid sensors [12]. PPAR are ligand-activated transcription factors with an important role in the inflammation and lipid and glucose metabolism [13, 14]. PPAR gamma activation diminished inflammatory response, increased survival, and attenuated neutrophil migration in different models of inflammation [81–84]. Moreover, we have shown that mice fed with omega-9 and submitted to sepsis produced less proinflammatory cytokines and more IL-10, which agrees with studies showing the activation of PPAR gamma-enhanced production of the anti-inflammatory cytokine IL-10 [17, 85, 86]. We showed that PPAR gamma decreases rolling and adhesion in brain microcirculation of septic mice [16]. Literature shows endothelial PPAR gamma downregulates P-selectin expression decreasing leukocyte-endothelial interactions [87]. Omega-9 binding to PPAR gamma may modulate P-selectin expression on leukocytes, decreasing their ability to roll. PPAR also increases bacterial elimination. Lack of PPAR alpha is linked with a high bacterial load in septic mice [88]. We showed that PPAR gamma rosiglitazone leads to increased bacterial clearance in septic mice. Leukocytes from PPAR gamma agonist-treated septic animals are activated; they increased intracellular ROS and increased the capacity of killing bacteria by NET formation [17].

PPAR gamma expression is decreased in many organs like lung, liver, and adipose tissue during endotoxemia and

sepsis [81, 89]. Interestingly, endotoxin decreased PPAR gamma through the increase of TNF release [90]. Based on the findings by Zhou et al. and our own results, we suggested the correlation between TNF production and decreased PPAR gamma expression. Studies with phytochemical curcumin have related its anti-inflammatory potential and mortality protection to increased PPAR gamma expression in the liver [91]. Our data showed that PPAR gamma expression in the liver decreases in septic animals and omega-9 treatment increases it, suggesting that PPAR gamma liver expression may be involved in omega-9-protective effects during sepsis.

Adipose tissue plays an essential role on the inflammatory response regulation in many metabolic diseases, including metabolic syndrome, obesity, diabetes, and sepsis [92, 93]. PPAR gamma controls adipocyte differentiation and function. LPS or TNF alpha decreased PPAR gamma expression in adipose tissue [94], as seen in our model of sepsis. The capacity of maintaining the anti-inflammatory grade of visceral adipose tissue by the PPAR gamma agonist is associated with the prevention of lung injury observed during sepsis. The PPAR gamma agonist pioglitazone decreased mortality of septic mice because it diminished inflammatory cytokine production in omental tissue, controlling visceral adipose tissue inflammation [93]. We reinforce the role of adipose tissue in negative modulation of exacerbated inflammation during sepsis. PPAR gamma expression in adipose tissue may be relevant because it was lower in septic animals and it was restored by omega-9 treatment. PPAR gamma expression is induced by its ligands (Frygiel-Górniak, 2014). Although omega-9 has other targets, we believe that omega-9 binding to PPAR gamma would restore PPAR gamma protein expression and account, at least partially, for omega-9-modulatory effect during sepsis.

In our previous report, we showed that omega-9 improves lipid metabolism in septic mice increasing their survival by

activating PPAR-regulated genes [19]. Accordingly, herein, we showed that omega-9 treatment dampens inflammation and increases bacterial clearance in septic mice possibly involving PPAR gamma. Therefore, omega-9 treatment has dual effect regulating lipid metabolism and inflammation.

4.1. Conclusion and Consideration. Omega-9 modulated the immune response in septic mice. Omega-9 decreased the production of proinflammatory cytokines, increased IL-10 production, reduced neutrophil migration and accumulation in the site of infection, and also improved bacterial clearance. Omega-9 treatment affected leukocyte trafficking in septic animals and in inflamed cremaster muscle postcapillary venules by decreasing selectin-dependent leukocyte rolling *in vivo*. Those effects controlling inflammation and increasing bacterial clearance likely contribute to the better outcome of sepsis. Therefore, omega-9-enriched diet, particularly olive oil, as supplemental food, may be advisable in patients with infections and might sum up with the other benefits of the ingestion of diets composed of unsaturated fatty acids.

Data Availability

All data used to support the findings of this work are included within the article and the supplementary information file.

Disclosure

The funders did not design the study, collect data analyzed, and prepare the manuscript.

Conflicts of Interest

The authors declare that there is no conflict of interest regarding the publication of this paper.

Authors' Contributions

Isabel Matos Medeiros-de-Moraes, Cassiano Felipe Gonçalves-de-Albuquerque, Hugo Caire de Castro-Faria-Neto, and Adriana Ribeiro Silva contributed equally to this work.

Acknowledgments

Our work was supported by grants from Fundação Carlos Chagas Filho de Amparo à Pesquisa do Estado do Rio de Janeiro (FAPERJ), Conselho Nacional de Desenvolvimento Científico e Tecnológico (CNPq), Programa Estratégico de Apoio à Pesquisa em Saúde (PAPES), Fundação Oswaldo Cruz, and Universidade Federal do Estado do Rio de Janeiro. We also acknowledge financial support by the European Community's Seventh Framework Programme (FP7-2007-2013) under grant agreement HEALTH-F4-2011-282095 (TARKINAID), and Programa de Produtividade Científica da Universidade Estácio de Sá. M. S. is supported by DFG grant SBF14, project B01.

Supplementary Materials

Supplementary 1. Supplemental videos from intravital microscopy in surgically prepared mouse cremaster muscle postcapillary venules in the trauma model are available. Video 1 was recorded from untreated animals and video 2 from the omega-9-treated group. Figure 4 shows the data.

Supplementary 2. Supplemental Table 1: hemodynamic conditions and systemic leukocyte counts from untreated or omega-9-treated Swiss mice in trauma and TNF models. We also treated animals of the trauma model with anti-P-selectin and of the TNF model with anti-P- and E-selectins.

Supplementary 3. Supplemental Figure 1: palmitic acid effect on neutrophil accumulation in the peritoneal cavity in septic mice. Animals were treated with palmitic acid for 14 days. On the 15th day, CLP was performed, and 24 h after, the peritoneal lavage was collected for the neutrophil counts. Control groups received saline. Results are mean \pm SEM from at least 6 animals. The experiment was repeated twice. * $p < 0.05$ compared to sham and sham + palmitic acid.

References

- [1] C. Adrie, C. Alberti, C. Chaix-Couturier et al., "Epidemiology and economic evaluation of severe sepsis in France: age, severity, infection site, and place of acquisition (community, hospital, or intensive care unit) as determinants of workload and cost," *Journal of Critical Care*, vol. 20, no. 1, pp. 46–58, 2005.
- [2] D. J. O'Brien and I. M. Gould, "Maximizing the impact of antimicrobial stewardship: the role of diagnostics, national and international efforts," *Current Opinion in Infectious Diseases*, vol. 26, no. 4, pp. 352–358, 2013.
- [3] M. Singer, C. S. Deutschman, C. W. Seymour et al., "The Third International Consensus Definitions for Sepsis and Septic Shock (Sepsis-3)," *JAMA*, vol. 315, no. 8, pp. 801–810, 2016.
- [4] K. N. Iskander, M. F. Osuchowski, D. J. Stearns-Kurosawa et al., "Sepsis: multiple abnormalities, heterogeneous responses, and evolving understanding," *Physiological Reviews*, vol. 93, no. 3, pp. 1247–1288, 2013.
- [5] P. C. Calder, "Polyunsaturated fatty acids and inflammation," *Prostaglandins, Leukotrienes, and Essential Fatty Acids*, vol. 75, no. 3, pp. 197–202, 2006.
- [6] E. Eschrich, R. Moral, and M. Solanas, "Olive oil, an essential component of the Mediterranean diet, and breast cancer," *Public Health Nutrition*, vol. 14, no. 12A, pp. 2323–2332, 2011.
- [7] D. B. Panagiotakos, K. Dimakopoulou, K. Katsouyanni et al., "Mediterranean diet and inflammatory response in myocardial infarction survivors," *International Journal of Epidemiology*, vol. 38, no. 3, pp. 856–866, 2009.
- [8] F. Sofi, F. Cesari, R. Abbate, G. F. Gensini, and A. Casini, "Adherence to Mediterranean diet and health status: meta-analysis," *BMJ*, vol. 337, p. a1344, 2008.
- [9] E. Tvřzicka, L. S. Kremmyda, B. Stankova, and A. Zak, "Fatty acids as biocompounds: their role in human metabolism, health and disease—a review. Part 1: classification, dietary sources and biological functions," *Biomedical Papers of the Medical Faculty of the University Palacky, Olomouc, Czech Republic*, vol. 155, no. 2, pp. 117–130, 2011.

- [10] E. Waterman and B. Lockwood, "Active components and clinical applications of olive oil," *Alternative Medicine Review*, vol. 12, no. 4, pp. 331–342, 2007.
- [11] M. S. Leite, P. Pacheco, R. N. Gomes et al., "Mechanisms of increased survival after lipopolysaccharide-induced endotoxic shock in mice consuming olive oil-enriched diet," *Shock*, vol. 23, no. 2, pp. 173–178, 2005.
- [12] H. E. Xu, M. H. Lambert, V. G. Montana et al., "Molecular recognition of fatty acids by peroxisome proliferator-activated receptors," *Molecular Cell*, vol. 3, no. 3, pp. 397–403, 1999.
- [13] S. J. Bensinger and P. Tontonoz, "Integration of metabolism and inflammation by lipid-activated nuclear receptors," *Nature*, vol. 454, no. 7203, pp. 470–477, 2008.
- [14] M. D. Neher, S. Weckbach, M. S. Huber-Lang, and P. F. Stahel, "New insights into the role of peroxisome proliferator-activated receptors in regulating the inflammatory response after tissue injury," *PPAR Research*, vol. 2012, Article ID 728461, 13 pages, 2012.
- [15] A. T. Reddy, S. P. Lakshmi, and R. C. Reddy, "PPAR γ in bacterial infections: a friend or foe?," *PPAR Research*, vol. 2016, Article ID 7963540, 7 pages, 2016.
- [16] C. V. Araujo, V. Estado, E. Tibirica, P. T. Bozza, H. C. Castro-Faria-Neto, and A. R. Silva, "PPAR gamma activation protects the brain against microvascular dysfunction in sepsis," *Microvascular Research*, vol. 84, no. 2, pp. 218–221, 2012.
- [17] C. V. Araujo, C. Campbell, C. F. Gonçalves-de-Albuquerque et al., "A PPAR γ agonist enhances bacterial clearance through neutrophil extracellular trap formation and improves survival in sepsis," *Shock*, vol. 45, no. 4, pp. 393–403, 2016.
- [18] C. F. Gonçalves de Albuquerque, P. Burth, M. Younes Ibrahim et al., "Reduced plasma nonesterified fatty acid levels and the advent of an acute lung injury in mice after intravenous or enteral oleic acid administration," *Mediators of Inflammation*, vol. 2012, Article ID 601032, 8 pages, 2012.
- [19] C. F. Gonçalves-de-Albuquerque, I. M. Medeiros-de-Moraes, F. M. d. J. Oliveira et al., "Omega-9 oleic acid induces fatty acid oxidation and decreases organ dysfunction and mortality in experimental sepsis," *Plos One*, vol. 11, no. 4, article e0153607, 2016.
- [20] C. Gonçalves-de-Albuquerque, P. Burth, A. Silva et al., "Oleic acid inhibits lung Na/K-ATPase in mice and induces injury with lipid body formation in leukocytes and eicosanoid production," *Journal of Inflammation*, vol. 10, no. 1, p. 34, 2013.
- [21] C. Gonçalves-de-Albuquerque, P. Burth, A. Silva et al., "Na/K-ATPase assay in the intact mice lung subjected to perfusion," *BMC Research Notes*, vol. 7, no. 1, p. 798, 2014.
- [22] C. F. Gonçalves-de-Albuquerque, A. R. Silva, P. Burth et al., "Oleic acid induces lung injury in mice through activation of the ERK pathway," *Mediators of Inflammation*, vol. 2012, Article ID 956509, 11 pages, 2012.
- [23] J. P. Prevatto, R. C. Torres, B. L. Diaz, P. M. R. Silva, M. A. Martins, and V. F. Carvalho, "Antioxidant treatment induces hyperactivation of the HPA axis by upregulating ACTH receptor in the adrenal and downregulating glucocorticoid receptors in the pituitary," *Oxidative Medicine and Cellular Longevity*, vol. 2017, Article ID 4156361, 10 pages, 2017.
- [24] R. C. Torres, N. S. Magalhães, P. M. R. e Silva, M. A. Martins, and V. F. Carvalho, "Activation of PPAR- γ reduces HPA axis activity in diabetic rats by up-regulating PI3K expression," *Experimental and Molecular Pathology*, vol. 101, no. 2, pp. 290–301, 2016.
- [25] A. R. M. Kurz, M. Pruenster, I. Rohwedder et al., "MST1-dependent vesicle trafficking regulates neutrophil transmigration through the vascular basement membrane," *Journal of Clinical Investigation*, vol. 126, no. 11, pp. 4125–4139, 2016.
- [26] M. Sperandio, J. Pickard, S. Unnikrishnan, S. T. Acton, and K. Ley, "Analysis of leukocyte rolling in vivo and in vitro," *Methods in Enzymology*, vol. 416, pp. 346–371, 2006.
- [27] D. C. Angus and T. van der Poll, "Severe sepsis and septic shock," *New England Journal of Medicine*, vol. 369, no. 9, pp. 840–851, 2013.
- [28] C. S. Deutschman and K. J. Tracey, "Sepsis: current dogma and new perspectives," *Immunity*, vol. 40, no. 4, pp. 463–475, 2014.
- [29] R. S. Hotchkiss, G. Monneret, and D. Payen, "Sepsis-induced immunosuppression: from cellular dysfunctions to immunotherapy," *Nature Reviews. Immunology*, vol. 13, no. 12, pp. 862–874, 2013.
- [30] A. Klinke, C. Nussbaum, L. Kubala et al., "Myeloperoxidase attracts neutrophils by physical forces," *Blood*, vol. 117, no. 4, pp. 1350–1358, 2011.
- [31] C. Nussbaum, S. Bannenberg, P. Keul et al., "Sphingosine-1-phosphate receptor 3 promotes leukocyte rolling by mobilizing endothelial P-selectin," *Nature Communications*, vol. 6, no. 1, p. 6416, 2015.
- [32] T. N. Mayadas, R. C. Johnson, H. Rayburn, R. O. Hynes, and D. D. Wagner, "Leukocyte rolling and extravasation are severely compromised in P selectin-deficient mice," *Cell*, vol. 74, no. 3, pp. 541–554, 1993.
- [33] J. Rivera-Nieves, T. L. Burcin, T. S. Olson et al., "Critical role of endothelial P-selectin glycoprotein ligand 1 in chronic murine ileitis," *The Journal of Experimental Medicine*, vol. 203, no. 4, pp. 907–917, 2006.
- [34] M. Sperandio, C. A. Gleissner, and K. Ley, "Glycosylation in immune cell trafficking," *Immunological Reviews*, vol. 230, no. 1, pp. 97–113, 2009.
- [35] M. Sperandio, M. L. Smith, S. B. Forlow et al., "P-selectin glycoprotein ligand-1 mediates L-selectin-dependent leukocyte rolling in venules," *The Journal of Experimental Medicine*, vol. 197, no. 10, pp. 1355–1363, 2003.
- [36] M. Bosmann and P. A. Ward, "The inflammatory response in sepsis," *Trends in Immunology*, vol. 34, no. 3, pp. 129–136, 2013.
- [37] C. M. Coopersmith, H. Wunsch, M. P. Fink et al., "A comparison of critical care research funding and the financial burden of critical illness in the United States," *Critical Care Medicine*, vol. 40, no. 4, pp. 1072–1079, 2012.
- [38] G. S. Martin, D. M. Mannino, S. Eaton, and M. Moss, "The epidemiology of sepsis in the United States from 1979 through 2000," *The New England Journal of Medicine*, vol. 348, no. 16, pp. 1546–1554, 2003.
- [39] K. A. Wood and D. C. Angus, "Pharmacoeconomic implications of new therapies in sepsis," *PharmacoEconomics*, vol. 22, no. 14, pp. 895–906, 2004.
- [40] D. F. Gaieski, J. M. Edwards, M. J. Kallan, and B. G. Carr, "Benchmarking the incidence and mortality of severe sepsis in the United States," *Critical Care Medicine*, vol. 41, no. 5, pp. 1167–1174, 2013.
- [41] J. Hawiger, R. A. Veach, and J. Zienkiewicz, "New paradigms in sepsis: from prevention to protection of failing microcirculation," *Journal of Thrombosis and Haemostasis*, vol. 13, no. 10, pp. 1743–1756, 2015.

- [42] N. R. London, W. Zhu, F. A. Bozza et al., "Targeting Robo4-dependent slit signaling to survive the cytokine storm in sepsis and influenza," *Science Translational Medicine*, vol. 2, no. 23, article 23ra19, 2010.
- [43] S. Skibsted, A. E. Jones, M. A. Puskarich et al., "Biomarkers of endothelial cell activation in early sepsis," *Shock*, vol. 39, no. 5, pp. 427–432, 2013.
- [44] S. Trzeciak, I. Cinel, R. Phillip Dellinger et al., "Resuscitating the microcirculation in sepsis: the central role of nitric oxide, emerging concepts for novel therapies, and challenges for clinical trials," *Academic Emergency Medicine*, vol. 15, no. 5, pp. 399–413, 2008.
- [45] X. Ye, J. Ding, X. Zhou, G. Chen, and S. F. Liu, "Divergent roles of endothelial NF- κ B in multiple organ injury and bacterial clearance in mouse models of sepsis," *The Journal of Experimental Medicine*, vol. 205, no. 6, pp. 1303–1315, 2008.
- [46] J. S. Boomer, K. To, K. C. Chang et al., "Immunosuppression in patients who die of sepsis and multiple organ failure," *JAMA*, vol. 306, no. 23, pp. 2594–2605, 2011.
- [47] E. Dolgin, "Trial failure prompts soul-searching for critical-care specialists," *Nature Medicine*, vol. 18, no. 7, p. 1000, 2012.
- [48] R. S. Hotchkiss, C. M. Coopersmith, J. E. McDunn, and T. A. Ferguson, "The sepsis seesaw: tilting toward immunosuppression," *Nature Medicine*, vol. 15, no. 5, pp. 496–497, 2009.
- [49] S. M. Opal, C. J. Fisher, J. F. A. Dhainaut et al., "Confirmatory interleukin-1 receptor antagonist trial in severe sepsis: a phase III, randomized, double-blind, placebo-controlled, multicenter trial," *Critical Care Medicine*, vol. 25, no. 7, pp. 1115–1124, 1997.
- [50] P. A. Ward, "Immunosuppression in sepsis," *JAMA*, vol. 306, no. 23, pp. 2618–2619, 2011.
- [51] G. F. Weber, B. G. Chousterman, S. He et al., "Interleukin-3 amplifies acute inflammation and is a potential therapeutic target in sepsis," *Science*, vol. 347, no. 6227, pp. 1260–1265, 2015.
- [52] L. Galland, "Diet and inflammation," *Nutrition in Clinical Practice*, vol. 25, no. 6, pp. 634–640, 2010.
- [53] J. M. Kremer, D. A. Lawrence, W. Jubiz et al., "Dietary fish oil and olive oil supplementation in patients with rheumatoid arthritis. Clinical and immunologic effects," *Arthritis and Rheumatism*, vol. 33, no. 6, pp. 810–820, 1990.
- [54] L. S. Kremmyda, E. Trvzicka, B. Stankova, and A. Zak, "Fatty acids as biocompounds: their role in human metabolism, health and disease: a review. Part 2: fatty acid physiological roles and applications in human health and disease," *Biomedical Papers of the Medical Faculty of the University Palacky, Olomouc, Czech Republic*, vol. 155, no. 3, pp. 195–218, 2011.
- [55] S. Rajaram, K. M. Connell, and J. Sabate, "Effect of almond-enriched high-monounsaturated fat diet on selected markers of inflammation: a randomised, controlled, crossover study," *The British Journal of Nutrition*, vol. 103, no. 6, pp. 907–912, 2010.
- [56] G. J. Wanten and P. C. Calder, "Immune modulation by parenteral lipid emulsions," *The American Journal of Clinical Nutrition*, vol. 85, no. 5, pp. 1171–1184, 2007.
- [57] P. Yaqoob, "Monounsaturated fatty acids and immune function," *European Journal of Clinical Nutrition*, vol. 56, Supplement 3, pp. S9–S13, 2002.
- [58] P. Perez-Martinez, J. Lopez-Miranda, L. Blanco-Colio et al., "The chronic intake of a Mediterranean diet enriched in virgin olive oil, decreases nuclear transcription factor κ B activation in peripheral blood mononuclear cells from healthy men," *Atherosclerosis*, vol. 194, no. 2, pp. e141–e146, 2007.
- [59] H. Gardener, C. B. Wright, Y. Gu et al., "Mediterranean-style diet and risk of ischemic stroke, myocardial infarction, and vascular death: the Northern Manhattan Study," *The American Journal of Clinical Nutrition*, vol. 94, no. 6, pp. 1458–1464, 2011.
- [60] L. Perdomo, N. Beneit, Y. F. Otero et al., "Protective role of oleic acid against cardiovascular insulin resistance and in the early and late cellular atherosclerotic process," *Cardiovascular Diabetology*, vol. 14, no. 1, p. 75, 2015.
- [61] H. G. Rodrigues, F. Takeo Sato, R. Curi, and M. A. R. Vinolo, "Fatty acids as modulators of neutrophil recruitment, function and survival," *European Journal of Pharmacology*, vol. 785, pp. 50–58, 2016.
- [62] E. Boonen, H. Vervenne, P. Meersseman et al., "Reduced cortisol metabolism during critical illness," *The New England Journal of Medicine*, vol. 368, no. 16, pp. 1477–1488, 2013.
- [63] W. Kanczkowski, M. Sue, K. Zacharowski, M. Reincke, and S. R. Bornstein, "The role of adrenal gland microenvironment in the HPA axis function and dysfunction during sepsis," *Molecular and Cellular Endocrinology*, vol. 408, pp. 241–248, 2015.
- [64] C. Summers, S. M. Rankin, A. M. Condliffe, N. Singh, A. M. Peters, and E. R. Chilvers, "Neutrophil kinetics in health and disease," *Trends in Immunology*, vol. 31, no. 8, pp. 318–324, 2010.
- [65] E. Kolaczowska and P. Kubes, "Neutrophil recruitment and function in health and inflammation," *Nature Reviews. Immunology*, vol. 13, no. 3, pp. 159–175, 2013.
- [66] P. Yaqoob, J. A. Knapper, D. H. Webb, C. M. Williams, E. A. Newsholme, and P. C. Calder, "Effect of olive oil on immune function in middle-aged men," *The American Journal of Clinical Nutrition*, vol. 67, no. 1, pp. 129–135, 1998.
- [67] M. A. Carluccio, M. Massaro, C. Bonfrate et al., "Oleic acid inhibits endothelial activation: a direct vascular antiatherogenic mechanism of a nutritional component in the Mediterranean diet," *Arteriosclerosis, Thrombosis, and Vascular Biology*, vol. 19, no. 2, pp. 220–228, 1999.
- [68] A. Mocsai, "Diverse novel functions of neutrophils in immunity, inflammation, and beyond," *The Journal of Experimental Medicine*, vol. 210, no. 7, pp. 1283–1299, 2013.
- [69] L. Fialkow, Y. Wang, and G. P. Downey, "Reactive oxygen and nitrogen species as signaling molecules regulating neutrophil function," *Free Radical Biology & Medicine*, vol. 42, no. 2, pp. 153–164, 2007.
- [70] M. E. Andrades, C. Ritter, and F. Dal-Pizzol, "The role of free radicals in sepsis development," *Frontiers in Bioscience (Elite Edition)*, vol. 1, pp. 277–287, 2009.
- [71] L. M. Hoesel, T. A. Neff, S. B. Neff et al., "Harmful and protective roles of neutrophils in sepsis," *Shock*, vol. 24, no. 1, pp. 40–47, 2005.
- [72] C. F. Gonçalves-de-Albuquerque, I. Rohwedder, A. R. Silva et al., "The yin and yang of tyrosine kinase inhibition during experimental polymicrobial sepsis," *Frontiers in Immunology*, vol. 9, p. 901, 2018.

- [73] E. Hatanaka, A. C. Levada-Pires, T. C. Pithon-Curi, and R. Curi, "Systematic study on ROS production induced by oleic, linoleic, and gamma-linolenic acids in human and rat neutrophils," *Free Radical Biology & Medicine*, vol. 41, no. 7, pp. 1124–1132, 2006.
- [74] H. G. Rodrigues, M. A. R. Vinolo, J. Magdalon et al., "Dietary free oleic and linoleic acid enhances neutrophil function and modulates the inflammatory response in rats," *Lipids*, vol. 45, no. 9, pp. 809–819, 2010.
- [75] R. Padovese and R. Curi, "Modulation of rat neutrophil function in vitro by cis- and trans-MUFA," *The British Journal of Nutrition*, vol. 101, no. 9, pp. 1351–1359, 2009.
- [76] B. S. Noriega, M. A. Sanchez-Gonzalez, D. Salyakina, and J. Coffman, "Understanding the impact of omega-3 rich diet on the gut microbiota," *Case Reports in Medicine*, vol. 2016, Article ID 3089303, 6 pages, 2016.
- [77] L. Costantini, R. Molinari, B. Farinon, and N. Merendino, "Impact of omega-3 fatty acids on the gut microbiota," *International Journal of Molecular Sciences*, vol. 18, no. 12, 2017.
- [78] C. Menni, J. Zierer, T. Pallister et al., "Omega-3 fatty acids correlate with gut microbiome diversity and production of N-carbamylglutamate in middle aged and elderly women," *Scientific Reports*, vol. 7, no. 1, article 11079, 2017.
- [79] L. M. Kumaratilake, A. Ferrante, B. S. Robinson, T. Jaeger, and A. Poulos, "Enhancement of neutrophil-mediated killing of *Plasmodium falciparum* asexual blood forms by fatty acids: importance of fatty acid structure," *Infection and Immunity*, vol. 65, no. 10, pp. 4152–4157, 1997.
- [80] S. L. Svahn, M. A. Ulleryd, L. Grahnemo et al., "Dietary omega-3 fatty acids increase survival and decrease bacterial load in mice subjected to *Staphylococcus aureus*-induced sepsis," *Infection and Immunity*, vol. 84, no. 4, pp. 1205–1213, 2016.
- [81] J. M. Kaplan, J. A. Cook, P. W. Hake, M. O'Connor, T. J. Burroughs, and B. Zingarelli, "15-Deoxy- Δ 12,14-prostaglandin J2 (15D-PGJ2), a peroxisome proliferator activated receptor γ ligand, reduces tissue leukosequestration and mortality in endotoxic shock," *Shock*, vol. 24, no. 1, pp. 59–65, 2005.
- [82] D. Liu, B. X. Zeng, S. H. Zhang et al., "Rosiglitazone, a peroxisome proliferator-activated receptor-gamma agonist, reduces acute lung injury in endotoxemic rats," *Critical Care Medicine*, vol. 33, no. 10, pp. 2309–2316, 2005.
- [83] D. Liu, B. X. Zeng, S. H. Zhang, and S. L. Yao, "Rosiglitazone, an agonist of peroxisome proliferator-activated receptor gamma, reduces pulmonary inflammatory response in a rat model of endotoxemia," *Inflammation Research*, vol. 54, no. 11, pp. 464–470, 2005.
- [84] G. Sener, A. O. Sehirli, N. Gedik, and G. A. Dulger, "Rosiglitazone, a PPAR-gamma ligand, protects against burn-induced oxidative injury of remote organs," *Burns*, vol. 33, no. 5, pp. 587–593, 2007.
- [85] A. E. Ferreira, F. Sisti, F. Sonego et al., "PPAR- γ /IL-10 axis inhibits MyD88 expression and ameliorates murine polymicrobial sepsis," *The Journal of Immunology*, vol. 192, no. 5, pp. 2357–2365, 2014.
- [86] S. R. Kim, K. S. Lee, H. S. Park et al., "Involvement of IL-10 in peroxisome proliferator-activated receptor gamma-mediated anti-inflammatory response in asthma," *Molecular Pharmacology*, vol. 68, no. 6, pp. 1568–1575, 2005.
- [87] H. Jin, M. A. Gebbska, I. O. Blokhin et al., "Endothelial PPAR- γ protects against vascular thrombosis by downregulating P-selectin expression," *Arteriosclerosis, Thrombosis, and Vascular Biology*, vol. 35, no. 4, pp. 838–844, 2015.
- [88] S. W. Standage, C. C. Caldwell, B. Zingarelli, and H. R. Wong, "Reduced peroxisome proliferator-activated receptor α expression is associated with decreased survival and increased tissue bacterial load in sepsis," *Shock*, vol. 37, no. 2, pp. 164–169, 2012.
- [89] H. Xiao, J. Siddiqui, and D. G. Remick, "Mechanisms of mortality in early and late sepsis," *Infection and Immunity*, vol. 74, no. 9, pp. 5227–5235, 2006.
- [90] M. Zhou, R. Wu, W. Dong, A. Jacob, and P. Wang, "Endotoxin downregulates peroxisome proliferator-activated receptor- γ via the increase in TNF- α release," *American Journal of Physiology-Regulatory, Integrative and Comparative Physiology*, vol. 294, no. 1, pp. R84–R92, 2008.
- [91] A. M. Siddiqui, X. Cui, R. Wu et al., "The anti-inflammatory effect of curcumin in an experimental model of sepsis is mediated by up-regulation of peroxisome proliferator-activated receptor-gamma," *Critical Care Medicine*, vol. 34, no. 7, pp. 1874–1882, 2006.
- [92] D. Frasca, B. B. Blomberg, and R. Paganelli, "Aging, obesity, and inflammatory age-related diseases," *Frontiers in Immunology*, vol. 8, p. 1745, 2017.
- [93] M. Kutsukake, T. Matsutani, K. Tamura et al., "Pioglitazone attenuates lung injury by modulating adipose inflammation," *The Journal of Surgical Research*, vol. 189, no. 2, pp. 295–303, 2014.
- [94] M. R. Hill, M. D. Young, C. M. McCurdy, and J. M. Gimble, "Decreased expression of murine PPARgamma in adipose tissue during endotoxemia," *Endocrinology*, vol. 138, no. 7, pp. 3073–3076, 1997.

Research Article

Anti-Inflammatory and Antioxidant Properties of Black Mulberry (*Morus nigra* L.) in a Model of LPS-Induced Sepsis

Karine de Pádua Lúcio,¹ Ana Carolina Silveira Rabelo ¹, Carolina Moraes Araújo,¹ Geraldo Célio Brandão,² Gustavo Henrique Bianco de Souza,² Regislainy Gomes da Silva,² Débora Maria Soares de Souza,³ André Talvani ³, Frank Silva Bezerra ⁴, Allan Jefferson Cruz Calsavara,⁵ and Daniela Caldeira Costa ¹

¹Laboratório de Bioquímica Metabólica (LBM), Departamento de Ciências Biológicas (DECBI), Programa de Pós-Graduação em Ciências Biológicas, Universidade Federal de Ouro Preto, Minas Gerais, Brazil

²Laboratório de Farmacognosia, Escola de Farmácia, Programa de Pós-graduação em Ciências Farmacêuticas, Universidade Federal de Ouro Preto, Ouro Preto, Minas Gerais, Brazil

³Laboratório de Imunobiologia da Inflamação, Departamento de Ciências Biológicas (DECBI), Programa de Pós-Graduação em Ciências Biológicas, Programa de Pós-Graduação em Saúde e Nutrição, Universidade Federal de Ouro Preto (UFOP), Ouro Preto, Minas Gerais, Brazil

⁴Laboratório de Fisiopatologia Experimental (LAFEx), Departamento de Ciências Biológicas (DECBI), Programa de Pós-Graduação em Ciências Biológicas, Universidade Federal de Ouro Preto (UFOP), Ouro Preto, Minas Gerais, Brazil

⁵Escola de Medicina, Universidade Federal de Ouro Preto (UFOP), Ouro Preto, Minas Gerais, Brazil

Correspondence should be addressed to Daniela Caldeira Costa; dani.caldeiracosta@gmail.com

Received 4 July 2018; Revised 14 September 2018; Accepted 20 September 2018; Published 7 November 2018

Guest Editor: Felipe L. de Oliveira

Copyright © 2018 Karine de Pádua Lúcio et al. This is an open access article distributed under the Creative Commons Attribution License, which permits unrestricted use, distribution, and reproduction in any medium, provided the original work is properly cited.

Sepsis is a complex disease and is the cause of many deaths worldwide. Sepsis pathogenesis involves a dysregulated inflammatory response with consequent production of inflammatory mediators and reactive species. The production and excessive release of these substances into the systemic circulation trigger various cellular and metabolic alterations that are observed during the disease evolution. Thus, more studies have been carried out to investigate the therapeutic potential of plants such as *Morus nigra* L., popularly known as black mulberry. Studies have shown that plants belonging to the *Morus* genus are rich in secondary metabolites such as flavonoids which are associated with important biological activities as antioxidant and anti-inflammatory actions. Based on this context, the objective of our study was to evaluate the anti-inflammatory and antioxidant properties of *Morus nigra* L. in a sepsis model induced by LPS. Male C57BL/6 mice were distributed in four groups: control, sepsis, sepsis treated with leaf extract of mulberry, and sepsis treated with mulberry pulp. The animals were treated with 100 μ L of their respective treatments for twenty-one days. Sepsis was induced at the 21st day with lipopolysaccharide (LPS) by intraperitoneal injection. The animals were euthanized 24 hours after receiving the LPS injection. The data obtained were analyzed in GraphPad Prism 6.0 software. Our results showed that treatment with either extract significantly decreased the number of leukocytes in the bronchoalveolar lavage fluid and serum levels of TNF in septic animals. Regarding the redox status, the treatments significantly decreased the antioxidant activity of the enzyme glutathione peroxidase. Regarding metalloproteinase type 2, it was observed that the treatment with black mulberry pulp was able to significantly reduce the activity of this enzyme concerning the sepsis group. Finally, these results together promoted an increase in the animal's survival that received the black mulberry leaf or pulp extract.

1. Introduction

Sepsis is an organ dysfunction that results from a dysregulated host response to infection [1]. The liver plays an important role in sepsis, being essential for microorganism and toxin clearance (such as endotoxins) [2]. Endotoxin, as lipopolysaccharide (LPS), a component of the outer membrane of Gram-negative bacteria, interacts with specific receptors on the host effector cells and induces the synthesis of a large number of proinflammatory cytokines. The overproduction of these cytokines can lead to an unregulated inflammatory reaction [3]. However, liver defense responses represent a double-edged sword which can contribute to the destruction and elimination of microbial products and can also lead to liver injury [2].

It is known that there is an interrelation between redox processes and inflammation and that reactive species can activate inflammatory signaling pathways and that inflammatory cells can produce more reactive species, resulting in a vicious cycle leading to a redox and inflammatory disequilibrium [4], and thus may be a determining factor in the sepsis outcome. Thus, the interaction between redox processes and inflammation would be a determining factor for the antioxidant selection with therapeutic potential to minimize systemic damage and improve the septic animal survival. Antioxidant therapies are widely used in diseases that have as main pathogenesis the redox imbalance and inflammatory processes. In this regard, many medicinal plants have an ability to protect the liver due to their antioxidant and anti-inflammatory effects [5].

Morus nigra L. (Moraceae family), known as black mulberry, is a tree distributed worldwide [6], including in different regions of Brazil and stands out for its medicinal properties [7]. Many studies have found that black mulberry is rich in polyphenols, flavonoids, and anthocyanins, which are responsible for their antioxidant [8, 9] and anti-inflammatory activities [10, 11]. Based on the fact that the fruits and leaves of *Morus nigra* have anti-inflammatory and antioxidant potential as well as on the fact that due to being a good therapeutic candidate to minimize systemic complications due to sepsis, it should contain both anti-inflammatory and antioxidant characteristics, the objective herein was to verify the potential of the leaf and pulp of *Morus nigra* in preventing or minimizing redox and inflammatory imbalance induced by sepsis.

2. Materials and Methods

2.1. Botanical Material. The aerial parts of *Morus nigra* were collected in the city of Ouro Preto, Minas Gerais, Brazil, in the year 2012. The specimen was identified by the number OUPR 27087 and deposited in the herbarium José Badini of the Federal University of Ouro Preto (UFOP).

2.2. Preparation of the Pulp and Hydroethanolic Leaf Extracts of *Morus nigra*. The ripe fruits were collected in September 2015, and the black mulberry extract was obtained after the fruits were pressed and subjected to filtration. The filtrate was stored in a freezer at -80°C . The black mulberry leaves were dehydrated in a drying oven at 37°C and then crushed.

The extraction was performed with a hydroalcoholic solution in a ratio of 1 : 1 by percolation for 24 hours at room temperature. The filtrate was concentrated in a rotary evaporator. The dried residue was dissolved in filtered water to the final concentration of $150\text{ mg}\cdot\text{mL}^{-1}$.

2.3. RP-UPLC-DAD-ESI-MS Analyses. Chemical characterization of the fluid extract of fruits and the hydroalcoholic extract of *Morus nigra* leaves was performed by ultra performance liquid chromatography (UPLC) coupled to a diode arrangement detector and mass spectrometry. The hydroethanolic extract was resuspended in a 98 : 2 (methanol : water) solution and then filtered through a $0.20\ \mu\text{m}$ PVDF syringe filter. Subsequently, it was injected into the liquid chromatograph. Chromatographic separation was performed in ACQUITY UPLC BEH RP-18 ($1.7\ \mu\text{m}$, $50\times 2\text{ mm i.d.}$) (Waters). The mobile phase consisted of water 0.1% formic acid (solvent A) and acetonitrile 0.1% formic acid (solvent B). The elution protocol was 0–11 min and linear gradient was ranging from 5% to 95% B. The flow rate was $0.3\text{ mL}\cdot\text{min}^{-1}$, and the sample injection volume was $4.0\ \mu\text{L}$. Analyses were performed using an ACQUITY UPLC (Waters) ion trap mass spectrometer in the following conditions: positive and negative ion mode; capillary voltage, 3500 V; capillary temperature, 320°C ; source voltage, 5 kV; vaporizer temperature, 320°C ; corona needle current, 5 mA; and sheath gas, nitrogen, 27 psi. Analyses were run in the full scan mode (100–2000 Da). The ESI-MS/MS analyses were additionally performed in an ACQUITY UPLC (Waters) with argon as the collision gas, and the collision energy was set at 30 eV. The UV spectra were registered from 190 to 450 nm.

2.4. Animal Protocol. Male C57BL6 mice were separated into 4 experimental groups: control group (C), sepsis group (S), sepsis group treated with leaf extract of *Morus nigra* (SL), and sepsis group treated with pulp of *Morus nigra* (SP). During 21 days, groups C and S received $100\ \mu\text{L}$ of water per gavage and the SL and SP groups received $100\ \mu\text{L}$ at a dose of $500\text{ mg}\cdot\text{kg}^{-1}$ of leaf extract and pulp extract, respectively, of *Morus nigra* [12, 13]. At the last day of the test, the animals received the treatments and 1 hour after the controls received intraperitoneal injection with saline solution and the other groups received LPS injection at a dose of $10\text{ mg}\cdot\text{kg}^{-1}$ (0111: B4, Sigma). The animals were euthanized 24 hours after sepsis induction, and through the trachea cannulation, the animals' lungs were perfused with saline solution (0.9% NaCl) to collect bronchoalveolar lavage. Blood and liver samples were collected and stored in the freezer at -80°C for further analysis, and the mortality rate was measured.

2.5. Biochemical Parameters. Serum glucose was obtained from blood samples taken from the animals' tail vein moments before their euthanasia using the Accu-Check® glycosimeter. Platelet quantification was obtained from a hemogram performed in an automated equipment.

2.6. Expression of Inflammatory Mediators. The real-time quantitative RT-PCR assay (RT-PCR) technique was used to evaluate the cytokine expression in liver samples. RNA

extraction was performed using the SV Total RNA Isolation System Kit (Promega Corporation, catalog # Z3100). The concentration and purity of RNA in the samples subjected to extraction were evaluated by tests in NanoVue (GE Healthcare, UK) using the A260/280 ratio. The cDNA molecule was formed using High-Capacity cDNA Reverse Transcription Kit (Applied Biosystems, catalog # 4368814) and oligo (dT) which is capable of converting 1 μ g of RNA to cDNA. Primers for IL-1 β , IL-6, and IL-10 were constructed from the Primer-BLAST program. DNA amplification, detection, and quantification reactions occurred at 50°C for 2 min, 95°C for 10 min in 40 cycles at 95°C for 15 sec, and 60°C for 1 min using the ABI Prism 7300 Sequence Detector (Applied Biosystems, CA, USA). Data were analyzed by comparative C_T method. Target gene expression was determined relative to the expression of β -actin gene. All analyses were performed in triplicate.

2.7. Analysis of Cytokine Level. The serum cytokine concentrations and also in hepatic tissue were determined using enzyme-linked immunosorbent assay kits ((PeproTech), Murine IL-6 Standard ABTS ELISA Development Kit (catalog # 900-K50), Murine TNF- α Standard ABTS ELISA Development Kit (catalog # 900-K54), Murine IL-1 β Mini ABTS ELISA Development Kit (catalog # 900-M47), and Murine IL-6 Mini ABTS ELISA Development Kit (catalog #900-M50)), according to the manufacturer's instructions.

2.8. Analyses of Antioxidant Defenses

2.8.1. Catalase Activity. The hepatic tissue (100 mg) was fractionated and homogenized with 1000 μ L of phosphate buffer (0.1 M, pH 7.2) and subsequently centrifuged at 10,000 rpm for 10 minutes. For the assay, 10 μ L of the obtained supernatant and 990 μ L of peroxide solution (6%) were mixed. Reading was performed in a spectrophotometer at 240 nm, and enzyme activity was measured by decaying the absorbances every 30 seconds during 3 minutes of reading as described previously by Aebi [14]. Hydrolysis of 1 μ mol of H₂O₂ per min was equivalent to one unit (U) of catalase.

2.8.2. Superoxide Dismutase Activity. The superoxide dismutase enzyme (SOD) activity was measured indirectly. As described previously by Marklund and Marklund [15], pyrogallol undergoes autooxidation producing the superoxide anion (O^{•-}). The SOD enzyme is able to compete for the superoxide anion by decreasing the MTT reduction ([3-(4,5-dimethyl-2-thiazolyl)-2,5-diphenyl-2H-tetrazolium bromide]) and consequently the formazan crystal formation. The reading was performed in a spectrophotometer at 570 nm. The results were expressed as U SOD/mg of protein, where one unit of SOD is defined as the amount of enzyme required for 50% inhibition of MTT reduction.

2.8.3. Total Glutathione, Oxidized Glutathione, and Reduced Glutathione. Total glutathione content (GSht) was determined by a kinetic assay using a protocol adapted from the commercial sigma kit (Sigma, catalog # CS0260). In this assay, DTNB [5,5'-dithiobis (2-nitrobenzoic acid)] is reduced to TNB (2-nitro-5-thiobenzoate) and this

reduction is directly proportional to the tripeptide concentration in the assessed tissue since reduced glutathione (GSH) is the cofactor of this reaction. To determine oxidized glutathione (GSSG) concentration, homogenate derivatization with 2,2',2''-nitrilotriethanol, tris(2-hydroxyethyl)amine (TEA), and vinylpyridine was performed. The concentrations of GSht and GSSH were obtained by a standard curve performed for each of these assays. The GSH concentration was obtained by subtracting the oxidized glutathione value from the total glutathione concentration.

2.8.4. Glutathione Reductase Activity. The activity of the glutathione reductase enzyme was measured by the Glutathione Reductase Assay Kit (Abcam, catalog # ab83461). The assay is based on the glutathione reduction by NADPH in the presence of glutathione reductase. The reading is carried out at 412 nm.

2.8.5. Glutathione Peroxidase Activity. The activity of the enzyme glutathione peroxidase was determined using the Glutathione Peroxidase Activity Kit (Assay Designs Inc., catalog # 900-158). The assay is based on the oxidation of GSH to GSSG by the enzymatic action of glutathione peroxidase coupled to the recycling of GSSG to GSH by glutathione reductase. The absorbance decay caused by the oxidation of the reduced coenzyme NADPH to NADP is measured at 340 nm being indicative of the activity of glutathione peroxidase since this enzyme is a limiting step of this reaction.

2.9. Gelatin Zymography. The activity of types 2 and 9 metalloproteinases was evaluated by electrophoresis in 8% polyacrylamide gel containing 2 mg•mL⁻¹ of porcine gelatin (Sigma Chem. Co., St. Louis, USA). Samples of hepatic extract at the concentration of 30 μ g of protein were applied to the gels, and the electrophoresis was performed for 120 minutes at 100 V. After the run, the gels were washed with 10% Triton-X solution and incubated in buffer composed of 50 mM of tris, 150 mM of NaCl, 5 mM of CaCl₂, and 0.05% of NaN₃ (pH 7.5) for 36 h at 37°C. After incubation, the gels were stained with 0.05% coomassie brilliant blue G-250 for 3 h and decolorized with methanol and acetic acid solution (4%–8%) as previously described by Sung et al. [16].

2.10. Histological Analysis. Fragments of the animal livers were fixed in 4% buffered formalin, and for the preparation of slides, they were subjected to serial dehydration with alcohols of decreasing concentrations and were subsequently immersed in paraffin. The paraffin sections of approximately 4 μ m were obtained in microtome, assembled, and stained by the hematoxylin and eosin (H&E) technique, to visualize the tissue structure. The photomicrographs were obtained using a Leica optical microscope coupled to the DM5000 digital camera using a 40x objective lens, and the morphometric analyzes were performed in the Leica Application Suite (Germany) analysis software.

2.11. Statistical Analysis. The normality of the distribution of each variable was assessed by means of the Kolmogorov-Smirnov test. Data that presented a normal distribution were analyzed through univariate analysis of variance (ANOVA-

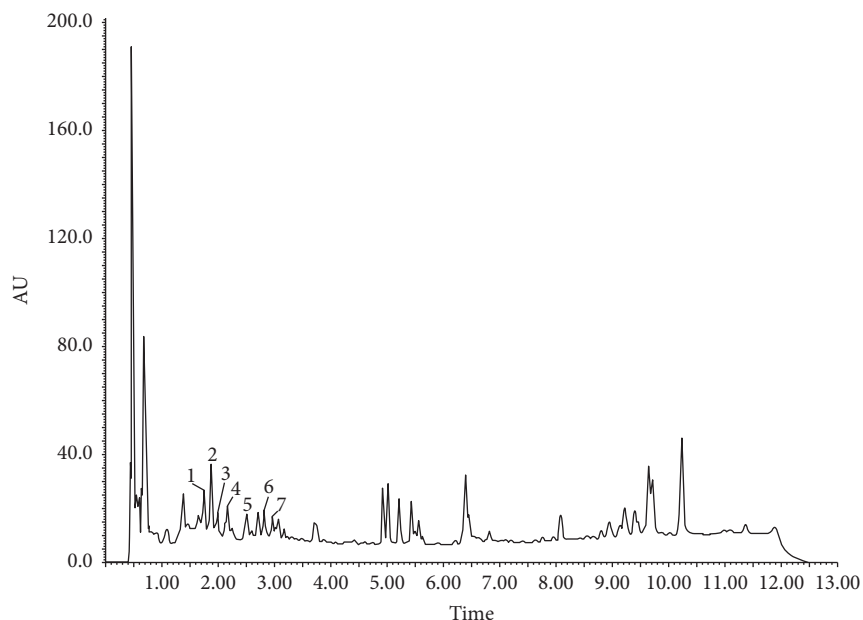


FIGURE 1: Profile of the leaf extract of *Morus nigra* L. 1: 3-O-Caffeoylquinic acid; 2: 4-O-caffeoylquinic acid; 3: 5-O-caffeoylquinic acid; 4: 6-hydroxy-luteolin-7-O-rutenoside; 5: quercetin-3-O-furanosyl-2-ramosil; 6: quercetin-3-O-rutenoside; 7: quercetin 3-O-glycoside.

one way), followed by Bonferroni's posttest to determine the differences among the C, SL, and SP groups in relation to the S group. Data were expressed as mean \pm standard error. Differences were considered significant when $p < 0.05$. All tests were performed on GraphPad Prism 6.0 software for Windows (San Diego, California, USA).

3. Results

3.1. RP-UPLC-DAD-ESI-MS Analyses. The results presented in Figures 1 and 2 and Tables 1 and 2 show the phenolic substances which have been identified in pulp extract and leaf extract, respectively, of *Morus nigra* including the glycosides of flavonoids. The mass spectra obtained were compared with the results described in the literature. The searches were performed on the data basis available for the m/z ratio obtained in the spectra.

3.2. Effect of *Morus nigra* on Survival and Biochemistry Parameters in Septic Mice. It is possible to observe that the animals pretreated with pulp and leaf extracts had a longer survival (78.5% and 71.4%, respectively) than the animals that did not receive treatment (Figure 3(a)). In addition, it was observed that the sepsis animal group showed a decrease in the total number of platelets (Figure 3(d)) and hypoglycemia (Figure 3(c)), in addition to an increase in the number of total leucocytes in the bronchoalveolar lavage fluid (BLF) (Figure 3(b)), being all of these manifestations characteristic of sepsis. Extracts from *Morus nigra* leaves as well as fruit pulp were able to decrease the number of inflammatory cells.

3.3. Effect of *Morus nigra* on the Inflammatory Profile in the Sepsis. Regarding the regulation of the expression of inflammatory mediators in the liver, no significant changes were observed in gene expression of IL-1 β (Figure 4(a)) and IL-6

(Figure 4(c)) in any of the experimental groups; however, a significant decrease was observed in hepatic levels of IL-1 β (Figure 4(b)) and IL-6 (Figure 4(c)) in septic animals. Concerning IL-10, an increase in the gene expression of this cytokine was observed in the sepsis group compared to the control as well as an increase in the expression of this gene in the group treated with pulp of black mulberry in relation to the sepsis group (Figure 4(e)); however, a decrease was observed in hepatic levels of IL-10 in septic animals compared to the control (Figure 4(f)). No alterations were observed in the levels of TNF and CCL2 in any of the experimental groups (Figures 4(g) and 4(h), respectively).

In relation to the systemic profile, a significant increase was observed in the levels of TNF, IL-6, and IL-10 in animals of the sepsis group compared to the control (Figures 5(a), 5(c), and 5(d), respectively). The treatment with the extracts of leaves and pulp reduced the levels of TNF in relation to the septic group without treatment (Figure 5(a)).

No significant alterations were observed in the level of IL-1 β in any of the experimental groups (Figure 5(b)).

3.4. Effect of *Morus nigra* on the Redox Status in the Sepsis Model. The results in this study show that animals with sepsis showed an increase in the superoxide dismutase (SOD) activity (Figure 6(a)) and a decrease in the catalase (CAT) activity (Figure 6(b)), which resulted in an increase in SOD/CAT (Figure 6(c)). No significant change was observed regarding the groups treated with the extract of leaves and pulp of black mulberry.

Concerning the glutathione metabolism, a reduction was observed in the total glutathione content (Figure 7(a)) and in the reduced fraction (Figure 7(b)), in addition to a significant increase in GPx activity (Figure 7(d)) and a decrease in the GR activity (Figure 7(e)) in the sepsis group when compared to the control group. The treatment with the black mulberry

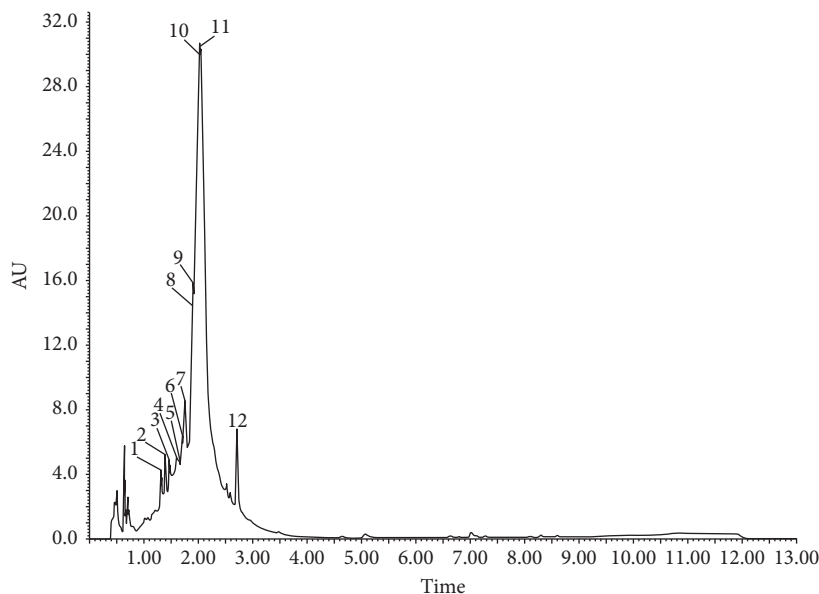


FIGURE 2: Profile of *Morus nigra* L. pulp. 1: 3-*O*-Caffeoylquinic acid; 2: 4-*O*-caffeoylquinic acid; 3: delphinidin 3-*O*-rutinoside; 4: 5-*O*-caffeoylquinic acid; 5: delphinidin 7-*O*-rutinoside; 6: delphinidin-3-*O*-glucoside; 7: cyanidin 3-*O*-glucoside; 8: delphinidin 7-*O*-glycoside; 9: cyanidin-*O*-glycosyl-aminosulfonate; 10: quercetin 3-*O*-rutinoside; 11: quercetin 3-*O*-glycoside/quercetin 7-*O*-glycoside; 12: quercetin 7-*O*-glycoside/quercetin 3-*O*-glycoside.

TABLE 1: Substances identified in the pulp of *Morus nigra* by LC-DAD-ESI-MS.

Peak	Compound	RT (min)	UV (nm)	LC-MS $[M - H]^-$ (m/z)	LC-MS $[M + H]^+$ (m/z)
1	3- <i>O</i> -Caffeoylquinic acid	1.76	323.1	353.3 (191.2; 179.3; 134.8)	355.4
2	4- <i>O</i> -Caffeoylquinic acid	1.88	321.1	353.4 (191.3; 179.2; 135.1)	355.7
3	5- <i>O</i> -Caffeoylquinic acid	1.99	323.1	353.5 (190.6; 179.2; 135.4)	355.9
4	6-Hydroxy-luteolin-7- <i>O</i> -rutenoside	2.17	265.3; 327.8	609.5 (301.1)	611.5
5	Quercetin-3- <i>O</i> -furanosyl-2''-ramnosyl	2.53	264.1; 357.8	579.2 (433.6; 301.0; 277.3)	581.7
6	Quercetin-3- <i>O</i> -rutenoside	2.70	255.3; 353.2	609.2 (301.0; 161.2)	611.2
7	Quercetin 3- <i>O</i> -glucoside	2.86	255.2; 355.3	463.1 (301.3)	465.2

TR (min): retention time in minutes; UV (nm): ultra violet in nanometers; LC-MS $[M - H]^-$ (m/z): liquid chromatography coupled to negative-mode mass spectrometry; LC-MS $[M + H]^+$ (m/z): liquid chromatography coupled to mass spectrometry in positive, mass/charge ratio.

TABLE 2: Substances identified in the extract of *Morus nigra* by LC-DAD-ESI-MS.

Peak	Compound	RT (min)	UV (nm)	LC-MS $[M - H]^-$ (m/z)	LC-MS $[M + H]^+$ (m/z)
1	3- <i>O</i> -Caffeoylquinic acid	1.46	323.1	353.4 (191.1; 179.0; 134.8)	355.39
2	4- <i>O</i> -Caffeoylquinic acid	1.74	321.1	353.4 (191.1; 179.0; 135.2)	355.72
3	Delphinidin 3- <i>O</i> -rutinoside	1.88	280.4	611.3 (285.0; 302.8; 474.8)	611.3
4	5- <i>O</i> -Caffeoylquinic acid	1.93	323.1	353.4 (190.8; 179.0; 135.0)	355.92
5	Delphinidin 7- <i>O</i> -rutinoside	1.98	281.1	611.3 (285.0; 302.8; 474.8)	611.3
6	Delphinidin 3- <i>O</i> -glucoside	1.97	280.4	465.3 (285.2; 301.3; 329.2)	465.34
7	Cyanidin 3- <i>O</i> -glucoside	1.99	280.1	447.3	449.38 (287.0)
8	Delphinidin 7- <i>O</i> -glucoside	2.05	281.4	465.3 (285.2; 301.3; 329.3)	465.35
9	Cyanidin 3- <i>O</i> -glucosyl-ramnoside	2.10	281.1	593.2	595.42 (449.1; 287.1)
10	Quercetin 3- <i>O</i> -rutinoside	2.70	255.4; 354.4	609.8 (301.3; 163.1)	611.60
11	Quercetin 3- <i>O</i> -glucoside/Quercetin 7- <i>O</i> -glucoside	2.71	255.1; 359.1	463.5 (301.1)	465.35 (303.2)
12	Quercetin 7- <i>O</i> -glucoside/Quercetin 3- <i>O</i> -glucoside	2.82	254.1; 358.1	463.2 (301.0)	465.48 (303.4)

TR (min): retention time in minutes; UV (nm): ultra violet in nanometers; LC-MS $[M - H]^-$ (m/z): liquid chromatography coupled to negative-mode mass spectrometry; LC-MS $[M + H]^+$ (m/z): liquid chromatography coupled to mass spectrometry in positive, mass/charge ratio.

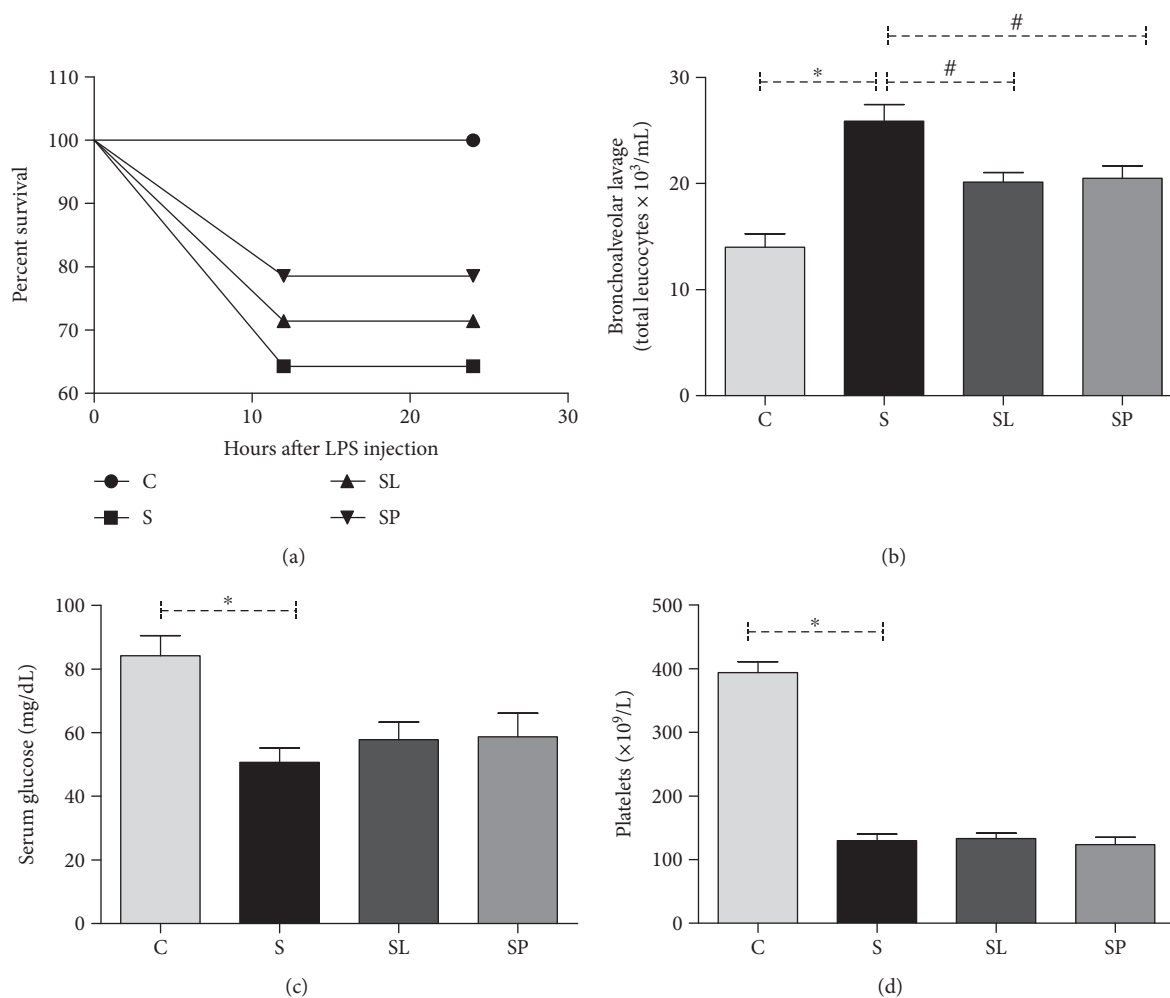


FIGURE 3: Effect of treatments with a pulp or leaf extract of *Morus nigra* on sepsis-induced percent survival (a) in C57BL/6 mice after 24 hours of LPS injection, influx cellular in bronchoalveolar lavage (b), serum glucose (c), and platelets (d). All data are shown as mean \pm SEM. * $P < 0.05$ indicates a significant difference between group S (sepsis) and group C (control). # $P < 0.05$ indicates a significant difference between S, SL (sepsis + leaf extract of mulberry), and SP (sepsis + mulberry pulp) groups.

pulp was able to restore the GSH levels to levels close to the control. In addition, a reduction was observed in the activity of GPx in the SL and SP groups. No significant differences were also observed among groups C, SL, and SP in relation to the activities of GR and GSSG levels (Figure 7(c)).

3.5. Effect of *Morus nigra* on the Liver Damage in the Sepsis Model. The results of Figure 8 show a decrease in the MMP2 activity in the sepsis animal group treated with pulp of black mulberry in relation to the nontreated sepsis group. In addition, it is possible to observe an increase in the MPP9 activity of septic animals compared to the control and no change was observed in animals treated with *Morus nigra*.

It was observed that there was no significant change in the liver histoarchitecture tissue in all the experimental groups (Figure 9(a)); however, a significant increase of inflammatory cells in the sepsis animal group and a reduction of 21% of inflammatory cells in the sepsis animal group treated with the pulp were observed, although this difference is not significant (Figure 9(b)).

4. Discussion

The present study demonstrated that pretreatment with black mulberry extracts was important to reduce the imbalance in the inflammatory and redox status of animals with sepsis induced by LPS, which could be seen through the reduction in the number of inflammatory cells present in the bronchoalveolar lavage, by the decrease in serum levels of TNF, GPx, and MMP2 activities and in the restoring of the GSH levels. These results analyzed in conjunction may justify the higher survival rate of animals that were pretreated with *Morus nigra*, suggesting that this plant presents a therapeutic potential to minimize the damage caused by sepsis.

It is known that leaves and fruits of *Morus nigra* exhibit a wide spectrum of biological activities, such as antimicrobial, antioxidant, and immunoregulatory properties [17, 18], due to the fact that they contain high levels of phenolic compounds [19]. Previous results from our research group demonstrated that *M. nigra* leaves present a higher content of phenolic compounds and antioxidant activity measured by the ability to neutralize the DPPH radical when compared

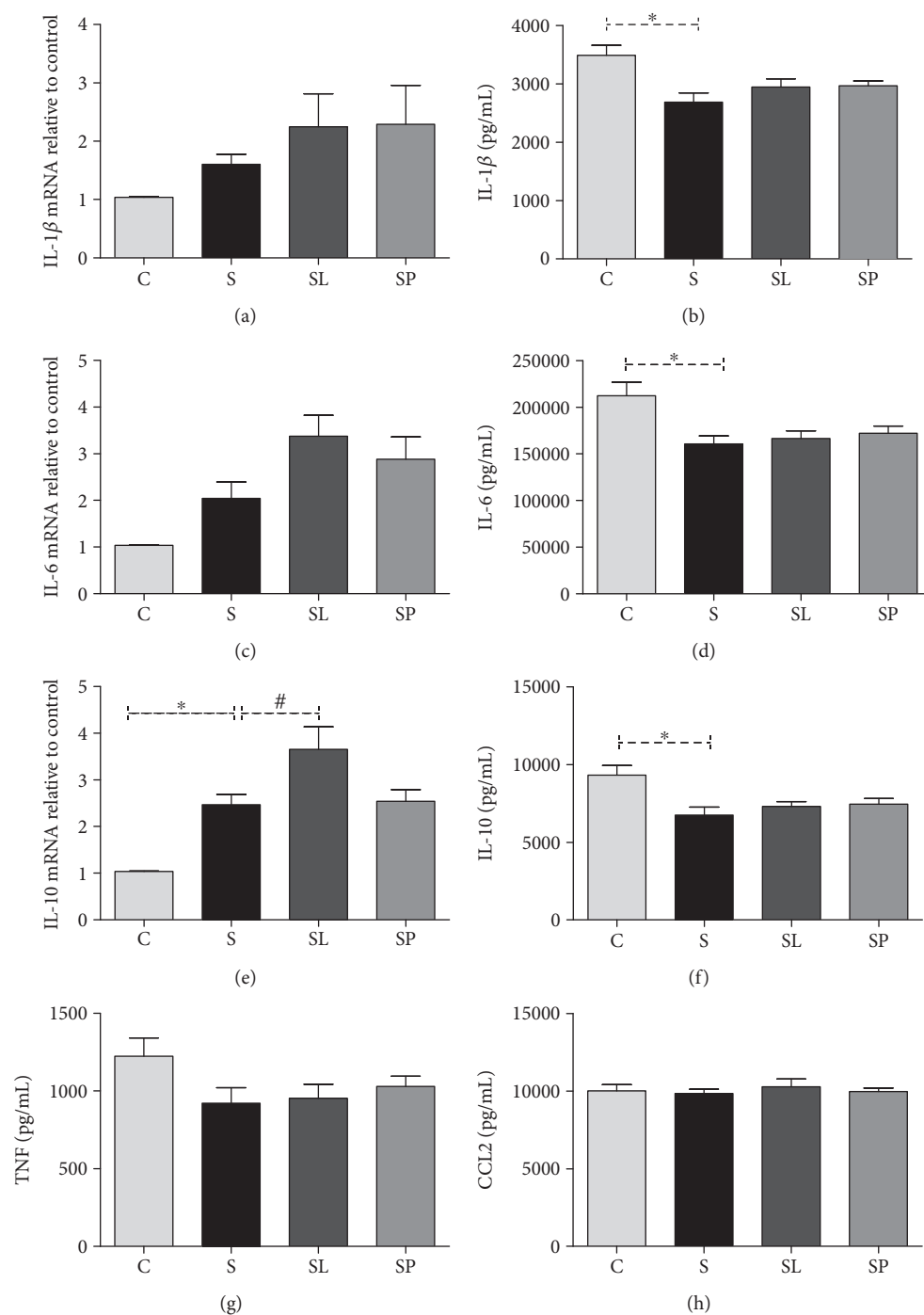


FIGURE 4: Effects of pulp and leaf extracts on expression and concentration of cytokines and interleukins in the liver samples from the C, S, SL, and SP groups. (a) IL-1 β expression, (b) IL-1 β levels, (c) IL-6 expression, (d) IL-6 levels, (e) IL-10 expression, (f) IL-10 levels, (g) TNF levels, and (h) CCL2 levels. All data are shown as mean \pm SEM. * $P < 0.05$ indicates a significant difference between group S (sepsis) and group C (control). # $P < 0.05$ indicates a significant difference between S, SL (sepsis + leaf extract of mulberry), and SP (sepsis + mulberry pulp) groups.

to its fruits, besides a distinct chromatographic profile between the extract of leaves and that of pulp of black mulberry [12]. In this study, a distinct chromatographic profile was also observed between the two preparations, being that in the fruit samples, the flavonoids delphinidin and cyanidin were observed. Delphinidin is derived from catechin and epicatechin [20], and it is widely found in plant-based food [21].

Its anti-inflammatory activities are well reported [22]. Cyanidin is an anthocyanin that has been extensively studied due to its antioxidant protection through the modulation of the Nrf2 transcription factor [23]. Although the berry production is more common in the Northern Hemisphere, the chromatographic profile observed in this study is in agreement with other studies of berries grown in Brazil [24].

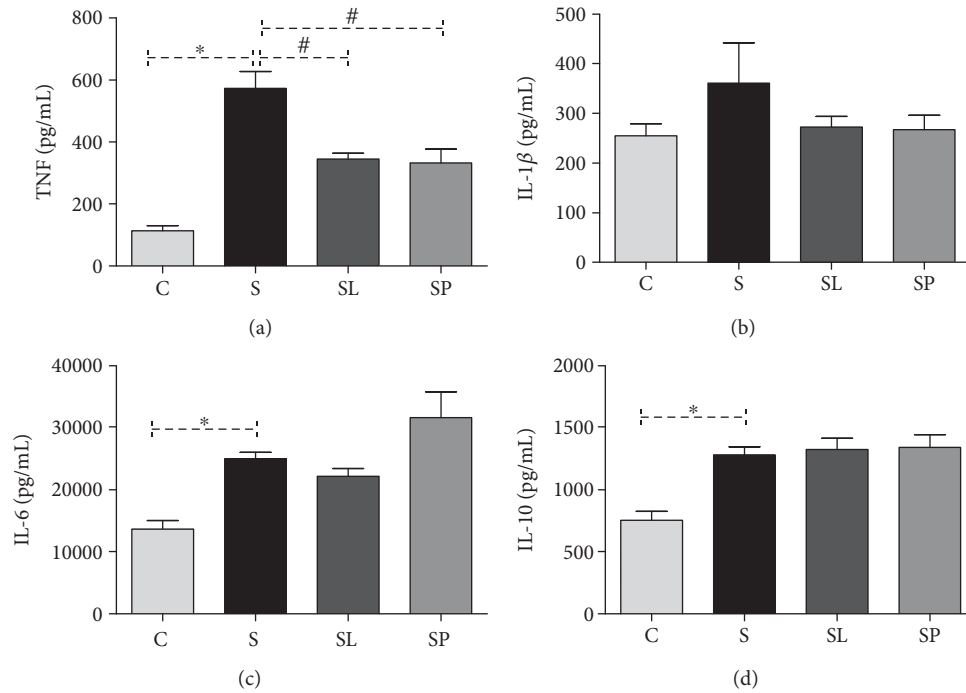


FIGURE 5: Effects of pulp and leaf extracts on serum cytokine levels. (a) TNF, (b) IL-1 β , (c) IL-6, and (d) IL-10. All data are shown as mean \pm SEM. * $P < 0.05$ indicates a significant difference between group S (sepsis) and group C (control). # $P < 0.05$ indicates a significant difference between S, SL (sepsis + leaf extract of mulberry), and SP (sepsis + mulberry pulp) groups.

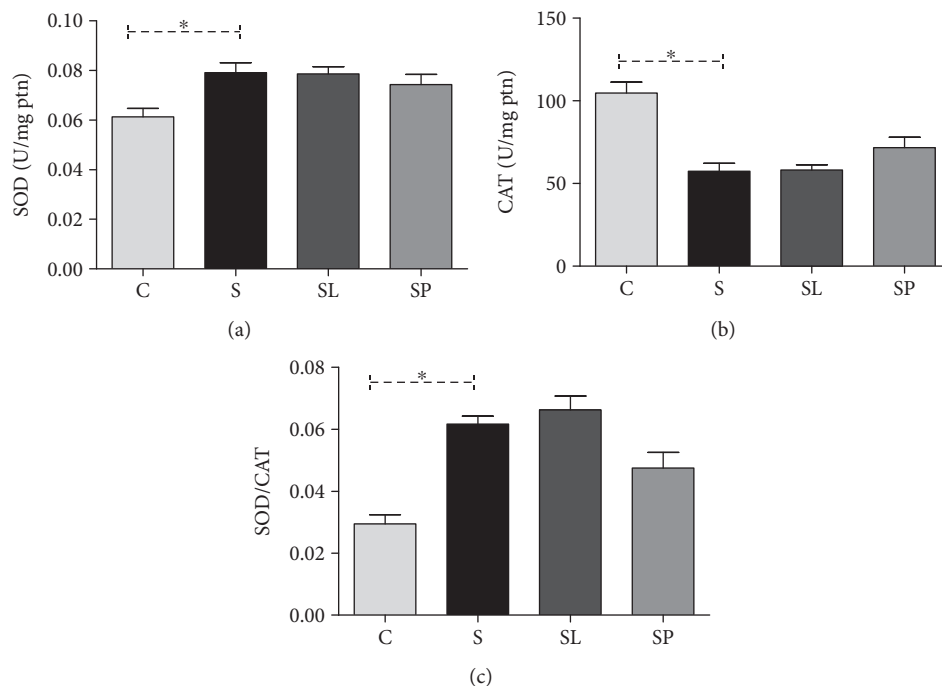


FIGURE 6: Effects of pulp and leaf extracts on the liver antioxidant enzymes. (a) SOD activity, (b) CAT activity, and (c) SOD/CAT ratio. All data are shown as mean \pm SEM. * $P < 0.05$ indicates a significant difference between group S (sepsis) and group C (control). # $P < 0.05$ indicates a significant difference between S, SL (sepsis + leaf extract of mulberry), and SP (sepsis + mulberry pulp) groups.

It is known that the anti-inflammatory and antioxidant properties of *Morus nigra* can be a determinant factor in the inflammatory processes and redox modulation induced

by sepsis. The inflammatory mediator activation in sepsis results in a metabolic imbalance [25]. Hypoglycemia observed in our study of a group of septic animals has also been observed

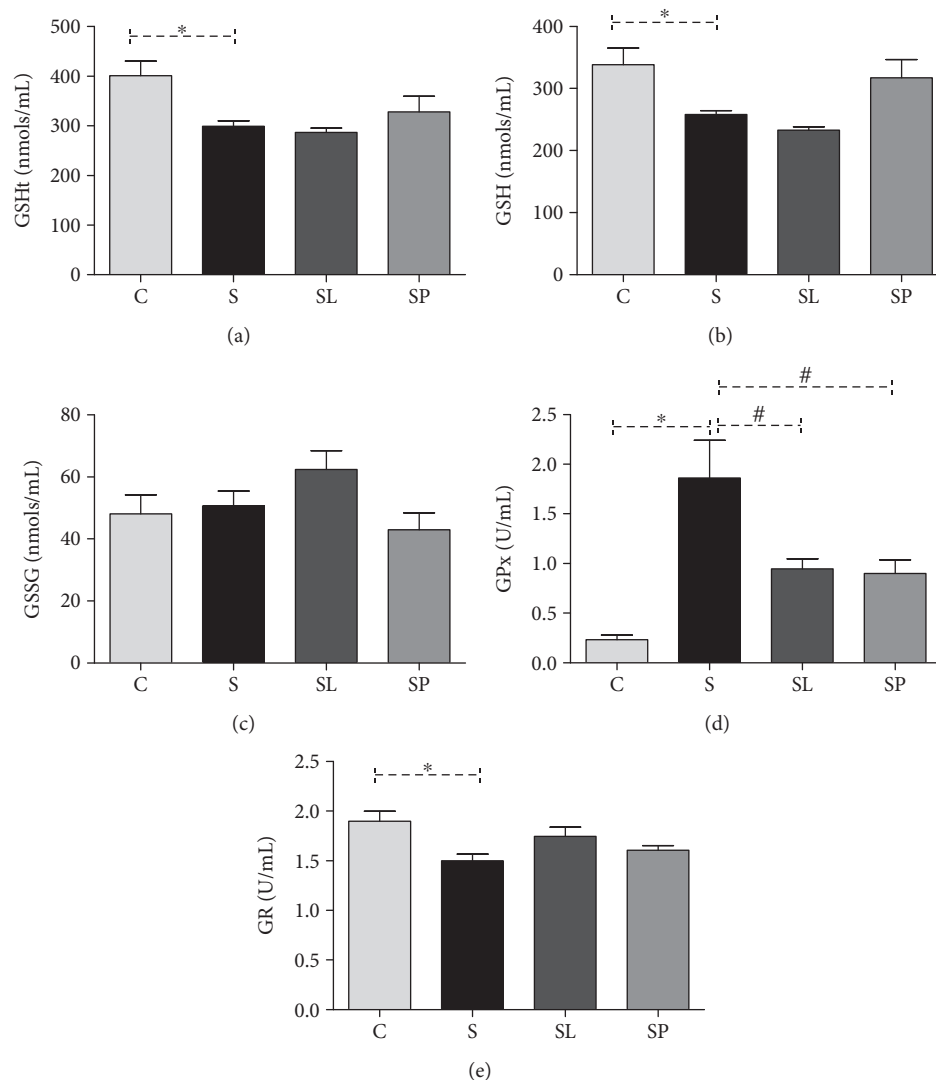


FIGURE 7: Effects of pulp and leaf extracts on hepatic glutathione metabolism. (a) Total glutathione (GSht), (b) reduced glutathione (GSH), (c) oxidated glutathione (GSSG), (d) glutathione peroxidase activity (GPx), and (e) glutathione reductase activity (GR). All data are shown as mean \pm SEM. * $P < 0.05$ indicates a significant difference between group S (sepsis) and group C (control). # $P < 0.05$ indicates a significant difference between S, SL (sepsis + leaf extract of mulberry), and SP (sepsis + mulberry pulp) groups.

in other studies [26, 27]. It is known that LPS is responsible to inhibit hepatic gluconeogenesis [28, 29]. In the same way, platelets are recognized to play an important role in innate and adaptive immunity [30], protecting against LPS-induced sepsis [31]. The treatment with *Morus nigra* did not alter the hypoglycemia and thrombocytopenia observed in septic animals. However, another well-studied parameter in sepsis is the inflammatory cell infiltration into the lungs. LPS induces lung microvascular injury, including leukocyte accumulation in the lung tissue, which plays an important role in the sepsis severity [32]. The results of this study show that the treatment with *Morus nigra* was able to reduce the inflammatory infiltrate in the lung. The presence and manifestations of immune activation are not uniform across the body spaces and organs. Thus, it is likely that a focus of infection at one site can produce organ damage at a distant site [33]. Based on this, levels of pro- and anti-inflammatory cytokines in the serum and the liver

were evaluated. The liver has an important role in bacterial and toxin clearance in sepsis [34]. Moreover, a major mechanism of sepsis immunosuppression is in liver desensitization, where the production of proinflammatory cytokines involves the concomitant induction of anti-inflammatory mediators, such as IL-10, in an attempt to protect the liver from injury [35]. The results showed an increase in the gene expression of IL-10 and a decrease in hepatic levels of IL-10, IL-6, and IL-1 β in septic animals when compared to the control, and the treatment with *Morus nigra* did not alter either the gene expression or the hepatic levels of cytokines. Analyzing these results, it is possible to infer that there was no association between the gene expression of cytokines and their hepatic levels, suggesting that posttranscriptional modification may be responsible for determining the levels of cytokines in the liver. Another point to be considered is that the host response to infection is a time- and space-compartmentalized process

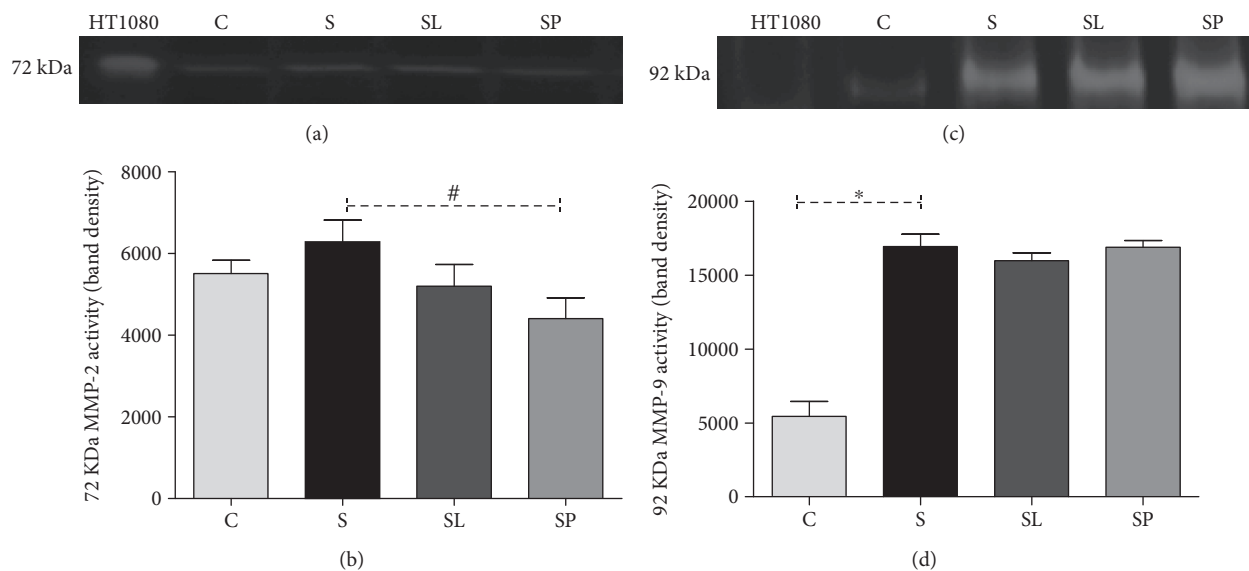


FIGURE 8: (a) Representative image of MMP-2 bands in the gel. (b) Effects of pulp extract and leaf extract on MMP-2 activity in hepatic homogenate. (c) Representative image of MMP-9 bands in the gel. (d) Effects of pulp and leaf extracts on MMP-9 activity in hepatic homogenate. C, S, SL, and SP; HT-1080 (Std.). All data are shown as mean \pm SEM. * $P < 0.05$ indicates a significant difference between group S (sepsis) and group C (control). # $P < 0.05$ indicates a significant difference between S, SL (sepsis + leaf extract of mulberry), and SP (sepsis + mulberry pulp) groups.

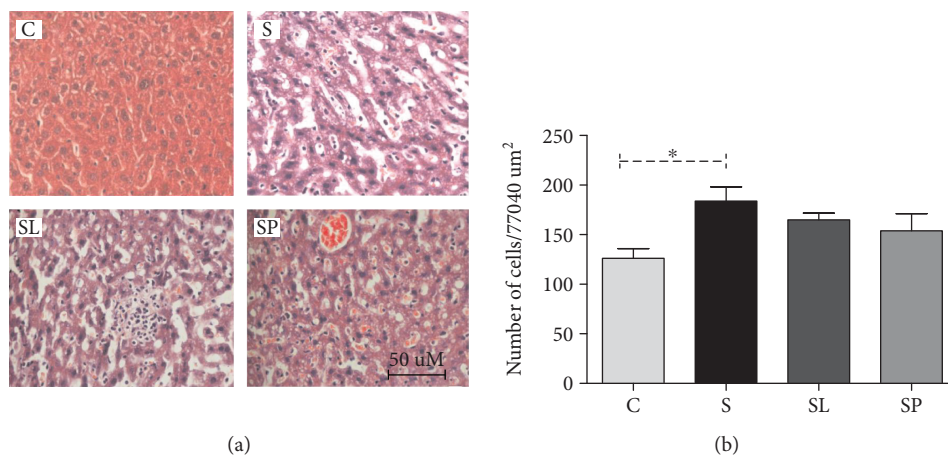


FIGURE 9: (a) Representative photomicrograph of hepatic tissue showing increased influx of leukocytes in septic mice (H&E $\times 40$). (b) Effect of pulp extract and leaf extract on the number of leukocytes in the hepatic tissue of septic mice. All data are shown as mean \pm SEM. * $P < 0.05$ indicates a significant difference between group S (sepsis) and group C (control). # $P < 0.05$ indicates a significant difference between S, SL (sepsis + leaf extract of mulberry), and SP (sepsis + mulberry pulp) groups.

that involves the inflammatory cytokine release that causes organ damage, being that the balance between proinflammatory and anti-inflammatory responses is a vital process in the liver during sepsis [35].

The events underlying the inflammatory response to lipopolysaccharide include the LPS detection by pattern recognition receptors, followed by the coordinated expression of proinflammatory cytokines (TNF, IL-1 β , and IL6) [36]. Regarding the serum levels of cytokines, an increase of TNF, IL-1 β , and IL6 was observed and both treatments were efficient to reduce the serum levels of TNF. TNF- α is key sepsis mediator [37] and is increased in circulation following

LPS administration [38]; thus, the serum decrease of TNF can have an important role in the sepsis outcome.

The antioxidant profile in the animals' liver was assessed as a means of evaluating the redox imbalance caused by sepsis and the effects of *Morus nigra* on the antioxidant defenses. Analyzing the ratio between the superoxide dismutase and catalase activities, it was observed that it remained significantly increased in animals belonging to the septic groups. This demonstrates that the increase in the SOD activity was not followed by an increase in the CAT activity. In this condition, the SOD activity does not usually protect the cell from a possible redox imbalance;

on the contrary, its activation results in an increase in hydrogen peroxide production that can mediate damage to the membranes and other biomolecules [39]. The glutathione system is another important component of the cellular antioxidant defense. Therefore, the enzyme glutathione peroxidase (GPx) has been proved to be an important oxidative stress biomarker in septic patients playing a critical role in the vital organ and tissue protection against oxidative damage. The increase in the SOD enzyme activity in all septic groups and the consequent increase in the hydrogen peroxide production were not followed by an increase in the catalase enzyme which is responsible for catalyzing the hydrolysis of this hydrogen peroxide into water and oxygen molecules. Thus, the accumulated peroxide may have been diverted to the glutathione system by the action of the enzyme glutathione peroxidase. This would justify the increase in the activity of this enzyme in septic animals. Many studies have already shown that LPS can raise the antioxidant enzyme activity as a response to the increase of reactive species caused by this substance [40, 41]. On the other hand, the activity of this enzyme in animals that received the treatments may have been reduced by the direct antioxidant action of phenolic compounds present in the two preparations of *Morus nigra* which were used in this study, in which the polyphenols are capable of reacting with the reactive species neutralizing their oxidant action in the organism [42].

It is known that LPS is able to induce the increase in the activity of several matrix metalloproteinases (MMPs), mainly MMP-2 and MMP-9 [43]. MMPs are a family of calcium- and zinc-dependent endopeptidases responsible for remodeling and degradation of extracellular matrix of basal membrane [44]. Our results show an increase in the MMP9 activity without a change in the MMP2 activity in the animals' liver of the sepsis group. It is known that MMP-2 is a constitutive expression enzyme, slightly responsive to the majority of stimuli, whereas MMP-9 is inducible, being considered a marker of systemic inflammation in animals [45]. Thus, it is possible to infer that the pretreatment with *Morus nigra* is able to inhibit the MMP2 constitutive expression without changing the MMP9 activity.

Concerning the liver histological analysis, a significant increase was observed in the influx of leukocytes in this tissue in septic animals when compared to control animals. It was also observed that the treatments were not capable of changing this parameter. The analysis of the liver tissue architecture revealed an apparent increase of sinusoidal capillaries in septic animals that can be explained by the influx of leukocytes in the organ. Sakurai et al. (2017) [46] also observed dilatation and congestion of the sinusoidal capillaries in septic animals in an experimental model of sepsis induced with LPS in the first hours after induction.

The results of this study made evident the complexity of sepsis, showing that this is a disease capable of compromising the function of several organs, especially the liver. This study also showed that the treatment with the extracts of leaves and the pulp of *Morus nigra* produced beneficial effects on the modulation of important parameters that are normally altered in sepsis. This shows that the chemical compounds

present in both preparations can modulate, at least in part, the damage caused by sepsis.

Data Availability

The results are available in the manuscript itself, but if any reader has any doubts, we are willing to respond.

Conflicts of Interest

The authors declare that they have no conflicts of interest.

Acknowledgments

This work was supported by Fundação de Amparo à Pesquisa do Estado de Minas Gerais (FAPEMIG), Conselho Nacional de Desenvolvimento Científico e Tecnológico (CNPq), and Universidade Federal de Ouro Preto (UFOP), Brazil. AT was supported by CNPq with the Fellowship of Research Productivity. FSB has been taking a Post-Doctoral Fellow (CAPES-PVEX-Process # 88881.172437/2018-01) in the Interdepartmental Division of Critical Care Medicine, St. Michael's Hospital, University of Toronto, Toronto, ON, Canada.

References

- [1] M. Singer, C. S. Deutschman, C. W. Seymour et al., "The third international consensus definitions for sepsis and septic shock (Sepsis-3)," *JAMA*, vol. 315, no. 8, pp. 801–810, 2016.
- [2] P. Strnad, F. Tacke, A. Koch, and C. Trautwein, "Liver - guardian, modifier and target of sepsis," *Nature Reviews Gastroenterology & Hepatology*, vol. 14, no. 1, pp. 55–66, 2017.
- [3] T. Solov'eva, V. Davydova, I. Krasikova, and I. Yermak, "Marine compounds with therapeutic potential in gram-negative sepsis," *Marine Drugs*, vol. 11, no. 6, pp. 2216–2229, 2013.
- [4] S. K. Biswas, "Does the interdependence between oxidative stress and inflammation explain the antioxidant paradox?," *Oxidative Medicine and Cellular Longevity*, vol. 2016, Article ID 5698931, 9 pages, 2016.
- [5] S. Li, M. Hong, H. Y. Tan, N. Wang, and Y. Feng, "Insights into the role and interdependence of oxidative stress and inflammation in liver diseases," *Oxidative Medicine and Cellular Longevity*, vol. 2016, Article ID 4234061, 21 pages, 2016.
- [6] M. Gundogdu, F. Muradoglu, R. I. G. Sensoy, and H. Yilmaz, "Determination of fruit chemical properties of *Morus nigra* L., *Morus alba* L. and *Morus rubra* L. by HPLC," *Scientia Horticulturae*, vol. 132, pp. 37–41, 2011.
- [7] M. A. Miranda, G. D. V. Vieira, M. S. Alves, C. H. Yamamoto, J. J. R. G. Pinho, and O. V. Sousa, "Uso etnomedicinal do chá de *Morus nigra* L. no tratamento dos sintomas do climatério de mulheres de Muriaé, Minas Gerais, Brasil," *HU Revista*, vol. 36, pp. 61–68, 2010.
- [8] M. Ozgen, S. Serce, and C. Kaya, "Phytochemical and antioxidant properties of anthocyanin-rich *Morus nigra* and *Morus rubra* fruits," *Scientia Horticulturae*, vol. 119, no. 3, pp. 275–279, 2009.
- [9] G. R. Souza, R. G. Oliveira-Junior, T. C. Diniz et al., "Assessment of the antibacterial, cytotoxic and antioxidant activities

- of *Morus nigra* L. (Moraceae),” *Brazilian Journal of Biology*, vol. 78, no. 2, pp. 248–254, 2018.
- [10] M. M. Padilha, F. C. Vilela, C. Q. Rocha et al., “Antiinflammatory properties of *Morus nigra* leaves,” *Phytotherapy Research*, vol. 24, no. 10, pp. 1496–1500, 2010.
 - [11] H. Chen, J. Pu, D. Liu et al., “Anti-inflammatory and antinociceptive properties of flavonoids from the fruits of black mulberry (*Morus nigra* L.),” *PLoS One*, vol. 11, no. 4, p. e0153080, 2016.
 - [12] C. M. Araujo, K. d. P. Lúcio, M. E. Silva et al., “*Morus nigra* leaf extract improves glycemic response and redox profile in the liver of diabetic rats,” *Food and Function*, vol. 6, no. 11, pp. 3490–3499, 2015.
 - [13] H. M. TAG, “Hepatoprotective effect of mulberry (*Morus nigra*) leaves extract against methotrexate induced hepatotoxicity in male albino rat,” *BMC Complementary and Alternative Medicine*, vol. 15, no. 1, pp. 252–261, 2015.
 - [14] H. Aebi, “[13] Catalase in vitro,” *Methods in Enzymology*, vol. 105, pp. 121–126, 1984.
 - [15] S. Marklund and G. Marklund, “Involvement of the superoxide anion radical in the autoxidation of pyrogallol and a convenient assay for superoxide dismutase,” *European Journal of Biochemistry*, vol. 47, no. 3, pp. 469–474, 1974.
 - [16] M. M. Sung, C. G. Schulz, W. Wang, G. Sawicki, N. L. Bautista-López, and R. Schulz, “Matrix metalloproteinase-2 degrades the cytoskeletal protein alpha-actinin in peroxynitrite mediated myocardial injury,” *Journal of Molecular and Cellular Cardiology*, vol. 43, no. 4, pp. 429–436, 2007.
 - [17] G. A. Naderi, S. Asgary, N. Sarraf-Zadegan, H. Oroojy, and F. Afshin-Nia, “Antioxidant activity of three extracts of *Morus nigra*,” *Phytotherapy Research*, vol. 18, no. 5, pp. 365–369, 2004.
 - [18] C. A. Simões, E. P. Schenkel, G. Gosmann, J. C. Mello, L. A. Mentz, and P. R. Petrovick, *Farmacognosia da planta ao medicamento*, Florianópolis: Editora da UFSC, 6^a edition, 2007.
 - [19] Y. Kimura, H. Okuda, T. Nomura, T. Fukai, and S. Arichi, “Effects of phenolic constituents from the mulberry tree on arachidonate metabolism in rat platelets,” *Journal of Natural Products*, vol. 49, no. 4, pp. 639–644, 1986.
 - [20] J. S. Cho, J. H. Kang, J. M. Shin, I. H. Park, and H. M. Lee, “Inhibitory effect of delphinidin on extracellular matrix production via the MAPK/NF- κ B pathway in nasal polyp-derived fibroblasts,” *Allergy, Asthma & Immunology Research*, vol. 7, no. 3, pp. 276–282, 2015.
 - [21] O. Dayoub, R. Andriantsitohaina, and N. Clere, “Pleiotropic beneficial effects of epigallocatechin gallate, quercetin and delphinidin on cardiovascular diseases associated with endothelial dysfunction,” *Cardiovascular & Hematological Agents in Medicinal Chemistry*, vol. 11, no. 4, pp. 249–264, 2013.
 - [22] C.-H. Wang, L.-L. Zhu, K.-F. Ju, J.-L. Liu, and K.-P. Li, “Anti-inflammatory effect of delphinidin on intramedullary spinal pressure in a spinal cord injury rat model,” *Experimental and Therapeutic Medicine*, vol. 14, pp. 583–5588, 2017.
 - [23] P. H. Shih, C. T. Yeh, and G. C. Yen, “Anthocyanins induce the activation of phase II enzymes through the antioxidant response element pathway against oxidative stress-induced apoptosis,” *Journal of Agricultural and Food Chemistry*, vol. 55, no. 23, pp. 9427–9435, 2007.
 - [24] V. C. Chaves, L. Boff, M. Vizzotto, E. Calvete, F. H. Reginatto, and C. M. O. Simões, “Berries grown in Brazil: anthocyanin profiles and biological properties,” *Journal of the Science of Food and Agriculture*, vol. 98, no. 11, pp. 4331–4338, 2018.
 - [25] I. Matot and C. L. Sprung, “Definition of sepsis,” *Intensive Care Medicine*, vol. 27, no. 14, pp. S3–S9, 2001.
 - [26] A. Suzuki, M. Uno, K. Arima et al., “A case report: sepsis associated with hypoglycemia,” *Kansenshogaku zasshi The Journal of the Japanese Association for Infectious Diseases*, vol. 68, no. 8, pp. 986–989, 1994.
 - [27] H. Tanaka, Y. Nishikawa, T. Fukushima et al., “Lipopolysaccharide inhibits hepatic gluconeogenesis in rats: the role of immune cells,” *Journal of Diabetes Investigation*, vol. 9, no. 3, pp. 494–504, 2018.
 - [28] K. F. LaNoue, A. D. Mason Jr, and J. P. Daniels, “The impairment of glucogenesis by Gram negative infection,” *Metabolism*, vol. 17, no. 7, pp. 606–611, 1968.
 - [29] J. P. Filkins and R. P. Cornell, “Depression of hepatic gluconeogenesis and the hypoglycemia of endotoxin shock,” *American Journal of Physiology*, vol. 227, no. 4, pp. 778–781, 1974.
 - [30] J. W. Semple, J. E. Italiano, and J. Freedman, “Platelets and the immune continuum,” *Nature Reviews Immunology*, vol. 11, no. 4, pp. 264–274, 2011.
 - [31] B. Xiang, G. Zhang, L. Guo et al., “Platelets protect from septic shock by inhibiting macrophage-dependent inflammation via the cyclooxygenase 1 signalling pathway,” *Nature Communications*, vol. 4, no. 1, pp. 2657–2684, 2013.
 - [32] X. Peng, P. M. Hassoun, S. Sammani et al., “Protective effects of sphingosine 1-phosphate in murine endotoxin-induced inflammatory lung injury,” *American Journal of Respiratory and Critical Care Medicine*, vol. 169, no. 11, pp. 1245–1251, 2004.
 - [33] J. M. Cavillon and D. Annane, “Compartmentalization of the inflammatory response in sepsis and SIRS,” *Journal of Endotoxin Research*, vol. 12, no. 3, pp. 151–170, 2006.
 - [34] U. Protzer, M. K. Maini, and P. A. Knolle, “Living in the liver: hepatic infections,” *Nature Reviews Immunology*, vol. 12, no. 3, pp. 201–213, 2012.
 - [35] J. Yan, S. Li, and S. Li, “The role of the liver in sepsis,” *International Reviews of Immunology*, vol. 33, no. 6, pp. 498–510, 2014.
 - [36] K. H. Lee, M. H. Yeh, S. T. Kao et al., “Xia-bai-san inhibits lipopolysaccharide-induced activation of intercellular adhesion molecule-1 and nuclear factor-kappa B in human lung cells,” *Journal of Ethnopharmacology*, vol. 124, no. 3, pp. 530–538, 2009.
 - [37] R. Lucas, J. Lou, D. R. Morel, B. Ricou, P. M. Suter, and G. E. Grau, “TNF receptors in the microvascular pathology of acute respiratory distress syndrome and cerebral malaria,” *Journal of Leukocyte Biology*, vol. 61, no. 5, pp. 551–558, 1997.
 - [38] N. Tsao, C. C. Liu, C. M. Wu, H. P. Hsu, and H. Y. Lei, “Tumour necrosis factor- α causes an increase in blood-brain barrier permeability during sepsis,” *Journal of Medical Microbiology*, vol. 50, no. 9, pp. 812–821, 2001.
 - [39] K. M. Stepien, R. Heaton, S. Rankin et al., “Evidence of oxidative stress and secondary mitochondrial dysfunction in metabolic and non-metabolic disorders,” *Journal of Clinical Medicine*, vol. 6, no. 7, 2017.
 - [40] D. M. El-Tanbouly, R. M. Abdelsalam, A. S. Attia, and M. T. Abdel-Aziz, “Pretreatment with magnesium ameliorates lipopolysaccharide-induced liver injury in mice,” *Pharmacological Reports*, vol. 67, no. 5, pp. 914–920, 2015.

- [41] R. El Kebbjaj, P. Andreoletti, H. I. El Hajj et al., "Argan oil prevents down-regulation induced by endotoxin on liver fatty acid oxidation and gluconeogenesis and on peroxisome proliferator-activated receptor gamma coactivator-1 α , (PGC-1 α), peroxisome proliferator-activated receptor α (PPAR α) and estrogen related receptor α (ERR α)," *Biochimie Open*, vol. 1, pp. 51–59, 2015.
- [42] F. A. Paiva, L. de Freitas Bonomo, P. F. Boasquivis et al., "Carqueja (*Baccharis trimera*) protects against oxidative stress and β -amyloid-induced toxicity in *Caenorhabditis elegans*," *Oxidative Medicine and Cellular Longevity*, vol. 2015, Article ID 740162, 15 pages, 2015.
- [43] M. A. Bellavance, M. Blanchette, and D. Fortin, "Recent advances in blood-brain barrier disruption as a CNS delivery strategy," *American Association of Pharmaceutical Scientists Journal*, vol. 10, no. 1, pp. 166–177, 2008.
- [44] W. Pengbo, H. Yonglong, T. Shiyun, L. Ming, S. Yongxiang, and F. Guo, "Interactions of central obesity with rs3918242 on risk of non-alcoholic fat liver disease: a preliminary case-control study," *International Journal of Clinical and Experimental Pathology*, vol. 8, pp. 4165–4170, 2015.
- [45] G. Opdenakker, P. E. Van den Steen, and J. Van Damme, "Gelatinase B: a tuner and amplifier of immune functions," *Trends in Immunology*, vol. 22, no. 10, pp. 571–579, 2001.
- [46] K. Sakurai, T. Miyashita, M. Okazaki et al., "Role for neutrophil extracellular traps (NETs) and platelet aggregation in early sepsis-induced hepatic dysfunction," *In Vivo*, vol. 31, no. 6, pp. 1051–1058, 2017.

Research Article

Polysiphonia japonica Extract Attenuates Palmitate-Induced Toxicity and Enhances Insulin Secretion in Pancreatic Beta-Cells

Seon-Heui Cha ^{1,2,3}, Hyun-Soo Kim,⁴ Yongha Hwang,^{1,2} You-Jin Jeon,⁴ and Hee-Sook Jun ^{1,2,3}

¹College of Pharmacy, Gachon University, Incheon 21936, Republic of Korea

²Lee Gil Ya Cancer and Diabetes Institute, Gachon University, Incheon 21936, Republic of Korea

³Gachon Medical and Convergence Institute, Gachon Gil Medical Center, Incheon 21565, Republic of Korea

⁴Department of Marine Life Science, School of Marine Biomedical Sciences, Jeju National University, Jeju 63243, Republic of Korea

Correspondence should be addressed to Hee-Sook Jun; hsjun@gachon.ac.kr

Received 18 May 2018; Revised 18 September 2018; Accepted 19 September 2018; Published 28 October 2018

Guest Editor: Anderson J. Teodoro

Copyright © 2018 Seon-Heui Cha et al. This is an open access article distributed under the Creative Commons Attribution License, which permits unrestricted use, distribution, and reproduction in any medium, provided the original work is properly cited.

Beta-cell loss is a major cause of the pathogenesis of diabetes. Elevated levels of free fatty acids may contribute to the loss of β -cells. Using a transgenic zebrafish, we screened ~50 seaweed crude extracts to identify materials that protect β -cells from free fatty acid damage. We found that an extract of the red seaweed *Polysiphonia japonica* (PJE) had a β -cell protective effect. We examined the protective effect of PJE on palmitate-induced damage in β -cells. PJE was found to preserve cell viability and glucose-induced insulin secretion in a pancreatic β -cell line, Ins-1, treated with palmitate. Additionally, PJE prevented palmitate-induced insulin secretion dysfunction in zebrafish embryos and mouse primary islets and improved insulin secretion in β -cells against palmitate treatment. These findings suggest that PJE protects pancreatic β -cells from palmitate-induced damage. PJE may be a potential therapeutic functional food for diabetes.

1. Introduction

It was estimated that 415 million people had diabetes mellitus (DM) in 2015, and this number is projected to increase to 642 million by 2040 (IDF diabetes atlas, 7th edition). DM is a group of chronic metabolic disorders characterized by a deficiency in circulating insulin levels, which results in high blood sugar levels over a prolonged period. Insulin deficiency is caused by a reduction in the number of insulin-producing β -cells in both type 1 and type 2 diabetes [1].

In type 2 diabetes, pancreatic β -cells are required to secrete increasing amounts of insulin to compensate for increasing insulin resistance. This places β -cells under increasing metabolic stress, eventually deteriorating their function and numbers [2–4]. Thus, it is important to preserve the health of β -cells. Preventing β -cell degeneration is an essential approach for treating DM.

Phytochemicals are regarded as an important source for treating human health problems, including DM. Seaweeds

are composed of a variety of bioactive substances such as polysaccharides, pigments, minerals, peptides, and polyphenols, which have valuable pharmaceutical and biomedical potential [5–10]. Numerous studies have demonstrated the beneficial effects of seaweeds for managing DM in animal models of diabetes and human patients [11–16].

Polysiphonia japonica is a red seaweed, and some members of its family were shown to have antioxidant [17, 18], antimycobacterial [19], and anticancer [20] activities. However, no studies have examined the effect of *P. japonica* on β -cell mass and function. Therefore, in this study, we evaluated whether PJE prevents palmitate-induced β -cell dysfunction following exposure to high levels of fatty acids such as those observed in DM.

2. Materials and Methods

2.1. *Polysiphonia japonica* Extract (PJE). *Polysiphonia japonica* was collected, rinsed with freshwater to remove the salt,

epiphytes, and sand, and stored at -75°C . The frozen samples were lyophilized and finely ground. To prepare the extract, 1 g (dry weight) of the alga was solubilized in 100 mL of 80% methanol for 24 h under continuous shaking at 20°C , and then the extracts were filtered and concentrated under a vacuum in a rotary evaporator (EYELA, Tokyo, Japan) at 40°C .

2.2. Cell Culture. The rat pancreatic β -cell line Ins-1 was cultured in RPMI 1640 supplemented with 10% fetal bovine serum, 100 U/mL penicillin, 100 $\mu\text{g}/\text{mL}$ streptomycin, and 55 μM β -mercaptoethanol and was maintained in a humidified incubator with 5% CO_2 .

2.3. Isolation of Islets. Islets were isolated from 10-week-old male C57BL/6 mice (Orient Bio, Kyunggi-do, Korea) using the liberase digestion method as described previously [21]. Briefly, after injection of liberase (Roche, Basel, Switzerland) into the bile duct, the swollen pancreas was excised and incubated at 37°C for 20 min. The islets were then separated by Ficoll (Sigma, St. Louis, MO, USA) gradient centrifugation at $2000 \times g$ for 10 min. Size-matched healthy islets were hand-picked under a stereomicroscope and maintained in RPMI 1640 containing 5.5 mM glucose supplemented with 10% fetal bovine serum, 100 U/mL penicillin, and 100 $\mu\text{g}/\text{mL}$ streptomycin for 24 h.

2.4. Assessment of Cell Viability. Cell viability was estimated using a cell counting kit (CCK-8; Dojindo Laboratories, Kumamoto, Japan), which measures mitochondrial dehydrogenase activity. For the CCK-8 assay, Ins-1 cells (5×10^4 cells/well) were seeded into 96-well plates. After 16 h, the cells were incubated with 1 or 2 $\mu\text{g}/\text{mL}$ PJE or 0.1, 0.2, 0.4, or 0.8 mM palmitate for 24 h to check the toxicity. To examine the protective effect of PJE, the cells were pre-treated with 2 $\mu\text{g}/\text{mL}$ PJE for 1 h and then incubated with or without 0.2 mM palmitate (Sigma, St. Louis, MO, USA) for 24 h at 37°C . CCK-8 solution was then added to the wells to a total reaction volume of 110 μL . After 2 h of incubation, the absorbance was measured at a wavelength of 450 nm. The optical density of the formazan generated in the control cells was considered to represent 100% viability.

2.5. Measurement of Insulin Secretion. Ins-1 cells (1×10^5 cells/well) or isolated islets (5 or 8 islets) were plated into 24-well plates for insulin secretion measurements as previously described [22]. Briefly, the cells were incubated with KRB buffer containing 3 or 17 mM glucose for 2 h at 37°C . The supernatants were collected, and released insulin was measured using an enzyme-linked immunosorbent assay (ELISA) kit according to the manufacturer's protocol (ALPCO, Salem, NH, USA). Insulin content was normalized to DNA (for islets) or protein (for Ins-1 cells) levels, which was determined using a DCTM protein assay kit (Bio-Rad, Hercules, CA, USA).

2.6. Treatment of Zebrafish Embryos with PJE and Palmitate. Transgenic zebrafish expressing enhanced green fluorescent protein under control of the insulin promoter $Tg(ins-egfp)$ were obtained from Korean Zebrafish Organogenesis Mutant

Bank and used in the experiment. Approximately 3 days postfertilization (dpf), embryos ($n = 6-8$) were transferred into a 24-well plate and maintained in 1 mL of embryo media. To determine the effect of PJE on insulin expression, embryos were incubated with or without PJE for 1 day. For palmitate treatment, embryos were incubated in the presence of PJE for 1 h prior to adding palmitate (0.2 mM) for 24 h. Next, the embryos were further incubated with basal glucose (3 mM) or stimulatory glucose (20 mM) for 3.5 h. The embryos were rinsed in embryo media and anesthetized with 2-phenoxyethanol (Sigma) to observe phase and fluorescence images (Leica, Wetzlar, Germany). For confocal microscopy, the embryos were fixed in 4% paraformaldehyde overnight at 4°C and washed with phosphate-buffered saline for 5 min at room temperature. After washing several times with phosphate-buffered saline, the pancreata were isolated from the embryos, stained with DAPI (Invitrogen, Carlsbad, CA, USA) for 5 min, mounted on slides with Vectashield (Vector Laboratories, Burlingame, CA, USA), and observed with a confocal microscope (Zeiss, Oberkochen, Germany). ImageJ software (NIH, Bethesda, MD, USA) was used to quantify the fluorescence and number of cells in the zebrafish. Zebrafish embryos were handled in accordance with the guidelines of Gachon University.

2.7. Measurement of Heart Rates. Zebrafish embryos were incubated with 10 $\mu\text{g}/\text{mL}$ PJE from 3 to 4 dpf, and heart rates were measured as an indicator of possible PJE toxicity [23]. Counting and recording of atrial and ventricular contractions were performed for 3 min under a microscope, and the results were presented as the average heart rate per minute.

2.8. Polyphenol, Carbohydrate, Lipid, and Protein Analysis. To quantify the polyphenol content of PJE, the total phenolic content was estimated using the Folin-Ciocalteu phenol method [24]. The total carbohydrate content of PJE was quantified using the phenol-sulfuric acid method [25]. The lipid content of PJE was determined using a colorimetric sulfo-phospho-vanillin method [26]. The protein concentration of PJE was measured using a DC protein assay kit (Bio-Rad, Hercules, CA).

2.9. High-Performance Liquid Chromatography (HPLC) Analysis. Liquid chromatography analysis of PJE was performed on a Waters HPLC system HPLC analysis. A Sunfire C18 ODS 4.6×150 mm column (Waters Corporation, Milford, MA, USA) was employed for reverse-phase separations. The mobile phases were 0.1% v/v formic acid in water and 0.1% v/v formic acid in acetonitrile at a flow rate of 1 mL/min. The elution gradient for the Sunfire C18 ODS condition was programmed as an increasing percentage from 5% to 100% over 60 min, holding at 100% for 10 min, and finally reequilibrating the column at 5% for 10 min. A standard solution containing DMH1 (Tocris, Bristol, UK) was prepared by dissolving DMH1 in distilled water (5 mg/mL). The solution was filtered through a 0.45 μm membrane filter, after which HPLC was performed.

2.10. Statistical Analysis. All measurements were carried out in triplicate, and all values are represented as the

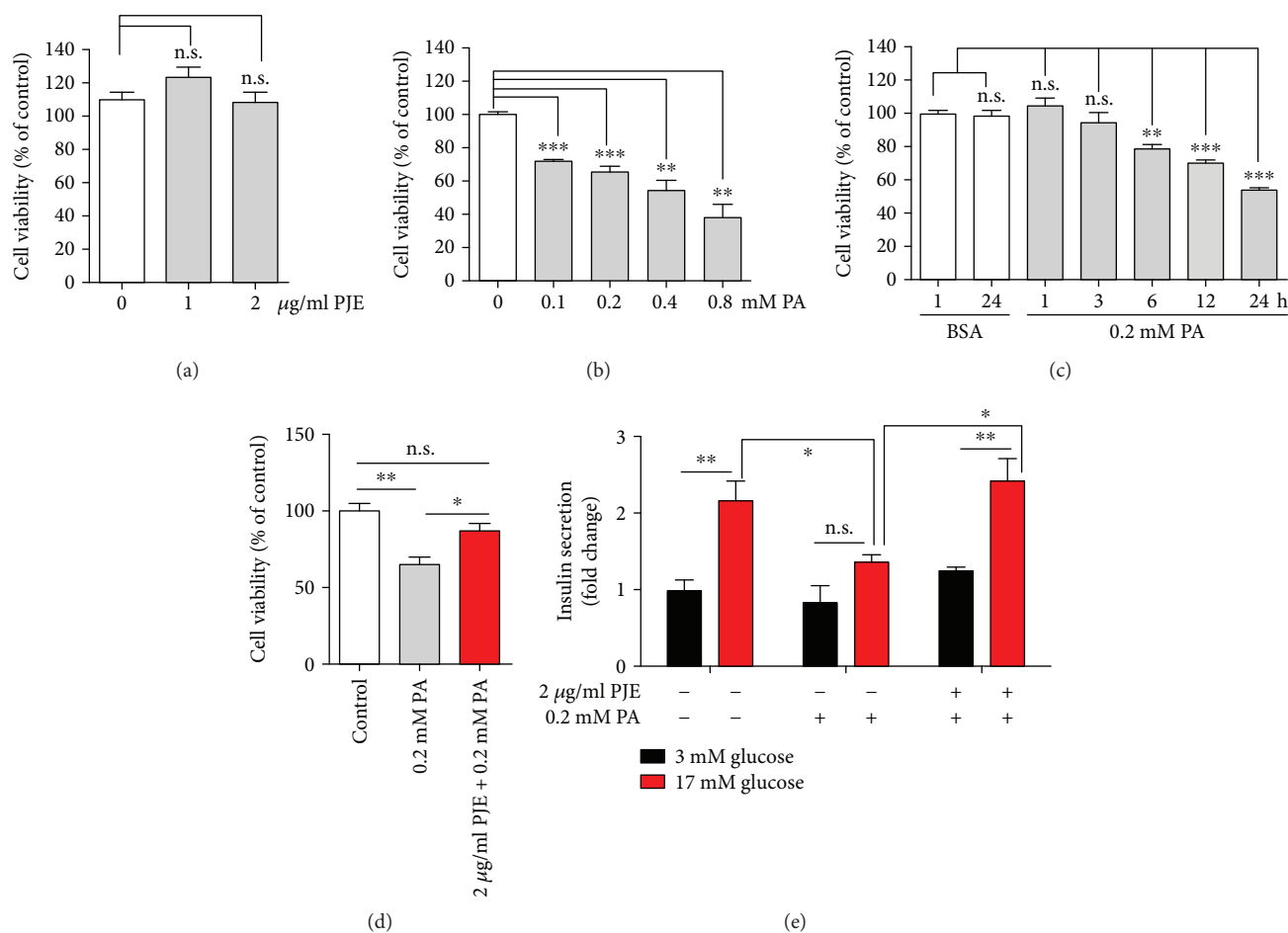


FIGURE 1: *Polysiphonia japonica* extract (PJE) protects against palmitate-induced lipotoxicity and dysfunction in Ins-1 cells. (a) Ins-1 cells were incubated with the indicated concentrations of PJE for 24 h. (b) Ins-1 cells were incubated with the indicated concentrations of palmitate (PA) for 24 h. (c) Ins-1 cells were incubated with 0.2 mM PA for the indicated times. (d) Ins-1 cells were incubated with 2 µg/mL PJE for 1 h and then further incubated with or without 0.2 mM PA for 24 h. CCK-8 assays were subsequently performed. (e) Ins-1 cells were incubated with 2 µg/mL PJE in 5 mM glucose media for 1 h and then further incubated with or without 0.2 mM palmitate (PA) for 24 h. Thereafter, the cells were starved in 0.2 mM glucose-containing KRB buffer for 2 h. Insulin release was measured after 2 h of incubation in either 3 mM glucose or 17 mM glucose. ELISA assays for insulin were subsequently performed. Data are expressed as the fold change from untreated cells in 3 mM glucose. Experiments were performed in triplicate. * $p < 0.05$, ** $p < 0.01$, and *** $p < 0.001$. n.s.: no significance.

mean \pm S.E. The results were subjected to an analysis of variance with the two-way and Tukey tests to analyze the differences (more than three samples), or Student's t -test (two samples) was applied. Values of $p < 0.05$ were considered significant.

3. Results

3.1. PJE Attenuates Palmitate-Induced Lipotoxicity in Ins-1 Cells. In order to find substances that increase insulin secretion, over 50 seaweed crude extracts were screened. Among them, PJE was the most prominent to insulin secretion.

First, to determine whether PJE protects against palmitate-induced cytotoxicity, Ins-1 cells were treated with either PJE or palmitate alone or were preincubated with PJE for 1 h and then further incubated with palmitate for various doses and times. PJE alone showed no cytotoxicity towards Ins-1 cells in the concentration range tested (1–2 µg/mL) (Figure 1(a)). Significantly lower cell viability

was observed in Ins-1 cells treated with palmitate in dose- and time-dependent manners (Figures 1(b) and 1(c)). Pre-treatment with 2 µg/mL PJE increased the cell viability to approximately 85% in the presence of 0.2 mM palmitate for 24 h compared to that in the presence of 0.2 mM palmitate alone (Figure 1(d)), indicating that PJE has cytoprotective effects against palmitate-induced damage in Ins-1 cells.

3.2. PJE Protects against Palmitate-Induced β -Cell Dysfunction in Ins-1 Cells. To investigate whether PJE protects against palmitate-induced β -cell dysfunction, we measured insulin secretion from PJE-treated Ins-1 cells in the presence of palmitate. Although palmitate had no effect on basal insulin secretion (3 mM glucose), insulin secretion stimulated by a high glucose concentration (17 mM) was inhibited by treatment with palmitate. When Ins-1 cells were preincubated with 2 µg/mL PJE prior to palmitate treatment, the suppressed insulin secretion was restored to normal levels

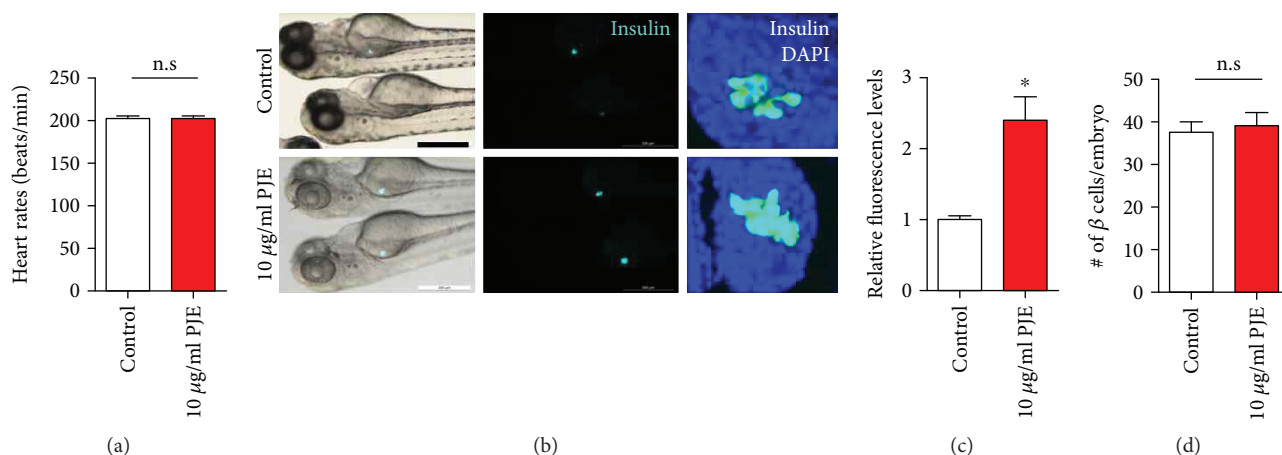


FIGURE 2: *Polysiphonia japonica* extract (PJE) promotes insulin secretion in zebrafish. Zebrafish were incubated with 10 µg/mL PJE from 3 to 4 days postfertilization. (a) Heart rates of embryos were measured for 3 min. (b) Phase contrast images of zebrafish and fluorescence and confocal microscopy images of the β-cell mass of zebrafish. Scale bar: 200 µm. (c) Relative EGFP fluorescence levels from (b). (d) Number of β-cells per embryo from (b). $n = 17-24$. * $p < 0.05$; n.s.: no significance.

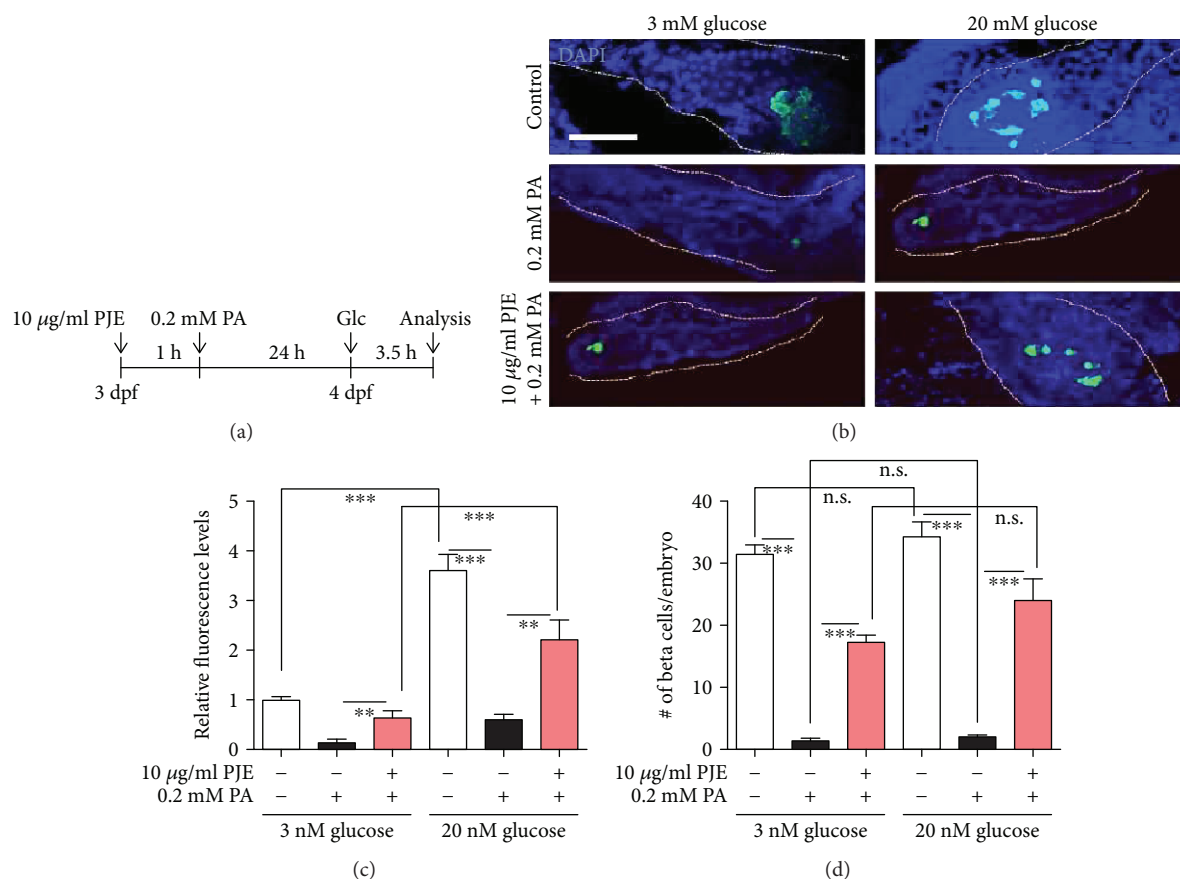


FIGURE 3: *Polysiphonia japonica* extract (PJE) protects against palmitate-induced β-cell dysfunction in zebrafish. (a) Zebrafish were incubated with 10 µg/mL PJE and 0.2 mM palmitate (PA) from 3 to 4 days postfertilization (dpf). PJE was added 1 h prior to PA treatment. Thereafter, the zebrafish incubated with 3 or 20 mM glucose for 3.5 h. (b) Confocal microscopy images of the pancreas of zebrafish. Scale bar: 100 µm. (c) Relative EGFP fluorescence levels from (b). (d) Number of β-cells per embryo from (b). $n = 4-6$. * $p < 0.05$ and *** $p < 0.001$. n.s.: no significance.

(Figure 1(e)), suggesting that the PJE has protective effects on the inhibition of insulin secretion in the presence of palmitate in Ins-1 cells.

3.3. PJE Promotes Insulin Secretion, but Not β-Cell Proliferation, in Zebrafish. To determine whether PJE directly affects insulin secretion *in vivo*, we used transgenic zebrafish

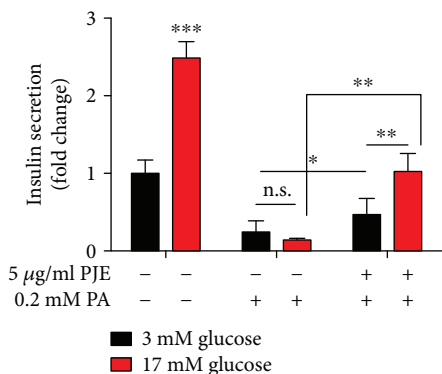


FIGURE 4: *Polysiphonia japonica* extract (PJE) protects against palmitate-induced β -cell dysfunction in mouse primary islets. Islets were incubated with the 5 $\mu\text{g}/\text{mL}$ PJE for 1 h and then further incubated with or without 0.2 mM palmitate (PA) for 24 h. Thereafter, the islets were starved in 0.2 mM glucose-containing KRB buffer for 2 h. Insulin release was measured after further incubation with 3 mM glucose or 17 mM glucose by ELISA. Experiments were performed in triplicate. * $p < 0.05$, ** $p < 0.01$, and *** $p < 0.001$; n.s.: no significance.

expressing enhanced green fluorescent protein (EGFP) under control of the insulin promoter. Incubation of embryos with 10 $\mu\text{g}/\text{mL}$ PJE for 24 h showed no toxic effects, as determined by heart rate measurements (Figure 2(a)). A significantly increased intensity of EGFP was observed in PJE-treated zebrafish embryos (Figures 2(b) and 2(c)). Interestingly, PJE treatment did not alter the number of EGFP-positive β -cells (Figure 2(d)). These data suggest that PJE promotes insulin secretion in zebrafish embryos.

3.4. PJE Protects against Palmitate-Induced β -Cell Dysfunction in Zebrafish. Next, we examined whether PJE has a protective effect against palmitate in zebrafish embryos. Embryos were preincubated with 10 $\mu\text{g}/\text{mL}$ PJE for 1 h, further incubated with 0.2 mM palmitate for 24 h, and stimulated with 3 or 20 mM glucose for 3.5 h (Figure 3(a)). We found that EGFP-expressing β -cells were reduced by palmitate treatment, whereas higher expression of EGFP was observed in PJE-pretreated embryos (Figure 3(b)). Palmitate-treatment decreased both basal insulin secretion (3 mM glucose) and insulin secretion after stimulation with high glucose concentrations (20 mM), while insulin secretion was recovered by PJE pretreatment in zebrafish embryos (Figure 3(c)), suggesting that PJE protects against palmitate-induced insulin secretion dysfunction in zebrafish embryos. Similarly, the number of EGFP-positive (insulin secreting) β -cells was reduced by palmitate treatment, and these numbers were recovered by PJE pretreatment under both the 3 and 20 mM glucose conditions (Figure 3(d)).

3.5. PJE Protects against Palmitate-Induced β -Cell Dysfunction in Mouse Primary Islets. As PJE protected against palmitate-induced insulin secretion dysfunction in both the cell line and zebrafish, we next investigated whether PJE protects mouse primary islets. As expected, insulin secretion was decreased by treatment with palmitate, whereas 5 $\mu\text{g}/\text{mL}$

TABLE 1: Proximate composition of *Polysiphonia japonica* extract (PJE).

Total phenols	Total carbohydrates	Lipid	Protein
38.0 \pm 2.1 mg/g	20.3 \pm 1.8 mg/g	2.9 \pm 0.4 mg/g	26.5 \pm 1.4 mg/g

Data are the mean values of triplicate measurements and expressed as the mean \pm standard deviation.

PJE pretreatment significantly rescued insulin secretion in palmitate-treated islets (Figure 4). These data suggest that PJE has protective effects on palmitate-induced β -cell dysfunction in primary islets.

3.6. Chemical Components, Chromatogram, and DMH1 Composition in PJE. We determined the levels of chemical components including polyphenol, carbohydrate, lipid, and protein contents of PJE. As shown in Table 1, the proximate composition of PJE was 38.0 \pm 2.1 mg/g total phenols, 20.3 \pm 1.8 mg/g carbohydrate, 2.9 \pm 0.4 mg/g lipid, and 26.5 \pm 1.4 mg/g protein. To identify the functional components in PJE, we targeted 4-[6-(4-isopropoxyphenyl)pyrazolo[1,5-a]pyrimidin-3-yl]quinolone (DMH1), a bone morphogenetic protein (BMP) receptor inhibitor [27], as inhibition of BMP has been suggested to affect insulin-secreting β -cell growth and function [28]. Thus, we examined whether DMH1 is present in the PJE (5 mg/mL). PJE was evaluated by HPLC, and DMH 1 was separated and eluted at 44 min (Figure 5).

4. Discussion

Natural products have been used as alternative treatments for diabetes in many countries [29–34]. Additionally, constituents of seaweeds show antidiabetic potential [35, 36], specifically inhibition of protein tyrosine phosphatase, α -glucosidase, and aldose reductase. However, it is unknown whether *P. japonica*, an edible seaweed, can be used to treat diabetic-related diseases at all. In the present study, first, we investigated the protective effects of PJE on palmitate-induced β -cell dysfunction.

Increased levels of free fatty acids (FFAs), alone or with hyperglycemia, have been shown to trigger the loss of β -cells in both type 1 and type 2 diabetes [37, 38]. In addition, lipotoxicity induced by prolonged elevated FFAs, particularly saturated FFAs such as palmitate, leads to β -cell apoptosis and dysfunction [39, 40]. In agreement with previous studies [41, 42], our results showed that exposure to palmitate-induced significant cell death of Ins-1 cells. In addition, palmitate treatment reduced insulin secretion in Ins-1 cells, zebrafish β -cells, and isolated mouse islets. In this study, we provide evidence that PJE can prevent β -cell death in Ins-1 cells and zebrafish β -cells, as well as preserve the dysfunction of insulin secretion both *in vitro* and *in vivo* after exposure to palmitate.

Saturated fatty acids such as palmitate can induce adverse effects, including reduced glucose-stimulated insulin release, suppressed proinsulin biosynthesis, and consequently apoptotic β -cell death [39, 43–46]. Several intracellular

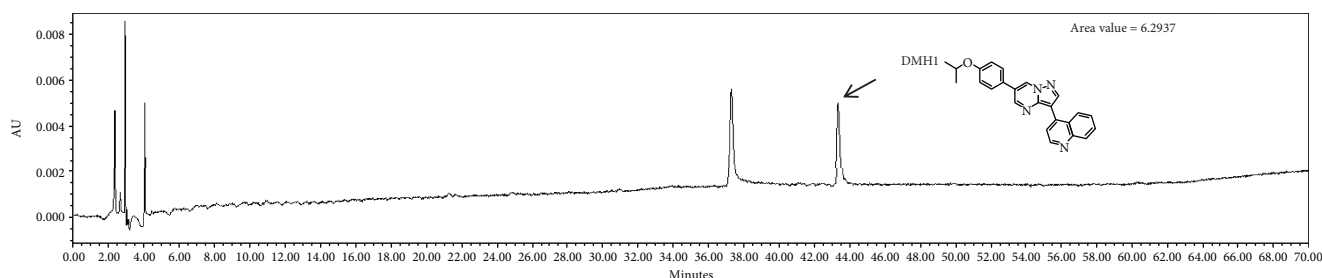


FIGURE 5: DMH1 was present in *Polysiphonia japonica* extract (PJE).

mediators of fatty acid-induced lipotoxicity have been reported. Palmitate-induced lipotoxicity increases oxidative stress due to intracellular reactive oxygen species accumulation [47–49]. Therefore, PJE may contain components with antioxidative effects, contributing to the prevention of palmitate-induced β -cell death and dysfunction. Another possible mechanism is that inhibition of BMP signaling by components in PJE such as DMH1 affects the increase in insulin secretion, as BMP inhibitor is known to improve β -cell function [28]. Another possibility is that the increase in or stimulation of glucagon-like peptide-1 receptor by PJE protects against palmitate-induced β -cell death and function. Glucagon-like peptide-1 receptor agonists such as exendin-4 are known to prevent palmitate- or H_2O_2 -induced β -cell dysfunction [50, 51]. Further studies are required to clarify the mechanisms for these beneficial effects of PJE on β -cell damage.

In conclusion, we found that PJE can effectively protect insulin-secreting β -cells from toxicity induced by palmitate. Moreover, PJE improves insulin secretion in Ins-1 cells, zebrafish, and mouse primary islets against palmitate treatment. These results suggest that PJE can be added to functional foods for DM patients and may be useful as a pharmaceutical agent for treating DM.

Abbreviations

PJE: *Polysiphonia japonica* extract
 DM: Diabetes mellitus
 FFAs: Free fatty acids
 GLP-1: Glucagon-like peptide.

Data Availability

The graphical summary used to support the findings of this study is included in the article.

Conflicts of Interest

The authors declare that there are no conflicts of interest.

Authors' Contributions

SHC participated in the experimental design, extract PJE, carried out all assays for the cells and zebrafish, performed statistical analysis, and participated in drafting the manuscript. HSK performed HPLC and chemical composition

analysis. YH carried out mouse primary islet assays. YJJ participated in analyzing the HPLC results and determination of chemical composition. HSJ conceived the study, participated in its design and coordination, and prepared the manuscript. All authors read and approved the final manuscript.

Acknowledgments

This work was supported by the Basic Science Research Program through the National Research Foundation of Korea (NRF) funded by the Ministry of Science, ICT, & Future Planning (2017R1D1A1B03033794) and by a grant from the Korea Health Technology RnD project through the Ministry of Health and Welfare (HI14C1135).

Supplementary Materials

Supplementary figure 1: free fatty acid; palmitate-induced DNA damage consequently impaired insulin secretion; interestingly, pretreatment of *Polysiphonia japonica* extract preserved insulin secretion impairment. (*Supplementary Materials*)

References

- [1] G. C. Weir and S. Bonner-Weir, "Islet β cell mass in diabetes and how it relates to function, birth, and death," *Annals of the New York Academy of Sciences*, vol. 1281, no. 1, pp. 92–105, 2013.
- [2] M. K. Garg, N. Mahalle, and M. K. Dutta, "Study of beta-cell function (by HOMA model) in metabolic syndrome," *Indian Journal of Endocrinology and Metabolism*, vol. 15, no. 5, p. 44, 2011.
- [3] S. G. Tattikota, T. Rathjen, J. Hausser et al., "miR-184 regulates pancreatic β -cell function according to glucose metabolism," *Journal of Biological Chemistry*, vol. 290, no. 33, pp. 20284–20294, 2015.
- [4] K. Nyalakonda, T. Sharma, and F. Ismail-Beigi, "Preservation of beta-cell function in type 2 diabetes," *Endocrine Practice*, vol. 16, no. 6, pp. 1038–1055, 2010.
- [5] T. Kuda, M. Tsunekawa, H. Goto, and Y. Araki, "Antioxidant properties of four edible algae harvested in the Noto Peninsula, Japan," *Journal of Food Composition and Analysis*, vol. 18, no. 7, pp. 625–633, 2005.
- [6] G.-N. Ahn, K. N. Kim, S. H. Cha et al., "Antioxidant activities of phlorotannins purified from *Ecklonia cava* on free radical scavenging using ESR and H_2O_2 -mediated DNA damage,"

- European Food Research and Technology*, vol. 226, no. 1-2, pp. 71–79, 2007.
- [7] Y. Athukorala and Y.-J. Jeon, “Screening for angiotensin 1 - converting enzyme inhibitory activity of *Ecklonia cava*,” *Preventive Nutrition and Food Science*, vol. 10, no. 2, pp. 134–139, 2005.
- [8] T. Shibata, K. Ishimaru, S. Kawaguchi, H. Yoshikawa, and Y. Hama, “Antioxidant activities of phlorotannins isolated from Japanese Laminariaceae,” *Journal of Applied Phycology*, vol. 20, no. 5, pp. 705–711, 2008.
- [9] S.-Y. Shim, L. Quang-To, S.-H. Lee, and S.-K. Kim, “*Ecklonia cava* extract suppresses the high-affinity IgE receptor, FcεRI expression,” *Food and Chemical Toxicology*, vol. 47, no. 3, pp. 555–560, 2009.
- [10] H. A. Jung, S. E. Jin, B. R. Ahn, C. M. Lee, and J. S. Choi, “Anti-inflammatory activity of edible brown alga *Eisenia bicyclis* and its constituents fucosterol and phlorotannins in LPS-stimulated RAW264.7 macrophages,” *Food and Chemical Toxicology*, vol. 59, pp. 199–206, 2013.
- [11] A. Ghorbani, “Best herbs for managing diabetes: a review of clinical studies,” *Brazilian Journal of Pharmaceutical Sciences*, vol. 49, no. 3, pp. 413–422, 2013.
- [12] M. S. Kim, J. Y. Kim, W. H. Choi, and S. S. Lee, “Effects of seaweed supplementation on blood glucose concentration, lipid profile, and antioxidant enzyme activities in patients with type 2 diabetes mellitus,” *Nutrition Research and Practice*, vol. 2, no. 2, pp. 62–67, 2008.
- [13] T.-H. Yang, H.-T. Yao, and M.-T. Chiang, “Red algae (*Gelidium amansii*) reduces adiposity via activation of lipolysis in rats with diabetes induced by streptozotocin-nicotinamide,” *Journal of Food and Drug Analysis*, vol. 23, no. 4, pp. 758–765, 2015.
- [14] J. S. Choi, H. J. Seo, Y. R. Lee et al., “Characteristics and in vitro anti-diabetic properties of the Korean rice wine, Makgeolli fermented with *Laminaria japonica*,” *Preventive Nutrition and Food Science*, vol. 19, no. 2, pp. 98–107, 2014.
- [15] M. J. Kim and H. K. Kim, “Insulinotropic and hypolipidemic effects of *Ecklonia cava* in streptozotocin-induced diabetic mice,” *Asian Pacific Journal of Tropical Medicine*, vol. 5, no. 5, pp. 374–379, 2012.
- [16] S.-H. Long, Z. Q. Yu, L. Shuai et al., “The hypoglycemic effect of the kelp on diabetes mellitus model induced by alloxan in rats,” *International Journal of Molecular Sciences*, vol. 13, no. 3, pp. 3354–3365, 2012.
- [17] X.-J. Duan, W.-W. Zhang, X.-M. Li, and B.-G. Wang, “Evaluation of antioxidant property of extract and fractions obtained from a red alga, *Polysiphonia urceolata*,” *Food Chemistry*, vol. 95, no. 1, pp. 37–43, 2006.
- [18] K. Li, X. M. Li, N. Y. Ji, and B. G. Wang, “Bromophenols from the marine red alga *Polysiphonia urceolata* with DPPH radical scavenging activity,” *Journal of Natural Products*, vol. 71, no. 1, pp. 28–30, 2008.
- [19] D. E. M. Saravanakumar, P. I. Folb, B. W. Campbell, and P. Smith, “Antimycobacterial activity of the red alga *Polysiphonia virgata*,” *Pharmaceutical Biology*, vol. 46, no. 4, pp. 254–260, 2008.
- [20] J. Gwak, S. Park, M. Cho et al., “*Polysiphonia japonica* extract suppresses the Wnt/ β -catenin pathway in colon cancer cells by activation of NF- κ B,” *International Journal of Molecular Medicine*, vol. 17, no. 6, pp. 1005–1010, 2006.
- [21] N. Téllez, M. Montolio, E. Estil-les, J. Escoriza, J. Soler, and E. Montanya, “Adenoviral overproduction of interleukin-1 receptor antagonist increases beta cell replication and mass in syngeneically transplanted islets, and improves metabolic outcome,” *Diabetologia*, vol. 50, no. 3, pp. 602–611, 2007.
- [22] Y. S. Oh, Y. J. Lee, E. Y. Park, and H. S. Jun, “Interleukin-6 treatment induces beta-cell apoptosis via STAT-3-mediated nitric oxide production,” *Diabetes/Metabolism Research and Reviews*, vol. 27, no. 8, pp. 813–819, 2011.
- [23] S.-H. Cha, J.-H. Lee, E.-A. Kim, C. H. Shin, H.-S. Jun, and Y.-J. Jeon, “Phloroglucinol accelerates the regeneration of liver damaged by H₂O₂ or MNZ treatment in zebrafish,” *RSC Advances*, vol. 7, no. 73, pp. 46164–46170, 2017.
- [24] J. Burns, P. T. Gardner, J. O’Neil et al., “Relationship among antioxidant activity, vasodilation capacity, and phenolic content of red wines,” *Journal of Agricultural and Food Chemistry*, vol. 48, no. 2, pp. 220–230, 2000.
- [25] S. S. Nielsen, “Phenol-sulfuric acid method for total carbohydrates,” in *Food Analysis Laboratory Manual*, pp. 47–53, Springer, Boston, MA, USA, 2010.
- [26] Y.-S. Cheng, Y. Zheng, and J. S. VanderGheynst, “Rapid quantitative analysis of lipids using a colorimetric method in a microplate format,” *Lipids*, vol. 46, no. 1, pp. 95–103, 2011.
- [27] L. D. Hover, C. D. Young, N. E. Bhola et al., “Small molecule inhibitor of the bone morphogenetic protein pathway DMH1 reduces ovarian cancer cell growth,” *Cancer Letters*, vol. 368, no. 1, pp. 79–87, 2015.
- [28] C. Bruun, G. L. Christensen, M. L. B. Jacobsen et al., “Inhibition of beta cell growth and function by bone morphogenetic proteins,” *Diabetologia*, vol. 57, no. 12, pp. 2546–2554, 2014.
- [29] G. Grosso, U. Stepaniak, A. Micek et al., “Dietary polyphenol intake and risk of type 2 diabetes in the polish arm of the health, alcohol and psychosocial factors in Eastern Europe (HAPIEE) study,” *British Journal of Nutrition*, vol. 118, no. 1, pp. 60–68, 2017.
- [30] S.-J. Heo, J.-Y. Hwang, J.-I. Choi, J.-S. Han, H.-J. Kim, and Y.-J. Jeon, “Diphlorethohydroxycarmalol isolated from *Ishige okamurae*, a brown algae, a potent α -glucosidase and α -amylase inhibitor, alleviates postprandial hyperglycemia in diabetic mice,” *European Journal of Pharmacology*, vol. 615, no. 1-3, pp. 252–256, 2009.
- [31] J. L. Rios, F. Francini, and G. R. Schinella, “Natural products for the treatment of type 2 diabetes mellitus,” *Planta Medica*, vol. 81, no. 12-13, pp. 975–994, 2015.
- [32] M. Salimifar, Z. Fatehi-Hassanabad, and M. Fatehi, “A review on natural products for controlling type 2 diabetes with an emphasis on their mechanisms of actions,” *Current Diabetes Reviews*, vol. 9, no. 5, pp. 402–411, 2013.
- [33] J. B. Xiao and P. Hogger, “Dietary polyphenols and type 2 diabetes: current insights and future perspectives,” *Current Medicinal Chemistry*, vol. 22, no. 1, pp. 23–38, 2015.
- [34] K. Shapiro and W. C. Gong, “Natural products used for diabetes,” *Journal of the American Pharmaceutical Association (1996)*, vol. 42, no. 2, pp. 217–226, 2002.
- [35] X. Lin and M. Liu, “Bromophenols from marine algae with potential anti-diabetic activities,” *Journal of Ocean University of China*, vol. 11, no. 4, pp. 533–538, 2012.
- [36] M. Liu, P. E. Hansen, and X. Lin, “Bromophenols in marine algae and their bioactivities,” *Marine Drugs*, vol. 9, no. 7, pp. 1273–1292, 2011.

- [37] O. Leonardi, G. Mints, and M. Hussain, "Beta-cell apoptosis in the pathogenesis of human type 2 diabetes mellitus," *European Journal of Endocrinology*, vol. 149, no. 2, pp. 99–102, 2003.
- [38] G. Shi, C. Sun, W. Gu et al., "Free fatty acid receptor 2, a candidate target for type 1 diabetes, induces cell apoptosis through ERK signaling," *Journal of Molecular Endocrinology*, vol. 53, no. 3, pp. 367–380, 2014.
- [39] R. Lupi, F. Dotta, L. Marselli et al., "Prolonged exposure to free fatty acids has cytostatic and pro-apoptotic effects on human pancreatic islets: evidence that β -cell death is caspase mediated, partially dependent on ceramide pathway, and Bcl-2 regulated," *Diabetes*, vol. 51, no. 5, pp. 1437–1442, 2002.
- [40] K. Maedler, G. A. Spinas, D. Dyntar, W. Moritz, N. Kaiser, and M. Y. Donath, "Distinct effects of saturated and monounsaturated fatty acids on β -cell turnover and function," *Diabetes*, vol. 50, no. 1, pp. 69–76, 2001.
- [41] F. Luo, Y. Feng, H. Ma et al., "Neutral ceramidase activity inhibition is involved in palmitate-induced apoptosis in INS-1 cells," *Endocrine Journal*, vol. 64, no. 8, pp. 767–776, 2017.
- [42] M. Hu, H. Lin, L. Yang, Y. Cheng, and H. Zhang, "Interleukin-22 restored mitochondrial damage and impaired glucose-stimulated insulin secretion through down-regulation of uncoupling protein-2 in INS-1 cells," *The Journal of Biochemistry*, vol. 161, no. 5, pp. 433–439, 2017.
- [43] M. Shimabukuro, Y.-T. Zhou, M. Levi, and R. H. Unger, "Fatty acid-induced β cell apoptosis: a link between obesity and diabetes," *Proceedings of the National Academy of Sciences of the United States of America*, vol. 95, no. 5, pp. 2498–2502, 1998.
- [44] R. H. Unger and Y. Zhou, "Lipotoxicity of beta-cells in obesity and in other causes of fatty acid spillover," *Diabetes*, vol. 50, Supplement 1, pp. S118–S121, 2001.
- [45] M. L. Elks, "Chronic perfusion of rat islets with palmitate suppresses glucose-stimulated insulin release," *Endocrinology*, vol. 133, no. 1, pp. 208–214, 1993.
- [46] I. Kharroubi, L. Ladrière, A. K. Cardozo, Z. Dogusan, M. Cnop, and D. L. Eizirik, "Free fatty acids and cytokines induce pancreatic β -cell apoptosis by different mechanisms: role of nuclear factor- κ B and endoplasmic reticulum stress," *Endocrinology*, vol. 145, no. 11, pp. 5087–5096, 2004.
- [47] Y. Liu, N. Wang, S. Zhang, and Q. Liang, "Autophagy protects bone marrow mesenchymal stem cells from palmitate-induced apoptosis through the ROS-JNK/p38 MAPK signaling pathways," *Molecular Medicine Reports*, vol. 18, no. 2, pp. 1485–1494, 2018.
- [48] S. W. Lee, J. B. Park, H. J. Kim et al., "Palmitate induces lipopoptosis in Schwann cells through ROS generation-mediated STAMP2 downregulation," *Biochemical and Biophysical Research Communications*, vol. 503, no. 3, pp. 1260–1266, 2018.
- [49] A. Sadeghi, A. Rostamirad, S. Seyyedebrahimi, and R. Meshkani, "Curcumin ameliorates palmitate-induced inflammation in skeletal muscle cells by regulating JNK/NF- κ B pathway and ROS production," *Inflammopharmacology*, vol. 26, no. 5, pp. 1265–1272, 2018.
- [50] Q. Wei, Y. Q. Sun, and J. Zhang, "Exendin-4, a glucagon-like peptide-1 receptor agonist, inhibits cell apoptosis induced by lipotoxicity in pancreatic β -cell line," *Peptides*, vol. 37, no. 1, pp. 18–24, 2012.
- [51] J.-Y. Kim, D.-M. Lim, C. I. Moon et al., "Exendin-4 protects oxidative stress-induced β -cell apoptosis through reduced JNK and GSK3 β activity," *Journal of Korean Medical Science*, vol. 25, no. 11, pp. 1626–1632, 2010.

Research Article

Procyanidins Extracted from Lotus Seedpod Ameliorate Amyloid- β -Induced Toxicity in Rat Pheochromocytoma Cells

Hao Huang,^{1,2} Peipei Yan,³ Taoping Sun,^{1,2} Xiaoxing Mo,^{1,2} Jiawei Yin,^{1,2} Peiyun Li,^{1,2} Yalun Zhu,^{1,2} Shuang Rong,⁴ Wei Yang,^{1,2} Xiaoyi Chen^{ID},⁵ and Liegang Liu^{ID}^{1,2}

¹Department of Nutrition and Food Hygiene, Hubei Key Laboratory of Food Nutrition and Safety, Tongji Medical College, Huazhong University of Science and Technology, Wuhan 430030, China

²Ministry of Education Key Lab of Environment and Health, School of Public Health, Tongji Medical College, China

³Chongqing Center for Disease Control and Prevention, Chongqing 400000, China

⁴Department of Nutrition and Food Hygiene, School of Public Health, Medical College, Wuhan University of Science and Technology, Wuhan 430065, China

⁵School of Public Health, Guangzhou Medical University, Guangzhou 511436, China

Correspondence should be addressed to Xiaoyi Chen; wwchenxy1@163.com and Liegang Liu; lgliu@mails.tjmu.edu.cn

Received 30 March 2018; Revised 26 July 2018; Accepted 6 August 2018; Published 28 October 2018

Academic Editor: Felipe L. de Oliveira

Copyright © 2018 Hao Huang et al. This is an open access article distributed under the Creative Commons Attribution License, which permits unrestricted use, distribution, and reproduction in any medium, provided the original work is properly cited.

Alzheimer's disease (AD) is a progressive neurodegenerative disease, which is characterized by extracellular senile plaque deposits, intracellular neurofibrillary tangles, and neuronal apoptosis. Amyloid- β ($A\beta$) plays a critical role in AD that may cause oxidative stress and downregulation of CREB/BDNF signaling. Anti- $A\beta$ effect has been discussed as a potential therapeutic strategy for AD. This study aimed to identify the amelioration of procyanidins extracted from lotus seedpod (LSPC) on $A\beta$ -induced damage with associated pathways for AD treatment. Rat pheochromocytoma (PC12) cells incubated with $A\beta_{25-35}$ serve as an $A\beta$ damage model to evaluate the effect of LSPC *in vitro*. Our findings illustrated that LSPC maintained the cellular morphology from deformation and reduced apoptosis rates of cells induced by $A\beta_{25-35}$. The mechanisms of LSPC to protect cells from $A\beta$ -induced damage were based on its regulation of oxidation index and activation of CREB/BDNF signaling, including brain-derived neurotrophic factor (BDNF) and phosphorylation of cAMP-responsive element-binding (CREB), protein kinase B (also known as AKT), and the extracellular signal-regulated kinase (ERK). Of note, by high-performance liquid chromatography-tandem mass spectroscopy (LC-MS/MS), several metabolites were detected to accumulate *in vivo*, part of which could take primary responsibility for the amelioration of $A\beta$ -induced damage on PC12 cells. Taken together, our research elucidated the effect of LSPC on neuroprotection through anti- $A\beta$, indicating it as a potential pretreatment for Alzheimer's disease.

1. Introduction

Alzheimer's disease (AD), a progressive neurodegenerative disease, is characterized by extracellular senile plaque deposits, intracellular neurofibrillary tangles, and neuronal apoptosis. Progressive loss of memory and other cognitive functions are typical symptoms in AD [1]. According to the amyloid hypothesis, amyloid- β ($A\beta$ -) related toxicity and imbalance are cardinal reasons that contribute to synaptic dysfunction and subsequent neurodegeneration in AD [2, 3]. $A\beta$ has been, therefore, suggested as a potential therapeutic target for AD treatment [4].

As similar to other age-related diseases, exorbitant oxidative stress is the fundamental feature of AD since $A\beta$ may lead to oxidative stress and macroautophagy [5]. Oxidative stress induced by $A\beta$ may disorder the membrane ion function and glutamate transporters of synapses, resulting in their dysfunction and degeneration [5]. Antioxidant compounds hence may have a positive effect on the mitigation of $A\beta$ -induced damages. AKT (also known as protein kinase B) and extracellular signal-regulated kinase (ERK) are two key kinases in modulating brain-derived neurotrophic factor (BDNF) transcription by activating phosphorylation of cAMP-responsive element-binding (CREB) [6, 7], both of

which could be attenuated by $A\beta$ [8, 9]. BDNF, a pivotal role in learning and memory [10, 11], is downregulated by $A\beta$ in AD [12]. The underlying mechanism of $A\beta$ on CREB/BDNF signaling is possible that $A\beta$ inhibits the activation of AKT and ERK, resulting in decreasing phosphorylation of CREB, the upstream of BDNF [13], and then, attenuating both transcriptions of BDNF mRNA and expression of BDNF protein [14]. Therefore, simulating CREB/BDNF signaling against $A\beta$ -induced damage is a promising therapeutic tactic for AD. CREB activators, BDNF imitators, or flavonoid-high dietary habit have been identified to ameliorate AD [15–17]. BDNF and oxidative stress also have an interactive influence *in vivo* [18, 19] so nature compounds are beneficial for AD treatment, which can modulate oxidative stress and CREB/BDNF signaling.

Lotus has been usually used as a Chinese traditional medicine, including its leaf, embryo loti, and seedpod [20, 21]. Procyanidins, as flavonoids, are highly correlated to learning and memory improvement [22, 23] and exhibit the potential for AD treatment [16, 24]. Procyanidins extracted from the lotus seedpod (LSPC) is the fresh and abundant resource of flavonoids [25]. In age-related mice, LSPC has been reported to enhance the abilities of learning and memory [26, 27]. Consequently, we put forward the assumption that LSPC might display the property of anti- $A\beta$ in AD while there was no definitive evidence for its anti- $A\beta$ toxicity function and its main pathways. LSPC, as a complex mixture, is composed of oligomeric procyanidins and polymeric procyanidins such as epicatechin, procyanidins dimers, and quercetin glucuronide [25] while it was insufficient in research exploring its distribution *in vivo*, which might be conducive to expound its impact.

In this study, we aimed to verify its anti- $A\beta$ effects and protective mechanisms as a promising nature production for AD treatment. We evaluated amelioration of LSPC in $A\beta_{25-35}$ -induced damage on rat pheochromocytoma (PC12) cells. CREB/BDNF signaling and antioxidant activity were studied as possible pathways. We used LC-MS/MS to analyze its distribution *in vivo*.

2. Materials and Methods

2.1. Cells and Reagents. PC12 cells were from Tongji Medical College, Huazhong Science and Technology University. LSPC was provided by Huazhong Agriculture University (China). Cell Counting Kit-8 (CCK-8) was purchased from Dojindo (Japan); anti-BDNF antibody was purchased from Elabscience (China); anti-CREB antibody, anti-phospho-CREB (Ser¹³³) antibody, anti-AKT antibody, anti-phospho-AKT (Ser⁴⁷³) antibody, anti-ERK1/2 antibody, anti-phospho-ERK1/2 (Thr202/Tyr²⁰⁴) antibody, and anti-GAPDH antibody were purchased from cell signaling; LY294002 inhibitor for PI3K and PD98059 inhibitor for ERK1/2 were purchased from Selleckchem; lactate dehydrogenase (LDH), superoxide dismutase (SOD), and malonaldehyde (MDA) were from Nanjing Jiancheng Bioengineering Institute (Nanjing, China); gallic acid was purchased from DRE; procyanidin dimer B (PDB) was purchased from Fluka Co.; epigallocatechin gallate (ECG) was purchased from

Chromadex; Annexin V-FITC for flow cytometry was purchased from BestBio; Hoechst staining for apoptosis analysis, BCA protein assay kit, and RIPA lysis solution was purchased from Beyotime; all other reagents were purchased from Sigma.

2.2. Cells Culture and Dosages of $A\beta_{25-35}$ and LSPC. PC12 cells were cultured in Roswell Park Memorial Institute (RPMI) 1640 medium with 10% fetal bovine serum in an atmosphere containing 5% CO₂ at 37°C. To decide an intervention dose of $A\beta_{25-35}$, we added different doses of $A\beta_{25-35}$ (0, 5, 10, 20, and 40 μ M) into cells and incubated for six periods of time (6, 12, 24, 48, and 72 h), respectively. $A\beta_{25-35}$ was prepared by dissolved in sterile PBS and aggregated through incubation at 37°C for 4 days. In order to choose an intervention dose of LSPC, we added six dosages of LSPC (1, 2.5, 5, 10, 20, and 40 μ g/mL) into 96-well plates 30 minutes before incubation with $A\beta_{25-35}$ for 24 h or without $A\beta_{25-35}$ for 24 h. Dosages for both $A\beta_{25-35}$ and LSPC were determined through measuring cell viability by CCK-8 according to the instruction. In brief, 10 μ L CCK-8 was added to each sample (100 μ L) with 2 h incubation under 37°C, and absorbance value of each sample was measured by an enzyme immunoassay analyzer (Bio-Tek, USA) at 570 nm.

2.3. PC12 Cells Imaging. After determination of $A\beta_{25-35}$ and LSPC doses, cells were cultured as three groups (PC12 cells, PC12 cells with 20 μ M $A\beta_{25-35}$, and PC12 cells with 20 μ M $A\beta_{25-35}$ and 10 μ g/mL LSPC), which were seeded on 6-well plates at a density of 1×10^6 cells/mL. Cells after treatment were fixed by paraformaldehyde and observed morphology under a microscope (Olympus Corporation, Japan).

2.4. Hoechst Staining. Cells were seeded on 6-well plates. After intervention as three groups, each group was washed with PBS twice before 800 μ L staining buffer was added and subsequently stained with Hoechst staining solution (5 μ L) for 30 min in the dark. Cells were imaged on a fluorescence microscope (Olympus Corporation, Japan). Hoechst staining was executed according to the instructions (Beyotime, China).

2.5. Flow Cytometry. Cells seeded on 6-well plates were washed with cold PBS twice. The number of cells was kept closing to 1×10^6 /mL in each sample and 400 μ L 1 \times Annexin V was provided. Each sample was incubated with 5 μ L Annexin V-FITC staining for 5 min at 4°C. Then 10 μ L propidium iodide (PI) staining was added for 5 min at 4°C. Samples were detected by a flow cytometry (Becton Dickinson, USA) and analyzed by FlowJo software (version 7.6). All procedures were consistent with the instructions (BestBio, China). Cells containing Annexin V-positive staining merely were defined to be in early apoptosis (EA), whereas cells stained with both Annexin V and PI were defined to be in late apoptosis (LA). Total apoptosis (TA) consisted of EA and LA.

2.6. Determination of Antioxidant Activity. Cells were divided into six groups (PC12 cells, PC12 cells with 20 μ M $A\beta_{25-35}$, PC12 cells with 20 μ M $A\beta_{25-35}$ and 5 μ g/mL LSPC,

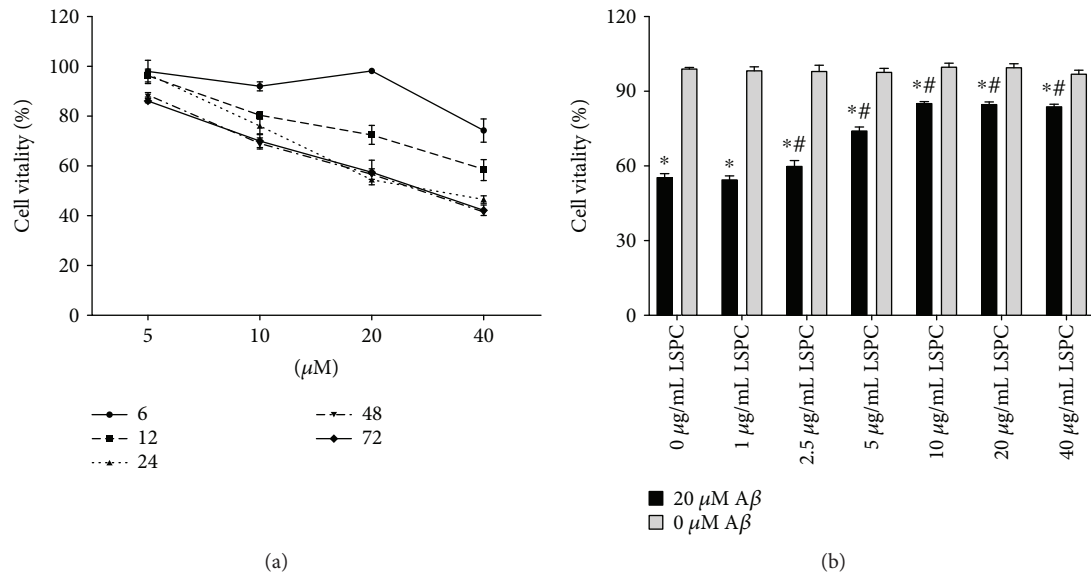


FIGURE 1: Determination for both $A\beta_{25-35}$ and LSPC through measuring survival rates of cells by CCK-8. (a) Survival rate of cells under variable dosage of $A\beta_{25-35}$ with different intervene time ($\bar{x} \pm \text{SEM}$, $n = 6$, %). (b) Survival rates of cells under different dosages of LSPC with $20 \mu\text{M } A\beta_{25-35}$ (black) and without $A\beta_{25-35}$ (gray) ($\bar{x} \pm \text{SEM}$, $n = 6$, %). $0 \mu\text{g/mL LSPC}$, PC12 cells with $20 \mu\text{M } A\beta_{25-35}$ group, and without $A\beta_{25-35}$; $1 \mu\text{g/mL LSPC}$, PC12 cells with $1 \mu\text{g/mL LSPC}$ for 30 minutes before incubation with $20 \mu\text{M } A\beta_{25-35}$ group, and without $A\beta_{25-35}$; $2.5 \mu\text{g/mL LSPC}$, PC12 cells with $2.5 \mu\text{g/mL LSPC}$ for 30 minutes before incubation with $20 \mu\text{M } A\beta_{25-35}$ group, and without $A\beta_{25-35}$; $5 \mu\text{g/mL LSPC}$, PC12 cells with $5 \mu\text{g/mL LSPC}$ for 30 minutes before incubation with $20 \mu\text{M } A\beta_{25-35}$ group, and without $A\beta_{25-35}$; $10 \mu\text{g/mL LSPC}$, PC12 cells with $10 \mu\text{g/mL LSPC}$ for 30 minutes before incubation with $20 \mu\text{M } A\beta_{25-35}$ group, and without $A\beta_{25-35}$; $20 \mu\text{g/mL LSPC}$, PC12 cells with $20 \mu\text{g/mL LSPC}$ for 30 minutes before incubation with $20 \mu\text{M } A\beta_{25-35}$ group and without $A\beta_{25-35}$; $40 \mu\text{g/mL LSPC}$, PC12 cells with $40 \mu\text{g/mL LSPC}$ for 30 minutes before incubation with $20 \mu\text{M } A\beta_{25-35}$ group and without $A\beta_{25-35}$; * $P < 0.05$ for groups vs PC12 cells without $A\beta_{25-35}$ and LSPC; # $P < 0.05$ for groups vs PC12 cells with $A\beta_{25-35}$ but without LSPC. All the results above are the representative of the three independent experiments.

PC12 cells with $20 \mu\text{M } A\beta_{25-35}$ and $10 \mu\text{g/mL LSPC}$, and PC12 cells with $20 \mu\text{M } A\beta_{25-35}$ and $20 \mu\text{g/mL LSPC}$. The levels of LDH, T-SOD, and MDA were measured depending on the methods [28] and instructions recommended by Nanjing Jiancheng Bioengineering Institute (Nanjing, China). LDH activity of each sample was detected by an enzyme immunoassay analyzer (Bio-Tek, USA) at 450 nm, and the values were expressed as units per liter. For T-SOD, a BCA protein assay kit (Beyotime, China) was applied to determine the values of proteins expression. The absorbance value of each sample was measured at 570 nm, and the values of T-SOD activity was calculated as units per mg protein. Quantification of MDA was stated as nanomoles per mg protein by testing absorbance values at 532 nm.

2.7. Western Blot. Cells were cultured as seven groups (PC12 cells, PC12 cells with $20 \mu\text{M } A\beta_{25-35}$, PC12 cells added with $10 \mu\text{g/mL LSPC}$ 30 minutes before incubation with $20 \mu\text{M } A\beta_{25-35}$, PC12 cells with $10 \mu\text{M LY294002}$, PC12 cells added $10 \mu\text{g/mL LSPC}$ 30 minutes before incubation with $10 \mu\text{M LY294002}$, PC12 cells with $30 \mu\text{M PD98059}$, and PC12 cells added with $10 \mu\text{g/mL LSPC}$ 30 minutes before incubation with $30 \mu\text{M PD98059}$). After intervention, cells were washed three times using cold PBS. After centrifugation ($14000 \times \text{rpm}$, 5 min), each sample was collected excluding the supernatant and lysed in $300 \mu\text{L}$ lysis buffer for 2 h, following centrifugation for 10 min at $14000 \times \text{rpm}$. The proteins in the supernatant were quantified using the BCA

method as above. For blot analysis, samples ($20 \mu\text{L}$, each) were boiled, separated on 7.5%–12% SDS-PAGE, and transferred to polyvinylidene difluoride (PVDF) membranes. The membranes were hybridized with various antibodies overnight at 4°C , including anti-BDNF antibody (1:1000), anti-CREB antibody (1:1000), anti-phospho-CREB (Ser¹³³) antibody (1:1000), anti-AKT antibody (1:1000), anti-phospho-AKT (Ser⁴⁷³) antibody (1:1000), anti-ERK1/2 antibody (1:1000), anti-phospho-ERK1/2 (Thr202/Tyr²⁰⁴) antibody (1:1000), and anti-GAPDH antibody (1:3000) as internal standard and then incubated with secondary antibodies for 1 h at room temperature. The images were obtained through a Fluorescence Chemical Imaging Analysis System (Syngene, British). The intensities of the bands were analyzed by the ImageJ software.

2.8. Quantitative Real-Time PCR (qRT-PCR). Total RNA was isolated from cells via RNAiso Plus (TaKaRa, China), and cRNA was extracted using the PrimeScript™ RT reagent Kit (TaKaRa, China), all of which were based on the instructions. qRT-PCR was carried out using the SYBR® Premix Ex Taq™ (TaKaRa, China) with an ABI 7900HT real-time thermocycler (Applied Biosystems, CA), as previously described [29]. The correlated expressions of genes were calculated by $2^{-\Delta\Delta\text{CT}}$ methods. Primers of specific genes, including BDNF (forward: 5'-AGCAGGCTCTGGAATGATGT-3'; reverse: 5'-GGATTTGAGTGTGGTTCTCCA-3') and

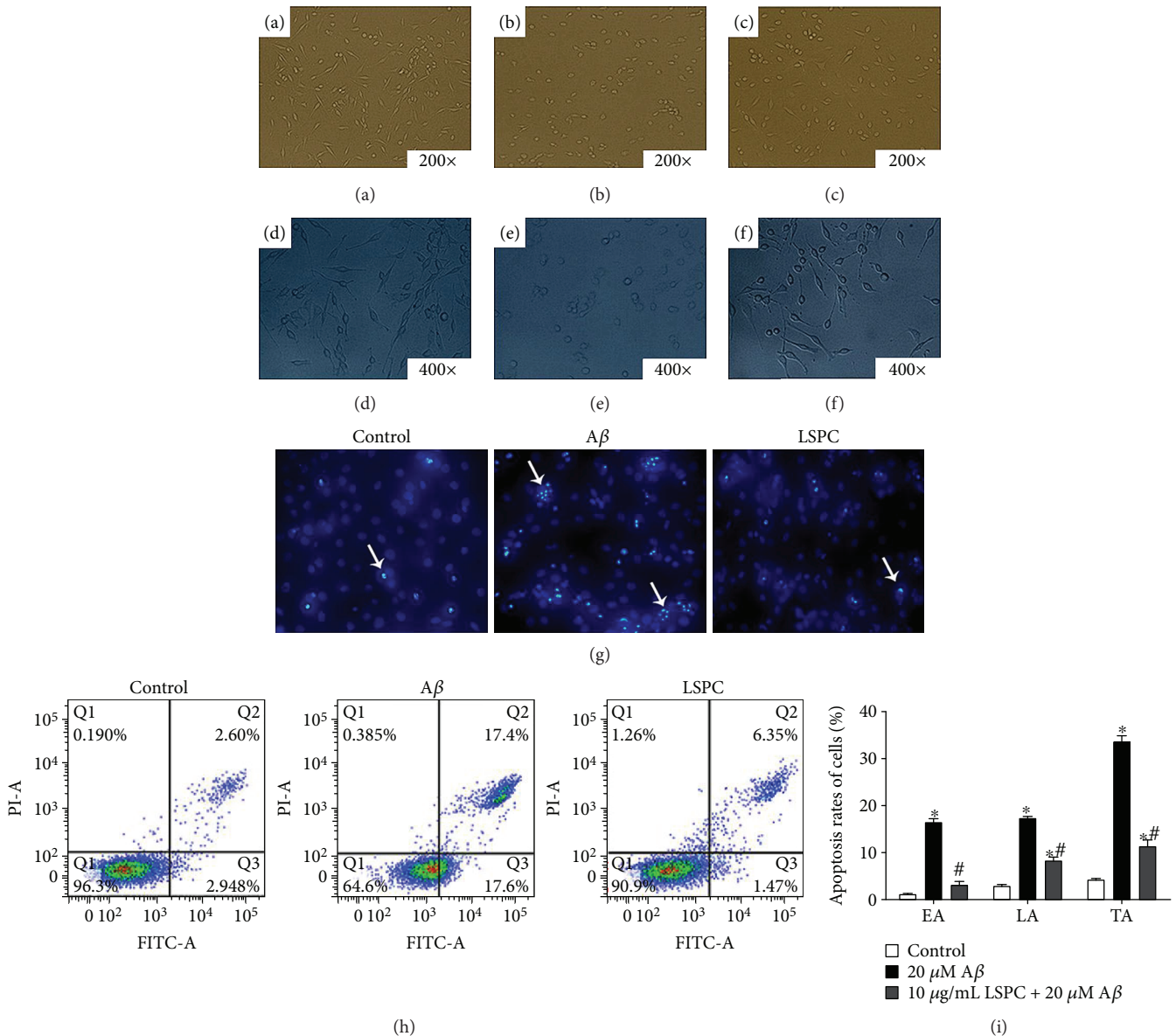


FIGURE 2: The effect of LSPC against Aβ₂₅₋₃₅-induced apoptosis on PC12 cells. (a–f) Cellular morphology of different groups under an electron microscope. (a) Control (200×); (b) control (400×); (c) Aβ (200×); (d) Aβ (400×); (e) LSPC (200×); (f) LSPC (400×). Control, PC12 cells; Aβ, PC12 cells with 20 μM Aβ₂₅₋₃₅; LSPC, PC12 cells added into 10 μg/mL LSPC 30 minutes before incubation with 20 μM Aβ₂₅₋₃₅. In the electron microscope, PC12 cells with 10 μg/mL LSPC and 20 μM Aβ₂₅₋₃₅ (e, f) showed the approximate number of cells and identical cellular morphology as a control group (a, b), while Aβ group (c, d) illustrated the reduction of cells number and abnormal morphology. (g) Hoechst staining reflects the apoptosis of cells in each group; apoptosis cells are pointed out by white arrows. (h and i) Flow cytometry calculates apoptosis rates of different groups after Annexin V/PI staining. Apoptosis rate of each group are mean ± SEM; **P* < 0.05 for groups vs control; #*P* < 0.05 for groups vs Aβ₂₅₋₃₅ group. Control, PC12 cells; Aβ, PC12 cells with 20 μM Aβ₂₅₋₃₅; LSPC, PC12 cells added into 10 μg/mL LSPC 30 minutes before incubation with 20 μM Aβ₂₅₋₃₅. All the results above are the representative of the three independent experiments run in quadruplicate.

GAPDH (forward: 5'-GCCAGCAAGGATACTGAGA-3'; reverse: 5'-GGATGGAATTGTGAGGGAGA-3') as control, were synthesized by Sangon Corp. (Sangon Biotech Co., Ltd., China).

2.9. Animals. Fourteen male Sprague-Dawley rats (226 ± 35 g, obtained from the Experimental Animal Center of Tongji Medical College, Huazhong Science and Technology University) with two or three per cage were kept in a

controlled temperature (23 ± 1°C) under a 12 h dark-light cycle. All rats were free access to deionized water and diet for 1 week. All procedures were in accordance with the guidelines of Tongji Medical College Council on Animal Care Committee, Huazhong Science and Technology University (IACUC number: S407, approval date was 28 March 2015).

2.10. LSPC Treatment. Prior to administration of LSPC, rats were randomly divided into two groups (*n* = 7 per group)

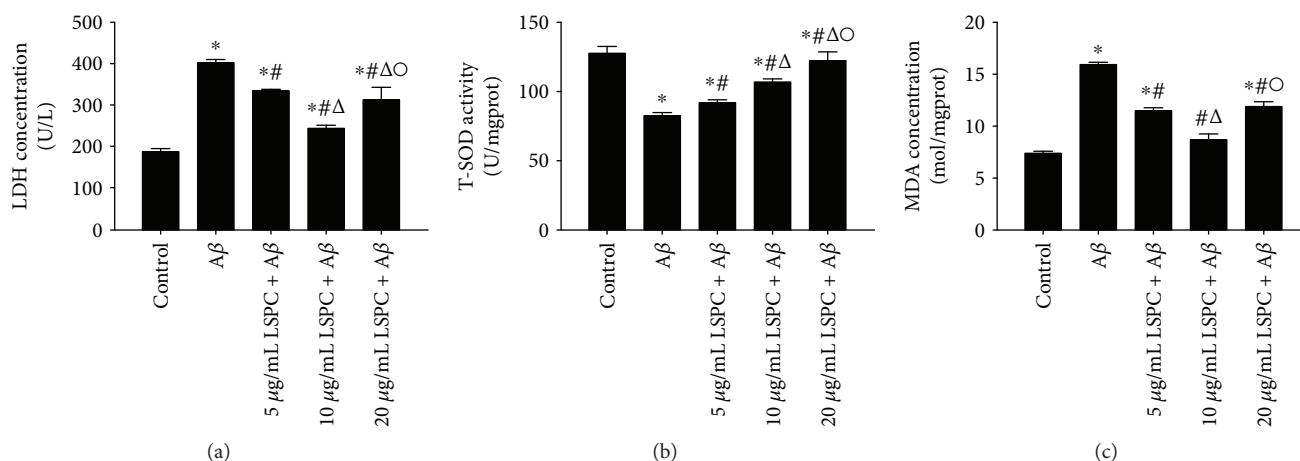


FIGURE 3: Oxidative index of different groups ($\bar{x} \pm \text{SEM}$, $n = 6$, %). (a–c) The LDH concentration, T-SOD activity, and MDA concentration of different groups, respectively. Control, PC12 cells; A β , PC12 cells with 20 μM A β_{25-35} ; 5 $\mu\text{g}/\text{mL}$ LSPC + A β , PC12 cells added into 5 $\mu\text{g}/\text{mL}$ LSPC 30 minutes before incubation with 20 μM A β_{25-35} ; 10 $\mu\text{g}/\text{mL}$ LSPC + A β , PC12 cells added into 10 $\mu\text{g}/\text{mL}$ LSPC 30 minutes before incubation with 20 μM A β_{25-35} ; 20 $\mu\text{g}/\text{mL}$ LSPC + A β , PC12 cells added into 20 $\mu\text{g}/\text{mL}$ LSPC 30 minutes before incubation with 20 μM A β_{25-35} . All data are mean \pm SEM. * $P < 0.05$ for groups vs control; # $P < 0.05$ for groups vs A β group; $\Delta P < 0.05$ for groups vs 5 $\mu\text{g}/\text{mL}$ LSPC+20 μM A β_{25-35} ; $^{\circ}P < 0.05$ for groups vs 10 $\mu\text{g}/\text{mL}$ LSPC+20 μM A β_{25-35} . All the results above are the representative of the three independent experiments.

and fasted for 12 h but had access to deionized water. For the control group, physiological saline was given by oral gavage daily; for LSPC group, LSPC (a brownish red powder) was dissolved in physiological saline (20 mg/mL) and administered to rats at a dose of 200 mg/kg body weight by oral gavage daily for two weeks. Body weights were measured every two days. Rats were sacrificed two hours later after a final dose. Tissues (brain, cardiac, liver, kidney, spleen, and pancreas), intestine content, and plasma were harvested and stored at -80°C until analysis.

2.11. LC-MS/MS. For the extraction of LSPC and its metabolites, tissues (60 mg) were homogenized with 300 μL mixture (50 μL 1% (w/v) aqueous ascorbic solution and 250 μL 0.1% formic acid). Ethyl gallate was an internal standard. Each sample was hydrolyzed with a β -glucuronidase/sulfatase type H1 (1500 U/mL) from *H. pomatia* (Sigma, USA) for two hours at 37°C . Then, methanol (200 μL) was added to each sample followed by vibration (30 s) and centrifugation (12000 rpm, 10 min, 4°C), and the supernatant was collected. The extraction was repeated once. The combined supernatants were evaporated to dryness under vacuum at 35°C . The residue was reconstituted in 50 μL of solvent (methanol/water, 1:1, v/v) for LC-MS/MS analysis.

The analysis was performed on a high-performance liquid chromatography-tandem mass spectrometry (LC-MS/MS, AB Sciex QTrap 4500, Applied Biosystems, Foster City, CA, USA). This method was in accordance with the reported studies [30–32]. Briefly, 5 μL samples were injected for LC-MS/MS, and the analytes were separated by BETASIL Phenyl Column (2.1 mm \times 150 mm, 3 μm ; Thermo Scientific, USA) at 35°C . The mobile phases composed (a) water with 0.2% acetic acid and (b) methanol with 0.2% acetic acid. Ionization was carried out by electrospray in the negative mode. The calibration curves of respective standards were utilized to quantify compounds. Transition ions, retention

times, and mass-spectrometry parameters for all compounds were shown in Table S1; chemical structures of all compounds were exhibited in Figure S1.

2.12. Statistical Analysis. The data are presented as mean values \pm standard error of the mean (SEM) and analyzed by ANOVA with Student-Newman-Keuls (SNK) or student t -test on SPSS software version 19.0. The level of significance was set for P value < 0.05 .

3. Results

3.1. Dosages of A β_{25-35} and LSPC. Figure 1(a) demonstrated that 20 μM A β_{25-35} had a significant effect on the survival rate of PC12 cells after 24 h intervention that was consistent with the previous report [33]. Thus, we chose the dosage of 20 μM A β_{25-35} with the intervention period of 24 h on PC12 cells for further study. In order to testify a dose-dependent manner of LSPC, we added 1, 2.5, 5, 10, 20, and 40 $\mu\text{g}/\text{mL}$ LSPC into PC12 cells before A β_{25-35} intervention, respectively. As shown in Figure 1(b), the survival rates of PC12 cells under the damage of 20 μM A β_{25-35} were gradually improved following the increasing dosages of LSPC until it reached 10 $\mu\text{g}/\text{mL}$. Moreover, there was no toxicity *in vitro* for any dosage of LSPC. 10 $\mu\text{g}/\text{mL}$ LSPC was chosen for further study since it exhibited the strongest protection on PC12 cells against the damage harvested from 20 μM A β_{25-35} .

3.2. LSPC Inhibit A β_{25-35} -Induced Morphology Changes and Apoptosis on PC12 Cells. Cells were cultured in three groups: control group, PC12 cells with 20 μM A β_{25-35} , and PC12 cells were added 10 $\mu\text{g}/\text{mL}$ LSPC 30 minutes before incubation with 20 μM A β_{25-35} . In electron microscope (Figures 2(a)–2(f)), PC12 cells with 10 $\mu\text{g}/\text{mL}$ LSPC and 20 μM A β_{25-35} showed the approximate number of cells and identical cellular morphology as control group,

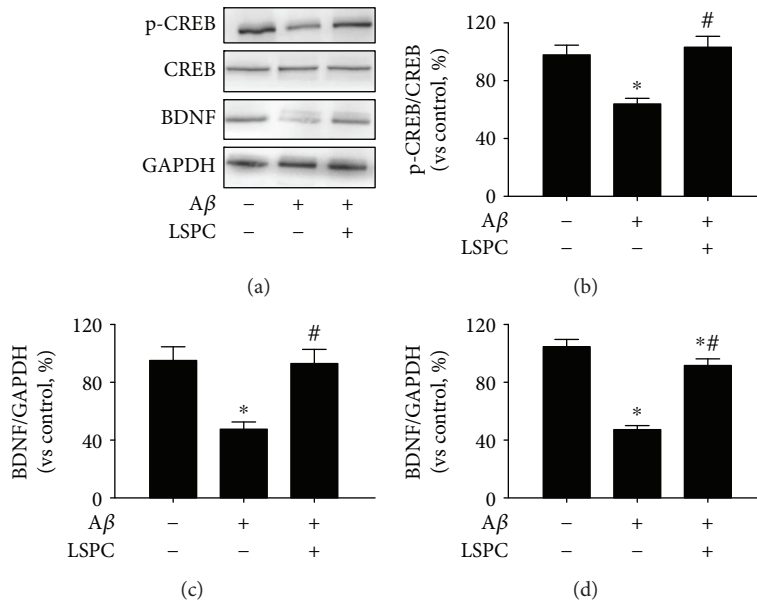


FIGURE 4: CREB/BDNF proteins expressions and mRNA expressions of intracellular BDNF in three groups (% of control, $n = 4$). (a) CREB/BDNF proteins expressions by Western blotting; (b) p-CREB/CREB proteins expressions by Western blotting in (a) (each group vs control, %); (c) BDNF protein expressions by Western blotting in (a) (each group vs control, %). Control, PC cells; A β , PC12 cells with 20 μM A β_{25-35} group; LSPC, PC12 cells with 10 $\mu\text{g}/\text{mL}$ LSPC and 20 μM A β_{25-35} group. All data are mean \pm SEM. * $P < 0.05$ for groups vs control group; # $P < 0.05$ for groups vs A β groups. (d) mRNA expression of intracellular BDNF in each group by qRT-PCR analysis. Cells were cultured as three groups as above, including control, A β , and LSPC. All data are mean \pm SEM. * $P < 0.05$ for groups vs control groups; # $P < 0.05$ for groups vs A β groups. All the results above are the representative of the three independent experiments.

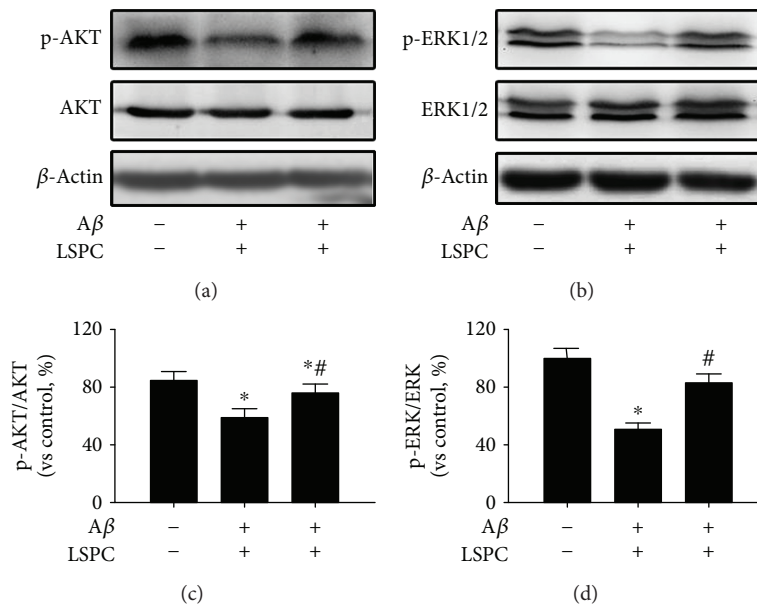


FIGURE 5: p-AKT/AKT and p-ERK/ERK proteins in each group (% of control, $n = 4$). (a) p-AKT/AKT proteins expressions by Western blotting; (b) p-ERK/ERK proteins expressions by Western blotting; (c) p-AKT/AKT proteins expressions by western blotting in (a) (each group vs control, %); (d) p-ERK/ERK proteins expressions by Western blotting in (b) (each group vs control, %). Control, PC cells; A β , PC12 cells with 20 μM A β_{25-35} group; LSPC, PC12 cells with 10 $\mu\text{g}/\text{mL}$ LSPC and 20 μM A β_{25-35} group. All data are mean \pm SEM. * $P < 0.05$ for groups vs control groups; # $P < 0.05$ for groups vs A β groups. All the results above are the representative of the three independent experiments.

while PC12 cells with 20 μM A β_{25-35} exhibited decreased cells number as well as abnormal morphology that PC12 cells shortened and shrank. As Hoechst staining (Figure 2(g))

demonstrated, PC12 cells in 20 μM A β_{25-35} group suggested conspicuous karyopyknosis and cell apoptosis compared to control group while addition of 10 $\mu\text{g}/\text{mL}$ LSPC prevented

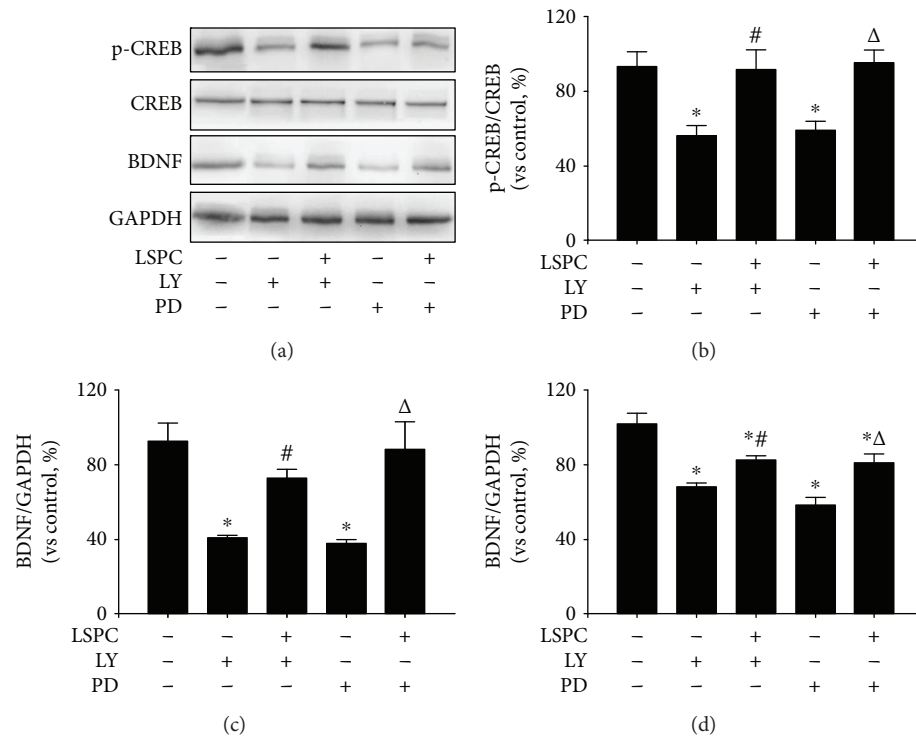


FIGURE 6: CREB/BDNF proteins expressions and mRNA expression of intracellular BDNF in five groups (% of control, $n = 4$). (a) CREB/BDNF proteins expressions by Western blotting; (b) p-CREB/CREB proteins expressions by Western blotting in (a) (each group vs control, %); (c) BDNF protein expressions by Western blotting in (a) (each group vs control, %). Control, PC cells; LY, PC12 cells with $10 \mu\text{M}$ LY294002; LSPC + LY, PC12 cells with $10 \mu\text{g/mL}$ LSPC and $10 \mu\text{M}$ LY294002; PD, PC12 cells with $30 \mu\text{M}$ PD98059; LSPC + PD, PC12 cells with $10 \mu\text{g/mL}$ LSPC and $30 \mu\text{M}$ PD98059. All data are mean \pm SEM. * $P < 0.05$ for groups vs control groups; # $P < 0.05$ for groups vs LY groups; $\Delta P < 0.05$ for groups vs PD groups. (d) mRNA expression of intracellular BDNF in each group by qRT-PCR analysis. Cells were cultured as five groups as above, including control, LY, LSPC + LY, PD, and LSPC + PD. All data are mean \pm SEM. * $P < 0.05$ for groups vs control group; # $P < 0.05$ for groups vs LY groups; $\Delta P < 0.05$ for groups vs PD groups. All the results above are the representative of the three independent experiments.

the damage from $A\beta_{25-35}$ remarkably. In flow cytometry analysis (Figures 2(h) and 2(i)), we further validated that the apoptosis rates of PC12 cells with $20 \mu\text{M}$ $A\beta_{25-35}$, including early apoptosis rates (AE), later apoptosis rates (LA), and total apoptosis rates (TA), were higher than that in the control ($P < 0.05$), and addition of $10 \mu\text{g/mL}$ LSPC significantly lessened apoptosis rates augmented by $A\beta_{25-35}$ ($P < 0.05$).

3.3. LSPC Protect PC12 Cells from $A\beta_{25-35}$ -Induced Oxidative Stress. The antioxidant activity of LSPC against the $A\beta_{25-35}$ -induced damage on PC12 cells was determined by evaluating levels of LDH, MDA, and T-SOD. As shown in Figures 3(a)–3(c), compared to control group, PC12 cells with $20 \mu\text{M}$ $A\beta_{25-35}$ had higher levels of intracellular MDA ($P < 0.05$) and extracellular LDH ($P < 0.05$) and a lower enzyme activity of T-SOD ($P < 0.05$). 5, 10, and $20 \mu\text{g/mL}$ LSPC all exhibited antioxidant activity. $10 \mu\text{g/mL}$ LSPC significantly reduced the levels of MDA and LDH among all groups and improved the activity of T-SOD on PC12 cells.

3.4. LSPC Ameliorate $A\beta_{25-35}$ -Induced Downregulation of CREB/BDNF Signaling in PC12 Cells. To substantiate the alleviation effect by LSPC on $A\beta_{25-35}$ -induced damage via CREB/BDNF signaling, we employed three groups: control

group, PC12 cells with $20 \mu\text{M}$ $A\beta_{25-35}$ ($A\beta$ group), and PC12 cells with $20 \mu\text{M}$ $A\beta_{25-35}$ after incubation with $10 \mu\text{g/mL}$ LSPC for 30 minutes (LSPC group). There was a significant discrepancy in p-CREB/CREB and BDNF expressions between the control group and $A\beta$ group ($P < 0.05$) (Figure 4). LSPC promoted phosphorylation of CREB (Figures 4(a) and 4(b)) and augmented BDNF expression (Figures 4(a) and 4(c)), indicating that LSPC could mitigate $A\beta_{25-35}$ -induced diminishment of CREB phosphorylation and BDNF expression. qRT-PCR analysis of BDNF mRNA (Figure 4(d)) demonstrated that $A\beta_{25-35}$ significantly attenuated BDNF mRNA expression compared with control group ($P < 0.05$) while LSPC counteracted the effect of $A\beta_{25-35}$ on BDNF mRNA expression.

Upstream signaling of CREB/BDNF including PI3K/AKT and Raf/ERK1/2 were analyzed through Western blotting (Figure 5). Both AKT and ERK phosphorylation were diminished after $A\beta_{25-35}$ treatment. LSPC could conspicuously reverse the effects induced by $A\beta$ ($P < 0.05$).

To further identify CREB/BDNF signaling in neuroprotection of LSPC, we applied LY294002, an inhibitor of the PI3K/AKT pathway, and PD98059, an inhibitor of the ERK pathway. Cells were cultured as five groups: PC12 cells, PC12 cells with $10 \mu\text{M}$ LY294002, PC12 cells with $10 \mu\text{g/mL}$

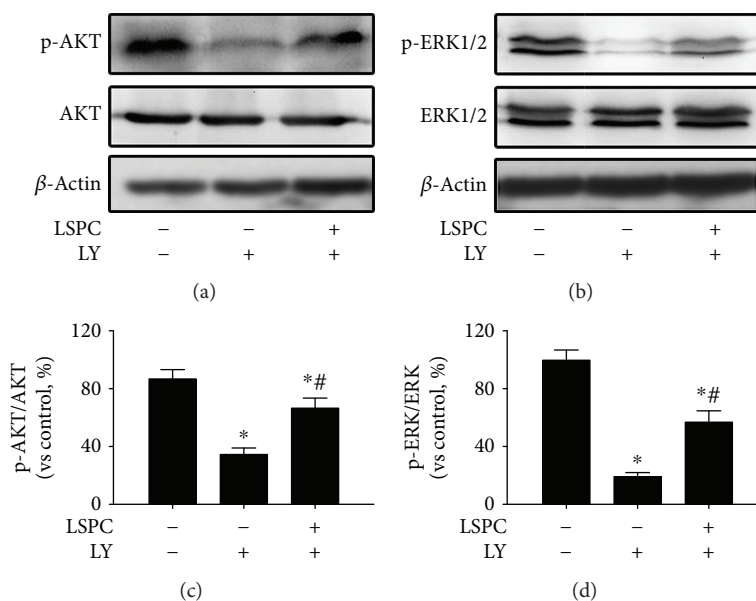


FIGURE 7: p-AKT/AKT and p-ERK/ERK proteins in each group (% of control, $n = 4$). (a) p-AKT/AKT proteins expressions by Western blotting; (b) p-ERK/ERK proteins expressions by Western blotting; (c) p-AKT/AKT proteins expressions by Western blotting in (a) (each group vs control, %); (d) p-ERK/ERK proteins expressions by western blotting in (b) (each group vs control, %). Control, PC cells; LY, PC12 cells with $10 \mu\text{M}$ LY294002; LSPC+LY, PC12 cells with $10 \mu\text{g/mL}$ LSPC and $10 \mu\text{M}$ LY294002; PD, PC12 cells with $30 \mu\text{M}$ PD98059; LSPC+PD, PC12 cells with $10 \mu\text{g/mL}$ LSPC and $30 \mu\text{M}$ PD98059. All data are mean \pm SEM. * $P < 0.05$ for groups vs control groups; # $P < 0.05$ for groups vs LY or PD groups. All the results above are the representative of the three independent experiments.

LSPC for 30 minutes before incubation with $10 \mu\text{M}$ LY294002, PC12 cells with $30 \mu\text{M}$ PD98059, PC12 cells with $10 \mu\text{g/mL}$ LSPC for 30 minutes before incubation with $30 \mu\text{M}$ PD98059. In Figures 6(a)–6(c), LY294002 and PD98059 inhibited the expression of phosphorylation of CREB and BDNF while LSPC reversed the inhibition of LY294002 and PD98059 significantly ($P < 0.05$). In a qRT-PCR analysis of BDNF mRNA (Figure 6(d)), LY294002 and PD98059 notably lessened BDNF mRNA expression and LSPC enhanced BDNF mRNA expression in PC12 cells. Additionally, LSPC counteracted the reduction of AKT and ERK phosphorylation after LY294002 or PD98059 intervention (Figure 7).

3.5. Distribution of LSPC and Its Metabolites in Rat Tissues.

As Tables 1(a) and 1(b), and 2 illustrated, after two weeks of consecutive LSPC administration, the quantities and formations of compounds varied in rat tissues and plasma. Summarily, PDB, epigallocatechin (EGC), and ECG were not detected in any rat tissues; syringic acid (1.98 ± 0.34) was slightly presented in plasma. After enzyme incubation, there were statistically significant differences ($P < 0.05$) about ferulic acid in pancreas and plasma, m-coumaric acid in the brain tissue, pancreas, and plasma, and protocatechuic acid (PCC) in the brain tissue and plasma.

In brain (Table 1(a) and 1(b)), the quantities of quercetin, epicatechin, gallic acid, vanillic acid, m-coumaric acid, protocatechuic, 3-hydroxyphenylacetic acid (3-HPAA), and pyrocatechol significantly accrued in LSPC group. The enhancement of four compounds was verified after enzyme preprocess with LSPC intervention, these being quercetin, epicatechin, caffeic acid, and 3-HPAA, in both cardiac and liver. Besides, catechin accumulated in the cardiac

tissues due to LSPC treatment; in the liver, homovanillic acid (HVA), gallic acid, and 3-hydroxybenzoic acid (3-HBA) increased markedly. Diverse compounds in the kidney (Table 1(a) and 1(b)) indicated significant differences between control and LSPC groups after enzyme disposal, including quercetin, catechin, epicatechin, HVA, caffeic acid, vanillic acid, 3,4-dihydroxyphenylacetic acid (3, 4-DHPA), 3-HBA, and pyrocatechol. In the pancreas (Table 1(a) and 1(b)), there was a remarkable increase in quercetin, ferulic acid, gallic acid, and m-coumaric acid, resulting from LSPC treatment. Apart from quercetin, 3, 4-DHPA alone in the spleen was confirmed to be significantly accrued after enzymolysis. LSPC administration contributed to the accumulations of quercetin, epicatechin, ferulic acid, HVA, caffeic acid, vanillic acid, 3-HBA, syringic acid, p-HPPA, m-coumaric, PCC, and pyrocatechol in plasma (Table 2).

There was no significant difference in body weight between the control group and LSPC group after LSPC treatment (Figure S2). Catechin and epicatechin were distinguished by LC-MS/MS according to distinctive retention time and transition ions.

4. Discussion

Recently, there has been an increasing interest in the discovery of potential flavonoids for preventing dementia or AD; nevertheless, the complexity and diversity of flavonoids restrict the understanding of their value on AD treatment. This study comprehensively verified its anti- $A\beta$ neurotoxicity *in vitro* that could alleviate AD-related symptoms.

In AD, $A\beta$ may contribute to oxidative stress in the brain [1, 34] while the antioxidant activity is an outstanding feature

TABLE 1: Quantities of compounds in rat tissues of control and LSPC groups.

(a)

Compound (ng/g)	Brain		Cardiac		Liver	
	Control Mean \pm SEM	LSPC Mean \pm SEM	Control Mean \pm SEM	LSPC Mean \pm SEM	Control Mean \pm SEM	LSPC Mean \pm SEM
PDB	ND	ND	ND	ND	ND	ND
ECG	ND	ND	ND	ND	ND	ND
EGC	ND	ND	ND	ND	ND	ND
Quercetin	35.84 \pm 2.63	46.72 \pm 2.57*	29.29 \pm 1.54	40.96 \pm 2.54**	27.71 \pm 1.45	49.12 \pm 3.63***
Catechin	ND	ND	ND	7.96 \pm 3.47*	ND	7.59 \pm 6.59
Epicatechin	ND	82.36 \pm 7.79***	ND	66.36 \pm 31.51	ND	55.50 \pm 9.13***
Syringic acid	ND	ND	ND	ND	ND	ND
Ferulic acid	54.21 \pm 3.81	84.45 \pm 8.96	ND	ND	ND	ND
HVA	142.07 \pm 12.50	236.36 \pm 63.98	ND	ND	1.52 \pm 0.94	19.36 \pm 2.53***
Caffeic acid	109.07 \pm 3.95	120.93 \pm 5.73	86.50 \pm 1.70	96.00 \pm 3.57*	79.50 \pm 1.70	92.50 \pm 4.98*
Gallic acid	39.88 \pm 2.83	69.36 \pm 4.72***	12.44 \pm 1.44	20.48 \pm 3.30	17.74 \pm 3.15	30.13 \pm 4.09*
Vanillic acid	67.92 \pm 11.19	122.50 \pm 17.15*	ND	ND	ND	ND
3,4-DHPA	154.21 \pm 22.81	361.71 \pm 162.66	18.64 \pm 1.92	21.89 \pm 2.08	ND	ND
p-HPPA	14.29 \pm 2.75	22.29 \pm 3.66	22.31 \pm 13.30	9.43 \pm 3.24	8.99 \pm 6.41	28.09 \pm 7.20
m-Coumaric acid	9.26 \pm 0.98	13.20 \pm 0.97*	ND	ND	ND	ND
PCC	183.64 \pm 11.80	231.29 \pm 16.06*	211.21 \pm 12.03	279.43 \pm 40.98	112.14 \pm 6.73	152.93 \pm 19.14
3-HPAA	16.03 \pm 1.16	25.47 \pm 2.65**	18.81 \pm 0.77	26.89 \pm 3.00*	104.00 \pm 9.17	170.86 \pm 13.76**
3-HBA	58.11 \pm 12.87	83.49 \pm 38.02	10.53 \pm 4.37	8.26 \pm 1.81	ND	4.13 \pm 0.73**
Pyrocatechol	94.21 \pm 5.88	124.79 \pm 9.49*	54.54 \pm 2.66	63.49 \pm 5.27	13.46 \pm 1.94	21.16 \pm 2.92

(b)

Compound (ng/g)	Kidney		Spleen		Pancreas	
	Control Mean \pm SEM	LSPC Mean \pm SEM	Control Mean \pm SEM	LSPC Mean \pm SEM	Control Mean \pm SEM	LSPC Mean \pm SEM
PDB	ND	ND	ND	ND	ND	ND
ECG	ND	ND	ND	ND	ND	ND
EGC	ND	ND	ND	ND	ND	ND
Quercetin	20.40 \pm 1.27	49.55 \pm 2.99***	29.13 \pm 1.56	38.49 \pm 3.66*	17.55 \pm 6.23	50.78 \pm 3.15***
Catechin	ND	7.01 \pm 1.66**	ND	ND	ND	ND
Epicatechin	ND	32.40 \pm 4.37***	ND	33.71 \pm 21.76	ND	ND
Syringic acid	ND	ND	ND	ND	ND	ND
Ferulic acid	ND	ND	ND	ND	18.49 \pm 7.86	41.51 \pm 3.58*
HVA	14.46 \pm 3.31	73.71 \pm 9.05***	ND	ND	ND	ND
Caffeic acid	71.00 \pm 2.25	101.50 \pm 5.90**	51.88 \pm 2.60	52.31 \pm 2.93	114.43 \pm 6.23	126.86 \pm 7.82
Gallic acid	25.64 \pm 1.35	51.12 \pm 17.29	22.47 \pm 1.69	26.72 \pm 1.16	30.32 \pm 5.58	47.08 \pm 1.43*
Vanillic acid	ND	21.83 \pm 7.41*	ND	ND	23.72 \pm 6.33	44.05 \pm 7.34
3,4-DHPA	9.34 \pm 1.83	20.89 \pm 2.45**	9.19 \pm 2.48	19.31 \pm 1.24**	ND	ND
p-HPPA	85.69 \pm 61.94	279.71 \pm 67.66	5.65 \pm 2.74	12.77 \pm 3.75	ND	ND
m-Coumaric acid	ND	20.05 \pm 13.39	ND	ND	17.88 \pm 3.71	36.21 \pm 4.51**
PCC	118.43 \pm 10.88	134.29 \pm 8.74	145.71 \pm 16.17	152.14 \pm 17.77	216.86 \pm 17.69	229.21 \pm 12.45
3-HPAA	15.31 \pm 1.37	21.62 \pm 3.21	2.82 \pm 1.11	2.14 \pm 0.73	40.83 \pm 3.56	49.78 \pm 4.52

TABLE 1: Continued.

Compound (ng/g)	Kidney		Spleen		Pancreas	
	Control Mean \pm SEM	LSPC Mean \pm SEM	Control Mean \pm SEM	LSPC Mean \pm SEM	Control Mean \pm SEM	LSPC Mean \pm SEM
3-HBA	5.40 \pm 0.68	26.16 \pm 2.60***	3.12 \pm 0.87	4.29 \pm 0.99	ND	ND
Pyrocatechol	19.98 \pm 1.67	33.25 \pm 3.60**	16.56 \pm 2.84	16.81 \pm 3.78	69.26 \pm 5.06	70.64 \pm 3.89

Note: control and LSPC represent different intervention groups, respectively. PDB, ECG, EGC, HVA, 3,4-DHPA, p-HPPA, PCC, 3-HPAA, and 3-HBA stand for procyanidin dimer B, epicatechin gallate, epigallocatechin, homovanillic acid, 3,4-dihydroxyphenylacetic acid, 3-(4-hydroxyphenyl)propionic acid, protocatechuic acid, 3-hydroxyphenylacetic acid, and 3-hydroxybenzoic acid, respectively. Values represent the concentrations of metabolites in different rat tissues, and they were all presented as the means \pm SEM ($n = 7$); ND = not detected; *, **, *** indicates significant differences between two groups with or without LSPC ($p < 0.05$, $p < 0.01$, and $p < 0.001$), respectively.

TABLE 2: Quantities of compounds in rat plasma of control and LSPC groups.

Compound (ng/mL)	Plasma	
	Control Mean \pm SEM	LSPC Mean \pm SEM
PDB	ND	ND
ECG	ND	ND
EGC	ND	ND
Quercetin	5.83 \pm 0.31	7.70 \pm 0.73*
Catechin	ND	ND
Epicatechin	ND	9.38 \pm 3.45*
Syringic acid	ND	1.98 \pm 0.34***
Ferulic acid	8.95 \pm 3.59	31.77 \pm 4.24**
HVA	6.64 \pm 0.40	29.59 \pm 3.63***
Caffeic acid	10.36 \pm 1.48	40.44 \pm 9.68**
Gallic acid	ND	ND
Vanillic acid	39.97 \pm 2.52	86.96 \pm 7.60***
3,4-DHPA	ND	ND
p-HPPA	23.22 \pm 16.84	122.97 \pm 10.64***
m-Coumaric acid	7.86 \pm 5.63	24.90 \pm 3.00*
PCC	2.21 \pm 0.36	10.95 \pm 2.55**
3-HPAA	4.63 \pm 0.41	6.77 \pm 0.94
3-HBA	4.10 \pm 0.26	13.86 \pm 0.90***
Pyrocatechol	1.27 \pm 0.47	4.73 \pm 0.68**

Note: control and LSPC represent different intervention groups, respectively. PDB, ECG, EGC, HVA, 3,4-DHPA, p-HPPA, PCC, 3-HPAA, and 3-HBA stand for procyanidin dimer B, epicatechin gallate, epigallocatechin, homovanillic acid, 3,4-dihydroxyphenylacetic acid, 3-(4-hydroxyphenyl)propionic acid, protocatechuic acid, 3-hydroxyphenylacetic acid, and 3-hydroxybenzoic acid, respectively. Values represent the concentrations of metabolites in different rat tissues, and they were all presented as the means \pm SEM ($n = 7$); ND = not detected; *, **, *** indicates significant differences between two groups with or without LSPC ($p < 0.05$, $p < 0.01$, and $p < 0.001$), respectively.

of flavonoids. PC12 cells with A β _{25–35}, as an AD-like model, were performed to testify the abilities about anti-A β neurotoxicity of LSPC [35, 36]. LSPC has no toxicity *in vitro* and *in vivo* that coincided with previous studies [27, 37]. LSPC has exhibited its antioxidation effect *in vitro* that was consistent with Xu et al. [27]. Interestingly, a higher concentration

of LSPC (20 mg/L) seemed to be less efficient in the decrease of MDA and LDH, and a dose-response could be seen regarding the SOD activity. This result could be partly due to the difference in antioxidant activity associated with doses of procyanidins, cell type, and time of exposure [38]. The inconsistency of different antioxidant enzymes activities has been reported by Puiggròs et al. [39]. Antioxidant reactions of flavonoids, as illustrated by many studies, may benefit the treatment and precaution of cancer [40], cardiovascular diseases [41, 42], type 2 diabetes [41, 42], and neurodegenerative diseases [43]. Since periphery anti-A β has been proposed as potential approaches to ameliorate impairment of A β [44, 45] in the central nervous system that the liver and kidney have been tightly related to it [44, 46], it is a high possibility that antioxidant effect of LSPC could contribute to alleviate A β toxicity in this pathway.

Not only oxidative stress is attributed to accumulation and neurotoxicity of A β in AD but also downregulation of CREB/BDNF signaling [5, 12–14]. Several studies have shed the light on anti-A β effect of flavonoids [47–49]. Lin et al. have reported that A β could induce the death of cells [50], and in AD, it is a major damage resulted from A β aggregation [51]. According to Hoechst staining and flow cytometry in the present study, LSPC kept cellular morphology from deformation and suppressed the apoptosis of cells induced by A β . In addition, A β can reduce the expression of BDNF in AD [52], and CREB can mediate A β -induced BDNF downregulation [53] that are in accordance with our results. CREB/BDNF signaling was downregulated by A β but upregulated by LSPC. Through targeting phosphorylation of CREB, AKT, and ERK, the upstream of CREB/BDNF signaling can affect BDNF transcription [6, 7]. Activations of both AKT and ERK were restrained by A β [8, 9] but increased with treatment of LSPC in our study. CREB/BDNF signaling plays a vital role in neuron survival, and BDNF-based synaptic repair is proposed as a therapeutic strategy for AD [54]. LSPC could hence ameliorate A β -induced damage in AD through CREB/BDNF signaling. Notably, an interaction between CREB/BDNF signaling and oxidative stress has been confirmed [18, 19]. Valvassori et al. have reported that increased BDNF in the brain can modulate oxidative stress [55]. Taken together, LSPC has both antioxidative effects and the ability to regulate CREB/BDNF signaling as a potential AD pretreatment. Several researches focusing on lotus also support that compounds from lotus may show neuroprotection [20].

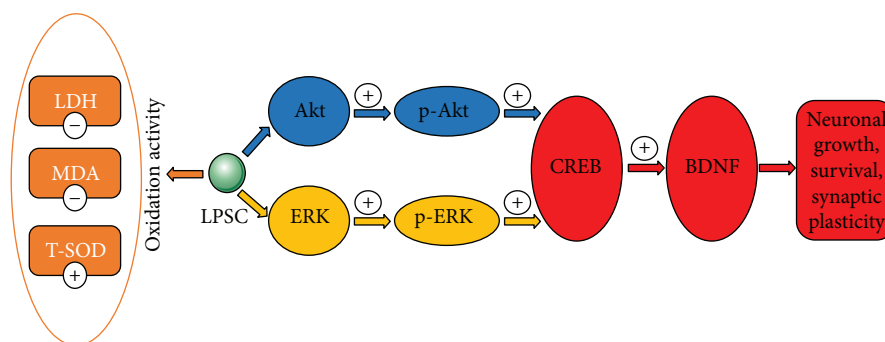


FIGURE 8: Schematic diagram shows anti- $A\beta$ effects of LSPC on PC12 cells. CREB/BDNF signaling plays a significant role in neuronal growth, survival, and synaptic plasticity. $A\beta$ can increase the apoptosis rates of cells and deform the cellular morphology since $A\beta$ may lead to downregulation of CREB phosphorylation and BDNF expression. LSPC can reverse the effect of $A\beta$ that it can improve the survival rates of cells and maintain the cellular morphology. LSPC may promote the upstream signaling of CREB/BDNF, including AKT and ERK phosphorylation, which can enhance CREB phosphorylation and BDNF expression. Additionally, $A\beta$ may contribute to higher levels of MDA and LDH and the lower activity of T-SOD. LSPC can mitigate $A\beta$ -induced damage through reducing the level of MDA and LDH and improving the activity of T-SOD. LSPC, procyanidins extracted from the lotus seedpod; $A\beta$, amyloid- β ; PC12, rat pheochromocytoma cells; BDNF, brain-derived neurotrophic factor; CREB, cAMP-responsive element-binding; LDH, lactate dehydrogenase; SOD, superoxide dismutase; MDA, malonaldehyde.

By LC-MS/MS, we found several detectable compositions accumulated *in vivo* and quantities of them were varied in rat tissues and plasma after consecutive LSPC administration. As reported, $A\beta$ can aggravate in both central and periphery tissues and the relationship between AD and the peripheral system is indivisible [56, 57]. AD has been called as “type 3 diabetes”, concerning its association with insulin resistance [58]; it also has been related to the gut-brain axis [59]. The distribution of LSPC was only measured in rat urine before so it was profound to confirm the distribution of it *in vivo*. In the LSPC group, epicatechin and quercetin, resulted from quercetin-3-O-glucuronide in LSPC [25], were found to accumulate in the brain. Wang et al. [16] have reported 3'-O-methyl-epicatechin-5-O- β -glucuronide, the major metabolites of epicatechin in the brain, may promote long-term potentiation (LTP) through CREB signaling. Quercetin-3-O-glucuronide has been reported to cross the blood-brain barrier and accumulate in the brain [60, 61]; deconjugation of it may contribute to the appearance of quercetin in tissues [61]. Quercetin-3-O-glucuronide has also been identified to inhibit $A\beta$ aggregation [60] and reduce oxidative stress [61, 62]. The increment of BDNF protein and AKT phosphorylation in the rat by quercetin-3-O-glucuronide has been observed by Baral et al. [63]. Serra et al. [64] have discussed the distribution of procyanidins from hazelnut extract after treatment once, reporting only p-HPPA is significantly increased in the brain. Conversely, our results showed that LSPC could lead to the accumulation of quercetin, epicatechin, gallic acid, vanillic acid, m-coumaric acid, protocatechuic, 3-HPAA, and pyrocatechol. This inconsistency could be ascribed to the difference between LSPC and hazelnut extract and intervention time.

Other compounds in the brain detected to increase in LSPC group, including gallic acid [65], vanillic acid [66], and protocatechuic acid [67], have been discussed to anti- $A\beta$ neurotoxicity through multifarious pathways. Gallic acid could inhibit $A\beta$ neurotoxicity through suppressing

neuroinflammation [65]; vanillic acid is found to attenuate oxidative stress induced by $A\beta$ [66]; protocatechuic acid may also minimize inflammatory response [67]. But evidences about these materials are insufficient. Further studies are required to discern and compare the effects of different compounds after LSPC treatment as an integral or as separated components.

5. Conclusion

Our research firstly affirmed anti- $A\beta$ effectiveness of LSPC that indicated it as a promising pretreatment for AD and expounded LSPC distribution *in vivo*. Through cell experiments, our study not only proved anti- $A\beta$ effects of LSPC through evaluation of cell viability and cellular morphology but also identified the antioxidant effect of LSPC and BDNF/CREB signaling in its anti- $A\beta$ mechanisms (Figure 8). We also applied LC-MS/MS in the detection of LSPC *in vivo* that contributed to explain its effect. Future studies still need to enrich our scientific recognition of LSPC and then establish the novel therapeutic strategies for AD.

Abbreviations

AD:	Alzheimer's disease
LSPC:	Procyanidins extracted from the lotus seedpod
$A\beta$:	Amyloid- β
LC-MS/MS:	High-performance liquid chromatography-tandem mass spectroscopy
PC12:	Rat pheochromocytoma cells
BDNF:	Brain-derived neurotrophic factor
CREB:	cAMP-responsive element-binding
AKT:	Protein kinase B
ERK:	Extracellular signal-regulated kinase
CCK-8:	Cell counting Kit-8

LDH:	Lactate dehydrogenase
SOD:	Superoxide dismutase
MDA:	Malonaldehyde
RPMI:	Roswell Park Memorial Institute
PI:	Propidium iodide
EA:	Early apoptosis
LA:	Late apoptosis
TA:	Total apoptosis
PVDF:	Polyvinylidene difluoride
qRT-PCR:	Quantitative reverse transcription PCR
SEM:	Standard error of mean
SNK:	Student-Newman-Keuls
PDB, ECG, EGC, HVA, 3,4-DHPA, p-HPPA, PCC, 3-HPAA, and 3-HBA:	Procyanidin dimer B, epicatechin gallate, epigallocatechin, homovanillic acid, 3,4- dihydroxyphenylacetic acid, 3-(4-hydro- xyphenyl)propionic acid, protocatechuic acid, 3-hydroxyphenylacetic acid, and 3-hydroxybenzoic acid, respectively
LTP:	Long-term potentiation.

Data Availability

The data is available on the website of Figshare and the access is <https://figshare.com/s/fb5f71daf2ef08cdf42>.

Conflicts of Interest

The authors declare that there is no conflict of interest regarding the publication of this paper.

Acknowledgments

We are thankful for the help from Professor Keqiang Ye (Department of Pathology and Laboratory Medicine, Emory University School of Medicine, Atlanta, USA). This study was supported by the National Natural Science Foundation of China (81472978).

Supplementary Materials

Figure S1: chemical structures of all analytes. Figure S2: body weights of rats fed as control group and LSPC group. Table S1: formula, transition ions, retention times, and mass spectrometry parameters for all compounds. (*Supplementary Materials*)

References

- [1] Y. Huang and L. Mucke, "Alzheimer mechanisms and therapeutic strategies," *Cell*, vol. 148, no. 6, pp. 1204–1222, 2012.
- [2] J. A. Hardy and G. A. Higgins, "Alzheimer's disease: the amyloid cascade hypothesis," *Science*, vol. 256, no. 5054, pp. 184–185, 1992.
- [3] J. Hardy and D. J. Selkoe, "The amyloid hypothesis of Alzheimer's disease: progress and problems on the road to therapeutics," *Science*, vol. 297, no. 5580, pp. 353–356, 2002.
- [4] C. Ising, M. Stanley, and D. M. Holtzman, "Current thinking on the mechanistic basis of Alzheimer's and implications for drug development," *Clinical Pharmacology & Therapeutics*, vol. 98, no. 5, pp. 469–471, 2015.
- [5] M. P. Mattson, "Pathways towards and away from Alzheimer's disease," *Nature*, vol. 430, no. 7000, pp. 631–639, 2004.
- [6] B. Bozon, A. Kelly, S. A. Josselyn, A. J. Silva, S. Davis, and S. Laroche, "MAPK, CREB and zif268 are all required for the consolidation of recognition memory," *Philosophical Transactions of the Royal Society of London. Series B, Biological Sciences*, vol. 358, no. 1432, pp. 805–814, 2003.
- [7] W. Wang, Y. Lu, Z. Xue et al., "Rapid-acting antidepressant-like effects of acetyl-L-carnitine mediated by PI3K/AKT/BDNF/VGF signaling pathway in mice," *Neuroscience*, vol. 285, pp. 281–291, 2015.
- [8] S. Jimenez, M. Torres, M. Vizuet et al., "Age-dependent accumulation of soluble amyloid beta (A β) oligomers reverses the neuroprotective effect of soluble amyloid precursor protein- α (sAPP α) by modulating phosphatidylinositol 3-kinase (PI3K)/Akt-GSK-3 β pathway in Alzheimer mouse model," *The Journal of Biological Chemistry*, vol. 286, no. 21, pp. 18414–18425, 2011.
- [9] C. Lu, Y. Wang, D. Wang et al., "Neuroprotective effects of soy isoflavones on scopolamine-induced amnesia in mice," *Nutrients*, vol. 10, no. 7, 2018.
- [10] C. R. Bramham and E. Messaoudi, "BDNF function in adult synaptic plasticity: the synaptic consolidation hypothesis," *Progress in Neurobiology*, vol. 76, no. 2, pp. 99–125, 2005.
- [11] C. G. Causing, A. Gloster, R. Aloyz et al., "Synaptic innervation density is regulated by neuron-derived BDNF," *Neuron*, vol. 18, no. 2, pp. 257–267, 1997.
- [12] M. Fahnstock, "Brain-derived neurotrophic factor: the link between amyloid- β and memory loss," *Future Neurology*, vol. 6, no. 5, pp. 627–639, 2011.
- [13] D. J. Garzon and M. Fahnstock, "Oligomeric amyloid decreases basal levels of brain-derived neurotrophic factor (BDNF) mRNA via specific downregulation of BDNF transcripts IV and V in differentiated human neuroblastoma cells," *The Journal of Neuroscience*, vol. 27, no. 10, pp. 2628–2635, 2007.
- [14] S. Peng, D. J. Garzon, M. Marchese et al., "Decreased brain-derived neurotrophic factor depends on amyloid aggregation state in transgenic mouse models of Alzheimer's disease," *The Journal of Neuroscience*, vol. 29, no. 29, pp. 9321–9329, 2009.
- [15] C. M. Williams, M. A. el Mohsen, D. Vauzour et al., "Blueberry-induced changes in spatial working memory correlate with changes in hippocampal CREB phosphorylation and brain-derived neurotrophic factor (BDNF) levels," *Free Radical Biology & Medicine*, vol. 45, no. 3, pp. 295–305, 2008.
- [16] J. Wang, M. G. Ferruzzi, L. Ho et al., "Brain-targeted proanthocyanidin metabolites for Alzheimer's disease treatment," *The Journal of Neuroscience*, vol. 32, no. 15, pp. 5144–5150, 2012.
- [17] S. M. Massa, T. Yang, Y. Xie et al., "Small molecule BDNF mimetics activate TrkB signaling and prevent neuronal degeneration in rodents," *The Journal of Clinical Investigation*, vol. 120, no. 5, pp. 1774–1785, 2010.
- [18] A. Wu, Z. Ying, and F. Gomez-Pinilla, "The interplay between oxidative stress and brain-derived neurotrophic factor modulates the outcome of a saturated fat diet on synaptic plasticity and cognition," *The European Journal of Neuroscience*, vol. 19, no. 7, pp. 1699–1707, 2004.
- [19] F. Kapczinski, B. N. Frey, A. C. Andreazza, M. Kauer-Sant'Anna, Á. B. M. Cunha, and R. M. Post, "Increased

- oxidative stress as a mechanism for decreased BDNF levels in acute manic episodes,” *Revista Brasileira de Psiquiatria*, vol. 30, no. 3, pp. 243–245, 2008.
- [20] A. Kumaran, C. C. Ho, and L. S. Hwang, “Protective effect of *Nelumbo nucifera* extracts on beta amyloid protein induced apoptosis in PC12 cells, in vitro model of Alzheimer’s disease,” *Journal of Food and Drug Analysis*, vol. 26, no. 1, pp. 172–181, 2018.
- [21] Y. Liu, P. Chaturvedi, J. Fu, Q. Cai, W. Weckwerth, and P. Yang, “Induction and quantitative proteomic analysis of cell dedifferentiation during callus formation of lotus (*Nelumbo nucifera* Gaertn.spp. baijianlian),” *Journal of Proteomics*, vol. 131, pp. 61–70, 2016.
- [22] D. Mastroiacovo, C. Kwik-Uribe, D. Grassi et al., “Cocoa flavanol consumption improves cognitive function, blood pressure control, and metabolic profile in elderly subjects: the Cocoa, Cognition, and Aging (CoCoA) Study—a randomized controlled trial,” *The American Journal of Clinical Nutrition*, vol. 101, no. 3, pp. 538–548, 2015.
- [23] A. H. Shinichi Kuriyama, K. Ohmori, T. Shimazu et al., “Green tea consumption and cognitive function: a cross-sectional study from the Tsurugaya Project,” *The American Journal of Clinical Nutrition*, vol. 83, no. 2, pp. 355–361, 2006.
- [24] Z. Zhang, X. Liu, J. P. Schroeder et al., “7,8-dihydroxyflavone prevents synaptic loss and memory deficits in a mouse model of Alzheimer’s disease,” *Neuropsychopharmacology*, vol. 39, no. 3, pp. 638–650, 2014.
- [25] J. S. Xiao, B. J. Xie, Y. P. Cao, H. Wu, Z. D. Sun, and D. Xiao, “Characterization of oligomeric procyanidins and identification of quercetin glucuronide from lotus (*Nelumbo nucifera* Gaertn.) seedpod,” *Journal of Agricultural and Food Chemistry*, vol. 60, no. 11, pp. 2825–2829, 2012.
- [26] J. Xu, S. Rong, B. Xie et al., “Memory impairment in cognitively impaired aged rats associated with decreased hippocampal CREB phosphorylation: reversal by procyanidins extracted from the lotus seedpod,” *The Journals of Gerontology Series A*, vol. 65A, no. 9, pp. 933–940, 2010.
- [27] J. Xu, S. Rong, B. Xie et al., “Procyanidins extracted from the lotus seedpod ameliorate age-related antioxidant deficit in aged rats,” *The Journals of Gerontology Series A*, vol. 65A, no. 3, pp. 236–241, 2010.
- [28] G. X. Mao, L. D. Zheng, Y. B. Cao et al., “Antiaging effect of pine pollen in human diploid fibroblasts and in a mouse model induced by D-galactose,” *Oxidative Medicine and Cellular Longevity*, vol. 2012, Article ID 750963, 10 pages, 2012.
- [29] Y. Gao, J. Chen, K. Li et al., “Replacement of Oct4 by Tet1 during iPSC induction reveals an important role of DNA methylation and hydroxymethylation in reprogramming,” *Cell Stem Cell*, vol. 12, no. 4, pp. 453–469, 2013.
- [30] D. Achaintre, A. Buleté, C. Cren-Olivé, L. Li, S. Rinaldi, and A. Scalbert, “Differential isotope labeling of 38 dietary polyphenols and their quantification in urine by liquid chromatography electrospray ionization tandem mass spectrometry,” *Analytical Chemistry*, vol. 88, no. 5, pp. 2637–2644, 2016.
- [31] Q. Wu, S. Li, X. Li et al., “Inhibition of advanced glycation end-product formation by lotus seedpod oligomeric procyanidins through RAGE–MAPK signaling and NF- κ B activation in high-fat-diet rats,” *Journal of Agricultural and Food Chemistry*, vol. 63, no. 31, pp. 6989–6998, 2015.
- [32] M. Urpi-Sarda, M. Monagas, N. Khan et al., “Targeted metabolic profiling of phenolics in urine and plasma after regular consumption of cocoa by liquid chromatography-tandem mass spectrometry,” *Journal of Chromatography. A*, vol. 1216, no. 43, pp. 7258–7267, 2009.
- [33] F. You, Q. Li, G. Jin, Y. Zheng, J. Chen, and H. Yang, “Genistein protects against $A\beta_{25-35}$ induced apoptosis of PC12 cells through JNK signaling and modulation of Bcl-2 family messengers,” *BMC Neuroscience*, vol. 18, no. 1, p. 12, 2017.
- [34] G. Perry, A. D. Cash, and M. A. Smith, “Alzheimer disease and oxidative stress,” *Journal of Biomedicine & Biotechnology*, vol. 2, no. 3, 123 pages, 2002.
- [35] S. Y. Park and D. S. Kim, “Discovery of natural products from *Curcuma longa* that protect cells from beta-amyloid insult: a drug discovery effort against Alzheimer’s disease,” *Journal of Natural Products*, vol. 65, no. 9, pp. 1227–1231, 2002.
- [36] S. Y. Lee, J. W. Lee, H. Lee et al., “Inhibitory effect of green tea extract on β -amyloid-induced PC12 cell death by inhibition of the activation of NF- κ B and ERK/p38 MAP kinase pathway through antioxidant mechanisms,” *Brain Research. Molecular Brain Research*, vol. 140, no. 1-2, pp. 45–54, 2005.
- [37] Q. Wu, S. Li, X. Li et al., “A significant inhibitory effect on advanced glycation end product formation by catechin as the major metabolite of lotus seedpod oligomeric procyanidins,” *Nutrients*, vol. 6, no. 8, pp. 3230–3244, 2014.
- [38] C. F. Skibola and M. T. Smith, “Potential health impacts of excessive flavonoid intake,” *Free Radical Biology & Medicine*, vol. 29, no. 3-4, pp. 375–383, 2000.
- [39] F. Puiggròs, N. Llopiz, A. Ardévol, C. Bladé, L. Arola, and M. Josepa Salvadó, “Grape seed procyanidins prevent oxidative injury by modulating the expression of antioxidant enzyme systems,” *Journal of Agricultural and Food Chemistry*, vol. 53, no. 15, pp. 6080–6086, 2005.
- [40] C. S. Yang, X. Wang, G. Lu, and S. C. Picinich, “Cancer prevention by tea: animal studies, molecular mechanisms and human relevance,” *Nature Reviews. Cancer*, vol. 9, no. 6, pp. 429–439, 2009.
- [41] R. M. van Dam, N. Naidoo, and R. Landberg, “Dietary flavonoids and the development of type 2 diabetes and cardiovascular diseases: review of recent findings,” *Current Opinion in Lipidology*, vol. 24, no. 1, pp. 25–33, 2013.
- [42] F. Perez-Vizcaino and J. Duarte, “Flavonols and cardiovascular disease,” *Molecular Aspects of Medicine*, vol. 31, no. 6, pp. 478–494, 2010.
- [43] R. Meeusen, “Exercise, nutrition and the brain,” *Sports Medicine*, vol. 44, Supplement 1, pp. 47–56, 2014.
- [44] Y. R. Wang, Q. H. Wang, T. Zhang et al., “Associations between hepatic functions and plasma amyloid-beta levels—implications for the capacity of liver in peripheral amyloid-beta clearance,” *Molecular Neurobiology*, vol. 54, no. 3, pp. 2338–2344, 2017.
- [45] Y. H. Liu, Y. R. Wang, Y. Xiang et al., “Clearance of amyloid-beta in Alzheimer’s disease: shifting the action site from center to periphery,” *Molecular Neurobiology*, vol. 51, no. 1, pp. 1–7, 2015.
- [46] S. L. Seliger, “Moderate renal impairment and risk of dementia among older adults: the cardiovascular health cognition study,” *Journal of the American Society of Nephrology*, vol. 15, no. 7, pp. 1904–1911, 2004.
- [47] J. Wang, L. Ho, W. Zhao et al., “Grape-derived polyphenolics prevent A β oligomerization and attenuate cognitive deterioration in a mouse model of Alzheimer’s disease,” *The Journal of Neuroscience*, vol. 28, no. 25, pp. 6388–6392, 2008.

- [48] T. Hamaguchi, K. Ono, A. Murase, and M. Yamada, "Phenolic compounds prevent Alzheimer's pathology through different effects on the amyloid-beta aggregation pathway," *The American Journal of Pathology*, vol. 175, no. 6, pp. 2557–2565, 2009.
- [49] X. Zhang, J. Hu, L. Zhong et al., "Quercetin stabilizes apolipoprotein E and reduces brain A β levels in amyloid model mice," *Neuropharmacology*, vol. 108, pp. 179–192, 2016.
- [50] J. Lin, J. Yu, J. Zhao et al., "Fucoxanthin, a marine carotenoid, attenuates β -amyloid oligomer-induced neurotoxicity possibly via regulating the PI3K/Akt and the ERK pathways in SH-SY5Y cells," *Oxidative Medicine and Cellular Longevity*, vol. 2017, Article ID 6792543, 10 pages, 2017.
- [51] B. T. Hyman, "Caspase activation without apoptosis: insight into A β initiation of neurodegeneration," *Nature Neuroscience*, vol. 14, no. 1, pp. 5–6, 2011.
- [52] A. Sen, T. J. Nelson, and D. L. Alkon, "ApoE4 and A β oligomers reduce BDNF expression via HDAC nuclear translocation," *The Journal of Neuroscience*, vol. 35, no. 19, pp. 7538–7551, 2015.
- [53] E. Rosa and M. Fahnstock, "CREB expression mediates amyloid β -induced basal BDNF downregulation," *Neurobiology of Aging*, vol. 36, no. 8, pp. 2406–2413, 2015.
- [54] B. Lu, G. Nagappan, X. Guan, P. J. Nathan, and P. Wren, "BDNF-based synaptic repair as a disease-modifying strategy for neurodegenerative diseases," *Nature Reviews Neuroscience*, vol. 14, no. 6, pp. 401–416, 2013.
- [55] S. S. Valvassori, C. O. Arent, A. V. Steckert et al., "Intracerebral administration of BDNF protects rat brain against oxidative stress induced by ouabain in an animal model of mania," *Molecular Neurobiology*, vol. 52, no. 1, pp. 353–362, 2015.
- [56] A. E. Roher, C. L. Esh, T. A. Kokjohn et al., "Amyloid beta peptides in human plasma and tissues and their significance for Alzheimer's disease," *Alzheimers Dement*, vol. 5, no. 1, pp. 18–29, 2009.
- [57] J. Wang, B. J. Gu, C. L. Masters, and Y. J. Wang, "A systemic view of Alzheimer disease — insights from amyloid- β metabolism beyond the brain," *Nature Reviews Neurology*, vol. 13, no. 10, pp. 612–623, 2017.
- [58] S. M. de la Monte, "Type 3 diabetes is sporadic Alzheimer's disease: mini-review," *European Neuropsychopharmacology*, vol. 24, no. 12, pp. 1954–1960, 2014.
- [59] C. Jiang, G. Li, P. Huang, Z. Liu, and B. Zhao, "The gut microbiota and Alzheimer's disease," *Journal of Alzheimer's Disease*, vol. 58, no. 1, pp. 1–15, 2017.
- [60] L. Ho, M. G. Ferruzzi, E. M. Janle et al., "Identification of brain-targeted bioactive dietary quercetin-3-O-glucuronide as a novel intervention for Alzheimer's disease," *The FASEB Journal*, vol. 27, no. 2, pp. 769–781, 2013.
- [61] A. Ishisaka, R. Mukai, J. Terao, N. Shibata, and Y. Kawai, "Specific localization of quercetin-3-O-glucuronide in human brain," *Archives of Biochemistry and Biophysics*, vol. 557, pp. 11–17, 2014.
- [62] A. Ishisaka, S. Ichikawa, H. Sakakibara et al., "Accumulation of orally administered quercetin in brain tissue and its antioxidative effects in rats," *Free Radical Biology & Medicine*, vol. 51, no. 7, pp. 1329–1336, 2011.
- [63] S. Baral, R. Pariyar, J. Kim, H. S. Lee, and J. Seo, "Quercetin-3-O-glucuronide promotes the proliferation and migration of neural stem cells," *Neurobiology of Aging*, vol. 52, pp. 39–52, 2017.
- [64] A. Serra, A. Macià, M. P. Romero, N. Anglès, J. R. Morelló, and M. J. Motilva, "Distribution of procyanidins and their metabolites in rat plasma and tissues after an acute intake of hazelnut extract," *Food & Function*, vol. 2, no. 9, pp. 562–568, 2011.
- [65] M. J. Kim, A. R. Seong, J. Y. Yoo et al., "Gallic acid, a histone acetyltransferase inhibitor, suppresses β -amyloid neurotoxicity by inhibiting microglial-mediated neuroinflammation," *Molecular Nutrition & Food Research*, vol. 55, no. 12, pp. 1798–1808, 2011.
- [66] F. U. Amin, S. A. Shah, and M. O. Kim, "Vanillic acid attenuates A β _{1–42}-induced oxidative stress and cognitive impairment in mice," *Scientific Reports*, vol. 7, no. 1, article 40753, 2017.
- [67] Y. Song, T. Cui, N. Xie, X. Zhang, Z. Qian, and J. Liu, "Protocatechuic acid improves cognitive deficits and attenuates amyloid deposits, inflammatory response in aged A β PP/PS1 double transgenic mice," *International Immunopharmacology*, vol. 20, no. 1, pp. 276–281, 2014.

Research Article

Multifunctional Phytochemicals in *Cotoneaster* Fruits: Phytochemical Profiling, Cellular Safety, Anti-Inflammatory and Antioxidant Effects in Chemical and Human Plasma Models *In Vitro*

Agnieszka Kicel ¹, Joanna Kolodziejczyk-Czepas,² Aleksandra Owczarek,¹ Magdalena Rutkowska,¹ Anna Wajs-Bonikowska,³ Sebastian Granica,⁴ Pawel Nowak,² and Monika A. Olszewska ¹

¹Department of Pharmacognosy, Faculty of Pharmacy, Medical University of Lodz, 1 Muszynskiego, 90-151 Lodz, Poland

²Department of General Biochemistry, Faculty of Biology and Environmental Protection, University of Lodz, Pomorska 141/143, 90-236 Lodz, Poland

³Institute of General Food Chemistry, Faculty of Biotechnology and Food Sciences, Lodz University of Technology, 4/10 Stefanowskiego, 90-924 Lodz, Poland

⁴Department of Pharmacognosy and Molecular Basis of Phytotherapy, Faculty of Pharmacy, Medical University of Warsaw, 1 Banacha, 02-097 Warsaw, Poland

Correspondence should be addressed to Agnieszka Kicel; agnieszka.kicel@umed.lodz.pl

Received 22 June 2018; Accepted 30 August 2018; Published 24 October 2018

Academic Editor: Felipe L. de Oliveira

Copyright © 2018 Agnieszka Kicel et al. This is an open access article distributed under the Creative Commons Attribution License, which permits unrestricted use, distribution, and reproduction in any medium, provided the original work is properly cited.

The work presents the results of an investigation into the molecular background of the activity of *Cotoneaster* fruits, providing a detailed description of their phytochemical composition and some of the mechanisms of their anti-inflammatory and antioxidant effects. GS-FID-MS and UHPLC-PDA-ESI-MS³ methods were applied to identify the potentially health-beneficial constituents of lipophilic and hydrophilic fractions, leading to the identification of fourteen unsaturated fatty acids (with dominant linoleic acid, 375.4–1690.2 mg/100 g dw), three phytosterols (with dominant β -sitosterol, 132.2–463.3 mg/100 g), two triterpenoid acids (10.9–54.5 mg/100 g), and twenty-six polyphenols (26.0–43.5 mg GAE/g dw). The most promising polyphenolic fractions exhibited dose-dependent anti-inflammatory activity in *in vitro* tests of lipoxygenase (IC₅₀ in the range of 7.7–24.9 μ g/U) and hyaluronidase (IC₅₀ in the range of 16.4–29.3 μ g/U) inhibition. They were also demonstrated to be a source of effective antioxidants, both in *in vitro* chemical tests (DPPH, FRAP, and TBARS) and in a biological model, in which at *in vivo*-relevant levels (1–5 μ g/mL) they normalized/enhanced the nonenzymatic antioxidant capacity of human plasma and efficiently protected protein and lipid components of plasma against peroxynitrite-induced oxidative/nitrative damage. Moreover, the investigated extracts did not exhibit cytotoxicity towards human PMBCs. Among the nine *Cotoneaster* species tested, *C. hjelmqvistii*, *C. zabelii*, *C. splendens*, and *C. bullatus* possess the highest bioactive potential and might be recommended as dietary and functional food products.

1. Introduction

Edible fruits are widely recognized as a valuable source of structurally diverse phytochemicals with a broad spectrum of health-promoting properties. Decreased cholesterol levels, lower blood pressure, better mental health, and protection

against cancer are only a few of the many benefits associated with the regular intake of fruit products, as indicated by numerous epidemiological studies [1]. Among the different fruit-bearing families, the Rosaceae seems to be of special importance. With over 3000 species, the family provides numerous types and varieties of fruits, some of which, such



FIGURE 1: The fruits of *C. bullatus* (a) and *C. splendens* (b).

as apples, pears, strawberries and cherries, have great economic and dietary importance, and are frequently and willingly consumed due to their excellent flavors and proven nutritional value [2]. Many other taxa (e.g., *Aronia* sp., *Sorbus* sp., *Pyracantha* sp., and *Prunus spinosa* L.) produce fruits, that while less attractive in taste and appearance, are, nonetheless, distinguished by especially high quantities of bioactive constituents, which makes them perfect candidates for more specialized food applications, for example, as functional food products or food additives [3–6].

The chemical diversity of health-beneficial phytochemicals contained in rosaceous plant materials is immense and ranges from highly lipophilic to strongly polar constituents. Unsaturated fatty acids of almond oil, the cholesterol-regulating phytosterols of *Prunus africana* (Hook.f.) Kalkman, and the pentacyclic triterpenes, ubiquitous throughout the Rosaceae, with proven anti-inflammatory activity are some examples of the possible structures from the hydrophobic end of the spectrum [7, 8]. On the other hand, the hydrophilic fractions often contain an abundance of highly-valued polyphenol antioxidants belonging to numerous chemical classes, such as flavonoids, phenolic acids, and tannins. The bioactive potential of Rosaceae fruits is, therefore, associated not with a single fraction but rather is an effect of the presence of a range of phytochemicals.

The genus *Cotoneaster* Medikus is one of the largest genera of the Rosaceae family (subfamily Spiraeoideae, tribe Pyreae) comprising about 500 species of shrubs or small trees. Its members are native to the Palearctic region (temperate Asia, Europe, north Africa) but are often cultivated throughout Europe as ornamental plants due to their decorative bright red fruits (Figure 1). The center of diversity of the taxon are the mountains of southwestern China and the Himalayas [9, 10], where the fruits have been used for culinary purposes by the local communities. The nutritional value of the fruits as a source of vitamins and minerals has been confirmed [11, 12] and additional beneficial health effects of the fruit consumption have been also reported in the traditional medicine for the treatment of diabetes mellitus, cardiovascular diseases, nasal hemorrhage, excessive menstruation, fever, and cough [9, 10]. The phytochemical research on the subject is scarce, but the available data indicate the tendency of the fruits to accumulate a wide range of active metabolites. In particular, the fruits of *Cotoneaster pannosus* Franch. are a source of linoleic acid, those of

Cotoneaster microphylla Wall ex Lindl contain pentacyclic triterpenoids, and the polyphenolic fractions of *C. pannosus* and *Cotoneaster integerrimus* Medik. fruits are rich in epicatechin, shikimic acid, and chlorogenic acid [9, 11, 12]. However, broader generalization of their properties is troublesome, and the possible wider application of the fruits, for example, as functional food products, is hindered by a lack of systematic studies. Similarly limited is the information on the activity of *Cotoneaster* fruits. Preliminary studies have been performed on the fruits of *C. integerrimus* and *C. pannosus* with regard to their antioxidant, anticholinesterase, antityrosinase, anti-amylase, and antiglycosidase properties, and their free radical-scavenging potential was proven to be the most promising [9, 12]. Still, the research was carried out using only simple *in vitro* chemical tests and did not cover *in vivo*-relevant antioxidant mechanisms.

The aim of this study was, therefore, to provide a more detailed insight into the chemical composition and activity of *Cotoneaster* fruits. To this end, the fruits from nine species of *Cotoneaster* cultivated in Poland were analyzed for a range of lipophilic and hydrophilic (polyphenolic) constituents with acknowledged health-promoting properties using a combination of chromatographic and spectroscopic methods (GC-FID-MS, UHPLC-PDA-ESI-MS³, and UV-Vis spectrophotometry). The most promising polyphenolic fractions were then subjected to an analysis of antioxidant activity comprising eight complementary *in vitro* tests (both chemical and biological plasma models) covering some of the mechanisms crucial for reducing the level of oxidative damage in the human organism, that is, scavenging of free radicals, enhancement of the nonenzymatic antioxidant capacity of blood plasma, and protection of its lipid and protein components against oxidative/nitrative changes. Additionally, the inhibitory effects of the fruit extracts on the proinflammatory enzymes, that is, lipoxygenase and hyaluronidase, were also measured. Finally, the cellular safety of the extracts was evaluated in cytotoxicity tests employing human peripheral blood mononuclear cells (PMBCs).

2. Materials and Methods

2.1. Plant Material. The fruit samples of nine selected *Cotoneaster* Medik. species, that is, *C. lucidus* Schltld. (AR), *C. divaricatus* Rehder et E.H. Wilson (BG), *C. horizontalis* Decne. (BG), *C. nanshan* Mottet (BG), *C. hjelmqvistii* Flink

et B. Hylmö (BG), *C. dielsianus* E. Pritz. (BG), *C. splendens* Flinck et B. Hylmö (BG), *C. bullatus* Bois (BG), and *C. zabelii* C.K. Schneid. (BG) were collected in September 2013, in the Botanical Garden (BG; 51°45'N 19°24'E) in Lodz (Poland) and in the Arboretum (AR; 51°49'N 19°53'E), Forestry Experimental Station of Warsaw University of Life Sciences (SGGW) in Rogow (Poland). The voucher specimens were deposited in the Herbarium of the Department of Pharmacognosy, Medical University of Lodz (Poland). The raw materials were powdered with an electric grinder, sieved through a 0.315 mm sieve, and stored in airtight containers until use.

2.2. General. Reagents and standards of analytical or HPLC grade such as 2,2-diphenyl-1-picrylhydrazyl (DPPH), 2,4,6-tris-(2-pyridyl)-s-triazine (TPTZ), 2,2'-azobis-(2-amidinopropane)-dihydrochloride (AAPH), linoleic acid, 2-thiobarbituric acid, Tween® 40, 5,5'-dithiobis-(2-nitrobenzoic acid) (DNTB), xylol orange disodium salt, Histopaque®-1077 medium *N,O*-bis-(trimethylsilyl)-trifluoroacetamide with 1% 1-trimethylchlorosilane (BSTFA + TMCS), boron trifluoride, bovine testis hyaluronidase, lipoxigenase from soybean, reference standards of fatty acid methyl esters (FAMES), ethyl oleate, 5- α -cholesterol, (\pm)-6-hydroxy-2,5,7,8-tetramethylchromane-2-carboxylic acid (Trolox®), butylated hydroxyanisole (BHA), 2,6-di-*tert*-butyl-4-methylphenol (BHT), gallic acid monohydrate, quercetin dehydrate, chlorogenic acid hemihydrate (5-*O*-caffeoylquinic acid), 3-*O*- and 4-*O*-caffeoylquinic acids, hyperoside semihydrate, isoquercitrin, rutin trihydrate, procyanidins B-2 and C-1, (-)-epicatechin, and indomethacin were purchased from Sigma-Aldrich (St. Louis, MO, USA). The standards of quercetin 3-*O*- β -D-(2''-*O*- β -D-xylosyl)-galactoside and quercitrin (quercetin 3-*O*- α -L-rhamnoside) have previously been isolated in our laboratory from *C. bullatus* and *C. zabelii* leaves with at least 95% HPLC purity (unpublished results). A (Ca²⁺ and Mg²⁺)-free phosphate buffered saline (PBS) was purchased from Biomed (Lublin, Poland). Peroxynitrite was synthesized according to Pryor et al. [13]. Anti-3-nitrotyrosine polyclonal antibody, biotin-conjugated secondary antibody, and streptavidin/HRP were purchased from Abcam (Cambridge, UK). HPLC grade solvents such as acetonitrile and formic acid were from Avantor Performance Materials (Gliwice, Poland). For chemical tests, the samples were incubated at a constant temperature using a BD 23 incubator (BINDER, Tuttlingen, Germany) and measured using a UV-1601 Rayleigh spectrophotometer (Beijing, China). Activity tests in blood plasma models and enzyme inhibitory assays were performed using 96-well plates and monitored using a SPECTROStar Nano microplate reader (BMG LABTECH, Ortenberg, Germany).

2.3. Phytochemical Profiling

2.3.1. Extraction and Derivatization of Lipophilic Phytochemicals. The fruit samples (7.0 g) were exhaustively extracted in a Soxhlet apparatus with chloroform (150 mL, 24 h), to give lipid extracts (288–467 mg dw), which were then subjected to quantification of lipophilic compounds.

Fatty acids were assayed as fatty acid methyl esters (FAMES) prepared according to a method described earlier [14]. Phytosterols and triterpenes were assayed after their transformation to trimethylsilyl ethers (TMSs) according to Thanh et al. [15]. The FAME and TMS mixtures were independently analyzed by GC-FID-MS.

2.3.2. GC-FID-MS Analysis. The analyses of lipophilic fractions were performed on a Trace GC Ultra instrument coupled with a DSQII mass spectrometer (Thermo Electron, Waltham, MA, USA) and a MS-FID splitter (SGE Analytical Science, Trajan Scientific Americas, Austin, TX, USA). The applied mass range was 33–550 amu, ion source-heating was 200°C, and ionization energy was 70 eV. The conditions for FAMES were as follows: capillary column: TG-WaxMS (30 m \times 0.25 mm i.d., film thickness 0.25 μ m; Thermo Fisher Scientific, Waltham, MA, USA); temperature program: 3–30 min: 50–240°C at 4°C/min; and injector and detector temperatures: 250°C and 260°C, respectively. The conditions for TMSs were as follows: capillary column: HP-5 (30 m \times 0.25 mm i.d., film thickness 0.25 μ m; Agilent Technologies, Santa Clara, CA, USA); temperature program: 1–15 min: 100–250°C, at 10°C/min; 15–30 min: 250–300°C, at 4°C/min; and injector and detector temperatures: 310°C and 300°C, respectively. In all cases, the carrier gas was helium (constant pressure: 300 kPa). The lipophilic analytes were identified by comparison of their MS profiles with those stored in the libraries NIST 2012 and Wiley Registry of Mass Spectral Data (10th and 11th eds). Retention times (t_R) of FAMES were also compared with those of the commercial FAME mixture. The analyte levels were expressed as mg/100 g fruit dry weight (dw), calculated using the internal standards of ethyl oleate and 5- α -cholesterol (for the fatty acids as well as phytosterols and triterpenoids, respectively) and it was recalculated to the content in the plant material taking into account the extraction yield.

2.3.3. Extraction of Polyphenolic Compounds. The fruit samples (100–500 mg) were first defatted by preextraction with chloroform (20 mL, 15 min; the chloroform extracts were discarded), then refluxed for 30 min with 30 mL of 70% (*v/v*) aqueous methanol, and twice for 15 min with 20 mL of the same solvent. The combined extracts were diluted with the extractant to 100 mL. Each sample was extracted in triplicate to give the test extracts, which were analyzed for their total phenolic contents (TPCs) and antioxidant activity in chemical models. For UHPLC analyses and antioxidant activity evaluation in the human plasma models, the test extracts were evaporated *in vacuo* and lyophilized using an Alpha 1-2/LDplus freeze dryer (Christ, Osterode am Harz, Germany) before weighing.

2.3.4. UHPLC-PDA-ESI-MS³ Analysis. Metabolite profiling was performed on an UltiMate 3000 RS UHPLC system (Dionex, Dreieich, Germany) with PDA detector scanning in the wavelength range of 220–450 nm and an amaZon SL ion trap mass spectrometer with ESI interface (Bruker Daltonics, Bremen, Germany). Separations were carried out on a Kinetex XB-C18 column (150 \times 2.1 mm, 1.7 μ m;

Phenomenex Inc., Torrance, CA, USA). The mobile phase consisted of solvent A (water-formic acid, 100:0.1, v/v) and solvent B (acetonitrile-formic acid, 100:0.1, v/v) with the following elution profile: 0–45 min, 6–26% (v/v) B; 45–55 min, 26–95% B; 55–60 min, 95% B; and 60–63 min, 95–6% B. The flow rate was 0.3 mL/min. The column temperature was 25°C. Before injections, samples of dry extracts (15 mg) were dissolved in 1.5 mL of 70% aqueous methanol, filtered through PTFE syringe filters (25 mm, 0.2 µm, Vitrum, Czech Republic) and injected (3 µL) into the UHPLC system. UV-Vis spectra were recorded over a range of 200–600 nm, and chromatograms were acquired at 280, 325, and 350 nm. The LC eluate was introduced directly into the ESI interface without splitting and analyzed in a negative ion mode using a scan from m/z 70 to 2200. The MS² and MS³ fragmentations were obtained in Auto MS/MS mode for the most abundant ions at the time. The nebulizer pressure was 40 psi, dry gas flow was 9 L/min, dry temperature was 300°C, and capillary voltage was 4.5 kV.

2.3.5. Determination of Total Phenolic Content (TPC). The TPC levels were determined according to the Folin-Ciocalteu method as described previously [16]. The results were expressed as mg of gallic acid equivalents (GAE) per g of dry weight of the plant material (mg GAE/g dw).

2.4. Lipoxygenase (LOX) and Hyaluronidase (HYAL) Inhibition Tests. The ability of the fruit extracts to inhibit lipoxygenase (LOX) and hyaluronidase (HYAL) was evaluated according to the method optimized earlier [17]. The results of both tests were expressed as IC₅₀ values (µg/mL) from concentration-inhibition curves.

2.5. Antioxidant Activity in Chemical Models. The DPPH free-radical scavenging activity was determined according to a previously optimized method [16] and expressed as normalized EC₅₀ values calculated from concentration-inhibition curves. The FRAP (ferric reducing antioxidant power) was determined according to [16] and expressed in µmol of ferrous ions (Fe²⁺) produced by 1 g of the dry extract or standard, which was calculated from the calibration curve of ferrous sulfate. The ability of the extracts to inhibit AAPH-induced peroxidation of linoleic acid was assayed as described previously [18] with peroxidation monitored by quantification of thiobarbituric acid-reactive substances (TBARS) according to a previously optimized method [19], and the antioxidant activity was expressed as IC₅₀ values calculated from concentration-inhibition curves. Additionally, the activity parameters in all of the assays were also expressed as µmol Trolox® equivalents (TE) per g of dry weight of the plant material (µmol TE/g dw).

2.6. Antioxidant Activity in Human Plasma Models

2.6.1. Isolation of Blood Plasma and Sample Preparation. Blood (buffy coat units) from eight healthy volunteers, received from the Regional Centre of Blood Donation and Blood Treatment in Lodz (Poland), was centrifuged to obtain plasma [20]. All experiments were approved by the committee on the Ethics of Research at the Medical University of

Lodz RNN/347/17/KE. Plasma samples, diluted with 0.01 M Tris/HCl pH 7.4 (1:4 v/v), were preincubated for 15 min at 37°C with the examined extracts, added to the final concentration range of 1–50 µg/mL, and then exposed to 100 or 150 µM peroxynitrite (ONOO⁻). Control samples were prepared with plasma untreated with the extracts and/or peroxynitrite. To eliminate the possibility of direct interactions of the extracts with plasma proteins and lipids, several experiments with blood plasma and the extracts only (without adding ONOO⁻) were also performed and no prooxidative effect was found.

2.6.2. Determination of 3-Nitrotyrosine and Thiols in Human Plasma Proteins. The peroxynitrite-induced protein damage in blood plasma was determined by the use of 3-nitrotyrosine and protein thiol levels (–SH) as biomarkers of oxidative stress. Immunodetection of 3-nitrotyrosine-containing proteins by the competitive ELISA (C-ELISA) method in plasma samples (control or antioxidants and 100 µM ONOO⁻-treated plasma) was performed according to [20]. The nitrofibrinogen (3NT-Fg, at a concentration of 0.5 µg/mL and 3–6 mol nitrotyrosine/mol protein) was prepared for use in the standard curve. The concentrations of nitrated proteins that inhibit antinitrotyrosine antibody binding were estimated from the standard curve and are expressed as the 3NT-Fg equivalents (in nmol/mg of plasma protein). The concentration of free thiol groups (–SH) in plasma samples (control or antioxidants and 100 µM ONOO⁻-treated plasma) was measured spectrophotometrically according to Ellman's method [20]. The free thiol group concentration was calculated from the standard curve of glutathione (GSH) and expressed as µmol/mL of plasma.

2.6.3. Determination of Lipid Hydroperoxides and TBARS in Human Blood Plasma. The peroxynitrite-induced lipid peroxidation in blood plasma was determined spectrophotometrically by evaluation of the level of lipid hydroperoxides and TBARS. The concentration of hydroperoxides in plasma samples (control or antioxidants and 100 µM ONOO⁻-treated plasma) was determined by a ferric-xylenol orange (FOX-1) protocol with a later modification [20]. The amount of lipid hydroperoxides was calculated from the standard curve of hydrogen peroxide and expressed in nmol/mg of plasma proteins. Determination of TBARS in plasma samples (control or antioxidants and 100 µM ONOO⁻-treated plasma) was performed according to [20]. The TBARS values were expressed in µmol TBARS/mL of plasma.

2.6.4. Ferric Reducing Ability of Human Blood Plasma (FRAP). The influence of the extracts on the nonenzymatic antioxidant status of plasma was conducted by measurements of their ability to reduce ferric ions (Fe³⁺) to ferrous ions (Fe²⁺). The experiments were performed according to Benzie and Strain [21] and modified by Kolodziejczyk-Czepas et al. [20]. The FRAP values of plasma samples (control or antioxidants and 150 µM ONOO⁻-treated plasma) were expressed in mM Fe²⁺ in plasma as calculated from the calibration curve of ferrous sulphate.

2.7. Cellular Safety Testing. The cytotoxicity of the examined extracts was conducted in an experimental system of peripheral blood mononuclear cells (PBMCs). PBMCs were isolated from fresh human blood using the Histopaque®-1077 medium, according to a procedure described in our previous work [19]. Then, the cells (1×10^6 PBMCs/mL, suspended in PBS) were incubated with *Cotoneaster* fruit extracts at the final concentrations of 5, 25, and 50 μ g/mL. Measurements of cell viability were executed after two, four, and six hours of incubation (at 37°C) in a routine dye excluding test, based on a staining with 0.4% Trypan blue. The procedure was carried out according to the manufacturer's protocol using a microchip-type automatic cell counter Bio-Rad (Hercules, CA, USA).

2.8. Statistical and Data Analysis. The statistical analysis was performed using STATISTICA 13Pl software for Windows (StatSoft Inc., Krakow, Poland). The results were reported as means \pm standard deviation (SD) or \pm standard error (SE) for the indicated number of experiments. The significance of differences between the samples and controls were analyzed by one-way ANOVA, followed by the post hoc Tukey's test for multiple comparison. A level of $p < 0.05$ was accepted as statistically significant.

3. Results and Discussion

3.1. GC-FID-MS Analysis of Fatty Acids. The fatty acid profiles of the lipophilic fractions in the chloroform extracts of the *Cotoneaster* fruits were determined by GC-FID-MS analysis of methyl ester derivatives (FAMES). As shown in Table 1 and Figure 2, fourteen fatty acids were identified, including saturated, mono-, and polyunsaturated acids with chain lengths ranging from 6 to 22 carbon atoms. Their total content (TFA) varied among the *Cotoneaster* species from 902.5 to 2683.8 mg/100 g of fruit dry weight (dw) with the highest levels noted for *C. zabelii* (2683.8 mg/100 g dw) and *C. splendens* (2024.1 mg/100 g dw). All analyzed fruits contained primarily poly- and monounsaturated acids, constituting 41.6–66.8% and 18.6–29.6% of TFA, respectively. The major component in each sample was linoleic acid C18:2 $\Delta^{9,12}$, the sole representative of the polyunsaturated acids. Its content varied among species from 375.4 to 1690.2 mg/100 g fruit dw with the highest amounts (above 10 mg/g dw) recorded for the fruits of *C. zabelii*, *C. splendens*, *C. hjelmqvistii*, and *C. horizontalis*. Relatively high levels of oleic acid C18:1 Δ^9 , a monounsaturated acid, were also noted, especially for the *C. zabelii* and *C. splendens* (649.7 and 473.7 mg/100 g dw, respectively). Regarding saturated acids, they accounted for only 12.3–28.8% of TFA. The highest content of this group was observed in the fruits of *C. zabelii*, *C. splendens*, and *C. nanshan*, with palmitic acid C16:0 being the dominant compound (226.5, 212.6 and 168.7 mg/100 g dw, respectively).

The present work is the first comparison of several *Cotoneaster* fruits in terms of their fatty acid profile. Despite some quantitative differences observed between the investigated fruits, a high level of consistency can be noticed in the qualitative composition of this fraction. The results

are in accordance with previous reports for the fruits of *C. pannosus* from Italy, as well as the branches of *C. horizontalis* Decke. of Egyptian origin and the seeds of *C. bullatus*, *C. dielsianus*, *C. francheti* Bois, *C. moupinensis* Franch., and *C. simonsii* Baker cultivated in Germany, in which linoleic and palmitic acids were also detected as the major fatty acid components [9, 22, 23].

The unsaturated fatty acids are known factors associated with the prevention of various chronic and acute diseases, such as cardiovascular diseases, osteoporosis, immune disorders, and cancer [7]. Linoleic acid, the representative of the omega-6 fatty acid family (essential fatty acids (EFA)), is considered a vital constituent of a healthy human diet, due to its contribution to cholesterol metabolism (regulation of plasma total cholesterol and low-density lipoprotein cholesterol levels and HDL-LDL ratio) and its association with a lower risk of atherosclerosis [24]. Main sources of this compound are plant oils, derived, inter alia, from the seeds of safflower, sunflower, grape, pumpkin, and corn. The available literature data [25, 26] indicate that whole fruits of some Rosaceae members, such as *Crataegus monogyna* Jacq., *Prunus spinosa* L., and *Rubus ulmifolius* Schott., might be considered as abundant in linoleic acid, constituting over 10% of their lipophilic fraction [26]. Our present results indicate that the analyzed *Cotoneaster* fruits also deserve more attention as rich sources of this compound.

3.2. GC-FID-MS Analysis of Phytosterols and Triterpenoids. Apart from fatty acids, three phytosterols (campesterol, β -sitosterol, and stigmasterol) and four triterpenes (α - and β -amyriins, ursolic and oleanolic acids) were identified in the chloroform extracts of the *Cotoneaster* fruits, based on GC-FID-MS analysis of their trimethylsilyl ether derivatives (TMSs). As reported in Table 2 and Figure 2, the total content of sterols and triterpenoids, depending on the tested species, was in the range of 154.6–515.6 mg/100 g of fruit (dw) with the highest levels observed for *C. splendens* (515.6 mg/100 g dw) and *C. nanshan* (438.0 mg/100 g dw). The dominant compound in all samples was β -sitosterol, with the levels ranging from 132.2 to 463.3 mg/100 g dw (76.5–89.3% of the total sterols and triterpenes). The highest content of β -sitosterol was observed for the fruit of *C. splendens* (463.3 mg/100 g dw) followed by those of *C. nanshan* (391.3 mg/100 g dw) and *C. horizontalis* (316.3 mg/100 g dw). Other individual components were observed at much lower concentrations, reaching at most 42 mg/100 g dw.

Regarding the phytosterol and triterpenoid profile, the present results are generally similar to the data obtained previously for different organs of *Cotoneaster* species, although some differences can be noticed in relative proportions of particular compounds. Among the sterols and triterpenoids identified earlier for the *C. horizontalis* branches collected in Egypt, α -amyrin was the dominant compound, constituting 14.4% of the total lipophilic constituents, followed by β -sitosterol (8.5%) and stigmasterol (1.1%) [23]. The ursolic acid was isolated previously from *C. simonsii* twigs [27], *C. racemiflora* Desf. twigs [28], and *C. microphylla* fruits [11], but the present work is the first to describe its quantitative levels in the *Cotoneaster* plants.

TABLE 1: Content of fatty acids (mg/100 g dw) in the *Cotoneaster* fruits.^a

Fruit sample	6:0	8:0	12:0	14:0	15:0	16:0	17:0	16:1 Δ^9	18:0	18:1 Δ^9	20:0	18:2 $\Delta^{9,12}$	20:1 Δ^{11}	22:0
<i>C. lucidus</i>	3.41 ± 0.10 ^B	2.35 ± 0.10 ^F	2.77 ± 0.01 ^F	5.97 ± 0.30 ^E	nd	126.25 ± 5.23 ^A	tr	8.96 ± 0.51 ^E	92.98 ± 5.12 ^F	258.05 ± 12.11 ^{A,B}	6.02 ± 0.20 ^A	375.35 ± 18.01 ^A	tr	18.77 ± 0.80 ^B
<i>C. divaricatus</i>	2.24 ± 0.11 ^A	0.61 ± 0.03 ^{A,B}	0.82 ± 0.05 ^A	2.86 ± 0.15 ^A	tr	136.65 ± 6.20 ^A	0.82 ± 0.01 ^B	4.90 ± 0.21 ^C	63.23 ± 2.45 ^E	262.09 ± 10.09 ^B	6.73 ± 0.31 ^A	566.60 ± 25.03 ^B	2.04 ± 0.08 ^B	7.55 ± 0.22 ^A
<i>C. horizontalis</i>	tr	0.69 ± 0.01 ^B	2.28 ± 0.10 ^E	4.80 ± 0.25 ^D	tr	174.10 ± 5.40 ^B	1.37 ± 0.05 ^C	8.68 ± 0.43 ^E	38.38 ± 2.10 ^{B,C}	294.05 ± 13.01 ^{B,C}	13.25 ± 0.60 ^C	1012.83 ± 45.02 ^D	tr	26.05 ± 1.00 ^C
<i>C. nanshan</i>	nd	0.65 ± 0.01 ^B	1.73 ± 0.10 ^{C,D}	4.33 ± 0.20 ^{C,D}	0.65 ± 0.01 ^A	168.68 ± 6.40 ^B	2.16 ± 0.12 ^D	8.22 ± 0.38 ^{D,E}	87.58 ± 3.54 ^F	384.72 ± 18.12 ^D	17.30 ± 0.75 ^D	736.79 ± 30.01 ^C	3.89 ± 0.20 ^D	19.25 ± 0.95 ^B
<i>C. hjelmqvistii</i>	tr	1.12 ± 0.04 ^C	1.96 ± 0.10 ^D	4.48 ± 0.32 ^D	nd	174.55 ± 8.00 ^B	0.56 ± 0.03 ^A	3.36 ± 0.16 ^{A,B}	41.19 ± 2.05 ^C	335.10 ± 14.10 ^C	17.09 ± 0.71 ^D	1216.27 ± 50.01 ^E	0.56 ± 0.02 ^A	24.38 ± 1.05 ^C
<i>C. dielsianus</i>	6.11 ± 0.20 ^C	1.77 ± 0.03 ^E	1.58 ± 0.08 ^C	4.14 ± 0.25 ^{B,C,D}	0.59 ± 0.02 ^A	177.81 ± 6.43 ^B	3.15 ± 0.16 ^E	4.14 ± 0.19 ^{B,C}	37.85 ± 1.04 ^{B,C}	273.21 ± 15.02 ^B	16.76 ± 0.80 ^D	643.22 ± 15.15 ^{B,C}	0.79 ± 0.03 ^A	19.91 ± 0.55 ^B
<i>C. splendens</i>	tr	1.55 ± 0.04 ^D	2.80 ± 0.15 ^F	5.59 ± 0.32 ^E	nd	212.60 ± 11.00 ^C	2.18 ± 0.11 ^D	8.39 ± 0.50 ^{D,E}	32.95 ± 1.14 ^{A,B}	473.70 ± 20.01 ^E	18.34 ± 0.61 ^D	1225.89 ± 30.12 ^E	2.49 ± 0.11 ^C	37.30 ± 1.85 ^E
<i>C. bullatus</i>	tr	0.51 ± 0.01 ^A	1.53 ± 0.04 ^C	3.73 ± 0.22 ^{B,C}	0.51 ± 0.03 ^A	120.49 ± 5.20 ^A	2.37 ± 0.10 ^D	2.54 ± 0.12 ^A	29.83 ± 1.10 ^A	215.22 ± 10.00 ^A	10.85 ± 0.55 ^B	677.53 ± 16.15 ^C	4.07 ± 0.15 ^D	30.33 ± 1.10 ^D
<i>C. zabelii</i>	3.25 ± 0.11 ^B	1.44 ± 0.05 ^D	1.08 ± 0.05 ^B	3.61 ± 0.15 ^B	nd	226.45 ± 5.40 ^C	1.44 ± 0.06 ^C	7.58 ± 0.35 ^D	53.09 ± 2.70 ^D	649.73 ± 25.05 ^F	30.34 ± 1.32 ^E	1690.23 ± 55.01 ^F	5.78 ± 0.21 ^E	9.75 ± 0.20 ^A

^aValues presented as means ± SD calculated per dw of the plant material ($n = 3$); tr—trace, the content less than 0.5 mg/100 g dw; nd—not detected; different capital letters within the same row indicate significant differences at $\alpha = 0.05$ in HSD Tukey's test; 6:0—caproic acid, 8:0—caprylic acid, 12:0—lauric acid, 14:0—myristic acid, 15:0—pentadecylic acid, 16:0—palmitic acid, 17:0—margaric acid, 18:0—palmitoleic acid, 18:1 Δ^9 —oleic acid, 18:2 $\Delta^{9,12}$ —linoleic acid, 20:1 Δ^{11} —eicosenoic acid and 22:0—behenic acid.

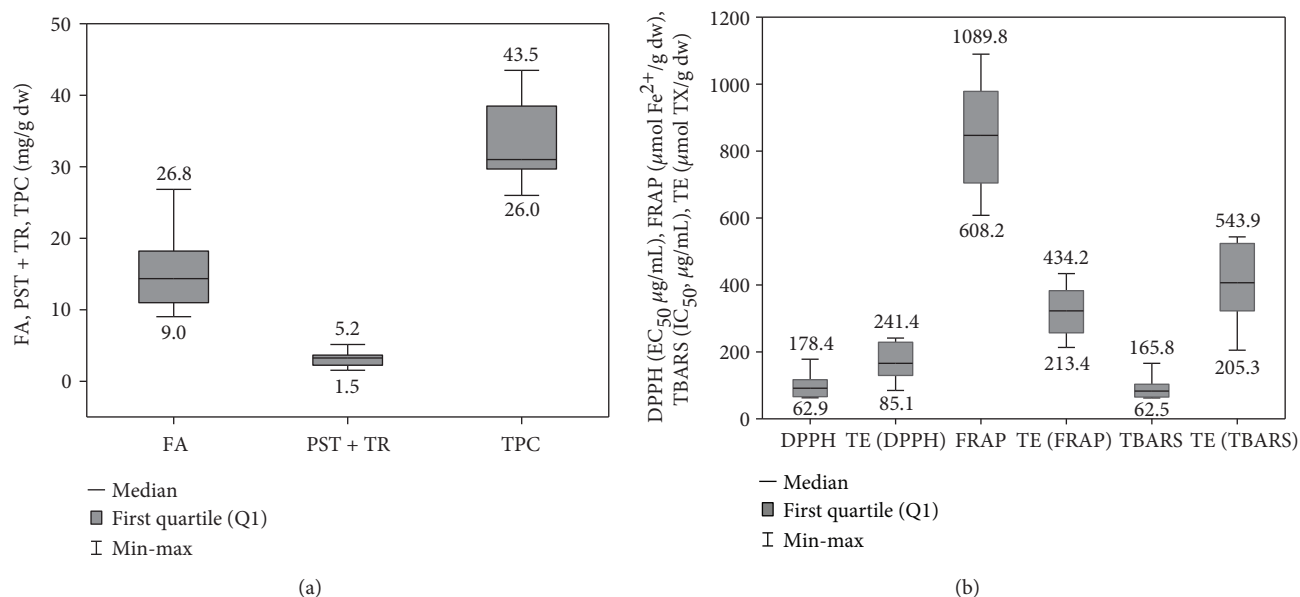


FIGURE 2: Variability of the measured quantitative and activity parameters among the investigated *Cotoneaster* fruits. (a) FA, total fatty acids; PS + TR, sum of phytosterols and triterpenes; TPC, total phenolic content, expressed in gallic acid equivalents (GAE). (b) DPPH, radical scavenging activity expressed as EC₅₀ value; FRAP, ferric reducing antioxidant power; TBARS, inhibition of linoleic acid peroxidation; TE, Trolox® equivalent antioxidant activity.

TABLE 2: Content of phytosterols and triterpenes (mg/100 g dw) in the *Cotoneaster* fruits.^a

Fruit sample	Campesterol	β -Sitosterol	Stigmasterol	β -Amyrin	α -Amyrin	Ursolic acid	Oleanolic acid
<i>C. lucidus</i>	6.83 ± 0.30 ^C	195.31 ± 5.31 ^B	nd	nd	1.05 ± 0.05 ^A	6.61 ± 0.30 ^B	15.52 ± 0.53 ^D
<i>C. divaricatus</i>	9.06 ± 0.31 ^E	132.19 ± 4.23 ^A	nd	nd	2.48 ± 0.07 ^B	2.21 ± 0.04 ^A	8.65 ± 0.32 ^{A,B}
<i>C. horizontalis</i>	6.04 ± 0.22 ^{B,C}	316.31 ± 15.03 ^D	nd	nd	0.88 ± 0.02 ^A	25.45 ± 1.10 ^F	17.24 ± 0.50 ^E
<i>C. nanshan</i>	8.94 ± 0.40 ^E	391.26 ± 17.02 ^E	nd	nd	5.26 ± 0.21 ^C	6.04 ± 0.22 ^B	26.52 ± 1.05 ^F
<i>C. hjelmqvistii</i>	4.31 ± 0.12 ^A	211.99 ± 10.13 ^B	nd	1.17 ± 0.05 ^A	14.37 ± 0.61 ^F	27.03 ± 0.98 ^F	18.41 ± 0.50 ^E
<i>C. dielsianus</i>	5.38 ± 0.21 ^B	181.96 ± 5.22 ^B	tr	2.12 ± 0.10 ^B	6.32 ± 0.24 ^D	10.49 ± 0.35 ^C	7.30 ± 0.18 ^A
<i>C. splendens</i>	13.11 ± 0.56 ^F	463.26 ± 15.10 ^F	nd	nd	8.79 ± 0.30 ^E	13.42 ± 0.45 ^D	17.05 ± 0.45 ^{D,E}
<i>C. bullatus</i>	7.98 ± 0.31 ^D	274.47 ± 12.15 ^C	2.70 ± 0.07 ^B	0.88 ± 0.04 ^A	14.15 ± 0.50 ^F	41.45 ± 1.50 ^G	13.05 ± 0.52 ^C
<i>C. zabelii</i>	6.77 ± 0.30 ^C	273.25 ± 10.22 ^C	1.00 ± 0.01 ^A	nd	14.89 ± 0.22 ^F	20.70 ± 1.03 ^E	9.27 ± 0.36 ^B

^aValues presented as means ± SD calculated per dw of the plant material ($n = 3$); tr—trace, the content less than 0.5 mg/100 g dw; nd—not detected; different capital letters within the same row indicate significant differences at $\alpha = 0.05$ in HSD Tukey's test.

On the other hand, betulinic acid, reported earlier for *C. microphylla* fruits [11], was not detected during the present study in any fruit sample.

Phytosterols (β -sitosterol, stigmasterol, and their analogues) are important dietary components which help regulate serum lipid profile, reduce total- and LDL-cholesterol levels, and increase HDL/LDL ratio. In addition, plant sterols possess anticancer, anti-inflammatory, and moderate antioxidant activities [29]. For instance, β -sitosterol, the most abundant plant sterol in the human diet, displays significant effects on reducing the symptoms of benign prostatic hyperplasia and prostate cancer. Moreover, this compound has been associated with antidiabetic, immunomodulatory, and analgesic properties [30]. Phytosterols are found abundantly in nonpolar fractions of plants, and their daily consumption is estimated in the range of 200–400 mg with the main dietary sources being vegetable oils, nuts, cereal

products, vegetables, fruits, and berries [30]. They are also known to be present in abundance in the fruits derived from numerous genera of Rosaceae, including *Prunus*, *Crataegus*, and *Rosa* [25]. In the lipid fraction of rosaceous fruits, β -sitosterol was often identified as the predominant lipophilic compound, constituting usually more than 60% of the total sterols. As the daily intake of phytosterols (1.5–2.4 g) required for beneficial health effects, especially for cardiovascular and antiatherogenic protection, is usually higher than consumed with the common diet [30], dietary supplementation is a rational solution, and new plant sources of these biomolecules, such as the *Cotoneaster* fruits, offer promise in this aspect.

3.3. Polyphenolic Profiling of Fruit Extracts. LC-MS analysis of the hydrophilic (70% aqueous methanolic) extracts of the *Cotoneaster* fruits revealed the presence of a number of

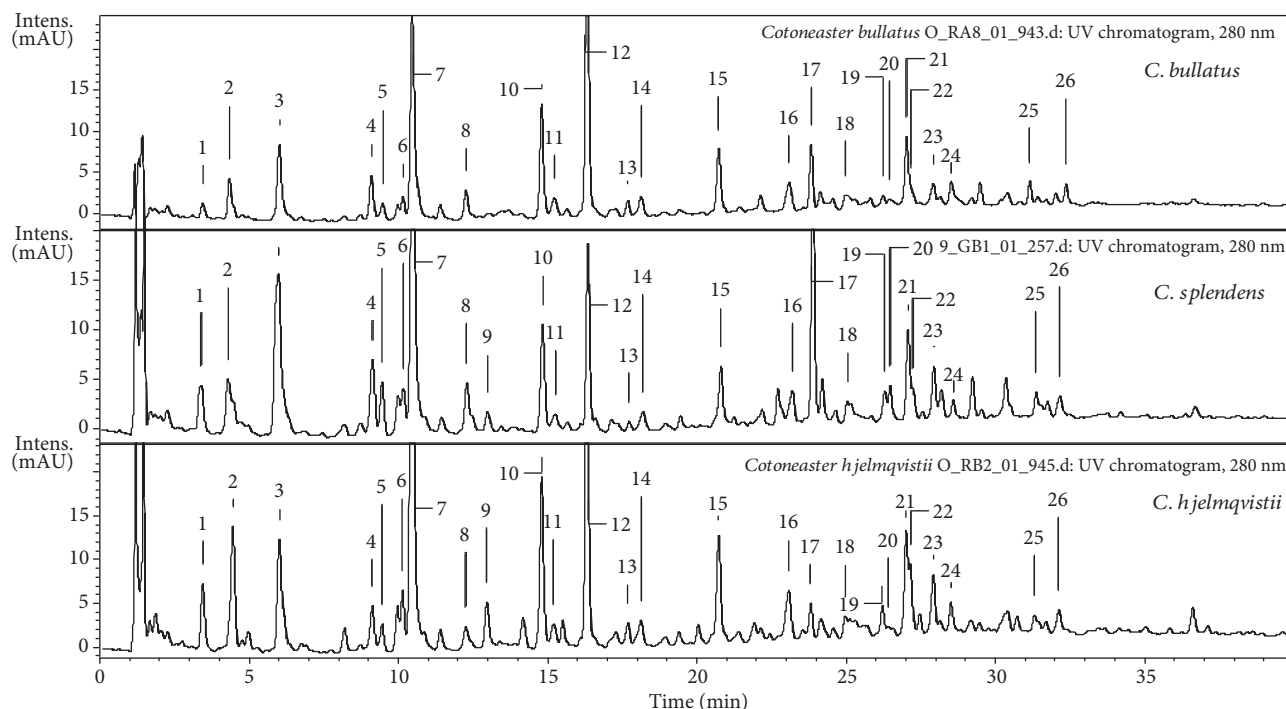


FIGURE 3: Representative UHPLC-UV chromatograms of the *C. bullatus*, *C. splendens*, and *C. hjelmqvistii* fruit polar extracts ($\lambda = 280$ nm). The peak numbers refer to those applied in Table 3.

polyphenols (UHPLC peaks 1–26, Figure 3, Table 3) that were fully or tentatively identified by comparison of their chromatographic behavior and ESI-MS³ fragmentation pattern with authentic standards or literature values. Three major groups of polyphenols were recognized, including phenolic acids (3, 7, and 8) and their derivatives (1, 4, 5, and 11), flavan-3-ols including proanthocyanidins (9, 10, 12–16, 18, and 24), and flavonoids (17, 20, 21–23, 25, and 26). The recorded UHPLC fingerprints (Table 3) indicate that the phenolic profiles of all nine *Cotoneaster* fruits were qualitatively similar. However, noticeable differences were found in the proportions of individual polyphenols, which allowed the subgroups of species to be distinguished depending on the prevalent phenolic class. A distinctive feature of most *Cotoneaster* samples, especially *C. divaricatus*, *C. horizontalis*, and *C. nanshan*, was the predominance of phenolic acid derivatives (1, 3–5, 7, 8, and 11), mainly caffeoylquinic acids, with the dominant peak being chlorogenic acid (7). On the other hand, *C. zabelii*, *C. bullatus*, and *C. hjelmqvistii* contained relatively high amounts of flavan-3-ols and proanthocyanidins (9, 10, 12–16, 18, and 24), with dominating (–)-epicatechin (12). The contribution of flavonoids (17, 20, 21–23, 25, and 26) to the overall phenolic fraction was generally the lowest, but *C. splendens* was distinguished by a particularly large proportion of quercetin 3-(2''-xylosyl)-galactoside (17), and *C. dielsianus* contained a relatively higher level of hyperoside (21).

This report is the first comprehensive study of the LC-MS characteristics of the *Cotoneaster* fruits; the previous studies on *C. integerrimus* and *C. pannosus* have focused only on a selected aspect (HPLC-PDA) of their polyphenolic profiles [9, 12]. In contrast to the present results,

the occurrence of low-molecular phenolic acids, including shikimic, *p*-coumaric, and benzoic acids, has been previously reported, and this phenomenon may be explained by the individual attributes of the tested samples or by differences in the methodology employed for the structural identification. On the other hand, the reported high level of (–)-epicatechin in the fruits of *C. integerrimus* [12] indicates its similarity to those of *C. zabelii* and *C. bullatus* analyzed in the present study.

The total phenolic content (TPC) of the 70% aqueous methanolic extracts of the *Cotoneaster* fruits was determined by the Folin-Ciocalteu photometric assay, commonly used to estimate phenolic metabolites as gallic acid equivalents (GAE). As shown in Table 4 and Figure 2, the TPC values in the analyzed fruits varied from 26.0 to 43.5 mg GAE/g of fruit dw. The highest phenolic content was found for the fruits of *C. hjelmqvistii* and *C. zabelii* (43.5 and 43.0 mg/g dw, respectively), followed by those of *C. splendens* and *C. bullatus* (38.5 and 37.3 mg/g dw, respectively). The level of phenolics in these species is comparable with those observed for other Rosaceae fruits reported in the literature as rich sources of natural polyphenols, for example, *Aronia melanocarpa* (Michx.) Elliott (34.4–78.5 mg GAE/g dw; [3]) and *Sorbus* species (22.4–29.8 mg GAE/g dw; [16]).

The presence of polyphenolic compounds in fruits and vegetables is strongly linked with the beneficial effects of these food products for human health, and the influence of polyphenols on closely intertwined processes of inflammation and oxidative stress is recognized as the most feasible mode of this action. As free radical scavengers, metal chelators, prooxidant and proinflammatory enzyme inhibitors, and modifiers of cell signaling pathways, polyphenols are

TABLE 3: UHPLC-PDA-ESI-MS³ data of polyphenols identified in the polar extracts from *Cotoneaster* fruits.

Number	Compounds	t_R	UV	(M-H) ⁻ m/z	MS/MS m/z (% base peak)	CL	CDV	GHR	GN	CH % ^b	CDL	CS	CB	CZ
1	Vanillic acid-hexoside	3.5	250, 290	329	MS ² : 167 (100); 123 (2); 107 (4)	3.8	3.1	3.4	3.4	2.5	1.4	2.3	0.9	1.7
2	Unidentified	4.4	250, 295	255	MS ² : 165 (23)	33.9	3.1	2.1	16.1	5.7	5.0	2.6	3.1	3.2
3	3-O-Caffeoylquinic acid	6.0	294, 325	353	MS ² : 191 (100); 179 (47); 135 (6)	1.8	10.4	5.3	15.1	5.1	5.1	8.1	5.7	1.9
4	3-O- <i>p</i> -Coumaroylquinic acid	9.4	285, 310	337	MS ² : 163 (100); 119 (10)	2.1	5.0	4.0	2.3	1.9	2.4	3.7	3.3	2.5
5	Caffeic acid hexoside	9.8	290, 323	341	MS ² : 179 (100); 135 (10)	2.3	8.2	2.7	5.1	1.2	0.6	2.5	1.0	2.8
6	Unidentified	10.0	285, 323	439	MS ² : 391 (100); 338 (17); 243 (10); 195 (55)	3.9	1.9	4.3	4.8	2.3	1.2	2.0	1.3	1.3
7	5-O-Caffeoylquinic acid (chlorogenic acid) ^a	10.4	294, 325	353	MS ² : 191 (100); 179 (6)	29.4	28.3	29.5	26.0	23.5	23.0	17.9	17.3	10.8
8	4-O-Caffeoylquinic acid	10.9	294, 325	353	MS ² : 191 (21); 179 (47); 173 (100)	1.1	4.1	2.4	5.1	1.0	1.4	2.4	2.1	2.0
9	Procyanidin B-type dimer	13.7	280	577	MS ² : 451 (30); 425 (100); 407 (55); 289 (10)	0.7	1.6	0.5	1.2	1.1	1.2	0.9	nd	0.7
					MS ³ (425): 407 (80); 273 (13)									
10	Procyanidin B-2 ^a	14.9	280	577	MS ² : 451 (25); 425 (100); 407 (62); 289 (14);	0.3	2.5	4.6	0.8	8.0	6.2	5.5	9.3	10.2
					MS ³ (425): 407 (95); 273 (9)									
11	5-O- <i>p</i> -Coumaroylquinic acid	15.7	285, 310	337	MS ² : 191 (100); 163 (7)	11.7	3.1	1.2	3.6	1.2	0.6	0.8	1.4	1.9
12	(-)-Epicatechin ^a	16.4	280	289	MS ² : 245 (100); 205 (28)	2.4	4.4	8.5	2.1	15.8	12.3	9.7	18.6	34.4
13	Procyanidin B-type dimer	17.3	280	577	MS ² : 451 (25); 425 (100); 407 (45); 289 (6);	nd	nd	nd	nd	0.4	nd	0.6	0.9	1.2
					MS ³ (425): 407 (75); 273 (9)									
14	Procyanidin B-type tetramer	18.3	280	1153	MS ² : 1027 (15); 863 (80); 739 (15); 501 (05); 491 (58); 289 (100)	nd	nd	nd	nd	1.0	nd	0.6	1.1	1.4

TABLE 3: Continued.

Number	Compounds	t_R	UV	(M-H) ⁻ m/z	MS/MS m/z (% base peak)	CL	CDV	CHR	CN	CH % ^b	CDL	CS	CB	CZ
15	Procyanidin C-1 ^a	20.6	280	865	MS ² : 847 (19); 739 (77); 713 (51); 695 (100); 577 (26); MS ³ (713): 695 (100); 561 (30); 543 (31); 425 (32); 407 (36)	0.5	1.9	3.2	nd	5.3	3.7	3.3	5.6	7.3
16	Procyanidin B-type tetramer	23.3	280	1153	MS ² : 863 (90); 739 (10); 501 (65); 491 (62); 289 (100)	nd	nd	2.1	nd	2.7	2.2	2.0	2.7	3.5
17	Quercetin 3-O- β -D-(2''-O- β -D-xylosyl)galactoside ^a	23.9	268, 355	595	MS ² : 463 (10); 445 (14); 300 (85); MS ³ (463): 343 (62); 301 (100)	nd	nd	4.0	nd	2.0	2.6	16.1	5.9	nd
18	Epicatechin derivative	26.2	280	739	MS ² : 587 (100); 451 (19); 339 (40); 289 (35)	nd	2.2	2.0	nd	1.1	nd	1.5	1.2	nd
19	Unidentified	26.3	280	451	MS ² : 341 (100); 217 (8)	nd	2.5	2.6	2.4	1.5	2.0	2.0	1.2	1.2
20	Quercetin rhamnoside-hexoside	26.7	275, 350	609	MS ² : 301 (100)	0.6	0.4	1.4	nd	0.7	3.2	2.3	0.9	1.8
21	Quercetin 3-O- β -D-galactoside (hyperoside) ^a	27.1	265, 355	463	MS ² : 301 (100)	2.5	5.0	4.9	5.5	5.5	9.5	5.2	6.6	2.4
22	Quercetin 3-O- β -D-(6''-O- α -L-Rhamnosyl)glucoside (rutin) ^a	27.3	260, 355	609	MS ² : 301 (100)	0.8	2.5	2.6	2.8	3.8	2.5	2.0	nd	2.2
23	Quercetin 3-O- β -D-glucoside (isoquercitrin) ^a	28.0	265, 355	463	MS ² : 301 (100)	1.6	3.1	2.4	2.4	3.5	2.5	3.3	2.6	3.2
24	Procyanidin B-type dimer	28.6	280	577	MS ² : 425 (100); 407 (52); 289 (18)	0.6	1.6	2.0	1.0	1.6	2.0	1.6	2.0	2.4
25	Quercetin rhamnoside-hexoside	31.3	276, 350	609	MS ² : 301 (100)	nd	2.2	2.2	nd	0.4	4.1	nd	2.9	nd
26	Quercetin 3-O- α -L-rhamnoside (quercitrin) ^a	32.4	276, 350	447	MS ² : 301 (100)	nd	2.8	2.2	nd	1.4	5.1	1.8	2.6	nd

^aIdentified with the corresponding standards; ^brelative contribution based on peak area on the UHPLC chromatograms ($\lambda = 280$ nm) recorded at the extract concentration of 10 mg/mL and injection volume of 3 μ L; nd—not detected; the values are means ($n = 3$); with RSD $\leq 5\%$. CL, *C. lucidus*; CHR, *C. divaricatus*; CDV, *C. horizontalis*; CN, *C. nanshan*; CH, *C. hylmiquistii*; CDL, *C. dtelsianus*; CS, *C. splendens*; CB, *C. bullatus*; CZ, *C. zabelii*.

TABLE 4: Total phenolic content (TPC) and antioxidant activity (DPPH, FRAP, and TBARS tests) of the *Cotoneaster* fruits and standard antioxidants.

Fruit sample/ standard	TPC ^a (mg GAE/g)	Radical scavenging activity DPPH ^b		Reducing power ^c		LA-peroxidation TBARS ^d	
		EC ₅₀ (μ g/mL)	TE (μ mol TE/g)	FRAP (mmol Fe ²⁺ /g)	TE (μ mol TE/g)	IC ₅₀ (μ g/mL)	TE (μ mol TE/g)
<i>C. lucidus</i>	28.70 \pm 1.01 ^B	123.41 \pm 1.70 ^E	122.75 \pm 1.69 ^C	0.70 \pm 0.01 ^B	257.22 \pm 4.96 ^{B,C}	108.70 \pm 4.11 ^F	314.84 \pm 6.03 ^C
<i>C. divaricatus</i>	29.71 \pm 0.91 ^B	91.47 \pm 2.01 ^C	165.58 \pm 3.62 ^D	0.76 \pm 0.01 ^C	281.61 \pm 4.43 ^C	83.16 \pm 0.58 ^D	406.94 \pm 1.43 ^D
<i>C. horizontalis</i>	30.50 \pm 0.72 ^B	93.32 \pm 1.90 ^C	162.38 \pm 3.31 ^D	0.85 \pm 0.01 ^D	322.75 \pm 4.06 ^D	84.89 \pm 2.11 ^D	401.23 \pm 5.03 ^D
<i>C. nanshan</i>	26.02 \pm 0.74 ^A	178.35 \pm 2.81 ^F	84.91 \pm 1.33 ^B	0.61 \pm 0.01 ^A	213.41 \pm 4.42 ^A	165.76 \pm 3.74 ^G	205.30 \pm 2.33 ^B
<i>C. hjelmqvistii</i>	43.50 \pm 1.21 ^D	64.51 \pm 0.84 ^B	234.84 \pm 2.91 ^{E,F}	1.05 \pm 0.02 ^F	414.38 \pm 11.14 ^{F,G}	62.96 \pm 1.10 ^C	532.92 \pm 4.63 ^{E,F}
<i>C. dielsianus</i>	31.02 \pm 1.02 ^B	117.10 \pm 2.40 ^D	129.37 \pm 2.65 ^C	0.67 \pm 0.03 ^B	240.90 \pm 13.83 ^{A,B}	103.72 \pm 2.58 ^E	322.66 \pm 3.98 ^C
<i>C. splendens</i>	38.51 \pm 0.81 ^C	67.15 \pm 1.80 ^B	225.49 \pm 6.04 ^E	0.98 \pm 0.01 ^E	383.06 \pm 6.24 ^{E,F}	66.21 \pm 2.94 ^C	518.18 \pm 11.79 ^E
<i>C. bullatus</i>	37.31 \pm 0.80 ^C	66.31 \pm 1.70 ^B	228.54 \pm 5.86 ^E	0.97 \pm 0.01 ^E	378.87 \pm 2.90 ^E	64.99 \pm 1.55 ^C	523.90 \pm 6.30 ^{E,F}
<i>C. zabelii</i>	43.02 \pm 1.11 ^D	62.93 \pm 1.91 ^B	240.93 \pm 7.28 ^F	1.09 \pm 0.04 ^G	434.27 \pm 20.50 ^G	62.54 \pm 1.32 ^C	543.86 \pm 5.76 ^F
QU	—	1.70 \pm 0.11 ^A	8.96 \pm 0.58 ^A	31.20 \pm 0.98 ^K	11878.15 \pm 15.20 ^J	1.85 \pm 0.12 ^A	18.37 \pm 1.69 ^A
BHA	—	2.90 \pm 0.15 ^A	5.24 \pm 0.27 ^A	16.14 \pm 0.77 ^I	7726.31 \pm 10.52 ^H	3.16 \pm 0.22 ^A	10.76 \pm 1.06 ^A
BHT	—	6.50 \pm 0.13 ^A	2.34 \pm 0.05 ^A	18.89 \pm 0.45 ^J	9247.66 \pm 12.30 ^I	9.31 \pm 0.16 ^B	3.64 \pm 0.09 ^A
TX	—	3.80 \pm 0.20 ^A	—	9.34 \pm 0.35 ^H	—	8.47 \pm 0.45 ^B	—

^{a-d}Results expressed as means \pm SD calculated per dw of the plant material ($n = 3$); different capital letters within the same row indicate significant differences at $\alpha = 0.05$ in HSD Tukey's test. ^aTotal phenolic content (TPC), expressed in gallic acid equivalents (GAE). ^bScavenging efficiency in the DPPH test, the amount of the plant materials or standards required for 50% reduction of the initial DPPH concentration expressed as EC₅₀, effective concentration. ^cFerric reducing antioxidant power. ^dAbility to inhibit linoleic acid (LA) peroxidation monitored by TBARS test and expressed as IC₅₀, concentration of plant materials or standards needed to decrease the LA-peroxidation by 50%; TE, Trolox[®] equivalent antioxidant activity. Standards: QU, quercetin; BHA, butylated hydroxyanisole; BHT, 2,6-di-*tert*-butyl-4-methylphenol; TX, Trolox[®].

effective agents preventing damages related to the oxidative stress and inflammation implicated in the etiology and progression of numerous chronic diseases, including cardiovascular diseases, diabetes mellitus, neurodegenerative disorders, and cancer [31–33]. The occurrence of polyphenolic compounds in the investigated fruits might thus largely define their bioactivity, especially that *Cotoneaster*-derived polyphenols have been previously linked with strong antioxidant capacity in our earlier study regarding the leaves [34].

3.4. Biological Activity. The above presented phytochemical studies proved that fruits of *Cotoneaster* species are indeed a rich source of diverse phytochemicals with a wide spectrum of recognized biological properties. However, based on the results of the quantitative studies, the polyphenolic fraction with the highest content would appear to have the greatest beneficial health effects of the fruits in a human organism. Thus, further studies were focused on providing a more detailed insight into potential mechanisms of the activity of the hydrophilic components, that is, their anti-inflammatory and antioxidant effects.

3.4.1. Inhibitory Effects on Two Enzymes Involved in Inflammation. Inflammation is a complex process that constitutes a part of the immune system defense against harmful stimuli, but may lead to negative effects if uncontrolled. The inflammatory response is regulated by numerous enzymes and mediators and thus can be intercepted at different points, and several of these key enzymes, including lipoxygenases (LOX) and hyaluronidases (HYAL), are most often used to determine the anti-inflammatory potential of natural

products [35]. LOX catalyze the dioxygenation of arachidonic acid to form hydroperoxides, the first step in the biosynthesis of several proinflammatory mediators [36]. HYAL, on the other hand, are highly specific hydrolases that degrade hyaluronic acid, an important component of the extracellular matrix, thus increasing the permeability of the tissues and facilitating the spread of inflammation [37]. Our present findings indicate that all fruit extracts inhibit the activity of LOX and HYAL in a dose-dependent manner (Table 5). The strongest inhibitory effect towards LOX was demonstrated by the leaf extracts of *C. hjelmqvistii* and *C. zabelii* (IC₅₀ = 7.70 and 9.97 μ g/U, respectively), while the activity of HYAL was most strongly hindered by the leaf extract of *C. lucidus* (IC₅₀ = 16.44 μ g/U). The activity of the extracts was weaker in comparison to indomethacin (IC₅₀ = 1.89 μ g/U for LOX and 5.60 μ g/U for HYAL), but after recalculating the results to adjust for the actual polyphenol content (which gives IC₅₀ values in the range of 0.33–0.77 μ g/U for LOX and 0.47–1.93 μ g/U for HYAL inhibition), the activity of the extracts looks quite advantageous in comparison to the positive standard. The anti-inflammatory potential of *Cotoneaster* polyphenols is further confirmed by the high activity of (–)-epicatechin, quercetin, and chlorogenic acid, the main constituents of the investigated leaf extracts.

3.4.2. Antioxidant Activity in Chemical Models. The basic antioxidant mechanism of *Cotoneaster* polyphenols was verified in chemical models using three complementary *in vitro* assays: DPPH and FRAP tests, two of the most frequently

TABLE 5: Inhibitory effects of *Cotoneaster* fruit extracts and standards towards lipoxygenase (LOX) and hyaluronidase (HYAL).

Fruit sample/standard	LOX		HYAL	
	IC ₅₀ ^a ($\mu\text{g}/\text{mL}$)	IC ₅₀ ^b ($\mu\text{g}/\text{U}$)	IC ₅₀ ^a ($\mu\text{g}/\text{mL}$)	IC ₅₀ ^b ($\mu\text{g}/\text{U}$)
<i>C. lucidus</i>	487.75 \pm 6.57 ^F	13.29 \pm 0.18 ^F	25.65 \pm 0.95 ^C	16.44 \pm 0.61 ^C
<i>C. divaricatus</i>	479.98 \pm 12.79 ^F	13.08 \pm 0.35 ^F	34.22 \pm 1.48 ^D	21.93 \pm 0.95 ^D
<i>C. horizontalis</i>	421.85 \pm 5.78 ^E	11.50 \pm 0.16 ^E	40.51 \pm 2.11 ^{E,F,G}	25.97 \pm 1.35 ^{E,F,G}
<i>C. nanshan</i>	626.16 \pm 5.04 ^H	17.07 \pm 0.14 ^H	45.64 \pm 0.76 ^G	29.25 \pm 0.49 ^G
<i>C. hjelmqvistii</i>	290 \pm 2.75 ^C	7.70 \pm 0.07 ^C	44.44 \pm 1.72 ^{F,G}	28.48 \pm 1.10 ^{F,G}
<i>C. dielsianus</i>	914.97 \pm 2.15 ^J	24.94 \pm 0.06 ^J	35.07 \pm 2.60 ^{D,E}	22.48 \pm 1.66 ^{D,E}
<i>C. splendens</i>	734.25 \pm 5.86 ^I	20.01 \pm 0.16 ^I	34.36 \pm 0.11 ^D	22.03 \pm 0.07 ^D
<i>C. bullatus</i>	585.43 \pm 16.14 ^G	15.96 \pm 0.44 ^G	39.04 \pm 0.82 ^{D,E,F}	25.03 \pm 0.53 ^{D,E,F}
<i>C. zabelii</i>	375.87 \pm 9.89 ^D	9.97 \pm 0.26 ^D	33.33 \pm 2.12 ^D	21.37 \pm 1.36 ^D
QU	69.60 \pm 2.62 ^A	2.46 \pm 0.01 ^A	21.04 \pm 1.03 ^C	13.87 \pm 0.06 ^C
ECA	124.38 \pm 1.56 ^B	3.39 \pm 0.04 ^B	18.51 \pm 0.50 ^B	11.87 \pm 0.32 ^B
CHA	151.71 \pm 7.52 ^B	4.14 \pm 0.21 ^B	20.35 \pm 0.36 ^B	13.05 \pm 0.23 ^B
IND	90.12 \pm 0.40 ^A	1.89 \pm 0.10 ^A	8.61 \pm 0.22 ^A	5.60 \pm 0.07 ^A

Results expressed as means \pm SD calculated per dry weight (dw) of the extracts; different capital letters within the same row indicate significant differences at $\alpha = 0.05$ in HSD Tukey's test. Standards: QU, quercetin; ECA, (-)-epicatechin; CHA, chlorogenic acid; IND, indomethacin. Ability to inhibit lipoxygenase (LOX) and hyaluronidase (HYAL) calculated as the amount of analyte needed for 50% inhibition of enzyme activity was expressed as follows: ^a μg of the dry extracts or standards/mL of the enzyme solution and ^b μg of the extracts/enzyme units (U).

employed SET (single electron transfer) type methods, and the inhibition of AAPH-induced linoleic acid peroxidation test (monitored by TBARS assay), a more physiologically relevant system which involves the HAT (hydrogen atom transfer) mechanism. In all of the applied tests, the investigated fruits displayed concentration-dependent activity with the capacity parameters (expressed in $\mu\text{mol TE/g dw}$) of a similar order of magnitude, which shows that *Cotoneaster* antioxidants can effectively act via both basic mechanisms. The highest activity in comparison to the natural (quercetin) and synthetic standards (BHA and BHT) were observed in the FRAP and TBARS assays for all fruits (Table 4 and Figure 2). In all tests, the fruits of *C. zabelii*, *C. hjelmqvistii*, *C. bullatus*, and *C. splendens*, indicated in the present study as the richest sources of polyphenols, displayed the highest antioxidant efficiency, with the activity parameters varying in the narrow range of 225.5–240.9 $\mu\text{mol TE/g dw}$ (DPPH), 378.9–434.3 $\mu\text{mol TE/g}$ (FRAP), and 518.2–543.9 $\mu\text{mol TE/g}$ (TBARS), respectively. Interestingly, these were the species that also exhibited the relatively largest proportions of proanthocyanidins/flavan-3-ols (*C. zabelii*, *C. bullatus*, *C. splendens*) or quercetin 3-(2''-xylosyl)-glucoside (*C. hjelmqvistii*), which suggest that these polyphenols play a significant role in the activity of fruits. Additionally, the close connection between the phenolic levels and antioxidant parameters was also evidenced by statistically significant linear correlations between TPCs and the results of the DPPH ($|r| = 0.9352$, $p < 0.001$), FRAP ($|r| = 0.9491$, $p < 0.001$), and TBARS ($|r| = 0.9116$, $p < 0.001$) tests.

3.4.3. Protective Effects on Human Plasma Components Exposed to Oxidative Stress. To provide a more detailed insight into the antioxidant effects of *Cotoneaster* polyphenols, the four most promising species (*C. zabelii*, *C. bullatus*,

C. splendens, and *C. hjelmqvistii*) were selected for further studies in a biological model. Since according to traditional application and our present results, *Cotoneaster* fruits appear to be promising sources of phytochemicals with properties especially advantageous for the circulatory system (i.e., linoleic acid and β -sitosterol), a human plasma model was selected to evaluate their additional benefits for cardiovascular health, this time mediated by polyphenols. This approach allowed for the *in vitro* monitoring of the protective effects of the extracts towards human plasma components under oxidative stress conditions. The peroxynitrite (ONOO⁻) used for inducing oxidative stress is a known *in vivo*-operating oxidant, responsible for structural changes in plasma proteins and lipids and implicated in numerous oxidative stress-related disorders [38]. The concentrations of ONOO⁻ (100 and 150 μM) selected for the study enabled quantitative measurements of the resulting modifications in plasma components, but may be also regarded as physiologically-relevant as they can be reached *in vivo* in local compartments, for example, during a serious inflammation of blood vessels [39].

The addition of ONOO⁻ to the plasma samples resulted in an overall decrease ($p < 0.001$) in the nonenzymatic antioxidant capacity of the plasma, measured as the FRAP parameter, and in oxidative and nitrative alterations of its protein and lipid components, which was evidenced by a significant increase ($p < 0.001$) in lipid peroxidation biomarkers (lipid hydroperoxides and TBARS), a noticeable rise ($p < 0.001$) in 3-nitrotyrosine level (marker of protein nitration), and a decrease ($p < 0.001$) in the level of thiol groups (marker of protein oxidation). On the other hand, in the plasma samples incubated with ONOO⁻ in the presence of *Cotoneaster* extracts (1–50 $\mu\text{g}/\text{mL}$), the extent of oxidative/nitrative damage to both proteins and lipids was noticeably limited ($p < 0.05$), regardless of the tested species and the

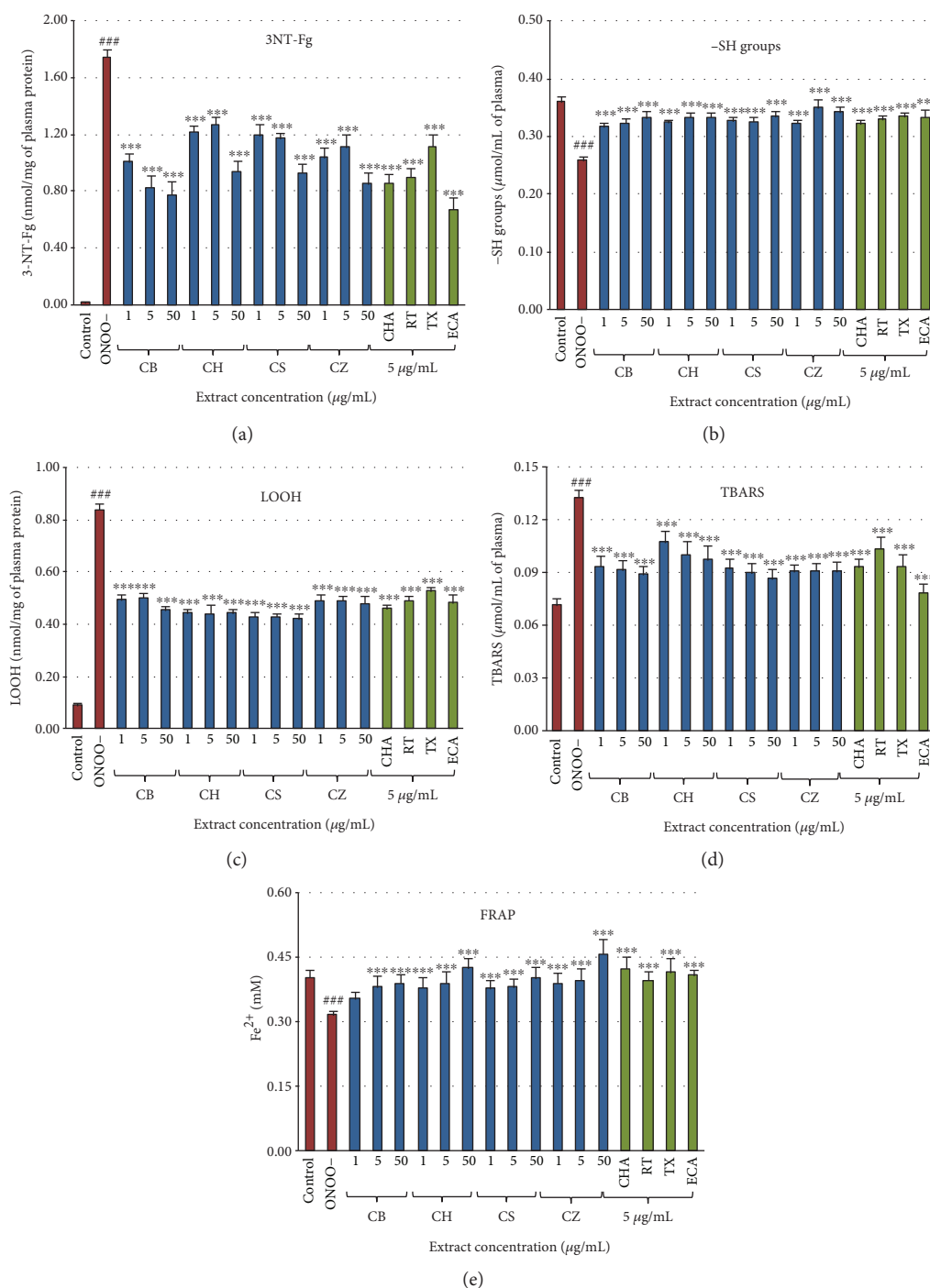


FIGURE 4: Effects of the *Cotoneaster* fruit extracts on human plasma exposed to oxidative stress: (a) effects on the nitration of tyrosine residues in plasma proteins and formation of 3-nitrotyrosine (3-NT-Fg); (b) effects on the oxidation of free thiol groups (-SH); effects on the peroxidation of plasma lipids including (c) formation of lipid hydroperoxides (LOOH), and (d) thiobarbituric acid-reactive substances (TBARS); (e) effects on ferric reducing ability of blood plasma (FRAP). Results expressed as means \pm SE ($n = 8$) for repeated measures: ### $p < 0.001$, for ONOO⁻-treated plasma (without the extracts) versus control plasma, and *** $p < 0.001$ for plasma treated with ONOO⁻ in the presence of the investigated extracts (1–50 $\mu\text{g/mL}$) or the standards (5 $\mu\text{g/mL}$). CB, *C. bullatus*; CH, *C. hjelmqvistii*; CS, *C. splendens*; CZ, *C. zabelii*. Standards: CHA, chlorogenic acid; RT, rutin; TX, Trolox®; ECA, (-)-epicatechin.

extract concentration. As shown in Figures 4(a) and 4(b), even at the lowest concentrations of 1 $\mu\text{g/mL}$, the extracts were able to reduce tyrosine nitration by about 29–42% and thiol group oxidation by about 24–26%, while at the

concentration of 50 $\mu\text{g/mL}$ the effectiveness rose to 46–55% and 29–32%, respectively. Moreover, as demonstrated in Figures 4(c) and 4(d), all fruit samples inhibited the generation of plasma lipid hydroperoxides by 40–50% and reduced

TBARS levels by 19–35%. All extract-treated samples, apart from those fortified with 1 $\mu\text{g}/\text{mL}$ of *C. bullatus* extract, demonstrated a statistically significant ($p < 0.001$) improvement in the nonenzymatic antioxidant capacity of blood plasma of up to 44% in comparison to the samples not protected by the extracts (Figure 4(e)). In most cases, little difference was observed in the activity between the tested fruits; however, the inhibition of tyrosine nitration assay found *C. bullatus* and *C. zabelii* displaying stronger activity than the other two extracts at all concentrations tested ($p < 0.05$). A dose dependency was noticeable for *C. bullatus* and *C. splendens* in antinitrative activity (Figure 4(a)) and for most *Cotoneaster* species in the TBARS test, with the exception of *C. zabelii* (Figure 4(d)). Some significant correlations were also found, between the TPCs and the activity parameters. The most prominent was the relationship for the FRAP assay ($|r| = 0.7587$, $p < 0.01$). In the tests for protein protection, the correlation between the percentage inhibition of tyrosine nitration and phenolic level was stronger ($|r| = 0.6774$, $p < 0.05$) than the analogous relationship for the reduction of thiol group oxidation ($|r| = 0.4885$, $p < 0.05$). Contrastingly, the correlations in the lipid peroxidation assays were not statistically significant ($p > 0.05$).

The effectiveness of the extracts was further supported by the fact that in all of the tests, the observed antioxidant effects of the fruit extracts at the corresponding concentration levels (5 $\mu\text{g}/\text{mL}$) were similar or higher to that of Trolox[®], a synthetic analog of vitamin E often used as a positive standard in antioxidant studies. Moreover, the significant activity of rutin, chlorogenic acid, and, especially, (–)-epicatechin confirm the important role of polyphenols in the capacity of the extracts.

The wide range of the extract concentrations tested (1–50 $\mu\text{g}/\text{mL}$) was in accordance with the general practice of *in vitro* studies [20] and allowed for the study of different interactions in the system. Additionally, the lower levels (1–5 $\mu\text{g}/\text{mL}$) might be considered physiologically-relevant as they correspond to the levels of phenolics attainable *in vivo* after consumption of polyphenol-rich plant materials. For example, according to the accumulated research [40, 41], the maximal achievable concentration of plant phenolics in blood plasma can reach up to 5–10 μM , which generally corresponds to less than 5 $\mu\text{g}/\text{mL}$. Taking into account the TPC levels evaluated for *Cotoneaster* fruits in the present study and the extraction efficiency (15–30%, depending on the species), the levels of phenolics corresponding to the applied extract concentration of 1–5 $\mu\text{g}/\text{mL}$ are about 0.13–1.25 $\mu\text{g}/\text{mL}$: well within the obtainable plasma range. This suggests that the protective activity of the *Cotoneaster* extracts towards ONOO[–]-induced changes observed *in vitro* may translate to their positive *in vivo* effects.

The harmful influence of ONOO[–] is often associated with serious pathological consequences in many organs and systems of the human body. The nitration/oxidation of biomolecules such as enzymes, receptors, lipoproteins, fatty acids, or nucleic acids changes their function and may impair cellular signalization pathways, induce inflammatory responses, or even promote cell apoptosis [38, 39]. In the case of the

circulatory system, the negative effects of ONOO[–] result in a higher risk of cardiovascular disorders, such as stroke, myocardial infarction, or chronic heart failure [38], and are connected with the direct modifications of plasma proteins and lipids. For instance, the formation of 3-nitrotyrosine in fibrinogen might contribute to prothrombotic events in the blood coagulation cascade and fibrinolysis process [42], while thiol oxidation in platelet proteins leads to the inhibition of platelet function [43]. Additionally, oxidation of low-molecular-weight thiols, such as reduced glutathione, diminishes the endogenous antioxidant capacity of plasma and primes further oxidative damage in the system [38]. Similarly, lipid peroxidation initiated by ONOO[–] may propagate platelet aggregation [44], while peroxynitrite-modified LDL binds with high affinity to macrophage scavenger receptors leading to foam cell formation, which represent a key early event in atherogenesis [38, 45]. The prevention of these processes partially explains the beneficial effects of *Cotoneaster* fruits reported by traditional medicine and might be regarded as a good strategy in prophylaxis of various cardiovascular complaints.

3.5. Cellular Safety. Due to its long tradition of consumption and application in folk medicine, the *Cotoneaster* fruits might be regarded as nontoxic. However, in the case of the concentrated extracts, a more detailed evaluation of their safety is required. Therefore, the next step of our research was a viability test on PMBCs which assessed the cytotoxicity of the extracts. After two, four, and six-hour incubation periods with the plant extracts at concentrations of 5, 25, and 50 $\mu\text{g}/\text{mL}$, the viability of the extract-treated cells constituted 97.3–101.7% of that of the control (non-treated cells) and no statistically significant differences were found ($p > 0.05$) between the two values (Figure 5). These findings suggest that the *Cotoneaster* extracts do not have cytotoxic effects at these concentrations.

4. Conclusion

The current paper presents the first comprehensive phytochemical and activity study of *Cotoneaster* fruits. The fruits were found to possess distinct lipophilic and phenolic profiles, significant antioxidant activity in both chemical and biological models, noticeable inhibitory effects on the proinflammatory enzymes, and cellular safety. Hence, *Cotoneaster* fruits appear to be promising candidates for the production of pharma- and nutraceuticals associated with preventing and treating oxidative stress and inflammatory-related chronic diseases; they may also contribute to a balanced and varied diet comprising food rich in bioactive compounds. Furthermore, the protective effects against ONOO[–]-induced modifications in the plasma components, demonstrated by the polyphenolic fractions from the fruits of *C. hjelmqvistii*, *C. zabelii*, *C. splendens*, and *C. bullatus* at *in vivo*-relevant levels, may be considered as a molecular basis for the beneficial effects of *Cotoneaster* fruits within the cardiovascular system reported by traditional medicine. The biological activity demonstrated in the present study might therefore be a starting point of more extensive investigation on the nutritional

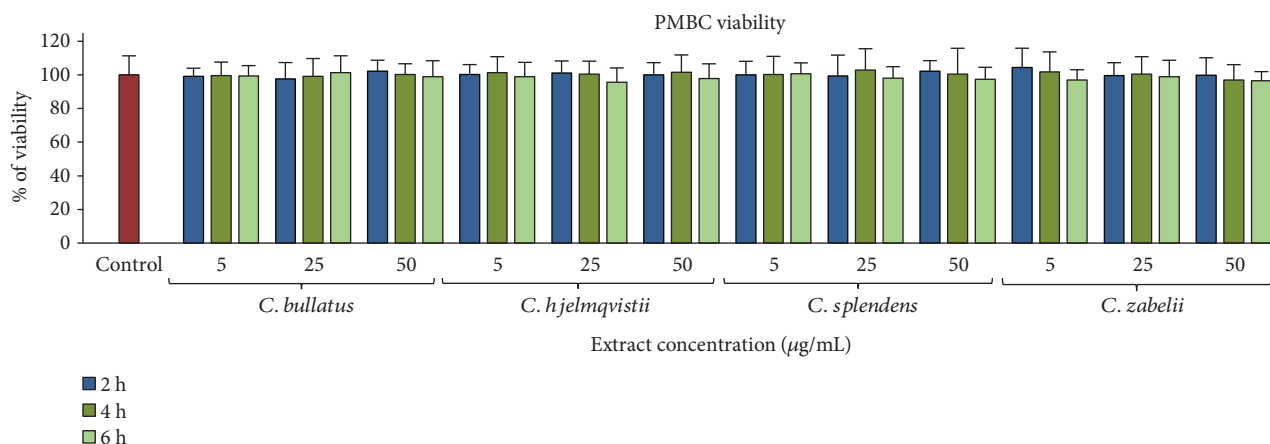


FIGURE 5: Viability of peripheral blood mononuclear cells (PMBCs) after 2, 4, and 6 h incubation with the *Cotoneaster* fruit extracts at 5, 25, and 50 µg/mL. Results are presented as means ± SD ($n = 14$).

value and bioactivity of *Cotoneaster* fruits, including their effects in *in vivo* systems.

Data Availability

The data used to support the findings of this study are available from the corresponding author upon request.

Conflicts of Interest

The authors report no conflicts of interest.

Acknowledgments

This work was financially supported by the University of Lodz, Poland through Grant no. 506/1136 (the synthesis of peroxynitrite, ONOO⁻), the Medical University of Lodz, Poland through Grant no. 503/3-022-01/503-31-001 (the phytochemical and anti-inflammatory activity studies), and the National Science Centre, Poland through Grant no. 2017/01/X/NZ7/00520 (all other costs). The authors would like to thank the staff of the Botanical Garden in Lodz and the Forestry Experimental Station of the Warsaw University of Life Sciences in Rogow for providing and authenticating the plant material.

References

- [1] H. Boeing, A. Bechthold, A. Bub et al., "Critical review: vegetables and fruit in the prevention of chronic diseases," *European Journal of Nutrition*, vol. 51, no. 6, pp. 637–663, 2012.
- [2] O. Ogah, C. S. Watkins, B. E. Ubi, and N. C. Oraguzie, "Phenolic compounds in Rosaceae fruit and nut crops," *Journal of Agricultural and Food Chemistry*, vol. 62, no. 39, pp. 9369–9386, 2014.
- [3] P. N. Denev, C. G. Kratchanov, M. Ciz, A. Lojek, and M. G. Kratchanova, "Bioavailability and antioxidant activity of black chokeberry (*Aronia melanocarpa*) polyphenols: in vitro and in vivo evidences and possible mechanisms of action: a review," *Comprehensive Reviews in Food Science and Food Safety*, vol. 11, no. 5, pp. 471–489, 2012.
- [4] R. Raudonis, L. Raudonė, K. Gaivelytė, P. Viškelis, and V. Janulis, "Phenolic and antioxidant profiles of rowan (*Sorbus L.*) fruits," *Natural Product Research*, vol. 28, no. 16, pp. 1231–1240, 2014.
- [5] C. F. Zhao, S. Li, S. J. Li, G. H. Song, L. J. Yu, and H. Zhang, "Extraction optimization approach to improve accessibility of functional fraction based on combination of total polyphenol, chromatographic profiling and antioxidant activity evaluation: *Pyracantha fortuneana* fruit as an example," *Journal of Functional Foods*, vol. 5, no. 2, pp. 715–728, 2013.
- [6] R. Pinacho, R. Y. Caverro, I. Astiasarán, D. Ansorena, and M. I. Calvo, "Phenolic compounds of blackthorn (*Prunus spinosa L.*) and influence of in vitro digestion on their antioxidant capacity," *Journal of Functional Foods*, vol. 19, pp. 49–62, 2015.
- [7] J. M. Lee, H. Lee, S. B. Kang, and W. J. Park, "Fatty acid desaturases, polyunsaturated fatty acid regulation, and biotechnological advances," *Nutrients*, vol. 8, no. 1, p. 23, 2016.
- [8] Z. Ovesná, A. Vachálková, K. Horváthová, and D. Tóthová, "Pentacyclic triterpenic acids: new chemoprotective compounds. Minireview," *Neoplasma*, vol. 51, no. 5, pp. 327–333, 2004.
- [9] F. Les, V. López, G. Caprioli et al., "Chemical constituents, radical scavenging activity and enzyme inhibitory capacity of fruits from *Cotoneaster pannosus* Franch.," *Food & Function*, vol. 8, no. 5, pp. 1775–1784, 2017.
- [10] G. Zengin, A. Uysal, E. Gunes, and A. Aktumsek, "Survey of phytochemical composition and biological effects of three extracts from a wild plant (*Cotoneaster nummularia* Fisch. et Mey.): a potential source for functional food ingredients and drug formulations," *PLoS One*, vol. 9, no. 11, article e113527, 2014.
- [11] G. Bisht, "Chemical constituents from the fruits of *Cotoneaster microphylla* Wall ex Lindl.," *Asian Journal of Chemistry*, vol. 7, pp. 455–456, 1995.
- [12] A. Uysal, G. Zengin, A. Mollica et al., "Chemical and biological insights on *Cotoneaster integerrimus*: a new (–)-epicatechin source for food and medicinal applications," *Phytomedicine*, vol. 23, no. 10, pp. 979–988, 2016.
- [13] W. A. Pryor, R. Cueto, X. Jin et al., "A practical method for preparing peroxynitrite solutions of low ionic strength and free of hydrogen peroxide," *Free Radical Biology & Medicine*, vol. 18, no. 1, pp. 75–83, 1995.

- [14] J. Nazaruk, A. Wajs-Bonikowska, and R. Bonikowski, "Components and antioxidant activity of fruits of *Cirsium palustre* and *C. rivulare*," *Chemistry of Natural Compounds*, vol. 48, pp. 9-10, 2012.
- [15] T. T. Thanh, M. F. Vergnes, J. Kaloustian, T. F. El-Moselhy, M. J. Amiot-Carlin, and H. Portugal, "Effect of storage and heating on phytosterol concentrations in vegetable oils determined by GC/MS," *Journal of the Science of Food and Agriculture*, vol. 86, no. 2, pp. 220-225, 2006.
- [16] M. A. Olszewska and P. Michel, "Antioxidant activity of inflorescences, leaves and fruits of three *Sorbus* species in relation to their polyphenolic composition," *Natural Product Research*, vol. 23, no. 16, pp. 1507-1521, 2009.
- [17] P. Michel, A. Owczarek, M. Matczak et al., "Metabolite profiling of eastern teaberry (*Gaultheria procumbens* L.) lipophilic leaf extracts with hyaluronidase and lipoxygenase inhibitory activity," *Molecules*, vol. 22, no. 3, p. 412, 2017.
- [18] M. A. Olszewska, A. Presler, and P. Michel, "Profiling of phenolic compounds and antioxidant activity of dry extracts from the selected *Sorbus* species," *Molecules*, vol. 17, no. 3, pp. 3093-3113, 2012.
- [19] M. Matczak, A. Marchelak, P. Michel et al., "*Sorbus domestica* L. leaf extracts as functional products: phytochemical profiling, cellular safety, pro-inflammatory enzymes inhibition and protective effects against oxidative stress in vitro," *Journal of Functional Foods*, vol. 40, pp. 207-218, 2018.
- [20] J. Kolodziejczyk-Czepas, P. Nowak, B. Wachowicz et al., "Antioxidant efficacy of *Kalanchoe daigremontiana* bufadienolide-rich fraction in blood plasma in vitro," *Pharmaceutical Biology*, vol. 54, no. 12, pp. 3182-3188, 2016.
- [21] I. F. F. Benzie and J. J. Strain, "The ferric reducing ability of plasma (FRAP) as a measure of "antioxidant power": the FRAP assay," *Analytical Biochemistry*, vol. 239, no. 1, pp. 70-76, 1996.
- [22] B. Matthaus and M. M. Özcan, "Fatty acid, tocopherol and squalene contents of Rosaceae seed oils," *Botanical Studies*, vol. 55, no. 1, p. 48, 2014.
- [23] S. A. Mohamed, N. M. Sokkar, O. El-Gindi, Z. Y. Ali, and I. A. Alfshawy, "Phytoconstituents investigation, anti-diabetic and anti-dyslipidemic activities of *Cotoneaster horizontalis* Decne cultivated in Egypt," *Life Science Journal*, vol. 9, pp. 394-403, 2012.
- [24] J. Lunn and H. E. Theobald, "The health effects of dietary unsaturated fatty acids," *Nutrition Bulletin*, vol. 31, no. 3, pp. 178-224, 2006.
- [25] F. Anwar, R. Przybylski, M. Rudzinska, E. Gruczynska, and J. Bain, "Fatty acid, tocopherol and sterol compositions of Canadian prairie fruit seed lipids," *Journal of the American Oil Chemists' Society*, vol. 85, no. 10, pp. 953-959, 2008.
- [26] P. Morales, I. C. F. R. Ferreira, A. M. Carvalho et al., "Wild edible fruits as a potential source of phytochemicals with capacity to inhibit lipid peroxidation," *European Journal of Lipid Science and Technology*, vol. 115, no. 2, pp. 176-185, 2013.
- [27] E. Palme, A. R. Bilia, and I. Morelli, "Flavonols and isoflavones from *Cotoneaster simonsii*," *Phytochemistry*, vol. 42, no. 3, pp. 903-905, 1996.
- [28] S. Khan, N. Riaz, Aziz-Ur-Rehman, N. Riaz, N. Afza, and A. Malik, "Isolation studies on *Cotoneaster racemiflora*," *Journal of the Chemical Society of Pakistan*, vol. 29, pp. 620-623, 2007.
- [29] P. J. H. Jones and S. S. AbuMweis, "Phytosterols as functional food ingredients: linkages to cardiovascular disease and cancer," *Current Opinion in Clinical Nutrition and Metabolic Care*, vol. 12, no. 2, pp. 147-151, 2009.
- [30] S. Saeidnia, A. Manayi, A. R. Gohari, and M. Abdollahi, "The story of beta-sitosterol—a review," *European Journal of Medicinal Plants*, vol. 4, no. 5, pp. 590-609, 2014.
- [31] D. Vauzour, A. Rodriguez-Mateos, G. Corona, M. J. Oruna-Concha, and J. P. E. Spencer, "Polyphenols and human health: prevention of disease and mechanisms of action," *Nutrients*, vol. 2, no. 11, pp. 1106-1131, 2010.
- [32] M. Locatelli, G. Zengin, A. Uysal et al., "Multicomponent pattern and biological activities of seven *Asphodeline* taxa: potential sources of natural-functional ingredients for bioactive formulations," *Journal of Enzyme Inhibition and Medicinal Chemistry*, vol. 32, no. 1, pp. 60-67, 2017.
- [33] G. Zengin, S. Nithiyanantham, M. Locatelli et al., "Screening of in vitro antioxidant and enzyme inhibitory activities of different extracts from two uninvestigated wild plants: *Centranthus longiflorus* subsp. *longiflorus* and *Cerintho minor* subsp. *Auriculata*," *European Journal of Integrative Medicine*, vol. 8, no. 3, pp. 286-292, 2016.
- [34] A. Kicel, P. Michel, A. Owczarek et al., "Phenolic profile and antioxidant potential of leaves from selected *Cotoneaster* Medik. species," *Molecules*, vol. 21, no. 6, p. 688, 2016.
- [35] R. Medzhitov, "Origin and physiological roles of inflammation," *Nature*, vol. 454, no. 7203, pp. 428-435, 2008.
- [36] S. T. Prigge, J. C. Boyington, M. Faig, K. S. Doctor, B. J. Gaffney, and L. M. Amzel, "Structure and mechanism of lipoxygenases," *Biochimie*, vol. 79, no. 11, pp. 629-636, 1997.
- [37] N. S. El-Safory, A. E. Fazary, and C. K. Lee, "Hyaluronidases, a group of glycosidases: current and future perspectives," *Carbohydrate Polymers*, vol. 81, no. 2, pp. 165-181, 2010.
- [38] P. Pacher, J. S. Beckman, and L. Liaudet, "Nitric oxide and peroxynitrite in health and disease," *Physiological Reviews*, vol. 87, no. 1, pp. 315-424, 2007.
- [39] C. Szabó, H. Ischiropoulos, and R. Radi, "Peroxynitrite: biochemistry, pathophysiology and development of therapeutics," *Nature Reviews Drug Discovery*, vol. 6, no. 8, pp. 662-680, 2007.
- [40] S. Baba, N. Osakabe, M. Natsume, Y. Muto, T. Takizawa, and J. Terao, "In vivo comparison of the bioavailability of (+)-catechin, (-)-epicatechin and their mixture in orally administered rats," *Journal of Nutrition*, vol. 131, no. 11, pp. 2885-2891, 2001.
- [41] C. Burak, V. Brüll, P. Langguth et al., "Higher plasma quercetin levels following oral administration of an onion skin extract compared with pure quercetin dihydrate in humans," *European Journal of Nutrition*, vol. 56, no. 1, pp. 343-353, 2017.
- [42] J. Kolodziejczyk-Czepas, M. B. Ponczek, and P. Nowak, "Peroxynitrite and fibrinolytic system—the effects of peroxynitrite on t-PA-induced plasmin activity," *International Journal of Biological Macromolecules*, vol. 81, pp. 212-219, 2015.
- [43] P. Nowak, B. Olas, E. Bald, R. Głowacki, and B. Wachowicz, "Peroxynitrite-induced changes of thiol groups in human blood platelets," *Platelets*, vol. 14, no. 6, pp. 375-379, 2003.
- [44] C. Calzada, E. Vericel, and M. Lagarde, "Low concentrations of lipid hydroperoxides prime human platelet aggregation specifically via cyclo-oxygenase activation," *Biochemical Journal*, vol. 325, no. 2, pp. 495-500, 1997.
- [45] N. Hogg, V. M. Darley-Usmar, A. Graham, and S. Moncada, "Peroxynitrite and atherosclerosis," *Biochemical Society Transactions*, vol. 21, no. 2, pp. 358-362, 1993.

Review Article

An Overview on the Anti-inflammatory Potential and Antioxidant Profile of Eugenol

Joice Nascimento Barboza,¹ Carlos da Silva Maia Bezerra Filho,¹ Renan Oliveira Silva,² Jand Venes R. Medeiros ,³ and Damião Pergentino de Sousa ¹

¹Department of Pharmaceutical Sciences, Universidade Federal da Paraíba, 58051-970 João Pessoa, Paraíba, Brazil

²Department of Biomedicine, University Center INTA-UNINTA, 62050-130 Sobral, Ceará, Brazil

³Laboratory of Pharmacology of Inflammation and Gastrointestinal Disorders-LAFIDG, Federal University of Piauí, Parnaíba, Piauí, Brazil

Correspondence should be addressed to Damião Pergentino de Sousa; damiaio_desousa@yahoo.com.br

Received 6 July 2018; Accepted 3 October 2018; Published 22 October 2018

Guest Editor: Anderson J. Teodoro

Copyright © 2018 Joice Nascimento Barboza et al. This is an open access article distributed under the Creative Commons Attribution License, which permits unrestricted use, distribution, and reproduction in any medium, provided the original work is properly cited.

The bioactive compounds found in foods and medicinal plants are attractive molecules for the development of new drugs with action against several diseases, such as those associated with inflammatory processes, which are commonly related to oxidative stress. Many of these compounds have an appreciable inhibitory effect on oxidative stress and inflammatory response, and may contribute in a preventive way to improve the quality of life through the use of a diet rich in these compounds. Eugenol is a natural compound that has several pharmacological activities, action on the redox status, and applications in the food and pharmaceutical industry. Considering the importance of this compound, the present review discusses its anti-inflammatory and antioxidant properties, demonstrating its mechanisms of action and therapeutic potential for the treatment of inflammatory diseases.

1. Introduction

Eugenol (4-allyl-2-methoxyphenol) is a phenolic compound from the class of phenylpropanoids and the main component of clove (*Syzygium aromaticum* (L.) Merr. & L. M. Perry.). It consists of 45–90% of its essential oil [1]. It is used in the food industry as a preservative, mainly due to its antioxidant property [2], and as a flavoring agent for foods and cosmetics [3]. It can also be found in soybean (*Glycine max* (L.) Merr.), beans [4], coffee [5], cinnamon (*Cinnamomum verum* J. Presl), basil (*Ocimum basilicum* L.) [6], “canelinha” (*Croton zehntneri* Pax et Hoffm) [7], banana [8, 9], bay laurel (*Laurus nobilis* L.), and other foods [10]. Among the plants that contain eugenol, soybeans, cloves, beans, and cinnamon also present the antioxidant activity, possibly performed by this compound and other constituents [11–14]. In addition, clove is also known by anti-inflammatory activity [15], which may be related to anti-inflammatory action of eugenol (Figure 1).

Inflammation is a complex protective response of the body against harmful agents, such as microorganisms or damaged cells [16, 17], which the biological system objective to remove harmful stimuli from the body and promote healing. However, this response needs to be controlled and last for a short period; otherwise, it may provide the appearance of pathological disorders related to the immune system [18]. Classically, inflammation can be classified in acute and chronic. The acute inflammation is an initial response, which is characterized by resident cell activation, with liberation of proinflammatory cytokines and chemokines, culminating in the recruitment of polymorphonuclear, primarily neutrophils, from the innate immune system to the injury site. This response complex act to promote cardinal signs of inflammation, such as pain, edema, and heat [19]. On the other hand, chronic inflammation is a prolonged response characterized by a gradual change in the cells type found at the inflammatory site, which over time cause both

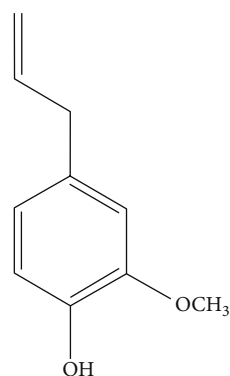


FIGURE 1: Chemical structure of eugenol.

permanent damage and healing of the tissue. In both types of inflammation occur increased local blood flow, vasodilation, fluid extravasation, and liberation of proinflammatory mediators [17, 20].

The nuclear factor-kappa B (NF- κ B) signaling pathway is a key part of the immune response. It is essential to inflammatory processes due to its importance in the transcription of cytokines, such as tumor necrosis factor- α (TNF- α), interleukin-1 β (IL-1 β), interleukin-6 (IL-6), and nitric oxide (NO). Like eugenol, substances that inhibit this pathway are of interest to the pharmaceutical industry [21–23]. In general, patients with inflammatory disorders use clinically glucocorticoids or nonsteroidal anti-inflammatory drugs (NSAIDs). However, these drugs are associated with critical side effects (i.e., gastrointestinal ulcers and bleeding) and limited therapeutic efficacy, which often leads patients to abandon the treatment [24]. In this context, the pharmaceutical industry has directed efforts in the attempt to find new bioactive molecules.

Medicinal plants have been important sources of constituents with pharmacological activities. Phenylpropanoids are considered a group of secondary compounds found in a variety of plants and usually in the oxidized form, presenting a hydroxyl at the aromatic ring [25]. Studies recently demonstrated that phenylpropanoids and their synthetic derivatives have a variety of pharmacologic activities, including anti-inflammatory action [26, 27].

Several pharmacological activities have been reported to eugenol: anti-inflammatory [28], antitumor [29], antibacterial [30], antifungal [31, 32], antipyretic [33], anesthetic [34], and analgesic activities [35]. Considering the importance of eugenol as bioactive molecule and its presence in various foods and medicinal plants, this review discusses its role in the inflammatory response in experimental models, including animals and cell culture tests, demonstrating its antioxidant profile and potential therapeutical application against inflammatory diseases.

2. Methodology

The present review was based on the data search performed in the scientific literature database PubMed, using the publication from January 2008 to January 2018, using the following keywords: eugenol, asthma, antiasthmatic

effect, allergy, antiallergic effect, inflammation, anti-inflammatory, immune response, lymphocytes, cytokines, immunoglobulins, immunoregulatory, and antioxidant. Table 1 shows the studies reported for this review and summarizes the results obtained, indicating the dose/concentration of eugenol administered, experimental model, parameters evaluated, and biological effect.

3. Results and Discussion

3.1. Antioxidant Action of Eugenol. The free radical scavenger effect of diphenyl-1-picrylhydrazyl (DPPH) is due to the ability of certain substances to donate hydrogen, especially those with a phenolic group in their structure. Thus, eugenol's ability to sequester free radicals in the DPPH assay ($IC_{50} = 11.7 \mu\text{g/mL}$), as well as to inhibit reactive oxygen species (ROS) ($IC_{50} = 1.6 \mu\text{g/mL}$), H_2O_2 ($IC_{50} = 22.6 \mu\text{g/mL}$ and $27.1 \mu\text{g/mL}$), and NO ($IC_{50} < 50.0 \mu\text{g/mL}$) [36]. These data corroborate with other studies in which eugenol demonstrated DPPH sequestering activity with EC_{50} of $22.6 \mu\text{g/mL}$ [37]. In another study, it was able to eliminate about 81% of the DPPH radicals and reduce the potency of the radicals when the concentration decreased from $1.0 \mu\text{M/mL}$ to $0.1 \mu\text{M/mL}$ [38]. Similar data were described in the study by Kim et al., in which eugenol performed the elimination of ABTS free radicals (76.9% at a dose of $20 \mu\text{g/mL}$) and DPPH (90.8% at a dose of $20 \mu\text{g/mL}$) in L-ascorbic acid in 76.9% and 89.9%, respectively [14].

In a comparative study of the antioxidant activity of clove and eugenol, both showed similar activities, with values of sequestering radicals DPPH and ABTS, respectively, $IC_{50} = 0.3257$ and 0.1595 mg/mL for the clove and of $IC_{50} = 0.1967$ and 0.1492 mg/mL for eugenol. Therefore, the antioxidant properties of this essential oil are related to the antioxidant action of its chemical constituent, which is eugenol [13]. The biochemical profile of this compound was confirmed in a study in which the antioxidant activity of eugenol was associated with anti-inflammatory activity. In this approach, Yogalakshmi et al. showed that pretreatment with eugenol ($10.7 \text{ mg/kg.bw/day}$) in rats for 15 days resulted in a decrease in lipid peroxidation indices, protein oxidation, and inflammatory markers (reduction in the expression of COX-2, TNF- α , and IL-6) and by improving antioxidant status by maintaining antioxidants such as glutathione peroxidase (GPx), superoxide dismutase (SOD), catalase (CAT), and glutathione-S-transferase (GST) [39]. Confirming these findings, a study by Kaur et al. showed that pretreatment with eugenol in male Swiss albino mice inhibited the expression of inflammatory markers such as iNOS and COX-2 and the cytokines IL-6, TNF- α , and PGE2, as well as prevented the depletion of antioxidant enzymes and reduced lipid peroxidation (LPO), acting both as anti-inflammatory and antioxidant agents [40]. In fact, eugenol pretreatment, in addition to reducing inflammation caused by lung exposure to LPS, was also able to significantly improve the levels of SOD1, CAT, Gpx1, and GST. Thus, eugenol can be used as an anti-inflammatory agent, as well as protecting the damage caused by oxidative stress [41].

TABLE 1: Modulation of inflammatory response mediated by eugenol.

Experimental model	Animal and/or cells lines	Dose or concentration of eugenol	Inflammatory parameters evaluated	Biological effect	References
<i>In vitro</i> and <i>in vivo</i> leukocyte migration induced by fMLP, LTB ₄ , and carrageenan	BALB/c mice	0.5, 1, 3, 9, or 27 $\mu\text{g}/\text{mL}$ 62.5, 125, or 250 mg/kg	Leukocyte migration	Decreased the number of leukocytes that rolled, adhered, and migrated to perivascular tissue	[50]
Model of allergic asthma	BALB/c mice	10 or 20 mg/kg	Cytokines (IL-4 and IL-5) levels, histological assessment, and VDUP1/NF- κ B signaling pathways	Inhibited OVA-induced eosinophilia, recovered IL-4 and IL-5 levels, inhibited P-I κ B α , NF- κ BP65, and p-NF- κ BP65 protein levels, and increased VDUP1 and I κ B α protein levels.	[51]
LPS-induced inflammatory reaction in acute lung injury	BALB/c mice	5 or 10 mg/kg	Activities of antioxidant enzymes (CAT, SOD, GPx, and GST) and inflammatory markers (MPO, IL-6, and TNF- α) and inflammatory cells recruitment	Reduced the IL-6 and TNF- α expression, suppressed NF- κ B signaling, decreased the leukocyte recruitment, and increased the protein levels (SOD, CAT, GPx, and GST)	[41]
LPS-induced lung injury	BALB/c mice	160 mg/kg body	Inflammatory cells, TNF- α , and NF- κ B levels	Reduced the neutrophil recruitment, macrophages, TNF- α , and NF- κ B expression	[52]
Diesel exhaust particles induced pulmonary damage	BALB/c mice	164 mg/kg	Amounts of polymorpho (PMN) and mononuclear cells, apoptosis, and oxidative stress	Prevented the PMN infiltration, reduced apoptosis through caspase-3 cleavage, but limited the effects on oxidative stress	[53]
Ischemia/reperfusion (I/R) injury	Wistar rats	10 or 100 mg/kg	Inflammatory markers (MPO, TNF- α , and NF- κ B p65) and oxidative stress (GSH and MDA)	Reduced MPO, TNF- α , NF- κ B, and MDA. Eugenol also increased GSH levels.	[54]
Isoproterenol-induced myocardial infarction	Wistar rats	100 mg/kg	Cells inflammatory infiltration, oxidative stress, and protein biomarker (α 1, α 2, β 1, β 2, and γ globulin)	Reduction of inflammatory cells infiltration and mediators proteins, increased SOD, GPx, and GSH, with reduction of TBARS	[55]
LPS-induced inflammatory signaling	Macrophage RAW 264.7	1, 10, 50, or 100 μM	Inflammatory markers (NO, TNF- α , IL-1 β , and NF- κ B), regulatory enzymes (iNOS), and signal transduction (Akt, ERK1/2, JNK, and p38 MAPK)	Reduced NO, TNF- α , IL-1 β , NF- κ B, and iNOS expression. Eugenol also decreased the ERK1/2 and p38 MAPK signaling pathways	[57]
LPS-activated peritoneal macrophages	BALB/c mice	0.31, 0.62, 1.24, or 2.48 $\mu\text{g}/\text{mL}$	COX-2, NF- κ B, and TNF- α expression in resting macrophages	Promoted hypoexpression of TNF- α , but not COX-2 or NF- κ B	[58]
RANKL-induced osteoclast formation	RAW264.7 murine macrophages	50, 100, or 200 μM	Degradation of I κ B α and NF- κ B, MAPK activation	Attenuated the degradation of I κ B α , activation of NF- κ B and MAPK pathways	[5]
Alveolar bone deformities in an ovariectomized (OVX) rodent model	Wistar rats	2.5 or 5 mg/kg	Histopathology and inflammatory mediators (IL-1 β , IL-6, and TNF- α)	Reduced the inflammatory cell infiltrate, IL-1 β , IL-6, and TNF- α levels	[60]
LPS-induced inflammation	Human dental pulp fibroblasts	13 μM	Genes expression (NF- κ B, IL-1 β , and TNF- α)	Inhibition of TNF- α expression and NF- κ B signaling pathway, but not IL-1 β levels	[62]
Cutaneous chemical carcinogenesis	Swiss mice	15% (v/v)	Inflammatory markers (IL-6, TNF- α , PGE ₂ , COX-2, and iNOS) and oxidative stress (MDA, GSH, GPx, GR, CAT, and GST)	Reduced the IL-6, TNF- α , PGE ₂ , COX, and iNOS levels. Eugenol also decreased the MDA levels and increased the GSH content and activities of GR, CAT, GPx, and GST	[40]

TABLE 1: Continued.

Experimental model	Animal and/or cells lines	Dose or concentration of eugenol	Inflammatory parameters evaluated	Biological effect	References
Ability to interfere with cell growth	HeLa cells	300 μ M	Genes expression (COX-2 and IL-1 β)	Reduced the COX-2 and IL-1 β expression	[63]
Cisplatin-mediated toxicity	MDA-MB-231, MDA-MB-468, and BT-20 cells	0.25, 0.50, 0.75, 1.0, or 1.5 μ M	Gene expression (NF- κ B, IL-1 β , and TNF- α)	Reduced NF- κ B, IL-1 β , and TNF- α expression	[23]
Postoperative alveolar osteitis in patients having third molars extracted	Human	0.2% chlorhexidine gel, a eugenol-based paste	Postoperative pain, inflammation, infection, and wound healing	Reduced the incidence of alveolar osteitis, pain, inflammation, infection, and better wound healing compared to control group	[65]
Carrageenan-induced paw edema	Rats	1, 2, or 4%	Paw edema	Inhibited the inflammation, reducing the edema	[64]

3.2. Can Eugenol Reduce the Inflammatory Response via Its Antioxidant Action? Oxidative stress is a condition that reflect an imbalance between biological defensive and aggressive system, mediated by excessive production of reactive oxygen species (ROS), e.g., O²⁻ (superoxide radical), \cdot OH (hydroxyl radical), and H₂O₂ (hydrogen peroxide), in which there is an inability of the antioxidant mechanisms to neutralize them [42]. This process results in toxic effects and alterations of the normal redox state, which is associated with cellular damage and lipid peroxidation [43].

Studies have shown that inflammation and oxidative stress are interconnected phenomena, which are involved in pathological conditions as cardiovascular [44], kidney [45], liver disease [46], and cancer [47]. In this way, during inflammatory events occur exacerbated production of ROS in the damaged inflammatory tissue, which can stimulate and had a critical role in the signaling pathway for inflammatory mediators production, such as proinflammatory cytokines and chemokines, resulting in inflammatory cell migration [48].

Thus, compounds capable of modulating oxidative stress may contribute to reduce critical mediators in inflammatory events act as anti-inflammatory agents, even by indirect way. So, several research groups have demonstrated that eugenol has anti-inflammatory and antioxidant capacity, and therefore, be more effective in reducing inflammation.

3.3. Eugenol Reduces the Inflammatory Response and Ameliorate the Function of Specific Organ. The anti-inflammatory effect of eugenol has been investigated in the leukocytes migration using different stimuli, such as N-formyl-methionyl-leucyl-phenylalanine (fMPLP), leukotriene B₄ (LTB₄), and carrageenan. Polymorphonuclear (PMN) recruitment to the inflammatory site occurs dependent on a complex response involving the endothelium-leukocyte interactions and subsequent extravasation to the inflamed site [49]. In this background, Estevão-Silva and colleagues [50] demonstrated that eugenol significantly decreased the *in vitro* and *in vivo* leukocytes migration in response to chemotactic factors by the modulation of rolling and adherence to perivascular tissue. In addition, the authors showed that

eugenol did not induce changes in cell viability, which suggest absence of toxic effect [50].

Additionally, Pan and Dong [51], using an experimental model of allergic asthma induced by ovalbumin (OVA), demonstrated that eugenol administration inhibited the OVA-induced eosinophilia in the lung tissue, prevented the increased of IL-4 and IL-5 levels, and reduced the NF- κ B signaling pathways. According to the authors, the inflammatory response reduction had a pivot role in the antiasthmatic effect of eugenol, resulting in the decrease of airway resistance (AWR) [51]. This data suggests that eugenol can be a therapeutic and strategic agent in patients with asthma.

Eugenol also has anti-inflammatory activity on lipopolysaccharide- (LPS-) induced acute lung injury. Pretreatment with eugenol inhibited the inflammatory response and leukocyte recruitment into the lung tissue by the downregulation of proinflammatory cytokines (IL-6 and TNF- α) expression and NF- κ B signaling. In addition, eugenol also increased the superoxide dismutase (SOD), catalase (CAT), glutathione peroxidase (GPx), and glutathione-S-transferase (GST), which are important antioxidative enzymes [41]. Similarly, Magalhães and colleagues [52], using an animal model of LPS-induced lung injury for 6 hours, demonstrated that eugenol significantly reduced neutrophil infiltration, TNF- α , and the NF- κ B-mediated signaling pathway, decreasing the lung inflammation, resulting in an improved lung structure and function, which suggest an important drug to treat disorders of lung inflammatory diseases [52].

So, eugenol reduces the inflammatory response in animal model pulmonary damage caused by diesel exhaust particles. Eugenol administration reduced the pulmonary inflammation by inhibiting the PMN infiltration and apoptosis through caspase-3 cleavage but limited the effects against oxidative stress. This resulted in the improvement of airspace collapse and pulmonary mechanics, which are evaluated by pneumotachography and altered by diesel particles [53]. These data demonstrated the potential of eugenol as an agent to treat the damage effects of air pollutant exposure, by mechanisms mediated, at the last in part, of its anti-inflammatory effects.

Motteleb and colleagues (2014) conducted a study using eugenol to assess its efficacy in the prevention of liver damage in a model of ischemia and reperfusion (I/R). In this work, eugenol abolished the inflammation, reduced myeloperoxidase (MPO) activity, TNF- α levels, and NF- κ B expression, and altered oxidative marker. It also reduced malondialdehyde (MDA) and increased GSH levels. This potent effect of eugenol resulted in the amelioration of hepatic structural and functional damage [54]. Thus, eugenol reduced the liver damage by the reduction of inflammatory mediators and modulation of redox status, suggesting a possible application against hepatic I/R injury.

Eugenol also was evaluated as preventive agent against cardiac remodeling following myocardial infarction. This pathology was induced using isoproterenol, which eugenol reduced inflammatory mediator's proteins and lipid peroxidation as well as increased antioxidative enzymes markers (i.e., SOD, GPx, and GSH). In this study, eugenol reduced cardiac injury biomarkers, such as troponin-T, creatine kinase-muscle/brain (CK-MB), and LDH, resulting in the improvement of electrocardiographic and hemodynamic parameters, and great potential antithrombotic, anti-inflammatory, and anti-ischemic activities [55].

3.4. Eugenol Inhibits the Liberation of Inflammatory Mediators from Macrophages. Macrophage is one of the immune system cells that contribute to the production of mediators (i.e., proinflammatory cytokines and nitric oxide), which are important to cellular and vascular events during the installation and progression of inflammatory process [56]. Thus, studies have demonstrated that eugenol can modulate the macrophage functions and regulates negatively the inflammation.

Yeh and colleagues demonstrated that eugenol inhibits the inducible nitric oxide synthase (iNOS) expression from macrophages in response to LPS, culminating in the reduction of NO levels. Additionally, eugenol also reduced the TNF- α and IL-1 β as well as the NF- κ B, ERK1/2, and p38 MAPK signaling pathways [57]. In other study, de Paula Porto and colleagues [58] also reported that eugenol promotes the downregulation of TNF- α in LPS-activated macrophages, which are associated with antigenotoxic activity when DNA damage was induced with doxorubicin (DXR) [58]. Thus, this data suggests that the molecular mechanisms to anti-inflammatory effects of eugenol are mediated by the regulation of inflammatory mediators production from macrophages.

3.5. Anti-inflammatory Effect of Eugenol Modulates the Bone Remodeling. Several research groups have described the effect of eugenol as anti-inflammatory agent and its role modulator on bone remodeling. Deepak and colleagues [59], using cell culture preexposed to RANKL (a receptor activator of NF- κ B ligand), demonstrated that eugenol prevented the osteoclast differentiation in a dose-dependent manner. Among the molecular mechanisms involved, the authors emphasized the downregulation of NF- κ B and MAPKs signaling pathways, which suggest its use in bone remodeling disorders, such as osteoporosis [59]. A recent study demonstrated that

eugenol administration for twelve weeks attenuated the alveolar bone loss and remodeling associated with estrogen insufficiency using an ovariectomized (OVX) rat model, which is similar to what occurs after menopause in humans. The authors suggested that anti-inflammatory effect of eugenol had primary importance, since it was accompanied by the reduction of IL-1 β , IL-6, and TNF- α levels resulting in the reduction of inflammatory cell [60].

Additionally, the effects of eugenol against inflammatory response also have been investigated in dental pulp fibroblasts from extracted third molars. During permanent teeth extractions arise postoperative complications, such as alveolar osteitis, an inflammatory condition with delayed healing and persistent pain [61]. In this context, Martínez-Herrera and colleagues [62] reported that eugenol inhibited TNF- α expression and NF- κ B signaling pathway, but not IL-1 β , when fibroblasts was exposed to LPS, confirming its anti-inflammatory property in bone disorders. Curiously, eugenol also induced inflammatory gene mild expression in fibroblasts absence of previous inflammation [62].

3.6. The Antitumor Effect of Eugenol Appears to Be Mediated, in Part, by Its Anti-inflammatory Activity. Kaur and colleagues [40] demonstrated that eugenol prevents the 7,12-dimethylbenz[a]anthracene- (DMBA-) and 12-O-tetradecanoylphorbol-13-acetate- (TPA-) promoted skin carcinogenesis. According to the authors, the molecular mechanism of eugenol is related to its anti-inflammatory properties, since reduced proinflammatory cytokine levels (i.e., IL-6 and TNF- α) and inflammation enzymes marker (COX and iNOS) are associated with the modulation of redox status (Figure 2) with reduced MDA and increased antioxidative enzymes [40]. Thus, these data strongly suggest the chemotherapeutic potential of eugenol against carcinogenesis. In accordance with these data, studies have evaluated the efficacy of eugenol alone or combined with other agents. Using HeLa cells, a human cervical cancer line, Hussain and colleagues [63] demonstrated that eugenol alone promoted cell growth inhibition and increase the therapeutic efficacy when combined with gemcitabine (a standard drug). In the clinical use, it can decrease the side effects promoted by gemcitabine administration. These beneficial effects appear to be mediated by its antiapoptotic and anti-inflammatory effects, since it were associated with increased caspase-3 activity and reduction of COX-2 and IL-1 β expression, respectively [63]. Additionally, a recent study reported that eugenol promotes cytotoxicity against breast cancer cells (TNBC) and animal model and synergistic chemotherapeutic effects with cisplatin. A key point in this effect was the inhibition of the NF- κ B signaling pathway, which resulted in the inhibition of the p50 and p65 subunits phosphorylation, and its consequence migration to the cellular nucleus, reducing IL-6 and IL-8 levels [23].

3.7. Eugenol-Based Pharmaceutical Formulation and Its Anti-inflammatory Effects. From the pharmacological potential of eugenol in the modulation of inflammation, its use has also been tested in pharmaceutical formulations. Experimentally, Esmaeili and colleagues [64], using an animal model of

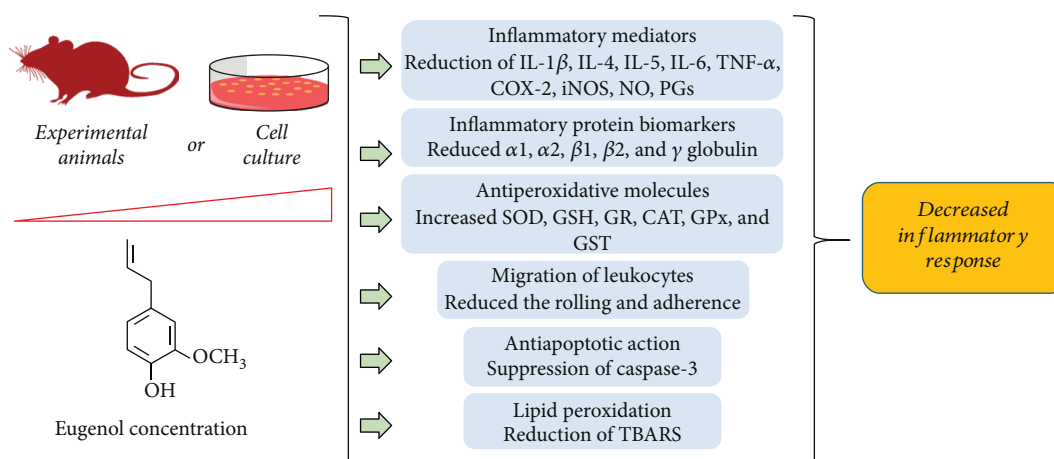


FIGURE 2: The effect of eugenol in the inflammation control.

carrageenan-induced edema, reported that a nano-emulsion containing 1%, 2%, and 4% of eugenol reduced the edema formation and has increased efficacy when combined with piroxicam, revealing a synergistic anti-inflammatory effect.

Additionally, a clinical dental study involving 270 patients having third molars extracted demonstrated that 0.2% chlorhexidine gel, a eugenol-based paste, reduced post-operative alveolar osteitis, pain, and time of wound healing compared to control group, but with better results when applied in two interventions [65].

3.8. Toxicity of Eugenol. Eugenol is known for its antioxidant, anti-inflammatory, antimicrobial, and antitumor activities; however, it may present some toxicity depending on the type of histological structure exposed to this compound and the concentration used [66]. Thus, eugenol toxicity was observed in human dental pulp fibroblasts from deciduous teeth, with DNA damage at concentrations ranging from 0.06–5.1 μ M, which was not observed at higher interval concentrations of 320 to 818 μ M [67]. Eugenol was also able to induce genotoxicity by inducing DNA damage of mouse peritoneal macrophages at all concentrations tested (0.62, 1.24, and 2.48 mg/mL). However, it has demonstrated antigenotoxic potential depending on the treatment protocol, which may be interlinked with its effect on drug metabolism [58]. Therefore, eugenol can modulate inflammatory and oxidizing processes. However, its use must be made according to the therapeutic safety evidenced in toxicity.

4. Conclusions

This review demonstrates that eugenol exerts a beneficial action on oxidative stress through the inhibition of enzymes and oxidative processes, which is related to the anti-inflammatory drug profile of this compound. The set of pharmacological studies reported evidences of the clinical potential of eugenol for the treatment of diseases associated with oxidative stress and inflammatory response. Considering the presence of this compound in foods and medicinal plants, the use of these vegetables can result in health benefits and consequently improvement in the quality of life.

However, advanced investigations are needed to understand its metabolism in the body and the contribution of metabolites in antioxidant action and possible interactions in receptors related to inflammation.

Abbreviations

ALDH:	Aldehyde dehydrogenase
AP-I:	Activating protein 1
AWR:	Airway resistance
Bcl-2:	B-cell lymphoma 2, apoptosis regulator
CAT:	Catalase
CK-MB:	Creatine kinase-muscle/brain
COX-2:	Cyclooxygenase-2
DNA:	Deoxyribonucleic acid
DMBA:	7,12-dimethylbenz[a]anthracene
DXR:	Doxorubicin
EC ₃ :	Estimated concentration
fMLP:	Formyl-methionyl-leucyl-phenylalanine
GPx:	Glutathione peroxidase
GSH:	Reduced glutathione
GST:	Glutathione-S-transferase
IFN- γ :	Interferon gamma
IL-1:	Interleukin-1
IL-2:	Interleukin-2
IL-4:	Interleukin-4
IL-5:	Interleukin-5
IL-6:	Interleukin-6
IL-8:	Interleukin-8
IL-18:	Interleukin-18
IL-1 β :	Interleukin 1 beta
iNOS:	Inducible nitric oxide synthase
LPS:	Lipopolysaccharide
LTB ₄ :	Leukotriene B ₄
MAPK:	Mitogen-activated protein kinase pathways
MDA:	Malondialdehyde
MPO:	Myeloperoxidase
NSAIDs:	Nonsteroidal anti-inflammatory drugs
NF- κ B:	Nuclear factor kappa B
NO:	Nitric oxide
OVA:	Ovalbumin

OVX: Ovariectomized
 PGE: Prostaglandins
 PGE2: Prostaglandins-2
 PMN: Polymorphonuclear
 RANKL: Receptor activator of NF- κ B ligand
 SI: Stimulation indices
 SOD: Dismutase
 TH1: T helper type 1
 TH2: T helper type 2
 TNF- α : Tumor necrosis factor α
 TNBC: Cytotoxicity against breast cancer cells
 TPA: 12-O-tetradecanoylphorbol-13-acetate
 TRAP: Acid phosphatase assay.

Conflicts of Interest

The authors declare that there is no conflict of interest regarding the publication of this paper.

Acknowledgments

This work was supported by the Brazilian agencies: Conselho Nacional de Desenvolvimento Científico e Tecnológico (CNPq) and Coordenação de Aperfeiçoamento de Pessoal de Nível Superior (CAPES).

References

- [1] P. Zhang, E. Zhang, M. Xiao, C. Chen, and W. Xu, "Study of anti-inflammatory activities of α -d-glucosylated eugenol," *Archives of Pharmacol Research*, vol. 36, no. 1, pp. 109–115, 2013.
- [2] H. Zhang, X. Chen, and J. J. He, "Pharmacological action of clove oil and its application in oral care products," *Oral Care Industry*, vol. 19, pp. 23–24, 2009.
- [3] D. Chatterjee and P. Bhattacharjee, "Use of eugenol-lean clove extract as a flavoring agent and natural antioxidant in mayonnaise: product characterization and storage study," *Journal of Food Science and Technology*, vol. 52, no. 8, pp. 4945–4954, 2015.
- [4] K. G. Lee and T. Shibamoto, "Antioxidant properties of aroma compounds isolated from soybeans and mung beans," *Journal of Agricultural and Food Chemistry*, vol. 48, no. 9, pp. 4290–4293, 2000.
- [5] G. Charalambous, Ed., *The Quality of Foods and Beverages VI: Chemistry and Technology*, Elsevier, 2012.
- [6] M. Marotti, R. Piccaglia, and E. Giovanelli, "Differences in essential oil composition of basil (*Ocimum basilicum* L.) Italian cultivars related to morphological characteristics," *Journal of Agricultural and Food Chemistry*, vol. 44, no. 12, pp. 3926–3929, 2005.
- [7] W. Bin-Nan, H. Tsong-Long, L. Ching-Fong, and C. Ing-Jun, "Vaninolol: a new selective β 1-adrenoceptor antagonist derived from vanillin," *Biochemical Pharmacology*, vol. 48, no. 1, pp. 101–109, 1994.
- [8] D. P. Bezerra, G. C. G. Militão, M. C. de Moraes, and D. P. de Sousa, "The dual antioxidant/prooxidant effect of eugenol and its action in cancer development and treatment," *Nutrients*, vol. 9, no. 12, p. 1367, 2017.
- [9] M. J. Jordán, K. Tandon, P. E. Shaw, and K. L. Goodner, "Aromatic profile of aqueous banana essence and banana fruit by gas chromatography-mass spectrometry (GC-MS) and gas chromatography-olfactometry (GC-O)," *Journal of Agricultural and Food Chemistry*, vol. 49, no. 10, pp. 4813–4817, 2001.
- [10] M. J. N. Diógenes and F. J. A. Matos, "Dermatite de contato por plantas (DCP)," *Anais Brasileiros De Dermatologia*, vol. 74, no. 6, pp. 629–634, 1999.
- [11] M. Sedighi, A. Nazari, M. Faghihi et al., "Protective effects of cinnamon bark extract against ischemia-reperfusion injury and arrhythmias in rat," *Phytotherapy Research*, vol. 32, no. 10, pp. 1983–1991, 2018.
- [12] S. J. Lee and K. G. Lee, "Inhibitory effects of volatile antioxidants found in various beans on malonaldehyde formation in horse blood plasma," *Food and Chemical Toxicology*, vol. 43, no. 4, pp. 515–520, 2005.
- [13] A. L. Dawidowicz and M. Olszowy, "Does antioxidant properties of the main component of essential oil reflect its antioxidant properties? The comparison of antioxidant properties of essential oils and their main components," *Natural Product Research*, vol. 28, no. 22, pp. 1952–1963, 2014.
- [14] D.-Y. Kim, K.-J. Won, D. I. Hwan, S. M. Park, B. Kim, and H. M. Lee, "Chemical composition, antioxidant and anti-melanogenic activities of essential oils from *Chrysanthemum boreale* Makino at different harvesting stages," *Chemistry & Biodiversity*, vol. 15, no. 2, article e1700506, 2018.
- [15] X. Han and T. L. Parker, "Anti-inflammatory activity of clove (*Eugenia caryophyllata*) essential oil in human dermal fibroblasts," *Pharmaceutical Biology*, vol. 55, no. 1, pp. 1619–1622, 2017.
- [16] L. Ferrero-Miliani, O. H. Nielsen, P. S. Andersen, and S. E. Girardin, "Chronic inflammation: importance of NOD2 and NALP3 in interleukin-1 β generation," *Clinical and Experimental Immunology*, vol. 147, no. 2, pp. 227–235, 2007.
- [17] R. de Cássia da Silveira e Sá, L. N. Andrade, and D. P. de Sousa, "A review on anti-inflammatory activity of monoterpenes," *Molecules*, vol. 18, no. 1, pp. 1227–1254, 2013.
- [18] R. Cássia da Silveira e Sá, L. N. Andrade, and D. P. de Sousa, "Anti-inflammation activities of essential oil and its constituents from indigenous cinnamon (*Cinnamomum osmophloeum*) twigs," *Bioresource Technology*, vol. 99, no. 9, pp. 3908–3913, 2008.
- [19] M. J. Stone, "Regulation of chemokine-receptor interactions and functions," *International Journal of Molecular Sciences*, vol. 18, no. 11, article 2415, 2017.
- [20] I. T. Nizamutdinova, G. F. Dusio, O. Y. Gasheva et al., "Mast cells and histamine are triggering the NF- κ B-mediated reactions of adult and aged perilymphatic mesenteric tissues to acute inflammation," *Aging*, vol. 8, no. 11, article 3065, 3090 pages, 2016.
- [21] J. Wang, Y. T. Liu, L. Xiao, L. Zhu, Q. Wang, and T. Yan, "Anti-inflammatory effects of apigenin in lipopolysaccharide-induced inflammatory in acute lung injury by suppressing COX-2 and NF- κ B pathway," *Inflammation*, vol. 37, no. 6, pp. 2085–2090, 2014.
- [22] F. Polesso, M. Sarker, A. Anderson, D. C. Parker, and S. E. Murray, "Constitutive expression of NF- κ B inducing kinase in regulatory T cells impairs suppressive function and promotes instability and pro-inflammatory cytokine production," *Scientific Reports*, vol. 7, no. 1, article 14779, 2017.
- [23] S. S. Islam, I. Al-Sharif, A. Sultan, A. Al-Mazrou, A. Remmal, and A. Aboussekhra, "Eugenol potentiates cisplatin anti-cancer activity through inhibition of ALDH-positive breast

- cancer stem cells and the NF- κ B signaling pathway," *Molecular Carcinogenesis*, vol. 57, no. 3, pp. 333–346, 2018.
- [24] B. L. Bermas, "Non-steroidal anti-inflammatory drugs, glucocorticoids and disease modifying anti-rheumatic drugs for the management of rheumatoid arthritis before and during pregnancy," *Current Opinion in Rheumatology*, vol. 26, no. 3, pp. 334–340, 2014.
- [25] J. D. Rajput, S. D. Bagul, U. D. Pete, C. M. Zade, S. B. Padhye, and R. S. Bendre, "Perspectives on medicinal properties of natural phenolic monoterpenoids and their hybrids," *Molecular Diversity*, vol. 22, no. 1, pp. 225–245, 2018.
- [26] D. P. Sousa, *Medicinal Essential Oils: Chemical, Pharmacological and Therapeutic Aspects*, Nova Science Publishers, 2012.
- [27] R. de Cássia da Silveira e Sá, L. N. Andrade, R. dos Reis Barreto de Oliveira, and D. P. de Sousa, "A review on anti-inflammatory activity of phenylpropanoids found in essential oils," *Molecules*, vol. 19, no. 2, pp. 1459–1480, 2014.
- [28] S. S. Kim, O. J. Oh, H. Y. Min et al., "Eugenol suppresses cyclooxygenase-2 expression in lipopolysaccharide-stimulated mouse macrophage RAW264. 7 cells," *Life Sciences*, vol. 73, no. 3, pp. 337–348, 2003.
- [29] E. Dervis, A. Yurt Kilcar, E. I. Medine et al., "In vitro incorporation of radioiodinated eugenol on adenocarcinoma cell lines (Caco2, MCF7, and PC3)," *Cancer Biotherapy & Radiopharmaceuticals*, vol. 32, no. 3, pp. 75–81, 2017.
- [30] S. F. Hamed, Z. Sadek, and A. Edris, "Antioxidant and antimicrobial activities of clove bud essential oil and eugenol nanoparticles in alcohol-free microemulsion," *Journal of Oleo Science*, vol. 61, no. 11, pp. 641–648, 2012.
- [31] E. Darvishi, M. Omid, A. A. S. Bushehri, A. Golshani, and M. L. Smith, "The antifungal eugenol perturbs dual aromatic and branched-chain amino acid permeases in the cytoplasmic membrane of yeast," *PLoS One*, vol. 8, no. 10, p. e76028, 2013.
- [32] J.-P. Dai, X. F. Zhao, J. Zeng et al., "Drug screening for autophagy inhibitors based on the dissociation of Beclin1-Bcl2 complex using BiFC technique and mechanism of eugenol on anti-influenza A virus activity," *PLoS One*, vol. 8, no. 4, article e61026, 2013.
- [33] Y. A. Taher, A. M. Samud, F. E. El-Taher et al., "Experimental evaluation of anti-inflammatory, antinociceptive and antipyretic activities of clove oil in mice," *Libyan Journal of Medicine*, vol. 10, no. 1, article 28685, 2015.
- [34] H. Tsuchiya, "Anesthetic agents of plant origin: a review of phytochemicals with anesthetic activity," *Molecules*, vol. 22, no. 8, p. 1369, 2017.
- [35] B. Baldisserotto, T. V. Parodi, and E. D. Stevens, "Lack of post-exposure analgesic efficacy of low concentrations of eugenol in zebrafish," *Veterinary Anaesthesia and Analgesia*, vol. 45, no. 1, pp. 48–56, 2018.
- [36] R. Perez-Roses, E. Risco, R. Vila, P. Penalver, and S. Canigual, "Biological and nonbiological antioxidant activity of some essential oils," *Journal of Agricultural and Food Chemistry*, vol. 64, no. 23, pp. 4716–4724, 2016.
- [37] L. L. Zhang, L. F. Zhang, J. G. Xu, and Q. P. Hu, "Comparison study on antioxidant, DNA damage protective and antibacterial activities of eugenol and isoeugenol against several food-borne pathogens," *Food & Nutrition Research*, vol. 61, no. 1, article 1353356, 2017.
- [38] U. K. Sharma, A. K. Sharma, and A. K. Pandey, "Medicinal attributes of major phenylpropanoids present in cinnamon," *BMC Complementary and Alternative Medicine*, vol. 16, no. 1, p. 156, 2016.
- [39] B. Yogalakshmi, P. Viswanathan, and C. V. Anuradha, "Investigation of antioxidant, anti-inflammatory and DNA-protective properties of eugenol in thioacetamide-induced liver injury in rats," *Toxicology*, vol. 268, no. 3, pp. 204–212, 2010.
- [40] G. Kaur, M. Athar, and M. S. Alam, "Eugenol precludes cutaneous chemical carcinogenesis in mouse by preventing oxidative stress and inflammation and by inducing apoptosis," *Molecular Carcinogenesis*, vol. 49, no. 3, pp. 290–301, 2010.
- [41] X. Huang, Y. Liu, Y. Lu, and C. Ma, "Anti-inflammatory effects of eugenol on lipopolysaccharide-induced inflammatory reaction in acute lung injury via regulating inflammation and redox status," *International Immunopharmacology*, vol. 26, no. 1, pp. 265–271, 2015.
- [42] P. Patlevič, J. Vašková, P. Švorc Jr, L. Vaško, and P. Švorc, "Reactive oxygen species and antioxidant defense in human gastrointestinal diseases," *Integrative Medicine Research*, vol. 5, no. 4, pp. 250–258, 2016.
- [43] A. Ayala, M. F. Muñoz, and S. Argüelles, "Lipid peroxidation: production, metabolism, and signaling mechanisms of malondialdehyde and 4-hydroxy-2-nonenal," *Oxidative Medicine and Cellular Longevity*, vol. 2014, Article ID 360438, 31 pages, 2014.
- [44] N. García, C. Zazueta, and L. Aguilera-Aguirre, "Oxidative stress and inflammation in cardiovascular disease," *Oxidative Medicine and Cellular Longevity*, vol. 2017, Article ID 5853238, 2 pages, 2017.
- [45] S. K. Biswas, J. B. Lopes De Faria, S. K. Biswas, and J. B. Lopes De Faria, "Which comes first: renal inflammation or oxidative stress in spontaneously hypertensive rats?," *Free Radical Research*, vol. 41, no. 2, pp. 216–224, 2007.
- [46] A. Ambade and P. Mandrekar, "Oxidative stress and inflammation: essential partners in alcoholic liver disease," *International Journal of Hepatology*, vol. 2012, Article ID 853175, 9 pages, 2012.
- [47] S. Reuter, S. C. Gupta, M. M. Chaturvedi, and B. B. Aggarwal, "Oxidative stress, inflammation, and cancer: how are they linked?," *Free Radical Biology and Medicine*, vol. 49, no. 11, pp. 1603–1616, 2010.
- [48] T. Hussain, B. Tan, Y. Yin, F. Blachier, M. C. B. Tossou, and N. Rahu, "Oxidative stress and inflammation: what polyphenols can do for us?," *Oxidative Medicine and Cellular Longevity*, vol. 2016, Article ID 7432797, 9 pages, 2016.
- [49] H. U. von Andrian, J. D. Chambers, L. M. McEvoy, R. F. Bargatzke, K. E. Arfors, and E. C. Butcher, "Two-step model of leukocyte-endothelial cell interaction in inflammation: distinct roles for LECAM-1 and the leukocyte beta 2 integrins in vivo," *Proceedings of the National Academy of Sciences*, vol. 88, no. 17, pp. 7538–7542, 1991.
- [50] C. F. Estevão-Silva, R. Kummer, F. C. Fachini-Queiroz et al., "Anethole and eugenol reduce in vitro and in vivo leukocyte migration induced by fMLP, LTB₄, and carrageenan," *Journal of Natural Medicines*, vol. 68, no. 3, pp. 567–575, 2014.
- [51] C. Pan and Z. Dong, "Antiasthmatic effects of eugenol in a mouse model of allergic asthma by regulation of vitamin D₃ upregulated protein 1/NF- κ B pathway," *Inflammation*, vol. 38, no. 4, pp. 1385–1393, 2015.
- [52] C. B. Magalhães, D. R. Riva, L. J. DePaula et al., "In vivo anti-inflammatory action of eugenol on lipopolysaccharide-

- induced lung injury,” *Journal of Applied Physiology*, vol. 108, no. 4, pp. 845–851, 2010.
- [53] W. A. Zin, A. G. L. S. Silva, C. B. Magalhães et al., “Eugenol attenuates pulmonary damage induced by diesel exhaust particles,” *Journal of Applied Physiology*, vol. 112, no. 5, pp. 911–917, 2012.
- [54] D. M. Abd el Motteleb, S. A. Selim, and A. M. Mohamed, “Differential effects of eugenol against hepatic inflammation and overall damage induced by ischemia/re-perfusion injury,” *Journal of Immunotoxicology*, vol. 11, no. 3, pp. 238–245, 2014.
- [55] K. Mnafigui, R. Hajji, F. Derbali et al., “Anti-inflammatory, antithrombotic and cardiac remodeling preventive effects of eugenol in isoproterenol-induced myocardial infarction in Wistar rat,” *Cardiovascular Toxicology*, vol. 16, no. 4, pp. 336–344, 2016.
- [56] G. Arango Duque and A. Descoteaux, “Macrophage cytokines: involvement in immunity and infectious diseases,” *Frontiers in Immunology*, vol. 5, p. 491, 2014.
- [57] J. L. Yeh, J. H. Hsu, Y. S. Hong et al., “Eugenol and glyceryl-isoegenol suppress LPS-induced iNOS expression by down-regulating NF- κ B AND AP-1 through inhibition of MAPKS and AKT/ κ B α signaling pathways in macrophages,” *International Journal of Immunopathology and Pharmacology*, vol. 24, no. 2, pp. 345–356, 2011.
- [58] M. de Paula Porto, G. N. Da Silva, B. C. O. Luperini et al., “Citral and eugenol modulate DNA damage and pro-inflammatory mediator genes in murine peritoneal macrophages,” *Molecular Biology Reports*, vol. 41, no. 11, pp. 7043–7051, 2014.
- [59] V. Deepak, A. Kasonga, M. C. Kruger, and M. Coetzee, “Inhibitory effects of eugenol on RANKL-induced osteoclast formation via attenuation of NF- κ B and MAPK pathways,” *Connective Tissue Research*, vol. 56, no. 3, pp. 195–203, 2015.
- [60] H. M. Abuohashish, D. A. Khairy, M. M. Abdelsalam, A. Alsayyah, M. M. Ahmed, and S. S. Al-Rejaie, “In-vivo assessment of the osteo-protective effects of eugenol in alveolar bone tissues,” *Biomedicine & Pharmacotherapy*, vol. 97, pp. 1303–1310, 2018.
- [61] S. Faizel, S. Thomas, V. Yuvaraj, S. Prabhu, and G. Tripathi, “Comparison between neocone, alvogyl and zinc oxide eugenol packing for the treatment of dry socket: a double blind randomised control trial,” *Journal of Maxillofacial and Oral Surgery*, vol. 14, no. 2, pp. 312–320, 2015.
- [62] A. Martínez-Herrera, A. Pozos-Guillén, S. Ruiz-Rodríguez, A. Garrocho-Rangel, A. Vértiz-Hernández, and D. M. Escobar-García, “Effect of 4-allyl-1-hydroxy-2-methoxybenzene (eugenol) on inflammatory and apoptosis processes in dental pulp fibroblasts,” *Mediators of Inflammation*, vol. 2016, Article ID 9371403, 7 pages, 2016.
- [63] A. Hussain, K. Brahmabhatt, A. Priyani, M. Ahmed, T. A. Rizvi, and C. Sharma, “Eugenol enhances the chemotherapeutic potential of gemcitabine and induces anticarcinogenic and anti-inflammatory activity in human cervical cancer cells,” *Cancer Biotherapy and Radiopharmaceuticals*, vol. 26, no. 5, pp. 519–527, 2011.
- [64] F. Esmaeili, S. Rajabnejhad, A. R. Partoazar et al., “Anti-inflammatory effects of eugenol nanoemulsion as a topical delivery system,” *Pharmaceutical Development and Technology*, vol. 21, no. 7, pp. 887–893, 2016.
- [65] J. S. Jesudasan, P. U. A. Wahab, and M. R. M. Sekhar, “Effectiveness of 0.2% chlorhexidine gel and a eugenol-based paste on postoperative alveolar osteitis in patients having third molars extracted: a randomised controlled clinical trial,” *British Journal of Oral and Maxillofacial Surgery*, vol. 53, no. 9, pp. 826–830, 2015.
- [66] Y. H. Shih, D. J. Lin, K. W. Chang et al., “Evaluation physical characteristics and comparison antimicrobial and anti-inflammation potentials of dental root canal sealers containing hinokitiol *in vitro*,” *PLoS One*, vol. 9, no. 6, article e94941, 2014.
- [67] M. Escobar-García, K. Rodríguez-Contreras, S. Ruiz-Rodríguez, M. Pierdant-Pérez, B. Cerda-Cristerna, and A. Pozos-Guillén, “Eugenol toxicity in human dental pulp fibroblasts of primary teeth,” *Journal of Clinical Pediatric Dentistry*, vol. 40, no. 4, pp. 312–318, 2016.

Research Article

Falcarinol Is a Potent Inducer of Heme Oxygenase-1 and Was More Effective than Sulforaphane in Attenuating Intestinal Inflammation at Diet-Achievable Doses

Amanda L. Stefanson  and Marica Bakovic 

Department of Human Health and Nutritional Sciences, 50 Stone Rd E, University of Guelph, Guelph, ON, Canada N1G 2W1

Correspondence should be addressed to Marica Bakovic; mbakovic@uoguelph.ca

Received 11 May 2018; Revised 20 August 2018; Accepted 2 September 2018; Published 21 October 2018

Guest Editor: Felipe L. de Oliveira

Copyright © 2018 Amanda L. Stefanson and Marica Bakovic. This is an open access article distributed under the Creative Commons Attribution License, which permits unrestricted use, distribution, and reproduction in any medium, provided the original work is properly cited.

Nuclear factor- (erythroid-derived 2) like 2 (Nrf2) is a transcription factor that regulates the expression of a battery of antioxidant, anti-inflammatory, and cytoprotective enzymes including heme oxygenase-1 (Hmox1, Ho-1) and NADPH:quinone oxidoreductase-1 (Nqo1). The isothiocyanate sulforaphane (SF) is widely understood to be the most effective natural activator of the Nrf2 pathway. Falcarinol (FA) is a lesser studied natural compound abundant in medicinal plants as well as dietary plants from the *Apiaceae* family such as carrot. We evaluated the protective effects of FA and SF (5 mg/kg twice per day in CB57BL/6 mice) pretreatment for one week against acute intestinal and systemic inflammation. The phytochemical pretreatment effectively reduced the magnitude of intestinal proinflammatory gene expression (IL-6, $Tnf\alpha/Tnf\alpha$, $Infy$, STAT3, and IL-10/IL-10r) with FA showing more potency than SF. FA was also more effective in upregulating Ho-1 at mRNA and protein levels in both the mouse liver and the intestine. FA but not SF attenuated plasma chemokine eotaxin and white blood cell growth factor GM-CSF, which are involved in the recruitment and stabilization of first-responder immune cells. Phytochemicals generally did not attenuate plasma proinflammatory cytokines. Plasma and intestinal lipid peroxidation was also not significantly changed 4 h after LPS injection; however, FA did reduce basal lipid peroxidation in the mesentery. Both phytochemical pretreatments protected against LPS-induced reduction in intestinal barrier integrity, but FA additionally reduced inflammatory cell infiltration even below negative control.

1. Introduction

The gastrointestinal (GI) tract is the largest interface between the body and the environment, followed by the lung and the integument, with ratios of an estimated surface area approximately 150 : 50 : 1. The small intestine is the majority component of the GI tract; its surface was composed of a single monolayer of intestinal epithelial cells which secrete a glycocalyx matrix and a layer of mucous. This delicate barrier performs the diametric roles of digestion and absorption of nutrients and protection against pathogenic microorganisms and innumerable xenobiotic compounds from the environment [1]. In addition, the small intestine is the organ of first pass detoxification [2] and provides the milieu for a large proportion of the immune system [1, 3]. Likely due to this

challenging physiological role, small intestinal epithelial cells have the highest turnover rates and are replaced every 2–6 days [4]. It is recognized that chronic and degenerative disease is rooted in early deviations from normal homeostasis that underpin the development of a wide variety of disparate disease pathologies. For example, unresolved inflammation contributes to cardiovascular disease, type 2 diabetes, metabolic syndrome, and neurodegenerative disease to name only a few. Intestinal barrier integrity is a lesser appreciated early deviation from homeostasis that contributes to many intestinal diseases (IBD, IBS, and celiac disease to name a few [5–7]) but also many other widely divergent pathologies. Barrier integrity has been implicated in autoimmune diseases, food allergies, obesity, endotoxemia, and chronic inflammation [5, 8, 9]. In fact, intestinal barrier function is very

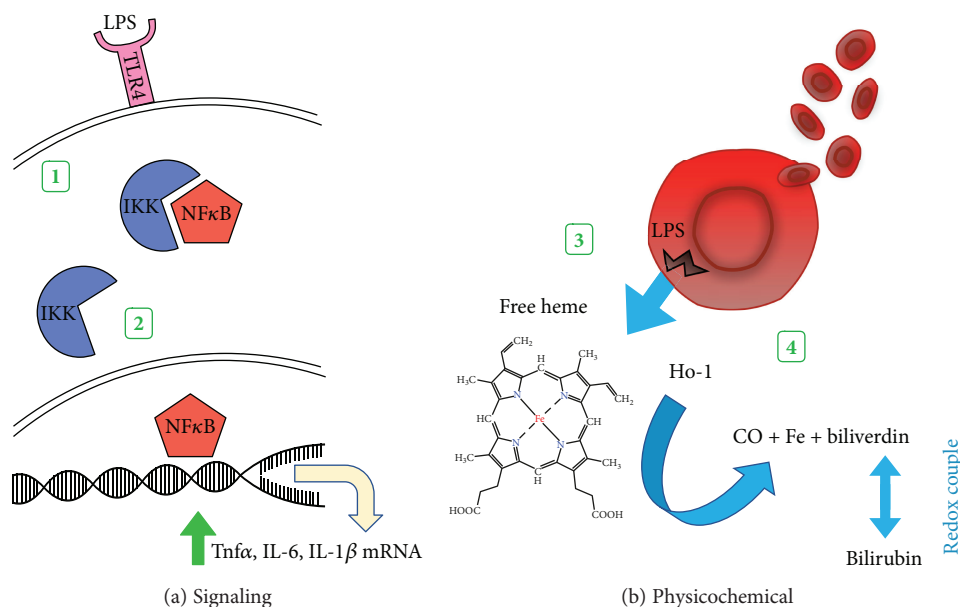


FIGURE 1: Effects of LPS. (1) LPS binding to the toll-like receptor-4 (TLR4) receptor initiates signaling to disrupt the inhibitor protein IKK association with proinflammation transcription factor NFκB. (2) Free NFκB translocates to the nucleus to increase the transcription of proinflammatory cytokines Tnfα, IL-6, IL-1β, etc. (3) LPS causes plasma membrane disruption in red blood cells releasing free heme. (4) Ho-1 breaks down free heme to equimolar amounts of CO, Fe, and biliverdin which is enzymatically converted to bilirubin, forming a redox couple.

sensitive to seemingly unrelated traumas such as burn injury [10–12], hemorrhagic shock [13, 14], and even intense exercise [15–19].

Intraperitoneal lipopolysaccharide (LPS) is absorbed in the tissues of the peritoneal space, making its way into systemic circulation, where it is rapidly cleared from the bloodstream (minutes to hours [20, 21]) and slowly (over days [22, 23]) excreted from the organism in bile through liver metabolism, in the urine through kidney filtration, but also through the shedding of epithelial cells at the villus tip in the small intestine. The liver clears two thirds of circulating LPS via sinusoidal endothelial cells and Kupffer cells [21], which is then secreted into the intestine via the bile [24]; in the luminal environment of the intestine, there is a high tolerance for LPS due to the constant interaction with gram-negative bacteria in the microbiome [25, 26] and it does not trigger inflammation [27, 28]. LPS is ultimately excreted in feces [29, 30]. Some LPS loses occur via urinary excretion [30]. But another route of excretion is via the small intestine, where LPS appears first in the crypts and then concentrates in the small intestinal epithelial cells of the villus tips [31, 32], which are ultimately shed contributing another pool of LPS to fecal excretion. Intraperitoneal LPS causes shedding of small intestinal epithelial cells in a Tnf receptor-(Tnfr-) dependent manner within 1.5 hours at doses as low as 0.125 mg/kg [27]. The rapid manifestation of epithelial shedding, preceded by the crypt appearance of LPS, suggests transmigration of intraperitoneal LPS across the visceral peritoneum and not only derived from circulation. The amelioration of splenic injury from the introduction of normal mesenteric lymph into LPS-treated mice indicates a role for mesenteric fluids in systemic inflammation [33]. Intestinal

clearance of LPS causes intestinal permeability, oxidative stress, and intestinal mitochondrial damage and increases lipid peroxidation [34].

As shown in Figure 1, LPS initiates inflammation through toll-like receptor (TLR4) signaling that activates NFκB-mediated cytokine production including Tnfα, IL-6 and IL-1β [35]. Keap1 is a redox-sensing cytosolic inhibitor protein for the transcription factor Nrf2 that upregulates the expression a battery of antioxidant, anti-inflammatory, and DNA repair genes including heme oxygenase-1 (Ho-1) [36, 37]. In response to increasing intracellular oxidation status or the binding of other electrophiles, the conformation of Keap1 is altered, releasing Nrf2 to translocate to the nucleus, binding the antioxidant response element (ARE) in the promoter regions of target genes (Figure 2) [38]. Priming the Keap1-Nrf2-ARE pathway with dietary electrophilic phytochemicals increases the threshold to the initiation of inflammation and delays the activation of proinflammatory transcription factor NFκB [39–41]. The inhibitory role of Nrf2 has also been demonstrated in macrophages where it can bind ARE-independent DNA sequences in the promoter region of *IL-6* and *IL-1β*, suppressing their transcription [42]. Additionally, LPS can physically disrupt red blood cell membranes releasing free heme with prooxidant potential [43]. In its enzyme role, inducible heme oxygenase-1 (Ho-1) degrades free heme to equimolar amounts of carbon monoxide (CO), free iron, and biliverdin. Biliverdin is enzymatically converted to bilirubin which forms an antioxidant redox couple, while CO is independently anti-inflammatory [44]. Upregulating Ho-1 is protective against intestinal inflammation and loss of barrier integrity [45–47] and maintains alternatively activated/M2 macrophage polarization [48–50],

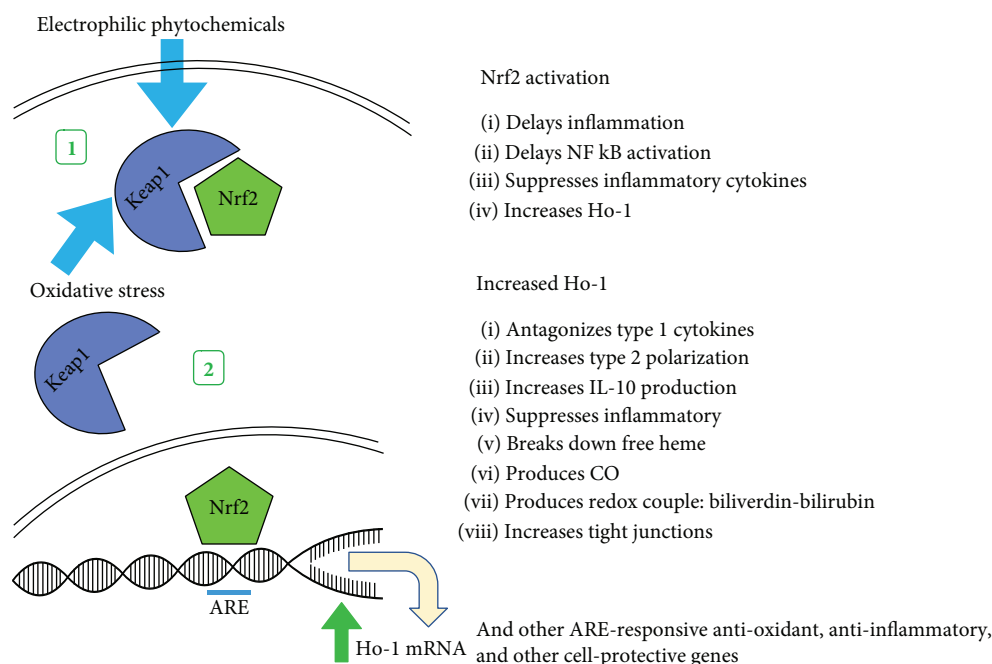


FIGURE 2: Effects of dietary electrophilic compounds on redox sensor Keap1. (1) Redox-sensing protein Keap1 is activated by intracellular oxidative stress or other electrophilic compounds, changing its conformation. (2) Keap1 releases transcription factor Nrf2 to translocate to the nucleus and upregulate the expression of a battery of antioxidant, anti-inflammatory, and cell protective genes including heme oxygenase-1 (Ho-1).

shifting the polarization of intestinal T cells towards a regulatory phenotype [51–53].

Polyacetylenes are bioactive bisacetylenic phytooxylypins abundant not only in medicinal plants such as *Notopterygium incisum* (Qiang Huo) [54], *Angelica sinensis* (Dong Quai) [55, 56], and ginseng [57] but also in agricultural crops from the *Apiaceae* family [58], the most widely consumed of which is carrot [59, 60]. Falcarinol (FA) and falcarindiol (FD) are the most abundant carrot-derived polyacetylenes and have a demonstrated anti-inflammatory effect [60–62], in part by the suppression of NF-κB [63]. FD has been shown to activate Nrf2 by S-alkylation of its inhibitor protein Keap1 [64]. FD pretreatment upregulated the antioxidant enzymes NADPH:quinone oxidoreductase (Nqo1) and glutathione-S-transferase (GST), protecting against a later oxidative challenge in both normal liver cells [65] and an in vivo mouse model examining the activity of these enzymes in the liver, small intestine, kidney, and lung, in part by reducing lipid peroxidation [66]. Ginseng-derived panaxynol, structurally identical to carrot-derived falcarinol, is an anti-inflammatory compound and potent activator of cardiac Nrf2 [57]. In humans, panaxynol reduces oxidative stress-induced plasma lipid peroxidation [67]. We set out to evaluate for the first time the protective effect of diet-achievable levels of FA against intestinal inflammation in comparison to sulforaphane (SF)—widely recognized as the most potent natural compound activator of the Nrf2/ARE pathway.

2. Methods

2.1. Animal Treatment. Three-month-old male CB57BL/6 mice (Charles River, St. Constant, QC, Canada) were

individually housed in a temperature-controlled room on a reverse (12:12) light-dark cycle, fed a standard chow diet (Harlan Teklad, Mississauga, ON, Canada), with access to water *ad libitum*. Phytochemicals were prepared in 100% ethanol immediately before individual doses were prepared in peanut butter and allowed to evaporate overnight, refrigerated in a light-proof container. Twice per day for 7 days, 4 groups of mice received peanut butter (166 mg ± 0.01) with 5 mg/kg FA (CAS# 21852-80-2, Quality Phytochemicals LLC, East Brunswick, NJ, USA) (FA group), 5 mg/kg SF (CAS# 142825-10-3, Cayman Chemical, Ann Arbor, MI, USA) (SF group), or ethanol vehicle for the two control groups: a negative control (NC group) that was saline-treated and a positive control (PC group) that was lipopolysaccharide- (LPS-) treated. The chemical structures of FA and SF are shown in Figure 3. To elicit an immune response, the FA, SF, and PC groups of fasted animals ($n = 3$ per group) received an intraperitoneal injection of 5 mg/kg LPS on the eighth day and were sacrificed after 4 hours—a time point chosen for maximal intestinal inflammatory response [68, 69]. Plasma was collected by cardiac puncture, and tissues were removed and snap frozen in liquid nitrogen. All of the procedures conducted were approved by the University of Guelph Animal Care Committee and were in accordance with the guidelines of the Canadian Council on Animal Care.

2.2. Histological Analysis. Upper duodenal sections were flushed with saline and fixed in phosphate-buffered 10% formalin solution for 24 hours. Paraffin blocks were embedded, and 5 μm sections in longitudinal orientation were slide-mounted, and haematoxylin and eosin (H&E) staining was performed by the Animal Health Laboratory

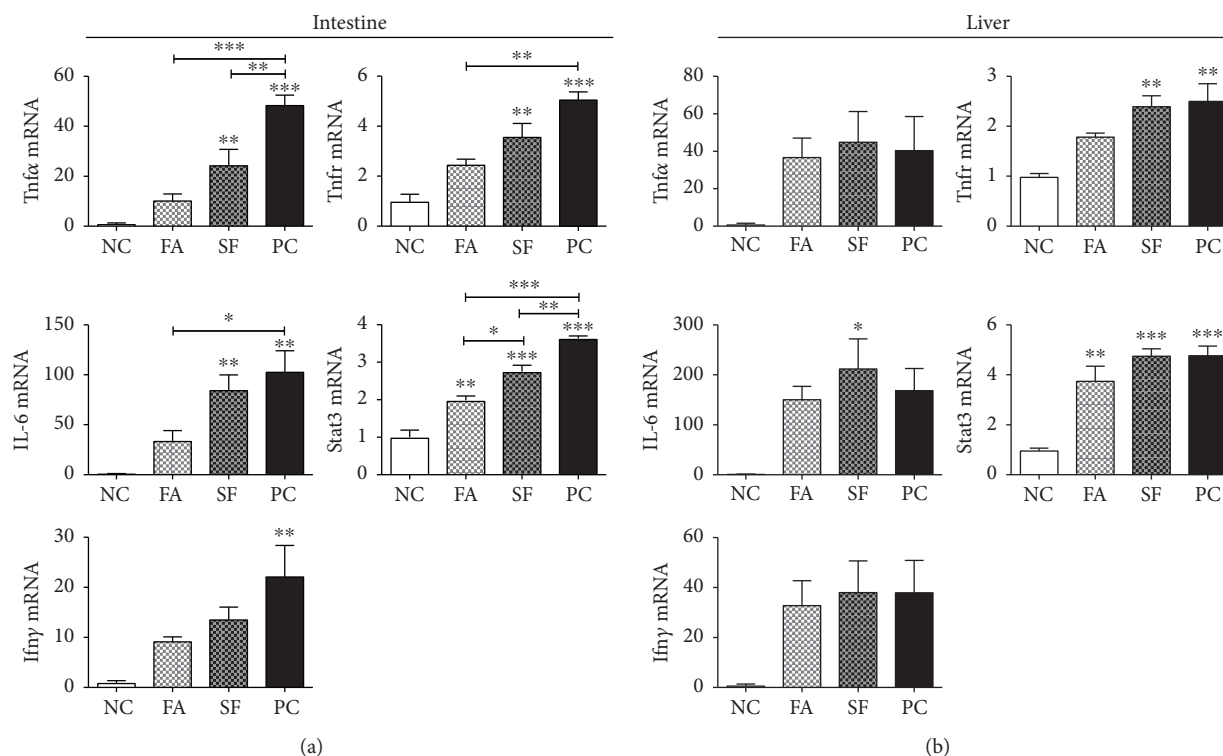


FIGURE 4: Intestinal and hepatic inflammatory gene expressions. Gene expression is expressed as mRNA fold change relative to negative control (NC). (a) Intestinal gene expression and (b) hepatic gene expression. Statistical significance is expressed as follows: * $p < 0.05$, ** $p < 0.01$, *** $p < 0.001$, and **** $p < 0.0001$.

of LPS-induced proinflammatory genes, but FA was consistently more effective than SF. *IL-6* showed the greatest magnitude of change among the inflammatory genes, increasing 103.6-fold for LPS treatment alone (positive control (PC)) and 85.2-fold for SF ($p < 0.01$ for both), whereas for FA, the increase was prevented and the expression was not significantly different from the LPS-untreated negative control (NC). This pattern repeated for *Tnfa*, its receptor (*Tnfr*), and *Ifny*. *Tnfa* expression increased by 48.8-fold for PC ($p < 0.0001$) and 24.6-fold for SF ($p < 0.01$), and *Tnfr* was increased by 5.1-fold in PC ($p < 0.001$) and 2.6-fold in SF ($p < 0.01$), but for FA-treated mice, the increases were prevented and not significantly different from the negative control group. *Ifny* mRNA increased by 22.3-fold in PC ($p < 0.001$), but there was no significant increase for either phytochemical-treated groups. *Stat3* increased in all LPS-treated groups, increasing by 3.6-fold in PC, 2.8-fold in SF (both $p < 0.0001$), and 2-fold in FA ($p = 0.0051$). *Stat3* was significantly lower for FA than both PC and SF ($p = 0.0002$ and $p = 0.0208$, respectively). As shown in Figure 5, *IL-10* and its receptor (*IL-10R*) were also significantly increased by LPS treatment and the LPS response was reduced by both phytochemical treatments. *IL-10* expression was increased by 17.7-, 13.1-, and 9.5-fold in PC, SF, and FA, respectively ($P < 0.0001$), whereas its receptor increased only for PC (by 1.6-fold) and decreased with phytochemical treatment (both to 0.7-fold, $P = 0.0176$). Altogether, the phytochemical pretreatment effectively reduced the magnitude of intestinal

proinflammatory gene expression with FA showing more potency than SF.

3.2. Phytochemicals Had a Minor Effect on Hepatic Inflammation. At 4 hours of post LPS injection, the effect on hepatic inflammatory gene expression was more subdued than in the intestine. As shown in Figure 4(b), the main inflammatory genes (*IL-6*, *Tnfa*, and *Ifny*) were all increased by LPS treatment and the phytochemical pretreatments showed no reductions in their expression. In fact, *IL-6* had the greatest magnitude of increase for all LPS groups with the highest increase for SF ($p = 0.0172$). *Tnfr* mRNA was upregulated by 2.4-fold and 2.5-fold for SF and PC, respectively (both $p < 0.01$), that was presented in the FA group. *Stat3* was significantly upregulated in all LPS-treated groups ($P = 0.0002$). SF and PC both increased by 4.8-fold (both $p = 0.0003$). Differently from SF, FA caused the most conservative increase in *Stat3* (3.8-fold, $p = 0.0022$), showing some reducing effects.

3.3. Downregulated Expression of Intestinal Nrf2 Pathway Genes Was Not Rescued with Pretreatments. We also evaluated the effect of phytochemicals on the expression of Nrf2, Keap1, and their responsive genes *Hmox1* and *Nqo1* in both the intestine and the liver (Figure 6). In the intestine, the expression of *Nrf2* was 3-fold downregulated by LPS ($p < 0.0001$) and not rescued by phytochemical pretreatment at 4 hours of postinjection. *Keap1* was significantly

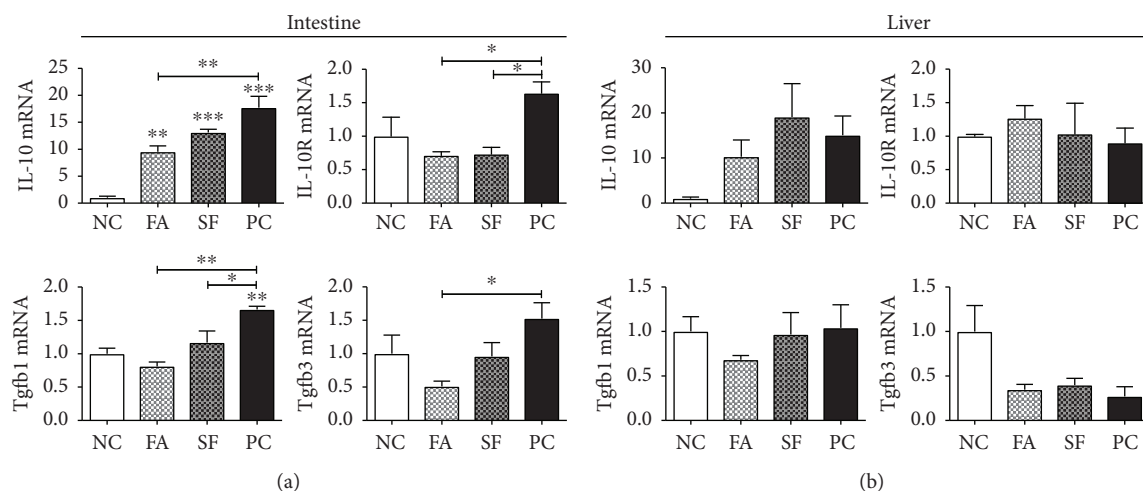


FIGURE 5: Intestinal and hepatic regulatory gene expressions. Gene expression is expressed as mRNA fold change relative to negative control (NC). (a) Intestinal gene expression and (b) hepatic gene expression. Statistical significance is expressed as follows: * $p < 0.05$, ** $p < 0.01$, *** $p < 0.001$, and **** $p < 0.0001$.

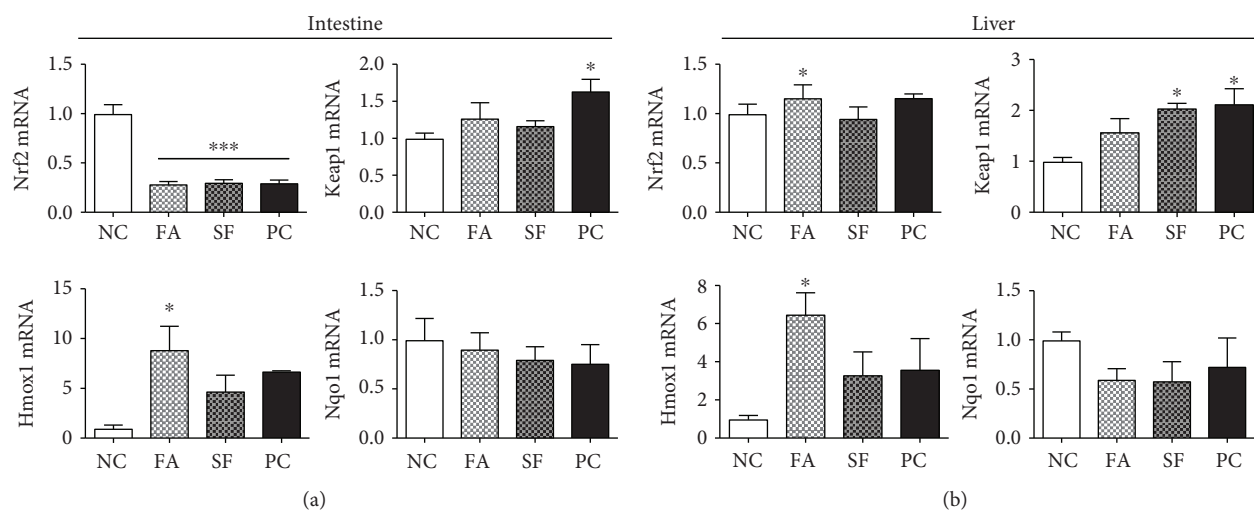


FIGURE 6: Intestinal and hepatic gene expressions of the Nrf2 pathway. Gene expression is expressed as mRNA fold change relative to negative control (NC). (a) Intestinal gene expression and (b) hepatic gene expression. Statistical significance is expressed as follows: * $p < 0.05$, ** $p < 0.01$, *** $p < 0.001$, and **** $p < 0.0001$.

upregulated only in PC by 1.6-fold ($p = 0.045$). We anticipated an increased expression of Nrf2 target genes by both phytochemical pretreatments but observed that only heme oxygenase-1 (*Hmox1*) was significantly increased only for FA by 8.9-fold above control ($p = 0.0184$). *Nqo1* (Figure 6) and *Muc-2* (not shown) gene expression also were not significantly changed by LPS with or without phytochemical pretreatments.

3.4. Falcarinol but Not Sulforaphane Stimulated Expression of Hepatic Nrf2 Pathway. In contrast, in the liver, LPS had no impact on the Nrf2 pathway (Figure 6(b)). In fact, the FA pretreatment resulted in a significant increase of Nrf2 mRNA ($p < 0.05$), and Keap1 was significantly upregulated only in the SF and PC groups (2.0- and 2.1-fold, respectively; both $p < 0.05$). Similarly, *Hmox1* was significantly increased only

in the FA-treated group (by 6.5-fold, $p < 0.05$), and there was no difference in expression between the SF and PC groups. *Nqo1* expression was not significantly affected by either LPS or phytochemicals in the liver.

3.5. Falcarinol but Not Sulforaphane Increased Intestinal and Liver Heme Oxygenase-1 Protein. Interestingly, Ho-1 and Nqo1 proteins followed a similar expression pattern with respect to mRNA in both the intestine and the liver (Figure 7). The intestinal Ho-1 protein was significantly increased with FA (1.83-fold, $p < 0.05$), while there was no effect of SF or PC on Ho-1 protein. Similarly, the largest increase in hepatic Ho-1 protein was obtained only with FA (16.4-fold; $p = 0.0806$). On the other hand, the intestinal Nqo1 protein was increased with all treatments but was significant only in the LPS PC group (2.18-fold, $p < 0.05$). There

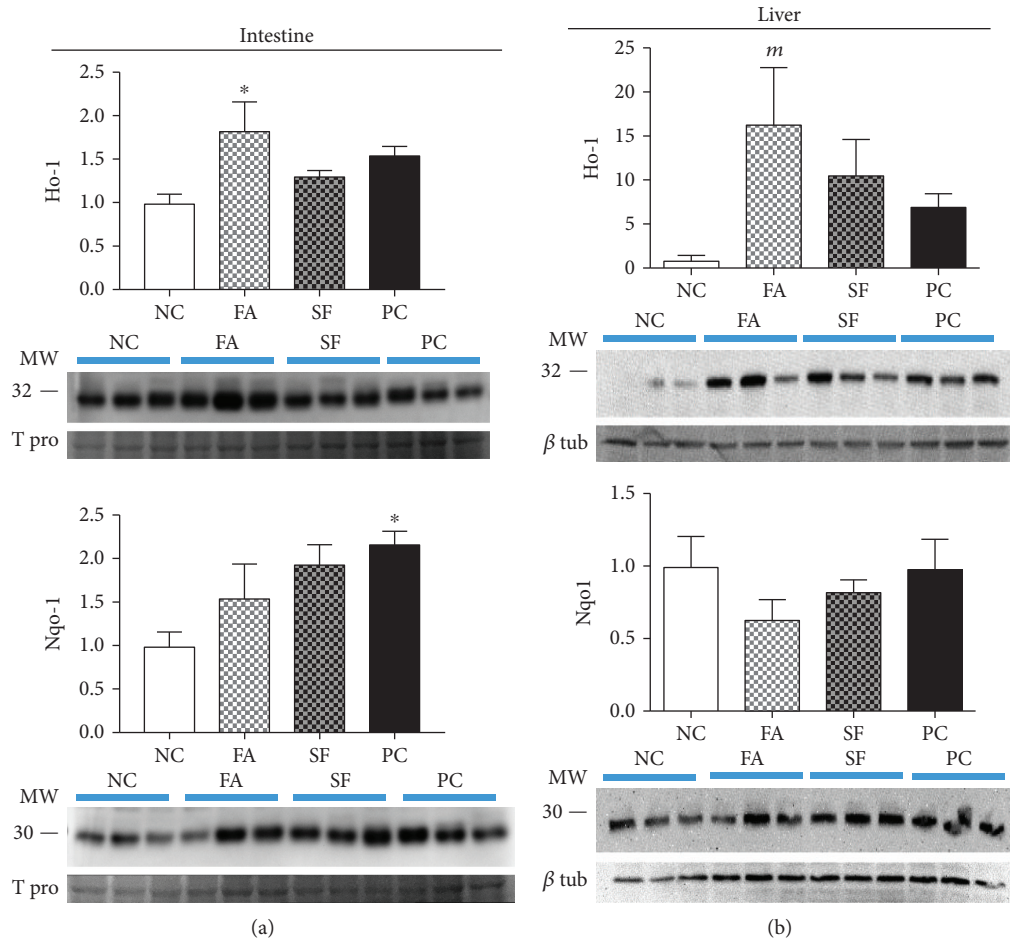


FIGURE 7: Intestinal and hepatic protein expressions of the Nrf2 pathway. Protein expression is expressed as fold change relative to negative control (NC). (a) Intestinal protein expression and (b) hepatic protein expression. Statistical significance is expressed as follows: * $p < 0.05$, ** $p < 0.01$, *** $p < 0.001$, and **** $p < 0.0001$; marginally significant results (^m $p < 0.1$) are also noted.

was no effect of either phytochemical or LPS treatment on the liver Nqo1 protein.

3.6. Falcarinol Pretreatment Specifically Reduced Initial-Phase Plasma Cytokines. Eosinophils are the first immune cells to be recruited to the site of injury in response to locally produced eotaxin, and are followed by more numerous neutrophils and macrophages [73]. As shown in Figure 8, eotaxin increased 5.4-fold for LPS alone ($p < 0.001$, PC) and it was attenuated with FA, which only showed a 4.1-fold increase ($p < 0.01$), but not with SF (5.0-fold, $p < 0.001$) demonstrating that FA was able to show some protective effects in the initial phases of the LPS response. Granulocyte-macrophage colony-stimulating factor (GM-CSF) acts to recruit eosinophils and macrophages but is inhibitory to neutrophils [74]; GM-CSF was significantly increased only for SF and PC, by 5.6-fold and 6.7-fold, respectively ($p < 0.05$). IL-12p40 was significantly upregulated only for SF (by 90.2-fold, $p < 0.05$).

The plasma inflammatory cytokines (IL-1 α , IL-1 β , IL-6, and Ifn γ) were all significantly upregulated by LPS treatment, but there was no effect of phytochemical pretreatment on the magnitude of the response seen at the 4-hour time point. Tnf α was significantly increased only in the FA group (by

8.4-fold, $p < 0.05$). Other inflammatory factors IL-13, MIP-1 α , and MIP-1 β were significantly increased but without a protective effect of phytochemical treatment; similarly, the regulatory cytokines IL-3, IL-4, and IL-10 were all significantly upregulated by LPS with no effect of phytochemical pretreatment. All cytokines were increased in the plasma after LPS injection, with the exception of IL-9 which was not detectable in all samples. Changes were not significant for IL-2, IL-5, IL-17, KC, MCP-1, RANTES, or IL-12p70.

3.7. Falcarinol Specifically Reduced Lipid Peroxidation in the Mesentery. As shown in Figure 8, LPS had no significant effect on lipid peroxidation in the plasma, jejunum, or mesentery at 4 hours of postinjection; however, TBARS was significantly lower in the mesentery of the FA-treated mice ($p < 0.05$).

3.8. Falcarinol Completely Attenuated Inflammatory Cell Infiltration and Reduced Epithelial Turnover in the Intestine. Qualitative scores for inflammatory cell infiltrate and epithelial damage were moderate 4 h after LPS treatment, ranging from 0 to 3 on a scale of 8. FA however completely attenuated LPS-induced inflammatory cell infiltration in the duodenum

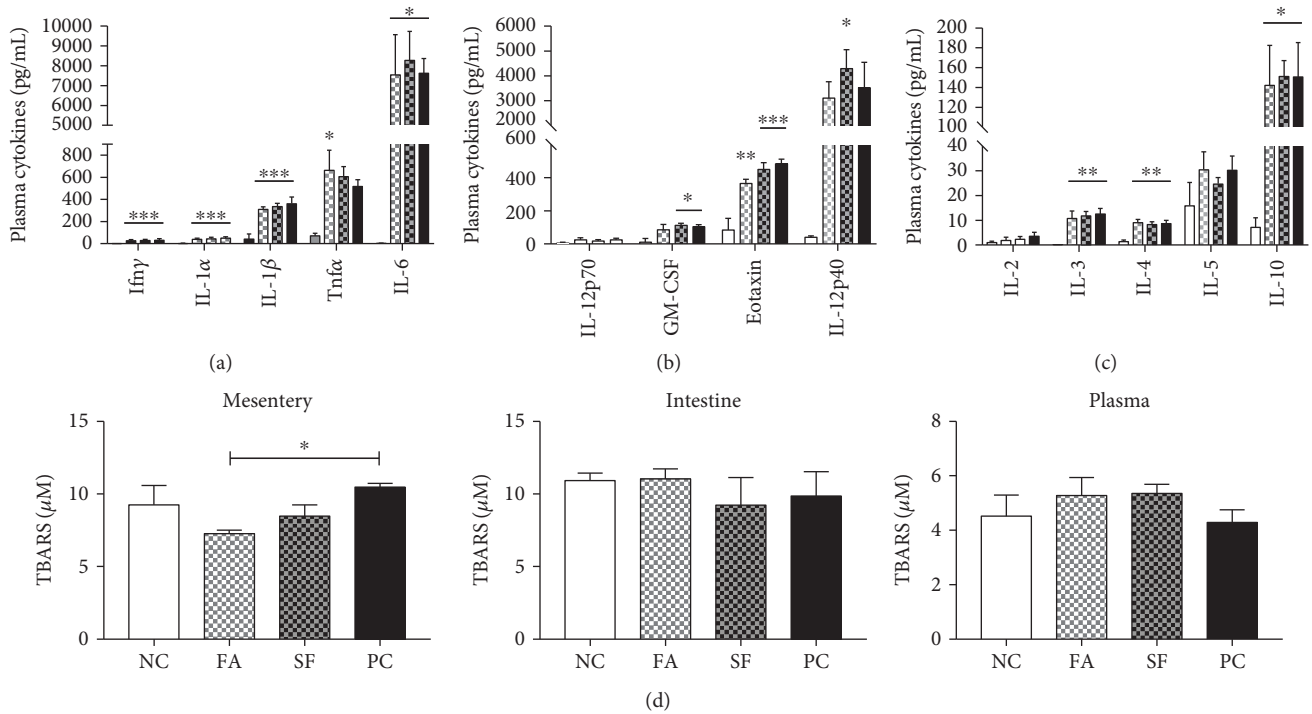


FIGURE 8: Plasma cytokines and lipid peroxidation. Circulating plasma cytokines 4 hours after LPS injection are expressed in pg/mL. (a) Classic inflammatory cytokines. (b) Other inflammatory cytokines. (c) Regulatory cytokines. (d) Lipid peroxidation measured by TBARS in the jejunal-associated mesentery, jejunum, and plasma 4 hours after LPS injection. Statistical significance is expressed as follows: * $p < 0.05$, ** $p < 0.01$, *** $p < 0.001$, and **** $p < 0.0001$.

(Figure 9). Remarkably, despite LPS treatment, the score for FA was lower even than saline-treated NC. Both SF and PC scored similarly to NC; differences were only significant between FA and SF (mean ranks: 2.5 and 9.0, respectively, $p < 0.05$). The number of mitotic cells in the intestinal epithelium is a marker for the epithelial cell turnover rate [32, 75]. Results only approached significance between NC and PC ($p = 0.0522$). The mean numbers of mitotic cells counted in 10 contiguous 400x fields were 24, 33, 45, and 63 for NC, FA, SF, and PC, respectively (Figure 9). This study did not observe shedding directly, but histology revealed the architecture of PC duodenum to be so poor due to shortened villi (crypt:villus ratio is $\sim 1:3$ for PC as compared to 7–12 for the other groups) in which further morphological study was not possible. This effect was not seen in the LPS-treated groups that received phytochemical pretreatment.

4. Discussion

The anticancer effects of FA are its best characterized bioactive property [76–83]. FA also has positive metabolic effects. *In vitro*, FA improves insulin signaling in insulin-resistant porcine myotubes [84] and increases glucose uptake in normal porcine myotubes and adipocytes, as well as inhibiting adipocyte differentiation [85]. Interestingly, falcariindiol does not inhibit adipocyte differentiation but is a more potent PPAR γ agonist than FA which requires a higher dose to initiate an effect [54, 85]. FA stimulates normal intestinal cell growth at physiological doses, whereas carotenoids have no effect [86], and carrot juice has an anti-inflammatory effect

in *in vitro* intestinal cells [87]. FA also has anticomplement activity [88] and modulates GABA $_A$ receptor activation [89].

In this study, we observed that the local effect of LPS on the intestine produced a greater response of inflammatory gene expression than in the liver, which would be expected to experience a lower dose of LPS derived from systemic circulation as opposed to directly from the intraperitoneal space. Additionally, the protective effect of the phytochemicals and falcariinol, in particular, was more pronounced in the intestine than in the liver. Intestinal cells would have been exposed to the full phytochemical dose over a short amount of time—a higher effective dose that would be available to cells relying on systemic circulation for phytochemical exposure such as the liver. The novel finding in this study is that falcariinol was more effective than sulforaphane in attenuating inflammatory gene expression in the intestine and to a lesser degree in the liver.

We also examined the effect of phytochemicals on Nrf2-activated targets, Ho-1 and Nqo1. Heme oxygenase-1 (Ho-1, *Hmox1*) has an emerging role in attenuating intestinal inflammation and protecting intestinal barrier integrity by upregulating the expression of tight junction proteins [47] and attenuating inflammation-induced intestinal permeability [46]. Prior Ho-1 upregulation protected intestinal barrier integrity by upregulating tight junction proteins, reducing apoptosis, activating Nrf2, and reducing NF κ B activation resulting from abdominal surgery in a rat model [90] and associated oxidative stress [91, 92]. FA, but not SF, significantly upregulated *Hmox1* in both the liver and intestine, whereas *Nqo1* expression was not affected by phytochemical.

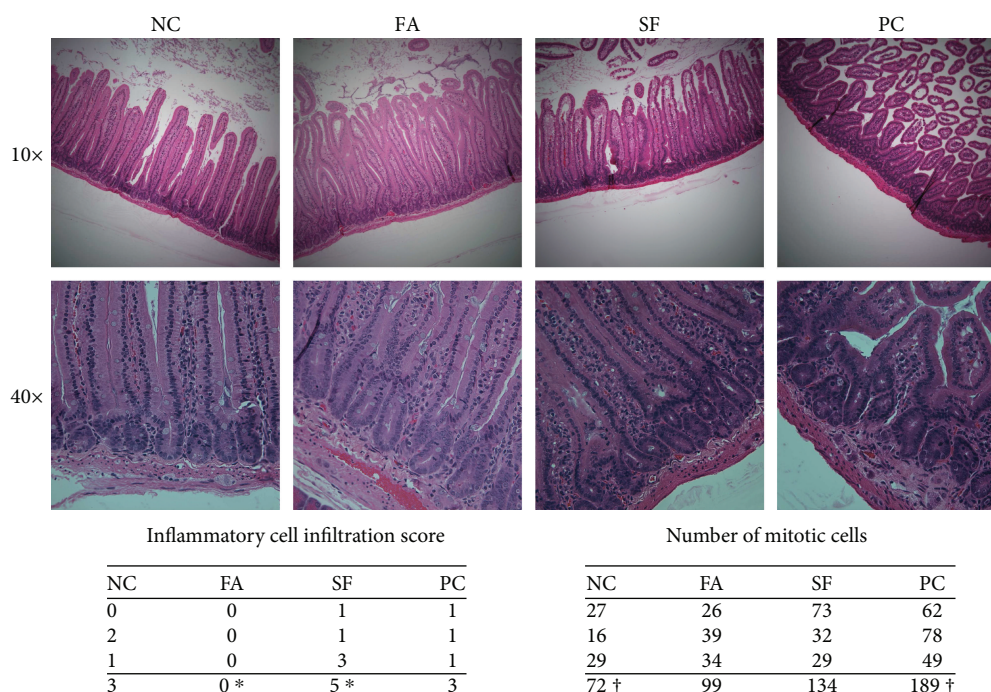


FIGURE 9: Histomorphological evaluation. Duodenal sections were slide-mounted and H&E stained. Histomorphological evaluation was performed blinded by a professional veterinary pathologist. Statistical significance is expressed as follows: * $p < 0.05$, ** $p < 0.01$, *** $p < 0.001$, and **** $p < 0.0001$; marginally significant results are also noted ($†p = 0.0522$).

A unique characteristic of the *Nqo1* promoter is the number of ARE sequences. Rather than rendering *Nqo1* more Nrf2-sensitive due to the increased number of ARE contributing to its regulation, it appears that it is more likely that *Nqo1* requires more intense Nrf2 exposure to affect transcriptional activation than *Hmox1*. We demonstrated that *Hmox1* is more sensitive to Nrf2 activation than *Nqo1* in the liver and intestine which was also reflected in protein levels. *Nqo1* protein levels were only significantly elevated in the intestine of PC, whereas in the liver, neither LPS nor phytochemical pretreatment showed an effect. Ho-1 protein levels were significantly increased from NC in both the liver and the intestine only in FA-treated mice, with no difference between the SF and the PC groups. Notably, this effect was only seen with FA-treated mice and not those treated with SF. This unique effect of FA is another novel finding in this study.

FA attenuated circulating eotaxin and GM-CSF (a proinflammatory inducer of M1 phenotype [93]) as compared to other LPS-treated groups, which could potentially translate to reduced immune cell recruitment, but cell trafficking was not evaluated in this study. Lipid peroxidation was not increased at 4 hours after LPS injection in any of the plasma, intestine, or mesentery; however, FA pretreatment reduced basal lipid peroxidation in the mesentery, which may be a contributing factor to the surprising reduction of inflammatory cell infiltration in FA duodena.

Glutathione-S-transferase is a phase II detoxification enzyme that conjugates electrophiles [94]. Sulforaphane is absorbed into intestinal cells as a glutathione conjugate [95], an interaction that is promoted by intracellular glutathione transferases [96] or a direct interaction with luminal

glutathione derived from the diet [97] or bile [98]. It is known that a portion of absorbed sulforaphane is secreted back into the intestine as a glutathione conjugate, reducing its bioavailability to 74% by some estimates [99]. The bioavailability of polyacetylenes has been demonstrated [100, 101], and they have been shown to bind human serum albumin for circulatory distribution [102], but we are not aware of any studies specific to their uptake mechanisms. Due to the electrophilicity of polyacetylenes; these mechanisms may be similar to SF, and possibly differential uptake efficiencies may contribute to the greater effectiveness of FA *in vivo*.

Normal epithelial cell loss from the villi tips is replaced by cells newly differentiated from crypt stem cells; a balance between cell loss and regeneration maintains intestinal barrier integrity. Accelerated mitosis in the epithelial layer is suggestive of shedding since there would be an increased need for regeneration to replace lost cells at the villus tip. LPS-treated groups had more mitotic cells than NC (1.38- and 1.88-fold more for FA and SF, respectively); PC had the most mitotic cells (2.63-fold more than NC) but did not reach significance ($p = 0.0522$), demonstrating the superior effect of FA over SF in protecting intestinal integrity. While LPS treatment did not substantively increase the qualitative score of inflammatory cell infiltration (mild to moderate infiltration in NC, SF, and PC), remarkably, FA did not show any infiltration despite LPS treatment (score = 0).

While it is possible that FA is a more potent activator of Nrf2 than sulforaphane, there may be other effects of FA that are responsible. Endocannabinoid signaling is involved in maintaining intestinal barrier integrity. Antagonism of cannabinoid type 1 receptor (CB₁R) reduced intestinal

inflammation and permeability in a diet-induced obesity model, attenuating metabolic endotoxemia and adipose inflammation and improving insulin resistance [103]. Pre-treatment of the apical but not basolateral side of a Caco-2 cell monolayer prevented the cytokine-induced increase in intestinal permeability mediated by the antagonism of CB₁R [104]. Dietary (apical side exposure) FA is likely protective of the intestinal epithelium since it is a covalent CB₁R antagonist [105]; we are unaware of any studies directly evaluating sulforaphane for potential CB₁R antagonism.

The current study evaluated the anti-inflammatory and antioxidant effects of isolated bioactive compounds available in the diet and their role in the prevention of inflammation (commonly understood to play an important role in the development of most chronic diseases) and more specifically in the context of intestinal inflammation and the maintenance of intestinal barrier integrity. Intestinal inflammation is particularly relevant since it provides the milieu for the polarization of naive T cells and other immune cells which have wider implications for the overall immune tone. The degradation of the intestinal barrier is gaining recognition as another early deviation from homeostasis contributing to the development of more serious and widely divergent diseases including some autoimmune conditions, food allergies, obesity, endotoxemia, chronic inflammation, and even intense exercise. Furthermore, our use of low/diet-achievable doses (5 mg/kg) as opposed to the commonly used default for studies of this type (100 mg/kg), which is a pharmaceutical or supplemental dose, make our findings all the more relevant since these effects are seen at dietary levels of exposure.

In conclusion, we have demonstrated the superior effectiveness of FA over SF at attenuating LPS-induced intestinal gene expression and to a lesser degree in the liver. FA was uniquely effective at upregulating Nrf2-target Ho-1 in both the intestine and the liver and attenuating some initial phase proinflammatory cytokines. FA also reduced inflammatory cell infiltration in the duodenum below even negative control and reduced basal mesenteric lipid peroxidation. These results suggest that the efficacy of FA may be fruitful to explore for prevention and treatment in inflammatory pathologies of the GI tract and in supporting the maintenance of intestinal barrier integrity due to the superiority of FA at upregulating Ho-1 to the anti-inflammatory and antioxidant effect demonstrated in the current study.

Data Availability

The data used to support the findings of this study are available from the corresponding author upon request.

Conflicts of Interest

The authors declare that there is no conflict of interest regarding the publication of this paper.

Acknowledgments

This research is funded by the Agri-Innovation Program of Agriculture and Agri-Food Canada's Growing Forward 2

Policy Framework (a federal-provincial-territorial initiative), Loblaw Companies Ltd., and the Carrot Common through the Organic Science Cluster II, an industry-supported research and development endeavour initiated by the Organic Agriculture Centre of Canada at Dalhousie University in collaboration with the Organic Federation of Canada.

References

- [1] J. R. Turner, "Intestinal mucosal barrier function in health and disease," *Nature Reviews. Immunology*, vol. 9, no. 11, pp. 799–809, 2009.
- [2] L. S. Kaminsky and Q.-Y. Zhang, "The small intestine as a xenobiotic-metabolizing organ," *Drug Metabolism and Disposition*, vol. 31, no. 12, pp. 1520–1525, 2003.
- [3] P. Brandtzaeg, "The gut as communicator between environment and host: immunological consequences," *European Journal of Pharmacology*, vol. 668, pp. S16–S32, 2011.
- [4] C. Lopez-Garcia, A. M. Klein, B. D. Simons, and D. J. Winton, "Intestinal stem cell replacement follows a pattern of neutral drift," *Science*, vol. 330, no. 6005, pp. 822–825, 2010.
- [5] J. Visser, J. Rozing, A. Sapone, K. Lammers, and A. Fasano, "Tight junctions, intestinal permeability, and autoimmunity," *Annals of the New York Academy of Sciences*, vol. 1165, no. 1, pp. 195–205, 2009.
- [6] R. Kiesslich, C. A. Duckworth, D. Moussata et al., "Local barrier dysfunction identified by confocal laser endomicroscopy predicts relapse in inflammatory bowel disease," *Gut*, vol. 61, no. 8, pp. 1146–1153, 2012.
- [7] J.-F. Turcotte, K. Wong, S. J. Mah et al., "Increased epithelial gaps in the small intestine are predictive of hospitalization and surgery in patients with inflammatory bowel disease," *Clinical and Translational Gastroenterology*, vol. 3, no. 7, pp. e19–e16, 2012.
- [8] Q. Mu, J. Kirby, C. M. Reilly, and X. M. Luo, "Leaky gut as a danger signal for autoimmune diseases," *Frontiers in Immunology*, vol. 8, p. 598, 2017.
- [9] C. Bleau, A. D. Karelis, D. H. St-Pierre, and L. Lamontagne, "Crosstalk between intestinal microbiota, adipose tissue and skeletal muscle as an early event in systemic low-grade inflammation and the development of obesity and diabetes," *Diabetes/Metabolism Research and Reviews*, vol. 31, no. 6, pp. 545–561, 2015.
- [10] E. A. Deitch, "Intestinal permeability is increased in burn patients shortly after injury," *British Journal of Surgery*, vol. 77, no. 5, pp. 587–592, 1990.
- [11] D. S. Walsh, P. Thavichaiarn, C. Dheeradhada et al., "Prolonged alteration in gut permeability following nonthermal injury," *Injury*, vol. 27, no. 7, pp. 491–494, 1996.
- [12] Z. M. Earley, S. Akhtar, S. J. Green et al., "Burn injury alters the intestinal microbiome and increases gut permeability and bacterial translocation," *PLoS One*, vol. 10, no. 7, pp. e0129996–e0129916, 2015.
- [13] J. S. Aranow and M. P. Fink, "Determinants of intestinal barrier failure in critical illness," *British Journal of Anaesthesia*, vol. 77, no. 1, pp. 71–81, 1996.
- [14] X. Gao, J. Zhang, D. Yang, Q. Tao, L. Liu, and J. Guo, "Effects of heme oxygenase-1 in the intestine on the intestinal barrier function of rats with hemorrhagic shock," *International Journal of Clinical and Experimental Medicine*, vol. 9, no. 9, pp. 17367–17376, 2016.

- [15] M. Lamprecht, S. Bogner, K. Steinbauer et al., "Effects of zeolite supplementation on parameters of intestinal barrier integrity, inflammation, redoxbiology and performance in aerobically trained subjects," *Journal of the International Society of Sports Nutrition*, vol. 12, no. 1, p. 40, 2015.
- [16] N. Vargas and F. Marino, "Heat stress, gastrointestinal permeability and interleukin-6 signaling — implications for exercise performance and fatigue," *Temperature*, vol. 3, no. 2, pp. 240–251, 2016.
- [17] K. Dokladny, M. N. Zuhl, and P. L. Moseley, "Intestinal epithelial barrier function and tight junction proteins with heat and exercise," *Journal of Applied Physiology*, vol. 120, no. 6, pp. 692–701, 2016.
- [18] L. M. JanssenDuijghuijsen, M. Mensink, K. Lenaerts et al., "The effect of endurance exercise on intestinal integrity in well-trained healthy men," *Physiological Reports*, vol. 4, no. 20, article e12994, 2016.
- [19] D. S. March, T. Marchbank, R. J. Playford, A. W. Jones, R. Thatcher, and G. Davison, "Intestinal fatty acid-binding protein and gut permeability responses to exercise," *European Journal of Applied Physiology*, vol. 117, no. 5, pp. 931–941, 2017.
- [20] J. C. Mathison and R. J. Ulevitch, "The clearance, tissue distribution, and cellular localization of intravenously injected lipopolysaccharide in rabbits," *The Journal of Immunology*, vol. 123, no. 5, pp. 2133–2143, 1979.
- [21] Z. Yao, J. M. Mates, A. M. Cheplowitz et al., "Blood-borne lipopolysaccharide is rapidly eliminated by liver sinusoidal endothelial cells via high-density lipoprotein," *The Journal of Immunology*, vol. 197, no. 6, pp. 2390–2399, 2016.
- [22] M. A. Freudenberg, N. Freudenberg, and C. Galanos, "Time course of cellular distribution of endotoxin in liver, lungs and kidneys of rats," *British Journal of Experimental Pathology*, vol. 63, no. 1, pp. 56–65, 1982.
- [23] B. Shao, M. Lu, S. C. Katz et al., "A host lipase detoxifies bacterial lipopolysaccharides in the liver and spleen," *The Journal of Biological Chemistry*, vol. 282, no. 18, pp. 13726–13735, 2007.
- [24] Y. Mimura, S. Sakisaka, M. Harada, M. Sata, and K. Tanikawa, "Role of hepatocytes in direct clearance of lipopolysaccharide in rats," *Gastroenterology*, vol. 109, no. 6, pp. 1969–1976, 1995.
- [25] E. d'Hennezel, S. Abubucker, L. O. Murphy, and T. W. Cullen, "Total lipopolysaccharide from the human gut microbiome silences toll-like receptor signaling," *mSystems*, vol. 2, no. 6, article e00046-17, 2017.
- [26] A. Gnauck, R. G. Lentle, and M. C. Kruger, "The characteristics and function of bacterial lipopolysaccharides and their endotoxic potential in humans," *International Reviews of Immunology*, vol. 35, no. 3, pp. 189–218, 2016.
- [27] J. M. Williams, C. A. Duckworth, A. J. M. Watson et al., "A mouse model of pathological small intestinal epithelial cell apoptosis and shedding induced by systemic administration of lipopolysaccharide," *Disease Models & Mechanisms*, vol. 6, no. 6, pp. 1388–1399, 2013.
- [28] H. Inagawa, C. Kohchi, and G. Soma, "Oral administration of lipopolysaccharides for the prevention of various diseases: benefit and usefulness," *Anticancer Research*, vol. 31, no. 7, pp. 2431–2436, 2011.
- [29] B. Kleine, M. A. Freudenberg, and C. Galanos, "Excretion of radioactivity in faeces and urine of rats injected with 3H,14C-lipopolysaccharide," *British Journal of Experimental Pathology*, vol. 66, no. 3, pp. 303–308, 1985.
- [30] M. A. Freudenberg, B. Kleine, and C. Galanos, "The fate of lipopolysaccharide in rats: evidence for chemical alteration in the molecule," *Reviews of Infectious Diseases*, vol. 6, no. 4, pp. 483–487, 1984.
- [31] Y. Ge, R. M. Ezzell, and H. S. Warren, "Localization of endotoxin in the rat intestinal epithelium," *The Journal of Infectious Diseases*, vol. 182, no. 3, pp. 873–881, 2000.
- [32] C.-W. Lai, T.-L. Sun, W. Lo et al., "Shedding-induced gap formation contributes to gut barrier dysfunction in endotoxemia," *Journal of Trauma and Acute Care Surgery*, vol. 74, no. 1, pp. 203–213, 2013.
- [33] L.-M. Zhang, W. Song, H. Cui et al., "Normal mesenteric lymph ameliorates lipopolysaccharide challenge-induced spleen injury," *Acta Cirúrgica Brasileira*, vol. 30, no. 9, pp. 604–610, 2015.
- [34] S. Cao, Q. Zhang, C. C. Wang et al., "LPS challenge increased intestinal permeability, disrupted mitochondrial function and triggered mitophagy of piglets," *Innate Immunity*, vol. 24, no. 4, pp. 221–230, 2018.
- [35] Y.-C. Lu, W.-C. Yeh, and P. S. Ohashi, "LPS/TLR4 signal transduction pathway," *Cytokine*, vol. 42, no. 2, pp. 145–151, 2008.
- [36] A. Kobayashi, M. I. Kang, H. Okawa et al., "Oxidative stress sensor Keap1 functions as an adaptor for Cul3-based E3 ligase to regulate proteasomal degradation of Nrf2," *Molecular and Cellular Biology*, vol. 24, no. 16, pp. 7130–7139, 2004.
- [37] A. T. Dinkova-Kostova, R. V. Kostov, and P. Canning, "Keap1, the cysteine-based mammalian intracellular sensor for electrophiles and oxidants," *Archives of Biochemistry and Biophysics*, vol. 617, pp. 84–93, 2017.
- [38] Y. Watai, A. Kobayashi, H. Nagase et al., "Subcellular localization and cytoplasmic complex status of endogenous Keap1," *Genes to Cells*, vol. 12, no. 10, pp. 1163–1178, 2007.
- [39] Y.-J. Surh, J. Kundu, and H.-K. Na, "Nrf2 as a master redox switch in turning on the cellular signaling involved in the induction of cytoprotective genes by some chemopreventive phytochemicals," *Planta Medica*, vol. 74, no. 13, pp. 1526–1539, 2008.
- [40] W. Li, T. O. Khor, C. Xu et al., "Activation of Nrf2-antioxidant signaling attenuates NFκB-inflammatory response and elicits apoptosis," *Biochemical Pharmacology*, vol. 76, no. 11, pp. 1485–1489, 2008.
- [41] A. Stefanson and M. Bakovic, "Dietary regulation of Keap1/Nrf2/ARE pathway: focus on plant-derived compounds and trace minerals," *Nutrients*, vol. 6, no. 9, pp. 3777–3801, 2014.
- [42] E. H. Kobayashi, T. Suzuki, R. Funayama et al., "Nrf2 suppresses macrophage inflammatory response by blocking proinflammatory cytokine transcription," *Nature Communications*, vol. 7, article 11624, 2016.
- [43] S. Brauckmann, K. Effenberger-Neidnicht, H. de Groot et al., "Lipopolysaccharide-induced hemolysis: evidence for direct membrane interactions," *Scientific Reports*, vol. 6, no. 1, article 35508, 2016.
- [44] S. Z. Sheikh, R. A. Hegazi, T. Kobayashi et al., "An anti-inflammatory role for carbon monoxide and heme oxygenase-1 in chronic Th2-mediated murine colitis," *The Journal of Immunology*, vol. 186, no. 9, pp. 5506–5513, 2011.
- [45] F. Tamion, V. Richard, S. Renet, and C. Thuillez, "Intestinal preconditioning prevents inflammatory response by

- modulating heme oxygenase-1 expression in endotoxic shock model,” *American Journal of Physiology-Gastrointestinal and Liver Physiology*, vol. 293, no. 6, pp. G1308–G1314, 2007.
- [46] R. Akagi, M. Akagi, Y. Hatori, and S. Inouye, “Prevention of barrier disruption by heme oxygenase-1 in intestinal bleeding model,” *Biological & Pharmaceutical Bulletin*, vol. 39, no. 6, pp. 1007–1012, 2016.
- [47] L. Zhang and Z. Zhang, “The protective effect of heme oxygenase-1 against intestinal barrier dysfunction in cholestatic liver injury is associated with NF- κ B inhibition,” *Molecular Medicine*, vol. 23, no. 1, p. 1, 2017.
- [48] C. Chauveau, S. Rémy, P. J. Royer et al., “Heme oxygenase-1 expression inhibits dendritic cell maturation and proinflammatory function but conserves IL-10 expression,” *Blood*, vol. 106, no. 5, pp. 1694–1702, 2005.
- [49] E. Sierra-Filardi, M. A. Vega, P. Sánchez-Mateos, A. L. Corbí, and A. Puig-Kröger, “Heme oxygenase-1 expression in M-CSF-polarized M2 macrophages contributes to LPS-induced IL-10 release,” *Immunobiology*, vol. 215, no. 9–10, pp. 788–795, 2010.
- [50] Y. Naito, T. Takagi, and Y. Higashimura, “Heme oxygenase-1 and anti-inflammatory M2 macrophages,” *Archives of Biochemistry and Biophysics*, vol. 564, pp. 83–88, 2014.
- [51] S. S. Lee, W. Gao, S. Mazzola et al., “Heme oxygenase-1, carbon monoxide, and bilirubin induce tolerance in recipients toward islet allografts by modulating T regulatory cells,” *The FASEB Journal*, vol. 21, no. 13, pp. 3450–3457, 2007.
- [52] S. Schulz, K. M. Chisholm, H. Zhao et al., “Heme oxygenase-1 confers protection and alters T-cell populations in a mouse model of neonatal intestinal inflammation,” *Pediatric Research*, vol. 77, no. 5, pp. 640–648, 2015.
- [53] V. Vijayan, F. A. D. T. G. Wagener, and S. Immenschuh, “The macrophage heme-heme oxygenase-1 system and its role in inflammation,” *Biochemical Pharmacology*, vol. 153, pp. 159–167, 2018.
- [54] A. G. Atanasov, M. Blunder, N. Fakhrudin et al., “Polyacetylenes from *Notopterygium incisum*—new selective partial agonists of peroxisome proliferator-activated receptor- γ ,” *PLoS One*, vol. 8, no. 4, pp. e61755–e61759, 2013.
- [55] J. Liu, S. Zschocke, E. Reiningger, and R. Bauer, “Inhibitory effects of *Angelica pubescens* f. *biserrata* on 5-lipoxygenase and cyclooxygenase,” *Planta Medica*, vol. 64, no. 06, pp. 525–529, 1998.
- [56] T. Uto, N. H. Tung, R. Taniyama, T. Miyanowaki, O. Morinaga, and Y. Shoyama, “Anti-inflammatory activity of constituents isolated from aerial part of *Angelica acutiloba* Kitagawa,” *Phytotherapy Research*, vol. 29, no. 12, pp. 1956–1963, 2015.
- [57] C. Qu, B. Li, Y. Lai et al., “Identifying panaxynol, a natural activator of nuclear factor erythroid-2 related factor 2 (Nrf2) from American ginseng as a suppressor of inflamed macrophage-induced cardiomyocyte hypertrophy,” *Journal of Ethnopharmacology*, vol. 168, pp. 326–336, 2015.
- [58] C. Zidorn, K. Jöhrer, M. Ganzera et al., “Polyacetylenes from the Apiaceae vegetables carrot, celery, fennel, parsley, and parsnip and their cytotoxic activities,” *Journal of Agricultural and Food Chemistry*, vol. 53, no. 7, pp. 2518–2523, 2005.
- [59] L. Schmiech, C. Alayrac, B. Witulski, and T. Hofmann, “Structure determination of bisacetylenic oxylipins in carrots (*Daucus carota*L.) and enantioselective synthesis of falcarindiol,” *Journal of Agricultural and Food Chemistry*, vol. 57, no. 22, pp. 11030–11040, 2009.
- [60] C. Dawid, F. Dunemann, W. Schwab, T. Nothnagel, and T. Hofmann, “Bioactive C₁₇-polyacetylenes in carrots (*Daucus carota* L.): current knowledge and future perspectives,” *Journal of Agricultural and Food Chemistry*, vol. 63, no. 42, pp. 9211–9222, 2015.
- [61] B. T. Metzger, D. M. Barnes, and J. D. Reed, “Purple carrot (*Daucus carota* L.) polyacetylenes decrease lipopolysaccharide-induced expression of inflammatory proteins in macrophage and endothelial cells,” *Journal of Agricultural and Food Chemistry*, vol. 56, no. 10, pp. 3554–3560, 2008.
- [62] H. Kang, T. S. Bang, J. W. Lee et al., “Protective effect of the methanol extract from *Cryptotaenia japonica* Hassk. against lipopolysaccharide-induced inflammation in vitro and in vivo,” *BMC Complementary and Alternative Medicine*, vol. 12, no. 1, p. 199, 2012.
- [63] Y.-J. Shiao, Y. L. Lin, Y. H. Sun, C. W. Chi, C. F. Chen, and C. N. Wang, “Falcarindiol impairs the expression of inducible nitric oxide synthase by abrogating the activation of IKK and JAK in rat primary astrocytes,” *British Journal of Pharmacology*, vol. 144, no. 1, pp. 42–51, 2009.
- [64] T. Ohnuma, S. Nakayama, E. Anan, T. Nishiyama, K. Ogura, and A. Hiratsuka, “Activation of the Nrf2/ARE pathway via S-alkylation of cysteine 151 in the chemopreventive agent-sensor Keap1 protein by falcarindiol, a conjugated diacetylene compound,” *Toxicology and Applied Pharmacology*, vol. 244, no. 1, pp. 27–36, 2010.
- [65] T. Ohnuma, T. Komatsu, S. Nakayama, T. Nishiyama, K. Ogura, and A. Hiratsuka, “Induction of antioxidant and phase 2 drug-metabolizing enzymes by falcarindiol isolated from *Notopterygium incisum* extract, which activates the Nrf2/ARE pathway, leads to cytoprotection against oxidative and electrophilic stress,” *Archives of Biochemistry and Biophysics*, vol. 488, no. 1, pp. 34–41, 2009.
- [66] T. Ohnuma, E. Anan, R. Hoashi et al., “Dietary diacetylene falcarindiol induces phase 2 drug-metabolizing enzymes and blocks carbon tetrachloride-induced hepatotoxicity in mice through suppression of lipid peroxidation,” *Biological & Pharmaceutical Bulletin*, vol. 34, no. 3, pp. 371–378, 2011.
- [67] H. M. Al-Kuraishy and A. I. Al-Gareeb, “Eustress and malondialdehyde (MDA): role of Panax ginseng: randomized placebo controlled study,” *Iranian Journal of Psychiatry*, vol. 12, no. 3, pp. 194–200, 2017.
- [68] K. Tateda, T. Matsumoto, S. Miyazaki, and K. Yamaguchi, “Lipopolysaccharide-induced lethality and cytokine production in aged mice,” *Infection and Immunity*, vol. 64, no. 3, pp. 769–774, 1996.
- [69] H. Vedder, W. Schreiber, A. Yassouridis, S. Gudewill, C. Galanos, and T. Pollmächer, “Dose-dependence of bacterial lipopolysaccharide (LPS) effects on peak response and time course of the immune-endocrine host response in humans,” *Inflammation Research*, vol. 48, no. 2, pp. 67–74, 1999.
- [70] U. Erben, C. Loddenkemper, K. Doerfel et al., “A guide to histomorphological evaluation of intestinal inflammation in mouse models,” *International Journal of Clinical and Experimental Pathology*, vol. 7, no. 8, pp. 4557–4576, 2014.
- [71] M. R. Saban, H. Hellmich, N. B. Nguyen, J. Winston, T. G. Hammond, and R. Saban, “Time course of LPS-induced gene

- expression in a mouse model of genitourinary inflammation,” *Physiological Genomics*, vol. 5, no. 3, pp. 147–160, 2001.
- [72] M. R. Dillingh, E. P. van Poelgeest, K. E. Malone et al., “Characterization of inflammation and immune cell modulation induced by low-dose LPS administration to healthy volunteers,” *Journal of Inflammation*, vol. 11, no. 1, p. 28, 2014.
- [73] R. A. Luz, P. Xavier-Elsas, B. de Luca et al., “5-Lipoxygenase-dependent recruitment of neutrophils and macrophages by eotaxin-stimulated murine eosinophils,” *Mediators of Inflammation*, vol. 2014, Article ID 102160, 13 pages, 2014.
- [74] M. Derouet, L. Thomas, A. Cross, R. J. Moots, and S. W. Edwards, “Granulocyte macrophage colony-stimulating factor signaling and proteasome inhibition delay neutrophil apoptosis by increasing the stability of Mcl-1,” *The Journal of Biological Chemistry*, vol. 279, no. 26, pp. 26915–26921, 2004.
- [75] J. M. Williams, C. A. Duckworth, M. D. Burkitt, A. J. M. Watson, B. J. Campbell, and D. M. Pritchard, “Epithelial cell shedding and barrier function,” *Veterinary Pathology*, vol. 52, no. 3, pp. 445–455, 2015.
- [76] M. W. Bernart, J. H. Cardellina, M. S. Balaschak, M. R. Alexander, R. H. Shoemaker, and M. R. Boyd, “Cytotoxic falcariinol oxylipins from *Dendropanax arboreus*,” *Journal of Natural Products*, vol. 59, no. 8, pp. 748–753, 1996.
- [77] L. P. Christensen, W. Vach, J. Ritskes-Hoitinga, and K. Brandt, “Inhibitory effects of feeding with carrots or (–)-falcariinol on development of azoxymethane-induced preneoplastic lesions in the rat colon,” *Journal of Agricultural and Food Chemistry*, vol. 53, no. 5, pp. 1823–1827, 2005.
- [78] L.-P. Jiang, Y. Lu, B.-M. Nie, and H.-Z. Chen, “Antiproliferative effect of panaxynol on RASMCs via inhibition of ERK1/2 and CREB,” *Chemico-Biological Interactions*, vol. 171, no. 3, pp. 348–354, 2008.
- [79] Z. Yan, R. Yang, Y. Jiang et al., “Induction of apoptosis in human promyelocytic leukemia HL60 cells by panaxynol and panaxydol,” *Molecules*, vol. 16, no. 7, pp. 5561–5573, 2011.
- [80] K. W. Tan, D. P. Killeen, Y. Li, J. W. Paxton, N. P. Birch, and A. Scheepens, “Dietary polyacetylenes of the falcariinol type are inhibitors of breast cancer resistance protein (BCRP/ABCG2),” *European Journal of Pharmacology*, vol. 723, pp. 346–352, 2014.
- [81] Z. R. Haywood Small, “Differential interactions of falcariinol combined with anti-tumour agents on cellular proliferation and apoptosis in human lymphoid leukaemia cell lines,” *Journal of Blood Disorders & Transfusion*, vol. 6, no. 2, 2015.
- [82] M. Kobaek-Larsen, R. B. El-Houri, L. P. Christensen, I. Al-Najami, X. Fretté, and G. Baatrup, “Dietary polyacetylenes, falcariinol and falcariindiol, isolated from carrots prevents the formation of neoplastic lesions in the colon of azoxymethane-induced rats,” *Food & Function*, vol. 8, no. 3, pp. 964–974, 2017.
- [83] H. T. Le, H. T. Nguyen, H. Y. Min et al., “Panaxynol, a natural Hsp90 inhibitor, effectively targets both lung cancer stem and non-stem cells,” *Cancer Letters*, vol. 412, pp. 297–307, 2018.
- [84] S. Bhattacharya, M. K. Rasmussen, L. P. Christensen, J. F. Young, K. Kristiansen, and N. Oksbjerg, “Naringenin and falcariinol stimulate glucose uptake and TBC1D1 phosphorylation in porcine myotube cultures,” *Journal of Biochemical and Pharmacological Research*, vol. 2, no. 2, pp. 91–98, 2014.
- [85] R. B. El-Houri, D. Kotowska, K. B. Christensen et al., “Polyacetylenes from carrots (*Daucus carota*) improve glucose uptake in vitro in adipocytes and myotubes,” *Food & Function*, vol. 6, no. 7, pp. 2135–2144, 2015.
- [86] S. Purup, E. Larsen, and L. P. Christensen, “Differential effects of falcariinol and related aliphatic C₁₇-polyacetylenes on intestinal cell proliferation,” *Journal of Agricultural and Food Chemistry*, vol. 57, no. 18, pp. 8290–8296, 2009.
- [87] S. Kamiloglu, C. Grootaert, E. Capanoglu et al., “Anti-inflammatory potential of black carrot (*Daucus carota* L.) polyphenols in a co-culture model of intestinal Caco-2 and endothelial EA.hy926 cells,” *Molecular Nutrition & Food Research*, vol. 61, no. 2, 2017.
- [88] I.-M. Chung, H. K. Song, S. J. Kim, and H. I. Moon, “Anticomplement activity of polyacetylenes from leaves of *Dendropanax morbifera* Leveille,” *Phytotherapy Research*, vol. 25, no. 5, pp. 784–786, 2011.
- [89] M. M. Czyzewska, L. Chrobok, A. Kania et al., “Dietary acetylenic oxylipin falcariinol differentially modulates GABAA receptors,” *Journal of Natural Products*, vol. 77, no. 12, pp. 2671–2677, 2014.
- [90] X. Chi, W. Yao, H. Xia et al., “Elevation of HO-1 expression mitigates intestinal ischemia-reperfusion injury and restores tight junction function in a rat liver transplantation model,” *Oxidative Medicine and Cellular Longevity*, vol. 2015, 12 pages, 2015.
- [91] N. Wang, G. Wang, J. Hao et al., “Curcumin ameliorates hydrogen peroxide-induced epithelial barrier disruption by upregulating heme oxygenase-1 expression in human intestinal epithelial cells,” *Digestive Diseases and Sciences*, vol. 57, no. 7, pp. 1792–1801, 2012.
- [92] N. Wang, Q. Han, G. Wang et al., “Resveratrol protects oxidative stress-induced intestinal epithelial barrier dysfunction by upregulating heme oxygenase-1 expression,” *Digestive Diseases and Sciences*, vol. 61, no. 9, pp. 2522–2534, 2016.
- [93] F. O. Martinez and S. Gordon, “The M1 and M2 paradigm of macrophage activation: time for reassessment,” *F1000Prime Reports*, vol. 6, 2014.
- [94] J. Nishihira, M. Sakai, S. Nishi, and Y. Hatanaka, “Identification of the electrophilic substrate-binding site of glutathione S-transferase P by photoaffinity labeling,” *European Journal of Biochemistry*, vol. 232, no. 1, pp. 106–110, 1995.
- [95] Y. Zhang, “The molecular basis that unifies the metabolism, cellular uptake and chemopreventive activities of dietary isothiocyanates,” *Carcinogenesis*, vol. 33, no. 1, pp. 2–9, 2011.
- [96] Y. Zhang, “Molecular mechanism of rapid cellular accumulation of anticarcinogenic isothiocyanates,” *Carcinogenesis*, vol. 22, no. 3, pp. 425–431, 2001.
- [97] H. Yamada, S. Ono, S. Wada et al., “Statuses of food-derived glutathione in intestine, blood, and liver of rat,” *npj Science of Food*, vol. 2, no. 1, p. 3, 2018.
- [98] T. Y. Aw, “Biliary glutathione promotes the mucosal metabolism of luminal peroxidized lipids by rat small intestine in vivo,” *The Journal of Clinical Investigation*, vol. 94, no. 3, pp. 1218–1225, 1994.
- [99] N. Petri, C. Tannergren, B. Holst et al., “Absorption-metabolism of sulforaphane and quercetin, and regulation of phase II enzymes, in human jejunum in vivo,” *Drug Metabolism and Disposition*, vol. 31, no. >6, pp. 805–813, 2003.
- [100] J. Hansen-Moller, S. L. Hansen, L. P. Christensen, L. Jespersen, K. Brandt, and J. Haraldsdottir, *Quantification*

of Polyacetylenes by LC-MS in Human Plasma after Intake of Fresh Carrot Juice, Danish Institute of Agricultural Sciences, 2002.

- [101] J. Haraldsdottir, L. Jespersen, J. Hansen-Moller, S. L. Hansen, L. P. Christensen, and K. Brandt, *Recent Developments in the Bioavailability of Falcarinol*, Danish Institute of Agricultural Sciences, 2002.
- [102] Y. Wang, J. Liu, M. Zhu et al., "Biophysical characterization of interactions between falcarinol-type polyacetylenes and human serum albumin via multispectroscopy and molecular docking techniques," *Journal of Luminescence*, vol. 200, pp. 111–119, 2018.
- [103] P. Mehrpouya-Bahrami, K. N. Chitrala, M. S. Ganewatta et al., "Blockade of CB1 cannabinoid receptor alters gut microbiota and attenuates inflammation and diet-induced obesity," *Scientific Reports*, vol. 7, no. 1, article 15645, 2017.
- [104] A. Alhamoruni, K. L. Wright, M. Larvin, and S. E. O'Sullivan, "Cannabinoids mediate opposing effects on inflammation-induced intestinal permeability," *British Journal of Pharmacology*, vol. 165, no. 8, pp. 2598–2610, 2012.
- [105] M. Leonti, L. Casu, S. Raduner et al., "Falcarinol is a covalent cannabinoid CB1 receptor antagonist and induces pro-allergic effects in skin," *Biochemical Pharmacology*, vol. 79, no. 12, pp. 1815–1826, 2010.

Research Article

Neuroprotective Effect of *Caryocar brasiliense* Camb. Leaves Is Associated with Anticholinesterase and Antioxidant Properties

Thiago Sardinha de Oliveira,¹ Douglas Vieira Thomaz,² Hiasmin Franciely da Silva Neri,¹ Letícia Bonancio Cerqueira,³ Luane Ferreira Garcia,² Henric Pietro Vicente Gil,⁴ Roberto Pontarolo ,³ Francinete Ramos Campos,³ Elson Alves Costa,¹ Fernanda Cristina Alcantara dos Santos,¹ Eric de Souza Gil ,² and Paulo César Ghedini ¹

¹Institute of Biological Sciences, Federal University of Goiás, Goiânia, Brazil

²Faculty of Pharmacy, Federal University of Goiás, Goiânia, Brazil

³Department of Pharmacy, Federal University of Paraná, Curitiba, Brazil

⁴Federal Institute of Goiás, Trindade, Brazil

Correspondence should be addressed to Eric de Souza Gil; ericsgil@gmail.com and Paulo César Ghedini; pcghedini@gmail.com

Received 27 February 2018; Revised 9 July 2018; Accepted 9 August 2018; Published 21 October 2018

Academic Editor: Felipe L. de Oliveira

Copyright © 2018 Thiago Sardinha de Oliveira et al. This is an open access article distributed under the Creative Commons Attribution License, which permits unrestricted use, distribution, and reproduction in any medium, provided the original work is properly cited.

Pequi (*Caryocar brasiliense*) is an endemic species from Brazilian Cerrado, and their fruits are widely used in regional cuisine. In this work, a crude hydroalcoholic extract (CHE) of *C. brasiliense* leaves and its resulting fractions in hexane (HF), chloroform (CF), ethyl acetate (EAF), and butanol (BF) were investigated for their antioxidant properties and anticholinesterase activities. The antioxidant properties were evaluated by free radical scavenging and electroanalytical assays, which were further correlated with the total phenolic content and LC-MS results. The acetylcholinesterase and butyrylcholinesterase inhibitory activities were examined using Ellman's colorimetric method. The LC-MS analysis of EAF revealed the presence of gallic acid and quercetin. CHE and its fractions, EAF and BF, showed anticholinesterase and antioxidant activities, suggesting the association of both effects with the phenolic content. In addition, behavioral tests performed with CHE (10, 100, and 300 mg/kg) showed that it prevented mice memory impairment which resulted from aluminium intake. Moreover, CHE inhibited brain lipid peroxidation and acetyl and butyryl-cholinesterase activities and the extract's neuroprotective effect was reflected at the microscopic level. Therefore, the leaves of pequi are a potential source of phenolic antioxidants and can be potentially used in treatments of memory dysfunctions, such as those associated with neurodegenerative disorders.

1. Introduction

Neurodegenerative disorders, such as Alzheimer's disease (AD), present features of memory and cognitive impairment. Literature reports that AD is characterized by a combined loss of cholinergic neurons and their projections to the basal nucleus and associated areas of the brain stream. Given that neurotransmission is nonetheless sensitive to beta-amyloid peptide toxicity, the progressive deterioration of cholinergic innervation leads to signaling impairment, therefore contributing to the cognitive and behavioral dysfunctions seen in AD [1, 2].

Oxidative damage is known to play an important role in neuronal damage, due to the neurodegeneration promoted by highly reactive compounds. Since brain tissue is particularly sensitive to reactive oxygen species- (ROS-) mediated cell damage, ROS build up may lead to lipid peroxidation. This process inhibits henceforth neurotransmitter production, such as that of acetylcholine, which is deeply involved in memory and learning [3, 4].

Considering the overall aspects of AD pathogenesis, the identification of antioxidant bioactive compounds presenting complementary anticholinesterase (AChE) activities is an important step to aid neuroprotector treatments, due to the

possibility of synergistically mopping up ROS and allowing proper acetylcholine build up in the synaptic cleft. In this context, Brazilian Cerrado trees are known to possess myriads of antioxidant secondary metabolites which may also hinder different forms of cholinesterase enzymes [5, 6].

Amongst potential neuroprotective phytochemicals is *Caryocar brasiliense* (Camb), a Caryocaraceae family member popularly known as “pequi.” This tree plays a significant role in central western Brazilian culture and is a source of raw material for small- and middle-sized industries. In folk medicine, the fruit pulp is used as stomachic and for flu treatment, whereas a decoction of the leaves and flowers is used as energetic, tonic, aphrodisiac, and treatment for liver diseases. *C. brasiliense* is also known to be rich in flavonoids which may display leishmanicidal, antifungal, antioxidant, and vasorelaxant properties [7–10].

Studies concerning *C. brasiliense* leaves reported the presence of antioxidant compounds such as gallic acid, quinic acid, quercetin, and quercetin 3-*o*-arabinose [9, 10]. However, literature reports on the extent of neuroprotection related to *C. brasiliense* extract ingestion, as well as anticholinesterase activities, are still limited [11].

This study therefore is aimed at evaluating the antioxidant and anticholinesterase activities as well as neuroprotective effects of *C. brasiliense* leaves, in order to provide new information on the potential use of this plant against neurodegenerative disorders.

2. Material and Methods

2.1. Reagents. Bovine serum albumin, gallic acid, rutin and quercetin, aluminium chloride, acetylcholine, 5,5'-dithio-bis(2-nitrobenzoic acid) (DNTB), 1,5-bis(4-allyldimethylammoniumphenyl)pentan-3-one dibromide (BW284c51), tetraisopropyl pyrophosphoramidate (iso-OMPA), acetylthiocholine iodide, S-butyrylthiocholine iodide, epinephrine bitartrate, and eosin were purchased from Sigma.

This work also made use of hydrogen peroxide (CRQ), trichloroacetic acid (TCA) (Vetec), thiobarbituric acid (TBA) (TediaBrasil), n-butanol (Synth), glycine (Vetec), NaH₂PO₄H₂O (Cromoline), Na₂HPO₄ (Synth), coomassie brilliant blue (Amresco), ethyl alcohol (Synth), xylene (Vetec), Paraplast (Merck), and hematoxylin (Merck).

All electrolyte salts, solvents and reagents were of analytical grade. Electrolyte solutions were prepared with double distilled Milli-Q water (conductivity $\leq 0.1 \mu\text{S}\cdot\text{cm}^{-1}$) (Millipore S. A., Molsheim, France).

2.2. Animals. Male Swiss mice (25–30 g) from the colony of the Federal University of Goiás were used in this study. The animals were housed under a controlled 12 h light/dark cycle and stable temperature (22–23°C) with free access to food and water. All experiments were conducted in accordance with the Sociedade Brasileira de Ciência em Animais de Laboratório (SBCAL) and were approved by the local Ethics in Research Committee (protocol number: 140/10).

2.3. Extract Preparation. *C. brasiliense* dried leaves were collected in September 2010 in Gurupi, Tocantins, Brazil.

The plant was authenticated by Professor Aristônio Magalhães Teles, and a voucher sample was deposited in the herbarium of the Institute of Biological Sciences of the Federal University of Goiás under the code 1353 [10].

The extract was prepared focusing on polyphenol extraction; henceforth, CHE was obtained by immersion and sonication of leaf powder in ethanol-water solution (70:30) for 1 h. The resulting extract was lyophilized and stored in a dark container at 4°C.

Organic fractions (OFs) were obtained by fractionation of crude hydroalcoholic lyophilized extract using organic solvents with crescent degrees of polarity (hexane—chloroform—ethyl acetate—butanol). Thereafter, solvents were evaporated under reduced pressure to produce a hexane fraction (HF), a chloroform fraction (CF), an ethyl acetate fraction (EAF), and a butanol fraction (BF).

2.4. Determination of In Vitro Anticholinesterase Activity. Acetylcholinesterase (AChE) and butyrylcholinesterase (BChE) inhibitory activities were measured by the spectrophotometric method developed by Ellman et al. [12]. AChE and BChE from whole mice brain homogenates were used, while acetylthiocholine iodide (ATC) and butyrylthiocholine chloride (BTC) were employed as substrates of the reaction. In order to distinguish if pequi extracts had preferential action between AChE and BChE, tests were performed using ATC as a substrate in the presence of iso-OMPA (an inhibitor of BChE).

DTNB was used for the measurement of anticholinesterase activity. CHE and OFs (1–500 $\mu\text{g}/\text{mL}$) were preincubated with the homogenates for 30 min before addition of DTNB and ATC or BTC. Neostigmine was used as a reference compound.

2.5. Antioxidant Assays

2.5.1. DPPH Free Radical Scavenging Assay. The free radical scavenging activity was determined spectrophotometrically by reaction with 2,2-diphenyl-1-picrylhydrazyl (DPPH), as described by Blois [13]. CHE and OFs (1–500 $\mu\text{g}/\text{mL}$) were preincubated for 30 min in the presence of DPPH before spectrophotometric analysis. Quercetin was used as an antioxidant standard.

2.5.2. Voltammetric Determination of Redox Behavior. The electroanalytical profile of CHE and OFs was performed according to the method described by Lino et al. [14]. The electrochemical analysis was performed in phosphate buffer 0.1 M (pH 7.0). Voltammetric experiments were carried out using a potentiostat/galvanostat $\mu\text{Autolab III}^{\circledR}$ integrated to the GPES 4.9[®] software (Eco Chemie, Utrecht, Netherlands).

Measurements were carried out in a 5 mL one-compartment electrochemical cell, using a three-electrode system consisting of a glassy carbon electrode (GCE) ($\varnothing = 2 \text{ mm}$) as the working electrode, Pt wire as the counter electrode, and Ag/AgCl (3 mol·L⁻¹ KCl) as the reference electrode. The experimental conditions for differential pulse voltammetry (DPV) and square wave voltammetry (SWV) were a pulse amplitude of 50 mV, pulse width of 0.4 s, and scan rate of 5 mV·s⁻¹.

Measurements of pH were carried out in a QUIMIS® pH meter. All experiments were done at room temperature. All voltammograms presented were background subtracted and baseline corrected using the moving average application with a step window of 2 mV included in the GPES software herein employed. This mathematical treatment improves the visualization and the identification of peaks over the baseline without introducing any artifacts, even though the peak intensity is in some cases reduced (<10%) in relation to the untreated curve. Nevertheless, this mathematical treatment was used in the presentation of all experimental voltammograms for a better and clearer identification of the peaks. The values for the peak current presented in all plots were determined from the original untreated voltammograms after subtraction of the baseline.

The antioxidant capacity was presented by electrochemical index (EI), obtained by index I_{pa}/E_{pa} , using the mathematical calculation:

$$EI = \frac{I_{pa1}}{E_{pa1}} + \frac{I_{pa2}}{E_{pa2}} + \dots + \frac{I_{pan}}{E_{pan}}. \quad (1)$$

2.5.3. Phenolic Content. The total phenolic content was estimated using the Folin-Ciocalteu reaction. Briefly, 2.5 mL of diluted Folin-Ciocalteu reagent (1/10) was added to a small volume of sample (usually between 25 and 100 μ L), which was then treated with sodium carbonate solution as described in Georgé et al. [15]. The absorbance was measured at 760 nm, and the total phenolic content was calculated as a gallic acid equivalent (GAE) based on a standard curve of gallic acid. All of the experiments were performed in triplicate. Results were expressed as milligrams of GAE/mL in both CHE and OFs.

2.6. MS Analysis

2.6.1. Standards and EAF Preparation for LC-MS Analysis. Stock solutions of gallic acid and quercetin standards were prepared separately in methanol at concentrations of 1 mg/mL. All stock solutions were stored under refrigeration at 4°C. Working solutions were obtained from stock solutions by appropriate dilution in methanol/water solution (70:30 v/v) containing 1 mM ammonium formate to the final concentration of 0.5 μ g/mL, 50 μ g/mL, and 2 mg/mL of gallic acid, quercetin standards and EAF solutions, respectively. All working standard solutions and samples were filtered through a polyvinylidene fluoride syringe filter (11 mm and 0.45 mm; Millipore Millex, Billerica, MA, USA) before injection into the liquid chromatography coupled to mass spectrometry (LC-MS).

2.6.2. LC-MS Instrumentation and Conditions. LC-ESI-MS analysis was performed using an Agilent 1200 RRHT system (Wilmington, NC, USA) that consisted of a G1311A binary pump, G1379A degasser, and G1316A column oven. These were connected with a CTC sample manager (model 2777, Waters, Milford, CT, USA). The system was coupled to an Applied Biosystems MDS Sciex API 3200 triple quadrupole mass spectrometer (Toronto, Canada) equipped

with a syringe pump Harvard 22 Dual Model (Harvard Apparatus, South Natick, MA, USA) and an electrospray ionization (ESI) source. The ESI source was operated in the negative ion mode for quercetin and gallic acid standards monitoring in the ethyl acetate fraction. For the negative ion mode, the mobile phase consisted of methanol/water solution (10:90 v/v) (A) and acetonitrile (B) both containing 1 mM ammonium formate. Analyte separations were carried out according to method established by Oliveira et al. [10]. Chromatographic analysis was performed on an XBridge C18 150 \times 2.1 mm (5 mm particle size) column coupled with an XBridge C18 10 \times 2.1 mm (5 mm particle size) guard column. The injection volume was 20 μ L, and the column temperature was maintained at 25°C. Data acquisition was achieved with the MS Workstation by Analyst 1.4 software (ABI/Sciex). The high-purity nitrogen and zero grade air that were used as the CUR, GS1, and GS2 gases were produced by a high-purity nitrogen generator from PEAK Scientific Instruments (Chicago, IL, USA).

2.7. Animal Studies

2.7.1. Experimental Design. Animals were segregated in 6 groups (I to VI) ($n = 10$ each group) and undergone chronic treatment for 90 days. Treatment solutions were administered through gavage (0.1 mL/10 g). Treatment I was designed as a control group (vehicle-distilled water); therefore, only water was administered, while treatments II to VI were test groups; henceforth, AlCl₃ solution (100 mg/kg) was administered, on the morning, from day 0 to day 90. After the 45th day, a second treatment was orally administered in the afternoon. The second treatment consisted of distilled water (groups I and III), quercetin 30 mg/kg (II), CHE 10 mg/kg (IV), CHE 100 mg/kg (V), and CHE 300 mg/kg (VI). After the treatment period, behavior was evaluated (memory and locomotor activity) and then the animals were sacrificed by cervical dislocation and total brain was removed and stored at 4°C for biochemical and histopathological assays.

2.7.2. Behavioral Studies. Twenty-four hours after the end of the treatment period (91° day), in order to assess the neuroprotective properties of CHE against aluminium-induced neurotoxicity, three behavioral tests were conducted, namely, the step-down test to evaluate short- and long-term memories [16] and open field and chimney tests to evaluate locomotor activity [17, 18].

2.7.3. Biochemical Assays. Twenty-four hours after the last behavioral test, the animals were anesthetized with isoflurane. Subsequently, mice were euthanized by blood extraction through cardiac puncture and the cerebral tissue was removed. Animal's whole brains were immersed in phosphate buffer solution pH 7.4 at a proportion of 1:5 w/v. Dispersion was homogenized in tissue homogenizer (Homo Mix). The resulting colloid was centrifuged at 4492 \times g for 20 minutes at 4°C, and the supernatant (biological sample) was assessed on its protein content by Bradford method [19]. Thereafter, the supernatant was also used to assess thiobarbituric acid-reactive species (TBARS)

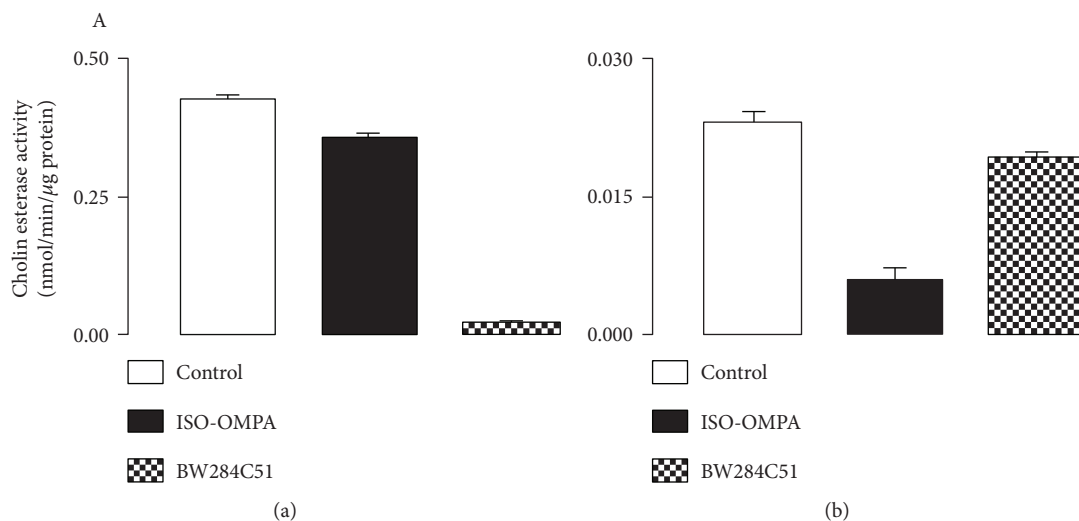


FIGURE 1: Determination of cholinesterase activity (nmol/min/μg protein) in mice brain homogenate using acetylthiocholine 1.5 mM (a) and butyrylthiocholine 1.5 mM (b) as enzyme substrates and in the presence of iso-OMPA 10 μM (an inhibitor of butyrylcholinesterase) or BW284c51 10 μM (an inhibitor of acetylcholinesterase). Control samples represent the total cholinesterase activity obtained in the absence of enzyme inhibitors. Data were obtained as a mean ± epm of 3 different samples in triplicate.

TABLE 1: Values of IC₅₀ for AChE, AChE in the presence of iso-OMPA (10⁻⁵ M) and BChE activities, and DPPH free radical formation of CHE and OFs (HF, CF, EAF, and BF) of *C. brasiliense* leaves. Values of EI and total phenolic content (GAE) to the samples are listed as well.

	AChE (μg/mL)	AChE + iso-OMPA (μg/mL)	BChE (μg/mL)	DPPH (μg/mL)	EI (μA/V)	GAE (mg/mL)
CHE	202.4 ± 7.9	233.6 ± 12.2	204.3 ± 12.4	4.6 ± 1.0	46.6 ± 3.9	1.2 ± 0.3
HF	ND	ND	ND	25.6 ± 1.5***	27.3 ± 2.5**	0.6 ± 0.1
CF	ND	ND	ND	76.4 ± 0.4***	4.4 ± 0.5***	0.1 ± 0.1*
EAF	81.5 ± 14.7***	128.9 ± 16.8***	118.6 ± 11.3***	5.9 ± 0.2	119.8 ± 4.0***	4.0 ± 0.2***
BF	235.9 ± 17.4	292.5 ± 22.3	225.7 ± 15.2	9.3 ± 0.6*	58.1 ± 2.7	1.9 ± 0.3

Values are expressed as mean ± SEM of three experiments. * $P < 0.05$, ** $P < 0.01$, and *** $P < 0.001$ when compared with CHE. ND: not determined.

[20], acetylcholinesterase (AChE), and butyrylcholinesterase (BChE) activities [12].

2.7.4. Histopathological Analysis. Animal's cortices were fixed in methanol/chloroform/acetic acid solution (6:3:1) and then dehydrated with increasing concentrations of ethanol. The dehydrated material was clarified with xylol and embedded in Paraplast (Histosec, Merck). After inclusion, the material was sectioned at 6 μm and stained by hematoxylin-eosin method. Histological sections were examined and digitized using a Zeiss Axio Scope A1 light microscope (Zeiss, Germany). The frontal cortex sections were submitted to morphometric analysis. We quantified the number of viable neurons and the percentage (%) of necrotic eosinophilic neurons per photomicrography (20 fields/group; 40x objective magnification). All analyses were performed using Image Pro-Plus program version 6.1 (Media Cybernetics Inc., Silver Spring, MD, USA). Values were presented as arithmetic mean ± standard deviation of the mean.

2.8. Statistical Analysis. Values of IC₅₀ were expressed as mean ± the standard error of the mean (SEM) and were obtained by construction of concentration-effect curves (1–500 μg/mL) of three experiments in triplicate using linear regression analysis. Statistical significance was determined

using Student's *t*-test or one-way analysis of variance (ANOVA) followed by Tukey's post hoc test, when appropriate. AP value of <0.05 was considered statistically significant. Analyses were performed using GraphPad Prism version 5.00 for Windows (San Diego, CA, USA).

3. Results and Discussion

3.1. In Vitro Anticholinesterase Activity. In order to cross-check whether all cholinesterase activities are fully blocked, control tests were performed for the AChE and BChE activities in mice brain samples incubated with iso-OMPA (an inhibitor of butyrylcholinesterase) or BW284c51 (an inhibitor of acetylcholinesterase) and using ATC or BTC as substrates (Figure 1).

The CHE inhibited the AChE and BChE activities, showing IC₅₀ of 202.4 ± 7.9 μg/mL and 204.3 ± 12.4 μg/mL, respectively. The EAF and BF inhibited the enzymes with IC₅₀ values of 81.5 ± 14.7 μg/mL and 235.9 ± 17.4 μg/mL for AChE and 118.6 ± 11.3 μg/mL and 225.7 ± 15.2 μg/mL for BChE, respectively. The HF and CF did not show an in vitro anticholinesterase effect (Table 1).

Considering that BChE hydrolyzes ATC, we performed assays using ATC as substrate in the presence

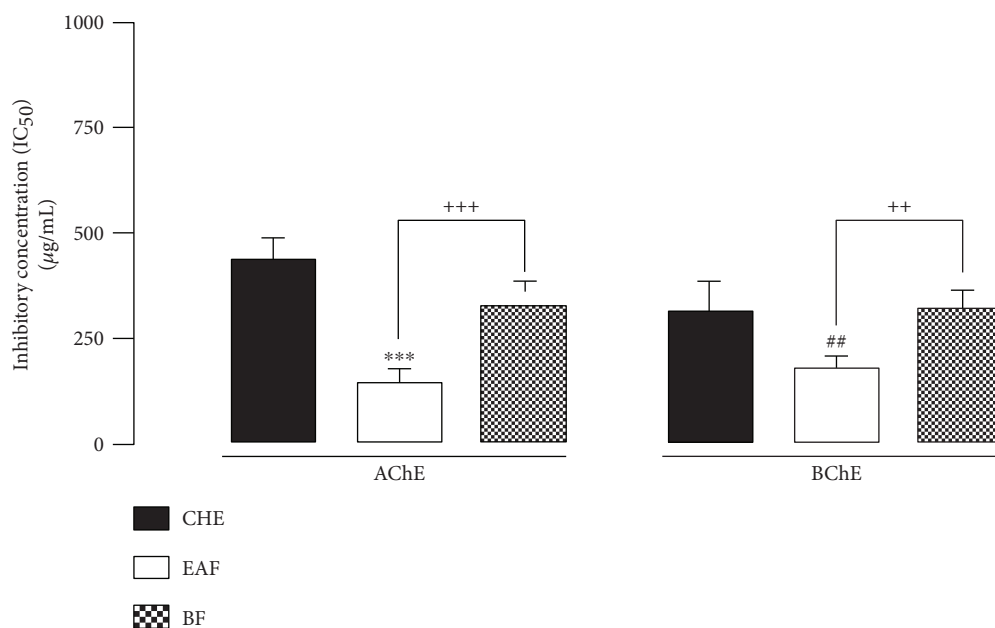


FIGURE 2: Representative figure of IC₅₀ of crude hydroalcoholic extract (CHE), ethyl acetate fraction (EAF), and butanol fraction (BF) of *Caryocar brasiliense* leaves on mice brain acetylcholinesterase and butyrylcholinesterase activities of 3 experiments in triplicate. *** $P < 0.001$ or ## $P < 0.01$ when compared to CHE; ++ $P < 0.01$ or +++ $P < 0.001$ when compared to EAF.

of iso-OMPA (an inhibitor of BChE) and the results were not different when compared with those without iso-OMPA (Table 1). Neostigmine, herein used as standard, inhibited AChE and BChE, with IC₅₀ values of 88 ± 19.7 ng/mL and 752.5 ± 121 ng/mL, respectively.

Acetylcholine is responsible for cholinergic neurotransmission, released by nervous presynaptic terminations, and it is the agonist of nicotinic and muscarinic receptors. Normally, AChE rapidly degrades ACh, ending its cellular action [20, 21]. In addition to AChE, another enzyme related to ACh degradation is the BChE enzyme [12]. It has been shown that, in AD, brain BChE activity increases progressively as the severity of dementia progresses, while the AChE activity decreases [2]. In this study, the results showed that CHE, EAF, and BF inhibited both in vitro cholinesterase enzymes, without preferential or selective actions between these two enzymes. On other hand, EAF showed a better cholinesterase inhibitory effect, suggesting that this fraction concentrates the anticholinesterase compounds present in *C. brasiliense* leaves (Figure 2).

3.2. Antioxidant Assays

3.2.1. DPPH Assay. CHE inhibited the DPPH oxidation, showing IC₅₀ values of 4.6 ± 1.0 µg/mL. HF, CF, EAF, and BF inhibited radical formation with values of IC₅₀ of 25.6 ± 1.5 µg/mL, 76.4 ± 0.4 µg/mL, 5.9 ± 0.2 µg/mL, and 9.3 ± 0.6 µg/mL, respectively (Table 1). Quercetin inhibited DPPH oxidation, with an IC₅₀ value of 1.46 ± 0.2 µg/mL.

3.2.2. Voltammetric Determination of Redox Behavior. The EI values obtained for the samples studied were 46.6 µA/V (CHE), 27.3 µA/V (HF), 4.4 µA/V (CF), 119.8 µA/V (EAF), and 58.1 µA/V (BF) (Table 1). The order of EI values

corresponded to EAF > BF > CHE > HF > CF, indicating that polar fractions showed higher antioxidant potentials. This result agrees with the DPPH results, where the EAF and BF were the fractions that showed higher antioxidant activity.

Figure 3(a) shows the DPV voltammograms obtained for CHE and OFs in a 0.1 M phosphate buffer with a pH of 7.0. The DPV voltammogram shows three consecutive oxidation peaks: 1a, at $E_{p1a} \cong +0.26$ V; 2a, at $E_{p2a} \cong +0.59$ V; and 3a, at $E_{p3a} \cong +0.87$ V. These peaks were present in all analyzed samples. In the case of complex samples, such as plant extracts, the formation of current peaks can be the result of contribution of one or more electroactive species in that redox process occurring at similar potentials. This affirmation is illustrated by the peak 2a observed for CHE, EAF, and BF or by peak broadening observed for the other fractions (HF and CF).

In order to establish a better correlation between the aforementioned peaks and the redox profile of potential phytochemicals to which they could be related, a DP voltammetry was conducted with the same standards used in MS analysis, namely, quercetin and gallic acid (Figure 3(a), inset). The peaks 1a at $E_{p1a} \cong +0.18$ V and 2a at $E_{p2a} \cong +0.5$ V present in both quercetin and gallic acid are correlated to the redox process that were also observed in all extracts (Figure 3(a)), which is correlated to catechol moiety present in a myriad of natural phenolic compounds with recognized antioxidant performance [18].

Figure 3(b) shows the SWV voltammogram obtained for CHE in the 0.1 M phosphate buffer with a pH of 7.0. The continuous line corresponds to the total current (I_t), which is the sum of the currents related to the oxidation (I_f , forward current) and reduction processes (I_b , backward current), represented by dotted lines. The similarity between the 1a and 1c

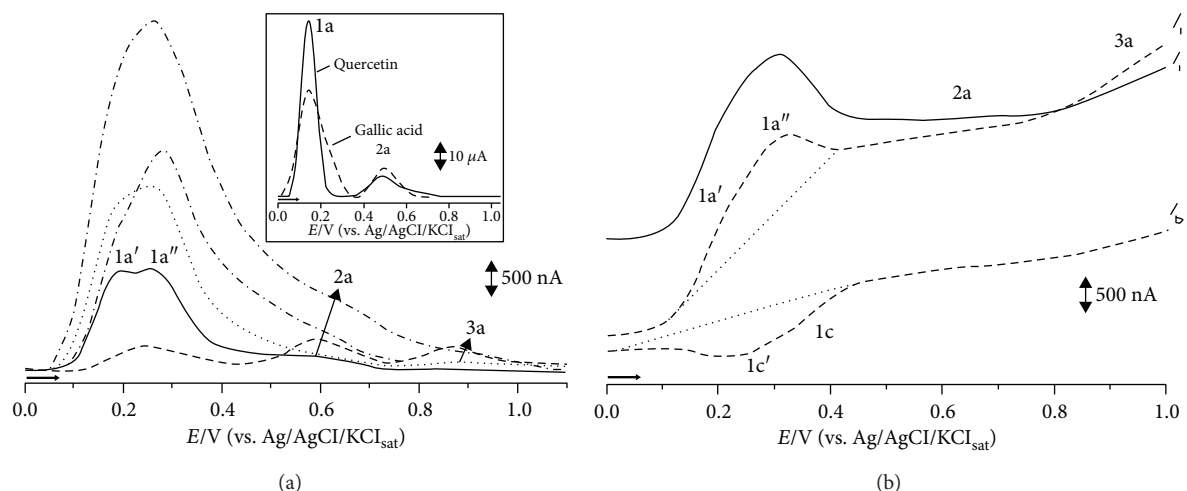


FIGURE 3: (a) DP voltammograms obtained for of EAF, BF, CHE, HF, and CF extracts. Inset: DP voltammogram of quercetin and gallic acid standards; (b) SWV voltammogram obtained for CHE in pH 7.0 0.1 M phosphate buffer total current (I_t : solid line), forward current (I_f : dashed line) and backward current (I_b : dotted line).

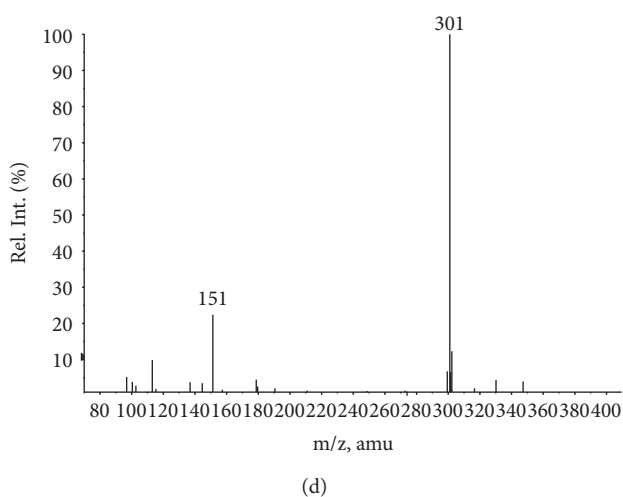
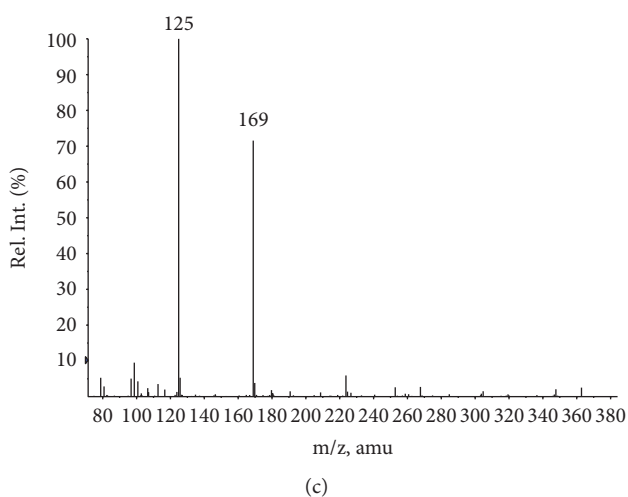
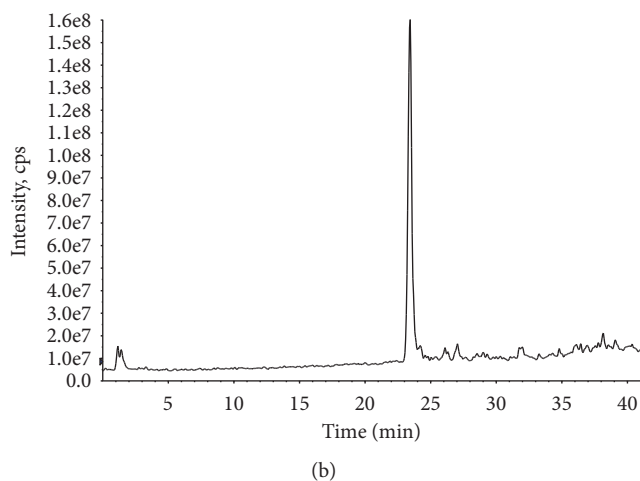
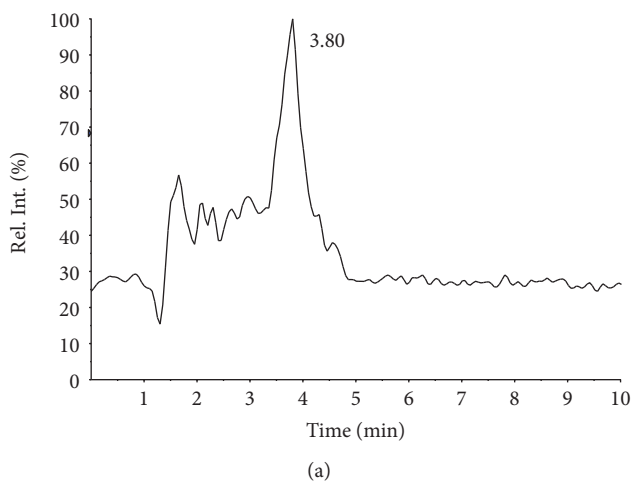


FIGURE 4: LC-ESI(-)-MS analysis of gallic acid and quercetin standards. Total ion chromatogram of standards: (a) gallic acid, (b) quercetin, (c) MS spectrum of peak extracted in $R_t = 3.8$ min of gallic acid standard, and (d) MS spectrum of peak extracted in $R_t = 23.8$ min of quercetin standard.

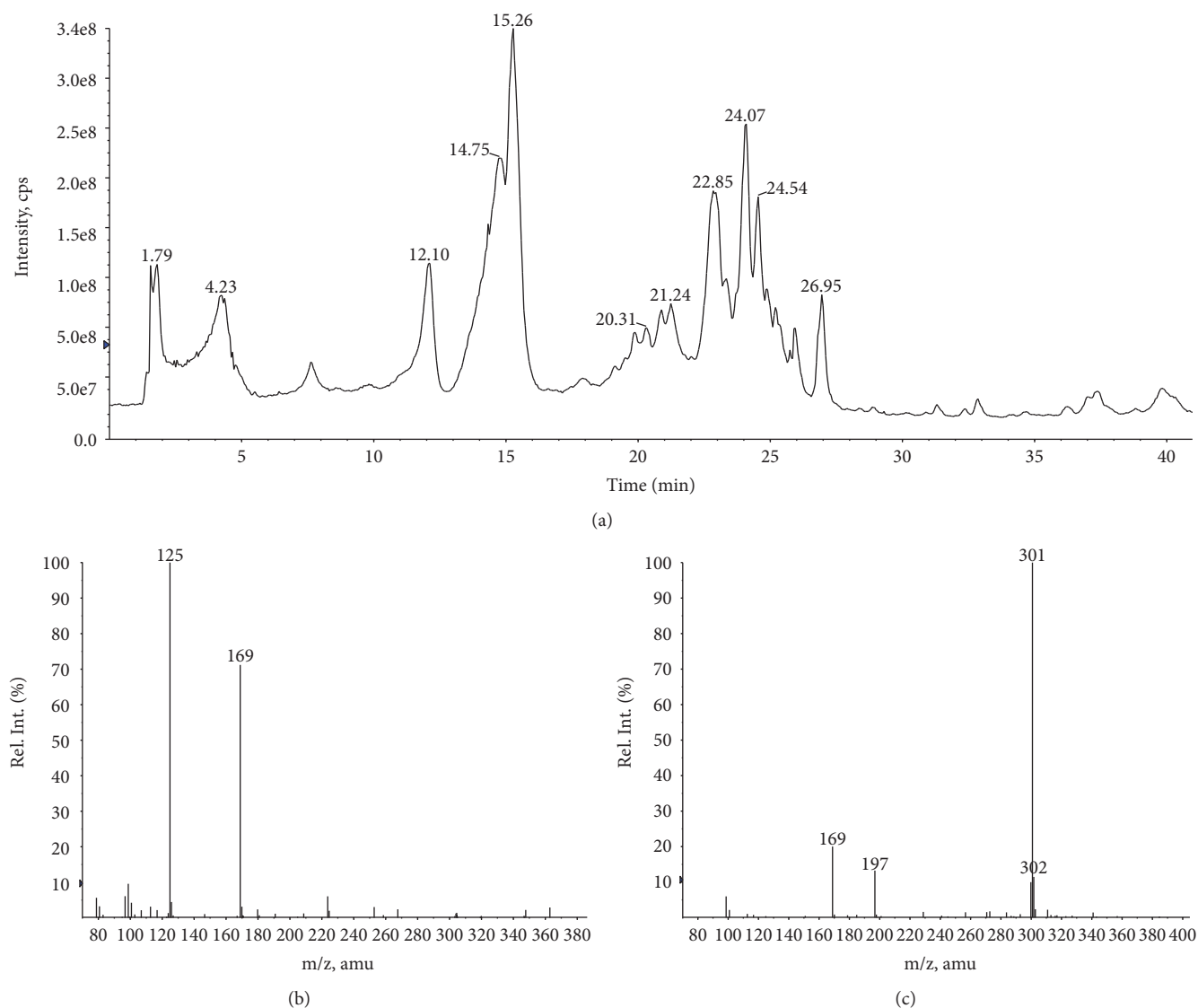


FIGURE 5: LC-ESI(-)-MS analysis for ethyl acetate fraction (EAF) from leaves of *Caryocar brasiliense*. (a) Total ion chromatogram of EAF, (b) MS spectrum of peak extracted in $R_t = 3.8$ min, and (c) MS spectrum of peak extracted in $R_t = 23.8$ min.

peaks indicates the reversibility of the system. In the case of antioxidants, the reversibility of a redox process is particularly useful as it relates to its stability and ability to restore the involved species.

3.3. Phenolic Content. The levels of phenols were 1.2 ± 0.3 (CHE), 0.6 ± 0.1 (HF), 0.1 ± 0.1 (CF), 4.0 ± 0.2 (EAF), and 1.9 ± 0.3 (BF), where all units are in mg-GAE/mL (Table 1). The highest concentrations of phenolic content were in EAF and BF, fractions that present anticholinesterase and antioxidant activities. It is well established that phenolic compounds, such as flavonoids, are antioxidants and some of them exhibit anticholinesterase activity [13–15]. Therefore, it is possible to suggest that the antioxidant and anticholinesterase activities herein observed are associated, at least in part, to the phenolic compounds.

Ethyl acetate and butanol are higher polarity solvents and extract phenolic compounds (i.e., flavonoids), among other

chemical substances [10, 22]. In a previous study, we showed the presence of gallic acid and quercetin in *C. brasiliense* leaves using LC-ESI-MS analysis [10]. In addition to being a well-known antioxidant agent [23], quercetin shows inhibitory activity against AChE and BChE [14, 24] and it was suggested that it may provide a promising approach for the treatment of AD and other oxidative stress-related neurodegenerative diseases [25].

Concerning gallic acid, despite it being an antioxidant agent [26], the anticholinesterase effect is nonsignificant [14]. Regarding these approaches, the presence of quercetin in *C. brasiliense* leaves can shed light on the anticholinesterase and antioxidant effects of *C. brasiliense*. However, further studies should be conducted in order to identify other possible compounds present in the polar OFs of *C. brasiliense* leaves that possess both effects. Furthermore, the differences between the results of colorimetric (DDPH and ABTS) and electrochemical methods can be attributed to the higher

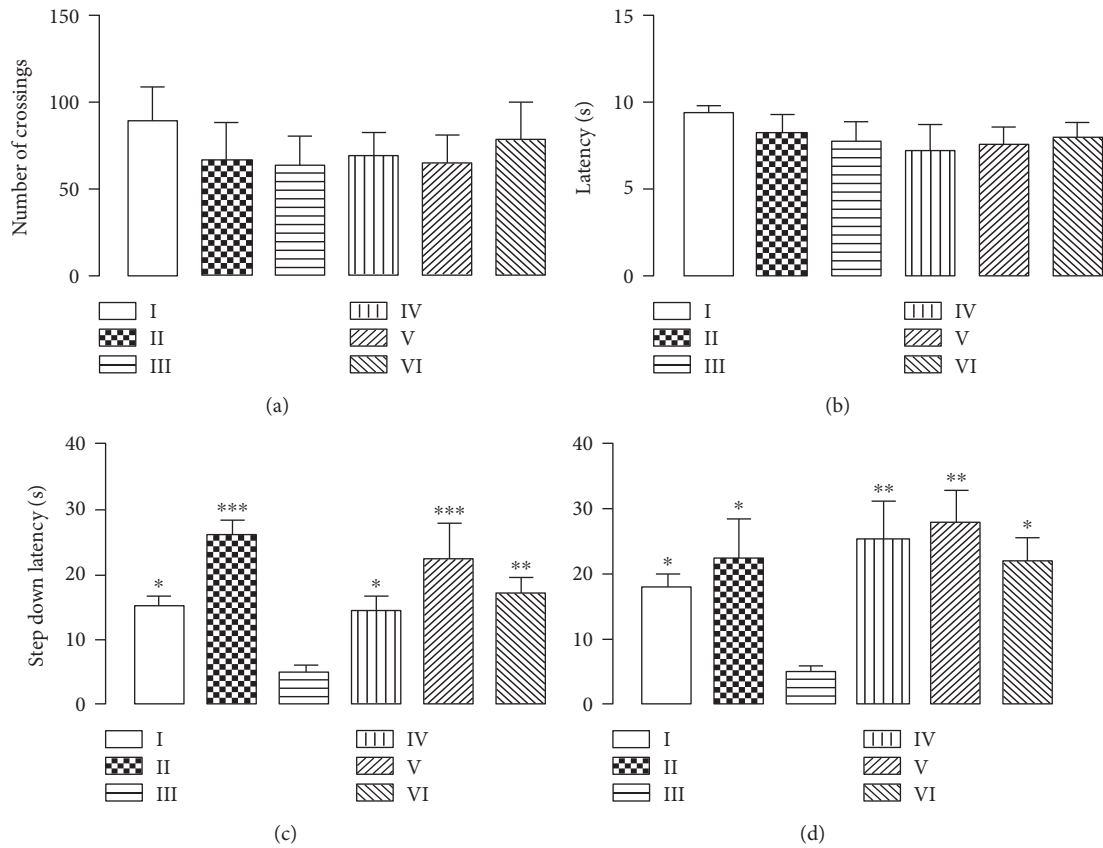


FIGURE 6: Effect of CHE treatment on locomotor activity (a, b) and memory (c, d) of mice subjected to 90 days of aluminium exposure. (a) Number of crossings of mice groups as evaluated in the open-field test. (b) Time (s) to climb backwards out of the tube within 30 sec for the examined animals in the chimney test. Latencies of retention time (s) in mice as evaluated in the step-down test at 90 min (c) and 24 h (d) after shock challenge. Each column represents mean \pm SEM of 10 animals. (* $P < 0.05$, ** $P < 0.01$, and *** $P < 0.001$ in comparison to group III). I: control group; II: quercetin 30 mg/kg; III: aluminium group; IV: CHE 10 mg/kg; V: CHE 100 mg/kg; VI: CHE 300 mg/kg.

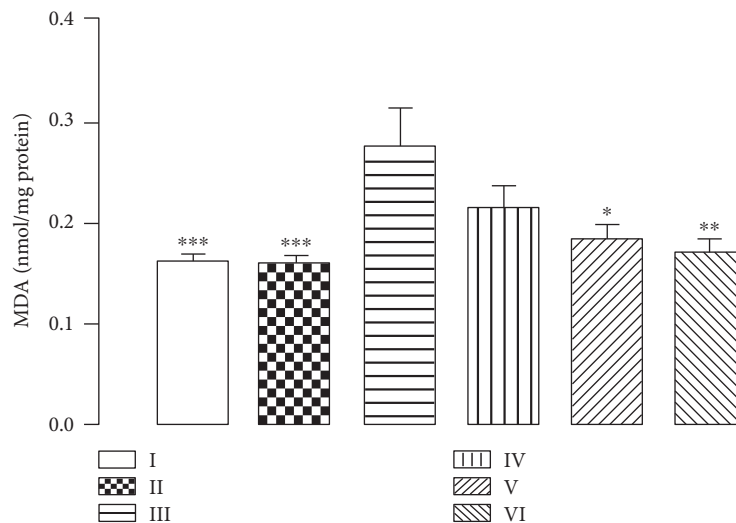


FIGURE 7: Effect of CHE treatment on malondialdehyde (MDA) concentration in animal whole brains of mice subjected to 90 days of aluminium exposure and treated with CHE (10, 100, and 300 mg/kg). Each column represents mean \pm SEM of 10 animals. (* $P < 0.05$, ** $P < 0.01$, and *** $P < 0.001$ in comparison to group III). I: control group; II: quercetin 30 mg/kg; III: aluminium group; IV: CHE 10 mg/kg; V: CHE 100 mg/kg; VI: CHE 300 mg/kg.

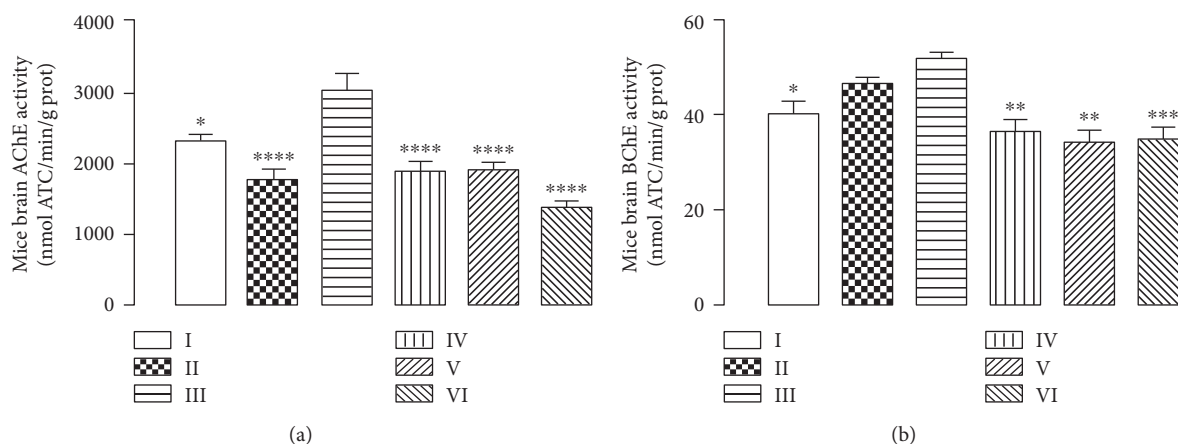


FIGURE 8: (a) Measure of acetylcholinesterase (AChE) and (b) butyrylcholinesterase (BChE) activities in mice whole brain subjected to 90 days of aluminium exposure and treated with CHE (10, 100, and 300 mg/kg). Each column represents mean \pm SEM of 10 animals. (* $P < 0.05$, ** $P < 0.01$, and *** $P < 0.001$ in comparison to group III). I: control group; II: quercetin 30 mg/kg; III: aluminium group; IV: CHE 10 mg/kg; V: CHE 100 mg/kg; VI: CHE 300 mg/kg.

selectivity of electroanalytical-based assays, since the color of the samples does influence the readings taken in the spectrophotometer [27, 28].

3.4. LC-ESI-MS Analysis. LC-ESI-MS analysis was performed in order to confirm the presence of gallic acid and quercetin in ethyl acetate fraction (EAF) from leaves of *C. brasiliense*. Since EAF and BF fractions originated from CHE, the presence of the markers is nonetheless stated to both extracts. We showed in a previous study the vasorelaxant effects of BF, which were associated with the presence of polyphenols such as gallic acid and quercetin in *C. brasiliense* leaves [10]. These compounds are also described as antioxidant agents, and quercetin presents moreover anticholinesterase effects too. Henceforth, these two compounds were herein selected for a preliminary chromatographic fingerprint analysis of EAF, because this fraction presented the best *in vitro* antioxidant and anticholinesterase effects.

The LC-ESI-MS analysis of EAF was realized in the negative mode to confirm the presence of the gallic acid and quercetin, comparing the results with those obtained from the spectra of the standard substances under the same analysis conditions (Figures 4 and 5). The MS spectrum obtained for total ion chromatogram of the EAF sample shows that $R_t = 3.8$ min (Figure 5(a)) and $R_t = 23.8$ min (Figures 5(b) and 4(c)). These results prove the presence of gallic acid and quercetin (Figures 4(c) and 4(d)) and are consistent with previously data reported in the literature [29]. In addition, the characteristic of the ion fragment at m/z 125 [$M-H-CO_2$] $^-$, that results of the fragmentation in ESI source of molecular ion [$M-H$] $^-$, m/z 169, was observed for both EAF and gallic acid standard in MS spectra. Therefore, the presence of these powerful antioxidants (acid galic and quercetin) in the leaves of *C. brasiliense* is irrefutable.

3.5. Behavioral Studies. Owing to the remarkable antioxidant capacity and promising AChE and BChE inhibitor activities of CHE, FB, and EAF extracts, *in vivo*

behavioral tests were performed to elucidate the potentialities of this potential herbal candidate to treat memory impairment disorders.

Although EAF exhibited best *in vitro* effects, we used CHE in this step because it was available in the lab in the amount required to treat the animals in all periods of the study. Since behavioral studies allow the assessment of aspects regarding memory retention and locomotor and exploratory capabilities, tests concerning these parameters were conducted. Therefore, behavior was studied with step-down, open field, and chimney tests.

Results indicate that CHE promotes memory retention without impairing locomotion (Figure 6). The aluminium-treated group presented both short- and long-term memory impairments, while the control group presented results akin to the literature. However, both the quercetin- and extract-treated groups (IV to VI) presented better memory retention, which implies that CHE do indeed promote neuroprotection and somehow improve murine memory retention. Literature reports that flavonoids exert neuroprotective activities mainly due to their ROS scavenging potential, which corroborates to the results seen in both LC-ESI-MS analysis and the aforementioned tests [22, 23].

3.6. TBAR Evaluation. It is established that aluminium neurotoxicity involves oxidative stress and neurodegeneration and that polyphenolic compounds, such as quercetin, attenuate neuronal death against aluminium-induced neurodegeneration [30].

Knowing that lipid peroxidation is one of the main manifestations of oxidative damage, we evaluated the CHE protective effect on mice brain cells measuring thiobarbituric acid reactive substances. Figure 7 shows the CHE-exerted protective effect against neuronal damage promoted by aluminium by minimizing lipid peroxidation. This result is a clear indicator of the extract antioxidant power, which promotes ROS reduction and therefore is implicated in lipid protection against oxidative damage.

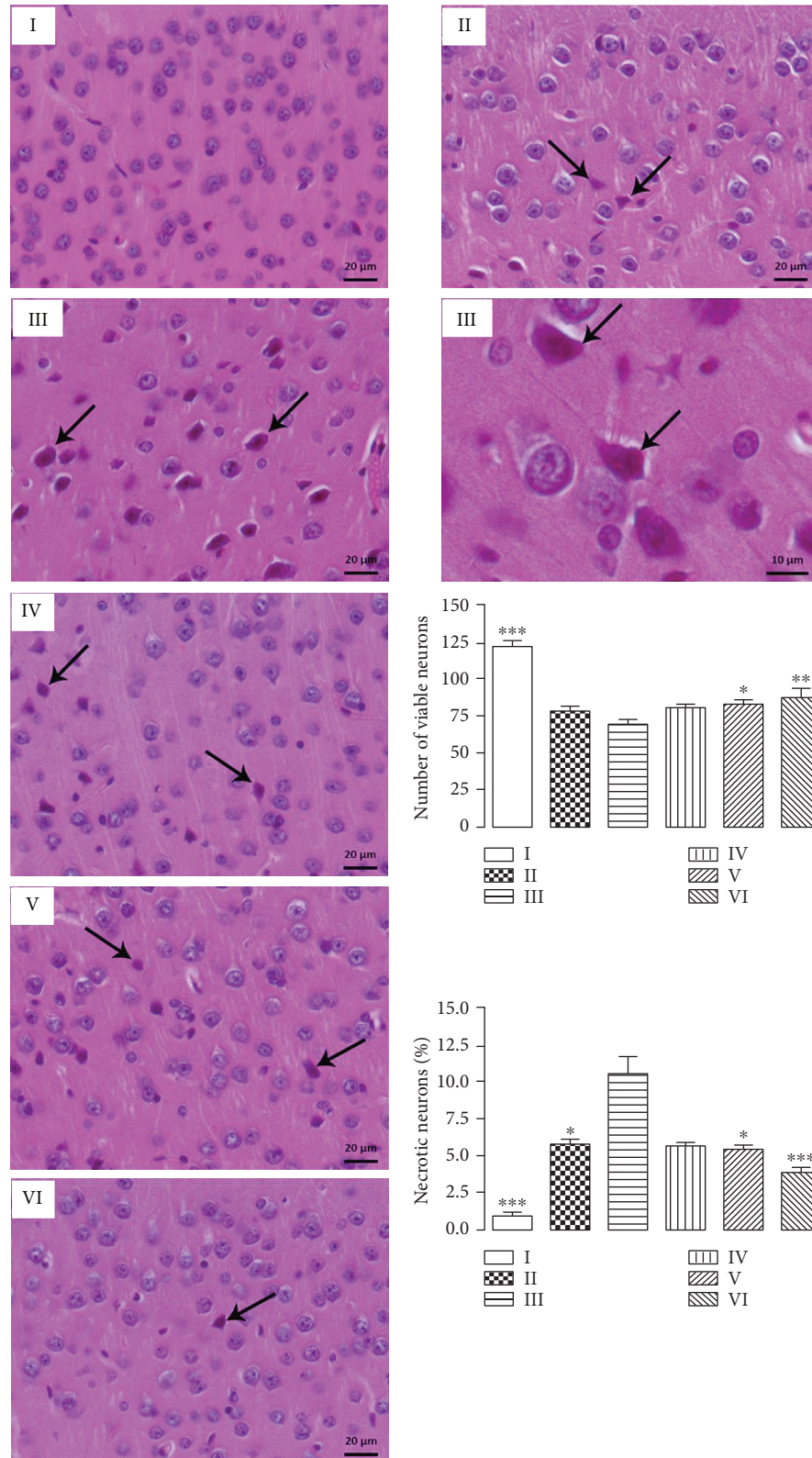


FIGURE 9: Histological sections of the frontal cerebral cortex stained by hematoxylin-eosin method. I: control group; II: quercetin 30 mg/kg; III: aluminium group; IV: CHE 10 mg/kg; V: CHE 100 mg/kg; VI: CHE 300 mg/kg. All aluminium-exposed groups presented shrunken neurons with cytoplasm being intensely eosinophilic (arrows). These necrotic neurons presented pyknotic nucleus with no discernible nucleolus. In the graphs, each column represents mean \pm SEM of 3 animals per group. (* $P < 0.01$, ** $P < 0.001$, and *** $P < 0.0001$ in comparison to group III).

3.7. Determination of Brain AChE and BChE Activities in Mice Treated with CHE. Considering our previous in vitro tests showing the inhibitory effect of pequi leaf extracts on AChE and BChE activities, we aimed to analyze if this effect would be present in animals treated with CHE. In accordance with results of in vitro tests, we observed the CHE inhibitory effect on cholinesterase enzymes in brain tissue of aluminium-intoxicated mice (Figure 8).

Since it is described that the increase of brain acetylcholine levels attenuates memory deficits [31] and, in opposition, aluminium chloride treatment increases the activity of mouse brain cholinesterase [32], we hypothesize that the inhibition of cholinesterase activity by CHE is a mechanism involved in the protection against memory impairment produced by aluminium.

3.8. Histopathological and Morphometrical Analyses. Morphoquantitative data demonstrated that aluminium decreased the number of viable neurons in the cerebral cortex, promoting a high percentage of eosinophilic neuronal necrosis (Figure 9). CHE (V and VI groups) increased the number of viable neurons and decreased the rate of neuronal death (Figure 9). These effects may be correlated to the neuroprotection exerted by phenolic compounds present in CHE, which were nonetheless detected in LC-MS. The results therefore show the potential of pequi leaves in counteracting the damage inflicted by aluminium on mice brain.

4. Conclusions

This study reports for the first time the anticholinesterase properties of *C. brasiliense*. The higher polarity fractions of *C. brasiliense* leaves presented high levels of phenols and both antioxidant and anticholinesterase activities. Behavioral tests revealed that pequi leaf extract protects against aluminium-induced memory impairment and inhibits lipid peroxidation and cholinesterase activity. Further histopathological studies revealed that pequi attenuates aluminium-induced cell necrosis, increasing neuronal viability. Taken together, these results indicate that pequi leaves may represent a new approach towards treatments to reverse the neuronal death, in order to slow down the progression of neurodegenerative diseases such as Alzheimer disease.

Abbreviations

AChE:	Acetylcholinesterase
AD:	Alzheimer's disease
BChE:	Butyrylcholinesterase
BF:	Butanol fraction
CF:	Chloroform fraction
CHE:	Crude hydroalcoholic extract
DPPH:	2,2-Diphenyl-1-picrylhydrazyl
DPV:	Differential pulse voltammetry
DTNB:	5,5'-Dithiobis(2-nitrobenzoic acid)
EAF:	Ethyl acetate fraction
EI:	Electrochemical index
E_{pa} :	Potentials of anodic peaks
ESI:	Electrospray ionization

GAE:	Gallic acid equivalent
GCE:	Glassy carbon electrode
HF:	Hexane fraction
I_b :	Backward current
I_f :	Forward current
I_{pa} :	Currents of anodic peaks
I_t :	Total current
LC-MS:	Liquid chromatography coupled to mass spectrometry
OFs:	Organic fractions
ROS:	Reactive oxygen compounds
SEM:	Standard error of the mean
SWV:	Square wave voltammetry.

Data Availability

All data used to support the findings of this study are included within the article.

Conflicts of Interest

The authors declare that there is no conflict of interest.

Acknowledgments

We thank the Fundação de Amparo à Pesquisa do Estado de Goiás (FAPEG) for the financial support (process number 20090064010955), Conselho Nacional de Desenvolvimento Científico e Tecnológico (Conselho Nacional de Pesquisa), and Coordenação de Aperfeiçoamento de Pessoal de Nível Superior (Coordenadoria de Aperfeiçoamento Pessoal) for the conceived scholarships.

References

- [1] P. T. Francis, A. M. Palmer, M. Snape, and G. K. Wilcock, "The cholinergic hypothesis of Alzheimer's disease: a review of progress," *Neurology, Neurosurgery & Psychiatry*, vol. 66, no. 2, pp. 137–147, 1999.
- [2] R. M. Lane, S. G. Potkin, and A. Enz, "Targeting acetylcholinesterase and butyrylcholinesterase in dementia," *The International Journal of Neuropsychopharmacology*, vol. 9, no. 1, pp. 101–124, 2006.
- [3] C. Cheignon, M. Tomas, D. Bonnefont-Rousselot, P. Faller, C. Hureau, and F. Collin, "Oxidative stress and the amyloid beta peptide in Alzheimer's disease," *Redox Biology*, vol. 14, pp. 450–464, 2018.
- [4] F. Tang, S. Nag, S. Y. W. Shiu, and S. F. Pang, "The effects of melatonin and Ginkgo biloba extract on memory loss and choline acetyltransferase activities in the brain of rats infused intracerebroventricularly with β -amyloid 1-40," *Life Sciences*, vol. 71, no. 22, pp. 2625–2631, 2002.
- [5] R. B. Giordani, L. B. Pagliosa, A. T. Henriques, J. A. S. Zuanazzi, and J. H. A. Dutilh, "Investigação do potencial antioxidante e anticolinesterásico de *Hippeastrum* (Amaryllidaceae)," *Química Nova*, vol. 31, no. 8, pp. 2042–2046, 2008.
- [6] F. D. de Araujo, "A review of *Caryocar brasiliense* (Caryocaraceae)—an economically valuable species of the central Brazilian cerrados," *Economic Botany*, vol. 49, no. 1, pp. 40–48, 1995.

- [7] K. C. Geórcze, L. C. A. Barbosa, P. H. Fidêncio et al., "Essential oils from pequi fruits from the Brazilian Cerrado ecosystem," *Food Research International*, vol. 54, no. 1, pp. 1–8, 2013.
- [8] W. de Paula-Júnior, F. H. Rocha, L. Donatti, C. M. T. Fadel-Picheth, and A. M. Weffort-Santos, "Leishmanicidal, antibacterial, and antioxidant activities of *Caryocar brasiliense* Cambess leaves hydroethanolic extract," *Revista Brasileira de Farmacognosia*, vol. 16, pp. 625–630, 2006.
- [9] C. A. Breda, A. M. Gasperini, V. L. Garcia et al., "Phytochemical analysis and antifungal activity of extracts from leaves and fruit residues of Brazilian savanna plants aiming its use as safe fungicides," *Natural Products and Bioprospecting*, vol. 6, no. 4, pp. 195–204, 2016.
- [10] L. M. de Oliveira, A. G. Rodrigues, E. F. da Silva et al., "Endothelium-dependent vasorelaxant effect of butanolic fraction from *Caryocar brasiliense* Camb. leaves in rat thoracic aorta," *Evidence-based Complementary and Alternative Medicine*, vol. 2012, Article ID 934142, 9 pages, 2012.
- [11] D. P. Leão, A. S. Franca, L. S. Oliveira, R. Bastos, and M. A. Coimbra, "Physicochemical characterization, antioxidant capacity, total phenolic and proanthocyanidin content of flours prepared from pequi (*Caryocar brasiliense* Camb.) fruit by-products," *Food Chemistry*, vol. 225, pp. 146–153, 2017.
- [12] G. L. Ellman, K. D. Courtney, V. Andres jr., and R. M. Featherstone, "A new and rapid colorimetric determination of acetylcholinesterase activity," *Biochemical Pharmacology*, vol. 7, no. 2, pp. 88–95, 1961.
- [13] M. S. Blois, "Antioxidant determinations by the use of a stable free radical," *Nature*, vol. 181, no. 4617, pp. 1199–1200, 1958.
- [14] F. M. A. Lino, L. Z. de Sá, I. M. S. Torres et al., "Voltammetric and spectrometric determination of antioxidant capacity of selected wines," *Electrochimica Acta*, vol. 128, pp. 25–31, 2014.
- [15] S. Georgé, P. Brat, P. Alter, and M. J. Amiot, "Rapid determination of polyphenols and vitamin C in plant-derived products," *Journal of Agricultural and Food Chemistry*, vol. 53, no. 5, pp. 1370–1373, 2005.
- [16] D. Martí Barros, M. R. Ramirez, E. A. dos Reis, and I. Izquierdo, "Participation of hippocampal nicotinic receptors in acquisition, consolidation and retrieval of memory for one trial inhibitory avoidance in rats," *Neuroscience*, vol. 126, no. 3, pp. 651–656, 2004.
- [17] K. C. Montgomery, "The relation between fear induced by novel stimulation and exploratory behavior," *Journal of Comparative and Physiological Psychology*, vol. 48, no. 4, pp. 254–260, 1955.
- [18] I. Groticke, K. Hoffmann, and W. Loscher, "Behavioral alterations in the pilocarpine model of temporal lobe epilepsy in mice," *Experimental Neurology*, vol. 207, no. 2, pp. 329–349, 2007.
- [19] M. M. Bradford, "A rapid and sensitive method for the quantitation of microgram quantities of protein utilizing the principle of protein-dye binding," *Analytical Biochemistry*, vol. 72, no. 1–2, pp. 248–254, 1976.
- [20] H. Ohkawa, N. Ohishi, and K. Yagi, "Assay for lipid peroxides in animal-tissues by thiobarbituric acid reaction," *Analytical Biochemistry*, vol. 95, no. 2, pp. 351–358, 1979.
- [21] E. R. Weibel, "Principles and methods for the morphometric study of the lung and other organs," *Laboratory Investigation*, vol. 12, pp. 131–155, 1978.
- [22] V. Kumar and K. D. Gill, "Oxidative stress and mitochondrial dysfunction in aluminium neurotoxicity and its amelioration: a review," *Neurotoxicology*, vol. 41, pp. 154–166, 2014.
- [23] D.-Y. Choi, Y.-J. Lee, J. T. Hong, and W.-J. Lee, "Antioxidant properties of natural polyphenols and their therapeutic potentials for Alzheimer's disease," *Brain Research Bulletin*, vol. 87, no. 2–3, pp. 144–153, 2012.
- [24] S. Sontadsakul, A. Prakongsantikul, W. Kitphati, J. Pratuangdejkul, and V. Nukoolkarn, "Quercetin and derivatives as butyrylcholinesterase inhibitors," *Thai Journal of Pharmaceutical Sciences*, vol. 36, pp. 31–34, 2012.
- [25] M. A. Ansari, H. M. Abdul, G. Joshi, W. O. Opii, and D. A. Butterfield, "Protective effect of quercetin in primary neurons against A β (1–42): relevance to Alzheimer's disease," *The Journal of Nutritional Biochemistry*, vol. 20, no. 4, pp. 269–275, 2009.
- [26] C. Jayasinghe, N. Gotoh, and S. Wada, "Pro-oxidant/antioxidant behaviours of ascorbic acid, tocopherol, and plant extracts in n-3 highly unsaturated fatty acid rich oil-in-water emulsions," *Food Chemistry*, vol. 141, no. 3, pp. 3077–3084, 2013.
- [27] D. V. Thomaz, K. C. S. Leite, E. K. G. Moreno et al., "Electrochemical study of commercial black tea samples," *International Journal of Electrochemical Science*, vol. 13, pp. 5433–5439, 2018.
- [28] K. C. de Siqueira Leite, L. F. Garcia, G. S. Lobón et al., "Antioxidant activity evaluation of dried herbal extracts: an electroanalytical approach," *Revista Brasileira de Farmacognosia*, vol. 28, no. 3, pp. 325–332, 2018.
- [29] I. K. Selvi and S. Nagarajan, "Separation of catechins from green tea (*Camellia sinensis* L.) by microwave assisted acetylation, evaluation of antioxidant potential of individual components and spectroscopic analysis –electrospray ionization mass spectrometry," *LWT*, vol. 91, pp. 391–397, 2018.
- [30] D. R. Sharma, W. Y. Wani, A. Sunkaria et al., "Quercetin attenuates neuronal death against aluminum-induced neurodegeneration in the rat hippocampus," *Neuroscience*, vol. 324, pp. 163–176, 2016.
- [31] Z. Batool, S. Sadir, L. Liaquat et al., "Repeated administration of almonds increases brain acetylcholine levels and enhances memory function in healthy rats while attenuates memory deficits in animal model of amnesia," *Brain Research Bulletin*, vol. 120, pp. 63–74, 2016.
- [32] P. Zatta, M. Ibn-Lkhatay-Idrissi, P. Zambenedetti, M. Kilyen, and T. Kiss, "In vivo and in vitro effects of aluminum on the activity of mouse brain acetylcholinesterase," *Brain Research Bulletin*, vol. 59, no. 1, pp. 41–45, 2002.

Research Article

Inhibitory Effects of Momordicine I on High-Glucose-Induced Cell Proliferation and Collagen Synthesis in Rat Cardiac Fibroblasts

Po-Yuan Chen ¹, Neng-Lang Shih,² Wen-Rui Hao,³ Chun-Chao Chen ³, Ju-Chi Liu ^{3,4}, and Li-Chin Sung ^{3,4}

¹Department of Biological Science and Technology, College of Biopharmaceutical and Food Sciences, China Medical University, Taichung 40402, Taiwan

²Department of Life Sciences, College of Science, National University of Kaohsiung, Kaohsiung 811, Taiwan

³Division of Cardiology, Department of Internal Medicine, Shuang Ho Hospital, Taipei Medical University, New Taipei City 23561, Taiwan

⁴Department of Internal Medicine, School of Medicine, College of Medicine, Taipei Medical University, Taipei 11031, Taiwan

Correspondence should be addressed to Li-Chin Sung; 10204@s.tmu.edu.tw

Received 2 July 2018; Accepted 2 September 2018; Published 8 October 2018

Guest Editor: Felipe L. de Oliveira

Copyright © 2018 Po-Yuan Chen et al. This is an open access article distributed under the Creative Commons Attribution License, which permits unrestricted use, distribution, and reproduction in any medium, provided the original work is properly cited.

Diabetes-associated cardiac fibrosis is a severe cardiovascular complication. Momordicine I, a bioactive triterpenoid isolated from bitter melon, has been demonstrated to have antidiabetic properties. This study investigated the effects of momordicine I on high-glucose-induced cardiac fibroblast activation. Rat cardiac fibroblasts were cultured in a high-glucose (25 mM) medium in the absence or presence of momordicine I, and the changes in collagen synthesis, transforming growth factor- β 1 (TGF- β 1) production, and related signaling molecules were assessed. Increased oxidative stress plays a critical role in the development of high-glucose-induced cardiac fibrosis; we further explored momordicine I's antioxidant activity and its effect on fibroblasts. Our data revealed that a high-glucose condition promoted fibroblast proliferation and collagen synthesis and these effects were abolished by momordicine I (0.3 and 1 μ M) pretreatment. Furthermore, the inhibitory effect of momordicine I on high-glucose-induced fibroblast activation may be associated with its activation of nuclear factor erythroid 2-related factor 2 (Nrf2) and the inhibition of reactive oxygen species formation, TGF- β 1 production, and Smad2/3 phosphorylation. The addition of brusatol (a selective inhibitor of Nrf2) or Nrf2 siRNA significantly abolished the inhibitory effect of momordicine I on fibroblast activation. Our findings revealed that the antifibrotic effect of momordicine I was mediated, at least partially, by the inhibition of the TGF- β 1/Smad pathway, fibroblast proliferation, and collagen synthesis through Nrf2 activation. Thus, this work provides crucial insights into the molecular pathways for the clinical application of momordicine I for treating diabetes-associated cardiac fibrosis.

1. Introduction

The prevalence of diabetes mellitus (DM) is rapidly increasing, and cardiovascular complications are the principal causes of morbidity and mortality among patients with DM. The Framingham study reported a 2.4-fold increase in the incidence of heart failure in diabetic men and a 5-fold increase in diabetic women [1, 2]. Diabetic cardiomyopathy (DCM), which was first introduced in 1972 by Rubler et al.,

is one of the most severe irreversible complications of DM [3]. DCM is characterized by myocardial fibrosis, left ventricular hypertrophy, and compromised left ventricular systolic and diastolic functions [2, 4, 5]. Left ventricular diastolic dysfunction is a major characteristic of DCM, and recent studies revealed that over 50% of asymptomatic diabetic patients have diastolic dysfunction [1, 6]. Cardiac fibroblasts are enmeshed in the myocardium and play a crucial role in maintaining the integrity and homeostasis of the interstitial

matrix in the adult heart [7–9]. In patients with diabetes, profibrotic myofibroblasts are mainly differentiated from cardiac fibroblasts, resulting in inefficiently organized fibrotic matrices, which can lead to myocardial fibrosis, stiffness, and diastolic dysfunction [4]. However, the mechanisms involved in the pathological changes of DCM are not completely understood. Because fibrosis plays a critical role in the pathology of DCM, we focused on the molecular mechanism involved in cardiac fibrosis in DM [5, 10].

Oxidative stress may play a fundamental role in inducing cardiomyopathy in patients with chronic DM [5, 11–14]. Various studies have demonstrated that DM is associated with increased formation of reactive oxygen species (ROS) and a decrease in antioxidant potential [14, 15]. An animal study revealed that ROS could directly induce fibrosis by promoting fibroblast proliferation and collagen synthesis in the setting of DM [15]. The transcription factor nuclear factor erythroid 2-related factor 2 (Nrf2), a basic leucine zipper protein, plays a fundamental role in antioxidant response element- (ARE-) dependent heme oxygenase-1 (HO-1) gene expression. HO-1 is considered a critical endogenous antioxidant and cytoprotective enzyme, which may be upregulated by Nrf2 [16]. The Nrf2/HO-1 signaling pathway has been recognized as the most crucial cellular defense mechanism against oxidative stress [17].

Transforming growth factor- β 1 (TGF- β 1) is involved in cardiac fibrosis in DCM [4, 10, 18, 19]. Small mothers against decapentaplegic (Smad) is an intracellular signal transduction protein of the TGF- β 1 pathway and is involved in these pathological changes [19]. ROS can induce TGF- β 1 activation, thus resulting in cardiac fibrosis. Euler demonstrated a reduction in TGF- β 1 levels in patients treated with N-acetylcysteine (NAC) [20].

Clinical studies have demonstrated that hyperglycemia is a crucial etiologic factor leading to diabetic complications [21]. Diastolic dysfunction is correlated with the degree of hyperglycemia; however, intensive glucose-lowering therapy does not always reduce the risk of DCM [1, 22]. Oxidative stress may be a target for intervention. Other than DM drugs, *Momordica charantia* (bitter melon or bitter melon), a member of the Cucurbitaceae family, has been used to manage hyperglycemia and the early signs of DM since ancient times in some countries [23–26]. Momordicine I (Figure 1(a)), a bioactive saponin and cucurbitane-type triterpenoid, has been isolated from *Momordica charantia* [27–29]. Momordicine I was reported to be a beneficial natural source of antioxidants [30]. Treatment with momordicine I might have therapeutic potential in improving diabetic myocardial dysfunction. However, little information is available about the effect of momordicine I on the cell proliferation and collagen synthesis of cardiac fibroblasts induced by high glucose.

Thus, we hypothesized that momordicine I is particularly capable of suppressing high-glucose-induced cell proliferation and collagen synthesis in cardiac fibroblasts and therefore decelerates the progression of DCM. The specific aims of this study are to delineate how momordicine I inhibits high-glucose-induced cardiac fibroblast activation through the modulation of ROS, Nrf2/HO-1 pathway, and TGF- β 1/Smad pathway.

2. Material and Methods

2.1. Antibodies and Reagents. Dulbecco's modified Eagle's medium (DMEM), fetal calf serum, and tissue culture reagents were obtained from Invitrogen/GIBCO (Grand Island, NY, USA). Momordicine I (>99% purity, kindly provided by Dr. Shi-Yie Cheng, Department of Life Sciences, College of Science, National University of Kaohsiung, Kaohsiung, Taiwan, ROC) was dissolved in dimethyl sulfoxide (DMSO), and the DMSO content in all groups was 0.1%. Anti-p-Smad2/3, anti-Smad2/3, anti-GAPDH, and anti-PARP antibodies were purchased from Cell Signaling Technology (Boston, MA, USA). Anti-HO-1 and anti-Nrf2 antibodies were purchased from Santa Cruz Biotechnology (Santa Cruz, CA, USA). Brusatol, the Nrf2-specific inhibitor, and all other reagent-grade chemicals were acquired from Sigma-Aldrich Chemical Co. (St. Louis, MO, USA).

2.2. Culture of Rat Cardiac Fibroblasts. Primary cultures of neonatal rat cardiac fibroblasts were isolated from the hearts of 1-day-old Sprague–Dawley rat pups as previously described [8]. The investigation conformed to the Guide for the Care and Use of Laboratory Animals published by the US National Institutes of Health (NIH publication no. 85–23, revised 1996) and was approved by the Institutional Animal Care and Use Committee of Taipei Medical University. Cardiac fibroblasts grown in culture dishes from the second to fourth passages were used in the experiments and were >99% positive for vimentin antibodies (Sigma-Aldrich). Serum-containing medium from the cultured cells was replaced with serum-free medium, and the cells were subsequently exposed to the treatments as indicated. For fibroblast proliferation assay and TGF- β 1 secretion assay, following incubation with momordicine I for 12 h, cardiac fibroblasts were then exposed to a serum-free normal-glucose medium (5.6 mM glucose) or high-glucose medium (25 mM glucose) for another 24 h before analyses.

2.3. 3-(4,5-Dimethylthiazol-2-yl)-2,5-diphenyltetrazolium Bromide (MTT) Assay. MTT assay was used to measure cell viability. After 24 h incubation with various concentrations of momordicine I as indicated, MTT (50 μ L) was added and cells were cultured for additional 4 h. Subsequently, cells were lysed using DMSO and the absorbance was measured at 490 nm by a spectrophotometer.

2.4. Proliferation Assay. Proliferation was assessed through quantifying 5-bromo-2'-deoxyuridine (BrdU) incorporation [7]. Cells were removed from the culture dishes by adding trypsin and were subsequently centrifuged. Cell proliferation was assessed through the incorporation of BrdU. BrdU incorporation was determined using a cell proliferation enzyme-linked immunosorbent assay (ELISA) kit (Roche Diagnostics, Mannheim, Germany) in accordance with the manufacturer's instructions.

2.5. 3 H-Proline Incorporation Assay. Cardiac fibroblasts were incubated using 3 H-proline (1 mCi/well, L-[2,3,4,5- 3 H]-proline; Amersham Biosciences, Little Chalfont, Buckinghamshire, United Kingdom) for 24 h; subsequently exogenous

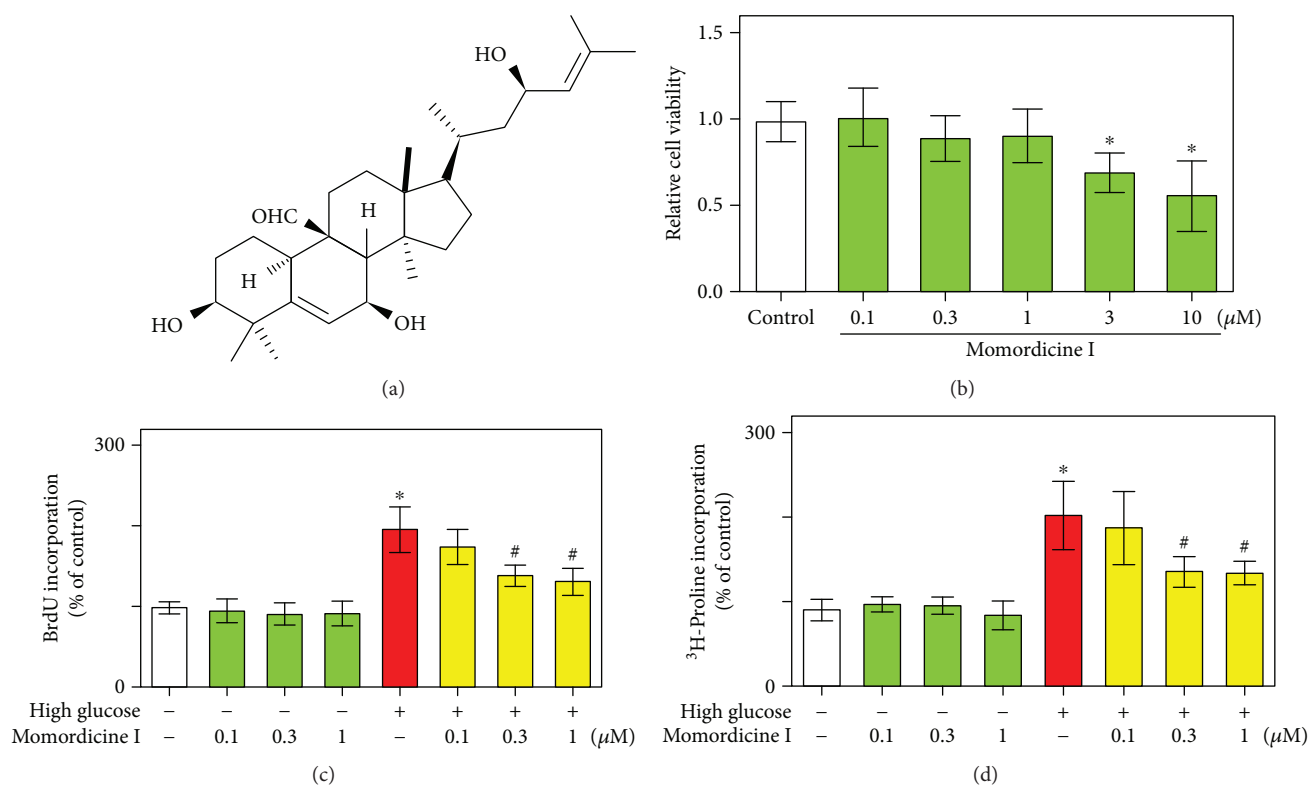


FIGURE 1: Effects of momordicine I on high-glucose-induced cell proliferation and collagen synthesis in rat cardiac fibroblasts. (a) Chemical structure of momordicine I. (b) Effect of momordicine I (0.1, 0.3, 1, 3, and 10 μM) on cell viability in cardiac fibroblasts. Cell viability was quantified through MTT assay. Effects of momordicine I on high-glucose-stimulated fibroblast proliferation (c) and collagen synthesis (d) were assessed through BrdU and ^3H -proline incorporation. Rat cardiac fibroblasts were cultured in a serum-free normal-glucose medium (5.6 mM glucose) or high-glucose medium (25 mM glucose) in the absence or presence of momordicine I (0.1, 0.3, and 1 μM) for 24 h. Results were presented as mean \pm SEM ($n = 4$). * $P < 0.05$ versus the control group; # $P < 0.05$ versus the high-glucose group.

^3H -proline incorporation was determined through scintillation counting.

2.6. Measurement of TGF- β 1 Concentrations. TGF- β 1 levels were measured in a culture medium using a commercial ELISA kit (R&D Systems Inc., Minneapolis, MN, USA) in accordance with the manufacturer's protocols. Results were normalized to cellular protein content in all experiments and expressed as percentages relative to the control group.

2.7. Western Blot Analysis. Nuclear proteins were prepared as previously described [31]. Western blot analysis was performed in accordance with a previously described method [8]. Whole-cell extracts were obtained in a radioimmunoprecipitation assay buffer (Roche Diagnostics GmbH, Germany). Extracts or proteins were separated through sodium dodecyl sulfate polyacrylamide gel electrophoresis followed by electrotransfer to polyvinylidene difluoride membranes and probed with antisera before the introduction of horseradish peroxidase-conjugated secondary antibodies. The proteins were visualized through chemiluminescence in accordance with the manufacturer's instructions (Pierce Biotechnology Inc., Rockford, IL, USA). Images were quantified through densitometry. The densitometry for each band of the phosphorylated form of specific protein (e.g., Smad2/3), the total level of specific protein (e.g., Smad2/3), and loading

control (e.g., GAPDH) were measured separately. The specific nonphosphorylated total protein (e.g., Smad2/3) was then normalized against the loading control (e.g., GAPDH) and used the normalized total protein for normalization of the specific phosphoprotein (e.g., Smad2/3). Each control group's value was used to normalize the values of the individual groups obtained in the same experiment. Independent values of control data were normalized on the control mean value, with the control mean value equal to 1, to generate control values in the bar graph.

2.8. Flow Cytometric Assay of 2',7'-Dichlorodihydrofluorescein Oxidation. Intracellular ROS production was determined based on the oxidation of 2',7'-dichlorodihydrofluorescein (DCFH) to a fluorescent 2',7'-dichlorofluorescein (DCF) as previously described [32]. DCFH was added at a final concentration of 10 μM and incubated for 30 min at 37°C. Cellular fluorescence was determined through flow cytometry (FACS-SCAN, Becton Dickinson, Franklin Lakes, NJ, USA). Subsequently, the cells were excited using an argon laser operating at 488 nm and measured at 510–540 nm.

2.9. Nrf2 Short Interfering (Si) RNA Transfection. Cardiac fibroblasts were transfected with either Nrf2 siRNA or control siRNA (obtained from Santa Cruz) by using the Lipofectamine reagent as described previously [31].

2.10. Statistical Analysis. Results were expressed as mean \pm standard error of the mean (SEM) for at least three experiments unless otherwise stated. Statistical analysis was performed using Student's *t*-test or analysis of variance followed by Tukey's multiple comparisons using GraphPad Prism software (GraphPad Software, San Diego, CA, USA). $P < 0.05$ was considered statistically significant.

3. Results

3.1. Inhibitory Effect of Momordicine I on High-Glucose-Induced Cell Proliferation and Collagen Synthesis in Rat Cardiac Fibroblasts. Rat cardiac fibroblasts were treated with various concentrations of momordicine I, and cell viability was determined through MTT assay. The effects of momordicine I on cell viability in cultures are presented in Figure 1(b). Momordicine I had no toxic effect on rat cardiac fibroblasts at concentrations of 0.1–1 μM , so concentrations of 0.1, 0.3, and 1 μM momordicine I were used for further analysis. We subsequently tested the effect of momordicine I on cardiac fibroblast proliferation and collagen synthesis. Isolated cardiac fibroblast cells were cultured in normal- and high-glucose media. The effects of momordicine I on high-glucose-stimulated cardiac fibroblast proliferation and collagen synthesis were assessed by incorporating BrdU and ^3H -proline. Compared with culturing in the normal-glucose medium, culturing in the high-glucose (25 mM) medium for 24 h slightly stimulated fibroblast proliferation and collagen synthesis (Figures 1(c) and 1(d)). Pretreatment of cardiac fibroblasts with momordicine I (0.3 and 1 μM) for 12 h followed by exposure to a high-glucose medium resulted in a significant decrease in high-glucose-induced cell proliferation and collagen synthesis (Figures 1(c) and 1(d)). These data demonstrate that momordicine I inhibited high-glucose-induced cardiac fibroblast activation.

3.2. Inhibitory Effect of Momordicine I on High-Glucose-Induced TGF- β 1 Secretion and Smad2/3 Phosphorylation in Rat Cardiac Fibroblasts. To investigate whether momordicine I affects TGF- β 1 in cardiac fibroblasts exposed to high-glucose medium, cardiac fibroblasts were treated with momordicine I under high-glucose conditions. TGF- β 1 secretion was determined through ELISA. As depicted in Figure 2(a), the ELISA results revealed that the cardiac fibroblasts treated with high-glucose medium exhibited increased TGF- β 1 secretion compared with the cardiac fibroblasts treated with a normal-glucose (5.6 mM) medium. However, high-glucose medium-induced TGF- β 1 secretion was prevented by treating cardiac fibroblasts with momordicine I (0.3 and 1 μM).

TGF- β receptor activation may increase Smad-2/3 phosphorylation and deploy many of their effects [20]. Therefore, phosphorylated Smad2/3 was also detected. Following incubation with momordicine I (1 μM) for 12 h, cells were exposed to a high-glucose medium for 24 h or human-recombinant TGF- β 1 (10 ng/mL) for 2 h. After the aforementioned treatment, total cell proteins were extracted and subjected to Western blotting. As illustrated in Figure 2(b), levels of total Smad2/3 protein in cardiac fibroblasts

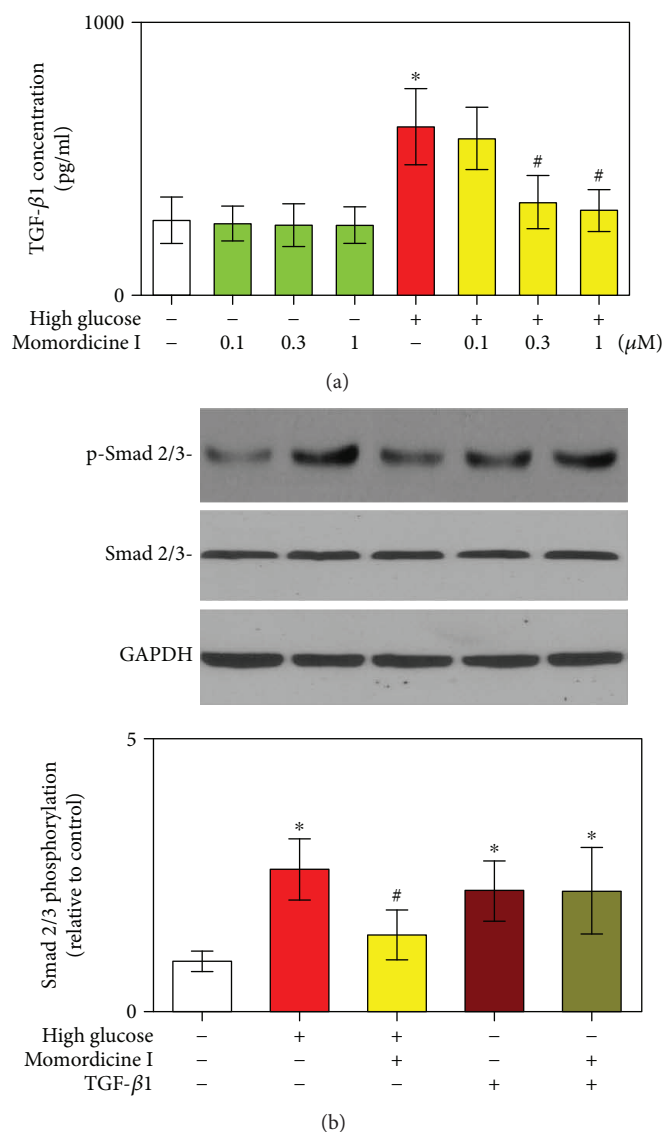


FIGURE 2: Effects of momordicine I on high-glucose-induced TGF- β 1 secretion and Smad2/3 phosphorylation in rat cardiac fibroblasts. (a) Cardiac fibroblasts treated using a normal-glucose medium or high-glucose medium in the absence or the presence of momordicine I (0.1, 0.3, 1 μM) for 24 h and the secretion of TGF- β 1 in cardiac fibroblast supernatants measured through ELISA. Results are presented as mean \pm SEM ($n = 5$). (b) Effect of momordicine I on high-glucose- or TGF- β 1-induced Smad2/3 phosphorylation. The protein expression levels of Smad2/3 and p-Smad2/3 were detected using Western blotting following incubation with momordicine I (1 μM) for 12 h; cardiac fibroblasts were exposed to high glucose for 24 h or TGF- β 1 (10 ng/mL) for 2 h. Representative micrographs of Smad2/3 and p-Smad2/3 expression in Western blot analysis (upper) and quantitative results (lower). Results are presented as mean \pm SEM ($n = 3$). * $P < 0.05$ versus the control group; # $P < 0.05$ versus the high-glucose group.

remained unchanged after exposure to a high-glucose medium for 24 h or TGF- β 1 for 2 h. However, the level of p-Smad2/3 was notably increased in high-glucose or TGF- β 1-treated cardiac fibroblasts as compared to that in cells

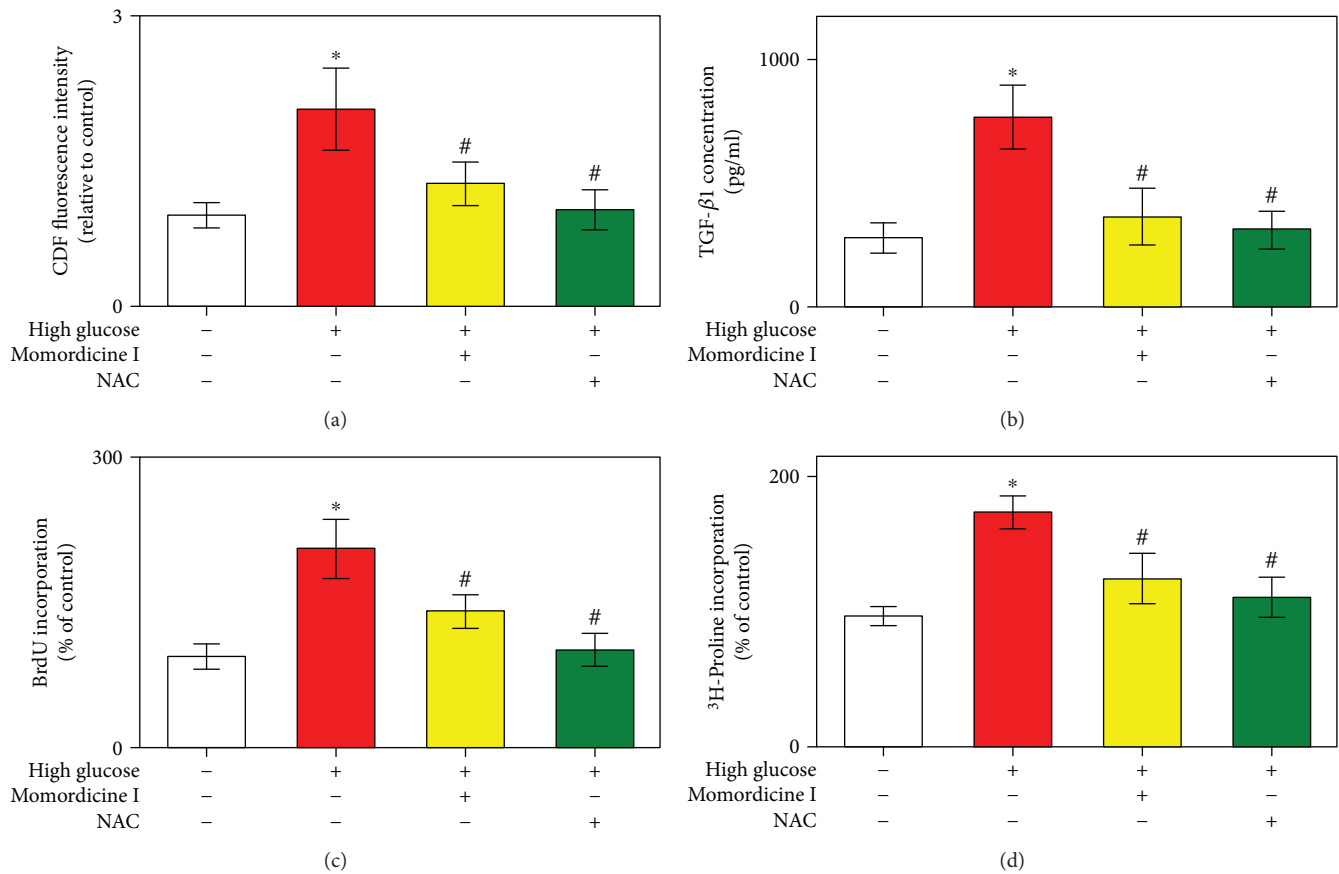


FIGURE 3: Momordicine I inhibits high-glucose-induced ROS in rat cardiac fibroblasts. (a) Effects of momordicine I on high-glucose-induced ROS generation. Cardiac fibroblasts were cultured in a normal-glucose medium or high-glucose medium for 30 min or preincubated with momordicine I ($1 \mu\text{M}$, for 12 h) or NAC (5 mM, for 30 min) and then stimulated with the high-glucose medium for 30 min. Column bar graph of mean cell fluorescence for DCF. The fluorescence intensities in the control cells are expressed as 100%. (b) Effects of momordicine I and NAC on the high-glucose-induced secretion of TGF- β 1 in cardiac fibroblasts. Effects of momordicine I and NAC on high-glucose-induced fibroblast proliferation (c) and collagen synthesis (d). Cardiac fibroblast cells were cultured in the control medium or high-glucose medium in the absence or presence of momordicine I ($1 \mu\text{M}$) or NAC (5 mM) for 24 h. Results are presented as mean \pm SEM ($n = 4$). * $P < 0.05$ versus the control group; # $P < 0.05$ versus the high-glucose group.

treated with a normal-glucose medium. Preincubation with momordicine I ($1 \mu\text{M}$) partially but significantly suppressed high-glucose-induced phosphorylation of Smad2/3 protein. However, momordicine I ($1 \mu\text{M}$) had no significant effect on TGF- β 1-induced Smad2/3 phosphorylation. These observations indicated that momordicine I may inhibit the high-glucose-mediated fibrotic response by regulating the TGF- β 1/Smad signaling pathway and suggested that momordicine I was able to suppress high-glucose-induced cardiac fibroblast activation through inhibition of TGF- β 1 secretion, which was independent of its direct effect on the TGF- β 1/Smad signaling pathway.

3.3. Antioxidant Effects of Momordicine I on High-Glucose-Induced ROS Production in Rat Cardiac Fibroblasts. Increased ROS plays a critical role in the development of DM-related cardiac fibrosis [4, 5, 11, 14, 15, 19]. We subsequently explored the role of momordicine I's antioxidant activity in the inhibition of the high-glucose-induced collagen synthesis. The ROS levels were detected from the

fluorescence intensity of the ROS, which was analyzed using DCFH-DA assay and a flow cytometer [32]. Our data revealed that the fluorescence intensity enhanced by high glucose was significantly reduced by momordicine I ($1 \mu\text{M}$) (Figure 3(a)). Notably, pretreatment with NAC (5 mM) for 2 h also substantially alleviated the ROS triggered by the high-glucose medium. As presented in Figure 3(b), cardiac fibroblasts treated with a high-glucose medium also exhibited increased TGF- β 1 secretion compared with cardiac fibroblasts in the normal-glucose medium. However, high-glucose-induced TGF- β 1 secretion was prevented by preincubation with momordicine I ($1 \mu\text{M}$) or NAC (5 mM). Additionally, we analyzed the effect of momordicine I and NAC on cardiac fibroblast proliferation and collagen synthesis. Compared with the normal-glucose medium, the high-glucose medium stimulated fibroblast proliferation, which was significantly blocked by treatment with momordicine I or NAC (Figure 3(c)). In addition to the inhibition of the proliferative effect of the high-glucose medium on cardiac fibroblasts, momordicine I or NAC attenuated the

collagen synthesis induced by the high-glucose-medium (Figure 3(d)). The effects of momordicine I on the high-glucose-induced ROS generation, TGF- β 1 secretion, and fibroblast activation are similar to the effects of NAC, implicating its possible antioxidant role. These findings suggested that the antioxidant effect of momordicine I is related to the reduced oxidative stress induced by the high-glucose medium.

3.4. Activation of the Nrf2 Signaling Pathway by Momordicine I in Rat Cardiac Fibroblasts. The Nrf2/HO-1 signaling pathway is also associated with antifibrotic actions [33, 34]. To more thoroughly understand the possible signaling pathways and mechanisms in the action of momordicine I, we ascertained the expression of Nrf2 and Nrf2 downstream HO-1 in cardiac fibroblasts in high-glucose conditions. Our data revealed that a high-glucose condition slightly elevated the translocation of Nrf2 from the cytoplasm to the nucleus and the enhanced HO-1 expression; however, this modulatory effect was further augmented by momordicine I treatment (Figures 4(a) and 4(b)). These data implicated that momordicine I can activate the Nrf2/HO-1 signaling pathway in cardiac fibroblasts *in vitro*.

3.5. Nrf2 Inhibitor Brusatol or Nrf2 siRNA Abrogated the Inhibitory Effect of Momordicine I on High-Glucose-Induced TGF- β 1 Secretion, Cell Proliferation, and Collagen Synthesis in Rat Cardiac Fibroblasts. To further verify the role of Nrf2 in the antifibrotic effect of momordicine I, brusatol, a specific Nrf2 inhibitor [35], was used to determine the role of Nrf2 in the effects of momordicine I on high-glucose medium-induced TGF- β 1 secretion and cardiac fibroblast activation. Cells were treated with brusatol (10 nM, 30 min), followed by 1 μ M momordicine I for 12 h, and were subsequently cultured in a high-glucose medium for 24 h. The levels of TGF- β 1 secretion significantly increased under high-glucose conditions compared with the normal-glucose control group (Figure 5(a)). However, these increases were inhibited by momordicine I. However, brusatol significantly abolished momordicine I's inhibitory effect on high-glucose-induced TGF- β 1 secretion. As expected, momordicine I significantly reduced the high-glucose-induced fibroblast proliferation and collagen synthesis, which was also significantly reversed by brusatol (Figures 5(b) and 5(c)). The role of Nrf2 in the inhibition of high-glucose-induced TGF- β 1 secretion, fibroblast proliferation, and collagen synthesis by momordicine I was also examined by silencing of Nrf2 (Figures 5(d)–5(f)). Cardiac fibroblasts transfected with Nrf2 siRNA (100 nM), followed by treatment with momordicine I (1 μ M) for 12 h, prevented the inhibitory effect of momordicine I on high-glucose-induced TGF- β 1 secretion, fibroblast proliferation, and collagen synthesis. In contrast, the control siRNA (100 nM) failed to block the inhibitory effect of momordicine I. Collectively, these data indicated that momordicine I inhibited TGF- β 1 pathway activation and proliferation and collagen synthesis of cardiac fibroblasts under a high-glucose condition in an Nrf-2 dependent manner.

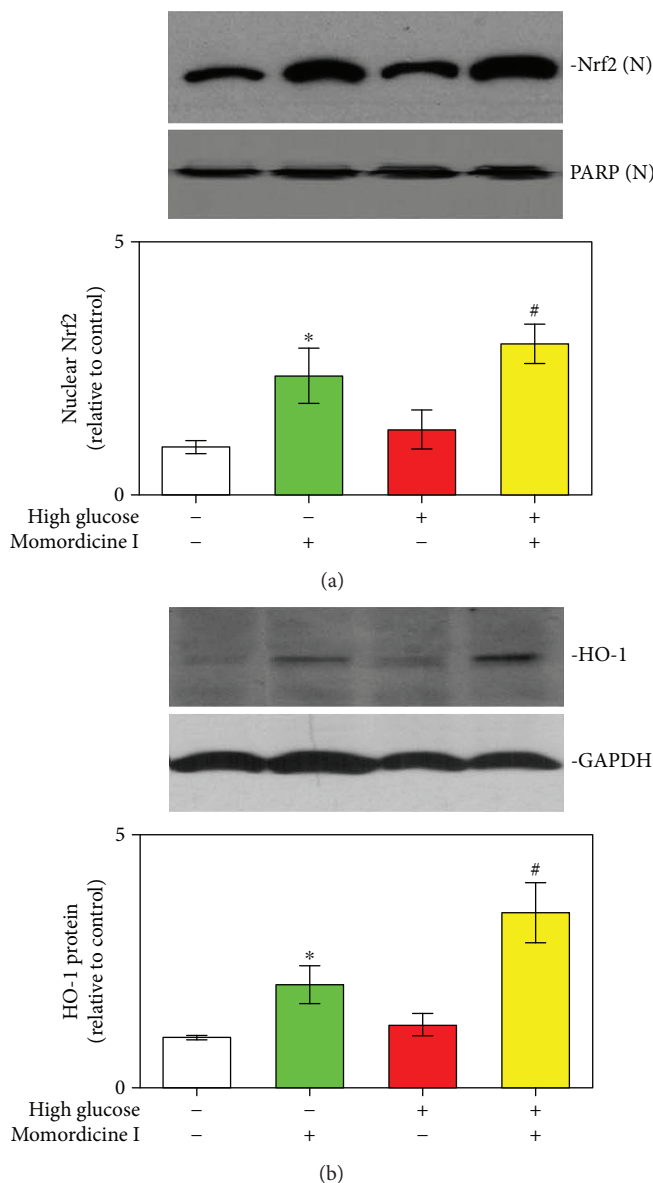


FIGURE 4: Momordicine I increases Nrf2 translocation and HO-1 protein expression in rat cardiac fibroblasts. (a) Effect of momordicine I on Nrf2 translocation. Cells were treated with or without momordicine I (1 μ M) for 12 h, followed by a normal-glucose medium or high-glucose medium for 12 h. N: nuclear extract. Results are presented as the mean \pm SEM ($n = 4$). (b) HO-1 expression was determined through Western blotting. Cells were pretreated with momordicine I (1 μ M) or not for 12 h, followed by the control medium or high-glucose medium for 24 h. Results are presented as the mean \pm SEM ($n = 3$). The relative protein expression of nuclear Nrf2 to PARP and HO-1 to GAPDH are presented in the bar graphs. * $P < 0.05$ versus the control group; # $P < 0.05$ versus the high-glucose group.

4. Discussion

Through a series of *in vitro* experiments, we determined that a high-glucose condition led to an increase in cell proliferation, collagen synthesis, and the expression of TGF- β 1 and Smad2/3 phosphorylation in cardiac fibroblasts.

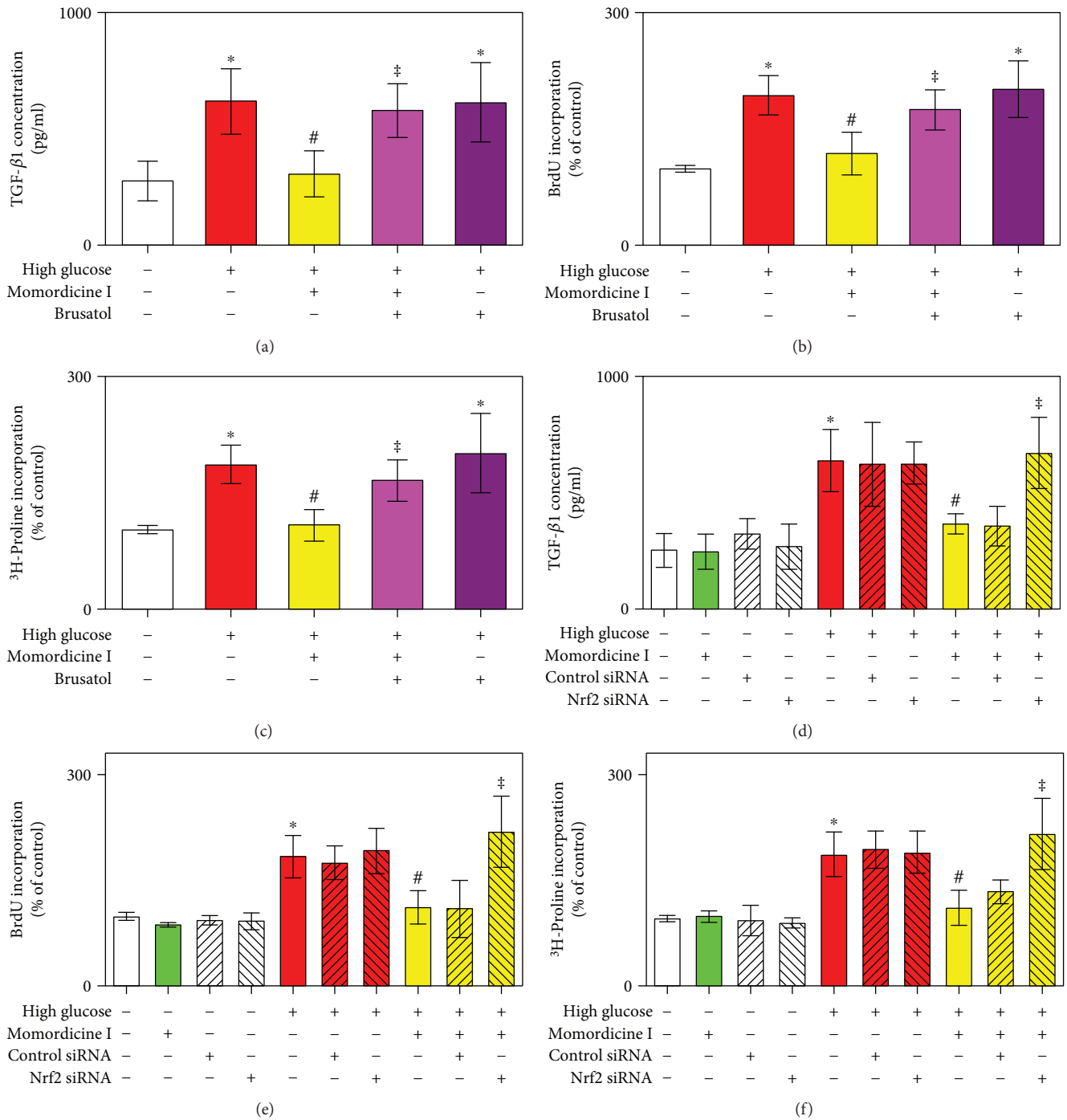


FIGURE 5: Momordicine I inhibits high-glucose-induced TGF-β1 secretion, cell proliferation, and collagen synthesis in rat cardiac fibroblasts in an Nrf2-dependent manner. (a) The Nrf2 inhibitor brusatol prevents the inhibitory effect of momordicine I on high-glucose-induced TGF-β1 secretion. Results are expressed as means ± SEM (*n* = 4). (b) Brusatol prevents the inhibitory effect of momordicine I on high-glucose-induced cell proliferation. Results are expressed as means ± SEM (*n* = 4). (c) Brusatol prevents the inhibitory effect of momordicine I on high-glucose-induced collagen synthesis. Cells were treated with brusatol (10 nM) for 30 min, followed by 1 μM momordicine I for 12 h, and were subsequently cultured in high-glucose medium for 24 h. Results are expressed as means ± SEM (*n* = 4). (d) Nrf2 siRNA prevents the inhibitory effect of momordicine I on high-glucose-induced TGF-β1 secretion. Results are expressed as means ± SEM (*n* = 3). (e) Nrf2 siRNA prevents the inhibitory effect of momordicine I on high-glucose-induced cell proliferation. Results are expressed as means ± SEM (*n* = 3). (f) Nrf2 siRNA prevents the inhibitory effect of momordicine I on high-glucose-induced collagen synthesis. Results are expressed as means ± SEM (*n* = 3). **P* < 0.05 compared with the control group; #*P* < 0.05 versus the high-glucose group; ‡*P* < 0.05 versus momordicine I treatment in the high-glucose group.

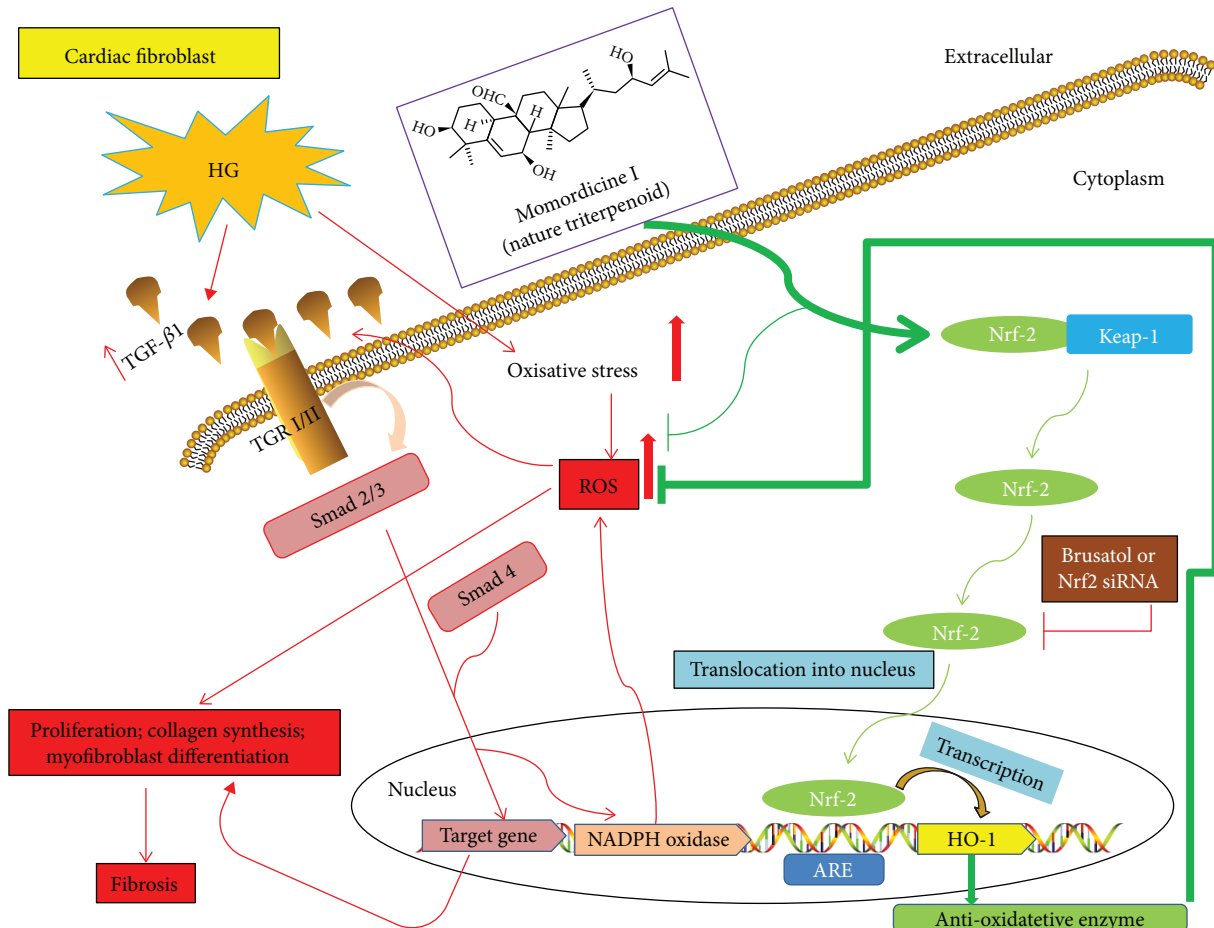


FIGURE 6: Schematic illustration of the proposed mechanism for high-glucose-induced rat cardiac fibroblast activation and momordicine I-inhibited fibrogenesis through the Nrf2-mediated inhibition of oxidative stress and TGF- β 1 signaling.

Momordicine I pretreatment significantly reduced the high-glucose-induced fibroblast activation by inhibiting the TGF- β 1-Smad2/3 signaling pathway. We further demonstrated that momordicine I can ameliorate high-glucose-induced ROS by activating the Nrf2/HO-1 pathway. Furthermore, brusatol (an Nrf2 inhibitor) or Nrf2 siRNA abrogated the inhibitory effect of momordicine I on high-glucose-induced TGF- β 1 secretion. These results suggested that momordicine I inhibits fibrogenesis through the Nrf2-mediated modulation of TGF- β 1-Smad2/3 signal transduction (Figures 6).

Consumption of food containing antioxidants has been revealed to protect against diseases such as cancer, cardiovascular diseases, and DM [25, 36]. *Momordica charantia*, commonly known as bitter melon, is a climbing perennial characterized by an elongated, warty fruit-like gourd and has been reported to have medicinal qualities in treating DM [25, 30, 37–39]. A principal therapeutic constituent of bitter melon known as momordicine has long been used in traditional Asian medicine [30]. Momordicine I belongs to cucurbitane-type triterpenoids, the major bioactive components of bitter melon. These have anticancer, antioxidant, antidiabetic, hypoglycemic, and anti-inflammatory properties [27, 30, 39–41]. With literature review and our study, we suppose that momordicine I may be used

as complementary treatment targeting cardiac fibrosis in patients with DM.

The pathophysiological mechanisms of DCM are multifactorial; substantial evidence from both clinical data and animal models has indicated that increased cardiac inflammation, oxidative stress, and enhanced cardiac fibrosis contribute to the development of DCM [42]. Therefore, anti-inflammatory, antioxidant, and antifibrotic therapeutic approaches may be beneficial for treating DCM. Fibrogenesis is the most critical factor in the progression of DCM. However, specific pharmaceuticals directly targeting fibrosis are still lacking. In this study, despite clearly acting as an antifibrotic result, momordicine I has been shown to demonstrate antioxidant effects. Furthermore, extensive evidence has indicated that oxidative stress mediates the initiation and development of fibrosis in relation to chronic inflammation [18]. Although our main focus was the modification of ROS levels as a mediator of downstream high-glucose-induced TGF- β 1 signaling [20], we discovered that momordicine I alleviated the production of hyperglycemia-induced ROS and might block the activation of high-glucose-induced cardiac fibroblast by inhibiting ROS and its downstream TGF- β 1 signal. Additionally, studies have indicated that TGF- β 1 increases ROS generation by inducing NADPH oxidase and suppressing antioxidant enzymes; in turn, ROS

activates TGF- β 1 signaling and mediates several of its fibrogenic effects, in a vicious cycle [2, 15, 18, 20]. These results further strengthen the evidence for the antioxidant properties of momordicine I through its inhibition of ROS. To confirm the role of oxidative stress in high-glucose-induced cardiac fibroblast activation, we treated cardiac fibroblasts with the antioxidant NAC. Similarly, the ROS scavenger NAC also decreased high-glucose-induced cardiac fibroblast activation. However, whether any antioxidant could have the beneficial effects of momordicine I in decreasing high-glucose-induced cardiac fibroblast activation remains to be examined in future studies.

The TGF- β family of growth factors is the most extensively studied mediator of fibroblast activation, of which TGF- β 1 likely plays a crucial role in pathological fibrosis [9]. The profibrotic actions of TGF- β 1 on cardiac fibroblasts are mediated, at least partially, by Smad3 [20, 43, 44]. Bujak et al. demonstrated that the loss of Smad3 prevents interstitial fibrosis in the noninfarcted remodeling of the myocardium [44]. TGF- β 1/Smad signaling appears to be responsible for cardiac fibrosis [20]. The canonical pathway of TGF- β 1 signaling involves the phosphorylation of Smad2/3, which subsequently binds to Smad4 and translocates to the nucleus. Here, transcriptional reprogramming is conducted to promote myofibroblast formation and extracellular matrix production, eventually leading to cardiac fibrosis [9, 20, 45]. Our paper suggests that momordicine I at nontoxic concentrations (0.1–1 μ M) effectively attenuates the profibrogenic TGF- β 1-Smad2/3 signaling pathway and is thus an effective therapy for diabetes-associated cardiac fibrosis. Several natural compounds, including matrine, resveratrol, and tanshinone, also suppressed cardiac fibrosis by inhibiting the TGF- β /Smad pathway [46–48].

Under normal conditions, Nrf2 is retained within the cytoplasm, forming a complex with its protein inhibitor Keap1 [36]. On activation, Keap1 cysteine residues undergo oxidoreduction resulting in the release of Nrf2, which subsequently translocates into the nucleus where it binds to ARE and controls the transcription of genes encoding antioxidant enzymes [49]. Nrf2 governs innate immune, antioxidant, and cytoprotective responses, and its deregulation is pivotal in the chronic inflammatory status [33]. Nrf2 has long been recognized to resist oxygen-free radicals and reduce ROS in the alleviation of cardiac fibrosis [34]. A study reported that the forced expression of Nrf2 in normal fibroblasts resulted in the abrogated stimulation of collagen synthesis, myofibroblast differentiation, and ROS generation through the disruption of canonical TGF- β 1 signaling [33]. Our study revealed that momordicine I not only ameliorates high-glucose-induced ROS but also effectively promotes Nrf2 translocation to the nucleus, which in turn upregulates HO-1. In this study, by using a selective Nrf2 inhibitor or Nrf2 knockdown, we confirmed that the antifibrotic effects of momordicine I on cardiac fibroblasts under high-glucose conditions were Nrf2 dependent. He et al. investigated the role of Nrf2 in the development of DCM using Nrf2-knockout mice. There was an increased level of ROS in the cardiomyocytes of Nrf2-knockout mice [50]. Notably, Nrf2 attenuated dystrophic muscle fibrosis by inhibiting the TGF- β 1/Smad

pathway [51]. Our study demonstrated that brusatol or Nrf2 siRNA significantly reversed the inhibitory effect of momordicine I on high-glucose-induced fibroblast activation and TGF- β 1 expression. Thus, momordicine I might reduce high-glucose-induced TGF- β 1 expression, cell proliferation, and collagen synthesis through the direct antifibrotic effects of Nrf2 and indirect downregulation of ROS levels. However, the exact molecular mechanism of Nrf2-mediated gene regulation in cardiac fibroblasts under high-glucose conditions by momordicine I remains unknown and warrants further investigation. Moreover, the induction of HO-1 is widely recognized as an effective cellular strategy to counteract a variety of cellular damage and inflammation. These effects may be mediated by multiple functions of HO-1. Although the exact mechanisms involved in the antifibrotic effects of HO-1 have not been fully elucidated, momordicine I, as confirmed in this study, can induce the expression of HO-1 in cardiac fibroblasts; the observed antifibrotic effects of momordicine I might be mediated, at least in part, by one or more of HO-1 by-products. However, whether inhibition of HO-1 activity could block momordicine I-induced antifibrotic action to suggest the role of HO-1 on the antifibrotic effect of momordicine I in cardiac fibroblasts remains to be elucidated.

A limitation of our study is that the antifibrotic efficacy of momordicine I was determined using a single TGF- β 1-dependent *in vitro* fibrosis model. Furthermore, the momordicine I-reduced high-glucose-induced collagen production from its inhibitory effect on proliferation cannot be excluded. The exact mechanism and potential role of momordicine I in fibroblast collagen synthesis remain to be investigated. The present *in vitro* model may not be directly translatable to clinical investigations of DCM. However, our preliminary results may encourage further research on determining the molecular mechanisms underlying high-glucose-induced fibroblast activation and cardiac fibrosis. While these results are promising, a lot of work needs to be done in elucidating the signal pathways involved in the action of momordicine I on these cells. Moreover, *in vivo* experiments in animal models are essential to establish the validity of these *in vitro* results in the future.

5. Conclusions

On the basis of this study, we propose that through Nrf2 activation, momordicine I can partially block intracellular TGF- β 1 signal transduction and inhibit the proliferation and collagen synthesis of cardiac fibroblasts. Through this activity, momordicine I reduces collagen synthesis and TGF- β 1 expression induced by high-glucose treatment, suggesting its potential for clinical application in preventing and treating diabetic myocardial fibrosis. Our study demonstrated that momordicine I attenuates high-glucose-induced fibroblast activation and its antifibrotic effects, at least partially, appear to reduce the expression of the profibrogenic cytokine TGF- β 1 and inhibit TGF- β 1-Smad2/3 signaling. This suggests that momordicine I has therapeutic potential in treating diabetes-induced cardiac fibrosis.

Data Availability

The data of materials and methods and conclusions to support the findings of this study are included within the article. If any other data may be needed, please contact the corresponding author upon request.

Conflicts of Interest

The authors declare that there is no conflict of interests.

Authors' Contributions

Po-Yuan Chen and Li-Chin Sung conceived and designed the experiments, Wen-Rui Hao and Po-Yuan Chen performed the experiments, Wen-Rui Hao, Chun-Chao Chen, Ju-Chi Liu, and Li-Chin Sung analyzed the data, Neng-Lang Shih and Li-Chin Sung contributed the reagents and materials, and Po-Yuan Chen and Li-Chin Sung wrote the paper. All authors read and approved the final manuscript.

Acknowledgments

This study was supported in part by research grants from Taipei Medical University (TMU105-AE1-B21), Taipei, Taiwan.

References

- [1] T. H. Marwick, R. Ritchie, J. E. Shaw, and D. Kaye, "Implications of underlying mechanisms for the recognition and management of diabetic cardiomyopathy," *Journal of the American College of Cardiology*, vol. 71, no. 3, pp. 339–351, 2018.
- [2] J. Tian, Y. Zhao, Y. Liu, Y. Liu, K. Chen, and S. Lyu, "Roles and mechanisms of herbal medicine for diabetic cardiomyopathy: current status and perspective," *Oxidative Medicine and Cellular Longevity*, vol. 2017, Article ID 8214541, 15 pages, 2017.
- [3] T. Miki, S. Yuda, H. Kouzu, and T. Miura, "Diabetic cardiomyopathy: pathophysiology and clinical features," *Heart Failure Reviews*, vol. 18, no. 2, pp. 149–166, 2013.
- [4] N. Shen, X. Li, T. Zhou et al., "Shensong Yangxin capsule prevents diabetic myocardial fibrosis by inhibiting TGF- β 1/Smad signaling," *Journal of Ethnopharmacology*, vol. 157, pp. 161–170, 2014.
- [5] X. T. Wang, Y. Gong, B. Zhou et al., "Ursolic acid ameliorates oxidative stress, inflammation and fibrosis in diabetic cardiomyopathy rats," *Biomedicine & Pharmacotherapy*, vol. 97, pp. 1461–1467, 2018.
- [6] J. S. Felício, C. C. Koury, C. T. Carvalho et al., "Present insights on cardiomyopathy in diabetic patients," *Current Diabetes Reviews*, vol. 12, no. 4, pp. 384–395, 2016.
- [7] J. Y. Liou, Y. L. Chen, S. H. Loh et al., "Magnolol depresses urotensin-II-induced cell proliferation in rat cardiac fibroblasts," *Clinical and Experimental Pharmacology & Physiology*, vol. 36, no. 7, pp. 711–716, 2009.
- [8] T. H. Cheng, P. Y. Cheng, N. L. Shih, I. B. Chen, D. L. Wang, and J. J. Chen, "Involvement of reactive oxygen species in angiotensin II-induced endothelin-1 gene expression in rat cardiac fibroblasts," *Journal of the American College of Cardiology*, vol. 42, no. 10, pp. 1845–1854, 2003.
- [9] J. G. Travers, F. A. Kamal, J. Robbins, K. E. Yutzey, and B. C. Blaxall, "Cardiac fibrosis: the fibroblast awakens," *Circulation Research*, vol. 118, no. 6, pp. 1021–1040, 2016.
- [10] Y. Yue, K. Meng, Y. Pu, and X. Zhang, "Transforming growth factor beta (TGF- β) mediates cardiac fibrosis and induces diabetic cardiomyopathy," *Diabetes Research and Clinical Practice*, vol. 133, pp. 124–130, 2017.
- [11] H. Wu, G. N. Li, J. Xie et al., "Resveratrol ameliorates myocardial fibrosis by inhibiting ROS/ERK/TGF- β /periostin pathway in STZ-induced diabetic mice," *BMC Cardiovascular Disorders*, vol. 16, no. 1, p. 5, 2016.
- [12] Y. J. Xu, P. S. Tappia, N. S. Neki, and N. S. Dhalla, "Prevention of diabetes-induced cardiovascular complications upon treatment with antioxidants," *Heart Failure Reviews*, vol. 19, no. 1, pp. 113–121, 2014.
- [13] A. Ceriello and E. Motz, "Is oxidative stress the pathogenic mechanism underlying insulin resistance, diabetes, and cardiovascular disease? The common soil hypothesis revisited," *Arteriosclerosis, Thrombosis, and Vascular Biology*, vol. 24, no. 5, pp. 816–823, 2004.
- [14] D. Zheng, S. Dong, T. Li et al., "Exogenous hydrogen sulfide attenuates cardiac fibrosis through reactive oxygen species signal pathways in experimental diabetes mellitus models," *Cellular Physiology and Biochemistry*, vol. 36, no. 3, pp. 917–929, 2015.
- [15] C. Liu, X. Z. Lu, M. Z. Shen et al., "N-acetyl cysteine improves the diabetic cardiac function: possible role of fibrosis inhibition," *BMC Cardiovascular Disorders*, vol. 15, no. 1, p. 84, 2015.
- [16] Z. Wang, H. Zhang, X. Sun, and L. Ren, "The protective role of vitamin D3 in a murine model of asthma via the suppression of TGF- β /Smad signaling and activation of the Nrf 2/HO-1 pathway," *Molecular Medicine Reports*, vol. 14, no. 3, pp. 2389–2396, 2016.
- [17] W. J. Bae, G. Q. Zhu, S. W. Choi et al., "Antioxidant and antifibrotic effect of a herbal formulation *in vitro* and in the experimental andropause via Nrf 2/HO-1 signaling pathway," *Oxidative Medicine and Cellular Longevity*, vol. 2017, Article ID 6024839, 10 pages, 2017.
- [18] G. Latella, "Redox imbalance in intestinal fibrosis: beware of the TGF β -1, ROS, and Nrf 2 connection," *Digestive Diseases and Sciences*, vol. 63, no. 2, pp. 312–320, 2018.
- [19] X. Liu, X. Song, J. Lu et al., "Neferine inhibits proliferation and collagen synthesis induced by high glucose in cardiac fibroblasts and reduces cardiac fibrosis in diabetic mice," *Oncotarget*, vol. 7, no. 38, pp. 61703–61715, 2016.
- [20] G. Euler, "Good and bad sides of TGF β -signaling in myocardial infarction," *Frontiers in Physiology*, vol. 6, p. 66, 2015.
- [21] H. Y. Lo, T. Y. Ho, C. C. Li, J. C. Chen, J. J. Liu, and C. Y. Hsiang, "A novel insulin receptor-binding protein from *Momordica charantia* enhances glucose uptake and glucose clearance *in vitro* and *in vivo* through triggering insulin receptor signaling pathway," *Journal of Agricultural and Food Chemistry*, vol. 62, no. 36, pp. 8952–8961, 2014.
- [22] H. Yamada, A. Tanaka, K. Kusunose et al., "Effect of sitagliptin on the echocardiographic parameters of left ventricular diastolic function in patients with type 2 diabetes: a subgroup analysis of the PROLOGUE study," *Cardiovascular Diabetology*, vol. 16, no. 1, p. 63, 2017.
- [23] C. Ma, H. Yu, Y. Xiao, and H. Wang, "*Momordica charantia* extracts ameliorate insulin resistance by regulating the

- expression of SOCS-3 and JNK in type 2 diabetes mellitus rats,” *Pharmaceutical Biology*, vol. 55, no. 1, pp. 2170–2177, 2017.
- [24] A. Raman and C. Lau, “Anti-diabetic properties and phytochemistry of *Momordica charantia* L. (Cucurbitaceae),” *Phytomedicine*, vol. 2, no. 4, pp. 349–362, 1996.
- [25] B. C. Panda, S. Mondal, K. S. P. Devi et al., “Pectic polysaccharide from the green fruits of *Momordica charantia* (Karela): structural characterization and study of immunoenhancing and antioxidant properties,” *Carbohydrate Research*, vol. 401, pp. 24–31, 2015.
- [26] H. Z. Gu, R. R. Lin, H. C. Wang, X. J. Zhu, Y. Hu, and F. Y. Zheng, “Effect of *Momordica charantia* protein on proliferation, apoptosis and the AKT signal transduction pathway in the human endometrial carcinoma Ishikawa H cell line in vitro,” *Oncology Letters*, vol. 13, no. 5, pp. 3032–3038, 2017.
- [27] S.-B. Wu, G. G. L. Yue, M.-H. To, A. C. Keller, C. B. S. Lau, and E. J. Kennelly, “Transport in Caco-2 cell monolayers of anti-diabetic cucurbitane triterpenoids from *Momordica charantia* fruits,” *Planta Medica*, vol. 80, no. 11, pp. 907–911, 2014.
- [28] M. J. Tan, J. M. Ye, N. Turner et al., “Antidiabetic activities of triterpenoids isolated from bitter melon associated with activation of the AMPK pathway,” *Chemistry & Biology*, vol. 15, no. 3, pp. 263–273, 2008.
- [29] A. C. Keller, J. Ma, A. Kavalier, K. He, A. M. B. Brillantes, and E. J. Kennelly, “Saponins from the traditional medicinal plant *Momordica charantia* stimulate insulin secretion in vitro,” *Phytomedicine*, vol. 19, no. 1, pp. 32–37, 2011.
- [30] S. Jia, M. Shen, F. Zhang, and J. Xie, “Recent advances in *Momordica charantia*: functional components and biological activities,” *International Journal of Molecular Sciences*, vol. 18, no. 12, 2017.
- [31] S. Zhuang, T. H. Cheng, N. L. Shih et al., “Tanshinone IIA induces heme oxygenase 1 expression and inhibits cyclic strain-induced interleukin 8 expression in vascular endothelial cells,” *The American Journal of Chinese Medicine*, vol. 44, no. 2, pp. 377–388, 2016.
- [32] J. C. Liu, C. H. Chen, J. J. Chen, and T. H. Cheng, “Urotensin II induces rat cardiomyocyte hypertrophy via the transient oxidation of Src homology 2-containing tyrosine phosphatase and transactivation of epidermal growth factor receptor,” *Molecular Pharmacology*, vol. 76, no. 6, pp. 1186–1195, 2009.
- [33] J. Wei, H. Zhu, G. Lord et al., “Nrf 2 exerts cell-autonomous antifibrotic effects: compromised function in systemic sclerosis and therapeutic rescue with a novel heterocyclic chalcone derivative,” *Translational Research*, vol. 183, pp. 71–86.e1, 2017.
- [34] S. M. Swamy, N. S. Rajasekaran, and V. J. Thannickal, “Nuclear factor-erythroid-2-related factor 2 in aging and lung fibrosis,” *The American Journal of Pathology*, vol. 186, no. 7, pp. 1712–1723, 2016.
- [35] D. Ren, N. F. Villeneuve, T. Jiang et al., “Brusatol enhances the efficacy of chemotherapy by inhibiting the Nrf2-mediated defense mechanism,” *Proceedings of the National Academy of Sciences of the United States of America*, vol. 108, no. 4, pp. 1433–1438, 2011.
- [36] L. C. Sung, H. H. Chao, C. H. Chen et al., “Lycopene inhibits cyclic strain-induced endothelin-1 expression through the suppression of reactive oxygen species generation and induction of heme oxygenase-1 in human umbilical vein endothelial cells,” *Clinical and Experimental Pharmacology & Physiology*, vol. 42, no. 6, pp. 632–639, 2015.
- [37] M. F. Mahmoud, F. E. El Ashry, N. N. El Maraghy, and A. Fahmy, “Studies on the antidiabetic activities of *Momordica charantia* fruit juice in streptozotocin-induced diabetic rats,” *Pharmaceutical Biology*, vol. 55, no. 1, pp. 758–765, 2017.
- [38] S. J. Yang, J. M. Choi, S. E. Park et al., “Preventive effects of bitter melon (*Momordica charantia*) against insulin resistance and diabetes are associated with the inhibition of NF- κ B and JNK pathways in high-fat-fed OLETF rats,” *The Journal of Nutritional Biochemistry*, vol. 26, no. 3, pp. 234–240, 2015.
- [39] A. Ota and N. P. Ulrih, “An overview of herbal products and secondary metabolites used for management of type two diabetes,” *Frontiers in Pharmacology*, vol. 8, p. 436, 2017.
- [40] J. Ma, P. Whittaker, A. Keller et al., “Cucurbitane-type triterpenoids from *Momordica charantia*,” *Planta Medica*, vol. 76, no. 15, pp. 1758–1761, 2010.
- [41] H. Liu, G. C. Wang, M. X. Zhang, and B. Ling, “The cytotoxicology of momordicins I and II on *Spodoptera litura* cultured cell line SL-1,” *Pesticide Biochemistry and Physiology*, vol. 122, pp. 110–118, 2015.
- [42] L. M. D. Delbridge, V. L. Benson, R. H. Ritchie, and K. M. Mellor, “Diabetic cardiomyopathy: the case for a role of fructose in disease etiology,” *Diabetes*, vol. 65, no. 12, pp. 3521–3528, 2016.
- [43] M. Bujak and N. G. Frangogiannis, “The role of TGF- β signaling in myocardial infarction and cardiac remodeling,” *Cardiovascular Research*, vol. 74, no. 2, pp. 184–195, 2007.
- [44] M. Bujak, G. Ren, H. J. Kweon et al., “Essential role of Smad 3 in infarct healing and in the pathogenesis of cardiac remodeling,” *Circulation*, vol. 116, no. 19, pp. 2127–2138, 2007.
- [45] G. Liu, C. Ma, H. Yang, and P. Y. Zhang, “Transforming growth factor β and its role in heart disease,” *Experimental and Therapeutic Medicine*, vol. 13, no. 5, pp. 2123–2128, 2017.
- [46] C.-Y. Zhan, J.-H. Tang, D.-X. Zhou, and Z.-H. Li, “Effects of tanshinone IIA on the transforming growth factor β 1/Smad signaling pathway in rat cardiac fibroblasts,” *Indian Journal of Pharmacology*, vol. 46, no. 6, pp. 633–638, 2014.
- [47] T. Chen, J. Li, J. Liu et al., “Activation of SIRT3 by resveratrol ameliorates cardiac fibrosis and improves cardiac function via the TGF- β /Smad 3 pathway,” *American Journal of Physiology. Heart and Circulatory Physiology*, vol. 308, no. 5, pp. H424–H434, 2015.
- [48] Y. Zhang, L. Cui, G. Guan et al., “Matrine suppresses cardiac fibrosis by inhibiting the TGF- β /Smad pathway in experimental diabetic cardiomyopathy,” *Molecular Medicine Reports*, vol. 17, no. 1, pp. 1775–1781, 2018.
- [49] Q. Ma, “Role of Nrf2 in oxidative stress and toxicity,” *Annual Review of Pharmacology and Toxicology*, vol. 53, no. 1, pp. 401–426, 2013.
- [50] X. He, H. Kan, L. Cai, and Q. Ma, “Nrf2 is critical in defense against high glucose-induced oxidative damage in cardiomyocytes,” *Journal of Molecular and Cellular Cardiology*, vol. 46, no. 1, pp. 47–58, 2009.
- [51] C. Sun, S. Li, and D. Li, “Sulforaphane mitigates muscle fibrosis in *mdx* mice via Nrf2-mediated inhibition of TGF- β /Smad signaling,” *Journal of Applied Physiology*, vol. 120, no. 4, pp. 377–390, 2016.

Research Article

Gamma Oryzanol Treats Obesity-Induced Kidney Injuries by Modulating the Adiponectin Receptor 2/PPAR- α Axis

Fabiane Valentini Francisqueti ¹, Artur Junio Togneri Ferron,¹
Fabiana Kurokawa Hasimoto,² Pedro Henrique Rizzi Alves,² Jéssica Leite Garcia,¹
Klinsmann Carolo dos Santos ¹, Fernando Moreto,¹ Vanessa dos Santos Silva ¹,
Ana Lúcia A. Ferreira,¹ Igor Otávio Minatel,² and Camila Renata Corrêa ¹

¹Medical School, São Paulo State University (UNESP), Botucatu, SP, Brazil

²Institute of Biosciences, São Paulo State University (UNESP), Botucatu, SP, Brazil

Correspondence should be addressed to Fabiane Valentini Francisqueti; fabiane_vf@yahoo.com.br

Received 17 May 2018; Accepted 22 July 2018; Published 9 September 2018

Academic Editor: Germán Gil

Copyright © 2018 Fabiane Valentini Francisqueti et al. This is an open access article distributed under the Creative Commons Attribution License, which permits unrestricted use, distribution, and reproduction in any medium, provided the original work is properly cited.

The kidney is an important organ in the maintenance of body homeostasis. Dietary compounds, reactive metabolites, obesity, and metabolic syndrome (MetS) can affect renal filtration and whole body homeostasis, increasing the risk of chronic kidney disease (CKD) development. Gamma oryzanol (γ Oz) is a compound with antioxidant and anti-inflammatory activity that has shown a positive action in the treatment of obesity and metabolic diseases. *Aim.* To evaluate the effect of γ Oz to recover renal function in obese animals by high sugar-fat diet by modulation of adiponectin receptor 2/PPAR- α axis. *Methods.* Male Wistar rats were initially randomly divided into 2 experimental groups: control and high sugar-fat diet (HSF) for 20 weeks. When proteinuria was detected, HSF animals were allocated to receive γ Oz or maintain HSF for more than 10 weeks. The following were analyzed: nutritional and biochemical parameters, systolic blood pressure, and renal function. In the kidney, the following were evaluated: inflammation, oxidative stress, and protein expression by Western blot. *Results.* After 10 weeks of γ Oz treatment, γ Oz was effective to improve inflammation, increase antioxidant enzyme activities, increase the protein expression of adiponectin receptor 2 and PPAR- α , and recover renal function. *Conclusion.* These results permit us to confirm that γ Oz is able to modulate PPAR- α expression, inflammation, and oxidative stress pathways improving obesity-induced renal disease.

1. Introduction

Kidneys exert a central role in the maintenance of body homeostasis by regulating electrolyte concentrations, blood pressure, degradation of hormones, lipid metabolism, and excretion of waste metabolites [1]. Despite many factors leading to kidney disease, such as age, gender, smoking status, alcohol use, physical inactivity, diabetes mellitus, and hypertension, studies reveal that obesity is an independent risk factor for development of CKD [1–3].

The pathways activated by obesity to induce kidney disease are not fully understood. Studies have identified several new injurious pathways in the kidney led by insulin resistance (IR), chronic inflammation (a major contributor

to microvascular remodeling), dyslipidemia and excessive nutrient availability (both may induce mitochondrial dysfunction and oxidative stress), and adipokine production unbalance [4–6].

Adiponectin is an adipocyte-derived protein hormone which plays a role in the suppression of inflammation-associated metabolic disorders. Adiponectin receptor 1 (Adipo-R1) and adiponectin receptor 2 (Adipo-R2) are the two major receptors for adiponectin and appear to be integral membrane proteins [7], expressed in different tissues, among them the kidney [8]. Kadowaki et al. [7] reported previously that the receptor expression levels are reduced in obesity, apparently in correlation with reduced adiponectin sensitivity. Moreover, the authors relate that Adipo-R1 may be more

tightly linked to activation of AMPK pathways, whereas Adipo-R2 seems to be associated with the activation of PPAR- α pathways and the inhibition of inflammation. So, the modulation of these pathways could be important to treat renal injuries.

Considering this situation, natural compounds have received attention as a promising pool of substances to treat diseases [9]. Rice bran is rich in gamma oryzanol (γ Oz), a natural compound with antioxidant and anti-inflammatory activities that showed a positive action in the treatment of hyperlipidemia, hyperglycemia, insulin resistance, and increased levels of adiponectin [10–14]. So, considering that obesity, inflammation, and oxidative stress are able to induce renal disease and there are no studies that evaluate the effect of γ Oz in renal disease, the aim of this study was to evaluate the effect of γ Oz in the recovery of renal function in obese animals by high sugar-fat diet by modulation of the adiponectin receptor 2/PPAR- α axis.

2. Methods

2.1. Experimental Protocol. All of the experiments and procedures were approved by the Animal Ethics Committee of Botucatu Medical School (1150/2015) and were performed in accordance with the National Institute of Health's Guide for the Care and Use of Laboratory Animals. Male Wistar rats (± 187 g) were kept in an environmental controlled room ($22^{\circ}\text{C} \pm 3^{\circ}\text{C}$, 12 h light-dark cycle, and relative humidity of $60 \pm 5\%$) and initially randomly divided into 2 experimental groups (control, $n = 15$, and high sugar-fat diet (HSF), $n = 30$) for 20 weeks. HSF groups also received water + sucrose (25%). The diets and water were provided ad libitum. The HSF diet contained soybean meal, sorghum, soybean peel, dextrin, sucrose, fructose, lard, vitamins, and minerals, plus 25% sucrose in drinking water; the control diet contained soybean meal, sorghum, soybean peel, dextrin, soy oil, vitamins, and minerals. The nutrients and nutritional composition of each diet was described in our previous study [15]. At week 20 of this study, when proteinuria was detected in the HSF groups, animals were divided to begin the treatment with γ Oz or continue receiving HSF for 10 more weeks as described below.

2.2. Group Characterization. After 20 weeks of experimental protocol, a 95% confidence interval (CI) was built for the protein/creatinine ratio from the HSF and control groups and was adopted as the separation point (SP) between the groups, the midpoint between the upper limit of the control group and the lower limit of the HSF group. The protein/creatinine ratio was adopted since it reflects proteinuria and is considered a marker of kidney function [16]. From this point, the control animals with a protein/creatinine ratio above of SP and the HSF animals with a protein/creatinine ratio below the SP were excluded from the control and HSF groups, respectively, ensuring the homogeneity of the treated and control groups. About the remaining animals in the HSF group, they were randomly divided to receive γ Oz or only diet. This criterion was adopted because animals submitted to different diet models do not always present the expected

response. This fact can lead to erroneous animal classification and, consequently, false conclusions. The values for protein/creatinine ratio on the 20th week were 2.5 for the control group and 3.3 for the HSF group ($p = 0.0006$).

2.3. Treatment with Gamma Oryzanol. After the characterization on the 20th week, the groups were the following: control diet (control, $n = 8$), high sugar-fat diet (HSF, $n = 8$), and HSF/HSF + gamma oryzanol (HSF/HSF + γ Oz, $n = 8$). The treatment duration was 10 weeks, totaling 30 weeks of experiment. The γ Oz dose used in this study was added in the chow (0.5 w/w) according to our previous study [15].

2.4. Body Composition and Caloric Ingestion. The nutritional profile was evaluated according to the following parameters: caloric intake, body weight, and adiposity index. Caloric intake was determined by multiplying the energy value of each diet ($\text{g} \times \text{kcal}$) by the daily food consumption. For the HSF group, caloric intake also included calories from water ($0.25 \times 4 \times \text{mL}$ consumed). Body weight was measured weekly. After euthanasia, fat deposits (visceral (VAT), epididymal (EAT), and retroperitoneal (RAT)) were used to calculate the adiposity index (AI) by the following formula: $[(\text{VAT} + \text{EAT} + \text{RAT})/\text{FBW}] \times 100$.

2.5. Metabolic and Hormonal Analysis. After 12 h fasting, blood was collected and the plasma was used to measure insulin and biochemical parameters. Glucose concentration was determined by using a glucometer (Accu-Chek Performa, Roche Diagnostics Brazil Limited); triglycerides were measured with an automatic enzymatic analyzer system (Chemistry Analyzer BS-200, Mindray Medical International Limited, Shenzhen, China). The insulin and adiponectin levels were measured using enzyme-linked immunosorbent assay (ELISA) methods using commercial kits (EMD Millipore Corporation, Billerica, MA, USA). The homeostatic model of insulin resistance (HOMA-IR) was used as an insulin resistance index, calculated according to the following formula: $\text{HOMA-IR} = (\text{fasting glucose (mmol/L)} \times \text{fasting insulin } (\mu\text{U/mL}))/22.5$.

2.6. Systolic Blood Pressure. Systolic blood pressure (SBP) evaluation was assessed in conscious rats by the noninvasive tail-cuff method with a Narco Bio-Systems[®] electrospphygmomanometer (International Biomedical, Austin, TX, USA). The animals were kept in a wooden box (50×40 cm) between 38 and 40°C for 4–5 minutes to stimulate arterial vasodilation [17]. After this procedure, a cuff with a pneumatic pulse sensor was attached to the tail of each animal. The cuff was inflated to 200 mmHg pressure and subsequently deflated. The blood pressure values were recorded on a Gould RS 3200 polygraph (Gould Instrumental Valley View, Ohio, USA). The average of three pressure readings was recorded for each animal.

2.7. Renal Function. Renal function was evaluated by measurements of plasma and urine. At twenty-four hours, urine was collected from the metabolic cages to measure the excretion of creatinine and the total protein. The urea and creatinine content of the plasma were measured. All

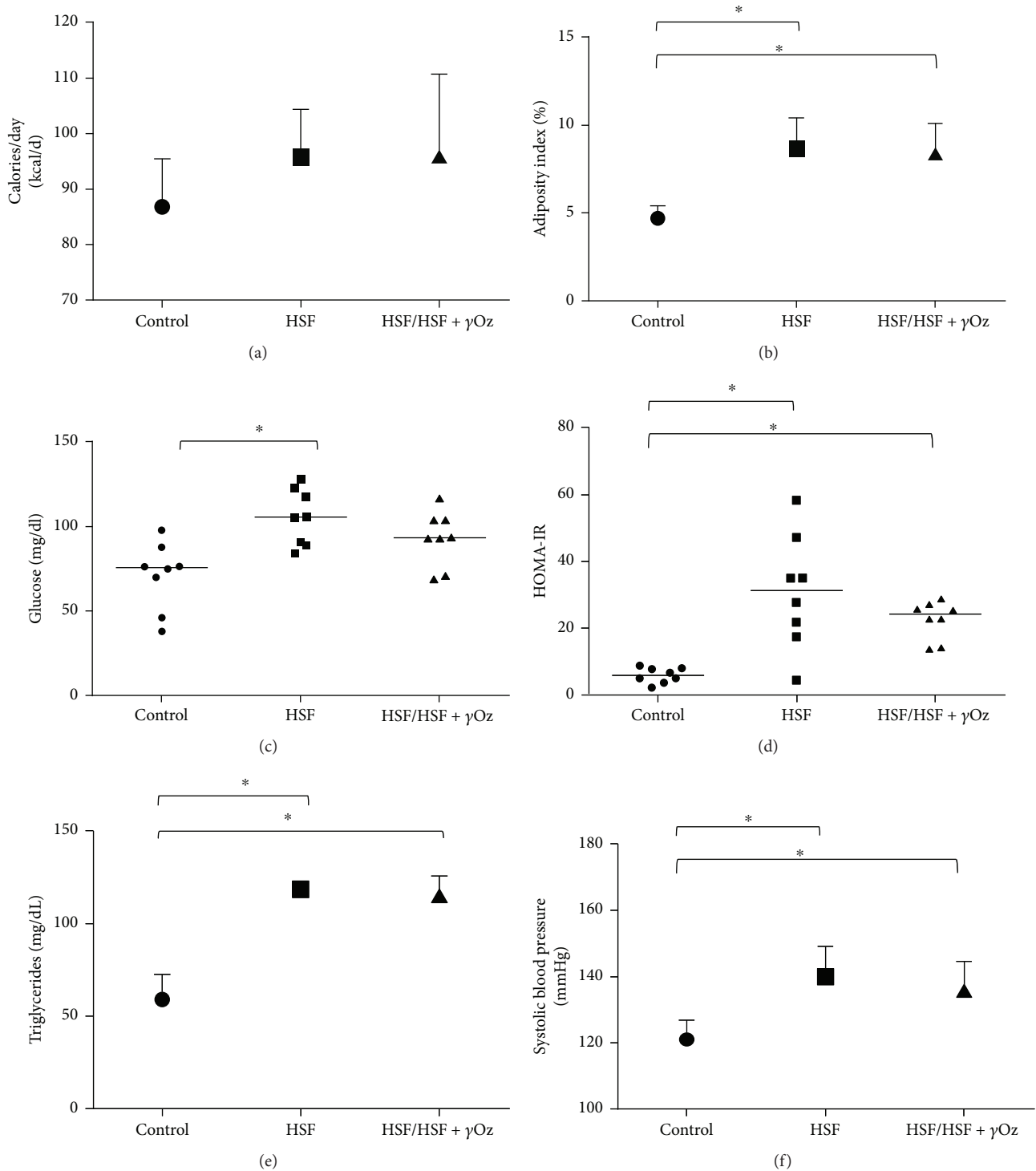


FIGURE 1: Nutritional, metabolic, and cardiovascular parameters: (a) caloric intake (kcal/day); (b) adiposity index (%); (c) glucose (mg/dL); (d) HOMA-IR; (e) triglycerides (mg/dL); (f) systolic blood pressure (mmHg). Data expressed in mean \pm standard deviation or median. Comparison by one-way ANOVA with Tukey post hoc. HSF: high sugar-fat diet; γ Oz: gamma oryzanol. * indicates $p < 0.05$; $n = 8$ animals/group.

analyses were performed with an automatic enzymatic analyzer system (biochemical analyzer BS-200, Mindray, China). The glomerular filtration rate ($GFR = (\text{urine creatinine} \times \text{flux}) / \text{plasma creatinine}$) and proteinuria were also calculated.

2.8. Renal Tissue Analysis

2.8.1. Inflammatory Parameters. Renal tissue (± 150 mg) was homogenized (ULTRA-TURRAX® T 25 basic IKA® Werke, Staufen, Germany) in 1.0 mL of phosphate-buffered saline

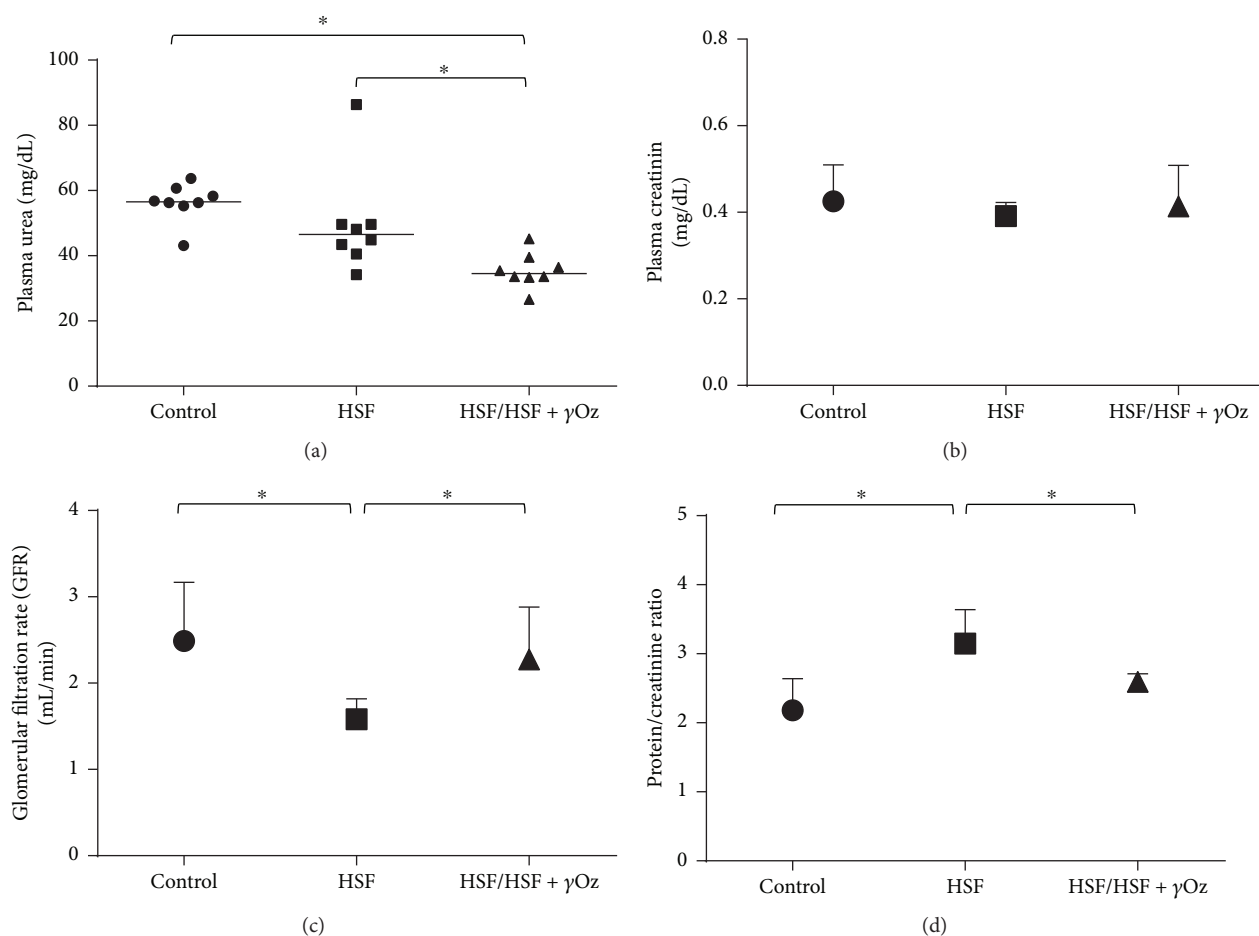


FIGURE 2: Renal function parameters: (a) plasma urea (mg/dL); (b) plasma creatinine (mg/dL); (c) glomerular filtration rate (GFR) (mL/min); (d) protein/creatinine ratio. Data expressed in mean \pm standard deviation or median. Comparison by one-way ANOVA with Tukey post hoc. * indicates $p < 0.05$; $n = 8$ animals/group.

(PBS) pH 7.4 cold solution and centrifuged at 800g at 4°C for 10 min. The supernatant (100 μ L) was used in analysis. Tumor necrosis factor- α (TNF- α), interleukin-6 (IL-6), and monocyte chemoattractant protein-1 (MCP-1) levels were measured using the enzyme-linked immunosorbent assay (ELISA) method using commercial kits from R&D System, Minneapolis, USA. The supernatant (100 μ L) was used for analysis, and the results were corrected by the protein amount.

2.8.2. Hydrophilic Antioxidant Capacity. The hydrophilic antioxidant capacity in the kidney was in the prepared supernatant as described in the previous item. It was determined fluorometrically, using a VICTOR X2 reader (PerkinElmer, Boston, MA). The antioxidant activity was quantitated by comparing the area under the curve relating to the oxidation kinetics of the suspension phosphatidylcholine (PC), which was used as the reference biological matrix. The peroxy radical 2',2'-azobis-(2-amidinopropane) dihydrochloride (AAPH) was used as an initiator of the reaction. The results represent the percent inhibition (4,4-difluoro-5-(4-phenyl 1-3 butadiene)-4-bora-3,4-diaza-s-indacene) (BODIPY) 581/591 plasma with respect to the control

sample of BODIPY 581/591 PC liposome. All analyses were performed in triplicate. The results are reported as a percentage of protection [18].

2.8.3. Antioxidant Enzyme Activity. For these analyses, a 100 mg kidney was homogenized (1:10 v/v) in KH_2PO_4 (10 mmol/L)/KCl (120 mmol/L), pH 7.4, and centrifuged at 2,000 \times g for 20 min. Superoxide dismutase (SOD) activity was measured based on the inhibition of a superoxide radical reaction with pyrogallol, and the absorbance values were measured at 420 nm [19]. Catalase activity was evaluated by following the decrease in the levels of hydrogen peroxide in 240 nm [20]. The activity is expressed as pmol of H_2O_2 reduced/min/mg protein. Glutathione peroxidase (GP) activity was measured by following β -nicotinamide adenine dinucleotide phosphate (NADPH) oxidation at 340 nm as described by Flohé and Günzler [21]. The results were expressed as μ mol hydroperoxide-reduced/min/mg protein. Protein was quantified based on Lowry et al.'s method [22] using bovine serum albumin as the standard. The absorbance values for all analyses were measured in a UV/VIS spectrophotometer (Pharmacia Biotech, Houston, Texas, USA), and the values are expressed as units per milligram of protein.

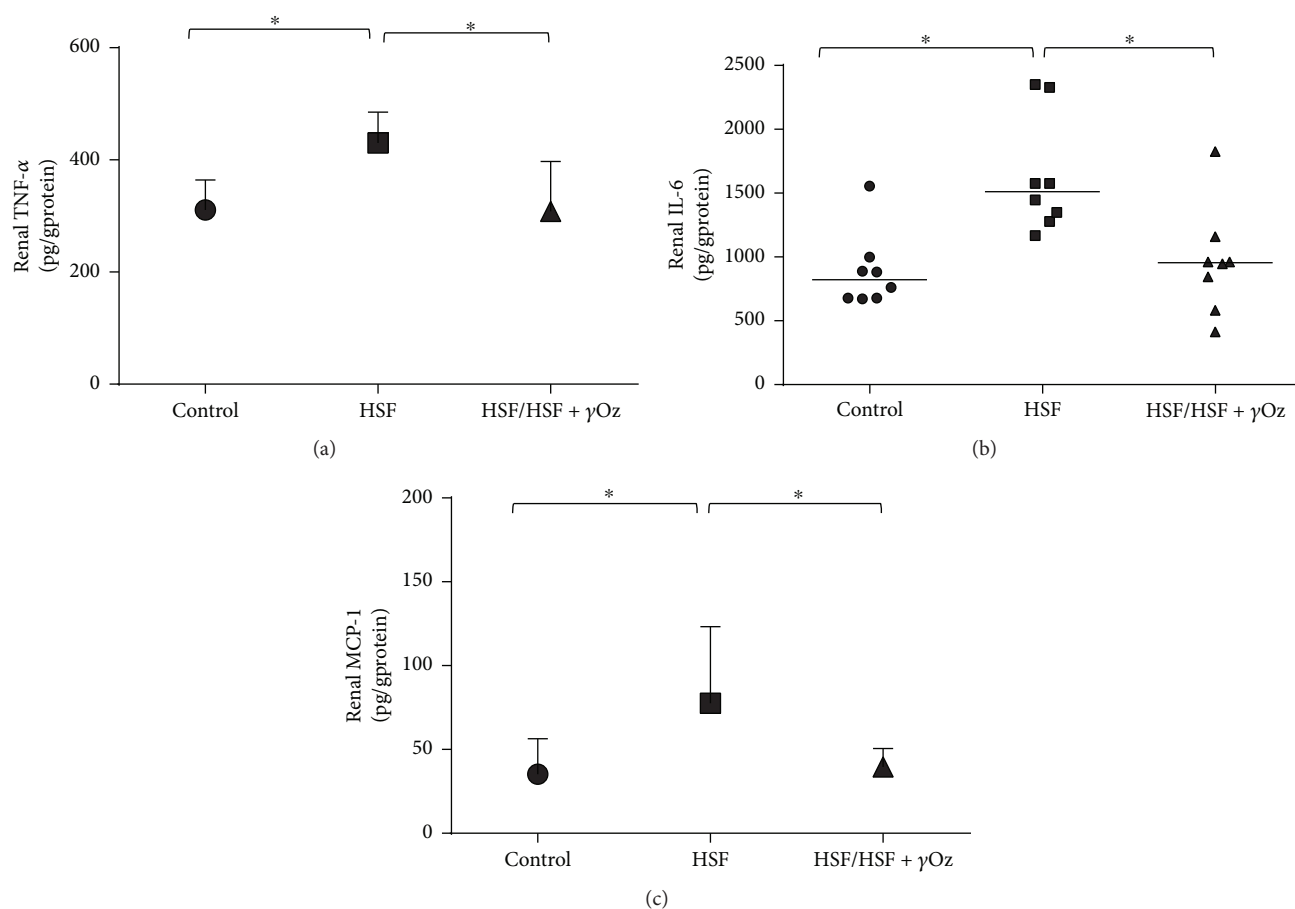


FIGURE 3: Inflammatory parameters in kidney tissue: (a) tumor necrosis factor-alpha (TNF- α ; pg/g protein); (b) interleukin-6 (IL-6; pg/g protein); (c) monocyte chemoattractant protein-1 (MCP-1; pg/g protein). Data expressed in mean \pm standard deviation or median. Comparison by one-way ANOVA with Tukey post hoc. * indicates $p < 0.05$; $n = 8$ animals/group.

2.8.4. Western Blot. Renal samples were homogenized in RIPA buffer with a protease and phosphatase cocktail inhibitor. After determination of protein concentration by the Bradford method [23], samples were diluted in Laemmli buffer and loaded (50 μ g of protein) into a 10% SDS-polyacrylamide gel. Transfer to a nitrocellulose membrane was carried out using Trans-Blot Turbo-Transfer System (BioRad). Incubation with the primary antibodies was performed overnight at 4°C in Tris-buffered saline solution containing Tween 20 (TBS-T) and 3% bovine serum albumin. Antibody dilutions were 1:1000 for Adipo-R1 (ABCAM ab126611), 1:1000 for Adipo-R2 (ABCAM ab77612), 1:500 for PPAR- α (ABCAM ab8934), 1:1000 for total AMPK (Cell Signaling #2532), 1:1000 for phospho-AMPH (Thr172) (Cell Signaling #2531), and 1:1000 for beta-actin (ABCAM ab8227). After incubation overnight at 4°C in TBS-T containing 1% nonfat dried milk with the Abcam secondary antibodies (dilution 1:3000 for anti-goat and 1:1000 for anti-rabbit). Protein was revealed using the chemiluminescence method according to the manufacturer's instructions (ECL SuperSignal® West Pico Chemiluminescent Substrate, Thermo Scientific). Band intensities were evaluated using ImageQuant TL 1D Version 8.1 (GE Healthcare Life Sciences).

2.9. Statistical Analysis. Data are presented as means \pm standard deviation (SD) or median (interquartile range). Differences among the groups were determined by one-way analysis of variance. Statistically significant variables were subjected to the Tukey post hoc test to compare all the groups. Statistical analyses were performed using Sigma Stat for Windows Version 3.5 (Systat Software Inc., San Jose, CA, USA). A p value of 0.05 was considered statistically significant.

3. Results

Figure 1 shows caloric intake, adiposity index, and cardiometabolic risk factors for kidney disease (glucose, HOMA-IR, triglycerides, and systolic blood pressure). It is possible to verify that both HSF groups presented higher values for all the parameters. There was no difference for caloric intake.

Figure 2 shows renal function parameters. Gamma oryzanol was effective for recovery of renal function of the HSF/HSF + γ Oz group, characterized by lower proteinuria and high glomerular filtration rate compared to the HSF group.

Figure 3 shows inflammatory parameters in kidney tissue. γ Oz was effective to reduce the inflammatory response for levels similar to those observed in the control group.

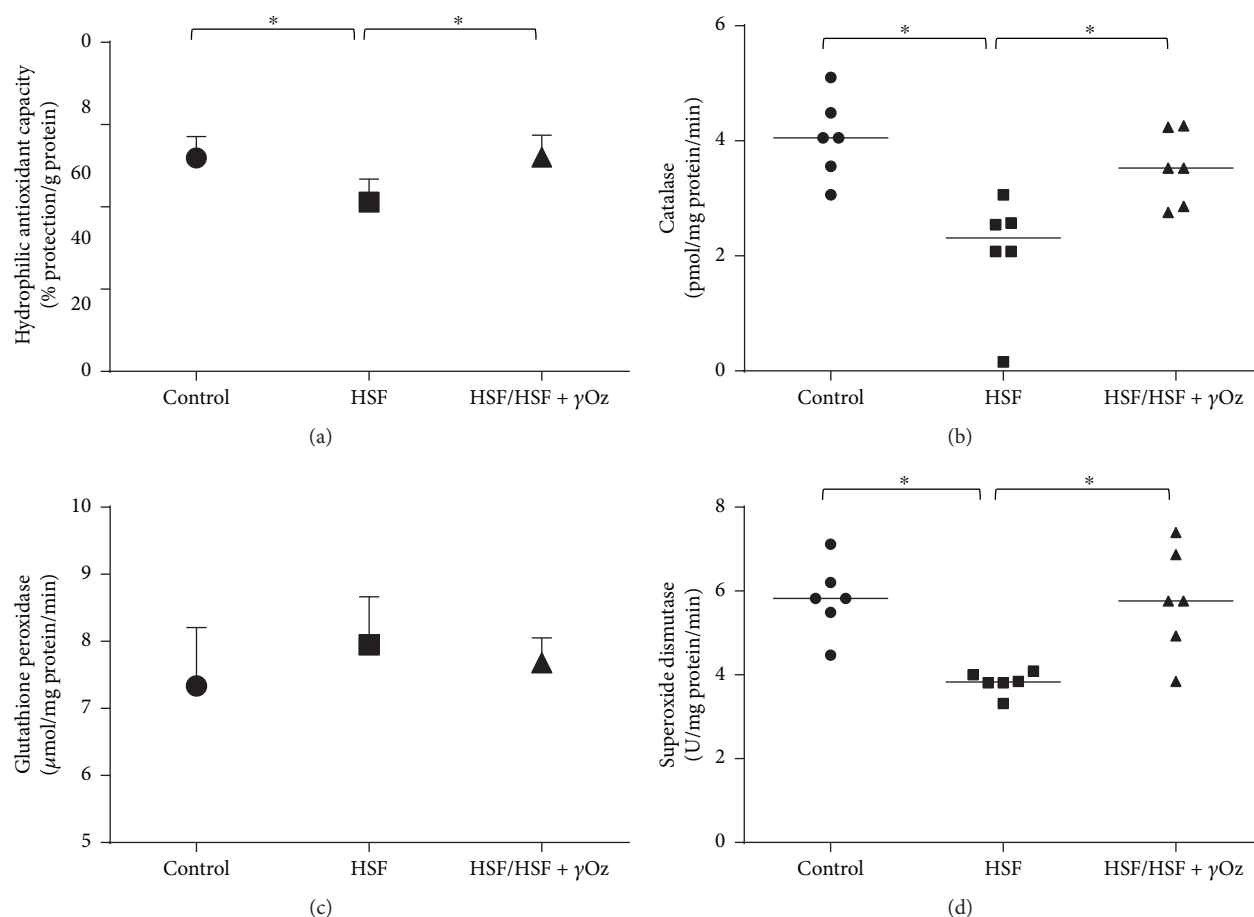


FIGURE 4: Redox state parameters in the kidney: (a) hydrophilic antioxidant capacity (% protection/g protein); (b) catalase (pmol/mg protein/min); (c) glutathione peroxidase (μ mol/mg protein/min); (d) superoxide dismutase (U/mg protein/min). Data expressed in mean \pm standard deviation. Comparison by one-way ANOVA with Tukey post hoc. * indicates $p < 0.05$; $n = 6$ animals/group.

Figure 4 shows redox state parameters in the kidney. It is possible to verify a positive action of γ Oz on the HSF/HSF + γ Oz group to increase hydrophilic antioxidant protection, catalase, and superoxide dismutase levels compared to HSF.

Figure 5 presents plasma adiponectin levels. The HSF group presented higher levels while the treatment with gamma oryzanol was able to reduce the levels.

Figure 6 shows protein expression of Adipo-R1, Adipo-R2, phosphorylated and total AMPK, and PPAR- α in the kidney. It is possible to note the effect of γ Oz which increased the expression of Adipo-R2 and PPAR- α when compared to HSF.

4. Discussion

The aim of this study was to evaluate the potential of γ Oz to recover renal function in obese animals by high sugar-fat diet consumption. In this study, the animals feeding on a HSF diet developed obesity and signals of kidney injury, characterized by proteinuria and decreased glomerular filtration rate. Obesity, insulin resistance, hypertension, chronic inflammation, dyslipidemia, and oxidative stress are

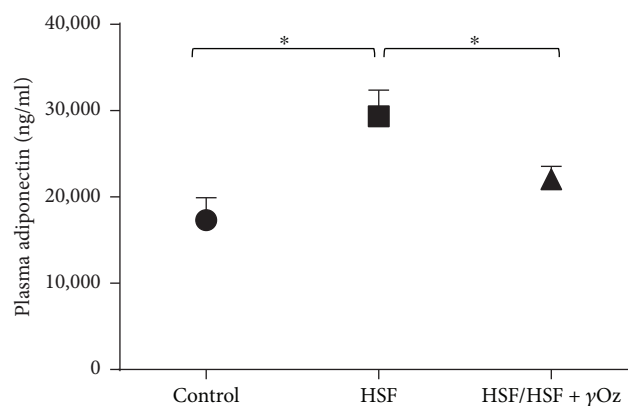


FIGURE 5: Plasma adiponectin levels (ng/mL). Data expressed in mean \pm standard deviation. Comparison by one-way ANOVA with Tukey post hoc. * indicates $p < 0.05$; $n = 8$ animals/group.

considered the major risk factors for renal disease [1, 4, 6]. The HSF group developed all these risk factors, which were expected considering the diet used in this study, rich in sugar and fat [15], but the noneffect of γ Oz on these parameters was observed. In opposition to our results, Wang et al. and

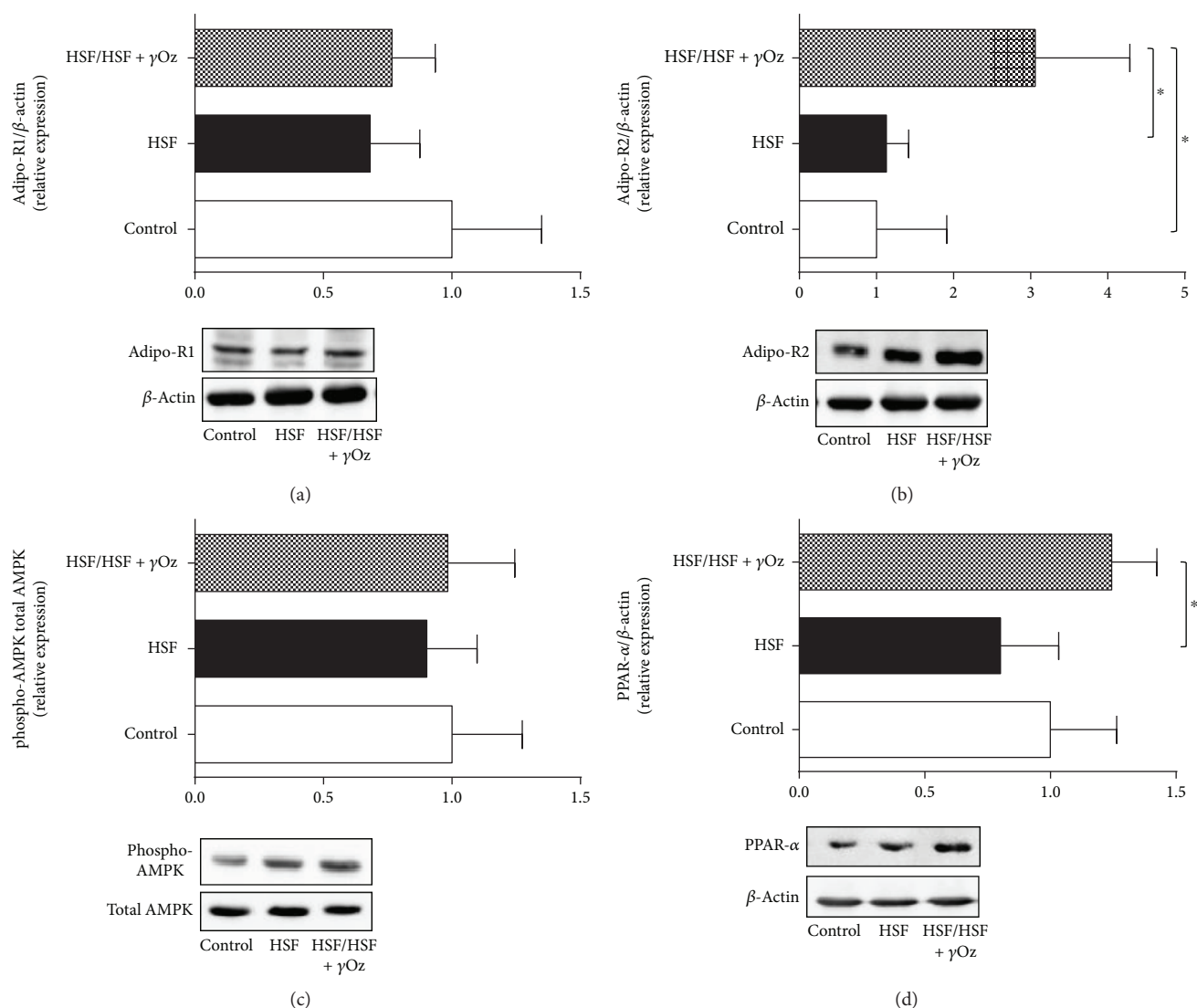


FIGURE 6: Relative protein expression in kidney tissue: (a) Adipo-R1; (b) Adipo-R2; (c) phospho-AMPK; (d) PPAR- α . Data expressed in mean \pm standard deviation. Comparison by one-way ANOVA with Tukey post hoc. * indicates $p < 0.05$; $n = 6$ animals/group.

Justo et al. found in their studies improvement in some parameters after treatment with γ Oz [10, 24]. It is important to emphasize that in these studies, animal models and the dose of γ Oz were different from ours, which can explain these opposite results.

Once metabolic disorders are risk factors for renal disease, it would be expected that both HSF groups presented renal function impairment. However, analyzing the clinical signals of renal disease (proteinuria, most conveniently performed by estimation of the protein/creatinine ratio and glomerular filtration rate) [25], we can note an improvement in the treatment group with γ Oz characterized by lower proteinuria and higher GFR. Therefore, better understanding of the mechanisms by which γ Oz acted in this group is very important to enable novel therapeutic target development.

Oxidative stress is one condition associated with impaired renal function [8, 26]. Kidney disease progression is related with a significant increase of ROS, which influences cell function and damages proteins, lipids, and nucleic acids,

and can also inhibit enzymatic activities of the cellular respiratory chains. On the other hand, endogenous enzymatic and nonenzymatic antioxidant mechanisms protect against damaging effects of oxidative products [27]. The first line of enzymatic antioxidant defense is SOD, which accelerates the dismutation rate of oxygen to H_2O_2 , but the catalase reduces H_2O_2 to water. Glutathione peroxidase reduces H_2O_2 and other organic peroxides to water and oxygen and requires glutathione as a hydrogen donor which is a scavenger for H_2O_2 , hydroxyl radicals, and chlorinated oxidants [27]. Usually, patients suffering from renal insufficiency have diminished antioxidant defense when compared to healthy controls [28]. In the case of this study, the results showed an increase of antioxidant capacity, SOD, and catalase activities after treatment with gamma oryzanol, confirming the potential of the compound to improve the antioxidant system. But some authors relate difficulty in establishing a pattern of antioxidant status in kidney disease due to assessment by different measurement techniques [28]. In this case,

information associating various parameters can give a better representation of a patient's current antioxidant status.

The literature reports that the renoprotection can also be related to some mechanisms involving improvement of the endothelial dysfunction, reduction of oxidative stress, and upregulation of endothelial nitric oxide synthase expression, all effects dependent on adiponectin receptor activation [29]. In contrast, the dysfunction regulation of adiponectin and its receptors has been observed in the development of various diseases, including obesity, insulin resistance, type 1 and type 2 diabetes, and chronic kidney disease [29].

Adiponectin is secreted primarily by adipose tissue and plays a key role in kidney disease. In obesity, reduced adiponectin levels are also associated with insulin resistance and cardiovascular disease. However, in conditions of established chronic kidney disease, adiponectin levels are elevated and positively predict progression of disease [30, 31]. Corroborating these findings, the HSF group presented higher levels of adiponectin associated with reduced GFR which confirms kidney disease. In opposition, the HSF group that received the compound showed reduction in the levels, which can be explained by the amelioration of glomerular filtration rate by γ Oz in these animals, since adiponectin is excreted via kidney glomerular filtration [32].

Adipo-R1 and Adipo-R2 are expressed in many tissues [8], but in the specific case of the kidneys, no studies evaluated the effect of γ Oz in this pathway and its role on renal function. The compound showed capacity to upregulate the Adipo-R2/PPAR- α axis. PPAR- α is highly expressed in tissues that possess high mitochondrial and β -oxidation activity, as the kidney. Decreased renal PPAR- α expression might contribute to the pathogenesis of kidney injuries [33], whereas its high expression is associated with metabolic control in the organ [34]. Moreover, PPAR- α activation can attenuate or inhibit several mediators of vascular injury involved in renal damage, such as lipotoxicity, reactive species oxygen (ROS) generation, and inflammation [34, 35]. Corroborating this information, our animals of the HSF/HSF+ γ Oz group did not present inflammation in the kidney, showing lower levels of TNF- α , IL-6, and MCP-1 compared to the HSF group.

In summary, this study introduces very important findings since γ Oz was effective in ameliorating renal dysfunction by acting on the Adipo-R2/PPAR- α axis and also by improving the antioxidant response in the organ. γ Oz could be a therapeutic alternative for restoring/ameliorating metabolic dysfunctions, in special renal injuries that are developed in an obese individual. These results permit us to confirm that γ Oz is able to modulate PPAR- α expression, inflammation, and oxidative stress pathways improving obesity-induced renal disease.

Data Availability

The data used to support the findings of this study are available from the corresponding author upon request.

Conflicts of Interest

The authors declare no conflict of interest.

Acknowledgments

This work was supported by Fundação de Amparo à Pesquisa do Estado de São Paulo (FAPESP) (2015/10626-0 and 2018/15288-3).

References

- [1] A. Odermatt, "The Western-style diet: a major risk factor for impaired kidney function and chronic kidney disease," *American Journal of Physiology - Renal Physiology*, vol. 301, no. 5, pp. F919–F931, 2011.
- [2] Y. Wang, X. Chen, Y. Song, B. Caballero, and L. J. Cheskin, "Association between obesity and kidney disease: a systematic review and meta-analysis," *Kidney International*, vol. 73, no. 1, pp. 19–33, 2008.
- [3] C. Wickman and H. Kramer, "Obesity and kidney disease: potential mechanisms," *Seminars in Nephrology*, vol. 33, no. 1, pp. 14–22, 2013.
- [4] X. Zhang and L. O. Lerman, "The metabolic syndrome and chronic kidney disease," *Translational Research*, vol. 183, pp. 14–25, 2017.
- [5] M. F. Gregor and G. S. Hotamisligil, "Inflammatory mechanisms in obesity," *Annual Review of Immunology*, vol. 29, no. 1, pp. 415–445, 2011.
- [6] M. Tesauro, M. P. Canale, G. Rodia et al., "Metabolic syndrome, chronic kidney, and cardiovascular diseases: role of adipokines," *Cardiology Research and Practice*, vol. 2011, Article ID 653182, 11 pages, 2011.
- [7] T. Kadowaki, T. Yamauchi, and N. Kubota, "The physiological and pathophysiological role of adiponectin and adiponectin receptors in the peripheral tissues and CNS," *FEBS Letters*, vol. 582, no. 1, pp. 74–80, 2008.
- [8] K. Sharma, "Obesity, oxidative stress, and fibrosis in chronic kidney disease," *Kidney International Supplements*, vol. 4, no. 1, pp. 113–117, 2014.
- [9] L. Wang, B. Waltenberger, E. M. Pferschy-Wenzig et al., "Natural product agonists of peroxisome proliferator-activated receptor gamma (PPAR γ): a review," *Biochemical Pharmacology*, vol. 92, no. 1, pp. 73–89, 2014.
- [10] O. Wang, J. Liu, Q. Cheng et al., "Effects of ferulic acid and γ -oryzanol on metabolic syndrome in rats," *PLoS One*, vol. 10, no. 2, article e0118135, 2015.
- [11] C. Schwartz, P. A. M. J. Scholtens, A. Lalanne, H. Weenen, and S. Nicklaus, "Development of healthy eating habits early in life. Review of recent evidence and selected guidelines," *Appetite*, vol. 57, no. 3, pp. 796–807, 2011.
- [12] T.-Y. Ha, S. Han, S.-R. Kim, I.-H. Kim, H.-Y. Lee, and H.-K. Kim, "Bioactive components in rice bran oil improve lipid profiles in rats fed a high-cholesterol diet," *Nutrition Research*, vol. 25, no. 6, pp. 597–606, 2005.
- [13] T. A. Wilson, R. J. Nicolosi, B. Woolfrey, and D. Kritchevsky, "Rice bran oil and oryzanol reduce plasma lipid and lipoprotein cholesterol concentrations and aortic cholesterol ester accumulation to a greater extent than ferulic acid in hypercholesterolemic hamsters," *The Journal of Nutritional Biochemistry*, vol. 18, no. 2, pp. 105–112, 2007.
- [14] M. J. Son, C. W. Rico, S. H. Nam, and M. Y. Kang, "Effect of oryzanol and ferulic acid on the glucose metabolism of mice fed with a high-fat diet," *Journal of Food Science*, vol. 76, no. 1, pp. H7–H10, 2011.

- [15] F. Francisqueti, I. Minatel, A. Ferron et al., "Effect of gamma-oryzanol as therapeutic agent to prevent cardiorenal metabolic syndrome in animals submitted to high sugar-fat diet," *Nutrients*, vol. 9, no. 12, 2017.
- [16] V. O. Anna, J. Mátyus, E. Sárkány, A. Horváth, and B. Fodor, "New trends in the laboratory diagnostics of proteinuria and albuminuria," *Orvosi Hetilap*, vol. 151, no. 21, pp. 864–869, 2010.
- [17] P. P. dos Santos, B. P. M. Rafacho, A. de Freitas Gonçalves et al., "Vitamin D induces increased systolic arterial pressure via vascular reactivity and mechanical properties," *PLoS One*, vol. 9, no. 6, pp. e98895–e98899, 2014.
- [18] G. Beretta, G. Aldini, R. M. Facino, R. M. Russell, N. I. Krinsky, and K. J. Yeum, "Total antioxidant performance: a validated fluorescence assay for the measurement of plasma oxidizability," *Analytical Biochemistry*, vol. 354, no. 2, pp. 290–298, 2006.
- [19] S. L. Marklund, "Product of extracellular-superoxide dismutase catalysis," *FEBS Letters*, vol. 184, no. 2, pp. 237–239, 1985.
- [20] H. Aebi, "[13] catalase in vitro," *Methods in Enzymology*, vol. 105, no. C, pp. 121–126, 1984.
- [21] L. Flohé and W. A. Günzler, "[12] assays of glutathione peroxidase," *Methods in Enzymology*, vol. 105, pp. 114–120, 1984.
- [22] O. H. Lowry, N. J. Rosebrough, A. L. Farr, and R. J. Randall, "Protein measurement with the folin phenol reagent," *Readings*, vol. 193, no. 1, pp. 265–275, 1951.
- [23] M. M. Bradford, "A rapid and sensitive method for the quantitation of microgram quantities of protein utilizing the principle of protein-dye binding," *Analytical Biochemistry*, vol. 72, no. 1-2, pp. 248–254, 1976.
- [24] M. L. Justo, R. Rodriguez-Rodriguez, C. M. Claro, M. A. de Sotomayor, J. Parrado, and M. D. Herrera, "Water-soluble rice bran enzymatic extract attenuates dyslipidemia, hypertension and insulin resistance in obese Zucker rats," *European Journal of Nutrition*, vol. 52, no. 2, pp. 789–797, 2013.
- [25] R. Fielding and K. Farrington, "Clinical presentation of renal disease," in *Oxford Textbook of Medicine*, pp. 2010–2005, Oxford Medicine, Oxford, UK, 2018.
- [26] N. Chueakula, K. Jaikumkao, P. Arjinajarn et al., "Diacerein alleviates kidney injury through attenuating inflammation and oxidative stress in obese insulin-resistant rats," *Free Radical Biology and Medicine*, vol. 115, pp. 146–155, 2018.
- [27] A. Modaresi, M. Nafar, and Z. Sahraei, "Oxidative stress in chronic kidney disease," *Iranian Journal of Kidney Diseases*, vol. 9, no. 3, pp. 165–179, 2015.
- [28] P. S. Tucker, V. J. Dalbo, T. Han, and M. I. Kingsley, "Clinical and research markers of oxidative stress in chronic kidney disease," *Biomarkers*, vol. 18, no. 2, pp. 103–115, 2013.
- [29] D. Zha, X. Wu, and P. Gao, "Adiponectin and its receptors in diabetic kidney disease: molecular mechanisms and clinical potential," *Endocrinology*, vol. 158, no. 7, pp. 2022–2034, 2017.
- [30] M. Heidari, P. Nasri, and H. Nasri, "Adiponectin and chronic kidney disease; a review on recent findings," *Journal of Nephro pharmacology*, vol. 4, no. 2, pp. 63–68, 2015.
- [31] N. Sweiss and K. Sharma, "Adiponectin effects on the kidney," *Best Practice & Research Clinical Endocrinology & Metabolism*, vol. 28, no. 1, pp. 71–79, 2014.
- [32] A. Markaki, E. Psylinakis, and A. Spyridaki, "Adiponectin and end-stage renal disease," *Hormones*, vol. 15, no. 3, pp. 345–354, 2016.
- [33] Y. Tanaka, S. Kume, S. I. Araki et al., "Fenofibrate, a PPAR α agonist, has renoprotective effects in mice by enhancing renal lipolysis," *Kidney International*, vol. 79, no. 8, pp. 871–882, 2011.
- [34] E. N. Kim, J. H. Lim, M. Y. Kim et al., "PPAR α agonist, fenofibrate, ameliorates age-related renal injury," *Experimental Gerontology*, vol. 81, pp. 42–50, 2016.
- [35] R. Stienstra, C. Duval, M. Müller, and S. Kersten, "PPARs, obesity, and inflammation," *PPAR Research*, vol. 2007, Article ID 95974, 10 pages, 2007.

Research Article

The Protective Effect of the Total Flavonoids of *Abelmoschus esculentus* L. Flowers on Transient Cerebral Ischemia-Reperfusion Injury Is due to Activation of the Nrf2-ARE Pathway

Yang Luo,¹ Hong-Xin Cui ,² An Jia,³ Shan-Shan Jia,¹ and Ke Yuan ^{1,4}

¹Zhejiang Agriculture and Forestry University, Lin'an 311300, China

²College of Pharmacy, Henan University of Chinese Medicine, Zhengzhou 450046, China

³College of Medicine, Huanghe S & T University, Zhengzhou 450063, China

⁴Jiyang College, Zhejiang Agriculture and Forestry University, Zhuji 311800, China

Correspondence should be addressed to Ke Yuan; yuan_ke001@126.com

Received 1 April 2018; Revised 14 June 2018; Accepted 23 June 2018; Published 5 August 2018

Academic Editor: Germán Gil

Copyright © 2018 Yang Luo et al. This is an open access article distributed under the Creative Commons Attribution License, which permits unrestricted use, distribution, and reproduction in any medium, provided the original work is properly cited.

Abelmoschus esculentus L. has favorable nutritional/medicinal features. We found the content of total flavonoids in flower extract to be the highest (788.56 mg/g) of all the different parts of *A. esculentus*; according to high-performance liquid chromatography, the quercetin-3-O- $[\beta$ -D-glu-(1 \rightarrow 6)]- β -D-glucopyranoside content was 122.13 mg/g. Protective effects of an extract of the total flavonoids of *A. esculentus* flowers (AFF) on transient cerebral ischemia-reperfusion injury (TCI-RI) were investigated. Compared with the model group, mice treated with AFF (300 mg/kg) for 7 days showed significantly reduced neurologic deficits, infarct area, and histologic changes in brain tissue, accompanied by increased contents of superoxide dismutase, whereas contents of nitric oxide and malondialdehyde decreased. AFF upregulated the expression of Nrf2, HO-1, and NQO1. These data suggest that AFF protects against TCI-RI by scavenging free radicals and activating the Nrf2-ARE pathway.

1. Introduction

Ischemic cardiovascular disease (also known as “ischemic stroke”) is the third leading cause of death and disability worldwide [1]. The number of patients suffering from cerebral ischemic disease worldwide has increased by 2 million per year, and the morbidity associated with this disease can affect young people [2].

At present, several of the synthetic drugs used for the treatment of transient ischemic attack have side effects. “Natural” medicines have good curative effects and few side effects. In addition, cerebral ischemic disease is an emergency, difficult to predict, and its pathogenesis is complex [3]. During reperfusion after a transient ischemic attack, a combination of oxidative stress and release of excitatory neurotransmitters causes irreversible damage, inflammation, and even apoptosis of nerve cells [4, 5]. Therefore, searching

for natural products for protection and treatment of transient cerebral ischemia-reperfusion injury (TCI-RI) and exploring their mechanism of action are a rational approach.

Nuclear factor-E2-related factor 2 (Nrf2) is a key regulator of defense against endogenous antioxidants. Most genes encoding antioxidant enzymes have antioxidant response element (ARE) sequences in their promoter regions. Studies have demonstrated that the activation of the Nrf2-ARE pathway contributes to neuroprotection following ischemic injury [6–8].

Abelmoschus esculentus L. commonly known as “lady’s fingers,” “okra,” or “bhindi” is an important vegetable crop cultivated in many countries [9, 10]. The fruits are beneficial to the digestive and immune systems due to the high content of glycoproteins and microelements and are used as food additives because of their antigestric acid, antifatigue, antioxidant, and anti-inflammation properties [11]. The seeds of

A. esculentus are a good source of many high-quality proteins and unsaturated fatty acids and have anticancer, antidiabetes mellitus, and antihyperlipidemia properties [12–14]. The flowering period of *A. esculentus* is long, and the yield is high, but *A. esculentus* flowers wither rapidly, so they tend not to be studied. *A. esculentus* flowers are good sources of flavonoids and polysaccharides and are involved in modulation of the immune system [15]. However, studies on the protective effects of an extract of the total flavonoids of *A. esculentus* flowers (AFF) on TCI-RI and its mechanism of action are lacking.

Therefore, we explore the protective effect of AFF on TCI-RI and its potential mechanism.

2. Material and Methods

2.1. Materials. The reference samples of quercetin-3-O- $[\beta$ -D-glu-(1 \rightarrow 6)]- β -D-glucopyranoside (AFG-1), quercetin-3-O- $[\beta$ -D-xyl-(1 \rightarrow 2)]- β -D-glucopyranoside (AFG-2), and quercetin-4''-O-methy-3-O- β -D-glucopyranoside (AFG-3) at a purity of >98% were separated by our research team [16]. Rutin reference sample was purchased from China Pharmaceutical and Biological Products Testing Institute. *A. esculentus* flower, fruit, and seed samples were picked up in vegetable test base of Zhejiang Agricultural and Forestry University in 2016. Nitric oxide (NO), malondialdehyde (MDA), superoxide dismutase (SOD), and Coomassie Brilliant Blue kit were purchased from Nanjing Jiancheng Biological Technology Co. Ltd. Antibodies against Nrf2, heme oxygenase-1 (HO-1), NAD(P)H:quinone oxidoreductase-1 (NQO1), and β -actin were purchased from Wanlei Biological Technology Co. Ltd. Chloral hydrate was purchased from Zhejiang Academy of Medical Sciences. All the reagents were of analytical or HPLC grade.

2.2. Extraction and Purification of Total Flavonoids from *A. esculentus*. Fresh samples of the flowers, fruits, and seeds of *A. esculentus* were weighed (10 kg), dried at 40°C, crushed, and passed through a 60-mesh sieve. These powders were reextracted by ultrasonication thrice with 70% ethanol: water at a 1:30 ratio (*w*:*v*) for 30 min each at room temperature. The extracts were combined and concentrated into a paste using a rotary evaporator. Then, the concentrated solution was extracted with ethyl acetate to remove fat-soluble components. The remaining extract was added to a column with resin (Diaion HP-20, Mitsubishi, Japan). The resin was washed with distilled water to remove proteins, polysaccharides, and other water-soluble impurities. Then, the eluate was collected with 50% methanol and dried by a rotary evaporator at 50°C. Powdered extracts of the total flavonoids of the flowers (258.8 g), fruits (186.3 g), and seeds (160.6 g) of *A. esculentus* were obtained and stored at 4°C.

2.3. Determination of the Composition of Total Flavonoids in Extracts. Each sample extract (10.0 mg), AFG-1 (31.6 mg), AFG-2 (3.25 mg), AFG-3 (5.08 mg), and rutin (10.0 mg) were dissolved in methanol and made up to 10 mL to provide samples and standard solutions. We measured the contents of total flavonoids using an AlCl₃-colorimetric assay [17]. The

absorbance was measured at 510 nm, and the content was expressed as milligram rutin equivalent per gram dry weight (mg RE/g DW). All samples were assayed thrice.

AFG-1, AFG-2, and AFG-3 contents were analyzed on a high-performance liquid chromatography (HPLC) system (2695; Waters, Milford, MA, USA) with a photodiode array detector (2996; Waters) under specific HPLC conditions: SunFire C18 column (4.6 mm \times 250 mm, 5.4 μ m), column temperature = 28°C, flow rate = 0.8 mL/min, mobile phase = methanol (solvent A):0.1% phosphoric acid water (solvent B), and ratio of gradient elution, 47:53. These solutions were determined at an absorbance of 255.6 nm with sample feeding of 10 μ L. Identification of unknown peaks was based on comparison of the retention times with those of known standards.

2.4. Animal Experiments. All procedures were approved by the Committee on the Ethics of Animal Experiments at Zhejiang Agriculture and Forestry University (Zhejiang, China).

Male Kunming mice (18–22 g) were purchased from the Animal Experiment Center of Zhejiang Academy of Medical Sciences (Zhejiang, China; number SC 2008-3344). Before experimentation, all mice were maintained in a well-ventilated environment (23–24°C; humidity, 56–59%) with a 12 h light-dark cycle and had free access to food and water for 1 week.

Mice (*n* = 75) were divided randomly into five groups, normal group (sham operation), model group, as well as high (300 mg/kg), medium (150 mg/kg), and low (75 mg/kg) AFF dose groups. 300 mg/kg has proven to be safe [18]. Mice in normal and model groups were given an equal volume of water, and in the other groups, the corresponding amounts of AFF were given once daily for 7 days. One hour after the final administration, mice in model and AFF groups were anesthetized (3.5% chloral hydrate, i.p.) and placed on a mouse fixator. Creation of the TCI-RI model is shown in Figure 1. The neck was disinfected with 75% alcohol. A mid-line incision was made, and skin was separated bluntly to allow exposure of bilateral common carotid arteries. Using an arterial clip, blood flow to bilateral common carotid arteries was blocked for 30 min. Subsequently, the arterial clip was loosened to recover this blood supply and the incision was sutured. In the normal group, bilateral common carotid arteries were not blocked and only suturing of the incision was done. After 24 h of reperfusion, the neurologic damage was evaluated. Then, 10 survived mice in each group were sacrificed, and their brain tissues were removed rapidly and stored at 20°C.

2.5. Survival and Neurologic Function Score. After TCI-RI for 24 h, the survival rate in each group was determined as the ratio of the number of survived mice to the total number of mice. An evaluator blinded to the treatment protocol undertook neurologic scoring as described by Longa et al. [19]. The scoring criteria are the following: 0 = no neurological deficits, 1 = failure to extend contralateral forepaw fully, 2 = circling to paretic side, 3 = falling to contralateral side, and 4 = did not walk spontaneously and has a depressed level of consciousness.

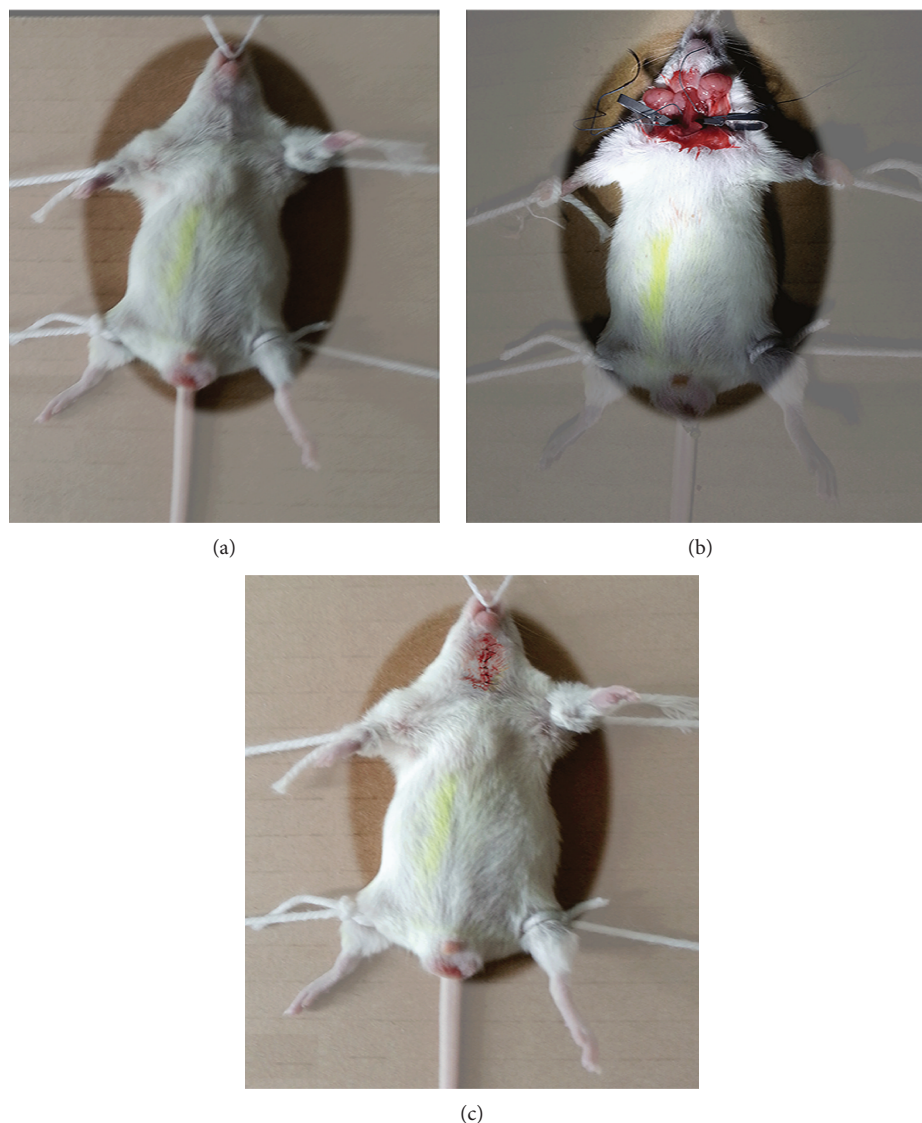


FIGURE 1: The process of TCI-RI operation. (a) The mouse was narcotized and fixed. (b) The middle neck of the mouse was cut, and the bilateral carotid artery was tied with thread and clamped with the arterial clip for 30 min. (c) After removal of the arterial clip and the line, the mouse wound was sutured and the mouse was reperused for 24 h.

2.6. Evaluation of the Infarct Area. The brain tissues in each group ($n_1 = 3$) were obtained in a random manner. Then, the cerebrums were cut into five coronal sections of thickness 2 mm. They were incubated immediately in 2% 2,3,5-triphenyltetrazolium chloride (TTC) solution at 37°C for 30 min in the dark and fixed in 10% formalin. After that, the stained slices were photographed using a camera (EOS30, Canon, Japan). The infarct area in each section was calculated using an image analyzer (Image-Pro Plus 6.0). The percentage of the infarct area was calculated using the following formula:

$$\text{Infarct area (\%)} = \frac{\text{total infarct area}}{\text{total section area}} \times 100. \quad (1)$$

2.7. Histopathology. The whole brain tissues of each group ($n_2 = 3$) after reperfusion for 24 h were fixed with 4%

paraformaldehyde for 24 h, stained with hematoxylin and eosin (H&E), and then observed with an optical microscope (BX20, Olympus, Tokyo, Japan).

2.8. TUNEL Assay. The whole brain tissues of each group ($n_2 = 3$) after reperfusion for 24 h were fixed with 4% paraformaldehyde for 24 h, regularly embedded in paraffin, sectioned at a thickness of 4 μm , deparaffinized, stained with terminal deoxynucleotidyl transferase-mediated (dUTP) nick end labeling (TUNEL) reagents and DAPI solution, washed, and then photographed using a fluorescence microscope (Nikon Eclipse C1, Nikon, Japan). The positive cells (green spots) were identified and counted by an investigator blinded to the grouping. Three mice and 10 regions of the fluorescent images were used to obtain the apoptotic cell data.

TABLE 1: Results for the determination of three kinds of flavonoid glycosides and total flavonoids in different parts extract of *A. esculentus*.

Part	AFG-1 (content/mg/g DW)	AFG-2 (content/mg/g DW)	AFG-3 (content/mg/g DW)	Total flavones (content/mg/g DW)	Powder yield
Flower	122.13	9.54	16.86	788.56	2.59%
Seed	53.16	3.01	28.06	627.04	1.86%
Fruit	35.96	2.66	25.59	520.83	1.61%

2.9. Biochemical Analyses of Brain Tissue. The brain tissues in each group ($n_3 = 4$) were homogenized with nine-fold physiological saline. The 10% homogenate was centrifuged at 3000 rpm for 10 min at room temperature. The 10% supernatants (100 μ L) were made into 2% concentration with cold physiological saline (400 μ L) to determine the protein content with Coomassie Brilliant Blue kit (standard solution: 0.563 g/L embryonic bovine serum BSA). The 10% supernatants were used to determine the contents of nitric oxide (NO), superoxide dismutase (SOD), and malondialdehyde (MDA) with the commercially available kits, and their results were expressed as equivalent per gram protein concentration.

2.10. Western Blotting. To analyze protein expression, brain tissue homogenates ($n_3 = 4$) were centrifuged at 14,000 rpm for 30 min at 4°C to obtain total protein. Protein content was quantified using a bicinchoninic acid protein assay kit. Equal amounts of protein (50 μ g per lane) were resolved on 12% polyacrylamide gels, transferred to polyvinylidene fluoride (PVDF) membranes (Millipore, Marlborough, MA, USA), and probed with primary antibodies against Nrf2, HO-1, NQO1, and β -actin. PVDF membranes were washed thrice for 10 min each and incubated for 2 h at 4°C with horseradish peroxidase-conjugated secondary antibody (anti-rat). Proteins were visualized using an enhanced chemiluminescence detection system (Amersham Pharmacia, Piscataway, NJ, USA).

2.11. Statistical Analysis. Data were analyzed by one-way ANOVA with Duncan's test and intergroup comparison using SPSS statistical software (SPSS 19.0 Inc., Chicago, IL, USA) and expressed as mean \pm standard deviation (SD). *P* values below 0.05 were considered statistically significant.

3. Results and Discussion

3.1. Contents of Total Flavonoids and Flavonoid Glycosides in Different Parts of *A. esculentus*. The fruits, seeds, roots, stems, leaves, and flowers of *A. esculentus* are used widely as traditional medicines in China because of their anticancer and anti-inflammatory effects [20]. It has been reported that the flowers, fruits, and seeds of *A. esculentus* are good sources of flavonoids and that the total content of flavonoids is different in different parts of *A. esculentus*.

The total content of flavonoids in flower extract was highest in different parts of *A. esculentus*, and the highest amount was 788.56 mg/g (Table 1). The three flavonoid glycosides, AFG-1, AFG-2 and AFG-3, the structures of which are shown in Figure 2, were the main components in different parts of *A. esculentus* (Figure 2). In AFF, the AFG-

1 content was 122.13 mg/g. Therefore, the potential protective effect of AFF upon TCI-RI was investigated.

3.2. Effect of AFF on the Survival Rate and Neurologic Damage. Transient cerebral ischemia is associated with high mortality and morbidity. Transient cerebral ischemia changes the cerebral ultrastructure and induces hypoxia and ischemia in the middle cerebral artery, which damages the nervous system [6, 21]. Only 52.6% of mice in the model group survived (Table 2). After AFF treatment, the survival rate was improved significantly depending on the AFF dose ($P < 0.05$). According to the observation of behavior and neurologic scores, mice in the normal group (which did not suffer damage to the nervous system) could move normally. The score of the model group was significantly different from that of the normal group ($P < 0.01$); the contralateral forepaw could not be extended forward or circled around, and athletic ability was weakened (neurologic score = 2.8 ± 0.79). The neurologic scores of the AFF (300 and 150 mg/kg) groups were significantly higher than those of the model group ($P < 0.01$), and mice did not fall to one side or suffer dyskinesia.

These results suggested that AFF could protect the nervous system from the effects of cerebral ischemic attack. Studies have shown that flavonoids have antioxidant functions [22]. Yuan et al. found that the total flavonoid extracts of flowers, fruits, leaves, and seeds all have free radical scavenging activity and antioxidant capacity and the free radicals scavenging capacity of AFF is relatively strong *in vitro* [23]. Neural cells in the brain have been more vulnerable to oxidative stress because they have high oxygen consumption and contain high levels of unsaturated fatty acids, essential prooxidants for lipid peroxidation, and low levels of antioxidant defense capacities [24]. Thereby, AFF scavenged free radicals to protect nerve cells from oxidative damage.

3.3. Effect of AFF on the Cerebral Infarction Area. Transient cerebral ischemia does not necessarily result in disability or death if timely return of oxygen and blood supply is initiated. Most cases of ischemic cardiovascular disease are caused by more severe reperfusion injury due to prolonged ischemia or hypoxia in the brain and heart [25, 26]. In patients with cerebral infarction, the infarct area of the middle cerebral arterial trunk is 82.12% [27]. Therefore, we used a method based on occlusion of the internal carotid artery to cause TCI-RI in mice, which results in symptoms similar to those of cerebral ischemia in humans.

Brain tissues were stained by TTC (Figures 3(a) and 3(b)), with red regions indicated normal tissue and white regions representing infarction. Compared with the normal

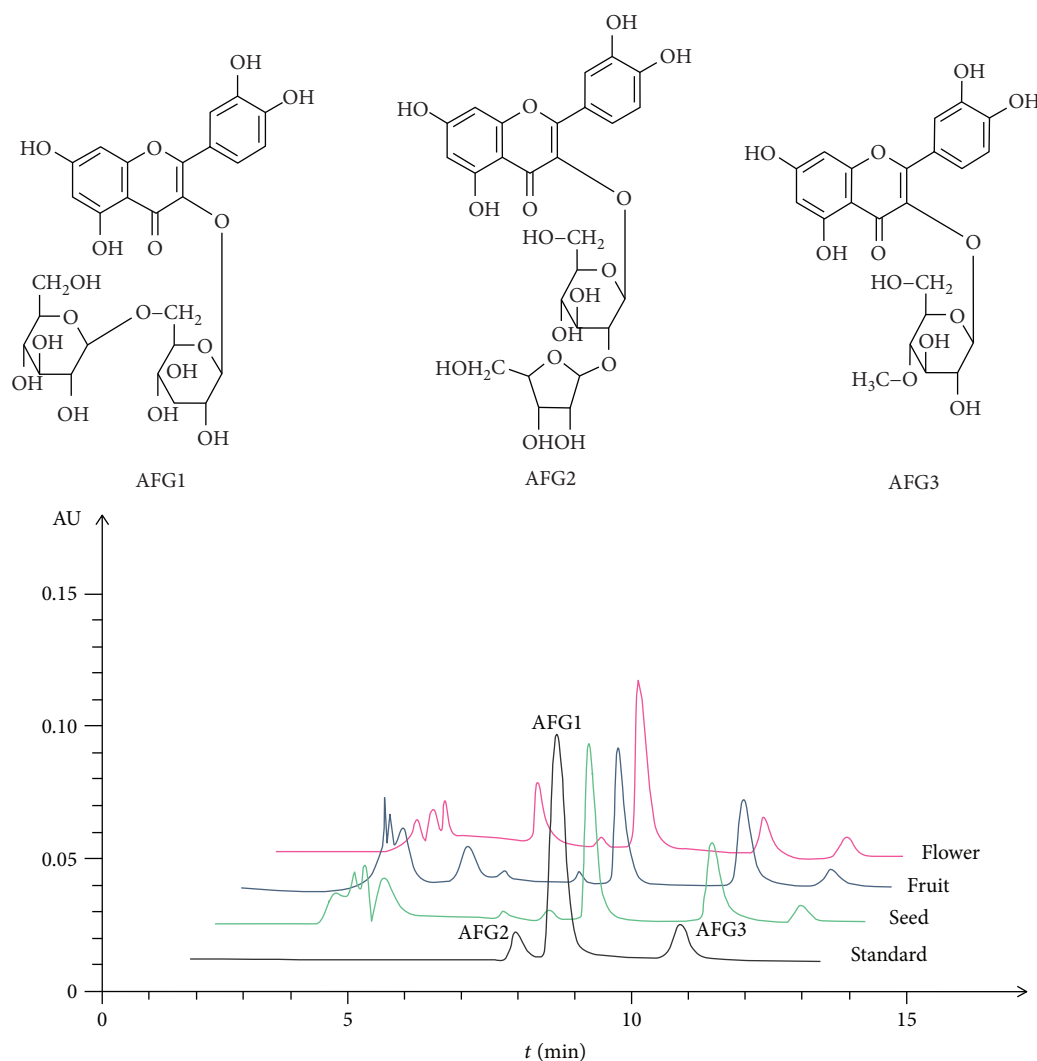


FIGURE 2: The structures and HPLC chromatogram of AFG-1, AFG-2, and AFG-3 in the flower, fruit, and seed of *A. esculentus*.

TABLE 2: Effect of AFF on the survival rate and neurologic score in mice subjected to TCI-RI.

Group	Dose (mg/kg/D)	<i>n</i>	<i>n</i> (survived mice)	Survival rate (%)	Neurologic score
Normal	0	10	10	100	0
Model	0	19	10	52.6	2.8 ± 0.79 ^{##}
AFF (300 mg/kg)	300	12	10	83.3	1.2 ± 0.63 ^{**}
AFF (150 mg/kg)	150	16	10	62.5	1.5 ± 0.53 ^{**}
AFF (75 mg/kg)	75	18	10	55.5	1.9 ± 0.74 [*]

Values are mean ± SD. **P* < 0.05 and ***P* < 0.01 versus the model group; ^{##}*P* < 0.01 versus the normal group.

group, mice in the model group had obvious cerebral infarction (39.13% ± 1.49). Pretreatment with AFF (300 and 150 mg/kg) reduced the cerebral infarct area markedly (*P* < 0.05). The results suggested a neuroprotective effect of AFF on TCI-RI mice. After subsection to cerebral ischemia and reperfusion, aerobic respiration gets compromised and the imbalance of Ca²⁺, Na⁺, and ADP ion homeostasis in the nerve cells stimulates the excessive production of mitochondrial oxygen radical [28]. Abnormal production of free radicals increases stress on cellular structures and

damages intracellular macromolecules, such as lipids, proteins, and nucleic acids, leading to inactivation of enzymes, destruction of cell membranes, and dysfunction and eventually leading to death of brain tissue cells and excitotoxicity to aggravate the cerebral infarction area [29]. Elevated levels of lipid peroxidation and cytotoxins caused by oxidative stress after ischemia disrupt the tight junctions of endothelial cells, accompanying with increasing permeability of the blood-brain barrier (BBB) and worsening of the infarct severity [30]. Members of the flavonoid family have been

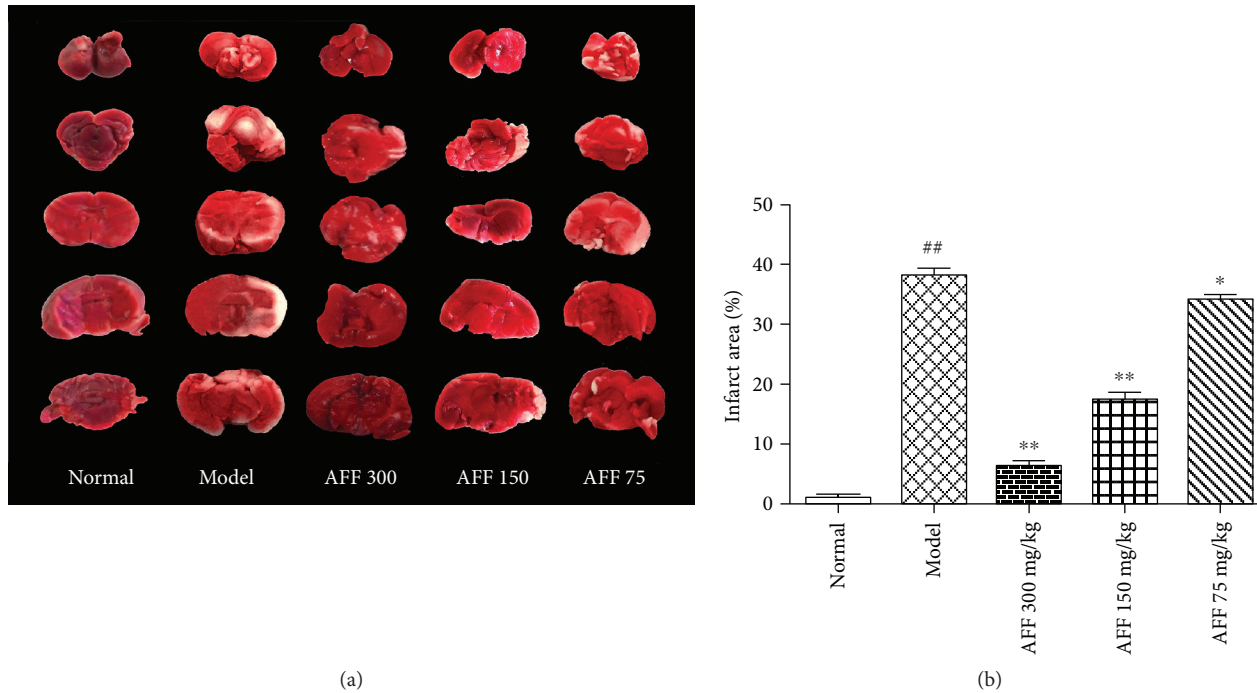


FIGURE 3: Effect of AFF on infarct areas in mice ($n_1 = 3$) after TCI-RI. (a) Representative brain sections of TTC staining. The infarct areas were white. (b) Quantitative results of the infarction area. Values are mean \pm SD. * $P < 0.05$ and ** $P < 0.01$ versus the model group; ## $P < 0.01$ versus the normal group.

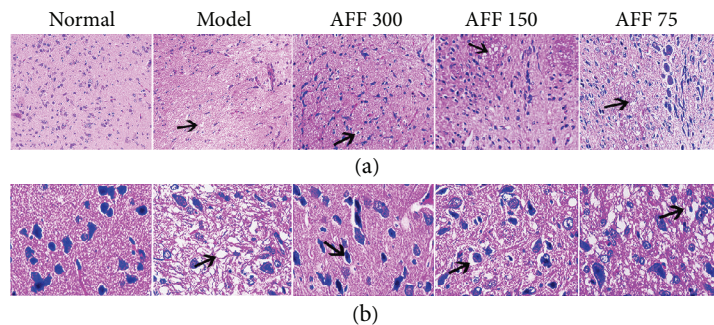


FIGURE 4: Effects of AFF on cortical area histopathologic changes in the brain of mice ($n_2 = 3$) stained with H&E ($\times 200$; $\times 400$). (a) HE-stained cerebral cortex of TCI-RI brain ($\times 200$). (b) HE-stained cerebral cortex of TCI-RI ($\times 400$). The arrows showed a gradual improvement on cellular edema and atrophic nucleolus.

reported to transverse BBB [31]. In AFF treatment groups, due to disruption of BBB after the TCI-RI event, AFF accumulated in TCI-RI regions improved neurologic function score and reduced the brain tissue infarct area through antioxidant activity, thereby promoting functional recovery of nerve cells. He et al. had demonstrated that Danhong injection promotes the recovery of neurological function with cerebral infarction by its antioxidant activities [32]. The previous study reported that flavonoids can also improve neurological function and protect brain tissue from cerebral ischemia-reperfusion injury by inhibiting oxidative stress to reduce the damage of the brain microvascular endothelial cell barrier and BBB function [6, 33].

3.4. Histopathology. Transient cerebral ischemia and hypoxia resulted in damage or necrosis of brain tissue accompanied

by complex histopathologic changes [34]. Different lesions were observed according to the duration of ischemic insult. Upon ischemia for 30 min, the main damage was to neuronal cells [35]. After the whole brain tissue had been stained with H&E, histopathologic changes were clearly visible (Figures 4(a) and 4(b)). Compared with the normal group, cerebral cortical cells in the model group showed edematous cells, nucleolus atrophy, or cell loss, which were associated with histopathologic changes. Pretreatment with AFF for 7 days prevented neuronal cells from the damage induced by TCI-RI, and the high-dose group had the best effect.

3.5. Effect of the AFF on Cellular Apoptosis Detected by TUNEL Assay. Abnormal formation of reactive oxygen species after reperfusion is one of the major factors inducing apoptosis in neuronal cells [36]. TUNEL

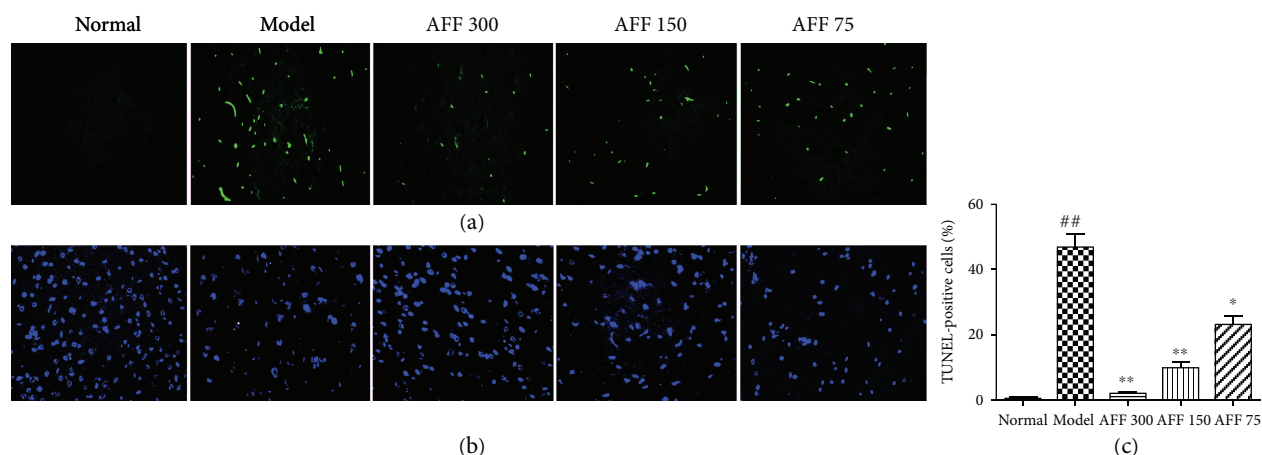


FIGURE 5: Effects of AFF on cortical area cellular apoptosis in the brain of mice ($n_2 = 3$) with TUNEL assay ($\times 400$). (a) TUNEL-stained cerebral cortex of TCI-RI brain, the green fluorescence represented the apoptotic cells. (b) DAPI-stained cerebral cortex of TCI-RI. (c) Quantitative data on TUNEL-positive cells in cerebral cortex were obtained. Values are mean \pm SD. ^{##} $P < 0.01$ versus the normal group; ^{*} $P < 0.05$ and ^{**} $P < 0.01$ versus the model group.

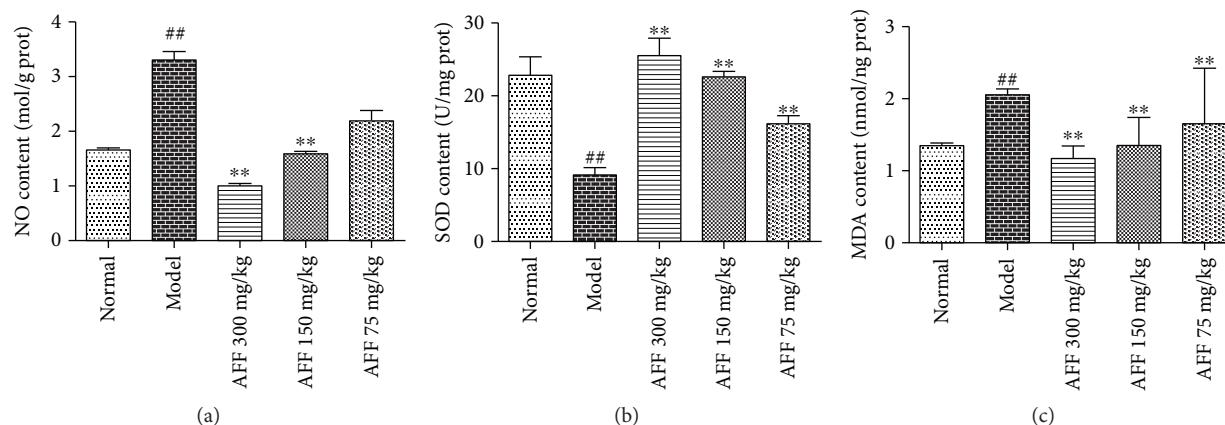


FIGURE 6: Effects of AFF on NO (a), SOD (b), and MDA (c) content in the brain tissue of mice ($n_3 = 4$) after TCI-RI. Values are mean \pm SD. ^{##} $P < 0.01$ versus the normal group; ^{**} $P < 0.01$ versus the model group.

staining was used to detect apoptotic cells on the basis of DNA fragmentation. The TUNEL-positive cells emitted green fluorescence after fluorescein labeling (Figure 5(a)). The normal group had no TUNEL-positive cells, and apoptotic cells in the model group increased significantly compared with the normal group. After AFF treatment (150 and 300 mg/kg BW), TUNEL-positive cells had significantly reduced when compared with the model group (Figure 5(c), $P < 0.01$). AFF had the potential action to protect the brain from TCI-RI damage by decreasing apoptotic cells. Zhang et al. found that pretreatment of flavonoid-rich extract from *Rosa laevigata* Michx fruit markedly inhibited neuron apoptosis by its antioxidant properties after TCI-RI [37].

3.6. Effect of AFF on the Contents of Protein, NO, SOD, and MDA in Brain Tissue. Several studies have shown that TCI-RI can cause severe reperfusion injury and produce a series of cascade reactions: energy depletion, oxidative stress with

release of large amounts of free radicals, activation of apoptosis-related genes, calcium overload, release of excitatory neurotransmitters, and inflammation [38]. Oxidative stress is a major cause of secondary injury after TCI-RI. If brain tissue is subjected to ischemic stimulation, oxidative stress causes an imbalance of oxidants and antioxidants in tissue cells and produces excess reactive oxygen species (ROS) [39]. The latter damage the structure and function and inactivate enzymes within mitochondria, resulting in reduced production of adenosine monophosphate (ATP) within them [40]. Intracellular deficiency of ATP reduces the pH, inhibits the activity of $\text{Na}^+/\text{Ca}^{2+}$ exchange proteins, increases intracellular levels of Na^+ and Ca^{2+} , and reduces levels of K^+ . These ion disorders damage brain cell defense systems, resulting in the apoptosis or death of nerve cells [6, 28]. Ca^{2+} overload increases the expression of nitric oxide synthase (NOS) and Ca^{2+} -dependent proteases. Then, NOS degrades glutamate to produce the nontraditional neurotransmitter NO. Subsequently, xanthine dehydrogenase is

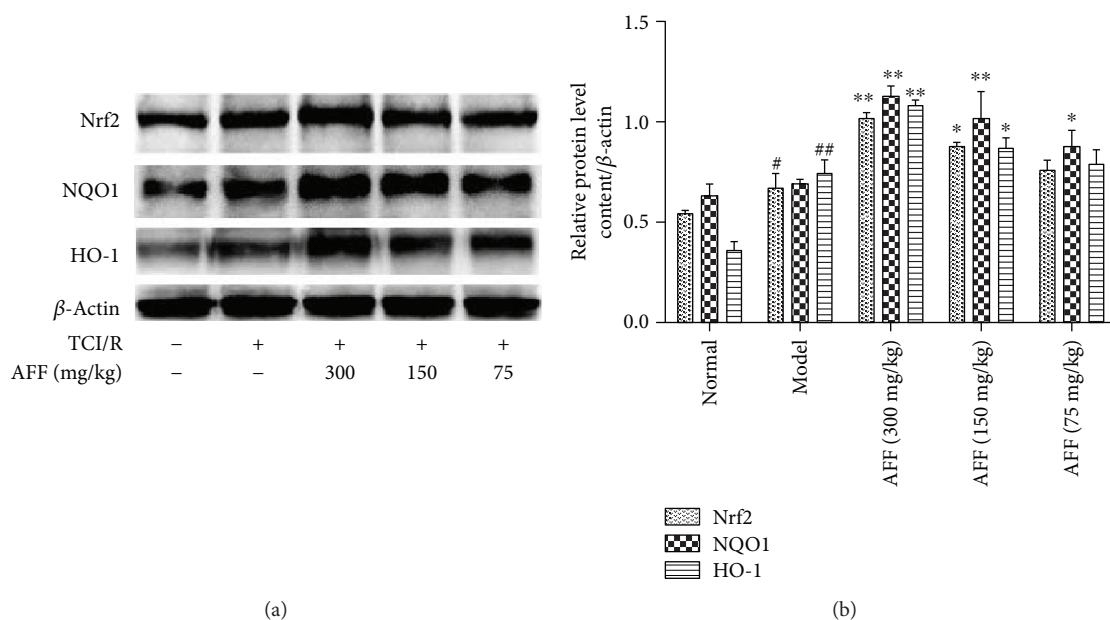


FIGURE 7: Effects of AFF on the expression level of Nrf2, NQO1, and HO-1 ($n_3 = 4$). (a) The expression levels of Nrf2, NQO1, and HO-1 were analyzed by Western blotting. (b) Quantitative results of the expression levels. Values are mean \pm SD. * $P < 0.05$ and ** $P < 0.01$ versus the model group; # $P < 0.05$ and ## $P < 0.01$ versus the normal group.

transformed to xanthine oxidase, which increases the levels of NO and oxygen free radicals [39, 41]. NO has complex roles in many diseases, including inhibition of mitochondrial function, and has toxic responses to induce cell death [42, 43]. The determination of the protein concentration in the tissue homogenate supernatant is not of a direct clinical value and used for the calculation of the relative content of other biochemical parameters [6, 37, 44]. The NO content increased markedly in mice of the model group compared with those in the normal group, and it was reduced significantly in AFF groups (300 and 150 mg/kg) compared with the model group; these differences were significant (Figure 6(a), $P < 0.05$).

The enzyme SOD scavenges superoxide anion radicals *in vivo* and can scavenge ROS, including superoxide anion radicals [45]. Decreased activity of SOD can cause massive accumulation of free radicals in brain tissue, which induces the lipid peroxidation of phospholipids and unsaturated fatty acids in cell membranes [6]. Then, levels of the final product of lipid peroxidation, MDA, increase accordingly, resulting in destruction of the structure and function of cell membranes and damage to neurons [46, 47]. Due to the scavenging of oxygen free radicals, SOD content is reduced and MDA content is increased after TCI-RI. Therefore, measuring the content of SOD and MDA can, indirectly, reflect the ability of the body to scavenge free radicals and the degree of damage caused by these chemicals [48]. Compared with the normal group, the SOD level in the brain tissue of mice in the model group was reduced significantly by 59.7% ($P < 0.01$) whereas the MDA content was increased by 51.9%. Pretreatment with AFF protected mice from TCI-RI, and levels of SOD and MDA

were increased significantly and decreased, respectively (Figures 6(b) and 6(c), $P < 0.01$).

3.7. Effect of AFF on the Expression of Nrf2, NQO1, and HO-1. TCI-RI is a very complex pathologic process, so the mechanism is also complex. Several studies have shown that oxidative stress is one of the major causes of TCI-RI. Mechanisms of antioxidant stress include direct scavenging of free radicals as well as indirect antioxidant activity through modulation of the pathways involved in the expression of cytoprotective enzymes and molecules [7]. Chen et al. [49] reported that the extent of scavenging of the DPPH radical of flavonoids in *A. esculentus* flowers was greater than that of vitamin C at the same concentration. The inducible Nrf2-ARE pathway helps to regulate the expression of phase II-detoxifying and antioxidant enzymes. In a normal physiologic environment, Nrf2 is in the cytoplasm bound to its “natural restrainer,” Kelch-like ECH-associated protein 1 (Keap1), which induces the ubiquitination and constitutive degradation of Nrf2. If subjected to oxidative stress, Nrf2 dissociates from Keap1 and moves to the nucleus. Here, it binds to small musculoaponeurotic fibrosarcoma (Maf) protein to form a heterodimer and recognizes the appropriate ARE sequence to promote transcription of the antioxidant genes *SOD*, *HO-1*, and *NQO1* [8, 50–52].

Previous studies had demonstrated that total flavonoids have a protective effect on PC12 cells and through PC12 cells; it can be visually seen that Nrf2 is transferred from the cytoplasm to the nucleus when exposed to oxidative stress [53]. Huang et al. [54] found that the addition of HO-1 inhibitors (ZnPP) significantly reduces the protective effect on PC12 cells. Wu et al. [7] showed that

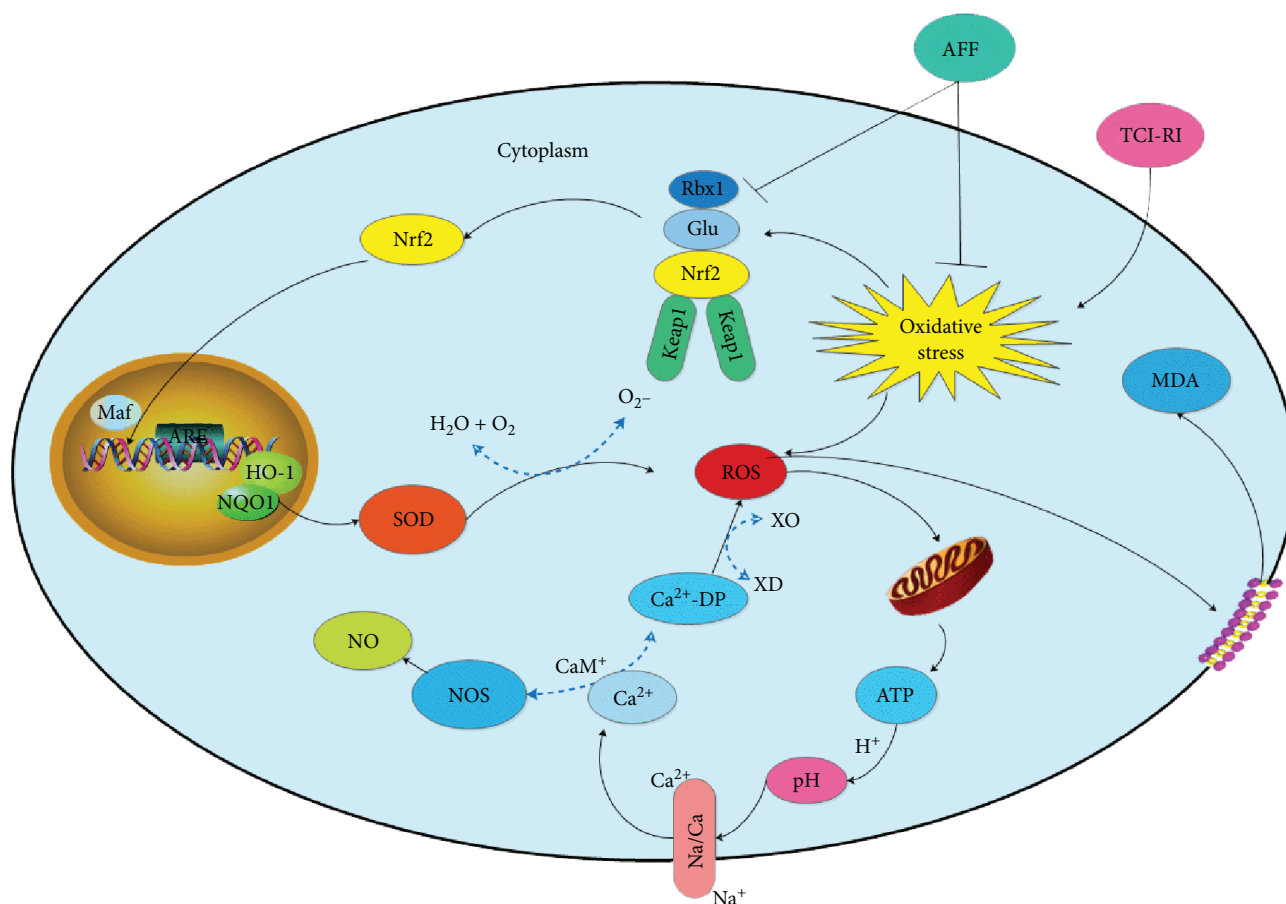


FIGURE 8: Mechanism of TCI-RI and protective effect of AFF on TCI-RI in nerve cells. AFF directly scavenged free radicals and indirectly activated the Nrf2-ARE pathway to enhance the expressions of antioxidant NQO1 and HO-1 and increase SOD content, against oxidative stress, which significantly reduced the content of NO, MDA, and protected TCI-RI.

mice lacking *Nrf2* are more susceptible to oxidative stress. Therefore, we investigated if AFF has a neuroprotective role by inducing the Nrf2-ARE pathway in TCI-RI *in vivo*. Compared with the model group, the expression of Nrf2, NQO1, and HO-1 in AFF-treated mice was upregulated significantly (Figures 7(a) and 7(b), $P < 0.01$). These results corresponded with the study [8]. Hence, the underlying molecular mechanism of the therapeutic effects of AFF on cerebral ischemic stroke was its antioxidant activity and modulation of the Nrf2-ARE pathway in response to oxidative stress (Figure 8). Nrf2 is a promising therapeutic target for defense against oxidative stress in stroke, and AFF will be an excellent medicine to protect against TCI-RI by activating the Nrf2-ARE pathway.

4. Conclusions

Our study demonstrated that AFF had protective effects against TCI-RI possibly by direct (scavenging free radicals) and indirect (activating the neuronal Nrf2-ARE pathway to modulate damage by oxidative stress) actions. This research provides a theoretical basis for the development of AFF as a

functional food and its therapeutic effects on ischemic cardiovascular diseases.

Data Availability

The data used to support the findings of this study are included within the article.

Additional Points

Chemical Compounds. Rutin (PubChem CID: 5280805), 2,3,5-triphenyltetrazolium chloride (PubChem CID: 9283), and chloral hydrate (PubChem CID: 2707) are the chemical compounds used in the study.

Conflicts of Interest

The authors have no conflict of interest in this research.

Acknowledgments

This project is sponsored by Zhejiang Provincial Natural Science Foundation of China (LY13H280011).

Supplementary Materials

The corresponding experimental data associated with this article can be seen from the supplementary materials' files. (*Supplementary Materials*)

References

- [1] J. F. Meschia, C. Bushnell, B. Boden-Albala et al., "Guidelines for the primary prevention of stroke: a statement for health-care professionals from the American Heart Association/American Stroke Association," *Stroke*, vol. 45, no. 12, pp. 3754–3832, 2014.
- [2] Y. Yang and H. Sun, "Research progress of acupuncture for cerebral ischemia reperfusion injury in recent 10 years," *Zhongguo zhen jiu= Chinese acupuncture & moxibustion*, vol. 35, no. 7, pp. 749–752, 2015.
- [3] X. L. Hou, Q. Tong, W. Q. Wang et al., "Suppression of inflammatory responses by dihydromyricetin, a flavonoid from *Ampelopsis grossedentata*, via inhibiting the activation of NF- κ B and MAPK signaling pathways," *Journal of Natural Products*, vol. 78, no. 7, pp. 1689–1696, 2015.
- [4] Y. Gursoy-Ozdemir, A. Can, and T. Dalkara, "Reperfusion-induced oxidative/nitrative injury to neurovascular unit after focal cerebral ischemia," *Stroke*, vol. 35, no. 6, pp. 1449–1453, 2004.
- [5] H. Pradeep, J. B. Diya, S. Shashikumar, and G. K. Rajanikant, "Oxidative stress - assassin behind the ischemic stroke," *Folia Neuropathologica*, vol. 50, no. 3, pp. 219–230, 2012.
- [6] Y. Liu, L. Zhang, and J. Liang, "Activation of the Nrf2 defense pathway contributes to neuroprotective effects of phloretin on oxidative stress injury after cerebral ischemia/reperfusion in rats," *Journal of the Neurological Sciences*, vol. 351, no. 1–2, pp. 88–92, 2015.
- [7] G. Wu, L. Zhu, X. Yuan et al., "Britanin ameliorates cerebral ischemia-reperfusion injury by inducing the Nrf2 protective pathway," *Antioxidants & Redox Signaling*, vol. 27, no. 11, pp. 754–768, 2017.
- [8] R. Zhang, M. Xu, Y. Wang, F. Xie, G. Zhang, and X. Qin, "Nrf2—a promising therapeutic target for defending against oxidative stress in stroke," *Molecular Neurobiology*, vol. 54, no. 8, pp. 6006–6017, 2016.
- [9] P. Arapitsas, "Identification and quantification of polyphenolic compounds from okra seeds and skins," *Food Chemistry*, vol. 110, no. 4, pp. 1041–1045, 2008.
- [10] H. Al-Wandawi, "Chemical composition of seeds of two okra cultivars," *Journal of Agricultural and Food Chemistry*, vol. 31, no. 6, pp. 1355–1358, 1983.
- [11] S. C. Sheu and M. H. Lai, "Composition analysis and immunomodulatory effect of okra (*Abelmoschus esculentus* L.) extract," *Food Chemistry*, vol. 134, no. 4, pp. 1906–1911, 2012.
- [12] Y. Okada, M. Okada, and Y. Sagesaka, "Screening of dried plant seed extracts for adiponectin production activity and tumor necrosis factor- α inhibitory activity on 3T3-L1 adipocytes," *Plant Foods for Human Nutrition*, vol. 65, no. 3, pp. 225–232, 2010.
- [13] K. Panneerselvam, S. Ramachandran, V. Sabitha, and K. R. Naveen, "Antidiabetic and antihyperlipidemic potential of *Abelmoschus esculentus* (L.) Moench. in streptozotocin-induced diabetic rats," *Journal of Pharmacy and Bioallied Sciences*, vol. 3, no. 3, pp. 397–402, 2011.
- [14] O. J. Oyelade, B. I. O. Ade-Omowaye, and V. F. Adeomi, "Influence of variety on protein, fat contents and some physical characteristics of okra seeds," *Journal of Food Engineering*, vol. 57, no. 2, pp. 111–114, 2003.
- [15] W. Zheng, T. Zhao, W. Feng et al., "Purification, characterization and immunomodulating activity of a polysaccharide from flowers of *Abelmoschus esculentus*," *Carbohydrate Polymers*, vol. 106, pp. 335–342, 2014.
- [16] Y. Lin, M. F. Lu, H. B. Liao, Y. X. Li, W. Han, and K. Yuan, "Content determination of the flavonoids in the different parts and different species of *Abelmoschus esculentus* L. by reversed phase-high performance liquid chromatograph and colorimetric method," *Pharmacognosy Magazine*, vol. 10, no. 39, pp. 278–284, 2014.
- [17] A. Akrouf, L. A. Gonzalez, H. El Jani, and P. C. Madrid, "Antioxidant and antitumor activities of *Artemisia campestris* and *Thymelaea hirsuta* from southern Tunisia," *Food and Chemical Toxicology*, vol. 49, no. 2, pp. 342–347, 2011.
- [18] G. Ai, Q. Liu, W. Hua, Z. Huang, and D. Wang, "Hepatoprotective evaluation of the total flavonoids extracted from flowers of *Abelmoschus manihot* (L.) Medic: *in vitro* and *in vivo* studies," *Journal of Ethnopharmacology*, vol. 146, no. 3, pp. 794–802, 2013.
- [19] E. Z. Longa, P. R. Weinstein, S. Carlson, and R. Cummins, "Reversible middle cerebral artery occlusion without craniectomy in rats," *Stroke*, vol. 20, no. 1, pp. 84–91, 1989.
- [20] L. Gao, D. Liu, and L. Xu, "Research progress and prospects of okra," *Chinese Journal of Tropical Agriculture*, vol. 34, pp. 22–29, 2014.
- [21] A. Ahmad, M. M. Khan, S. S. Raza et al., "*Ocimum sanctum* attenuates oxidative damage and neurological deficits following focal cerebral ischemia/reperfusion injury in rats," *Neurological Sciences*, vol. 33, no. 6, pp. 1239–1247, 2012.
- [22] J. Cao, X. Xia, X. Chen, J. Xiao, and Q. Wang, "Characterization of flavonoids from *Dryopteris erythrosora* and evaluation of their antioxidant, anticancer and acetylcholinesterase inhibition activities," *Food and Chemical Toxicology*, vol. 51, pp. 242–250, 2013.
- [23] K. Yuan, H. Liao, W. Dong, X. Shi, and H. Liu, "Analysis and comparison of the active components and antioxidant activities of extracts from *Abelmoschus esculentus* L.," *Pharmacognosy Magazine*, vol. 8, no. 30, pp. 156–161, 2012.
- [24] B. Halliwell, "Reactive oxygen species and the central nervous system," *Journal of Neurochemistry*, vol. 59, no. 5, pp. 1609–1623, 1992.
- [25] H. Y. Meng, "New clinical development of transient ischemic attacks," *Chinese Journal of Coal Industry Medicine*, vol. 3, pp. 487–488, 2010.
- [26] M. Miao, X. Yan, L. Guo, and S. Shao, "Effects of the *Rabdosia rubescens* total flavonoids on focal cerebral ischemia reperfusion model in rats," *Saudi Pharmaceutical Journal*, vol. 25, no. 4, pp. 607–614, 2017.
- [27] R. Tsuchidate, Q.-P. He, M.-L. Smith, and B. K. Siesjö, "Regional cerebral blood flow during and after 2 hours of middle cerebral artery occlusion in the rat," *Journal of Cerebral Blood Flow & Metabolism*, vol. 17, no. 10, pp. 1066–1073, 1997.
- [28] Y. C. Zhang, F. F. Gan, S. B. Shelar, K. Y. Ng, and E. H. Chew, "Antioxidant and Nrf2 inducing activities of luteolin, a flavonoid constituent in *Ixeris sonchifolia* Hance, provide

- neuroprotective effects against ischemia-induced cellular injury," *Food and Chemical Toxicology*, vol. 59, pp. 272–280, 2013.
- [29] L. S. Zhang, J. J. Li, and C. Y. Wu, "Research progress of injury mechanism and related signal pathways of cerebral ischemia," *Chinese Journal of Neuroanatomy*, vol. 30, pp. 729–732, 2014.
- [30] X. K. Tu, W. Z. Yang, R. S. Liang et al., "Effect of baicalin on matrix metalloproteinase-9 expression and blood–brain barrier permeability following focal cerebral ischemia in rats," *Neurochemical Research*, vol. 36, no. 11, pp. 2022–2028, 2011.
- [31] K. A. Youdim, M. S. Dobbie, G. Kuhnle, A. R. Proteggente, N. J. Abbott, and C. Rice-Evans, "Interaction between flavonoids and the blood–brain barrier: *in vitro* studies," *Journal of Neurochemistry*, vol. 85, no. 1, pp. 180–192, 2003.
- [32] Y. He, H. Wan, Y. du et al., "Protective effect of Danhong injection on cerebral ischemia–reperfusion injury in rats," *Journal of Ethnopharmacology*, vol. 144, no. 2, pp. 387–394, 2012.
- [33] A. Ülken, G. Fauler, E. Bernhart et al., "Phloretin ameliorates 2-chlorohexadecanal-mediated brain microvascular endothelial cell dysfunction *in vitro*," *Free Radical Biology and Medicine*, vol. 53, no. 9, pp. 1770–1781, 2012.
- [34] C. C. Wang, R. Liu, S. H. Yuan, Q. X. Liu, and J. B. Chen, "The role of CXCL12 on the ultra-early time of transient focal brain ischemic injury in rats," *Journal of Apoplexy and Neurological Diseases*, vol. 12, pp. 1095–1098, 2015.
- [35] Y. J. Wang, W. W. He, and Q. E. Lang, "Pathological changes of brain tissue after cerebral ischemia," *Progress of Anatomical Sciences*, vol. 3, pp. 264–270, 1995.
- [36] I. Olmez and H. Ozyurt, "Reactive oxygen species and ischemic cerebrovascular disease," *Neurochemistry International*, vol. 60, no. 2, pp. 208–212, 2012.
- [37] S. Zhang, Y. Qi, Y. Xu et al., "Protective effect of flavonoid-rich extract from *Rosa laevigata* Michx on cerebral ischemia–reperfusion injury through suppression of apoptosis and inflammation," *Neurochemistry International*, vol. 63, no. 5, pp. 522–532, 2013.
- [38] N. Cho, J. H. Choi, H. Yang et al., "Neuroprotective and anti-inflammatory effects of flavonoids isolated from *Rhus verniciflua* in neuronal HT22 and microglial BV2 cell lines," *Food and Chemical Toxicology*, vol. 50, no. 6, pp. 1940–1945, 2012.
- [39] M. J. O'Neill, T. K. Murray, D. R. McCarty et al., "ARL 17477, a selective nitric oxide synthase inhibitor, with neuroprotective effects in animal models of global and focal cerebral ischemia," *Brain Research*, vol. 871, no. 2, pp. 234–244, 2000.
- [40] M. F. Anderson and N. R. Sims, "The effects of focal ischemia and reperfusion on the glutathione content of mitochondria from rat brain subregions," *Journal of Neurochemistry*, vol. 81, no. 3, pp. 541–549, 2002.
- [41] Y. Chen, T. Chen, and H. Feng, "Present situation of injury mechanism and treatment of cerebral ischemia reperfusion," *Medical Research Education*, vol. 6, pp. 47–54, 2012.
- [42] S. Ashwal, D. J. Cole, S. Osborne, T. N. Osborne, and W. J. Pearce, "L-NAME reduces infarct volume in a filament model of transient middle cerebral artery occlusion in the rat pup," *Pediatric Research*, vol. 38, no. 5, pp. 652–656, 1995.
- [43] M. Ozaki, S. Kawashima, T. Hirase et al., "Overexpression of endothelial nitric oxide synthase in endothelial cells is protective against ischemia-reperfusion injury in mouse skeletal muscle," *The American Journal of Pathology*, vol. 160, no. 4, pp. 1335–1344, 2002.
- [44] N. X. Zhang, J. Q. Yi, L. Y. Feng, X. P. Gong, and Y. F. Sun, "Study on the determination of protein content in tissue homogenate supernatant," *Hebei Medical Journal*, vol. 5, pp. 408–409, 1999.
- [45] H. J. Wang, Y. Y. Jiang, P. Lu, Q. Wang, and T. Ikejima, "An updated review at molecular pharmacological level for the mechanism of anti-tumor, antioxidant and immunoregulatory action of silibinin," *Yao Xue Xue Bao*, vol. 45, no. 4, pp. 413–421, 2010.
- [46] Y. Zhao, L. D. Lu, and X. H. Zhen, "Effect of chuanxiong polysaccharide on cerebral ischemia and reperfusion injury and expression of high mobility group box protein B1 in rats," *Chinese Journal of Gerontology*, vol. 37, pp. 2878–2880, 2017.
- [47] I. M. Cojocaru, M. Cojocaru, V. Sapira, and A. Ionescu, "Evaluation of oxidative stress in patients with acute ischemic stroke," *Romanian journal of internal medicine= Revue roumaine de medecine interne*, vol. 51, no. 2, pp. 97–106, 2013.
- [48] D. S. Warner, H. Sheng, and I. Batinić-Haberle, "Oxidants, antioxidants and the ischemic brain," *Journal of Experimental Biology*, vol. 207, no. 18, pp. 3221–3231, 2004.
- [49] B. Chen, Z. Ma, and Y. Sun, "Analysis of extraction and antioxidant of flavonoids in *Abelmoschus esculents* L. flower," *Jiangsu Condiment and Subsidiary Food*, vol. 3, pp. 20–23, 2017.
- [50] K. Itoh, N. Wakabayashi, Y. Katoh, T. Ishii, T. O'Connor, and M. Yamamoto, "Keap1 regulates both cytoplasmic-nuclear shuttling and degradation of Nrf2 in response to electrophiles," *Genes to Cells*, vol. 8, no. 4, pp. 379–391, 2003.
- [51] M. Kobayashi and M. Yamamoto, "Nrf2-Keap1 regulation of cellular defense mechanisms against electrophiles and reactive oxygen species," *Advances in Enzyme Regulation*, vol. 46, no. 1, pp. 113–140, 2006.
- [52] S. K. Niture, R. Khatri, and A. K. Jaiswal, "Regulation of Nrf2 - an update," *Free Radical Biology and Medicine*, vol. 66, pp. 36–44, 2014.
- [53] M. Liu, Y. Xu, X. Han et al., "Potent effects of flavonoid-rich extract from *Rosa laevigata* Michx fruit against hydrogen peroxide-induced damage in PC12 cells via attenuation of oxidative stress, inflammation and apoptosis," *Molecules*, vol. 19, no. 8, pp. 11816–11832, 2014.
- [54] L. Huang, J. Wang, L. Chen et al., "Design, synthesis, and evaluation of NDGA analogues as potential anti-ischemic stroke agents," *European Journal of Medicinal Chemistry*, vol. 143, pp. 1165–1173, 2018.

Research Article

Protocatechuic Acid Attenuates Trabecular Bone Loss in Ovariectomized Mice

Seon-A Jang,¹ Hae Seong Song,¹ Jeong Eun Kwon,¹ Hyun Jin Baek,¹ Hyun Jung Koo,² Eun-Hwa Sohn,³ Sung Ryul Lee ,⁴ and Se Chan Kang ¹

¹Department of Oriental Medicine Biotechnology, College of Life Sciences, Kyung Hee University, Yongin 17104, Republic of Korea

²Department of Medicinal and Industrial Crops, Korea National College of Agriculture and Fisheries, Jeonju 54874, Republic of Korea

³Department of Herbal Medicine Resources, Kangwon National University, Samcheok 25949, Republic of Korea

⁴Department of Convergence Biomedical Science, Cardiovascular and Metabolic Disease Center, College of Medicine, Inje University, Busan 47392, Republic of Korea

Correspondence should be addressed to Sung Ryul Lee; lsr1113@inje.ac.kr and Se Chan Kang; स्कang@khu.ac.kr

Received 25 April 2018; Accepted 27 June 2018; Published 29 July 2018

Academic Editor: Felipe L. de Oliveira

Copyright © 2018 Seon-A Jang et al. This is an open access article distributed under the Creative Commons Attribution License, which permits unrestricted use, distribution, and reproduction in any medium, provided the original work is properly cited.

Primary osteoporosis is a disease related to excessive bone resorption due to estrogen insufficiency that occurs postmenopause. Protocatechuic acid (PCA), or 3,4-dihydroxybenzoic acid, is a common compound present in numerous plants. Although numerous biological activities of PCA have been identified, its antiosteoporotic function has not been well established. In this study, the antiosteoporotic activity of PCA supplementation was determined in ovariectomized (OVX) female ICR mice at 12 weeks after OVX. The biomechanical properties of a bone were evaluated by microcomputed tomography. The signaling molecules associated with osteoclast differentiation were determined in bone marrow cells through immunoblot or RT-PCR. Oral supplementation with PCA (20 mg/kg/day) significantly ameliorated the OVX-mediated stimulation of osteoclast activity based on decreases in serum levels of receptor activator of nuclear factor κ B ligand (RANKL), osteocalcin, and bone alkaline phosphatase and increase in serum osteoprotegerin (each group, $n = 6$; $p < 0.05$). In addition, the OVX-induced decreases in mRNA expression levels of cathepsin K, calcitonin receptor, nuclear factor of activated T cell cytoplasmic 1 (NFATc1), and tumor necrosis factor (TNF) receptor-associated factor-6 (TRAF6) in bone marrow cells were significantly attenuated (each group, $n = 6$; $p < 0.05$). Finally, the loss of trabecular bone and changes in biomechanical properties of a bone were significantly improved by supplementation with 20 mg/kg PCA (each group, $n = 6$; $p < 0.05$). Collectively, our results show that PCA supplement suppressed trabecular bone loss in OVX mice and therefore might be an effective alternative approach for preventing the progression of postmenopausal osteoporosis.

1. Introduction

Protocatechuic acid (PCA) is a 3,4-dihydroxybenzoic acid that occurs in nature and has a similar structure to gallic acid, caffeic acid, and vanillic acid [1]. PCA is a very common compound that is present in numerous plants, including *Rubus coreanus* Miquel, *Astragalus membranaceus* Bunge, cinnamon, star anise, medicinal rosemary, and *Sorghum bicolor* L, and in fruits and products of plant origin. PCA possesses biological activity against diabetes, infection, ageing, and inflammation, as reviewed elsewhere [1–3]. PCA is

traditionally considered to be nontoxic and a relatively safe compound for oral administration [1].

Bone is a type of dense connective tissue that is composed of ~80% cortical bone (outer layer, compact bone) and ~20% trabecular bone (inner layer, cancellous bone). Based on porosity and unit microstructure, a bone is basically classified as either cortical, which is a compact and dense form, or trabecular, which is a cancellous or sponge form [4]. A bone undergoes continuous remodeling through resorption of old bone and formation of the same amount of newly formed bone at the same place [5, 6]. Bone mineral density (BMD)

has been regarded as a surrogate marker for bone strength and an important factor in bone quality [7]. In addition to BMD, bone volume fraction (BV/TV) and bone microstructure are important factors determining bone strength [8]. Osteoporosis is associated with increased risk of a broken bone due to loss of bone mass and deterioration of bone microarchitecture, which increase bone fragility and susceptibility to hip and spine fractures [9, 10]. Osteoporosis can be classified as either primary or secondary osteoporosis according to cause, which includes age, sex hormones, medical conditions, and diseases [10, 11]. Primary osteoporosis, which is classified as type I (postmenopausal osteoporosis) and is frequently associated with fenestrated trabecular bone resorption, occurs between the ages of 50 and 65 years in postmenopausal women [12]. Estrogen deficiency induces receptor activator of nuclear factor κ B ligand (RANKL), the key molecule required for osteoclast differentiation, leading to enhanced osteoclast activation and reduced osteoclast apoptosis [13–15]. In the bone environment, upregulated RANKL, RANK, and osteoprotegerin (OPG) expression and increased RANKL/OPG ratio are important determinants of bone mass in normal and pathological conditions [16]. In addition, quantitative analysis of osteoclast-specific gene markers such as tartrate-resistant acid phosphatase (TRAP), cathepsin K, and calcitonin receptor has been an important and reliable method for identifying osteoclastogenic capability [17–19]. Although hormone replacement therapy (HRT) is effective in the prevention and treatment of postmenopausal osteoporosis, it is associated with a high risk of blood clotting, biliary disease, and breast or endometrium cancer. Therefore, it is important to develop safer compounds with fewer adverse effects than estrogen mimetics [20].

Several studies have shown that PCA has beneficial effects on osteoblast and osteoclast cells *in vitro* [21–23]. In *in vitro* experiments, PCA has an inhibitory effect on osteoclast differentiation [21] and a proliferative effect on osteoblasts [23]. Wu et al. reported that PCA reduced the RANKL-induced TRAP activity and osteoclast-specific gene expression such as TRAP, tumor necrosis factor receptor-associated factor-6 (TRAF6), and cathepsin K in RAW264.7 murine macrophage cells [21]. In addition, the RANKL-mediated signaling pathways including mitogen-activated protein kinases, nuclear factor κ B, and cyclooxygenase-2 could be attenuated by PCA treatment [21]. Park et al. have shown that PCA inhibits RANKL-induced osteoclast differentiation in mouse bone marrow macrophages and lipopolysaccharide-induced inflammatory bone loss in mice [24]. In contrast, Rivera-Piza et al. suggested in 2017 that PCA might enhance osteogenesis in C3H10T1/2 and 3T3-L1 cells [22]. The antiosteoporotic effect of PCA in the ovariectomized state that leads to estrogen deficiency, one of the etiological factors of postmenopausal osteoporosis, has not been confirmed. In the present study, we investigated the preventive effect of PCA against deterioration of bone structural architecture *in vivo* in an ovariectomized (OVX) mouse model using microcomputed tomography (CT) bone analysis. We also examined the suppressive effects of PCA on levels of biological markers involved in activation of osteoclasts, such as bone alkaline phosphatase (BALP), RANKL, OPG, TRAF6, nuclear factor

of activated T cell cytoplasmic 1 (NFATc1), cathepsin K, and calcitonin receptor, in the serum or bone marrow from experimental groups.

2. Materials and Methods

2.1. Reagents. Protocatechuic acid (PCA), RANKL, and 17β -estradiol (E_2) were purchased from Sigma Chemical Co. (St. Louis, MO). Phosphate-buffered saline (PBS) was purchased from Welgene Inc. (Seoul, Korea). Other chemicals not specified were obtained from Sigma. Enzyme-linked immunosorbent assay (ELISA) kits for RANKL and OPG were purchased from R&D Systems (Minneapolis, MN). ELISA kits for osteocalcin and BALP were obtained from Biomedical Technologies Inc. (Stoughton, MA).

2.2. Experimental Animals. Six-week-old female ICR mice were purchased from Korea Laboratory Animal Co. (Daejeon, Korea) and acclimatized for 1 week before the experiments. The mice were housed in controlled environments of temperature ($22 \pm 2^\circ\text{C}$) and humidity ($53 \pm 5^\circ\text{C}$) under a 12 h light/dark cycle. The mice were provided with sterile standard mouse chow and water *ad libitum* during the acclimation and experimental periods. All animal experiments were performed strictly according to the Guide for the Humane Use and Care of Laboratory Animals and in accordance with the current ethical regulations for animal care and use at Kyung Hee University (KHUASP (SE)-16-003).

2.3. Experimental Model. The mice underwent either bilateral laparotomy (sham, $n = 6$) or bilateral OVX ($n = 24$) under anesthesia with tiletamine/zolazepam (Virbac Korea, Seoul, Korea) and xylazine HCl (Bayer Korea, Kyungkido, Korea) using a ventral approach at 7 weeks of age. The surgical procedure was performed under aseptic conditions following ethical regulations for animal care and use. At 1 week after surgery, the mice were randomly divided into five groups ($n = 6$ per group): (1) sham-operated mice orally administered an equivalent volume of PBS to treatment groups (sham control); (2) OVX mice with daily oral administration of PBS (OVX); (3) OVX mice with daily oral administration of PCA at 10 mg/kg body weight (b.w.); (4) OVX mice with daily oral administration of PCA at 20 mg/kg b.w.; and (5) OVX with intraperitoneal injection (i.p.) of 17β -estradiol (E_2) at 0.1 mg/kg b.w./day three times per week. Body weight was measured weekly, and the PCA or E_2 dose was adjusted accordingly. All experimental mice received their respective treatment for 12 weeks. There was no treatment-related mortality during the experimental course.

2.4. Micro-CT Bone Analysis. To determine structural loss of bone architecture, the proximal and distal parts of the right tibiae were scanned by *in vivo* microcomputed tomography (micro-CT, Skyscan1076, Skyscan, Antwerp, Belgium), as previously reported [25]. The scan conditions were set at an aluminum filter of 0.5 mm, X-ray voltage of 50 kV, X-ray current of 200 mA, and exposure time of 360 ms. During each scan, the mice were maintained under anesthesia via

TABLE 1: Primer sequences used for real-time PCR.

Gene name	Primer sequences
Cathepsin K	5'-CACCCAGTGGGAGCTATGGAA-3' (forward) 5'-GCCTCCAGGTTATGGGCAGA-3' (reverse)
Calcitonin receptor	5'-AGGCAGACCCAAATGCTGTAATG-3' (forward) 5'-TTGGTGATAGGTTCTTGGTGACCTC-3' (reverse)
TRAF6 (tumor necrosis factor receptor-associated factor-6)	5'-TTAAATGTCCGCATTCTCAGGGTA-3' (forward) 5'-TTGTGACCCGAGACTCTCCCAAG-3' (reverse)
NFATc1 (nuclear factor of activated T cell cytoplasmic 1)	5'-GCTTCACCCATTTGCTCCAG-3' (forward) 5'-ATGGTGTGGAAATACGGTTGGTC-3' (reverse)
β -Actin	5'-TCACCCACACTGTGCCCATCTACGA-3' (forward) 5'-GGATGCCACAGGATCCATACCCA-3' (reverse)

inhalation of isoflurane (Hana Pharm, Seoul, Korea). The mice were placed in a chamber filled with 5% carbon dioxide for 5 min, and then the isoflurane was adjusted to 1.5% to keep the mice anesthetized. The data were digitalized with a frame grabber, and the resulting images were transmitted to a computer for analysis using Comprehensive TeX Archive Network (CTAN) topographic reconstruction software. The total volume (TV) indicated the inner area of cortical bone. The trabecular bone volume (BV) indicated the total trabecular bone within the total volume. The bone volume percentage was calculated by dividing the trabecular bone volume by the total volume. Cortical bone parameters assessed were bone volume fraction (BV, mm^3), mean polar moment of inertia (MMI, mm^4), cross-section thickness (Cs.Th, mm), and bone mineral density (BMD, g/cm^3). Trabecular bone parameters assessed were bone volume fraction (BV/TV, %), trabecular thickness (Tb.Th, mm), trabecular separation (Tb.Sp), trabecular number (Tb.N, 1/mm), trabecular bone pattern factor (Tb.Pf, mm^{-1}), and specific bone surface (BS/BV, 1/mm). Structure model index (SMI), ranging from 0 to 3, characterizes the type of 3D structure of a bone based on a certain amount of rods and plates [26].

2.5. Enzyme-Linked Immunosorbent Assay. At the end of the experiment, all animals were fasted for 6 h, and then blood was collected from the abdominal vena cava under anesthesia with diethyl ether. The blood was allowed to clot for 30 min at room temperature, and sera were obtained after centrifugation at $3000 \times g$ for 10 min at 4°C . The serum levels of RANKL, osteocalcin, and BALP were determined using commercial ELISA assay kits according to the manufacturer's instructions.

2.6. Quantitative Real-Time Polymerase Chain Reaction. Total RNA was extracted from the bone marrow isolated from experimental mice using Trizol reagent according to the manufacturer's protocols. A total of $1 \mu\text{g}$ of total RNA was reverse transcribed in a $20 \mu\text{l}$ total volume using oligo (dT) primers with the enzyme and buffer supplied in the PrimeScript® II 1st strand cDNA synthesis kit (Takara, Japan). Quantitative real-time PCR was conducted with an MX3005P (Stratagene, USA) using the primers listed in

Table 1. For quantitative real-time PCR, SYBR Premix Ex Taq II (Takara, Japan) was used in a $25 \mu\text{l}$ reaction mixture containing $2 \mu\text{l}$ cDNA template, $1 \mu\text{l}$ forward and reverse primer, $12.5 \mu\text{l}$ master mix, and $8.5 \mu\text{l}$ sterile distilled water. The thermal cycling profile consisted of a preincubation step at 95°C for 10 min, followed by 35 cycles at 95°C for 15 sec and 59°C for 1 min. Relative quantitative mRNA levels of cathepsin K, calcitonin receptor, TRAF6, NFATc1, and β -actin were determined by the comparative cycle threshold method.

2.7. Statistical Analysis. Data are represented as mean \pm standard deviation (SD). Group differences were assessed with one-way analysis of variance (ANOVA) followed by a modified *t*-test with Bonferroni correction using SigmaPlot software (Systat Software Inc., San Jose, CA, USA). A statistical probability of $p < 0.05$ was considered significant.

3. Results

3.1. Effects of PCA on Body, Uterus, and Tissue Weight in OVX Mice. There were no clinical signs or abnormalities in behavior during the experiment. The body weight of OVX mice was higher than that of the sham controls (Figure 1(a)), but relative uterus weight per body weight was decreased compared to the sham controls (Figure 1(b)). The uterus is one of the most estrogen-responsive reproductive tissues and therefore can easily become atrophied in the absence of estrogen. E_2 treatment with $0.1 \text{ mg}/\text{kg}$ body weight/day administered i.p. significantly increased the relative uterus weight per body weight ($n = 6$, $p < 0.05$). In contrast, PCA supplementation at the dose of 10 and $20 \text{ mg}/\text{kg}$ body weight/day did not recover the relative uterus weight (Figure 1(b)). The spleen and thymus, major organs of the immune system, are also highly susceptible to estrogen insufficiency. In the OVX group, the weight of the thymus was significantly increased, but that of the spleen was decreased compared to the sham controls (each group $n = 6$, $p < 0.05$; Table 2). Changes in weight of the spleen and thymus were significantly attenuated by E_2 supplementation. A similar

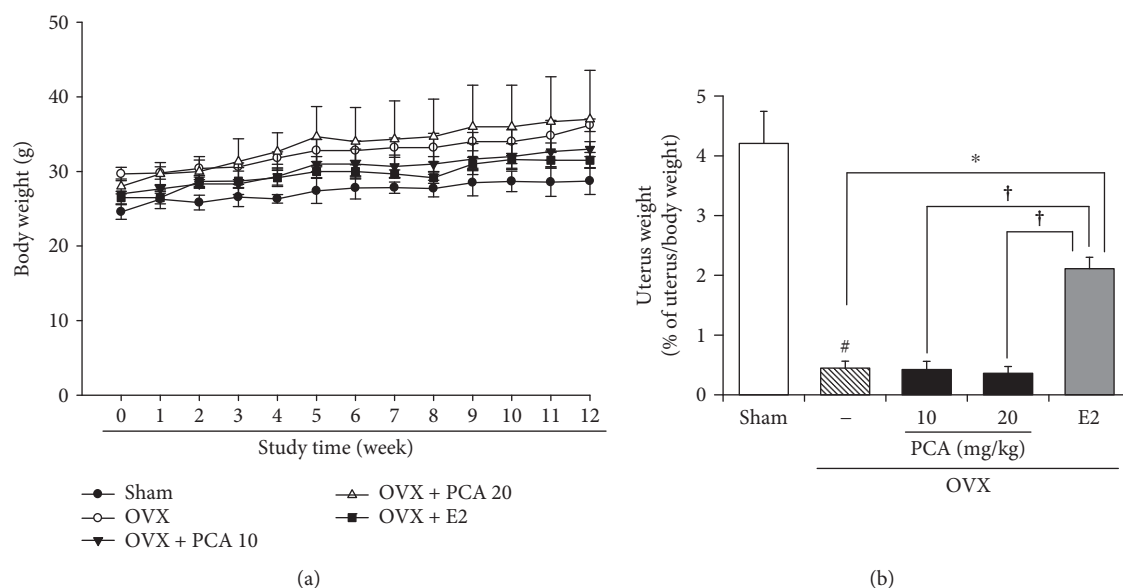


FIGURE 1: Effects of PCA on changes of body weight and uterus weight in OVX mice. Sham or OVX mice were orally administered vehicle or PCA (10 and 20 mg/kg b.w./day) for 12 weeks. As a positive control group, E₂ (0.1 mg/kg b.w./day) was administered three times a week for 12 weeks via i.p. injection. Body weight was measured once a week (a). At the end of the experiment, the uterus was removed and weighed (b). Results are expressed as relative ratio per body weight. Data are mean \pm SD (each group, $n = 6$). # $p < 0.05$ between the sham and OVX-alone group. * $p < 0.05$ among OVX groups with or without interventions. † $p < 0.05$ among OVX groups with interventions. b.w.: body weight; i.p.: intraperitoneal; E₂: 17 β -estradiol; OVX: ovariectomized; PCA: protocatechuic acid.

TABLE 2: Effects of PCA on weight of the thymus and spleen in OVX mice.

Tissue (mg)	Sham	—	OVX PCA (mg/kg b.w.)		E ₂ (0.1 mg/kg b.w.)
			10	20	
Thymus	47.75 \pm 2.06	61.66 \pm 5.68 [#]	61.33 \pm 18.50	36.0 \pm 1.41 [*]	44.0 \pm 2.45 [*]
Spleen	151.65 \pm 0.71	94.42 \pm 3.79 [#]	88.08 \pm 2.65	117.11 \pm 1.41 [*]	137.14 \pm 8.47 [*]

Data are mean \pm SD (each group, $n = 6$). # $p < 0.05$ between the sham and OVX-alone group. * $p < 0.05$ among OVX groups with or without interventions. b.w.: body weight; E₂: 17 β -estradiol; OVX: ovariectomized; PCA: protocatechuic acid.

effect was achieved with PCA supplementation at 20 mg/kg (Table 2).

3.2. Effect of PCA on the Structural Properties of Cortical Bone.

To identify the effect of PCA on structural characteristics of a bone induced by OVX, we analyzed structural parameters for the entire cortical bone of the tibia (BV, MMI, Cs.Th, and BMD) using micro-CT images after scanning the tibia of each mouse (Figures 2(a) and 3). In the OVX group, the values of BV ($n = 6$, $p > 0.05$), MMI ($n = 6$, $p > 0.05$), Cs.Th ($n = 6$, $p > 0.05$), and BMD ($n = 6$, $p > 0.05$) did not change compared to those of the sham controls (Figure 3). In addition, treatment with PCA (10 and 20 mg/kg) or E₂ did not induce any significant changes in structural parameters of cortical bone of the tibia (Figure 3).

3.3. Effects of PCA on the Mechanical Properties of Trabecular Bone.

Alteration of trabecular architecture is considered an important component of postmenopausal osteoporosis that influences bone strength [6, 13]. Unlike cortical bone (shown

in Figure 3), the trabecular bone structure was significantly affected by OVX. The values of BV/TV, Tb.Th, Tb.N, Tb.Pf, BS/BV, and BMD in trabecular bones were significantly decreased, whereas the values of Tb.Sp and SMI were markedly higher than those of the sham controls (Figures 2(b) and 4). Osteoporotic trabecular bone shows less connectivity and thinner rod-like structures than normal trabecular bone, indicating that the value of SMI is negatively correlated with trabecular bone strength [27]. The trabecular bone of PCA- (10 and 20 mg/kg) treated OVX mice had a more compact trabecular bone structure, with higher bone volume fraction (Tb. BV/TV) and increased trabecular number (Tb.N) and thickness (Tb.Th) with less trabecular separation (Tb.Sp) at both the radius and tibia compared with that of the untreated OVX group (Figure 4) [28]. When compared to the OVX group, BV/TV, Tb.Th, Tb.N, BS/BV, and BMD (Tb) were enhanced, and Tb.Sp and SMI were suppressed in the PCA- (10 and 20 mg/kg) and E₂-treated groups, whereas Tb.Pf was not significantly different from that in the OVX group (Figure 4(e)). In view of improving BV/TV

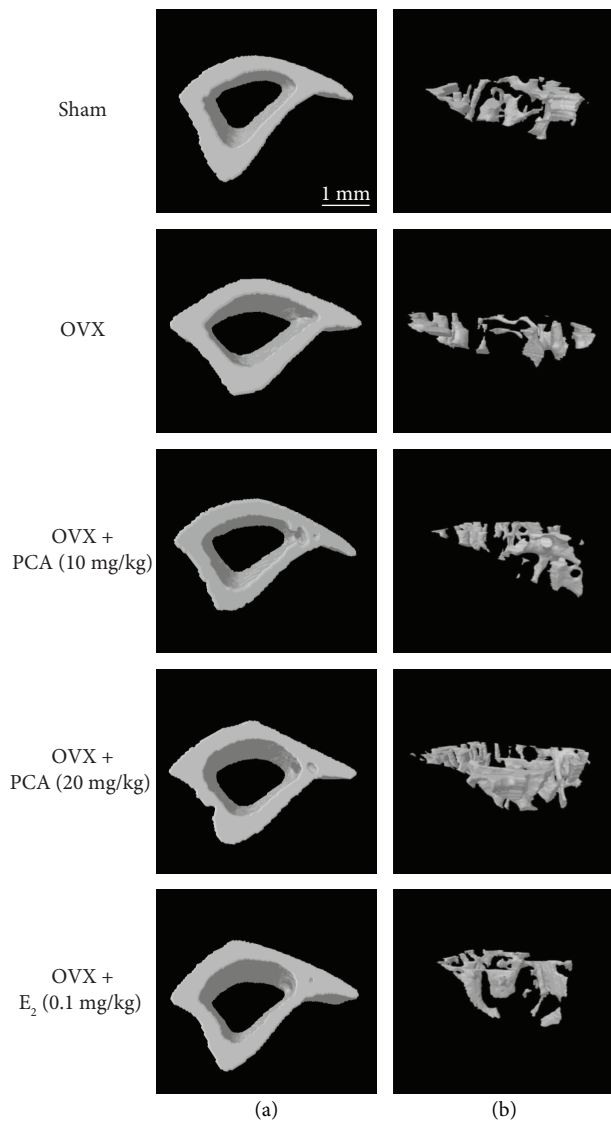


FIGURE 2: Micro-CT analysis of the cortical and trabecular bone. OVX mice received PBS as a vehicle, PCA (10 mg/kg and 20 mg/kg), or E_2 (0.1 mg/kg) for 12 weeks. Vehicle and PCA were delivered orally, and E_2 was given by intraperitoneal injection. The proximal and distal parts of the right tibias were scanned by *in vivo* μ -computed tomography (CT). Representative images of the cortical (a) and trabecular bone (b) reconstructed using Comprehensive TeX Archive Network (CTAN) topographic reconstruction software are presented. E_2 : 17β -estradiol; OVX: ovariectomized; PCA: protocatechuic acid.

(Figure 4(a)), Tb.N (Figure 4(d)), and BMD (Figure 4(h)) of trabecular bones, PCA treatment at the dose of 20 mg/kg was better than E_2 treatment. These results indicate that PCA might be preventive against OVX-mediated deterioration of trabecular bone architecture.

3.4. Effects of PCA on Serum RANKL, OPG, and RANKL/OPG Ratio in OVX Mice. Excessive bone resorption would be ameliorated by inhibiting the activity of osteoclasts and osteoclast differentiation. Similar to E_2 , PCA supplementation effectively attenuated OVX-mediated trabecular bone destruction (Figure 4). Bone resorption is controlled by

regulatory factors involving the tumor necrosis factor (TNF)/TNF receptor families, RANK, RANKL, and OPG [14, 15]. In addition, the balance between OPG and RANKL produced by osteoblasts is important for osteoclast regulation. The antiosteoporotic effect of PCA might be associated with its suppressive effect on bone resorption. To test this hypothesis, we examined changes in serum levels of OPG and RANKL, important regulators of the bone resorption process, in OVX mice in the presence or absence of PCA (each group, $n = 6$). The serum level of RANKL was significantly increased in OVX mice (Figure 5(a)), whereas the OPG level was significantly decreased (Figure 5(b)). As a result, the RANKL/OPG ratio was significantly higher than that of the sham controls (sham versus OVX group, 0.51 ± 0.02 versus 2.78 ± 0.41 , $p < 0.05$). These results indicate that deterioration of trabecular bones observed in OVX mice is, at least in part, associated with enhancement of bone resorption. Like E_2 , PCA treatment at the dose of 20 mg/kg not only significantly decreased the serum level of RANKL but also increased the OPG level. Thereby, the RANKL/OPG ratio was significantly decreased compared to that of OVX mice (Figure 5(c)).

3.5. Effects of PCA on the Expression of TRAF6 and NFATc1 in OVX Mice. During osteoclast differentiation, binding of RANKL to its receptor RANK results in recruitment of TRAF6, leading to activation of downstream signaling molecules such as NFATc1 [15]. As shown in Figure 5(a), PCA supplementation (20 mg/kg) significantly reduced the serum level of RANKL in OVX mice. We therefore assumed that the expression level of TRAF6 and NFATc1 would be repressed in the presence of PCA. Indeed, both TRAF6 and NFATc1 mRNA levels in bone marrow cells of PCA- (20 mg/kg) supplemented OVX mice were significantly lower than those in OVX mice ($p < 0.05$, Figure 6). Collectively, these data show that PCA supplement suppressed the signaling pathways involved in osteoclast differentiation and thereby reduced the impairment of trabecular bone architecture in OVX mice (Figure 4).

3.6. Effects of PCA on Expression of Cathepsin K and Calcitonin Receptor in OVX Mice. To further test the suppressive effects of PCA on osteoclast differentiation, the expression levels of cathepsin K and calcitonin receptor, osteoclast-specific markers in the bone marrow cells, were determined in OVX mice (each group, $n = 6$). The OVX mice showed an approximately 2-fold increase in the mRNA expression levels of cathepsin K and calcitonin receptor compared to the sham controls ($p < 0.05$). However, supplementation with PCA at the dose of 20 mg/kg or E_2 significantly suppressed the increase in both cathepsin K and calcitonin receptor (Figure 7).

3.7. Effects of PCA on Serum Levels of Osteocalcin and BALP in OVX Mice. Osteocalcin and BALP, which are synthesized by osteoblasts, are released into the circulation during the bone resorption process [10]. Increased levels of osteocalcin and BALP in serum indirectly reflect progression toward bone resorption. As shown in Figure 8, the levels of both

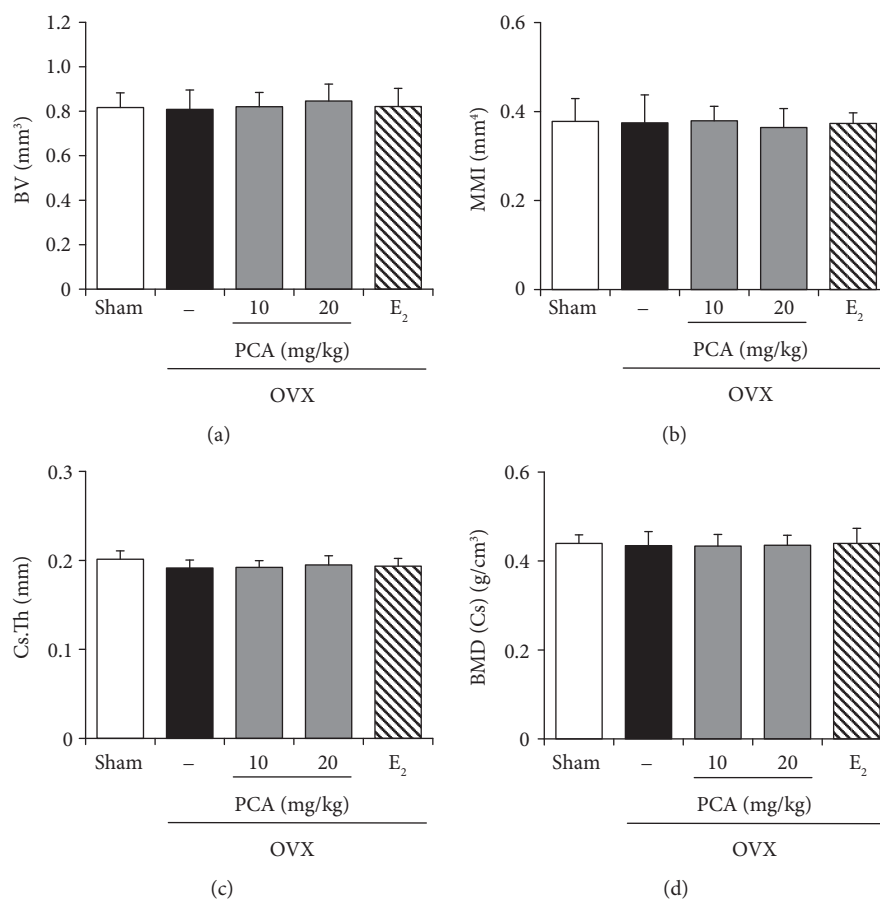


FIGURE 3: Effect of PCA on the cortical bone in OVX mice. After obtaining the three-dimensional image shown in Figure 3(a), changes in the following parameters of the cortical bone were analyzed: (a) bone volume density (BV), (b) mean polar moment of inertia (MMI), (c) cross-section thickness (Cs.Th), and (d) bone mineral density (BMD). The results are expressed as mean \pm SD (each group, $n = 6$). There was no statistical significance among the groups. E₂: 17 β -estradiol; OVX: ovariectomized; PCA: protocatechuic acid.

osteocalcin and BALP were significantly increased in the OVX group, but these effects were significantly suppressed in the presence of PCA (20 mg/kg) and E₂ ($p < 0.05$). The inhibitory potential of 20 mg/kg PCA against BALP was comparable to that of E₂. These results suggest that PCA supplementation can suppress bone resorption initiated by osteoblasts in OVX mice.

4. Discussion

In this study, oral administration of PCA to OVX mice prevented loss of the tibial bone, preserved trabecular bone microarchitecture, and improved bone biomechanical properties. In conjunction with this result, administration of PCA (20 mg/kg body weight) normalized serum levels of RANKL, OPG, and osteocalcin in OVX mice. The mRNA expression levels of TRAF6 and NFATc1, which are involved in the RANKL-RANK signaling pathway, were significantly suppressed by PCA administration. In addition, the mRNA expression levels of calcitonin receptor and cathepsin K were also significantly suppressed by PCA. Thus, PCA reduced the bone resorption caused by estrogen deficiency through

suppression of signaling pathways involved in the activation of osteoclasts.

It has been suggested that the degeneration of the uterus observed in OVX mice represents a model for the bone loss due to estrogen deficiency that occurs in women after menopause [29]. Ovariectomy results in a significant decrease in uterine weight, BMD of trabecular bone, and biomechanical strength, in part due to estrogen deficiency. In our study, the body weight of mice was increased in the OVX group (Figure 1(a)), which is consistent with previous reports [30]. The uterus is one of the most estrogen-responsive reproductive tissues and predominantly expresses estrogen receptor (ER) α [31]. In contrast to the increase in body weight, the OVX mice showed initial atrophy of the uterus that was recovered by treatment with E₂ (Figure 1(b)). Considering that supplementation with PCA had no significant effect on the uterus but could ameliorate the impaired density and architecture of trabecular bone with similar potential to E₂ supplementation (Figure 4), it is assumed that PCA has less estrogenic activity or suppresses loss of bone in a different manner.

In the evaluation of bone structure, BV/TV and BMD are known to be critical parameters for determining the fragility

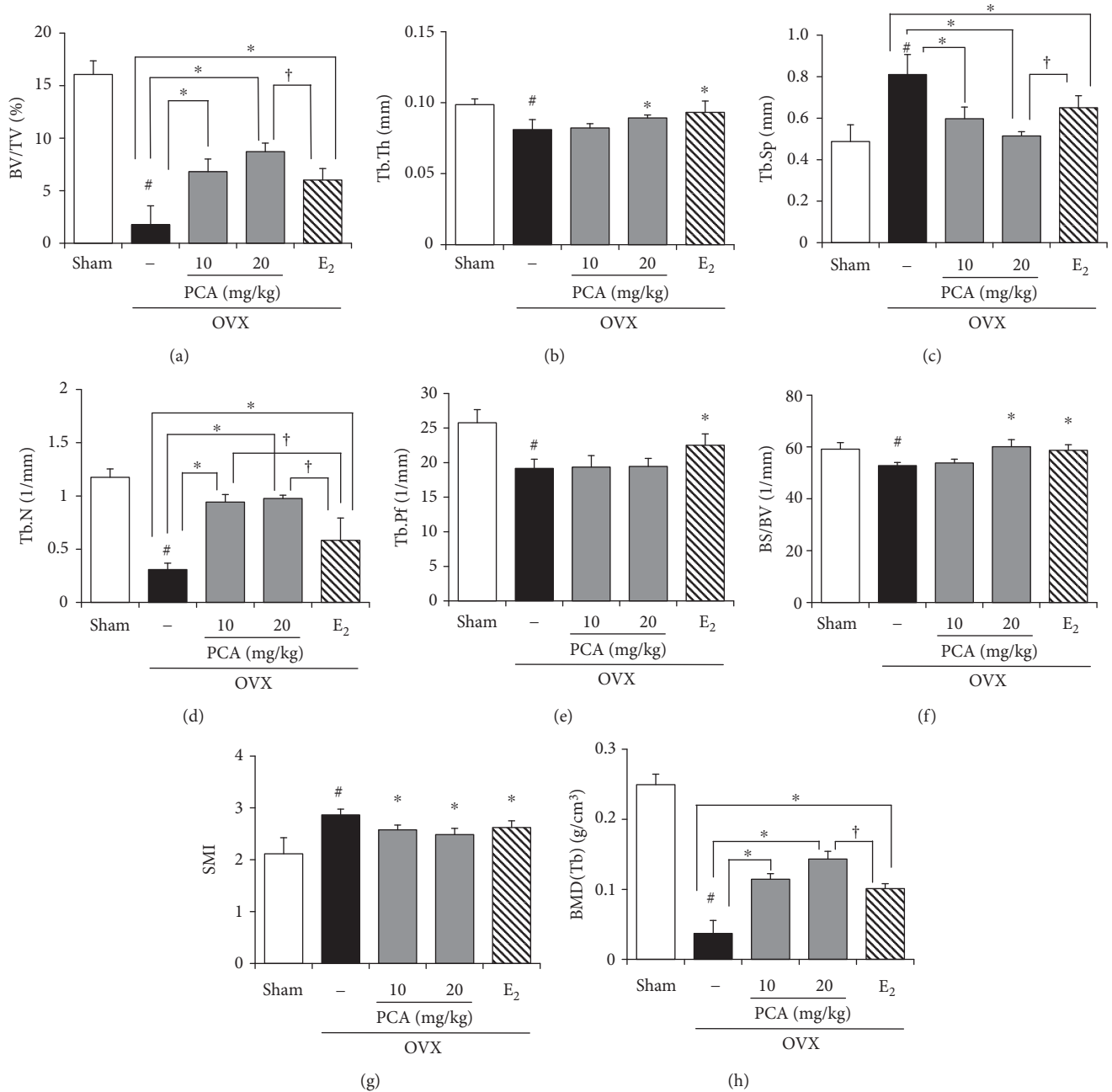


FIGURE 4: Effect of PCA on the trabecular bone in OVX mice. After obtaining the 3-dimensional image shown in Figure 3(b), changes in the following parameters of the trabecular bone were analyzed: (a) bone volume fraction (BV/TV), (b) trabecular thickness (Tb.Th), (c) trabecular separation (Tb.Sp), (d) trabecular number (Tb.N), (e) trabecular bone pattern factor (Tb.Pf), (f) specific bone surface (BS/BV), (g) structure model index (SMI), and (h) bone mineral density (BMD). The results are expressed as mean \pm SD (each group, $n = 6$). [#] $p < 0.05$ between the sham and OVX-alone group. ^{*} $p < 0.05$ among OVX groups with or without interventions. [†] $p < 0.05$ among OVX groups with interventions. E₂: 17 β -estradiol; OVX: ovariectomized; PCA: protocatechuic acid.

of trabecular bone [8]. Thus, a lower value of BV/TV not only indicates fewer trabecular bones but also is associated with morphological features such as rod-shaped and disconnected trabecular bones [32]. PCA administration resulted in increased BV/TV (bone volume ratio), consistent with the improvement in BMD (Tb). In addition, PCA supplementation restored the trabecular connectivity by increasing Tb.N (trabecular number) and reducing Tb.Sp (trabecular spacing).

PCA increased both BS/BV (bone surface to volume) and Tb.Th (trabecular thickness) compared to the OVX group (Figure 4).

Osteoclasts are specialized cells involved in degradation of bone matrix. Among more than 24 involved genes or loci, osteoclast differentiation and activation are largely regulated by the action of OPG, RANK, and RANKL [33, 34]. OPG and RANKL are produced by osteoblastic cells, with a balance

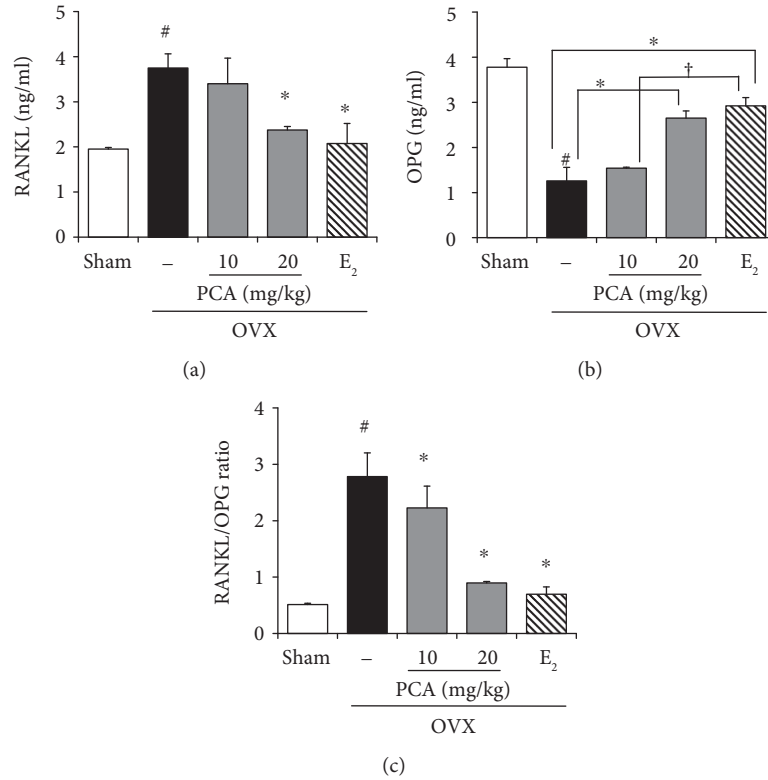


FIGURE 5: Effects of PCA on serum levels of RANKL and OPG and RANKL/OPG ratio. OVX mice received vehicle, PCA (10 and 20 mg/kg b.w./day), or E₂ for 12 weeks. At the end of the experiment, sera were obtained; RANKL (a) and OPG (b) levels were determined using commercial ELISA kits; and the RANKL/OPG ratio was calculated (c). The results are expressed as mean \pm SD (each group, $n = 6$). [#] $p < 0.05$ between the sham and OVX-alone group. ^{*} $p < 0.05$ among OVX groups with or without interventions. [†] $p < 0.05$ among OVX groups with interventions. b.w.: body weight; E₂: 17 β -estradiol; OVX: ovariectomized; PCA: protocatechuic acid; RANKL: receptor activator of nuclear factor κ B ligand.

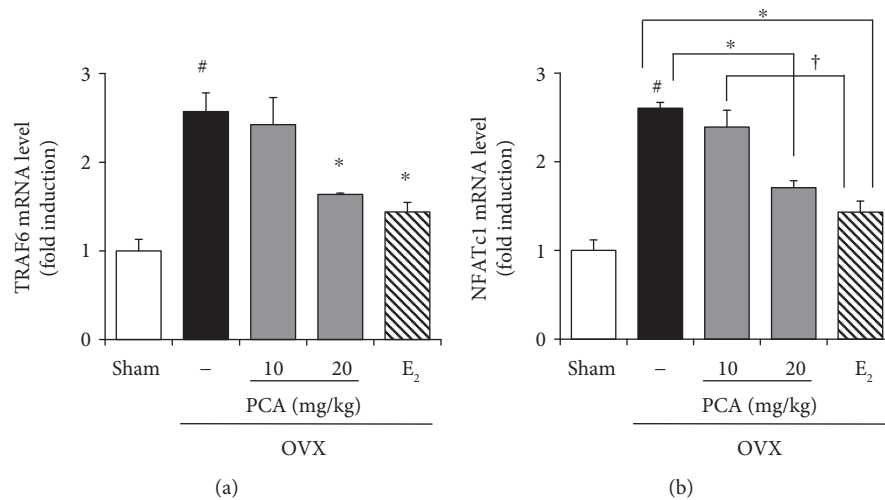


FIGURE 6: Effects of PCA on mRNA expression level of TRAF6 and NFATc1. OVX mice received vehicle, PCA (10 and 20 mg/kg b.w./day), or E₂ for 12 weeks. At the end of the experiment, bone marrow cells were isolated, and the mRNA expression levels of cathepsin K (a) and calcitonin receptor (b) were measured by real-time RT-PCR. β -Actin was used as a loading control for RT-PCR. The results are expressed as a mean \pm SD (each group, $n = 6$). [#] $p < 0.05$ between the sham and OVX-alone group. ^{*} $p < 0.05$ among OVX groups with or without interventions. [†] $p < 0.05$ among OVX groups with interventions. b.w.: body weight; E₂: 17 β -estradiol; OVX: ovariectomized; PCA: protocatechuic acid; TRAF6: TNF receptor-associated factor-6; NFATc1: nuclear factor of activated T cell cytoplasmic 1.

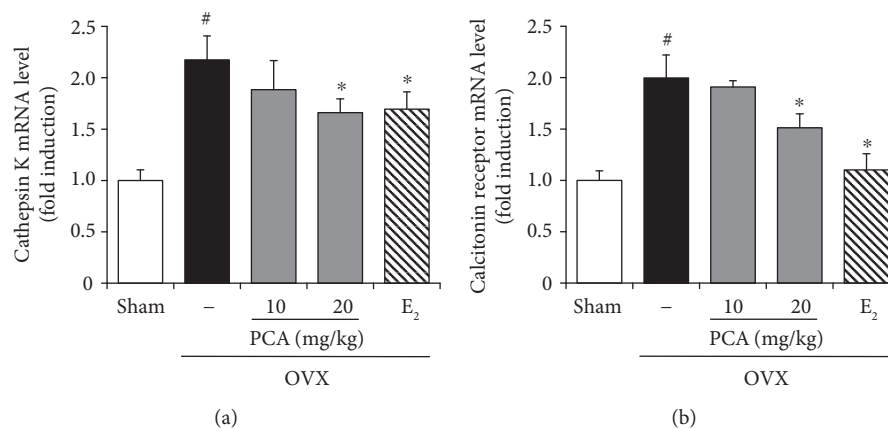


FIGURE 7: Effects of PCA on the mRNA expression level of cathepsin K and calcitonin receptor. OVX mice received vehicle, PCA (10 and 20 mg/kg b.w./day), or E₂ for 12 weeks. At the end of the experiment, bone marrow cells were isolated, and mRNA expression levels of cathepsin K (a) and calcitonin receptor (b) were measured by real-time RT-PCR. β -Actin was used as a loading control for RT-PCR. The results are expressed as mean \pm SD (each group, $n = 6$). # $p < 0.05$ between the sham and OVX-alone group. * $p < 0.05$ among OVX groups with or without interventions. b.w.: body weight; E₂: 17 β -estradiol; OVX; ovariectomized; PCA: protocatechuic acid.

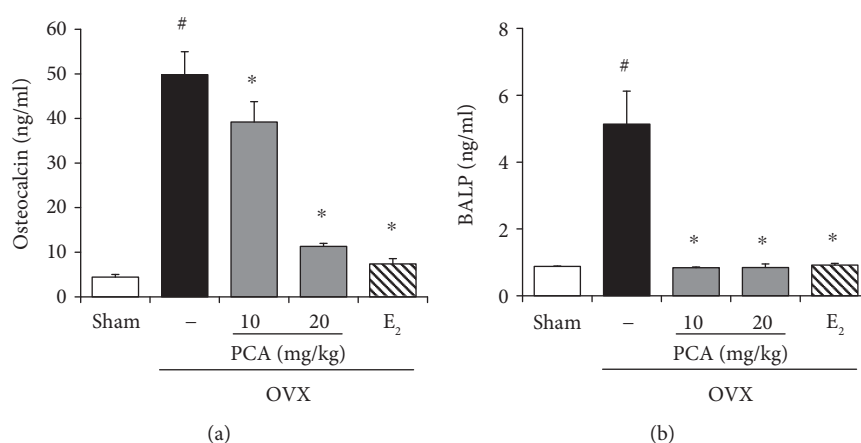


FIGURE 8: Effects of PCA on serum levels of osteocalcin and BALP. OVX mice received vehicle, PCA (10 and 20 mg/kg b.w./day), or E₂ for 12 weeks. At the end of experiment, sera were obtained, and osteocalcin (a) and BALP (b) levels were determined using commercial ELISA kits. The results are expressed as mean \pm SD (each group, $n = 6$). # $p < 0.05$ between the sham and OVX-alone group. * $p < 0.05$ among OVX groups with or without interventions. BALP: bone alkaline phosphatase; b.w.: body weight; E₂: 17 β -estradiol; OVX; ovariectomized; PCA: protocatechuic acid.

between membrane-bound RANKL and secreted OPG decoy receptor. The RANK signaling pathway is negatively regulated by OPG [35]. The differentiation of osteoclast cell precursors is induced upon the binding of RANKL and RANK, which promotes the activation of mature osteoclasts. Therefore, RANKL is an essential factor for differentiation, activation, and survival of osteoclasts in bone remodeling, whereas OPG is a soluble decoy receptor and inhibitor of RANKL action. It seems that loss of trabecular bone induced by OVX or estrogen insufficiency might be associated with signaling pathways involved in the acceleration of bone resorption. From this view of point, supplementation of PCA normalized the RANKL/OPG ratio, which is a good marker of severe osteolysis, by increasing the production of OPG and downregulating the production of RANKL

(Figure 5). Alternatively, increased levels of osteocalcin and BALP, which are synthesized by osteoblasts and considered markers of bone turnover, were significantly attenuated by treatment with PCA or E₂ compared to the OVX control group (Figure 8). It seems that the administration of PCA might also affect osteoblast activity, although the underlying mechanisms require further study.

TRAF6 has been shown to be a major adaptor molecule in signal transduction of RANK-RANKL, leading to activation of NFATc1 [36, 37], which functions as a major regulator of osteoclastogenesis via upregulation of osteoclast-specific genes such as cathepsin K, calcitonin receptor, osteoclast-associated receptor (OSCAR), and $\beta 3$ integrin, in concert with transcription factors such as activator protein-1 (AP-1), PU.1, microphthalmia-associated

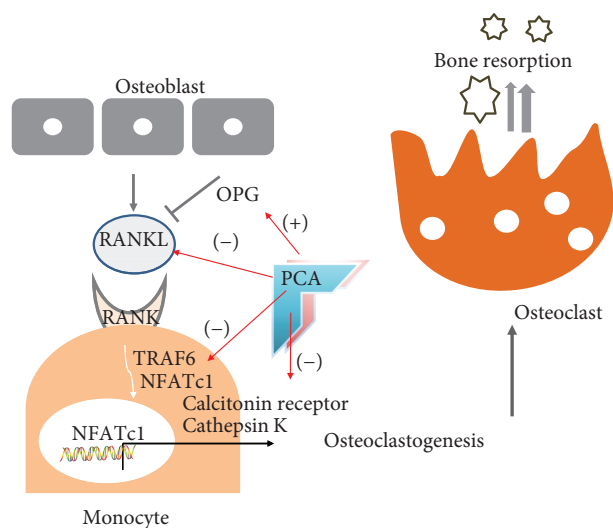


FIGURE 9: Summary of inhibitory potential of PCA against osteoclastogenesis in OVX mice. NFATc1: nuclear factor of activated T cell cytoplasmic 1; OPG: osteoprotegerin; PCA: protocatechuic acid; RANK: receptor activator of nuclear factor κ B; RANKL: RANK ligand; TRAF6: TNF receptor-associated factor-6; (+): increase; (-): decrease.

transcription factor [36]. In the present study, the mRNA expression levels of TRAF6 and NFATc1 were significantly increased in OVX mice, but these increases were suppressed by administration of PCA (Figure 6). The expression of other signaling molecules involved in osteoclast differentiation, such as cathepsin K and calcitonin receptor, in OVX mice was significantly inhibited by supplementation with PCA (Figure 7).

In summary, the inhibitory potential of PCA against osteoclastogenesis, which augments bone resorption in OVX or postmenopausal conditions, was demonstrated in the OVX mouse model. As summarized in Figure 9, the underlying mechanism of PCA in the suppression of bone loss in OVX mice may be associated with the following effects: (1) reduction of serum level of RANKL and increase in OPG; (2) blocking the RANK signaling pathway via downregulation of TRAF6 and NFATc1 expression; and (3) attenuation of cathepsin K and calcitonin receptor expression. PCA shows promise as a starting compound or alternative to estrogenic constituents in the development of antiosteoporotic compounds with improved safety. The exact signaling target of PCA involved in the suppression of osteoclastogenesis and/or improved bone formation mediated by osteoblasts in OVX mice remains unclear. This issue should be further investigated in future research to develop new antiosteoporotic compounds based on the action of PCA.

Abbreviations

BALP:	Bone alkaline phosphatase
BMD:	Bone mineral density
CT:	Computed tomography
E2:	17 β -estradiol
OPG:	Osteoprotegerin

NFATc1:	Nuclear factor of activated T cell cytoplasmic 1
OVX:	Ovariectomized
PBS:	Phosphate-buffered saline
PCA:	Protocatechuic acid
RANK:	Receptor activator of nuclear factor kappa B
RANKL:	Receptor activator of nuclear factor κ B ligand
RT-PCR:	Reverse transcription polymerase chain reaction
TARP:	Tartrate-resistant acid phosphatase
TRAF6:	Tumor necrosis factor receptor-associated factor-6
b.w.:	Body weight
i.p.:	Intraperitoneal.

Data Availability

The data used to support the findings of this study are available from the corresponding author upon request.

Conflicts of Interest

The authors declare that they have no conflict of interest.

Acknowledgments

This research was supported by the Ministry of Trade, Industry & Energy (MOTIE) and Korea Institute for Advancement of Technology (KIAT) through the Encouragement Program for the Industries of Economic Cooperation Region (R0000429).

References

- [1] S. Kakkar and S. Bais, "A review on protocatechuic acid and its pharmacological potential," *ISRN Pharmacology*, vol. 2014, Article ID 952943, 9 pages, 2014.
- [2] Y. Semaming, P. Pannengetch, S. C. Chattipakorn, and N. Chattipakorn, "Pharmacological properties of protocatechuic acid and its potential roles as complementary medicine," *Evidence-based Complementary and Alternative Medicine*, vol. 2015, Article ID 593902, 11 pages, 2015.
- [3] A. K. Khan, R. Rashid, N. Fatima et al., "Pharmacological activities of protocatechuic acid," *Acta Poloniae Pharmaceutica*, vol. 72, no. 4, pp. 643–650, 2015.
- [4] H. Chen and K. Y. Kubo, "Bone three-dimensional microstructural features of the common osteoporotic fracture sites," *World Journal of Orthopedics*, vol. 5, no. 4, pp. 486–495, 2014.
- [5] H. K. Vaananen, "Mechanism of bone turnover," *Annals of Medicine*, vol. 25, no. 4, pp. 353–359, 1993.
- [6] M. J. Seibel, "Biochemical markers of bone turnover: part I: biochemistry and variability," *The Clinical Biochemist Reviews*, vol. 26, no. 4, pp. 97–122, 2005.
- [7] M. L. Bouxsein, "Mechanisms of osteoporosis therapy: a bone strength perspective," *Clinical Cornerstone*, vol. 5, Supplement 2, pp. S13–S21, 2003.
- [8] A. Nazarian, D. von Stechow, D. Zurakowski, R. Müller, and B. D. Snyder, "Bone volume fraction explains the variation in strength and stiffness of cancellous bone affected by metastatic cancer and osteoporosis," *Calcified Tissue International*, vol. 83, no. 6, pp. 368–379, 2008.

- [9] C. H. Wilkins, "Osteoporosis screening and risk management," *Clinical Interventions in Aging*, vol. 2, no. 3, pp. 389–394, 2007.
- [10] N. E. Lane, "Epidemiology, etiology, and diagnosis of osteoporosis," *American Journal of Obstetrics and Gynecology*, vol. 194, no. 2, pp. S3–11, 2006.
- [11] R. G. Josse, "Osteoporosis: an update on pathogenesis and treatment," *Canadian Family Physician*, vol. 29, no. 11, pp. 2113–2118, 1983.
- [12] M. M. Iqbal, "Osteoporosis: epidemiology, diagnosis, and treatment," *Southern Medical Journal*, vol. 93, no. 1, pp. 2–18, 2000.
- [13] B. L. Riggs, S. Khosla, and L. J. Melton III, "A unitary model for involutional osteoporosis: estrogen deficiency causes both type I and type II osteoporosis in postmenopausal women and contributes to bone loss in aging men," *Journal of Bone and Mineral Research*, vol. 13, no. 5, pp. 763–773, 1998.
- [14] S. C. Manolagas, "Birth and death of bone cells: basic regulatory mechanisms and implications for the pathogenesis and treatment of osteoporosis," *Endocrine Reviews*, vol. 21, no. 2, pp. 115–137, 2000.
- [15] V. Nagy and J. M. Penninger, "The RANKL-RANK story," *Gerontology*, vol. 61, no. 6, pp. 534–542, 2015.
- [16] S. L. Teitelbaum, "Bone resorption by osteoclasts," *Science*, vol. 289, no. 5484, pp. 1504–1508, 2000.
- [17] H. Takayanagi, K. Ogasawara, S. Hida et al., "T-cell-mediated regulation of osteoclastogenesis by signalling cross-talk between RANKL and IFN- γ ," *Nature*, vol. 408, no. 6812, pp. 600–605, 2000.
- [18] J. H. Kim and N. Kim, "Regulation of NFATc1 in osteoclast differentiation," *Journal of Bone Metabolism*, vol. 21, no. 4, pp. 233–241, 2014.
- [19] S. Boonen, E. Rosenberg, F. Claessens, D. Vanderschueren, and S. Papapoulos, "Inhibition of cathepsin K for treatment of osteoporosis," *Current Osteoporosis Reports*, vol. 10, no. 1, pp. 73–79, 2012.
- [20] J. Marsden, "The menopause, hormone replacement therapy and breast cancer," *The Journal of Steroid Biochemistry and Molecular Biology*, vol. 83, no. 1–5, pp. 123–132, 2002.
- [21] Y. X. Wu, T. Y. Wu, B. B. Xu et al., "Protocatechuic acid inhibits osteoclast differentiation and stimulates apoptosis in mature osteoclasts," *Biomedicine & Pharmacotherapy*, vol. 82, no. 8, pp. 399–405, 2016.
- [22] A. Rivera-Piza, Y. J. An, D. K. Kim et al., "Protocatechuic acid enhances osteogenesis, but inhibits adipogenesis in C3H10T1/2 and 3T3-L1 cells," *Journal of Medicinal Food*, vol. 20, no. 3, pp. 309–319, 2017.
- [23] G. Xu, Q. Y. Pei, C. G. Ju, F. Zhang, and T. Z. Jia, "Detection on effect of different processed *Cibotium barometz* on osteoblasts by CCK-8," *Zhongguo Zhong Yao Za Zhi*, vol. 38, no. 24, pp. 4319–4323, 2013.
- [24] S. H. Park, J. Y. Kim, Y. H. Cheon et al., "Protocatechuic acid attenuates osteoclastogenesis by downregulating JNK/c-Fos/NFATc1 signaling and prevents inflammatory bone loss in mice," *Phytotherapy Research*, vol. 30, no. 4, pp. 604–612, 2016.
- [25] H. Jung Koo, E. H. Sohn, Y. J. Kim, S. A. Jang, S. Namkoong, and S. Chan Kang, "Effect of the combinatory mixture of *Rubus coreanus* Miquel and *Astragalus membranaceus* Bunge extracts on ovariectomy-induced osteoporosis in mice and anti-RANK signaling effect," *Journal of Ethnopharmacology*, vol. 151, no. 2, pp. 951–959, 2014.
- [26] S. S. Henriksen, M. Ding, M. Vinther Juhl, N. Theilgaard, and S. Overgaard, "Mechanical strength of ceramic scaffolds reinforced with biopolymers is comparable to that of human bone," *Journal of Materials Science: Materials in Medicine*, vol. 22, no. 5, pp. 1111–1118, 2011.
- [27] M. L. Brandi, "Microarchitecture, the key to bone quality," *Rheumatology*, vol. 48, Supplement 4, pp. iv3–iv8, 2009.
- [28] Y. Yang, F. Pan, F. Wu et al., "Familial resemblance in trabecular and cortical volumetric bone mineral density and bone microarchitecture as measured by HRpQCT," *Bone*, vol. 110, no. 5, pp. 76–83, 2018.
- [29] A. Sakai, S. Nishida, N. Okimoto et al., "Bone marrow cell development and trabecular bone dynamics after ovariectomy in ddy mice," *Bone*, vol. 23, no. 5, pp. 443–451, 1998.
- [30] J. Hong, R. E. Stubbins, R. R. Smith, A. E. Harvey, and N. P. Núñez, "Differential susceptibility to obesity between male, female and ovariectomized female mice," *Nutrition Journal*, vol. 8, no. 1, p. 11, 2009.
- [31] S. Nilsson, S. Mäkelä, E. Treuter et al., "Mechanisms of estrogen action," *Physiological Reviews*, vol. 81, no. 4, pp. 1535–1565, 2001.
- [32] T. Kataoka, M. Tamura, A. Maeno, S. Wakana, and T. Shiroishi, "Genetic dissection of trabecular bone structure with mouse intersubspecific consomic strains," *G3: Genes, Genomes, Genetics*, vol. 7, no. 10, pp. 3449–3457, 2017.
- [33] S. Khosla, "Minireview: the OPG/RANKL/RANK system," *Endocrinology*, vol. 142, no. 12, pp. 5050–5055, 2001.
- [34] W. J. Boyle, W. S. Simonet, and D. L. Lacey, "Osteoclast differentiation and activation," *Nature*, vol. 423, no. 6937, pp. 337–342, 2003.
- [35] T. L. Burgess, Y. Qian, S. Kaufman et al., "The ligand for osteoprotegerin (OPGL) directly activates mature osteoclasts," *The Journal of Cell Biology*, vol. 145, no. 3, pp. 527–538, 1999.
- [36] Q. Zhao, J. Shao, W. Chen, and Y.-P. Li, "Osteoclast differentiation and gene regulation," *Frontiers in Bioscience*, vol. 12, no. 1, pp. 2519–2529, 2007.
- [37] Q. Zhao, X. Wang, Y. Liu, A. He, and R. Jia, "NFATc1: functions in osteoclasts," *The International Journal of Biochemistry & Cell Biology*, vol. 42, no. 5, pp. 576–579, 2010.

Research Article

The Antidiabetic and Antinephritic Activities of *Tuber melanosporum* via Modulation of Nrf2-Mediated Oxidative Stress in the db/db Mouse

Xue Jiang, Shanshan Teng, Xue Wang, Shan Li, Yaqin Zhang, and Di Wang 

School of Life Sciences, Jilin University, Changchun 130012, China

Correspondence should be addressed to Di Wang; jluwangdi@outlook.com

Received 11 February 2018; Revised 15 June 2018; Accepted 26 June 2018; Published 29 July 2018

Academic Editor: Anderson J. Teodoro

Copyright © 2018 Xue Jiang et al. This is an open access article distributed under the Creative Commons Attribution License, which permits unrestricted use, distribution, and reproduction in any medium, provided the original work is properly cited.

Tuber melanosporum (TM), a valuable edible fungus, contains 19 types of fatty acid, 17 types of amino acid, 6 vitamins, and 7 minerals. The antidiabetic and antinephritic effects of TM and the underlying mechanisms related to oxidative stress were investigated in db/db mice. Eight-week oral administration of metformin (Met) at 0.1 g/kg and TM at doses of 0.2 and 0.4 g/kg decreased body weight, plasma glucose, serum levels of glycated hemoglobin, triglyceride, and total cholesterol and increased serum levels of high-density lipoprotein cholesterol in the mice, suggesting hypoglycemic and hypolipidemic effects. TM promoted glucose metabolism by increasing the levels of pyruvate kinase and hepatic glycogen. It also regulated the levels of inflammatory factors and oxidative enzymes in serum and/or the kidneys of the mice. Additionally, TM increased the expression of nuclear respiratory factor 2 (Nrf2), catalase, heme oxygenase 1, heme oxygenase 2, and manganese superoxide dismutase 2 and decreased the expression of protein kinase C alpha, phosphor-janus kinase 2, phosphor-signal transducer and activator of transcription 3, and phosphor-nuclear factor- κ B in the kidneys. The results of this study reveal the antidiabetic and antidiabetic nephritic properties of TM via modulating oxidative stress and inflammation-related cytokines through improving the Nrf2 signaling pathway.

1. Introduction

The incidence of diabetes mellitus (DM), a metabolic disturbance disease characterized by chronic hyperglycemia [1], has increased rapidly worldwide. Currently, a global population of 382 million people are diagnosed with DM and this number is predicted to rise to 592 million by 2035 [2]. Type 2 diabetes mellitus (T2DM), which is associated with β -cell dysfunction and insulin resistance and/or insulin secretion deficiency, is the most common form of DM [3]. Prolonged hyperglycemia in DM results in various secondary complications including nephropathy, hepatic damage, retinopathy, neuropathy, and cardiovascular disease [4–6]. Diabetic nephropathy (DN), a leading cause of end-stage renal disease, is the most common diabetic microvascular complication with high mortality and morbidity [7]. The progression of DN is associated with hyperglycemia, hyperlipidemia, and oxidative stress [8]. Renal inflammation

resulting from the accumulation of inflammatory cells in the kidney has been reported as a key factor in the development of DN [9]. Furthermore, mesangial expansion and renal tubule damage, the major morphological alterations of DN, are associated with oxidative stress [10]. Hyperglycemia leads to the overproduction of mitochondrial superoxide, which causes the accumulation of intracellular reactive oxygen species (ROS) that are responsible for the defective angiogenesis and inflammatory pathway activation [11].

Current antidiabetic therapies have some limitations. Moreover, DM is a chronic disease with miscellaneous complications that require long-term treatment. Some effective Western medicines for diabetes are associated with high cost and adverse effects [12]. Furthermore, many treatments, such as oral antihyperglycemic agents and insulin injections, only address blood glucose regulation and β -cell function and have little therapeutic effect on complications [13]. Therefore, it is necessary to find alternative agents for the treatment

of diabetes and its complications that have lower costs and fewer side effects.

Edible fungi have been used as folk tonic foods and/or medicines to prevent and/or treat diseases due to their efficacy and auxiliary therapeutic effects with few adverse effects [14, 15]. *Tuber melanosporum* (TM), an edible fungus containing many nutritional components [16], has been shown to exhibit antiviral, antimutagenic, antimicrobial, and anti-inflammatory activities [17]. However, the antidiabetic and antinephritic activities of TM and their underlying mechanisms have not yet been reported.

In this study, leptin receptor deficient (db/db) mice, which are systemic mutation mice that develop hyperinsulinemia and insulin resistance at 2 weeks old and then exhibit β -cell failure and hyperglycemia after 4 weeks [18], were used as a model to observe the effects of TM on diabetes and diabetic nephropathy and expose underlying mechanisms related to oxidative stress. Our results provide the first experimental evidence to support the development of TM as functional food for adjuvant therapy for diabetes and diabetic nephropathy.

2. Materials and Methods

2.1. Measurement of the TM Components. A TM fruiting body (purchased from Senzhong Co. Ltd., Yunnan, China) was pulverized in a crushing machine and stored in a dryer for the subsequent experiment.

2.1.1. Main Component Analysis. The quantities of the main TM components including total sugar, reducing sugar, protein, total ash, crude fat, crude fiber, and total polyphenols were measured using the phenol-sulfuric acid method [19], direct titration [20], the Kjeldahl method [21], combustion [22], Soxhlet extraction [23], double differences method [24], and the Folin-Ciocalteu method [25], respectively. The quantities of triterpenoids, mannitol, and vitamins were measured using high-performance liquid chromatography (HPLC) [26–28]. Total flavonoids, carotenoids, and sterols were measured using UV spectrophotometry [29–31].

2.1.2. Fatty Acid Analysis. TM was extracted via reflux extraction at 80°C with 2% NaOH in a methanol solution, and then a 14% BF₃ solution was added and the mixture was incubated for another 10 min. After cooling to room temperature, a saturated solution of NaCl and n-heptane was added. The collected supernatant was mixed with anhydrous sodium sulfate, and the levels of fatty acids were analyzed using gas chromatography (GC, Agilent 7890A) [32].

2.1.3. Amino Acid Analysis. TM was hydrolyzed using 6 mol/L of HCl at 110°C for 24 h. After vacuum drying, the samples were dissolved in 1 mL hydrochloric acid (HCl) solution (0.02 mol/L), which was mixed with triethylamine acetonitrile (1 mol/L) and phenyl isothiocyanate (0.1 mol/L) in a ratio of 2:1:1 (V:V:V). After the addition of 2 mL n-hexane for 10 min, a quantitative analysis of the amino acids was carried out by HPLC (Agilent 1260; column: Agilent C18 (4.6 × 250 mm × 5 μ m); mobile phase A: 0.1 mol/L sodium

acetate solution/acetonitrile (1:1); mobile phase B: acetonitrile/ultrapure water (8:2); flow rate: 1.0 mL/min) [33].

2.1.4. Mineral Analysis. After pretreating the TM with hydrogen nitrate for 27 min (3 min at 100°C, 3 min at 140°C, 3 min at 160°C, 3 min at 180°C, and 15 min at 190°C), the levels of zinc, iron, manganese, calcium, copper, sodium, and potassium were detected using inductively coupled plasma optical emission spectrometry (ICP-OES, Optima 8000) [34], and lead, mercury, chromium, arsenic, cadmium, and selenium were analyzed using inductively coupled plasma mass spectrometry (ICP-MS, Thermo Fisher Scientific ICAPQ) [35].

2.2. Animal Care and Experimental Design. The experimental animal protocol was approved by the Ethical Committee of Animal Research of Jilin University (20170301). All efforts were made to minimize animal suffering and reduce the number of animals used, according to the recommendations of Laboratory Animal Care and Use. The db/db mice and wild db/+ littermates (8 weeks, male, SCXK (Su) 2015-0001) were purchased from the Nanjing Biomedical Research Institute of Nanjing University, Nanjing, China. The db/db mice develop hyperinsulinemia and insulin resistance at 2 weeks age and then exhibit β -cell failure and hyperglycemia after 4 weeks. Therefore, the db/db mice were chosen to be a common diabetes model to accurately reflect the pathophysiology of diabetes [18]. All of the mice were housed on a 12-h light-dark cycle (lights on 07:00–19:00) and food available (growth and reproduction fodder of mice) ad libitum in a quiet room at a temperature of 23 ± 1°C and humidity of 60%.

The drug administration and study protocol are shown in Figure 1(a). Doses and the administration route were selected based on preliminary experiments performed in our laboratory. After one week adaptation, the db/+ mice were given physiological saline by oral administration for eight weeks and served as the control group ($n = 12$). The db/db mice with blood glucose levels > 11.1 mmol/L were randomly divided into four groups ($n = 12$ /group) and orally administered with physiological saline (model group), Met at 0.1 g/kg (positive control group), and TM at doses of 0.2 and 0.4 g/kg once a day for eight weeks.

2.3. Oral Glucose Tolerance Test in db/db Mice. The oral glucose tolerance test (OGTT) was performed in overnight-fasted db/db mice after the last drug administration. All mice were orally administered with 2.0 g/kg of glucose. Blood samples were collected from the tail vein at 0, 30, 60, 120, and 240 min and assayed using a fast blood glucose meter [36]. The formula used for determining the area under the blood glucose curve (AUC) was as follows [37]: $AUC = (\text{basal glycemia} + \text{glycemia } 0.5 \text{ h}) \times 0.25 + (\text{glycemia } 0.5 \text{ h} + \text{glycemia } 1 \text{ h}) \times 0.25 + (\text{glycemia } 1 \text{ h} + \text{glycemia } 2 \text{ h}) \times 0.5$.

2.4. Sample Collection and Parameter Determination. Blood was sampled via the tail vein before the mice were sacrificed. After centrifugation of the blood samples at 3000 rpm for 10 min, the serum was collected and stored at -80°C for further use. After sacrifice, the kidney and liver tissues were collected and one part of the tissues was washed in ice-cold

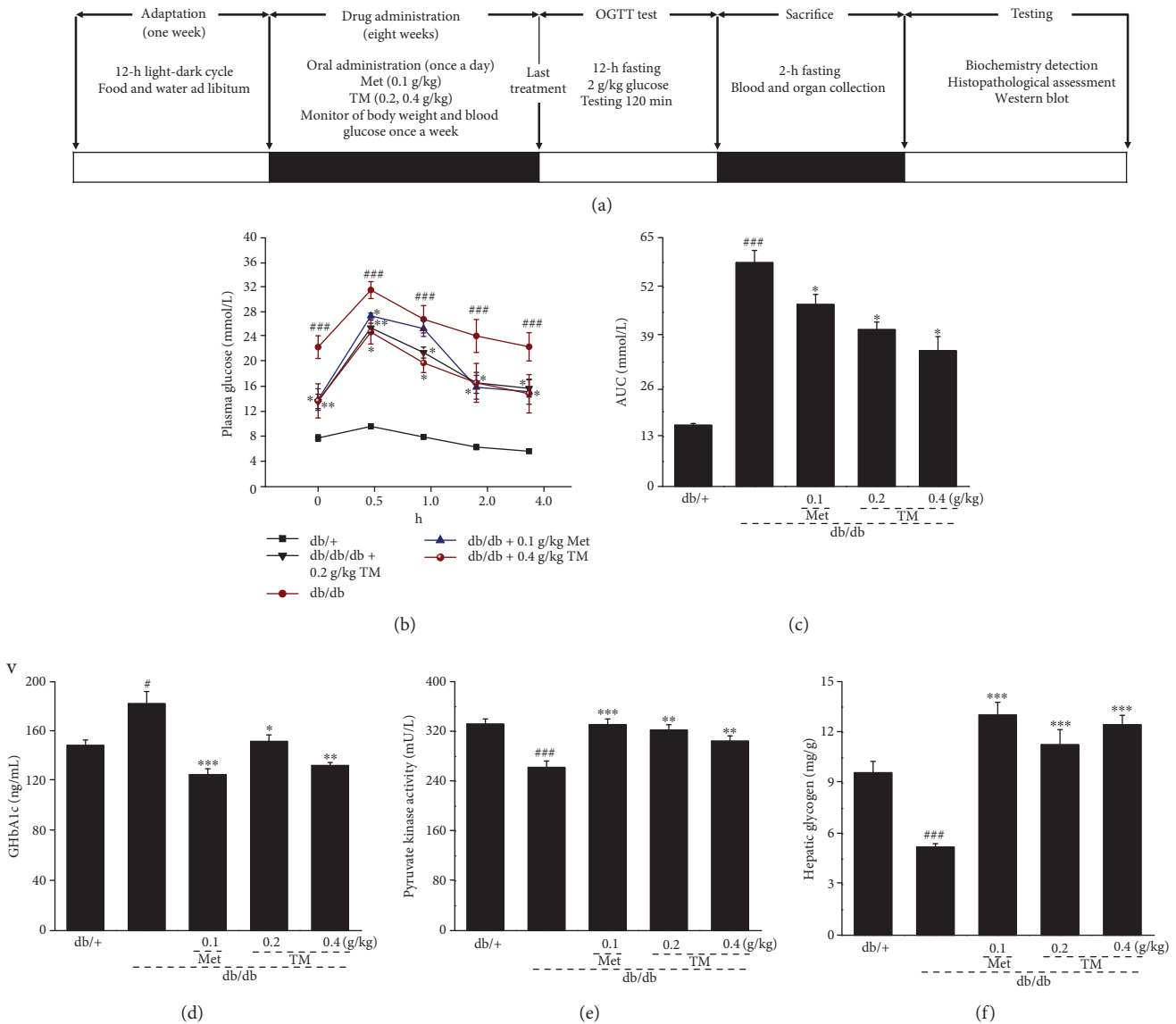


FIGURE 1: (a) The drug administration and study protocol. Eight-week TM treatment affected the (b) oral glucose tolerance, (c) AUC, (d) the serum levels of GHbA1c, (e) the serum levels of PK, and (f) the content of hepatic glycogen in db/db mice compared to db/+ mice. The data were analyzed using post hoc test of Holm-Sidak, and they are expressed as means \pm SEMs ($n = 10$). # $p < 0.05$ and ### $p < 0.001$ versus db/+ mice; * $p < 0.05$, ** $p < 0.01$, and *** $p < 0.001$ versus nontreated db/db mice. TM: *T. melanosporum*; AUC: the area under the curve of glucose of oral glucose tolerance; GHbA1c: glycosylated hemoglobin A1c; PK: pyruvate kinase.

physiological saline solution and then homogenized in double-distilled water and/or a radioimmunoprecipitation assay buffer (RIPA; Sigma-Aldrich, USA) containing 1% protease inhibitor cocktail and 2% phenylmethanesulfonyl fluoride (Sigma-Aldrich, USA).

The levels of interleukins (ILs) IL-2 (cat. number CK-E20010), IL-6 (cat. number CK-E20012), and IL-10 (cat. number CK-E20005), 6-keto-prostaglandin F1 α (6-K-PGF1 α ; cat. number CK-E30144), monocyte chemoattractant protein-5 (MCP-5; cat. number CK-E95264), matrix metalloproteinase-9 (MMP-9; cat. number CK-E90157), urine N-acetyl- β -D-glucosidase (NAG; cat. number CK-E20276), and ROS (cat. number CK-E91516) in the kidney; the levels of glycated hemoglobin A1c (GhbA1c; cat. number CK-E20512), triglyceride (TG; cat. number CK-E91733),

total cholesterol (TC; cat. number CK-E91839), high-density lipoprotein cholesterol (HDL-C; cat. number CK-E93031), low-density lipoprotein cholesterol (LDL-C; cat. number CK-E93032), and pyruvate kinase (PK; cat. number CK-E20312) in serum; and the levels of superoxide dismutase (SOD; cat. number CK-E20348), glutathione peroxidase (GSH-Px; cat. number CK-E92669), and catalase (CAT; cat. number CK-E92636) in the kidney and serum were detected by enzyme-linked immunosorbent assay (ELISA) according to the manufacturer's instructions (Shanghai Yuanye Bio-Technology Co. Ltd., Shanghai, China). The concentration of hepatic glycogen (HG; cat. number A043) was detected by the procedures provided by the manufacturer of the assay kit (Nanjing Jiancheng Bioengineering Institute, Nanjing, China) [38].

2.5. Histopathological Observation of the Kidneys. Histologic assessment of the kidneys was carried out as in a previous study [39]. Briefly, tissues were fixed with 10% neutral phosphate-buffered formalin for 48 h, embedded in paraffin, and sliced into 5 μm thick sections. After staining with hematoxylin and eosin (H&E) and periodic acid Schiff (PAS), histopathological examination was carried out using optical microscopy.

2.6. Western Blot. One part of the collected kidney tissue was homogenized in RIPA containing 1% protease inhibitor cocktail and 2% phenylmethanesulfonyl fluoride. Protein concentrations were determined by the Bradford method, and 40 μg of protein was separated using 12% SDS-PAGE gel and electroblotted onto a nitrocellulose membrane (0.45 μm ; Bio Basic Inc., USA). After blocking with 5% BSA for 4 h, the transferred membranes were incubated with the following primary antibodies overnight at 4°C at a dilution of 1:2000: phosphor-janus kinase 2 (p-JAK2, ab68268), total-janus kinase 2 (t-JAK2, ab39636), phosphor-nuclear factor- κB (p-NF- κB , ab86299), total-NF- κB (t-NF- κB , ab32536), phosphor-signal transducer and activator of transcription 3 (p-STAT3, ab76315), total-STAT3 (t-STAT3, M06-596), catalase (CAT, ab16731), heme oxygenase 1 (HO-1, ab68477), nuclear respiratory factor 2 (Nrf2, ab137550), manganese superoxide dismutase 2 (SOD2, ab13533), heme oxygenase 2 (HO-2, ab90492), protein kinase C alpha (PKC- α , ab23513) (Abcam, Cambridge, USA), and glyceraldehyde-3-phosphate dehydrogenase (GAPDH; ABS16) (Merck Millipore, Darmstadt, Germany). After 5 washes with TBST buffer, the transferred membranes were incubated with horseradish peroxidase-conjugated goat anti-rabbit secondary antibody (sc-3836) (Santa Cruz Biotechnology, Santa Cruz, USA) for 4 h at 4°C. Chemiluminescence was detected using Immobilon Western HRP substrate (Millipore Corporation, Billerica, USA). The intensity of the bands was quantified by scanning densitometry using an imaging system (Ultra-Violet Products Ltd., Cambridge, UK).

2.7. Statistical Analysis. Data were analyzed using SPSS 16.0 software (IBM Corporation, Armonk, USA), and continuous variables were expressed as mean \pm SEM. A homoscedasticity test was carried out. A post hoc Holm-Sidak test was used to calculate statistical significance. A p value under 0.05 was considered statistically significant.

3. Results

3.1. Composition of TM. The TM contained 35.60% total sugars, 2.90% reducing sugar, 13.10% protein, 6.60% total ash, 7.30% crude fat, 5.00% crude fiber, 0.59% total flavones, 0.04% total triterpenoids, 1.25% mannitol, 0.67% total polyphenols, $3.20 \times 10^{-4}\%$ carotenoids, and 3.58% total sterols (Table 1). Among the 35 types of fatty acid detected, only 19 were found in the TM sample (Table 2). Among 17 types of detected amino acid, glutamic acid, aspartic acid, and lysine were present at higher concentrations than others (Table 3). Among 9 detected vitamins, the three most common were vitamins C, B₃, and D₂ (Table 4). The minerals

TABLE 1: Main components of TM.

Compounds	Contents (%)
Total sugar	35.60
Reducing sugar	2.90
Protein	13.10
Total ash	6.60
Crude fat	7.30
Crude fiber	5.00
Total flavones	0.59
Total triterpenoids	0.04
Mannitol	1.25
Total polyphenol	0.67
Carotenoid ($\times 10^{-4}$)	3.20
Total sterol	3.58

TM: *T. melanosporum*.

Zn, Fe, Mn, Ca, Cu, Na, and K were also detected (Table 5), and the concentrations of the heavy metals Pb, Hg, Cr, As, and Cd were lower than the detection limits of traditional analytical techniques, which indicates the safety of using TM (Table 5).

3.2. The Hypoglycemic Effect of TM on db/db Mice. Compared with the db/+ mice, the db/db mice had increased body weights and plasma glucose levels and reduced organ indexes of the spleen and kidney ($p < 0.001$, Table 6). After 8 weeks oral administration, 0.4 g/kg of TM reduced body weight by over 11% and plasma glucose by over 30% ($p < 0.05$, Table 6). The reduced indexes of the spleen and kidneys of the db/db mice were strongly improved by 0.4 g/kg of TM administration ($p < 0.05$, Table 6).

As a more sensitive indicator of early abnormalities of glucose regulation than fasting blood glucose, the OGGT was conducted after 8 weeks administration of TM to confirm its antihyperglycemic capacity [40]. The concentration of fasting blood glucose in the db/db mice was significantly higher than that of the db/+ mice within 4 h of 2.0 g/kg glucose administration. Similar to the Met group, the TM-treated db/db mice showed a significant reduction in blood glucose levels from 30 min to 4 h ($p < 0.05$, Figure 1(b)). Compared to the db/db mice, a significantly low AUC was noted in the TM and Met-treated mice ($p < 0.05$, Figure 1(c)). High serum levels of GHbA1c were observed in the db/db mice ($p < 0.05$, Figure 1(d)); 0.1 g/kg of Met and 0.2 g/kg and 0.4 g/kg of TM reduced GHbA1c levels by 31.2% ($p < 0.001$), 16.6% ($p < 0.05$), and 27.2% ($p < 0.01$), respectively (Figure 1(d)).

PK can promote carbohydrate metabolism by contributing to the glycolytic pathway [41]. Compared to the non-treated db/db mice, the mice that received 8 weeks TM administration exhibited a >16.1% increase in serum PK levels ($p < 0.01$, Figure 1(e)) and an increase in HG content of >120% ($p < 0.001$, Figure 1(f)).

3.3. The Hypolipidemic Effects of TM in db/db Mice. As diabetes mellitus is commonly accompanied by hyperlipidemia

TABLE 2: The compositions and percentage content of fatty acids in TM.

Compounds	Contents (%)	Compounds	Contents (%)	Compounds	Contents (%)
Octoic acid (C8:0)	ND ^I	Heptadecenoic acid (C17:1) ($\times 10^{-2}$)	0.20	Docosanoic acid (C22:0) ($\times 10^{-3}$)	0.02
Capric acid (C10:0)	ND ^{II}	Stearic acid (C18:0)	0.46	Eicosatrienoic acid (C20:3n6)	ND ^X
Undecanoic acid (C11:0)	ND ^{III}	<i>trans</i> -Oleic acid (C18:1n9t) ($\times 10^{-2}$)	0.20	Erucic acid (C22:1n9) ($\times 10^{-2}$)	0.30
Lauric acid (C12:0)	ND ^{IV}	Oleic acid (C18:1n9c)	1.79	Eicosatrienoic acid (C20:3n3)	ND ^{XI}
Tridecanoic acid (C13:0)	ND ^V	<i>trans</i> -Linoleic acid (C18:2n6t)	ND ^{VII}	Arachidonic acid (C20:4n6)	ND ^{XII}
Myristic acid (C14:0) ($\times 10^{-2}$)	0.40	Linoleic acid (C18:2n6c)	3.85	Tricosanoic acid (C23:0) ($\times 10^{-2}$)	0.40
Myristoleic acid (C14:1)	ND ^{VI}	Arachidic acid (C20:0)	0.05	Docosadienoic acid (C22:2n6)	ND ^{XIII}
Pentadecanoic acid (C15:0) ($\times 10^{-2}$)	0.10	γ -Linolenic acid (C18:3n6)	ND ^{VIII}	Eicosapentaenoic acid (C20:5n3)	ND ^{XIV}
Pentadecenoic acid (C15:1)	ND ^{VII}	Eicosaenoic acid (C20:1n9)	0.03	Tetracosanoic acid (C24:0)	0.02
Hexadecanoic acid (C16:0)	0.64	α -Linolenic acid (C18:3n3)	ND ^{IX}	Nervonic acid (C24:1n9)	0.01
Palmitoleic acid (C16:1)	0.01	Heneicosanoic acid (C21:0) ($\times 10^{-2}$)	0.30	Docosahexaenoic acid (C22:6n3)	ND ^{XV}
Heptadecanoic acid (C17:0) ($\times 10^{-2}$)	0.70	Eicosadienoic acid (C20:2)	0.04		

ND: not detected; ND^I: the detection limit was 4.20 mg/kg; ND^{II}: the detection limit was 3.83 mg/kg; ND^{III}: the detection limit was 3.54 mg/kg; ND^{IV}: the detection limit was 2.99 mg/kg; ND^V: the detection limit was 2.91 mg/kg; ND^{VI}: the detection limit was 2.82 mg/kg; ND^{VII}: the detection limit was 2.64 mg/kg; ND^{VIII}: the detection limit was 2.51 mg/kg; ND^{IX}: the detection limit was 2.36 mg/kg; ND^X: the detection limit was 2.68 mg/kg; ND^{XI}: the detection limit was 3.21 mg/kg; ND^{XII}: the detection limit was 4.66 mg/kg; ND^{XIII}: the detection limit was 2.88 mg/kg; ND^{XIV}: the detection limit was 3.31 mg/kg; ND^{XV}: the detection limit was 4.33 mg/kg.

TABLE 3: The compositions and percentage content of amino acids in TM.

Compounds	Contents (%)	Compounds	Contents (%)
Aspartic acid (Asp)	12.69	Proline (Pro)	5.77
Glutamic acid (Glu)	20.46	Tyrosine (Tyr)	5.53
Cystine (Cys)	5.75	Valine (Val)	5.76
Serine (Ser)	6.45	DL-methionine (Met)	1.61
Glycine (Gly)	7.48	Isoleucine (Ile)	4.38
Histidine (His)	3.69	Leucine (Leu)	6.48
Arginine (Arg)	9.94	Phenylalanine (Phe)	4.16
L-Threonine (Thr)	5.95	Lysine (Lys)	10.48
Alanine (Ala)	7.36		

TM: *T. melanosporum*.

TABLE 4: The compositions and percentage content of vitamins in TM.

Compounds	Contents (mg/kg)	Compounds	Contents (mg/kg)
Vitamin A	0.07	Vitamin B ₁	70.43
Vitamin B ₂	24.62	Vitamin B ₃	1533.01
Vitamin B ₆	ND ^{XVI}	Vitamin C	1706.52
Vitamin D ₂	196.64	Vitamin D ₃	ND ^{XVIII}
Vitamin E	ND ^{XVII}		

TM: *T. melanosporum*. ND^{XVI}: the detection limit was 2.92 mg/kg; ND^{XVII}: the detection limit was 1.32 mg/kg; ND^{XVIII}: the detection limit was 0.084 mg/kg.

TABLE 5: The compositions and percentage content of minerals (including heavy metals) in TM.

Compounds	Contents (‰)	Compounds	Contents (μ g/kg)
Zinc (Zn)	1.04	Lead (Pb)	119.70
Iron (Fe)	1.03	Mercury (Hg)	219.62
Manganese (Mn)	0.08	Chromium (Cr)	5595.99
Calcium (Ca)	9.67	Arsenic (As)	75.06
Copper (Cu)	0.68	Cadmium (Cd)	1417.40
Sodium (Na)	0.65	Selenium (Se)	ND ^{XIX}
Potassium (K)	208.10		

TM: *T. melanosporum*. ND^{XIX}: not detected (the detection limit was 20 μ g/kg).

TABLE 6: Effects of 8-week TM treatment on the bodyweight, plasma glucose, and organ indices of mice.

	Week	db/+	db/db	0.1 g/kg Met	0.2 g/kg TM	0.4 g/kg TM
Body weights (g)	1	20.2 ± 0.4	43.2 ± 0.4 ^{###}	42.9 ± 0.8	43.3 ± 0.8	43.6 ± 0.7
	3	21.4 ± 0.4	45.0 ± 0.7 ^{###}	44.8 ± 0.7	46.5 ± 0.8	44.8 ± 0.7
	5	20.9 ± 0.4	48.0 ± 1.1 ^{###}	43.9 ± 0.9*	45.3 ± 1.2	43.6 ± 0.8*
	7	21.7 ± 0.3	51.7 ± 1.0 ^{###}	47.5 ± 1.2*	50.2 ± 1.3	47.6 ± 0.8*
	9	21.1 ± 0.7	55.7 ± 0.9 ^{###}	52.9 ± 0.4*	52.8 ± 1.4	49.5 ± 1.2**
Plasma glucose (mmol/L)	1	5.6 ± 0.4	19.1 ± 1.4 ^{###}	19.6 ± 1.2	17.4 ± 0.9	18.8 ± 2.1
	3	6.9 ± 0.4	19.6 ± 1.5 ^{###}	18.8 ± 1.8	17.2 ± 0.9	18.8 ± 2.3
	5	6.5 ± 0.3	18.8 ± 1.2 ^{###}	16.6 ± 1.1	15.8 ± 1.0	16.0 ± 1.5
	7	6.6 ± 0.4	21.7 ± 1.2 ^{###}	16.8 ± 1.2*	12.9 ± 1.2**	15.1 ± 1.6*
	9	6.5 ± 0.5	21.3 ± 1.1 ^{###}	13.8 ± 1.5*	14.0 ± 1.2*	13.7 ± 1.7*
Organ indexes (%)	Spleen	0.32 ± 0.06	0.11 ± 0.01 ^{###}	0.13 ± 0.01**	0.15 ± 0.02**	0.17 ± 0.02***
	Kidney	1.27 ± 0.07	0.70 ± 0.07 ^{###}	0.79 ± 0.08*	0.73 ± 0.07	0.84 ± 0.13*

The data were analyzed using a one-way ANOVA and they are expressed as means ± SEMs ($n = 10$). ^{###} $p < 0.001$ versus db/+ mice; * $p < 0.05$, ** $p < 0.01$, and *** $p < 0.001$ versus nontreated db/db mice. TM: *T. melanosporum*.

[42], we determined the levels of serum TG, TC, HDL-C, and LDL-C to analyze the antihyperlipidemic activities of TM. Compared to the nontreated db/db mice, except for LDL-C, TM reduced the levels of TG ($p < 0.01$, Figure 2(a)) and TC ($p < 0.05$, Figure 2(b)) and enhanced the levels of HDL-C ($p < 0.05$, Figure 2(c)) in serum.

3.4. Renal Protective Effects of TM in db/db Mice. NAG is a lysosomal enzyme in proximal tubular cells and serves as an index of intense tubular damage in the early stages [43]. Similar to Met treatment, 0.4 g/kg of TM reduced the levels of NAG in the kidneys of the db/db mice by 37.6% ($p < 0.01$, Figure 3(a)). 6-keto-PGF1 α , MCP-5, and MMP-9 can also be used as valuable indicators of renal injury in DN. The 0.4 g/kg of TM treatment caused a 27.6% reduction in serum levels of 6-keto-PGF1 α in the db/db mice ($p < 0.05$, Figure 3(b)); 0.2 g/kg of TM treatment led to 50.6% and 47.6% increases in MCP-5 ($p < 0.01$, Figure 3(c)) and MMP-9 ($p < 0.001$, Figure 3(d)) serum levels in the db/db mice. Treatment with TM at 0.2 g/kg exhibited better effects on MCP-5 and MMP-9 levels in the kidney than did 0.4 g/kg ($p < 0.01$, Figures 3(c) and 3(d)). H&E and PAS staining of the kidney further confirmed the renal protective effect of TM. Many neutrophil infiltrations in the kidney calices and renal papillae were observed in the db/db mice, which significantly improved after TM and Met administration (Figure 3(e)). The PAS staining results showed that the thickened basement membrane of renal tubular epithelial cells and inflammatory cell infiltrations in the db/db mice were relieved by Met and TM (Figure 3(f)).

Typical hyperglycemia and hyperlipidemia of DN always result in glomerular injury associated with severe inflammation [44]. The release of inflammatory cytokines in the kidneys of the db/db mice was regulated by the 8-week TM treatment: 0.2 g/kg of TM strongly reduced the level of IL-2 by 20.2% ($p < 0.05$, Figure 4(a)) and increased the levels of IL-6 and IL-10 by 27.9% ($p < 0.05$, Figure 4(b)) and 74.4%

($p < 0.01$, Figure 4(c)), respectively. Only TM at 0.2 g/kg significantly improved IL-6 levels in the kidney.

3.5. The Antioxidative Effects of TM in the db/db Mice. Overproduction of ROS and hypoactivities of SOD, GSH-Px, and CAT were observed in the serum and/or kidneys of the db/db mice ($p < 0.05$, Table 7). TM, especially at 0.4 g/kg, increased serum levels of SOD and CAT by 12.9% and 17.5%, respectively ($p < 0.001$, Table 7); however, no significant influence on the serum levels of GSH-Px was noted in the TM-treated db/db mice. Additionally, TM significantly reduced the high levels of ROS in the kidney by 30.1% after 8 weeks administration ($p < 0.05$, Table 7).

3.6. Regulation of Nrf2 and NF- κ B Signaling by TM in db/db Mice. To understand the underlying mechanisms of the antidiabetic and antidiabetic nephritic effects of TM, the expression levels of proteins related to Nrf2 and NF- κ B signaling in the kidney were assessed by Western blotting. Compared with the db/db mice, TM visibly upregulated the expressions of CAT, HO-1, HO-2, SOD2, and Nrf2 ($p < 0.001$, Figure 5(a)) and downregulated the expressions of PKC- α ($p < 0.01$, Figure 5(a)), p-JAK2, p-STAT3, and p-NF- κ B in the kidneys ($p < 0.001$, Figure 5(b)).

4. Discussion

In the present study, we first confirmed the antidiabetic and antidiabetic nephritic effects of TM in db/db mice and clarified the underlying mechanisms associated with oxidative stress. Compared with currently used effective medicines (such as Met), TM contains various nutritional ingredients including 19 types of fatty acid, 17 types of amino acid, 6 vitamins, and 7 minerals. Its nature as a crude agent suggests that it has multieffective components, which might target many molecules in the signaling of inflammation and oxidative stress. This “systemic targeting” will eliminate the inflammation and oxidative stress in a much more “natural” way, so

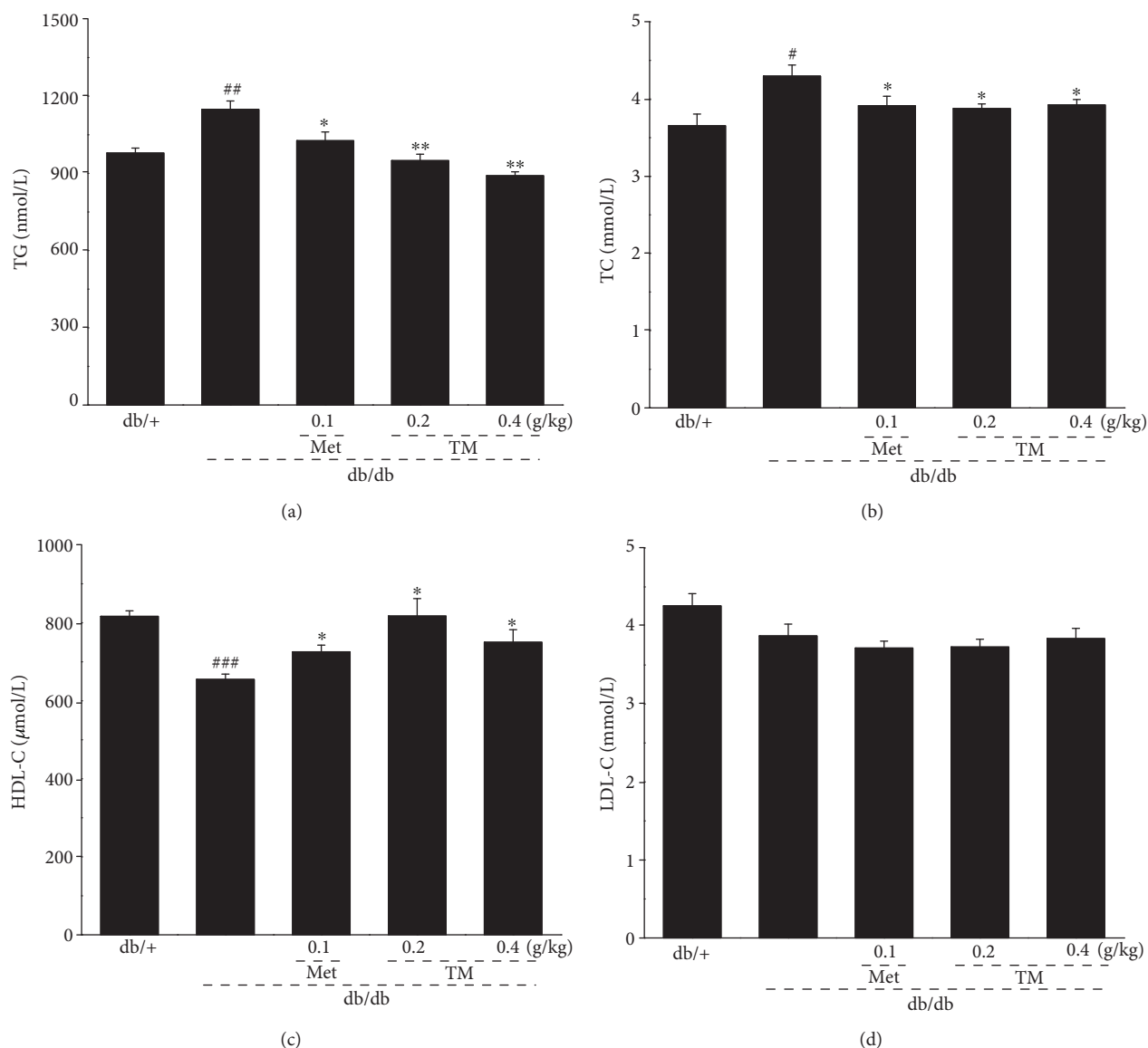


FIGURE 2: Eight-week TM treatment regulated the levels of the (a) TG, (b) TC, (c) HDL-C, and (d) LDL-C in the serum of db/db mice. The data were analyzed using post hoc test of Holm-Sidak, and they are expressed as means \pm SEMs ($n = 10$). # $p < 0.05$, ## $p < 0.01$, and ### $p < 0.001$ versus db/+ mice; * $p < 0.05$ and ** $p < 0.01$ versus nontreated db/db mice. TM: *T. melanosporum*; TG: triglyceride; TC: total cholesterol; HDL-C: high-density lipoprotein cholesterol; LDL-C: low-density lipoprotein cholesterol.

fewer adverse side effects are expected. The use of TM as a folk tonic food has been practiced by Europeans for thousands of years, which further emphasizes its safety and lack of adverse side effects. The “systemic targeting” may also explain the nondose-dependent manner by which TM displayed its antidiabetic and antidiabetic nephritic effects. A number of natural products are reported to show various pharmacological activities in a nondose-dependent manner [45, 46].

TM effectively decreased the body weights and food intakes of the db/db mice. The hypoglycemic activity of TM was confirmed by the reduction in blood glucose and the modulation of the OGTT and GHbA1c levels. TM enhanced the levels of HG and PK in serum. PK promotes carbohydrate metabolism via its contribution to the glycolytic pathway and

is a key glycolytic enzyme in glucose homeostasis [47]. As glycogen is the main intracellular storable form of glucose, the induction of glycogen accumulation in hepatocytes is an important antihyperglycemic phenomenon [38]. Furthermore, as a popular type 2 diabetic model, db/db mice develop insulin resistance, which leads to hyperglycemia and hyperinsulinemia [48]. Although the etiologies of DN are complex, dyslipidemia, characterized by abnormal lipid profiles, has been reported as a crucial factor in kidney damage [49, 50]. The characteristic features of diabetic lipid profiles are high levels of TG, TC, or LDL-C in serum and tissues [51]. Eight-week TM administration exhibited strongly hypolipidemic effects in db/db mice, suggesting renal protection.

Our data show that TM exerted strong renal protection by regulating the levels of NAG, 6-keto-PGF1 α , MCP-5,

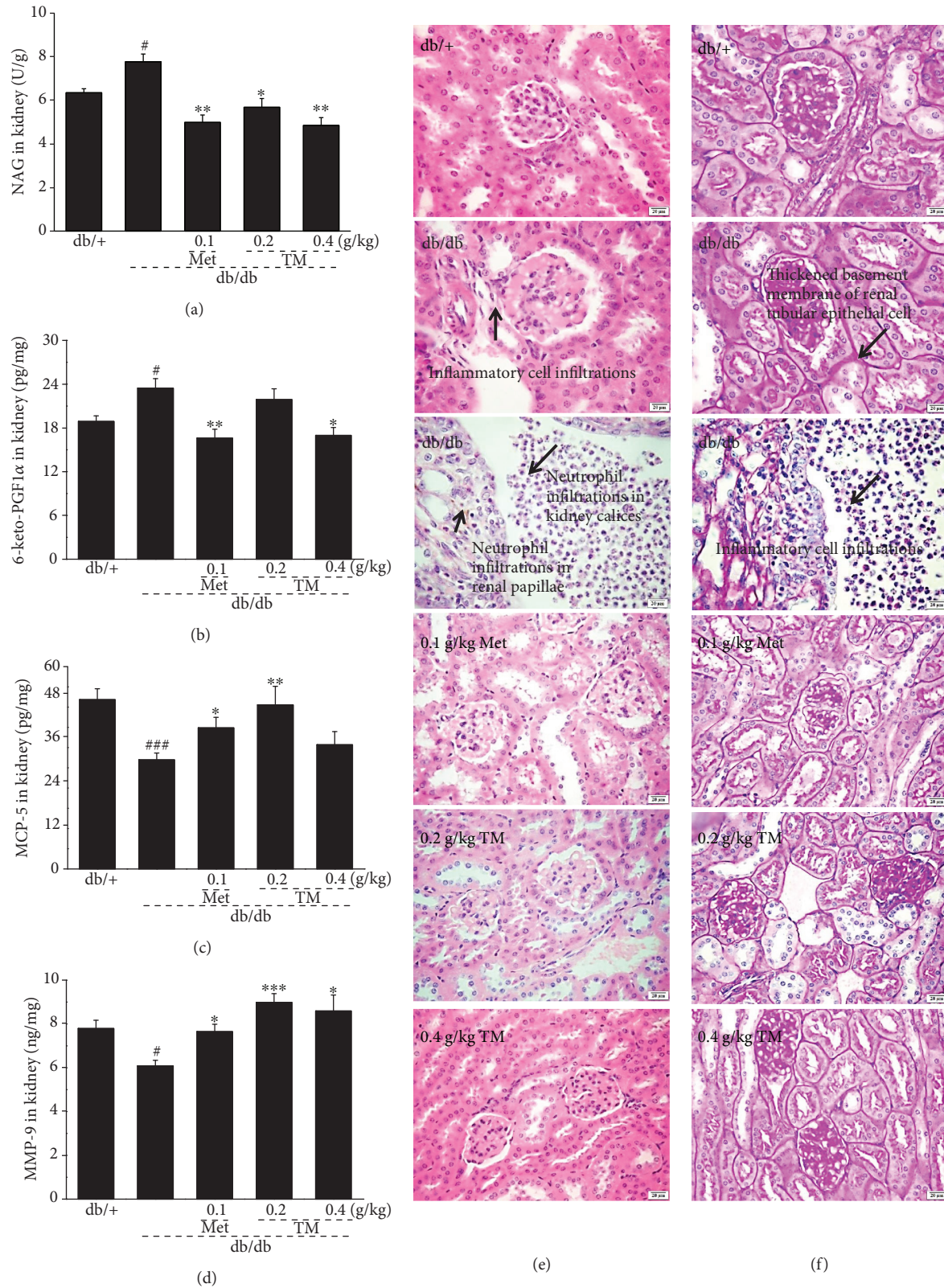


FIGURE 3: Eight-week TM treatment affected the levels of the (a) NAG, (b) 6-keto-PGF1 α , (c) MCP-5, and (d) MMP-9 in the kidney of db/db mice. The data were analyzed using post hoc test of Holm-Sidak, and they are expressed as means \pm SEMs ($n = 10$). [#] $p < 0.05$ and ^{###} $p < 0.001$ versus db/+ mice; ^{*} $p < 0.05$, ^{**} $p < 0.01$, and ^{***} $p < 0.001$ versus nontreated db/db mice. Histopathological analysis in kidney was shown by (e) H&E staining (scale bar: 20 μ m; magnification: 400x) and (f) PAS staining (scale bar: 20 μ m; magnification: 400x). TM: *T. melanosporum*; NAG: n-acetyl- β -d-glucosaminidase; 6-keto-PGF1 α : 6-keto prostaglandin F1 α ; MCP-5: monocyte chemotactic protein-5; MMP-9: matrix metalloproteinase-9; H&E: Hematoxylin and eosin; PAS: periodic acid Schiff.

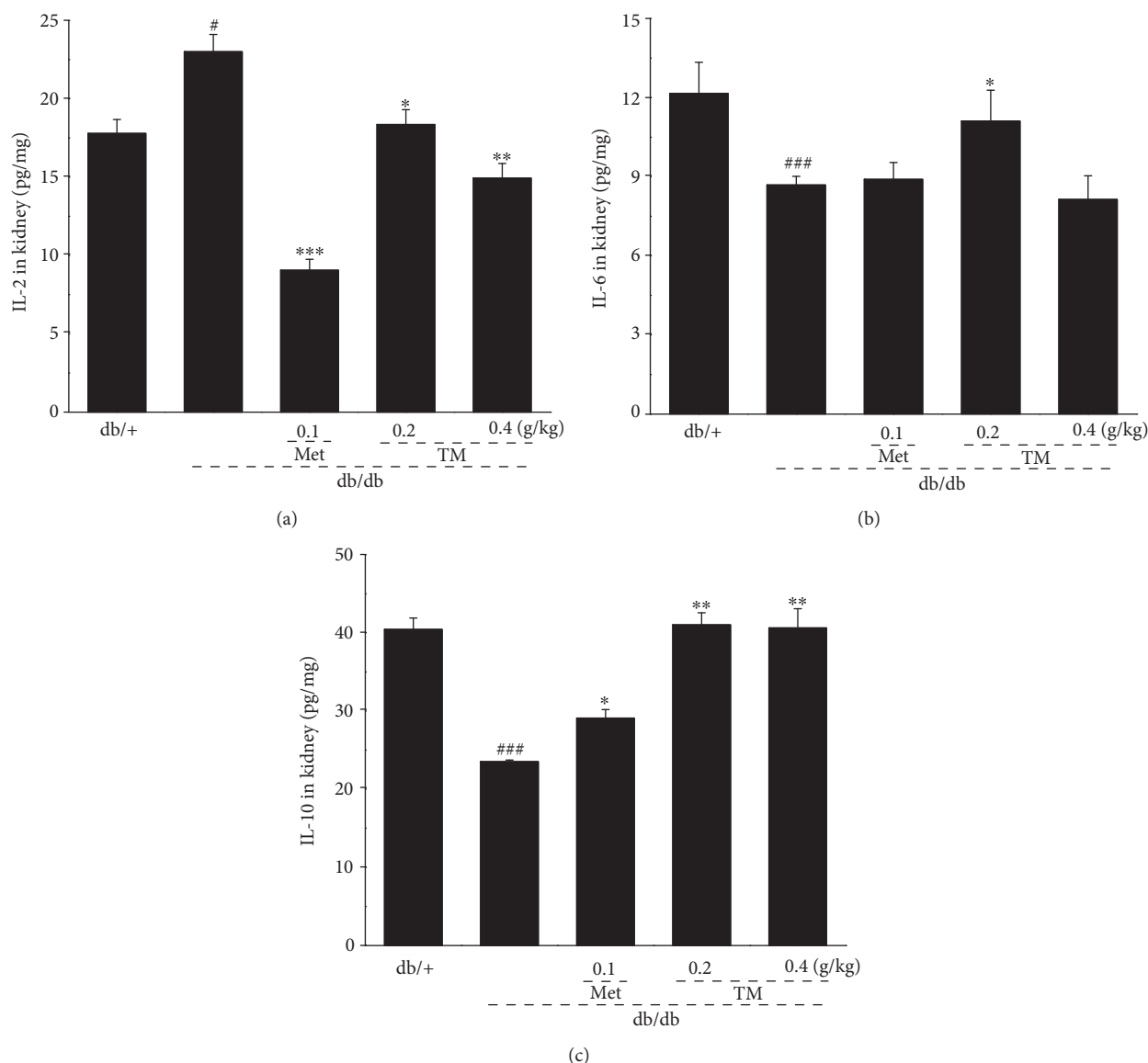


FIGURE 4: Eight-week TM treatment affected the levels of the (a) IL-2, (b) IL-6, and (c) IL-10 in the kidney of db/db mice. The data were analyzed using post hoc test of Holm-Sidak, and they are expressed as means \pm SEMs ($n = 10$). # $p < 0.05$ and ### $p < 0.001$ versus db/+ mice; * $p < 0.05$, ** $p < 0.01$, and *** $p < 0.001$ versus nontreated db/db mice. TM: *T. melanosporum*; IL-2: interleukin-2; IL-6: interleukin-6; IL-10: interleukin-10.

TABLE 7: The effects of *Tuber melanosporum* powder on oxidative stress-related factors in the serum and kidney of mice.

		db/+	db/db	0.1 g/kg Met	0.2 g/kg TM	0.4 g/kg TM
Serum	SOD (U/mL)	240.3 \pm 5.0	193.6 \pm 2.5###	245.7 \pm 3.9***	206.1 \pm 3.9*	218.6 \pm 5.5***
	GSH-Px (U/mL)	304.4 \pm 9.5	230.8 \pm 3.7###	227.2 \pm 6.0	248.8 \pm 11.6	236.5 \pm 5.3
	CAT (U/mL)	54.6 \pm 1.3	41.2 \pm 0.9###	45.2 \pm 1.5*	48.3 \pm 1.9**	48.4 \pm 1.1***
Kidney	ROS (U/mg)	46.1 \pm 1.7	62.6 \pm 4.1#	42.1 \pm 2.1***	51.1 \pm 0.5	43.3 \pm 3.2*
	SOD (U/mg)	34.9 \pm 2.8	23.3 \pm 1.3##	29.4 \pm 2.6*	37.0 \pm 5.0*	34.1 \pm 4.8*
	GSH-Px (mg/mL)	75.7 \pm 3.9	42.3 \pm 1.3###	50.8 \pm 3.0*	71.6 \pm 6.9**	67.7 \pm 6.4**
	CAT (U/mg)	8.7 \pm 0.5	7.0 \pm 0.3#	8.8 \pm 0.5*	8.9 \pm 0.4**	9.0 \pm 0.3**

The data were analyzed using a one-way ANOVA and they are expressed as means \pm SEMs ($n = 10$). # $p < 0.05$, ## $p < 0.01$, and ### $p < 0.001$ versus db/+ mice; * $p < 0.05$, ** $p < 0.01$, and *** $p < 0.001$ versus nontreated db/db mice. TM: *T. melanosporum*.

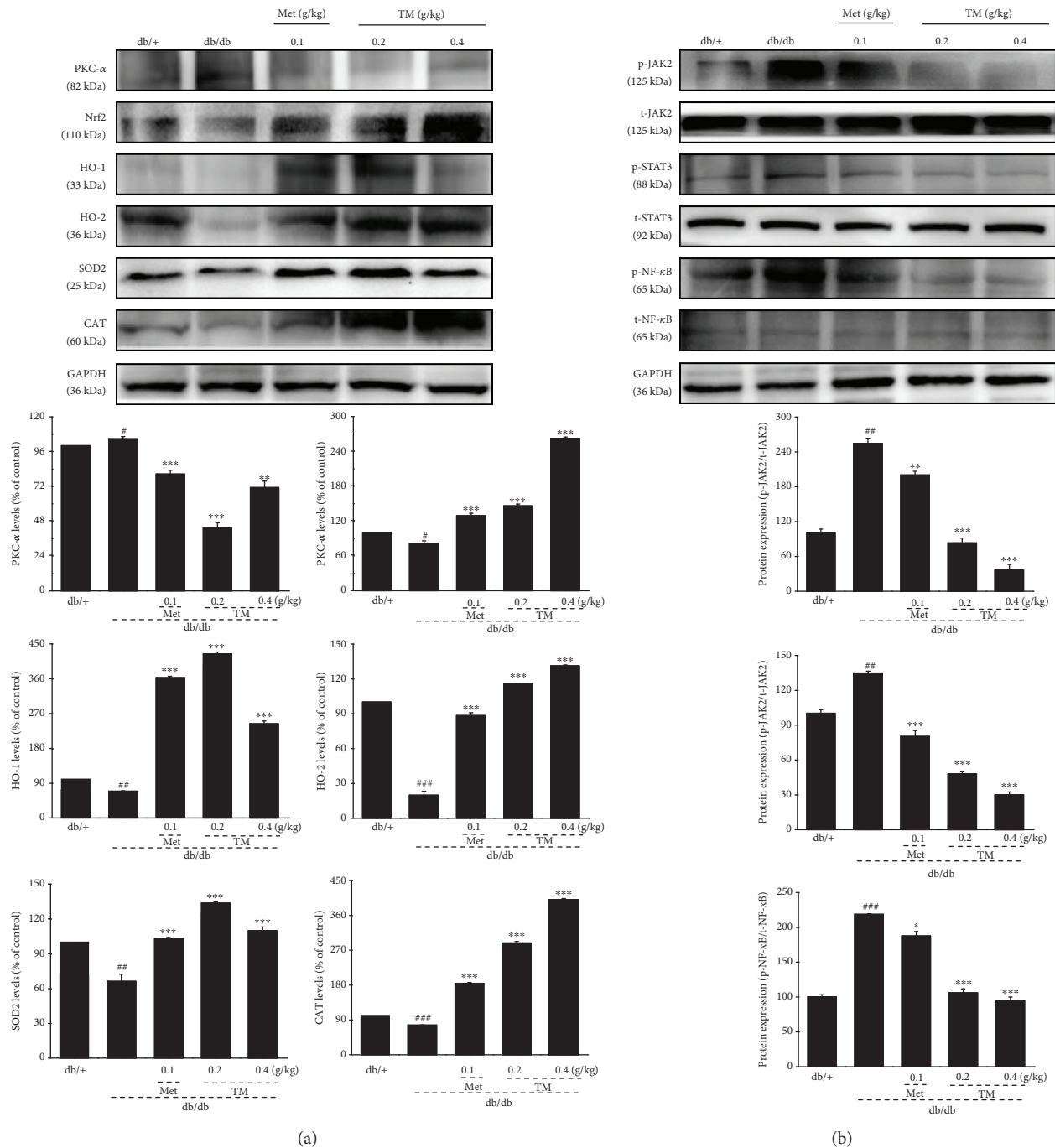


FIGURE 5: Eight-week TM treatment regulated the expressions of (a) CAT, HO-1, HO-2, SOD2, Nrf2, and PKC- α and (b) phosphor-JAK2, phosphor-NF- κ B, and phosphor-STAT3 in the kidney of db/db mice. The data on quantified protein expressions were normalized to the levels of GAPDH and related total proteins. The data were analyzed using post hoc test of Holm-Sidak, and they are expressed as means \pm SEMs ($n = 10$). $^{\#}p < 0.05$, $^{\#\#}p < 0.01$, and $^{\#\#\#}p < 0.001$ versus db/+ mice; $^*p < 0.05$, $^{**}p < 0.01$, and $^{***}p < 0.001$ versus nontreated db/db mice. TM: *T. melanosporum*; CAT: catalase; HO-1: heme oxygenase 1; HO-2: heme oxygenase 2; SOD2: superoxide dismutase 2; Nrf2: nuclear respiratory factor 2; PKC- α : protein kinase C alpha; JAK2: janus kinase 2; NF- κ B: nuclear factor- κ B; STAT3: signal transducers and activators of transcription 3.

and MMP-9. NAG and 6-keto-PGF1 α serve as specific and sensitive indicators of the extent of oxidative damage and acute kidney damage [52, 53]. The accumulation of extracellular matrix is a pathological characteristic of DN. MMP-9 protects mice by promoting the decomposition of glomeruli

fibrin caps during glomerulonephritis via fibrinolytic activity [54]. MCP-5 is reported to be a murine homolog of human MCP-1, which is secreted by renal tubular epithelial cells and kidney mesangial cells during the process of inflammation and is differentially expressed in the kidneys [55].

Cytokines, as small proteins with multipotent biological features, including interleukins and interferons, show anti-inflammatory or proinflammatory properties [56]. Interleukins play an important role during the development of inflammation. The overproduction of IL-2 activates proinflammatory CD4+, which exacerbates glomerular damage via recruiting macrophages and neutrophils [57]. IL-6 can enhance basic and insulin-stimulated glucose uptake and has favorable effects on energy metabolism [58]. As an inhibitor of TNF- α expression, IL-10 is recognized as an efficient anti-inflammatory cytokine, which can ameliorate insulin resistance and hyperglycemia [59, 60]. Eight-week TM administration successfully regulated the levels of interleukins in the kidneys of db/db mice, further confirming its renal protective effects. In diabetes, hyperglycemia activates protein kinase C (PKC), which increases the expression of NF- κ B and induces both cytokines and chemokines [61], which contribute to the accumulation of the extracellular matrix and injury of podocytes in diabetic animals [62]. The JAK/STAT system mediates abnormal kidney diseases, and suppression of JAK2 expression can relieve DN progression [63]. Phosphorylated JAKs result in the activation of full STAT activities [63]. It has been reported that NF- κ B activates STAT3 on tyrosine residues indirectly [64]. Our data suggest that TM-mediated renal protection in db/db mice may be related to its modulation of NF- κ B activation.

Oxidative stress, which is related to the overproduction of ROS, has been identified as a general pathogenic factor in DN [62, 65]. In contrast, antioxidant enzymes including SOD, GSH-Px, and CAT scavenge free radicals and prevent oxidative injury [66]. TM exhibited significant antioxidative effects in db/db mice by reducing ROS levels and increasing SOD, CAT, and GSH-Px levels in the kidneys and/or serum. Nrf2 is an important inducible transcription factor that protects redox homeostasis from oxidative injury [67]. Nrf2 combines with antioxidant response element (ARE) and mediates the expression of downstream genes HO-1 and SOD-1, which encode detoxifying and antioxidant enzymes in consort with relevant proteins [68, 69]. Subsequently, the overproduced ROS is scavenged via the activation of Nrf2 [70]. The inactivation of Nrf2 signaling is reported to be beneficial for the overactivation of NF- κ B [71].

In summary, we successfully explored the antidiabetic and antidiabetic nephritic properties of TM in db/db diabetic mice and found that these effects may be related to the modulation of oxidative stress and inflammation-related cytokines via Nrf2 signaling. The effects of TM are similar to those of Met, a commonly used hyperglycemic drug, which supports TM as a candidate nutritious natural product for DN adjunctive therapy.

Data Availability

The data used to support the findings of this study are available from the corresponding author upon request.

Conflicts of Interest

The authors have declared that there is no conflict of interest.

Acknowledgments

This work was supported by the Science and Technology Key Project in Jilin Province of China (Grant nos. 20150203002NY and 20160204029YY) and the Special Projects of the cooperation between Jilin University and Jilin Province (Grant no. SXGJSF2017-1).

References

- [1] F. F. Chen, J. T. Wang, L. X. Zhang et al., "Oleanolic acid derivative DKS26 exerts antidiabetic and hepatoprotective effects in diabetic mice and promotes glucagon-like peptide-1 secretion and expression in intestinal cells," *British Journal of Pharmacology*, vol. 174, no. 17, pp. 2912–2928, 2017.
- [2] M. R. Jain, A. A. Joharapurkar, S. G. Kshirsagar et al., "ZY15557, a novel, long acting inhibitor of dipeptidyl peptidase-4, for the treatment of type 2 diabetes mellitus," *British Journal of Pharmacology*, vol. 174, no. 14, pp. 2346–2357, 2017.
- [3] S. Y. Park, B. Jin, J. H. Shin, S. Adisakwattana, and O. Kwon, "Standardized *Mori ramulus* extract improves insulin secretion and insulin sensitivity in C57BLKS/J db/db mice and INS-1 cells," *Biomedicine & Pharmacotherapy*, vol. 92, pp. 308–315, 2017.
- [4] J. Wang, L. Teng, Y. Liu et al., "Studies on the antidiabetic and antinephritic activities of *Paecilomyces hepiali* water extract in diet-streptozotocin-induced diabetic Sprague Dawley rats," *Journal of Diabetes Research*, vol. 2016, Article ID 4368380, 10 pages, 2016.
- [5] V. Gowd, Z. Jia, and W. Chen, "Anthocyanins as promising molecules and dietary bioactive components against diabetes – a review of recent advances," *Trends in Food Science & Technology*, vol. 68, pp. 1–13, 2017.
- [6] L. Ang, L. Yuguang, W. Liying, Z. Shuying, X. Liting, and W. Shumin, "Ergosterol alleviates kidney injury in streptozotocin-induced diabetic mice," *Evidence-based Complementary and Alternative Medicine*, vol. 2015, Article ID 691594, 8 pages, 2015.
- [7] R. el Boustany, C. Taveau, C. Chollet et al., "Antagonism of vasopressin V2 receptor improves albuminuria at the early stage of diabetic nephropathy in a mouse model of type 2 diabetes," *Journal of Diabetes and its Complications*, vol. 31, no. 6, pp. 929–932, 2017.
- [8] C. S. Lo, Y. Shi, I. Chenier et al., "Heterogeneous nuclear ribonucleoprotein F stimulates sirtuin-1 gene expression and attenuates nephropathy progression in diabetic mice," *Diabetes*, vol. 66, no. 7, pp. 1964–1978, 2017.
- [9] E. S. Lee, M. Y. Lee, M. H. Kwon et al., "Sarpogrelate hydrochloride ameliorates diabetic nephropathy associated with inhibition of macrophage activity and inflammatory reaction in db/db mice," *PLoS One*, vol. 12, no. 6, article e0179221, 2017.
- [10] C. Ying, Y. Mao, L. Chen et al., "Bamboo leaf extract ameliorates diabetic nephropathy through activating the AKT signaling pathway in rats," *International Journal of Biological Macromolecules*, vol. 105, Part 3, pp. 1587–1594, 2017.
- [11] F. Giacco and M. Brownlee, "Oxidative stress and diabetic complications," *Circulation Research*, vol. 107, no. 9, pp. 1058–1070, 2010.
- [12] W. Sun, G. Xu, X. Guo et al., "Protective effects of asiatic acid in a spontaneous type 2 diabetic mouse model," *Molecular Medicine Reports*, vol. 16, no. 2, pp. 1333–1339, 2017.

- [13] L. Ding, S. Lu, Y. Wang et al., "BPI-3016, a novel long-acting hGLP-1 analogue for the treatment of type 2 diabetes mellitus," *Pharmacological Research*, vol. 122, pp. 130–139, 2017.
- [14] Y. Liu, Y. You, Y. Li et al., "The characterization, selenylation and antidiabetic activity of mycelial polysaccharides from *Catathelasma ventricosum*," *Carbohydrate Polymers*, vol. 174, pp. 72–81, 2017.
- [15] P. Kamtchouing, S. M. Kahpui, P. D. D. Dzeufiet, L. Tédong, E. A. Asongalem, and T. Dimo, "Anti-diabetic activity of methanol/methylene chloride stem bark extracts of *Terminalia superba* and *Canarium schweinfurthii* on streptozotocin-induced diabetic rats," *Journal of Ethnopharmacology*, vol. 104, no. 3, pp. 306–309, 2006.
- [16] R. S. Liu and Y. J. Tang, "*Tuber melanosporum* fermentation medium optimization by Plackett-Burman design coupled with Draper-Lin small composite design and desirability function," *Bioresource Technology*, vol. 101, no. 9, pp. 3139–3146, 2010.
- [17] S. Wang and M. F. Marcone, "The biochemistry and biological properties of the world's most expensive underground edible mushroom: truffles," *Food Research International*, vol. 44, no. 9, pp. 2567–2581, 2011.
- [18] B. Senturk, B. M. Demircan, A. D. Ozkan et al., "Diabetic wound regeneration using heparin-mimetic peptide amphiphile gel in db/db mice," *Biomaterials Science*, vol. 5, no. 7, pp. 1293–1303, 2017.
- [19] P. S. Chow and S. M. Landhauser, "A method for routine measurements of total sugar and starch content in woody plant tissues," *Tree Physiology*, vol. 24, no. 10, pp. 1129–1136, 2004.
- [20] P. Xue, Y. Zhao, C. Wen, S. Cheng, and S. Lin, "Effects of electron beam irradiation on physicochemical properties of corn flour and improvement of the gelatinization inhibition," *Food Chemistry*, vol. 233, pp. 467–475, 2017.
- [21] P. Sáez-Plaza, T. Michałowski, M. J. Navas, A. G. Asuero, and S. Wybraniec, "An overview of the Kjeldahl method of nitrogen determination. Part I. Early history, chemistry of the procedure, and titrimetric finish," *Critical Reviews in Analytical Chemistry*, vol. 43, no. 4, pp. 178–223, 2013.
- [22] E. Jurak, A. M. Punt, W. Arts, M. A. Kabel, and H. Gruppen, "Fate of carbohydrates and lignin during composting and mycelium growth of *Agaricus bisporus* on wheat straw based compost," *PLoS One*, vol. 10, no. 10, article e0138909, 2015.
- [23] E. de Santiago, M. Domínguez-Fernández, C. Cid, and M. P. de Peña, "Impact of cooking process on nutritional composition and antioxidants of cactus cladodes (*Opuntia ficus-indica*)," *Food Chemistry*, vol. 240, pp. 1055–1062, 2018.
- [24] T. Tesfaye, B. Sithole, D. Ramjugernath, and V. Chunilall, "Valorisation of chicken feathers: characterisation of chemical properties," *Waste Management*, vol. 68, pp. 626–635, 2017.
- [25] V. L. Singleton, R. Orthofer, and R. M. Lamuela-Raventos, "[14] Analysis of total phenols and other oxidation substrates and antioxidants by means of Folin-Ciocalteu reagent," *Methods in Enzymology*, vol. 299, pp. 152–178, 1999.
- [26] B. Chen, B. Ke, L. Ye et al., "Isolation and varietal characterization of *Ganoderma resinaceum* from areas of *Ganoderma lucidum* production in China," *Scientia Horticulturae*, vol. 224, pp. 109–114, 2017.
- [27] X. Wang, X. Wang, and Y. Guo, "Rapidly simultaneous determination of six effective components in *Cistanche tubulosa* by near infrared spectroscopy," *Molecules*, vol. 22, no. 5, 2017.
- [28] P. Mattila, K. Könkö, M. Eurola et al., "Contents of vitamins, mineral elements, and some phenolic compounds in cultivated mushrooms," *Journal of Agricultural and Food Chemistry*, vol. 49, no. 5, pp. 2343–2348, 2001.
- [29] C. Zhao, X. Zhao, J. Zhang et al., "Screening of *Bacillus* strains from sun vinegar for efficient production of flavonoid and phenol," *Indian Journal of Microbiology*, vol. 56, no. 4, pp. 498–503, 2016.
- [30] J. R. Bertolín, M. Joy, P. J. Rufino-Moya, S. Lobón, and M. Blanco, "Simultaneous determination of carotenoids, tocopherols, retinol and cholesterol in ovine lyophilised samples of milk, meat, and liver and in unprocessed/raw samples of fat," *Food Chemistry*, vol. 257, pp. 182–188, 2018.
- [31] L. B. D. C. Araújo, S. L. Silva, M. A. M. Galvão et al., "Total phytoester content in drug materials and extracts from roots of *Acanthospermum hispidum* by UV-VIS spectrophotometry," *Revista Brasileira de Farmacognosia*, vol. 23, no. 5, pp. 736–742, 2013.
- [32] T. Massouras, K. A. Triantaphyllopoulos, and I. Theodossiou, "Chemical composition, protein fraction and fatty acid profile of donkey milk during lactation," *International Dairy Journal*, vol. 75, pp. 83–90, 2017.
- [33] C. Canoura, M. T. Kelly, and H. Ojeda, "Effect of irrigation and timing and type of nitrogen application on the biochemical composition of *Vitis vinifera* L. cv. Chardonnay and Syrah grapeberries," *Food Chemistry*, vol. 241, pp. 171–181, 2018.
- [34] D. P. Peyton, M. G. Healy, G. T. A. Fleming et al., "Nutrient, metal and microbial loss in surface runoff following treated sludge and dairy cattle slurry application to an Irish grassland soil," *Science of The Total Environment*, vol. 541, pp. 218–229, 2016.
- [35] W. P. C. Santos, N. M. Ribeiro, D. C. M. B. Santos, M. G. A. Korn, and M. V. Lopes, "Bioaccessibility assessment of toxic and essential elements in produced pulses, Bahia, Brazil," *Food Chemistry*, vol. 240, pp. 112–122, 2018.
- [36] Y. F. Gao, M. N. Zhang, T. X. Wang, T. C. Wu, R. D. Ai, and Z. S. Zhang, "Hypoglycemic effect of D-chiro-inositol in type 2 diabetes mellitus rats through the PI3K/Akt signaling pathway," *Molecular and Cellular Endocrinology*, vol. 433, pp. 26–34, 2016.
- [37] R. Subramanian, M. Z. Asmawi, and A. Sadikun, "In vitro α -glucosidase and α -amylase enzyme inhibitory effects of *Andrographis paniculata* extract and andrographolide," *Acta Chimica Polonica*, vol. 55, no. 2, pp. 391–398, 2008.
- [38] C.-W. Liu, Y. C. Wang, C. C. Hsieh, H. C. Lu, and W. D. Chiang, "Guava (*Psidium guajava* Linn.) leaf extract promotes glucose uptake and glycogen accumulation by modulating the insulin signaling pathway in high-glucose-induced insulin-resistant mouse FL83B cells," *Process Biochemistry*, vol. 50, no. 7, pp. 1128–1135, 2015.
- [39] J. Wang, W. Hu, L. Li et al., "Antidiabetic activities of polysaccharides separated from *Inonotus obliquus* via the modulation of oxidative stress in mice with streptozotocin-induced diabetes," *PLoS One*, vol. 12, no. 6, article e0180476, 2017.
- [40] B. A. Sheikh, L. Pari, A. Rathinam, and R. Chandramohan, "Trans-anethole, a terpenoid ameliorates hyperglycemia by regulating key enzymes of carbohydrate metabolism in streptozotocin induced diabetic rats," *Biochimie*, vol. 112, pp. 57–65, 2015.
- [41] Y. Horiuchi, D. Nakatsu, F. Kano, and M. Murata, "Pyruvate kinase M1 interacts with A-Raf and inhibits endoplasmic

- reticulum stress-induced apoptosis by activating MEK1/ERK pathway in mouse insulinoma cells," *Cellular Signalling*, vol. 38, pp. 212–222, 2017.
- [42] J. Yu, P. J. Cui, W. L. Zeng et al., "Protective effect of selenium-polysaccharides from the mycelia of *Coprinus comatus* on alloxan-induced oxidative stress in mice," *Food Chemistry*, vol. 117, no. 1, pp. 42–47, 2009.
- [43] O. S. Mohamed Ali, S. S. Elshaer, H. M. Anwar, and M. S. E. L. D. Zohni, "Relevance of cystatin-C, N-acetylglucosaminidase, and interleukin-18 with the diagnosis of acute kidney injury induced by cadmium in rats," *Journal of Biochemical and Molecular Toxicology*, vol. 31, no. 11, 2017.
- [44] Y. Birnbaum, M. Bajaj, J. Qian, and Y. Ye, "Dipeptidyl peptidase-4 inhibition by saxagliptin prevents inflammation and renal injury by targeting the Nlrp 3/ASC inflammasome," *BMJ Open Diabetes Research & Care*, vol. 4, no. 1, article e000227, 2016.
- [45] J. Wei, S. Wang, G. Liu et al., "Polysaccharides from *Enteromorpha prolifera* enhance the immunity of normal mice," *International Journal of Biological Macromolecules*, vol. 64, pp. 1–5, 2014.
- [46] L. Ma, S. Zhang, and M. Du, "Cordycepin from *Cordyceps militaris* prevents hyperglycemia in alloxan-induced diabetic mice," *Nutrition Research*, vol. 35, no. 5, pp. 431–439, 2015.
- [47] Y. C. Kim, J. H. Kim, D. Y. Cheung et al., "The usefulness of a novel screening kit for colorectal cancer using the immunochromatographic fecal tumor M2 pyruvate kinase test," *Gut and Liver*, vol. 9, no. 5, pp. 641–648, 2015.
- [48] I. M. Wahba and R. H. Mak, "Obesity and obesity-initiated metabolic syndrome: mechanistic links to chronic kidney disease," *Clinical Journal of the American Society of Nephrology*, vol. 2, no. 3, pp. 550–562, 2007.
- [49] T. Wu, Z. Yu, Q. Tang et al., "Honeysuckle anthocyanin supplementation prevents diet-induced obesity in C57BL/6 mice," *Food & Function*, vol. 4, no. 11, pp. 1654–1661, 2013.
- [50] T. Wu, Q. Tang, Z. Gao et al., "Blueberry and mulberry juice prevent obesity development in C57BL/6 mice," *PLoS One*, vol. 8, no. 10, article e77585, 2013.
- [51] S. Palazhy and V. Viswanathan, "Lipid abnormalities in type 2 diabetes mellitus patients with overt nephropathy," *Diabetes and Metabolism Journal*, vol. 41, no. 2, pp. 128–134, 2017.
- [52] N. E. el-Ashmawy, E. G. Khedr, H. A. el-Bahrawy, and S. A. el-Berashy, "Effect of human umbilical cord blood-derived mononuclear cells on diabetic nephropathy in rats," *Biomedicine & Pharmacotherapy*, vol. 97, pp. 1040–1045, 2018.
- [53] D. Liu, P. Huang, X. Li, M. Ge, G. Luo, and Z. Hei, "Using inflammatory and oxidative biomarkers in urine to predict early acute kidney injury in patients undergoing liver transplantation," *Biomarkers*, vol. 19, no. 5, pp. 424–429, 2014.
- [54] B. Lelongt, S. Bengatta, M. Delauche, L. R. Lund, Z. Werb, and P. M. Ronco, "Matrix metalloproteinase 9 protects mice from anti-glomerular basement membrane nephritis through its fibrinolytic activity," *Journal of Experimental Medicine*, vol. 193, no. 7, pp. 793–802, 2001.
- [55] J. M. Chung, B. K. Park, J. H. Kim, H. J. Lee, and S. D. Lee, "Impact of repeated extracorporeal shock wave lithotripsy on prepubertal rat kidney," *Urolithiasis*, pp. 1–10, 2017.
- [56] W. Eik Filho, S. S. Marcon, T. Krupek et al., "Blood levels of pro-inflammatory and anti-inflammatory cytokines during an oral glucose tolerance test in patients with symptoms suggesting reactive hypoglycemia," *Brazilian Journal of Medical and Biological Research*, vol. 49, no. 8, 2016.
- [57] R. Bertelli, A. Di Donato, M. Cioni et al., "LPS nephropathy in mice is ameliorated by IL-2 independently of regulatory T cells activity," *PLoS One*, vol. 9, no. 10, article e111285, 2014.
- [58] J. K. Ihalainen, J. P. Ahtainen, S. Walker et al., "Resistance training status modifies inflammatory response to explosive and hypertrophic resistance exercise bouts," *Journal of Physiology and Biochemistry*, vol. 73, no. 4, pp. 595–604, 2017.
- [59] A. Denys, I. A. Udalova, C. Smith et al., "Evidence for a dual mechanism for IL-10 suppression of TNF- α production that does not involve inhibition of p38 mitogen-activated protein kinase or NF- κ B in primary human macrophages," *The Journal of Immunology*, vol. 168, no. 10, pp. 4837–4845, 2002.
- [60] J. Zhang, Z. Deng, L. Jin et al., "Spleen-derived anti-inflammatory cytokine IL-10 stimulated by adipose tissue-derived stem cells protects against type 2 diabetes," *Stem Cells and Development*, vol. 26, no. 24, pp. 1749–1758, 2017.
- [61] M. Hamzawy, S. A. A. Gouda, L. Rashid, M. Attia Morcos, H. Shoukry, and N. Sharawy, "The cellular selection between apoptosis and autophagy: roles of vitamin D, glucose and immune response in diabetic nephropathy," *Endocrine*, vol. 58, no. 1, pp. 66–80, 2017.
- [62] W. Wadie and D. M. El-Tanbouly, "Vinpocetine mitigates proteinuria and podocytes injury in a rat model of diabetic nephropathy," *European Journal of Pharmacology*, vol. 814, pp. 187–195, 2017.
- [63] C. Guo, L. Yang, C. X. Wan et al., "Anti-neuroinflammatory effect of sophoraflavanone G from *Sophora alopecuroides* in LPS-activated BV2 microglia by MAPK, JAK/STAT and Nrf2/HO-1 signaling pathways," *Phytomedicine*, vol. 23, no. 13, pp. 1629–1637, 2016.
- [64] U. Rozovski, D. M. Harris, P. Li et al., "Activation of the B-cell receptor successively activates NF- κ B and STAT3 in chronic lymphocytic leukemia cells," *International Journal of Cancer*, vol. 141, no. 10, pp. 2076–2081, 2017.
- [65] S. Y. Nam, H. M. Kim, and H. J. Jeong, "Anti-fatigue effect by active dipeptides of fermented porcine placenta through inhibiting the inflammatory and oxidative reactions," *Biomedicine & Pharmacotherapy*, vol. 84, pp. 51–59, 2016.
- [66] R. Liang, Z. Zhang, and S. Lin, "Effects of pulsed electric field on intracellular antioxidant activity and antioxidant enzyme regulating capacities of pine nut (*Pinus koraiensis*) peptide QDHCH in HepG2 cells," *Food Chemistry*, vol. 237, pp. 793–802, 2017.
- [67] X. Sun, Y. Yang, J. Shi, C. Wang, Z. Yu, and H. Zhang, "NOX4 and Nrf2-mediated oxidative stress induced by silver nanoparticles in vascular endothelial cells," *Journal of Applied Toxicology*, vol. 37, no. 12, pp. 1428–1437, 2017.
- [68] D. F. Engel, J. de Oliveira, V. Lieberknecht, A. L. S. Rodrigues, A. F. de Bem, and N. H. Gabilan, "Duloxetine protects human neuroblastoma cells from oxidative stress-induced cell death through Akt/Nrf-2/HO-1 pathway," *Neurochemical Research*, vol. 43, no. 2, pp. 387–396, 2018.
- [69] W. Liao, Z. Fu, Y. Zou et al., "MicroRNA-140-5p attenuated oxidative stress in cisplatin induced acute kidney injury by activating Nrf2/ARE pathway through a Keap1-independent mechanism," *Experimental Cell Research*, vol. 360, no. 2, pp. 292–302, 2017.

- [70] K. Ha Kim, R. T. Sadikot, J. Yeon Lee et al., "Suppressed ubiquitination of Nrf2 by p47^{phox} contributes to Nrf2 activation," *Free Radical Biology & Medicine*, vol. 113, pp. 48–58, 2017.
- [71] L. R. Aldaba-Muruato, M. H. Muñoz-Ortega, J. R. Macías-Pérez, J. Pulido-Ortega, S. L. Martínez-Hernández, and J. Ventura-Juárez, "Adrenergic regulation during acute hepatic infection with *Entamoeba histolytica* in the hamster: involvement of oxidative stress, Nrf2 and NF- κ B," *Parasite*, vol. 24, p. 46, 2017.